Sun. Jun 15, 2025

| Main conference：Main conference

Sun. Jun 15, 2025 1:50 PM - 5:30 PM JST | Sun. Jun 15, 2025 4:50 AM - 8:30 AM UTC Centennial Hall (Clock Tower Centennial Hall)

[15tu] Tutorials

Chair: Kazuhiro Yanagi

1:50 PM - 2:30 PM JST | 4:50 AM - 5:30 AM UTC

[15tu-01]

Dispersion and Structure Sorting of Single-Wall Carbon Nanotubes

*Hiromichi Kataura[1] (1. AIST until March (Japan))

2:50 PM - 3:30 PM JST | 5:50 AM - 6:30 AM UTC

[15tu-02]

Synthesis of Single-Walled Carbon Nanotubes

Yan Li[1] (1. Peking University (China))

3:50 PM - 4:30 PM JST | 6:50 AM - 7:30 AM UTC

[15tu-03]

Contemporary challenges in van der Waals layered semiconductors

*Young Hee Lee[1] (1. Sungkyunkwan University (Korea))

4:50 PM - 5:30 PM JST | 7:50 AM - 8:30 AM UTC

[15tu-04]

Tutorial: How do we analyze Raman spectra?

*Riichiro Saito[1,2] (1. Tohoku University, (Japan), 2. National Taiwan Normal University (Taiwan))

Mon. Jun 16, 2025

| Main conference：Main conference

Mon. Jun 16, 2025 9:30 AM - 12:10 PM JST | Mon. Jun 16, 2025 12:30 AM - 3:10 AM UTC Centennial Hall (Clock Tower Centennial Hall)

[16ma] Main Conference

Chair: Yutaka Ohno, Keigo Otsuka

9:30 AM - 10:10 AM JST | 12:30 AM - 1:10 AM UTC

[16ma-01]

Towards fab-compatible low-dimensional semiconductor electronics

*Lian-Mao Peng[1] (1. Peking University (China))

10:10 AM - 10:40 AM JST | 1:10 AM - 1:40 AM UTC

[16ma-02]

Carbon nanotube-based flexible amplifier

*Youfan Hu[1] (1. Peking University (China))

11:00 AM - 11:30 AM JST | 2:00 AM - 2:30 AM UTC

[16ma-03]

TRANSFORMING PRECURSOR MOLECULES INTO 1D CARBON NANOMATERIALS INSIDE CARBON NANOTUBES

Huiju Cao[1], Yingzhi Chen[1], Kunpeng Tang[1], Yanghao Feng[1], Weili Cui[1], Wendi Zhang[2], Kecheng Cao[2], *Lei Shi[1] (1. Sun Yat-sen University (China), 2. ShanghaiTech University (China))

11:30 AM - 11:50 AM JST | 2:30 AM - 2:50 AM UTC

[16ma-04]

Confined carbyne is a tailored hybrid system with vibronic properties solely driven by anharmonic interactions.

*Thomas Pichler[1] (1. University of Vienna (Austria))

11:50 AM - 12:10 PM JST | 2:50 AM - 3:10 AM UTC

[16ma-05]

BNNT as molecular template : from single molecule chains to superradiant light emitters

Jean-Baptiste Marceau[1], Juliette Le Balle[1,2], Duc-Minh Ta[4], Alberto Aguilar[4], Annick Loiseau[2], Richard Martel[5], Pierre Bon[4], Raphael Voituriez[3], Gaelle Recher[1], *Etienne Gaufrès[1] (1. CNRS-Université de Bordeaux (France), 2. CNRS-Onera (France), 3. Sorbonne University (France), 4. CNRS- University of Limoges (France), 5. Université de Montréal (Canada))

| Parallel Symposia：Symposium on Nanomaterials for Energy and Electronics

Mon. Jun 16, 2025 2:00 PM - 5:20 PM JST | Mon. Jun 16, 2025 5:00 AM - 8:20 AM UTC Conference room 5a/5b(INNOVATION BLDG., 5F)

[16en] Energy & Electronics

Chair:Suguru Noda, Yoshiyuki Nonoguchi

2:00 PM - 2:40 PM JST | 5:00 AM - 5:40 AM UTC

[16en-01]

Recent Advances towards High-Performance Carbon Nanotube FETs

*Nathaniel Safron[1], Matthias Passlack[1], Hsin-Yuan Chiu[2], Tzu-Ang Chao[2], Carlo Gilardi[1], H.-S. Philip Wong[2], Marvin M.-F. Chang[2], Gregory Pitner[1], Iuliana Radu[2] (1. TSMC Corporate Research (United States of America), 2. TSMC Corporate Research (Taiwan))

2:40 PM - 3:00 PM JST | 5:40 AM - 6:00 AM UTC

[16en-02]

Exploring aligned CNT material for device application: variability and polymer cleaning

*Marina Y. Timmermans[1], Luca Mana[1,2], Himanshu Sharma[1], Dennis Lin[1], Jean-François de Marneffe[1], Patrick Kelp[1], Atefeh Fathzadeh[1,2], Philippe Bezard[1], Xiangyu Wu[1], Han Han[1], Lijun Liu[1,2], Katherine R. Jinkins[3], Michael S. Arnold[3], Claudia Fleischmann[1,2], Steven Brems[1], Cesar J. L. de la Rosa[1], Gouri S. Kar[1] (1. imec (Belgium), 2. KU Leuven (Belgium), 3. SixLine Semiconductor (United States of America))

3:00 PM - 3:20 PM JST | 6:00 AM - 6:20 AM UTC

[16en-03]

Nanomaterials-based Monolithic 3D Integration for Energy-Efficient Computing

*Jianshi Tang[1] (1. School of Integrated Circuits, Tsinghua University (China))

4:00 PM - 4:20 PM JST | 7:00 AM - 7:20 AM UTC

[16en-04]

CNT sorting using block copolymers and removal of wrapped polymers from CNTs for improved electrical performance

*Sean Foradori[1], Stephanie Oliveras-Santos[1], Nilabja Maity[1], Michael S Arnold[1], Padma Gopalan[1] (1. University of Wisconsin – Madison (United States of America))

4:20 PM - 4:40 PM JST | 7:20 AM - 7:40 AM UTC

[16en-05]

Preparation of Single-Walled Carbon Nanotubes as Electronic Materials

*Yan Li[1,2] (1. Beijing National Laboratory for Molecular Science, College of Chemistry and Molecular Engineering, Peking University (China), 2. Institute of Carbon-Based Thin Film Electronics, Peking University (China))

4:40 PM - 5:00 PM JST | 7:40 AM - 8:00 AM UTC

[16en-06]

Interface properties of carbon nanotube thin film transistors

*Yutaka Ohno[1] (1. Nagoya University (Japan))

5:00 PM - 5:20 PM JST | 8:00 AM - 8:20 AM UTC

[16en-07]

High-Performance N-type Aligned Carbon Nanotube Field-Effect Transistors and Their Scaling Behavior

*Yu Cao[1] (1. Peking University (China))

| Parallel Symposia：17th Symposium on Computational Challenges in Nanotubes, 2D Materials, and Their Macroscopic Assemblies

Mon. Jun 16, 2025 2:00 PM - 5:20 PM JST | Mon. Jun 16, 2025 5:00 AM - 8:20 AM UTC Conference Room IV(Clock Tower Centennial Hall, 2F)

[16ct] Computation and Theory

Chair:Vincent Meunier, Christophe Bichara

2:00 PM - 2:40 PM JST | 5:00 AM - 5:40 AM UTC

[16ct-01]

Moiré Band Engineering in Twisted Trilayer Transition Metal Dichalcogenide

Naoto Nakatsuji[1], Takuto Kawakami[1], Hayato Tateishi[2], Koichiro Kato[2], *Mikito Koshino[1] (1. University of Osaka (Japan), 2. Kyushu University (Japan))

2:40 PM - 3:00 PM JST | 5:40 AM - 6:00 AM UTC

[16ct-02]

Theoretical prediction of magnetic interaction at homo- or hetero-interfaces of two-dimensional materials

*Cong Wang[1], Wei Ji[1] (1. Renmin University of China (China))

3:00 PM - 3:20 PM JST | 6:00 AM - 6:20 AM UTC

[16ct-03]

Theory of Sigma Bond Resonance in Flat Boron Materials

*Lu Qiu[1], Feng Ding[2] (1. City University of Hong Kong (Hong Kong), 2. Suzhou Laboratory (China))

4:00 PM - 4:40 PM JST | 7:00 AM - 7:40 AM UTC

[16ct-04]

An Overview of Machine Learning Force Fields for Nanotube Growth Simulations

*Daniel Hedman[1] (1. Center for Multidimensional Carbon Materials (CMCM), Institute for Basic Science (IBS) (Korea))

4:40 PM - 5:00 PM JST | 7:40 AM - 8:00 AM UTC

[16ct-05]

Growth Simulations of Single-Walled Carbon Nanotubes Using Carbon Monoxide with Machine-Learning Force Fields

*Sida Sun[1], Yan Li[1] (1. Peking University (China))

5:00 PM - 5:20 PM JST | 8:00 AM - 8:20 AM UTC

[16ct-06]

Oxygen modulates the catalytic activity of iron for CNT Nucleation

*Ben McLean[1], Alister J. Page[2], Feng Ding[3] (1. RMIT University (Australia), 2. University of Newcastle (Australia), 3. Shenzhen Institute of Advanced Technology, Chinese Academy of Sciences (China))

| Parallel Symposia：6th Symposium on Synthesis, Purification, Functionalization, and Manufacturing of Carbon Nanotubes and Low-Dimensional Materials

Mon. Jun 16, 2025 2:00 PM - 5:20 PM JST | Mon. Jun 16, 2025 5:00 AM - 8:20 AM UTC HORIBA Symposium Hall (INNOVATION BLDG., 5F)

[16sy] Synthesis

Chair:Yan Li, Alister J Page

2:00 PM - 2:40 PM JST | 5:00 AM - 5:40 AM UTC

[16sy-01]

NEW SYNTHESES OF GRAPHENE AND DIAMOND

*Rodney Ruoff[1] (1. UNIST and IBS CMCM (Korea))

2:40 PM - 3:00 PM JST | 5:40 AM - 6:00 AM UTC

[16sy-02]

High-Melting Point Bimetallic Icosahedral Clusters for Carbon Nanotube Growth

*Shigeo Maruyama[1,2], Daniel Hedman[3], Daisuke Asa[1], Ikuma Kohata[1], Kaoru Hisama[4], Qingmei Hu[1], Wanyu Dai[1], Keigo Ostuka[1], Rong Xiang[2], Christophe Bichara[5] (1. The University of Tokyo (Japan), 2. Zhejiang University (China), 3. Institute for Basic Science (IBS) (Korea), 4. Shinshu University (Japan), 5. Aix-Marseille Univ (France))

3:00 PM - 3:20 PM JST | 6:00 AM - 6:20 AM UTC

[16sy-03]

Synthesis of Diamond in Liquid Metal at 1 Atmosphere Pressure

*Da Luo[1] (1. The Chinese University of Hong Kong, Shenzhen (China))

4:00 PM - 4:20 PM JST | 7:00 AM - 7:20 AM UTC

[16sy-04]

Synthesis and Electronic Applications of Wafer-Scale 2.5D Materials

*Hiroki Ago[1] (1. Kyushu University (Japan))

4:20 PM - 4:40 PM JST | 7:20 AM - 7:40 AM UTC

[16sy-05]

Orienting-Stitched Graphene is Permeable

Zhien Wang[2], Chi Cheng[3], *Jiangtao Wang[1], Jing Kong[2] (1. Peking University (China), 2. Massachusetts Institute of Technology (United States of America), 3. The University of New South Wales (Australia))

4:40 PM - 5:00 PM JST | 7:40 AM - 8:00 AM UTC

[16sy-06]

Highly efficient weakly confined carbyne (wCC) synthesis inside single-walled carbon nanotubes (SWCNTs)

*Bowen Zhang[1], Xiyang Qiu[1], Wanyu Dai[1], Qingmei Hu[1], Yongjia Zheng[2], Aina Fitó-Parer[3], Dmitry I. Levshov[3], Keigo Otsuka[1], Shohei Chiashi[1], Rong Xiang[2], Feng Yang[4], Yan Li[5], Sofie Cambré[3], Shigeo Maaruyama[1] (1. University of Tokyo (Japan), 2. Zhejiang University (China), 3. University of Antwerp (Belgium), 4. Southern University of Science and Technology (China), 5. Peking University (China))

5:00 PM - 5:20 PM JST | 8:00 AM - 8:20 AM UTC

[16sy-07]

Solving the Secondary Nucleation Problem that Causes Misoriented Islands during the Wafer-Scale Epitaxy of Single-Crystal Graphene on Ge

*Michael S. Arnold[1] (1. University of Wisconsin-Madison (United States of America))

| Parallel Symposia：Symposium on Fundamental, Structural and Optical Properties of 1D and 2D Materials and their Heterostructures

Mon. Jun 16, 2025 2:00 PM - 5:20 PM JST | Mon. Jun 16, 2025 5:00 AM - 8:20 AM UTC International Exchange Hall III (Clock Tower Centennial Hall, 2F)

[16fn] Fundamental Properties

Chair:Jana Zaumseil, Thomas Pichler

2:00 PM - 2:20 PM JST | 5:00 AM - 5:20 AM UTC

[16fn-01]

Valley-Hybridized Gate-Tunable 1D Exciton Confinement in $MoSe_2$

*Antoine RESERBAT-PLANTEY[1] (1. Université Côte d'Azur, CNRS, CRHEA. (France))

2:20 PM - 2:40 PM JST | 5:20 AM - 5:40 AM UTC

[16fn-02]

ISOTOPE ENGINEERING OF TRANSITION METAL DICHALCOGENIDES

Rahul Kesarwani[1,2], Vaibhav Varade[1], Artur Slobodeniuk[1], Martin Kalbac[2], *Jana Kalbacova Vejpravova[1] (1. Charles University (Czech Republic), 2. J Heyrovsky Institute (Czech Republic))

2:40 PM - 3:00 PM JST | 5:40 AM - 6:00 AM UTC

[16fn-03]

Collective optical states in one- and two-dimensional molecular lattice

*Sabrina Juergensen[1], José A. Arcos Pareja[1], Chantal Mueller[1], Jean-Baptiste Marceau[2], Niclas S. Mueller[3], Nikolai Severin[4], Eduardo B. Barros[5,6], Patryk Kusch[1], Antonio Setaro[1,7], Jürgen P. Rabe[4], Etienne Gaufrès[2], Stephanie Reich[1] (1. Freie Universität Berlin (Germany), 2. Université de Bordeaux (France), 3. Fritz-Haber-Institut, Berlin (Germany), 4. Humboldt Univerität zu Berlin (Germany), 5. Federal University of Ceará, Fortaleza (Brazil), 6. Technische Universität Berlin (Germany), 7. Pegaso University (Italy))

3:00 PM - 3:20 PM JST | 6:00 AM - 6:20 AM UTC

[16fn-04]

Raman Spectroscopy of Twisted Graphene

*Lianming Tong[1] (1. Peking University Shenzhen Graduate School (China))

4:00 PM - 4:20 PM JST | 7:00 AM - 7:20 AM UTC

[16fn-05]

Moiré effects and dielectric coupling in one-dimensional heterostructures

*Georgy Gordeev Gordeev[1,2] (1. University of Luxembourg (Luxembourg), 2. Freie Universität Berlin (Germany))

4:20 PM - 4:40 PM JST | 7:20 AM - 7:40 AM UTC

[16fn-06]

Free Carrier Infrared Response of Intrinsic and Doped Carbon Nanotubes

Daniel Noll[1], Klaus Eckstein[1], Taras Abramovic[1], Friedrich Schöppler[1], Han Li[2], *Tobias Hertel[1] (1. Institute of Physical and Theoretical Chemistry (Germany), 2. Turku University (Finland))

4:40 PM - 5:00 PM JST | 7:40 AM - 8:00 AM UTC

[16fn-07]

MAGNETIC FIELD EFFECT ON QUATERNION EXCITONIC COMPLEXES IN BILAYER STRUCTURES NEAR METALS

*Igor V Bondarev[1], David W Snoke[2] (1. North Carolina Central University (United States of America), 2. University of Pittsburgh (United States of America))

5:00 PM - 5:20 PM JST | 8:00 AM - 8:20 AM UTC

[16fn-08]

Superconducting Diodes Based on the Structural Design of $NbSe_2$

*zhaolong chen[1], Jinpei Zhao[2], Konstantin Novoselov[2] (1. Peking University ShenZhen Graduate School (China), 2. National University of Singapore (China))

| Parallel Symposia：15th Symposium on Carbon Nanomaterials, Biology, Medicine and Toxicology

Mon. Jun 16, 2025 2:00 PM - 5:00 PM JST | Mon. Jun 16, 2025 5:00 AM - 8:00 AM UTC Meeting Room E/F(INNOVATION BLDG., 5F)

[16nb] NanoBio

Chair:Markita Landry, Sanghwa Jeong, Ching-Wei Lin

2:00 PM - 2:40 PM JST | 5:00 AM - 5:40 AM UTC

[16nb-01]

Near-infrared fluorescence probe using oxygen-doped carbon nanotubes and carbon nanotube degradation for safety

*Toshiya Okazaki[1] (1. AIST (Japan))

2:40 PM - 3:00 PM JST | 5:40 AM - 6:00 AM UTC

[16nb-02]

Short-wave infrared fluorescence cytometry

*Ching-Wei Lin[1], Te-I Liu[1], Jhih-Shan Wang[1,2,5], Ai-Phuong Nguyen[1,3], Marco Raabe[1], Carlos Jose Quiroz Reyes[1,4], Chih-Hsin Lin[4] (1. Academia Sinica (Taiwan), 2. National Taiwan University (Taiwan), 3. National Tsing Hua University (Taiwan), 4. Taipei Medical University (Taiwan), 5. University of Stuttgart (Germany))

3:00 PM - 3:20 PM JST | 6:00 AM - 6:20 AM UTC

[16nb-03]

Imaging oxytocin signaling in prairie voles to study social relationships with carbon nanotube based fluorescent sensors

*Natsumi Komatsu[1], Alexis Marie Black[1], Devanand Manoli[2], Annaliese Beery[1], Markita Landry[1] (1. University of California, Berkeley (United States of America), 2. University of California, San Francisco (United States of America))

4:00 PM - 4:20 PM JST | 7:00 AM - 7:20 AM UTC

[16nb-04]

Carbon Nanomaterials as Nanocarriers and Optical Nanosensors for Plant Biotechnology

*Tedrick Thomas Salim Lew[1], Biao Huang[1], Suppanat Puangpathumanond[1] (1. National University of Singapore (Singapore))

4:20 PM - 4:40 PM JST | 7:20 AM - 7:40 AM UTC

[16nb-05]

Pattern Recognition-derived Optical SWCNT Nanosensor Array for Liquid Biopsy

*Sanghwa Jeong[1], Dakyeon Lee[1] (1. Pusan National University (Korea))

4:40 PM - 5:00 PM JST | 7:40 AM - 8:00 AM UTC

[16nb-06]

Using Molecular Probe Adsorption (MPA) to Characterize the Nanoparticle Corona Phase and Molecular Recognition

*Gabriel Sánchez-Velázquez[1], Duc Thinh Khong[2], Minkyung Park[1], Xiaojia Jin[1], Zhe Yuan[1], Xun Gong[1], Mervin Chun-Yi Ang[2], Michael S Strano[1,2] (1. Department of Chemical Engineering, Massachusetts Institute of Technology (United States of America), 2. Disruptive & Sustainable Technologies for Agricultural Precision IRG, Singapore-MIT Alliance for Research and Technology (Singapore))

| Main conference：Main conference

Mon. Jun 16, 2025 6:00 PM - 8:00 PM JST | Mon. Jun 16, 2025 9:00 AM - 11:00 AM UTC Poster 1(International Exchange Hall III, Clock Tower Centennial Hall, 2F)

[16psa] Poster 1

[16psa-01]

Light Emission, Structure-Phase Evolution, and Photocatalytic Behavior in Full-Series Multilayered $GaTe_{1-x}S_x$ (0<=x<=1) with Direct-Transition Edge

*Ching-Hwa Ho[1], Luthviyah Choirotul Muhimmah[1] (1. National Taiwan University of Science and Technology, Graduate Institute of Applied Science and Technology (Taiwan))

[16psa-02]

Hydrophobicity and space confinement effect of carbon nanotube-alumina support on the Cu-Co catalysts for CO2 methanation

*Weizhong Qian[1], mingyu Ma[1], chaojie Cui[1] (1. Tsinghua University (China))

[16psa-03]

Double-Walled Carbon Nanotubes with Dynamic Strength of Over 90 GPa Enhanced by Intershell Friction

*Hongjie Yue[1], Fei Wei[1] (1. Tsinghua University (China))

[16psa-04]

Pd-based nanoparticles on reduced graphene oxide for formic acid electro-oxidation

*Patraporn Luksirikul[1], Pacharapon Kankla[1], Teera Butburee[2], Narong Chanlek[3], Suchinda Sattayaporn[4] (1. Kasetsart University (Thailand), 2. National Science and Technology Development Agency (Thailand), 3. Synchrotron Light Research Institute (Public Organization) (Thailand), 4. King Mongkut's University of Technology North Bangkok (Rayong Campus) (Thailand))

[16psa-05]

Half-Full Filled Aerogels with A 348% Increment in Energy Absorption and A Retained High Electromagnetic Shielding Performance

*zhengqiang lyu[1] (1. Suzhou Institute of Nano-Tech and Nano-Bionics, Chinese Academy of Sciences (China))

[16psa-06]

3D-structured carbon nanotube fibers as ultra-robust fabrics for adaptive electromagnetic shielding

*dongmei Hu[1] (1. Suzhou Institute of Nano-Tech and Nano-Bionics, Chinese Academy of Sciences (China))

[16psa-07]

Study on structure of carbon nanotubes for electrochemical electrodes

*Daichi Suzuki[1], Takemura Kenshin[1], Nao Terasaki[1] (1. AIST (Japan))

[16psa-08]

Mass density effects on thermal resistance of CNT forests

*Yamato Watanabe[1], Takayuki Nakano[1], Yoku Inoue[1] (1. Shizuoka Univ. (Japan))

[16psa-09]

Novel CNT-based thermal interface films: Design, fabrication, and evaluation

*Tomoki Okumura[1], Takayuki Nakano[1], Yoku Inoue[1] (1. Shizuoka Univ. (Japan))

[16psa-10]

Wafer-Scale Characterization of Macroscopic Defects in Aligned Carbon Nanotube Arrays Fabricated by Dimension-Limited Self-Alignment

*Bing Gao[1], Chuanhong Jin[1] (1. Zhejiang University (China))

[16psa-11]

Morphological evolution of atomic layer deposited hafnium oxide on aligned carbon nanotube arrays

*Sujuan Ding[1], Yifan Liu[2], Bing Gao[1], Bo Wang[1], Zhiyong Zhang[2], Chuanhong Jin[1] (1. Zhejiang Univ. (China), 2. Peking Univ. (China))

[16psa-12]

Bond based spectral map of oligomers in machine learning algorithm for MD vibrational spectra in graphene SERS sensor

*Tatiana Zolotoukhina[1], Haruto Goto[1], Yasuhiro Yamamoto[1] (1. Dep. of Mech. Engineering, Faculty of Eng., Toyama University (Japan))

[16psa-13]

Effective Fabrication of Suspended Graphene Nanoribbon Transistors for Width-Dependent Transition from Quantum Interference to Coulomb Blockade

*Yuan-Liang Zhong[1] (1. CYCU Univ. (Taiwan))

[16psa-14]

Strongly hybridized phonons and spontaneous electric polarizations in low-dimensional graphitic multilayers

Shaoqi Sun[1], Zhou Zhou[1], Xiyao Peng[1], Qingyun Lin[1], Yihuan Li[1], Daichi Kozawa[2], Huizhen Wu[1], Shigeo Maruyama[3], Pilkyung Moon[4], Toshikaze Kariyado[2], Ryo Kitaura[2], *Sihan Zhao[1] (1. Zhejiang University (China), 2. National Institute for Materials Science (Japan), 3. The University of Tokyo (Japan), 4. NYU Shanghai (China))

[16psa-15]

High-performance Transparent and Conductive CNT Films from Dilute Organic Dispersions

*Tsuyoshi Endo[1], Seiya Nishida[1], Hiroaki Kahara[1], Satoshi Yamazaki[2], Takashi Kodama[3], Yoko Iizumi[4], Toshiya Okazaki[4], Keigo Otsuka[1], Shigeo Maruyama[1], Shohei Chiashi[1] (1. Department of Mechanical Engineering, the University of Tokyo (Japan), 2. Furukawa Electric Co., Ltd. (Japan), 3. Dept. of Mech. and Control Eng., Kyushu Institute of technology (Japan), 4. National Institute of Advanced Industrial Science and Technology (Japan))

[16psa-16]

Mxene/metal Composites for Hydrogen Evolution Application

*Sergii A Sergiienko[1] (1. University of Chemistry and Technology, Prague (Czech Republic))

[16psa-17]

High near-field noise suppression in the 5G frequency bands for graphene sheets printed by jet-dispensing

*Masato Watanabe[1] (1. Research Institute for Electromagnetic Materials (Japan))

[16psa-18]

Flavin-Wrapped Carbon Nanotubes for Fundamentals and Applications

*Sang-Yong Ju[1], Hangil Lee[2], Seongjoo Hwang[1] (1. Department of Chemistry, Yonsei University (Korea), 2. Department of Chemistry, Sookmyung Women's University (Korea))

[16psa-19]

Monocyclic Aromatic Molecule-Driven Confined Synthesis of 6-Armchair Graphene Nanoribbons

*Huiju Cao[1], Yingzhi Chen[1], Kunpeng Tang[1], Wendi Zhang[2], Kecheng Cao[2], Lei Shi[1] (1. Sun Yat-sen University (China), 2. ShanghaiTech University (China))

[16psa-20]

Inner Doping of Carbon Nanotubes with Perovskites and Charge Detection for High Performance Nanoelectronics

*Huimin Yin[1], Chuanhong Jin[1] (1. zhejiang university (China))

[16psa-21]

UHV exfoliation and rational functionalization of 2D materials

*Martin Kalbac[1] (1. J. Heyrovsky Institute of Physical Chemistry of the Czech Academy of Sciences (Czech Republic))

[16psa-22]

Microscopic Understanding of Metal Contacts to Aligned Carbon Nanotubes Arrays: Wetting and Coverage

*Haozhe Lu[1], Chuanhong Jin[1] (1. Zhejiang University (China))

[16psa-23]

Encapsulation and Electronic Modulation of Tungsten-Alloyed MoS_2 Nanoribbons in Carbon Nanotubes

*Yuanfang Zhang[1], Wenqi Lv[3], Fenfa Yao[2], Yanning Zhang[3], Xin Chen[1], Chuanhong Jin[2] (1. East China University of Science and Technology (China), 2. Zhejiang University (China), 3. University of Electronic Science and Technology (China))

[16psa-24]

Synthesis of carbon nanotubes using higher alkanes as a carbon source

*Łukasz Nowicki[1], Sandra Lepak-Kuc[2,1], Agnieszka Lekawa-Raus[1] (1. Centre for Advanced Materials and Technologies (CEZAMAT), Warsaw University of Technology (Poland), 2. Faculty of Mechanical and Industrial Engineering, Warsaw University of Technology (Poland))

[16psa-25]

Symmetry and asymmetry in carbon nanotube mutations and memory retention in long- and short-range

*Lin Chai[1], Fei Wei[1] (1. Tsinghua University (China))

[16psa-26]

Observation of strongly hybridized phonons in one-dimensional van der Waals crystals

*Shaoqi Sun[1], Qingyun Lin[1], Yihuan Li[1], Daichi Kozawa[2], Huizhen Wu[1], Shigeo Maruyama[3], Pilkyung Moon[4], Toshikaze Kariyado[2], Ryo Kitaura[2], Sihan Zhao[1] (1. Zhejiang Univ. (China), 2. National Institute for Materials Science (NIMS) (Japan), 3. The University of Tokyo (Japan), 4. NYU Shanghai (China))

[16psa-27]

Optical Modeling, Solver, and Design of Single-Enantiomer Carbon Nanotube Film and Reconfigurable Chiral Photonic Device

Jichao Fan[1], *Benjamin Hillam[1], Cheng Guo[2], Hiroyuki Fujinami[3], Koki Shiba[3], Haoyu Xie[1], Ruiyang Chen[1], Kazuhiro Yanagi[3], Weilu Gao[1] (1. Univ. of Utah (United States of America), 2. Stanford Univ. (United States of America), 3. Tokyo Metropolitan Univ. (Japan))

[16psa-28]

Anomalous Interfacial Electron Transfer Kinetics in Moiré Graphene

*Meg Grace Takezawa[1], Yun Yu[1], Kaidi Zhang[1], Sonal Maroo[1], Daniel Kwabena Bediako[1,2] (1. University of California, Berkeley (United States of America), 2. Lawrence Berkeley National Laboratory (United States of

[16psa-29]

Photoluminescence of gated mixed-dimensional heterostructures

*Ufuk Erkilic[1,2], Nan Fang[1], Chee Fai Fong[1], Yih-Ren Chang[1,2,3], Yuichiro K. Kato[1,2] (1. RIKEN Cluster for Pioneering Research (Japan), 2. RIKEN Center for Advanced Photonics (Japan), 3. Kobe Univ. (Japan))

[16psa-30]

Thermal Conductivity of Solution-Spun Carbon Nanotube Fibers with Different Draw Ratios

*Jiun-Hung Yi[1,2], Ognyan Stefanov[1,2], Michelle Durán-Chaves[2,3], Eldar Khabushev[2,4], Matteo Pasquali[2,3,4], Geoff Wehmeyer[1,2] (1. Department of Mechanical Engineering, William Marsh Rice University (United States of America), 2. The Carbon Hub, William Marsh Rice University (United States of America), 3. Department of Chemistry, William Marsh Rice University (United States of America), 4. Department of Chemical and Biomolecular Engineering, William Marsh Rice University (United States of America))

[16psa-31]

APPLICATION OF MULTIWALL CARBON NANOTUBES TO ENHANCE THE LUBRICATION PERFORMANCE OF MACHINE ELEMENTS

*Amarnath Muniyappa[1], Santhosh Kamarapu[1], Kamlesh Shivvedi[1], Chella durai[1] (1. Tribology and Machine Dynamics Laboratory, Department of Mechanical Engineering, Indian Institute of Information Technology, Design, and Manufacturing, Jabalpur, Madhya Pradesh, 482005, India (India))

[16psa-32]

Synthesis of single-unit-cell thin perovskites by liquid-phase confined assembly for high-performance ultrastable X-ray detectors

*Meihui Song[1], Feng Yang[1] (1. Southern University of Science and Technology (China))

[16psa-33]

Low power NO_2 sensing by MoS_2 photoactivated sensor with integrated micro-LED light source

*Hiroshi Tabata[1], Kotaro Fujii[1], Shuhei Ichikawa[1], Toshihiro Ishihara[1], Kazunobu Kojima[1], Yasufumi Fujiwara[1,2], Mitsuhiro Katayama[1] (1. Osaka Univ. (Japan), 2. Ritsumeikan Univ. (Japan))

[16psa-34]

Extraction of the true topography of carbon nanotubes on SiO_2/Si substrates by scanning electron microscopy

*Boxiang Zhang[1], Chuanhong Jin[1] (1. Zhejiang University (China))

[16psa-35]

High performance aligned carbon nanotube thin film transistors for mini- and micro-LED driving

*Xi Mei qi[1,2], Liu Fang[1], Zhu Xue hao[1], Li Yi[1], Bai Lan[1,2], Peng Lian mao[1,2], Cao Yu[1,2], Liang Xue Lei[1,2] (1. Peking University (China), 2. ICTFE-PKU (China))

[16psa-36]

Synthesis of a Hybrid Flexible Thermoelectric Device with Carbon Nanotubes and Chalcogenide-based Thermoelectric Materials

*Aarti Bisht[1], Bhasker Gahtori , Sanjay R. Dhakate, Bhanu Pratap Singh (1. Research Scholar (India))

[16psa-37]

The cross-scale assembly and mechanical behavior of super-strong carbon nanotubes

*Yukang Zhu[1], Fei Wei[1] (1. Tsinghua University (China))

[16psa-38]

Effects of Y on stabilizing Fe catalyst in carbon nanotube growth

*Duy Huy Khuong Le[1], Takayuki Nakano[1], Hisashi Sugime[2], Yoku Inoue[1] (1. Shizuoka University (Japan), 2. Kindai University (Japan))

[16psa-39]

Reinforcement of Polyimine Covalent Adaptable Networks with Mechanically Interlocked Derivatives of SWNTs

*ALEJANDRO LOPEZ-MORENO[1], ION ISASTI[1], SILVIA MIRANDA[1], DAVID M. JIMENEZ[1], SYLWIA PARZYSZEK[1], NATALIA MARTÍN SABANÉS[1], HENRIK PEDERSEN[2], EMILIO M. PEREZ[1] (1. IMDEA NANOSCIENCE (Spain), 2. Nanocore ApS (Denmark))

[16psa-40]

Overcoming the Yield-Quality Trade-off for Aerosol-CVD-Synthesized Single-Walled Carbon Nanotubes by Diameter Control

*Ilya V. Novikov[1], Yasir Shafi Mir[1], Il Hyun Lee[1], Jeong-Seok Nam[1], Il Jeon[1] (1. Sungkyunkwan University (Korea))

[16psa-41]

Boosted thermal conductivity of single-walled carbon nanotube films via BN welding and encapsulation

*Changping Yu[1,2], Feng Zhang[1,2], Chang Liu[1,2] (1. Shenyang National Laboratory for Materials Science, Institute of Metal Research, Chinese Academy of Sciences (China), 2. School of Materials Science and Engineering, University of Science and Technology of China (China))

[16psa-42]

Enhanced Efficiency in Dye-Sensitized Solar Cells Using Carbon Nanotube Composite Papers via Multiple Dye Fixation

*YI KOU[1], Takahide Oya[1,2] (1. Graduate School of Engineering Science, Yokohama National Univ. (Japan), 2. Semiconductor and Quantum Integrated Electronics Research Center, Institute for Multidisciplinary Sciences, Yokohama National Univ. (Japan))

[16psa-43]

Confined synthesis of nitrogen-doped graphene nanoribbons transformed from nitrogen-containing precursors

*Kunpeng Tang[1], Yingzhi Chen[1], Huiju Cao[1], Wendi Zhang[2], Kecheng Cao[2], Lei Shi[1] (1. Sun Yat-sen University (China), 2. ShanghaiTech University (China))

[16psa-44]

Annealing and Doping Effects on Axial Thermal Transport Properties of Solution-Spun Carbon Nanotube Fibers

*Ognyan Stefanov[1,2], Michelle Duran-Chaves[2,3], Aosheen Anand[2,3], Eldar Khabushev[2,4], Matteo Pasquali[2,3,4], Geoff Wehmeyer[1,2] (1. Department of Mechanical Engineering, William Marsh Rice University (United States of America), 2. The Carbon Hub, William Marsh Rice University (United States of America), 3. Department of Chemistry, William Marsh Rice University (United States of America), 4. Department of Chemical and Biomolecular Engineering, William Marsh Rice University (United States of America))

[16psa-45]

Cathodes based on V_2O_5 are an excellent material for fabricating symmetric supercapacitors for lithium-ion batteries

*Kaviyarasu Kasinathan[1] (1. UNESCO Africa Chair Nanoscience & Nanotechnology, University of South Africa. (South Africa))

[16psa-46]

Replica higher-order topology of Hofstadter butterflies in twisted bilayer graphene

*Youngkuk Kim[1] (1. Department of Physics, Sungkyunkwan University (Korea))

[16psa-47]

Bright trion emission in carbon-nanotube/tungsten-diselenide mixed-dimensional heterostructures

*Nan Fang[1], Ufuk Erkilic[1], Yih-Ren Chang[1], Shun Fujii[1,2], Daiki Yamashita[1,3], Chee Fai Fong[1], Yuichiro K. Kato[1] (1. RIKEN (Japan), 2. Keio Univ. (Japan), 3. AIST (Japan))

[16psa-48]

Diameter Controllable Separation of Single-Walled Carbon Nanotubes by Simply Changing the Metal in Phenanthroline-Based Supramolecular Polymers

*Xinyi Fu[1], Takuya Hayashi[2], Guoqing Cheng[1], Naoki Komatsu[1] (1. Graduate School of Human and Environmental Studies, Kyoto University (Japan), 2. Carbon Science Division, Research Institute for Supra Materials, Shinshu University (Japan))

[16psa-49]

High-Frequency Current Noise in Carbon Nanotubes due to Phonon Scattering

*Raimu Akimoto[1], Aina Sumiyoshi[1], Takahiro Yamamoto[1,2] (1. Department of Physics, Tokyo University of Science (Japan), 2. RIST, Tokyo University of Science (Japan))

[16psa-50]

Ceramic Cold Cathode X-ray Tubes with a Compact Size and High Performance Fabricated by CNT Film Field Elelctron Emitter

Cheol Jin LEE[1,2], *Hyunjea LEE[2], Jun Young Lee[2], Hosan Shin[2], Yejin Kong[2] (1. School of Electrical Engineering, Korea University (Korea), 2. LuminaX Co., Ltd (Korea))

[16psa-51]

Fully recyclable carbon nanotube fibers

*Michelle Duran-Chaves[1,2], Ivan Rosa Siqueira [1,2], Oliver Scott Dewey[1,2], Steven Williams[1,2], Cedric J. S. Ginestra [1,2], Juan de la Garza [1], Yingru Song [1], Geoff Wehmeyer [1,2,3], Matteo Pasquali[1,2,3] (1. Rice University (United States of America), 2. The Carbon Hub (United States of America), 3. The Smalley-Curl Institute (United States of America))

[16psa-52]

High-Sensitivity UV Photodetector Using 2D WS2/Ti2N MXene Quantum Dot Hybrid Structure

*Shamima Afroz[1], Annas Syhukri Ariffin[1], Anir Syahmi Sharbirin[1], Jeongyong Kim[1] (1. Sungkyunkwan University (Korea))

[16psa-53]

Integration of single-defect carbon nanotube photon sources into waveguide circuits for quantum applications

*Clement Deleau[1], Chee Fai Fong[1,2], Finn Sebastian[3], Jana Zaumseil[3], Yuichiro Kato[1,2] (1. Quantum Optoelectronics research team, RIKEN Center for Advanced Photonics (Japan), 2. Nanoscale Quantum Photonics Laboratory, RIKEN Cluster for Pioneering Research (Japan), 3. Institute for Physical Chemistry, Universität Heidelberg (Germany))

[16psa-54]

ENTANGLED EXITON EMISSION FROM EXCITON QUANTUM BITS MADE WITH CARBON NANOTUBES BY CONTROLLED-NOT GATE OPERATION

*Akira Hida[1], Koji Ishibashi[1] (1. RIKEN (Japan))

[16psa-55]

Electrospray deposition of single-walled carbon nanotube films for gas sensors

*Yuto Nishizono[1], Ryo Kuchino[1], Shuhei Ichikawa[1], Kazunobu Kojima[1], Mitsuhiro Katayama[1], Hiroshi tabata[1] (1. Osaka university (Japan))

| Main conference：Main conference

Mon. Jun 16, 2025 6:00 PM - 8:00 PM JST | Mon. Jun 16, 2025 9:00 AM - 11:00 AM UTC Poster 2(International Exchange Hall I&II, Clock Tower Centennial Hall, 2F)

[16psb] Poster 2

[16psb-01]

Exciton Behaviors in Monolayer $MoSe_2$-SWCNT Mixed-Dimensional Heterostructures

*Yih-Ren CHANG[1,2], Nang Fang[1], Chee Fai Fong[1], Shun Fujii[1,3], Yuichiro K. Kato[1] (1. RIKEN (Japan), 2. Kobe University (Japan), 3. Keio University (Japan))

[16psb-02]

Unique structure and thermodynamics of adsorbed water on CNT surface

Yuki Maekawa[1], Yusei Kioka[1], Kenji Sasaoka[1], *Yoshikazu Homma[1], Takahiro Yamamoto[1] (1. Tokyo University of Science (Japan))

[16psb-03]

Cinematographic Electron Microscopic Study on Formation Processes of Carbon Materials

*Koji Harano[1] (1. NIMS (Japan))

[16psb-04]

In-situ monitoring of single-molecule functionalization in vapor-phase for air-suspended single-walled carbon nanotubes

*Mengyue Wang[1,2], Daichi Kozawa[1,2,3], Yuichiro K. Kato[1,2] (1. RIKEN Center for Advanced Photonics (Japan), 2. RIKEN Cluster for Pioneering Research (Japan), 3. National Institute for Materials Science (Japan))

[16psb-05]

Development of Carbon-Based Xerogels and Aqueous Dispersions Inspired by Japanese-Solid-Ink

*Sakurako Kubota[1], Kotone Masuda[1], Junpei Hayakawa[1] (1. Nara Prefectural Seiwaseiryo Senior High School (Japan))

[16psb-06]

Relationship between the interfacial adhesion and microscopic interface structures in CNT/epoxy resin nanocomposites

*Tomoe Yayama[1], Tenma Hiraishi[2], Fumiko Akagi[1,2] (1. Department of Applied Physics, Kogakuin University (Japan), 2. Electronics and Electron Engineering Program, Kogakuin University (Japan))

[16psb-07]

Diameter Controllable Synthesis of Single-walled Carbon Nanotubes by Arc Discharge Using Ni-based Catalysts

Yixi Yao[1,2], *Zeyao Zhang[1,2], Yan Li[1,2] (1. Peking University (China), 2. Institute of Carbon-Based Thin Film Electronics, Peking University, Shanxi (China))

[16psb-08]

Diameter Specific Bandgap Modulation in MoS_2 Nanotubes Grown via Template Reaction

Zhen Han[1,2], *Runze Lai[2], Jian Sheng[2], Chengping Lian[2], Yan Li[1,2] (1. Academy for Advanced Interdisciplinary Studies, Peking University, Beijing 100871 (China), 2. College of Chemistry and Molecular Engineering, , Peking University, Beijing 100871 (China))

[16psb-09]

Green conversion of low quality chemical feedstock to hydrogen and carbon nanotubes

*Chaojie Cui[1], Bofan Li[1], Ruijing Jiao[1], Weizhong Qian[1] (1. Tsinghua University (China))

[16psb-10]

Hybrid Fibers incorporating Carbon Nanotubes

*Erica F Antunes[1], Daiana Pimenta[1], Rayza Gonçalves[1], Manuela Mourthe[1], Thiago Cançado[1], Felipe Murta[1], Alexander Kasama[2], Luiz Ladeira[1], Myriano Oliveira Jr.[1], Glaura Silva[1] (1. CTNANO/UFMG (Brazil), 2. CENPES/PETROBRAS (Brazil))

[16psb-11]

Harnessing Multiscale Engineering for Advancing CNT Technology: From AI for Synthesis to Functional Nanocarbon Assembly

*DEWU LIN[1], Don N. Futaba[2], Kenji Hata[2], Wenjun Zhang[3] (1. Peking University Shenzhen Graduate School (China), 2. National Institute of Advanced Industrial Science and Technology (Japan), 3. City University of Hong Kong (Hong Kong))

[16psb-12]

Mass Production of Two-Dimensional Materials by Bubbling Chemical Vapor Deposition

*Zhiyuan Shi[1] (1. Shanghai Institute of Microsystem and Information Technology, CAS (China))

[16psb-13]

Precise structural regulation of carbon crystals by electron doping

Fei Pan[1], Kun Ni[1], *Yanwu Zhu[1] (1. University of Science and Technology of China (China))

[16psb-14]

Autonomous Multi-Objective Bayesian Optimization of Carbon Nanotube Yield and Diameter Control at Synthesis from Disordered Catalyst

*Robert Waelder[1,2], Woojae Kim[3], Mark Pitt[4], Jay Myung[4], Benji Maruyama[1] (1. Air Force Research Lab (United States of America), 2. BlueHalo LLC (United States of America), 3. Howard University (United States of America), 4. Ohio State University (United States of America))

[16psb-15]

Towards a More Complete Empirical Thermodynamic Understanding and Control of Supported Catalyst Carbon Nanotube Synthesis

*Robert Waelder[1,2], Arthur Sloan[3], Benji Maruyama[1] (1. Air Force Research Lab (United States of America), 2. BlueHalo LLC (United States of America), 3. National Research Council (United States of America))

[16psb-16]

Evolution of Carbon atoms to Chiral Carbon Nanotubes on metal free template

*Shuchen Zhang[1] (1. State Key Laboratory of Precision and Intelligent Chemistry Department of Materials Science and Engineering School of Chemistry and Materials Science University of Science and Technology of China (China))

[16psb-17]

Synthesis of isolated pentagonal h-BN crystals by atmospheric pressure CVD

*Kamal Prasad Sharma[1], Takahiro Maruyama[1] (1. Meijo University (Japan))

[16psb-18]

Synthesis of Long Carbon Nanotubes by Br-assisted Floating Catalyst Chemical Vapor Deposition

*Hirotaka Inoue[1,2], Anastasios Karakassides[2], Toshihiko Fujimori[1,3], Akira Takakura[1], Soichiro Okubo[1], Hua Jiang[2], Ghulam Yasin[2], Kazuhiro Ikeda[1], Takamasa Onoki[1], Yoku Inoue[4], Esko I. Kauppinen[2] (1. Sumitomo Electric Industries (Japan), 2. Aalto University (Finland), 3. University of Tsukuba (Japan), 4. Shizuoka University (Japan))

[16psb-19]

Glaphene: a hybridization of 2D silica glass and graphene

*Sathvik Ajay Iyengar[1], Manoj Tripathi[2], Anchal Srivastava[3], Abhijit Biswas[1], Tia Gray[1], Mauricio Terrones[4], Alan B Dalton[2], Marcos A. Pimenta[5], Robert Vajtai[1], Vincent Meunier[4], Pulickel Ajayan[1] (1. Rice University (United States of America), 2. University of Sussex (UK), 3. Banaras Hindu University (India), 4. The Pennsylvania State University (United States of America), 5. Universidade Federal de Minas Gerais (Brazil))

[16psb-20]

Controlled Growth of Horizontally Aligned Single-Walled Carbon Nanotube Arrays

*Liu Qian[1], Ying Xie[1], Yue Li[1], Jin Zhang[1] (1. Peking University (China))

[16psb-21]

Preparation of semiconducting single-wall carbon nanotube arrays with a narrow band-gap distribution

*Jia-Yang Zhang[1], Lingtong Ding[2], Chen Xie[2], Lili Zhang[1], Meng-Ke Zou[1], Xiao Wang[2], Chang Liu[1] (1. Institute of Metal Research, Chinese Academy of Sciences (China), 2. Shenzhen Institute of Advanced Technology, Chinese Academy of Sciences (China))

[16psb-22]

Engineering Luminescent Defects in Polymer-Wrapped SWCNTs using Benzoyl Peroxide Chemistry

*Andrzej Dzienia[1], Patrycja Taborowska[1], Pawel Kubica-Cypek[1], Dawid Janas[1] (1. Silesian University of Technology (Poland))

[16psb-23]

Unleashing Ultra-Efficient Heat Transfer: The Magic of Graphene-Skinned Powders Synthesized by FB-CVD in Nanoelectronic Thermal Management

*Yuqing Song[1] (1. Beijing Graphene Institute (BGI) 13 Cuihu Nanhuan Road, Sujiatuo Town, Haidian District Beijing 100095, P. R. China (China))

[16psb-24]

Controlled Growth of Graphene-skinned Al_2O_3 Powdersby Fluidized Bed-Chemical Vapor Deposition for Heat Dissipation

*Yuzhu Wu[1,2], Yuqing Song[2] (1. College of Chemistry and Molecular Engineering, Peking University, Beijing (P.R.China) (China), 2. Beijing Graphene Institute (BGI), Beijing 100095 (P.R.China) (China))

[16psb-25]

Sorting and brightening of single-walled carbon nanotubes using organic derivatives of hydrazine

*Dominik Sebastian Just[1], Ryszard Siedlecki[1], Błażej Podleśny[1], Dawid Janas[1] (1. Silesian University of Technology (Poland))

[16psb-26]

Single-walled carbon nanotube growth by CVD with high-entropy alloy catalysts composed of platinum-group elements

*Takahiro Maruyama[1], Shu Matsuoka[1], Kamal Prasad Sharma[1], Takahiro Saida[1], Kohei Kusada[2], Hiroshi Kitagawa[2] (1. Meijo University (Japan), 2. Kyoto University (Japan))

[16psb-27]

Molecule Super-Transport through Macroscopic Length of Individual Carbon Nanotube

*Jingwei Wu[1], Fei Wei[1] (1. Tsinghua University (China))

[16psb-28]

BSTCIM: A Balanced Symmetry Ternary Fully Digital In-MRAM Computing Macro for Energy Efficiency Neural Network

*Zhongzhen Tong[1,2], Chenghang Li[1,2], Chao Wang[1,2], Daming Zhou[2], Xiaoyang Lin[1,2] (1. National Key Lab of Spintronics, International Innovation Institute, Beihang University (China), 2. School of Integrated Circuit Science and Engineering, Fert Beijing Institute, Beihang University (China))

[16psb-29]

Monolithic 3D integration of CNTFET and SOT-MTJ for high-performance non-volatility memories

Ke Zhang[1], Ningfei Gao[2], *Daming Zhou[1], Zhongzhen Tong[1], Hongxi Liu[3], Xiaoyang Lin[1], Haitao Xu[2,4], Lianmao Peng[2], Weisheng Zhao[1] (1. Fert Beijing Institute, School of Integrated Circuit Science and Engineering, Beihang University (China), 2. Key Laboratory for the Physics and Chemistry of Nanodevices, Center for Carbon-based Electronics, School of Electronics, Peking University (China), 3. Truth Memory Technology Corporation Limited (China), 4. Institute of Carbon-based Thin Film Electronics, Peking University (China))

[16psb-30]

Interlayer Stacking Sensitivity of Anisotropic Thermoelectric Transport Properties of $NbSe_2$ Polymorphs based on First-Principles Band Calculations

*Mark Edwin Jr Roa Cleofe[1], Koichi Nakamura[1], Tetsuro Habe[1] (1. Kyoto University of Advanced Science (Japan))

[16psb-31]

Solution Processed Carbon Nanotube Integrated Circuits for Multi-Modal Edge Computing

*Jingfang Pei[1], Songwei Liu[1], Yingyi Wen[1], Lekai Song[1], Guohua Hu[1] (1. The Chinese University of Hong Kong (China))

[16psb-32]

Multi-functional Data Processing by Solution-processed 2D Material Ferroelectric Junction Devices

*Songwei Liu[1], Yingyi Wen[1], Jingfang Pei[1], Guohua Hu[1] (1. The Chinese University of Hong Kong (Hong Kong))

[16psb-33]

Temporal Signal Processing by Physical Reservoir Computing Using Solution Processed MoS_2 Charge-Trapping Transistors

*Yingyi Wen[1], Songwei Liu[1], Teng Ma[2], Guohua Hu[1] (1. The Chinese University of Hong Kong (Hong Kong), 2. Hong Kong Polytechnic University (Hong Kong))

[16psb-34]

Application of aerosol-synthesized single-walled carbon nanotubes for binder-free Nickel-rich positive electrodes via a solvent-free fabrication

*Alisa Bogdanova[1], Filipp Obrezkov[1], Seyedabolfazl Mousavihashemi[1], Eldar Khabushev[1], Tanja Kallio[1] (1. Aalto University School of Chemical Engineering (Finland))

[16psb-35]

High-Energy-Density Quasi-Solid-State Lithium-Sulfur Batteries: Reliable Energy Storage Solutions in Extreme Environments

*Haifa Taoum[1], Mariam Ezzedine[1], Costel-Sorin Cojocaru[1] (1. LPICM-CNRS (France))

[16psb-36]

$Pt@WS_2$ -an Extrinsic 2D Dilute Ferromagnetic Semiconductor Beyond Room Temperature

*Yu-Xiang Chen[1,2,3], Mario Hofmann[4], Ya-Ping Hsieh[1] (1. Institute of Atomic and Molecular Sciences, Academia Sinica (Taiwan), 2. International Graduate Program of Molecular Science and Technology, National Taiwan

University (Taiwan), 3. Molecular Science and Technology ProgramTaiwan International Graduate Program, Academia Sinica (Taiwan), 4. Department of Physics, National Taiwan University (Taiwan))

[16psb-37]

Two-Dimensional Electronic Transport and Surface Electron Accumulation in Transition Metal Dichalcogenides

*Hemanth Kumar Bangolla[1], Ruei-San Chen[1] (1. Taiwan Tech (Taiwan))

[16psb-38]

Efficient Field-free Switching of Perpendicular Magnetization induced by Dominant out-of-plane Torque Generated by $NbIrTe_4$

*Wei Yang[1,2,3], Juan-Carlos Rojas-Sánchez[3], Xiaoyang Lin[1,2], Weisheng Zhao[1,2] (1. National Key Lab of Spintronics, Hangzhou International Innovation Institute of Beihang University (China), 2. Fert Beijing Institute, Beihang University (China), 3. Insititut Jean Lamour, Université de Lorraine (France))

[16psb-39]

Enhanced Surface Properties of WS_2 via Cryogenic Exfoliation and High-Pressure Dispersion for Catalysis

*Yejin Choi[1], Myeung-Jin Lee[1], Bora Jeong[1], Hong-Dae Kim[1] (1. Korea Institute of Industrial Technology (Korea))

[16psb-40]

Hot-electron Injection Enabled High-performance Broadband Photodetection Based on WO_{3-x}/Bi_2O_2Se Hybrid structure

*Xinlei Zhang[1], Yuanfang Yu[2], Junpeng Lv[1], Zhenhua Ni[1] (1. Southeast University (China), 2. Nanjing University of Posts and Telecommunications (China))

[16psb-41]

First-principles Calculations on Oxygen Functional Group Interactions on Graphene and Their Modulation by Surface Normal Electric Fields

*Takazumi Kawai[1], Yoshiyuki Miyamoto[2] (1. Tokyo City University (Japan), 2. National Institute of Advanced Industrial Science and Technology (Japan))

[16psb-42]

Ambipolar Doping of Single-Walled CarbonNanotubes via Covalent Charge-Transfer Engineering

*Antonio Setaro[1,2], Alphonse Fiebor[1], Mohsen Adeli[1], Stephanie Reich[1] (1. Freie Universität Berlin (Germany), 2. Pegaso University (Italy))

[16psb-43]

Intrinsic temperature dependence of Raman-active modes in individual isolated single- and double-walled carbon nanotubes

*Ya Feng[1,2], Dmitry I. Levshov[3], Yuta Sato[4], Taiki Inoue[5], Sofie Cambré[3], Wim Wenseleers[3], Rong Xiang[6], Kazu Suenaga[5], Shigeo Maruyama[2,6] (1. Dalian University of Technology (China), 2. The University of Tokyo (Japan), 3. University of Antwerp (Belgium), 4. National Institute of Advanced Industrial Science and Technology (Japan), 5. Osaka University (Japan), 6. Zhejiang University (China))

Tue. Jun 17, 2025

| Main conference：Main conference

Tue. Jun 17, 2025 9:30 AM - 12:10 PM JST | Tue. Jun 17, 2025 12:30 AM - 3:10 AM UTC Centennial Hall (Clock Tower Centennial Hall)

[17ma] Main Conference

Chair: Shoei Chiashi, Yuichiro K. Kato

9:30 AM - 10:10 AM JST | 12:30 AM - 1:10 AM UTC

[17ma-01]

Exciton transfer and interface excitons in mixed-dimensional heterostructures

Nan Fang[1], Yih-Ren Chang[1], Shun Fujii[1,2], Daiki Yamashita[1,3], Mina Maruyama[4], Yanlin Gao[4], Chee Fai Fong[1], Daichi Kozawa[5], Keigo Otsuka[6], Kosuke Nagashio[6], Susumu Okada[4], *Yuichiro K. Kato[1] (1. RIKEN (Japan), 2. Keio Univ. (Japan), 3. AIST (Japan), 4. Univ. of Tsukuba (Japan), 5. NIMS (Japan), 6. Univ. of Tokyo (Japan))

10:10 AM - 10:40 AM JST | 1:10 AM - 1:40 AM UTC

[17ma-02]

READOUT OF TRIPLET STATES IN SP^3-FUNCTIONALIZED CARBON NANOTUBES BY OPTICALLY-DETECTED MAGNETIC RESONANCE

J. Alejandro de Sousa[1,2], Simon Settele[3], Timur Biktagirov[4], Uwe Gerstmann[4], Etienne Goovaerts[1], Jana Zaumseil[3], Nuria Crivillers[2], *Sofie Cambré[1] (1. Theory and Spectroscopy of Molecules and Materials, University of Antwerp (Belgium), 2. Institut de Ciència de Materials de Barcelona (Spain), 3. Institute for Physical chemistry, Universität Heidelberg (Germany), 4. Lehrstuhlfür Theoretische Material physik, Universität Paderborn (Germany))

11:00 AM - 11:30 AM JST | 2:00 AM - 2:30 AM UTC

[17ma-03]

Computational modeling and design of DNA-carbon nanotube sensors of small molecular analytes

*Lela Vukovic[1] (1. University of Texas at El Paso (United States of America))

11:30 AM - 11:50 AM JST | 2:30 AM - 2:50 AM UTC

[17ma-04]

Chirality-Dependent Kinetics of Single-Walled Carbon Nanotubes from Machine-Learning Force Fields

*Sida Sun[1], Shigeo Maruyama[2], Yan Li[1] (1. Peking University (China), 2. The University of Tokyo (Japan))

11:50 AM - 12:10 PM JST | 2:50 AM - 3:10 AM UTC

[17ma-05]

DUV-Raman and photoluminescence studies of SWNT@BNNT hetero-nanotubes

*Hsiang-Lin Liu[1], Shigeo Maruyama[2], Riichiro Saito[1,3] (1. National Taiwan Normal University (Taiwan), 2. The University of Tokyo (Japan), 3. Tohoku University (Japan))

| Parallel Symposia：Symposium on Nanomaterials for Energy and Electronics

Tue. Jun 17, 2025 2:00 PM - 5:20 PM JST | Tue. Jun 17, 2025 5:00 AM - 8:20 AM UTC Conference room 5a/5b(INNOVATION BLDG., 5F)

[17en] Energy & Electronics

Chair:Yutaka Ohno, Esko Ilmari Kauppinen

2:00 PM - 2:20 PM JST | 5:00 AM - 5:20 AM UTC

[17en-01]

Transparent, Conductive Carbon Nanotube Thin Films via Direct, Dry Deposition from the Floating Catalyst Chemical Deposition Synthesis

*Esko Ilmari Kauppinen[1] (1. Department of Applied Physics, Aalto University School of Science, (Finland))

2:20 PM - 2:40 PM JST | 5:20 AM - 5:40 AM UTC

[17en-02]

Preparation and Electrocatalytic Property of Integrated W_2C Nanowires @ Single-Walled Carbon Nanotubes Films

*Feng Zhang[1], Chang Liu[1] (1. Institute of Metal Research, Chinese Academy of Sciences (China))

2:40 PM - 3:00 PM JST | 5:40 AM - 6:00 AM UTC

[17en-03]

Advancing Energy Applications with WSe_2 Based Materials: Doping and Hybridization Strategies

*Antonia Kagkoura[1], Zdeněk Sofer[1] (1. University of Chemistry and Technology, Prague (Czech Republic))

3:00 PM - 3:20 PM JST | 6:00 AM - 6:20 AM UTC

[17en-04]

Exploiting the Unique Properties of MXenes for Hydrogen Production via Dry Reforming of Methane

Joshua O Ighalo[1], AmirMohammad Ebrahimi[1], Davood B Pourkargar[1], *Placidus B Amama[1] (1. Kansas State University (United States of America))

4:00 PM - 4:20 PM JST | 7:00 AM - 7:20 AM UTC

[17en-05]

Highly Conductive Carbon Nanotube Fibers

Haozike Wang[1], Zhaoqing Gao[1], Pengxiang Hou[1], *Chang Liu[1] (1. Institute of Metal Research, Chinese Academy of Sciences (China))

4:20 PM - 4:40 PM JST | 7:20 AM - 7:40 AM UTC

[17en-06]

Synthesis of advanced carbon material graphdiyne and their applications in sustainable energy

*Xin Gao[1] (1. Peking University (China))

4:40 PM - 5:00 PM JST | 7:40 AM - 8:00 AM UTC

[17en-07]

Insights into the mechanism of carbon nanotubes in silicon-based anodes

*Ziying He[1], Fei Wei[1] (1. Tsinghua University (China))

5:00 PM - 5:20 PM JST | 8:00 AM - 8:20 AM UTC

[17en-08]

Fabrication and Performance Evaluation of Lithium-Sulfur Pouch Cells

*Mariam Ezzedine[1], Costel Sorin Cojocaru[1] (1. LPICM-Ecole Polytechnique (France))

| Parallel Symposia：Symposium on Thin Films, Fibers, 3-D Materials and their Properties

Tue. Jun 17, 2025 2:00 PM - 5:20 PM JST | Tue. Jun 17, 2025 5:00 AM - 8:20 AM UTC Conference Room III(Clock Tower Centennial Hall, 2F)

[17mm] Macromaterials

Chair:Suguru Noda, Yoshiyuki Nonoguchi

2:00 PM - 2:20 PM JST | 5:00 AM - 5:20 AM UTC

[17mm-01]

MESOPOROUS 3-D GRAHENE MATERIALS FOR ENERGY STORAGE

*Hirotomo Nishihara[1] (1. Tohoku University (Japan))

2:20 PM - 2:40 PM JST | 5:20 AM - 5:40 AM UTC

[17mm-02]

Application of 2D carbon materials in water: adsorption of dyes and viruses

*Yuta Nishina[1] (1. Okayama University (Japan))

2:40 PM - 3:00 PM JST | 5:40 AM - 6:00 AM UTC

[17mm-03]

2D Materials for Post-AI Era: Smart Fibers, Soft Robotics & Single Atom Catalysts

*Sang Ouk Kim[1] (1. Materials Science & Engineering, KAIST (Korea))

3:00 PM - 3:20 PM JST | 6:00 AM - 6:20 AM UTC

[17mm-04]

Shaping MXenes: Templated Guided Synthesis Using Carbon Fibers

*Filipa M. Oliveira[1], Zdenek Sofer[1], Jesus Gonzalez-Julian[2] (1. University of Chemistry and Technology Prague (Czech Republic), 2. CNRS - Laboratory of Thermo-Structural Composites (LCTS) (France))

4:00 PM - 4:20 PM JST | 7:00 AM - 7:20 AM UTC

[17mm-05]

A Universal Framework for Ultra-Sensitive Pressure Sensing Enabled by Electric Double-Layer Charge Redistribution Mechanism

*Ming XU[1], Huajian Li[1] (1. Huazhong University of Science and Technology (China))

4:20 PM - 4:40 PM JST | 7:20 AM - 7:40 AM UTC

[17mm-06]

Progress in CNT Pellicle Development and Future Prospects

*Yosuke Ono[1] (1. Mitsuichemicals, Inc. (Japan))

4:40 PM - 5:00 PM JST | 7:40 AM - 8:00 AM UTC

[17mm-07]

Nanofiller effect of single-walled carbon nanotube bundles to elongate and toughen cellulose fibers

*Kazufumi Kobashi[1], Takahiro Morimoto[1], Minfang Zhang[1], Takushi Sugino[1], Toshiya Okazaki[1], Junya Tsujino[2], Hideki Kajita[2], Yasuyuki Isojima[2], Yasuo Gotoh[3] (1. National Institute of Advanced Industrial Science and Technology (Japan), 2. Omikenshi Co., Ltd. (Japan), 3. Shinshu University (Japan))

5:00 PM - 5:20 PM JST | 8:00 AM - 8:20 AM UTC

[17mm-08]

A New Conductive Network in Concrete: Interfacial Nanoengineering by Graphene

*Jing Zhong[1] (1. Harbin Institute of Technology (China))

| Parallel Symposia：17th Symposium on Computational Challenges in Nanotubes, 2D Materials, and Their Macroscopic Assemblies

Tue. Jun 17, 2025 2:00 PM - 5:20 PM JST | Tue. Jun 17, 2025 5:00 AM - 8:20 AM UTC Conference Room IV(Clock Tower Centennial Hall, 2F)

[17ct] Computation and Theory

Chair:Vassili Perebeinos, Mikito Koshino

2:00 PM - 2:40 PM JST | 5:00 AM - 5:40 AM UTC

[17ct-01]

Many-body interactions in optical properties of low-dimensional materials

*Vasili Perebeinos[1] (1. University at Buffalo (United States of America))

2:40 PM - 3:00 PM JST | 5:40 AM - 6:00 AM UTC

[17ct-02]

Contacts to Low-Dimensional Semiconductors: Physics-Based Analytical Model

*Jimmy Qin[1], H. S. Philip Wong[1] (1. Stanford University (United States of America))

3:00 PM - 3:20 PM JST | 6:00 AM - 6:20 AM UTC

[17ct-03]

ELECTRONIC STRUCTURES OF THIN FILMS OF ATOMIC LAYER MATERIALS

*Mina Maruyama[1] (1. University of Tsukuba (Japan))

4:00 PM - 4:20 PM JST | 7:00 AM - 7:20 AM UTC

[17ct-04]

Simulating CVD Carbon Nanotube Growth on Alloy Nanoparticles

*Alister J Page[1] (1. University of Newcastle (Australia))

4:20 PM - 4:40 PM JST | 7:20 AM - 7:40 AM UTC

[17ct-05]

Transient C-O single bond by femtosecond laser on graphene oxide studied by the time-dependent density functional theory

*Yoshiyuki Miyamoto[1], Tokutaro Komatsu[2] (1. National Institute of Advanced Industrial Science and Technology (Japan), 2. School of Medicine, Nihon University (Japan))

4:40 PM - 5:00 PM JST | 7:40 AM - 8:00 AM UTC

[17ct-06]

Topological Design of Low-Dimensional Carbon Materials for Novel Spintronics - Carbon Nanotubes in the Natural Helical Crystal Lattice Scheme

*Elise Yu-Tzu Li[1] (1. National Taiwan Normal University (Taiwan))

5:00 PM - 5:20 PM JST | 8:00 AM - 8:20 AM UTC

[17ct-07]

Exascale transport simulations for the understanding of the switching mechanism in atomically thin memristors

*Liangbo Liang[1], Wenchang Lu[2], Jameela Fatheema[3], Emil Briggs[2], Deji Akinwande[3], Jerzy Bernholc[2], Panchapakesan Ganesh[1] (1. Oak Ridge National Lab (United States of America), 2. North Carolina State University (United States of America), 3. The University of Texas at Austin (United States of America))

| Parallel Symposia：6th Symposium on Synthesis, Purification, Functionalization, and Manufacturing of Carbon Nanotubes and Low-Dimensional Materials

Tue. Jun 17, 2025 2:00 PM - 5:20 PM JST | Tue. Jun 17, 2025 5:00 AM - 8:20 AM UTC HORIBA Symposium Hall (INNOVATION BLDG., 5F)

[17sy] Synthesis

Chair:Don N Futaba, Guohai Chen

2:00 PM - 2:20 PM JST | 5:00 AM - 5:20 AM UTC

[17sy-01]

Salt-Assisted Growth of Transition Metal Dichalcogenide Nanotubes: Mechanisms from Molecular Dynamics

*Alister J Page[1], Daniel S Vadseth[1], Shigeo Maruyama[2] (1. University of Newcastle (Australia), 2. Tokyo University (Japan))

2:20 PM - 2:40 PM JST | 5:20 AM - 5:40 AM UTC

[17sy-02]

Transforming the Synthesis of Carbon Nanotubes with Machine Learning Models and Automation

*Yue Yuri Li[1], Liu Qian[1], Jin Zhang[1] (1. Peking University (China))

2:40 PM - 3:00 PM JST | 5:40 AM - 6:00 AM UTC

[17sy-03]

An Autonomous, Closed Loop Experimentation system for Floating Catalyst Carbon Nanotube Synthesis

*Arthur William Newton Sloan[1,2], Morgen Smith[1,3,4], Robert Waelder[1,4], John Bulmer[1,2], Rahul Rao[1], Benji Maruyama[1] (1. Air Force Research Laboratory (United States of America), 2. National Research Council (United States of America), 3. Kansas State University (United States of America), 4. BlueHalo LLC (United States of America))

3:00 PM - 3:20 PM JST | 6:00 AM - 6:20 AM UTC

[17sy-04]

Carbon Nanotube Synthesis Mechanism for Deep-Injection Floating Catalyst Chemical Vapor Deposition

Raj Kumar[1,2], Ji Hong Park[1], Seung-Yeol Jeon[1,2], Young Shik Cho[1], *Seung Min Kim[1,2] (1. Korea Institute of Science and Technology (Korea), 2. Jeonbuk National Univ. (Korea))

4:00 PM - 4:20 PM JST | 7:00 AM - 7:20 AM UTC

[17sy-05]

High-speed screening of growth conditions for carbon nanotube thin films using an aerosol jet printing system

*Keigo Otsuka[1], Ryuji Fujiwara[1], Shigeo Maruyama[1] (1. The University of Tokyo (Japan))

4:20 PM - 4:40 PM JST | 7:20 AM - 7:40 AM UTC

[17sy-06]

Synthesis of boron nitride nanotubes and applications into electrochemical catalysis

*Myung Jong Kim[1] (1. Gachon University (Korea))

4:40 PM - 5:00 PM JST | 7:40 AM - 8:00 AM UTC

[17sy-07]

Controlled Synthesis of Single-Walled Carbon Nanotubes: Microplasma-Assisted Multi-Step Reactor and Catalyst Precursor Effects

*Guohai Chen[1], Takashi Tsuji[1], Jinping He[1], Maho Yamada[1], Yoshiki Shimizu[1], Hajime Sakakita[1], Kenji Hata[1], Don N. Futaba[1], Shunsuke Sakurai[1] (1. AIST (Japan))

5:00 PM - 5:20 PM JST | 8:00 AM - 8:20 AM UTC

[17sy-08]

Aerosol CVD Carbon Nanotube Thin Films: From Synthesis to Advanced Applications

*Ilya V. Novikov[1], Dmitry V. Krasnikov[2], Albert G. Nasibulin[2], Il Jeon[1] (1. Sungkyunkwan University (Korea), 2. Skolkovo Institute of Science and Technology (Russia))

| Parallel Symposia：Symposium on Fundamental, Structural and Optical Properties of 1D and 2D Materials and their Heterostructures

Tue. Jun 17, 2025 2:00 PM - 5:20 PM JST | Tue. Jun 17, 2025 5:00 AM - 8:20 AM UTC International Exchange Hall III (Clock Tower Centennial Hall, 2F)

[17fn] Fundamental Properties

Chair:Yasumitsu Miyata, Antoine RESERBAT-PLANTEY

2:00 PM - 2:40 PM JST | 5:00 AM - 5:40 AM UTC

[17fn-01]

TEM-EELS of low-D materials combining high energy and momentum resolution

*Thomas Pichler[1] (1. University of Vienna (Austria))

2:40 PM - 3:00 PM JST | 5:40 AM - 6:00 AM UTC

[17fn-02]

Energy transfer in mixed-dimension heterostructures based on super-radiant Dyes@BNNT and 2D semiconductors

*Juliette Le Balle[1,2], Jean-Baptiste Marceau[2], Frédéric Fossard[1], Gaëlle Recher [2], Annick Loiseau [1], Etienne Gaufrès[2] (1. Université Paris-Saclay, ONERA, CNRS, Laboratoire d'étude des microstructures (LEM), 92322 Châtillon, France. (France), 2. Laboratoire Photonique Numérique et Nanosciences, CNRS-Institut d'Optique - Université de Bordeaux, 33400 Talence, France. (France))

3:00 PM - 3:20 PM JST | 6:00 AM - 6:20 AM UTC

[17fn-03]

Creation and Control of Quantum Light Emitters in 2D Flatland

*Han Htoon[1] (1. Los Alamos National Laboratory (United States of America))

4:00 PM - 4:20 PM JST | 7:00 AM - 7:20 AM UTC

[17fn-04]

Anharmonicity and confinement effects in Carbyne-like Materials

*Sebastian Heeg[1] (1. Humboldt-Universität zu Berlin (Germany))

4:20 PM - 4:40 PM JST | 7:20 AM - 7:40 AM UTC

[17fn-05]

Unraveling the Origin of B-Type Photoluminescence Blinking at 2D/3D Heterojunction Interface

*Tao Zhou[1], Dongyang Wan[1], Junpeng lu[1], Zhenhua Ni[1] (1. Southeast University (China))

4:40 PM - 5:00 PM JST | 7:40 AM - 8:00 AM UTC

[17fn-06]

Strain and defects engineering in transition metal dichalcogenide nanostructures

*Yasumitsu Miyata[1] (1. Tokyo Metropolitan University (Japan))

5:00 PM - 5:20 PM JST | 8:00 AM - 8:20 AM UTC

[17fn-07]

Moiré Superlattice in Twisted Transition Metal Dichalcogenide Trilayers

*Hao Ou[1], Kota Tanaka[2], Koshi Oi[2], Jiang Pu[1], Taishi Takenobu[2] (1. Institute of Science Tokyo (Japan), 2. Nagoya Univ. (Japan))

| Main conference：Main conference

Tue. Jun 17, 2025 6:00 PM - 8:00 PM JST | Tue. Jun 17, 2025 9:00 AM - 11:00 AM UTC Poster 1(International Exchange Hall III, Clock Tower Centennial Hall, 2F)

[17psa] Poster 1

[17psa-01]

Hybrid silicon all-optical switching devices integrated with 2D material

*Daiki Yamashita[1,2], Nan Fang[1], Shun Fujii[1,3], Yuichiro K Kato[1] (1. RIKEN (Japan), 2. AIST (Japan), 3. Keio Univ. (Japan))

[17psa-02]

Optical resolution of single-walled carbon nanotubes through wrapping with chiral metal coordination polymers followed by interlocking with metal-tethered tetragonal nanobrackets

Sicong Dai[1], Guoqin Cheng[1], Takuya Hayashi[2], Xinyi Fu[1], *Naoki Komatsu[1] (1. Graduate School of Human and Environmental Studies, Kyoto University (Japan), 2. Carbon Science Division, Research Institute for Supra Materials, Shinshu University (Japan))

[17psa-03]

Perpendicular electronic transport in twisted 3D graphite and twisted 3D superconductors

*Tenta Tani[1], Takuto Kawakami[1], Mikito Koshino[1] (1. Osaka Univ. (Japan))

[17psa-04]

Correlation between Flow-induced Electricity Generation on Graphene and Flow Dynamics

*Takeru Okada[1], Mitsuhiro Honda[2], Masaki Tanemura[2], Ichiro Yamashita[3], Atsuki Komiya[4] (1. Graduate School of Engineering, Tohoku University (Japan), 2. Naogya Institute of Technology (Japan), 3. Osaka University (Japan), 4. Institute of Fluid Science, Tohoku University (Japan))

[17psa-05]

Surface-Dependent Graphene Growth Kinetics on Cu Foil in Low-Pressure Chemical Vapor Deposition

*Jiyun Kim[1], Ji-Yong Park[1] (1. Ajou Univ. (Korea))

[17psa-06]

Automated evaluation and counting of nanofibers in SEM micrographs

*Torben Peters[1], John Schumann[1], Asmus Meyer-Plath[1] (1. Federal Institute for Occupational Safety and Health (Germany))

[17psa-07]

Suspended SWCNT arrays by transfer with sublimable materials

*Yuuki Kanai[1], Kaito Sakakibara[1], Riku Fujiwara[1], Ryotaro Kaneda[1], Waka Miyata[1], Keigo Otsuka[1], Shigeo Maruyama[1], Chiashi Shohei[1] (1. The University of Tokyo (Japan))

[17psa-08]

Hydrogenolysis of Graphene Oxide

*Moe Kitamura[1], Akiho Horibe[1], Koji Nakabayashi[2], Toshihira Irisawa[3], Yoshiyuki Nonoguchi[1] (1. Kyoto Institute of Technology (Japan), 2. Kyushu University (Japan), 3. Gifu University (Japan))

[17psa-09]

Chemical Vapor Deposition of Large Area Single-Walled Carbon Nanotubes Films Using Ethanol as the Carbon Precursor

*Afzal Khan[1], Abid .[1], Lingfeng Wang[1], Yongjia Zheng[1], Nduwarugira Bill Herve[1], Salman Ullah[1], Hafiz Bilal Naveed[1], Rong Xiang[1] (1. Zhejiang University (China))

[17psa-10]

Viral detection platform: portable graphene-derived biosensor

*Ana Champi[1] (1. Federal University of ABC (Brazil))

[17psa-11]

Optimizing CVD Growth of Monolayer MoS 2 through Relative Configurations of Substrate and Gas flows

*hoyeon Jung[1], jiyong Park[1] (1. Ajou University (Korea))

[17psa-12]

Energetics and electronic property of Janus WSSe nanoscroll

*Yanlin Gao[1], Susumu Okada[1] (1. University of Tsukuba (Japan))

[17psa-13]

Electrical and thermal transport properties of individual carbon nanotubes by in situ TEM

*Daiming Tang[1,2], Hai-Bo Zhao[3,4], Ovidiu Cretu[1], Chang Liu[3,4] (1. National Institute for Materials Science (NIMS) (Japan), 2. Faculty of Pure and Applied Sciences, University of Tsukuba (Japan), 3. Institute of Metal Research (IMR), Chinese Academy of Sciences (CAS) (China), 4. School of Materials Science and Engineering, University of Science and Technology of China (China))

[17psa-14]

Investigation and Mitigation of the Electron-Hole Conduction Asymmetry in Graphene Field-Effect Transistors

*MINSANG KIM[1], Ji-Yong Park[1] (1. AJOU UNIV. (Korea))

[17psa-15]

Signle-step SH group termination of epitaxial graphene and graphene oxide

*Yuya Miyake[1], Jun Ishii[1], Taisei Suzuoka[1], Yoshiaki Matsuo[2], Kazuyuki Takai[1] (1. Hosei Univ. (Japan), 2. Univ. of Hyogo (Japan))

[17psa-16]

Aggregation effect on exciton binding energies of single-chirality single-walled carbon nanotubes

*Zhirui Liu[1], Taishi Nishihara[1], Vasili Perebeinos[2], Yuhei Miyauchi[1] (1. Institute of Advanced Energy, Kyoto University (Japan), 2. Department of Electrical Engineering and Center for Advanced Semiconductor Technologies, University at Buffalo (United States of America))

[17psa-17]

Solvent acoustic coupling governs non-covalent bonding at the interface of ultra-long carbon nanotubes

*Yuxuan Tian[1] (1. Beijing Key Laboratory of Green Chemical Reaction Engineering and Technology, Department of Chemical Engineering, Tsinghua University, Beijing 100084, China. (China))

[17psa-18]

Fabrication of Near-Infrared Perfect Absorber Using Chirality-Sorted Carbon Nanotubes

*Mioko Kawakami[1], Sota Takasu[1], Taishi Nishihara[1], Yuhei Miyauchi[1] (1. Kyoto University (Japan))

[17psa-19]

One-pot Electrochemical Exfoliation/Functionalization of graphite for N-Functionalized Graphene

Yuta Konno[1], Sota Ishizu[1], Ryo Watanabe[1], *Haruya Okimoto[1] (1. Yamagata University (Japan))

[17psa-20]

Self-winding ultra-long carbon nanotube rings and their potential functional applications

*Sibo Chen[1], Fei Wei[1] (1. Tsinghua University (China))

[17psa-21]

A High-Performance High-Temperature Accelerometer Based on the Improved Graphene Aerogel

*Yanchun Wang[1], Zibo Wang[1], Weiya Zhou[1] (1. Institute of Physics, Chinese Academy of Sciences (China))

[17psa-22]

Early-Stage Au Deposition Morphology on Graphene and Its Effect on Graphene Field Effect Transistors

*SungYeon Kim[1], Ji-Yong Park[1] (1. Ajou university (Korea))

[17psa-23]

A statistical assessment of the semiconducting proportion in single-wall carbon nanotubes based on electrostatic force microscopy

Yuki Kuwahara[1], Indra M Khoris[1], Fahmida Nasrin[1], *Ryota Yuge[2,1], Takeshi Saito[1] (1. AIST (Japan), 2. NEC (Japan))

[17psa-24]

Diameter Dependence of Phase Transition and Phases Coexistence of Water Confined Inside Carbon Nanotubes

*Wenjie Liu[1], Ikuma Kohata[1], Yuki Maekawa[2], Takihiro Yamamoto[2], Yoshikazu Homma[2], Shohei Chiashi[1] (1. The University of Tokyo (Japan), 2. Tokyo University of Science (Japan))

[17psa-25]

Carbon Nanotube-based Spectrally Selective Solar Absorber: Design and Fabrication

*Hengkai Wu[1], Taishi Nishihara[1], Takeshi Tanaka[2], Hiromichi Kataura[2], Yuhei Miyauchi[1] (1. Kyoto University (Japan), 2. National Institute of Advanced Industrial Science and Technology (AIST) (Japan))

[17psa-26]

Achieving High Thermal Conductivity with Lower Filler Loading: Direct CNT Growth on AlN in Silicone Rubber Composites

*Naoyuki Matsumoto[1], Don N. Futaba[1], Takeo Yamada[1], Ken Kokubo[1] (1. National Institute of Advanced Industrial Science and Technology (AIST) (Japan))

[17psa-27]

Oxidation Mechanism on Single-Walled Carbon Nanotubes Analyzed by Photo-Induced Force Microscopy

*Kaori Fujii[1], Kazufumi Kobashi[1], Yasuhiko Fujita[1], Takahiro Morimoto[1], Hideaki Nakajima[1], Toshiya Okazaki[1] (1. Advanced industrial science and technology (Japan))

[17psa-28]

Large-scale separation of micrometer-long single-chirality single-wall carbon nanotubes in aqueous surfactant systems

*Zimeng An[1], Sayuki Oka[1], Kazuki Nagashima[1], Yohei Yomogida[1] (1. Hokkaido University (Japan))

[17psa-29]

Automatic Transfer of Carbon Nanotubes: from Growth to Device Performance

*Luca Ornago[1], Frederik H. van Veen[2,3], Jorien van der Meulen[4,1], Seoho Jung[1], Natanael Lanz[1], Andre Butzerin[1], Marko Nikolic[1], Mikael L. Perrin[2,3], Maria El Abbassi[1] (1. Chiral Nano AG (Switzerland), 2. Empa (Switzerland), 3. ETH Zürich (Switzerland), 4. TU Delft (Netherlands))

[17psa-30]

Ultraclean carbon nanotube transistors via robotic assembly

*Seoho Jung[1], Frederik van Veen[2,3], Jorien van der Meulen[1,4], Luca Ornago[1], Marko Nikolic[1], Andre Butzerin[1], Natanael Lanz[1], Mickael Perrin[2,3], Maria El Abbassi[1] (1. Chiral Nano AG (Switzerland), 2. Empa (Switzerland), 3. ETH Zurich (Switzerland), 4. Delft Univ. of Technology (Netherlands))

[17psa-31]

NIR photoluminescence of single-wall carbon nanotubes by the biochemical reaction of luciferin/luciferase

*Takeshi Tanaka[1], Mahoko Higuchi[1], Mayumi Tsuzuki[1], Atsunori Hiratsuka[1], Hiromichi Kataura[1] (1. Nanomaterials Research Institute, National Institute of Advanced Industrial Science and Technology (AIST) (Japan))

[17psa-32]

Reconfigurable physical unclonable functions from carbon nanotube transistors for secure vehicle communications

*Yang Liu[1], Jingfang Pei[1], Yingyi Wen[1], Lekai Song[1], Songwei Liu[1], Pengyu Liu[1], Teng Ma[2], Guohua Hu[1] (1. the Chinese University of Hong Kong (Hong Kong), 2. the Hong Kong Polytechnic University (Hong Kong))

[17psa-33]

MXene Quantum Dots/ Metal Organic Framework Hybrid for Photocatalytic Applications

*MUHAMMAD ANNAS SYHUKRI BIN MOHD ARIFFIN[1], ANIR SYAHMI BIN SHARBIRIN[1], AFRIZAL LATHIFUL FADLI[1], JEONGYONG KIM[1] (1. SUNGKYUNKWAN UNIVERSITY (Korea))

[17psa-34]

Theoretical study on photo thermoacoustic phenomena in carbon nanotubes based on Tyndall model

*Akari Sudo[1], Takahiro Yamamoto[1] (1. Tokyo University of Science (Japan))

[17psa-35]

Semiconducting Transport Characteristics and Performance of Large-Bundle SWCNT FETs

*Md Abu Taher Khan[1], Nan Wei[2], Esko I. Kauppinen[1] (1. Aalto University (Finland), 2. Peking University (China))

[17psa-36]

Armchair-Oriented Synthesis of Tin Disulfide Nanotubes (SnS_2 NT)

*Abid .[1], Yongjia Zheng[1], Luneng Zhao[2], Ju Huang[3,4], Yuta Sato[5], Qingyun Lin[6], Zheng Han[7], Chunxia .[1], Tianyu Wang[1], Kazu Suenaga[10], Yige Zheng[1], Hang Wang[1], Salman Ullah[1], Mohd Taazeem Ansari[8], Feng Ding[9], Afzal Khan[1], Wenbin Li[3,4], Junfeng Gao[2], Shigeo Maruyama[11], Rong Xiang[1] (1. State Key Laboratory of Fluid Power and Mechatronic Systems, Zhejiang Provincial Key Laboratory for Atomic-level Manufacturing, School of Mechanical Engineering, Zhejiang University (China), 2. Key Laboratory of Material Modification by Laser, Ion and Electron Beams (Dalian University of Technology), Ministry of Education, Dalian, 116024, China (China), 3. Key Laboratory of 3D Micro/Nano Fabrication and Characterization of Zhejiang Province, School of Engineering, Westlake University, 310030, Hangzhou, China (China), 4. Institute of Advanced Technology, Westlake Institute for Advanced Study, 310024, Hangzhou, China (China), 5. Nanomaterials Research Institute, National Institute of Advanced Industrial Science and Technology (AIST), Tsukuba 305-8565, Japan (Japan), 6. Center of Electron Microscopy, State Key Laboratory of Silicon and Advanced Semiconductor Materials, School of Material Science and Engineering, Zhejiang University, Hangzhou 310027, China (China), 7. College of Chemistry and Molecular Engineering, Peking University, Beijing 100871, P. R. China (China), 8. Department of Applied Sciences & Humanities, Faculty of Engineering & Technology, Jamia Millia Islamia, New Delhi, India (India), 9. Institute of

Technology for Carbon Neutrality, Shenzhen Institute of Advanced Technology, Chinese Academy of Sciences, Shenzhen, China (China), 10. The Institute of Scientific and Industrial Research, Osaka University, 8-1 Mihogaoka, Ibaraki, Osaka, Japan (Japan), 11. Department of Mechanical Engineering, The University of Tokyo, Tokyo 113-8656, Japan (Japan))

[17psa-37]

Overcoming Van der Waals Bundling: Molecular Wedges Enable Sonication-Free Dispersion of Single-Walled Carbon Nanotubes

*Seungyeop Lee Lee[1], Ziyi Wang[1], Ebenezer Afriyie[1], Jiajun Wang[2], Ayman Alibrahim[1], Anand Jagota[2], YuHuang Wang[1] (1. University of Maryland, College Park (United States of America), 2. Lehigh University (United States of America))

[17psa-38]

Hydrogen storage by carbon nanohorns enhanced by dispersion with metallic nanoparticles

*Noriaki Sano[1] (1. Kyoto Univerisity (Japan))

[17psa-39]

Synthesis of H_2-rich syngas and CNTs from CH_4/CO_2 using Ni-Mo_2C/MgO catalyst: Impact of biogas impurities and catalyst regeneration

*Supanida Saconsint[1], Noriaki Sano[1], Sakhon Ratchahat[2] (1. Kyoto Univerisity (Japan), 2. Mahidol University (Thailand))

[17psa-40]

Geometric structure and electronic properties of bilayer graphene with a Moire superlattice by interlayer asymmetric tensile strain

Mina Maruyama[1], Nadia Sultana[1], Yanlin Gao[1], *Susumu Okada[1] (1. UNiversity of Tsukuba (Japan))

[17psa-41]

Structural and Electrical Properties of 3D CNT Networks in CNT-Oxide Ceramic Composites

*Akinobu Shibuya[1,2], Tomo Tanaka[1,2], Noriyuki Tonouchi[1,2], Toshie Miyamoto[1,2], Ryota Yuge[1,2] (1. NEC Corporation (Japan), 2. National Institute of Advanced Industrial Science and Technology (Japan))

[17psa-42]

Composite of Carbon Nanotubes and Activated Carbon as Air Electrode in Zn-air Battery

*Munsuree Kalong[1], Noriaki Sano[1], Tetsuo Suzuki[1] (1. Kyoto Univerisity (Japan))

[17psa-43]

Quantitative insights into the correlation between sp^3 defects and functional groups in oxidized single-walled carbon nanotubes

*Hideaki Nakajima[1], Kazufumi Kobashi[1], Ying Zhou[1], Minfang Zhang[1], Toshiya Okazaki[1] (1. National Institute of Advanced Industrial Science and Technology (Japan))

[17psa-44]

Preferential growth of (7,5) SWCNTs by enhanced direct-injection pyrolytic synthesis method

Yuki Kuwahara[1], Yuta Nishiwaki[2], Kei Takano[2], *Takeshi Hashimoto[2], Ryota Yuge[1,3], Takeshi Saito[1] (1. AIST (Japan), 2. Meijo Nano Carbon Co. Ltd. (Japan), 3. NEC (Japan))

[17psa-45]

Vacuum electronics of carbon nanotubes and its applications in aerospace

*Peng Liu[1], Lian Liu[1], Kaili Jiang[1], Shoushan Fan[1] (1. Tsinghua University (China))

[17psa-46]

Machine learning force field driven exploration of 992 binary alloy metal clusters for carbon nanotube growth

*Daniel Hedman[1], Daisuke Asa[2], Ryo Yoshikawa[2], Ikuma Kohata[2], Kaoru Hisama[3], Christophe Bichara[4], Keigo Otsuka[2], Shigeo Maruyama[2] (1. Center for Multidimensional Carbon Materials (CMCM), Institute for Basic Science (IBS) (Korea), 2. Department of Mechanical Engineering, The University of Tokyo (Japan), 3. Center for Research Initiative for Supra-Materials, Shinshu University (Japan), 4. Aix-Marseille Univ, CNRS, CINaM (France))

[17psa-47]

Impact of Twisted angle on Thermal Transport Property of Graphene/h-BN Moiré Superlattice

*SHINICHIRO MOURI[1], Yusuke Kodama[1], Abdul Kuddus[2] (1. Graduate of School of Science and Engineering (Japan), 2. R-GIRO, Ritsumeikan University (Japan))

[17psa-48]

Structure and Fabrication Process Optimization of Microbolometer Array using Semi-conducting Single-walled Carbon Nanotube Networks

*Tomo Tanaka[1,2], Masahiko Sano[1], Masataka Noguchi[1,2], Megumi Kanaori[2], Toshie Miyamoto[1,2], Ryota Yuge[1,2] (1. NEC Corporation (Japan), 2. AIST (Japan))

[17psa-49]

Gate Voltage Dependence of Low-Frequency Noise in Carbon Nanotube Networks

*Noriyuki Tonouchi[1,2], Norika Fukuda[2], Tomo Tanaka[1,2], Ryota Yuge[1,2] (1. NEC (Japan), 2. AIST (Japan))

[17psa-50]

Terahertz wave detection using P/N carbon nanotube fiber at room temperature

*Koki Shiba[1], Shigeki Saito[1], Satoshi Kusaba[1,2], Ryo Tamaki[2], Shizuka Tsuduki[3], Tsukasa Matsuura[3], Jun Takeda[2], Ikufumi Katayama[2], Kazuhiro Yanagi[1] (1. Tokyo Metroplitan Univ. (Japan), 2. Yokohama National Univ. (Japan), 3. TOKAI RIKA Co., LTD. (Japan))

[17psa-51]

Growth of Isolated Carbon Nanotubes Wrapped by Homogeneous Amorphous Carbon

Zeyu Liu[1], Xinrui Zhang[1], Yanzhao Liu[1], Zilong Qiu[1], Jian Sheng[1], Zeyao Zhang[1], *Yan Li[1] (1. Peking University (China))

[17psa-52]

DIRECT GRAPHENE GROWTH BETWEEN ELECTRODES BY JOULE HEATING

*Koki Nakane[1], Agus Subagyo[1], Kazuhisa Sueoka[1] (1. Graduate School of Information Science and Technology, Hokkaido University (Japan))

| Main conference：Main conference

Tue. Jun 17, 2025 6:00 PM - 8:00 PM JST | Tue. Jun 17, 2025 9:00 AM - 11:00 AM UTC Poster 2(International Exchange Hall I&II, Clock Tower Centennial Hall, 2F)

[17psb] Poster 2

[17psb-01]

Fabrication of High-Density Arrays of Single-Chirality and Enantiomer-Pure Single-Walled Carbon Nanotubes

*Yanzhao Liu[1], Zilong Qiu[1], Yiran Ma[1], Min Lyu[1], Zeyao Zhang[1,2], Yan Li[1,2] (1. Peking University (China), 2. Institute of Carbon-Based Thin Film Electronics, Peking University, Shanxi (China))

[17psb-02]

Photovoltaic devices with wide operating temperature ranges based on large-area, freestanding, transparent and conductive G-SWCNT films

*Weiya Zhou[1,2], Ying Yue[1,2], Mingming Li[1,2] (1. Beijing National Laboratory for Condensed Matter Physics and Institute of Physics, Chinese Academy of Sciences (China), 2. University of Chinese Academy of Sciences (China))

[17psb-03]

Multi-level organization of carbon nanotubes for advanced THz optics

*Dmitry V. Krasnikov[1], Nikita I. Raginov[1], Arina V. Radivon[2], Alexey S. Ezersky[3], Gleb M. Katyba[4,5], Sergey A. Kuznetsov[6], Maria G. Burdanova[2], Albert G. Nasibulin[1] (1. Skolkovo Institute of Science and Technology (Russia), 2. Moscow Institute of Physics and Technology (Russia), 3. ITMO University (Russia), 4. Prokhorov Institute of General Physics of the Russian Academy of Sciences (Russia), 5. Institute of Solid State Physics of the Russian Academy of Sciences (Russia), 6. Novosibirsk State University (Russia))

[17psb-04]

Coupling TiO_2 with Low-Dimensional Materials for Efficient Photocatalytic Oxidation of NOx

Morgen L Smith[1], Brian M Everhart[1], Ahmed Al Mayyahi[1], *Placidus B Amama[1] (1. Kansas State University (United States of America))

[17psb-05]

Continuous Synthesis and Fiber Spinning of Nitrogen-Doped SWCNTs

*Zhikai Li[1], Toshihiko Fujimori[1,2], Samuel Jeong[1], Jun-ichi Fujita[1] (1. University of Tsukuba (Japan), 2. Sumitomo Electric Industries, Ltd (Japan))

[17psb-06]

Dielectric-assisted transfer using single-crystal antimony oxide for two-dimensional material devices

*Junhao Liao[1] (1. Peking University (China))

[17psb-07]

Graphene Tamed Supercooling in Plastic Crystals

*Xinyu Zhang[1], Yuanlong Shao[1,2], Jin Zhang[1,2] (1. Peking University (China), 2. Beijing Graphene Institute (China))

[17psb-08]

Nano-seeding method for preparing arrays of horizontally aligned carbon nanotube wafers

*Ying Xie[1], Yue Li[1], Zhisheng Peng[1], Liu Qian[1], Ziqiang Zhao[1], Jin Zhang[1] (1. Peking University (China))

[17psb-09]

Direct Crystallization of one-dimensional Van der Waals Semiconductor WTe_2 Nanowires via Chemical Vapor Transport

*Hang Wang[1], Tianyu Wang[1], Yongjia Zheng[1], Shanhe Xue[2], Abid .[1], Yige Zheng[1], Qingyun Lin[1], Afzal Khan[1], Qi Zhang[2], Rong Xiang[1] (1. Zhejiang Univ (China), 2. Hangzhou Dianzi Univ (China))

[17psb-10]

Janus MoSSe nanotubes on one-dimensional SWCNT-BNNT van der Waals heterostructures

*Chunxia Yang[1,2], Qingyun Lin[2], Yuta Sato[3], Yanlin Gao[4], Yongjia Zheng[2], Tianyu Wang[2], Yicheng Ma[2], Wanyu Dai[1], Wenbin Li[5], Mina Maruyama[4], Susumu Okada[4], Kazu Suenaga[6], Shigeo Maruyama[1,2], Rong Xiang[2] (1. The University of Tokyo (Japan), 2. Zhejiang University (China), 3. National Institute of Advanced Industrial Science and Technology (AIST) (Japan), 4. University of Tsukuba (Japan), 5. Westlake University (China), 6. Osaka University (Japan))

[17psb-11]

A Simple Equipment-Free Method for Length Sorting of Carbon Nanotubes

*Xiaojun Wei[1,2], Shuang Ling[1,3], Xin Luo[1], Xiao Li[1,2], Feibing Xiong[3], Weiya Zhou[1,2], Sishen Xie[1,2], Huaping Liu[1,2] (1. Institute of Physics, Chinese Academy of Sciences (China), 2. University of Chinese Academy of Sciences (China), 3. Xiamen University of Technology (China))

[17psb-12]

In-Situ Observation of Vapor-Liquid-Solid Growth of WS_2 in a Substrate-Stacked Microreactor for Mechanistic Investigation

*Hiroo Suzuki[1], Yutaro Senda[1], Yuta Takahashi[2], Shun Fujii[2], Yasuhiko Hayashi[1] (1. Okayama Univ. (Japan), 2. Keio Univ. (Japan))

[17psb-13]

Tailoring Oxidation States for Selective CVD Growth of Boron Nitride Nanotubes on Supported Catalysts

*Chunghun Kim[1], Myung Jong Kim[1] (1. Gachon university (Korea))

[17psb-14]

Interlocking of SWNTs with Metal-Tethered Tetragonal Nanobrackets to Enrich a Few Hundredths of Nanometer Range in Their Diameters

*Guoqing Cheng[1], Takuya Hayashi[2], Hiroshi Tabata[3], Mitsuhiro Katayama[3], Naoki Komatsu[4] (1. SINANO, CAS (China), 2. Shinshu Univ. (Japan), 3. Osaka Univ. (Japan), 4. Kyoto Univ. (Japan))

[17psb-15]

Novel BNNT-Tungsten Oxide Hybrid Structures for Enhanced Energy Storage Applications

*Honggu Kim[1], Chandan Kumar Maity[1], Myung Jong Kim[1] (1. Gachon University (Korea))

[17psb-16]

Reductive functionalization and purification of single-walled carbon nanotubes for controlling near-infrared photoluminescence properties

*Yutaka Maeda[1], Kentaro Kawada[1], Atsushi Suwa[1], Yui Iguchi[1], Yasuhiro Suzuki[1], Yui Konno[1], Michio Yamada[1], Pei Zhao[2], Masahiro Ehara[2] (1. Tokyo Gakugei University (Japan), 2. Institute for Molecular Science (Japan))

[17psb-17]

Divide and Functionalize: Sorting and Brightening of Single-Walled Carbon Nanotubes

Dominik Just[1], Patrycja Taborowska[1], Andrzej Dzienia[1], *Dawid Janas[1] (1. Silesian University of Technology (Poland))

[17psb-18]

Ultra clean (6,5) SWCNT film with perfect vdW spacing and its 1D heterostructures

*Lingfeng Wang[1], Yicheng Ma[1], Zhirui Liu[2], Yongjia Zheng[1], Tianyu Wang[1], Yuhei Miyauchi[2], Rong Xiang[1] (1. Zhejiang University (China), 2. Kyoto University (Japan))

[17psb-19]

Metal chloride-intercalated pnictogens. Unexplored field full of possibilities

*Cristina Madrona[1], Gonzalo Abellán[1] (1. ICMol - Universidad de Valencia (Spain))

[17psb-20]

TERPYRIDINE-FUNCTIONALIZED SINGLE-WALLED CARBON NANOTUBES AS SELECTIVE ELECTROCATALYST

*Ioanna Sideri[1], Nikos Tagmatarchis[1] (1. National Hellenic Research Foundation, Theoretical and Physical Chemistry Institute (Greece))

[17psb-21]

FUNCTIONALIZED MoS_2 ELECTROSTATICALLY ASSOCIATED WITH PHOTOACTIVE CHROMOPHORES

*Eleni Nikoli[1], Marina Tsigkou[1], Ioanna Sideri[1], Michalis Kardaras[1], Hiram Joazet Ojeda Galvan[2], Mildred Quintana[2], Nikos Tagmatarchis[1] (1. National Hellenic Research Foundation, Theoretical and Physical Chemistry Institute (Greece), 2. Universidad Autonóma de San Luis Potosi, High Resolution Microscopy-CICSaB and Faculty of Science (Mexico))

[17psb-22]

Transition Metal Dichalcogenide Nanotubes with Diameters Below 3 nm

*Runze Lai[1], Zhen Han[1], Xinrui Zhang[1], Yan Li[1] (1. College of Chemistry and Molecular Engineering, Peking University (China))

[17psb-23]

Large-scale complementary carbon nanotube integrated circuits for harsh radiation environments

Ke Zhang[1], *Daming Zhou[1], Ningfei Gao[2,3], Zhongzhen Tong[1], Xiaoyang Lin[1], Haitao Xu[2,3,4], Lianmao Peng[2], Weisheng Zhao[1] (1. School of Integrated Circuit Science and Engineering, Beihang University (China), 2. Key Laboratory for the Physics and Chemistry of Nanodevices, Center for Carbon-based Electronics, School of Electronics, Peking University (China), 3. Beijing Institute of Carbon-based Integrated Circuits (China), 4. Institute of Carbon-based Thin Film Electronics, Peking University (China))

[17psb-24]

Architecting Host−Guest Synergistic Solid-State Electrolytes Enables Unobstructed Li-Ion Interphase Migration for Lithium Metal Batteries

*lixiang li[1] (1. University of Science & Technology Liaoning (China))

[17psb-25]

Optimizing Metal Contacts for Low Contact Resistance in Graphene Field Effect Transistors

*Duc Chung Nguyen[1], Yi Yong Park[1] (1. Ajou University (Korea))

[17psb-26]

Diameter Adjustment of Single-Walled Carbon Nanotubes by Ni-Based Bimetallic Catalysts in Laser Ablation

Shaochuang Chen[1], *Zeyao Zhang[1,2], Yan Li[1,2] (1. Peking University (China), 2. Institute of Carbon-Based Thin Film Electronics, Peking University, Shanxi (China))

[17psb-27]

Marangoni-Flow-Induced Self-Assembly of Single Walled Carbon Nanotubes into High Density Arrays

Zilong Qiu[1], Yuguang Chen[1], *Yanzhao Liu[1], Zeyao Zhang[1,2], Yan Li[1,2] (1. Peking University (China), 2. Institute of Carbon-Based Thin Film Electronics, Peking University, Shanxi (China))

[17psb-28]

Intrinsic High-Semiconducting-Purity Carbon Nanotube Array Films for High-Performance Electronics

*Lan Bai[1,2] (1. Peking University (China), 2. Shanxi Institute of Carbon-Based Thin Film Electronics, Peking University (China))

[17psb-29]

h-BN/Graphene Heterostructure-Decorated Copper Current Collector for Long-Cycle Anode-Free Lithium Metal Batteries

*Lingchen Kong[1], Chaofan Zhou[1], Xuanguang Ren[1], Li Lin[1,2], Xin Gao[1,2] (1. Peking University (China), 2. Beijing Graphene Institute (China))

[17psb-30]

Research on Semiconducting SWCNTs with clean surfaces in Dispersions and Thin-Films

*Song Qiu[1] (1. Suzhou Institute of Nano-Tech and Nano-Bionics, Chinese Academy of Sciences (China))

[17psb-31]

Gas Phase Chemistry of Salt Assisted MoS_2 Growth

*Daniel Stormer Vadseth[1], Shigeo Maruyama[2], Alister Page[1] (1. University of Newcastle (UoN) (Australia), 2. University of Tokyo (UTokyo) (Japan))

[17psb-32]

On the use of seeding for chirality-controlled growth of carbon nanotubes

*Kim-Jonas Mikael Ylivainio[1], Daniel Hedman[2], Andreas Larsson[1] (1. Luleå university of technology (Sweden), 2. Institute for basic science (Korea))

[17psb-33]

Super graphene-skinned material: From epitaxial growth to property calculations

*Sun Xiu cai[1], Liu Zhong fan[2,1] (1. Beijing Graphene Institute (BGI) (China), 2. Peking University (China))

[17psb-34]

Graphene Layers Folded Many Times

*Kazuyuki Uchida[1] (1. Kyoto Sangyo University (Japan))

[17psb-35]

Anomalous Electrostatic Properties of Double-walled BN Nanotubes

*Nadia Sultana[1], Yanlin Gao[1], Mina Maruyama[1], Susumu Okada[1] (1. University of Tsukuba (Japan))

[17psb-36]

Machine Learning-Assisted Computational Exploration of the Electronic Structures of MoS_2 Nanotubes

*Wenbin Li[1], Ju Huang[1] (1. Westlake University (China))

[17psb-37]

Observation of Topological Nodal-Ring Phonons in Monolayer Hexagonal Boron Nitride

*Zhiyu Tao[1] (1. Institute of Physics, Chinese Academy of Sciences (China))

[17psb-38]

On-Chip Metasurface-Mediated $MoTe_2$ Photodetector with Electrically Tunable Polarization-Sensitivity

*Ruizhi Li[1], Xinlei Zhang[1], Fan Zhong[1], Zhenhua Ni[1] (1. Southeast University (China))

[17psb-39]

Synthesis of Rhenium Doped WS_2 Nanotubes and their electrical properties

*Abdul Ahad[1,2], M. A. Afzal[1], R. Higashinaka[1], M. Kikuchi[1], S. Saito[1], S. Kusaba[1], Z. Liu[4], Y. Miyata[1], Y. Hirose[3], K. Yanagi[1] (1. Department of Physics, Tokyo Metropolitan University (Japan), 2. Department of Physics, Comilla University (Bangladesh), 3. Department of Chemistry, Tokyo Metropolitan University (Japan), 4. National Institute of Advanced Industrial Science and Technology (AIST) (Japan))

[17psb-40]

Interband Scattering via Effective-Diameter Modulation in Single-Wall Carbon Nanotubes

*Nikita Gavrilov[1], Eden Levi[1], Alon Strugatsky[1], Michael Shlafman[1], Kenji Watanabe[2], Takashi Taniguchi[2], Yuval E. Yaish[1] (1. Technion - Israel Institute of Technology (Israel), 2. National Institute for Materials Science (Japan))

[17psb-41]

Thermal characterization of highly thermally conductive SWCNT films employing two-laser Raman thermometry

*Timm Swoboda[1], Martin Magg[2], Cristian Borja Peña[3], Pu Tan[1], Jiaqi Yang[1], Daniel Capolat Palomar[1], Wim Wenseleers[4], Sofie Cambré[3], Benjamin Flavel[2], Javier Rodriguez-Viejo[1,5], Marianna Sledzinska[1] (1. Catalan Institute of Nanoscience and Nanotechnology (ICN2), 08193, Barcelona, Spain (Spain), 2. Institute of Nanotechnology, Karlsruhe Institute of Technology, 76344, Eggenstein-Leopoldshafen, Germany (Germany), 3. Theory and Spectroscopy of Molecules and Materials, Department of Physics, University of Antwerp, 2610. Antwerp, Belgium (Belgium), 4. Nanostructured and Organic Optical and Electronic Materials, Department of Physics, University of Antwerp, 2610, Antwerp, Belgium (Belgium), 5. Physics department, Autonomous University of Barcelona (UAB) Campus UAB, Bellaterra, 08193, Barcelona, Spain (Spain))

[17psb-42]

ANISOTROPIC OPTICAL PROPERTIES OF MONOLAYER ALIGNED SINGLE-WALLED CARBON NANOTUBES

G A Ermolayev[1], M G Burdanova[2], Y Xie[3], L Qian[3], M Tatmyshevskiy[2], A Slavich[2], A Arsenin[1], V Volkov[1], J Zhang[3], *Alexander Chernov[2,4] (1. Emerging Technologies Research Center XPANCEO Emmay Tower (United Arab Emirates), 2. Moscow Institute of Physics and Technology (Russia), 3. Peking University (China), 4. Russian Quantum Center (Russia))

[17psb-43]

Fluctuations, dynamics and structure of the crystal edge of growing carbon nanotubes

Daniel Hedman[1], *Christophe Bichara[2] (1. CNRS and Aix-Marseille Univ. (Korea), 2. Institute for Basic Science (France))

Wed. Jun 18, 2025

| Main conference：Main conference

Wed. Jun 18, 2025 9:30 AM - 10:40 AM JST | Wed. Jun 18, 2025 12:30 AM - 1:40 AM UTC Centennial Hall (Clock Tower Centennial Hall)

[18ma] Main Conference

Chair: Toshiaki Kato

9:30 AM - 10:10 AM JST | 12:30 AM - 1:10 AM UTC

[18ma-01]

Ultra-clean interfaces in atomically thin materials for electronics

*Manish Chhowalla[1] (1. University of Cambridge (UK))

10:10 AM - 10:40 AM JST | 1:10 AM - 1:40 AM UTC

[18ma-02]

Flexoelectricity in Self-Assembled Graphene Nanowrinkles

Sathvik Ajay Iyengar[2,3], James G McHugh[3], Jonathan P Salvage[4], Alan Dalton[5], Manoj Tripathi[5], P M Ajayan[2], *Vincent Meunier[1] (1. The Pennsylvania State University (United States of America), 2. Rice University (United States of America), 3. University of Manchester (UK), 4. University of Brighton (UK), 5. University of Sussex (UK))

| Main conference：Main conference

Wed. Jun 18, 2025 11:00 AM - 12:10 PM JST | Wed. Jun 18, 2025 2:00 AM - 3:10 AM UTC Centennial Hall (Clock Tower Centennial Hall)

[18ss] Special panel session of 35 Years of Carbon Nanotubes –Past, current and future applications in industry—

Kenji Hata (AIST)
Shigeo Maruyama (Zhejiang University, The University of Tokyo, Nagoya University)

Thu. Jun 19, 2025

| Main conference：Main conference

Thu. Jun 19, 2025 9:30 AM - 12:10 PM JST | Thu. Jun 19, 2025 12:30 AM - 3:10 AM UTC Centennial Hall (Clock Tower Centennial Hall)

[19ma] Main Conference

Chair: Ryo Kitaura, Susumu Okada

9:30 AM - 10:10 AM JST | 12:30 AM - 1:10 AM UTC

[19ma-01]

Luminescent Defects in Single-Wall Carbon Nanotubes: Chemistry & Applications

*Jana Zaumseil[1] (1. Heidelberg University (Germany))

10:10 AM - 10:40 AM JST | 1:10 AM - 1:40 AM UTC

[19ma-02]

Electroluminescence From Monochiral Carbon Nanotubes With Quantum Defects

*Ralph Krupke[1] (1. Institute of Nanotechnology, Karlsruhe Institute of Technology (Germany))

11:00 AM - 11:30 AM JST | 2:00 AM - 2:30 AM UTC

[19ma-03]

Infrared Image Sensor using Carbon Nanotubes

*Ryota Yuge[1,2], Tomo Tanaka[1,2], Masahiko Sano[1], Noriyuki Tonouchi[1,2], Akinobu Shibuya[1,2], Taizo Shibuya[1,2], Masataka Noguchi[1,2], Toshie Miyamoto[1,2], Naoki Oda[1] (1. NEC Corporation (Japan), 2. National Institute of Advanced Industrial Science and Technology (Japan))

11:30 AM - 11:50 AM JST | 2:30 AM - 2:50 AM UTC

[19ma-04]

Nanofluidic transport in narrow single-wall carbon nanotube pores

*Aleksandr Noy[1] (1. Lawrence Livermore National Laboratory (United States of America))

11:50 AM - 12:10 PM JST | 2:50 AM - 3:10 AM UTC

[19ma-05]

Thermal rectification using Tesla valve structure in graphite microribbon

*Masahiro Nomura[1,3], Roman Anufriev[2,3], Laurent Jalabert[3], Kenji Watanabe[4], Takashi Taniguchi[4], Sebastian Volz[3] (1. The University of Tokyo (Japan), 2. Universite de Lyon (France), 3. LIMMS, CNRS-IIS UTokyo (Japan), 4. NIMS (Japan))

| Parallel Symposia：Symposium on Nanomaterials for Energy and Electronics

Thu. Jun 19, 2025 2:00 PM - 5:20 PM JST | Thu. Jun 19, 2025 5:00 AM - 8:20 AM UTC Conference room 5a/5b(INNOVATION BLDG., 5F)

[19en] Energy & Electronics

Chair:Yutaka Matsuo, Yutaka Takaguchi

2:00 PM - 2:40 PM JST | 5:00 AM - 5:40 AM UTC

[19en-01]

MIXED-DIMENSIONAL HETEROSTRUCTURES FOR ELECTRONIC AND ENERGY TECHNOLOGIES

*Mark Hersam[1] (1. Northwestern University (United States of America))

2:40 PM - 3:00 PM JST | 5:40 AM - 6:00 AM UTC

[19en-02]

Automated processing and transfer of two-dimensional materials with robotics

*Yixuan Zhao[1] (1. Peking university (China))

3:00 PM - 3:20 PM JST | 6:00 AM - 6:20 AM UTC

[19en-03]

Single-Walled Carbon Nanotubes in Artificial Photosynthesis

*Yutaka Takaguchi[1], Linh Thi Pham[1], Kazushi Mukai[1], Kazutaka Gomado[1] (1. University of Toyama (Japan))

4:00 PM - 4:20 PM JST | 7:00 AM - 7:20 AM UTC

[19en-04]

Semiconducting Carbon Nanotube-Polythiophene Composites Showing Large Thermoelectric Power Factors

*Yoshiyuki Nonoguchi[1] (1. Kyoto Inst. Tech. (Japan))

4:20 PM - 4:40 PM JST | 7:20 AM - 7:40 AM UTC

[19en-05]

Suspended carbon nanotube quantum dot heat engines

*Frederik van Veen[1,2], Jordi Picó Cortés[3], Seoho Jung[4], Bhaskar Ghawri[1], Natanael Lanz[4], Marko Nikolic[4], Andre Butzerin[4], Luca Ornago[4], Michel Calame[1,6], Andrea Donarini[3], Milena Grifoni[3], Herre van der Zant[5], Maria El Abbassi[4], Mickael Perrin[1,2] (1. Transport at Nanoscale Interfaces Laboratory, Empa (Switzerland), 2. Department of Information Technology and Electrical Engineering, ETH Zurich (Switzerland), 3. Institute for Theoretical Physics, University of Regensburg (Germany), 4. Chiral Nano AG (Switzerland), 5. Delft University of Technology (Netherlands), 6. Department of Physics, University of Basel, (Switzerland))

4:40 PM - 5:00 PM JST | 7:40 AM - 8:00 AM UTC

[19en-06]

STRUCTURE-DEFINED THERMOELECTRIC PERFORMANCE OF THIN SINGLE-WALLED CARBON NANOTUBE FILMS

*Dmitry V. Krasnikov[1], Jiraphat Khongthong[1], Nikita I. Raginov[1], Anastasia E. Goldt[1], Vladislav A. Kondrashov[1], Albert G. Nasibulin[1] (1. Skolkovo Institute of Science and Technology (Russia))

5:00 PM - 5:20 PM JST | 8:00 AM - 8:20 AM UTC

[19en-07]

SiO-$LiNi_{0.8}Co_{0.1}Mn_{0.1}O_2$ Full Cell Realized by Three-Dimensional Current Collectors of Carbon Nanotubes

*Tomotaro Mae[1], Suguru Noda[1] (1. Waseda University (Japan))

| Parallel Symposia：Symposium on Thin Films, Fibers, 3-D Materials and their Properties

Thu. Jun 19, 2025 2:00 PM - 5:00 PM JST | Thu. Jun 19, 2025 5:00 AM - 8:00 AM UTC Conference Room III(Clock Tower Centennial Hall, 2F)

[19mm] Macromaterials

Chair:Yoshiyuki Nonoguchi, Suguru Noda

2:00 PM - 2:40 PM JST | 5:00 AM - 5:40 AM UTC

[19mm-01]

Multifunctional Carbon Nanotube Films for Advanced Protective Applications

*Qingwen Li[1] (1. Suzhou Institute of Nano-Tech and Nano-Bionics, Chinese Academy of Sciences (China))

2:40 PM - 3:00 PM JST | 5:40 AM - 6:00 AM UTC

[19mm-02]

Large-area and long-length single-wall carbon nanotube transparent conductive film strengthened by carbon welding

*Peng-Xiang Hou[1], Yi-Ming Zhao[1], Chang Liu[1], Hui-Ming Cheng[2] (1. Shenyang National Laboratory for Materials Science, Institute of Metal Research, Chinese Academy of Sciences (China), 2. Shenzhen Key Laboratory of Energy Materials for Carbon Neutrality, Shenzhen Institute of Advanced Technology, Chinese Academy of Sciences (China))

3:00 PM - 3:20 PM JST | 6:00 AM - 6:20 AM UTC

[19mm-03]

Aerosol-synthesized Surfactant-free Single-walled Carbon Nanotube-based chemical sensors: Unprecedentedly High Sensitivity, Fast Recovery, and In-fluid (transformer oil) Applicability

*IL JEON[1] (1. Sungkyunkwan University (SKKU) (Korea))

4:00 PM - 4:20 PM JST | 7:00 AM - 7:20 AM UTC

[19mm-04]

Unlocking the Full Potential of Carbon Nanotubes: A Trans-Scale Approach from Nanoscale to Macroscale

*Yasuhiko Hayashi[1], Hiroo Suzuki[1] (1. Okayama University (Japan))

4:20 PM - 4:40 PM JST | 7:20 AM - 7:40 AM UTC

[19mm-05]

Electrical and Thermal Properties of Aligned CNT Materials at Extreme Temperatures

*Kadyn Tackett[1], Brice Hall[1], Jake Blue[1], Sabrina Eddy[1], Timothy Haugan[1], John Bulmer[1,2] (1. Air Force Research Laboratory (United States of America), 2. National Research Council (United States of America))

4:40 PM - 5:00 PM JST | 7:40 AM - 8:00 AM UTC

[19mm-06]

High-performance carbon nanotube fiber actuators driven by electrochemical intercalation

*Jiangtao Di[1] (1. Suzhou Institute of Nano-Tech and Nano-Bionics, Chinese Academy of Sciences (China))

| Parallel Symposia：6th Symposium on Synthesis, Purification, Functionalization, and Manufacturing of Carbon Nanotubes and Low-Dimensional Materials

Thu. Jun 19, 2025 2:00 PM - 5:20 PM JST | Thu. Jun 19, 2025 5:00 AM - 8:20 AM UTC HORIBA Symposium Hall (INNOVATION BLDG., 5F)

[19sy] Synthesis

Chair:Minfang Zhang, Shigeo Maruyama

2:00 PM - 2:20 PM JST | 5:00 AM - 5:20 AM UTC

[19sy-01]

Ultra-Pure Synthesis of (6,5) Carbon Nanotubes with Multiphase Catalysts

*Toshiaki Kato[1] (1. Tohoku Univ. (Japan))

2:20 PM - 2:40 PM JST | 5:20 AM - 5:40 AM UTC

[19sy-02]

Catalytic rapid Joule heating synthesis of carbon nanotubes in seconds

*Jian Sheng[1], Yifan Xu[1], Yan Li[1] (1. Peking University (China))

2:40 PM - 3:00 PM JST | 5:40 AM - 6:00 AM UTC

[19sy-03]

Synthesis and Characterization of One-Dimensional van der Waals Heterostructures with Radial, Axial and Alloy Configurations

*Yongjia Zheng[1], Wanyu Dai[2], Akihito Kumamoto[3], Yuta Sato[4], Keigo Otsuka[2], Qiang Zhang[5], Esko I. Kauppinen[5], Yuichi Ikuhara[3], Kazu Suenaga[6], Shigeo Maruyama[2], Rong Xiang[1] (1. State Key Laboratory of Fluid Power and Mechatronic Systems, School of Mechanical Engineering, Zhejiang University (China), 2. Department of Mechanical Engineering, The University of Tokyo (Japan), 3. Institute of Engineering Innovation, The University of Tokyo (Japan), 4. Nanomaterials Research Institute, AIST (Japan), 5. Department of Applied Physics, Aalto University School of Science (Finland), 6. The Institute of Scientific and Industrial Research (ISIR), Osaka University (Japan))

3:00 PM - 3:20 PM JST | 6:00 AM - 6:20 AM UTC

[19sy-04]

Preparation of Highly Ordered CNT Fiber and Its Application on Nanofiltration

*Xiao Zhang[1], Weiya Zhou[1], Huaping Liu[1], Michael De Volder[2], Adam Boies[2] (1. Institute of Physics, Chinese Academy of Sciences (China), 2. Department of Engineering, University of Cambridge (UK))

4:00 PM - 4:20 PM JST | 7:00 AM - 7:20 AM UTC

[19sy-05]

Oxidation Saturation in Carbon Nanotubes: General Understanding of Functionalization Methods

*Minfang Zhang[1], Mei Yang[1], Makoto Yaguchi[1], Hirokuni Jintoku[1], Shunsuke Sakurai[1], Don Futaba[1] (1. National Institute of Advanced Industrial Science and Technology (AIST) (Japan))

4:20 PM - 4:40 PM JST | 7:20 AM - 7:40 AM UTC

[19sy-06]

Confined Assembling Chemistry within Single-Walled Carbon Nanotubes

*Feng Yang[1] (1. Southern University of Science and Technology (China))

4:40 PM - 5:00 PM JST | 7:40 AM - 8:00 AM UTC

[19sy-07]

Precise Partitioning of Single-Wall Carbon Nanotubes and Enantiomers Through Aqueous Two-Phase Extraction

*Han Li[1], Ming Zheng[2], Jeffrey Fagan[2] (1. University of Turku (Finland), 2. National Institute of Standards and Technology (United States of America))

5:00 PM - 5:20 PM JST | 8:00 AM - 8:20 AM UTC

[19sy-08]

Quantifying Enantiomeric Purity Of Sorted Single-Walled Carbon Nanotubes Using Combined Chiroptical Spectroscopy And Hyperspectral Fluorescence Microscopy

Miguel Ángel López Carrillo[1], Filip Desmet[1], Maksiem Erkens[2], Jeffrey A. Fagan[3], Ming Zheng[3], Han Li[4,5], Benjamin S. Flavel[4], Wim Wenseleers[2], Wouter Herrebout[1], Sofie Cambré[1], *Dmitry Levshov[1] (1. Theory and Spectroscopy of Molecules and Materials, Department of Chemistry and Department of Physics, University of Antwerp, Antwerp (Belgium), 2. Nanostructured and Organic Optical and Electronic Materials, Department of Physics, University of Antwerp, Antwerp (Belgium), 3. Materials Science and Engineering Division, National Institute of Standards and Technology, 20899 Gaithersburg, Maryland (United States of America), 4. Institute of Nanotechnology, Karlsruhe Institute of Technology, 76344 Eggenstein-Leopoldshafen (Germany), 5. Department of Mechanical and Materials Engineering, University of Turku, FI-20014 Turku (Finland))

| Parallel Symposia：Symposium on Fundamental, Structural and Optical Properties of 1D and 2D Materials and their Heterostructures

Thu. Jun 19, 2025 2:00 PM - 5:00 PM JST | Thu. Jun 19, 2025 5:00 AM - 8:00 AM UTC International Exchange Hall III (Clock Tower Centennial Hall, 2F)

[19fn] Fundamental Properties

Chair:Sebastian Heeg, Shohei Chiashi

2:00 PM - 2:20 PM JST | 5:00 AM - 5:20 AM UTC

[19fn-01]

Optical Absorption in Layered Semiconductor to Semimetal Platinum Diselenide

*Marin Tharrault[1], Sabrine Ayari[1,2], Mehdi Arfaoui[3], Eva Desgué[4], Romaric Le Goff[1], Sihem Jaziri[3,5], Bernard Plaçais[1], Pierre Legagneux[4], Francesca Carosella[1], Christophe Voisin[1], Robson Ferreira[1], Emmanuel Baudin[1] (1. Laboratoire de Physique de l'Ecole normale supérieure, ENS, Université PSL, CNRS, Sorbonne Université, Université Paris Cité (France), 2. De Vinci Higher Education, Research Center (France), 3. Laboratoire de Physique de la Matière Condensée, Faculté des Sciences de Tunis, Université Tunis El Manar (Tunisia), 4. Thales Research & Technology (France), 5. Laboratoire de Physique des Matériaux : Structure et Propriétés, Faculté des Sciences de Bizerte, Université de Carthage (Tunisia))

2:20 PM - 2:40 PM JST | 5:20 AM - 5:40 AM UTC

[19fn-02]

THERMAL TRANSPORT ACROSS TWISTED BI-LAYERS OF 2D TRANSITION METAL DICHALCOGENIDES

*Marianna Sledzinska[1], Jiaqi Yang[1,2], Daniel Capolat Palomar[1], Onurcan Kaya[1], Aron W Cummings[1], Aitor Lopeandia[1,2], Javier Rodríguez Viejo[1,2], Stephan Roche[1,3] (1. Catalan Institute of Nanoscience and Nanotechnology (ICN2) (Spain), 2. UAB (Spain), 3. ICREA (Spain))

2:40 PM - 3:00 PM JST | 5:40 AM - 6:00 AM UTC

[19fn-03]

Chiral Stacking Identification of Two-Dimensional Triclinic Crystals Enabled by Machine Learning

*He Hao[1], Kangshu Li[1], Xujing Ji[1], Xiaoxu Zhao[1], Lianming Tong[1], Jin Zhang[1] (1. Peking University (China))

3:00 PM - 3:20 PM JST | 6:00 AM - 6:20 AM UTC

[19fn-04]

Probing strong electron-phonon coupling in graphene by resonance Raman spectroscopy with infrared excitation energy

*Simone Sotgiu[1,2], Tommaso Venanzi[2], Lorenzo Graziotto[2], Francesco Macheda[3], Taoufiq Ouaj[1], Elena Stellino[2], Guglielmo Marchese[2], Claudia Fasolato[4], Paolo Postorino[2], Vaidotas Mišeikis[3], Marvin Metzelaars[1], Paul Kögerler[1], Bernd Beschoten[1], Camilla Coletti[3], Stefano Roddaro[5], Matteo Calandra[6], Michele Ortolani[2], Christoph Stampfer[1], Francesco Mauri[2], Leonetta Baldassarre[2] (1. RWTH Aachen Univ. (Germany), 2. Sapienza Univ. (Italy), 3. IIT (Italy), 4. CNR (Italy), 5. Pisa Univ. (Italy), 6. Trento Univ. (Italy))

4:00 PM - 4:20 PM JST | 7:00 AM - 7:20 AM UTC

[19fn-05]

Intrinsic process for upconversion photoluminescence via *K*-momentum phonon coupling in carbon nanotubes

*Daichi Kozawa[1,2], Shun Fujii[1,3], Yuichiro K. Kato[1] (1. RIKEN (Japan), 2. NIMS (Japan), 3. Keio University (Japan))

4:20 PM - 4:40 PM JST | 7:20 AM - 7:40 AM UTC

[19fn-06]

EXPERIMENTAL DETERMINATION OF PHASE TRANSITIONS OF WATER MOLECULES ENCAPSULATED INSIDE THIN SWCNTs

*Aina Fitó-Parera[1], Miles Martinati[1,2], Wim Wenseleers[2], Sofie Cambré[1] (1. TSM2, University of Antwerp (Belgium), 2. NANOrOPT, University of Antwerp (Belgium))

4:40 PM - 5:00 PM JST | 7:40 AM - 8:00 AM UTC

[19fn-07]

Multi-modal carbon nanotube characterization for nano-confined thermodynamics

*Matthias Kuehne[1] (1. Brown University (United States of America))

| Parallel Symposia：15th Symposium on Carbon Nanomaterials, Biology, Medicine and Toxicology

Thu. Jun 19, 2025 2:00 PM - 5:00 PM JST | Thu. Jun 19, 2025 5:00 AM - 8:00 AM UTC Meeting Room E/F(INNOVATION BLDG., 5F)

[19nb] NanoBio

Chair:Tomohiro Shiraki, Anton Naumov, Mijin Kim

2:00 PM - 2:40 PM JST | 5:00 AM - 5:40 AM UTC

[19nb-01]

Functionally Programmed Medical Nanodevices for Cancer

*Naoki Komatsu[1] (1. Kyoto University (Japan))

2:40 PM - 3:00 PM JST | 5:40 AM - 6:00 AM UTC

[19nb-02]

Engineered Muti-Walled Carbon Nanotubes for tumor microenvironment modulation and melanoma metastasis suppression

*LORENA GARCÍA HEVIA[1], Rym Soltani[2], Jesús González[3], Olivier Chaloin[2], Cecilia Ménard-Moyon[2], Alberto Bianco[2], Mónica L. Fanarraga[3] (1. CINBIO, UNIVERSITY OF VIGO, IISGS (Spain), 2. University of Strasbourg (France), 3. Universidad de Cantabria-IDIVAL (Spain))

3:00 PM - 3:20 PM JST | 6:00 AM - 6:20 AM UTC

[19nb-03]

Evidence-based, systematic design of machine perception nanosensors for disease detection

*Mijin Kim[1] (1. Georgia Institute of Technology (United States of America))

4:00 PM - 4:20 PM JST | 7:00 AM - 7:20 AM UTC

[19nb-04]

Wrapping Polymer-dependent Microenvironment Responses of Near-infrared Photoluminescence from Color Centers in Single-walled Carbon Nanotubes

*Tomohiro Shiraki[1,2], Yoshiaki Niidome[1], Ryo Hamano[1], Hiromu Matsumoto[1], Koichiro Kato[1,3], Tsuyohiko Fujigaya[1,2,3] (1. Dept. of Applied Chem., Kyushu Univ. (Japan), 2. WPI-I2CNER, Kyushu Univ. (Japan), 3. CMS, Kyushu Univ. (Japan))

4:20 PM - 4:40 PM JST | 7:20 AM - 7:40 AM UTC

[19nb-05]

Toward Non-Invasive Real-Time Detection of Neurotransmitters and Hormones Using Near-Infrared Fluorescent Graphene Quantum Dots

*Anton Naumov[1], Floyd Wormley[1], Alina Valimukhametova[1], Natalia Castro Lopez[1], Alyssa Dickens[1], Pramita Sharma[1] (1. Texas Christian University (United States of America))

4:40 PM - 5:00 PM JST | 7:40 AM - 8:00 AM UTC

[19nb-06]

The Design and Application of Carbon Dots-Based Prodrug Conjugates

*Jia-Yaw Chang[1] (1. National Taiwan University of Science and Technology (Taiwan))

| Main conference：Main conference

Thu. Jun 19, 2025 6:00 PM - 8:00 PM JST | Thu. Jun 19, 2025 9:00 AM - 11:00 AM UTC Poster 1(International Exchange Hall III, Clock Tower Centennial Hall, 2F)

[19psa] Poster 1

[19psa-01]

Laser fabrication of hBN single photon emitters on silicon nitride waveguides

*Daiki Yamashita[1], Masaki Yumoto[1], Aiko Narazaki[1], Makoto Okano[1] (1. AIST (Japan))

[19psa-02]

Sorting of Single-Walled Carbon Nanotubes in the Tri-Surfactant System Using Aqueous Two-Phase Extraction

Cheng Li[1], Min Lyu[1], *Yan Li[1,2] (1. Peking Univ. (China), 2. Institute of Carbon-Based Thin Film Electronics, Peking University, Shanxi (China))

[19psa-03]

Evaluation of cross-plane Seebeck coefficient of single-walled carbon nanotube thin films using AC heating

*Shigeki Saito[1], Yoshihiko Kaneko[1], Shojiro Asatori[1], Satoshi Kusaba[1], Kan Ueji[1,2], Takashi Yagi[2], Kazuhiro Yanagi[1] (1. Tokyo Metropolitan University (Japan), 2. National Institute of Advanced Industrial Science and Technology (Japan))

[19psa-04]

The origin of the negative linear temperature dependence of resistance in nano-carbon materials

*Takahiro Morimoto[1], Takumi Inaba[1], Satoshi Yamazaki[2], Kazufumi Kobashi[1], Toshiya Okazaki[1] (1. AIST (Japan), 2. ADMAT (Japan))

[19psa-05]

Visualization of exciton modulation in monolayer WSe2 under dynamic strain

*Yuta Takahashi[1], Takumi Yamamoto[1], Kazuki Maezawa[1], Hajime Kumazaki[1], Shinichi Watanabe[1], Shun Fujii[1] (1. Keio University (Japan))

[19psa-06]

Non-catalytic direct synthesis of graphene and h-BN on sapphire substrates

*Waka Miyata[1], Hodaka Nishimura[1], Keigo Otsuka[1], Shigeo Maruyama[1], Shohei Chiashi[1] (1. Department of Mechanical Engineering, the University of Tokyo (Japan))

[19psa-07]

Development of In-Situ Electrical Observation System for Janus TMDs

*Dingkun Bi[1,2], Tianyishan Sun[1,2], Weizi Lu[1,2], Hiroto Ogura[1,2], Toshiaki Kato[1,2] (1. Grad. School of Engineering, Tohoku Univ. (Japan), 2. WPI-AIMR, Tohoku Univ. (Japan))

[19psa-08]

Formation of hBN-Encapsulated Janus TMDs without Air Exposure

*Tianyishan Sun[1,2], Dingkun Bi[1,2], Hiroto Ogura[1,2], Weizi Lu[1,2], Toshiaki Kato[1,2] (1. Grad. School of Engineering, Tohoku Univversity (Japan), 2. WPI-AIMR, Tohoku University (Japan))

[19psa-09]

Direct Fabrication of Graphene-Bridged Superconductor Junctions

*Zhuoqun Li[1,2], Yuto Tsukidate[1,2], Hiroto Ogura[1,2], Toshiaki Kato[1,2] (1. Grad. School of Engineering, Tohoku Univ. (Japan), 2. WPI-AIMR, Tohoku Univ. (Japan))

[19psa-10]

Boundary-Directed Epitaxy of Block Copolymers Guided by Graphene Nanoribbon Templates via Boundary-Directed Epitaxy

*Michael S. Arnold[1] (1. University of Wisconsin-Madison (United States of America))

[19psa-11]

Electrical contact formation of CNT@BNNT heteronanotubes with metal electrodes through heat treatment

*Atsutaka Watanabe[1], Makoto Shimizu[1], Yoshinori Murase[1], Taiki Inoue[1], Yoshihiro Kobayashi[1] (1. Osaka University (Japan))

[19psa-12]

Synthesis and Evaluation of High-Quality BNNT Growth on SWCNTs

*Xiyang Qiu[1], Shuhui Wang[1], Dmitry I Levshov[2], Ming Liu[1], Waka Miyata[1], Bowen Zhang[1], Yongjia Zheng[1,3], Esko I Kauppinen[4], Keigo Otsuka[1], Vasili Perebeinos[5], Shohei Chiashi[1], Rong Xiang[1,3], Shigeo Maruyama[1,3,6] (1. The University of Tokyo (Japan), 2. University of Antwerp (Belgium), 3. Zhejiang University (China), 4. Aalto University (Finland), 5. University at Buffalo (United States of America), 6. Nagoya University (Japan))

[19psa-13]

Weighing Transport of CNT Conductors in Extreme Environments

*John Bulmer[1,7], Chris Kovacs[1,8], Thomas Bullard[1,5], Charlie Ebbing[1,6], Kadyn Tackett[1], Sabrina Eddy[1], Michael Susner[1], Ganesh Pokharel[2,4], Stephen Wilson[2], Fedor Balakirev[3], Oscar Valenzuela[3], Timothy Haugan[1] (1. Air Force Research Laboratory (United States of America), 2. University of California, Santa Barbara (United States of America), 3. National High Magnetic Field Laboratory, Los Alamos (United States of America), 4. University of West Georgia (United States of America), 5. Blue Halo (United States of America), 6. University of Dayton Research Institute (United States of America), 7. National Research Council (United States of America), 8. Scintillating Solutions LLC (United States of America))

[19psa-14]

SAW-guided Reconfigurable Memristor using 2D MoS_2

*Sihyeok Kim[1], Jang Woo Lee[1], Hyeonseung Ryu[2], Taehoon Kim[1], Il Hyun Lee[1], Soo Ho Choi[1], Hyunho Lee[2], Yeong Hwan Ahn[2], Keekeun Lee[2], Il Jeon[1] (1. Sungkunkwan university (Korea), 2. Ajou university (Korea))

[19psa-15]

CNT-PP composite spacers for Reverse Osmosis Technology: A promising strategy to reduce positive organic fouling

*Armando David Martinez Iniesta[1], Kenji Takeuchi[1], Juan Fajardo-Diaz[1], Hiroki Kitano[3], Takahiro Kawakatsu[4], Syogo Tejima[5], Rodolfo Cruz-Silva[1,6], Morinobu Endo[1,2] (1. Institute for Aqua Regeneration, Shinshu University (Japan), 2. Global Aqua Innovation Center, Shinshu University (Japan), 3. Kitagawa Industries Co. (Japan), 4. Kurita Water Industries Ltd (Japan), 5. Research Organization for Information Science & Technology. (Japan), 6. Center for Applied Research in Chemistry, Plastic Transformation department (Mexico))

[19psa-16]

Efficient thermal defect healing of single-walled carbon nanotubes using a multiple-cycle approach

*Man Shen[1], Taiki Inoue[1], Yoshihiro Kobayashi[1] (1. Osaka Univ. (Japan))

[19psa-17]

Photo-induced thermal effects on the bandgap of monolayer WSe_2 integrated with ultrahigh-Q optical microcavities

*Hidetoshi Kanzawa[1], Ryo Sugano[1], Hajime Kumazaki[1], Shun Fujii[1] (1. Keio University (Japan))

[19psa-18]

Magnetic bulk photovoltaic effect in $MoS_2/CrPS_4$ artificial heterostructure device.

*Shuichi Asada[1], Keisuke Shinokita[1], Kazunari Matsuda[1] (1. Kyoto University Institute of Energy Science (Japan))

[19psa-19]

Magnetic brightening of defect-localized single-photon emission in monolayer WSe_2

*Yubei Xiang[1], Keisuke Shinokita[1], Kenji Watanabe[2], Takashi Taniguchi[3], Kazunari Matsuda[1] (1. Institute of Advanced Energy, Kyoto University (Japan), 2. Research Center for Electronic and Optical Materials, NIMS (Japan), 3. Research Center for Materials Nanoarchitectonics, NIMS (Japan))

[19psa-20]

Study on Alignment Control Method of Carbon Nanotube Network Films and Their Electrical Properties

*Norika Fukuda[1], Noriyuki Tonouchi[1,2], Tomo Tanaka[1,2], Toshie Miyamoto[1,2], Megumi Kanaori[1], Ryota Yuge[1,2] (1. National Institute of Advanced Industrial Science and Technology (Japan), 2. NEC Corporation (Japan))

[19psa-21]

Catalytic rapid Joule heating synthesis of one-dimensional nanomaterials in seconds

*Jian Sheng[1], Yifan Xu[1], Zhen Han[1], Xinrui Zhang[1], Chi Xu[1], Hai-Gang Lu[2], Si-Dian Li[2], Yan Li[1] (1. Peking University (China), 2. Shanxi University (China))

[19psa-22]

Stacking structure of epitaxial growth graphene on reduced graphene oxide

*Satoshi Kanda[1], Shunji Kurosu[2], Fumitaka Sakamoto[2], Tatsuro Hanajiri[1,2], Yuta Nishina[3], Ryota Negishi[1,2] (1. Graduate School of Toyo Univ. (Japan), 2. BNC (Japan), 3. Okayama univ. (Japan))

[19psa-23]

Circular dichroism of Trion in enantiopure carbon nanotubes

*Hiroyuki Fujinami[1], Koki Shiba[1], Yuya Hosokawa, Yohei Yomogida[2], Kazuhiro Yanagi[1] (1. Department of Physics, Tokyo Metropolitan University (Japan), 2. Department of Chemical Sciences and Engineering, Hokkaido University (Japan))

[19psa-24]

Direct Growth of Graphene on Hexagonal Boron Nitride under a Catalyst-Free Condition

*Yunosuke Miyashita[1], Hayato Watanabe[2], Yusei Terada[2], Aoi Sasanuma[2], Ryosuke Takatsuka[1], Keiichi Yanagisawa[3], Tomofumi Ukai[3], Shunji Kurosu[3], Kenji Watanabe[4], Takashi Taniguchi[4], Tatsuro Hanajiri[1,2,3], Toru Maekawa[1,2,3], Ryota Negishi[1,2,3] (1. Graduate School of Toyo Univ. (Japan), 2. Toyo Univ. (Japan), 3. BNC (Japan), 4. NIMS (Japan))

[19psa-25]

Doping-dependent valley polarization induced by Mott transition in WSe_2/WS_2 moiré superlattice

*Zhiwei Li[1], Kenji Watanabe[2], Takashi Taniguchi[3], Kazunari Matsuda[1] (1. Institute of Advanced Energy, Kyoto University, Uji, Kyoto (Japan), 2. Research Center for Electronic and Optical Materials, NIMS (Japan), 3. Research Center for Materials Nanoarchitectonics, NIMS (Japan))

[19psa-26]

Development of a Dual-Functional Device for Rapid Detection of NO_2 Gas and Long-Term Cumulative Exposure Memory using Optimized Single-Walled Carbon Nanotubes

*Sihyeok Kim[1], Ilya V. Novikov[1], Peng Liu[2], Jang Woo Lee[1], Il Hyun Lee[1], Artem Dudorov[3], Dmitry V. Krasnikov[3], Esko I. Kauppinen[2], Albert G. Nasibulin[3], Keekeun Lee[4], Il Jeon[1] (1. Sungkunkwan university (Korea), 2. Aalto

university (Finland), 3. Skolkovo Institute of Science and Technology (Russia), 4. Ajou university (Korea))

[19psa-27]

Bending Effect on Thermoelectric performance of carbon nanotubes

*Akari Yoshida[1], Takahiro Yamamoto[1,2] (1. Tokyo University of Science, Department of Physics (Japan), 2. RIST, Tokyo University of Science (Japan))

[19psa-28]

POROUS SILICON-BASED NANOCOMPOSITES FOR EFFICIENT ELECTROCHEMICAL SENSORS

*Abdullah Saeed Jalalah[1], Fahad Hussain Albaqami[1] (1. Institute of Microelectronics and Semiconductor Technologies, King Abdulaziz City for Science and Technology, Saudi Arabia (Saudi Arabia))

[19psa-29]

Optical Absorption of Fermi Level-Cotrolled Multilayer Graphene:Effects of Stacking Structure and Spacer Insertion

*Shinnosuke Yoshida[1], Takuo Mizuno[1], Taiki Inoue[1], Yuta Nishina[2], Yoshihiro Kobayashi[1] (1. Osaka Univ. (Japan), 2. Okayama Univ. (Japan))

[19psa-30]

EVALUATION OF MOLYBDENUM DISULFIDE PREPARED BY HEATING SULFUR-CAPPED MOLYBDENUM THIN FILMS

Kazushi Inoue[1], Yuto Kimura[1], Koki Nakane[1], *Agus Subagyo[1], Kazuhisa Sueoka[1] (1. Graduate School of Information Science and Technology, Hokkaido University (Japan))

[19psa-31]

Detection of process-induced contaminants on carbon nanotubes using Raman spectroscopy

*Haruki Uchiyama[1], Yudai Yoshikawa[1], Hiromichi Kataura[2], Yutaka Ohno[1,3] (1. Nagoya Univ. (Japan), 2. AIST (Japan), 3. IMaSS, Nagoya Univ. (Japan))

[19psa-32]

Peptide-modified Carbon Nanotube Biosensor

*Asahi Nagamine[1], Haruki Uchiyama[1], Hiromichi Kataura[2], Chishu Homma[3], Yuhei Hayamizu[3], Yutaka Ohno[1,4] (1. Department of Electronics, Nagoya Univ. (Japan), 2. Nanomaterials Research Institute, National Institute of Advanced Industrial Science and Technology (Japan), 3. Tokyo Institute of Technology (Japan), 4. Institute of Material and Systems for Sustainability, Nagoya Univ. (Japan))

[19psa-33]

METAL OXIDE/METAL SELENIDE NANOSTRUCTURE ELECTRODE FOR SOLID-STATE SYMMETRIC SUPERCAPACITOR WITH EXCELLENT CAPACITANCE RETENTION

*Mohammed Jalalah[1], Arpan Nayak[2] (1. Promising Centre for Sensors and Electronic Devices (PCSED), Najran University, P.O. Box: 1988, Najran 11001, Saudi Arabia (Saudi Arabia), 2. Department of Energy Engineering, Konkuk University, 120 Neungdong-ro, Seoul-05029, Republic of Korea (Korea))

[19psa-34]

Electronic transport in CNT thin films and PBTTT films:Crossover between weak and strong localization

*Yuki Hiyama[1], Hiroki Kaya[1], Manaho Matsubara[1], Hidetoshi Fukuyama[2], Takahiro Yamamoto[1] (1. Department of Physics, Tokyo University of Science (Japan), 2. RIST, Tokyo Univerity of Science (Japan))

[19psa-35]

Characterization of carbon nanotube thin-film transistors with inorganic polymer insulator

*Eito Kuromiya[1], Haruki Uchiyama[1], Masahiro Matsunaga[2], Shunto Arai[3], Hiromichi Kataura[4], Yutaka Ohno[1,2] (1. Department of Electronics, Nagoya University (Japan), 2. Institute of Material and Systems for Sustainability,

Nagoya University (Japan), 3. National Institute for Materials Science (Japan), 4. National Institute of Advanced Industrial Science and Technology (Jersey))

[19psa-36]

Floating Catalyst Chemical Vapour Deposition (FCCVD)-Based CNT Electrodes for Metal Halide Perovskite Memristors in Neuromorphic Synaptic Applications

*Jang Woo Lee[1], Yasir Shafi Mir[1], Taehoon Kim[1], Sihyeok Kim[1], Ilya Novikov[1], Sungjoo Lee[1], Il Jeon[1] (1. SKKU Advanced Institute of Nano-Tech. (Korea))

[19psa-37]

Durable Organic and Perovskite Solar Cells Using Single-walled Carbon Nanotubes Transparent Thin-film Electrodes

*Yutaka Matsuo[1] (1. Nagoya University (Japan))

[19psa-38]

Structural changes in semiconducting CNT networks by coating conditions

*Toshie Miyamoto[1,2], Tomo Tanaka[1,2], Megumi Kanaori[2], Norika Fukuda[2], Shunta Doi[1], Noriyuki Tonouchi[1,2], Ryota Yuge[1,2] (1. NEC Corporation (Japan), 2. National Institute of Advanced Industrial Science and Technology (Japan))

[19psa-39]

Bayesian optimization for the synthesis of small-diameter single-walled carbon nanotubes using the eDIPS method

*Taizo Shibuya[1,2], Noriyuki Tonouchi[1,2], Yuta Nishiwaki[3], Satoru Hashimoto[3], Takeshi Hashimoto[3], Takeshi Saito[2], Ryota Yuge[1,2] (1. NEC Corporation (Japan), 2. AIST (Japan), 3. Meijo Nano Carbon Co., Ltd (Japan))

[19psa-40]

POROUS SILICON-BASED NANOCOMPOSITES FOR EFFICIENT ELECTROCHEMICAL SENSORS

*Fahad Hussain Albaqami[1], Abdullah Saeed Jalalah[1] (1. Institute of Microelectronics and Semiconductor Technologies, King Abdulaziz City for Science and Technology, Riyadh, Saudi Arabia (Saudi Arabia))

[19psa-41]

Optical Properties of Interlayer Excitons in TMD-based vdw Stacks

*Sudhanshu Kumar Nayak[1,2], Hiroo Suzuki[3], Daichi Kozawa[2], Sai Santosh Kumar Raavi[1], Ryo Kitaura[2] (1. Ultrafast Photophysics and Photonics Laboratory, Department of Physics, Indian Institute of Technology Hyderabad, Kandi, Telangana, India (India), 2. Research Center for Materials Nanoarchitectonics (MANA)National Institute for Materials Science (NIMS)Tsukuba 305-0044, Japan (Japan), 3. Life, Natural Science and Technology, Institute of Academic and Research, Okayama University (Japan) (Japan))

[19psa-42]

Carbon Nanotube Electrode-Based Reconfigurable Metal Halide Perovskite Memristors for Reservoir Computing Applications

*Jang Woo Lee[1], Taehoon Kim[1], Naoumi Hasumi[2], Ryosuke Nakajima[2], Sihyeok Kim[1], Sungjoo Lee[1], Suguru Noda[2], Il Jeon[1] (1. SKKU Advanced Institute of Nano-Tech. (Korea), 2. Waseda University (Japan))

[19psa-43]

Collapsed carbon nanotubes: Raman signal and flattening control

*Emmanuel Picheau[1], Daiming Tang[1] (1. NIMS (Japan))

[19psa-44]

Exploration for the Optimized Double-Layer Catalyst Support Structure for the Synthesis of Vertically Aligned Carbon Nanotube Arrays

*Shunsuke Sakurai[1], Takashi Tsuji[1], Don N Futaba[1] (1. National Institute of Advanced Industrial Science and Technology (Japan))

[19psa-46]

Activated Diffusion of 1D J-Aggregates in Boron Nitride Nanotubes by Curvature Patterning

Jean-Baptiste Marceau[1], Juliette Le Balle[1,4], Duc-Minh Ta[2], Alberto Aguilar[2], Annick Loiseau[4], Richard Martel[5], Pierre Bon[2], Raphael Voituriez[3], Gaelle Recher[1], *Etienne Gaufrès[1] (1. CNRS-University of Bordeaux (France), 2. CNRS-University of Limoges (France), 3. CNRS-University of Sorbonne (France), 4. CNRS-Onera (France), 5. University of Montreal (Canada))

[19psa-47]

Flexible electronics based on conjugated polymers, oxides, and carbon nanostructures

*Lucimara Stolz Roman[1] (1. Universidade Federal do Paraná (Brazil))

[19psa-48]

Graphene nano-electromechanical mass sensor with high resolution at room temperature

*SangWook Lee[1], Dong-Hoon Shin[2,3], Sunghyun Kim[1], Peter Steeneken[3], Chirlmin Joo[3] (1. Ewha Womans University (Korea), 2. Korea University (Korea), 3. Delft University of Techology (Netherlands))

[19psa-49]

Carbon Nanotube Schottky Diode-Based Millimeter-Wave Frontends: Enabling Silicon-Compatible Flexible RF Systems from 10 GHz to W-Band

*Defu Wang[1] (1. Peking University (China))

[19psa-50]

Upcycling Waste Plastics into Carbon Nanotube Wirings and Synaptic Devices for Physical Reservoir Computing

*Takashi Ikuno[1], Kotaro Takanashi[1] (1. Tokyo University of Science (Japan))

[19psa-51]

CNTFET-Metal Contact Investigations via Voltage Controlled Material Deposition

*Martin Hartmann[1,2], Martin Ernst[1,2], Simon Böttger[1,2], Sascha Hermann[1,2] (1. Center for Microtechnologies, Chemnitz University of Technology (Germany), 2. Center for Materials Architecture and Integration of Nanomembranes, Chemnitz University of Technology (Germany))

[19psa-52]

AM I TOO FAT? CNT ASKED. DIFFERENCES IN MORPHOLOGY OF CARBON NANOTUBES FOR TRIBOLOGICAL APPLICATION

*Szymon Tomasz Ruczka[1,2,3], Adam Marek[1,4], Artur Terzyk[5], Magdalena Skrzypek[6], Łukasz Wojciechowski[6], Sławomir Boncel[1,2,3] (1. NanoCarbon Group; Department of Organic Chemistry, Bioorganic Chemistry and Biotechnology, Silesian University of Technology, Bolesława Krzywoustego 4, 44-100 Gliwice, Poland (Poland), 2. Centre for Organic and Nanohybrid Electronics (CONE), Silesian University of Technology, Stanisława Konarskiego 22B, 44-100 Gliwice, Poland (Poland), 3. NanoCarbonGroup.com Ltd., Ks. Marcina Strzody 7, 44-100 Gliwice, Poland (Poland), 4. Department of Chemical Organic Technology and Petrochemistry, Silesian University of Technology, Bolesława Krzywoustego 4, 44-100 Gliwice, Poland (Poland), 5. Department of Materials Chemistry, Adsorption and Catalysis, Nicolaus Copernicus University in Toruń, Gagarina 7, 87-100 Toruń, Poland (Poland), 6. Institute of Construction Machines and Automotive Vehicles, Poznań University of Technology, Piotrowo 3, 60-959 Poznań (Poland))

[19psa-53]

FROM DOTS TO TUBES – THE *REVERSE* SCENARIO OF BOTTOM-UP CATALYST-FREE SYNTHESIS OF *N*-DOPED CNTs

Program

NT 25（The 25th International Conference on the Science and Applications of Nanotubes and Low-

*Slawomir Boncel[1], Anna Kolanowska[1,2] (1. Silesian University of Technology (Poland), 2. University of Silesia (Poland))

| Main conference：Main conference

Thu. Jun 19, 2025 6:00 PM - 8:00 PM JST | Thu. Jun 19, 2025 9:00 AM - 11:00 AM UTC Poster 2(International Exchange Hall I&II, Clock Tower Centennial Hall, 2F)

[19psb] Poster 2

[19psb-01]

Investigation of Co Nanoparticle Formation Mechanisms on MgO and Al_2O_3 supports for Carbon Nanotube Synthesis

*Jiwoo Kim[1], Jaegeun Lee[1,2] (1. School of Chemical Engineering, Pusan National University (Korea), 2. Department of Organic Material Science and Engineering, Pusan National University (Korea))

[19psb-02]

Hybrid bismuthene hexagons by molecular interface engineering

*Gonzalo Abellán[1] (1. University of Valencia (Spain))

[19psb-03]

Carbon nano-onions: Potassium intercalation and reductive covalent functionalization

María Eugenia Pérez-Ojeda[1], Matteo Andrea Lucherelli[2], *Gonzalo Abellán[2] (1. FAU Erlangen-Nürnberg (Germany), 2. University of Valencia (Spain))

[19psb-04]

Orientation of MoS_2 Flakes Grown on Twisted Bilayer Graphene

*SHINICHIRO MOURI[1], Shun Tonegawa[1], Abdul Kuddus[2] (1. Graduate of School of Science and Engineering, Ritsumeikan University (Japan), 2. R-GIRO, Ritsumeikan University (Japan))

[19psb-05]

Growth of MoS_2 on $Al_{(1-x)}Ti_xO_y$ by Chemical Vapor Deposition

*Koshiro Kawakami[1], Syunsuke Yamamura[1], Abdul Kuddus[1], Shinichiro Mouri[1] (1. Ritsumeikan Univ. (Japan))

[19psb-06]

In situ XAFS measurements on the formation process of single-walled carbon nanotubes from Fe catalyst

*Jumpei Horiuchi[1], Shinya Mizuno[1], Takahiro Saida[1], Shigeya Naritsuka[1], Takahiro Maruyama[1] (1. Meijo Univ. (Japan))

[19psb-07]

Chirality Selective Growth of Bulk Single-walled Carbon NanotubesUsing Cobalt-sulfur Catalyst

Zihan Xu[1], *Zeyao Zhang[1,2], Yan Li[1,2] (1. Peking University (China), 2. Institute of Carbon-Based Thin Film Electronics, Peking University, Shanxi (China))

[19psb-08]

Understanding the role of molybdenum in carbon nanotube growth using layered double hydroxides

*Yeon Su Shin[1], Yoon Seo Kim[2], Seungho Cho[2,3], Jaegeun Lee[1,4] (1. School of Chemical Engineering, Pusan National University, Busan 46241 (Korea), 2. Department of Materials Science and Engineering, Ulsan National Institute of Science and Technology (UNIST), Ulsan 44919 (Korea), 3. Graduate School of Semiconductor Materials and Devices Engineering, Center for Future Semiconductor Technology (FUST), Ulsan National Institute of Science and Technology (UNIST), Ulsan 44919 (Korea), 4. Department of Organic Material Science and Engineering, Pusan National University, Busan 46241 (Korea))

[19psb-09]

Harnessing Metal-Support Interaction in Catalytic Synthesis of Carbon Nanotubes

Chi Xu[1], *Sida Sun[1], Zeyao Zhang[1], Yan Li[1] (1. Peking University (China))

[19psb-10]

Chirality and Enantiomer Based Sorting of Single-Walled Carbon Nanotubes by PEG/Salt Aqueous Two-Phase Systems

Min Lyu[1], Cheng Li[1], *Yanzhao Liu[1], Yan Li[1,2] (1. Peking University (China), 2. Institute of Carbon-Based Thin Film Electronics, Peking University, Shanxi (China))

[19psb-11]

General Synthesis Strategy of Alloy Transition Metal Dichalcogenide Nanotubes

*Runze Lai[1], Zhen Han[1], Xinrui Zhang[1], Yan Li[1] (1. College of Chemistry and Molecular Engineering, Peking University (China))

[19psb-12]

Remote salt enabling metallic NbS_2 one-dimensional van der Waals heterostructures

*Wanyu Dai[1], Yongjia Zheng[1,2], Akihito Kumamoto[3], Yanlin Gao[4], Sijie Fu[5], Sihan Zhao[5], Ryo Kitaura[6], Esko I Kauppinen[8], Keigo Otsuka[1], Slava V Rotkin[7], Yuichi Ikuhara[3], Mina Maruyama[4], Susumu Okada[4], Rong Xiang[1,2], Shigeo Maruyama[1,2] (1. Department of Mechanical Engineering, The University of Tokyo (Japan), 2. State Key Laboratory of Fluid Power and Mechatronic System, School of Mechanical Engineering, Zhejiang University (China), 3. Institute of Engineering Innovation, The University of Tokyo (Japan), 4. Department of Physics, Graduate School of Pure and Applied Sciences, University of Tsukuba (Japan), 5. School of Physics, Zhejiang University (China), 6. Research Center for Materials Nano architectonics (MANA), National Institute for Materials Science (NIMS) (Japan), 7. Materials Research Institute and Department of Engineering Science & Mechanics The Pennsylvania State University (United States of America), 8. Department of Applied Physics, Aalto University School of Science (Finland))

[19psb-14]

Fundamental investigation of monolayer graphene modification by low-pressure Argon Plasma

*Pierre Vinchon[1], Lucas Spiske[1], Nicolas Mauchamp[1], Yoshiyuki Miyamoto[2], Satoshi Hamaguchi[1] (1. Osaka University (Japan), 2. National Institute of Advanced Industrial Science and Technology (Japan))

[19psb-15]

Development of an autonomous 2D semiconductors production system driven by Bayesian optimization

*Wataru Idehara[1], Fan Yang[1], Keisuke Shinokita[1], Kazunari Matsuda[1] (1. Institute of Advanced Energy Science, Kyoto University (Japan))

[19psb-16]

Analysis roles of Fe and Co binary catalysts in chemical vapor deposition growth of single-walled carbon nanotubes

*Qingmei Hu[1], Ya Feng[2,1], Wanyu Dai[1], Daisuke Asa[1], Daniel Hedman[3], Aina Fitó Parera[4], Yixi Yao[5], Yongjia Zheng[6,1], Kaoru Hisama[7], Christophe Bichara[8], Shohei Chiashi[1], Yan Li[5], Wim Wenseleers[4], Dmitry Levshov[4], Sofie Cambré[4], Keigo Otsuka[1], Rong Xiang[1,6], Shigeo Maruyama[1,6] (1. The University of Tokyo (Japan), 2. Dalian University of Technology (China), 3. IBS-CMCM (Korea), 4. University of Antwerp (Belgium), 5. Peking University (China), 6. Zhejiang University (China), 7. Shinshu University (Japan), 8. Aix-Marseille University and CNRS (France))

[19psb-17]

Single-crystal Graphene Wafers: Controlled Synthesis and Mass Production

*Kaicheng Jia[1] (1. Beijing Graphene Institute (China))

[19psb-18]

HIGH-TEMPERATURE ADSORPTION OF NITROGEN DIOXIDE FOR STABLE, EFFICIENT, AND SCALABLE DOPING OF CARBON NANOTUBES

*Dmitry V. Krasnikov[1], Nikita I. Raginov[1], Anastasia E. Goldt[1], Stanislav S. Fedotov[1], Albert G. Nasibulin[1] (1. Skolkovo Institute of Science and Technology (Russia))

[19psb-19]

Synthesis of Tunable Fluorescent Carbon Dots from Dairy Whey for Advanced Cancer Nanomedicine: Bioimaging and Theranostic Applications

*Mónica L Fanarraga[1], Rafael Valiente[1], Jesús González[1], Marina Candela[1], Lorena García-Hevia[1] (1. Grupo de Nanomedicina, Universidad de Cantabria-IDIVAL (Spain))

[19psb-22]

Robust carbon nanotube composite coatings for perfect absorption in harshenvironmental applications

*Yuanhao Jin[1] (1. Tsinghua University (China))

[19psb-23]

Synthesis of Single-Walled Carbon Nanotubes/Graphene Nanoflakes Hybrid Nanostructures Utilizing Fe-Re Bimetallic Catalysts by Floating Catalyst Chemical Vapor Deposition

*Anastasios Karakasidis[1], Hirotaka Inoue[1,2], Ghulam Yasin[1], Hua Jiang[1], Esko I. Kauppinen[1] (1. Aalto University (Finland), 2. Sumitomo Electric Industries (Japan))

[19psb-24]

Magnetically Aligned All-Solid-State Ionic-Liquid Crystal Elastomer based Electrochemical Artificial Muscles

*Guang Yang[1,2] (1. University of Science and Technology of China (China), 2. Suzhou Institute of Nano-Tech and Nano-Bionics, Chinese Academy of Sciences (China))

[19psb-25]

Sequential Assembly of Low-Dimensional Materials on Arbitrary Fiber Substrates for Electromagnetic Interference Shielding

*Jiayi Liu[1,2], Quanfen Guo[1,2], Huahui Tian[2], He Hao[3], Xin Gao[1], Jin Zhang[3] (1. School of Materials Science and Engineering, Peking Univ. (China), 2. Beijing Graphene Institute (China), 3. Beijing Science and Engineering Center for Nanocarbons, Beijing National Laboratory for Molecular Sciences, College of Chemistry and Molecular Engineering, Peking Univ. (China))

[19psb-26]

Facile and scalable concentration method for surfactant-assisted carbon nanotube dispersion

*Jaegyun Im[1], Jaegeun Lee[1,2] (1. School of Chemical Engineering, Pusan National University (Korea), 2. Department of Organic Material Science and Engineering, Pusan National University (Korea))

[19psb-27]

Wet-spinning of high strength and high thermal conductivity carbon nanotube fibers

*Yuanlong Shao[1], Jin Zhang[1] (1. Peking University (China))

[19psb-28]

Exploring the Role of Sulfur Promoter from Carbon Disulfide in Carbon Nanotubes Synthesis

*Ghulam Yasin[1], Otto Salmela[1], Hirotaka Inoue[1,2], Anastasios Karakassides[1], Hua Jiang[1], Esko I. Kauppinen[1] (1. Aalto University (Finland), 2. Sumitomo Electric Industries (Japan))

[19psb-29]

Selective Semiconducting Carbon Nanotube Extraction with Cellulose Acetate

*Kazuhiro Yoshida[1], Yoshiyuki Nonoguchi[1] (1. Kyoto Institute of Technology (Japan))

[19psb-30]

Estimating key factors for self-organized, aligned CNT film formation by machine learning

*Miki Ikeda[1], Tomoyuki Miyao[2], Yoshiyuki Nonoguchi[1] (1. Kyoto Institute of Technology (Japan), 2. Nara Institute of Science and Technology (Japan))

[19psb-32]

Preparation, properties and applications of carbon nanomaterial flexible transparent conducting films

*Hong-Zhang Geng[1] (1. Tiangong University (China))

[19psb-33]

Beyond d-spacing: The critical role of defects in graphene oxide membranes

*Nima Zakeri[1], Kirill Levin[1], Marta Cerruti[1] (1. McGill University (Canada))

[19psb-34]

Structure Dependence of CNT Forests on the Lateral Memristive Resistance

*Hiroshi Furuta[1,2], Yuki Sato[1], Ryuichi Shinsei[1] (1. School of Systems Engineering, Kochi Univ. Technol. (Japan), 2. Research Inst., Kochi Univ. Technol. (Japan))

[19psb-35]

Direct identification and manipulation of valley coherence in monolayer semiconductor WSe_2

*Haonan Wang[1], Kenji Watanabe[2], Takashi Taniguchi[2], Satoru Konabe[3], Kazunari Matsuda[1] (1. Kyoto University (Japan), 2. NIMS (Japan), 3. Hosei University (Japan))

[19psb-36]

High-Density Polarization Dots in Short-Period Moiré Superlattices Enabled by Flexoelectric Effects

*Kota Tanaka[1], Hao Ou[2], Taishi Takenobu[1] (1. Nagoya University (Japan), 2. Institute of Science Tokyo (Japan))

[19psb-37]

High current density in electric double layer light-emitting devices of WSe_2 monolayers

*Koshi Oi[1], Taiga Aridome[1], Hao Ou[2], Jiang Pu[2], Takahiko Endo[3], Yasumitsu Miyata[3], Taishi Takenobu[1] (1. Department of Applied Physics, Nagoya University (Japan), 2. Department of Physics, Institute of Science Tokyo (Japan), 3. Department of Physics, Tokyo Metropolitan University (Japan))

[19psb-38]

Novel Interface Effects in Fe2O3@CNT

AAkanksha Kapoor[1], Avirup Dey[1], Sunil Nair[1], *Ashna Bajpai[1] (1. Indian Institute of science education and Research (India))

[19psb-39]

Reconfigurable nonlinear losses of nanomaterial covered waveguides

*Ayvaz Davletkhanov[1,2], Daniil Ilatovskii[3], Aram Mkrtchyan[4], Alexey Bunkov[4], Dmitry Krasnikov[4], Albert Nasibulin[4], Yuriy Gladush[4], Ralph Krupke[1,2,5] (1. Institute of Quantum Materials and Technologies, Karlsruhe Institute of Technology, 76131 Karlsruhe (Germany), 2. Institute of Materials Science, Technische Universität Darmstadt, 64827 Darmstadt (Germany), 3. Okinawa Institute of Science and Technology, 1919-1 Tancha, Onna-son, Kunigami-gun Okinawa (Japan), 4. Skolkovo Institute of Science and Technology, Moscow 121205 (Russia), 5. Institute of Nanotechnology, Karlsruhe Institute of Technology, 76131 Karlsruhe (Germany))

Fri. Jun 20, 2025

| Main conference：Main conference

Fri. Jun 20, 2025 9:30 AM - 12:10 PM JST | Fri. Jun 20, 2025 12:30 AM - 3:10 AM UTC Centennial Hall (Clock Tower Centennial Hall)

[20ma] Main Conference

Chair: Taishi Takenobu, Suguru Noda

9:30 AM - 10:10 AM JST | 12:30 AM - 1:10 AM UTC

[20ma-01]

Synthesis and Characterization of Janus Transition Metal Dichalcogenide Materials

*Jing Kong[1] (1. MIT (United States of America))

10:10 AM - 10:40 AM JST | 1:10 AM - 1:40 AM UTC

[20ma-02]

Synthesis and scalable transfer of research-grade CVD graphene

*James Hone[1] (1. Columbia University (United States of America))

11:00 AM - 11:30 AM JST | 2:00 AM - 2:30 AM UTC

[20ma-03]

CARBON-BASED MULTI-VIEW TERAHERTZ AND INFRARED IMAGERS

*Yukio Kawano[1,2,3], Kou Li[1] (1. Chuo University (Japan), 2. National Institute of Informatics (Japan), 3. Kanagawa Institute of Industrial Science and Technology (Japan))

11:30 AM - 11:50 AM JST | 2:30 AM - 2:50 AM UTC

[20ma-04]

Stepwise Engineering of van der Waals Heterostructures for High Current Density in Light Emitting Devices

Rei Usami[1], Koshi Oi[1], Keisuke Yamada[1], Jiang Pu[2], Hao Ou[2], Takahiko Endo[3], Yasumitsu Miyata[3], *Taishi Takenobu[1] (1. Nagoya University (Japan), 2. Institute of Science Tokyo (Japan), 3. Tokyo Metropolitan University (Japan))

11:50 AM - 12:10 PM JST | 2:50 AM - 3:10 AM UTC

[20ma-05]

CARBON AND BORON NITRIDE MATERIALS: BASIC SCIENCE AND BROADER IMPACT

*Rodney Ruoff[1,2] (1. IBS CMCM (Korea), 2. UNIST (Korea))

Session
NT 25（The 25th International Conference on the Science and Applications of Nanotubes and Low-

| Main conference：Main conference

Sun. Jun 15, 2025 1:50 PM - 5:30 PM JST | Sun. Jun 15, 2025 4:50 AM - 8:30 AM UTC Centennial Hall (Clock Tower Centennial Hall)

[15tu] Tutorials

Chair: Kazuhiro Yanagi

1:50 PM - 2:30 PM JST | 4:50 AM - 5:30 AM UTC

[15tu-01]

Dispersion and Structure Sorting of Single-Wall Carbon Nanotubes

*Hiromichi Kataura[1] (1. AIST until March (Japan))

2:50 PM - 3:30 PM JST | 5:50 AM - 6:30 AM UTC

[15tu-02]

Synthesis of Single-Walled Carbon Nanotubes

Yan Li[1] (1. Peking University (China))

3:50 PM - 4:30 PM JST | 6:50 AM - 7:30 AM UTC

[15tu-03]

Contemporary challenges in van der Waals layered semiconductors

*Young Hee Lee[1] (1. Sungkyunkwan University (Korea))

4:50 PM - 5:30 PM JST | 7:50 AM - 8:30 AM UTC

[15tu-04]

Tutorial: How do we analyze Raman spectra?

*Riichiro Saito[1,2] (1. Tohoku University, (Japan), 2. National Taiwan Normal University (Taiwan))

Dispersion and Structure Sorting of Single-Wall Carbon Nanotubes

H. Kataura

305-0032, Tsukuba, Ibaraki Japan

Because the physical properties of single-wall carbon nanotubes (SWCNTs) depend heavily on their structure, structure-selected (single-chirality) SWCNTs are needed for fundamental research and applications in electronic devices. However, the direct production of single-chirality SWCNTs has not yet been perfected, so structure sorting is still necessary. Many sorting methods have been reported so far, but the basic concepts are similar. In addition, most sorting methods require individually dispersed SWCNT solutions before sorting. Therefore, the dispersion process is also very important.

In this tutorial, we introduce our proprietary sorting technique, gel column chromatography, where nanoscale hydrophobic interactions play a key role. We also present a newly developed gentle dispersion method using a blade stirrer. We demonstrate that very low defect levels of SWCNTs can be selected from raw soot using "surfactant magic". This allows for the sorting of highly pure and highly crystalline semiconducting or single chirality species, depending on their diameter. We believe that this knowledge can also be applied to the dispersion or structural sorting of other nanomaterials, since the hydrophobic interactions used for sorting are not specific to SWCNTs but are thought to be universal for hydrophobic surfaces.

Outline of the tutorial is as follows.

1. Short introduction
2. Why sodium cholate? A special surfactant for SWCNT
3. Defect-free dispersion method
4. How to remove defective SWCNTs using “surfactant magic”
5. How to prepare a good blade for dispersion
6. Reliability of Raman G/D value of SWCNTs
7. Structure sorting using gel-column chromatography
8. What is the role of the gel?
9. Difference in sorting parameters between semiconducting and metallic species
10. Assignment of (n,m) index of metallic single chirality species
11. Appendix: Is defect healing possible?

Synthesis of Single-Walled Carbon Nanotubes

Yan Li
College of Chemistry and Molecular Engineering, Peking University, Beijing 100871, China

Single-walled carbon nanotubes (SWCNTs) present outstanding properties determined by their structures. The controlled synthesis of SWCNTs is of essential importance in the field. Varies methods such as arc-discharge, laser ablation, and chemical vapor deposition have been employed to synthesize SWCNTs. This tutorial talk will cover a wide range of topics including a general overview, the growth mechanisms, the strategy for structure-control, the challenges, and the perspective of SWCNT synthesis.

Contemporary challenges in van der Waals layered semiconductors

Young Hee Lee

Center for Integrated Nanostructure Physics, Sungkyunkwan University, Suwon, Korea

Since the advent of one-dimensional carbon nanotubes (CNTs) in 1991 and two-dimensional graphene in 2004, followed by transition metal dichalcogenides (TMDs), there has been an explosion of research exploring their unique fundamental science and technological applications. Among them, other 2D layered materials such as TMDs, hexagonal boron nitride (hBN), and black phosphorus (BP) have been extensively studied, opening new horizons in physics, electronics, and optoelectronics. These materials also offer exciting possibilities in emerging fields like valleytronics, spintronics, twistronics, and orbitronics. The key physics behind include strong Coulomb interactions, reduced charge screening, large exciton binding energies, and significant spin-orbit coupling, which present valuable opportunities for both fundamental research and practical applications. In this presentation, I will discuss recent and ongoing challenges in the field of vdW semiconductors and devices including Ohmic contact, mobility/on-current, ferromagnetic semiconductors at room temperature, hot-carrier solar cell, and Bose-Einstein condensation in electronics etc.

Tutorial: How do we analyze Raman spectra?

Riichiro Saito[1],[2]

[1]*National Taiwan Normal University, Taiwan,* [2]*Tohoku University, Japan*

In this tutorial, we will explain how to perform Raman spectroscopy measurements and analysis. In Raman spectroscopy, the intensity of inelastically scattered light in a material is observed as Raman spectra as a function of the light's energy loss (Raman shift) [1]. Nowadays, Raman spectra can be obtained by simply loading a sample into a Raman setup. However, you may need some theoretical support to analyze the observed Raman spectra. I am often asked to perform analyses, and in many cases I often wish that they had asked me before they performed the experiment so that we could have obtained better results.

By using polarized Raman spectroscopy (or helicity-dependent Raman spectroscopy) that uses linearly (or circularly) polarized lights, the symmetry of phonon modes can be obtained experimentally. In this case, it is necessary to understand how to set the geometry of sample, waveplate, and polarizer orientation for a given sample structure ***before*** conducting the experiment. Raman tensor calculation is useful for understanding polar plot of Raman intensity as a function of polarization directions [2].

By using deep-ultraviolet (DUV) laser whose photon energy is 4.66eV, most of Raman spectra becomes resonant, and the obtained Raman spectra becomes another world compared with those by visible light [3]. We will explain some results DUV Raman [3].

By using first-principles calculation such as Quantum Espresso [4], you can calculate phonon dispersion relation, non-resonant Raman spectra. You can obtain of animation of vibration of Raman active mode by using your note-PC. Further, when you use open-source of QERaman [5] or Q2R [6] codes, you can even calculate resonant Raman spectra of first-order and second-order Raman spectra, respectively. In this tutorial, we would like to introduce you how to use the first-principles calculation for beginner, too.

We all hope that everybody will enjoy the Raman spectroscopy in your research.

References:

[1] “Raman Spectroscopy in Graphene Related Systems” A. Jorio, M. S. Dresselhaus, R. Saito, G. Dresselhaus, Wiley-VCH, (2011).
[2] Lecture Notes of Raman spectroscopy at NTNU, https://web.phy.ntnu.edu.tw/~rsaito/Raman
[3] R. Saito, N. T. Hung, T. Yang, J. Huang, H-L. Liu, D. P. Gulo, S. Han, L. Tong, Small, 2308558, (2024).
[4] “Quantum ESPRESSO Course for Solid-State Physics”, N. T. Hung, A. R. T. Nugraha, R. Saito, Jenny Stanford Pub. (2022).
[5] N. T. Hung, J. Huang, Y. Tatsumi, T. Yang, R. Saito, Comp. Phys. Comm. 295, 108967, (2023)
[6] J. Huang et al. unpublished.

e-mail: r.saito.sendai@gmail.com

Session
NT 25（The 25th International Conference on the Science and Applications of Nanotubes and Low-

| Main conference：Main conference

Mon. Jun 16, 2025 9:30 AM - 12:10 PM JST | Mon. Jun 16, 2025 12:30 AM - 3:10 AM UTC Centennial Hall (Clock Tower Centennial Hall)

[16ma] Main Conference

Chair: Yutaka Ohno, Keigo Otsuka

9:30 AM - 10:10 AM JST | 12:30 AM - 1:10 AM UTC

[16ma-01]

Towards fab-compatible low-dimensional semiconductor electronics

*Lian-Mao Peng[1] (1. Peking University (China))

10:10 AM - 10:40 AM JST | 1:10 AM - 1:40 AM UTC

[16ma-02]

Carbon nanotube-based flexible amplifier

*Youfan Hu[1] (1. Peking University (China))

11:00 AM - 11:30 AM JST | 2:00 AM - 2:30 AM UTC

[16ma-03]

TRANSFORMING PRECURSOR MOLECULES INTO 1D CARBON NANOMATERIALS INSIDE CARBON NANOTUBES

Huiju Cao[1], Yingzhi Chen[1], Kunpeng Tang[1], Yanghao Feng[1], Weili Cui[1], Wendi Zhang[2], Kecheng Cao[2], *Lei Shi[1] (1. Sun Yat-sen University (China), 2. ShanghaiTech University (China))

11:30 AM - 11:50 AM JST | 2:30 AM - 2:50 AM UTC

[16ma-04]

Confined carbyne is a tailored hybrid system with vibronic properties solely driven by anharmonic interactions.

*Thomas Pichler[1] (1. University of Vienna (Austria))

11:50 AM - 12:10 PM JST | 2:50 AM - 3:10 AM UTC

[16ma-05]

BNNT as molecular template : from single molecule chains to superradiant light emitters

Jean-Baptiste Marceau[1], Juliette Le Balle[1,2], Duc-Minh Ta[4], Alberto Aguilar[4], Annick Loiseau[2], Richard Martel[5], Pierre Bon[4], Raphael Voituriez[3], Gaelle Recher[1], *Etienne Gaufrès[1] (1. CNRS-Université de Bordeaux (France), 2. CNRS-Onera (France), 3. Sorbonne University (France), 4. CNRS- University of Limoges (France), 5. Université de Montréal (Canada))

Towards fab-compatible low-dimensional semiconductor electronics

Lian-Mao Peng[1]

[1]*School of Electronics, Peking University (China)*

Low-dimensional semiconductors, represented by one-dimensional carbon nanotubes (CNTs), are ideal electronic materials that provide ultra-thin conductive channels, extremely high intrinsic carrier mobility, and ideal surfaces, making them perfect for building excellent electronic systems [1-6]. The rapid development of low-dimensional semiconductor materials suitable for integrated circuit applications in recent years has made it possible to construct large-scale carbon nanotube integrated circuits. Supported by the US DARPA project, a joint team from MIT and SkyWater Technology successfully produced 90nm carbon nanotube CMOS chips on a commercial 8-inch line, demonstrating million-gate carbon nanotube sensing and imaging arrays, thousands of gates of SRAM circuits, and carbon nanotube microprocessors of certain complexity [6]. In particular we have demonstrated excellent scalability of low-dimensional semiconductor devices down to sub-5nm and close to the theoretical limit [7], ultra-low power Dirac source transistors operating at 0.5V [8], flexible electronics [9], optoelectronics [10], RF transistors and amplifiers working at terahertz frequencies [11], unclonable cryptographic encoders and decoders [12], and carbon nanotube TPU [13]. These achievements fully demonstrate the potential for large-scale applications in the field of low-dimensional semiconductor electronics. However, compared to the mature silicon-based CMOS process, challenges remain in the uniformity of low-dimensional semiconductor materials and the stability of transistors. This report will analyze these challenges and possible coping strategies in conjunction with recent progress in the field.

References

[1] L.-M. Peng *et al*., Nature Electronics **2**, 499 (2019).
[2] L.J. Liu *et al*., Science **368**, 850 (2020).
[3] J.F. Jiang *et al.*, *Nature* **616**, 470 (2023).
[4] W. Peng *et al.*, *Nature Review Electrical Engineering* **1**, 629 (2024)
[5] J.F. Jiang *et al.*, *Nature Review Electrical Engineering* **2**, 6 (2025).
[6] G. Hills *et al.*, *Nature* **572**, 595 (2019).
[7] C. Qiu *et al.*, *Science* **255**, 271 (2017).
[8] C. Qiu *et al.*, *Science* **361**, 387 (2018).
[9] L. Xiang *et al*., *Nature Electronics* **1**, 273 (2018).
[10] Y. Liu *et al*., *Nature Electronics* **1**, 644 (2018).
[11] H.W. Shi *et al.*, *Nature Electronics* **4**, 405 (2020).
[12] D.L. Zhong *et al.*, *Nature Electronics* **5**, 424 (2022).
[13] J. Shi *et al.*, *Nature Electronics* **7**, 684 (2024).

Carbon nanotube-based flexible amplifier

Youfan Hu

School of Electronics and Center for Carbon-Based Electronics, Peking University, Beijing 100871, China

Abstract

In situ signal amplification is important for collecting weak physiological signals. Utilizing carbon nanotubes, we developed high-performance differential amplifiers featuring a voltage gain of 27 dB, a common-mode rejection ratio exceeding 43 dB, and a gain bandwidth product over 22 kHz, demonstrating successful in situ electrocardiography signal amplification. By adopting a dual-gate structure with electrical and mechanical co-design, excellent gate control efficiency and mechanical stability of thin film transistors (TFTs) were guaranteed simultaneously when fabricated on an ultrathin PI film (~125 nm thick), which exhibited high transconductance (8.96 mS/μm), high mobility (127 cm^2/Vs), and steep subthreshold swing (84 mV/dec). The obtained differential amplifier achieved a gain-bandwidth product of 1.83 MHz, enabling higher-gain amplification of weak signals over an extended frequency spectrum that is demonstrated by amplification of electromyography signals in situ.

Additionally, our recent work reported complementary carbon nanotube TFTs with negative differential resistance-induced current super-saturation for ultrahigh, exponentially variable intrinsic gain, resilient to degradation from scaling. The distinguished large-window, gate-modulated negative differential resistance behavior a characteristic of carbon nanotubes, enables its practical utilization in circuits. When approaching the singularity, the intrinsic gain varies by orders of magnitude, ranging from 10^2 to 10^6 at different operation points. We further demonstrate ultrahigh and exponentially variable gain in an operational amplifier, showing a tunable single-stage gain ranging from 35 to 60 dB.

References

[1] L. Xiang, Y. Wang, F. Xia, F. Liu, D. He, G. Long, X. Zeng, X. Liang, C. Jin, Y. Wang, A. Pan, L.-M. Peng, Y. Hu, Science Advances, 8, eabp8075 (2022).

[2] Y. Wang, T. Wang, L. Xiang, R. Huang, G. Long, W. Wang, M. Xi, J. Tian, W. Li, X. Deng, Q. Gong, T. Bai, Y. Chen, H. Liu, Y. Xia, X. Liang, Q. Chen, L.-M. Peng, Y. Hu, Science Advances, 10, eadq6022 (2024)

[3] G. Long, Y. Wang, T. Bai, W. Li, P. Zhang, X. Deng, X. Cai, M. Xi, Y. Lin, X. Cheng, C. Fan, F. Xia, X. Luo, Z. Zhang, X. Liang, Z. Zhang, N. Sun, L.-M. Peng, Y. Hu, Nature Communications (2025).

TRANSFORMING PRECURSOR MOLECULES INTO 1D CARBON NANOMATERIALS INSIDE CARBON NANOTUBES

Huiju Cao[1], Yingzhi Chen[1], Kunpeng Tang[1], Yanghao Feng[1], Weili Cui[1], Wendi Zhang[2], Kecheng Cao[2], Lei Shi[1]

[1]*Sun Yat-sen University (China),* [2]*ShanghaiTech University (China)*

The 1D nanospace of carbon nanotube is an ideal nanoreactor for synthesis of nonexistent or unusual materials. For example, previously we have synthesized ultra-long linear carbon chains [1]. Thanks to the confinement of the carbon nanotube and Raman Spectroscopy, the evolution or reactions of precursor molecules under high temperature or high pressure can be studied in detail. Here, as shown in Figure 1, our recent results discovered that some precursor molecules with/without hexatomic rings can be converted into quasi-1D graphene nanoribbons [2,3], whereas some aromatic molecules can be transformed into true 1D linear carbon chains [4]. These unusual phenomena are beyond the conventional chemical reaction. In addition, many kinds of 1D elemental or compound chains can be obtained by using the confined synthesis, which paves the way to create a library of novel 1D materials that do not exist or are yet to be explored.

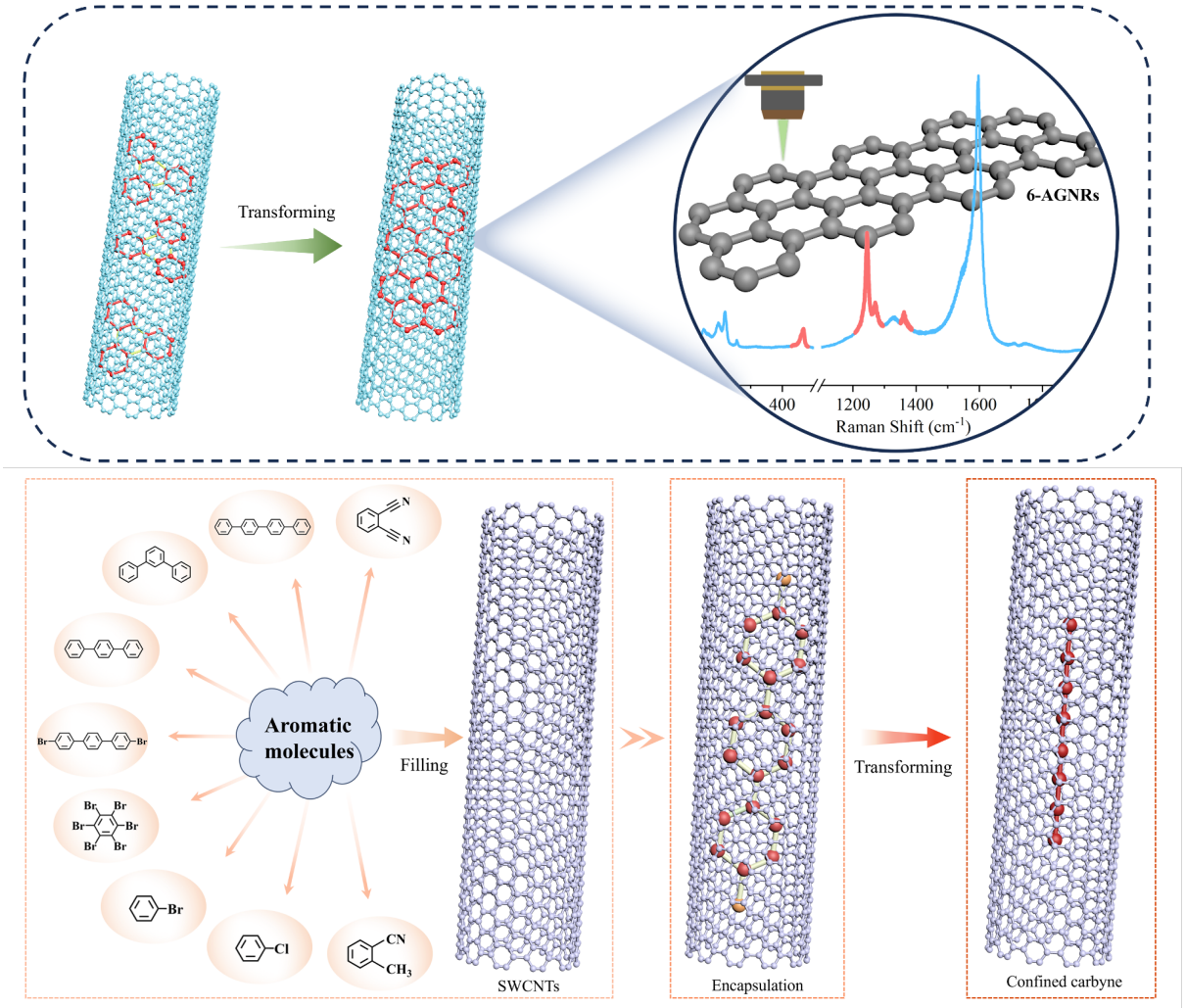

Figure 1: Schematics of confined transformations from precursor molecules into graphene nanoribbons [3] or linear carbon chains [4] inside carbon nanotubes.

References

[1] L. Shi, *et al.*, *Nat. Mater.* **15**, 634–639 (2016).
[2] H. Kuzmany, *et al.*, *Carbon* **171**, 221–229 (2021).
[3] H. Cao, *et al.*, *Submitted* (2025).
[4] Y. Chen, *et al.*, *Submitted* (2025).

Confined carbyne is a tailored hybrid system with vibronic properties solely driven by anharmonic interactions.

T. Pichler

[1] *University of Vienna, Faculty of Physics, Botzmanngasse 5, 1090 Vienna (Austria)*

Precise tailoring of the properties of carbon nanotubes yields to completely new properties. Especially tailoring 1D cylinders by encapsulating 1D chains yields new hybrid structures with novel properties. In this contribution I will present an overview of recent progress understanding the fundamental properties of these novel hybrid systems confining carbyne inside carbon nanotubes by using inelastic scattering as probe (resonance Raman and EELS). Stabilized by the encaging nanotubes allows high yield (stepwise) synthesis [1,2] and specific tailoring by doping and isotope engineering [3]. This enables tracing nano chemical reactions and unraveling their growth [4]. Anharmonic effects control interaction of carbynes confined in carbon nanotubes and shape their vibrational properties [5]. This holds for both the inner carbon nanotubes [5] and the carbyne chain [5,6]. This anharmonic effects lead to a peculiar Raman fingerprint of the nanotube modes which enables a reliable and fast determination of the carbyne bulk yield [7,8] without being influenced by the narrow resonance window of the carbyne chain which has the biggest resonance Raman cross section so far [9]. On the other hand, this huge Raman resonance of the chain makes them particularly suitable for sensing application such as truly local contact free temperature sensors [1,10]. In addition, I will show first results on complementary nanospectroscopic EELS inside a TEM [11] allow to directly assign the structure & properties of individual carbyne@CNT hybrids.

This project has received funding from the European Research Council (ERC) under the European Union's Horizon 2020 research and innovation program (MORE-TEM ERC-SYN project, grant agreement No 951215)

References

[1] L. Shi et al., Nature Materials, 15, 634 (2016); https://doi.org/10.1038/NMAT4617
[2] L. Shi et al., NanoLetters. 21, 1096 (2021); https://doi.org/10.1021/acs.nanolett.0c04482
[3] W. Cui et al., Angewandte Chemie 60, 9897 (2021); https://doi.org/10.1002/anie.202017356
[4] W. Cui et al., Advanced Functional Materials 32, 2206491 (2022) https://doi.org/10.1002/adfm.202206491
[5] E. Parth et al., Nature Communications (2025); https://doi.org/10.21203/rs.3.rs-5247129/v1
[6] J. Lechner et al., submitted; https://arxiv.org/abs/2410.14820
[7] C. Schuster et al., Carbon 234, 11997 (2025); https://doi.org/10.1016/j.carbon.2024.119979
[8] C Freytag et al.; submitted (2025).
[9] C.D. Tschannen et al. NanoLetters 20, 6750 (2020); https://doi.org/10.1021/acs.nanolett.0c02632
[10] C.D. Tschannen et al., ACS Nano 15, 12249(2021); https://doi.org/10.1021/acsnano.1c03893
[11] R. Senga, et al., NanoLetters 18, 3920 (2018), https://doi.org/10.1021/acs.nanolett.8b01284

BNNT as molecular template : from single molecule chains to superradiant light emitters

J.-B. Marceau[1], J. Le Balle[1,2], D.-M. Ta[3], A. Aguilar[3], A. Loiseau[2], R. Martel[4], P. Bon[3], R. Voituriez[5], G. Recher[1], and E. Gaufrès[1*]

[1] Laboratoire Photonique Numérique et Nanosciences, Institut d'Optique, CNRS, Université de Bordeaux, France, [2] Laboratoire d'Étude des Microstructures, ONERA-CNRS, Université Paris-Saclay, France, [3] XLIM, CNRS, Limoges, France, [4] Département de chimie et Institut Courtois, Université de Montréal, Canada, [5] Lab. de Physique Théorique de la Matière Condensée CNRS Sorbonne Université, Paris, France

Boron nitride nanotubes (BNNTs) have been identified as a promising dielectric host template for fluorescent molecules because of their wide-gap semiconductors of ~5.5 eV [1]. In this presentation we will focus on the different way to organize dyes light emitter inside BNNTs, from spaced single molecules in 1D arrays to periodic J-aggregates with highly polarized photoluminescence emission. Especially, we will show that a local bending of BNNT induce an activated diffusion of molecules from curved to straight parts of the BNNTs [2,3]. Finally, combining ac-HRTEM and time resolved fluorescence imaging we will demonstrate that assemblies of aligned and regularly spaced dyes in BNNTs lead to superradiant light emission at room temperature with shortened lifetime by more than a decade, while keeping high brightness [4]. These multifunctional nanohybrids open a new route toward robust and low cost materials platform for quantum technologies.

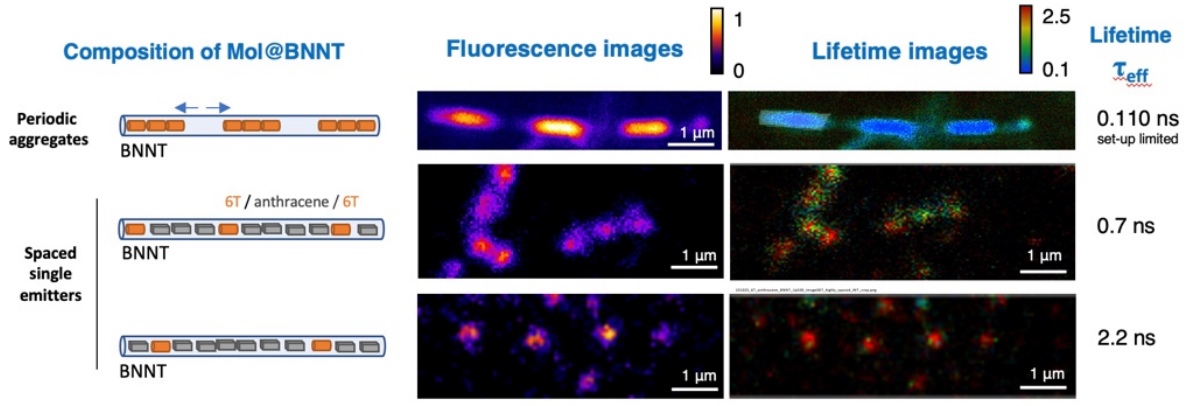

Figure caption: Room temperature time-resolved fluorescence images at 600 nm of single molecules and superradiant 1D aggregates confined inside an individual BNNT

References (if desired)
[1] C. Allard et al, Advanced Materials, 32,29 (2020)
[2] A. Badon & J.-B Marceau et al, Materials Horizons 10, 983-992 (2023)
[3] J-B Marceau et al, ACS Nano, just accepted (2025)
[4] J-B Marceau et al, Encoded Dipolar Chains : from single molecule arrays to superradiant emitters (submitted).

Session
NT 25（The 25th International Conference on the Science and Applications of Nanotubes and Low-

| Parallel Symposia：Symposium on Nanomaterials for Energy and Electronics

Mon. Jun 16, 2025 2:00 PM - 5:20 PM JST | Mon. Jun 16, 2025 5:00 AM - 8:20 AM UTC Conference room 5a/5b(INNOVATION BLDG., 5F)

[16en] Energy & Electronics

Chair:Suguru Noda, Yoshiyuki Nonoguchi

2:00 PM - 2:40 PM JST | 5:00 AM - 5:40 AM UTC

[16en-01]

Recent Advances towards High-Performance Carbon Nanotube FETs

*Nathaniel Safron[1], Matthias Passlack[1], Hsin-Yuan Chiu[2], Tzu-Ang Chao[2], Carlo Gilardi[1], H.-S. Philip Wong[2], Marvin M.-F. Chang[2], Gregory Pitner[1], Iuliana Radu[2] (1. TSMC Corporate Research (United States of America), 2. TSMC Corporate Research (Taiwan))

2:40 PM - 3:00 PM JST | 5:40 AM - 6:00 AM UTC

[16en-02]

Exploring aligned CNT material for device application: variability and polymer cleaning

*Marina Y. Timmermans[1], Luca Mana[1,2], Himanshu Sharma[1], Dennis Lin[1], Jean-François de Marneffe[1], Patrick Kelp[1], Atefeh Fathzadeh[1,2], Philippe Bezard[1], Xiangyu Wu[1], Han Han[1], Lijun Liu[1,2], Katherine R. Jinkins[3], Michael S. Arnold[3], Claudia Fleischmann[1,2], Steven Brems[1], Cesar J. L. de la Rosa[1], Gouri S. Kar[1] (1. imec (Belgium), 2. KU Leuven (Belgium), 3. SixLine Semiconductor (United States of America))

3:00 PM - 3:20 PM JST | 6:00 AM - 6:20 AM UTC

[16en-03]

Nanomaterials-based Monolithic 3D Integration for Energy-Efficient Computing

*Jianshi Tang[1] (1. School of Integrated Circuits, Tsinghua University (China))

4:00 PM - 4:20 PM JST | 7:00 AM - 7:20 AM UTC

[16en-04]

CNT sorting using block copolymers and removal of wrapped polymers from CNTs for improved electrical performance

*Sean Foradori[1], Stephanie Oliveras-Santos[1], Nilabja Maity[1], Michael S Arnold[1], Padma Gopalan[1] (1. University of Wisconsin – Madison (United States of America))

4:20 PM - 4:40 PM JST | 7:20 AM - 7:40 AM UTC

[16en-05]

Preparation of Single-Walled Carbon Nanotubes as Electronic Materials

*Yan Li[1,2] (1. Beijing National Laboratory for Molecular Science, College of Chemistry and Molecular Engineering, Peking University (China), 2. Institute of Carbon-Based Thin Film Electronics, Peking University (China))

4:40 PM - 5:00 PM JST | 7:40 AM - 8:00 AM UTC

[16en-06]

Interface properties of carbon nanotube thin film transistors

*Yutaka Ohno[1] (1. Nagoya University (Japan))

5:00 PM - 5:20 PM JST | 8:00 AM - 8:20 AM UTC

[16en-07]

High-Performance N-type Aligned Carbon Nanotube Field-Effect Transistors and Their Scaling Behavior

Session
NT 25 (The 25th International Conference on the Science and Applications of Nanotubes and Low-
*Yu Cao[1] (1. Peking University (China))

Recent Advances towards High-Performance Carbon Nanotube FETs

Nathaniel Safron[1*], Matthias Passlack[1], Hsin-Yuan Chiu[2], Tzu-Ang Chao[2], Carlo Gilardi[1], H.-S. Philip Wong[2], Marvin M.-F. Chang[2], Gregory Pitner[1*], Iuliana Radu[2]
[1]TSMC Corporate Research, San Jose, California, USA
[2]TSMC Corporate Research, Hsinchu, Taiwan
Email: nsafron@tsmc.com

Recent exploration for a suitable transistor channel material to deliver performance, scalability, and energy-efficiency benefits beyond Silicon CMOS in future technology nodes has focused on low-dimensional 1D and 2D channel materials. Until recently the performance of CNT transistors has underperformed $I_{D\text{-}SAT}$ requirements, suffered greatly from non-idealities such as high leakage current (I_{MIN} > 100 nA/ µm) and poor sub-V_T slope (> 100 mV/dec) at high V_{DS}, and have shown degraded performance in n-type devices [1,2]. We will summarize the recent fundamental advances of our team and collaborators including:

- The effect of CNT band gap on Contant Resistance (R_C) and leakage for both p- and n-type transistors [3]
- An impedance measurement technique to accurately measure CNT gate stack Density of Interface Traps (D_{IT}) and model the implications to CNT transistor performance [4]
- Iso-performance p- and n-type CNT transistors enabled by self-aligned extension doping [5]
- A novel CNT Nanosheet FET utilizing higher band gap CNTs with similar $I_{D\text{-}SAT}$, 1000× lower leakage, and <100 mV/dec sub-V_T slope at high V_{DS} (-0.5V) [2,6].

To conclude we will outline our perspective of the remaining fundamental challenges facing CNT devices and encourage future research directions in the scientific community.

[1] IRDS 2023. [2] N. Safron, *et al.*, VLSI 2024. [3] Chiu, Hsin-Yuan, *et al.*, Nano Letters, vol 35, p 3981 – 3988, 2025. [4] M. Passlack, *et al.*, IEDM 2024. [5] S. Li, *et al.*, IEDM 2024. [6] N. Safron, *et al.*, VLSI 2025.

References (if desired)

[1] M. S. Dresselhaus *et al.*, *Phys. Rep.* **409**, 47–99 (2005).
[2] A. K. Geim, *Science* **324**, 1530–1534 (2009).
[3] ….

Exploring aligned CNT material for device application: variability and polymer cleaning

Marina Y. Timmermans[1], Luca Mana[1,2], Himanshu Sharma[1], Dennis Lin[1], Jean-François de Marneffe[1], Patrick Kelp[1], Atefeh Fathzadeh[1], Philippe Bezard[1], Xiangyu Wu[1], Han Han[1], Lijun Liu[1,2], Katherine R. Jinkins[3], Michael S. Arnold[3], Claudia Fleischmann[1,2], Steven Brems[1], Cesar J. L. de la Rosa[1], Gouri S. Kar[1]

[1]imec, Kapeldreef 75, 3001 Leuven (Belgium),[2]KU Leuven, Celestijnenlaan 200D, 3001 Leuven (Belgium),[3]SixLine Semiconductor, Inc., 1509 University Ave., Madison, WI, 53706 (USA)

Continuous advancement in lithography technologies and innovations in transistor materials are required to further extend the logic device scaling roadmap and enable the continuation of Moore's law. Due to their remarkable electronic, thermal and mechanical properties, carbon nanotubes (CNTs) offer potential solutions to support technology scaling. An application where CNT material can make a difference in the near future is a CNT pellicle for extreme ultraviolet (EUV) lithography. A pellicle made of free-standing random CNT film is able to prevent photomask contamination from fall-on particles while demonstrating high EUV transmission and mechanical stability [1].

Another promising CNT application in the semiconductor industry is an active channel composed of aligned CNTs for next generation field-effect transistors (FETs). Recent progress in solution-based semiconducting CNT sorting and high-density alignment demonstrated technologically feasible approach to enable high-performance scaled transistors [2]. However, there are still a number of challenges that need to be solved when moving from a lab to a fab environment. A key requirement for industrial adoption is 300 mm wafer scale integration of CNT FETs. One of the main issues in the assembly of aligned CNT material at a wafer scale is morphology defects, e.g. variability in CNT alignment, pitch, CNT bundling [3]. CNT alignment has a significant impact on device performance and variability. Furthermore, the extraction of high purity semiconducting CNTs and their assembly into aligned arrays require CNT wrapping by conjugated polymers, which need to be removed afterwards without CNT damage. Additionally, CNT channel material can be further contaminated with the photoresist during device fabrication. We explore various CMOS compatible approaches aiming to remove the polymer residue with the focus on downstream hydrogen plasma treatment by means of Transient-Assisted Plasma etching (TAP) [4]. Optimization of TAP process parameters, including the substrate temperature and duration of hydrogen pulses, showed potential of this technique to reduce the polymer residue while minimizing CNT damage. Raman spectroscopy together with the electrical performance (G_m, I_{max}/I_{min}, SS) of the aligned CNT material highlight the effect of the cleaning processes on the CNT quality and device behavior. Further research in reducing the variability of high-density CNT alignment, scaling up the deposition processes and improving CNT post-deposition cleaning is important to enable the adoption of this material into wafer scale integration flows.

References

[1] M.Y.Timmermans *et al, J. Micro/Nanolith. MEMS MOEMS* **17**(4) 043504 (2018); M.Y.Timmermans *et al, J. Micro/Nanopattern. Mats. Metro*. **20**(3) 031010 (2021); M. van de Kerkhof *et al, Proc. SPIE* 12494, 124940D (2023); J. Bekaert et al, *Proc. SPIE 12494*, 124940E (2023)

[2] Liu *et al, Science* **368**, 850 (2020), Jinkins *et al, Sci. Adv*. **7** (2021); Lin *et al, Nat. Electron*, **6** (2023)

[3] Y.Ze *et al, Mater. Today* **79**, 97-111 (2024); B. Wang *et al, ACS Nano* **18** (33) (2024)

[4] A. Fathzadeh *et al, J. Vac. Sci. Technol. A* **42**, 033006 (2024)

Nanomaterials-based Monolithic 3D Integration for Energy-Efficient Computing

Jianshi Tang

School of Integrated Circuits, Tsinghua University, Beijing 100084, China

The fast development of artificial intelligence imposes an ever-increasing demand of computing power and energy efficiency for silicon chips. Amid the slowdown of Moore's law scaling, monolithic 3D integration (M3D) emerges as a promising solution to enhance the chip functionality and on-chip data flow. For this purpose, a variety of low-thermal budget nanomaterials, including carbon nanotubes and oxide semiconductors, and emerging memories, including resistive random-access memory (RRAM) and ferroelectric memory, are promising candidates for logic, memory, and computing-in-memory (CIM) building blocks that can be vertically stacked in the backend of the line (BEOL) of Si CMOS. In this talk, I will introduce our recent works on M3D of various BEOL-compatible functional layers on top of RRAM-based CIM array and Si CMOS circuits for energy-efficient computing. The associated material and processing challenges as well as device innovations will be discussed. A series of prototype M3D chips, including M3D-LIME, M3D-CCP, M3D-FACT, M3D-BRIC, M3D-CIM, M3D-CMIL, etc, will be presented. Finally, I will conclude my talk with a perspective on the challenges and opportunities in the field of M3D.

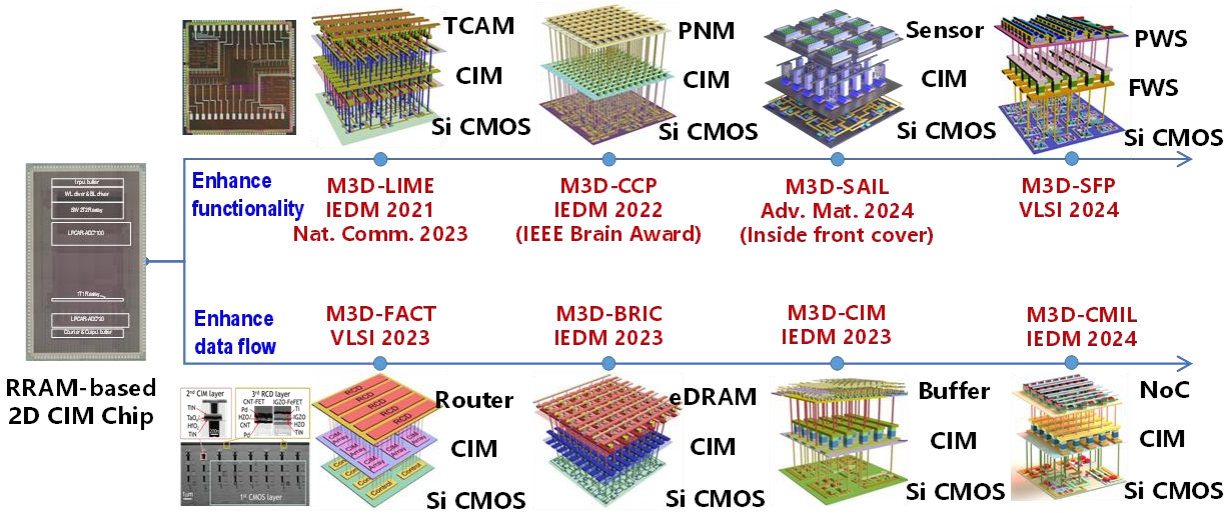

Figure caption: A series of M3D prototype chips based on CNT and RRAM demonstrated at Tsinghua to enhance the functionality and energy efficiency of computing-in-memory.

CNT sorting using block copolymers and removal of wrapped polymers from CNTs for improved electrical performance

S. M. Foradori[1], S. Oliveras-Santos[2], S. Li[1], N. Maity[1], M. S. Arnold[1], P. Gopalan[1,2]

[1] *Department of Materials Science and Engineering, University of Wisconsin – Madison, Madison Wisconsin 53706 (United States),*

[2] *Department of Chemistry, University of Wisconsin – Madison, Madison Wisconsin 53706 (United States),*

Aromatic conjugated polymers based on polyfluorenes and polythiophenes are commonly used to produce high-purity semiconducting carbon nanotube (CNT) inks. We have studied the design rules for these conjugated polymer dispersants to incorporate additional functions such as pitch control and to improve the yield and selectivity of the sorting process. [1] By using triblock ABA polymers with conjugated polymers as the B block and non-conjugated coiled polymers as the A blocks we have improved the sorting efficiency while maintaining the semiconducting selectivity even with relatively short length conjugated B blocks. The coiled A block can also potentially be used to control the pitch of aligned arrays of the polymer wrapped CNTs by acting as a buffer material between adjacent CNTs. We also explore methods of processing polymer wrapped CNTs to improve the contact resistance between CNTs and metal electrodes in field effect transistors. [2,3]

References

[1] S. Oliveras-Santos, S. Li, N. Maity, M. S. Arnold, P. Gopalan, *Macromolecules*, **57**, 3588-3594 (2024).
[2] S. M. Foradori, P. Gopalan, M. S. Arnold, *et al*, *Carbon,* **231**, 119709 (2025).
[3] S. M. Foradori, B. Prussack, A. Berson, M. S. Arnold, *ACS Nano*, **18**, 8259-8269 (2024)

Preparation of Single-Walled Carbon Nanotubes as Electronic Materials

Yan Li

Beijing National Laboratory for Molecular Science, College of Chemistry and Molecular Engineering, Peking University; Institute of Carbon-Based Thin Film Electronics, Peking University

Emai: yanli@pku.edu.cn

The unique structure of single-walled carbon nanotubes (SWCNTs) endows them excellent properties. Attributed to the very high and well-balanced carrier mobilities toward both electrons and holes and outstanding stability, SWCNTs have been considered as superior candidate channel materials for field-effect transistor and high-performance integrated circuits. For such applications, well-aligned SWCNTs with high semiconductor purity (99.9999%) and high density (100-200 tubes per micron) are needed. Therefore, the controlled preparation of SWCNTs becomes an essential requirement and also a key challenge. The possible route contains three steps: structure-controlled synthesis, solution phase separation and purification, and assembly [1]. We accordingly developed full-chain preparation methods: using arc-discharge to synthesizing SWCNTs with highly graphitized structure and tunable diameters; synthesized conjugated polymers to separate of semiconducting SWCNTs with the purity >99.9999%; by harnessing Marangoni flow, assembling the SWCNTs into well aligned single-layer arrays with tube density > 125 /μm. With these developments, we have initially formed a solution for SWCNTs as materials for high performance chips.

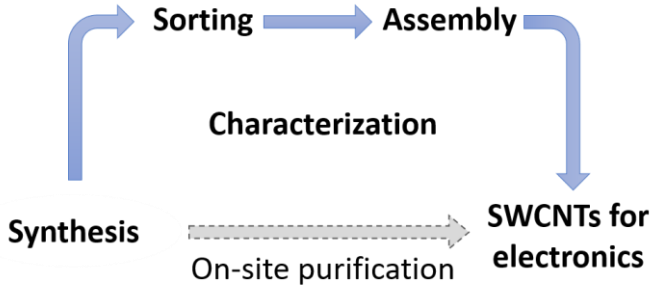

Figure 1. The possible route for the preparation of SWCNTs as electronic materials.

References

[1] Yan Li *et al*., *ACS Cent. Sci.* **2022**, 8 (11), 1490–1505.

Interface properties of carbon nanotube thin film transistors

Yutaka Ohno

[1]*Institute of Materials and Systems for Sustainability, Nagoya University (Japan)*

The reliability of semiconductor devices is determined by the ability to control the interface. In silicon, the excellent insulator/semiconductor interface obtained through thermal oxidation has made it possible to manufacture highly reliable large-scale integrated circuits, and the high-k gate insulator introduced with miniaturization has been achieved based on an understanding and control of interface phenomena, contributing to ultra-high density integration and low power consumption.

In contrast, in carbon nanotube devices, it is known that there is a significant degree of instability in the characteristics (hysteresis and current drift) and low-frequency noise due to traps at/near the gate insulator interface, and that the carrier polarity and threshold voltage change due to fixed charges near the interface. However, there are no examples of completely removing defects and contamination from the surface of the material to form a clean, controlled interface, and so the design and demonstration experiments of integrated circuits are being carried out using ready-made characteristics.

In this work, the interface characteristics of CNT TFTs, in particular, the structure, electrical property, and traps of the oxide/CNT interface, based on various characterization methods. We also report a flexible CNT TFT with an inorganic polymer as the gate insulator, which show ionic conduction at very low frequency. The result suggests a new possibility for the suppression of low-frequency noise through the screening of trap charges by accumulated ions.

High-Performance N-type Aligned Carbon Nanotube Field-Effect Transistors and Their Scaling Behavior

Yu Cao[1]

[1]*Center for Carbon-based Electronics, School of Electronics, Peking University (China)*

Aligned semiconducting carbon nanotube (A-CNT) field-effect transistors (FETs) are emerging as a promising alternative to conventional silicon transistors for advanced integrated circuit (IC) technology, owing to their potential for miniaturization and high energy efficiency. High-performance A-CNT p-type FETs (PFETs) at the 90 nm node have already outperformed their silicon counterparts and hold promise for sub-10 nm nodes with a full contact scheme [1]. However, A-CNT n-type FETs (NFETs) have lagged in performance, limiting the development of complementary metal-oxide-semiconductor (CMOS) technology. We identify the primary cause of this performance gap as the oxidation of the low-work-function scandium-CNT interface, induced by H_2O precursors during atomic layer deposition (ALD) of the dielectric. This issue can be mitigated by enhancing substrate hydrophobicity before A-CNT deposition and employing low-density A-CNTs (~120 tubes/μm). By implementing these strategies, we achieve high-performance A-CNT NFETs with an on-current (I_{on}) of 600 μA/μm and a peak transconductance (g_m) of 225 μS/μm [2]. However, these NFETs exhibited abnormal scaling behavior due to lateral oxidation of the low-work function source/drain contacts, posing significant challenges for simultaneously scaling of gate length (L_g) and contact length (L_c). The best device demonstrated a record I_{on} exceeding 1 mA/μm and g_m of 0.4 mS/μm with L_g of 100 nm but a long L_c of 800 nm [3]. These findings provide critical insights for enhancing A-CNT NFET performance and advancing CNT-based CMOS digital IC technology.

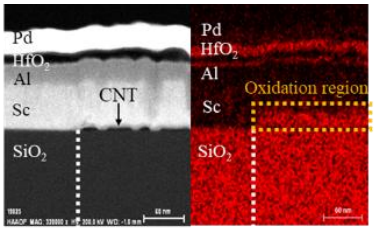

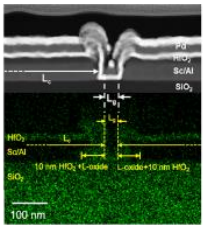

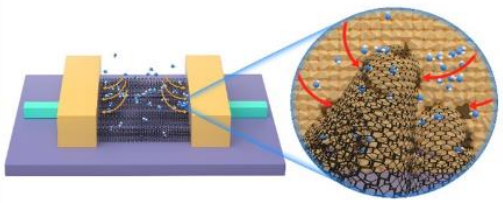

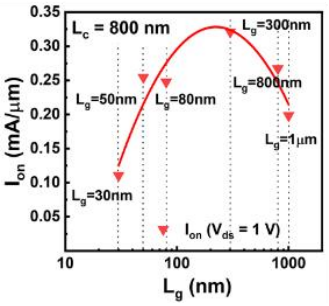

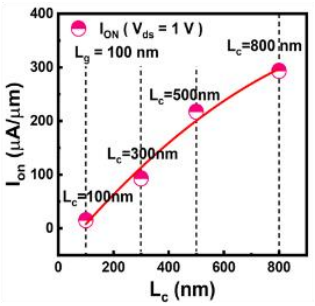

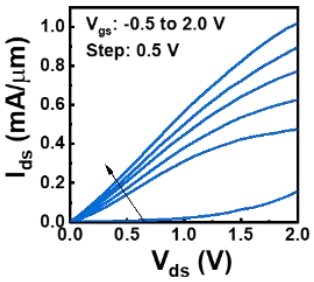

References

[1] Lin, Y.;Cao, Y.;Ding, S.;Zhang, P.;Xu, L.;Liu, C.;Hu, Q.;Jin, C.;Peng, L.-M.; Zhang, Z. Scaling aligned carbon nanotube transistors to a sub-10 nm node. ***Nature Electronics*** 2023, 6, 506-515.

[2] Liu, C.;Cao, Y.;Wang, B.;Zhang, Z.;Lin, Y.;Xu, L.;Yang, Y.;Jin, C.;Peng, L. M.; Zhang, Z. Complementary Transistors Based on Aligned Semiconducting Carbon Nanotube Arrays. ***ACS Nano*** 2022, 16, 21482-21490.

[3] Liu, C.;Cao, Y.;Lu, H.;Lin, Y.;Jin, C.; Zhang, Z. Scaling of N-Type Field-Effect Transistors Based on Aligned Carbon Nanotube Arrays. ***ACS Applied Materials & Interfaces*** 2024, 16, 41, 55964–55969.

Session
NT 25（The 25th International Conference on the Science and Applications of Nanotubes and Low-

| Parallel Symposia：17th Symposium on Computational Challenges in Nanotubes, 2D Materials, and Their Macroscopic Assemblies

Mon. Jun 16, 2025 2:00 PM - 5:20 PM JST | Mon. Jun 16, 2025 5:00 AM - 8:20 AM UTC Conference Room IV(Clock Tower Centennial Hall, 2F)

[16ct] Computation and Theory

Chair:Vincent Meunier, Christophe Bichara

2:00 PM - 2:40 PM JST | 5:00 AM - 5:40 AM UTC

[16ct-01]

Moiré Band Engineering in Twisted Trilayer Transition Metal Dichalcogenide

Naoto Nakatsuji[1], Takuto Kawakami[1], Hayato Tateishi[2], Koichiro Kato[2], *Mikito Koshino[1] (1. University of Osaka (Japan), 2. Kyushu University (Japan))

2:40 PM - 3:00 PM JST | 5:40 AM - 6:00 AM UTC

[16ct-02]

Theoretical prediction of magnetic interaction at homo- or hetero-interfaces of two-dimensional materials

*Cong Wang[1], Wei Ji[1] (1. Renmin University of China (China))

3:00 PM - 3:20 PM JST | 6:00 AM - 6:20 AM UTC

[16ct-03]

Theory of Sigma Bond Resonance in Flat Boron Materials

*Lu Qiu[1], Feng Ding[2] (1. City University of Hong Kong (Hong Kong), 2. Suzhou Laboratory (China))

4:00 PM - 4:40 PM JST | 7:00 AM - 7:40 AM UTC

[16ct-04]

An Overview of Machine Learning Force Fields for Nanotube Growth Simulations

*Daniel Hedman[1] (1. Center for Multidimensional Carbon Materials (CMCM), Institute for Basic Science (IBS) (Korea))

4:40 PM - 5:00 PM JST | 7:40 AM - 8:00 AM UTC

[16ct-05]

Growth Simulations of Single-Walled Carbon Nanotubes Using Carbon Monoxide with Machine-Learning Force Fields

*Sida Sun[1], Yan Li[1] (1. Peking University (China))

5:00 PM - 5:20 PM JST | 8:00 AM - 8:20 AM UTC

[16ct-06]

Oxygen modulates the catalytic activity of iron for CNT Nucleation

*Ben McLean[1], Alister J. Page[2], Feng Ding[3] (1. RMIT University (Australia), 2. University of Newcastle (Australia), 3. Shenzhen Institute of Advanced Technology, Chinese Academy of Sciences (China))

Moiré Band Engineering in Twisted Trilayer Transition Metal Dichalcogenide

Naoto Nakatsuji,[1] Takuto Kawakami, [1] Hayato Tateishi, [2] Koichiro Kato, [2]
and Mikito Koshino[1]

[1]*1Department of Physics, University of Osaka (Japan)*

2Department of Applied Chemistry, Kyushu University (Japan)

We present a systematic theoretical study on the structural and electronic properties of twisted trilayer transition metal dichalcogenide (TMD) WSe2, where two independent moiré patterns interplay to form a “moiré-of-moiré” structure. Using a continuum approach, we investigate the optimized lattice structure and the resulting energy band structure, revealing fundamentally different electronic behaviors between helical and alternating twist configurations.

A key distinction of trilayer TMDs from bilayers is that the moiré potentials from the bottom and top layers are effectively summed onto the middle layer, leading to a remarkable diversity of potential landscapes depending on the stacking structure. In a helical stacking configuration, where the three layers are arranged in a spiral form, the middle layer experiences a Kagome lattice potential—a structure rarely realized in other moiré systems. The resulting electronic structure exhibits a singular flat band characteristic of Kagome physics, providing a platform to explore strongly correlated states and topological phases associated with flat-band Kagome lattices. In the alternate stacking configuration, by contrast, we find a triangular array of quantum dots with a potential depth approximately twice that of twisted bilayers, which could be advantageous for achieving longer coherence times for moiré excitons.

Furthermore, we demonstrate that a moderate perpendicular electric field can switch the layer polarization near the valence band edge, providing an additional degree of tunability. It enables tuning of the hybridization between orbitals on different layers, allowing for the engineering of diverse and controllable electronic band structures. Our findings highlight the unique role of moiré potential summation in trilayer systems, offering a broader platform for designing moiré-based electronic and excitonic phenomena beyond those achievable in bilayer TMDs.

References

[1] N. Nakatsuji, T. Kawakami, H. Tateishi, K. Kato, and M. Koshino, in prepration (2025).

Theoretical prediction of magnetic interaction at homo- or hetero-interfaces of two-dimensional materials

Cong Wang,[1] Wei Ji[1],*

[1] *Beijing Key Laboratory of Optoelectronic Functional Materials & Micro-Nano Devices, Department of Physics, Renmin University of China, Beijing 100872, China…*

Emergent two-dimensional (2D) magnetic materials, characterized by atomic-scale thickness and surface dangling-bond-free features, eliminate lattice mismatch constraints in heterogeneous integration while exhibiting sensitive tunability under external fields. These attributes establish a novel material platform for fundamental research and potential spintronic applications. Interlayer interactions in 2D materials were predominantly attributed to van der Waals (vdW) forces, significantly underestimating the role of interlayer coupling in modulating electronic structures and magnetism. Understanding interlayer magnetic coupling mechanisms may unlock low-energy-consumption, high-speed magnetic modulation strategies.

We predicted performance modulation and magnetic phase transitions in selected 2D layered material systems. By leveraging interlayer coupling, strain, and intercalation, we demonstrated precise control over their electronic structures, confirming the critical role of interlayer interactions in regulating 2D magnetism. In strongly interlayer-coupled systems such as CrS_2 and $CrSe_2$, we revealed that interlayer wavefunction overlap induces charge transfer between Cr t_2g and eg orbitals, driving an in-plane antiferromagnetic-to-ferromagnetic transition in bilayer configurations. Collaborative experiments identified and confirmed novel magnetic transitions in monolayer $CrTe_2$, including spin-reorientation under external fields and real-space intrinsic antiferromagnetic ordering—previously unreported phenomena. Furthermore, we demonstrated that epitaxial strain, interlayer intercalation, and heterointerface engineering can effectively modulate 2D magnetism. Remarkably, magnetic state alterations in 2D materials reciprocally regulate adjacent vdW material properties. For example, intercalation enabled in situ tuning of magnetic anisotropy energy and Curie temperature in Fe_3GeTe_2. Theoretically predicted strain-modulated phase diagrams for monolayer and bilayer $CrSe_2/CrTe_2$ magnetic structures align with experimental observations in heterostructures.

Theory of Sigma Bond Resonance in Flat Boron Materials

L. Qiu[1], F. Ding[2]

[1]*City University of Hong Kong (China),* [2]*Suzhou Laboratory (China)*

Recent discoveries of novel boron materials, such as planar boron clusters, boron cages, boron nanotubes, and monolayer boron sheets (borophene), have generated widespread interest due to their unique chemical and physical properties, such as the preference for hexagonal holes in planar boron lattice, unexpected high stability of pristine edges, and unusual double aromaticity. Despite extensive research, key insights into the bonding, stability, and properties of these boron allotropes remains limited, which constrains their design, synthesis, and applications.

In the development of carbon materials, the concept of π bond resonance (aromaticity) plays a central role in intuitively understanding the stability and properties of organic molecules. In this talk, I would like to present an analogue theory of σ bond resonance to understand the bonding configurations of flat boron materials without relying on extensive quantum calculations[1]. This theory enables the determination of the distribution of the two-center two-electron (2c-2e) and three-center two-electron (3c-2e) bonds in a boron triangular lattice. Consequently, the Kekulé-like bonding configurations of various flat boron materials, such as borophene, boron nanoribbons, and boron clusters, can be drawn straightforwardly.

With this new understanding of the bonding structures of flat boron materials, the origins of their unique properties are revealed. Major puzzles, such as how hexagonal holes stabilize the triangular boron lattice, why neutral borophene with 1/9 holes are energetically most stable, and how substrate doping affects the hole concentration in borophene, are well understood for the first time[1]. Further study shows that borophene edges, such as flat edges, can be effectively self-terminated and further stabilized by edge resonance, explaining the high stability of borophene nanoribbons and other planar boron structures[2]. Finally, we propose a general bonding model with four simple rules that enables an intuitive description of bonding configurations in various planar boron structures[3], which serves as a tool for evaluating the stability of boron materials and predicting novel boron structures. Like the aromaticity theory for carbon materials, this theory significantly advances our understanding of boron-based materials, offering a foundation for their rational design and paving the way for future applications.

References

[1] L. Qiu *et al.*, *Nat. Commun.* **14**, 1804 (2023).
[2] L. Qiu *et al.*, *JACS Au* **4**, 116 (2024).
[3] L. Qiu *et al.*, *under review*

An Overview of Machine Learning Force Fields for Nanotube Growth Simulations

Daniel Hedman[1]

[1]*Center for Multidimensional Carbon Materials (CMCM), Institute for Basic Science (IBS), Ulsan, 44919 (Korea)*

Machine learning force fields (MLFFs) have transformed computational materials science by enabling simulations that combine quantum mechanical accuracy with the speed of classical force fields. Here an overview of MLFFs and their impact on understanding material growth mechanisms is given, with a particular focus on carbon nanotube (CNT) growth—a longstanding challenge due to the need for both accuracy and efficiency.

Neural network-based MLFFs have emerged as powerful tools for simulating material growth, offering unprecedented insights into atomic-scale processes. Recent advancements, such as DeepCNT-22 for CNT growth on iron catalysts [1] and similar models for cobalt catalysts [2], have enabled near microsecond-scale simulations while maintaining DFT accuracy. These models overcome the limitations of conventional force fields, which often lack the expressiveness required to capture complex energy landscapes involved in nucleation and growth. However, applying MLFFs to CNT growth presents unique challenges, including the need to accurately describe substantial structural evolution, reactive events, and dispersion interactions while ensuring high computational efficiency for long-timescale simulations under realistic chemical potentials. By shifting complexity from the MLFF architecture to the training data, these challenges can be addressed through active learning and carefully curated datasets.

MLFF-driven simulations have provided significant insights into CNT growth mechanisms [1-3], revealing: (1) the role of configurational entropy at the CNT-edge, (2) the formation and healing of defects at the tube-catalyst interface, (3) how growth rate and temperature influence defect-free growth, (4) mechanisms governing diameter control and chirality distribution shifts, and (5) chirality-dependent growth and etching rates. These findings shed new light on growth mechanisms at the atomic scale which can help explain experimental trends, including chirality shifts between different catalysts, the correlation between growth conditions and tube quality, and the potential for chirality-selective growth via controlled etching.

Looking ahead, MLFF-driven simulations will extend beyond CNTs, enhancing our understanding of diverse material synthesis processes. They could enable predictive catalyst design and growth-condition optimization, bridging atomic-scale mechanisms with macroscopic material properties. However, significant challenges remain: MLFFs must become orders of magnitude faster to access longer timescales, particularly for growth on solid catalysts or at low temperatures. More efficient architectures, improved learning algorithms, and transferable representations are needed to reduce data requirements and enhance generalization, ensuring reliable simulations of structural evolution. Addressing these challenges will push the boundaries of computational materials design, paving the way for precise control over nanomaterial synthesis.

References

[1] D. Hedman, B. McLean, C. Bichara et al., Nat Commun **15** (2024) 4076.
[2] S. Sun, S. Maruyama, Y. Li, J Am Chem Soc (2025).
[3] I. Kohata, R. Yoshikawa, K. Hisama et al., arXiv (2024).

GROWTH SIMULATIONS OF SINGLE-WALLED CARBON NANOTUBES USING CARBON MONOXIDE WITH MACHINE-LEARNING FORCE FIELDS

Sida Sun[1], Yan Li[1,*]

[1]*College of Chemistry and Molecular Engineering, Peking University, China*

Molecular dynamics (MD) simulations of the growth of single-walled carbon nanotubes (SWCNTs) have been consistently relying on carbon atoms as carbon sources, which is not the case in experiments. Here, we develop a new machine-learning force field of the iron–carbon–oxygen system. Using it to drive MD simulations under CO (and CO_2) atmosphere, we achieve the defect-free continued growth simulations of SWCNTs from carbon feedstock gas molecules for the first time. The edge pattern distributions of the SWCNTs simulated align well with our previously proposed growth models [1].

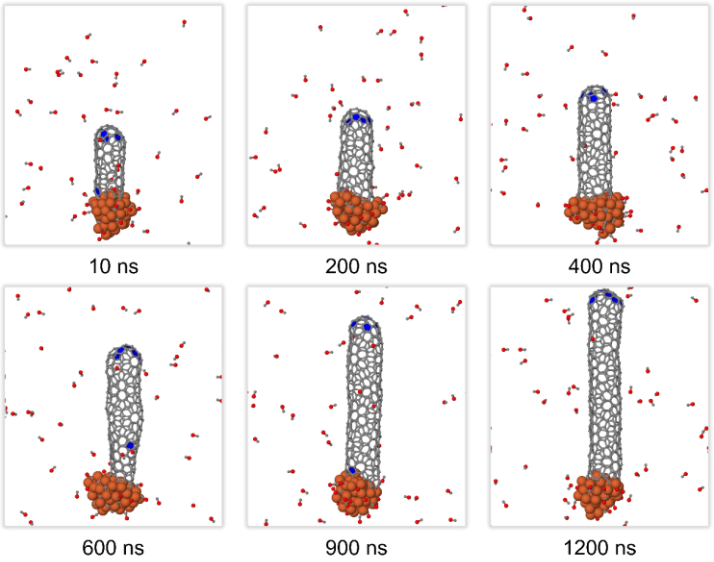

Figure caption: Snapshots of the continued-growth of a (7,4) SWCNT on an Fe_{55} cluster in pure CO gas. The defect encapsulated at 600 ns is healed afterwards.

References

[1] S. Sun, S. Maruyama, Y. Li. *J. Am. Chem. Soc.* **147**, 7103 (2025).

Oxygen modulates the catalytic activity of iron for CNT Nucleation

B. McLean[1],* A. J. Page[2], F. Ding[3]

[1]RMIT University, Melbourne (Australia), [2]University of Newcastle, Newcastle (Australia), [3]Shenzhen Institute of Advanced Technology, Chinese Academy of Sciences, Shenzhen (China)

email: ben.mclean2@rmit.edu.au

Extensive theoretical and experimental investigations have created a rich framework of catalytic chemical vapor deposition (CVD) synthesis of single-walled carbon nanotubes (CNTs). A wide array of transition metals are effective catalysts, with iron the most routinely studied, while oxides and alloys have demonstrated great promise for structure-controlled growth. The mechanisms of CNT nucleation in the case of carbon atoms on a pure metal nanoparticle are well understood, though knowledge of how these mechanisms differ for a mixed catalyst remains elusive. Iron oxide has proved a prominent growth catalyst for long CNTs with controlled diameter and alcohol CVD is long-established for effective synthesis, as is the inclusion of H_2O, CO and CO_2 as growth promoters. Despite this, and prior investigations into decomposition pathways that lead to catalyst oxidation, the precise role of oxygen during growth lacks understanding. In this work, *how* oxygen influences the catalytic properties of iron nanoparticles is demonstrated using quantum chemical density functional tight binding (DFTB) molecular dynamics (MD) simulations and density functional theory (DFT) calculations.

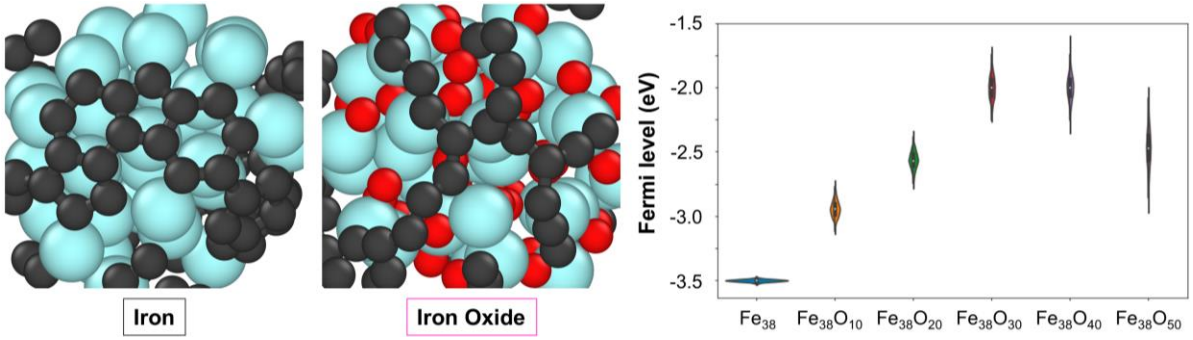

Figure: (Left) Carbon networks formed during MD simulations at 1000 °C, comprising rings on an iron catalyst and chains on an iron oxide catalyst. Cyan, red, and black spheres represent iron, oxygen and carbon respectively. (Right) Fermi level distributions for iron oxide catalysts with varying oxygen content.

Session
NT 25（The 25th International Conference on the Science and Applications of Nanotubes and Low-

| Parallel Symposia：6th Symposium on Synthesis, Purification, Functionalization, and Manufacturing of Carbon Nanotubes and Low-Dimensional Materials

Mon. Jun 16, 2025 2:00 PM - 5:20 PM JST | Mon. Jun 16, 2025 5:00 AM - 8:20 AM UTC HORIBA Symposium Hall (INNOVATION BLDG., 5F)

[16sy] Synthesis

Chair:Yan Li, Alister J Page

2:00 PM - 2:40 PM JST | 5:00 AM - 5:40 AM UTC

[16sy-01]

NEW SYNTHESES OF GRAPHENE AND DIAMOND

*Rodney Ruoff[1] (1. UNIST and IBS CMCM (Korea))

2:40 PM - 3:00 PM JST | 5:40 AM - 6:00 AM UTC

[16sy-02]

High-Melting Point Bimetallic Icosahedral Clusters for Carbon Nanotube Growth

*Shigeo Maruyama[1,2], Daniel Hedman[3], Daisuke Asa[1], Ikuma Kohata[1], Kaoru Hisama[4], Qingmei Hu[1], Wanyu Dai[1], Keigo Ostuka[1], Rong Xiang[2], Christophe Bichara[5] (1. The University of Tokyo (Japan), 2. Zhejiang University (China), 3. Institute for Basic Science (IBS) (Korea), 4. Shinshu University (Japan), 5. Aix-Marseille Univ (France))

3:00 PM - 3:20 PM JST | 6:00 AM - 6:20 AM UTC

[16sy-03]

Synthesis of Diamond in Liquid Metal at 1 Atmosphere Pressure

*Da Luo[1] (1. The Chinese University of Hong Kong, Shenzhen (China))

4:00 PM - 4:20 PM JST | 7:00 AM - 7:20 AM UTC

[16sy-04]

Synthesis and Electronic Applications of Wafer-Scale 2.5D Materials

*Hiroki Ago[1] (1. Kyushu University (Japan))

4:20 PM - 4:40 PM JST | 7:20 AM - 7:40 AM UTC

[16sy-05]

Orienting-Stitched Graphene is Permeable

Zhien Wang[2], Chi Cheng[3], *Jiangtao Wang[1], Jing Kong[2] (1. Peking University (China), 2. Massachusetts Institute of Technology (United States of America), 3. The University of New South Wales (Australia))

4:40 PM - 5:00 PM JST | 7:40 AM - 8:00 AM UTC

[16sy-06]

Highly efficient weakly confined carbyne (wCC) synthesis inside single-walled carbon nanotubes (SWCNTs)

*Bowen Zhang[1], Xiyang Qiu[1], Wanyu Dai[1], Qingmei Hu[1], Yongjia Zheng[2], Aina Fitó-Parer[3], Dmitry I. Levshov[3], Keigo Otsuka[1], Shohei Chiashi[1], Rong Xiang[2], Feng Yang[4], Yan Li[5], Sofie Cambré[3], Shigeo Maaruyama[1] (1. University of Tokyo (Japan), 2. Zhejiang University (China), 3. University of Antwerp (Belgium), 4. Southern University of Science and Technology (China), 5. Peking University (China))

5:00 PM - 5:20 PM JST | 8:00 AM - 8:20 AM UTC

[16sy-07]

Session

NT 25（The 25th International Conference on the Science and Applications of Nanotubes and Low-

Solving the Secondary Nucleation Problem that Causes Misoriented Islands during the Wafer-Scale Epitaxy of Single-Crystal Graphene on Ge

*Michael S. Arnold[1] (1. University of Wisconsin-Madison (United States of America))

NEW SYNTHESES OF GRAPHENE AND DIAMOND

Rodney S. Ruoff[1,2]

[1]*Center for Multidimensional Carbon Materials (CMCM), Institute for Basic Science (IBS) (Republic of Korea),*
[2]*Department of Chemistry, Ulsan National Institute of Science and Technology (UNIST) (Republic of Korea)*

We have discovered a new way (using a home-built system) to synthesize single crystal, fold- and wrinkle-free, and extremely flat, monolayer graphene ('SCG') films that are epitaxial to Ni(111) foil surfaces (both sides). These Ni(111) foils are generated by a high temperature anneal in argon and hydrogen gas mixture from as-received polycrystalline Ni foils.[1] Synthesis is 'very fast' and the Ni(111) foil yields high quality SCG on both sides within a few minutes—and 'over and over'. I'll explain about our method and some implications of growing such high quality SCG, and rapidly, at least from our perspective.

Diamond & graphite are essentially isoenergetic at STP (298K, 1 atm) as is true at higher temperatures (and the same is true for hBN and cBN). *If at chemical equilibrium* a sample containing only graphite and diamond would have a mass percentage of ~50 wt% diamond and ~50 wt% graphite. Why then the widely held perception that it 'must be' more difficult to form diamond (or cubic boron nitride) than graphite (or hBN) respectively? Well, to date, this has been true! Also (on Earth) there seems to be much more natural graphite than natural diamond, and there is (now) much more synthetic graphite annually produced than synthetic diamond. But must this always be so, going forward? I will describe how one might synthesize diamond and cBN in new ways; and see [2]. *Supported by the Institute for Basic Science (IBS-R019D1).*

References

[1] Sunghwan Jin, Ming Huang, Youngwoo Kwon, Leining Zhang, Bao-Wen Li, Sangjun Oh, Jichen Dong, Da Luo, Mandakini Biswal, Benjamin V. Cunning, Pavel V. Bakharev, Inyong Moon, Won Jong Yoo, Dulce C. Camacho-Mojica, Yong-Jin Kim, Sun Hwa Lee, Bin Wang, Won Kyung Seong, Manav Saxena, Feng Ding, Hyung-Joon Shin, Rodney S. Ruoff. Colossal grain growth yields single crystal metal foils by contact-free annealing. *Science*. (2018), 362(6418), 1021-1025.

[2] Yan Gong, Da Luo, Myeonggi Choe, Won Kyung Seong, Pavel Bakharev, Meihui Wang, Seulyi Lee, Tae Joo Shin Zonghoon Lee, Rodney Ruoff. Growth of diamond in liquid metal at 1 atmosphere pressure. *Nature*. 2023, 629, 348-354.

Synthesis of 1D van der Waals Heterostructures Based on Single-Walled Carbon Nanotubes

Shigeo Maruyama[1,2], Yongjia Zheng[2,1], Wanyu Dai[1], Chunxia Yang[1], Keigo Otsuka[1], Rong Xiang[2,1]

[1] *Department of Mechanical Engineering, The University of Tokyo (Japan),*
[2] *School of Mechanical Engineering, Zhejiang University (China)*

Single-walled carbon nanotubes (SWCNTs) with diverse optical and electronic properties (metallic or semiconducting) depending on chiral indices (n, m) have been the critical nanomaterials in advanced applications [1,2]. Even though a mixture of metallic and semiconducting SWCNT can be used for bulk and film-form applications such as batteries and solar cells [3], the controlled growth of (n, m) or the sorting of (n, m) is essential for electronics applications such as field effect transistors (FET) [4]. On the other hand, the controlled modulation of properties can also be possible either by employing the inner space of the SWCNTs to encapsulate various materials or by externally wrapping the SWCNT template with additional atomic layers [5]. Here, we mainly discuss the latter case as a one-dimensional (1D) van der Waals (vdW) heterostructure based on SWCNT [6]. We have demonstrated the atomically precise one-dimensional (1D) van der Waals (vdW) heterostructure -- SWCNTs, boron nitride nanotubes (BNNTs), and molybdenum disulfide (MoS_2) sequentially wrapped in radial direction -- by chemical vapor deposition in 2020 [6]. One of the obvious extensions of this work is the use of BNNT-SWCNT [7], which have superior semiconductor properties such as field effect transistors [8,9]. We have developed various characterization techniques for BNNT-SWCNT for the growth optimization and quality control of BNNT in several types of SWCNTs [10-12].

Yet another extension is the various kinds of transition metal dichalcogenides (TMD) nanotubes. We have optimized CVD conditions for various metal dichalcogenides such as tungsten disulfide (WS_2), niobium disulfide (NbS_2), and molybdenum diselenide ($MoSe_2$) so far in addition to the original MoS_2. Here, we further broaden the concept of 1D vdW heterostructure by combining 2 transition metal species. By setting WS_2 growth right after the MoS_2 growth, we can observe the axial junction of the outermost tube, MoS_2 - WS_2. The junction is atomically smooth within a few nanometers. On the other hand, by setting the 2 transition metal species at the same CVD time, we can observe $\{W_xMo_{(1-x)}\}S_2$ alloy nanotube. Both axial junction and alloy nanotubes are preferentially monolayers. Various Yanus TMD nanotubes, such as MoSSe, are also composed by employing the hydrogen plasma technique. They can be preferentially monolayer or bilayer tubes. At this stage, sulfur at the center side is preferred.

Part of this work was supported by JSPS KAKENHI Grant Numbers JP23H00174, JP23H05443 and by JST, CREST Grant Number JPMJCR20B5, Japan.

References

[1] Y. Li, S. Maruyama, Single-Walled Carbon Nanotubes, Springer (2019).
[2] S. Maruyama, M. S. Arnold, R. Krupke, L.-M. Peng, *J. Appl. Phys.* **131**, 080401 (2022).
[3] J.-M. Choi, J. Han, J. Yoon, S. Kim, I. Jeon, S. Maruyama, *Adv. Funct. Mater.* **32**, 2204594 (2022).
[4] D.-M. Tang, O. Cretu, S. Ishihara, Y. Zheng, K. Otsuka, R. Xiang, S. Maruyama, H.-M. Cheng, C. Liu, D. Golberg, *Nat. Rev. Electr. Eng.*, [DOI:10.1038/s44287-023-00011-8] (2024).
[5] S. Cambre, M. Liu, D. Levshov, K. Otsuka, S. Maruyama, R. Xiang, *Small* **17**, 2102585 (2021).
[6] R. Xiang, et al., *Science* **367**, 537 (2020).
[7] Y. Zheng, et al., *P. Natl. Acad. Sci.* **118**, e2107295118 (2021).
[8] S. Matsushita, et al., *ACS Appl. Mater. Inter.* **15**, 10965 (2023).
[9] K. Otsuka, et al., *Nano Res.* **16**, 12840 (2023).
[10] M. Liu, et al., *ACS Nano* **15**, 8418 (2021).
[11] R. Zhang, et al., *Carbon* **199**, 407 (2022).
[12] S. Wang, et al., *ACS Nano*, (2024) in press.

Synthesis of Diamond in Liquid Metal at 1 Atmosphere Pressure

Da Luo[1]

[1]*The Chinese University of Hong Kong, Shenzhen (China)*

There are two conventional methods for growing synthetic diamonds on a scale of one centimeter or larger. One is the chemical vapor deposition (CVD) method, which includes plasma-assisted and hot-filament CVD and is used to create diamond films. The other method is high-pressure high-temperature (HPHT) growth, which accounts for approximately 99% of the synthetic diamonds produced annually[1]. In the HPHT method, carbon dissolved in liquid metals forms diamonds under pressures of 5-10 GPa and at temperatures ranging from 1300-1600 °C.

There is a prevailing paradigm that diamond can be formed in liquid metals only under HPHT conditions because diamond is thermodynamically stable in this regime. It's worth noting that the diamonds produced using HPHT are usually limited to sizes of about one cubic centimeter due to the components involved. Discovering alternative methods to make diamonds in liquid metals under lower pressures is an intriguing basic science challenge that, if achieved, could revolutionize diamond manufacturing.

In this talk, I would like to present our recent results on growing diamonds using liquid metals. We developed a liquid metal alloy composed of 77.75/11.00/11.00/0.25 atomic percentages of Ga/Ni/Fe/Si, which facilitates the growth of diamond crystals (hundreds of nanometers in size) and polycrystalline diamond films (a few millimeters in lateral size) using methane at 1 atm pressure and 1025 °C. This challenges the traditional growth model of diamonds[2]. The diamonds were observed growing within the subsurface regions of the liquid metal. We found that carbon becomes 'supersaturated' in the subsurface, leading to the nucleation and growth of diamonds, and that Si atoms play a critical role in stabilizing sp^3-bonded carbon clusters, which triggers nucleation.

Our growth method offers significant flexibility in the composition of liquid metals; for example, diamonds can also be grown using Ga/Co/Fe/Si and Ga/In/Ni/Fe/Si liquid alloys. It is likely that liquid metal alloys of other compositions would also work for growing diamonds.

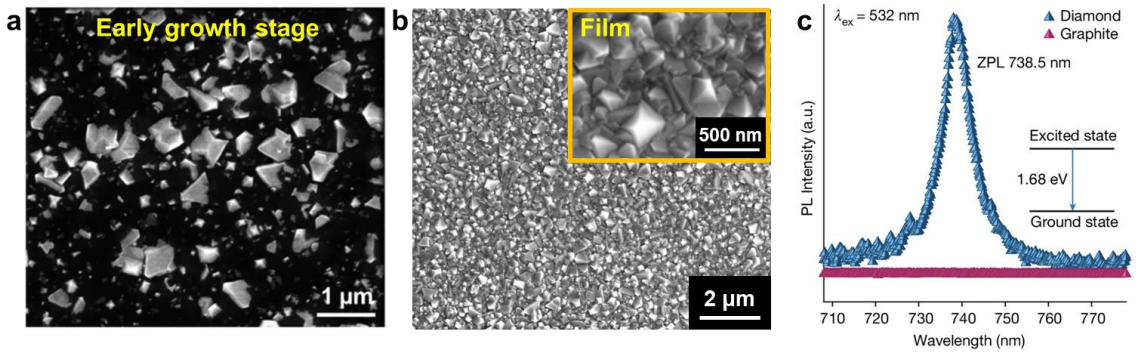

Figure 1: (a) SEM image of the as-grown diamond crystals at early growth stage. Many crystals are buried inside the solidified liquid metal alloy. (b) SEM image of the as-grown polycrystalline diamond film. (c) Photoluminescence spectrum of the as-grown diamond film showing the presence of SiV^- in the diamond structure.

References

[1] Olya Linde *et al.*, The Global Diamond Industry 2018, Bain & Company.
[2] Y. Gong, D. Luo, R. S. Ruoff *et al.*, *Nature* **629**, 348–354 (2024).

Synthesis and Electronic Applications of Wafer-Scale 2.5D Materials

Hiroki Ago

Faculty of Engineering Sciences, Kyushu University,

Center for Semiconductor and Device Ecosystem (CSeDE), Kyushu University

Two-dimensional (2D) materials have intriguing properties and many potential applications due to their unique 2D structures with atom-level thicknesses. The control of van der Waals (vdW) interaction and utilization of vdW nanospace are expected to extend the field of materials science, and such research direction can be expressed with a new concept of "Science of 2.5D materials" [1].

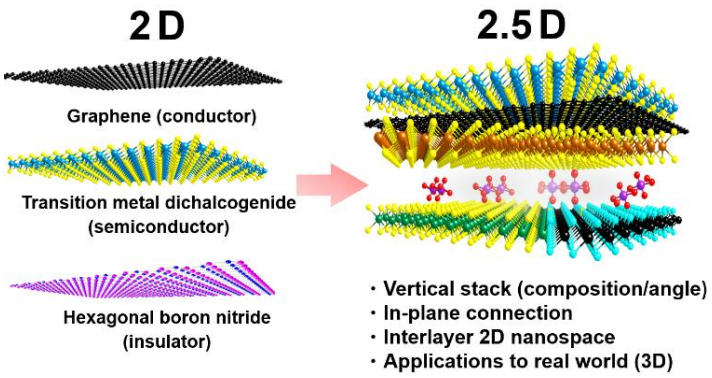

Figure 1. Concept of 2.5D materials.

In this presentation, our recent research is introduced based on this 2.5D concept, first showing the controlled CVD growth of bilayer graphene (BLG) and the intercalation of metal chloride molecules and alkaline metal ions, revealing new unique 2D structures with increased electrical conductivity [2,3]. We have also developed the CVD growth of high-quality and large-area multilayer hBN to be used as a building block of various 2.5D materials, such as graphene field-effect transistors (FETs) [4] and magnetic tunnel junction (MTJ) devices [5].

In addition, our recent development on the synthesis of high density, self-aligned MoS_2 nanoribbons is also presented [6]. Different from previous research, we do not need to make atomic steps on substrate surface to align MoS_2 nanoribbons. A high catalytic activity of the edges of the nanoribbon are visualized, signifying the potential application of MoS_2 nanoribbons in the hydrogen evolution reaction (HER), due to their high edge-to-surface ratios. Such high density MoS_2 array is also promising for channels of high-performance semiconductor devices.

I will also introduce our new result of the tape transfer of 2D materials, which is expected to accelerate the 2D/2.5D materials research and applications [7]. We achieved clean and user-friendly transfer of graphene, MoS_2, WS_2, and hBN using the UV tapes whose adhesive force can be decreased about 1/10 by UV light illumination. We do not need to use organic solvent so that we can transfer them onto plastics, and the robust tape allows "cut-and-transfer" for site-selective transfer, which saves 2D materials and production cost.

Finally, our national project named, "Science of 2.5 Dimensional Materials: Paradigm Shift of Materials Science Toward Future Social Innovation (2021-2026)", supported by MEXT, Japan is briefly introduced [8,9].

References

[1] H. Ago, P. Solís-Fernández, *NPG Asia Mater.*, **16**, 31 (2024).
[2] Y.-C. Lin *et al.*, *Adv. Mater.*, **33**, 2105898 (2021).
[3] Y.-C. Lin *et al.*, *Nat. Commun.*, **15**, 425 (2024).
[4] S. Fukamachi *et al.*, *Nat. Electron.*, **6**, 126 (2023).
[5] S. Emoto *et al.*, *ACS Appl. Mater. Interfaces*, **16**, 31458 (2024).
[6] Z. Ma et al., *Sci. Adv.*, **5**, eaau3407 (2025).
[7] M. Nakatani *et al.*, *Nat. Electron.*, **7**, 119 (2024).
[8] H. Ago *et al.*, *Sci. Tech. Adv. Mater. (STAM)*, **23**, 275 (2022).
[9] https://25d-materials.jp/en/

Orienting-Stitched Graphene is Permeable

Z. Wang[1], C. Cheng[2], J. Wang[3], J. Kong[1]

[1]Massachusetts Institute of Technology (USA), [2]The University of New South Wales (Australia), [3]Peking University (China)

Oriented-stitching of graphene has emerged as the predominant method for growth of large-area, high-quality graphene films. Particularly noteworthy is graphene grown on single-crystalline Cu(111)/sapphire substrates, which exhibits exceptionally planar oriented stitching due to the atomically smooth substrate, facilitating the formation of continuous, high-quality graphene monolayer. These oriented stitches have conventionally been regarded as seamless with negligible defect concentrations. In this report, we present novel experimental observations regarding graphene grown on single-crystalline Cu(111)/sapphire substrates. Our findings reveal two major stitching mechanisms: one producing the expected seamless integration, and another unexpectedly generating structural defects that create nanoscale pathways permitting water permeation. This discovery challenges the conventional paradigm of oriented-stitched graphene films as uniformly impermeable barriers and offers significant implications for applications in molecular sieving, selective filtration membranes, and protective coatings.

Highly efficient weakly confined carbyne (wCC) synthesis inside single-walled carbon nanotubes (SWCNTs)

Bo-Wen Zhang[1], Xi-Yang Qiu[1], Wanyu Dai[1], Yongjia Zheng[2], Dmitry I. Levshov[3], Keigo Otsuka[1], Shohei Chiashi[1], Rong Xiang[2], Feng Yang[4], Yan Li[5], Sofie Cambré[3], Shigeo Maruyama[1,2,*]

[1]*Department of Mechanical Engineering, The University of Tokyo (Japan)*

[2]*State Key Laboratory of Fluid Power and Mechatronic Systems, School of Mechanical Engineering, Zhejiang University (China)*

[3]*Departments of Chemistry and Physics, University of Antwerp (Belgium)*

[4]*Department of Chemistry, Southern University of Science and Technology (China)*

[5]*College of Chemistry and Molecular Engineering, Peking University (China)*

Confined carbyne (CC) has attracted much interest due to its unique structure and potential technological applications. CC possesses higher strength, elastic modulus, and stiffness than any known material. Yet, its chemical stability remains an issue [1], and efficient synthesis of CC has not been fully realized. A landmark study on CC synthesis has been achieved using double-walled carbon nanotubes (DWCNTs) as the template, though a high-temperature high-vacuum (HTHV) condition (1460°C) was required to attain long chains composed of more than 6,000 carbon atoms [2]. Recently, we developed a low-temperature synthesis method (1460°C) to synthesize CC inside single-walled carbon nanotubes [3]. By encapsulating ammonium deoxycholate (ADC) inside SWCNTs with a diameter large enough (over 0.95 nm), a weakly confined carbyne (wCC) was obtained because of the relatively weak interaction between CC and SWCNT walls. However, we found the ADC filling method resulted in large fluctuations in the yield of CC of our product, necessitating urgent improvements. Here, we report an enhanced synthesis method for highly efficient synthesis of CC@SWCNT. By employing the nano-extraction method [4], deoxycholic acid was encapsulated into ACCVD SWCNTs [5] in the liquid phase. Subsequently, using low-temperature annealing at 400°C, we successfully obtained a large quantity of CC@SWCNT products.

Raman mapping characterization (600 μm × 600 μm, step 60 μm) was conducted to evaluate the efficiency of CC synthesis. The characteristic peak of carbyne near 1860 cm^{-1}, known as the CC-mode, and the intensity ratio of this peak to the G band of SWCNT, I_{CC}/I_G, are used as indicators to measure the synthesis efficiency of CC. As shown in Figure 1a, our Raman mapping results indicate that the majority of the sample exhibited a CC-mode 6-14 times the intensity of the G band, significantly enhancing the uniformity of the results. Figure 1b represents the average result of all points from the Raman mapping (over 5) and the single point result of the highest I_{CC}/I_G (over 10), which demonstrates the high efficiency of this method in synthesizing CC@SWCNT. Furthermore, we have analyzed the positions of the CC-mode from all individual data points, as depicted in Figure 1c. The distribution of the CC-mode positions spans the range of 1856-1866 cm^{-1}, with the peak occurring at 1862 cm^{-1}. The presence of values exceeding 1860 cm^{-1} also corroborates that the CC-loaded SWCNTs possess larger diameters, consistent with our previous results observed for wCC [3].

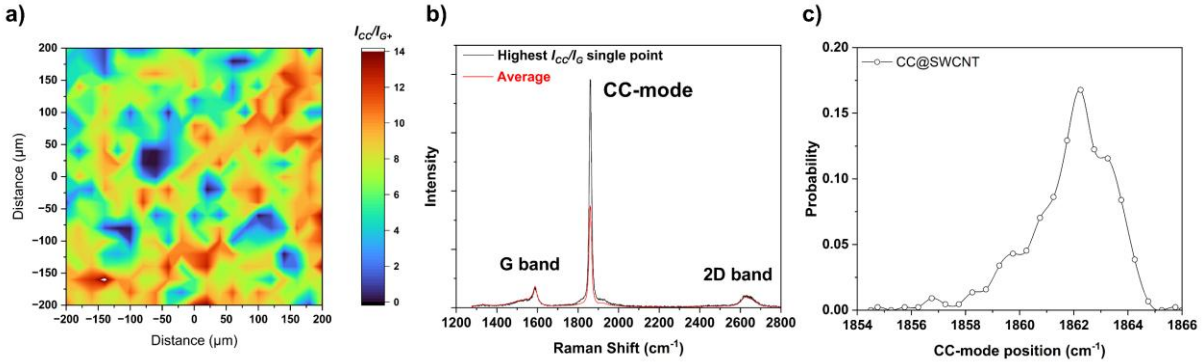

Figure 1. (a) Raman mapping of normalized CC-mode intensity (I_{CC}/I_{G+}) characterized by 532 nm laser wavelength (600 μm × 600 μm, step 60 μm). (b) Average Raman spectra of all points from Raman mapping (red) and single point result of the highest I_{CC}/I_{G+} characterized by 532 nm laser wavelength. (c) The distribution curve of CC-mode Raman shifts for CC@SWCNT.

References

[1] Liu, M. *et al.*, ACS Nano **7**, 10075–10082 (2013).
[2] Shi, L. *et al.*., Nature Mater **15**, 634–639 (2016).
[3] Zhang, B.-W. *et al.*, ACS Nano, in press (2025).
[4] Yudasaka, M. *et al.*, *Chem. Phys. Lett.*, **380**, 42–46 (2003).

Solving the Secondary Nucleation Problem that Causes Misoriented Islands during the Wafer-Scale Epitaxy of Single-Crystal Graphene on Ge

M. S. Arnold[1]

[1]*University of Wisconsin-Madison (USA)*

The large-area CVD synthesis of single-crystal graphene on substrates commonly used in the semiconductor electronics industry is a major challenge inhibiting the development of next-generation devices that harness the exceptional electronic, thermal, and mechanical properties of single-crystal graphene. Here, the factors controlling the island orientation of graphene grown epitaxially on Ge(110) by CVD are elucidated, and this insight is used to create graphene with minimal polycrystallinity. In the early stages of growth, most graphene islands have unidirectionally aligned lattices. However, we have discovered a secondary nucleation phenomenon in which misoriented graphene domains nucleate near/from the initial island edges, introducing defective grain boundaries and significantly increasing polycrystallinity throughout growth. We find that secondary nucleation occurs when islands grow over Ge steps, which form because of an interplay between the island growth and Ge surface topography evolution. Strategies for suppressing secondary nucleation are evidenced, enabling the synthesis of graphene in which the predominant crystal orientation has high coverage > 99% and low rotational spread < 0.6°. This work[1] overcomes the irreproducibility of graphene epitaxy on Ge(110) reported in the literature[2-4], providing a route towards the large-area synthesis of single-crystal graphene on technologically useful semiconductor wafers.

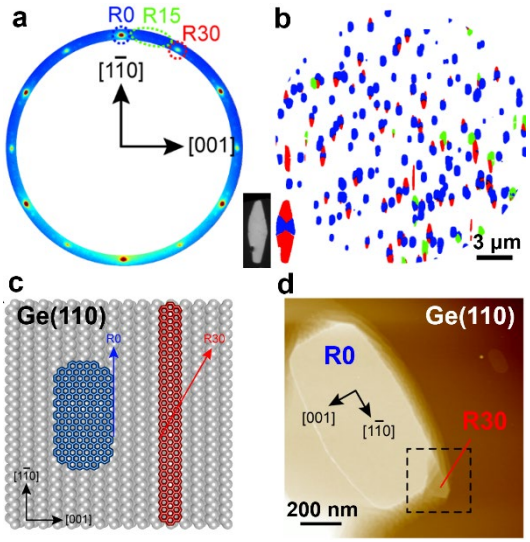

Fig. 1. LEEM/LEED/AFM characterization of graphene CVD on Ge(110). (a) LEED pattern on log-intensity scale evidencing a pronounced peak at the R30 orientation. **(b)** Corresponding color-coded DF-LEEM image. Most red R30 domains are found at the edges of blue R0 domains because they nucleate near/from the R0 edges. **(c)** Schematic of relative orientations. **(d)** AFM height image of R30 domain nucleating off/near the edge of an R0 domain.

References

1. Robert M. Jacobberger, Zichun Miao, Ka-Man Yu, Yin Hei Lam, Zizhong Li, Yangchen He, Jia Wang, Katherine A. Su, Yashwrdhan Pathaare, Vivek Saraswat, Daniel A. Rhodes, Max G. Lagally, Michael S. Altman, Michael S. Arnold, Submitted (2025).
2. Lee, J.-H.; Lee, E. K.; Joo, W.-J.; Jang, Y.; Kim, B.-S.; Lim, J. Y.; Choi, S.-H.; Ahn, S. J.; Ahn, J. R.; Park, M.-H.; Yang, C.-W.; Choi, B. L.; Hwang, S.-W.; Whang, D., Wafer-Scale Growth of Single-Crystal Monolayer Graphene on Reusable Hydrogen-Terminated Germanium. Science 2014, 344 (6181), 286-289.
3. Shen, T.-Z.; Hong, S.-H.; Lee, J.-H.; Kang, S.-G.; Lee, B.; Whang, D.; Song, J.-K., Selectivity of Threefold Symmetry in Epitaxial Alignment of Liquid Crystal Molecules on Macroscale Single-Crystal Graphene. Advanced Materials 2018, 30 (40), 1802441.
4. Ahn, S. J.; Kim, H. W.; Khadka, I. B.; Rai, K. B.; Ahn, J. R.; Lee, J.-H.; Kang, S. G.; Whang, D., Electronic Structure of Graphene Grown on a Hydrogen-terminated Ge (110) Wafer. Journal of the Korean Physical Society 2018, 73 (5), 656-660.

Session
NT 25（The 25th International Conference on the Science and Applications of Nanotubes and Low-

| Parallel Symposia：Symposium on Fundamental, Structural and Optical Properties of 1D and 2D Materials and their Heterostructures

Mon. Jun 16, 2025 2:00 PM - 5:20 PM JST | Mon. Jun 16, 2025 5:00 AM - 8:20 AM UTC International Exchange Hall III (Clock Tower Centennial Hall, 2F)

[16fn] Fundamental Properties

Chair:Jana Zaumseil, Thomas Pichler

2:00 PM - 2:20 PM JST | 5:00 AM - 5:20 AM UTC

[16fn-01]

Valley-Hybridized Gate-Tunable 1D Exciton Confinement in $MoSe_2$

*Antoine RESERBAT-PLANTEY[1] (1. Université Côte d'Azur, CNRS, CRHEA. (France))

2:20 PM - 2:40 PM JST | 5:20 AM - 5:40 AM UTC

[16fn-02]

ISOTOPE ENGINEERING OF TRANSITION METAL DICHALCOGENIDES

Rahul Kesarwani[1,2], Vaibhav Varade[1], Artur Slobodeniuk[1], Martin Kalbac[2], *Jana Kalbacova Vejpravova[1] (1. Charles University (Czech Republic), 2. J Heyrovsky Institute (Czech Republic))

2:40 PM - 3:00 PM JST | 5:40 AM - 6:00 AM UTC

[16fn-03]

Collective optical states in one- and two-dimensional molecular lattice

*Sabrina Juergensen[1], José A. Arcos Pareja[1], Chantal Mueller[1], Jean-Baptiste Marceau[2], Niclas S. Mueller[3], Nikolai Severin[4], Eduardo B. Barros[5,6], Patryk Kusch[1], Antonio Setaro[1,7], Jürgen P. Rabe[4], Etienne Gaufrès[2], Stephanie Reich[1] (1. Freie Universität Berlin (Germany), 2. Université de Bordeaux (France), 3. Fritz-Haber-Institut, Berlin (Germany), 4. Humboldt Univerität zu Berlin (Germany), 5. Federal University of Ceará, Fortaleza (Brazil), 6. Technische Universität Berlin (Germany), 7. Pegaso University (Italy))

3:00 PM - 3:20 PM JST | 6:00 AM - 6:20 AM UTC

[16fn-04]

Raman Spectroscopy of Twisted Graphene

*Lianming Tong[1] (1. Peking University Shenzhen Graduate School (China))

4:00 PM - 4:20 PM JST | 7:00 AM - 7:20 AM UTC

[16fn-05]

Moiré effects and dielectric coupling in one-dimensional heterostructures

*Georgy Gordeev Gordeev[1,2] (1. University of Luxembourg (Luxembourg), 2. Freie Universität Berlin (Germany))

4:20 PM - 4:40 PM JST | 7:20 AM - 7:40 AM UTC

[16fn-06]

Free Carrier Infrared Response of Intrinsic and Doped Carbon Nanotubes

Daniel Noll[1], Klaus Eckstein[1], Taras Abramovic[1], Friedrich Schöppler[1], Han Li[2], *Tobias Hertel[1] (1. Institute of Physical and Theoretical Chemistry (Germany), 2. Turku University (Finland))

4:40 PM - 5:00 PM JST | 7:40 AM - 8:00 AM UTC

[16fn-07]

MAGNETIC FIELD EFFECT ON QUATERNION EXCITONIC COMPLEXES IN BILAYER STRUCTURES NEAR METALS

Session

NT 25 (The 25th International Conference on the Science and Applications of Nanotubes and Low-

*Igor V Bondarev[1], David W Snoke[2] (1. North Carolina Central University (United States of America), 2. University of Pittsburgh (United States of America))

5:00 PM - 5:20 PM JST | 8:00 AM - 8:20 AM UTC

[16fn-08]

Superconducting Diodes Based on the Structural Design of $NbSe_2$

*zhaolong chen[1], Jinpei Zhao[2], Konstantin Novoselov[2] (1. Peking University ShenZhen Graduate School (China), 2. National University of Singapore (China))

Valley-Hybridized Gate-Tunable 1D Exciton Confinement in $MoSe_2$

Antoine Reserbat-Plantey[1]

[1] *Université Côte d'Azur, CNRS, CRHEA (France)*

Controlling excitons at the nanoscale in semiconductor materials represents a formidable challenge in quantum photonics and optoelectronics fields. Achieving this control holds excellent potential for unlocking strong exciton-exciton interaction regimes, enabling exciton-based logic operations, exploring exotic quantum phases of matter, facilitating deterministic positioning and tuning of quantum emitters, and designing advanced optoelectronic devices. Monolayers of transition metal dichalcogenides (TMDs) offer inherent two-dimensional confinement and possess significant binding energies, making them promising candidates for achieving electric-field-based confinement of excitons without dissociation. While previous exciton engineering strategies have predominantly focused on local strain gradients [1], the recent emergence of electrically confined states in TMDs has paved the way for novel approaches [2-3]. Exploiting the valley degree of freedom associated with these confined states further broadens the prospects for exciton engineering. In this talk, I will show electric control of light polarization emitted from one-dimensional (1D) quantum confined states in $MoSe_2$. By employing non-uniform in-plane electric fields, we demonstrate the in-situ tuning of the trapping potential and reveal how gate-tunable valley-hybridization gives rise to linearly polarized emission from these localized states. Remarkably, the polarization of the localized states can be entirely engineered through either the spatial geometry of the 1D confinement potential or the application of an out-of-plane magnetic field [4].

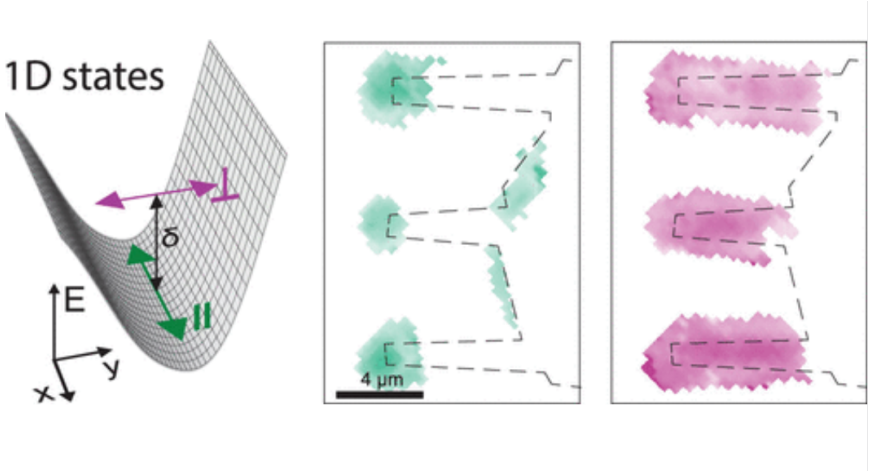

Figure1: 1D confined excitons show fine structure splitting, with lower/upper branches (green and purple, respectively). These states are linearly polarized, aligned either parallel ∥ or perpendicular ⊥ to the channel axis. On the right panel, we show the fitted weight of localized states' spectral components in reflection contrast when excitation polarization is set vertically.

References

[1] Dirnberger, F. et al. Quasi-1D exciton channels in strain-engineered 2D materials. Science Advances 7, (2021).
[2] Thureja, D. et al. Electrically tunable quantum confinement of neutral excitons. Nature 606, 298–304 (2022).
[3] Hu, J. et al. Quantum control of exciton wavefunctions in 2D semiconductors. (2023) doi:10.48550/arxiv.2308.06361.
[4] Heithoff, M. et al. Valley-hybridized gate-tunable 1D exciton confinement in MoSe2. (2023) ACS Nano. 18,44. (2024)

ISOTOPE ENGINEERING OF TRANSITION METAL DICHALCOGENIDES

R. Kesarwani[1,2#], V. Varade[1#], A. Slobodeniuk[1], M. Kalbac[2], J. Vejpravova[1]

[1]Faculty of Mathematics and Physics, Charles University (Czech Republic), [2]J Heyrovsky Institute of Physical Chemistry, Czech Academy of Sciences (Czech Republic)

#These authors contributed equally.

Isotope engineering provides a unique approach to tuning the optoelectronic and vibrational properties of transition metal dichalcogenides (TMDs) without extrinsic and chemical modifications. By leveraging sulfur isotope labeling in MoS_2 and WS_2, we demonstrate its impact on interlayer interactions, charge distribution, exciton dynamics, and valley scattering phenomena.

Using chemical vapor deposition (CVD), we first synthesized MoS_2 and WS_2 monolayers with natural sulfur and isotopically pure ^{34}S and ^{32}S [1, 2]. We explored isotope-dependent phonon renormalization, and exciton and valley scattering as a function of temperature and magnetic fields. The phonon modes as detected by the Raman spectroscopy follow the expected variation of the frequency depending on the mass of the Sulphur isotopes. Moreover, mixed-isotope WS_2 exhibited a single-phonon up-conversion process, while pure-isotope WS_2 ($W^{32}S_2$, $W^{34}S_2$) revealed two-phonon processes. Magnetic-field-dependent photoluminescence (PL) measurements further revealed distinct exciton polarization trends, emphasizing variations in valley scattering mechanisms.

We further fabricated isotopically resolved MoS_2 bilayers using a two-step CVD [3] and a conventional transfer process [4], respectively. It enabled us to probe the phononic and electronic properties of the individual layers through Raman and PL spectroscopy. We observed strong interlayer coupling, as evidenced by low-frequency Raman modes. Time-resolved PL indicated faster exciton lifetimes in isotope-engineered heterostructures, highlighting the role of isotopic modification in exciton and phonon dynamics.

Our findings demonstrate the potential of isotope engineering in van der Waals heterostructures for controlling vibrational properties, charge transport, exciton recombination, and valley polarization. This approach offers new possibilities for designing TMD-based optoelectronic and valleytronic devices, paving the way for advanced quantum materials and energy conversion applications.

References

[1] V. Varade et al, *2D Mater.* **10**, 025024 (2023)
[2] R. Kesarwani et al, *2D Mater.* (2025), accepted.
[3] V. Varade et al, *Nanoscale Adv.* (2025).
[4] A. Kralik *et al.*, *J. Phys. Chem. C* **128**, 12575–12581 (2024).

Collective optical states in one- and two-dimensional molecular lattices

S. Juergensen[1], José A. Arcos Pareja[1], C. Mueller[1], J.-B. Marceau[2], N. S. Mueller[3], N. Severin[4], E. Barros[5,6], P. Kusch[1], A. Setaro[1;7], J. Rabe[4], E. Gaufrès[2], S. Reich[1]

[1]Freie Universität Berlin (Germany), [2] Laboratoire Photonique Numérique et Nanosciences, Institut d'Optique, Université de Bordeaux (France), [3]Fritz-Haber-Institut (Germany), [4]Humboldt Univerität zu Berlin (Germany), [5]Federal University of Ceará, Fortaleza (Brazil), [6]Technische Universität Berlin (Germany), [7]Engineering Department, Pegaso University (Italy)

Nanomaterials such as two-dimensional layers and one-dimensional nanotubes can act as templates and containers for the formation of highly ordered molecular lattices in one or two dimensions. These ordered molecular systems show fascinating optical properties, arising from the Coulomb coupling of the molecules' transition dipole moments which result in a delocalized collective optical state.

We investigate the formation of well-ordered one-dimensional molecular chains inside nanotubes [1] and two-dimensional lattices on atomically flat two-dimensional substrates. [2] Using organic α-sexithiophene, MePTCDI (perylene derivate) and phthalocyanine molecules, we show the formation of large ordered domains of collective coupled molecules, as well as the change in the optical response of the molecules upon the coupling of their transition dipole moments. It is characteristic for collective states to have a strong and narrow emission, shifted emission/absorption, and a vanishing Stokes shift.

We study how the interaction of the different organic molecules with the one- and two-dimensional hosts and substrates induce hybridized states with focus on changes in the molecule-related response. Further, we study a bundle of boron nitride nanotubes (BNNT) that contain molecular chains. The difference in the optical response of single- and multi-file filled tubes gives us the opportunity to investigate the optical response of the bundle yielding unexpected strong red shifts for tubes with small inner diameter that are only filled with one chain of molecules.

The high transition energy tunability of the molecular systems makes them promising candidates for components in future optoelectronic devices and for analytic spectroscopy.

References

[1] S. Juergensen, S. Reich *et al.*, *J. Phys. Chem. Letters.*, accepted (2025).
[2] S. Juergensen, S. Reich *et al.*, *ACS Nano* **17**, 17350–17358 (2023).

Raman Spectroscopy of Twisted Graphene

Lianming Tong[1]

[1]*School of Advanced Materials, Peking University Shenzhen Graduate School, Shenzhen 518055, P.R. China*

Email: tonglm@pku.edu.cn

Twisted graphene has attracted widespread attention due to the twist-angle-dependent band structures and exceptional properties such as superconductivity and magnetism. Great efforts have been made in understanding the physical picture behind the superior properties and revealing the structural information of twisted graphene. Raman spectroscopy is a rapid and non-destructive characterization technique for material structure and properties, and has been extensively employed to study the resonance effects, layer numbers, and interlayer interactions in twisted graphene systems.

In this talk, we will introduce circularly polarized Raman spectroscopy and helicity-dependent Raman spectroscopy for the measurement of twisted graphene. We show that helicity-dependent Raman spectroscopy can be used to reveal new Raman modes in twisted bilayer graphene and measure the orientation angle of vertical graphene arrays. Furthermore, we also investigated the interlayer electron-phonon coupling in twisted bilayer graphene heterostructures and observed chirality transfer within the twisted graphene system (Figure 1).

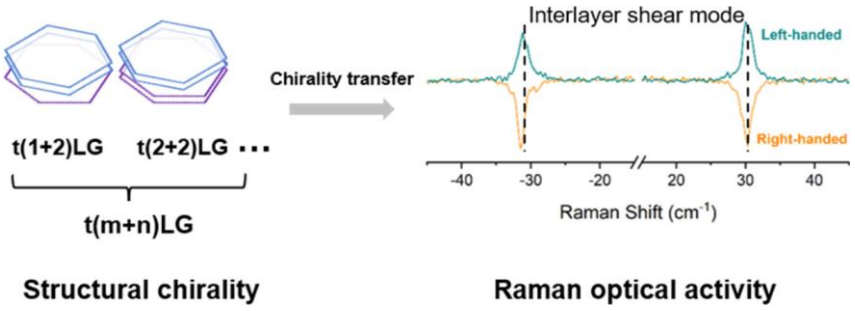

Figure 1: Chirality transfer in twisted graphene**.**

References

[1] Song, G.; Hong, H.; Ma, C. J.; Hao, H.; Yan, S. W.; Liu, K. H.; Tong, L. M.*; Zhang, J., *J Am Chem Soc* **147**, 473-479 (2025).
[2] Yan, S. W.; Huang, J. Q.; Hao, H.; Song, G.; Wang, Y. C.; Peng, H. L.; Yang, T.; Zhang, J.; Tong, L. M.*, *Nano Lett* **24**, 7879-7885 (2024).
[3] Song, G.; Hao, H.; Yan, S. W.; Fang, S. S.; Xu, W. G.; Tong, L. M.*; Zhang, J., *ACS Nano* **18**, 17578-17585 (2024).
[4] Han, S. Y.; Hung, N. T.; Xie, Y.; Saito, R.*; Zhang, J.; Tong, L. M.*, *Nano Lett* **23**, 8454-8459 (2023).
[5] Hao, H. †; Lin, M. L.†; Xu, B. †; Wu, H.; Wang, Y. C.; Peng, H. L.; Tan, P. H.*; Tong, L. M.*; Zhang, J. , *ACS Nano* **17**, 10142-10151 (2023).
[6] Xu, B. †; Hao, H. †; Huang, J. Q.; Zhao, Y.; Yang, T.; Zhang, J.; Tong, L. M.*, *J Phys Chem C* **126**, 25, 10487-10493 (2022)
[7] Han, S. Y.; Zhao, Y.; Hung, N. T.; Xu, B.; Saito, R.*; Zhang, J.; Tong, L. M.*, *J Phys Chem C* **13**, 1241-1248 (2022).
[8] Zhao, Y.; Xu, B.; Tong, L. M.*; Zhang, J.*, *Sci China Chem* **65**, 269-283 (2022).
[9] Xu, B.; Xu, S. C.; Zhao, Y.; Zhang, S. S.; Feng, R.; Zhang, J.; Tong, L. M.*, *J Phys Chem C* **125**, 8353-8359 (2021).
[10] Zhao, Y.; Zhang, S. S.; Shi, Y. P.; Zhang, Y. F.; Saito, R.; Zhang, J.; Tong, L. M.*, *ACS Nano* **14**, 10527-10535 (2020).

Moiré effects and dielectric coupling in one-dimensional heterostructures

G. Gordeev[1,2]
[1]Materials Research and Technology Department, University of Luxembourg, 41 rue du Brill, L-4422 Belvaux, Luxembourg
[2]Freie Universität Berlin, Department of Physics, Arnimallee 14, 14195 Berlin, Germany

Double-walled carbon nanotube (DWCNT) is a fascinating system hosting one-dimensional moiré and van-der Waals Coulomb physics. In this talk I will discuss different physical phenomena, that can be achieved by the 1D the moiré potential, that interconnects the electronic states between the inner and outer walls. Such coupling has chiral and radial components, the chiral component is predefined by the DWCNT chirality while radial component by the wall separation distance. That has immediate consequences for the vibrational properties of DWCNTs, for instance during the oscillation of the radial breathing modes the atoms undergo a change in the moiré potential and their frequency shifts. We provide a tight-binding based model linearly relating the RBM frequency shifts with the energy shifts of the electronic transitions. This model is verified experimentally using resonance Raman spectroscopy of RBM modes with a system containing semiconducting inner and outer walls.[1,2] Further we use dielectric properties of the outer wall to control the many-body physics is the inner one, which is regulated by strong electron-hole correlations. The metallic walls provide substantially higher dielectric coupling compared to semiconducting ones and screen the inner walls exciton. We show that in the case of small diameter metallic@metallic system the excitonic effects can be fully suppressed.[3] Further the metallic outer wall provides a dense dielectric shell which alters electric field reaching the inner wall. We study these experimentally by analyzing Raman matrix elements and establish theoretically using quasi-static approximation. Lastly, I explore the potential for generating novel excitonic phases through the utilization of moiré-coupled states.

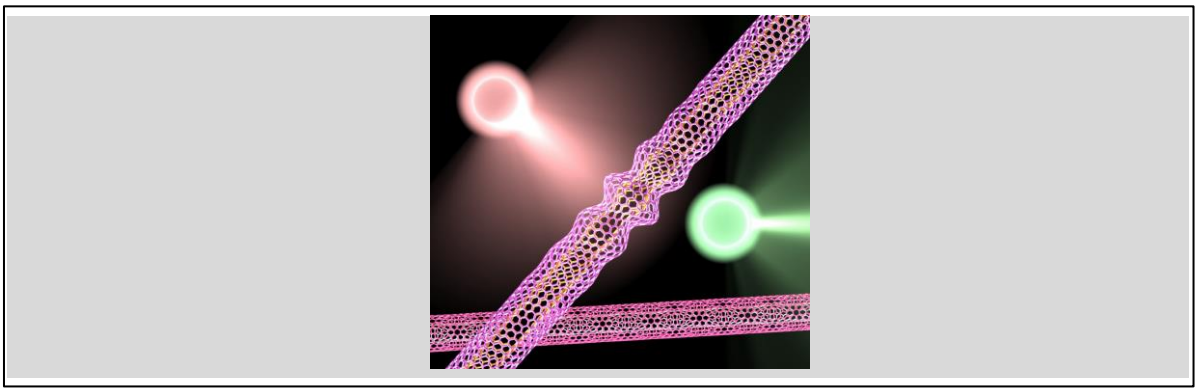

Figure caption: Radial breathing oscillation regulated by moiré pattern

References (if desired)

[1] Li, H. et al. Inner- and outer-wall sorting of double-walled carbon nanotubes. Nat. Nanotechnol. 12, 1176–1182 (2017).
[2] Gordeev, G., Wasserroth, S., Li, H., Flavel, B. & Reich, S. Moiré-Induced Vibrational Coupling in Double-Walled Carbon Nanotubes. Nano Lett. 21, 6732–6739 (2021).
[3] Gordeev, G. et al. Dielectric Screening inside Carbon Nanotubes. Nano Lett. 24, 8030–8037 (2024).

Free Carrier Infrared Response of Intrinsic and Doped Carbon Nanotubes

Daniel Noll[1], Klaus Eckstein[1], Taras Abramovic[1], Friedrich Schöppler[1], Han Li[2], Tobias Hertel[1,2]

[1]Institute of Physical and Theoretical Chemistry, Julius-Maximilans-University Würzburg (Germany), [2]University of Turku (Finland)

Infrared spectroscopy of single-wall carbon nanotubes (SWNTs) offers a unique perspective for studying carrier dynamics, doping-induced changes to many particle phenomena, and interactions between electronic and vibrational degrees of freedom in these low-dimensional systems. A critical challenge remains in differentiating intrinsic carrier behaviors from doping- and chemical functionalization-induced effects, which is essential for controlled modifications of nanotube electronic and optical properties. Additionally, we are interested in clarifying the nature of Fano-like resonances in the infrared spectra of doped SWNTs, specifically to determine if and how the discrete vibrational modes involved couple to the free carrier continuum.

Here, we present the results of infrared spectroscopy studies on intrinsic, redox-chemically doped, as well as chemically functionalized and subsequently redox-doped semiconducting SWNTs. p-doping significantly modifies infrared absorption signatures in semiconducting SWNTs, transitioning with increasing doping level from weak discrete vibrational bands toward a superposition with a pronounced Drude–Smith-type and, at higher doping levels, Drude-type optical conductivity, indicative of doping-dependent changes in free-carrier concentrations, mobilities and scattering processes. We compare these results with the doping dependence of spectra from pre-functionalized SWNTs containing organic color centers.

In contrast, preliminary data from chirality enriched metallic SWNTs exhibit fundamentally different infrared spectral responses to p-doping. This allows to probe the role of many-particle interactions and screening versus independent particle effects for the observed spectral phenomena. Additional insights can here be gained from the doping-dependence of excitonic resonances in the visible spectral range of the metallic SWNTs.

Moreover, prominent Fano-like resonances appearing in the spectral range of vibrational modes typically observed only in Raman spectra are tentatively attributed to the coupling between discrete vibrational modes and the continuum of free-carrier excitations. These resonances are believed to reflect both intramolecular interactions within the SWNTs and intermolecular interactions between the SWNTs and the wrapping polymer.

We will also discuss how Monte Carlo trajectory simulations of carrier transport can be used to model experimental IR spectra, offering insights into how doping and chemical functionalization affect free carrier abundance, mobility, and scattering.

MAGNETIC FIELD EFFECT ON QUATERNION EXCITONIC COMPLEXES IN BILAYER STRUCTURES NEAR METALS

I.V. Bondarev[1] and D.W. Snoke[2]

[1]*Department of Mathematics & Physics, North Carolina Central University, Durham, NC 27707, USA*
[2]*Department of Physics, University of Pittsburgh, Pittsburgh, PA 15218, USA*

Two-dimensional monolayer structures of transition metal dichalcogenides (TMDCs) have been shown to allow many higher order excitonic bound states such as trions (charged excitons), biexcitons (excitonic molecules), and charged biexcitons. Recently [1], an atom-like excitonic structure was reported experimentally in bilayer TMDCs in accord with theory predictions – the quaternion (Fig.1, left) – a complex of a free charge carrier in top layer bound to a like-charge trion in bottom layer placed close to a parallel metal layer to screen the excessive repulsive interaction in the system. Because they carry two net charges and are also bosonic, a Bose-Einstein condensate (BEC) of these would be a superfluid, and therefore also a Schafroth superconductor [2,3]. Here, we develop a theoretical framework to explain the latest experimental observations of the Zeeman effect for quaternion complexes in perpendicular magnetostatic field [4]. Our theory is based on group theoretical analysis and spin-Hamiltonian formalism. We show that, contrary to the linear Zeeman shift known for excitons/trions in TMDC monolayers [5], the quaternion ground state is the spin triplet to exhibit a quadratic magnetic field shift (Fig1, right) similar to that known for hydrogen-like atoms (with difference being that their ground state is singlet). In addition to a novel superconductivity mechanism, another fascinating possibility is that, since quaternion complexes have long-range Coulomb repulsion, they could form a bosonic Wigner crystal at low temperature, and in principle, could become an 'atom-like' supersolid. For an ensemble of charged particles the process of Wigner crystallization is controlled by the ratio of the Coulomb repulsion energy over the mean kinetic energy per particle [6]. Due to their double charge and triple mass as compared to electrons, this ratio is at least 10 times greater for quaternions, suggesting a much higher Wigner crystallization temperature than that of the order of 10 K recently reported for quasi-2D electrons in TMDC nanostructures [7].

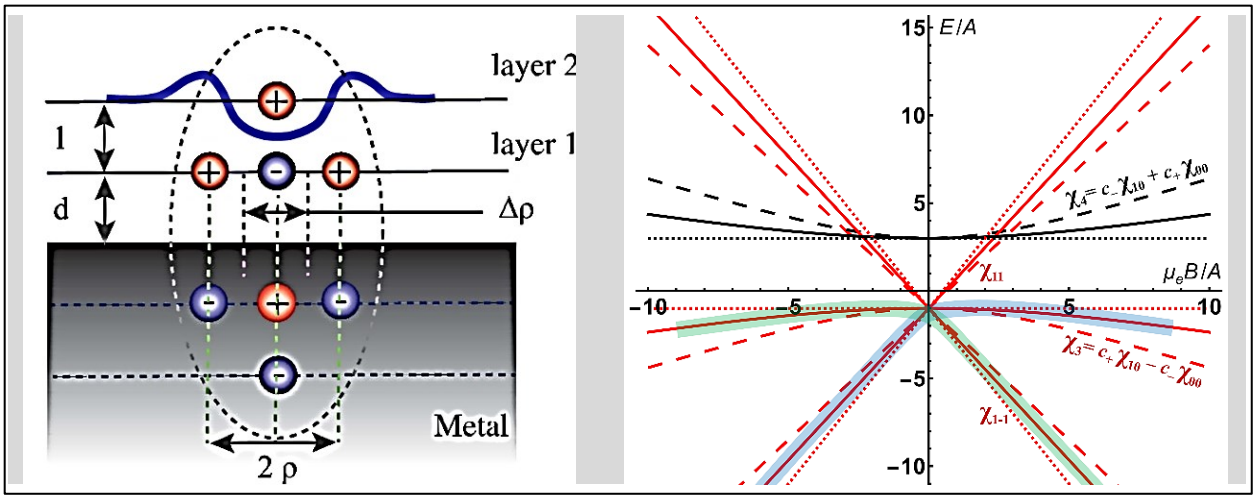

Figure 1: (*Left*) Schematic of the quaternion excitonic complex formed by an electron and three holes near metallic surface due to the partial screening of excessive repulsion by image charges inside metal [1]. (*Right*) Theoretical magnetic field dependences for the spin states (indicated) of the quaternion treated as coupled (with constant A) system of spin-1/2-trion and electron in bottom and top layer, respectively [4]. Shown are the triplet (red) and singlet (black) quaternion energy levels calculated for trion-to-electron magnetic moment ratio $\zeta = 0.5$, 0.73 and 1 (dashed, solid and dotted lines, respectively). The green and purple bands show the lowest energy quaternion states that emit photons of right and left circular polarizations measured experimentally [4].

Acknowledgments
This research is supported by the U.S. Army Research Office grant No. W911NF-24-1-0237.

References

[1] Z. Sun, et al., *Nano Lett*. **21**, 7669 (2021).
[2] M. Schafroth, *Physical Review* **96**, 1442 (1954).
[3] Y. E. Lozovik and V. Yudson, *Zh. Eksp. Teor. Fiz.* **71**, 738 (1976).
[4] Q. Wan, et al., *Science Adv. (under review)*; see arXiv:2412.06941 (12 Dec 2024).
[5] D. MacNeill, et al., *Phys. Rev. Lett*. **114**, 037401 (2015).
[6] P. M. Platzman and H. Fukuyama, *Phys. Rev. B* **10**, 3150 (1974).
[7] T. Smoleński, et al., *Nature* **595**, 53 (2021); Y. Zhou, et al., *ibid*. **595**, 48 (2021).

Superconducting Diodes Based on the Structural Design of $NbSe_2$

Zhaolong Chen[1,2*], Jinpei Zhao[2], Kostya Novoselov[2]
[1]School of Advanced Materials, Peking University Shenzhen Graduate School, Shenzhen, 518071, China
[2]Institute of Functional Intelligent Materials, National University of Singapore, Singapore, 117544
*Email: chenzhaolong@pku.edu.cn

Compared to traditional semiconductor diodes, superconducting diodes can achieve unidirectional conduction in a zero-resistance state, potentially advancing low-energy electronics, quantum computing, and high-sensitivity sensors[1,2]. These devices typically utilize the Rashba effect to induce inversion symmetry breaking at the surface interface of superconductors[3]. With the advent of 2D superconducting materials and van der Waals stacking techniques, we can design more complex structures to fabricate superconducting diodes by tuning local crystal symmetry[4, 5]. This talk, I will discuss our work on fabricating superconducting diode devices in few-layer niobium diselenide by breaking inversion symmetry through structural design. Notably, in systems with twisting angles, Moiré superlattice reconstruction and interface dipole moments can influence the order parameter of 2D superconductors, altering the superconducting flux pinning effect and enhancing diode characteristics.

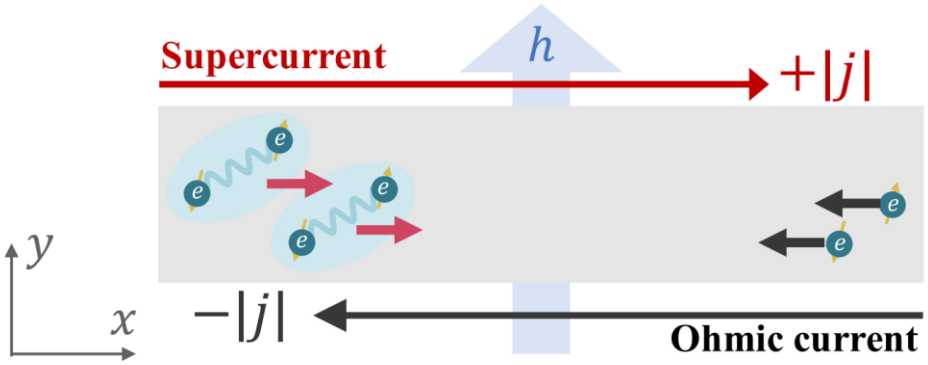

Fig. 1 Schematic figure for the superconducting diode effect [1]

References

[1] Daido A, Ikeda Y, Yanase Y. *Phys. Rev. Lett.,* **128**, 037001(2022).
[2] Nadeem M, Fuhrer M S, Wang X. *Nat. Rev. Phys.*, **5**, 558-577(2023).
[3] Narita H, Ishizuka J, Kawarazaki R, et al. *Nat. Nanotechnol.,* **17,** 823-828(2022).
[4] Díez-Mérida J, Díez-Carlón A, Yang S Y, et al. *Nat. Commun.*, **14**, 2396(2023).
[5] Zhang N J, Lin J X, Chichinadze D V, et al. Nat. Mater., **23**, 356-362(2024).

Session
NT 25（The 25th International Conference on the Science and Applications of Nanotubes and Low-

| Parallel Symposia：15th Symposium on Carbon Nanomaterials, Biology, Medicine and Toxicology

Mon. Jun 16, 2025 2:00 PM - 5:00 PM JST | Mon. Jun 16, 2025 5:00 AM - 8:00 AM UTC Meeting Room E/F(INNOVATION BLDG., 5F)

[16nb] NanoBio

Chair:Markita Landry, Sanghwa Jeong, Ching-Wei Lin

2:00 PM - 2:40 PM JST | 5:00 AM - 5:40 AM UTC

[16nb-01]

Near-infrared fluorescence probe using oxygen-doped carbon nanotubes and carbon nanotube degradation for safety

*Toshiya Okazaki[1] (1. AIST (Japan))

2:40 PM - 3:00 PM JST | 5:40 AM - 6:00 AM UTC

[16nb-02]

Short-wave infrared fluorescence cytometry

*Ching-Wei Lin[1], Te-I Liu[1], Jhih-Shan Wang[1,2,5], Ai-Phuong Nguyen[1,3], Marco Raabe[1], Carlos Jose Quiroz Reyes[1,4], Chih-Hsin Lin[4] (1. Academia Sinica (Taiwan), 2. National Taiwan University (Taiwan), 3. National Tsing Hua University (Taiwan), 4. Taipei Medical University (Taiwan), 5. University of Stuttgart (Germany))

3:00 PM - 3:20 PM JST | 6:00 AM - 6:20 AM UTC

[16nb-03]

Imaging oxytocin signaling in prairie voles to study social relationships with carbon nanotube based fluorescent sensors

*Natsumi Komatsu[1], Alexis Marie Black[1], Devanand Manoli[2], Annaliese Beery[1], Markita Landry[1] (1. University of California, Berkeley (United States of America), 2. University of California, San Francisco (United States of America))

4:00 PM - 4:20 PM JST | 7:00 AM - 7:20 AM UTC

[16nb-04]

Carbon Nanomaterials as Nanocarriers and Optical Nanosensors for Plant Biotechnology

*Tedrick Thomas Salim Lew[1], Biao Huang[1], Suppanat Puangpathumanond[1] (1. National University of Singapore (Singapore))

4:20 PM - 4:40 PM JST | 7:20 AM - 7:40 AM UTC

[16nb-05]

Pattern Recognition-derived Optical SWCNT Nanosensor Array for Liquid Biopsy

*Sanghwa Jeong[1], Dakyeon Lee[1] (1. Pusan National University (Korea))

4:40 PM - 5:00 PM JST | 7:40 AM - 8:00 AM UTC

[16nb-06]

Using Molecular Probe Adsorption (MPA) to Characterize the Nanoparticle Corona Phase and Molecular Recognition

*Gabriel Sánchez-Velázquez[1], Duc Thinh Khong[2], Minkyung Park[1], Xiaojia Jin[1], Zhe Yuan[1], Xun Gong[1], Mervin Chun-Yi Ang[2], Michael S Strano[1,2] (1. Department of Chemical Engineering, Massachusetts Institute of Technology (United States of America), 2. Disruptive & Sustainable Technologies for Agricultural Precision IRG, Singapore-MIT Alliance for Research and Technology (Singapore))

Near-infrared fluorescence probe using oxygen-doped carbon nanotubes and carbon nanotube degradation for safety

Toshiya Okazaki[1]

[1]*National Institute of Advanced Industrial Science and Technology (AIST) (Japan)*

Single-walled carbon nanotubes (CNTs) fluoresce in the near-infrared (NIR) region; the fluorescence quantum yield of CNTs can be increased by moderate chemical functionalization, making the application of functionalized CNTs for bioimaging particularly interesting. In this talk, we will report on the synthesis of epoxide oxygen-doped CNTs (Ep-CNTs) and their application as near-infrared fluorescence probes, which has been carried out by our research group [1-3]. The treatment of these (6, 5) nanotubes produces photoluminescence at ~1280 nm, corresponding to one of the most transparent regions in biomaterials, and we have demonstrated immunoassays and fluorescent angiography in mice using Ep-CNTs as near-infrared fluorescent labels and imaging agents, respectively. The biodistribution of Ep-CNT imaging probes during mouse administration was then investigated in detail. In addition, the biological responses of mice after administration related to safety were also investigated. An immune response due to a certain amount of residual Ep-CNTs was observed, but not at a level that would disrupt biological homeostasis or affect animal health.

On the other hand, since CNTs are made of stable graphite, the possibility of their accumulation in the environment and in living organisms has been discussed. Therefore, elucidating the biodegradation properties of CNTs is an essential issue in discussing their long-term safety. In recent years, several reports on the biodegradability of CNTs have been published, but the results vary from report to report, and many details remain unclear. Under these circumstances, we clarified the biodegradability of CNTs in immune cells by using the near-infrared absorption property of CNTs to measure the amount of CNTs taken up into cells [4,5]. Furthermore, oxidation by hypochlorous acid produced during the enzymatic reaction is thought to be involved in the CNT biodegradation mechanism. When hypochlorite compounds were mixed with CNT dispersion, the CNT dispersion easily became transparent [5]. This decomposition method can be applied to single-walled carbon nanotubes, multi-walled carbon nanotubes, and even graphene [6,7]. We are currently working on international standardization activities for this method.

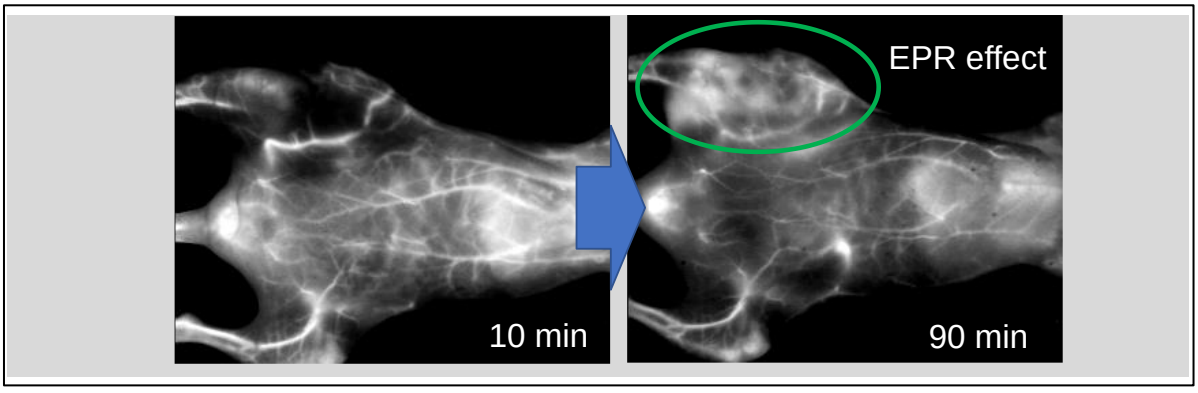

Figure 1: In vivo NIR images of a tumor-bearing mouse after injection of the Ep-CNT imaging probe.

References

[1] Y. Iizumi *et al.*, *Sci. Rep.*, **8**, 6272 (2018).
[2] T. Takeuchi *et al.*, *Bioconjugate Chem.*, **30**, 1323−1330 (2019). (Cover Article)
[3] K. Kojima, Y. Iizumi, M. Zhang, T. Okazaki, *Langmuir*, **38**, 1509-1513 (2022).
[4] M. Yang *et al.*, *Int. J. Nanomedicine*, **14**, 2797-2807 (2019).
[5] M. Zhang *et al.*, *Sci. Rep.* **9**, 1284 (2019).
[6] M. Zhang *et al.*, *ACS Appl. Nano Mater.*, **2**, 4293-4301 (2019).
[7] M. Zhang *et al.*, *Sci. Rep.*, **12**, 1541 (2022).

Short-wave infrared fluorescence cytometry

Ching-Wei Lin[1], Te-I Liu[1], Jhih-Shan Wang[1], Ai-Phuong Nguyen[1], Marco Raabe[1], Carlos Jose Quiroz Reyes[1], Chih-Hsin Lin

[1]Institute of Atomic and Molecular Sciences, Academia Sinica (Taiwan), [2]Department of Materials Science and Engineering, National Taiwan University (Taiwan), [3]Department of Physics, University of Stuttgart (Germany), [4]Department of Chemistry, National Tsing Hua University (Taiwan), [5]International Ph.D. Program in Biomedical Engineering, Taipei Medical University (Taiwan), [6]Graduate Institute of Nanomedicine and Medical Engineering, Taipei Medical University (Taiwan)

Fluorescence cytometry plays a crucial role in characterizing cellular properties such as immunophenotyping, but its restricted optical window (400–850 nm) limits the number of stained fluorophores that can be detected simultaneously and hampers the study and utilization of short-wave infrared (SWIR; 900–1700 nm) fluorophores in cells. In this talk, we will introduce two SWIR-based methods to address these limitations: SWIR flow cytometry and SWIR image cytometry.[1] We developed a quantification protocol for deducing cellular fluorophore mass. Both systems achieve a limit of detection of ~0.1 fg cell^{-1} within a 30 min experimental time frame, using individualized, high-purity (6,5) single-wall carbon nanotubes as a model fluorophore and macrophage-like RAW264.7 as a model cell line. This high-sensitivity feature reveals that low-dose (6,5) serves as an antioxidant, and cell morphology and oxidative stress dose-dependently correlate with (6,5) uptake. Our SWIR fluorescence cytometry holds immediate applicability for existing SWIR fluorophores and offers a solution to the issue of spectral overlapping in conventional cytometry. Finally, we will also mention our future goals and recent progresses on the SWIR fluorescence cytometry related work.

References

[1] T.-I Liu *et al.*, *ACS Nano* **18**, 18534–18547 (2024).

Imaging oxytocin signaling in prairie voles to study social relationships with carbon nanotube based fluorescent sensors

Natsumi Komatsu[1], Alexis M. Black[1], Devanand Manoli[2], Annaliese K. Beery[1], and Markita P. Landry[1]

[1]*University of California Berkeley (USA),* [2]*University of California San Francisco (USA)*

Neurochemicals are fundamental to communication between neurons and drive brain function, with their imbalance at the core of numerous neurodegenerative and psychiatric conditions. One such neurochemical, oxytocin, is a neuropeptide hypothesized to play a central role in social behaviors, and its dysregulation is implicated in developmental issues such as autism spectrum disorder. However, oxytocin has remained invisible due to a lack of real-time biosensors, hindering our understanding of when and where oxytocin is released, and how its release may be impaired (and thus treatable) in developmental disorders. To this end, we have developed a fluorescent oxytocin nanosensor based on single-walled carbon nanotubes noncovalently functionalized with single-stranded DNA, enabling real-time imaging of oxytocin in living brain tissue slices (Figure 1A) [1].

Utilizing newly developed carbon nanotube based nanosensors, we have developed a new assay to image oxytocin's role in social relationships in prairie voles, a rodent species ideal for social neuroscience studies because of the unique capacity of voles to form selective social bonds, as seen in humans. By imaging oxytocin signaling in transgenic voles lacking functional oxytocin receptors, we observed a reduced number of oxytocin releasing sites in the oxytocin receptor null mutant brain relative to wildtype (Figure 1B), suggesting that oxytocin signaling is not enhanced but rather decreased in the absence of functional receptors. Furthermore, behavioral tests revealed that mutant females showed no partner selectivity after 24 hours of cohabitation—a duration sufficient to induce partner preferences in wildtype animals. Taken together, our study not only enabled oxytocin imaging in non-model organisms, but also provided molecular insights into the role of oxytocin and its receptors in social relationships and aberrations thereof.

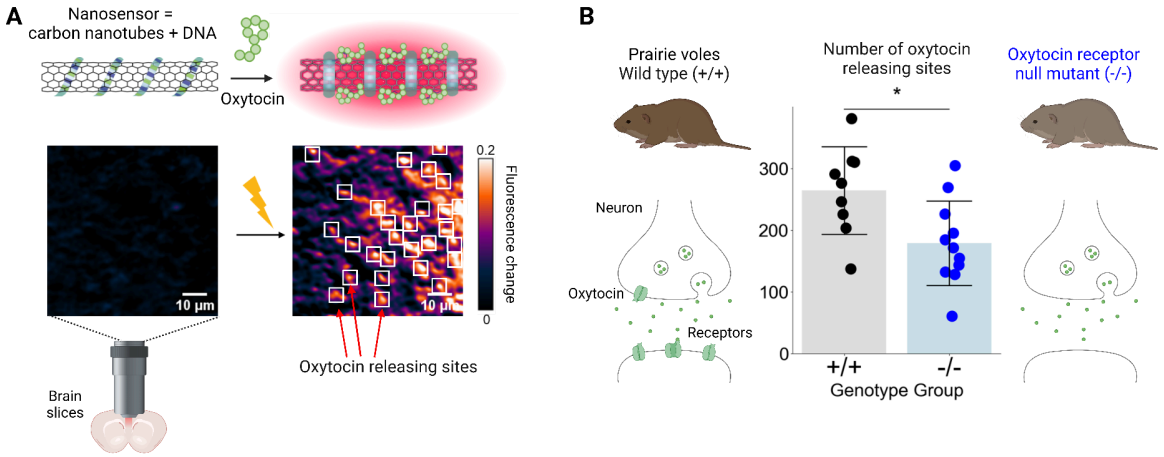

Figure 1: A) Nanosensor is based on near-infrared fluorescent carbon nanotubes functionalized with DNA, which 'turns on' upon analyte interaction. Ex vivo oxytocin imaging enables quantification of number of releasing sites. B) The number of oxytocin releasing sites was reduced in oxytocin receptor null mutant (-/-) compared to wild types (+/+), implying altered oxytocin regulation in the absence of receptors.

References

[1] J. A. M. Adams, N. Komatsu, *et al. bioRxiv,* 593556 (2024)

Carbon Nanomaterials as Nanocarriers and Optical Nanosensors for Plant Biotechnology

B. Huang[1], S. Puangpathumanond[1], T.T.S. Lew[1]

[1]*Department of Chemical and Biomolecular Engineering, National University of Singapore, Singapore 117585*

Plant engineering plays a pivotal role in enhancing the productivity and resilience of future agricultural practices. In this talk, I will present the development of nanoparticle-based analytical tools which can be interfaced with living plants of different species to enable diverse plant biotechnology and agricultural applications. I will first describe the engineering of single-walled carbon nanotubes as nanocarriers for plant genetic modification. These nanocarriers can deliver DNA into specific plant organelles for transient protein expression. Additionally, I will discuss the development of single-walled carbon nanotubes as optical nanosensors to monitor plant defense signaling pathways elicited by environmental stresses. By embedding nanosensors within plant tissues, the plant internal state can be accessed with portable electronics in a non-destructive and species-independent manner – a combination of features currently unattainable with existing analytical approaches. These advances highlight the potential of nanomaterial-enabled platforms as species-independent tools for plant engineering to bolster our agricultural sustainability efforts.

Pattern Recognition-derived Optical SWCNT Nanosensor Array for Liquid Biopsy

Dakyeon Lee, Jaehang Lee, Sunyoung Kwon, Sanghwa Jeong*

[1]*School of Biomedical Convergence Engineering, Pusan National University, Yangsan, Republic of Korea*

The functionalization of fluorescent single-walled carbon nanotubes (SWCNTs) with biopolymers represents a versatile platform for developing biosensors targeting small molecules, proteins, and environmental factors. Covalent and non-covalent functionalization of the SWCNT surface modulates the sensitivity and selectivity of its fluorescence to biomedical signals. Mimicking the olfactory system of organisms, each distinct SWCNT nanosensor can serve as an olfactory protein receptor, with the collective signal of multiple nanosensors functioning as a multi sensor array for patient's liquid samples such as blood. In this study, we introduce pattern recognition-derived SWCNT nanosensor arrays that differentiate disease states in patients using blood serum. We functionalized SWCNT surfaces using two methods: covalent modification with various amino acids and non-covalent modification with ssDNA sequences. Dozens of different SWCNT nanosensors were incubated with patient blood samples and samples from healthy individuals as controls. The fluorescence changes of all sensors to each sample were recorded and analyzed using both conventional and machine learning-aided methods. Our machine learning model distinguishes patient and control blood serum with >0.9 AUC, demonstrating the promising potential of patter recognition-based multisensory array. Future directions for this universal biomedical sensor technology will be discussed.

Additionally, we analyzed the toxicity of ssDNA-wrapped SWCNTs using zebrafish embryos to investigate the biological and environmental impact of colloidal SWCNT dispersions. The effects of ssDNA-SWCNT and several other nanomaterials were tested on zebrafish embryos over a 3-day period. Single-cell transcriptomic analysis was performed to uncover the fundamental mechanisms of toxicity-related responses from SWCNT dispersion. This research provides insights into the biocompatibility of ssDNA-SWCNTs and addresses potential environmental concerns.

Using Molecular Probe Adsorption (MPA) to Characterize the Nanoparticle Corona Phase and Molecular Recognition

Gabriel Sánchez-Velázquez[1†], Duc Thinh Khong[2†], Minkyung Park[1], Xiaojia Jin[1], Zhe Yuan[1], Xun Gong[1], Mervin Chun-Yi Ang[2], and Michael S. Strano[1,2]

[1]Department of Chemical Engineering, Massachusetts Institute of Technology, Cambridge, MA, [2]Disruptive & Sustainable Technologies for Agricultural Precision IRG, Singapore-MIT Alliance for Research and Technology, Singapore, [†]These authors contributed equally

The nanoparticle corona—a molecular layer adsorbed on nanoparticle surfaces—plays a crucial role in controlling molecular interactions and enabling applications in catalysis, nanoparticle separations, and sensing technologies. It underpins Corona Phase Molecular Recognition (CoPhMoRe), where the adsorbed layer adopts a conformation that selectively binds a specific molecular configuration. While tailoring the corona has enabled the molecular recognition of diverse analytes, quantitatively characterizing its properties remains challenging. Herein, we advance Molecular Probe Adsorption (MPA), applying it across a broad range of data sets to further validate and refine the technique. MPA utilizes a fluorescent probe quenched upon adsorption to quantify solvent-exposed surface area via adsorption isotherms. We leverage MPA to elucidate recognition mechanisms in five corona phases and expand the library of characterized CoPhMoRe constructs by 20, enabling comprehensive comparative analyses. Additionally, we examine how polymer stiffness, quantified by persistence length, influences corona formation on single-walled carbon nanotubes (SWCNTs). Our results reveal that as polymer persistence length increases from 1.16 nm to ~4 nm, the q/K_D value, a proxy for exposed surface area, rises from ~200 M^{-1} to 1,600 M^{-1}. In agreement with theoretical predictions, we find that sufficiently flexible polymers achieve greater SWCNT surface coverage, offering new insights for optimizing polymer-based corona phases. Furthermore, we establish structure–property relationships linking MPA-derived surface area to adsorption parameters, demonstrating that ssDNA and high molecular weight polymers exhibit differing probe–corona interactions, with binding affinities varying by a factor of ~2.7. Lastly, we show that MPA can be integrated with molecular dynamics simulations and thermodynamic modeling to predict analyte binding affinities for 42 phytohormones, enabling computational CoPhMoRe screening. This integration paves the way for rational sensor design without extensive experimental screening. Our findings underscore the utility of MPA in advancing nanomaterial-based sensing technologies through quantitative corona characterization and provide a framework for the rational design of selective nanosensors.

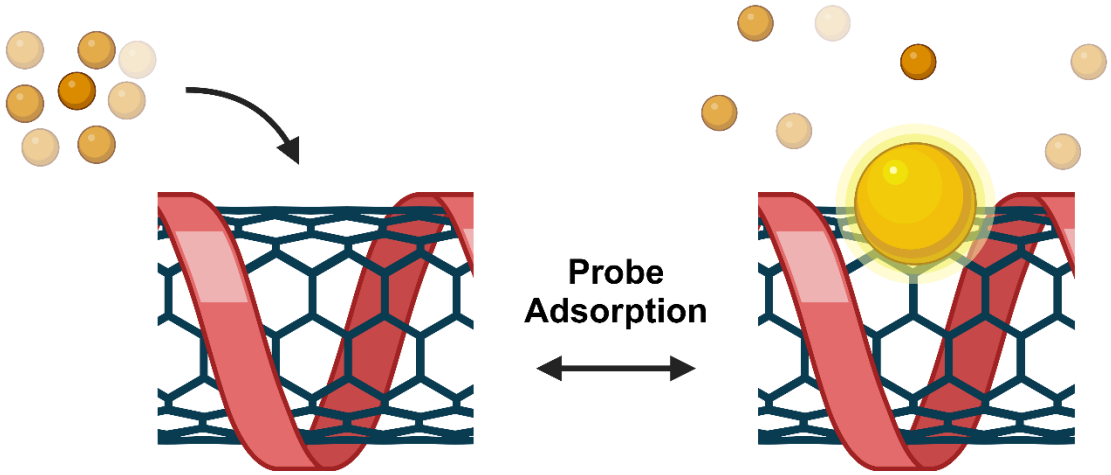

Figure 1. Schematic representation of the Molecular Probe Adsorption (MPA) technique. The probe (yellow) interacts with the nanotube surface, providing insight into the accessible surface area and the extent of corona (red) adsorption on the nanotube.

Session
NT 25（The 25th International Conference on the Science and Applications of Nanotubes and Low-

| Main conference：Main conference

Mon. Jun 16, 2025 6:00 PM - 8:00 PM JST | Mon. Jun 16, 2025 9:00 AM - 11:00 AM UTC Poster 1(International Exchange Hall III, Clock Tower Centennial Hall, 2F)

[16psa] Poster 1

[16psa-01]

Light Emission, Structure-Phase Evolution, and Photocatalytic Behavior in Full-Series Multilayered $GaTe_{1-x}S_x$ (0<=x<=1) with Direct-Transition Edge

*Ching-Hwa Ho[1], Luthviyah Choirotul Muhimmah[1] (1. National Taiwan University of Science and Technology, Graduate Institute of Applied Science and Technology (Taiwan))

[16psa-02]

Hydrophobicity and space confinement effect of carbon nanotube-alumina support on the Cu-Co catalysts for CO2 methanation

*Weizhong Qian[1], mingyu Ma[1], chaojie Cui[1] (1. Tsinghua University (China))

[16psa-03]

Double-Walled Carbon Nanotubes with Dynamic Strength of Over 90 GPa Enhanced by Intershell Friction

*Hongjie Yue[1], Fei Wei[1] (1. Tsinghua University (China))

[16psa-04]

Pd-based nanoparticles on reduced graphene oxide for formic acid electro-oxidation

*Patraporn Luksirikul[1], Pacharapon Kankla[1], Teera Butburee[2], Narong Chanlek[3], Suchinda Sattayaporn[4] (1. Kasetsart University (Thailand), 2. National Science and Technology Development Agency (Thailand), 3. Synchrotron Light Research Institute (Public Organization) (Thailand), 4. King Mongkut's University of Technology North Bangkok (Rayong Campus) (Thailand))

[16psa-05]

Half-Full Filled Aerogels with A 348% Increment in Energy Absorption and A Retained High Electromagnetic Shielding Performance

*zhengqiang lyu[1] (1. Suzhou Institute of Nano-Tech and Nano-Bionics, Chinese Academy of Sciences (China))

[16psa-06]

3D-structured carbon nanotube fibers as ultra-robust fabrics for adaptive electromagnetic shielding

*dongmei Hu[1] (1. Suzhou Institute of Nano-Tech and Nano-Bionics, Chinese Academy of Sciences (China))

[16psa-07]

Study on structure of carbon nanotubes for electrochemical electrodes

*Daichi Suzuki[1], Takemura Kenshin[1], Nao Terasaki[1] (1. AIST (Japan))

[16psa-08]

Mass density effects on thermal resistance of CNT forests

*Yamato Watanabe[1], Takayuki Nakano[1], Yoku Inoue[1] (1. Shizuoka Univ. (Japan))

[16psa-09]
Novel CNT-based thermal interface films: Design, fabrication, and evaluation

*Tomoki Okumura[1], Takayuki Nakano[1], Yoku Inoue[1] (1. Shizuoka Univ. (Japan))

[16psa-10]
Wafer-Scale Characterization of Macroscopic Defects in Aligned Carbon Nanotube Arrays Fabricated by Dimension-Limited Self-Alignment

*Bing Gao[1], Chuanhong Jin[1] (1. Zhejiang University (China))

[16psa-11]
Morphological evolution of atomic layer deposited hafnium oxide on aligned carbon nanotube arrays

*Sujuan Ding[1], Yifan Liu[2], Bing Gao[1], Bo Wang[1], Zhiyong Zhang[2], Chuanhong Jin[1] (1. Zhejiang Univ. (China), 2. Peking Univ. (China))

[16psa-12]
Bond based spectral map of oligomers in machine learning algorithm for MD vibrational spectra in graphene SERS sensor

*Tatiana Zolotoukhina[1], Haruto Goto[1], Yasuhiro Yamamoto[1] (1. Dep. of Mech. Engineering, Faculty of Eng., Toyama University (Japan))

[16psa-13]
Effective Fabrication of Suspended Graphene Nanoribbon Transistors for Width-Dependent Transition from Quantum Interference to Coulomb Blockade

*Yuan-Liang Zhong[1] (1. CYCU Univ. (Taiwan))

[16psa-14]
Strongly hybridized phonons and spontaneous electric polarizations in low-dimensional graphitic multilayers

Shaoqi Sun[1], Zhou Zhou[1], Xiyao Peng[1], Qingyun Lin[1], Yihuan Li[1], Daichi Kozawa[2], Huizhen Wu[1], Shigeo Maruyama[3], Pilkyung Moon[4], Toshikaze Kariyado[2], Ryo Kitaura[2], *Sihan Zhao[1] (1. Zhejiang University (China), 2. National Institute for Materials Science (Japan), 3. The University of Tokyo (Japan), 4. NYU Shanghai (China))

[16psa-15]
High-performance Transparent and Conductive CNT Films from Dilute Organic Dispersions

*Tsuyoshi Endo[1], Seiya Nishida[1], Hiroaki Kahara[1], Satoshi Yamazaki[2], Takashi Kodama[3], Yoko Iizumi[4], Toshiya Okazaki[4], Keigo Otsuka[1], Shigeo Maruyama[1], Shohei Chiashi[1] (1. Department of Mechanical Engineering, the University of Tokyo (Japan), 2. Furukawa Electric Co., Ltd. (Japan), 3. Dept. of Mech. and Control Eng., Kyushu Institute of technology (Japan), 4. National Institute of Advanced Industrial Science and Technology (Japan))

[16psa-16]
Mxene/metal Composites for Hydrogen Evolution Application

*Sergii A Sergiienko[1] (1. University of Chemistry and Technology, Prague (Czech Republic))

[16psa-17]
High near-field noise suppression in the 5G frequency bands for graphene sheets printed by jet-dispensing

*Masato Watanabe[1] (1. Research Institute for Electromagnetic Materials (Japan))

[16psa-18]

Session
NT 25 (The 25th International Conference on the Science and Applications of Nanotubes and Low-

Flavin-Wrapped Carbon Nanotubes for Fundamentals and Applications

*Sang-Yong Ju[1], Hangil Lee[2], Seongjoo Hwang[1] (1. Department of Chemistry, Yonsei University (Korea), 2. Department of Chemistry, Sookmyung Women's University (Korea))

[16psa-19]

Monocyclic Aromatic Molecule-Driven Confined Synthesis of 6-Armchair Graphene Nanoribbons

*Huiju Cao[1], Yingzhi Chen[1], Kunpeng Tang[1], Wendi Zhang[2], Kecheng Cao[2], Lei Shi[1] (1. Sun Yat-sen University (China), 2. ShanghaiTech University (China))

[16psa-20]

Inner Doping of Carbon Nanotubes with Perovskites and Charge Detection for High Performance Nanoelectronics

*Huimin Yin[1], Chuanhong Jin[1] (1. zhejiang university (China))

[16psa-21]

UHV exfoliation and rational functionalization of 2D materials

*Martin Kalbac[1] (1. J. Heyrovsky Institute of Physical Chemistry of the Czech Academy of Sciences (Czech Republic))

[16psa-22]

Microscopic Understanding of Metal Contacts to Aligned Carbon Nanotubes Arrays: Wetting and Coverage

*Haozhe Lu[1], Chuanhong Jin[1] (1. Zhejiang University (China))

[16psa-23]

Encapsulation and Electronic Modulation of Tungsten-Alloyed MoS_2 Nanoribbons in Carbon Nanotubes

*Yuanfang Zhang[1], Wenqi Lv[3], Fenfa Yao[2], Yanning Zhang[3], Xin Chen[1], Chuanhong Jin[2] (1. East China University of Science and Technology (China), 2. Zhejiang University (China), 3. University of Electronic Science and Technology (China))

[16psa-24]

Synthesis of carbon nanotubes using higher alkanes as a carbon source

*Łukasz Nowicki[1], Sandra Lepak-Kuc[2,1], Agnieszka Lekawa-Raus[1] (1. Centre for Advanced Materials and Technologies (CEZAMAT), Warsaw University of Technology (Poland), 2. Faculty of Mechanical and Industrial Engineering, Warsaw University of Technology (Poland))

[16psa-25]

Symmetry and asymmetry in carbon nanotube mutations and memory retention in long- and short-range

*Lin Chai[1], Fei Wei[1] (1. Tsinghua University (China))

[16psa-26]

Observation of strongly hybridized phonons in one-dimensional van der Waals crystals

*Shaoqi Sun[1], Qingyun Lin[1], Yihuan Li[1], Daichi Kozawa[2], Huizhen Wu[1], Shigeo Maruyama[3], Pilkyung Moon[4], Toshikaze Kariyado[2], Ryo Kitaura[2], Sihan Zhao[1] (1. Zhejiang Univ. (China), 2. National Institute for Materials Science (NIMS) (Japan), 3. The University of Tokyo (Japan), 4. NYU Shanghai (China))

[16psa-27]

Optical Modeling, Solver, and Design of Single-Enantiomer Carbon Nanotube Film and Reconfigurable Chiral Photonic Device

Jichao Fan[1], *Benjamin Hillam[1], Cheng Guo[2], Hiroyuki Fujinami[3], Koki Shiba[3], Haoyu Xie[1], Ruiyang Chen[1], Kazuhiro Yanagi[3], Weilu Gao[1] (1. Univ. of Utah (United States of America), 2. Stanford Univ. (United States of America), 3. Tokyo Metropolitan Univ. (Japan))

[16psa-28]

Anomalous Interfacial Electron Transfer Kinetics in Moiré Graphene

*Meg Grace Takezawa[1], Yun Yu[1], Kaidi Zhang[1], Sonal Maroo[1], Daniel Kwabena Bediako[1,2] (1. University of California, Berkeley (United States of America), 2. Lawrence Berkeley National Laboratory (United States of America))

[16psa-29]

Photoluminescence of gated mixed-dimensional heterostructures

*Ufuk Erkilic[1,2], Nan Fang[1], Chee Fai Fong[1], Yih-Ren Chang[1,2,3], Yuichiro K. Kato[1,2] (1. RIKEN Cluster for Pioneering Research (Japan), 2. RIKEN Center for Advanced Photonics (Japan), 3. Kobe Univ. (Japan))

[16psa-30]

Thermal Conductivity of Solution-Spun Carbon Nanotube Fibers with Different Draw Ratios

*Jiun-Hung Yi[1,2], Ognyan Stefanov[1,2], Michelle Durán-Chaves[2,3], Eldar Khabushev[2,4], Matteo Pasquali[2,3,4], Geoff Wehmeyer[1,2] (1. Department of Mechanical Engineering, William Marsh Rice University (United States of America), 2. The Carbon Hub, William Marsh Rice University (United States of America), 3. Department of Chemistry, William Marsh Rice University (United States of America), 4. Department of Chemical and Biomolecular Engineering, William Marsh Rice University (United States of America))

[16psa-31]

APPLICATION OF MULTIWALL CARBON NANOTUBES TO ENHANCE THE LUBRICATION PERFORMANCE OF MACHINE ELEMENTS

*Amarnath Muniyappa[1], Santhosh Kamarapu[1], Kamlesh Shivvedi[1], Chella durai[1] (1. Tribology and Machine Dynamics Laboratory, Department of Mechanical Engineering, Indian Institute of Information Technology, Design, and Manufacturing, Jabalpur, Madhya Pradesh, 482005, India (India))

[16psa-32]

Synthesis of single-unit-cell thin perovskites by liquid-phase confined assembly for high-performance ultrastable X-ray detectors

*Meihui Song[1], Feng Yang[1] (1. Southern University of Science and Technology (China))

[16psa-33]

Low power NO_2 sensing by MoS_2 photoactivated sensor with integrated micro-LED light source

*Hiroshi Tabata[1], Kotaro Fujii[1], Shuhei Ichikawa[1], Toshihiro Ishihara[1], Kazunobu Kojima[1], Yasufumi Fujiwara[1,2], Mitsuhiro Katayama[1] (1. Osaka Univ. (Japan), 2. Ritsumeikan Univ. (Japan))

[16psa-34]

Extraction of the true topography of carbon nanotubes on SiO_2/Si substrates by scanning electron microscopy

*Boxiang Zhang[1], Chuanhong Jin[1] (1. Zhejiang University (China))

[16psa-35]

High performance aligned carbon nanotube thin film transistors for mini- and micro-LED driving

*Xi Mei qi[1,2], Liu Fang[1], Zhu Xue hao[1], Li Yi[1], Bai Lan[1,2], Peng Lian mao[1,2], Cao Yu[1,2], Liang Xue Lei[1,2] (1. Peking University (China), 2. ICTFE-PKU (China))

[16psa-36]

Synthesis of a Hybrid Flexible Thermoelectric Device with Carbon Nanotubes and Chalcogenide-based Thermoelectric Materials

*Aarti Bisht[1], Bhasker Gahtori , Sanjay R. Dhakate, Bhanu Pratap Singh (1. Research Scholar (India))

[16psa-37]

The cross-scale assembly and mechanical behavior of super-strong carbon nanotubes

*Yukang Zhu[1], Fei Wei[1] (1. Tsinghua University (China))

[16psa-38]

Effects of Y on stabilizing Fe catalyst in carbon nanotube growth

*Duy Huy Khuong Le[1], Takayuki Nakano[1], Hisashi Sugime[2], Yoku Inoue[1] (1. Shizuoka University (Japan), 2. Kindai University (Japan))

[16psa-39]

Reinforcement of Polyimine Covalent Adaptable Networks with Mechanically Interlocked Derivatives of SWNTs

*ALEJANDRO LOPEZ-MORENO[1], ION ISASTI[1], SILVIA MIRANDA[1], DAVID M. JIMENEZ[1], SYLWIA PARZYSZEK[1], NATALIA MARTÍN SABANÉS[1], HENRIK PEDERSEN[2], EMILIO M. PEREZ[1] (1. IMDEA NANOSCIENCE (Spain), 2. Nanocore ApS (Denmark))

[16psa-40]

Overcoming the Yield-Quality Trade-off for Aerosol-CVD-Synthesized Single-Walled Carbon Nanotubes by Diameter Control

*Ilya V. Novikov[1], Yasir Shafi Mir[1], Il Hyun Lee[1], Jeong-Seok Nam[1], Il Jeon[1] (1. Sungkyunkwan University (Korea))

[16psa-41]

Boosted thermal conductivity of single-walled carbon nanotube films via BN welding and encapsulation

*Changping Yu[1,2], Feng Zhang[1,2], Chang Liu[1,2] (1. Shenyang National Laboratory for Materials Science, Institute of Metal Research, Chinese Academy of Sciences (China), 2. School of Materials Science and Engineering, University of Science and Technology of China (China))

[16psa-42]

Enhanced Efficiency in Dye-Sensitized Solar Cells Using Carbon Nanotube Composite Papers via Multiple Dye Fixation

*YI KOU[1], Takahide Oya[1,2] (1. Graduate School of Engineering Science, Yokohama National Univ. (Japan), 2. Semiconductor and Quantum Integrated Electronics Research Center, Institute for Multidisciplinary Sciences, Yokohama National Univ. (Japan))

[16psa-43]

Confined synthesis of nitrogen-doped graphene nanoribbons transformed from nitrogen-containing precursors

*Kunpeng Tang[1], Yingzhi Chen[1], Huiju Cao[1], Wendi Zhang[2], Kecheng Cao[2], Lei Shi[1] (1. Sun Yat-sen University (China), 2. ShanghaiTech University (China))

[16psa-44]

Annealing and Doping Effects on Axial Thermal Transport Properties of Solution-Spun Carbon Nanotube Fibers

*Ognyan Stefanov[1,2], Michelle Duran-Chaves[2,3], Aosheen Anand[2,3], Eldar Khabushev[2,4], Matteo Pasquali[2,3,4], Geoff Wehmeyer[1,2] (1. Department of Mechanical Engineering, William Marsh Rice University (United States of America), 2. The Carbon Hub, William Marsh Rice University (United States of America), 3. Department of Chemistry, William Marsh Rice University (United States of America), 4. Department of Chemical and Biomolecular Engineering, William Marsh Rice University (United States of America))

[16psa-45]

Cathodes based on V_2O_5 are an excellent material for fabricating symmetric supercapacitors for lithium-ion batteries

*Kaviyarasu Kasinathan[1] (1. UNESCO Africa Chair Nanoscience & Nanotechnology, University of South Africa. (South Africa))

[16psa-46]

Replica higher-order topology of Hofstadter butterflies in twisted bilayer graphene

*Youngkuk Kim[1] (1. Department of Physics, Sungkyunkwan University (Korea))

[16psa-47]

Bright trion emission in carbon-nanotube/tungsten-diselenide mixed-dimensional heterostructures

*Nan Fang[1], Ufuk Erkilic[1], Yih-Ren Chang[1], Shun Fujii[1,2], Daiki Yamashita[1,3], Chee Fai Fong[1], Yuichiro K. Kato[1] (1. RIKEN (Japan), 2. Keio Univ. (Japan), 3. AIST (Japan))

[16psa-48]

Diameter Controllable Separation of Single-Walled Carbon Nanotubes by Simply Changing the Metal in Phenanthroline-Based Supramolecular Polymers

*Xinyi Fu[1], Takuya Hayashi[2], Guoqing Cheng[1], Naoki Komatsu[1] (1. Graduate School of Human and Environmental Studies, Kyoto University (Japan), 2. Carbon Science Division, Research Institute for Supra Materials, Shinshu University (Japan))

[16psa-49]

High-Frequency Current Noise in Carbon Nanotubes due to Phonon Scattering

*Raimu Akimoto[1], Aina Sumiyoshi[1], Takahiro Yamamoto[1,2] (1. Department of Physics, Tokyo University of Science (Japan), 2. RIST, Tokyo University of Science (Japan))

[16psa-50]

Ceramic Cold Cathode X-ray Tubes with a Compact Size and High Performance Fabricated by CNT Film Field Elelctron Emitter

Cheol Jin LEE[1,2], *Hyunjea LEE[2], Jun Young Lee[2], Hosan Shin[2], Yejin Kong[2] (1. School of Electrical Engineering, Korea University (Korea), 2. LuminaX Co., Ltd (Korea))

[16psa-51]

Fully recyclable carbon nanotube fibers

*Michelle Duran-Chaves[1,2], Ivan Rosa Siqueira [1,2], Oliver Scott Dewey[1,2], Steven Williams[1,2], Cedric J. S. Ginestra [1,2], Juan de la Garza [1], Yingru Song [1], Geoff Wehmeyer [1,2,3], Matteo Pasquali[1,2,3] (1. Rice University (United States of America), 2. The Carbon Hub (United States of America), 3. The Smalley-Curl Institute (United States of America))

[16psa-52]

High-Sensitivity UV Photodetector Using 2D WS2/Ti2N MXene Quantum Dot Hybrid Structure

*Shamima Afroz[1], Annas Syhukri Ariffin[1], Anir Syahmi Sharbirin[1], Jeongyong Kim[1] (1. Sungkyunkwan University (Korea))

[16psa-53]

Integration of single-defect carbon nanotube photon sources into waveguide circuits for quantum applications

*Clement Deleau[1], Chee Fai Fong[1,2], Finn Sebastian[3], Jana Zaumseil[3], Yuichiro Kato[1,2] (1. Quantum Optoelectronics research team, RIKEN Center for Advanced Photonics (Japan), 2. Nanoscale Quantum Photonics Laboratory, RIKEN Cluster for Pioneering Research (Japan), 3. Institute for Physical Chemistry, Universität Heidelberg (Germany))

[16psa-54]

ENTANGLED EXITON EMISSION FROM EXCITON QUANTUM BITS MADE WITH CARBON NANOTUBES BY CONTROLLED-NOT GATE OPERATION

*Akira Hida[1], Koji Ishibashi[1] (1. RIKEN (Japan))

[16psa-55]

Electrospray deposition of single-walled carbon nanotube films
for gas sensors

*Yuto Nishizono[1], Ryo Kuchino[1], Shuhei Ichikawa[1], Kazunobu Kojima[1], Mitsuhiro Katayama[1], Hiroshi tabata[1] (1. Osaka university (Japan))

Light Emission, Structure-Phase Evolution, and Photocatalytic Behavior in Full-Series Multilayered $GaTe_{1-x}S_x$ ($0 \le x \le 1$) with Direct-Transition Edge

Ching-Hwa Ho[1], Luthviyah Choirotul Muhimmah[1]

[1]*Graduate Institute of Applied Science and Technology, National Taiwan University of Science and Technology, Taipei 106, Taiwan*

This work investigates multilayered $GaTe_{1-x}S_x$ semiconductors with a focus on its structural and optical analysis. High-purity single crystals of $GaTe_{1-x}S_x$ ($0 \le x \le 1$) were successfully grown by chemical vapor transport (CVT). The structural transformation was investigated using X-ray diffraction (XRD), scanning electron microscopy and energy-dispersive X-ray spectroscopy (SEM/EDS), and high-resolution transmission electron microscopy (HRTEM). The structural analyses reveal that the monoclinic (M) phase dominates for $0 \le x \le 0.4$, and the hexagonal (H) phase dominates for $0.425 \le x \le 1$. The M and H crystal phases of $GaTe_{1-x}S_x$ were analyzed. All GaTe with S-incorporation samples [$GaTe_{1-x}S_x$ ($0 \le x \le 0.9$) alloys] were discovered to consist of both M and H phases, whereas pure GaS crystal contained only the H phase. All lattice constants of the M- and H-$GaTe_{1-x}S_x$ series crystals were examined using HRTEM and XRD. Micro-Raman (μRaman), micro-photoluminescence (μPL), micro-time-resolved photoluminescence (μTRPL), micro-thermoreflectance (μTR), and area-fluoresce-lifetime mapping (AFLM) experiments were performed to characterize the band edge and optical properties of the multilayered $GaTe_{1-x}S_x$ samples in the M and H phases. The optical measurements revealed that the M phase dominates for $0 \le x \le 0.4$, whereas the H phase dominates for $0.425 \le x \le 1$. In the μTRPL experiment, the M phase exhibited higher energy and a shorter carrier recombination lifetime than those of the H phase in the same sample. The $GaTe_{1-x}S_x$ series containing both phases had band gaps ranging from NIR to blue light, starting from 1.588 eV (H-GaTe) to 2.5 eV (H-GaS, direct emission of the ε stacking fault). The emission range of M-$GaTe_{1-x}S_x$ ($0 \le x \le 0.4$) layers displays 1.65–1.77 eV (700–750 nm) and that of the H-$GaTe_{1-x}S_x$ ($0 \le x \le 1$) layers is 1.588–2.5 eV (496–780 nm). These monochalcogenides are promising for application in optoelectronic and light-emitting devices owing to their luminescence efficiency, two-color emission, and enhanced photodetection ability in the M- and H-$GaTe_{1-x}S_x$. Moreover, nanosheets of $GaTe_{1-x}S_x$ were developed as a photocatalyst to remove methylene blue (MB; $C_{16}H_{18}ClN_3S$) dye from water under visible light illumination. The photocatalytic results indicate that $GaTe_{1-x}S_x$ could be considered as a visible light water-splitting photocatalyst for further energy and environmental applications [1, 2].

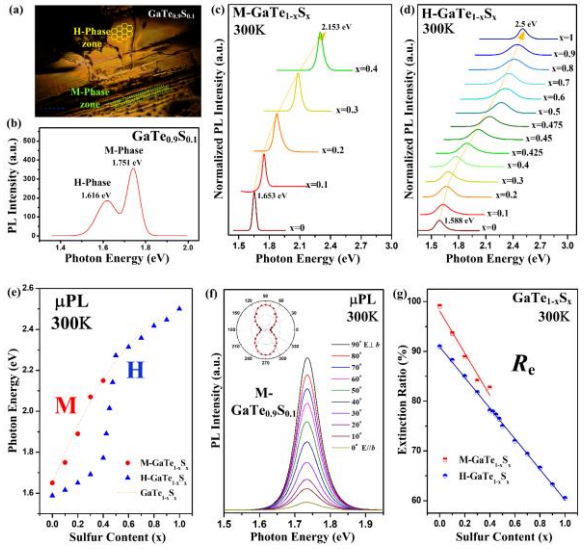

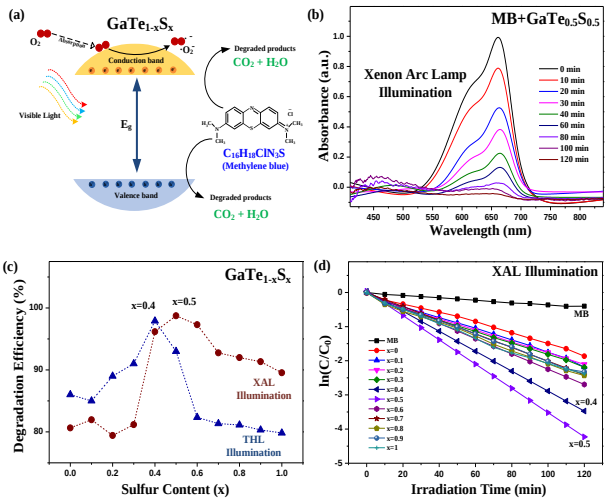

Fig. 2. Scheme and phtocatalytic degradation test of MB solutions. The x=0.4 and 0.5 own the best photocatalytic performance.

Fig. 1. (a) Microscope image of selective $GaTe_{0.9}S_{0.1}$. (b) The two-peak μPL spectrum combines the emissions of both the H- and M-phases of the multilayer $GaTe_{0.9}S_{0.1}$. The μPL spectra of each composition for (c) M-$GaTe_{1-x}S_x$ ($0 \le x \le 0.4$) and (d) H-$GaTe_{1-x}S_x$ ($0 \le x \le 1$) at 300 K. (e) Composition-dependent PL peak energies of multilayer M-$GaTe_{1-x}S_x$ ($0 \le x \le 4$) are indicated by red-solid circles and those of H-$GaTe_{1-x}S_x$ ($0 \le x \le 1$) are indicated by blue-solid triangles. (f) Angle-dependent polarized μPL spectra of M-$GaTe_{0.9}S_{0.1}$ measured at 300 K show the distinction of in-plane axial anisotropy. The inset shows the polar plot of the angle-dependent polarized PL intensity change of M-$GaTe_{0.9}S_{0.1}$. (g) Polarized extinction ratio (R_e) of μPL spectra in multilayered M-$GaTe_{1-x}S_x$ ($0 \le x \le 4$) and H-$GaTe_{1-x}S_x$ ($0 \le x \le 1$) at 300 K. The red line and blue line respectively show the linear fitted results of the polarized extinction ratios of the M- and H-phases..

[1] L. C. Muhimmah, Y. H. Peng, C. H. Ho, *Mater. Today Adv.* **21**, 100450 (2024).
[2] C. H. Ho, L. C. Muhimmah, *Mater. Sci. Engn. R* **161**, 100867 (2024).

Hydrophobicity and space confinement effect of carbon nanotube-alumina support on the Cu-Co catalysts for CO2 methanation

Weizhong Qian, Mingyu Ma, Chaojie Cui

Department of Chemical Engineering, Tsinghua University, Beijing, 100084. China

For the CO2 methanation reaction, the development of highly efficient catalysts at low temperatures is currently a key focus of research. This study investigated the space confinement effect of a carbon nanotube-alumina strip (CAS) support on Cu-Co bimetallic catalysts for CO2 methanation. CAS, prepared through extrusion of carbon nanotubes with an alumina precursor followed by high-temperature calcination, featured mesoporous structures and hydrophobic properties. The Cu-Co/CAS catalysts demonstrated superior catalytic performance compared to catalysts supported on individual carbon nanotubes or pure alumina. At 250°C and 1.5 MPa, the CO2 conversion reached 49.62%, with a CH4 selectivity of 95.98%. This enhanced performance was attributed to the hydrophobicity of the CAS support, which effectively removed water from the active sites, promoting equilibrium between the reverse water-gas shift and methanation reactions. Additionally, CAS support had a spatial confinement effect that increased the contact time of CO2 or intermediated with the active sites, compared with individual nanotube support. XPS and Raman spectroscopy confirmed the presence of oxygen vacancies in CAS, which facilitated CO2 methanation. Additionally, H2-TPR results, combined with DFT calculations, revealed that the CAS support altered the electronic structure of the Cu-Co active phase, enhancing its H2 adsorption and activation capabilities at low temperatures. As a result, it provided valuable insights for developing efficient low-temperature catalysts for CO2 methanation.

References

[1] Mingyu Ma *et al.*, Catalysis Today (2024) 437: 114781.

Double-Walled Carbon Nanotubes with Dynamic Strength of Over 90 GPa Enhanced by Intershell Friction

Hongjie Yue, Fei Wei

Beijing Key Laboratory of Green Chemical Reaction Engineering and Technology, Department of Chemical Engineering, Tsinghua University, Beijing, 100084, China

Email: hongjieyue23@outlook.com; wf-dce@tsinghua.edu.cn.

Low-dimensional ultra-strong nanomaterials have attracted great anticipation for applications under extreme dynamic conditions. A photocatalytic method is developed to selectively cut off the outer shell of double-walled carbon nanotubes (DWCNTs), achieving non-contact measurement of intershell friction with both high temporal and spatial resolutions at high sliding velocities under optical microscope. The intershell friction linearly increases with the sliding velocity, with a slope related to intershell distance and chirality of DWCNTs. The maximum measured friction reaches 194.1 ± 7.3 nN at a sliding velocity of 977 mm s^{-1}, a value comparable to the tensile force (~450 nN) for breaking the outer shell. Molecular dynamics simulations indicate that the velocity-dependent intershell friction is related to dynamic localized commensurate contacts. The friction-induced “intershell locking” enhances the effective dynamic strength of DWCNTs from 64.8 ± 3.4 GPa to 90.1 ± 4.0 GPa at a tensile strain rate of 3300 s^{-1}. This study reveals anomalous friction mechanisms at nanoscale and demonstrates promising application of DWCNTs as ultra-strong materials.

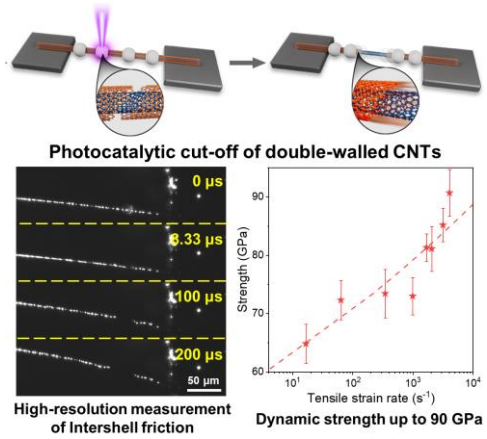

PD-BASED NANOPARTICLES ON REDUCED GRAPHENE OXIDE FOR FORMIC ACID ELECTRO-OXIDATION

P. Kankla[1,5], T. Butburee[2], N. Chanlek[3], S. Sattayaporn[4], P. Luksirikul[*1,5]

[1] Department of Chemistry, Faculty of Science, Kasetsart University (Thailand), [2] National Nanotechnology Center (NANOTEC), National Science and Technology Development Agency (NSTDA), (Thailand), [3] Synchrotron Light Research Institute (Public Organization) (Thailand), [4] Faculty of Science, Energy and Environment, King Mongkut's University of Technology North Bangkok (Rayong Campus) (Thailand), [5] Research Network NANOTEC-KU on Nanocatalysts and Nanomaterials for Sustainable Energy and Environment, Kasetsart University (Thailand)

Palladium-based catalyst is an attractive catalyst for a numerous low-temperature reaction, including automobile pollutants, CO oxidation, and electro-oxidation of formic acid. To maximize the capabilities of Pd-based catalysts in term of catalytic activity, durability and cost, the catalysts composition, structure, and support are necessary modified. In this study, Cr, Ni, Cu and Zn are chosen to rationalize with Pd-based catalysts composition on reduced graphene oxide (rGO) as carbon support. First, the mole proportion between Pd and metal (Ni) were studied in Pd_xNi series when x=1,2,4). The Pd_xNi/rGO were prepared in one-pot without the use of any surfactants. All Pd_xNi/rGO catalysts were characterized with the combination techniques of XRD, TEM/EDS, and XPS. The results confirmed the alloy of Pd_xNi nanoparticles with diameter of 5 nm decorated on rGO sheet. All the obtained catalysts are then used for the electro-oxidation of formic acid. The electro-oxidation measurements revealed that Pd_xNi/rGO samples exhibit superior electrocatalytic performance both in current densities and stabilities for formic acid oxidation (FAO) compared to Pd/rGO, and Pd_4Ni/rGO showed the electrocatalytic activity among the other Pd_xNi/rGO samples. With the same ratio, Pd_4Cr/rGO exhibited higher efficiency towards FAO than the other series in order of Pd_4Cr/rGO > Pd_4Ni/rGO > Pd_4Cu/rGO > Pd_4Zn/rGO.

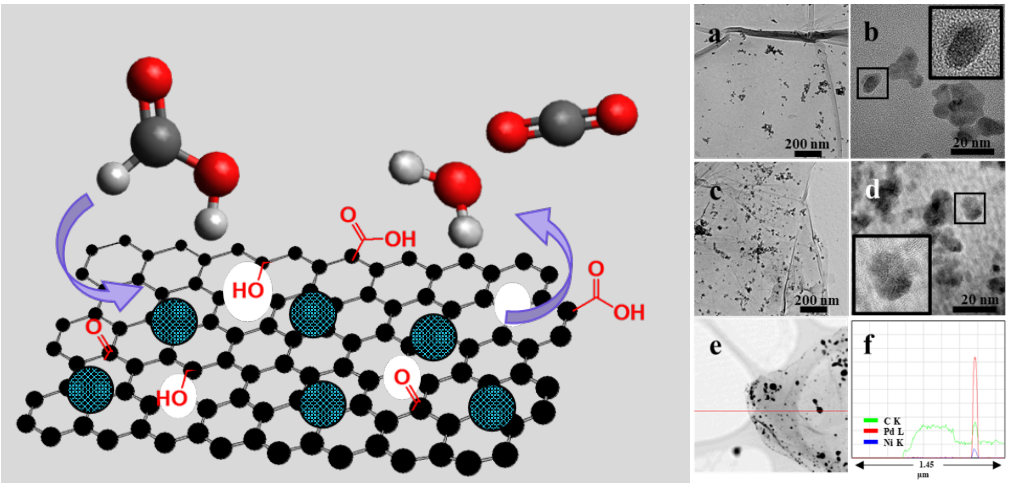

Figure1 Schematic showing formic acid oxidation over Pd-based on rGO catalyst. TEM and HR-TEM images of Pd/rGO (a,b), Pd_4Ni/rGO (c,d), and the close-up TEM of Pd_4Ni/rGO (e) with the corresponding line-scan to indicate distribution curve (f).

References

[1] X. Yu, P.G. Pickup, Recent Advances in Direct Formic Acid Fuel Cells (DFAFC). *J. Power Sources* **182**, 124−132 (2008).
[2] P. Kankla, J. Limtrakul, M.L.H Green, N. Chanlek, P. Luksirikul, *Applied Surface Science* **471**, 176–184 (2019).
[3] P. Kankla, T. Butburee, N. Chanlek, S. Sattayaporn. P. Luksirikul, *Topics in Catalysis* **66**, 1608–1618 (2023).

Half-Full Filled Aerogels with A 348% Increment in Energy Absorption and A Retained High Electromagnetic Shielding Performance

Ying Kong[1,2], Zhengqiang Lv[1], Jin Wang[1], Dongmei Hu[1]

[1]Key Laboratory of Multifunctional and Smart Systems, Suzhou Institute of Nano-Tech and Nano-Bionics, Chinese Academy of Science (China), [2]University of Shanghai for Science and Technology, School of Energy and Power Engineering (China)

Abstract

Aerogels, as kinetic energy absorbing materials, can find crucial applications for safeguarding in transportation, sports, buildings, construction, and aerospace. However, the highly porous structure makes it extremely fragile for endurance usage. In this study, a half-full filled structure has been proposed, and the concept has been demonstrated based on shear thickening fluid (STF) and chemically vapor deposited carbon nanotube aerogels (CNTAs), in which the outer part of CNTA is filled with STF while the inner core keeping unfilled. Chemical vapor deposition significantly enhances the elasticity and electromagnetic shielding performance of the native CNTA. The half-full filled aerogels (HFFA) show a 348% increase in energy absorption compared to the CNTA. At the same time, the density, electronic conductivity, and electromagnetic interference shielding effectiveness (EMI SE) of the HFFAs are 0.117 g cm^{-3}, 1213 S m^{-1}, and 69.52 dB (which is a neglectable reduction of 0.63% compared to native CNTA), respectively. The HFFA strategy provides an alternative route to fabricate robust aerogels with a remarkable increase of target properties while maintaining other properties, such as low density, high pore volume, and conductivity, with limited changes.

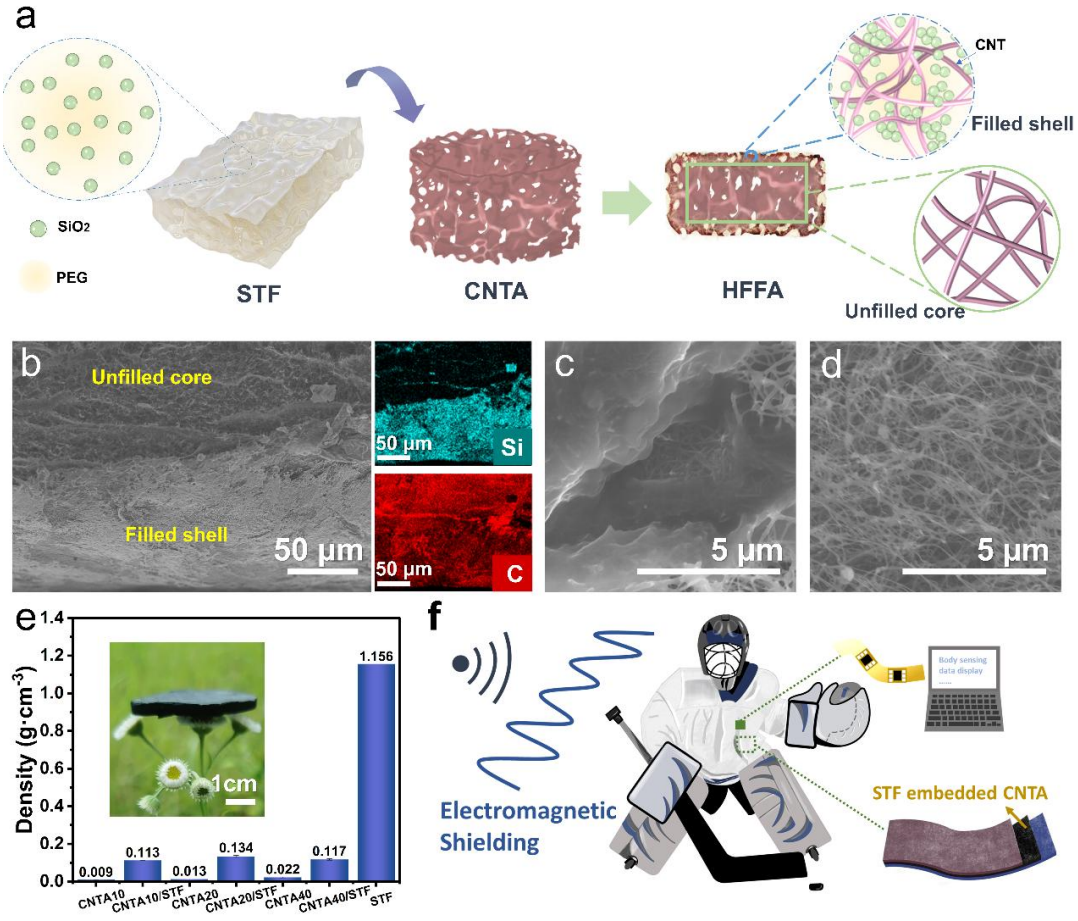

Figure: (a) Schematic diagram of the synthetic process of CNTA-based HFFA. (b) SEM and EDS images of the CNTA-based HFFA. (c) SEM of the outside layer of the CNTA-based HFFA. (d) SEM of the inner core of the CNTA-based HFFA. (e) The density of the CNTA-based HFFA and STF is as indicated. Inset is the photo image of HFFA. (f) Proposed applications of the HFFA for wearable and construction protection.

3D-structured carbon nanotube fibers as ultra-robust fabrics for adaptive electromagnetic shielding

Dongping Li[1,2], Ping Wang[2], Yan Zhang[2], Jin Wang[1], Dongmei Hu[1]

[1]Key Laboratory of Multifunctional and Smart Systems, Suzhou Institute of Nano-Tech and Nano-Bionics, Chinese Academy of Sciences (China), [2]College of Textile and Clothing Engineering of Soochow University (China)

Abstract

Wireless communication technology is indispensable in our daily lives, but it also results in serious electromagnetic radiation pollution. Hence, developing smart electromagnetic interference shielding materials with adjustable electromagnetic wave (EMW) responses holds significant promise for future electromagnetic shielding devices. In this study, we propose an electromagnetic shielding switch (ESS) characterized by tunable electromagnetic shielding performance achieved by fabricating a 3D carbon nanotube-based spacer fabric (CNT-SF) and modifying CNT-SF with chemical vapor deposition (CCNT-SF). The CCNT-SF displays direction-dependent electrical conductivity by manipulating the warp and weft density, measuring 128 S/m transversely and 447 S/m vertically. This characteristic allows the CCNT-SF to transmit or shield EMW by adjusting the angle of EMW incidence through fabric rotation, resulting in anisotropic electromagnetic shielding performance (33 dB transversely and 87 dB vertically). This feature enables switchable shielding with an on/off ratio of 2.64. Furthermore, the unique 3D structure confers excellent mechanical properties on the fabric, with compressive strength reaching 120 kPa. As a flexible, lightweight, and mechanically robust ESS, the CCNT-SF holds promising prospects for mitigating the challenges of increasingly severe and intricate electromagnetic environments.

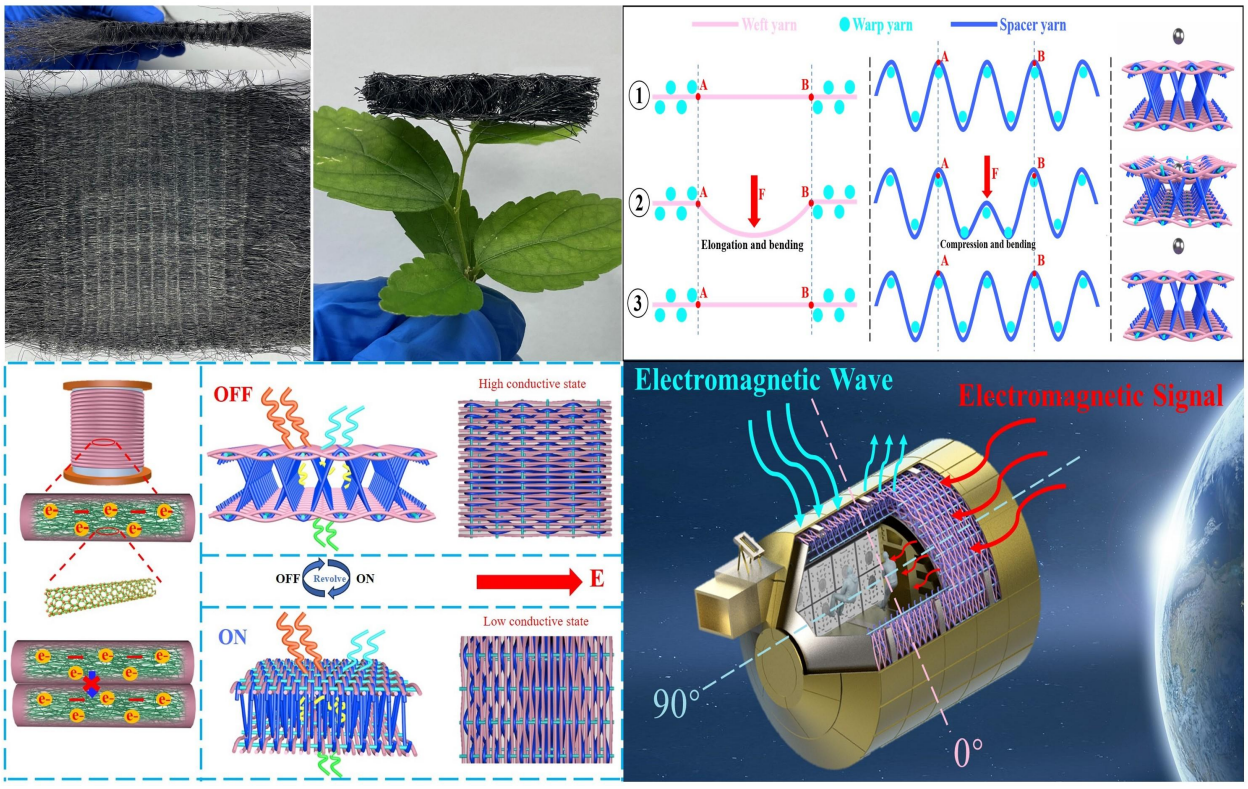

Figure: The Weaving of Carbon Nanotube Fibers and Their Application in Electromagnetic Shielding Switches.

Study on structure of carbon nanotubes for electrochemical electrodes

D. Suzuki, K. Takemura, N. Terasaki

Sensing System Research Center, National Institute of Advanced Industrial Science and Technology (AIST) (Japan)

Electrochemical detection by cyclic voltammetry (CV) measurements is the most common bioanalytical method that can measure target viruses in solution with high sensitivity and speed. Because CV measurements utilize chemical reactions on the electrode surface, the material and surface morphology of the electrode are important factors that determine the sensitivity. There have been many reports that utilizes carbon nanotube (CNT) films as electrochemical electrodes has improved the sensitivity of biosensing due to their physical/chemical robustness and large specific surface area. On the other hand, although the chemical reactions of CNTs change depending on their structure, such as diameter and chirality [1], the structure of CNTs suitable for use as electrochemical electrodes has not yet been elucidated.

Therefore, in this study, we investigated the effect of various CNT structures on their performance as electrochemical electrodes for virus detection. As a result of evaluating CNTs with different structures, we found that the amount of antibody modification is almost independent of the micro-morphology, but depends on the nano-morphology such as the synthesis method of CNTs and the dispersant used for their preparation. In addition, a comparison of antigen-antibody reactions by CV measurements revealed that two parameters, the amount of antibody modification and the electrical conductivity of CNTs, are important. By using the optimally structured CNT film as an electrochemical electrode, we achieved a limit of detection of 1 fg/mL for norovirus sensing. We also clarified the relationship between the structural factors of CNTs and their electrochemical reactions, which was previously unknown, providing an important guide for the development of CNT biosensors. This result is expected to contribute to the development of virus sensors and to the improvement of the performance of devices that use electrochemical electrodes, such as batteries and catalysts.

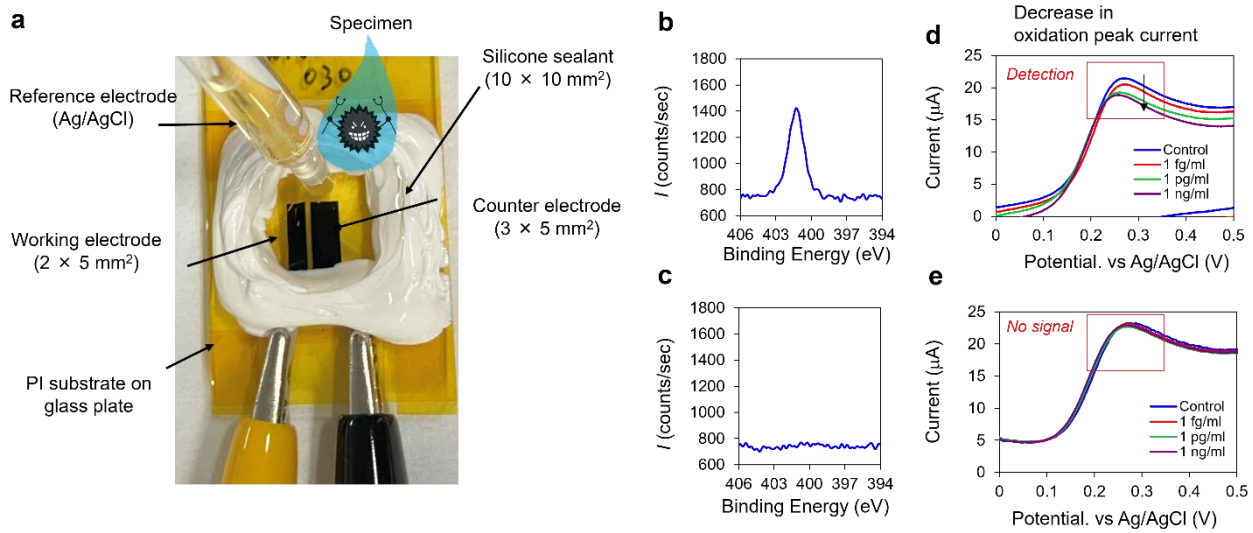

Figure 3. (a) Photographic image of the CNT electrochemical virus sensor. (b–c) XPS spectra in the N 1s region of (b) CNT film with well-adsorbed antibodies and (c) CNT film with no antibody adsorbed. (d-e) CVs of the electrochemical virus sensor of (d) CNT film with well-adsorbed antibodies and (e) CNT film with no antibody adsorbed.

References (if desired)

[1] D. Suzuki *et al.*, *AIP Advances* **15**, 015318 (2025).

Mass density effects on thermal resistance of CNT forests

Yamato Watanabe, Takayuki Nakano, Yoku Inoue

Shizuoka University (Japan)

Thermal interface materials (TIMs) are becoming increasingly crucial for enhancing heat dissipation efficiency in electronic devices. Among these materials, carbon nanotubes (CNTs) stand out for their exceptional thermal conductivity and mechanical flexibility. When CNTs are used as TIMs, it is crucial to consider interfacial thermal resistance alongside the material's thermal conductivity. In addition, there is a trade-off relationship where the mass density of CNTs tends to decrease with increasing length [1]. However, the topic of thermal resistance, particularly concerning the trade-off and the metal/CNT interface, has seldom been addressed. In this study, we investigated the thermal resistance of CNT forests as a function of length, with a focus on the impact of dynamic density decay during CNT growth.

We investigated the thermal properties of CNT forests and their interfacial thermal resistance using transient thermal response measurements. The high-density CNT forests were grown by chemical vapor deposition (CVD) with varying lengths (100-1100 μm). These CNT forests were subsequently detached and subjected to thermal transient response experiments. The resulting transient cooling curves were numerically converted into thermal structure functions, allowing for a detailed analysis of thermal resistance.

The thermal structure functions of CNTs of different lengths are shown in Fig. 1(a). Longer CNT forests have wider flat areas in the staircase-like structure function, indicating higher thermal resistance. Figure 1(b) shows the thermal resistance of CNT forests as a function of CNT height. We found that thermal resistance increases non linearly with height. The nonlinear increase suggests that the macroscopic thermal conductivity of the CNT forest decreases as the forest length increases. This is because, with longer CNT forests, the density at the root decreases, leading to a reduction in the thermal conduction pathways. Since the CNT catalyst becomes deactivated due to thermal diffusion during synthesis, the root density decreases as synthesis time increases. We proposed an equivalent circuit model using a dynamic density decay model [1], and calculations were performed for the nonlinear increase in Fig. 1(b). The calculation results indicate that the thermal conductivity of individual CNTs ranges from 120 to 150 W/m·K, which is comparative to reported values. We also studied the annealing effects (> 2000 °C) on thermal resistance, and it was found that the thermal resistance of CNT forests decreases with increasing crystallization, and the thermal conductivity increases by a factor of two or more.

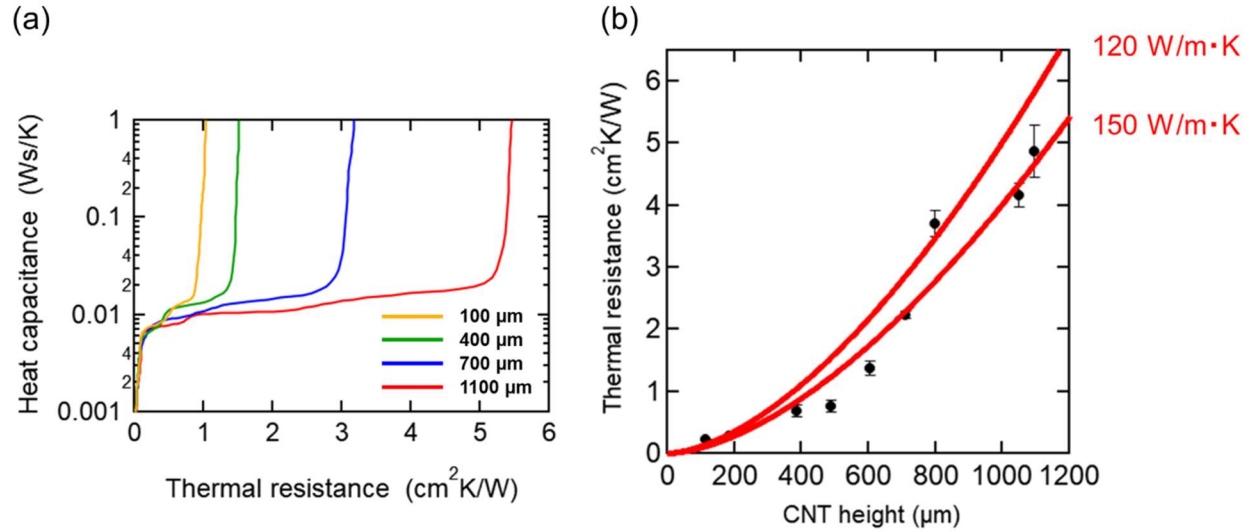

Figure 1: (a) Thermal structure function of CNTs of different lengths (100, 400, 700, 1100 μm). (b) Relationship between CNT height and thermal resistance.

References

[1] K. Tabata *et al.*, *J. Phys. Chem. C.* **126**, 20448–20455 (2022).

Novel CNT-based thermal interface films: Design, fabrication, and evaluation

Tomoki Okumura, Takayuki Nakano, Yoku Inoue

Shizuoka University (Japan)

The increasing power consumption of high-performance integrated circuits has driven the need for advanced heat dissipation technologies, particularly high-performance thermal interface materials (TIMs). Conventional thermally conductive greases suffer from pump-out issues at high temperatures and during long-term operation. In this context, carbon nanotube (CNT) forests, which combine high thermal conductivity, flexibility, and solid-state stability, have attracted significant attention.

In this study, we developed a high-density CNT-TIM film technology for next-generation TIM applications. Transient thermal response measurements were employed to evaluate heat transport within the TIMs and the overall heat dissipation system under simulated operating conditions.

CNT forests were synthesized on Si substrates, Cu foil, and graphite sheets. A multilayer $Fe/Al_2O_3/SiO_2$ catalyst was deposited via RF sputtering, covering both sides of Cu foil and graphite sheets. Using C_2H_2 as the carbon source, high-density CNT forests (~50 μm in length, 140 mg/cm^3 in density) were grown via a rapid-heating thermal chemical vapor deposition (CVD) process. To fabricate the CNT-TIM structures, CNTs were integrated with an inter-film layer, forming a CNT/inter-film/CNT configuration. Specifically, CNTs synthesized on a Si substrate were hot-pressed onto both sides of a polyphenylene sulfide (PPS) film, creating a robust CNT/PPS/CNT structure. Alternatively, CNT forests were directly grown on both sides of Cu foil and graphite sheets to form CNT/Cu/CNT and CNT/Graphite/CNT structures, respectively.

Transient thermal response measurements (Fig. 1(a)) were conducted to assess the thermal resistance of these TIMs. The obtained cooling curves were numerically converted into thermal structure functions, enabling an estimation of the thermal resistance via step-structure decomposition. A comparative analysis of CNT/PPS/CNT, CNT/Cu/CNT, and CNT/Graphite/CNT samples, each ~100 μm thick and in direct contact with a cold plate, is shown in Fig. 1(b), with pressure dependence results in Fig. 1(c). The CNT-TIMs on PPS and Cu foil exhibited relatively low thermal resistance (~1 cm^{2}K/W). Despite PPS having low intrinsic thermal conductivity, its minimal thickness prevented significant thermal resistance buildup, confirming its suitability for CNT-TIM integration. The pressure dependence analysis further revealed that even under low contact pressure (~100 kPa), CNT forest tips formed effective thermal contacts with metal surfaces, ensuring efficient heat dissipation.

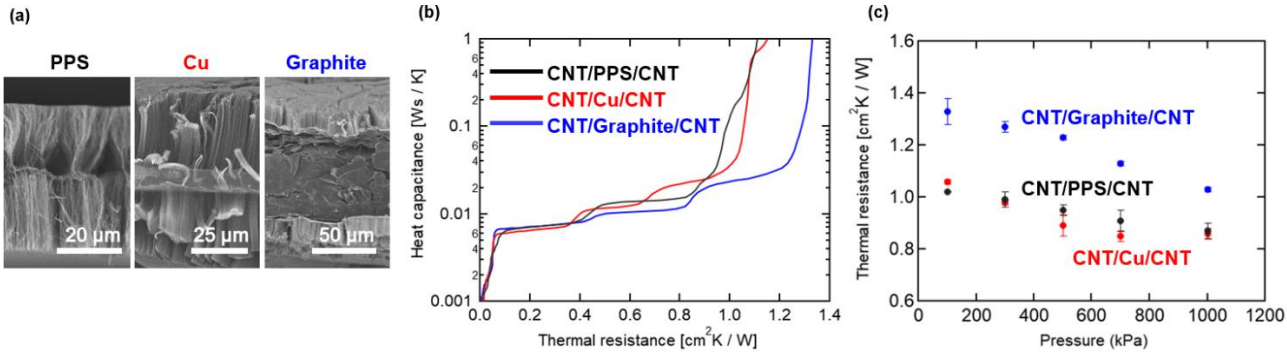

Fig.1: (a) Cross-sectional SEM images of CNT-TIMs. (b) Comparison of typical structure functions of the CNT-TIMs. (c) Pressure dependence of thermal resistance of CNT-TIMs.

Wafer-Scale Characterization of Macroscopic Defects in Aligned Carbon Nanotube Arrays Fabricated by Dimension-Limited Self-Alignment

Bing Gao[1*], Chuanhong Jin[1]

[1] *State Key Laboratory of Silicon and Advanced Semiconductor Materials, School of Materials Science and Engineering, Zhejiang University (China)*

**Correspondence to: binggao@zju.edu.cn*

Aligned carbon nanotube arrays (A-CNTs) with high density and semiconducting purity are critical for developing high-performance CNT-based devices. However, current solution-based assembly processes for A-CNTs[1][2] remain immature, often resulting in arrangement defects that dominate the wafer and degrade device performance[3][4]. To address this, understanding defect formation mechanisms and improving wafer quality require a wafer-scale characterization method with reasonable spatial resolution and throughput—a capability that remains elusive. In this study, we employed scanning electron microscopy (SEM) and polarized optical microscopy (POM) to comprehensively characterize macroscopic defects in A-CNTs fabricated via dimension-limited self-alignment (DLSA). We identified distinct defect types, including global misorientation, topological defects, and local defects, each exhibiting unique features and suggesting different formation mechanisms. Wafer-scale imaging and statistical sampling revealed a concentrated orientation distribution with a low defect-area ratio, though defect concentrations were notably higher at the wafer edges. These findings provide insights into defect origins and guide strategies for enhancing A-CNT wafer quality.

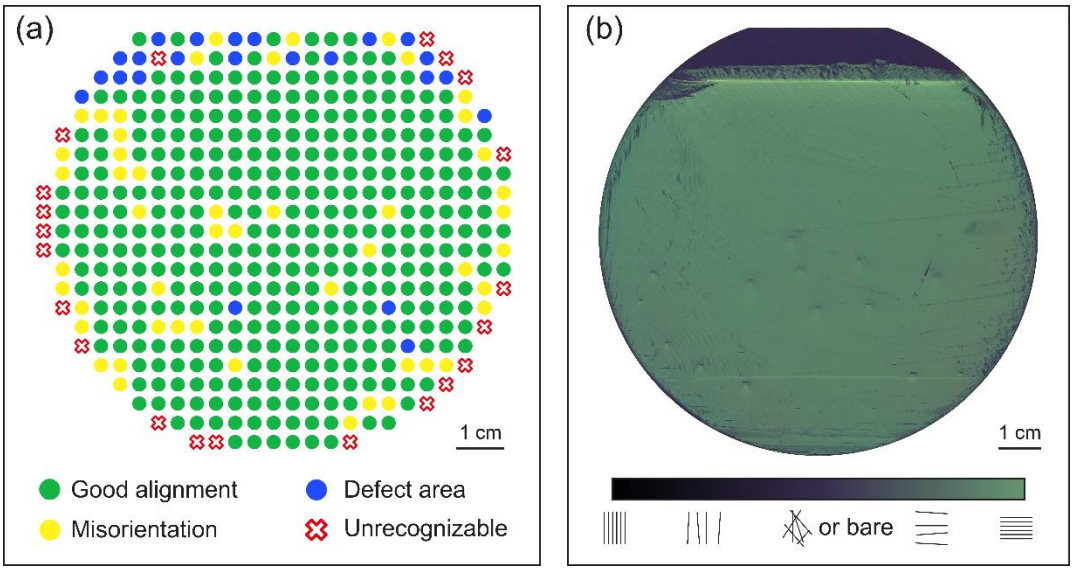

Figure1: Wafer-scale sampling and imaging of two A-CNTs wafers. (a) Sampling map of CNT alignment classification using SEM. Each point represents a single SEM image, with a 4 mm spacing between adjacent points. (b) POM image of an A-CNTs wafer. The two polarizing filters, positioned at the light source and before the camera, are oriented 1° to 4° from perpendicular to each other and aligned at ±45° relative to the vertical axis, respectively.

References

[1] L. Liu, *et al*., *Science* **368 (6493)**, 850-856 (2020).
[2] K. R. Jinkins, *et al*., *Science advances* **7 (37)**, eabh0640 (2021).
[3] B. Wang, *et al*., *ACS nano* **18 (33)**, 22474-22483 (2024).
[4] T. A. Chao, *et al*., *Advanced Materials Interfaces* 11(6) 2300684 (2024).

Morphological evolution of atomic layer deposited hafnium oxide on aligned carbon nanotube arrays

Sujuan Ding[1*], Yifan Liu[2], Bing Gao[1], Bo Wang[1], Zhiyong Zhang[2], Chuanhong Jin[1*]

[1] State Key Laboratory of Silicon and Advanced Semiconductor Materials, School of Materials Science and Engineering, Zhejiang University (China), [2] Key Laboratory for the Physics and Chemistry of Nanodevices and Center for Carbon-based Electronics, School of Electronics, Peking University (China)

**Correspondence to: dingsujuan@zju.edu.cn*

Semiconducting single-walled carbon nanotubes arrays (A-CNTs) are emerging as successors to silicon as the building block for next-generation high-performance devices [1,2]. However, issues on how to form high-quality high-κ dielectrics (like HfO_2) in CNTs seem to be unique, since the dangling-bond-free and thus chemical-inert surfaces of CNTs inherently unfavor the nucleation of HfO_2 through processes like atomic layer deposition (ALD) [3]. Microscopic study on the nucleation and growth of ALD dielectrics onto CNTs is an essential while challenging task. Here, we capture the morphological evolution and growth behaviors of ALD-HfO_2 onto SiO_2/Si-supported A-CNTs under three ALD recipes via cross-sectional high-resolution scanning transmission electron microscopy (STEM). The HfO_2 in ALD I (200℃) preferentially nucleates on SiO_2 substrate in heterogeneous growth mode, resulting in films with considerable pinholes. While ALD II (90℃) and III (90℃ and extra H_2O presoak) exhibit homogeneous growth with nucleation on both SiO_2 and CNTs, yielding uniform films. Arrangement defects in A-CNTs exacerbate non-uniformity of HfO_2 and tube-tube separation plays deterministic roles affecting the HfO_2-CNT interfacial morphology. Electrical measurements from A-CNT metal-oxide-semiconductor devices validate these findings. Our investigation contributes valuable insights for optimizing ALD processes for enhanced dielectric integration on A-CNTs in next-generation electronics [4].

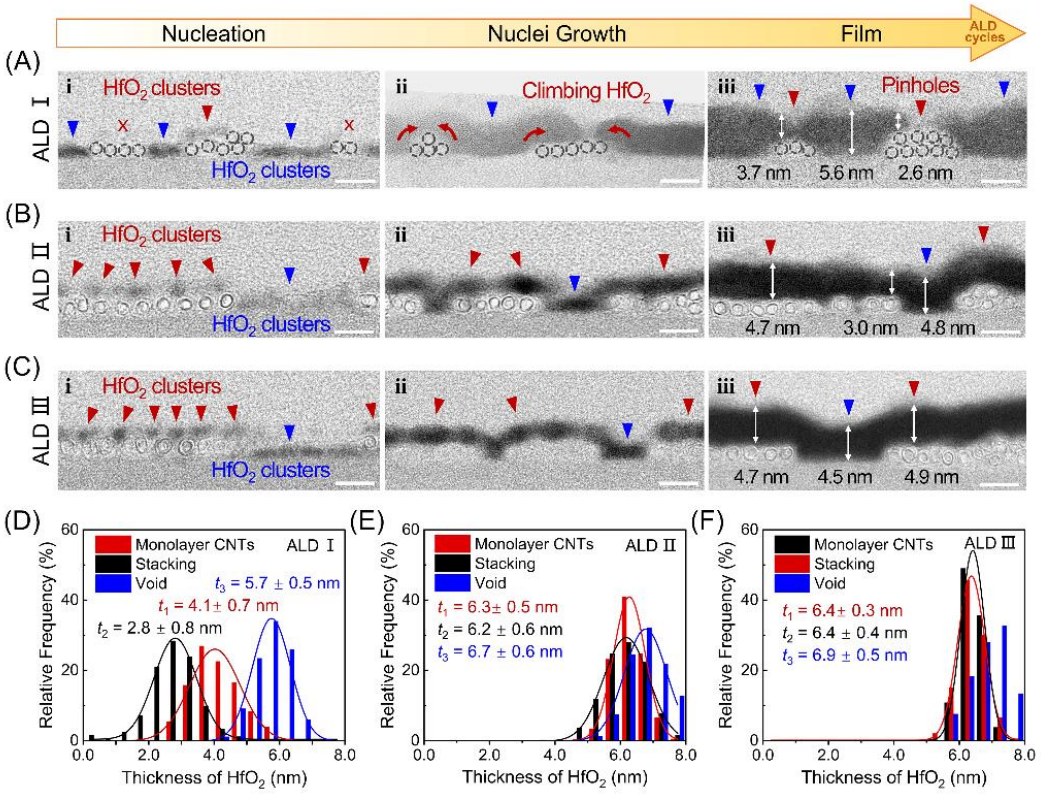

Nucleation and growth process of HfO_2 on A-CNTs under three different recipes.

References

[1] Liu, L. *et al.*, *Science*, 368 (6493), 850–856 (2020).
[2] Lin, Y. *et al.*, *Nat Electron.*, 6 (7), 506–515 (2023).
[3] Wang, X *et al.*, *JACS.*, 130 (26), 8152–8153 (2008).
[4] Ding, S. *et al.*, *Nano Letters* 24 (43), 13631-13637 (2024).

Bond based spectral map of oligomers in machine learning algorithm for MD vibrational spectra in graphene SERS sensor

T. Zolotoukhina[1], H. Goto[1], Y. Yamamoto[1].

[1] *Department of Mechanical Engineering, University of Toyama, Toyama 930-8555, (Japan)*

The use of machine learning (ML) algorithms in optical measurements correlates with the application of ML in molecular simulations, where applications were extended from potential predictions to models for machine learning tensorial properties, such as molecular dipole moments and polarizability tensors [1-3]. Such algorithms lead to calculations of the IR and Raman spectra and reconnect with corresponding measured spectra, respectively.

The contribution of the ML methods to the large-scale research on DNA/RNA and protein could lead to the automation of down to the single oligomer identification in simulation as well as in spectroscopic real-time experiments. The parallel utilization of ML in the surface-enhanced Raman scattering (SERS) sensors and their simulated models can improve the detectability of single oligomers through evaluation in the models of spectral variations related to interaction with environments and conformational motion.

Molecular dynamics (MD) provides simulated vibrational spectra in various interaction environments and molecular conformations through spectral maps of individual bonds. Identification of oligomers in varying environments can be done by the Random Forest (RF) algorithm in ML that has already shown high accuracy for the experimental Raman spectra. The MD model of the SERS sensor consisting of graphene film with nanopore and attached plasmon Au nanoparticles was used to propagate the target molecules of DNA nucleotides, which bond spectra were collected. To create an extended dataset from bond spectral data, the calculated MD spectra of nucleotide's base bonds with correlation decay component were simultaneously baseline corrected using SpectroChemPy package library with equivalent accuracy. The corrected spectral maps were then weighted with bond polarizabilities [4,5] for individual bond spectraa to reflect the quantum definition of Raman spectra as the Fourier transform of polarizability correlation. The bond spectral maps together with spectral ring average that corresponds to the measured Raman spectra were used for training and test datasets in Random Forest algorithms (80% to 20% split, selection of test data as random and fixed part) to reproduce the spectra of ring averages along with the reproduction of individual spectra of bonds included into datasets. For individual bonds in the datasets, the reproduction accuracy has reached the 0.5 ~1% mean absolute error, and therefore, the accuracy of the ring average can be estimated to be around 97-98%, which corresponds to the accuracy of the experimentally measured spectra treated with RF algorithms.

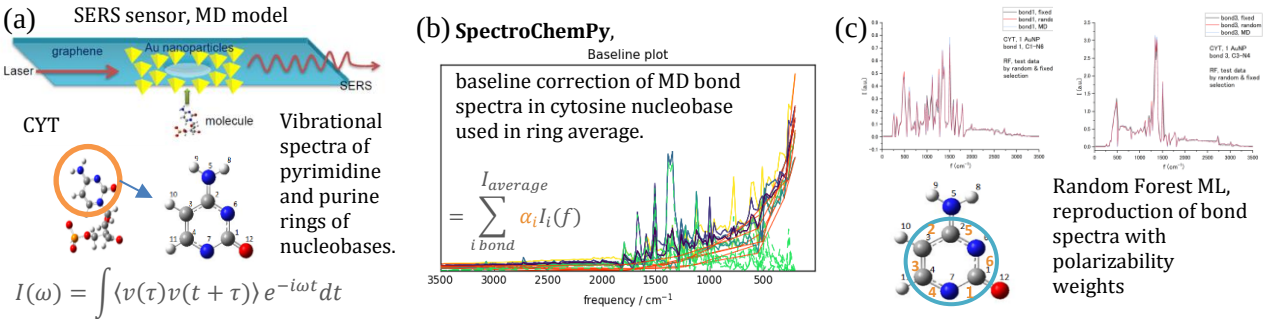

Figure 1. (a) MD model of the SERS sensor, (b) baseline correction of MD bond spectra in spectral map, (c) reproduction by RF algorithm of bond spectra for the bonds 1 & 3 in the pyrimidine cytosine ring [bond # in orange]**.**

References

[1] J. K. Sowa, P. J. Rossky, *J. Chem. Theory Comput*., **20**, 10071−10079 (2024)
[2] H. Zhou, L. Xu, Z. Ren, J. Zhu and C. Lee, *Nanoscale Adv*., **5**, 538 (2023).
[3] R. Ochoa, T. Fox, *J. of Mol. Graphics and Modelling*, **125**, 108608 (2023).
[4] D. Zarena, N. Jyothi, *Ind. J. of Advances in Chemical Science*, **11**(1), 55-57 (2023).
[5] D.W. Snoke, M. Cardona, S. Sanguinetti, G. Benedek, *Phys. Rev. B* **53**, 12641 (1996).
[6] T. Zolotoukhina, M. Yamada, S. Iwakura, *Biosensors*, **11**(2),37 (2021)

Effective Fabrication of Suspended Graphene Nanoribbon Transistors for Width-Dependent Transition from Quantum Interference to Coulomb Blockade

Yuan-Liang Zhong[1*], Jyun-Hong Chen[1, 2], Yann-Wen Lan[3], Lain-Jong Li[4], Chiashain Chuang[5]

[1]1Department of Physics and Quantum Information Center, Chung Yuan Christian University, Taoyuan 320, Taiwan

2National Applied Research Laboratories, National Taiwan Semiconductor Research Institute, Hsinchu 30078, Taiwan

3Department of Physics, National Taiwan Normal University, Taipei 11677, Taiwan.

4Department of Mechanical Engineering, The University of Hong Kong, Hong Kong 999077, China

5Department of Electronic Engineering and Research Center for Semiconductor Materials and Advanced Optics, Chung Yuan Christian University, Taoyuan 320, Taiwan

Quantum transport in graphene nanoribbons is crucial for various electronic and quantum device applications. For example, the Coulomb blockade effect in graphene nanoribbon devices could be utilized in quantum computing, single-electron transistors, and sensitive charge detectors. However, the wafer scale and mass production for high quality chemical vapor deposition graphene nanoribbons with effective costs and fabrications in order to perform quantum transport behaviors well remain a challenge. We effectively fabricated suspended chemical vapor deposition graphene nanoribbons varying widths ranging from 705 to 50 nm and approximately 150 nm in length to investigate electron transport characteristics concerning the sample scale. Our findings reveal a transition in electron transport behavior from observing magnetoresistance fluctuations due to quantum interference phenomena, such as weak localization, universal conductance fluctuations and to single electron transport, such as Coulomb blockade. Coulomb blockade behavior was observed, particularly pronounced in nanoribbons with a width of 50 nm, and evidenced by diamond-like structures in the source-drain versus back-gate voltage characteristics, a great advantage for applications in designs and applications in graphene-based electronic and quantum devices.

Strongly hybridized phonons and spontaneous electric polarizations in low-dimensional graphitic multilayers

S. Sun[1], Z. Zhou[1], X. Peng[1], Q. Lin[2], Y. Li[1], D. Kozawa[3], H. Wu[1], S. Maruyama[4], P. Moon[5], R. Kitaura[3], T. Kariyado[3], **S. Zhao**[1]

[1]School of Physics, Zhejiang University, Hangzhou 310058 (China) [2]Center of Electron Microscopy, School of Materials Science and Engineering, Zhejiang University, Hangzhou 310027 (China) [3]Research Center for Materials Nanoarchitectonics (MANA), National Institute for Materials Science (NIMS), 1-1 Namiki, Tsukuba 305-0044 (Japan) [4]Department of Mechanical Engineering, The University of Tokyo, Tokyo 113-8656 (Japan) [5]Arts and Sciences, NYU Shanghai, Shanghai 200124 (China)

The rich interlayer couplings in graphitic multilayers and versatile controlling knobs to tune their physical properties have led to significant advancements in condensed matter physics in recent years. In this talk, I will present two recent works in our study of two low-dimensional graphitic multilayer systems: the discovery of strongly hybridized phonons in one-dimensional (1D) double-walled carbon nanotubes (DWNTs) [1] and direct optical imaging of spontaneous electric polarizations and sliding dynamics in tetralayer graphene [2], both of which reveal new and intriguing physics.

In the first part of the talk [1], I will show the discovery of uncharted phonon modes in one commensurate and three incommensurate DWNT crystals, three of which concurrently exhibit strongly-reconstructed electronic band structures. Our density functional theory (DFT) calculations for the experimentally observed commensurate DWNT (7,7) @ (12,12) reveal that this new phonon mode originates from a (nearly) degenerate coupling between two transverse acoustic modes (ZA modes) of constituent inner and outer nanotubes having approximately trigonal and pentagonal rotational symmetry along the nanotube circumferences. Such coupling strongly hybridizes the two phonon modes in different layers and leads to the formation of a unique lattice motion featuring evenly distributed vibrational amplitudes over inner and outer nanotubes, distinct from any known phonon modes in 1D systems. All four DWNTs that exhibit the pronounced new phonon modes show small chiral angle twists, closely matched diameter ratios of 3/5 and decreased frequencies of new phonon modes with increased diameters, all supporting the uncovered coupling mechanism.

In the second part of the talk [2], I will share our direct optical imaging of spontaneous electric polarizations and polarization switching in tetralayer graphene. We visualize opposite out-of-plane electric polarizations in adjacent polar stacking orders of tetralayer graphene that lack inversion and mirror symmetries by their own but are mutually transformable by the two symmetries with the nanometer scale resolution. Particularly noteworthy is the observation of versatile DW sliding dynamics at different interfaces among multiple and distinct polytypes in gated tetralayer graphene, revealing a sliding ferroelectricity between two polar stackings driven by a cooperative sliding mechanism. This observation, in conjunction with our DFT calculations, further consolidates our assignment of the polar stacking orders in tetralayer graphene and rationalizes their formation and distribution we observed in other multilayer graphene samples. We also demonstrate a reversable polarization switching between two polar stacking orders in tetralayer graphene by an atomic force microscopy (AFM) tip manipulation.

References

[1] S. Sun *et al.*, *Phys. Rev. Lett.* (2025) (accepted).
[2] Z. Zhou, X. Peng *et al.*, manuscript to be submitted (2025)

High-performance Transparent and Conductive CNT Films from Dilute Organic Dispersions

Tsuyoshi Endo[1], Seiya Nishida[1], Hiroaki Kahara[1], Satoshi Yamazaki[2], Takashi Kodama[3], Yoko Iizumi[4], Toshiya Okazaki[4], Keigo Otsuka[1], Shigeo Maruyama[1]and Shohei Chiashi[1]

[1]*Department of Mechanical Engineering, the University of Tokyo (Japan),*
[2]*Furukawa Electric Co., Ltd. (Japan),*
[3]*Dept. of Mech. and Control Eng., Kyushu Institute of technology (Japan),*
[4]*National Institute of Advanced Industrial Science and Technology (Japan)*

CNT-based transparent conductive films (CNT-TCFs) are promising applications because of their high flexibility, mechanical strength, and thermal/chemical durability, in addition to their optical and electrical properties. As CNT-TCF fabrication methods, the wet methods are easier to handle and more scalable than the dry methods. However, since CNTs hardly disperse in pure water, sufficient dispersant and powerful ultrasonic treatment are essential for the preparation of CNT aqueous dispersion, and the residual impurities and damage to the CNTs are issues [1]. On the other hand, some organic solvents are known to be able to maintain the dispersion state of CNTs to a certain extent, although their saturation concentration and stability are not higher than those of the CNT aqueous dispersion. In this study, we focused on N-methyl-2-pyrrolidone (NMP) as an organic solvent for dispersing CNTs [2] and investigated appropriate methods for dispersing CNTs in NMP. Concurrently, a thin film fabrication method from the obtained dilute CNT dispersion was developed.

In the experiment, single- or double-walled commercial CNT samples were used. The samples were bath sonicated in NMP for 1 minute, and a dilute CNT-NMP dispersion (concentration: 10^{-4} -10^{-3} mg/mL) was obtained as the supernatant after 1 day. CNT thin films were prepared by conventional vacuum filtration and a liquid surface fabrication method (LSF) that we developed. In LSF, Polydimethylsiloxane (PDMS)/NMP and CNT/NMP dispersions were dropped in order against Dimethyl sulfoxide (DMSO) aqueous solution (35~40 vol%), and then PDMS forms a film on the water surface, stabilizing the liquid-liquid interface and acting as a filter to deposit CNT-TCF, as shown in Fig. 1.

The CNT thin film was annealed in Ar gas at 300 °C for 30 minutes to evaluate the effect of doping with nitric acid. The characteristics of the obtained CNT thin films are shown in Fig. 2. For example, using SWCNT sample (EC2.0) with an effective length of 1913 nm and G/D ratio of 52.0, we succeeded in producing an excellent transparent conductive film with a resistance of 535 Ω/sq (90%T) before doping and 74.8 Ω/sq (90%T) after doping. Furthermore, by adding PVP during dispersion, the performance of this SWCNT was improved to be 68.8 Ω/sq (90%T) after doping. As for LSF, we obtained 752 Ω/sq (90%T) before doping and 72.2 Ω/sq (90%T) after doping.

By premixing and short bath sonication, CNTs could be dispersed to the level of bundles consisting of several CNTs without any loss of their quality, and high-performance CNT-TCFs could be fabricated. The developed LSF had the potential to produce large-scale CNT thin films.

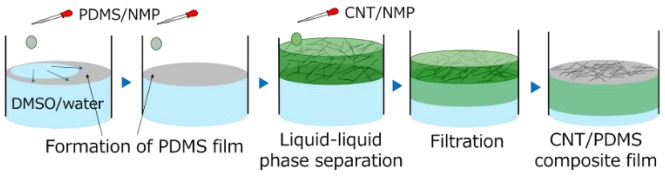

Fig. 1 Schematic images of the mechanism of the liquid surface fabrication method.

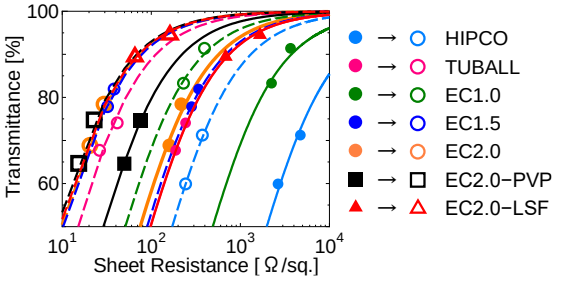

Fig. 2 Sheet resistance and Transmittance of CNT-TCFs prepared by vacuum filtration and LSF.
(filled marks：before doping, empty marks: after doping)

[1] J. Hirotani, et *al*., *Top. Curr. Chem*., **3**, 257 (2019).
[2] T. Hasen, *et al., J. Phys. Chem. C*, **111**, 12594 (2007).

Mxene/metal Composites for Hydrogen Evolution Application

S. A. Sergiienko

University of Chemistry and Technology Prague, Technick´a 5, 166 28 Prague 6, Czech Republic

Energy storage technologies, such as batteries, hydrogen production, and thermal storage, play a crucial role in balancing supply and demand, stabilizing the grid, and ensuring continuous energy availability. Among them, hydrogen storage offers a promising solution due to its high energy density and potential for long-term storage. The production of hydrogen by water electrolysis is now considered one of the most promising technologies. Ammonia is considered as a potential hydrogen carrier, while the NH_3 electrosynthesis from N_2 and H_2O looks attractive currently limited by its low efficiency. Electrochemical CO_2 reduction another attractive technology to production of liquid fuels. All these technologies require efficient and cheap electrocatalysts for successful industrial implementation.

The emergence of new multifunctional materials continuously increases the expectations for the performance of energy conversion and storage devices. MXenes, a family of two-dimensional transition metal carbides has been discovered as candidate for these applications [1], [2]. MXene/metal composites are considered as promising electrocatalysts for several processes. Ni and Ni-based alloy (Ni-Cu) electrodes have been employed as non-precious metal catalysts for hydrogen production owing to their substantial catalytic activity in hydrogen evolution reaction (HER) in alkaline media. However, in economical water-alkali electrolysers, the sluggish water dissociation kinetics (Volmer step) in platinum-free electrocatalysts results in poor hydrogen-production activity. MXene/nano-metal composites as electrocatalysts for hydrogen evolution reaction (HER) in an alkaline medium, demonstrate lower overpotential compared to balk metal electrode at high current densities. An enhanced catalytic activity of MXene/nano-metal composite attributed to the acceleration of the Volmer stage in HER process in alkaline media, by enhancing the water adsorption and dissociation on the catalyst surface where water dissociation is a rate-limiting step. This work proposes a concept of composite structures composed of MAX phase/metal-Al alloy and MXene/metal as functional materials. The concept is based on the combination of the initial MAX phase with metal alloys (Ni, Cu), tuning MAX phase and metal-Al alloy ratio, carbon content and synthesis conditions, followed by Al etching. In more details this work explores the possibilities for the processing of Ni-Al/MAX phase or Cu-Al/MAX phase and corresponding Ni/MXene or Cu/MXene - containing composite electrodes for energy conversion and storage application. Synthesis of powder mixtures with extra Ni or Cu and Al content (e.g. Cu:Ti:Al:C = 1:2:4.5:2) resulted in products containing modified titanium-based MAX phase material and Ni-Al or Cu-Al alloys [2]. It was found that the presence of Cu and Al excess in the reaction mixture promotes the formation process of conventional MAX phases (Ti_3AlC_2) due to generating Al-rich metal-Al alloys with a lower melting point. Further etching of these sintered products (Ni-Al or Cu-Al/ MAX phase) in HF or alkaline solution allowed the direct formation of electrodes with active surface containing MXene and nanoporous metal (Cu, Ni) composites [2, 3] with a well-developed 3D porous MXene/metal structure possessing good mechanical integrity, electrical conductivity and catalytic activity in hydrogen evolution reaction [2, 3].

References

[1] Yury Gogotsi *et al., ACS nano*., **13**, 8491–8494 (2019).
[2] Sergii A. Sergiienko *et al., RSC advances* **14**, 3052–3069 (2024).
[3] Sergii A. Sergiienko *et al., Int. J. of Hydrogen Energy,* **46**, 11636–11651 (2021).

High near-field noise suppression in the 5G frequency bands for graphene sheets printed by jet-dispensing

M. Watanabe[1]

[1]*Research Institute for Electromagnetic Materials (Japan)*

In order to suppress near-field electromagnetic interference (EMI) for various electronic or telecommunication devices in the 5G frequency bands, graphene noise suppression sheet (NSS) based on electromagnetic wave (EMW) absorption mainly by current losses has been proposed. Graphene NSS is light-weighted and has a possible availability from microwave to THz frequency range [1], different from traditional ferromagnetic NSS that has an advantage in the lower frequency range. Graphene sheets were prepared by mechanical-collision type jet-dispensing with water solution composed of physically exfoliated few-layer graphene flakes and cellulose nanofibers on flexible Kapton® sheets with a coated area of 10 cm square. The graphene flakes were found to have c-axis orientation with high dispersion from X-ray large-area reciprocal space mapping. Raman spectroscopy for the graphene sheet showed an unsymmetric G'(2D) peak, which is characteristic of few-layer graphene. Transmission attenuation power ratio R_{tp}, which can be derived from reflection coefficient S_{11} and transmission coefficient S_{21}, was measured up to 40 GHz using a vector network analyzer and a microstrip line with Z_0=50 Ω and a 122μm width conductive line. Figure 1 shows cross-sectional SEM images of the graphene sheet before and after press treatment, which caused an increase in density of graphene flakes and resistivity reduction. Typical noise suppression property of the graphene sheet before and after press treatment is shown in Fig. 2. Linear spectrum of R_{tp} in the sample before press is found to change into one with large sharp peak of R_{tp}=72.4dB at 26.8 GHz after press. R_{tp} of 72.4dB is more than two times larger than magnetic or nonmagnetic NSS commercial products. Since noise suppression effect in the graphene sheet is mainly influenced by R_S, the change in frequency dependence by press is considered to be due to change in state of current induced by incident EMW [2]. Addition to conventional current joule loss, other absorption mechanisms such as interband transition in Dirac cone [3] might contribute to the large EMW absorption found in the graphene sheet. Graphene NSS is very promising for various applications in the 5G or beyond 5G telecommunication network from its high R_{tp} in mm wave bands and light weight.

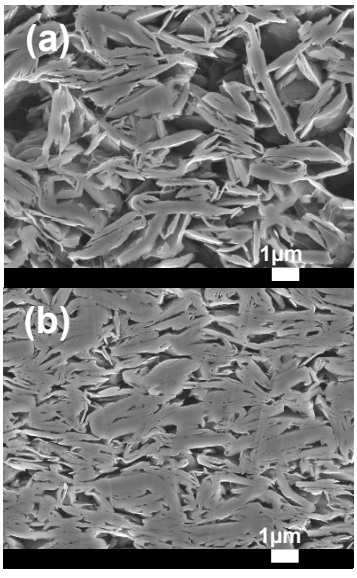

Fig.1 Cross-sectional SEM images for the graphene sheet before (a) and after press treatment of 0.5t (b).

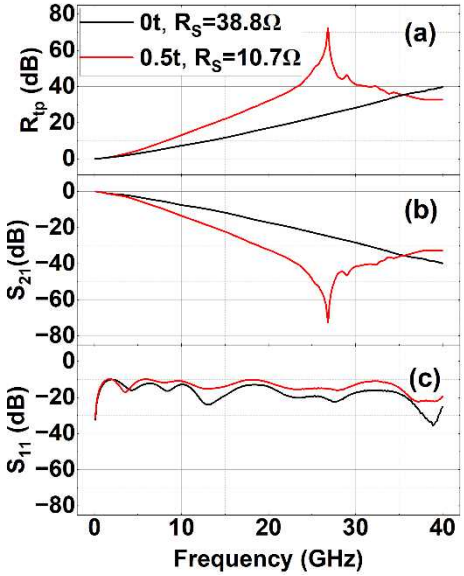

Fig.2 Frequency spectra of R_{tp} (a), S_{21} (b) and S_{11} for the graphene sheet before and after press treatment of 0.5t.

References

[1] K. Batrakov *et al.*, *Appl. Phys. Lett.* **108**, 123101 (2016).
[2] S. Muroga *et al.*, *IEEE Trans. Magn.* **45**, 4804-4807 (2009).
[3] Z. Zheng *et al.*, *Opt. Express* **20**, 23201-23214 (2012).

Flavin-Wrapped Carbon Nanotubes for Fundamentals and Applications

Sang-Yong Ju[1,*], Hangil Lee[2], Seongjoo Hwang[1]

[1]*Department of Chemistry, Yonsei University 03722 Seoul (Republic of Korea),* [2]*Department of Chemistry, Sookmyung Women's University, Seoul (Republic of Korea)*

Carbon nanotubes (CNTs) exhibit outstanding optical, electrical, and mechanical properties, making them highly suitable for various dispersion-based applications, including electronic ink, transparent electrodes, batteries, supercapacitors, nanocomposites, biosensors, and filters. In this study, we explore the potential of flavins as multifunctional dispersants for CNTs.

Flavins provide a well-defined self-assembly framework for dispersing CNTs and can be easily removed for high-end applications. The isoalloxazine ring in the flavin wrapping system forms strong π–π interactions with single-walled carbon nanotubes (SWCNTs) and establishes quadruple hydrogen bonding with adjacent isoalloxazine molecules, while its side chain enhances dispersibility. Flavin mononucleotide (FMN) and n-dodecyl flavin (FC12), which have distinct side chains, have been shown to effectively disperse CNTs in both aqueous and organic solvents. Due to these properties, flavin derivatives have been employed to sort SWCNTs based on chirality, handedness, and metallicity.

Additionally, flavins on flavin-wrapped CNTs form a tightly wound helical structure, providing oxygen resistance and tunability for nanocomposite components. Flavins also exhibit strong electronic interactions with underlying CNTs, leading to excitonic Fano scattering. Moreover, the straightforward extraction of monochiral (8,6)-SWCNTs enables a deeper understanding of the fundamental properties of SWCNTs.

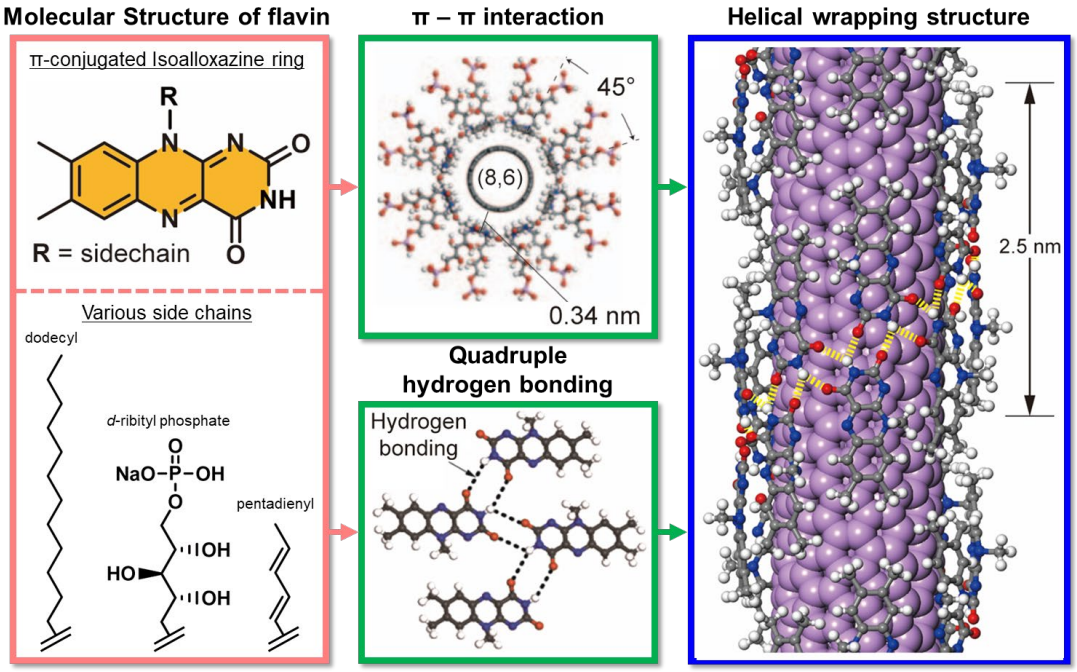

Figure caption: Flavin molecules form intrinsic helical wrapping structure on CNT surface.

Monocyclic Aromatic Molecule-Driven Confined Synthesis of 6-Armchair Graphene Nanoribbons

Huiju Cao[1], Yingzhi Chen[1], Kunpeng Tang[1], Wendi Zhang[2], Kecheng Cao[2], Lei Shi[1]

[1]*Sun Yat-sen University (China),* [2]*ShanghaiTech University (China)*

Abstract:

Armchair graphene nanoribbons (AGNRs) exhibit a width-dependent band gap, facilitating the tuning of their electronic properties. While various strategies have been developed to enhance the yield of AGNRs, achieving precise control over their dimensions—specifically length, width, and edge structures—remains an area with significant developmental potential. In this study, we present the confined synthesis of 6-AGNRs inside single-walled carbon nanotubes (SWCNTs). High-yield and uniform-width 6-AGNRs were synthesized using a range of mono-cyclic aromatic molecules, with no detectable presence of other AGNR widths in SWCNTs of varying diameters, as confirmed by resonance Raman spectroscopy and transmission electron microscopy. Our experiments indicated that aromatic molecules containing halogens exhibited a higher propensity to react, while the free rotation and polymerization capabilities of aromatic molecules with different substituents and substitution sites influenced the yield of 6-AGNRs inside SWCNTs. This method provides a novel confined synthesis pathway for 6-AGNRs based on molecular design precursors, featuring a straightforward reaction strategy that allows for large-scale preparation. This advancement holds promise for future applications in semiconductor technology.

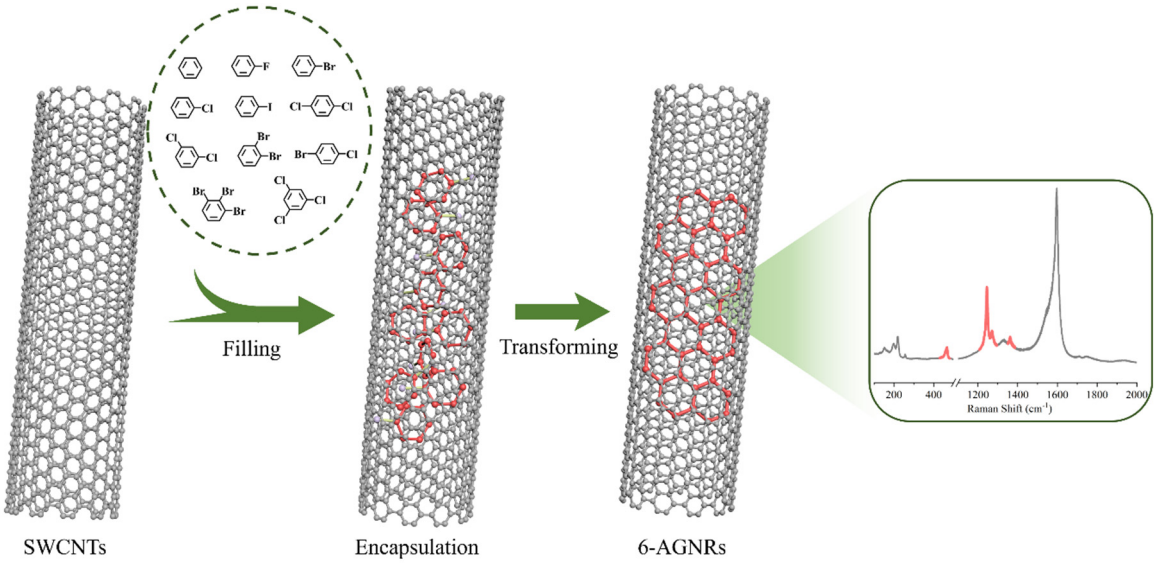

Figure 1: Schematics of confined transformations from precursor molecules into graphene nanoribbons inside carbon nanotubes.

Inner Doping of Carbon Nanotubes with Perovskites and charge detection for High performance Nanoelectronics

Huimin Yin, Chuanhong Jin

[1] *State Key Laboratory of Silicon Materials, School of Materials Science and Engineering, Zhejiang University, Hangzhou, Zhejiang 310024, P. R. China*

yinhuimin@zju.edu.cn;

Semiconducting carbon nanotubes (CNTs) are considered as the most promising channel material to construct ultra-scaled field-effect transistors (FETs)[1]. However, the perfect sp^2 carbon-carbon structure makes stable doping difficult, limiting the electrical designability of CNT devices[2]. In this study, an inner doping method is developed by filling CNTs with 1D halide perovskites, enabling precise tuning for nanoelectronics. Non-destructive characterization using Kelvin Probe Force Microscopy (KPFM), Raman spectroscopy, and SEM identifies doping type, fill status, and charge effects at the individual CNT level. Revealing diameter-dependent doping effects, structure transfer and charge transfer polarity, which enables a stable n-type field-effect transistor for constructing complementary metal–oxide–semiconductor electronics. Furthermore, a quasi-broken-gap tunnel FET based on $CsPbBr_3$@CNT demonstrated excellent subthreshold swing of 35 mV dec^{-1}, high on-state current at room temperature, and promising potential for low-power integrated circuits. These findings support the development of scalable, high-performance nanoelectronics[3].

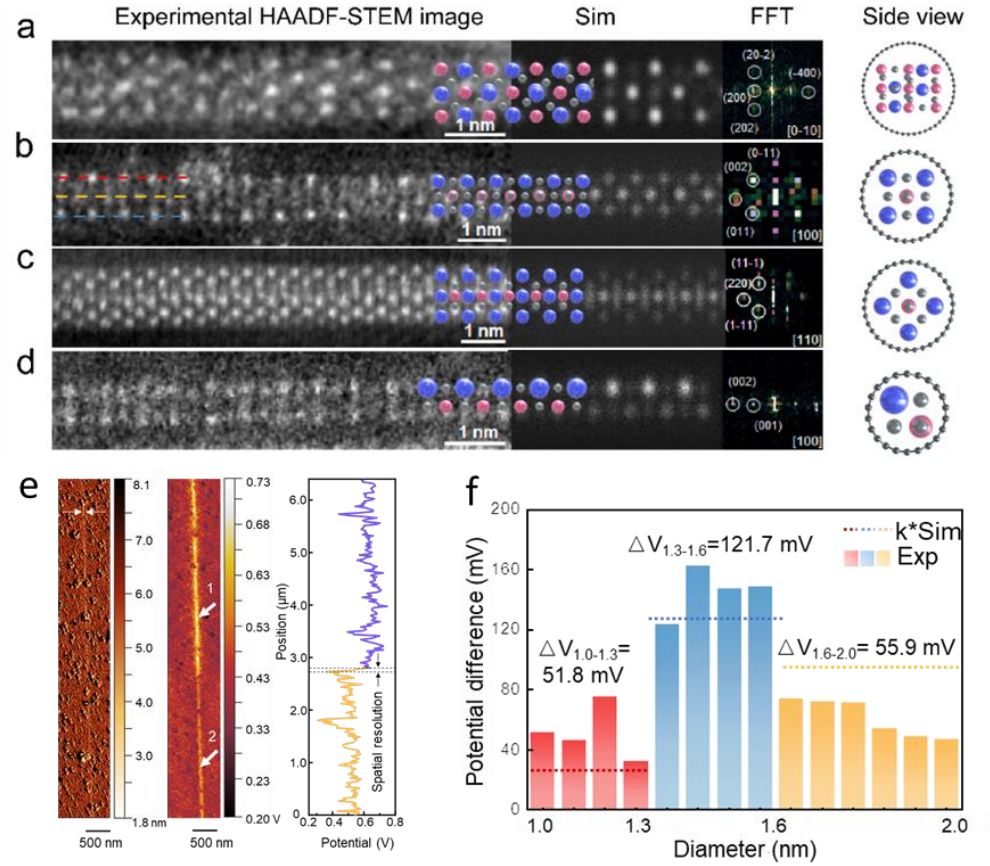

Figure1: Confined atomic structure of the $CsPbBr_3$@CNT and the typical measurements of electrical properties . (a-d) Orthogonal, cubic and the 1/2 unit cubic of $CsPbBr_3$ encapsulated in different diameter CNT. (e) Topography image , potential image characterized by KPFM and potential profile along the carbon nanotube, respective. f) Comparison between the experimental and simulation potential difference, illustrating the trend in potential difference with varying CNT diameters.

References

[1] L. J. Liu et al., *Science* **368**, 850-856 (2020).
[2] Maiti U N, Lee W J et al., *Adv. Mater* **26**, 40-67 (2014).
[3] M. G. Zhu, H. M. Yin, et al., *Adv. Mater* **36**, 2403743 (2024).
[4] H. M. Yin et al., *submitted work* (2025)

UHV exfoliation and rational functionalization of 2D materials

M. Kalbac[1]

[1]*Heyrovsky Institute of Physical Chemistry of the Czech Academy of Sciences, Dolejškova 2155/3, 182 23 Prague, Czech Republic.*

2D materials are very sensitive to their environment. This is because they do not have a bulk component and thus literally all atoms can interact with species adhering to the surface of the 2D material. In ambient conditions the surface gets immediately covered by impurities. In order to preserve a clean surface, we propose a method for exfoliation of the 2D materials in ultra-high vacuum conditions. This allowed us to explore the properties of these materials in a pristine state. To further tailor the properties of 2D materials one can exploit chemical functionalization. However, this process is generally not compatible with ultraclean environment like ultra-high vacuum. I will present our strategies which provides pathway to reach this challenging goal.

References (if desired)

[1] M. Thakur, G.Haider, F. J. Sonia, J.Plšek, M. Kalbáč et al. : *Small*, 2205575 (2023).
[2] G. Haider, M. Gastaldo, B. Karim, J. Plsek, V. Varade, O. Volochanskyi, J.Vejpravova, M. Kalbac, *ACS Applied Electronic Materials*,6, 2301 (2024).

Microscopic Understanding of Metal Contacts to Aligned Carbon Nanotubes Arrays: Wetting and Coverage

Haozhe Lu[1*], Chuanhong Jin[1]

[1] *State Key Laboratory of Silicon Materials, School of Materials Science and Engineering, Zhejiang University, Hangzhou, Zhejiang 310024, P. R. China*

haozhelu@zju.edu.cn

Semiconducting carbon nanotubes (CNTs) are a promising channel material for ultra-scaled field-effect transistors (FETs).[1] However, optimizing the performance of CNT FETs requires a detailed understanding of the interface between metal contacts and aligned, high-density CNT arrays (A-CNTs).[2] While previous research has focused on individual CNTs, the complexity increases with A-CNTs due to their dense arrangement, varying interactions with metals, and inherent alignment variations.[3] This study employs cross-sectional high-resolution transmission electron microscopy (X-TEM) to examine the interface between A-CNTs and five common contact metals (Pd, Pt, Au, Sc, Y) in both p-type and n-type FETs. We introduce a robust methodology to assess the wetting properties of the metal-CNT interface, using the wettability parameter ω_{CM}. By correlating wetting behavior with CNT spacing (linked to A-CNT density), we uncover a transition from wetting to non-wetting as array density increases, which is expected to impact device performance. Additionally, we establish a relationship between the coverage ratio, A-CNT density, and contact resistance, providing insights into the role of metal-CNT interfacial behavior. This work offers a framework for optimizing metal-CNT contacts, with direct applications for next-generation CMOS integrated circuits.[6]

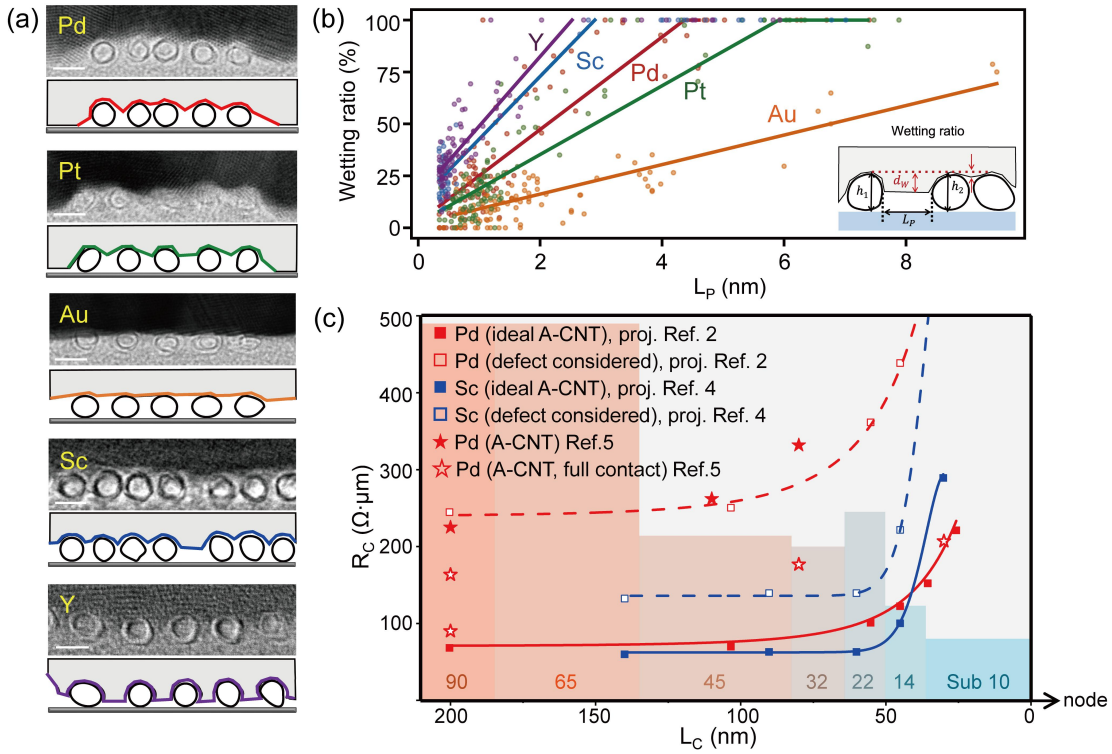

Figure 1: (a) Representative X-TEM images and their corresponding schematic diagrams showing the typical contact interface structures for each metal. Scale bar:2 nm; (b) Statistical data showing the relationship between wetting ratio and CNTs' pitches for five different metals, with linear fits (solid lines) applied to the data points (scattered dots). (c) Contact resistance comparison as a function of contact length. Square data points are obtained based on individual tube devices [2][4]. And red star in correspond to the experimental results in A-CNT devices with Pd contact.[5]

References

[1] J. Si *et al.*, *Natl. Sci. Rev.* **11**, nwad261 (2024).
[2] A. D. Franklin *et al.*, *ACS Nano* **8**, 7333–7339 (2014).
[3] B. Wang *et al.*, *ACS Nano* **18**, 22474-22483 (2024).
[4] L. J. Liu *et al.*, *Nanoscale* **9**, 9615–9621 (2017).
[5] Y. X. Lin *et al.*, *Nat Electron* **6**, 506–515 (2023).
[6] H. Z. Lu *et al.*, submitted work (2025).

Encapsulation and Electronic Modulation of Tungsten-Alloyed MoS_2 Nanoribbons in Carbon Nanotubes

Yuanfang Zhang[1,2*], Wenqi Lv[3], Fenfa Yao[2], Yanning Zhang[3], Xin Chen[1*], Chuanhong Jin[2]

[1] Key Laboratory for Ultrafine Materials of Ministry of Education and Shanghai Key Laboratory of Advanced Polymeric Materials, School of Materials Science and Engineering, East China University of Science and Technology (China), [2] State Key Laboratory of Silicon and Advanced Semiconductor Materials, School of Materials Science and Engineering, Zhejiang University (China), [3] Key Laboratory of Quantum Physics and Photonic Quantum Information, the Ministry of Education, Institute of Fundamental and Frontier Sciences, University of Electronic Science and Technology (China)

*Correspondence to: yuanfangzhang@mail.ecust.edu.cn; xinchen73@ecust.edu.cn.

One-dimensional transition metal dichalcogenides (TMDCs) are highly promising for applications in nanoelectronics and optoelectronics [1,2]. However, synthesizing sub-10 nm wide TMDC nanoribbons (NRs) with precise doping remains challenging [3]. We report a solution-based two-step method to synthesize atomically thin $Mo_{1-x}W_xS_2$ ($0<x<1$) nanoribbons within single-walled carbon nanotubes (SWCNTs). STEM imaging confirms controlled doping, revealing nanoribbons with widths ranging from 1–6 nm and thicknesses of 1–3 layers, depending on the SWCNT diameter. At a 1:1 doping ratio, tungsten atoms form highly ordered atomic-scale stripe structures. The Mo-Mo, W-W, and Mo-W bond lengths remain nearly unchanged across different doping concentrations, indicating structural stability. Spectroscopic analysis reveals electronic structure modulation within CNTs. Raman G-band redshift suggests electron transfer from CNTs to nanoribbons, while UV-vis-NIR peak shifts indicate doping-induced bandgap modulation. STS measurements show Fermi level shifts, attributed to the inhomogeneous distribution of Mo and W, leading to local electronic state reconstruction. DFT calculations predict a strong correlation between nanoribbon structure and SWCNT diameter, further revealing a significant interaction between the Mo and C atoms at the edges of the nanoribbons, leading to charge transfer effects that are critical for understanding the electronic properties of these encapsulated structures. This study demonstrates a controlled doping strategy for TMDC nanoribbons within CNTs and unveils the electronic modulation mechanism, laying the foundation for tunable nanoelectronic applications.

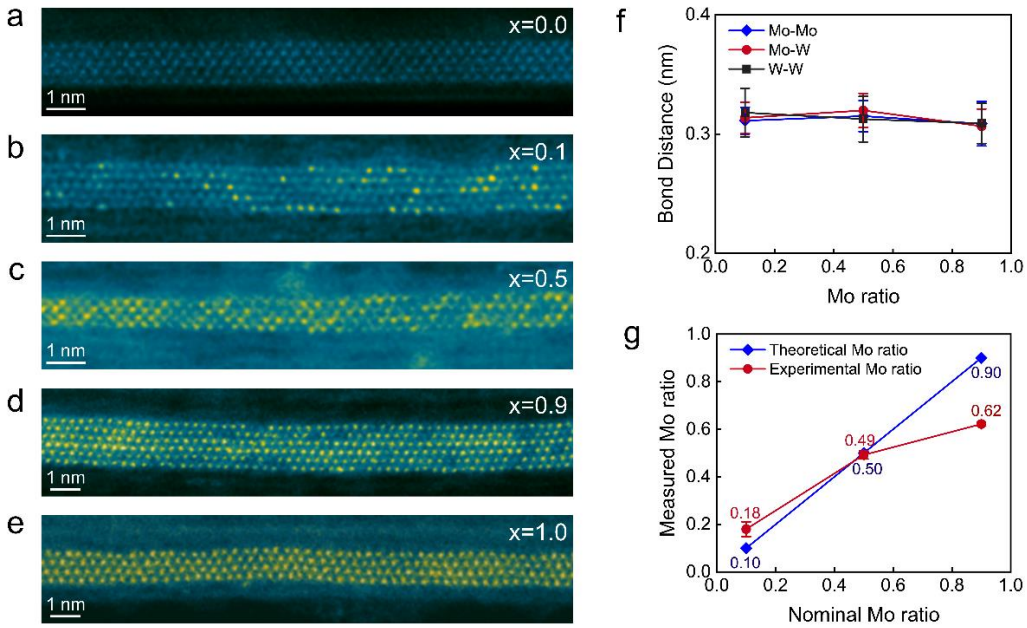

Atomic-resolution ADF-STEM images, bond length analysis, and Mo composition characterization of monolayer $Mo_{1-x}W_xS_2$ NRs encapsulated within CNTs. (a-e) ADF-STEM images of monolayer $Mo_{1-x}W_xS_2$ NRs encapsulated within CNTs with varying W concentrations, represented by x = 0, 0.1, 0.5, 0.9, and 1. (f) Experimentally measured Mo-Mo, Mo-W, and W-W bond lengths as a relationship of Mo ratio. (g) Experimentally measured Mo ratio versus nominal Mo ratio of monolayer $Mo_{1-x}W_xS_2$ NRs.

References

[1] Radisavljevic, B., *et al.*, *Nat Nanotechnol*. 6(3), 147-150 (2011).
[2] Yin, Z., *et al.*, *ACS nano*, 6(1), 74-80 (2012).
[3] Aljarb, A., *et al.*, *Nat. Mater.* 19(12), 1300-1306 (2020).

Synthesis of carbon nanotubes using higher alkanes as a carbon source

L. Nowicki[1], S. Lepak-Kuc[1,2], A. Lekawa-Raus[1]

[1]Centre for Advanced Materials and Technologies (CEZAMAT) Warsaw (Poland), [2]Faculty of Mechanical and Industrial Engineering, Warsaw University of Technology (Poland)

Although investigated for a long time now the synthesis of CNTs is still highly challenging. The game changer for further development of CNT applications would be the bulk production of CNTs with precisely controlled chirality, diameter, number of layers, and length [1-4]. In the following work we used a purpose designed Floating Catalyst Chemical Vapour Deposition (FC-CVD) method to perform a systematic study on the effect of the use of higher alkanes of increasing chain lengths as a carbon source in the synthesis CNTs, which to the best of our knowledge has not been reported by now. [5-9]. FC-CVD is a versatile method enabling a high yield synthesis of both MWCNTs and SWCNTs and their different assemblies [10-11]. Our purpose designed reactor enables the precise control of all basic synthesis parameters such as temperature, time of reaction or speed of injection and is set to manufacture CNT arrays. In this study we tested 6 higher alkanes - hexane, octane, decane, dodecane, tetradecane and hexadecane and investigated their decomposition at 4 different temperatures from 760˚C - 1060˚C. The feedstock comprised also ferrocene as a catalyst source and argon was used as carrier gas. The analysis of obtained materials showed clear differences in CNTs diameters, height of arrays, and amount of material, and temperature of decomposition in thermogravimetric analysis (TGA).

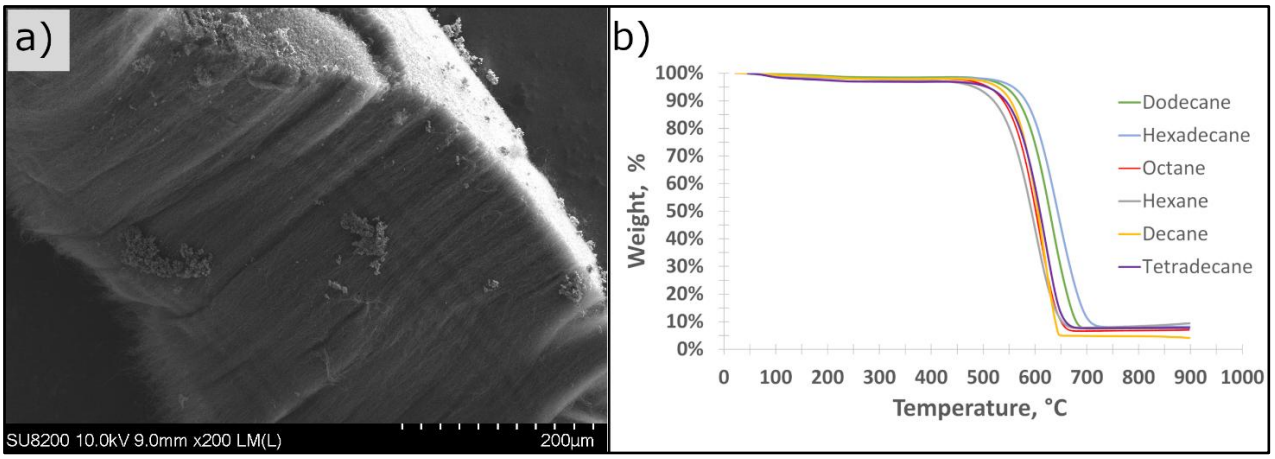

Figure 1: a) CNTs arrays with Octane as a carbon source. **b)** TGA for all tested alkanes synthesized in 760˚C

References

[1] S. Wang et al., *Nano Res.* **16**, 10342–10347 (2023)
[2] A. Aghaei, M. Shaterian, H. Hosseini-Monfared, and A. Farokhi, *Chem. Pap.* **77**, 249–258 (2023)
[3] X.-X. Lim, S.-C. Low, and W.-D. Oh, *Fuel Process. Technol*. **241**, 107624 (2023)
[4] M. J. Giannetto et al., *ACS Nanosci. Au* **3**, 182–191 (2023)
[5] S. S. Meysami, A. A. Koós, F. Dillon, and N. Grobert, *Carbon* **58**, 159–169 (2013)
[6] N. Sonoyama et al., *Carbon* **44**, 1754–1761 (2006)
[7] M. W. Brenner, V. M. Boddu, and A. Kumar, *Appl. Phys. A* **117**, 1849–1857 (2014)
[8] H. W. Zhu, C. L. Xu, D. H. Wu, B. Q. Wei, R. Vajtai, and P. M. Ajayan, *Science* **296**, 884–886 (2002)
[9] H. Li, D. He, T. Li, M. Genestoux, and J. Bai, *Carbon* **48**, 4330–4342 (2010)
[10] T. Zhao et al., *Appl. Surf. Sci*. **357**, 2136–2140 (2015)
[11] J. H. Park, J. Park, S.-H. Lee, and S. M. Kim, *Carbon Lett.* **30**, 613–619 (2020)

Symmetry and asymmetry in carbon nanotube mutations and memory retention in long- and short-range

Lin Chai, Fei Wei*

Beijing Key Laboratory of Green Chemical Reaction Engineering and Technology, Department of Chemical Engineering, Tsinghua University, Beijing 100084, China.

Symmetry is a motif featuring in almost all areas of science and understanding the mechanism of symmetry breaking is challenging. Similar to mutations that disrupt symmetry in evolution, defects in materials offer insights into symmetry breaking. Here, we investigate the symmetry in intragenerational mutations and the symmetry breaking in transgenerational mutations in the evolutionary growth system of carbon nanotubes (CNTs). Mutations caused by pentagon–heptagon (5–7) pairs in different conformations which are detected by four-dimensional scanning transmission electron microscope (4D-STEM), shorten the lifespans of single-walled carbon nanotubes (SWNTs) by acting as time markers during growth. Symmetric distributions are observed for intragenerational mutations from (n, m) to ($n\pm i$, $m\mp i$) with different appearance orders of pentagon and heptagon. Such symmetry breaks in transgenerational mutations. Intragenerational mutations occur multiple times on a SWNT, oscillating regularly between i and $-i$ until termination occurs. These types and effects are retained in the form of memory to encode SWNTs during subsequent growth, resulting in length reduction after each mutation.

Furthermore, we reveal that the memory retention for intragenerational mutations exists not only at the long-range scale (several micrometers), but also manifests significantly at the short-range (~ 2 nm), through atomic-scale imaging via 4D-STEM. Additionally, based on the projected charge density distribution derived from 4D-STEM, we observe that it is not related to chirality, but also associated with the electrical conductivity properties for the charge distribution on pentagons and heptagons in both intragenerational and transgenerational mutations.

Our results provide theoretical foundations for deeper understanding of symmetry breaking and memory retention of mutations in CNTs, meanwhile offering guidance for subsequent controllable synthesis.

References

[1] L. Chai, F. Wei*, *et al.*, *J. Am. Chem. Soc.,* 4c10400 (2024).

Observation of strongly hybridized phonons in one-dimensional van der Waals crystals

Shaoqi Sun[1], Qingyun lin[2], Yihuan Li[1], Daichi Kozawa[3], Huizhen Wu[1], Shigeo Maruyama[4], Pilkyung Moon[5], Toshikaze Kariyado[3], Ryo Kitaura[3] and Sihan Zhao[1]

[1]School of Physics, Interdisciplinary Center for Quantum Information, Zhejiang Key Laboratory of Micro-Nano Quantum Chips and Quantum Control, and State Key Laboratory of Silicon and Advanced Semiconductor Materials, Zhejiang University (China), [2]Center of Electron Microscopy, School of Materials Science and Engineering, Zhejiang University (China), [3]Research Center for Materials Nanoarchitectonics (MANA), National Institute for Materials Science (NIMS) (Japan), [4]Department of Mechanical Engineering, The University of Tokyo (Japan), [5]Arts and Sciences, NYU Shanghai (China); NYU-ECNU Institute of Physics at NYU Shanghai (China)

The phenomena of pronounced electron-electron and electron-phonon interactions in one-dimensional (1D) systems are ubiquitous, which are well described by frameworks of Luttinger liquid, Peierls instability and concomitant charge density wave. However, the experimental observation of strongly hybridized phonons in 1D was not demonstrated. Herein we report the first observation of strongly hybridized phonons in 1D condensed matters by using double-walled carbon nanotubes (DWNTs), representative 1D van der Waals crystals, with combining the spectroscopic and microscopic tools as well as the ab initio density functional theory (DFT) calculations. We observe uncharted phonon modes in one commensurate and three incommensurate DWNT crystals, three of which concurrently exhibit strongly-reconstructed electronic band structures. Our DFT calculations for the experimentally observed commensurate DWNT (7,7) @ (12,12) reveal that this new phonon mode originates from a (nearly) degenerate coupling between two transverse acoustic modes (ZA modes) of constituent inner and outer nanotubes having approximately trigonal and pentagonal rotational symmetry along the nanotube circumferences. Such coupling strongly hybridizes the two phonon modes in different shells and leads to the formation of a unique lattice motion featuring evenly distributed vibrational amplitudes over inner and outer nanotubes, distinct from any known phonon modes in 1D systems. All four DWNTs that exhibit the pronounced new phonon modes show small chiral angle twists, closely matched diameter ratios of 3/5 and decreased frequencies of new phonon modes with increased diameters, all supporting the uncovered coupling mechanism. Our discovery of strongly hybridized phonons in DWNTs open new opportunities for engineering phonons and exploring novel phonon-related phenomena in 1D condensed matters.

Optical Modeling, Solver, and Design of Macroscopic Single-Enantiomer Carbon Nanotube Film and Reconfigurable Chiral Photonic Device

J. Fan[1], B. Hillam[1], C Guo[2], H. Fujinami[3], K. Shiba[3], H. Xie[1], R. Chen[1], K. Yanagi[3], W. Gao[1*]

[1]*University of Utah (U.S.A),* [2]*Stanford University (U.S.A),* [3]*Tokyo Metropolitan University (Japan)*

**Email: weilu.gao@utah.edu*

The interaction of circularly polarized light with chiral materials and their functional devices has found broad applications in molecular sensing [1], 3D image generation [2], neuromorphic computing [3], and quantum technologies [4]. Single-enantiomer carbon nanotubes (CNTs) emerge as a promising chiral photonic material platform with quantum confinement-induced optical properties and quantum-engineered chirality, thanks to the recent progress in large-scale chirality and enantiomer separation [5]. However, optical modeling, solver, and device design tools for such materials are non-existent. Here, we prepare macroscopic single-enantiomer (6,5) and (11, -5) randomly oriented CNT films and create an optical material model based on measured experimental optical spectra (**Fig. 1**). We also implement a highly parallel graphic-processing-unit accelerated transfer matrix solver for general bi-anisotropic materials and layered structures. Further, we demonstrate reconfigurable chiral photonic devices in a heterostructure with phase change materials through machine learning-enabled efficient gradient-based inverse design and optimization. Our developed full stack of a chiral photonic material and device hardware platform and a corresponding high-performance differential-programming-enabled solver opens the door for future chiral photonic devices and applications based on single-enantiomer CNT films.

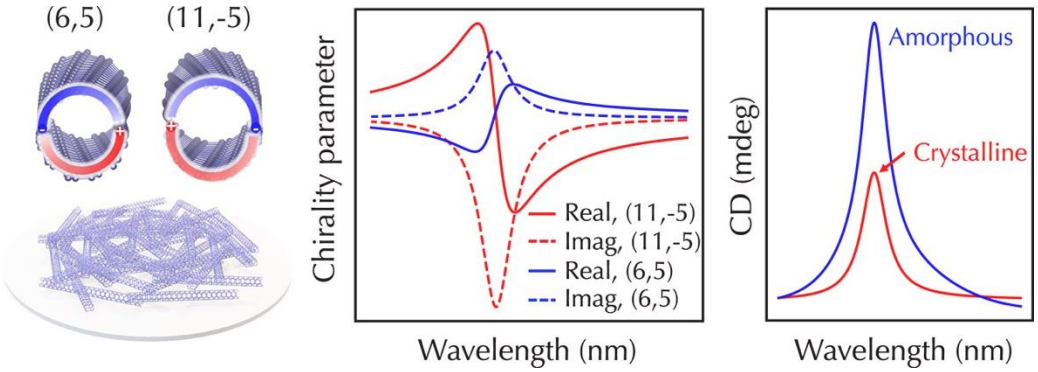

Fig. 1: Illustration of single-enantiomer (6,5) and (11, -5) CNT films (left), their extracted chirality parameters (middle), and their reconfigurable CD spectra with phase-change material (right).

References

[1] L.A. Warning, A.R. Miandashti, L.A. McCarthy, Q. Zhang, C.F. Landes, S. Link, Nanophotonic approaches for chirality sensing, ACS Nano 15, pp. 15538-15566 (2021).
[2] X. Zhan, F.-F. Xu, Z. Zhou, Y. Yan, J. Yao, Y.S. Zhao, 3D laser displays based on circularly polarized lasing from cholesteric liquid crystal arrays, Adv. Mater. 33, p. 2104418 (2021).
[3] S. Dan, S. Paramanik, A.J. Pal, Introducing chiro-optical activities in photonic synapses for neuromorphic computing and in-memory logic operations, ACS Nano 18, pp. 14457-14468 (2024).
[4] C.D. Aiello, J.M. Abendroth, M. Abbas, A. Afanasev, S. Agarwal, A.S. Banerjee, D.N. Beratan, J.N. Belling, B. Berche, A. Botana, et al., A chirality-based quantum leap, ACS Nano 16, pp. 4989-5035 (2022).
[5] X. Wei, T. Tanaka, T. Hirakawa, M. Tsuzuki, G. Wang, Y. Yomogida, A. Hirano, H. Kataura, High-yield and high-throughput single-chirality enantiomer separation of single-wall carbon nanotubes, Carbon 132, pp.1-7 (2018).

Anomalous Interfacial Electron Transfer Kinetics in Moiré Graphene

M.G. Takezawa[1], Y. Yu[1], K. Zhang[1], S. Maroo[1], D.K. Bediako[1]

[1]*University of California Berkeley (USA)*

Interfacial electron transfer (ET) reactions are critical for the conversion of electrical and chemical energy. Van der Waals materials are unique platforms to study such phenomena as they offer unprecedented freedom to modify the electronic and the physical structures, such as by introducing a slight lattice mismatch or inducing a relative twist angle between layers (Figure 1a). [1] For bilayers and trilayers, specific interlayer twist angles, known as “magic angles,” produce highly non-dispersive electronic bands in momentum space, giving rise to massively enhanced density of electronic states (DOS) near Fermi level [2] (Figure 1b).

We present studies from our group demonstrating a strong twist-angle dependence in interfacial ET kinetics due to the modulation of the electronic bands that align with the reduction potentials of the redox couple [3]. ET kinetics are shown to be significantly enhanced in AA stacking regions, compared to AB/BA and Saddle Point stacking regions (Figure 1c). These findings can be attributed to the fact that the prominent enhancement of DOS near the charge neutrality point is localized at AA sites whereas lower DOS is found at other sites [4]. These findings imply that the DOS of the electrode, specifically its variance across the spatial profile and near the Fermi level, can dictate the ET kinetics.

Interestingly, calculating the twist-angle dependence of the standard reduction rate constant, shows that the Marcus-Hush-Chidsey (MHC) model significantly underestimates the angle-dependence of ET rate constants. A key parameter that this anomalous behavior can be attributed to is the reorganization energy, which dictates the activation free energy in Marcus theory [5]. Conventionally, the reorganization energy is assumed to primarily come from the electrolyte and hence is usually treated as invariant in the MHC model, irrespective of electrode property. However, recent molecular dynamics simulations suggest that the electrostatic screening of the electrode may play a considerable role in the electron transfer rate, with lower values of the Thomas-Fermi screening length (or higher metallicity of the electrode) leading to a decrease in both the free energy of activation, owing to a reduction in the reorganization energy. [6] Future experimental and theoretical studies are needed to elucidate the microscopic origins of the anomalous ET rates and how they deviate from the MHC model. Nevertheless, these findings demonstrate that van der Waals materials are a versatile platform to systematically tune the physical and electronic structures of the material and control interfacial electrochemical behaviors, which can be harnessed for electrocatalytic processes and other energy conversion applications.

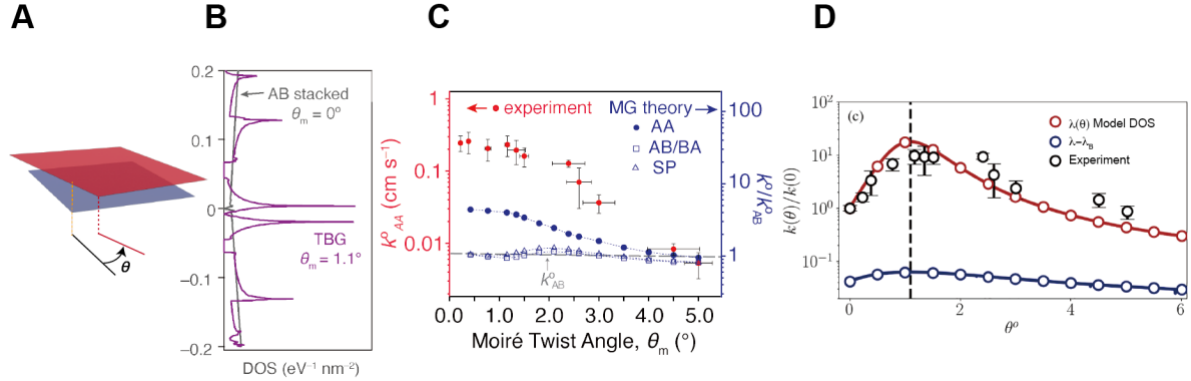

Figure 1: (a) A schematic of introducing a relative twist angle between two graphene layers. (b) Emergence of flat bands near that charge neutrality point at the magic angle of 1.1°. (c) The measured standard rate constant at AA stacking regions compared to values of the rate constant attributed to other stacking regions from the Gerischer-Marcus theory as a function of the twist angle. (d) ET rate dependence on the twist angle evaluated from the DOS and screening length (red line), the rate obtained with fixed reorganization energy (blue line), and experimental data from (c). [6]

References

[1] A. K. Geim, I. V. Grigorieva. *Nature*, **499**, 419–425 (2013).
[2] R. Bistritzer, *et al. Proc. Natl Acad. Sci. USA*, **108**, 12233–12237 (2011).
[3] Y. Yu, *et al. Nature Chemistry*, **14**, 267–273 (2022).
[4] A. Kerelsky, *et al. Nature*, **572**, 95–100 (2019).
[5] R. A. Marcus. *Angew. Chem. Int. Ed.*, **32**, 1111–1121 (1993).
[6] L. C. Escalante, D. T. Limmer. *Nano Lett*, **24**, 14868–14874. (2024).

Photoluminescence of gated mixed-dimensional heterostructures

U. Erkılıç[1,2], N. Fang[1], C. F. Fong[1], Y. R. Chang[1,2,3], Y. K. Kato[1,2]

[1]*Nanoscale Quantum Photonics Laboratory, RIKEN Cluster for Pioneering Research (Japan),*

[2]*Quantum Optoelectronics Research Team, RIKEN Center for Advanced Photonics (Japan)*

[3]*Department of Electrical and Electronic Engineering, Kobe University (Japan)*

Atomically thin two-dimensional (2D) semiconductors exhibit a wide range of novel physical phenomena. Mixed-dimensional 1D-2D heterostructures are expected to introduce unique electronic and optical properties, levitating the potential of 2D semiconductors through the interplay between the different dimensions at the interfaces. Our group has recently demonstrated efficient exciton transfer and the emergence of interlayer excitons in mixed-dimensional carbon nanotube (CNT) and 2D tungsten diselenide (WSe_2) heterostructures via band alignment engineering [1,2]. Additional degrees of freedom can be introduced into this system through doping and the application of an electric field, further enhancing the ability to manipulate interactions at the 1D-2D interface.

Here, we will discuss the photoluminescence (PL) emission in WSe_2/CNT heterostructures under the application of back-gate voltage. Measurements are conducted on air-suspended WSe_2/CNT field-effect transistors (Fig. 1). The field-effect device fabrication begins with the chemical vapor deposition growth of CNTs over the trenches with pre-deposited source and drain metal contacts. The mixed-dimensional heterostructure is formed by transferring an exfoliated WSe_2 flake on top of an air-suspended CNT using anthracene-assisted dry transfer method [3]. We performed photoluminescence excitation spectroscopy under different gate voltages. We investigated the vertical electric field dependence of PL emission under E_{22} excitation of CNT and A-exciton resonance excitation of WSe_2. We clarified the role of metal contacts on the chirality dependence of band alignments.

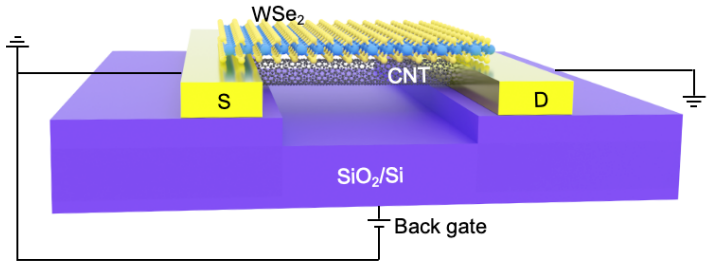

Figure 1: An illustration of an air-suspended WSe_2/CNT field-effect transistor.

References

[1] N. Fang, Y. R. Chang, D. Yamashita, S. Fujii, M. Maruyama, Y. Gao, C. F. Fong, K. Otsuka, K. Nagashio, S. Okada, Y. K. Kato, "Resonant exciton transfer in mixed-dimensional heterostructures for overcoming dimensional restrictions in optical processes," *Nature Commun.* **14**, 8152 (2023).

[2] N. Fang, Y. R. Chang, S. Fujii, D. Yamashita, M. Maruyama, Y. Gao, C. F. Fong, D. Kozawa, K. Otsuka, K. Nagashio, S. Okada, Y. K. Kato, "Room-temperature quantum emission from interface excitons in mixed-dimensional heterostructures," *Nature Commun.* ***15***, *2871 (2024).*

[3] K. Otsuka, N. Fang, D. Yamashita, T. Taniguchi, K. Watanabe, Y. K. Kato, "Deterministic transfer of optical-quality carbon nanotubes for atomically defined technology", *Nature Commun.* **12**, 3138 (2021).

Acknowledgments

This work is supported by JST (ASPIRE JPMJAP2310) and JSPS (KAKENHI JP23H00262, JP22K14623, JP22F22350, JP24K17627). C.F.F. is supported by the RIKEN Special Postdoctoral Researcher Program.

Thermal Conductivity of Solution-Spun Carbon Nanotube Fibers with Different Draw Ratios

Jiun-Hung Yi[1,2], Ognyan Stefanov[1,2], Michelle Durán-Chaves[2,3], Eldar Khabushev[2,4], Matteo Pasquali[2,3,4], Geoff Wehmeyer[1,2]

[1] Department of Mechanical Engineering, William Marsh Rice University (USA), [2] The Carbon Hub, William Marsh Rice University (USA), [3] Department of Chemistry, William Marsh Rice University (USA), [4]Department of Chemical and Biomolecular Engineering, William Marsh Rice University (USA)

Carbon nanotubes fibers (CNTFs) have been widely explored for electronic devices, thermal management applications, textiles, and wearable devices due to their high electrical and thermal conductivity, high mechanical strength, low density, and flexibility [1-5]. However, the wide variety of constituent carbon nanotube structures and processing methods results in a broad range of thermal properties for CNTFs [6, 7], motivating further investigation into the relevant thermal mechanisms and structure-property relations. When fabricating CNTFs through extrusion of a carbon nanotube (CNT)-chlorosulfonic acid solution into coagulant, the draw ratio *DR* (i.e., ratio of collection linear velocity to extrusion linear velocity) applied during collection influences the fiber morphology [8, 9]. Large *DR* can improve CNT alignment within the CNTF, potentially decreasing thermal resistances between CNT bundles and further enhancing the thermal conductivity of the CNTF. However, excessive *DR* can lead to instabilities in fiber collection and reduced residence time in the coagulant bath. Though prior work has quantified how the mechanical and electrical properties of solution-spun CNTF depend on *DR* [8, 9], the effect of *DR* on thermal conductivity of solution-spun CNTF is not known.

Here, we fabricated CNTFs using few-wall CNTs with viscosity-averaged molecular aspect ratios of 5500. The fibers were collected with different draw ratio (*DR*=2,3, and 4) and subjected to either a washing procedure, which removes the residual acid to stabilize fiber properties, or no washing. The electrical conductivity was measured using a four-probe method, while the thermal properties were measured using the self-heating three-omega [10, 11] method for suspended fibers. Both measurements were conducted in a vacuum chamber to minimize the effect of thermal convection. The cross-sectional areas of the fibers were measured by scanning electron microscope (SEM) after focused-ion beam (FIB) cutting. The G/D ratio and the order parameter of the fibers were measured by polarized Raman microscope [12, 13].

The electrical conductivity results show no strong dependence on the draw ratio, with values ranging from 2.5 - 5.6 MS/m. The washed fibers exhibited lower electrical conductivity than the unwashed fibers due to the removal of residual acid during washing. The thermal conductivity measurement results indicated that a higher *DR* could result in higher thermal conductivity, with the highest measured values occurring at *DR*=3 and 4. The largest measured value was 415±50 W/m.K observed at *DR* =3, which is similar to but larger than the reported prior value of ~390 W/m.K for pristine as-spun CNTF [7, 9]. However, the relatively high scatter in thermal conductivity for high-draw *DR*=4 samples indicates that excessive drawing might break the bundle-to-bundle connection, which increases the thermal resistance between bundles and causes instability or axial variation in the properties of CNTF. The fibers subjected to an additional washing procedure exhibit a different trend compared to unwashed samples in terms of specific electrical and thermal conductivity. For washed samples, the mass-normalized thermal conductivity increases with *DR*, whereas for unwashed samples, the optimal values occur at *DR*=3. To further investigate factors influencing electrical and thermal properties, additional measurements of the G/D ratio and order parameter were conducted. Results showed that the CNTFs exhibited high G/D ratios and high order parameter, indicating well-aligned CNTs within the fibers, though these results do not strongly correlate with *DR* over this range of *DR*.

In summary, we find that CNTFs made from high molecular aspect ratio CNT using moderate-to-high draw ratio have strong potential for achieving high (>400 W/m.K) room-temperature thermal conductivity. However, excessive draw can result in notable axial variations in thermal conductivity and incomplete acid removal without additional washing procedures. Thus, this work details the structure-property relation of high-performance CNTF and motivates further investigation into thermal transport mechanisms and CNT alignment.

References

[1] J.S. Bulmer, A. Kaniyoor, and J.A. Elliott, *A meta-analysis of conductive and strong carbon nanotube materials.* Advanced Materials, 2021. **33**(36): p. 2008432.

[2] N. Komatsu, et al., *Macroscopic weavable fibers of carbon nanotubes with giant thermoelectric power factor.* Nature Communications, 2021. **12**(1): p. 4931.

[3] A. Lekawa-Raus, et al., *Electrical properties of carbon nanotube based fibers and their future use in electrical wiring.* Advanced Functional Materials, 2014. **24**(24): p. 3661-3682.

[4] L.W. Taylor, et al., *Improved properties, increased production, and the path to broad adoption of carbon nanotube fibers.* Carbon, 2021. **171**: p. 689-694.

[5] H.Z. Wang, et al., *Highly Conductive Double-Wall Carbon Nanotube Fibers Produced by Dry-Jet Wet Spinning.* Advanced Functional Materials, 2024. **34**(39): p. 2404538.

[6] L. Qiu, et al., *Functionalization and densification of inter-bundle interfaces for improvement in electrical and thermal transport of carbon nanotube fibers.* Carbon, 2016. **105**: p. 248-259.

[7] N. Behabtu, et al., *Strong, light, multifunctional fibers of carbon nanotubes with ultrahigh conductivity.* science, 2013. **339**(6116): p. 182-186.

[8] X. Zhang, et al., *Simultaneously enhanced tenacity, rupture work, and thermal conductivity of carbon nanotube fibers by raising effective tube portion.* Science Advances, 2022. **8**(50): p. eabq3515.

[9] S.G. Kim, et al., *Hierarchical structure control in solution spinning for strong and multifunctional carbon nanotube fibers.* Carbon, 2022. **196**: p. 59-69.

[10] L. Lu, W. Yi, and D. Zhang, *3ω method for specific heat and thermal conductivity measurements.* Review of scientific instruments, 2001. **72**(7): p. 2996-3003.

[11] C. Dames and G. Chen, *1ω, 2ω, and 3ω methods for measurements of thermal properties.* Review of scientific Instruments, 2005. **76**(12).

[12] C. Zamora-Ledezma, et al., *Anisotropic thin films of single-wall carbon nanotubes from aligned lyotropic nematic suspensions.* Nano letters, 2008. **8**(12): p. 4103-4107.

[13] D.E. Tsentalovich, et al., *Influence of carbon nanotube characteristics on macroscopic fiber properties.* ACS applied materials & interfaces, 2017. **9**(41): p. 36189-36198.

APPLICATION OF MULTIWALL CARBON NANOTUBES TO ENHANCE THE LUBRICATION PERFORMANCE OF MACHINE ELEMENTS

Kamlesh Shivvedi[1], Santhosh Kumar Kamarapu[2], M Amarnath[1], H. Chelladurai[1]

1. *Tribology and Machine Dynamics Laboratory, Department of Mechanical Engineering, Indian Institute of Information Technology Design and Manufacturing, Jabalpur, Madhya Pradesh, 482005, India*
2. *Department of Mechanical Engineering, SR University, Warangal, Telangana 506371, India*

Abstract

The utilization of petroleum-based lubricants leads to several hazardous effects on environment viz. soil and water contamination and aquatic ecosystem damage which result in adverse impacts such as global warming, human health concerns. Vegetable oil-based lubricants are considered as one of the promising substitutes for the petroleum oil-based lubricants which possess several advantages, such as high flash point, viscosity index, boiling point, low environmental pollution, toxicity, bio degradability and excellent lubricity. Although vegetable oils generally exhibit superior biodegradability in comparison with mineral oil-based lubricants, some concerns such as thermal and oxidative instability limit their suitability to fulfill the requirements of industrial applications. In this context, the researchers have explored various options for enhancing the oxidation stability of vegetable oils, which include chemical treatments such as transesterification, epoxidation, and hydrogenation, as well as the addition of extreme performance additives viz. detergents, dispersants, antioxidizing additives, nanoparticles, viscosity enhancers, and wear resistance additives. This paper presents the results of experimental investigations carried out to enhance the performance of roller bearing system by using multiwall carbon nano tubes (MWCNT) blended vegetable oil-based lubricant. The results are compared with the bearing operated by using mineral oil-based lubricant to highlight the importance of MWCNT blended vegetable oil which enhanced the performance of roller bearing system by minimizing friction, wear, and dynamic response of roller bearing subjected to fatigue load cycles over a test duration of 1200 hrs.

Synthesis of single-unit-cell thin perovskites by liquid-phase confined assembly for high-performance ultrastable X-ray detectors

Meihui Song, Feng Yang*

Department of Chemistry, Southern University of Science and Technology, Shenzhen, China,

The instability of halide perovskites under working conditions or in complex postprocessing is challenging for practical applications. Herein we developed a room-temperature, two-phase assembling strategy to synthesize single-unit-cell perovskite chains within single-walled carbon nanotubes (SWCNTs). This approach is efficient, scalable, and tailorable, providing compatibility for assembling various single-chain perovskites.

The single-unit-cell-chain perovskites show unconventional stoichiometries (e.g., $[A_4BX_5]^+$) due to dimensionality reduction and are balanced by negatively charged nanotubes. The direct X-ray detector constructed by high-entropy-Cs_3MCl_6@SWCNT exhibits outstanding performance, with a high sensitivity of 1.22×10^4 $\mu C\cdot Gyair^{-1}\cdot cm^{-2}$, an incredibly low dark current density of 0.2 $nA\cdot cm^{-2}$, a negligible dark current drift of 8.5×10^{-7} $nA\cdot cm^{-1}\cdot s^{-1}\cdot V^{-1}$, and a superior detection limit of 16.6 $nGyair\cdot s^{-1}$. These surpass various common semiconductor and state-of-the-art perovskite detectors, due to the ionic character of perovskite@SWCNT inducing a strong cation-π interaction, suppressing ion migration. The device is quite stable under harsh conditions, including continuous X-ray irradiation, high temperatures, 91-day exposure in ambient air, and 96-hour immersion in water. This low-cost synthetic methodology paves the way for the commercialization of potential perovskite X-ray detectors for medical and industrial applications [1].

This cost-effective and scalable synthesis method unveils novel possibilities for the commercial viability of perovskite-based X-ray detectors. This breakthrough not only addresses the enduring challenges associated with perovskite instability but also paves the way for its widespread application in next-generation optoelectronic devices.

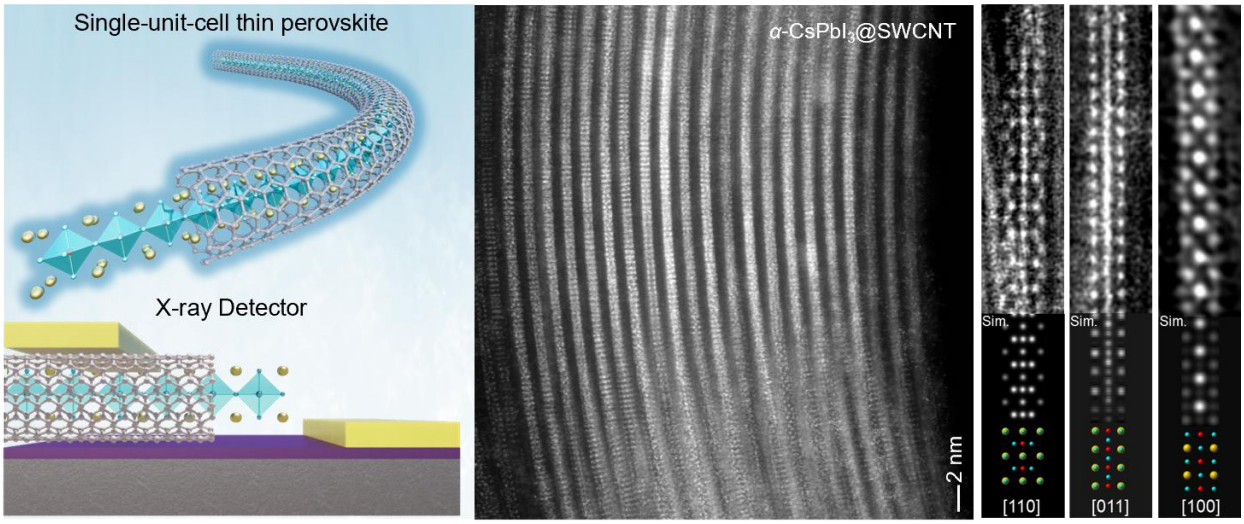

Figure 1: Assembling single-unit-cell perovskite chains within SWCNTs for X-ray detector.

References

[1] M. Song#, B. Zhao#, B. Li, K. Wang, Y. Jiang, G. Jia, X. Zhao, B. Yu, Y.-L. Li*, F. Yang* , *Nature Synthesis,* in press (2025).

Low power NO_2 sensing by MoS_2 photoactivated sensor with integrated micro-LED light source

H. Tabata[1], K. Fujii[1], S. Ichikawa[1], T. Ishihara[1], K. Kojima[1], Y. Fujiwara[1,2], M. Katayama[1]

[1]*Osaka University (Japan),* [2]*Ritsumeikan University (Japan)*

In recent years, increasing interest in environmental monitoring and personal health monitoring has necessitated the development of compact, cost-effective, energy-conserving gas sensors suitable for integration into portable devices. Photoactivated gas sensors, which demonstrate high sensitivity and rapid response/recovery under light irradiation, are promising candidates for low-power gas sensors capable of operating at room temperature. Transition metal dichalcogenides (TMDCs) are expected to be superior sensing materials for the photoactivated gas sensor using visible light compared to conventional metal oxide semiconductors [1] due to their higher surface-to-volume ratio and higher absorption coefficient in visible light spectrum, attributable to their smaller bandgap. Previously, we have fabricated photoactivated gas sensors using MoS_2 monolayer flakes and demonstrated their high photoactivated response to NO_2 under visible light illumination [2]. However, the experiment has utilized an external light source and has not demonstrated their capacity for reducing power consumption and achieving miniaturization, inclusive of the light source. The purpose of this study was to fabricate a monolithic gas sensor with MoS_2 gas sensor mounted on a micro-LED device to achieve low power consumption and miniaturization and evaluate sensor characteristics during low-power operation.

The planer micro-LEDs with an emission area of 30 μm × 30 μm were fabricated by forming ITO current spreading layer patterns on the top of the p-GaN layer of a GaN-based blue LED substrate with a multi-quantum well of InGaN/GaN as the emission layer. The MoS_2 sensors were fabricated through the deposition of a MoS_2 monolayer flake onto the micro-LEDs covered with a SiO_2 insulating layer and subsequently contacted with Bi/Au electrodes (Fig.1). The gas-sensing properties of the sensor were evaluated by exposing the sensor to NO_2 under conditions of constant irradiance (input power) with a constant voltage applied to the LED. Figure 2 shows the dynamic responses of sensor resistance to 100 ppb NO_2 exposure measured under different irradiance (input power) of the LED. A distinct photoactivation response was observed even at 52 μW, which is close to the minimum input power (~40 μW) determined by the leakage current of this LED. However, the response and recovery speeds exhibited a tendency to decrease at input power levels below approximately 230 μW. Based on these results, we determined that the minimum power consumption required to maintain photoactivation performance in this sensor is approximately 230 μW. This value could be further reduced by improving the luminous efficiency of the LEDs and the light utilization efficiency of the sensor.

Figure 1: Schematic of MoS_2/micro-LED device

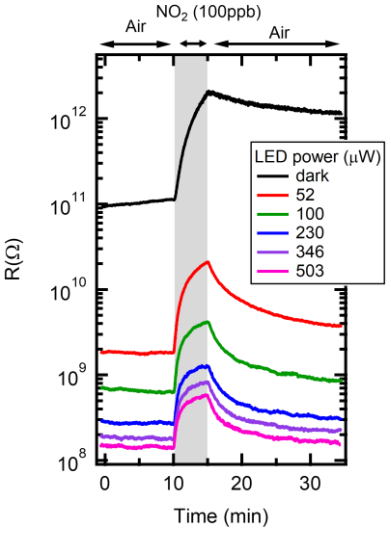

Figure 2: Sensor responses to 100 ppb NO_2 under various LED input power levels.

Acknowledgements: This work was supported by Iketani Science and Technology Foundation and JSAP KAKENHI (23H01805, 23K26498) .

References

[1] R. Kumar *et al*., Mano-Micro Lett. **12**, 164 (2020).
[2] H. Tabata *et al*., ACS Nano **15**, 2542 (2021).

Extraction of the true topography of carbon nanotubes on SiO_2/Si substrates by scanning electron microscopy.

Boxiang Zhang[1*], Chuanhong Jin[1]

[1] *State Key Laboratory of Silicon Materials, School of Materials Science and Engineering, Zhejiang University, Hangzhou, Zhejiang 310024, P. R. China*

*boxiang.zhang@zju.edu.cn

The apparent width (W_{CNT}) of single-walled carbon nanotubes (CNTs) on SiO_2/Si substrate measured by scanning electron microscopy (SEM) used to broaden from its intrinsic diameter of 1-2 nm to over 30 nm due to the charging effects [1] and electron-beam-induced current [2] (see Fig.1a). This hinders the extraction of the real diameter of CNTs, the resolving of CNT bundles with single CNTs, and most importantly, hinders the density extraction of high-density CNT arrays used for CNT-based integrated circuits.

To solve this problem, we developed two methods to narrow the W_{CNT} back to ~3 nm (see Fig.1b), thus making it possible to distinguish between individual CNT and CNT bundles (see Fig.1c), to locate isolated CNT fragments (see Fig. 1d) and to extract the density arrays up to 330 CNTs/um if 3 nm is taken as the limit of the resolvable pitch length. The core of both methods is to detect SEM images dominated by charging and topography information by separating electrons with different emission energies and angles. The first method draws on the SEM technique used in metals research [3], i.e., varying the working distance in Zeiss's compound lens. The second method involves varying the deceleration voltage in Hitachi's system.

In order to investigate the limiting factors that prevent the W_{CNT} from being further reduced, we have investigated the effects of beam size, landing energy, and residual charging on the W_{CNT}, and our results show that the beam size at low landing energy and the signal-to-noise ratio at high landing energy are currently the limiting factors for W_{CNT}. Therefore, better instrumentation (e.g., aberration-corrected SEMs) or methods for improving the signal-to-noise ratio of the detector are the future direction to move forward.

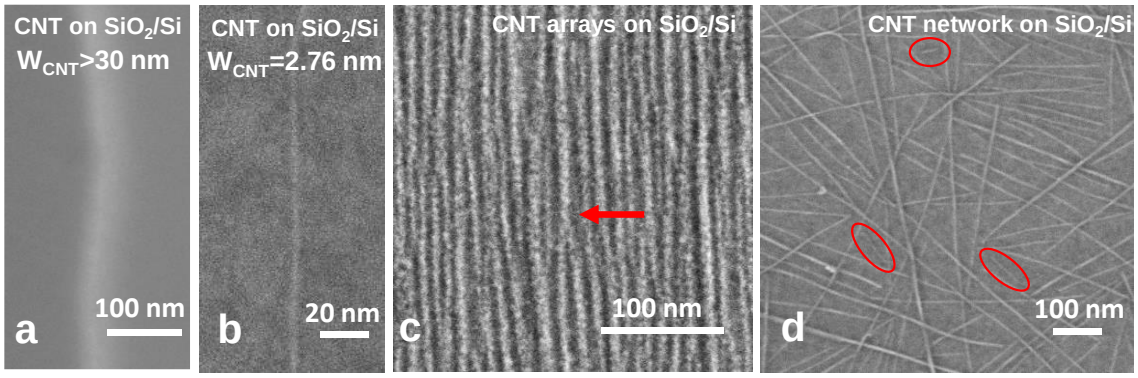

Figure 1: SEM images of (a-b) Individual CNT, (c) high-density CNT arrays, and (d) CNT networks on SiO_2/Si substrate recorded at a landing energy of 1 keV with Zeiss's Gemini 500. The working distance is 5 mm for (a) and 1 mm for (b-d). The red arrow indicates the branching behavior of CNT bundles in high-density CNT arrays, and the red circles indicates the isolated fragments of CNTs as short as 30 nm in length.

References

[1] T. Brintlinger *et al.*, *Appl. Phys. Lett.*, **81,** 2454–2456 (2002).
[2] Y. Homma et *al.*, *Appl. Phys. Lett.*, **84,** 1750–1752 (2004).
[3] M. Nagoshi *et al.*, *Surface and Interface Analysis*, **48,** 470–473 (2016).

High performance aligned carbon nanotube thin film transistors for mini- and micro-LED driving

Meiqi Xi[1,2], Fang Liu[1], Xuehao Zhu[1], Yi Li[1], Lan Bai[1,2], Lianmao Peng[1,2], Yu Cao[1,2]*, Xuelei Liang[1,2]*

[1] *Key Laboratory for the Physics and Chemistry of Nanodevices and Center for Carbon-Based Electronics, School of Electronics, Peking University (China),* [2] *Institute for Carbon-Based Thin Film Electronics, Peking University, Shanxi (ICTFE-PKU) (China)*

Mini-LED (mLEDs) and micro-LEDs (μLEDs) are inorganic solid-state self-emitting devices which outperform organic LEDs (OLEDs) on the ground of their longer lifetime, high luminous efficiency and superior stability[1]. Since the mLEDs/μLEDs are current driving devices, high mobility (~100 $cm^2/V·s$) and high current driving capability (μA to mA) are requisite for the driving thin film transistors (TFTs)[2]. S-CNTs possess excellent electronic and thermal properties, such as high carrier mobility (up to 100,000 cm^2/Vs), high current-carrying capability, and small intrinsic capacitance, making them promising candidates for future emissive display applications[3]. However, the reported results are mostly based on network type CNT films and the large amount of inter-tube junctions in the film hamper high field-effect mobility (>100 cm^2/Vs) and large current driving capability (>20 μA/μm) for devices with channel length of micrometer scale. Recently, with the progress of s-CNT material research, high-density and high-semiconducting-purity aligned s-CNT arrays (A-CNTs) can be obtained in wafer scale, and the performance of so fabricated devices at sub-100 nm scale have been proven to outperform the silicon MOSFETs[4].

In this work, TFTs were fabricated by using the A-CNTs with channel length (L) of 1-10 μm. The measured average current density ranges from 417 μA/μm for L = 1 μm to 17 μA/μm for L = 10 μm at source-drain voltage (V_{ds}) of -3.1 V. The average field-effect mobility ranges in 105-135 cm^2/Vs. Such high mobility and high current make the A-CNT TFTs suitable for mLEDs/μLEDs driving. As a proof of concept, 1T1D structured mLEDs driven by A-CNT TFTs were fabricated and driven successfully. A 2 × 2 mLED display module was developed, showcasing individual pixel control via scan and data line modulation, as depicted in Figure 1h. This work highlights the potential of A-CNT TFTs for next-generation mLEDs and μLEDs display technologies.

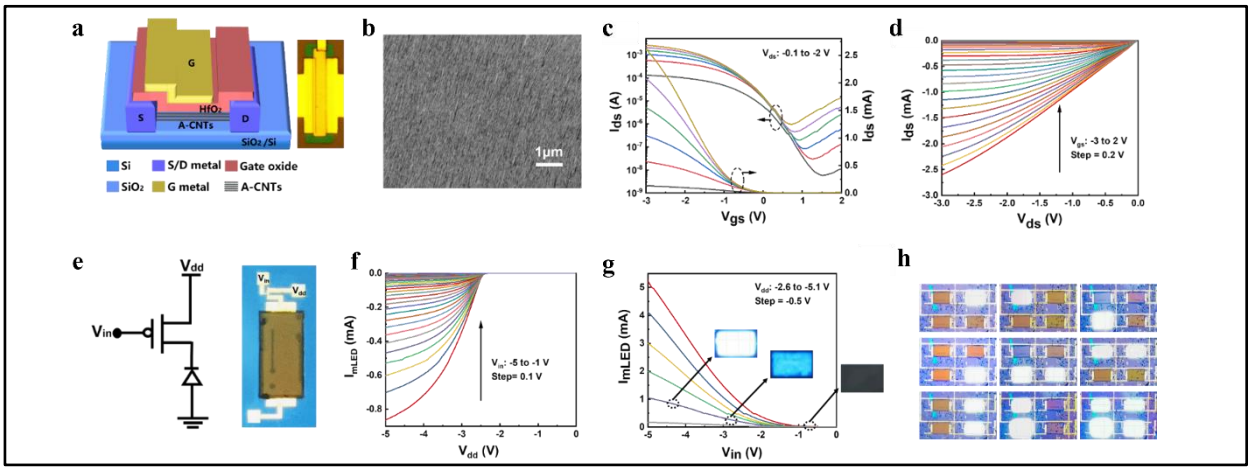

Figure1: (a) Schematic and optical image of A-CNT TFT；(b) SEM image of A-CNTs (density: 100–200 tubes/μm)；(c) Transfer characteristics of a typical A-CNT TFT(W=20 μm , L=3 μm)；(d) Output characteristics of the same device；(e) Schematic and optical image of a 1T1D single-pixel circuit；(f) Current–voltage characteristics of an mLED controlled by the single-pixel circuit, with I_{mLED} measured by sweeping V_{dd}；(g) Transfer characteristics (I_{mLED}-V_{in}) of the single-pixel circuit；(h) The switching properties of the 2 × 2 pixel array of mLEDs.

References

[1]Huang Y, Hsiang E L, Deng M Y, Wu S T et al., *Light Sci Appl*, **9:,** 105 (2020).
[2]Behrman K, Kymissis I et al., *Nat. Electron*, **5(9):** 564-73 (2022).
[3]Liang X, Xia J, Dong G et al., *Top Curr Chem (Cham)*, **374(6):** 80 (2016).
[4]Liu L J, Han J, Xu L et al., *Science*, 2020, **368(6493):** 850-+ (2020).

Synthesis of a Hybrid Flexible Thermoelectric Device with Carbon Nanotubes and Chalcogenide-based Thermoelectric Materials

Aarti[1,2], Bhasker Gahtori[1,2], S. R. Dhakate[1,2], Bhanu Pratap Singh[1,2]
[1]*Advanced Carbon Products and Metrology, CSIR-National Physical Laboratory, New Delhi -110012, India*
[2]*Academy of Scientific and Innovative Research (AcSIR), Ghaziabad- 201002, India*

Thermoelectric (TE) materials are pivotal in energy conversion processes, facilitating the transformation of thermal energy into electrical energy and vice versa, thereby enhancing energy efficiency and mitigating environmental pollution. Recent investigations have demonstrated that inorganic TE materials exhibit superior TE performance, however, their inherent rigidity and toxicity present significant challenges for practical applications. In contrast, organic TE materials, characterized by their flexibility, cost-effectiveness, lower toxicity, and ease of fabrication, typically exhibit inferior thermoelectric performance. To harness the advantages of both inorganic and organic TE materials, researchers are exploring hybrid systems that integrate both components to enhance flexibility and overall performance. Notably, a substantial portion of waste heat is generated within mid- to low-temperature ranges, where chalcogenide based materials are particularly effective for low temperature region. Concurrently, carbon nanotubes (CNTs) have emerged as promising organic TE materials due to their exceptional electrical conductivity; however, their thermoelectric performance remains suboptimal.

In this study, we present the development of a hybrid flexible TE structure composed of CNTs and chalcogenide based TE materials, fabricated via a dip-coating method. Initially, we synthesized a CNT sheet utilizing the floating catalyst chemical vapor deposition (FC-CVD) technique. To enhance the p-type thermoelectric performance of the CNT sheet, we incorporated a p-type TE material, silver antimony telluride ($AgSbTe_2$). Subsequently, we applied a coating of Bi_2Te_3 onto the CNT sheet, resulting in the formation of an n-type thermoelectric material.

We systematically characterized the synthesized materials through X-ray photoelectron spectroscopy (XPS), Raman spectroscopy, and electrical property measurements, assessing voltage, current, and resistance across a range of temperatures. Ultimately, we assembled a flexible thermoelectric device comprising 40 pairs of p-type and n-type materials, achieving a maximum output power of 50 μW and an open-circuit voltage of 321 mV at a temperature differential of 70 K. The detailed findings and performance results of this innovative hybrid thermoelectric material will be presented at the conference, underscoring its potential applications in energy harvesting and waste heat recovery systems.

Keywords: Thermoelectric, Carbon nanotubes, Bi2Te3, Dip coating.

1. Jin, H., et al., Hybrid organic–inorganic thermoelectric materials and devices. 2019. 58(43): p. 15206-15226.
2. Bano, S., et al., Room temperature Bi2Te3-based thermoelectric materials with high performance. 2020. 31(11): p. 8607-8617.
3. Zhao, W., et al., Flexible carbon nanotube papers with improved thermoelectric properties. 2012. 5(1): p. 5364-5369.
4. Ahmad, K. and Z.J.M.T.C. Almutairi, Enhanced thermoelectric properties of bismuth telluride (Bi2Te3) and multiwall carbon nanotube (MWCNT) composites. 2023. 35: p. 106228.
5. Sehrawat, M., M. Rani, and B.P.J.J.o.N. Singh, One Step Fabrication of Aligned Carbon Nanotube Sheet via FC-CVD Technique. 2022. 2022(1): p. 8318217.

The cross-scale assembly and mechanical behavior of super-strong carbon nanotubes

Yukang Zhu[1],Fei Wei[1*]

[1] *Green Chemical Reaction Engineering and Technology, Department of Chemical Engineering, Tsinghua University,Beijing 100084, China*

wf-dce@tsinghua.edu.cn

Carbon nanotubes (CNTs) with superior mechanical properties are expected to play a role in the next generation of critical engineering mechanical materials. Crucial advances have been made in CNTs, as it has been reported that the tensile strength of defect-free CNTs and CNT bundles can approach the theoretical limit[1]. However, the tensile strength of macro carbon nanotube fibers (CNTFs) is far lower than the theoretical level. On the other hand, the mechanical strength of CNTFs showed size effect, that is, the tensile strength of CNTFs decreased significantly with the increase of fiber diameter[2]. To gain deeper insights into the relationship between the mechanical properties and diameter of one-dimensional CNT assemblies, it is essential to achieve controlled fabrication of small-diameter bundle fiber structures composed of CNTs on the hundred-level scale. In this work, by integrating the gas-flow coalescence assembly technology of ultra-long CNT bundle with a floating catalyst system for density enhancement, we achieved the controlled fabrication of CNT bundle fibers with submicron-scale diameters. The effects of kinetic parameters, including reaction time, catalyst concentration, hydrogen dosage, and post-treatment annealing, on the diameter and crystallinity of the bundle fibers were investigated. Based on this, effective strengthening strategies for the mechanical properties of CNT assembly at different scales were developed. As a result, the tensile strength CNT bundle fiber composed of about 100 constituent tubes can reach 50 GPa. Then the mechanical properties of CNT bundle fibers of different scales were tested, and the size effect of the mechanical properties of CNT bundle fibers was further revealed. For bundle fibers with submicron-scale diameters, the highly aligned internal structure contributes to their strength. With each order of magnitude increase in size, the strength decreases by one-third. The introduction of macroscopic fibers with non-highly aligned internal structures results in a 50% reduction in strength with size scaling, underscoring the importance of microstructural alignment and microstress distribution in achieving effective cross-scale assembly of CNT mechanical properties.

References

[1] Bai, Y. *et al.*, *Acc. Mater. Res.* **2021,** *2* (11), 998-1009.
[2] Zhu, Y. *et al.*, *Nanomaterials* **2022,** *12* (19).

Effects of Y on stabilizing Fe catalyst in carbon nanotube growth

Le Huy Khuong Duy[1], Takayuki Nakano[1], Hisashi Sugime[2], Yoku Inoue[1]

[1]Shizuoka University (Japan), [2]Kindai University (Japan)

During the growth of carbon nanotubes (CNTs), maintaining long catalyst activity is challenging due to the thermal diffusion of Fe catalyst, which limits the synthesis of long CNTs. Previous studies have reported that introducing a Gd underlayer can suppress catalyst diffusion, likely due to the high standard Gibbs energy of formation (ΔG) of Gd oxide, which enhances catalyst stabilization [1]. In this study, we investigated the use of Y oxide, which has an even larger ΔG than Gd oxide, to further improve catalyst stability.

For CNT synthesis, a cold-gas chemical vapor deposition (CVD) method with limited gas preheating was employed alongside a conventional hot-wall CVD process. Si substrates were prepared with a multilayer structure of Fe/Y/Al_2O_3/SiO_2 via RF sputtering. During the CVD process, ferrocene (Fc) and aluminum isopropoxide (AIP), along with H_2O, were introduced to mitigate catalyst deactivation, in addition to process gases (C_2H_2, Ar, H_2, and CO_2).

The relationship between CNT forest growth time and length under cold-gas CVD is shown in Fig. 1. The Y underlayer significantly increased CNT length from 0.5 mm to 4 mm. Adding H_2O further extended the catalyst lifetime to ~9 hours, producing CNTs up to 9.5 mm long. Introducing Fc extended catalyst activity to ~18 hours, achieving CNT lengths of 13.8 mm. Moreover, the combined addition of Fc and AIP dramatically prolonged catalyst lifetime to ~25 hours, yielding CNTs up to 17.7 mm long.

These results demonstrate that incorporating Y, Fe, and Al into the CVD process significantly enhances catalyst stability, with the underlayer material's ΔG playing a key role. Additionally, the effects of the Y layer, along with Fe and Al additions, were examined in hot-wall CVD. Further details will be discussed in the presentation.

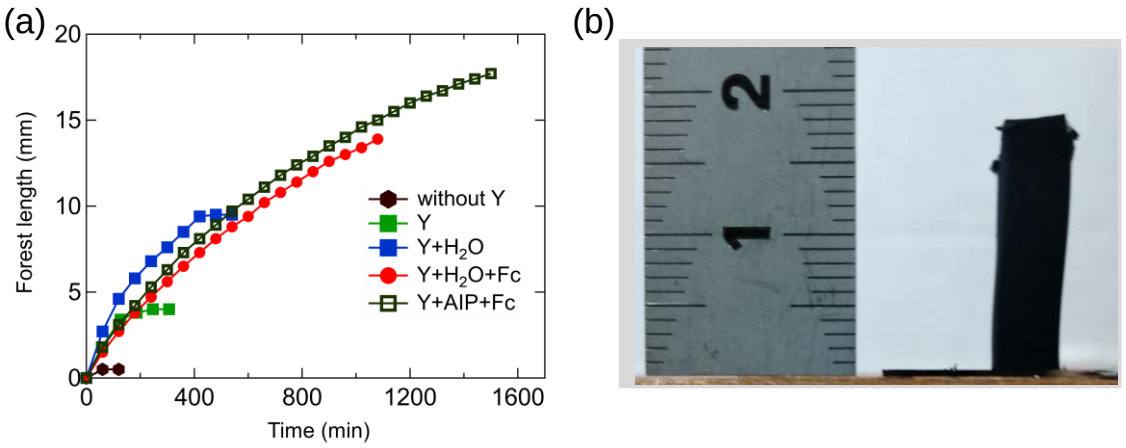

Fig1: (a) Growth profiles of the CNT forests without Y, with Y, with Y and H_2O, with Y and H_2O and ferrocene, with Y and AIP and ferrocene, and (b) CNT forest grown with Y, AIP and ferrocene.

References

[1] H. Sugime et al. ACS Nano **13**, 13208–13216 (2019).

Reinforcement of Polyimine Covalent Adaptable Networks with Mechanically Interlocked Derivatives of SWNTs

A. López-Moreno,[1] I. Isasti, [1] S. Miranda, [1] D. M. Jiménez, [1] S. Parzyszek, [1] N. Martín Sabanés, [1] H. Pedersen, [2] E. M. Pérez[1]

[1]IMDEA Nanociencia, Ciudad Universitaria de Cantoblanco, Faraday 9, Madrid, E28049 (Spain), [2]Nanocore ApS, Gothersgade 21, Copenhagen K, DK-1123 (Denmark)

The exceptional characteristics of single-walled carbon nanotubes (SWNTs) make them ideal polymer fillers, particularly for materials that are typically brittle or easily deformed. This potential has fueled extensive research into integrating SWNTs with polymers to develop high-performance composite materials. However, ensuring uniform dispersion of nanotubes by effectively debundling them is crucial to fully harness their advantageous properties.

Over the past decade, our research group [1] and others [2] have developed mechanically interlocked derivatives of SWNTs, known as MINTs. In these structures, macrocyclic molecules wrap around the nanotubes in a rotaxane-like fashion. Our proof-of-concept studies have shown that using MINTs to reinforce polymers not only reduces the tendency of SWNTs to aggregate but also creates more sites for interaction with the polymer, thereby improving load transfer. [3,4, 5]

Here we report that MINTs significantly enhance the mechanical properties of polyimine (PI) covalent adaptable networks (CANs), achieving near-optimal load transfer. Both stiffness and ultimate strength are markedly improved compared to composites made with pristine SWNTs. Additionally, the PI MINT CANs can be recycled thermally and chemically without any loss in mechanical performance. We have also fabricated and characterized prototype carbon fiber PI MINT laminar composites, which show a substantial boost in mechanical properties.

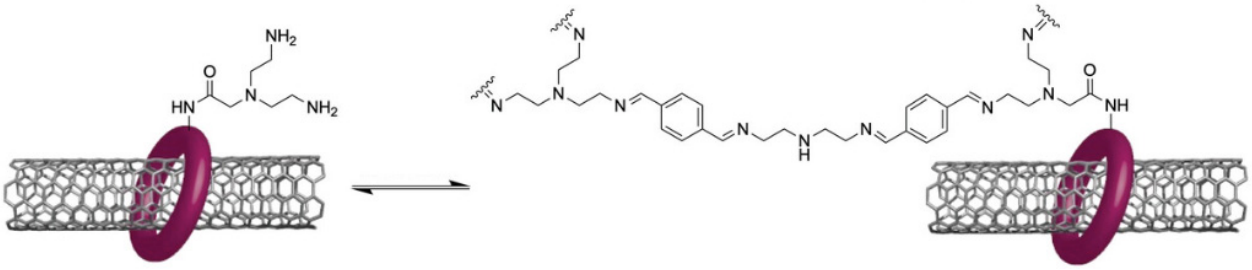

References

[1] A. de Juan, Y. Pouillon, L. Ruiz-Gonzalez, A. Torres-Pardo, S. Casado, N. Martin, A. Rubio, E. M. Perez, Angew. Chem., Int. Ed. 2014, 53, 5394

[2] A. López-Moreno, J. Villalva, E. M. Pérez, Chem. Soc. Rev. 2022, 51, 9433

[3] A. López-Moreno, B. Nieto-Ortega, M. Moffa, A. de Juan, M. M. Bernal, J. P. Fernández-Blázquez, J. J. Vilatela, D. Pisignano, E. M. Pérez, ACS Nano 2016, 10, 8012.

[4] S. Mena-Hernando, M. Eaton, J. P. Fernández-Blázquez, A. López-Moreno, H. Pedersen, E. M. Pérez, Chem. Eur. J. 2023, 29, 202301490

[5] J. Villalva, A. Rapakousiou, M. A. Monclús, J. P. Fernández Blázquez, J. de la Vega, A. Naranjo, M. Vera-Hidalgo, M. L. Ruiz-González, H. Pedersen, E. M. Pérez, ACS Nano 2023, 17, 16565

Overcoming the Yield-Quality Trade-off for Aerosol-CVD-Synthesized Single-Walled Carbon Nanotubes by Diameter Control

Ilya V. Novikov[1], Yasir Shafi Mir[1], Il Hyun Lee[1], Jeong-Seok Nam[1], Il Jeon[1]

[1] *Sungkyunkwan University (SKKU) (Republic of Korea)*

Carbon nanotube (CNT) thin films are a cutting-edge material being explored for next-generation electronic, semiconducting, and optical technologies [1]. Aerosol chemical vapor deposition (CVD), a particular case of floating catalyst CVD (FCCVD), beneficially stands out among other methods for CNT film production by enabling the one-step collection of high-quality isotropic films with easy-to-tune thickness and area as well as avoiding the use of any liquids and the treatment procedures associated with them [2]. Nevertheless, one of the most challenging and crucial obstacles to the full-scale realization of this method is the simultaneous maintenance of high yield and high quality of CNT films [2]. In this study, we propose a strategy for targeted synthesis of nanotubes with increased diameter and length that allows to improve both the conductivity and the yield of the produced CNT films. Since transparent electrodes are one of the most promising applications of CNT thin films, to demonstrate CNT film quality, we use the Yield/R_{90} (sheet resistance of 90% transparent conductive film) ratio as an indicator of CNT film performance and the productivity of aerosol CVD synthesis simultaneously. Utilizing toluene as a carbon source (demonstrated to result in improvement of both the properties and yield of CNTs [3,4]) for nanotube growth and finely tuning concentration of hydrogen (**Figure 1**), known to have a complex influence on the catalyst precursor decomposition, nanotube nucleation, and its growth stages [5-7], we managed to synthesize films of wide nanotubes with a diameter of *ca.* 2.5 nm and an I_G/I_D ratio higher than 60. The combination of large diameter and length, low defectiveness, and some other factors led to an ultrahigh Yield/R_{90} ratio of 1.1 mm^2 l^{-1} (Ω □$^{-1}$)$^{-1}$ for *pristine* nanotube films, more than two times higher than the best results of 0.40-0.45 mm^2 l^{-1} (Ω □$^{-1}$)$^{-1}$ reported so far for *doped* single-walled CNT films [2,3,8]. The approach to the targeted synthesis of wide, long, and low-defective CNTs for high-yield production of high-quality films enhances the prospects of aerosol-CVD-synthesized nanotubes for mass application in the forefront technologies.

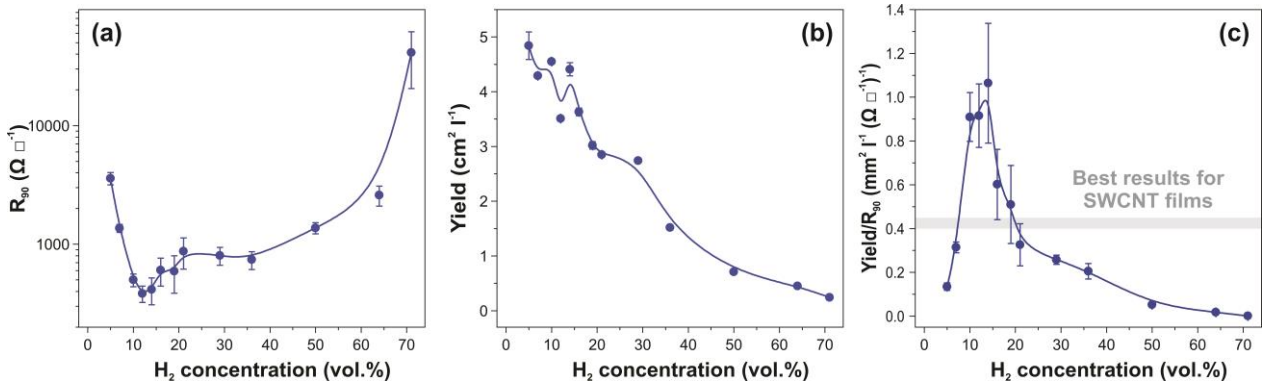

Figure 1. Dependency of **(a)** R_{90}, **(b)** Yield, and **(c)** Yield/R_{90} ratio on H_2 concentration in toluene-based aerosol CVD synthesis of CNTs. The grey line indicates the best values of the Yield/R_{90} ratio achieved for SWCNT films.

References

[1] A. Kaskela *et al.*, *Nano Lett.* **10**, 4349–4355 (2010).
[2] I.V. Novikov *et al.*, *Adv. Mat.* 2413777 (2025).
[3] E.M. Khabushev *et al.*, *Carbon* **189**, 474-483 (2022).
[4] E.X. Ding *et al.*, *Nano Res.* **13**, 112 (2020).
[5] J. Lei *et al.*, *J. Phys. Chem. Lett.* **14**, 4266-4272 (2023).
[6] A.R. Bogdanova *et al.*, *Nanomaterials* **13**, 154 (2023).
[7] P.X. Hou *et al.*, *ACS Nano* **8**, 7156-7162 (2014).
[8] E.X. Ding *et al.*, *Nanoscale* **9**, 17601 (2017).

Boosted thermal conductivity of single-walled carbon nanotube films via BN welding and encapsulation

Changping Yu [1,2], Feng Zhang [1,2], and Chang Liu [1,2]

[1] *Shenyang National Laboratory for Materials Science, Institute of Metal Research, Chinese Academy of Sciences, 72 Wenhua Road, Shenyang, China*

[2] *School of Materials Science and Engineering, University of Science and Technology of China, 96 Jinzhai Road, Hefei, China*

Owing to the ultrahigh thermal conductivity, excellent flexibility, and lightweight nature, single-walled carbon nanotubes (SWCNTs) exhibit great potential as thermal management materials, but the weak van der Waals interaction between the SWCNTs in their macroscopic assemblies leads to large thermal contact resistance at the tube-tube junctions. An epitaxial growth method enables the efficient integration of hexagonal boron nitride (h-BN) on SWCNTs [1] to provide an additional heat transfer path, but the thermal resistance at the junctions persists, which suggests limited efficacy in interfacial phonon coupling. To overcome these limitations, we propose a two-step atmospheric pressure chemical vapor deposition method [2] to weld SWCNT network junctions with amorphous BN while encapsulating SWCNT bundles with h-BN. By precisely modulating the partial pressures of BN precursors, we achieve controlled nucleation sites, microstructures, and compositions of BN phase, thereby enabling simultaneous BN welding and encapsulation. The welded SWCNT@h-BN (W-SWCNT@h-BN) film exhibits a 344% increase in in-plane thermal conductivity after BN welding and encapsulating. This approach highlights the critical role of interfacial phonon coupling optimization in advancing thermal management solutions for flexible electronics and energy devices.

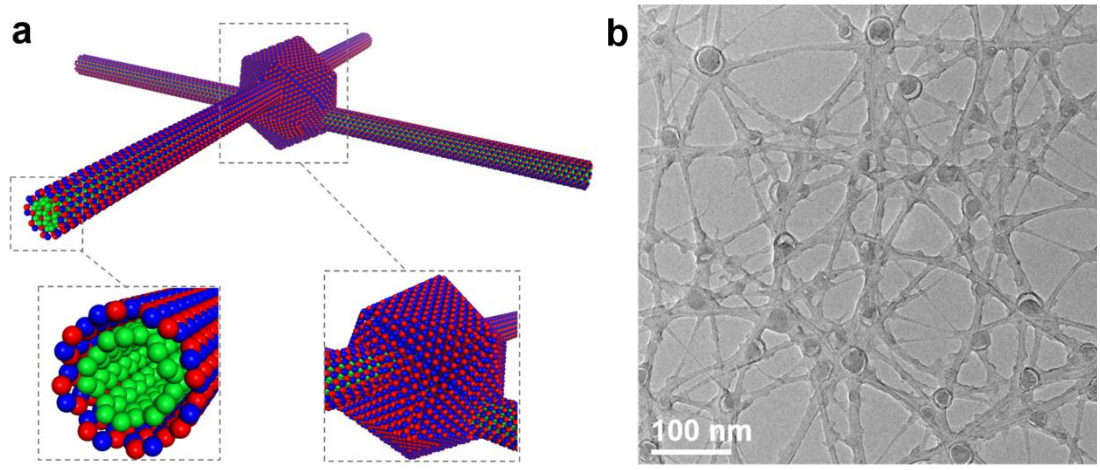

Figure 1. (a) Schematic of the atomic structure of W-SWCNT@h-BN, (b) Transmission electron microscopy image of W-SWCNT@h-BN.

References

[1] Yu, C, et al. *Materials*, **16**, 1864 (2023).

[2] Yu, C, et al. *Journal of Materials Science & Technology*, (2025) accepted.

Enhanced Efficiency in Dye-Sensitized Solar Cells Using Carbon Nanotube Composite Papers via Multiple Dye Fixation

Y. Kou[1], T. OYA[1, 2]

[1] *Graduate School of Engineering Science, Yokohama National University (Japan),*

[2] *Semiconductor and Quantum Integrated Electronics Research Center, Institute for Multidisciplinary Sciences, Yokohama National University (Japan)*

In recent years, as interest in environmental issues grows, renewable energy sources such as solar energy are gaining increasing attention. In this study, we focus on a novel type of solar cells called dye-sensitized solar cells (DSSCs) [1], which use the redox reaction of dyes to generate power. By utilizing carbon nanotube composite papers (CNTCPs), a composite material of CNT and paper that we have succeeded in developing, as the cathode and anode, low-cost and environmentally friendly paper-DSSCs can be realized. Recent studies have also shown that incorporating a gel electrolyte can extend the operating lifetime of the paper-DSSCs. However, challenges remain in improving the photoelectric conversion efficiency [2]. As a possible cause of the low photoelectric conversion efficiency, we hypothesized that there might be a problem in the relationship between the energy level of the ground state of the dye and the valence band level of the electrolyte, and the energy level of the excited state of the dye and the conduction band level of the semiconducting CNT. Therefore, in this study, we introduce Copper(II) 2,3-naphthalocyanine(CuPc) and ruthenium (N719, Ruthenizer 535-bisTBA) dyes, which are considered to have different energy levels than the purple sweet potato dyes[3,4] we have been using in our previous study and investigate their effect on paper-DSSCs. Concrete experimental methods in this study are described below.

To prepare metallic CNTCPs, single-walled CNTs and a dispersant are placed in water, followed by ultrasonic dispersion. A pulp dispersion is separately prepared by stirring pulp in water. After that the two dispersions are mixed, then the pulp fibers with CNT are scooped up by fine net by using the modified Japanese *washi* papermaking method. For semiconducting CNTCPs, semiconducting CNTs and selected dyes are dispersed in water under similar conditions. The resulting material is dried and shaped through heat pressing. The gel electrolyte was prepared by dissolving 0.05 M iodine and 0.5 M potassium iodide in acetonitrile, followed by the incorporation of 5%(w/v) polyvinylidene difluoride (PVDF) and 5%(w/v) polyethylene glycol (PEG) as polymer hosts. The mixture was homogenized under heating to form a gel electrolyte. To fix the dyes on the semiconducting CNTCPs, they are immersed in solutions of CuPc, N719 and purple sweet potato dyes for 12 hours at room temperature, respectively. As results, the CNTCPs as electrodes exhibit green, red, and purple appearances, corresponding to the adsorption of the respective dye molecules. The excess unanchored dye molecules are subsequently removed from the surface via ethanol rinsing and dried to ensure effective adsorption of dye molecules and reduce invalid sites[5]. In this study, to further improve the power generation efficiency by optimizing dye coverage and suppressing charge recombination[6], a second dye fixation was performed on semiconducting CNTCPs that had been previously fixed with the dyes described above. As a result, the proposed approach of conducting two times of dyeing was confirmed to be effective to some extent. For example, the power generation efficiency was 3.5×10^{-5}% and the fill factor (FF, power generation performance index) was 0.104 when the sample was dyed only with purple sweet potato dye, whereas the power generation efficiency and FF improved to 2.34×10^{-3}% and 0.228, respectively, when the sample was dyed with purple sweet potato dye and then dyed a second time with CuPc.

In this study, multiple fixations of dyes were attempted to improve power generation efficiency, and their effectiveness was confirmed. In the future, we will continue our research on better dye combinations and theoretical analysis of the energy level difference between each dye and CNTs.

References: [1] D. Duonghond, *et al.*, *Helvetica chimica acta.* **67**, 1012-1018 (1984).
[2] Y. Kou, T. Oya, *Journal of Composites Science* **7**, 232 (2023).
[3] W. Mekprasart, *et al.*, *Materials Science and Engineering: B* **172**(3), 231-236 (2010).
[4] J. Ahn, *et al.*, *Molecular Crystals and Liquid Crystals* **581**(1), 45-51 (2013).
[5] W. M. Tang, *et al.*, *Optical Materials*, **144**, 114308 (2023).
[6] R. Su, *et al.*, *Solar Energy*, **206**, 443-454 (2020).

Confined synthesis of nitrogen-doped graphene nanoribbons transformed from nitrogen-containing precursors

Kunpeng Tang[1], Yingzhi Chen[1], Huiju Cao[1], Wendi Zhang[2], Kecheng Cao[2], Lei Shi[1]*

[1] *Sun Yat-sen University (China),* [2] *ShanghaiTech University (China)*

In prior research, various types of graphene nanoribbons (GNRs) with limited widths and well-defined edges have been synthesized through on-surface synthesis[1,2], including nitrogen-doped GNRs[3,4]. However, the synthesis of nitrogen-doped 6-armchair GNRs (6-AGNRs) with subnanometer widths has remained a challenge due to difficulties in designing suitably small nitrogen-containing precursors. In this study, we employed a confined synthesis technique to successfully synthesize N-doped 6-AGNRs with a width of 0.62 nm from various precursor molecules via decomposition and recombination mechanism, rather than traditional polymerization and dehydrocyclization processes[5-7]. Raman spectroscopy and X-ray photoelectron spectroscopy (XPS) confirmed that both cyanoferrocene and aminoferrocene serve as effective precursor molecules for the synthesis of N-doped 6-AGNRs. Notably, Raman analysis indicated an upward shift of the C-H mode due to N-doping. XPS results identified nitrogen species corresponding to pyrrolic and pyridinic doping types, with a calculated nitrogen-to-carbon atomic ratio of 1.21 at%. Additionally, aberration-corrected high-resolution transmission electron microscopy was utilized to directly visualize the N-doped 6-AGNRs, allowing for quantitative estimation of the GNR widths and the diameters of encapsulating single-walled carbon nanotubes. These findings enhance our ability to achieve precise synthesis of GNRs with controlled edge configurations, widths, and doping levels, paving the way for further applications of N-doped GNRs.

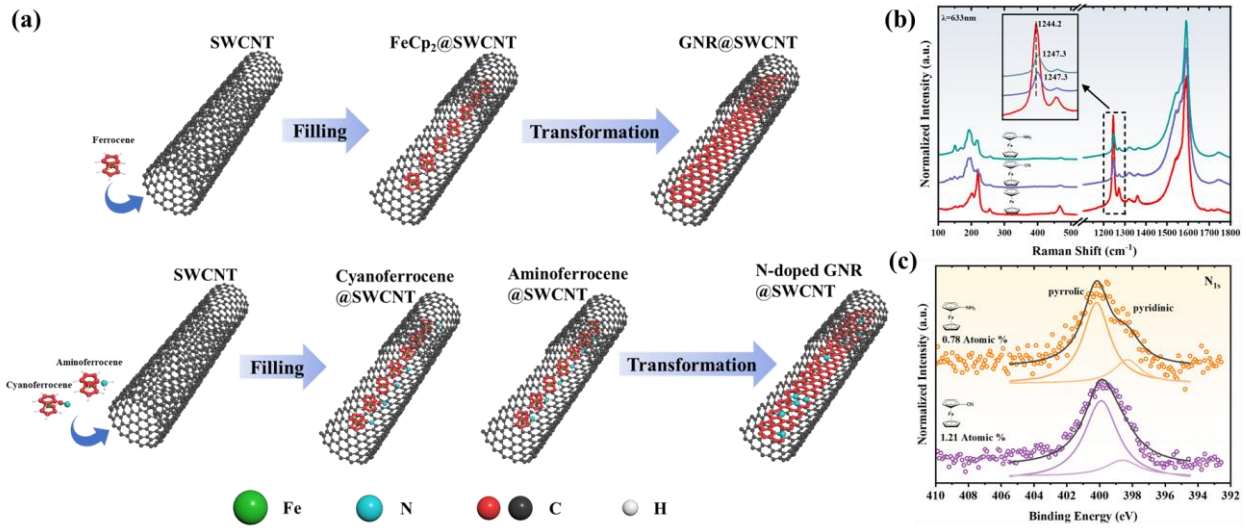

Figure (a) Schematic of confined synthesis of GNR using ferrocene (up panel) and nitrogen-containing molecules (bottom panel) as precursors. (b) Raman spectra of 6-AGNRs transformed from $FeCp_2$, cyanoferrocene and aminoferrocene as precursors. (c) N_{1s} signals with peak fitting of the N-doped 6-AGNRs.

References (if desired)

[1] Cai, J. M *et al.*, *Nature* **466**, 470–473 (2010).
[2] Merino-Diez, N. *et al.*, *ACS Nano* **11**, 11661–11668 (2017).
[3] Dibble, D. J. *et al.*, *Angew. Chem. Int. Ed.* **54**, 5883–5887 (2015).
[4] Pawlak, R. *et al.*, *Angew. Chem. Int. Ed.* **60**, 8370–8375 (2021).
[5] Hans Kuzmany, Lei Shi *et al.*, *Carbon* **171**, 221–229 (2021).
[6] Yifan Zhang *et al.*, *Nano Res.* **15**, 1709–1714 (2022).
[7] Kunpeng Tang *et al.*, Submitted (2025).

Annealing and Doping Effects on Axial Thermal Transport Properties of Solution-Spun Carbon Nanotube Fibers

Ognyan Stefanov[1,2], Michelle Durán-Chaves[2,3], Aosheen Anand[2,3], Eldar Khabushev[2,4], Matteo Pasquali[2,3,4], Geoff Wehmeyer[1,2]

[1] Department of Mechanical Engineering, William Marsh Rice University (USA), [2] The Carbon Hub, William Marsh Rice University (USA), [3] Department of Chemistry, William Marsh Rice University (USA), [4]Department of Chemical and Biomolecular Engineering, William Marsh Rice University (USA)

Solution spinning can be used to produce high-performance carbon nanotube fibers (CNTF) consisting of neat, aligned bundles of carbon nanotubes (CNTs). Solution-spun CNTF display appealing room-temperature axial thermal conductivity and thermal diffusivity for applications in lightweight axial heat spreading, flexible thermal connections, and thermoelectric active cooling.

Prior work has shown that remnant chlorosulfonic acid (CSA) or its derivatives within as-spun CNTF act as p-type dopants [1, 2]. De-doping of solution-spun CNTF through moderate temperature annealing (500-600 ℃) decreases the electrical conductivity by an order of magnitude [1, 2] and increases the thermal conductivity from 390 to 600 $W/m.K$ [1]. Moreover, annealing in the presence of iodine (p-dopant) gas further improved the thermal conductivity to 630 $W/m.K$ [1], while simultaneously doubling the electrical conductivity compared to the pristine fiber. Doping with vapor-phase iodine monochloride (ICl) has also been shown to improve the electrical conductivity of solution-spun CNTF [2], but the effects on thermal conductivity are unknown. Despite the prior work suggesting that annealing and doping can improve thermal conductivity, there has not been a systematic study that further explores the effects of these post-processing conditions on the CNTF axial thermal transport. In this study, we investigate the effects of (1) annealing at various temperatures well below the graphitization temperature of CNTs, and (2) vapor-phase ICl doping on the axial thermal conductivity and thermal diffusivity of solution-spun CNT fibers.

We fabricated solution-spun CNTF by dissolving commercially available few-wall, high molecular aspect ratio (3000-6000) CNTs in CSA and extruding through a spinneret into an acetone coagulant [1]. We annealed the as-spun fiber from 220 to 1085 ℃. Samples above 500 ℃ were annealed in nitrogen, while lower temperatures used a vacuum oven. For the vapor-phase doping procedure, we placed solution-spun CNTF inside an autoclave with 0.2 mL solution of ICl in dichloromethane (1 M). The autoclave was placed inside a vacuum oven at ~100 ℃ for 2 hours. Afterwards, we cooled the autoclave in an ice bath to crystallize remnant ICl that was not absorbed by the fiber. We measured the thermal conductivity and thermal diffusivity using the self-heating suspended configuration of the three-omega method [3, 4] in rough vacuum conditions. We measured the fiber cross-sectional areas by scanning electron microscope after focused-ion beam cutting.

Our electrical and thermal measurements show that annealing of as-spun fiber above 500 ℃ systematically reduces electrical conductivity by an order of magnitude, from approximately 6 to 0.6 MS/m, which qualitatively agrees with prior work. However, the relatively larger fractional decrease observed here as compared to prior work suggests that annealing above 600 ℃ more effectively de-dopes the as-spun CNTF by fully removing residual CSA or its derivatives. Annealing also systematically decreases the temperature coefficient of electrical resistance (TCR) of the as-spun fibers from 2800 ± 100 to 1000 ± 400 ppm/K. Measurements on the thermal conductivity of the annealed fibers display a wide range of values from 200 $W/m.K$ (comparable to the pristine value for this batch of fibers) to 565 $W/m.K$, with no systematic trend observed with annealing temperature. The thermal diffusivity ranges from 135 to 310 mm^2/s for these fibers, and the samples with the highest thermal diffusivity also have the highest thermal conductivity. Vapor-phase ICl doping enhances the thermal conductivity and reduces the thermal diffusivity of annealed CNTF; the diffusivity reduction is a new observation of this work and arises from the larger volumetric heat capacity of the halogen-doped CNTF.

In summary, this work quantifies the effects of annealing and vapor-phase doping on the axial thermal and electrical properties of solution-spun CNTF. These results provide insight into property optimization via post-processing for potential applications in thermal management or thermoelectric energy conversion.

References

[1] N. Behabtu, C. C. Young, D. E. Tsentalovich, O. Kleinerman, X. Wang, A. W. K. Ma, E. A. Bengio, R. F. ter Waarbeek, J. J. de Jong, R. E. Hoogerwerf, S. B. Fairchild, J. B. Ferguson, B. Maruyama, J. Kono, Y. Talmon, Y. Cohen, M. J. Otto, and M. Pasquali, "Strong, Light, Multifunctional Fibers of Carbon Nanotubes with Ultrahigh Conductivity," *Science*, vol. 339, no. 6116, pp. 182–186, Jan. 2013, doi: 10.1126/science.1228061.

[2] N. Komatsu, Y. Ichinose, O. S. Dewey, L. W. Taylor, M. A. Trafford, Y. Yomogida, G. Wehmeyer, M. Pasquali, K. Yanagi, and J. Kono, "Macroscopic weavable fibers of carbon nanotubes with giant thermoelectric power factor," *Nat Commun*, vol. 12, no. 1, p. 4931, Aug. 2021, doi: 10.1038/s41467-021-25208-z.

[3] L. Lu, W. Yi, and D. L. Zhang, "3 omega method for specific heat and thermal conductivity measurements," *Review of Scientific Instruments*, vol. 72, no. 7, pp. 2996–3003, Jul. 2001, doi: 10.1063/1.1378340.

[4] C. Dames and G. Chen, "1ω,2ω, and 3ω methods for measurements of thermal properties," *Review of Scientific Instruments*, vol. 76, no. 12, p. 124902, Dec. 2005, doi: 10.1063/1.2130718.

Cathodes based on V_2O_5 are an excellent material for fabricating symmetric supercapacitors for lithium-ion batteries

K. Kaviyarasu[1]

[1]UNESCO - UNISA Africa Chair in Nanosciences/Nanotechnology Laboratories, School of Interdisciplinary Research and Graduate Studies, University of South Africa (UNISA), Roodepoort, Johannesburg, (South Africa).

It is interesting to note that the V_2O_5 peak, where the symmetric counterpart can be found, contains a greater number of nanoflakes of intercalation. It has been confirmed through SEM analysis that the orthorhombic V_2O_5 diffraction plane corresponds to the faces of the 30.9° (110) and 41.2° (002) peaks [1]. There is an intriguing characteristic of LiBr nanoflakes doped with V_2O_5 that defines a peak at two points corresponding to lithium bromide concentrations in the JCPDS File No. 49-2101. In V_2O_5, oxygen could adsorb on its surface and form a V-O bond because of its large specific surface area. We also note that these samples were annealed at higher temperatures, at 600 °C, under the same inert atmosphere, leading to rapid grain growth and a low-frequency band. Additionally, SEM results demonstrate that the eutectic salt of V_2-O-LiBr is well absorbed by the V_2O_5 particles in the framework network, demonstrating the suitability of the ternary electrolyte for high-performance supercapacitors, as it is both affinity- and wettability-friendly [2]. A coin cell battery operates with molten salt electrolyte in a liquid state. LiBr does exist in a solid state doped with V_2O_5 that inhibits liquid electrolyte flow. Therefore, molten salt must be wettable with the flow inhibitor, which is also a prerequisite for stable battery operation [3]. Pure V_2O_5 has a surface area of 66.539 m^2/g and a pore volume of 0.024 g/cc as determined by the BET method. As shown by the BJH pore size distribution derived from the absorption data, pure V_2O_5 has an average pore size of 0.411 nm, indicating microporous structure. As measured by BJH, LiBr doped with V_2O_5 has a surface area of 62.410 m^2/g, a volume of 0.058 g/cc and an average pore size distribution of 0.425 nm [4]. The specific capacitance of V_2O_5 @ LiBr as a function of current densities calculated from GCD curves of 7908 Fg^{-1} at 1 Ag^{-1}. As a result of its remarkable cyclic stability, V_2O_5 is an excellent material to fabricate symmetric supercapacitors [5]. Interestingly, the specific capacitance of pure V_2O_5 and V_2O_5 @ LiBr derived from CV data shows a high capacitance for pure V_2O_5 flakes of 206 Fg^{-1} at Ag^{-1} and Li- V_2O_5 of 2380 Fg^{-1} at 1 Ag^{-1}. Incorporating the V_2O_5 electrode into a coin-cell supercapacitor assembly, it exhibits excellent electrochemical performance [6]. With a specific capacitance of 172 Fg^{-1}, an energy density of 1093 Wh kg^{-1}, a power density of 599 W kg^{-1}, and capacitance retention of ~98.4% after 2000 cycles.

References

[1] J.C. Valmalette, *et al., Materials Science and Engineering: B.* **54**, 168 -173 (1998).
[2] M. Tamilselvan, *et al., Ceramics International,* **47**, 29832 - 29839 (2021).
[3] K. Shiva Prasad, *et al., ChemistrySelect,* **3**, 3860 - 3865 (2013).
[4] T. Jayaraman, *et al., New J. Chem.,* **39**, 1367-1374 (2015).
[5] Z. Zou, *et al., Int. J. Electrochem. Sci.,* **13**, 8127-8136 (2018).
[6] I. Arockia Mary, *et al., Ionics,* **25**, 5839-5855 (2019).

Replica higher-order topology of Hofstadter butterflies in twisted bilayer graphene

Youngkuk Kim[1]

[1]*Department of Physics, Sungkyunkwan University (Korea)*

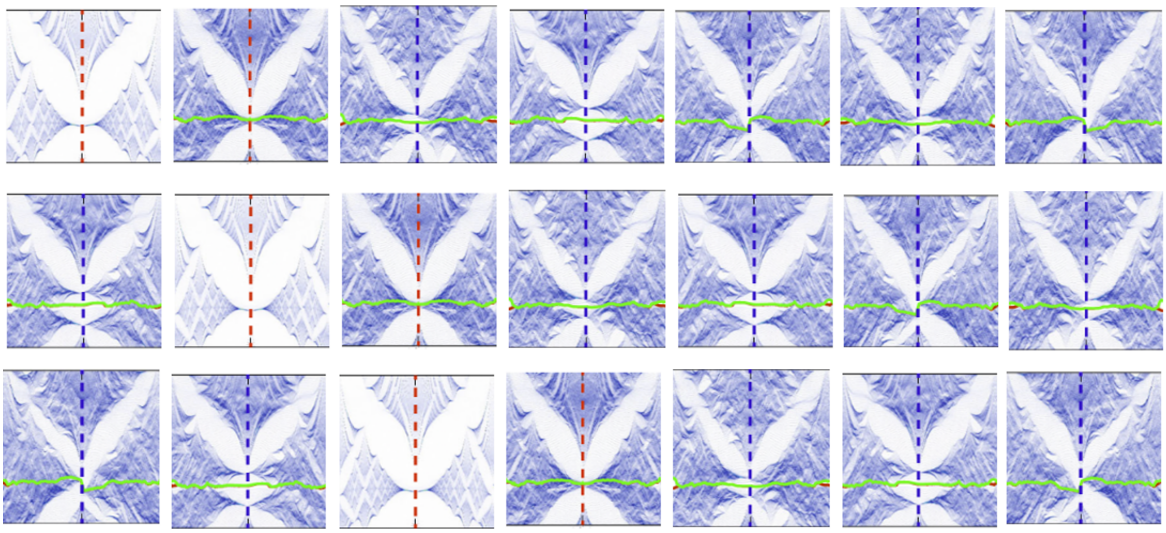

In this talk, we present our recent work on the Hofstadter energy spectrum of twisted bilayer graphene (TBG), which exhibits recursive higher-order topological phases [1]. We demonstrate that higher-order topological insulator (HOTI) phases, characterized by localized corner states, appear as replicas of the original HOTIs, maintaining the self-similarity of the Hofstadter spectrum. Our findings reveal the presence of exact flux translational symmetry in TBG across all commensurate angles. Building on this, we identify that the original HOTI phase at zero flux reappears at a half-flux periodicity, where effective twofold rotational symmetry is preserved. Additionally, multiple replicas of the original HOTIs emerge for fluxes that lack protective symmetries. Like the original HOTIs, these replica HOTIs exhibit localized corner states and edge-localized real-space topological markers. The emergence of these replica HOTIs is due to the different interaction scales, specifically the intralayer and interlayer couplings in TBG. Our results uncover the topological nature of Hofstadter butterflies, emphasizing symmetry-protected topology in quantum fractals.

References

[1] Replica higher-order topology of Hofstadter butterflies in twisted bilayer graphene Sun-Woo Kim, Sunam Jeon, Moon Jip Park, and Y. Kim, npj Comput. Mater. 9, 152 (2023)

Bright trion emission in carbon-nanotube/tungsten-diselenide mixed-dimensional heterostructures

Nan Fang[1,2], Ufuk Erkilic[1], Yih-Ren Chang[1,2], Shun Fujii[2,3], Daiki Yamashita[2,4], Chee Fai Fong[1,2], Yuichiro K. Kato[1,2]

[1]*Nanoscale Quantum Photonics Laboratory, RIKEN Cluster for Pioneering Research, Saitama, Japan*
[2]*Quantum Optoelectronics Research Team, RIKEN Center for Advanced Photonics, Saitama, Japan*
[3]*Department of Physics, Faculty of Science and Technology, Keio University, Yokohama, Japan*
[4]*Platform Photonics Research Center, National Institute of Advanced Industrial Science and Technology (AIST), Ibaraki, Japan*

Two-dimensional van der Waals heterostructures have unveiled unconventional phenomena that emerge at atomically precise interfaces, and further advancements are anticipated in mixed-dimensional heterostructures. The anthracene-assisted transfer technique [1] is utilized to form the clean and free-standing mixed-dimensional heterostructures consisting of one-dimensional carbon nanotubes and two-dimensional tungsten diselenide. Both the chirality and the layer number are identified before assembling, allowing for precise engineering of the band alignment.

The mixed-dimensional heterostructures exhibit strong excitonic interaction, thus leading to the observation of intriguing excitonic phenomena. For example, in type-I band alignment, resonant exciton transfer is observed [2], while interface excitons appear in type-II band alignment [3].

In this study, we observe bright trion emission in type-I band alignment. Through photoluminescence excitation, spatial imaging, and time-resolved measurements, we unveil a considerable dimensional heterogeneity effect that results in the enhancement of trion emission.

This work was supported in part by JSPS (KAKENHI JP22F22350, JP22K14624, JP22K14623, JP23H00262, JP24H01202, JP24K17627), JST (ASPIRE JPMJAP2310), and MEXT (ARIM JPMXP1222UT1135). C.F.F. is supported by the RIKEN Special Postdoctoral Researcher Program. The authors acknowledge the Advanced Manufacturing Support Team at RIKEN for technical assistance.

References

[1] K. Otsuka, N. Fang, D. Yamashita, T. Taniguchi, K. Watanabe, and Y. K. Kato, *Nat. Commun.* **12**, 3138 (2021).
[2] N. Fang, Y. R. Chang, D. Yamashita, S. Fujii, M. Maruyama, Y. Gao, C. F. Fong, K. Otsuka, K. Nagashio, S. Okada, and Y. K. Kato, *Nat. Commun.* **14**, 8152 (2023).
[3] N. Fang, Y. R. Chang, S. Fujii, D. Yamashita, M. Maruyama, Y. Gao, C. F. Fong, D. Kozawa, K. Otsuka, K. Nagashio, S. Okada, and Y. K. Kato, *Nat. Commun.* **15**, 2871 (2024).

Diameter Controllable Separation of Single-Walled Carbon Nanotubes by Simply Changing the Metal in Phenanthroline-Based Supramolecular Polymers

Xinyi Fu[1], Takuya Hayashi[2], Guoqing Cheng[1], Naoki Komatsu[1,*]

[1] *Graduate School of Human and Environmental Studies, Kyoto University (Japan),* [2] *Carbon Science Division, Research Institute for Supra Materials, Shinshu University (Japan)*

Carbon nanotubes (CNTs) possess unique electronic and optical properties which are highly dependent on their structures. Therefore, diameter selective synthesis and separation are meaningful for a wide range of their applications. Although various methods have been developed for CNT separations, challenges still remain in more efficient discrimination for diameters and more thorough removal of dispersants. In our previous works, the diameter, handedness and/or metallicity of CNTs have been separated through host-guest complexation by "nanotweezers" [1], "nanocalipers" [2] and "M-nanobrackets" [3]. In this work, we will describe a novel approach for size-tunable diameter separation of single-walled CNTs (SWNTs) by simply changing the metals in supramolecular polymers (SPs) consisting of phenanthroline-based nanobrackets and metal ions.

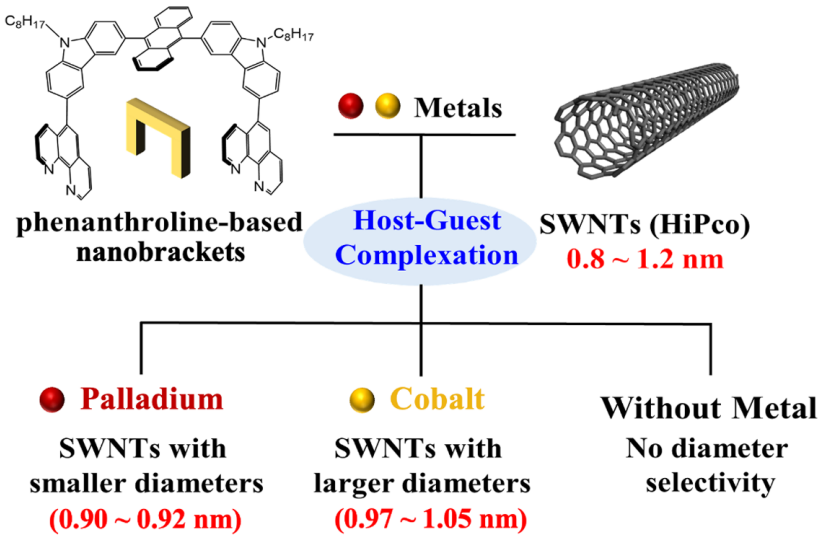

Figure 1: Structure of phenanthroline-based nanobrackets and their size-tunable diameter separation of SWNTs through host-guest complexation.

In the separation, SWNTs and phenanthroline-based nanobrackets were sonicated for 9 h, then $Pd(OAc)_2$ or $Co(acac)_2 \cdot 2H_2O$ was added and sonicated for another 15 h. After centrifugation, the precipitates including the SWNT-SP complexes were washed with dithiothreitol in THF to remove the SPs. The residual SWNTs were analyzed by Raman spectroscopy followed by UV–vis–NIR and photoluminescence spectroscopy after dispersing them in D_2O with the help of surfactant, SDBS. These spectra revealed that Pd and Co ions with phenanthroline-based SPs show the large difference in diameter preference to the smaller (0.90 ~ 0.92 nm) and the larger (0.97 ~ 1.05 nm) diameters, respectively. This method offers not only size-tunable diameter selectivity, but also significant improvements in extraction efficiency and facile and thorough removal of the host molecules as compared to previous techniques.

References

[1] X. Peng, N. Komatsu, et al., *Nat. Nanotechnol*. **2007**, 2, 361; X. Peng, N. Komatsu, et al., *J. Am. Chem. Soc*., **2007,** 129, 15947; F. Wang, N. Komatsu, et al., *J. Am. Chem. Soc*., **2010,** 132, 10876.
[2] G. Liu, N. Komatsu, et al., *J. Am. Chem. Soc*. **2013**, 135, 4805; G. Liu, N. Komatsu, et al., *J. Mater. Chem. A*, **2014**, 2, 19067; G. Liu, Y. Miyake, N. Komatsu, *Org. Chem. Front*, **2017**, 4, 911.
[3] G. Cheng, N. Komatsu, et al., *ACS Nano*, **2022,** 16, 12500; G. Cheng, N. Komatsu, et al., *Beilstein J. Org. Chem.*, **2024**, 20, 1298; G. Cheng, N. Komatsu, et al., *Carbon*, **2025,** 20, 120102.

High-Frequency Current Noise in Carbon Nanotubes due to Phonon Scattering

Raimu Akimoto[1], Aina Sumiyoshi[1], Takahiro Yamamoto[1,2]

[1]*Department of Physics, Tokyo University of Science, Tokyo, 162-8601, Japan*

[2]*RIST, Tokyo University of Science, Tokyo, 162-8601, Japan*

Carbon nanotubes (CNTs) are potential candidates for use in nanoelectronics due to their outstanding electrical and mechanical properties. In such nanomaterials, current noise as well as quantum effects are enhanced, strongly influencing device performance. Previously, the current noise was considered a hindrance, but with recent developments in nonequilibrium statistical mechanics (e.g., thermodynamic uncertainty relation [1] and fluctuation theorem [2]), it is now thought to contain laws and valuable material information. However, experimental studies on intrinsic source of noise are still lacking for nanoscale systems. Therefore, the quantitative evaluation of current noise in CNTs and similar nanomaterials using numerical simulations is an effective approach.

In this study, we focus on the current noise in CNTs originating from atomic thermal vibration (phonons) as an example of intrinsic noise. To compute the time-dependent current, including current noise, we apply the Landauer type model and an atomistic simulation method [3]. Fig.1 shows our simulation model. This method utilizes a time-dependent π-orbital tight binding model where the hopping integral between carbon atoms depend on the time, and the atomic vibration is calculated by the classical molecular dynamics simulation. The current flowing through a CNT is determined from the probability current density in the buffer layers, which is obtained by solving the time-dependent of Schrödinger equation for an open system placed between left lead and right lead. By applying this model and method, we evaluate the noise power spectral density (PSD) depends on frequencies ω for metallic CNTs with length of maximum the noise intensity. The obtained low-ω region of the noise PSD, which is lower than the characteristic frequency ω_c, can be well fitted by the Lorenz curve. This means that the low-ω electron transport process subject to phonon scattering is regarded as a Markov process. In the low-ω region, the acoustic phonon mode (TW) is dominant to the current noise from the selection rule [4] for electron phonon scattering. On the other hand, we found unique signals to SWCNTs that the noise PSD exhibits several sharp peaks that deviate from the Lorentz curve in high-ω region. To clarify the origin of these peaks, we compute the current for a CNT vibrating in an eigen-phonon mode derived from the dynamical matrix. As a result, we clarify that the peaks originate from the intra-valley (K-K) and inter-valley (K-K') scattering by the RBM phonons and E_2-mode (oTO branch) phonons.

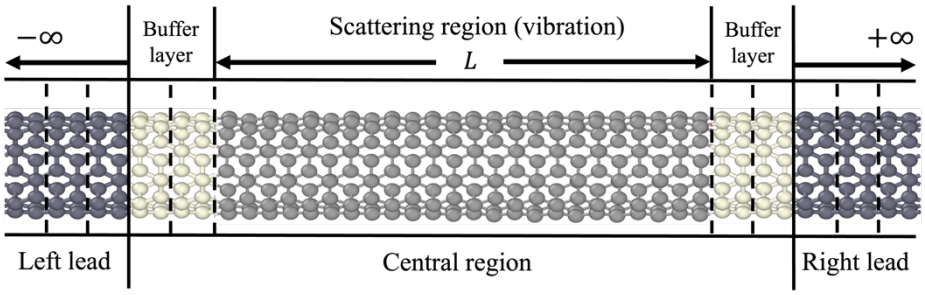

Figure 1: The simulation model based on Landauer type model and consists of three regions: the left lead, the central region, and the right lead. The central region is sandwiched between two semi-infinite leads without atomic vibration, and it consists of a scattering region with atomic vibration and two buffer layers without atomic vibration.

References

[1] Andre C. Barato, and Udo Seifert, *Phys. Rev. Lett.* **114**, 158101 (2015).
[2] D. J. Evans, E. G. D. Cohen, and G. P. Morriss, *Phys. Rev. Lett.* **71**, 2401 (1993).
[3] K. Ishizeki, K.Sasaoka, S. Konabe, S. Souma, T. Yamamoto, *Phys. Rev. B* **96**, 239908 (2017).
[4] J. Jiang *et al.*, *Phys. Rev. B* **72**, 235408 (2005).

Ceramic Cold Cathode X-ray Tubes with a Compact Size and High Performance Fabricated by CNT Film Field Elelctron Emitter

H. Lee[1], J. Y. Lee[1], Y. J. Kong[1], H. S. Shin[1], C. J. Lee[1,2]

[1]*Institute of Vacuum Nanoelectronics, LuminaX Co., Ltd., Seoul 02841 (Korea)*

[2]*School of Electrical Engineering, Korea University, Seoul 02841 (Korea)*

The cold cathode X-ray tubes have much interest due to a hihg operation speed, a low power consumption and a low X-ray exposion for medical doctors and patients, compared with hot filament thermionic X-ray tubes.[1] The ceramic tube based cold cathode x-ray tubes were fabricated using a carbon nanotube (CNT) film field electron emitter, which is composed of the CNT film emitter, the slit gate electrode, the focusing lens and the anode electrode. In this work, the ceramic cold cathode x-ray tube shows a compact size which is the length of 110 mm and the diameter of 42 mm. Compared with previous ceramic cold cathode X-ray tubes, this ceramic X-ray tube presents much high performance indicating a high tube current over 30 mA and a tube voltage of 110 kV.[2] In addition, it shows a high electron beam transmittance over 85 % and a small focal spot size less than 0.8 due to an optimized geometries of the line-shape CNT line emitter, the slit gate electrode and the oval-shape focusing lens.[2,3] The ceramic CNT cold cathode x-ray tube also indicates stable operation characteristics and good lifetime about 100,000 shots. We suggest that the proposed ceramic cold cathode X-ray tube is considered to be sufficiently applicable to not only various medical X-ray imaging systems and dental X-ray imaging systems but also non-distructive inspection systems and security check systems. It is also expected to have a very big ripple effect in the field of X-ray technology in the future.

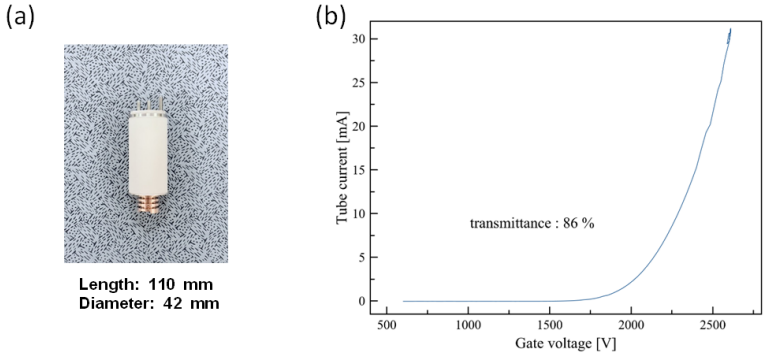

Figure (a) The optical image of the ceramic cold cathode X-ray tube, (b) The tube current according to the applied gate voltage.

References (if desired)

[1] C. J. Lee, S. H. Lee, J.-S. Han, *USA patent*, 10912180, 2021. 2
[2] J. S. Han, S. H. Lee, H. Go, S. J. Kim, J. H. Noh, C. J. Lee, *ACS Nano* 16, (2022) 10231
[3] S. E. Han, H. Go, H. Lee, C. J. Lee, *Nanotechnology 35, (2023) 065701*

Fully recyclable carbon nanotube fibers

M. Durán Chaves[1,6], I. R. Siqueira[2,6], O. S. Dewey[2,6], S. M. Williams[2,6], C. J. S. Ginestra[2,6], J. de la Garza[6], Y. Song[3], G. Wehmeyer[3,5,6], M. Pasquali[1,2,4,5,6]

[1]Department of Chemistry, Rice University (USA), [2]Department of Chemical and Biomolecular Engineering, Rice University (USA), [3]Department of Mechanical Engineering, Rice University (USA), [4]Department of Materials Science and Nanoengineering, Rice University (USA), [5]The Smalley-Curl Institute, Rice University (USA), [6]Carbon Hub, Rice University (USA),

Challenges and limitations in recycling metals, polymers, and carbon fibers have been a major concern to climate change and material circularity. With demonstrated property overlaps and increasingly efficient production, carbon nanotube (CNT) fibers can become a sustainable replacement for hard-to-decarbonize incumbent industrial materials. Here, we show that solution-spun CNT fibers can be fully and easily recycled without losing properties and irrespective of their constituent CNTs. Continuous segments of virgin, single-source CNT fibers made from different CNTs were mixed together in solution and reprocessed into a recycled, mixed-source CNT fiber with the same morphology, structure, alignment, and properties of the virgin, mixed-source CNT fiber made by directly mixing the raw CNTs. Following the ongoing improvements in CNT synthesis and CNT fiber manufacturing, recyclability further positions CNT fibers as a promising alternative to realize the transition to a greener future with a circular economy.

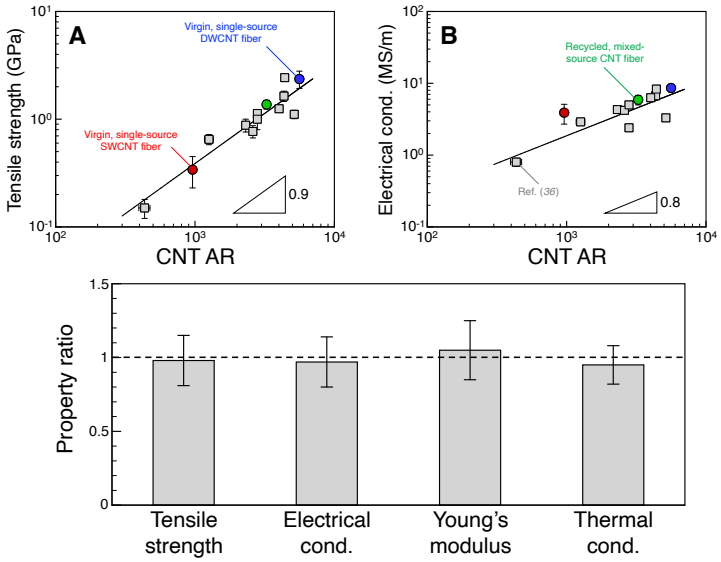

Figure 1. **CNT fiber properties. (A)** Tensile strength and **(B)** electrical conductivity of solution-spun CNT fibers as a function of CNT AR for the virgin, single-source SWCNT fiber (red circle), virgin, single-source DWCNT fiber (blue circle), and recycled, mixed-source CNT fiber (green circle) and **(C)** the ratio of properties of the recycled, mixed-source CNT fiber to properties of the virgin, mixed-source CNT fiber with the same CNT content.

References

[1] P. Ghisellini, *et al., Journal Cleaner Production* **114**, 11–32 (2016).
[2] D. Gielen, *et al., MRS Bulletin* **33**, 471–477 (2008).
[3] R. U. Ayres. *Resources, Conservation and Recycling* **21**, 145–173 (1997).
[4] I. A. Ignatyev, *et al., ChemSusChem* **7**, 1579–1593 (2014).
[5] G. Oliveux, *et al., Progress in Materials Science* **72**, 61–99 (2015).
[6] J. Zhang, *et al., Composites Part B: Engineering* **193**, 108053 (2020).
[7] N. Behabtu, *et al., Nano Today* **3**, 24–34 (2008).
[8] D. E. Tsentalovich, *et al., Macromolecules* **49**, 681–689 (2016).
[9] D. E. Tsentalovich, *et al., ACS Applied Materials & Interfaces* **9**, 36189–36198 (2017).
[10] L. W. Taylor, O. S. Dewey, R. *et al., Carbon* **171**, 689–694 (2021).
[11] F. Smail, *et al., Carbon* **152**, 218–232 (2019).
[12] R. J. Headrick, *et al., Advanced Materials* **30**, 1704482 (2018).
[13] A. Mikhalchan, *et al., Carbon* **220**, 118851 (2024).
[14] P. J. Flory. *The Journal of Chemical Physics* **10**, 51–61 (1942).

High-Sensitivity UV Photodetector Using 2D WS2/Ti2N MXene Quantum Dot Hybrid Structure

Shamima Afroz, Annas S. Ariffin, Anir S. Sharbirin, Jeongyong Kim[1]
Department of Energy Science, Sungkyunkwan University, Suwon 16417, Korea
**j.kim@skku.edu*

We report that the integration of transition metal dichalcogenides (TMDs) with MXene quantum dots offers a promising approach for developing high-performance ultraviolet (UV) photodetectors. This hybrid structure combines the strong light absorption and mechanical flexibility of TMDs with the superior electrical conductivity and environmental stability of MXenes [1]. Because of the wider bandgap of Mxene QDs, the 0D/2D mixed-dimensional hybrid plays a crucial role in enhancing the UV absorption of TMDs by interfacial energy transfer which makes such hybrid materials highly desirable for next-generation photodetectors, LEDs, and optical sensors [2]. Moreover, this photodetector feature is ideal for portable and wearable UV detection, ensuring low power consumption for extended use and convenience [3]. The hybrid photodetectors are expected to provide rapid response times, reduced dark current, and enhanced photodetection capability in the UV spectral range [4]. WS_2 stands out as a promising UV photodetector material among TMDs, due to its wider bandgap, high mobility, and strong excitonic effects. Our work explores the fabrication process of the 2D WS2/Ti2N MXene quantum dot hybrid photodetector, characterizes its optoelectronic properties, and evaluates its performance. The findings suggest that the hybrid device could outperform conventional photodetectors, offering a promising solution for future applications requiring efficient, low-power UV detection.

References

[1]. P. Sahatiya et al., Applied Materials Today 10: 106-114, (2018).
[2]. Sharbirin AS, Kong RE, Mato WB et al., Opto-Electron Adv 7, 240029, (2024).
[3]. Sun Yilin et al., IEEE Electron Device Letters, 42(12), pp.1814-1817, (2021).
[4]. Huang, Junyi, et al. J. Mater. Chem. C, 11, 17106, (2023).

Integration of single-defect carbon nanotube photon sources into waveguide circuits for quantum applications

Clement Deleau[1], Chee Fai Fong[1,2], Finn L. Sebastian[3], Jana Zaumseil[3] and Yuichiro K. Kato[1,2]

[1] *Quantum Optoelectronics Research Team, RIKEN Center for Advanced Photonics (Japan),*

[2] *Nanoscale Quantum Photonics Laboratory, RIKEN Cluster for Pioneering Research (Japan)*

[3]*Institute for Physical Chemistry, Universität Heidelberg (Germany)*

Currently a rapidly growing research field at the heart of many emerging technologies, photonic integrated circuits (PIC) have enabled the realization of mass-manufacturable, stable, resilient and compact optical circuits for a large panel of applications. However, quantum photonic integrated circuits development has remained limited due to the lack of scalable chip-integration techniques for implementing quantum light sources generating single photons at room temperature [1]. Carbon nanotubes (CNTs) have been proposed as promising candidates but have yet to be demonstrated in functional quantum photonics circuits due to the stringent conditions indispensable for producing and manipulating photons with pure states [2,3]. In this research we aim to develop such tools as a technological starting point for CNT-based quantum PIC applications.

Firstly, as a result of thorough excitonic analysis involving spectral, lifetime, polarization, brightness and autocorrelation measurements, (6,5) carbon-nanotubes with single defects have firstly been identified as a promising choice for chip integration [3]. A photonic integrated circuit characterization platform has been realized and implemented to a photoluminescence measurement set-up for CNT circuit coupling analysis. Following, different types of photonic circuit fabrication processes have been developed in cleanroom and used to realize a large variety of photonic nanostructures such as couplers, resonators, interferometers, waveguides, gratings or cavities. CNTs have then been implemented both by drop-casting or deterministic positioning techniques and coupled to these circuits on grating cavities that allow Purcell effect enhancement, demonstrating a sharpened and magnified photon-emission into waveguides. Finally, we also showed single-photon emission at room temperature and waveguide photonic coupling of a deterministically positioned CNT in a lithium niobate waveguide circuit, readily available for electro-optical modulator processing.

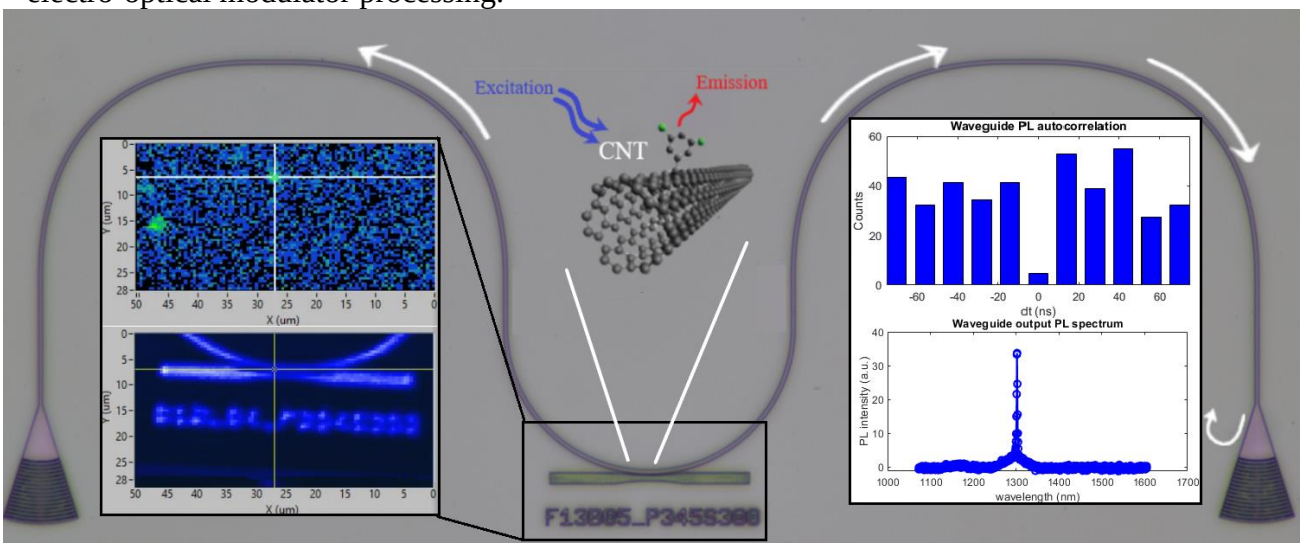

Circuit coupling principle of a single CNT, autocorrelation measurement and typical emission spectrum

References :

[1] Galan Moody et al J. Phys. Photonics 4 012501 2022.

[2] Baydin Andrey et al. Materials 15, 1535 2022.

[3] Finn L. Sebastian et al. Phys.Chem.Lett. 13 3542-3548,2022

Work supported by JSPS (KAKENHI JP24KF0092, JP24K17627 and JP23H00262), JST (ASPIRE JPMJAP2310) and MEXT (ARIM JPMXP1224UT1073). We thank the Advanced Manufacturing Support Team at RIKEN for technical assistance C.F.F. is supported by the RIKEN Special Postdoctoral Researcher Program.

ENTANGLED EXITON EMISSION FROM EXCITON QUANTUM BITS MADE WITH CARBON NANOTUBES BY CONTROLLED-NOT GATE OPERATION

A. Hida[1] and K. Ishibashi[1,2]

[1]Advanced Device Laboratory, RIKEN (JAPAN), [2]RIKEN Center for Emergent Matter Science (Japan)

A quantum light emitter is not only essential for a quantum information technology but also expected to lead to new findings in the fields of, for example, imaging and spectroscopy. We are investigating the use of exciton controlled-NOT (CNOT) gate scheme to generate quantum light. The CNOT gate is originally intended for the quantum computing and makes it possible to provide arbitrary quantum states in combination with the manipulations of individual quantum bits (qubits). The excitons in the quantum dots (QDs) act as exciton qubits [1-4], so if the CNOT gate operations are executable to them, we may be able to control excitonic states at will and eventually obtain desired exciton emissions.

The QD is formed in a single walled carbon nanotube (SWNT) when its both ends are terminated with collagen model peptides [5], and the exciton produced in it shows superior characteristics as an exciton qubit [6]. We constructed a laser pulse system for performing exciton CNOT gate operations and confirmed that the input/output relations observed in the experiments agree well with the truth table of an ideal CNOT gate [6]. One of the characteristic functions of the CNOT gate is to generate entanglement, which may allow us to obtain entangled exciton emissions from SWNT exciton qubits. First we evaluated the excitonic state produced after performing an entangling operation. By observing the state while changing the measurement bases, it was found that an entangled state surely exists. Then we investigated the emission from that entangled state by conducting quantum interference experiments. The entangled photons are, in principle, indistinguishable until the state of either of them is decided through the observation and hence show quantum interference. In fact, a clear dip expressing the occurrence of quantum interference was detected in the coincidence measurement of photons. On the other hand, the photons emitted when unentangled excitonic state was prepared by operation did not show any sign of being indistinguishable.

In this presentation, the current status and future outlook of our scheme are discussed from the perspective of entangled photon emitter while showing major experimental results.

References (if desired)

[1] T. H. Stievater *et al.*, *Phys. Rev. Lett.* **87**, 133603 (2001).
[2] H. Kamada *et al.*, *Phys. Rev. Lett.* **87**, 246401 (2001).
[3] Q. Q. Wang *et al.*, *Appl. Phys. Lett.* **87**, 031904 (2005).
[4] K. Kuroda *et al.*, *Appl. Phys. Lett.* **90**, 051909 (2007).
[5] A. Hida *et al.*, *Appl. Phys. Express* **8**, 045101 (2015).
[6] A. Hida *et al.*, *ACS Photonics* **9**, 3398 (2022).

Electrospray deposition of single-walled carbon nanotube films for gas sensors

Yuto Nishizono[1], Ryo Kuchino [1], Shuhei Ichikawa[1], Kazunobu Kojima[1], Mitsuhiro Katayama[1], and Hiroshi Tabata[1]

[1]*Osaka University (Japan)*

Single-walled carbon nanotubes (SWNTs) are promising gas-sensing materials owing to their large surface-to-volume ratio and ability to operate at room temperature. Semiconducting-enriched SWNTs (sc-SWNTs) and surface-modified SWNTs have been used to achieve high sensitivity and selectivity of gas sensors[1][2]. Such SWNTs are provided in the form of dispersions and are often scarce and expensive compared to as-synthesized SWNTs. Hence, a deposition method with a high usage efficiency of dispersion is required to form SWNT films for gas sensors.

In this study, we adopted the electrospray deposition (ESD) method for SWNT depositions on substrates. ESD is a technique widely used to deposit thin films or nanoparticles onto a grounded substrate by utilizing an electrically charged aerosol and is characterized by a high collection efficiency of dispersed substances. To evaluate the usefulness of this method for the deposition of SWNT films for gas sensors, the electrical characteristics and response properties to NH_3 gas of the deposited films were measured.

SWNTs were deposited on a grounded glass substrate with electrodes by applying a positive high voltage to the tip of a syringe filled with 9 mg/L semiconducting SWNT dispersion with water as a dispersant to generate an electrospray. The spray range was controlled by the voltage of a ring electrode placed between the syringe and substrate. Figure 1shows an SEM image of the SWNT films deposited by ESD. SWNTs were uniformly deposited without forming thick bundles between the electrodes. The amount of dispersion consumed in this process is approximately 1/20 that of the immersion method using a SWNT-dispersed droplet, giving this method a significant advantage in terms of dispersion usage efficiency. Raman spectra in Figure 2 show that the intensity ratio of the G and D bands, which indicate the defect density of SWNTs, is almost the same as that of the drop-casting method, indicating that the application of high voltage in the ESD process does not cause serious damage to SWNTs. Figure 3 shows the sensor response ($\Delta G/G_0 \times 100\%$) upon exposure to NH_3 at 20 ppb-200 ppm for 20 min. The fabricated gas sensor showed an 11.4% response to 5 ppm NH_3. This value was comparable to that of other group's report on the NH_3 response of sc-SWNTs gas sensors (18% @5 ppm)[1] and indicates that the SWNT films deposited by the ESD can be used for gas sensors.

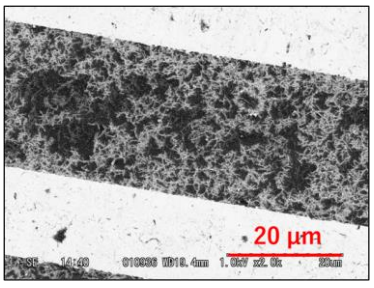

Fig. 1 SEM image of SWNT film deposited by ESD

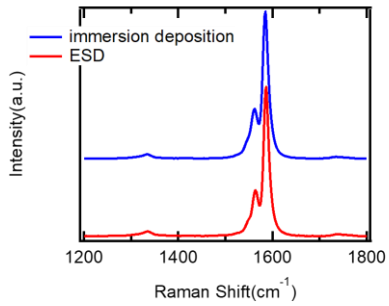

Fig. 2 Raman spectra of SWNT films prepared by immersion deposition and ESD

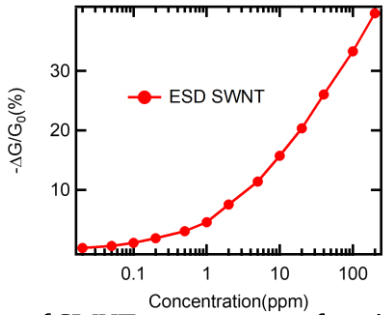

Fig. 3 Sensor response of SWNT gas sensor as a function of NH_3 concentration

References

[1] S. Abbas *et al.*, Phys. Status Solidi A. **219** 2100529 (2022).
[2] K. Tanaka. M.S. thesis, Osaka Univ. 1-97 (2024).

Session
NT 25（The 25th International Conference on the Science and Applications of Nanotubes and Low-

| Main conference：Main conference

Mon. Jun 16, 2025 6:00 PM - 8:00 PM JST | Mon. Jun 16, 2025 9:00 AM - 11:00 AM UTC Poster 2(International Exchange Hall I&II, Clock Tower Centennial Hall, 2F)

[16psb] Poster 2

[16psb-01]

Exciton Behaviors in Monolayer $MoSe_2$-SWCNT Mixed-Dimensional Heterostructures

*Yih-Ren CHANG[1,2], Nang Fang[1], Chee Fai Fong[1], Shun Fujii[1,3], Yuichiro K. Kato[1] (1. RIKEN (Japan), 2. Kobe University (Japan), 3. Keio University (Japan))

[16psb-02]

Unique structure and thermodynamics of adsorbed water on CNT surface

Yuki Maekawa[1], Yusei Kioka[1], Kenji Sasaoka[1], *Yoshikazu Homma[1], Takahiro Yamamoto[1] (1. Tokyo University of Science (Japan))

[16psb-03]

Cinematographic Electron Microscopic Study on Formation Processes of Carbon Materials

*Koji Harano[1] (1. NIMS (Japan))

[16psb-04]

In-situ monitoring of single-molecule functionalization in vapor-phase for air-suspended single-walled carbon nanotubes

*Mengyue Wang[1,2], Daichi Kozawa[1,2,3], Yuichiro K. Kato[1,2] (1. RIKEN Center for Advanced Photonics (Japan), 2. RIKEN Cluster for Pioneering Research (Japan), 3. National Institute for Materials Science (Japan))

[16psb-05]

Development of Carbon-Based Xerogels and Aqueous Dispersions Inspired by Japanese-Solid-Ink

*Sakurako Kubota[1], Kotone Masuda[1], Junpei Hayakawa[1] (1. Nara Prefectural Seiwaseiryo Senior High School (Japan))

[16psb-06]

Relationship between the interfacial adhesion and microscopic interface structures in CNT/epoxy resin nanocomposites

*Tomoe Yayama[1], Tenma Hiraishi[2], Fumiko Akagi[1,2] (1. Department of Applied Physics, Kogakuin University (Japan), 2. Electronics and Electron Engineering Program, Kogakuin University (Japan))

[16psb-07]

Diameter Controllable Synthesis of Single-walled Carbon Nanotubes by Arc Discharge Using Ni-based Catalysts

Yixi Yao[1,2], *Zeyao Zhang[1,2], Yan Li[1,2] (1. Peking University (China), 2. Institute of Carbon-Based Thin Film Electronics, Peking University, Shanxi (China))

[16psb-08]

Diameter Specific Bandgap Modulation in MoS_2 Nanotubes Grown via Template Reaction

Zhen Han[1,2], *Runze Lai[2], Jian Sheng[2], Chengping Lian[2], Yan Li[1,2] (1. Academy for Advanced Interdisciplinary Studies, Peking University, Beijing 100871 (China), 2. College of Chemistry and Molecular Engineering, , Peking University, Beijing 100871 (China))

[16psb-09]

Green conversion of low quality chemical feedstock to hydrogen and carbon nanotubes

*Chaojie Cui[1], Bofan Li[1], Ruijing Jiao[1], Weizhong Qian[1] (1. Tsinghua University (China))

[16psb-10]

Hybrid Fibers incorporating Carbon Nanotubes

*Erica F Antunes[1], Daiana Pimenta[1], Rayza Gonçalves[1], Manuela Mourthe[1], Thiago Cançado[1], Felipe Murta[1], Alexander Kasama[2], Luiz Ladeira[1], Myriano Oliveira Jr.[1], Glaura Silva[1] (1. CTNANO/UFMG (Brazil), 2. CENPES/PETROBRAS (Brazil))

[16psb-11]

Harnessing Multiscale Engineering for Advancing CNT Technology: From AI for Synthesis to Functional Nanocarbon Assembly

*DEWU LIN[1], Don N. Futaba[2], Kenji Hata[2], Wenjun Zhang[3] (1. Peking University Shenzhen Graduate School (China), 2. National Institute of Advanced Industrial Science and Technology (Japan), 3. City University of Hong Kong (Hong Kong))

[16psb-12]

Mass Production of Two-Dimensional Materials by Bubbling Chemical Vapor Deposition

*Zhiyuan Shi[1] (1. Shanghai Institute of Microsystem and Information Technology, CAS (China))

[16psb-13]

Precise structural regulation of carbon crystals by electron doping

Fei Pan[1], Kun Ni[1], *Yanwu Zhu[1] (1. University of Science and Technology of China (China))

[16psb-14]

Autonomous Multi-Objective Bayesian Optimization of Carbon Nanotube Yield and Diameter Control at Synthesis from Disordered Catalyst

*Robert Waelder[1,2], Woojae Kim[3], Mark Pitt[4], Jay Myung[4], Benji Maruyama[1] (1. Air Force Research Lab (United States of America), 2. BlueHalo LLC (United States of America), 3. Howard University (United States of America), 4. Ohio State University (United States of America))

[16psb-15]

Towards a More Complete Empirical Thermodynamic Understanding and Control of Supported Catalyst Carbon Nanotube Synthesis

*Robert Waelder[1,2], Arthur Sloan[3], Benji Maruyama[1] (1. Air Force Research Lab (United States of America), 2. BlueHalo LLC (United States of America), 3. National Research Council (United States of America))

[16psb-16]

Evolution of Carbon atoms to Chiral Carbon Nanotubes on metal free template

*Shuchen Zhang[1] (1. State Key Laboratory of Precision and Intelligent Chemistry Department of Materials Science and Engineering School of Chemistry and Materials Science University of Science and Technology of China (China))

[16psb-17]

Synthesis of isolated pentagonal h-BN crystals by atmospheric pressure CVD

*Kamal Prasad Sharma[1], Takahiro Maruyama[1] (1. Meijo University (Japan))

[16psb-18]

Synthesis of Long Carbon Nanotubes by Br-assisted Floating Catalyst Chemical Vapor Deposition

Session
NT 25（The 25th International Conference on the Science and Applications of Nanotubes and Low-
*Hirotaka Inoue[1,2], Anastasios Karakassides[2], Toshihiko Fujimori[1,3], Akira Takakura[1], Soichiro Okubo[1], Hua Jiang[2], Ghulam Yasin[2], Kazuhiro Ikeda[1], Takamasa Onoki[1], Yoku Inoue[4], Esko I. Kauppinen[2] (1. Sumitomo Electric Industries (Japan), 2. Aalto University (Finland), 3. University of Tsukuba (Japan), 4. Shizuoka University (Japan))

[16psb-19]

Glaphene: a hybridization of 2D silica glass and graphene

*Sathvik Ajay Iyengar[1], Manoj Tripathi[2], Anchal Srivastava[3], Abhijit Biswas[1], Tia Gray[1], Mauricio Terrones[4], Alan B Dalton[2], Marcos A. Pimenta[5], Robert Vajtai[1], Vincent Meunier[4], Pulickel Ajayan[1] (1. Rice University (United States of America), 2. University of Sussex (UK), 3. Banaras Hindu University (India), 4. The Pennsylvania State University (United States of America), 5. Universidade Federal de Minas Gerais (Brazil))

[16psb-20]

Controlled Growth of Horizontally Aligned Single-Walled Carbon Nanotube Arrays

*Liu Qian[1], Ying Xie[1], Yue Li[1], Jin Zhang[1] (1. Peking University (China))

[16psb-21]

Preparation of semiconducting single-wall carbon nanotube arrays with a narrow band-gap distribution

*Jia-Yang Zhang[1], Lingtong Ding[2], Chen Xie[2], Lili Zhang[1], Meng-Ke Zou[1], Xiao Wang[2], Chang Liu[1] (1. Institute of Metal Research, Chinese Academy of Sciences (China), 2. Shenzhen Institute of Advanced Technology, Chinese Academy of Sciences (China))

[16psb-22]

Engineering Luminescent Defects in Polymer-Wrapped SWCNTs using Benzoyl Peroxide Chemistry

*Andrzej Dzienia[1], Patrycja Taborowska[1], Pawel Kubica-Cypek[1], Dawid Janas[1] (1. Silesian University of Technology (Poland))

[16psb-23]

Unleashing Ultra-Efficient Heat Transfer: The Magic of Graphene-Skinned Powders Synthesized by FB-CVD in Nanoelectronic Thermal Management

*Yuqing Song[1] (1. Beijing Graphene Institute (BGI) 13 Cuihu Nanhuan Road, Sujiatuo Town, Haidian District Beijing 100095, P. R. China (China))

[16psb-24]

Controlled Growth of Graphene-skinned Al_2O_3 Powdersby Fluidized Bed-Chemical Vapor Deposition for Heat Dissipation

*Yuzhu Wu[1,2], Yuqing Song[2] (1. College of Chemistry and Molecular Engineering, Peking University, Beijing (P.R.China) (China), 2. Beijing Graphene Institute (BGI), Beijing 100095 (P.R.China) (China))

[16psb-25]

Sorting and brightening of single-walled carbon nanotubes using organic derivatives of hydrazine

*Dominik Sebastian Just[1], Ryszard Siedlecki[1], Błażej Podleśny[1], Dawid Janas[1] (1. Silesian University of Technology (Poland))

[16psb-26]

Single-walled carbon nanotube growth by CVD with high-entropy alloy catalysts composed of platinum-group elements

*Takahiro Maruyama[1], Shu Matsuoka[1], Kamal Prasad Sharma[1], Takahiro Saida[1], Kohei Kusada[2], Hiroshi Kitagawa[2] (1. Meijo University (Japan), 2. Kyoto University (Japan))

[16psb-27]

Molecule Super-Transport through Macroscopic Length of Individual Carbon Nanotube

*Jingwei Wu[1], Fei Wei[1] (1. Tsinghua University (China))

[16psb-28]

BSTCIM: A Balanced Symmetry Ternary Fully Digital In-MRAM Computing Macro for Energy Efficiency Neural Network

*Zhongzhen Tong[1,2], Chenghang Li[1,2], Chao Wang[1,2], Daming Zhou[2], Xiaoyang Lin[1,2] (1. National Key Lab of Spintronics, International Innovation Institute, Beihang University (China), 2. School of Integrated Circuit Science and Engineering, Fert Beijing Institute, Beihang University (China))

[16psb-29]

Monolithic 3D integration of CNTFET and SOT-MTJ for high-performance non-volatility memories

Ke Zhang[1], Ningfei Gao[2], *Daming Zhou[1], Zhongzhen Tong[1], Hongxi Liu[3], Xiaoyang Lin[1], Haitao Xu[2,4], Lianmao Peng[2], Weisheng Zhao[1] (1. Fert Beijing Institute, School of Integrated Circuit Science and Engineering, Beihang University (China), 2. Key Laboratory for the Physics and Chemistry of Nanodevices, Center for Carbon-based Electronics, School of Electronics, Peking University (China), 3. Truth Memory Technology Corporation Limited (China), 4. Institute of Carbon-based Thin Film Electronics, Peking University (China))

[16psb-30]

Interlayer Stacking Sensitivity of Anisotropic Thermoelectric Transport Properties of $NbSe_2$ Polymorphs based on First-Principles Band Calculations

*Mark Edwin Jr Roa Cleofe[1], Koichi Nakamura[1], Tetsuro Habe[1] (1. Kyoto University of Advanced Science (Japan))

[16psb-31]

Solution Processed Carbon Nanotube Integrated Circuits for Multi-Modal Edge Computing

*Jingfang Pei[1], Songwei Liu[1], Yingyi Wen[1], Lekai Song[1], Guohua Hu[1] (1. The Chinese University of Hong Kong (China))

[16psb-32]

Multi-functional Data Processing by Solution-processed 2D Material Ferroelectric Junction Devices

*Songwei Liu[1], Yingyi Wen[1], Jingfang Pei[1], Guohua Hu[1] (1. The Chinese University of Hong Kong (Hong Kong))

[16psb-33]

Temporal Signal Processing by Physical Reservoir Computing Using Solution Processed MoS_2 Charge-Trapping Transistors

*Yingyi Wen[1], Songwei Liu[1], Teng Ma[2], Guohua Hu[1] (1. The Chinese University of Hong Kong (Hong Kong), 2. Hong Kong Polytechnic University (Hong Kong))

[16psb-34]

Application of aerosol-synthesized single-walled carbon nanotubes for binder-free Nickel-rich positive electrodes via a solvent-free fabrication

*Alisa Bogdanova[1], Filipp Obrezkov[1], Seyedabolfazl Mousavihashemi[1], Eldar Khabushev[1], Tanja Kallio[1] (1. Aalto University School of Chemical Engineering (Finland))

[16psb-35]

High-Energy-Density Quasi-Solid-State Lithium-Sulfur Batteries: Reliable Energy Storage Solutions in Extreme Environments

*Haifa Taoum[1], Mariam Ezzedine[1], Costel-Sorin Cojocaru[1] (1. LPICM-CNRS (France))

[16psb-36]

Pt@WS_2 -an Extrinsic 2D Dilute Ferromagnetic Semiconductor Beyond Room Temperature

*Yu-Xiang Chen[1,2,3], Mario Hofmann[4], Ya-Ping Hsieh[1] (1. Institute of Atomic and Molecular Sciences, Academia Sinica (Taiwan), 2. International Graduate Program of Molecular Science and Technology, National Taiwan University (Taiwan), 3. Molecular Science and Technology ProgramTaiwan International Graduate Program, Academia Sinica (Taiwan), 4. Department of Physics, National Taiwan University (Taiwan))

[16psb-37]

Two-Dimensional Electronic Transport and Surface Electron Accumulation in Transition Metal Dichalcogenides

*Hemanth Kumar Bangolla[1], Ruei-San Chen[1] (1. Taiwan Tech (Taiwan))

[16psb-38]

Efficient Field-free Switching of Perpendicular Magnetization induced by Dominant out-of-plane Torque Generated by $NbIrTe_4$

*Wei Yang[1,2,3], Juan-Carlos Rojas-Sánchez[3], Xiaoyang Lin[1,2], Weisheng Zhao[1,2] (1. National Key Lab of Spintronics, Hangzhou International Innovation Institute of Beihang University (China), 2. Fert Beijing Institute, Beihang University (China), 3. Insititut Jean Lamour, Université de Lorraine (France))

[16psb-39]

Enhanced Surface Properties of WS_2 via Cryogenic Exfoliation and High-Pressure Dispersion for Catalysis

*Yejin Choi[1], Myeung-Jin Lee[1], Bora Jeong[1], Hong-Dae Kim[1] (1. Korea Institute of Industrial Technology (Korea))

[16psb-40]

Hot-electron Injection Enabled High-performance Broadband Photodetection Based on WO_{3-x}/Bi_2O_2Se Hybrid structure

*Xinlei Zhang[1], Yuanfang Yu[2], Junpeng Lv[1], Zhenhua Ni[1] (1. Southeast University (China), 2. Nanjing University of Posts and Telecommunications (China))

[16psb-41]

First-principles Calculations on Oxygen Functional Group Interactions on Graphene and Their Modulation by Surface Normal Electric Fields

*Takazumi Kawai[1], Yoshiyuki Miyamoto[2] (1. Tokyo City University (Japan), 2. National Institute of Advanced Industrial Science and Technology (Japan))

[16psb-42]

Ambipolar Doping of Single-Walled CarbonNanotubes via Covalent Charge-Transfer Engineering

*Antonio Setaro[1,2], Alphonse Fiebor[1], Mohsen Adeli[1], Stephanie Reich[1] (1. Freie Universität Berlin (Germany), 2. Pegaso University (Italy))

Session
NT 25 (The 25th International Conference on the Science and Applications of Nanotubes and Low-
[16psb-43]

Intrinsic temperature dependence of Raman-active modes in individual isolated single- and double-walled carbon nanotubes

*Ya Feng[1,2], Dmitry I. Levshov[3], Yuta Sato[4], Taiki Inoue[5], Sofie Cambré[3], Wim Wenseleers[3], Rong Xiang[6], Kazu Suenaga[5], Shigeo Maruyama[2,6] (1. Dalian University of Technology (China), 2. The University of Tokyo (Japan), 3. University of Antwerp (Belgium), 4. National Institute of Advanced Industrial Science and Technology (Japan), 5. Osaka University (Japan), 6. Zhejiang University (China))

Exciton Behaviors in Monolayer $MoSe_2$-SWCNT Mixed-Dimensional Heterostructures

Y.-R. Chang[1,2,3], N. Fang[1], C. F. Fong[1], U. Erkilic[1,2], S. Fujii[2,4], Y. K. Kato[1,2]

[1]Nanoscale Quantum Photonics Laboratory, RIKEN Cluster for Pioneering Research (Japan), [2]Quantum Optpelectronics Research Team, RIKEN Center for Advanced Photonics (Japan), [3]Department of electrical and electronic engineering, Kobe University (Japan), [4]Department of Physics, Keio University (Japan)

The formation of two-dimensional (2D) van der Waals heterostructures not only creates a new class of materials but also gives rise to a variety of novel properties, such as superconductivity, ferroelectricity, and interface excitons [1–3]. To gain a deeper understanding of interface excitons in these low-dimensional van der Waals heterostructure materials, mixed-dimensional heterostructures based on few-layer tungsten diselenide (WSe_2) and single-walled carbon nanotubes (SWCNTs) have been fabricated and investigated in our previous research [4–5]. Since the bandgap structures of both WSe_2 and SWCNTs vary depending on the number of layers in the 2D material and the chirality of the SWCNTs, van der Waals heterostructures with highly tunable band alignment between WSe_2 and SWCNTs can be achieved.

In the case of ~~Type~~ type I band alignment, where the smaller bandgap of the SWCNT is entirely encompassed by the bandgap of the 2D material, exciton transfer from the 2D material to the SWCNT can be observed [4]. On the other hand, when a ~~Type~~ type II band alignment is formed, new photoluminescence (PL) emission peaks appear, originating from the interface between the nanomaterials. These interface excitons have been confirmed as localized excitons due to their extended exciton lifetime, rapid saturation with increasing laser power, and antibunching behavior observed in photon correlation measurements [5].

In this research, van der Waals heterostructures based on monolayer molybdenum diselenide ($MoSe_2$) and SWCNTs are fabricated. Using anthracene dry transfer method [6], mechanically exfoliated monolayer $MoSe_2$ flakes are transferred onto suspended SWCNTs. The suspended structure can preserve the PL emission strength of the SWCNTs. The band alignment between $MoSe_2$ and SWCNTs with different chiralities is investigated using photoluminescence excitation measurements. Additionally, exciton characteristics of these heterostructures are verified through time-resolved PL measurements and PL mapping. Our results take a step further in understanding exciton behavior in mixed-dimensional van der Waals heterostructures from another point of view.

This work was supported in part by JSPS (KAKENHI JP22K14623, JP22K14625, JP22KF0407, JP23H00262, JP24H01202, JP24K17624 and JP24K17627), MEXT (ARIM JPMXP1223UT1132) and JST ASPIRE (JPMJAP2310). Y.-R.C. is supported by JSPS (International Research Fellow). C.F.F. is supported by the RIKEN Special Postdoctoral Researcher Program. The authors acknowledge the Advanced Manufacturing Support Team at RIKEN for technical assistance.

References

[1] Y. Cao, V. Fatemi, S. Fang, K. Watanabe, T. Taniguchi, E. Kaxiras & P. Jarillo-Herrero, *Nature, 556, 43–50 (2018).*
[2] K. Yasuda, X. Wang, K. Watanabe, T. Taniguchi, P. Jarillo-Herrero, *Science* 372, 1458–1462 (2021).
[3] Y. Jiang, S. Chen, W. Zheng, B. Zheng, A. Pan, *Light: Science & Applications*, 10, 72 (2021).
[4] N. Fang, Y. R. Chang, D. Yamashita, S. Fujii, M. Maruyama, Y. Gao, C. F. Fong, K. Otsuka, K. Nagashio, S. Okada, Y. K. Kato, *Nature Commun.* 14, 8152 (2023).
[5] N. Fang, Y. R. Chang, S. Fujii, D. Yamashita, M. Maruyama, Y. Gao, C. F. Fong, D. Kozawa, K. Otsuka, K. Nagashio, S. Okada, Y. K. Kato, *Nature Commun.* 15, 2871 (2024).
[6] K. Otsuka, N. Fang, D. Yamashita, T. Taniguchi, K. Watanabe, Y. K. Kato, *Nature Commun.* 12, 3138 (2021).

Unique structure and thermodynamics of adsorbed water on CNT surface

Yuki Maekawa[1], Yusei Kioka[1], Kenji Sasaoka[2] Yoshikazu Homma[1,2] and Takahiro Yamamoto[1,2]

[1]*Department of Physics, Faculty of Science, Tokyo University of Science, Shinjuku, Tokyo 162-8601, Japan*

[2]*Water Frontier Research Center, RIST, Tokyo University of Science, Shinjuku, Tokyo 162-8601, Japan*

Photoluminescence (PL) [1,2] has revealed that a stable thin film of water forms on the surface of CNTs under ambient conditions. Adsorbed water on CNTs exhibits unique thermodynamic properties; however, its structure and dynamics have not been fully clarified. In this study, we investigated the structure and dynamics of adsorbed water on different adsorption states using classical molecular dynamics (MD) simulations.

When the adsorbed water layer is a single (1L model), the adsorbed water forms a tetragonal crystalline ice structure, organizing into an ice nano-ring (iNR). iNR has structural similarities with ice nanotubes (iNT) formed inside CNTs [3]. While iNR undergoes a first-order phase transition into a liquid-like structure (Figure 1(a)), this structure is unstable and quickly undergoes dewetting from the CNT surface, transitioning into droplets. The melting point and dewetting temperature are dependent on the curvature and hydrogen bond distances.

When the adsorbed water layer is a double (2L model), on the other hand, the adsorbed water is an amorphous configuration primarily composed of pentamers and hexamers of water clusters. On the graphene surface, adsorbed water forms hexagonal ice at low temperatures [4]. However, on the CNT surface, the difference of occupied areas between first and second water-layers prevents the formation of hexagonal ice and results in an amorphous structure. Figure 1(b) shows the changes of the potential energy per water molecule. The slope of the potential curve below 160 K differs from the slope above 200 K, and the curve transitions continuously within these two temperature ranges. This potential change is characteristic of a glass transition, and a liquid-solid crossover appears. The rotational autocorrelation function (RACF) at 200 K, which is near the transition temperature, both slow and fast relaxation regions are observed as shown in Figure 1(c). This is considered to indicate dynamic heterogeneity, which appears in the glass transitions.

When the amount of adsorbed water molecules is insufficient to fully cover two layers (pre-2L model), the adsorbed water separates into a double water-layer region (amophous structure) and a single water-layer region (iNR) at low temperatures. Its thermodynamic properties also resemble a combination of amorphous water and iNR, with both the glass transition point and melting point being observed. The thermodynamics of 2L and pre-2L model are consistent with the experimental results obtained by PL [2].

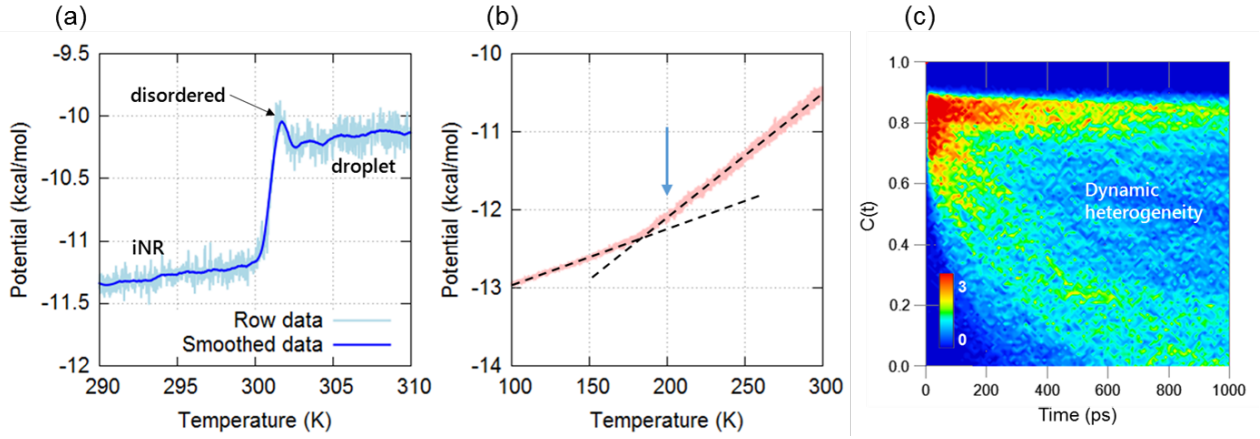

Figure 1: (a) Potential energy change per adsorbed water molecule in 1L model. (b) Potential energy change per adsorbed water molecule in 2L model. (c) RACF of adsorbed water in 2L model at 200 K (shown as an arrow in Fig.1(b))

References (if desired)

[1] Y. Homma *at al.*, *Phys. Rev. Lett.* 110, 157402 (2013).
[2] Y. Saito *at al.*, *J. Appl. Phys.* 129, 014301 (2021).
[3] K. Koga *et al.*, *Nature* 412, 802–805 (2001).
[4] R. Ma *et al.*, *Nature* 577, 60–63 (2020).

Cinematographic Electron Microscopic Study on Formation Processes of Carbon Materials

Koji Harano[1]

[1]*Center for Basic Research on Materials, National Institute for Materials Science (Japan)*

Among many analytical methods, atomic-resolution electron microscopy has the advantage of elucidating not only the static structure but also the dynamic behavior of molecules. However, in electron microscopic observation of molecular materials, sample damage caused by electron beam irradiation have hindered high-resolution imaging. In this study, based on a uniquely developed electron microscope sample preparation technique, single-molecule atomic-resolution time-resolved electron microscopy (SMART-EM), using nanocarbon materials (CNT, graphene, etc.) as specimen supports, we have succeeded in minimizing sample damage by the electron beam to reveal the structure of single molecules and molecular aggregates with atomic resolution [1]. This method also allows the tracking of time changes of molecules as atomic-resolution images, providing videos of three-dimensional structural transformations of complex organic molecules and molecular aggregates as well as chemical reactions induced by heat and electron beams, enabling the analysis of various chemical phenomena as statistical data on the behavior of individual molecules, which is not obtainable through bulk analysis.

For example, we successfully tracked the process of structural change at the level of single molecular chains in carbon fiber produced by heat treatment of polyacrylonitrile (PAN) as atomic-resolution images [2] (Figure). While the formation of a graphite structure consisting of carbon hexagonal rings occurs in the ordinary carbonization process, in the carbonization process using PAN as a starting material, a non-planar graphite structure containing five- and seven-membered rings is formed, which was shown to be the factor that causes the high mechanical strength of PAN-derived carbon fiber. We also demonstrated that cinematographic recordings of dimerization reactions of a van der Waals dimer of [60]fullerene (C_{60}) producing a short carbon nanotube individual molecules at a maximum frame rate of 1600 frames per second [4]. Using Chambolle total variation algorithm processing [4, 5] and automated cross-correlation image matching analysis, we identified several metastable intermediates of the multistep fusion reaction of C_{60} by their shape and size. We anticipate that the rapid technological development of microscopy and image processing will soon initiate an era of cinematographic studies of chemical reactions.

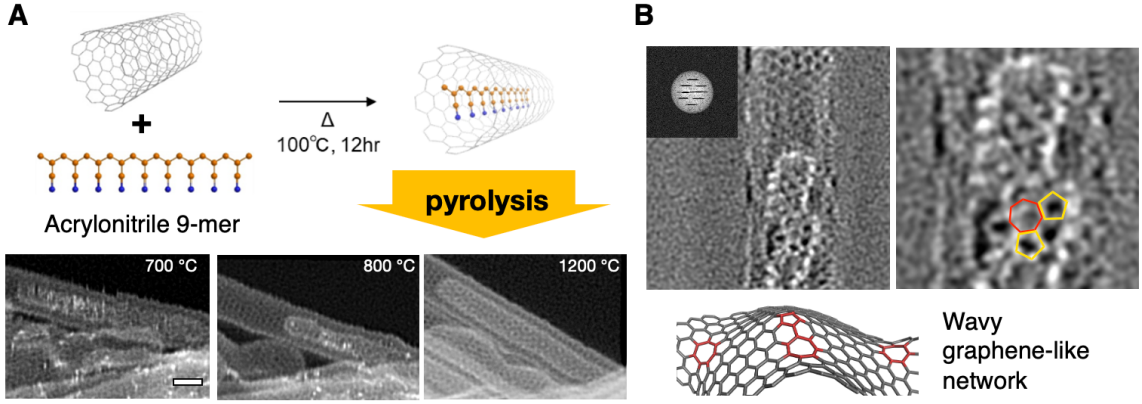

Figure. SMART-EM imaging of s single-chain carbon fiber formed upon pyrolysis of polyacrylonitrile in a single-walled carbon nanotube (CNT). (A) Sequential STEM images of an acrylonitrile 9-mer molecule (AN9) upon pyrolysis in CNT. Scale bar: 1 nm. (B) Image of AN9@CNT treated at 900 °C reconstructed by ptychography.

References

[1] K. Harano, T. Nakamuro, E. Nakamura, *Microscopy* **73**, 101 (2024).
[2] T. Ishikawa et al. *J. Am. Chem. Soc.* **145**, 12244 (2023).
[3] T. Shimizu, D. Lungerich, K. Harano, E. Nakamura, *J. Am. Chem. Soc.* **144**, 9797 (2022).
[4] T. Shimizu et al. *Bull. Chem. Soc. Jpn.* **93**, 1079 (2020).
[5] J. Stuckner et al. *Microsc. Microanal.* **26**, 667 (2020).

In-situ monitoring of single-molecule functionalization in vapor-phase for air-suspended single-walled carbon nanotubes

Mengyue Wang[1, 2*], Daichi Kozawa[1,2,3], Yuichiro K. Kato[1,2]

[1] *Quantum Optoelectronics Research Team, RIKEN Center for Advanced Photonics, Saitama, Japan*
[2] *Nanoscale Quantum Photonics Laboratory, RIKEN Cluster for Pioneering Research, Saitama, Japan*
[3] *Research Center for Materials Nanoarchitectonics, National Institute for Materials Science, Ibaraki, Japan*

Molecular devices are envisioned as the next generation of electronics, as traditional fabrication methods near their physical limits of miniaturization. Among the key approaches for incorporating sub-nanometer structures into molecular devices, functionalization reactions at the single-molecule level remain in their early stages, primarily due to limitations in characterization techniques.

In this work, we developed a setup to monitor and precisely control single-molecule functionalization, enabling the formation of organic color centers on single-walled carbon nanotubes (SWCNTs) via a vapor-phase photochemical reaction [1]. The setup consists of a reaction chamber and a focused UV laser to activate photochemical reactions on air-suspended SWCNTs. Real-time spectral evolution is monitored using an in-situ PL microscopy system, with a shutter mechanism in place to promptly block the UV light and stop the covalent modification process. The defect formation rate is investigated by varying the UV laser power. Additionally, this study explores changes in the binding configurations of pre-formed organic color centers on SWCNTs, as revealed by wavelength shifts in the defect emission peak of the time-resolved PL signal.

By understanding the vapor-phase functionalization process, single molecules can be reliably doped into air-suspended SWCNTs for single photon emission. Well-characterized single-molecule functionalization on SWCNTs also holds significant promise for molecular-scale electronics fabrication, potentially leading to breakthroughs in nanofabrication technology.

A part of this work was supported by JSPS (KAKENHI JP23H00262), JST (ASPIRE JPMJAP2310) and MEXT (ARIM JPMXP1224UT1071). We thank the Advanced Manufacturing Support Team at RIKEN for technical assistance.

References

[1] D. Kozawa, X. Wu, A. Ishii, J. Fortner, K. Otsuka, R. Xiang, T. Inoue, S. Maruyama, Y. Wang, and Y. K. Kato, *Nat. Commun.***13**, 2814 (2022).

Development of Carbon-Based Xerogels and Aqueous Dispersions Inspired by Japanese-Solid-Ink

Sakurako Kubota, Kotone Masuda, Junpei Hayakawa*

Nara Prefectural Seiwaseiryo Senior High School (Japan)

Japanese-solid-ink, traditionally produced from soot (susu) and glue (nikawa), has been used since the Nara Period for calligraphy and artistic purposes. Inspired by this ancient technique, we investigated novel methods to create carbon-based xerogels and aqueous dispersions by utilizing various carbon materials. This study aimed to develop simple, effective, and environmentally friendly approaches for the processing of carbon nanomaterials without the need for specialized equipment.

Firstly, carbon xerogels were prepared by replacing soot with multi-walled carbon nanotubes (MWCNTs), single-walled carbon nanotubes (SWCNTs) fullerenes C_{60}, graphite, graphene, and nanodiamonds (ND) (Fig. 1)[1]. These materials were mixed with glue in hot water, ground thoroughly, and dried under ambient conditions. The resulting xerogels exhibited robust structures and uniform distribution of carbon particles. Furthermore, composite xerogels using two carbon materials in a 1:1 mass ratio were successfully obtained, demonstrating the versatility of this method. This preparation technique enables the fabrication of novel xerogels with potential applications in electronic materials and environmental technologies.

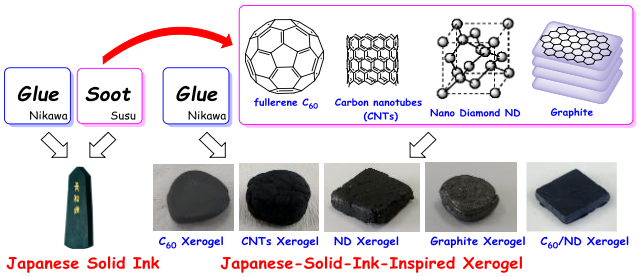

Figure 1: Xerogels of carbon materials

Secondly, aqueous dispersions of carbon materials such as MWCNTs, SWCNTs, fullerenes C_{60}, graphite, graphene, and ND were explored using glue as a natural dispersant (Fig. 2)[2]. The dispersion performance of several proteins, including cook gelatin, type-A gelatin, and collagen peptides, was evaluated. The results indicated that proteins with certain molecular weights were effective in dispersing carbon materials in water, irrespective of the surface charge of the dispersed particles. Glue was found to be rich in glycine, closely resembling gelatin in composition, which contributes to its dispersing ability. This study highlights the importance of molecular weight and protein structure in achieving stable aqueous dispersions of carbon materials. Furthermore, these prepared dispersions could be utilized to create ink paintings (Fig.3).

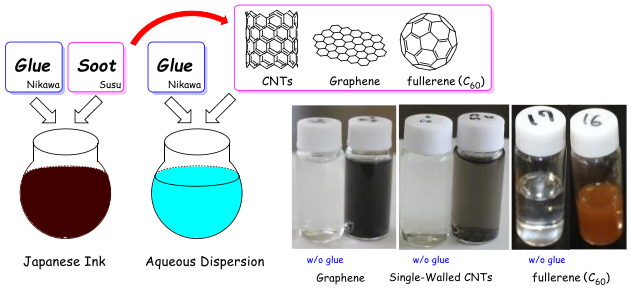

Figure 2: Aqueous dispersions of carbon materials

Figure 3: Ink paintings using prepared dispersions

These investigations provide a sustainable and accessible approach for processing carbon nanomaterials inspired by traditional Japanese craftsmanship. The combination of carbon xerogels and aqueous dispersions broadens the potential applications of carbon-based composites, contributing to future advancements in nanomaterial science.

References

[1] J. Hayakawa *et al.*, *Chem. Lett.* **53**, 183 (2024).
[2] J. Hayakawa *et al*, *Chem. Edu.* **98**, 1381–1388 (2021).

Relationship between the interfacial adhesion and microscopic interface structures in CNT/epoxy resin nanocomposites

T. Yayama[1], T. Hiraishi[2], F. Akagi[1,2]

[1] Department of Applied Physics, School of Advanced Engineering, Kogakuin University, *(Japan)*,

[2] Electronics and Electron Engineering Program, Graduate school of Engineering, Kogakuin University, *(Japan)*,

1. Introduction

Structural materials for satellites and rockets used in space must be both considerably lightweight and robust. Nanocomposites with carbon nanotubes (CNT) as the reinforcement are promising structural material for realizing next-generation satellites and rockets and the other space equipment due to the excellent mechanical properties. However, there still remains numerous challenges and especially the poor load transfer at the interface between CNT and polymetric matrix is critical issue. [1,2] We believe that covalent bonds between CNTs and resin are important for load transfer at the interface, and have investigated binding energies and other electronic properties using first-principles calculations. In particular, we have shown that strong covalent bonds are formed in the vicinity of a point defect in CNTs, and have proposed structures that lead to improved interfacial adhesion. [3] In this work, molecular dynamics (MD) is used to evaluate the interfacial shear strength (IFSS) using a model in which CNTs are embedded in numerous resin molecules. The microscopic structures, such as the density and arrangement of the resin molecules around the CNTs are analyzed, as the factor that causes the IFSS to change depending on the state of the CNTs.

2. Calculation models and method

MD simulations are conducted using LAMMPS. Interface models are made for composite consisting of (7,0) single wall CNT and 72 Bisphenol A diglycidyl ether (DGEBA) monomer. For the CNTs, the following three-types of models were used: A defect-free CNT, a CNT with a point defect, and a model with covalent bonds between a CNT and DGEBA. IFSS were evaluated by pull-out simulations, for interface models with each CNTs, shown in following procedure. Under NVE conditions, with the CNTs completely embedded in the resin as the initial state, the CNTs were given an initial velocity and ejected from the resin. The CNTs receive work from the resin due to friction, resulting in a decrease in kinetic energy. The IFSS was determined based on this decrease in kinetic energy. To describe the bond breaking, ReaxFF potential is used for interatomic potential. To further clarify the relationship between IFSS and structure, the density and shape of the resin near the CNTs were considered by classification using the K-means method.

3. Results and discussion

A model for pull-out simulation and the time dependence of the kinetic energy of CNT is shown in Fig. 1. It can be seen that the kinetic energy of the CNTs decreases with time and converges when they are completely pull-out from the matrix. The IFSSs calculated from the reduction in kinetic energy are 275.7 MPa, 284.6 MPa and 911.2 MPa for each model respectively. As expected, the IFSS for the bond model is extremely large and more than three times higher than that for the defect-free model where the only interfacial interaction thought to be the van der Waals force. On the other hand, the defect model also shows an increase in the IFSS, although not as much as the bond model. Analysis of the structure shows an increase in resin density near the interface and the effect of resin placement.

References

[1] I. A. Kinloch et al., *Science*, **362** (2018) 547-553.
[2] S. Bagchi, et. al., *Proc. R. Soc. A* **474** (2018) 20170705-1-19.
[3] T. Yayama et al., *J. Evol. Space Act.*, **2** (2024) 118-1-7.

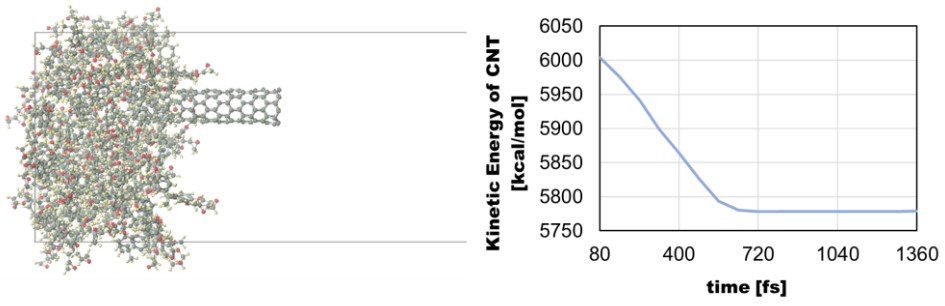

Fig. 1 : A model for pull-out simulation and the time dependence of the kinetic energy of CNT.

Diameter Controllable Synthesis of Single-walled Carbon Nanotubes by Arc Discharge Using Ni-based Catalysts

Yixi Yao[1,2], Zeyao Zhang[1,2,*], Yan Li[1,2,*]

[1]*Academy for Advanced Interdisciplinary Studies, Peking University, Beijing, China;*
[2]*Institute of Carbon-Based Thin Film Electronics, Peking University, Shanxi, Taiyuan, China;*

E-mail of corresponding author: zeyaozhang@pku.edu.cn; yanli@pku.edu.cn

Abstract: Single-walled carbon nanotube (SWCNT)-based nanoelectronic devices with ultra-high performance and low power consumption present a promising alternative to surpass the limitations of silicon-based devices in the post-Moore era. The intrinsic properties of SWCNTs are uniquely determined by their structures. According to the tight-binding model, the band gap (E_g) of semiconducting SWCNTs is approximately inversely proportional to the diameter. Thus, the diameter-controllable synthesis of SWCNTs is of great interest to offer ideal materials for various devices. Arc discharge has the advantage of higher degree of graphitization with fewer defects. However, the diameter control of arc synthesis is a critical challenge. In this work, we obtained SWCNTs with different diameter distributions by introducing MgO and adjusting the current and the pressure of helium during the arc discharge process. With the increase of MgO content, the average diameter of SWCNTs reduced from 1.47±0.15 nm to 1.26±0.10 nm using Ni-Y catalysts, and from 1.27±0.18 nm to 1.09±0.14 nm using Ni catalysts. In addition, the introduction of supports can greatly enhance the effect of arc current and He pressure on the diameter regulation of SWCNTs. Thus, by changing the ratio of MgO to catalysts, the current and the He pressure, we achieved diameter-controllable synthesis of SWCNTs with average diameters ranging from 1.09 nm to 1.47 nm, covering the required bandgaps for high performance SWCNT-based electronics. Our research provides a feasible way to controllable synthesis of SWCNTs by arc discharge.

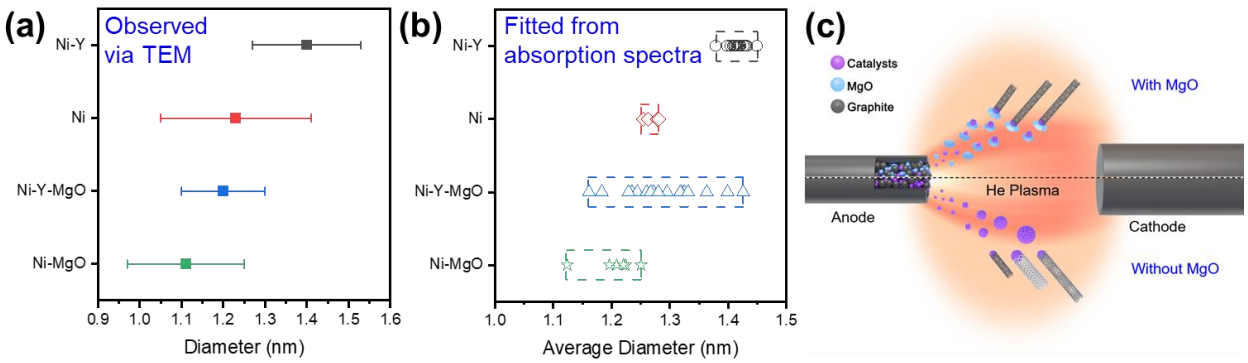

Fig. 1 Diameter controllable synthesis of SWCNTs by arc discharge. (a) Diameter distribution observed via TEM. (b) Average diameters fitted from absorption spectra of SWCNTs synthesized applying different conditions. (c) Effects of the introduction of MgO supports.

Diameter Specific Bandgap Modulation in MoS_2 Nanotubes Grown via Template Reaction

Zhen Han[1], Runze Lai[1], Jian Sheng[1], Chengping Lian[1], Yan Li[1*]

[1]*Beijing National Laboratory for Molecular Science, Key Laboratory for the Physics and Chemistry of Nanodevices, College of Chemistry and Molecular Engineering, and Academy for Advanced Interdisciplinary Studies, Peking University, Beijing 100871, China*

Compared with two-dimensional counterparts, one-dimensional MoS_2 nanotubes not only have degrees of freedom in number of layers, but also have additional degrees of freedom in diameter and chirality, which are expected to induce novel physical properties[1]. Theoretical results predicted that, as the diameter of a MoS_2 nanotube decreases, the combined effect of curvature-induced flexoelectricity and circumferential tensile strain causes a rapid narrowing of the bandgap.[2,3] In 2020, single-walled MoS_2 nanotubes were synthesized on SWCNT and BNNT via template reaction, endowing us opportunities to explore their structure-property relationships[4]. In this work, using SWCNT@BNNT as a template, we synthesized MoS_2 nanotubes with a diameter as small as 3.8 nm by chemical vapor deposition. The electronic structure of MoS_2 nanotubes was investigated by ultra-high energy resolution electron energy loss spectroscopy. The results show that the bandgap of MoS_2 nanotube is reduced by up to 210 meV compared with the monolayer MoS_2. In the range of diameters from 3.8 nm to 6.8 nm, the regulation mechanism of bandgap narrowing with decreasing diameter (-47 meV/nm) was experimentally revealed. This is the first experimental evidence of diameter specific bandgap modulation in MoS_2 nanotubes at individual tube scale.

References

[1] Guo, J., Xiang, R., Cheng, T., et al. *ACS Nanosci. Au* ***2***, 3-11 (2022).
[2] Zhao, S., Yang, C., Zhu, Z., et al. *Npj Comput. Mater.* ***9***, 92 (2023).
[3] Hisama, K., Maruyama, et al. *Jpn. J. Appl. Phys.* ***60***, 065002 (2021).
[4] Xiang, R., Inoue, T., Zheng, Y., et al. *Science* ***367***, 537-542 (2020).

Green conversion of low quality chemical feedstock to hydrogen and carbon nanotubes

Chaojie Cui, Bofan Li, Ruijing Jiao, Weizhong Qian

Tsinghua University, Beijing 100084, China

With the development of clean energy and the popularity of electric vehicles, the conversion and utilization of petrochemical resources such as diesel oil has become a new topic. At the same time, disposing waste from producing high-value cyano- or amino-chemicals or materials remains a significant challenge for environmental protection. Here, we propose a general catalytic conversion method to convert low-quality chemical feedstocks into carbon nanotubes (CNTs) with hydrogen production as a by-product, which is highly desirable for the sustainable development of human society in the era of carbon neutrality.

A direct catalytic decomposition of diesel to produce H2 with a nano-Fe-based catalyst and simultaneously fix carbon elements as CNTs is achieved. The carbon footprint value of the present technology is far lower than those of grey H2, blue H2, and other dehydrogenation technologies. Compared with most of the technologies mentioned above, the energy consumption (based on per molar H2) and reactor amplification all validate the high efficiency and high practical feasibility of the present technology.

The conversion of cyano-/amino- compounds to N-CNTs by the chemical vapor deposition (CVD) method is also achieved. One-step vapor deposition can effectively remove all cyanide, including HCN, for exhaust gases with low cyanide concentrations. For a model liquid waste with a high concentration of cyano- or amino-compounds in the temperature range of 700 - 850°C, toxic compounds are eliminated, and N-CNTs with different nitrogen doping ratios can also be prepared depending on the catalyst and operating conditions. These N-CNTs are attractive as electrodes for supercapacitors or adsorbents with hydrophilic properties and excellent electrical conductivity.

References

[1] Ruijing Jiao, et al., ACS Omega, 2024, 9, 1546-1553.
[2] Bofan Li, et al., Engineering (under review), 2025.

Hybrid Fibers incorporating Carbon Nanotubes

E. F. Antunes[1*], D. S. Pimenta[1*], R. B. R. Gonçalves[1], M. M. Mourthé[1], T. L. Cançado[1], F. Murta[1], A. H. Kasama[2], L. O. Ladeira[1], M. H. Oliveira[1], G. G. Silva[1]

[1]*Centro de Tecnologia de Nanomateriais e Grafeno – CTNANO, Universidade Federal de Minas Gerais – UFMG (Brazil),*

[2]*Centro de Pesquisas, Desenvolvimento e Inovação Leopoldo Américo Miguez de Mello - CENPES, Petróleo Brasileiro, S.A - PETROBRAS (Brazil)*

[*]Both authors contributed equally to this paper.

Abstract: The production of hybrid fibers incorporating carbon nanotubes (CNTs) has been widely explored in the literature and is expected to reach pilot-scale production in the near future. In this way, our research group has been studying potentially scalable chemical vapor deposition processes. Our approach utilizes a high-temperature furnace, where precursor solutions containing liquid hydrocarbons and metallocene catalysts drive CNT growth. To evaluate the quality and purity of our carbon nanotubes, we employed Raman spectroscopy, scanning electron microscopy (SEM), transmission electron microscopy (TEM), and thermogravimetric analysis (TGA). Our method enables the synthesis of high-quality single-walled and double-walled carbon nanotubes (SWCNTs/DWCNTs). Additionally, we performed electrical characterization to determine the fiber´s conductivity and specific conductivity ranges. We acknowledge the support of **PETROBRAS** for funding this project at CTNANO/UFMG (SAP PETROBRAS 0050.0126098.23.9 4600677416) and the "**Centro de Microscopia"**, as well as the **LCPNANO** and **CTNANO** characterization facilities at UFMG, for their assistance with electron microscopy imaging, Raman spectroscopy, and thermogravimetric analysis.

References

[1] J. Qin et al., Composite Science and Technology, 211, 108870 (2021)

Harnessing Multiscale Engineering for Advancing CNT Technology: From AI for Synthesis to Functional Nanocarbon Assembly

Dewu LIN[1], Don N. Futaba[2], Kenji Hata[2], Wenjun ZHANG[3]

[1]Peking University Shenzhen Graduate School (China), [2]AIST (Japan), [3]City University of Hong Kong (China)

Thirty years since their discovery, the quest to mass-produce single-walled carbon nanotubes (CNTs) while translating their superlative nanoscale properties into macroscopic functionality remains a critical challenge. While the supergrowth method enables scaled-up synthesis of vertically aligned nanotube forests, inherent kinetic-thermodynamic trade-offs between crystallinity and growth efficiency persists. To break this trade-off, we employed an automated synthesis reactor generating 585 experimental datasets to train an XGBoost regression machine learning model. Subsequent 16,000 parameter-space explorations identified optimal hydrocarbon reactivity ($\Delta_f G$ = 550-750 kJ/mol) and C/O ratios ($\log_{(C/O)}$=1-2), enabling 48% enhanced growth efficiency (980 µm in 10 min) while maintaining high crystallinity (G/D≈20), achieving coexistence of previously exclusive characteristics.[1] Furthermore, the ML-revealed hydrocarbon reactivity principles guided rational selection of butadiene feedstock, demonstrating how fundamental insights accelerate applied material design.

Harnessing the outstanding nanoscale properties of individual CNT into assemblies toward macroscale applications remains challenging. To cope with this problem, we developed microwave shock technology for direct hierarchical engineering of CNT assemblies, from electrical regulation to mesoscale bundle exfoliation and to macro performance enhancement. CNT films with lithiophilic N-doped interfaces (1 at. %) and opened bundle (15×SSA increase to 648 m^2/g) enabled dendrite-free lithium cycling (850 hours@2 mA/cm^2) when applied to battery anodes.[2] Further solvent-free grafting of CNTs following a microwave shock treatment facilitate the functional customization CNTs in arbitrary macroscopic assemblies, which complements conventional solution-based techniques.[3,4]

We believe that the symbiosis of AI-driven synthesis optimization and application-oriented structural engineering (Figure 1) represents a transformative approach. This paradigm shift from isolated optimizations to systemic co-design opens new frontiers in energy storage, flexible electronics, and catalytic systems where nanoscale design must meet macroscale functionality.

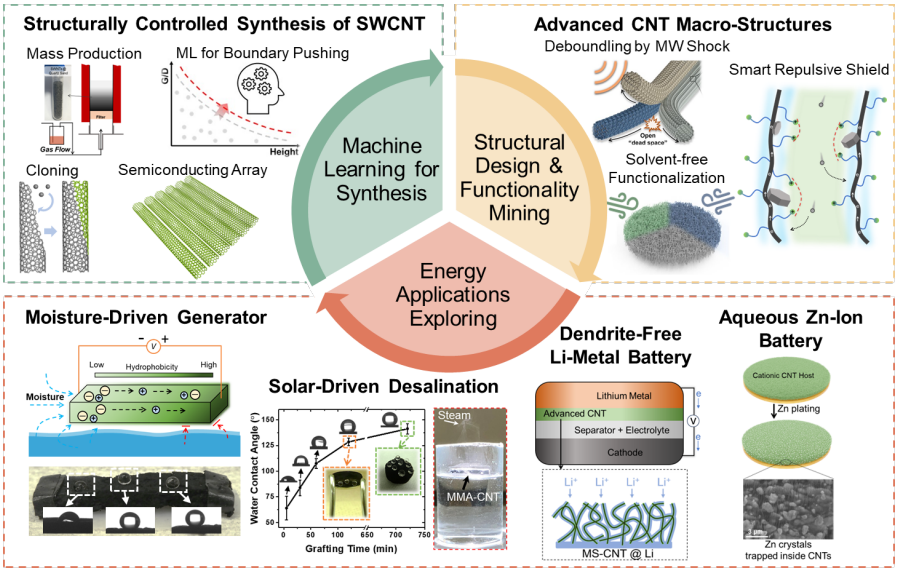

Figure 1. Study loop of "AI Driven Synthesis-Structural Engineering-Application".

References

[1] D. Lin, *ACS Nano*, 2023, 17, 22821.
[2] D. Lin, *Adv. Funct*. Mater., 2023, 33, 2211180.
[3] D. Lin, *ACS Nano*, 2023, 17, 3976.
[4] D. Lin, *Adv. Energy Mater.*, 2024, 14, 2304535.

MASS PRODUCTION OF TWO-DIMENSIONAL MATERIALS BY BUBBLING CHEMICAL VAPOR DEPOSITION

Zhiyuan Shi[1]

[1]*Shanghai institute of microsystem and information technology, CAS (China)*

Abstract

Fully exploiting the intrinsic characteristics and further promoting the large-scale industrial applications of two-dimensional (2D) materials highly depend on its mass production with efficiency (high-yield, time-saving, and low-cost) and controllability (high-quality, safe, and environmentally friendly). For the mass production of two-dimensional materials, the usage of bubbling as a new tool makes a big difference in multiple aspects of graphene production [1]. The molten media is employed as the transport media, and the catalyst, which is the crucical factor for the synthesis of 2D materials.

We suggested molten metal (Cu) or molten salt (NaKCl-$CuCl_2$) as the molten media and methane was introduced as the carbon source. One-pot synthesis of 0D (carbon black, CB)/2D (graphene, Gr) carbon materials was realized by bubbling chemical vapor deposition (B-CVD) method [2]. The confined space introduced by the bubble acts as a mini-reactor to define the product morphology and accelerate the growth. Beneficial to the synergistic effect between ionic complex promotion and bubble confined space, the mass production of CB/Gr simultaneously with high efficiency and low cost at relatively low temperature is achieved.

We proposed molten metal-boron alloy for the controllable synthesis of large-area 2D multilayered hexagonal boron nitride (h-BN) films. Combined molten $Fe_{82}B_{18}$ alloy with N_2, the vapor-liquid-solid (VLS) growth strategy was developed to realize the epitaxy-enabled growth of multilayered h-BN on c-facet sapphire substrate [3]. We further introduce molten Ni-B alloy wetting on W, the alloy serves as both the boron source and the growth substrate for synthesizing h-BN multilayers [4]. The full width of half maximum of Raman E_{2g} mode reaches 9.3 cm^{-1}, which is similar to the exfoliated h-BN flakes. Based on the molten metal-boron alloy, we realized mass production of two-dimensional h-BN nanopowders by B-CVD method. The collected h-BN nanopowders exhibit few-layered (less than 3 nm) feature with large lateral size (more than 100 μm).

The proposed B-CVD method promotes the mass production of two-dimensional materials with high quality and low cost, paving the way to potential applications.

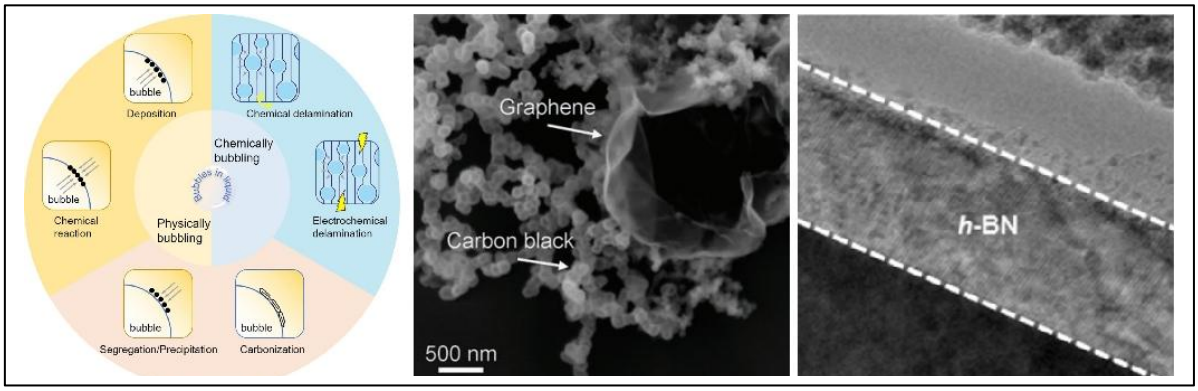

Figure caption: Synthesis of two-dimensional materials with the assistance of molten media.

References

[1] Z. Shi, *et al.*, *Adv. Funct. Mater.* **32**, 2203124 (2022).
[2] Y. Zhao, *et al.*, *Adv. Funct. Mater.* **32**, 2202381 (2022).
[3] Z. Shi, *et al.*, *Nat. Commun.* **11**, 849 (2020).
[4] Y. Zhu, *et al.*, *2D Mater.* **11**, 035033 (2024).

Precise structural regulation of carbon crystals by electron doping

Fei Pan[1,3], Kun Ni[1], Yanwu Zhu[1,2,3,*]
[1]*Department of Materials Science and Engineering, School of Chemistry and Materials Science, University of Science and Technology of China, Hefei, Anhui 230026, China;*
[2]*Hefei National Research Center for Physical Sciences at the Microscale, University of Science and Technology of China, Hefei, Anhui 230026, China;*
[3]*Key Laboratory of Precision and Intelligent Chemistry, University of Science and Technology of China, Hefei, Anhui 230026, China.*

Abstract text. The structural phase transition of carbon crystals, such as graphite to diamond, usually occurred under high temperature (above 1000 °C) and/or high pressure (above 1 GPa). Herein, we show two types of structural phase transition of carbon crystal induced by electron doping under atmospheric pressure and temperature below 600 °C. At first, we demonstrate that 3R to 2H phase transition of graphite can be promoted by changing the charged state of 3D graphite [1], which promotes the repulsion between the layers and significantly reduces the energy barrier between the 3R and 2H phases. The charge transfer from lithium nitride (α-Li_3N) to graphite can lower the transition temperature down to 350 °C. The proposed interlayer slipping model potentially offers the control over topological states at the interfaces between different phases of graphite. The charge transfer from alkali metals (Li, Na, K) have also been proven to promote the aforementioned stacking phase transition of graphite [2]. In addition, we demonstrate that the gram-scale preparation of a new type of carbon, long-range ordered porous carbon (LOPC), from fcc-C_{60} crystal catalyzed by the electron transfer from α-Li_3N to C_{60} under atmospheric pressure and temperature of 550 °C [3]. At a lower temperature of 480 °C, a well-known polymerized C_{60} crystal can be obtained. LOPC consists of connected broken C_{60} cages that maintain long-range periodicity of face-centered cubic (fcc) stacking. The carbon K-edge near-edge X-ray absorption fine structure shows a higher degree of delocalization of electrons in LOPC than in fcc-C_{60} crystal. Numerical simulations based on a neural network show that LOPC is a metastable structure produced during the transformation from fullerene-type to graphene-type carbons [4].

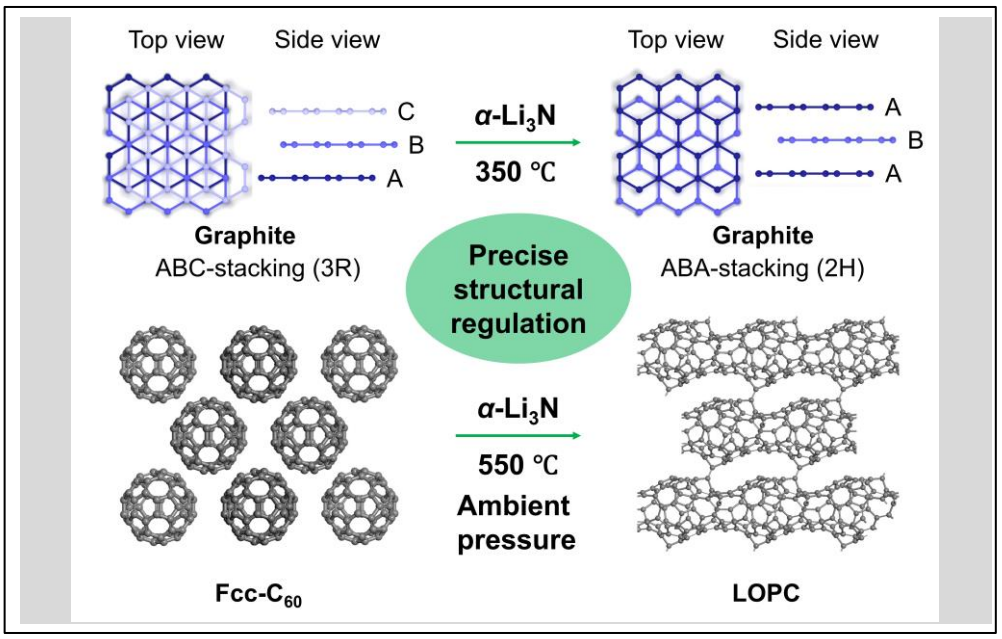

Figure caption: Under electron doping from α-Li_3N, the ABC stacking in graphite powder transforms to ABA stacking under 350 ℃ and the fcc-C_{60} crystal powder transforms to LOPC under 550 ℃ and ambient pressure.

References

[1] F. Pan,# K. Ni,# Y. Ma,# *et al.*, *Nano Lett.* **21**, 5648-5654 (2021).
[2] X. Wang,# W. Zhang,# K. Ni, *et al.*, *Carbon* **213**, 118295 (2023).
[3] F. Pan,# K. Ni,# T. Xu,# *et al.*, *Nature* **614**, 95–101 (2023).
[4] K. Ni,* F. Pan, Y. Zhu,* *Adv. Funct. Mater.* **32**, 2203894 (2022).

Autonomous Multi-Objective Bayesian Optimization of Carbon Nanotube Yield and Diameter Control at Synthesis from Disordered Catalyst

R. Waelder[1,2], W. Kim[3], M. Pitt[4], J. Myung[4], and B. Maruyama[1]

[1]Materials and Manufacturing Directorate, Air Force Research Laboratory (USA), [2]BlueHalo (USA), [3]Department of Psychology, Howard University (USA), [4]Department of Psychology, Ohio State University (USA)

Autonomous research systems combine automated execution of experiments, in-line characterization and analysis, and machine learning-based decision making to reliably, efficiently, and intelligently explore an experimental space in search of a scientific goal. These systems are of particular value for high-dimensional questions, such as materials synthesis where desired properties may be a function of many process inputs.

Single-walled carbon nanotube (SWCNT) synthesis is an ideal area for autonomous research: it is a high dimensional problem, with a large number of both discrete and continuous experimental inputs, and critically important outputs, due to the vast range of SWCNT properties. The electronic properties of SWCNTs in particular range from metallic through wide-bandgap semiconducting based on the diameter and helical angle of the structure. Diameter selection can be achieved post-growth, but is a lossy process, and diameter control should not come at the cost of yield. We present the first multi-objective autonomous research campaign for CNT synthesis, maximizing both overall CNT yield and diameter control. Many attempts at SWCNT diameter control do so via intensive engineering of the catalyst particles: tuning composition, diameters, packing densities, etc. Here we begin with a disordered film of oxidized cobalt on a defective alumina support. By varying the thermodynamic conditions of the synthesis environment, we can control the size distribution and population dynamics of the emergent nanoparticle catalyst bed, and therefore control the diameters of the resulting SWCNTs. Using this thermodynamic understanding, we identify regions of experimental space conducive to yield- and diameter control-optimized growth, demonstrating significant overlap, and that for the conditions tested here, that these objectives are independent, and arbitrary degrees of diameter control can be realized for all experimentally achieved yields.

Towards a More Complete Empirical Thermodynamic Understanding and Control of Supported Catalyst Carbon Nanotube Synthesis

R. Waelder[1,2], A. W. N. Sloan[1,3], R. Rao[1], and B. Maruyama[1]

[1]Materials and Manufacturing Directorate, Air Force Research Laboratory (USA), [2]BlueHalo LLC (USA), [3]National Research Council (USA)

Catalyst control is critical to CNT synthesis to enable property control and scalability. In supported catalyst CNT growth, the reduction of an oxidized metal catalyst enables growth, but its reduction also initiates catalyst deactivation via Ostwald ripening. In other words, a reduced catalyst is an active one, and an oxidized catalyst is a stable one. In order to maximize catalyst performance, we must balance activity and stability by controlling oxidative and reductive forces. This control can be achieved through the relationship between catalyst species, temperature, and growth gas concentration. We hypothesize that the appropriate balance is achieved, and catalyst performance maximized, at the minimum applied reducing potential that will reduce the catalyst oxide.

We have demonstrated this effect using two different thicknesses of an iron catalyst film in our LaserCNT Autonomous Research System. [1] LaserCNT was guided by an experimental planning algorithm called Jump Regression, which is specifically designed to identify discontinuous features in a response. Since oxidized catalyst does not promote CNT growth and metallic catalyst does, this phase transition will manifest as a jump discontinuity in our measured CNT yields as a function of the synthesis inputs. The Jump Regression algorithm identified a jump for each film thickness from no growth to the best overall observed growth as a function of these redox forces.

We have since applied this formalism to other catalysts, such as cobalt and nickel in the supported catalyst regime, with encouraging results. In addition, we have begun to extend these concepts to our floating catalyst reactor, a non-equilibrium system, and have observed promising preliminary results.

[1] Waelder, R. et al. *Carbon* **228**, 19356 (2024).

Evolution of Carbon atoms to Chiral Carbon Nanotubes on metal free template

Shuchen Zhang[1]

[1]*State Key Laboratory of Precision and Intelligent Chemistry, Department of Materials Science and Engineering, School of Chemistry and Materials Science, University of Science and Technology of China (China)*

The structural control of single-walled carbon nanotubes (SWNTs) has remained a critical challenge, hindering their application in microelectronics for over two decades. It is widely accepted that at high growth temperatures, a more rigid growth template is beneficial for controlling the structure of carbon nanotubes. In this study, we propose a simple yet effective strategy for controlling the chirality of as-grown SWNTs on a pure carbon-based template (e.g., fullerene) with enhanced efficiency by employing a single-site catalyst-modified substrate. Pure carbon templates generally exhibit low efficiency in SWNT growth due to the absence of catalytic sites necessary for decomposing carbon source molecules. Single-site catalysts, however, efficiently decompose carbon sources into carbon atoms while preventing the formation of large nanoparticles that could lead to unwanted nucleation. By modifying a sapphire substrate with single-site catalysts, a surface environment with a high concentration of carbon atoms is created. The generated carbon atoms are subsequently transferred and adsorbed onto the carbon-based template. Once a sufficient concentration of carbon atoms is reached, local surface fluctuations at high temperatures facilitate their assembly into ordered carbon fragments, forming a new carbon phase that undergoes downhill diffusion. The continuous accumulation of carbon atoms onto these fragments promotes their growth into nanotube caps, leading to their detachment from the template surface and the eventual formation of carbon nanotubes. Due to the specific pentagon-hexagon configurations within the carbon-based template, only (15, 7) tubes with near five-fold symmetry and (17, 6) tubes with near six-fold symmetry were selectively enriched, as confirmed by Raman spectroscopy. These findings provide compelling evidence that the structure of SWNTs can be controlled using a pure carbon template, offering new insights into the evolution of carbon atoms into SWNTs. This study paves the way for the experimental enrichment of chiral SWNTs using metal-free templates, presenting a promising direction for future research.

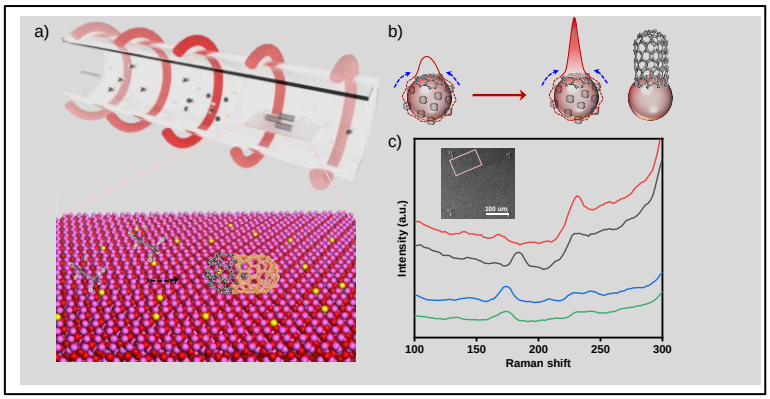

Figure 1: SWNTs growth by metal-free template. a) Schematic illustration of SWNTs growth on a metal-free template with single-site catalysts modified substrate. b) Proposed mechanism for carbon atom assembly into SWNTs. c) Representative Raman spectrum of as-grown SWNTs.

References

[1] S. C. Zhang et al. *Nature* **2017**, 543, 234-238.
[2] L. N. Chen et al. *Science* **2023**, 381, 857-861.
[3] S. C. Zhang et al. *Chem* **2019**, 5, 1182-1193.
[4] S. C. Zhang et al. *Nat. Sci. Rev.* **2018**, 5, 310-312.

Synthesis of isolated pentagonal h-BN crystals by atmospheric pressure CVD

K. P. Sharma[1, 2], T. Maruyama[1, 2]

[1]*Department of Applied Chemistry,* [2]*Nanomaterial Research center, Meijo University (Nagoya, Japan)*

Hexagonal boron nitride (h-BN), a structural analogue of graphene, is a wide bandgap 2D insulating layered material, consisting of alternating sp^2–bonded boron and nitrogen atoms [1]. h-BN shows appealing properties such as thermally stable in air up to 800ºC, chemical inertness, stable thermal conductivity, and superior elastic properties, and hence has drawn significant attention as a promising material in frontier applications [2]. Although chemical vapor deposition (CVD) technique has developed as the most scalable process to synthesize h-BN on transition metals, the formation of various polygonal-shaped single domain is unclear and are still limited to few microns in their edge length [3, 4]. In this research, we investigated the isolated pentagonal h-BN crystals grew onto various Cu facet in single crystallinity prospective [1].

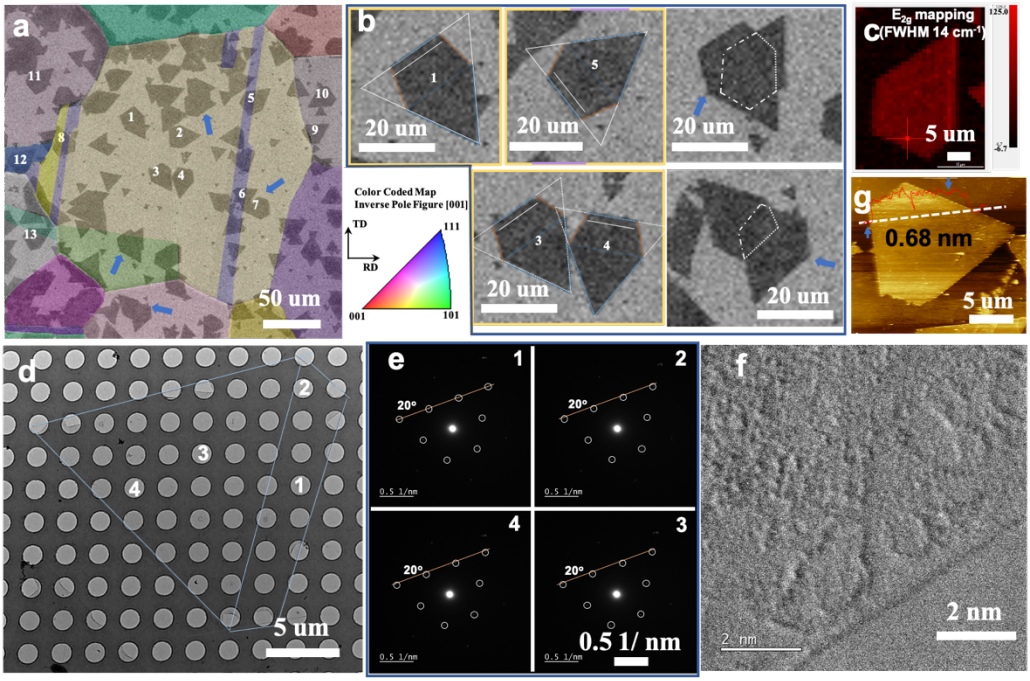

Figure: 1 (a) FESEM with false color overlaid EBSD mapping, **(b)** enlarged crystals in **(a)**, **(c)** Raman mapping (E2g vibration mode), and **(d)** TEM, and **(g)** AFM images of typical pentagonal h-BN crystals grown for 38 min with AB heated for 60-65ºC. **(e)** shows SAED taken around 1-4 spot in **(d)** and **(f)** shows HRTEM image of it onto edge.

For h-BN crystals synthesis, bare Cu foils were heated at 26 ºC/min to 1050 ºC with 100 sccm Ar in horizontal tubular furnace. After annealing the Cu foil for 30 min with 100 sccm Ar, ammonia borate (AB) was evaporated with 100:2 mixtures of Ar and H_2. To grow h-BN, 2 mg of AB was heated for various growth intervals with different supply rate to study the morphological transition and rapidly cooled down within 30 min. As synthesized h-BN crystals were analyzed by optical microscopy (OM), Raman spectroscopy, FESEM, XPS, AFM, EBSD, and HRTEM.

Pentagonal shaped (most dominance) along with regular triangular shaped h-BN crystals (**Figure 1(a)**) were grown for 38 min with AB heated for 60-65ºC. **Figure 1 b-d, g** shows the uniformity of pentagonal crystal with sharp and step edges comprising longer and shorter arms respectively. It is believed that merging of small triangular h-BN crystals in different fashion produced most of polygonal h-BN crystals and could be polycrystalline [3-4]. SAED were taken from 1-4 of an isolated pentagonal crystal shows no distinct difference in crystallographic orientations (see **Figure (e)**) and HRTEM image shows its high crystallinity.

This work was supported in part by Private University Research Branding Project from the Ministry of Education, Culture, Sports, Science and Technology (MEXT), Japan.

References

[1] K. K. Kim *et al., Nano Lett.,* **12**, 161 (2012).
[2] J. Sun *et al., Chem. Soc. Rev.* **47**, 4242 (2018).
[3] R. Y. Tay *et al., Nanoscale* **8**, 2434 (2016).
[4] K.P. Sharma *et al., CrysEngComm.* **20**, 550 (2018).

Synthesis of Long Carbon Nanotubes by Br-assisted Floating Catalyst Chemical Vapor Deposition

Hirotaka Inoue[1,2], Anastasios Karakassides[2], Toshihiko Fujimori[1,3], Akira Takakura[1], Soichiro Okubo[1], Hua Jiang[2], Ghulam Yasin[2], Kazuhiro Ikeda[1], Takamasa Onoki[1], Yoku Inoue[4], Esko I. Kauppinen[2]

[1]*Sumitomo Electric Industries (Japan),* [2]*Aalto University (Finland),* [3]*University of Tsukuba (Japan),* [4]*Shizuoka University (Japan)*

Carbon nanotubes (CNTs) have outstanding mechanical strength, electrical properties, and thermal conductivity along the axial direction of the tube, as demonstrated by experimental and theoretical studies over the past 30 years. CNT fibers in which CNTs are aligned along the tube axis maximize the unique properties of individual CNTs, and open the potential for applying them to macro-scale products such as electrical cables, high-tensile wires, and thermoelectric devices.

One of the key factors affecting CNT fibers is the length of individual CNTs, which directly impacts their strength, electrical conductivity, and thermal conductivity [1]. In order to synthesize long CNTs, various techniques have been developed, *e.g.*, water-assisted chemical vapor deposition (CVD) [2], Cl-assisted CVD [3,4], and bi-metallic catalyst systems [5]. However, it remains difficult to achieve both the high quality and high yield required for industrial applications, highlighting the need for new approaches to synthesize longer CNTs.

In this study, we demonstrate the impact of bromine (Br) addition in the floating catalyst CVD (FC-CVD) process for enhancing the CNT length. 6.9×10^{-7} mol/min of ferrocene as iron source, elemental sulfur as sulfur source, ethylene as main carbon source, and C_2H_5Br as Br source were introduced to the reactor by 1 L/min of pure hydrogen gas at 1200°C. Fig. 1 (a) shows a relationship between Br concentration and mean bundle length. It was found that adding C_2H_5Br up to 89 ppm significantly increased the length of CNT bundles by 2.7 times. Furthermore, the sheet resistance of CNT films at 90% transmittance improved from 5403 ± 3383 Ω/□ to 139 ± 33 Ω/□ with 89 ppm of C_2H_5Br (Fig. 1 (b)), and this effect was superior to that of other halogen elements such as Cl and I. To obtain long CNTs in high yield, the Br-assisted FC-CVD technique was applied to a system with quite different synthetic conditions: higher temperature (1350°C), larger carrier gas flow rate (9 L/min), and higher ferrocene introduction rate (4.0×10^{-4} mol/min). Comparison of the optimum amount of Br for the high- and low-yield systems showed that the optimal condition of Br had a stronger relationship to the amount of carbon source rather than that of catalyst. These results suggest that Br may influence carbon-related processes during synthesis, such as improving the efficient decomposition of carbon precursors. Further details of these findings will be discussed in the presentation.

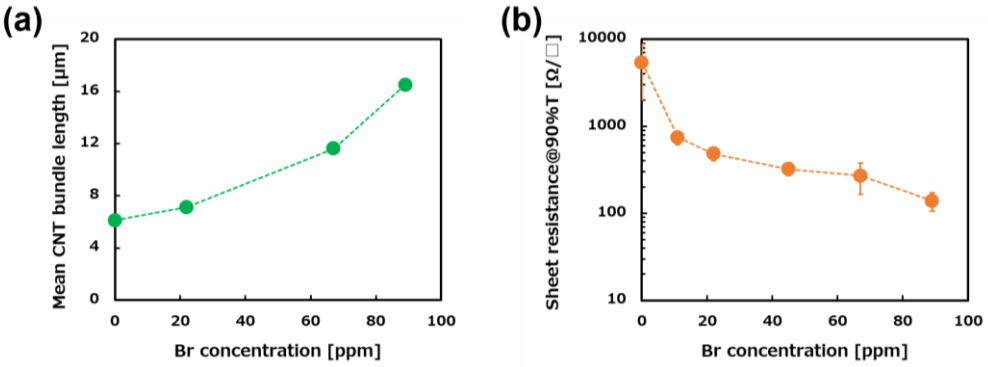

Figure 1. Relationship between Br concentration and (a) mean CNT bundle length, (b) sheet resistance.

References

[1] D. E. Tsentalovich *et al.*, *ACS Appl. Mater. Interfaces* **9** (41), 36189–36198 (2017).
[2] K. Hata *et al.*, *Science* **306** (5700), 1362–1364 (2004).
[3] T. Kinoshita *et al.*, *Carbon* **196**, 391-400 (2022).
[4] Z. Hu *et al.*, *J. Am. Chem. Soc.*, **146** (16), 11432–11439 (2024).
[5] H. Sugime *et al.*, *ACS Nano* **13** (11), 13208–13216 (2019).

Glaphene: a hybridization of 2D silica glass and graphene

Sathvik Ajay Iyengar[1], Manoj Tripathi[2], Anchal Srivastava[1, 3], Abhijit Biswas[1], Tia Gray[1], Mauricio Terrones[4], Alan B. Dalton[2], Marcos A. Pimenta[5, 6], Robert Vajtai[1], Vincent Meunier[7]*, Pulickel M. Ajayan[1]*

[1]Department of Materials Science and NanoEngineering, Rice University(USA); [2]Department of Physics and Astronomy, School of Mathematical and Physical Sciences, University of Sussex(UK); [3]Department of Physics, Banaras Hindu University (India); [4]Department of Physics, Department of Chemistry, Department of Materials Science and Engineering and Center for 2-Dimensional and Layered Materials, The Pennsylvania State University (USA); [5]Departamento de Física, Universidade Federal de Minas Gerais (Brazil); [6]Centro de Tecnologia em Nanomateriais e Grafeno (CTNano), Universidade Federal de Minas Gerais (Brazil); [7]Department of Engineering Science and Mechanics, Department of Physics, and Department of Materials Science and Engineering Pennsylvania State University (USA)

2D materials provide ideal platforms for breakthroughs in both fundamental science and practical, real-world applications. Although a vast array of 2D materials exists, efforts to combine them have been limited primarily to homo/hetero-structural stacking and Janus structures. In this presentation, we introduce 'glaphene'—a hybridization of two fundamentally different materials: 2D silica glass and graphene. [1] We propose a metastable hybrid structure based on first-principles calculations, synthesize the structure via scalable liquid precursor-based vapor-phase growth, and chemically validate the interlayer structure and hybridization through extensive optical and electron spectroscopy, mass spectrometry, and atomic-resolution electron microscopy. We demonstrate a material system that exhibits a strong electronic proximity effect and show, through probe microscopy, that a specific electronic cloud redistribution at the interface (beyond conventional van der Waals interactions) leads to interlayer hybridization. Furthermore, we theoretically and experimentally reconstruct the energy level diagram for glaphene, showing that the combination of semi-metallic graphene (E_g ~ 0 eV) and insulating 2D silica glass ($E_{g,\,exp}$ ~ 8.2 eV, $E_{g,\,th}$ ~ 7 eV) results in a semiconducting ‘glaphene’ ($E_{g,\,exp}$ ~ 3.6 eV, $E_{g,\,th}$ ~ 4 eV) formed through out-of-plane p_z hybridization. This work paves the way for scalable, bottom-up methodologies to bring interlayer hybridization and its emergent properties to the 2D materials toolbox.

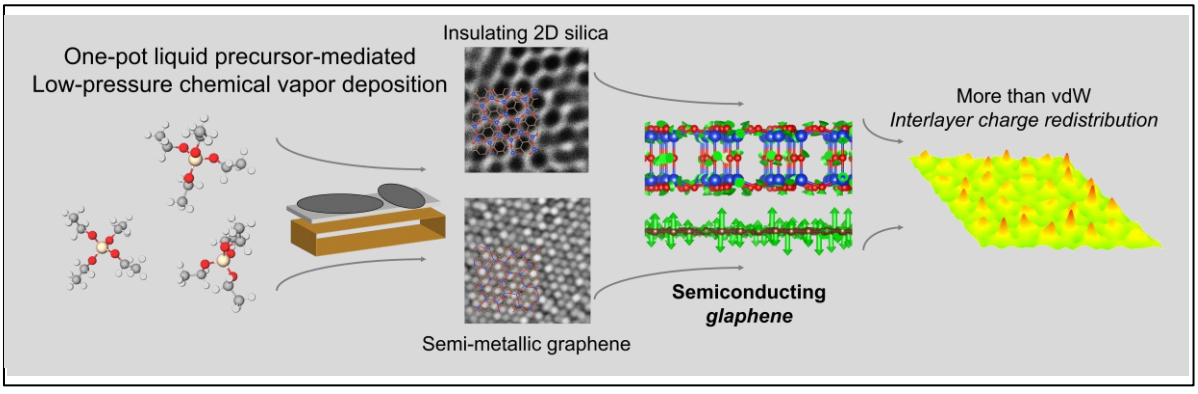

References

[1] Sathvik Ajay Iyengar et al, manuscript under review (2025)

Controlled Growth of Horizontally Aligned Single-Walled Carbon Nanotube Arrays

Liu Qian*, Ying Xie, Yue Li, Mingzhi Zou, Jin Zhang*

School of Materials Science and Engineering, Peking University (China)

Single-walled carbon nanotubes (SWNTs) are ideal for constructing field-effect transistors and logic circuits due to their exceptional mobility, current-carrying capacity, and operational stability. To achieve high device performance, however, horizontal carbon nanotube arrays must simultaneously demonstrate both high density and semiconducting purity. While significant progress has been made in controlling the density and structure of SWNT arrays, current materials remain far from practical industrial implementation. This report presents a comprehensive CVD synthesis framework for SWNT horizontal arrays, spanning precise structural control, large-area high-density preparation, and AI-assisted workflow integration.

By implementing ion implantation and vertical spray CVD systems, we developed a "nano-seeding" catalysts method to achieve direct preparation of wafer-scale uniform high-density SWNT horizontal arrays (up to 140 tubes/μm), complemented by polarized optical characterization techniques for large-area quality assessment.[1] Building on the floating solid catalyst method,[2] our spatially confined growth strategy enhanced titanium-based catalyst deposition efficiency to achieve semiconducting-enriched SWNT growth.[3] Leveraging intrinsic differences in energy band structures between semiconducting and metallic nanotubes, we developed AI-optimized photocatalyst designs for selective semiconducting SWNT synthesis. Simultaneously, plasma-enhanced CVD systems were adapted with electric-field-assisted growth methods to further enhance semiconducting purity. Besides, we also developed an AI-driven platform that integrates transformer-based language models tailored for carbon materials, robotic CVD, and data-driven machine learning models, empowering accelerating the research of CNT array synthesis.[4] Through this platform, we realized the innovation of a bi-metal catalyst, TiPt, for growth of high-density SWNT arrays, and the growth of arrays with desired density. From fine structure tuning to AI assisted new paradigm, we provide new ideas for the preparation of high-density, structure-specific SWNTs, aiming to realize the direct preparation of wafer-scale, high-density, structurally controllable horizontal arrays of SWNTs, and to promote the advancement of the carbon-based chip industry.

References

[1] Y. Xie, Y. Li, Z. Peng, L. Qian*, Z. Zhao*, J. Zhang* *et al.*, *Nat. Commun.* 2025, **16**, 149.
[2] L. Qian, J. Zhang* *et al.*, *Angew. Chem. Int. Ed*. 2020, **59**, 100884.
[3] L. Qian, J. Zhang* *et al.*, *Adv. Funct. Mater*. 2022, **32**, 2106643.
[4] Y. Li, S. Wang, L. Qian*, Z. Zhao*, J. Zhang* *et al.*, *Matter* 2025, **8**, 101913.

Preparation of semiconducting single-wall carbon nanotube arrays with a narrow band-gap distribution

Jia-Yang Zhang[1,2], Lingtong Ding[3], Chen Xie[3], Lili Zhang*[1], Meng-Ke Zou[1,2], Xiao Wang*[3], Chang Liu*[1]

[1]*Shenyang National Laboratory for Materials Science, Institute of Metal Research, Chinese Academy of Sciences (IMR), Shenyang 110016, P.R. (China),* [2]*School of Materials Science and Engineering, University of Science and Technology of China, Hefei 230026, P.R. (China),* [3]*Institute of Technology for Carbon Neutrality, Shenzhen Institute of Advanced Technology, Chinese Academy of Sciences, Shenzhen, 518055, Guangdong, (China).*

Horizontal semiconducting single-wall carbon nanotubes (s-SWCNTs) arrays have emerged as a promising candidate for next-generation integrated circuits, owing to their exceptional carrier mobility and unique one-dimensional quantum confinement characteristics. However, the synthesis of horizontal s-SWCNT arrays with a narrow band-gap distribution remains a big challenge, primarily due to the difficulties in precisely controlling the size of catalyst nanoparticles (NPs) and the small energy difference between SWCNTs with different chiralities. Herein, we developed a dual stage, i.e. during and post growth, strategy to control the structure of SWCNTs. Initially, a modulator-induced reactive metal-support interaction (RMSI) is engineered to prepare uniform ultrasmall catalytic NPs, enabling the growth of horizontal SWCNT arrays with a narrow diameter distribution.[1] Subsequently, we implemented a selective etching strategy involving pre-hydrogenation followed by oxidative etching, which significantly amplified the energy difference between metallic (m-) and semiconducting SWCNTs of similar diameters confirmed by density functional theory calculations, leading to efficient removal of m-SWCNTs.[2] *Quasi-in-situ* Raman spectroscopy further demonstrated that the selective etching mechanism originates from the structure-dependent hydrogenation of SWCNTs. Through this strategy, we obtained horizontal s-SWCNT arrays with a content up to 99.0 %, and the band-gap difference is less than 0.06 eV.

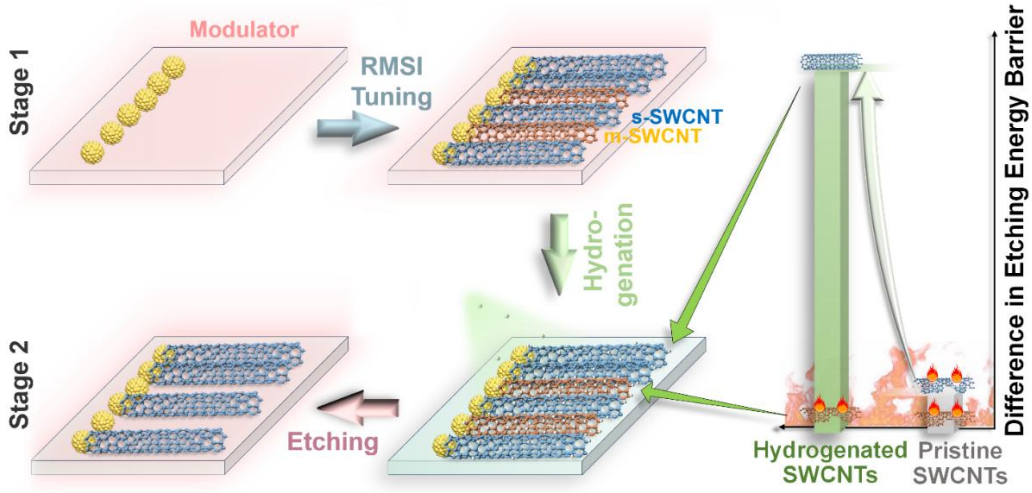

References

[1] Jia-Yang Zhang *et al.*, *In preparation.*
[2] Jia-Yang Zhang *et al.*, *J. Mater. Sci. Technol.* Accepted (2025).

Engineering Luminescent Defects in Polymer-Wrapped SWCNTs using Benzoyl Peroxide Chemistry

A. Dzienia [1], P. Taborowska [1], P. Kubica-Cypek [1], D. Janas [1]

[1] *Silesian University of Technology (Poland)*

Semiconducting single-walled carbon nanotubes (SWCNTs) are promising materials for optoelectronics and photonics due to their unique structure-dependent properties. Moreover, the material's performance can be further enhanced by using covalent modification. However, the practical application of functionalized monochiral SWCNTs is limited by challenges in scalable and efficient processing, often requiring complex system composition and unstable reagents like diazonium salts [1, 2].

Recently, in this context, benzoyl peroxide (BPO), has emerged as an appealing reactant, which can easily introduce luminescent defects into SWCNTs to modify their optical properties [3]. While BPO functionalization has shown significant potential, the underlying radical chemistry remains poorly understood, and the knowledge about the applicability of BPO derivatives for controlled defect engineering is lacking. Therefore, a systematic investigation into the radical chemistry of BPO and its derivatives in terms of their impact on polymer-wrapped SWCNT functionalization in non-polar solvents is crucial for achieving precise control over the formation of luminescent defects [4].

Here, we show that by systematically varying the substituents in a library of self-synthesized BPO derivatives, we achieved a high degree of control over the radical covalent functionalization of (6,5) and (7,5)-SWCNTs, enabling precise tuning of their photoluminescent emission [5]. We demonstrate that electronic and steric properties of substituents on BPO derivatives profoundly influence functionalization efficiency, with electron-withdrawing groups enhancing reactivity and enabling a tunable range of defect densities. Furthermore, we established a correlation between the substituents' Hammett constant and the emission wavelength from the luminescent defects, providing a predictive framework for the rational design of SWCNTs with tailored optical properties, potentially extending into the telecommunication window.

This systematic approach and the developed library of BPO derivatives provide a powerful toolbox for the controlled engineering of luminescent defects in SWCNTs dispersed by polymers in organic solvents, paving the way for their application in advanced optoelectronic devices, such as sensors and single-photon emitters. Our method achieves this control using facile radical chemistry preceded by simple organic chemistry without demanding purification steps, enhancing its practical scalability.

The authors thank for the support National Science Centre, Poland (under the SONATA program, Grant agreement UMO-2020/39/D/ST5/00285) and Metropolis GZM, Poland (under Metropolitan Science Support Fund, Grant agreement No. RW/61/2025).

References

[1] D. Janas, *Mater. Horiz.*, **7**, 2860-2881 (2020)
[2] F. Berger *et al.*, *ACS Nano*, **13**, 8, 9259–9269 (2019)
[3] L. Przypis *et al. Sci. Rep.*, **10**, 19877 (2020)
[4] P. Taborowska *et al. Chem. Sci.*, **16**, 1374-1389 (2025)
[5] A. Dzienia, P. Taborowska, P. Kubica-Cypek, D. Janas, Tailoring optical properties of single-walled carbon nanotubes with benzoyl peroxide derivatives, unpublished manuscript (2025)

Unleashing Ultra-Efficient Heat Transfer: The Magic of Graphene-Skinned Powders Synthesized by FB-CVD in Nanoelectronic Thermal Management

Y.Z. Wu[1,2], Y.Q. Song[2], Z.F. Liu[1,2]

[1]College of Chemistry and Molecular Engineering, Peking University, Beijing (P.R.China), [2] Beijing Graphene Institute (BGI), Beijing 100095 (P.R.China)

The demand for future-oriented high-performance chips, driven by the ongoing digitalization and intelligence advancements in the information society, is rapidly increasing. Nevertheless, this trend is accompanied by escalating power consumption, underscoring the critical importance of efficient heat dissipation for the sustainable advancement of the electronics industry. Graphene and its composites, characterized by their exceptionally high thermal conductivity, hold a distinctive position in this domain. The controlled synthesis of high-quality multilayer graphene composites, however, remains a significant challenge that hinders the full utilization of graphene's exceptional thermal conductivity. In this report, we will introduce an innovative composite structure featuring graphene as a conformal skin for ceramic (Al_2O_3, AlN, Diamond) powders, leading to graphene-skinned powders that exhibit markedly improved thermal conductivity and performance. This material is synthesized via the fluidized bed-chemical vapor deposition (FB-CVD) process, resulting in a continuous graphene skin consisting of multiple highly crystalline layers that are directly grown on the surface of the ceramic powder, forming an impeccable continuous and uniform structure.[1,2] The exceptional thermal conductivity of graphene on both the surface and interlayer, combined with the strong phonon coupling between graphene and ceramic powder, ensures efficient heat transfer at the interface. The heat flow within the graphene skin surpasses that within the ceramic powders by more than an order of magnitude, establishing a comprehensive heat transfer network in the composite system. Our findings provide a facile and scalable strategy for the synthesis of high-crystallinity, multilayer graphene-skinned composite for the applications in thermal management of nanoelectronics.

References

[1] Qi, Y., Sun, L.Z., Liu, Z.F. *ACS Nano* **18**, 4617-4623 (2024).
[2] Qi, Y., Sun, L.Z., Liu, Z.F. *Acta Phys. -Chim. Sin.* **39**, 2307028 (2009).

Controlled Growth of Graphene-skinned Al_2O_3 Powders by Fluidized Bed-Chemical Vapor Deposition for Heat Dissipation

Y.Z. Wu[1,2], Y.Q. Song[2], Z.F. Liu[1,2]

[1]College of Chemistry and Molecular Engineering, Peking University, Beijing (P.R.China), [2] Beijing Graphene Institute (BGI), Beijing 100095 (P.R.China)

The rapid development of digitalization and intelligent technologies has increased the demand for high-performance chips, yet their rising power consumption requires efficient thermal management solutions. Graphene-based composites, known for their ultrahigh thermal conductivity, are promising candidates for such applications. However, synthesizing high-quality multilayer graphene composites with controlled structures remains a critical challenge, limiting their practical deployment. This study proposes an innovative graphene-skinned alumina (Al_2O_3) composite fabricated via fluidized bed-chemical vapor deposition (FB-CVD). The composite features a continuous, uniform, and highly crystalline graphene layer in conformal contact with Al_2O_3 powders. This architecture capitalizes on graphene's exceptional in-plane and interlayer thermal transport properties to significantly enhance thermal conductivity. Experimental results reveal that heat flow within the graphene skin exceeds that in the Al_2O_3 matrix by over an order of magnitude, forming an interconnected thermal conduction network. Thermal interface materials (TIMs) incorporating this composite achieve a thermal conductivity of 6.44 $W \cdot m^{-1} \cdot K^{-1}$. In practical LED thermal management tests, the composite reduces device surface temperature by 17.7°C, demonstrating superior heat dissipation performance. This synthesis strategy is not only straightforward but also scalable, offering a promising new material solution for the thermal management of nanoelectronic devices, opening up new possibilities for addressing heat-related issues in the development of high-performance chips.

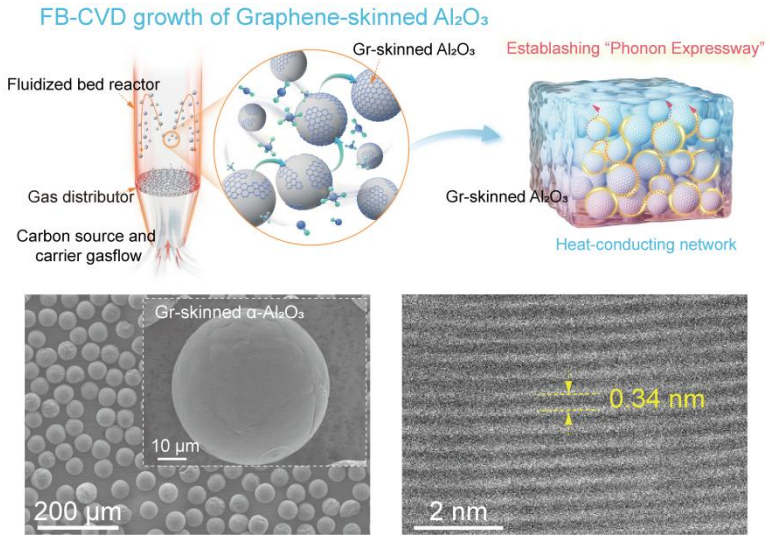

Figure caption: Schematic illustration for the preparation process of Gr-skinned Al_2O_3 powder based TIM. SEM image of the Gr-skinned Al_2O_3 powders. Cross-sectional high-magnification STEM image of continuous graphene skin.

References

[1] Qi, Y., Sun, L.Z., Liu, Z.F. *ACS Nano* **18**, 4617-4623 (2024).

[2] Qi, Y., Sun, L.Z., Liu, Z.F. *Acta Phys. -Chim. Sin.* **39**, 2307028 (2009).

Sorting and brightening of single-walled carbon nanotubes using organic derivatives of hydrazine

Dominik Just[1*], Ryszard Siedlecki[1], Błażej Podleśny [1], Dawid Janas[1*]
1 Department of Chemistry, Silesian University of Technology, B. Krzywoustego 4, 44–100, Gliwice, Poland
**Corresponding authors: dominik.just@polsl.pl, dawid.janas@polsl.pl*

Single-walled carbon nanotubes [SWCNTs] exhibit exceptional electronic and optical properties, making them highly promising for applications in optoelectronics, sensing, and biomedical imaging [1]. However, synthesis of SWCNTs yields heterogeneous mixtures of different chiral species, significantly limiting their practical deployment. Conjugated polymer extraction [CPE] has emerged as one of the leading techniques for sorting SWCNTs with high selectivity, but this method is typically constrained by low extraction yields [2,3]. We recently demonstrated that incorporating molecular enhancers, such as poly(9,9'-dioctylfluorenyl-2,7-diyl-alt-2,5-thiophene) oligomers or 2,5-dibromothiophene, into the extraction systems significantly improves the efficiency of SWCNT isolation without compromising purity [4]. Beyond selectivity and yield, another critical limitation of SWCNTs is their inherently low photoluminescence quantum yield [PLQY] [1], which restricts their application potential [5]. To address both of these problems, herein, we propose the use of organic derivatives of hydrazine. According to this contribution, such compounds can not only promote high-yield SWCNT extraction but also enable introduction of luminescent defects into SWCNTs in both organic and aqueous environments [6] to improve the PLQY of the material. The versatile nature of the reported approach and its rapid nature make it particularly attractive for making the SWCNTs more suitable for photonics.

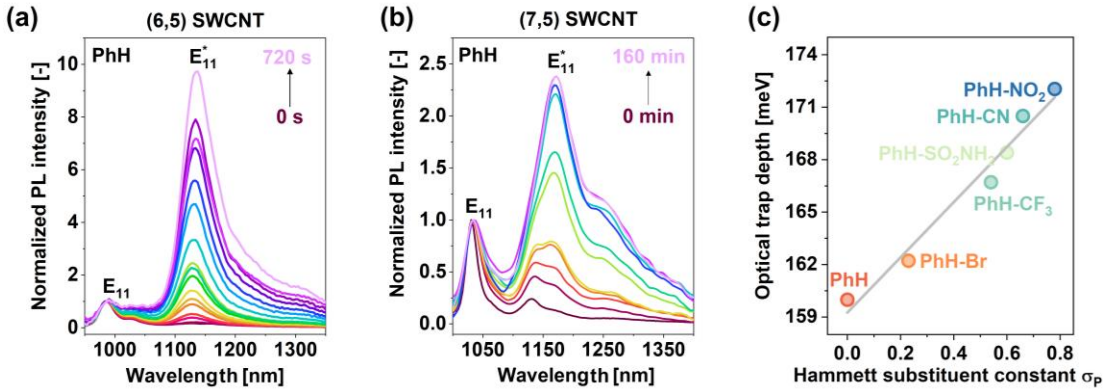

Figure Normalized PL intensity from (a) (6,5) and (b) (7,5) SWCNTs functionalized in water with PhH at the concentration of 0.1125 µg/mL over various treatment times, (c) correlation of the recorded optical trap depth with respect to the Hammet substituent constants of the respective functional groups attached.

References

[1] Janas, D. Perfectly Imperfect: A Review of Chemical Tools for Exciton Engineering in Single-Walled Carbon Nanotubes. *Mater. Horiz.* **2020**, *7* (11), 2860–2881. https://doi.org/10.1039/D0MH00845A.

[2] Dzienia, A.; Just, D.; Taborowska, P.; Mielanczyk, A.; Milowska, K. Z.; Yorozuya, S.; Naka, S.; Shiraki, T.; Janas, D. Mixed-Solvent Engineering as a Way around the Trade-Off between Yield and Purity of (7,3) Single-Walled Carbon Nanotubes Obtained Using Conjugated Polymer Extraction. *Small* **2023**, *19* (46). https://doi.org/10.1002/smll.202304211.

[3] Dzienia, A.; Just, D.; Wasiak, T.; Milowska, K. Z.; Mielańczyk, A.; Labedzki, N.; Kruss, S.; Janas, D. Size Matters in Conjugated Polymer Chirality-Selective SWCNT Extraction. *Advanced Science* **2024**, *11* (29). https://doi.org/10.1002/advs.202402176.

[4] Just, D.; Dzienia, A.; Milowska, K. Z.; Mielańczyk, A.; Janas, D. High-Yield and Chirality-Selective Isolation of Single-Walled Carbon Nanotubes Using Conjugated Polymers and Small Molecular Chaperones. *Mater Horiz* **2024**, *11* (3), 758--767. https://doi.org/10.1039/D3MH01687K.

[5] Brozena, A. H.; Kim, M.; Powell, L. R.; Wang, Y. Controlling the Optical Properties of Carbon Nanotubes with Organic Colour-Centre Quantum Defects. *Nat Rev Chem* **2019**, *3* (6), 375–392. https://doi.org/10.1038/s41570-019-0103-5.

[6] Just, D.; Siedlecki, R.; Podleśny, B.; Janas, D. Synchronous Sorting and Functionalization of Single-Walled Carbon Nanotubes Using Organic Derivatives of Hydrazine. *Adv Opt Mater* (under review).

Single-walled carbon nanotube growth by CVD with high-entropy alloy catalysts composed of platinum-group elements

T. Maruyama[1,2], S. Matsuoka[1], K. P Sharma[2], T. Saida[1,2], K. Kusada[3,4], H. Kitagawa[3]

[1]*Department of Applied Chemistry, Meijo University (Nagoya, Japan),*
[2]*Nanomaterial Research Center, Meijo University (Nagoya, Japan)*
[3]*Division of Chemistry, Graduate School of Science, Kyoto University (Kyoto, Japan)*
[4]*Tha Hakubi Center for Advanced Research, Kyoto University (Kyoto, Japan)*

Synthesis of SWCNTs with unique chirality has been anticipated to realize the application in the electronics field. However, SWCNTs grown with monometal catalyst particles generally show wide chirality distributions because of the Ostwald ripening of catalyst particles. In last decades, single-phase solid solution alloys have attracted attention as catalysts for SWCNT synthesis because of their robustness during the SWCNT growth. By using W-Co alloy, high-purity (12, 6) SWCNTs has been obtained [1].

Recently, high-entropy alloys (HEAs) that are single-phase solid solutions containing five or more metals in almost equal proportions have attracted tremendous attention in various fields because of their specific properties such as high hardness and strength [2-4]. In addition, the HEA nanoparticles (NPs) act as catalysts with high activities in many chemical reactions such as NH_3 oxidation, oxygen reduction, and ethanol oxidation [5-7].

In this study, we focused on HEA NPs as catalysts for SWCNT growth. Using HEA NPs composed of five platinum-group metals (5PGM; Ru, Rh, Pd, Ir, and Pt) as catalysts, we succeeded in growth of SWCNTs via chemical vapor deposition (CVD) with C_2H_2 feedstock. After CVD growth at 750 °C for 10 min, high-density SWCNTs with lengths of 1 μm or more were grown (Fig. 1). Transmission electron microscopy (TEM) and Raman results showed that their diameters were less than 1.0 nm. The SWCNT yield with 5PGM HEA NP catalysts were much higher than those with monometal PGM catalysts (Ru, Pd, Ir, and Pt). Scanning transmission electron microscopy (STEM) and energy-dispersive X-ray spectroscopy (STEM-EDS) showed that, even after SWCNT growth, each element was homogeneously distributed in the 5PGM HEA NPs and that their crystal structure was preserved. Our results demonstrated that the 5PGM HEA NPs act as highly active catalysts and their robustness would be useful to grow SWCNTs with unique chirality.

Part of this work was conducted at the Institute of Molecular Science (IMS), supported by ARIM. XAFS analysis was performed at Aichi SR in Japan.

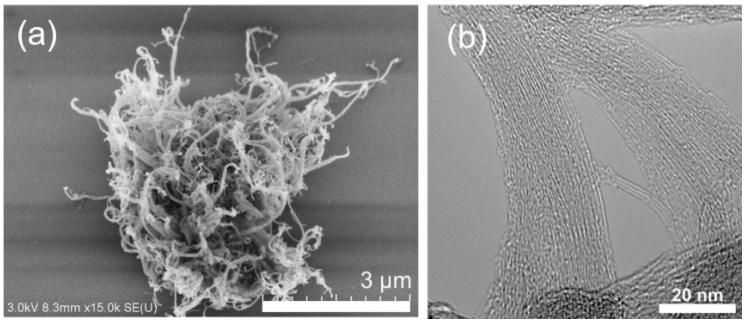

Figure 1: (a) SEM and (b)TEM images of SWCNTs grown at 750°C from 5PGM HEA NPs.

References (if desired)

[1] F. Yang *et al., Nature* **510**, 522 (2014).
[2] K. Kusada, D. We and H. Kitagawa, *Chem. Eur. J.* **26**, 5105 (2020).
[3] K. Kusada, H. Kitagawa *et al.*, *J. Phys. Chem. C* **125**, 458 (2021).
[4] D. Wu, K. Kusada, H. Kitagawa *et al., J. Am. Chem. Soc.* **144**, 3365 (2022).
[5] D. Wu, K. Kusada, H. Kitagawa *et al., J. Am. Chem. Soc.* **142**, 13833 (2020).
[6] Y. Yao *et al. Science* **359**, 1489 (2018).
[7] T. Löffler *et al. Energy Mater.* **8**, 1802259 (2018).

MOLECULE SUPER-TRANSPORT THROUGH MACROSCOPIC LENGTH OF INDIVIDUAL CARBON NANOTUBE

Jingwei Wu[1], Fei Wei[1]

[1]*Tsinghua University (China)*

The flow and transport in nanoscale channel pose challenges to the classic models. Herein, we establish a mass spectroscopy system to research the molecule transport in single ultra-long carbon nanotube. The measured water flow exceeds the values calculated from Poiseuille flow by more than six orders of magnitude. The measured gas flow exceeds predictions of Knudsen diffusion by more than an order magnitude. This surprising result highlights that the phenomenon of molecule super-transport is still efficient at the macroscopic length scales, reflecting a frictionless fluid-carbon interface. Besides, the molecular flow rate per nanotube remains constant with increasing length of carbon nanotube, which suggests ballistic molecule transport through the one-dimensional channel. Illustrated by the residence time distribution (RTD) profile, both gas and water molecule diffuse in carbon nanotube without any back mixing, indicating observation of single-file diffusion in carbon nanotube. Our report, for the first time, demonstrates molecule simultaneous single-file diffusion and ballistic transport in individual carbon nanotube. This work provides new insights into the super-transport of macroscopic length and demonstrates the possibility of a low energy-consumed process.

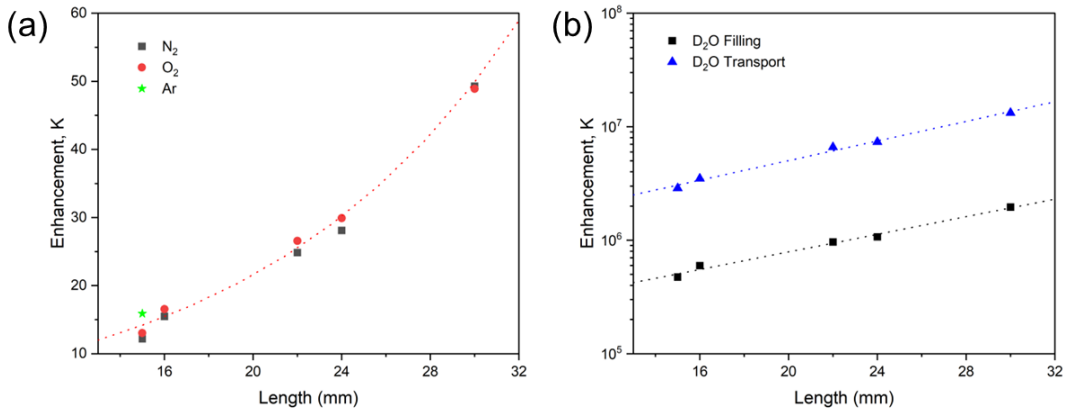

Enhanced molecule flow through single ultra-long carbon nanotube: Enhancement factor observed for different lengths of carbon nanotube for gas (a) and water (b).

BSTCIM: A Balanced Symmetry Ternary Fully Digital In-MRAM Computing Macro for Energy Efficiency Neural Network

Zhongzhen Tong[1,2], Chenghang Li[1,2], Chao Wang[1,2], Daming Zhou[2], Xiaoyang Lin[1,2], *Senior Member, IEEE*

[1]*National Key Lab of Spintronics, International Innovation Institute, Beihang University, Hangzhou, 311115, China and*
[2]*MIIT Key Laboratory of Spintronics, School of Integrated Circuit Science and Engineering, Fert Beijing Institute, Beihang University, Beijing 100191, China*

Silicon-based traditional binary computing in-memory (TBCIM) architectures are approaching their energy efficiency and throughput limits owing to challenges facing Moore's Law. Thus, it is essential to explore architecture based on novel devices and computing paradigms to fulfill data-centric applications, such as artificial intelligence. In this paper, we propose a balanced symmetry ternary (BST) fully digital in-MRAM computing macro (BSTCIM) using hybrid voltage-gated spin-orbit torque magnetic tunnel junctions (VGSOT-MTJ) and gate-all-around carbon nanotube field-effect-transistors (GAA-CNTFET) technology, as shown in **Figure 1**. The overall computing is based on the highest efficiency multi-bit ternary system. BSTCIM includes a ternary dot product (TDP) unit with 4 GAA-CNTFETs and 2 VGSOT-MTJs achieving TDP operation without complex logic circuits. The multi-bit ternary multiply-and-accumulate (MAC) operation is realized through the proposed ternary adder tree and ternary post adder which accumulate TDP results within the digital domain enabling high accuracy neural network inference. Furthermore, due to the advantages of BST, ternary signed MAC is more easily performed compared to TBCIM macros that adapt 2's complement or separate signed bit calculations. BSTCIM with 288 kb is simulated, achieving throughput and energy efficiency of 0.72 TOPS and 54.5 TOPS/W, respectively, at a 0.6 V supply voltage and 1.15 TOPS and 33.7 TOPS/W, respectively at a 0.8 V supply voltage with 8b-IN, 8b-W, and 20b-OUT. Moreover, the figure-of-merit for BSTCIM is 1.13–33.6 times higher than that of existing CIM macros.

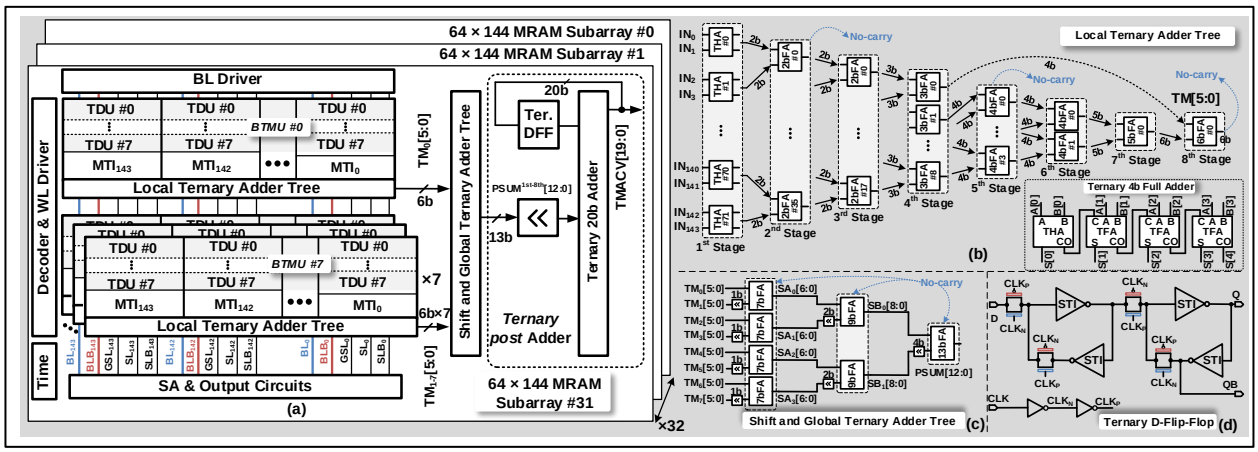

Figure 1: Overall structure of the balanced symmetry ternary fully digital in-MRAM computing macro.

References

[1] G. Zhao et al., *IEEE Transactions on Emerging Topics in Computing* 12. 826-839 (2024).
[2] K. Zhang et al., *IEEE Access* **8**, 50792-50800 (2020).
[3] F. Razi et al., *IEEE Transactions on Nanotechnology* **18**, 598-605 (2019).
[4] N. Yang et al., *IEEE Transactions on Electron Devices* **68**, 1975-1979 (2021).
[5] C. S. Lee et al., *IEEE Transactions on Electron Devices* **62**, 3061-3069 (2015).
[6] M. T. Nasab et al., *IEEE Transactions on Emerging Topics in Computing* **11**, 527-533 (2023).

Monolithic 3D integration of CNTFET and SOT-MTJ for high-performance non-volatility memories

Ke Zhang[1,#], Ningfei Gao[2,#], Daming Zhou[1,#], Zhongzhen Tong[1,#], Hongxi Liu[3], Xiaoyang Lin[1,*], Haitao Xu[2,4,*], Lianmao Peng[2], Weisheng Zhao[1,*]

[1]Fert Beijing Institute, School of Integrated Circuit Science and Engineering, Beihang University (Beijing, China), [2]Key Laboratory for the Physics and Chemistry of Nanodevices, Center for Carbon-based Electronics, School of Electronics, Peking University (Beijing, China), [3]Truth Memory Technology Corporation Limited (Beijing, China), [4]Institute of Carbon-based Thin Film Electronics, Peking University (Taiyuan, Shanxi, China).

The integration of monolithic three-dimensional (M3D) architecture is widely recognized as a promising approach in the post-Moore's era for addressing the storage capacity challenge [1-5]. This emerging technology enables direct connectivity between different units through extensive interlayer vias, facilitating high-bandwidth data transfer, low-latency data processing, and energy-efficient storage. However, integrating Si CMOS into M3D structure is generally considered challenging due to thermal budget constraints. Here, we demonstrate the M3D integration of carbon nanotube field-effect transistor (CNTFET, logic layer), and spin-orbit-torque magnetic tunnel junction (SOT-MTJ, memory layer), namely M3D-CM, as a potential solution to large-capacity, high-density, and radiation-hardened magnetic random access memory (MRAM). Using randomly oriented CNTs, an ultra-high current density of over 80 μA/μm was achieved for the CNTFET with a channel length of 3 μm. The SOT-MTJ can be effectively driven by the high performance CNTFET, enabling the M3D-CM to feature non-volatility (>10 years), fast write speed (10 ns), excellent endurance (1×10^{12} cycles), and reliable operation at 130 °C. To validate the M3D integration process of multilayer CNTFETs and SOT-MTJs, M3D-CCM, composed of a single layer of SOT-MTJ and double layers of CNTFETs, was successfully demonstrated. Further simulations indicate that CNTFETs offer substantial benefits for memory operations, reducing power consumption by 47.6% and time delay by 33.3% compared to FinFETs. Our work illustrates the feasibility and immense potential of such M3D architecture in advanced memory technologies.

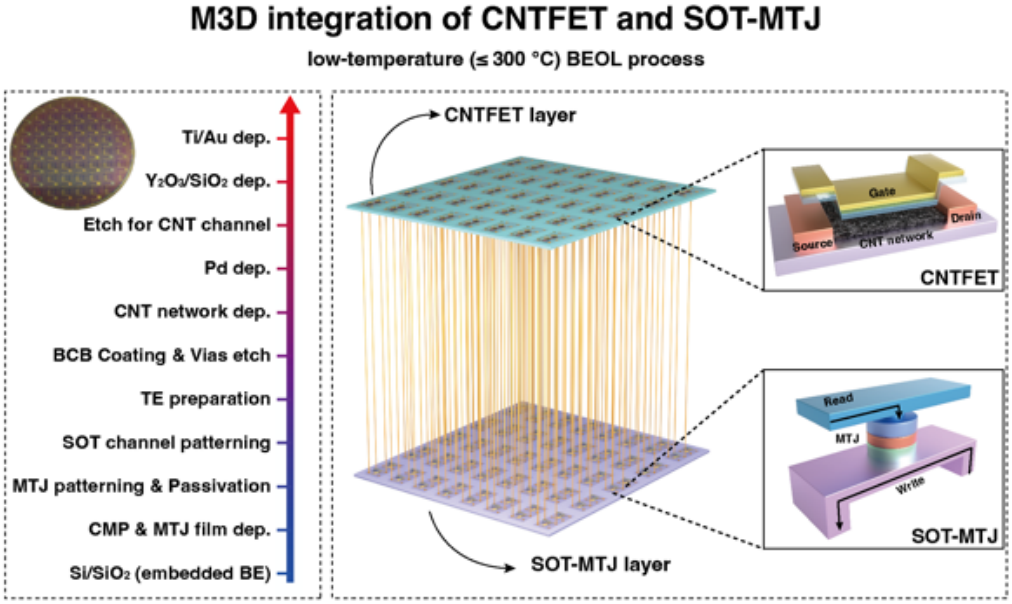

Figure 1: Schematic diagram of M3D integration of CNTFET and SOT-MTJ (M3D-CM).

References

[1] C. Qiu, *et al.*, *Science,* **355**, 271 (2017).
[2] L. Liu, et al., *Science,* **368**, 850 (2020).
[3] M. Zhu, et al., *Nat Electron*, **3**, 622 (2020).
[4] A. Du, et al., *Nat Electron*, **6**, 425 (2023).
[5] M. Wang, et al., *Nat Electron,* **1**, 582 (2018).

Interlayer Stacking Sensitivity of Anisotropic Thermoelectric Transport Properties of $NbSe_2$ Polymorphs based on First-Principles Band Calculations

M.E. Jr. Cleofe, K. Nakamura, T. Habe

Department of Mechanical and Electrical Systems Engineering, Kyoto University of Advanced Science (Japan)

Interlayer stacking provides a robust strategy for tuning the electronic properties of niobium diselenide ($NbSe_2$) by altering its crystal symmetry and van der Waals (vdW) interactions between the atomic layers [1]. Although the stable 2H phase has garnered most attention due to its unique physical properties, several metastable configurations, such as the 3R and hybrid 2H-3R phases remain relatively underexplored. This gap is significant because thermoelectric transport properties, such as Seebeck coefficient (S), electrical conductivity (σ), electronic thermal conductivity (κ_e), and power factor ($S^2\sigma$), are highly sensitive to both crystal symmetry and interlayer coupling [2]. In this study, we systematically investigate the in-plane and out-of-plane thermoelectric transport behaviors of **$2H_a$**, **$2H_c$**, **3R**, and **2H-3R** $NbSe_2$ polymorphs. By combining first-principles calculations with semi-empirical Boltzmann transport theory, we establish a direct correlation between stacking-induced symmetry variations and changes in the electronic structure that impact S, σ, and κ_e. Our results reveal a pronounced anisotropy in transport properties that is strongly influenced by the stacking sequence: while S_x undergoes sign reversal at varying carrier densities without significant amplitude change, S_z maintains its sign but varies in magnitude with different stacking orders. Temperature dependent measurements indicate that with increasing temperature, S_x becomes progressively more negative, while S_z increases in positive magnitude, with S_z exhibiting a significantly larger absolute value than S_x. Fermi velocity (v_F) contour analysis further shows that in-plane transport is dominated by the Γ- and K-centered cylindrical FS features, whereas the out-of-plane transport is governed by the pancake-shaped Fermi pocket at the Γ-point. Finally, v_F projection illustrates clearly that the spatial distribution of high $v_{F\parallel}$ and $v_{F\perp}$ across the FS critically influences directional transport. These findings underscore the potential of stacking-engineered $NbSe_2$ in developing high-efficiency thermoelectric devices and metastable TMD-based functional materials designs.

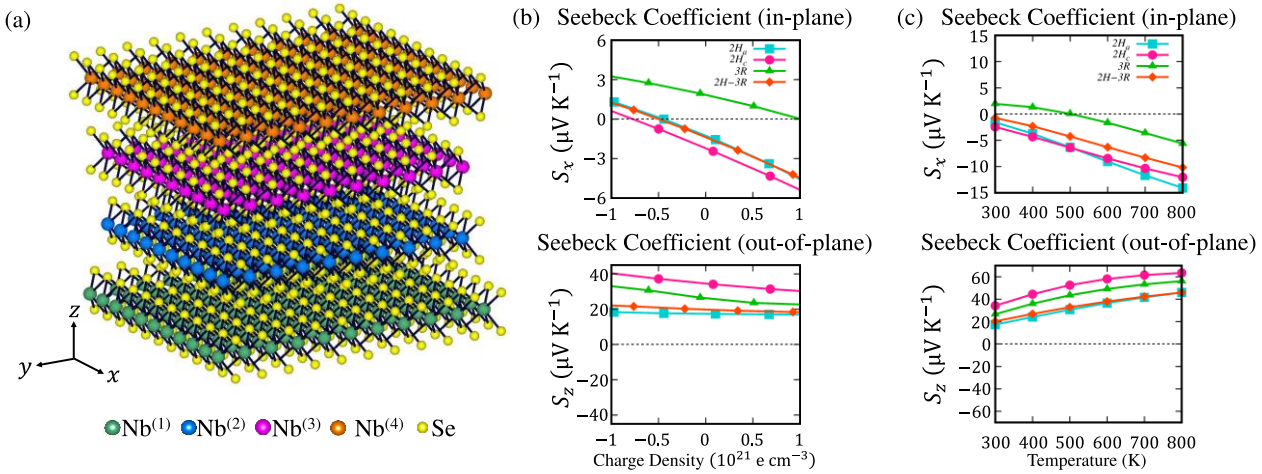

Fig.1: (a) 2H-3R-$NbSe_2$ stacking structure. Seebeck coefficients of various stacking orders of $NbSe_2$ along the in-plane and out-of-plane directions as functions of (b) charge density and (c) and temperature.

References

[1] F. Cossu *et al.*, *Phys. Rev. Research* **6**, 043111 (2024).
[2] F. Mamani Gonzalo *et al.*, *Sci. Rep.* **14**, 26844 (2024).

SOLUTION PROCESSED CARBON NANOTUBE INTEGRATED CIRCUITS FOR MULTI-MODAL EDGE COMPUTING

J. Pei[1], S. Liu[1], Y. Wen[1], L. Song[1], G. Hu[1]*

[1]*The Chinese University of Hong Kong (China),*

Edge computing, employing intelligent hardware for real-time pre-processing data at edge, can effectively accelerate big-data analysis in, for instance, autonomous driving, intelligent display, and internet-of-things. However, the edge computing hardware usually faces complex deployment conditions and limited resources in edge scenarios. Carbon nanotubes, with excellent electrical properties and scalabilities, are proven promising to facilitate versatile high-performance integrated electronics development for design and implementation of edge computing hardware. Here, we develop wafer-scale solution-processed integrated circuits using carbon nanotubes and demonstrate their capability in practical data processing at edge.

As basic bricks of integrated circuits, solution processed capacitors and thin-film transistors are fabricated, with sol-gel deposited silicon dioxide as the gate and capacitor dielectric, and solution sorted semiconducting single-walled carbon nanotube as the channel. The transistors exhibit an ON/OFF switching ratio of over 10^5 within an operating voltage range of $\pm$ 1 V. The transistors can be forged into complementary pairs to enable low power consumption logic operations. Given the scalability and versability of the solution processes, the devices can be fabricated on a large-scale (on a wafer scale) with a high yield (approaching a 100% success rate) on both glass and silicon wafer. Considering the request for multi-modal signal processing in practical edge scenarios, we demonstrate integration of the devices in developing key integrated circuit units, including i) the differential amplifier and current mirror to handle analog signal; ii) logic gates such as NAND, NOR, XOR and NOT to construct full-logic digital circuit; iii) electronic memories such as DRAM and SRAM; and iv) matrix multiplication unit by crossbar array. Integrated with peripheral circuits, the solution processed integrated circuit units are proven effective in performing not only conventional signal processing but also advanced neuromorphic computing in an analog mode, manifesting the potential for developing next-generation intelligent edge hardware.

Multi-functional Data Processing by Solution-processed 2D Material Ferroelectric Junction Devices

S. Liu[1,†], Y. Wen[1,†], J. Pei[1], G. Hu[1,*]

[1]*Department of Electronic Engineering, The Chinese University of Hong Kong (HKSAR, China),* [†]*These authors contributed equally.*

Solution-processed two-dimensional (2D) material electronics show promise in enabling information processing at edge, due to their cost-effective fabrication, capacity of mass production and, essentially, adaptability to versatile substrates beyond silicon [1,2]. In this work, we present scalable, high-yield fabrication of a ferroelectric-semiconductor junction device, based on solution-processed ferroelectric P(VDF-TrFE) and 2D semiconductor molybdenum disulfide (MoS_2), and demonstrate that the junction device can be used to perform multi-functional data processing for edge applications.

Here the P(VDF-TrFE)-MoS_2 junction devices are developed by a layer-by-layer deposition and annealing process, and form a distinct ferroelectric-MoS_2 heterogenous interface. The fabrication yields a 100 % success rate in sampling of over 750 devices. Upon operation of the devices, ferroelectric polarization builds up within P(VDF-TrFE), and leads to an effective Stark modulation of the electrical property of the MoS_2. Particularly, with varying operational voltage, the devices perform reversible transformation from nonlinear junction to memristor. Under the nonlinear junction mode, the devices exhibit repeatable nonlinear current output for over 10^5 voltage sweepings, while the frequency response of the device exceeds 1 MHz, promising for performing high-speed analog signal processing. Under the memristor mode, on the other hand, the devices present robust non-volatile switching for more than 10^5 write-read cycles. In addition, by fine-tuning the writing memory pulse width, the devices show highly linear long-term potentiation and depression process, potentially suitable for advancing in-memory computing hardware.

The results manifest the capability of our P(VDF-TrFE)-MoS_2 junction devices for performing multi-functional data processing, for instance, in both analog and in-memory schemes. To demonstrate this capability, we adopt the devices as physical nonlinear activation functions in facilitating the implementation of a physical reservoir with peripheral circuits. Specifically, integrating our devices with silicon circuits on PCBs, the as-implemented physical reservoir computing accurately reconstruct dynamical systems such as Mackey-Glass and more. Besides, the physical reservoir can embedded as encoder module for an edge-central variational auto-encoder paradigm, enabling sensory data pre-processing at edge.

References

[1] S. Pinilla, *et al.*, *Nat. Rev. Mater.*, **7**, 717-735 (2022).
[2] S. Pazos, *et al.*, *Nat. Rev. Mater.*, **9**, 358-373 (2024).

Temporal Signal Processing by Physical Reservoir Computing Using Solution Processed MoS_2 Charge-Trapping Transistors

Y. Wen[1], S. Liu[1], T. Ma[2], G. Hu*[1]

[1]*The Chinese University of Hong Kong (China),* [2]*Hong Kong Polytechnic University (China)*

Temporal signal processing plays a fundamental role in modern portable electronics, e.g. IoT sensors and electronics, wearables, robotics. The advancements now put a demand on these edge devices to perform complex tasks, such as temporal signal classification and regression. Deploying neural networks at the edge and enabling localized temporal signal processing is an emergent solution. [1] Among the many neural networks, reservoir computing with a lightweight recurrent neural network topology is particularly well-suited for temporal signal processing at the edge. Here we prototype a reservoir edge computing system based on volatile MoS_2 charge-trap transistors, and demonstrate its capability for real-time processing of multi-channel signals.

The fabrication of the MoS_2 charge-trapping transistors starts with scalable electrochemical exfoliation of MoS_2, followed by spin-coating and patterning via photolithography. The transistors exhibit an on-off ratio of ~10^4 and a large memory window of about 8 V with a low turn-on voltage of 4 V. Particularly, the transistors show a short-term memory effect with a time constant of several seconds. The short-term memory is ideal for the delay feedback connections in reservoir computing, while the non-linear transfer features make the transistors suitable for the implementation of non-linear analogue activation. [2] Considering these characteristics, we design a reservoir edge computing system using the MoS_2 charge-trap transistors as the physical reservoir nodes. Besides, an ARM SoC and analog-digital/digital-analog converters are used to accomplish the necessary digital operations. After highly efficient training, the system can achieve not only tracking of dynamic systems, but also classification on non-transformed raw electrocardiogram and multi-channel electromyography signals with accuracies over 80%. The reservoir power consumption is much lower than the typical neural networks running on the centralized computation facilities. Furthermore, using the reservoir edge computing system as a chaotic decoder, we achieve encrypted communication via visible light with a bit rate of tens of bps while no additional synchronization technique is required. Given the remarkable temporal signal processing performance, as well as the simplicity and power efficiency of the reservoir edge computing, we envisage realizing higher data throughput tasks, such as spectrum processing and video processing in human-machine interfaces, autonomous driving, etc.

References

[1] H. Purwins *et al., IEEE J. Sel. Top. Signal Process.* **13**, 206-219 (2019).
[2] G. Tanaka *et al., Neural Networks,* **115**, 100-123 (2019).

Application of aerosol-synthesized single-walled carbon nanotubes for binder-free Nickel-rich positive electrodes via a solvent-free fabrication

A. R. Bogdanova[1], F.A. Obrezkov[1], S. Mousavihashemi[1], E.M. Khabushev[1], T. Kallio[1]

[1]*Aalto University School of Chemical Engineering (Finland)*

Single-walled carbon nanotubes (SWCNTs) are a promising conductive additive for lithium-ion battery (LIB) due to their high electrical conductivity, flexibility, and mechanical robustness [1], improving the electrochemical performance of LIBs. Usually, SWCNTs are incorporated into positive electrodes of LIBs during slurry preparation, where they are dispersed in N-methyl-2-pyrrolidone with electrochemically inactive polymeric binders such as polyvinylidene fluoride [2]. This involves challenging homogenization of the SWCNT solution and energy-intensive solvent recovery/drying, resulting in less efficient electrode manufacturing process, and highlighting the need for solvent-free approaches development. Here, we investigate the fabrication of Ni-rich layered oxide positive electrodes: $LiNi_{0.8}Mn_{0.1}Co_{0.1}O_2$ (NMC811) and $LiNi_{0.6}Mn_{0.2}Co_{0.2}O_2$ (NMC622) by integrating aerosol chemical vapor deposition-synthesized SWCNTs using two distinct solvent-free approaches. In the first method, as-synthesized SWCNTs are directed through a fixed amount of fluidized NMC622 particles under mechanical vibration. In the second approach, in situ gas-phase mixing of synthesized SWCNTs with aerosolized NMC811 material is performed, resulting in a continuous process.

Both methods yield self-standing binder-free electrodes with 99–99.8 wt% of active material, containing only 0.2–1 wt% SWCNTs functioning both as a conductive additive and binder. Electrochemical cycling revealed that the NMC811-SWCNT electrode retains 75% of its initial capacity after 200 cycles at 1C, compared to only 55% for conventional slurry-based electrodes. Similarly, the NMC622-SWCNT electrode demonstrates over 97% capacity retention after 50 cycles compared to reference NMC622 with 95%. Electrochemical impedance spectroscopy confirms that the SWCNT network significantly enhances charge transport, while Raman spectroscopy indicates good structural integrity of the NMC-SWCNT electrodes after cycling. These findings contribute to the development of alternative approaches and the direct integration of CNTs into ready-to-use battery electrodes.

References

[1] S. Mousavihashemi *et al.*, *Adv. Mater. Technol.* **9**, 2301765 (2024).
[2] M. Guo *et al.*, *Advanced Science* **10**, 2207355 (2023).

High-Energy-Density Quasi-Solid-State Lithium-Sulfur Batteries: Reliable Energy Storage Solutions in Extreme Environments

H. Taoum[1], M. Ezzedine[1], C-S. Cojocaru[1]

[1]*Laboratoire de Physique des Interfaces et des Couches Minces (LPICM), CNRS, École Polytechnique, IP Paris, 91128, Palaiseau Cedex, France.*

The increasing demand for high-performance energy storage systems has driven extensive research into next-generation batteries that offer higher energy density, enhanced power output, and durability in extreme environments. As the world shifts toward electrification and advanced mobility, energy storage technologies must evolve to meet the stringent requirements of applications such as defense, deep-sea exploration, aerospace, and industrial surveying. Conventional lithium-ion batteries (LIBs) have dominated the market due to their high efficiency and reliability, but their limited thermal stability (−20 °C to 60 °C), safety concerns, and low energy density necessitate the development of alternative solutions [1]. Among advanced battery concepts, rechargeable lithium- sulfur (Li-S) batteries stand out due to their high theoretical gravimetric energy density, cost-effectiveness, environmental sustainability, efficiency, and reliability. However, despite their advantages, achieving long cycle stability, high power density, and survivability in extreme conditions remains a significant challenge. Harsh operational environments (e.g., radiation Exposure, mechanical Stress…), extreme temperatures, and vacuum conditions impose severe limitations on conventional Li-S batteries, requiring innovative design strategies to enhance their electrochemical stability and performance [2].

This study focuses on the practical development of quasi-all solid-state Li-S cells with an S-based cathode fabricated by vertically aligning tens of trillions of CNTs per cm² on standard aluminum foil, which acts as a current collector, and laminating the dense carpet of CNTs with S (S@VACNTs). The batteries have demonstrated survivability under harsh conditions of -100°C to 150°C and vacuum down to 10^{-3} mbar. Additionally, they demonstrate charge/discharge cycle stability across more than 80% of the survivability range, making them strong candidates for high-reliability energy storage applications. The proposed approach offers a step forward in achieving safe, high-performance, and durable energy storage solutions for the most demanding conditions.

References

[1] S. Ma et al., *Progress in Natural Science: Materials International* **28**, 653 (2018).
[2] W. Qu et al., *Energy & Environmental Materials* **6**, e12444 (2023).

Pt@WS_2 -an Extrinsic 2D Dilute Ferromagnetic Semiconductor Beyond Room Temperature

Yu-Xiang Chen[1,2,3*], Mario Hofmann[4], Ya-Ping Hsieh[1]

[1]*Institute of Atomic and Molecular Sciences, Academia Sinica, Taipei, Taiwan*

[2]*International Graduate Program of Molecular Science and Technology, National Taiwan University, Taipei, Taiwan*

[3]*Molecular Science and Technology Program Taiwan International Graduate Program, Academia Sinica, Taipei, Taiwan*

[4]*Department of Physics, National Taiwan University, Taipei, Taiwan*

Extrinsic dilute magnetic semiconductors achieve magnetic functionality through tailored interaction between a semiconducting matrix and a non-magnetic dopant. The absence of intrinsic magnetic impurities makes this approach promising to investigate the newly emerging field of 2D dilute magnetic semiconductors. Here the first realization of an extrinsic 2D DMS in Pt-doped WS_2 is demonstrated. A bottom-up synthesis approach yields a uniform and highly crystalline monolayer where platinum selectively occupies the tungsten sub-lattice. The orbital overlap between W 4d and Pt 5d results in spin-selective hybrid states that produce a strong valley-Zeeman splitting. Combined experimental and theoretical results show that this interaction yields a sizable ferromagnetic response with a Curie temperature ≈375 K. These results open up a new route toward 2D magnetic properties through tailoring of atomic interactions for future applications in spintronics and magnetic nanoactuation.

Two-Dimensional Electronic Transport and Surface Electron Accumulation in Transition Metal Dichalcogenides

Hemanth Kumar Bangolla and Ruei-San Chen*

Graduate Institute of Applied Science and Technology, Taiwan Tech, Taipei 106335, Taiwan.

**E-mail: rsc@mail.ntust.edu.tw*

Transition metal dichalcogenides (TMDs) have attracted substantial attention due to their facile two-dimensional (2D) structures are of interest for fundamental research and ultrathin electronic device applications. Understanding surface and defect characteristics is key for realistic control and application of layered semiconductors, especially their nanostructures. Generally, Van der Waals crystals are expected to have an inert surface because of the absence of dangling bonds. However, here we show that the surface of high-quality synthesized TMDs such as molybdenum disulfide [1], molybdenum diselenide [2], and rhenium disulfide [3] has a major n-doping source. The surface-dominant 2D transport was observed in TMD nanostructures. The surface electron accumulation (SEA) was found to be generated easily by mechanical exfoliation and room temperature deselenization. The presence of SEA in these materials has been confirmed by angle-resolved photoemission spectroscopy and scanning tunneling spectroscopy. The electron concentration ($\sim 10^{19}$ cm^{-3}) at the surface is over three orders of magnitude higher than that of the bulks. Sulfur and Selenium vacancies which are sensitive to air molecules are suggested to be the major factor resulting in SEA and high conductivity in TMD nanostructures.

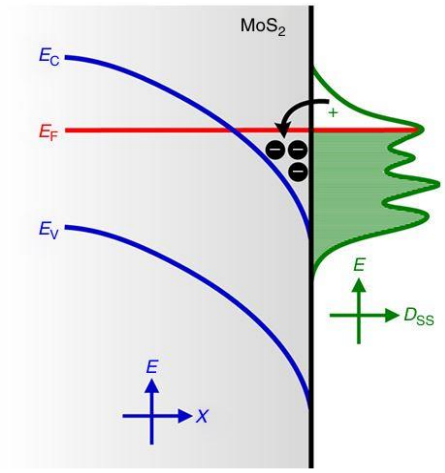

Figure 1: Schematic band bending and electron accumulation at MoS_2 surface [1]. The surface band bending and SEA induced by the presence of donor-like surface states are illustrated.

References:

[1] M. D. Siao *et al.*, *Nat. Commun.* **9**, 1442 (2018).
[2] Y. S. Chang, *Nano Energy*, **84**, 105922 (2021).
[3] H. K. Bangolla, *Nanoscale*, **15**, 19735-19745 (2023).

Efficient Field-free Switching of Perpendicular Magnetization induced by Dominant out-of-plane Torque Generated by $NbIrTe_4$

Wei Yang[1,2,3], Juan-Carlos Rojas-Sánchez[3], Xiaoyang Lin[1,2] and Weisheng Zhao[1,2]
[1]National Key Lab of Spintronics, Hangzhou International Innovation Institute, Beihang University, Yuhang District, Hangzhou, 311115, China,
[2]Fert Beijing Institute, Beihang University, Beijing, 100191, China,
[3]Insititut Jean Lamour, Université de Lorraine, Nancy, 7198, France,

Spin-orbit torque (SOT) has emerged as a promising mechanism for electrically manipulating magnetic states[1–3], which is vital for the development of high-speed, low-power memory technologies. Despite its potential, the traditional spin Hall effect (SHE) primarily produces in-plane spin currents due to symmetry constraints. This limitation necessitates the use of external magnetic fields or complex structures to achieve effective switching of perpendicular magnetization, hindering device efficiency and versatility.

In this study, we explore the unique properties of the Weyl semimetal $NbIrTe_4$, which can generate a significant out-of-plane spin current. This characteristic allows for reliable, field-free switching of perpendicular magnetization with improved efficiency. Through a combination of experimental results and theoretical analysis, we reveal that $NbIrTe_4$ exhibits substantial out-of-plane spin Hall conductance of $\sigma_{sh,z}\approx 9.05\pm1.5\times10^4\ \hbar/2e\cdot(\Omega m)^{-1}$,and $\sigma_{sh,y}\approx 1.78\pm0.08\times10^4\hbar/2e\cdot(\Omega m)^{-1}$. These insights into the spin-orbit coupling mechanisms of $NbIrTe_4$ highlight its potential in advancing scalable, energy-efficient spintronic devices, particularly for applications requiring robust and efficient control of perpendicular magnetization without external magnetic fields.

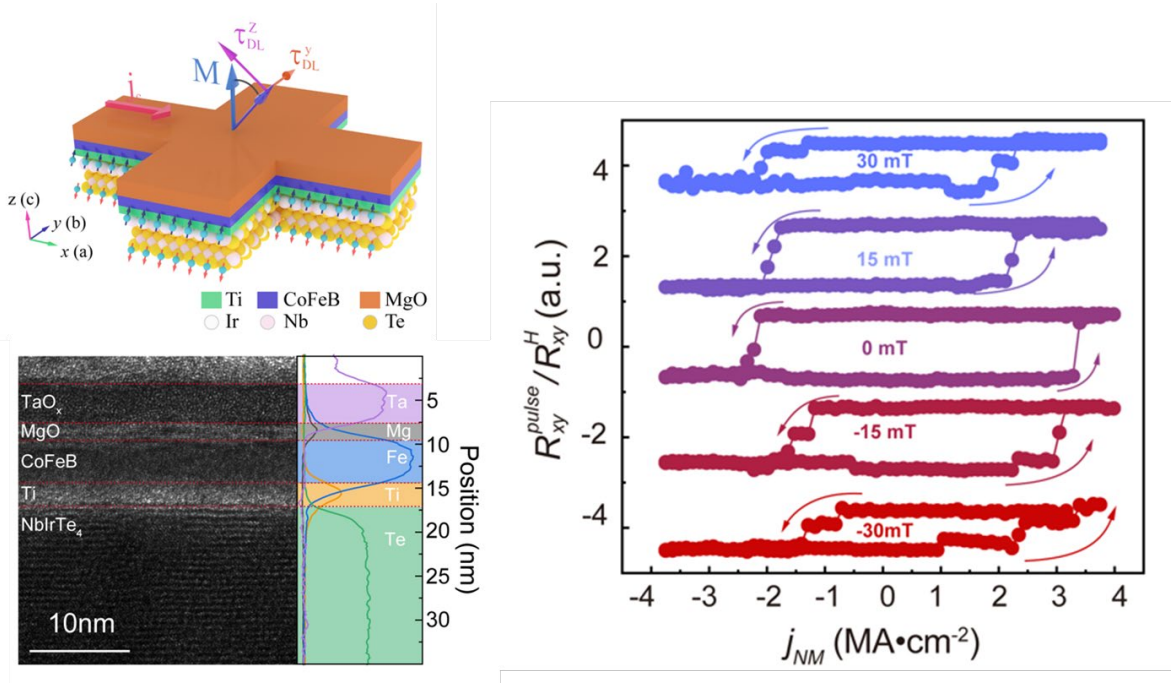

Fig. 1 Field free magnetization switching included by out-of-plane field of $NbIrTe_4$

References

[1] Liu, L. et al., Spin-torque switching with the giant spin Hall effect of Tantalum. SCIENCE 336 555 (2012).
[2] Yang, H. et al., Two-dimensional materials prospects for non-volatile spintronic memories. NATURE 606 663 (2022).
[3] Miron, I. M. et al., Perpendicular switching of a single ferromagnetic layer induced by in-plane current injection. NATURE 476 189 (2011).

Enhanced Surface Properties of WS_2 via Cryogenic Exfoliation and High-Pressure Dispersion for Catalysis

Yejin Choi[1], Myeung-Jin Lee[1], Bora Jeong[1], Hong-Dae Kim[*1]

[1]*Ulsan Division, Korea Institute of Industrial Technology, Ulsan, Republic of Korea*

Tungsten disulfide (WS_2), a promising transition metal dichalcogenides (TMDs), has attracted significant attention due to its unique structural and electronic properties. In particular, single- and few-layered WS_2 nanosheets provide a higher surface area and improved accessibility to active sites, making them attractive for various applications. Various exfoliation methods, including mechanical exfoliation, liquid-phase exfoliation, and chemical vapor deposition, have been explored to obtain WS_2 nanosheets. In this study, a cryogenic exfoliation process using liquid nitrogen was employed to effectively reduce the thickness of WS_2 and enhance its dispersion using high-pressure dispersion techniques. The exfoliation mechanism is driven by sudden temperature change. WS_2 was first heated to 200 ^oC to induce interlayer expansion and weaken van der Waals interactions. Upon immersion in liquid nitrogen, nitrogen molecules intercalated between the expanded layers, and the rapid temperature change facilitated layer separation. This process was repeated five times to achieve exfoliated WS_2 nanosheets (WS_2-NS). To further improve nanosheet dispersion and uniformity, a high-pressure disperser was applied, resulting in well-dispersed WS_2 nanosheets (WS_2-NS(HP)) with 1 to 4 layers, as confirmed by microscopic and spectroscopic analyses. Although the exfoliated WS_2 exhibited excellent dispersibility and chemical stability, dangling bonds were predominantly localized at the edge sites. To modify its surface properties and enhance charge transport characteristics, vanadium loading was performed on exfoliated WS_2. The structural, optical, and electronic properties of WS_2 were systematically analyzed, demonstrating its potential for catalytic applications. The exfoliated WS_2 was incorporated into a nanocomposite catalyst for NH_3-SCR (Selective Catalytic Reduction) applications, where its content was optimized. Catalytic performance was evaluated in a fixed bed reactor over a temperature range of 150-400 ^oC, comparing bulk WS_2, exfoliated WS_2 (WS_2-NS), and exfoliated and high-pressure dispersed WS_2 (WS_2-NS(HP)). Under SO_2-free conditions, the catalytic activities at 250 °C were 59.4%, 77.9%, and 84.7%, respectively, with the highest activity observed in catalysts treated with liquid nitrogen and high-pressure dispersion. Furthermore, despite SO_2-induced deactivation being a common issue in NH_3-SCR catalysts, the developed catalyst exhibited sulfur resistance, maintaining similar activity under SO_2-containing conditions.

Keywords : transition metal dichalcogenide (TMD), tungsten disulfide (WS_2), cryogenic exfoliation, catalyst

Hot-electron Injection Enabled High-performance Broadband Photodetection Based on WO_{3-x}/Bi_2O_2Se Hybrid structure

X. Zhang[1], Y. Yu[2], J. Lv[1,3*], Z. Ni[1,3*]

[1]1School of Physics, Key Laboratory of Quantum Materials and Devices of Ministry of Education, and Key Laboratory of MEMS of Ministry of Education, Southeast University, Nanjing 211189, China,

[2] State Key Laboratory for Organic Electronics and Information Displays, Institute of Advanced Materials, School of Materials Science and Engineering, Nanjing University of Posts and Telecommunications, Nanjing 210023, China

[3]School of Electronic Science and Engineering, Southeast University, Nanjing 210096, China

Two-dimensional (2D) Bi_2O_2Se has emerged as a promising candidate for broadband photodetection, owing to its superior carrier mobility, outstanding air-stability, and suitable bandgap (~ 0.8 eV) [1-3]. However, Bi_2O_2Se photodetectors suffer limited sensitivity at a near-infrared region due to the relatively weak light absorption at this band, while the construction of heterojunctions introduces adverse interfacial defects, leading to a trade-off between responsivity and response speed [4, 5]. Here, we demonstrate that integrating plasmonic nanostructures effectively enhances the performance of Bi_2O_2Se photodetectors at a broad spectral range of 532–1550 nm. The hybrid structure exhibits rapid hot-electron injection and enhanced light absorption in the visible and near-infrared regions. Due to plasmon-induced hot-electron injection and enhanced light absorption through LSPR effect, the WO_{3-x}/Bi_2O_2Se hybrid photodetector achieves a high responsivity of ~1.7×10^6 A/W at 700 nm and ~48 A/W at 1310 nm, nearly an order of magnitude higher than that of the pristine Bi_2O_2Se device. Moreover, benefiting from ultrafast hot-electron transfer and suppressed defect trapping, the device maintains a high-speed photoresponse. Our results demonstrate that 2D materials coupled with plasmonic nanostructures offer a promising architecture for developing next-generation broadband photodetectors.

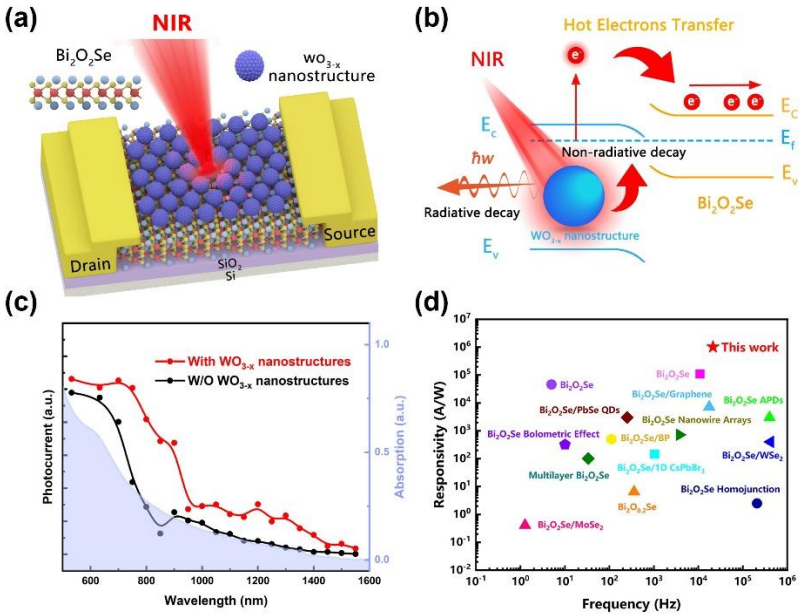

Device schematic and photoelectric characterization of WO_{3-x}/Bi_2O_2Se hybrid photodetector. (a) Schematic of the WO_{3-x}/Bi_2O_2Se hybrid photodetector. (b) Schematic diagram of the generation, transfer, and transportation of plasmon-induced hot electrons in the hybrid structure. (c) Spectrum-dependent absorption and photocurrent comparison. (d) Comparison of the responsivity and photoresponse speed of the WO_{3-x}/Bi_2O_2Se hybrid photodetector with other photodetectors based on Bi_2O_2Se.

References:

[1] J. Wu, *et al.*, *Nat. Nanotechnol.* **12**, 530-534, (2017).
[2] Y. Sun, et al., Adv. Funct. Mater. **30**, 2004480, (2020).
[3] J. Yin, *et al.*, *Nat. Commun.* **9**, 3311, (2018).
[4] P. Luo, *et al.*, *ACS Nano*, **13**, 9028−9037, (2019).
[5] M. D. Hossain, *et al.*, *J. Mater. Chem. C*, **11**, 6670, (2023).

First-principles Calculations on Oxygen Functional Group Interactions on Graphene and Their Modulation by Surface Normal Electric Fields

T. Kawai[1], Y. Miyamoto[2]

[1]Department of Design Data Science, Tokyo City University (Japan), [2]Advanced Power Electronics Research Center, National Institute of Advanced Industrial Science and Technology (AIST) (Japan)

Oxidized graphene can be formed inexpensively through a simple process, making it promising for various electronic devices such as resistive random-access memory (ReRAM)[1-2]. Additionally, the oxidation and reduction processes of graphene can not only manipulate the electronic states of graphene but also be utilized for atomic-scale processing, such as edge formation. Recent studies have reported that while both hydroxyl and epoxy groups contribute similarly to oxygen desorption during heat treatment, epoxy groups selectively desorb during photoreduction[3], which is very intriguing.

In this study, we investigated several stable adsorption structures and interactions of hydroxyl and epoxy groups using first-principles electronic state calculations based on density functional theory (DFT)[4]. Initially, molecular dynamics (MD) simulations were performed at approximately 300K on a 6x6 supercell structure where 18 out of 36 A-sites were occupied by oxygen atoms, with half forming hydroxyl groups (-OH) and half forming epoxy groups (-O-). We found that epoxy groups easily break one bond and migrate to the top site of graphene carbon atoms. The activation barrier for epoxy groups to transition across carbon top sites is approximately 0.9 eV or lower from previous calculations[5], but this appears to be influenced by the interactions between adsorbed oxygen atoms. In the presentation, we will also discuss the effects of external electric fields normal to the graphene surface on the activation barrier.

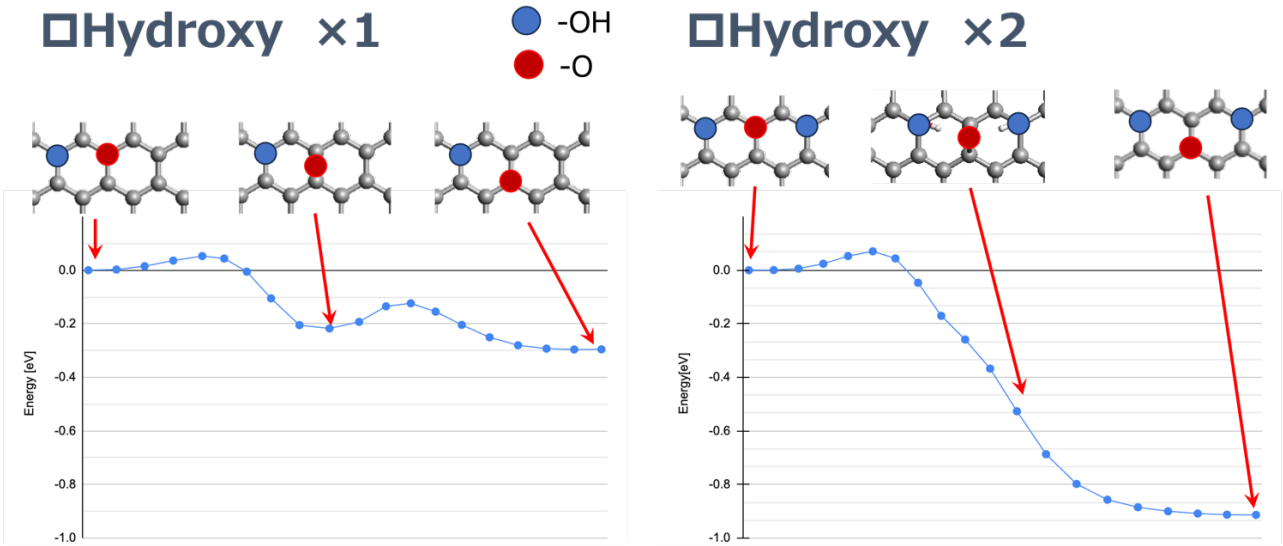

Figure: Energy profiles showing the migration of an epoxide group from one carbon top site to an adjacent site, in the presence of one or two nearby hydroxyl groups.

References

[1] H. Tian, *et al.*, *Nano Letters* **14,** 3214 (2014).
[2] A. Rani, *et al.*, *small* **12**, 6167 (2016).
[3] M. Hada, *et al*. *ACS Nano* **13**, 10103 (2019).
[4] P. Giannozzi *et al.*, J. Phys.:Condens. Matter **21**, 395502 (2009); P. Giannozzi *et al.*, J. Phys.:Condens. Matter **29**, 465901 (2017); P. Giannozzi *et al.*, J. Chem. Phys. **152**, 154105 (2020); URL http://www.quantum-espresso.org.
[5] T. Kawai, *et al., Current Applied Physics* **11**, S50eS54 (2011).
[6] T. Sun, *et al.*, *J. Phys. Chem. A* **120,** 2607 (2016).

Ambipolar Doping of Single-Walled Carbon Nanotubes via Covalent Charge-Transfer Engineering

A. Setaro[1,2], A. Fiebor[1], M. Adeli[1], S. Reich[1]

[1]*Physics Department, Freie Universität Berlin (Germany)*

[2]*Engineering Department, Pegaso University (Italy)*

Precisely controlling the doping level of single-walled carbon nanotubes at the individual scale unlocks new applications. Electrochemical gating finely tunes the Fermi level but is typically applied to nanotube ensembles, while charge-transfer by filling the tubes with molecules enable single-nanotube doping but lacks precise charge regulation. We propose an alternative approach using covalently attached, custom-synthesized charge-transfer compounds. This preserves π-conjugation and optoelectronic properties while enabling systematic charge transfer control by adjusting functional group attachment. Our rational ambipolar design employs the same molecular building blocks [1] —methoxy-substituted aniline rings—to achieve either electron donation or withdrawal, depending on the assembly configuration.

References

[1] A Fiebor *et al.*, *J. Phys. Chem. C* **125**, *19925* (2021).

Intrinsic temperature dependence of Raman-active modes in individual isolated single- and double-walled carbon nanotubes

Ya Feng[1,2*], Dmitry I. Levshov[3], Yuta Sato[4], Taiki Inoue[5], Sofie Cambré[3], Wim Wenseleers[6], Rong Xiang[7], Kazu Suenaga[8], Shigeo Maruyama[2*]

[1]*Key Laboratory of Ocean Energy Utilization and Energy Conservation of Ministry of Education, School of Energy and Power Engineering, Dalian University of Technology, Dalian 116024, China*
[2]*Department of Mechanical Engineering, School of Engineering, The University of Tokyo, Tokyo 113-8656, Japan*
[3]*Theory and Spectroscopy of Molecules and Materials, Department of Chemistry and Department of Physics, University of Antwerp, Antwerp 2610, Belgium*
[4]*Nanomaterials Research Institute, National Institute of Advanced Industrial Science and Technology (AIST), Tsukuba 305-8565, Japan*
[5]*Department of Applied Physics, Graduate School of Engineering, Osaka University, Osaka 565-0871, Japan*
[6]*Nanostructured and Organic Optical and Electronic Materials, Department of Physics, University of Antwerp, Antwerp 2610, Belgium*
[7]*State Key Laboratory of Fluid Power and Mechatronic Systems, School of Mechanical Engineering, Zhejiang University, Hangzhou 310027, China*
[8]*The Institute of Scientific and Industrial Research, Osaka University, Osaka 565-0047, Japan*

The intrinsic temperature dependence of Raman-active modes in carbon nanotubes (CNTs), particularly the radial breathing mode (RBM), has been a topic of long-standing controversy. In this study, we prepared suspended individual CNTs to investigate how their Raman spectra depend on temperature and to understand the environmental effects on this dependency. We analyzed the intrinsic temperature dependence of the main Raman-active modes, including the RBM, the moiré-activated R feature, and the G-band in a double-walled carbon nanotube (DWCNT) and single-walled carbon nanotubes (SWCNTs) after complete desorption of air. The inner tube of the DWCNT, like the desorbed SWCNTs, was free from environmental influences, resulting in minimal temperature-induced RBM frequency shifts. We show that the larger RBM shift of SWCNTs upon initial heating is not intrinsic but due to air desorption. The R feature, attributed to moiré-activated phonon scattering and non-dispersive in nature, demonstrated a quasi-linear temperature dependence, akin to the G-band but with a lower temperature coefficient. The G-band, largely unaffected by environmental conditions, exhibited a consistent temperature coefficient across SWCNTs, DWCNTs, and small SWCNT bundles [1].

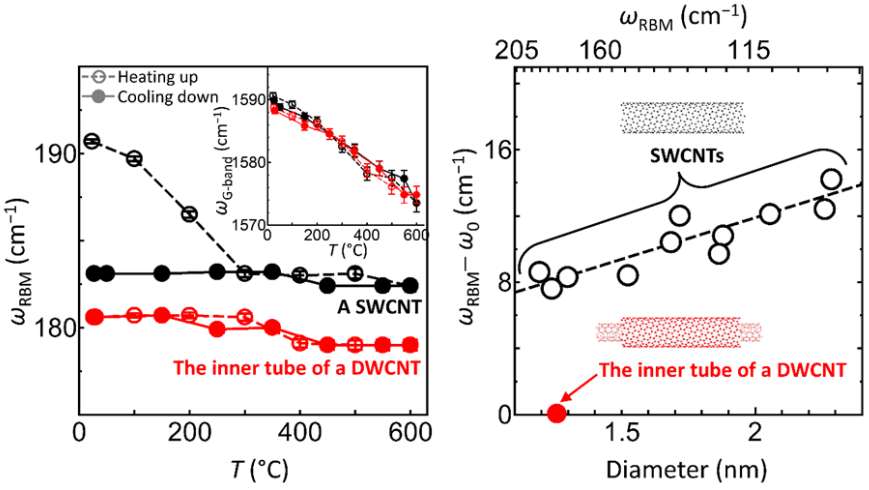

Figure 1: Heating in a protective flowing gas removes the adsorbates from SWCNTs, revealing that the intrinsic temperature dependence of the RBM frequency is minimal for both the desorbed SWCNT as well as the inner nanotube of DWCNT.

Reference

[1] Y. Feng *et al.*, *ACS Nano.* **19**(1), 1396–1404 (2025).

Session
NT 25（The 25th International Conference on the Science and Applications of Nanotubes and Low-

| Main conference：Main conference

Tue. Jun 17, 2025 9:30 AM - 12:10 PM JST | Tue. Jun 17, 2025 12:30 AM - 3:10 AM UTC Centennial Hall (Clock Tower Centennial Hall)

[17ma] Main Conference

Chair: Shoei Chiashi, Yuichiro K. Kato

9:30 AM - 10:10 AM JST | 12:30 AM - 1:10 AM UTC

[17ma-01]

Exciton transfer and interface excitons in mixed-dimensional heterostructures

Nan Fang[1], Yih-Ren Chang[1], Shun Fujii[1,2], Daiki Yamashita[1,3], Mina Maruyama[4], Yanlin Gao[4], Chee Fai Fong[1], Daichi Kozawa[5], Keigo Otsuka[6], Kosuke Nagashio[6], Susumu Okada[4], *Yuichiro K. Kato[1] (1. RIKEN (Japan), 2. Keio Univ. (Japan), 3. AIST (Japan), 4. Univ. of Tsukuba (Japan), 5. NIMS (Japan), 6. Univ. of Tokyo (Japan))

10:10 AM - 10:40 AM JST | 1:10 AM - 1:40 AM UTC

[17ma-02]

READOUT OF TRIPLET STATES IN SP^3-FUNCTIONALIZED CARBON NANOTUBES BY OPTICALLY-DETECTED MAGNETIC RESONANCE

J. Alejandro de Sousa[1,2], Simon Settele[3], Timur Biktagirov[4], Uwe Gerstmann[4], Etienne Goovaerts[1], Jana Zaumseil[3], Nuria Crivillers[2], *Sofie Cambré[1] (1. Theory and Spectroscopy of Molecules and Materials, University of Antwerp (Belgium), 2. Institut de Ciència de Materials de Barcelona (Spain), 3. Institute for Physical chemistry, Universität Heidelberg (Germany), 4. Lehrstuhlfür Theoretische Material physik, Universität Paderborn (Germany))

11:00 AM - 11:30 AM JST | 2:00 AM - 2:30 AM UTC

[17ma-03]

Computational modeling and design of DNA-carbon nanotube sensors of small molecular analytes

*Lela Vukovic[1] (1. University of Texas at El Paso (United States of America))

11:30 AM - 11:50 AM JST | 2:30 AM - 2:50 AM UTC

[17ma-04]

Chirality-Dependent Kinetics of Single-Walled Carbon Nanotubes from Machine-Learning Force Fields

*Sida Sun[1], Shigeo Maruyama[2], Yan Li[1] (1. Peking University (China), 2. The University of Tokyo (Japan))

11:50 AM - 12:10 PM JST | 2:50 AM - 3:10 AM UTC

[17ma-05]

DUV-Raman and photoluminescence studies of SWNT@BNNT hetero-nanotubes

*Hsiang-Lin Liu[1], Shigeo Maruyama[2], Riichiro Saito[1,3] (1. National Taiwan Normal University (Taiwan), 2. The University of Tokyo (Japan), 3. Tohoku University (Japan))

Exciton transfer and interface excitons in mixed-dimensional heterostructures

Nan Fang[1,2], Yih-Ren Chang[1], Shun Fujii[2,3], Daiki Yamashita[2,4], Mina Maruyama[5], Yanlin Gao[5], Chee Fai Fong[1], Daichi Kozawa[1,2,6], Keigo Otsuka[1,7], Kosuke Nagashio[8], Susumu Okada[5], Yuichiro K. Kato[1,2]

[1] Nanoscale Quantum Photonics Laboratory, RIKEN Cluster for Pioneering Research (Japan), [2] Quantum Optoelectronics Research Team, RIKEN Center for Advanced Photonics (Japan), [3] Department of Physics, Keio University (Japan), [4] Platform Photonics Research Center, National Institute of Advanced Industrial Science and Technology (AIST), (Japan), [5] Department of Physics, University of Tsukuba (Japan), [6] Research Center for Materials Nanoarchitectonics, National Institute for Materials Science (Japan), [7] Department of Mechanical Engineering, The University of Tokyo, Tokyo (Japan), [8] Department of Materials Engineering, The University of Tokyo, Tokyo (Japan)

Two-dimensional van der Waals heterostructures have introduced unconventional phenomena that emerge at atomically precise interfaces, and further development is expected in mixed-dimensional heterostructures. Here we discuss exciton physics in 1D-2D heterostructures consisting of one-dimensional carbon nanotubes and two-dimensional tungsten diselenide [1,2]. Both the chirality and the layer number are identified before assembling the free-standing heterostructures using the anthracene-assisted transfer [3], allowing for investigation of the band alignment effects. For small band gap nanotubes corresponding to type I band alignment, exciton transfer is observed [1]. With increasing the nanotube band gap, the transfer efficiency shows a pronounced enhancement indicating a resonance in the band alignment. For large band gap nanotubes corresponding to type II band alignment, exciton transfer diminishes whereas bright emission peaks originating from the interface are identified [2]. We assign the peaks to interface excitons as they only appear in type-II heterostructures. Localization of low-energy interface excitons is indicated by extended lifetimes as well as small excitation saturation powers, and photon correlation measurements confirm room-temperature quantum emission. With mixed-dimensional van der Waals heterostructures where band alignment can be engineered, new opportunities for quantum photonics are envisioned.

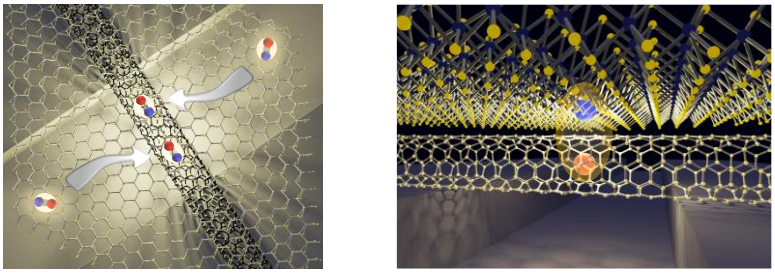

Figure 1: Illustrations of (left) exciton transfer and (right) an interface exciton in air-suspended WSe_2/CNT mixed dimensional heterostructures.

References

[1] N. Fang, Y. R. Chang, D. Yamashita, S. Fujii, M. Maruyama, Y. Gao, C. F. Fong, K. Otsuka, K. Nagashio, S. Okada, Y. K. Kato, “Resonant exciton transfer in mixed-dimensional heterostructures for overcoming dimensional restrictions in optical processes,” *Nature Commun.* **14**, 8152 (2023).

[2] N. Fang, Y. R. Chang, S. Fujii, D. Yamashita, M. Maruyama, Y. Gao, C. F. Fong, D. Kozawa, K. Otsuka, K. Nagashio, S. Okada, Y. K. Kato, “Room-temperature quantum emission from interface excitons in mixed-dimensional heterostructures,” *Nature Commun.* **15**, 2871 (2024).

[3] K. Otsuka, N. Fang, D. Yamashita, T. Taniguchi, K. Watanabe, Y. K. Kato, “Deterministic transfer of optical-quality carbon nanotubes for atomically defined technology”, *Nature Commun.* **12**, 3138 (2021).

Acknowledgments

Work supported by JSPS (KAKENHI JP22K14624, JP22K14625, JP21K14484, JP22K14623, JP22H01893, JP21H05233, JP22F22350, JP23H00262, JP20H02558), JST (ASPIRE JPMJAP2310), and MEXT (ARIM JPMXP1222UT1135). Y.R.C. is supported by JSPS (International Research Fellow). N.F. and C.F.F. are supported by the RIKEN Special Postdoctoral Researcher Program. We thank the Advanced Manufacturing Support Team at RIKEN for technical assistance.

READOUT OF TRIPLET STATES IN SP^3-FUNCTIONALIZED CARBON NANOTUBES BY OPTICALLY-DETECTED MAGNETIC RESONANCE

J. Alejandro de Sousa[1,2], Simon Settele[3], Timur Biktagirov[4], Uwe Gerstmann[4], Etienne Goovaerts[1], Jana Zaumseil[3], Nuria Crivillers[2], Sofie Cambré[1]

[1] Theory and Spectroscopy of Molecules and Materials, University of Antwerp (Belgium), [2] Institut de Ciència de Materials de Barcelona (Spain), [3]Institute for Physical chemistry, Universität Heidelberg (Germany), [4] Lehrstuhlfür Theoretische Material physik, Universität Paderborn (Germany)

Controlled *sp*^{3}-functionalization of single-wall carbon nanotubes (SWCNTs) has become a common route to enhance their emission efficiency [1]. While a lot of research focused on the effect of the functionalization on the bright singlet excitons, little information is available on how triplet excitons are affected by the creation of these *sp*^{3}-defects along the CNT wall.

Here we investigate such triplet excitons by optically detected magnetic resonance, a technique combining the sensitivity of emission spectroscopy with magnetic resonance transitions between the triplet sublevels in an external applied magnetic field [2,3]. We perform ODMR experiments on a series of samples with different functionalization densities and functional groups. Interestingly, we found significant differences in zero-field splitting, ODMR intensity and triplet spin-density distribution. Experimental results are corroborated by DFT calculations. While pristine SWCNTs hold triplet excitons with a purely axial symmetry and a zero-field splitting inversely proportional to the diameter of the SWCNT [3], the spin-density distribution of triplet excitons trapped in *sp*^{3}-defects changes significantly. Additionally, by changing the functional group on the SWCNTs to a electron spin-label group, we demonstrate strong coupling between the triplet state and the unpaired electron spin, leading to enhanced intersystem crossing and strong exchange coupling between the spin states. These results show the first steps towards exploiting *sp*^{3}-functionalization of CNTs to create optical readout of electron spin qubits.

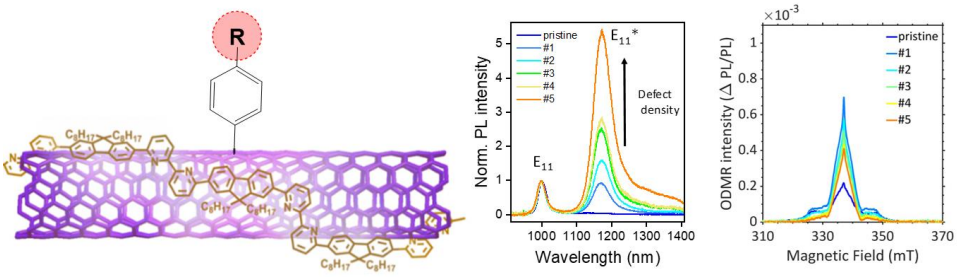

Figure: (left) Schematic drawing of a functionalised (6,5) SWCNT; (b) PL spectra of SWCNTs with different functionalisation density and (c) corresponding ODMR spectra.

References

[1] Y. Piao, B. Meany, L. R. Powell, N. Valley, H. Kwon, G. C. Schatz and Y. Wang, Brightening of carbon nanotube luminescence through the incorporation of sp3 defects, *Nature Chem* 5, 840. **2013**

[2] E. Goovaerts, Optically Detected Magnetic Resonance, *eMagRes* 6, 343. **2017**

[3] I. Sudakov, E. Goovaerts, W. Wenseleers, J.L. Blackburn. J. G. Duque and S. Cambré, Chirality dependence of triplet excitons in (6,5) and (7,5) single-wall carbon nanotubes revealed by optically detected magnetic resonance, *ACS Nano* 17, 2190. **2023**

Computational modeling and design of DNA-carbon nanotube sensors of small molecular analytes

L. Vukovic[1,2]

[1]*Department of Chemistry and Biochemistry, University of Texas at El Paso (United States)* [2]*Department of Physical Chemistry II, Ruhr University Bochum (Germany)*

Single-walled carbon nanotubes (SWNTs) functionalized with DNA exhibit unique optical properties that make them powerful tools for biosensing applications. These DNA-SWNT conjugates enable the detection of small biomolecules through analyte-induced modulation of their fluorescence emission. In this work, we use computational methodologies to design and optimize DNA-wrapped SWNT sensors for the selective detection of neuromodulators such as serotonin and oxytocin. Using machine learning approaches, we identify DNA sequences that exhibit strong binding affinity to target analytes while inducing distinct optical shifts in the SWNT fluorescence [1,2]. Additionally, we employ molecular simulations to elucidate the structural and energetic interactions governing DNA-SWNT-analyte recognition [3]. By integrating predictive modeling with atomistic characterization, we aim to advance the rational design of highly specific and sensitive carbon nanotube-based biosensors.

References

[1] P. Kelich, S. Jeong, N. Navarro, J. Adams, X. Sun, H. Zhao, M. Landry, L. Vuković. ACS Nano, **16**, 736-745 (2022).
[2] P. Kelich, J. Adams, S. Jeong, N. Navarro, M. P. Landry, L. Vukovic. J. Chem. Inf. Model. **10**, 3992-4001 (2024).
[3] A. Krasley, S. Chakraborty, L. Vukovic, A. Beyene. ACS Nano, **19**, 8, 7804–7820 (2025).

CHIRALITY-DEPENDENT KINETICS OF SINGLE-WALLED CARBON NANOTUBES FROM MACHINE-LEARNING FORCE FIELDS

Sida Sun[1], Shigeo Maruyama[2], Yan Li[1,*]

[1]*College of Chemistry and Molecular Engineering, Peking University, China,*
[2]*Department of Mechanical Engineering, The University of Tokyo, Japan*

The mechanism of the chiral selectivity of single-walled carbon nanotubes (SWCNTs) has been a long-standing dispute. Since no *in situ* experimental methods can characterize the atomic-level dynamics at the nanotube-catalyst interface, theoretical approaches to this problem are particularly valued. In recent years, the development of machine-learning force fields (MLFFs) enables the microsecond-scale, high-accuracy molecular dynamics (MD) simulations of the interface, providing a method for the direct investigation of the growth of SWCNTs [1,2].

Here, we develop a cobalt–carbon MLFF and use it to perform extensive growth simulations on Co_{55} clusters under the vapor–liquid–solid (VLS) regime. While initially the chirality distribution of the MD trajectories hardly depends on the chiral angle, it develops a bias towards (6,5) over time. We reveal that it is the immediate formation and resolution of pentagon defects after nucleation that shifts the chirality distribution in process. By proposing a method to label the unique nanotube edges, we develop microkinetic models of the growth and defect kinetics at the edge, reproduce the observed edge pattern distribution and defect lifetime statistics, and discuss their dependence on the chirality. Our work therefore highlights the defect kinetics as an important part of the chirality origin in the VLS growth of SWCNTs. [3]

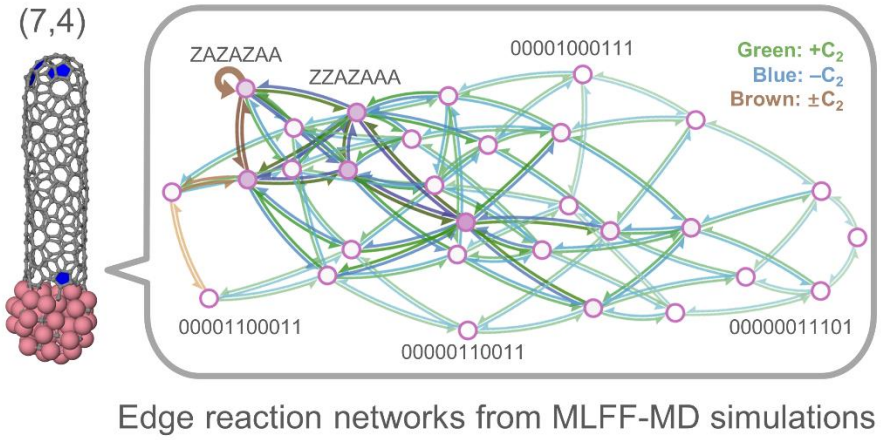

Figure caption: Reaction network of the growth and etching processes of a (7,4) SWCNT. Reprinted with permission from [3]. Copyright 2025 American Chemical Society.

References

[1] D. Hedman et al. *Nat. Commun.* **15**, 4076 (2024).
[2] I. Kohata et al. arXiv:2302.09264.
[3] S. Sun, S. Maruyama, Y. Li. *J. Am. Chem. Soc.* **147**, 7103 (2025).

DUV-Raman and photoluminescence studies of SWNT@BNNT hetero-nanotubes

Hsiang-Lin Liu[1], Shigeo Maruyama[2], Riichiro Saito[1,3]

[1]*Department of Physics, National Taiwan Normal University, Taipei 11677, Taiwan*
[2]*Department of Mechanical Engineering, The University of Tokyo, 113-8656, Japan*
[3]*Department of Physics, Tohoku University, Sendai 980-8578, Japan*

Using a 266 nm (4.66 eV) excitation laser, we simultaneously measure the Raman and photoluminescence (PL) spectra of a vertically aligned (VA) single-walled carbon nanotube (VA-SWNT) encapsulated by a boron nitride nanotube (hetero-nanotube, VA-SWNT@BNNT) [1,2]. By suppressing the D band intensity of the VA-SWNT, we observe the near-resonant BN E2g mode at 1370 cm^{-1} in the SWNT@BNNT. Notably, its intensity is 10 times smaller than the defect-induced PL spectrum, in contrast to the case of the h-BN single crystal. Furthermore, the larger PL intensity of the VA-BNNT compared to the h-BN single crystal suggests that the VA-BNNT contains more defect states than the h-BN single crystal. Additionally, the VA-SWNT@BNNT exhibits two multi-phonon Raman peaks at 3033 and 3142 cm^{-1} and four PL peaks at 4639, 5859, 6905, and 8293 cm^{-1}. The PL intensity of the VA-SWNT@BNNT is 20 times smaller than that of the VA-BNNT. For the VA-SWNT, an additional Raman peak is observed at 4677 cm^{-1}, along with peaks at 3040 and 3155 cm^{-1}. Given that the 4677 cm^{-1} Raman peak of the VA-SWNT is close to the 4639 cm^{-1} PL peak of the VA-SWNT@BNNT, we propose that the photo-excited electrons in the PL process in the VA-BNNT may transfer to the Raman process within the VA-SWNT component of the VA-SWNT@BNNT. The first-principles calculations identify possible donor and acceptor states in BN bilayers with substitutional defects (e.g., carbon replacing boron or nitrogen). These defect states are also relevant to understanding the origin of PL in BNNT.

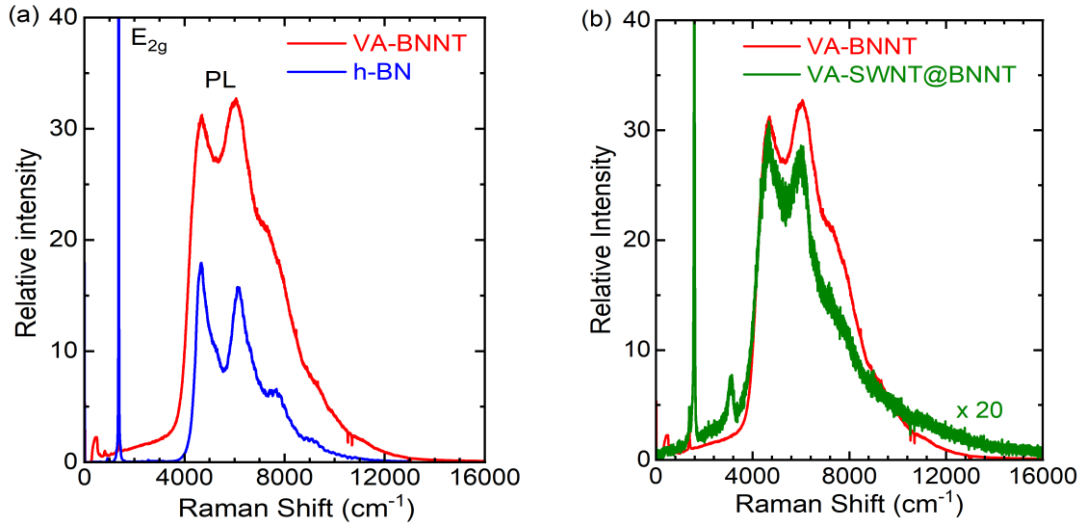

Figure 1 (a) The DUV-Raman and PL spectra of the VA-BNNT and h-BN single crystal. (b) The DUV-Raman and PL spectra of VA-BNNT and VA-SWNT@BNNT. The PL intensity of the VA-SWNT@BNNT scales up by a factor of 20 for comparison.

References

[1] D. P. Gulo *et al*. J. Phys. Chem. Lett. **14**, 10263 (2023).
[2] D. P. Gulo *et al*. J. Phys. Chem. Lett. **16**, 1711 (2025).

Session
NT 25（The 25th International Conference on the Science and Applications of Nanotubes and Low-

| Parallel Symposia：Symposium on Nanomaterials for Energy and Electronics

Tue. Jun 17, 2025 2:00 PM - 5:20 PM JST | Tue. Jun 17, 2025 5:00 AM - 8:20 AM UTC Conference room 5a/5b(INNOVATION BLDG., 5F)

[17en] Energy & Electronics

Chair:Yutaka Ohno, Esko Ilmari Kauppinen

2:00 PM - 2:20 PM JST | 5:00 AM - 5:20 AM UTC

[17en-01]

Transparent, Conductive Carbon Nanotube Thin Films via Direct, Dry Deposition from the Floating Catalyst Chemical Deposition Synthesis

*Esko Ilmari Kauppinen[1] (1. Department of Applied Physics, Aalto University School of Science, (Finland))

2:20 PM - 2:40 PM JST | 5:20 AM - 5:40 AM UTC

[17en-02]

Preparation and Electrocatalytic Property of Integrated W_2C Nanowires @ Single-Walled Carbon Nanotubes Films

*Feng Zhang[1], Chang Liu[1] (1. Institute of Metal Research, Chinese Academy of Sciences (China))

2:40 PM - 3:00 PM JST | 5:40 AM - 6:00 AM UTC

[17en-03]

Advancing Energy Applications with WSe_2 Based Materials: Doping and Hybridization Strategies

*Antonia Kagkoura[1], Zdeněk Sofer[1] (1. University of Chemistry and Technology, Prague (Czech Republic))

3:00 PM - 3:20 PM JST | 6:00 AM - 6:20 AM UTC

[17en-04]

Exploiting the Unique Properties of MXenes for Hydrogen Production via Dry Reforming of Methane

Joshua O Ighalo[1], AmirMohammad Ebrahimi[1], Davood B Pourkargar[1], *Placidus B Amama[1] (1. Kansas State University (United States of America))

4:00 PM - 4:20 PM JST | 7:00 AM - 7:20 AM UTC

[17en-05]

Highly Conductive Carbon Nanotube Fibers

Haozike Wang[1], Zhaoqing Gao[1], Pengxiang Hou[1], *Chang Liu[1] (1. Institute of Metal Research, Chinese Academy of Sciences (China))

4:20 PM - 4:40 PM JST | 7:20 AM - 7:40 AM UTC

[17en-06]

Synthesis of advanced carbon material graphdiyne and their applications in sustainable energy

*Xin Gao[1] (1. Peking University (China))

4:40 PM - 5:00 PM JST | 7:40 AM - 8:00 AM UTC

[17en-07]

Insights into the mechanism of carbon nanotubes in silicon-based anodes

*Ziying He[1], Fei Wei[1] (1. Tsinghua University (China))

Session

NT 25（The 25th International Conference on the Science and Applications of Nanotubes and Low-

5:00 PM - 5:20 PM JST | 8:00 AM - 8:20 AM UTC

[17en-08]

Fabrication and Performance Evaluation of Lithium-Sulfur Pouch Cells

*Mariam Ezzedine[1], Costel Sorin Cojocaru[1] (1. LPICM-Ecole Polytechnique (France))

Transparent, Conductive Carbon Nanotube Thin Films via Direct, Dry Deposition from the Floating Catalyst Chemical Deposition Synthesis

Esko I. Kauppinen

Aalto University (Finland)

We combined carbon nanotube (CNT) floating catalyst chemical vapor deposition (FC-CVD) synthesis with the direct deposition of CNTs to form a thin film. CNT thin films were directly deposited at the FC-CVD reactor outlet at the ambient temperature followed by the cooling of the FC-CVD readctor gas via membrane filtration followed by a simple press transfer onto a desired substrate [1]. When the substrate has an open area, free-standing CNT thin films can be directly manufactured [2]. Alternatively, CNTs can be directly deposited onto a desired substrate via thermophoretic as well as via electric field induced deposition. The film thickness can be controlled via the collection time as well as via the concentration of the CNTs in the FC-CVD synthesis reactor gas. The CNT film conductivity increases with increasing nanotube length and decreasing the bundle diameter [3]. As no post synthesis purification, sonication and surfactant addition is needed, and accordingly pristine CNTs will make the film, state-of-the-art conductive uniform films with the sheet resistance below 25 ohms/sq at 90 % transmittance have been manufactured with our direct, dry depositon method [4].

In this talk we will present the development steps of the dry depositon method to prodce CNT thin films as well as their applications as touch sensors, nanoparticle filters, gas sensors, solar cells as well as in thin film field effect transistors (TFT-FET).

References

[1] E.I. Kauppinen *et al. NanoLetters* **10**, 4349-4355 (2010)
[2] E.I. Kauppinen *et al. ACS Nano* **5**,3214-3221 (2011).
[3] E.I. Kauppinen *et al. Carbon* **103**, 228-235 (2016).
[4] E.I. Kauppinen, I. Jeon *et al. Adv. Funct. Mater.* **33**, 2213374 (2023).

Preparation and Electrocatalytic Property of Integrated W_2C Nanowires @ Single-Walled Carbon Nanotubes Films

F. Zhang, C. Liu

Shenyang National Laboratory for Materials Science, Institute of Metal Research, Chinese Academy of Sciences (China)

The hydrogen production industry achieved through water electrolysis is hindered by the lack of cost-effective, high-performance electrocatalysts.[1,2] Tungsten carbide (WC) with platinum-like electronic structure is recognized as a promising non-precious metal catalyst for the hydrogen evolution reaction (HER). However, traditional WC synthesized via high-temperature carbonization often faces challenges such as large particle sizes, poor structural uniformity, and the presence of impurity phases. To address these limitations, we developed a novel approach using single-walled carbon nanotubes (SWCNTs) as "nanoreactors" to synthesize ultrafine W_2C nanowires,[3] which were then used to fabricate a HER membrane electrode composed of W_2C@SWCNT. By combining in-situ transmission electron microscopy and density functional theory calculations, we elucidated the formation mechanism of W_2C nanowires within SWCNTs.[4] Guided by this mechanism, tungsten oxide were encapsulated into SWCNTs through a hydrothermal process, followed by rapid thermal annealing and high-temperature carbonization to produce a W_2C@SWCNT hybrid film. When employed as a self-supported HER membrane electrode, the film demonstrated exceptional performance under acidic conditions, achieving a current density of 4000 mA cm^{-2} at an overpotential of 373 mV. Moreover, it exhibited remarkable stability, maintaining its catalytic activity for over 500 hours at 3000 mA cm^{-2}.[5] This work provides a strategy for synthesizing high-performance HER catalysts and offers valuable insights into the design of advanced electrocatalytic materials for industrial applications.

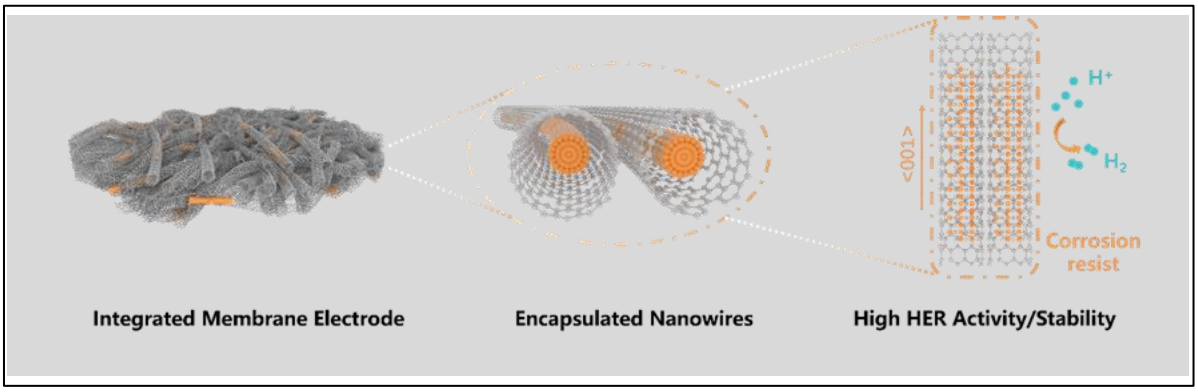

Figure caption: Schematic showing the hierarchical structural of W_2C NWs@SWCNT membrane electrode with high activity and excellent stability.

References

[1] J. Z. Zhang *et al.*, *Nano Lett.* **23**, 8331-8338 (2023)
[2] Z. C. Zhang *et al.*, *Nano Energy. 1***23**, 11 (2024)
[3] X. Zheng *et al.*, *Nanoscale.* **15**, 3931–3939 (2023).
[4] Z. C. Zhang *et al.*, *under review*
[5] Z. C. Zhang *et al.*, *under review*

Advancing Energy Applications with WSe_2-Based Materials: Doping and Hybridization Strategies

A. Kagkoura[1] and Z. Sofer[1]

[1]*Department of Inorganic Chemistry, Faculty of Chemical Technology, University of Chemistry and Technology Prague, Technická 5, 166 28 Prague 6, Czech Republic*

The increasing global energy demand, fueled by population growth and higher consumption, presents a major challenge. As fossil fuel reserves dwindle, the focus on renewable energy sources intensifies. Additionally, the high cost and limited availability of lithium present obstacles for lithium-ion batteries (LIBs). At the same time, while electrochemical water splitting for hydrogen and oxygen production is promising, the cost and scarcity of current electrocatalysts limit its broad adoption. Therefore, identifying alternative materials for these applications is essential.

Transition metal dichalcogenides (TMDs) have garnered attention as electrocatalysts in the hydrogen evolution reaction (HER), oxygen evolution reaction (OER), and as anodes in LIBs.[1-3] Among them, tungsten diselenide (WSe_2) offers unique advantages due to its improved electrical conductivity, cost-effectiveness, and environmental benefits compared to other TMDs. Doping atoms into WSe_2 further enhances its electrocatalytic activity by introducing new electronic states and modifying its electronic structure. However, conventional synthesis methods such as chemical vapor deposition or pyrolysis are often complex and require high temperatures.

In this study, we successfully doped WSe_2 with Mn, Co, and Ni using a simple hydrothermal method. Mn-doped WSe_2 exhibited excellent electrocatalytic activity for HER and performed exceptionally well as an LIB anode.[4] Similarly, Co- and Ni-doped WSe_2 demonstrated high electrocatalytic activity for water splitting and outstanding performance as cathode electrocatalysts in polymer electrolyte membrane water electrolyzers, showcasing strong potential for practical applications.[5]

Furthermore, we synthesized a $WSe_2/Ti_3C_2Cl_2$ MXene hybrid via a simple solvothermal approach.[6] The direct integration of WSe_2 onto $Ti_3C_2Cl_2$ enhances electron transfer, conductivity, and the availability of active sites, leading to exceptional HER activity with an overpotential of just -0.19 V vs RHE at -10 mA cm^{-2}. The hybrid's optimized composition also demonstrated remarkable energy storage capabilities, nearly doubling the initial discharge capacity of WSe_2 when used as an anode in LIBs (1255 mAh g^{-1}). Additionally, $WSe_2/Ti_3C_2Cl_2$ exhibited superior electrocatalytic performance for H_2O_2 reduction, with a two-fold higher response compared to pristine WSe_2, enabling sensitive amperometric H_2O_2 detection over the concentration range of 1-88 μM with a detection limit of 0.6 μM.

Overall, the in-situ hybridization of WSe_2 with MXenes and strategic doping strategies significantly enhance its electrochemical properties, making it a highly efficient material that bridges energy storage, conversion, and sensing applications.

References

[1] A. Mondal *et al.*, *Adv. Funct. Mater.* **32**, 2208994 (2022).
[2] Y. Li et al., *Nanoscale Adv.* **4**, 3142–3148 (2022).
[3] S. Cogal *et al.*, *Int J Hydrogen Energy* **49**, 689-700 (2024).
[4] A. Kagkoura et al., *Nanoscale* **17**, 947-954 (2025).
[5] A. Kagkoura et al., *J. Phys. Chem. C* **129**, 2893–2903 (2025).
[6] A. Kagkoura et al., npj 2D mater. appl. Submitted

Exploiting the Unique Properties of MXenes for Hydrogen Production via Dry Reforming of Methane

J.O. Ighalo, A. Ebrahimi, D.B. Pourkargar, P.B. Amama

Tim Taylor Department of Chemical Engineering, Kansas State University, United States

The development of coke-resistant catalysts for dry reforming of methane (DRM) is critical for sustainable syngas production. To suppress coking, this study investigates the use of $Ti_3C_2T_x$ and Nb_2CT_x MXenes as support for Ni catalysts in DRM and benchmarked their performance with conventional catalysts (Ni/γ-Al_2O_3, Ni/$MgAl_2O_4$, Ni/SiO_2). The MXenes were etched using NH_4HF_2 and a 10 wt.% Ni loading was achieved via wet impregnation synthesis. Ni/Nb_2CT_x showed the highest H_2 consumption (10.4 $mmol_{H2}/g_{cat}$). DRM was conducted at 700°C using a feed ratio of CH_4/CO_2 of 1:1 and a high space velocity (90,000 ml/g_{cat}.hr). The use of high space velocities helps to overcome diffusion limitations and achieve high throughput, features that are critical for scale-up conversion of two greenhouse gases to syngas. Unlike the other catalysts, Ni/Nb_2CT_x pre-reduced at 500°C exhibited a low normalized coking rate (4.41 $\mu g_{coke}/mmol_{CH4}$), a high overall reaction rate (104 ± 13 $mmol/g_{Ni}$.min), and the highest turnover frequency at 12.4 s^{-1}. The apparent CO_2 reaction rate at these conditions was similar to the CH_4 rate, suggesting that the low coking rate was due to the efficient utilization of dissociated oxygen. Molecular dynamics simulations performed on NbC(111) and TiC(111) surfaces at 700°C and atmospheric pressure reveal that the efficient utilization was mediated by rapid oxygen spillover. The average oxygen velocity from the simulations was slightly higher on NbC (0.0969 Å/fs) than on TiC (0.0961 Å/fs). Both MXene supports are transformed to stable oxycarbides during DRM, and Nb_2CT_x was stable for 50 h TOS. The study illuminates the catalytic properties of Ni/$Ti_3C_2T_x$ and Ni/Nb_2CT_x, such as textural properties, oxygen vacancies, metal-support interaction (MSI), and catalyst reducibility, and how they affect the catalytic performance (reaction rates, product selectivity, and resistance to catalyst deactivation) in methane reforming. The results highlight the potential of Ni/Nb_2CT_x as a coke-resistant catalyst and also demonstrate the critical role of MXene supports in the DRM process.

References

[1] J. O. Ighalo et al. *Chem. Eng. J.* **508,** 160707-16020 (2025).
[2] J.O. Ighalo et al. *2D Mater.* **12**, 022001 (2025).
[3] J.O. Ighalo, P.B. Amama *J. CO2 Util.* **81**, 102734-102751 (2024).
[4] J.O. Ighalo, P.B. Amama, *Int. J. Hydrogen Energy* **51**, 114965 (2023).

Highly Conductive Carbon Nanotube Fibers

Haozike Wang, Zhaoqing Gao, Pengxiang Hou, Chang Liu

Institute of Metal Research, Chinese Academy of Sciences (China)

Single-wall carbon nanotubes (SWCNTs) with unique one-dimensional tubular structure and excellent physical and chemical properties are considered ideal building block for the fabrication of high-performance fibers with a wide range of applications. We prepared high purity, highly crystallined SWCNTs efficiently by a floating catalyst CVD method [1]. Under optimum conditions, the conversion rate of the carbon source to SWCNTs reached ~30%, and the as-prepared SWCNTs had a purity higher than 96 wt.%. Using the as-prepared high-quality SWCNTs, we spun macroscopic SWCNT fibers with diameters of 10-20 microns by a wet-spinning process. The resulting fibers had a high electrical conductivity of 6.67×10^6 S/m [1]. We further developed a dry-jet wet spinning method, producing double-wall CNT Fibers with a high electrical conductivity of 1.1×10^7 S m^{-1} and an ampacity of 8.0×10^8 A m^{-2} [2]. A SWCNT/Cu core-shell fiber was prepared by a combined magnetron sputtering and electrochemical deposition method, which showed an ultra-high specific electrical conductivity of 1.15×10^4 S m^2 kg^{-1}, 56% higher than Cu [3]. In addition, a strong connection between the CNT fibers and Cu substrate was achieved by soldering [4].

References

[1] X. Y. Jiao *et al.*, *ACS Nano* **16**, 20263-20271 (2022).
[2] H. Z. K. Wang *et al.*, *Adv. Funct. Mate*r. **34**, 2404538 (2024).
[3] L. L. Xu *et al.*, *ACS Nano* **17**, 9245-9254 (2023).
[4] Z. Q. Gao *et al.*, *ACS Nano* **17**, 18290-18298 (2023).

Synthesis of advanced carbon material graphdiyne and their applications in sustainable energy

Xin Gao[1]

[1]*School of Materials Science and Engineering, Peking University (China)*

Designing and discovering novel nanomaterials and nanostructures and exploring their niche applications are crucial to materials science. Graphdiyne is an emerging two-dimensional carbon material, with unique *sp*-sp^2 carbon atoms and π-conjugated network. Its tunable sub-nanometer pore structure and high ion/electron mobility enable its great potential in sustainable energy, especially for batteries. However, the synthesis of high quality graphdiyne remains challenging because of the free rotation around alkyne-aryl single bonds and the lack of thickness control. Here, we developed facile synthesis methodology of high-quality, ultrathin single-crystalline graphdiyne film and graphdiyne nanowalls, including the solution-phase van der Waals epitaxial strategy and the copper envelope catalysis method. A hydrogen-substituted graphdiyne-assisted ultrafast sparking synthesis (GAUSS) platform for the preparation of metastable nanomaterials was also developed. Graphdiyne provides high density sites for supporting metastable nanomaterials. The unique structure of the graphdiyne-based metastable composites prepared by GAUSS provides abundant active sites for enhancing the sluggish Li-S redox reaction kinetics in high energy density batteries.

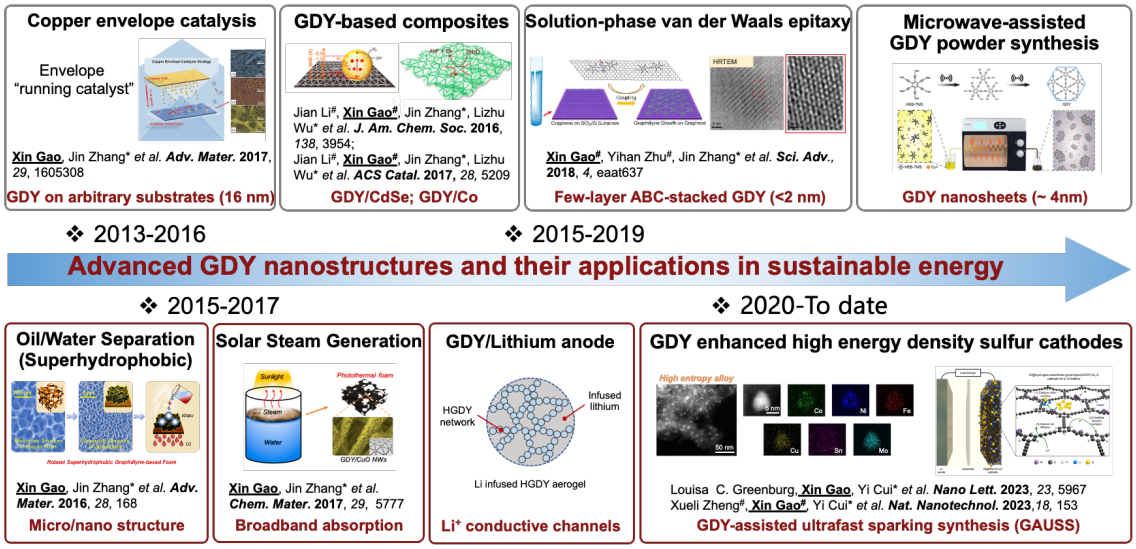

Figure 1 Advanced graphdiyne (GDY) nanostructures and their applications in sustainable energy.

References (if desired)

[1] **Xin Gao**, Jin Zhang* *et al.* ***Adv. Mater.*** **2017**, *29*, 1605308
[2] **Xin Gao**#, Yihan Zhu#, Jin Zhang* *et al.* ***Sci. Adv.*****2018**, *4,* eaat637.
[3] Xueli Zheng#, **Xin Gao**#, Yi Cui* *et al.* ***Nat. Nanotechnol.*** **2023**,*18,* 153.
[4] **Xin Gao**#, Xueli Zheng#*, Yusheng Ye#, Yi Cui* *et al.* ***Nano Lett.*** **2024**, *24*, 3044.
[5] Lianming Tong*, **Xin Gao***, Jin Zhang* *et al.* ***J. Am. Chem. Soc.*** **2024**, *146*, 14898.
[6] Lianming Tong*, **Xin Gao***, Jin Zhang* *et al.* ***Adv. Mater.*** 2024, 2405660.

Insights into the mechanism of carbon nanotubes in silicon-based anodes

Ziying He [1], Fei Wei [1,2]*

[1]*Department of Chemical Engineering and Technology, Tsinghua University, Beijing, China*

[2]*OrdosLaboratory, Ordos, Inner Mongolia, China*

Silicon-based anodes are considered ideal candidate materials for next generation lithium-ion batteries but suffer from poor electrical conductivity, large volume expansion and unstable SEI. The above issues can be effectively alleviated by adding carbon nanotubes (CNTs). However, the electrochemical performances vary significantly depending on the type of CNTs added, and the intrinsic mechanism remains unknown. Herein, we propose a non-destructive method to monitor the microscopic contact state and strain in silicon-based anodes based on in situ Raman spectroscopy. Then, we revealed that the large volume expansion of Si-based anodes leads to the acupuncture effect of short CNTs, with the compressive stress on the CNTs and the Li-ion (Li^+) diffusion energy barriers in the SEI exhibiting a linear correlation. Both the SEI and carbon-coating are penetrated by short, thick CNTs with gigapascal (GPa)-scale compressive stress, thereby accelerating electrolyte decomposition and leading to a LiF-rich SEI and an increased Li^+ diffusion barrier. Thus, long, slender CNTs are ideal for Si-based anodes. This work reveals the structure-property relationships among compressive stress, SEI components and Li^+ diffusion energy barriers, providing a novel perspective on the development of high-performance electrodes.

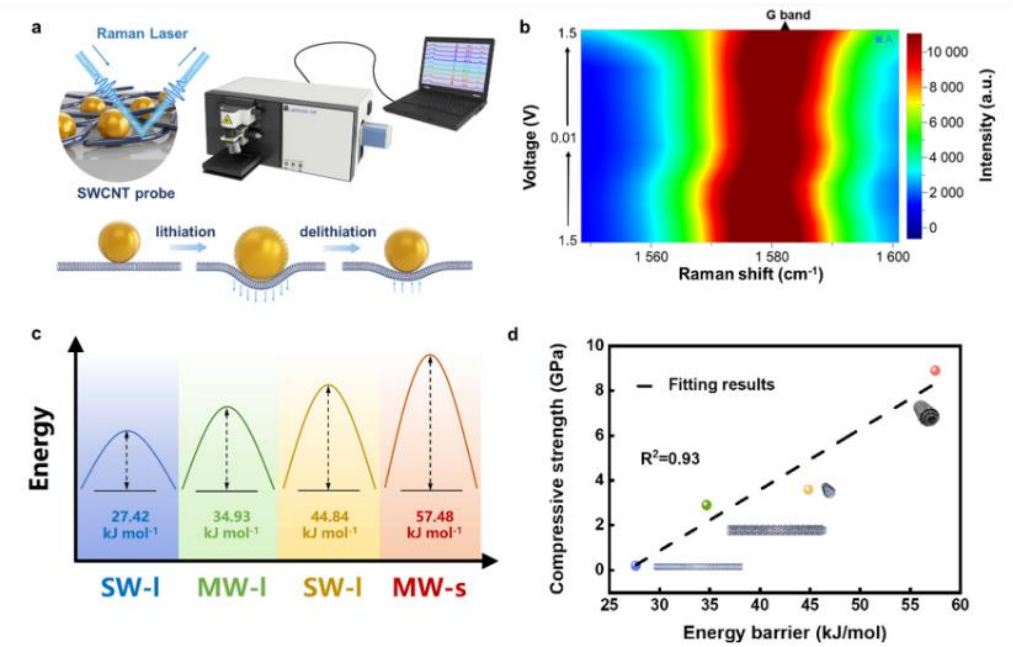

Fig. 1 The fabrication and characterization of the SiOx@C|SWCNT anode

References (if desired)

[1] Ziying He, Fei Wei* et al. Single-Walled Carbon Nanotube Film as an Efficient Conductive Network for Si-Based Anodes. Advanced Functional Materials 2023, 33, 2300094.

[2] Ziying He, Fei Wei* et al. The acupuncture effect of carbon nanotubes induced by the volume expansion of silicon-based anodes. Energy & Environmental Science 2024, 17, 3358.

[3] Ziying He, Fei Wei* et al. Advances in Carbon Nanotubes and Carbon Coatings as Conductive Networks in Silicon-Based Anodes. Advanced Functional Materials 2024, n/a (n/a), 2408285.

Fabrication and Performance Evaluation of Lithium-Sulfur Pouch Cells

M. Ezzedine[1], C-S. Cojocaru[1]

[1]*Laboratoire de Physique des Interfaces et des Couches Minces (LPICM), CNRS, École Polytechnique, IP Paris, 91128, Palaiseau Cedex, France.*

Lithium-sulfur battery (LSB) are being explored as a promising candidate to overcome the energy density limitations of traditional lithium-ion batteries (LIB). Conventional LSBs use elemental sulfur (S_8) as the cathode material due to its high theoretical specific capacity of 1672 mAh g^{-1}, world-wide abundance, and low-cost alternative to nickel and cobalt containing LIBs.[1] Metallic lithium serves as the anode, offering a theoretical specific capacity of 3860 mAh g^{-1}. The theoretical energy density of LSB is 2600 Wh kg^{-1}, which is three to five times higher than that of LIBs.[2] However, several critical challenges hinder the commercial competitiveness of the LSB, including the low conductivity of S, volume expansion, the lithium polysulfide (LiPS) shuttling effect, and sluggish reaction kinetics. To address these limitations, various advancements in electrolytes, separators, carbon materials, and electrode designs have been proposed.[3]

Despite significant research efforts demonstrating promising cell performance, most studies remain limited to small-scale coin cells, without considering for scalable designs. A considerable gap still exists between lab-scale scientific findings and practical advancements at the product level.

This work promotes the practical development of next-generation high-energy battery systems by bridging the gap between lab-scale cell assembly and prototype cell development. The proposed electrode design adopts a novel architecture, representing a disruptive approach compared to commercial LIBs. The electrodes consist of vertically aligned carbon nanotube (VACNT) carpet synthesized directly on a macroscopic metallic foil acting as a current collector. The dense VACNT carpet is decorated with S active material (S@VACNTs). Additionally, the unique architecture exploits the high electrical conductivity and large surface area of VACNTs to facilitate rapid charge transport, enabling repeated fast charging and improved power performance in high specific energy batteries.[4] Pouch cells have been successfully fabricated, demonstrating significantly enhanced performances with both liquid and quasi-solid electrolytes. Research on upscaled prototypes is imperative to identify and overcome key bottlenecks on the path toward commercialization of this technology.

References

[1] S. Dörfler, H. Althues, P. Härtel, T. Abendroth, B. Schumm, S. Kaskel, *Joule* **2020**, *4*, 539.
[2] K. Kakiage, T. Yano, H. Uehara, M. Kakiage, *Commun. Eng.* **2024**, *3*, 1.
[3] T. Cleaver, P. Kovacik, M. Marinescu, T. Zhang, G. Offer, *J. Electrochem. Soc.* **2017**, *165*, A6029.
[4] M. Ezzedine, F. Jardali, I. Florea, C.-S. Cojocaru, *J. Electrochem. Soc.* **2024**, *171*, 050531.

Session
NT 25（The 25th International Conference on the Science and Applications of Nanotubes and Low-

| Parallel Symposia：Symposium on Thin Films, Fibers, 3-D Materials and their Properties

Tue. Jun 17, 2025 2:00 PM - 5:20 PM JST | Tue. Jun 17, 2025 5:00 AM - 8:20 AM UTC Conference Room III(Clock Tower Centennial Hall, 2F)

[17mm] Macromaterials

Chair:Suguru Noda, Yoshiyuki Nonoguchi

2:00 PM - 2:20 PM JST | 5:00 AM - 5:20 AM UTC

[17mm-01]

MESOPOROUS 3-D GRAHENE MATERIALS FOR ENERGY STORAGE

*Hirotomo Nishihara[1] (1. Tohoku University (Japan))

2:20 PM - 2:40 PM JST | 5:20 AM - 5:40 AM UTC

[17mm-02]

Application of 2D carbon materials in water: adsorption of dyes and viruses

*Yuta Nishina[1] (1. Okayama University (Japan))

2:40 PM - 3:00 PM JST | 5:40 AM - 6:00 AM UTC

[17mm-03]

2D Materials for Post-AI Era: Smart Fibers, Soft Robotics & Single Atom Catalysts

*Sang Ouk Kim[1] (1. Materials Science & Engineering, KAIST (Korea))

3:00 PM - 3:20 PM JST | 6:00 AM - 6:20 AM UTC

[17mm-04]

Shaping MXenes: Templated Guided Synthesis Using Carbon Fibers

*Filipa M. Oliveira[1], Zdenek Sofer[1], Jesus Gonzalez-Julian[2] (1. University of Chemistry and Technology Prague (Czech Republic), 2. CNRS - Laboratory of Thermo-Structural Composites (LCTS) (France))

4:00 PM - 4:20 PM JST | 7:00 AM - 7:20 AM UTC

[17mm-05]

A Universal Framework for Ultra-Sensitive Pressure Sensing Enabled by Electric Double-Layer Charge Redistribution Mechanism

*Ming XU[1], Huajian Li[1] (1. Huazhong University of Science and Technology (China))

4:20 PM - 4:40 PM JST | 7:20 AM - 7:40 AM UTC

[17mm-06]

Progress in CNT Pellicle Development and Future Prospects

*Yosuke Ono[1] (1. Mitsuichemicals, Inc. (Japan))

4:40 PM - 5:00 PM JST | 7:40 AM - 8:00 AM UTC

[17mm-07]

Nanofiller effect of single-walled carbon nanotube bundles to elongate and toughen cellulose fibers

*Kazufumi Kobashi[1], Takahiro Morimoto[1], Minfang Zhang[1], Takushi Sugino[1], Toshiya Okazaki[1], Junya Tsujino[2], Hideki Kajita[2], Yasuyuki Isojima[2], Yasuo Gotoh[3] (1. National Institute of Advanced Industrial Science and Technology (Japan), 2. Omikenshi Co., Ltd. (Japan), 3. Shinshu University (Japan))

5:00 PM - 5:20 PM JST | 8:00 AM - 8:20 AM UTC

[17mm-08]

Session

NT 25（The 25th International Conference on the Science and Applications of Nanotubes and Low-

A New Conductive Network in Concrete: Interfacial Nanoengineering by Graphene

*Jing Zhong[1] (1. Harbin Institute of Technology (China))

MESOPOROUS 3-D GRAHENE MATERIALS FOR ENERGY STORAGE

H. Nishihara

Advanced Institute for Materials Research (WPI-AIMR), Tohoku University, Sendai, Japan.

To extend the application of two-dimensional (2-D) graphene in battery-related fields, significant efforts have been made by developing three-dimensional (3-D) frameworks based on graphene. Although 3-D graphene is expected to enhance battery performances, most materials reported thus far have encountered issues in precisely controlling graphene stacking, excluding graphene edge sites, and controlling nanoporous structures. This presentation will highlight a novel 3-D graphene material, customized for fast and durable energy storage, called Graphene MesoSponge® (GMS) [1].

GMS is a new type of graphene-based mesoporous material synthesized via template-directed chemical vapor deposition, followed by template removal and high-temperature annealing at 1800 °C [1,2]. GMS primarily consists of single-layer graphene walls with a minimal number of edge sites, exhibiting extreme elasticity (Fig. 1) [3]. Using in-house temperature-programmed desorption (TPD) up to 1800 °C, which can determine the number of edge sites in any sp^2-based carbon materials, it has been revealed that GMS has fewer edge sites than single-walled carbon nanotubes (SWCNTs). Consequently, GMS outperforms SWCNTs in terms of a wide voltage window, reaching up to 4.4 V when assembled in a supercapacitor [4].

Another unique feature of GMS is its topological-defect-rich framework. From the geometric requirements, GMS necessarily includes many carbon non-hexagon rings including 5- and 7-membered rings, which are called topological defects (Fig. 2) [5]. The topological defects can play the role of anchoring sites for metal nanoparticles such as Pt [6] and Ru [7], which are useful to fuel cell and Li-O_2 battery applications, respectively. Furthermore, GMS can be molded into self-standing sheets with controllable macroporosities. The optimized structure outperforms any carbon-based cathodes for Li-O_2 batteries [8].

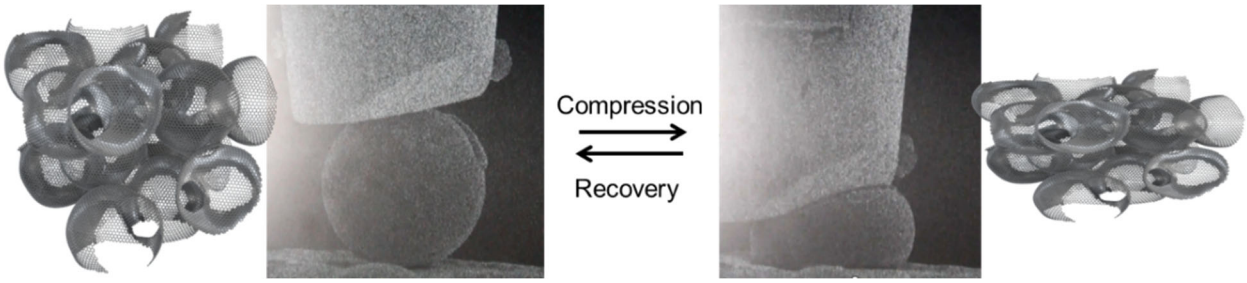

Figure 1: Unique mechanical elasticity of GMS.

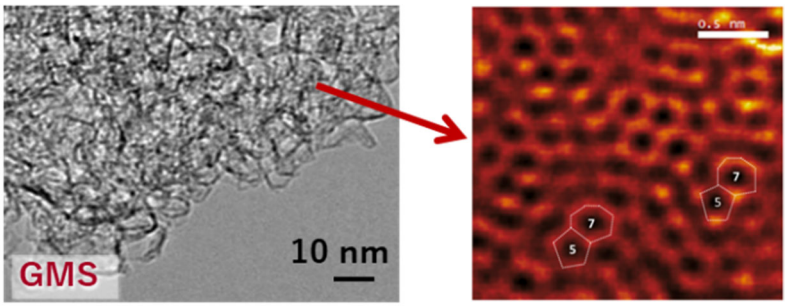

Figure 2: TEM photos of GMS.

References

[1] H. Nishihara et al., *Adv. Funct. Mater.* **26**, 6418 (2016).
[2] S. Sunahiro et al., *J. Mater. Chem. A* **9**, 14296 (2021).
[3] K. Nomura et al., *Nat. Commun.* **10**, 2559 (2019).
[4] K. Nomura et al., *Energy Environ. Sci.* **12**, 1542 (2019).
[5] W. Yu et al., *Adv. Sci.* **10**, 2300268 (2023).
[6] A. Ohma et al., *Electrochim. Acta* **370**, 137705 (2021).
[7] Z. Shen et al., *J. Phys. Chem. C* **127**, 6239-6247 (2023).
[8] W. Yu et al., *Adv. Energy Mater.* **14**, 2303055 (2024).

Application of 2D carbon materials in water: adsorption of dyes and viruses

Y. Nishina[1,2]

[1]*Okayama University (Japan)*, [2]*Shinshu University (Japan)*

Low-dimensional nanomaterials tend to stack together when dried, resulting in a very low active surface area. In contrast, when dispersed in a solvent, these materials exhibit a high surface area. To fully utilize their properties, it is preferable to handle nanomaterials in a solvent, ideally in water.

Sewage epidemiology surveys are attracting attention as an indicator of virus infection status. By analyzing sewage, it is possible to find signs of new infection clusters occurring and to identify them at an early stage before an outbreak of infection has occurred. Cotton and gauze, which are currently used as virus adsorbents, have a very low virus recovery rate (approximately 7%) and are not suitable for detecting low-concentration viruses. This study focused on developing materials that can be mass-produced and easily applied to large volumes of wastewater. Graphene oxide (GO) is a two-dimensional, high-specific-surface-area material obtained from the oxidation and exfoliation of graphite, and can be synthesized on a scale of more than 100 g even at the laboratory level. Furthermore, it is possible to adjust its physical properties by chemical modification. Although GO has shown promise in the adsorption of bacteria and viruses, it has not been applied to virus concentration. In this study, we aimed to use chemically modified GO to achieve concentration that enables the detection of viruses from low-concentration virus solutions, and to apply this to sewage epidemiological surveys.

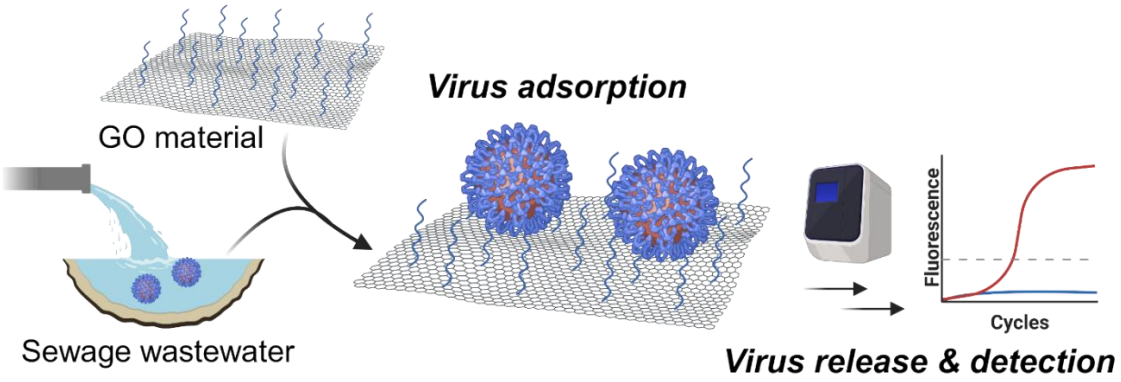

Figure. Protocol for viral detection in sewage water.

References

[1] Y. Nishina. *ACS Nano* **18**, 33264-33275(2024)

[2] P. Ferre-Pujol, S. Obata, J. Raya, A. Bianco, H. Katayama, T. Kato, Y. Nishina. *Carbon* **235**, 120015(2025)

2D Materials for Post-AI Era: Smart Fibers, Soft Robotics & Single Atom Catalysts

Sang Ouk Kim

National Creative Research Initiative Center for Multi-dimensional Directed Nanoscale Assembly, Department of Materials Science & Engineering, KAIST Institute for Nanocentury, KAIST, Daejeon 34125, Republic of Korea

Ever-expanding broad-spectrum library of 2D materials can address the critical challenges facing in the current technological trend of the 4th industrial revolution. This presentation will introduce three significant emerging application areas of 2D materials: smart fibers, soft robotics, and single atom catalysts (SACs), which hold immense potentials for the academic and technological advancements in the post-artificial intelligence (Post-AI) era [1]. Among many different types of 2D structures, Graphene Oxide Liquid Crystal (GOLC) is an intriguing 2D carbon based soft material exhibiting nematic type discotic liquid crystallinity in good solvents, such as water. Since our first discovery of GOLC at 2009 [2], this interesting mesophase has been utilized over world-wide for many different application areas, such as liquid crystalline graphene fiber spinning, highly ordered graphene membrane/film production for water treatment, nanoporous graphene assembly for energy/environmental applications and so on. Interestingly, GOLC allow us a valuable opportunity for the highly ordered molecular scale assembly of smart carbon based fibers and soft artificial muscles. Smart fibers showcase the unconventional functionalities including healthcare/environmental monitoring, energy storage/harvesting, and antipathogenic protection in the forms of wearable fibers and textiles [3]. Artificial muscle aligns with the technological trend to overcome the longstanding limitations of the hard-material based mechanics by introducing soft actuators and sensors. Noticeably, our recent development of the human muscle inspired graphene based nanocomposite fiber highlights the all-around superior performance of actuation parameters to attain the interesting demonstration of arbitrary biomimetic movements [4]. Lastly, my long-term research effort for the heteroelement-doping of graphene based structures yielded the world-first discovery of SACs [1,5,6], which are widely useful in energy storage/conversion and environmental management, principally contributing to the low carbon footprint for the sustainable post-AI era. Significance and unique values of the 2D materials in these emerging applications are highlighted, where my research group has devoted research efforts for more than a decade.

References

[1] G. S. Lee *et al.*, *Adv. Mater.* DOI: 10.1002/adma.202307689 –Hall of Fame review.
[2] S. P. Sasikala *et al*., *Chem. Soc. Rev.* **47**, 6013–6045 (2013) – Front Cover, Invited.
[3] H. J. Jung *et al*., *ACS Cent. Sci.* **6**, 1105-1114 (2020) – Front Cover.
[4] I. H. Kim *et al*., *Nat. Nanotechnol.* **17**, 1198-1205 (2022) – Front Cover.
[5] I. H. Kim *et al.*, *Acc. Mater. Res.* **2**, 394-406 (2021) – Front Cover.
[6] D. H. Lee *et al.*, *PRL* **106**, 175502 (2011).

Shaping MXenes: Templated Guided Synthesis Using Carbon Fibers

Filipa M. Oliveira*[1], Zdeněk Sofer[1], & Jesus Gonzalez-Julian[2]

[1] *Department of Inorganic Chemistry, Faculty of Chemical Technology, University of Chemistry and Technology Prague, Technická 5, 166 28 Prague 6, Czech Republic*

[2] *Laboratory of Thermo-Structural Composites (LCTS), 3, Allée La Boétie, F 33600, Pessac, France*

MXenes, a distinguished class of two-dimensional (2D) transition metal carbides and nitrides, exhibit exceptional properties that make them highly promising for electromagnetic shielding, catalysis, sensing, and energy storage applications. Their performance is intrinsically linked to their structure and morphology, necessitating precise control over their synthesis.

This study presents a versatile approach for synthesizing MXenes using carbon fibers (CF) as both a carbon source and a structural template. This method employs a molten salts shielded synthesis (MS3) process conducted entirely in air, eliminating the need for protective inert atmospheres and hazardous etching agents like hydrofluoric acid. CF enables the formation of a tubular MAX phase precursor, which retains its hollow morphology after selective etching to obtain the corresponding MXene.

Comprehensive structural and chemical characterization, including X-ray diffraction, X-ray photoelectron spectroscopy, and transmission electron microscopy, confirms the preservation of the tubular architecture and alignment of MXene layers. The methodology demonstrated here is adaptable to different MAX phases, offering a scalable and environmentally friendly route to tailoring MXene morphology. The ability to engineer MXenes with controlled structures expands their potential across various applications, including gas separation, liquid filtration, and ion transport systems. This study paves the way for further exploration of alternative templates and synthesis conditions to broaden the MXene material family.

A Universal Framework for Ultra-Sensitive Pressure Sensing Enabled by Electric Double-Layer Charge Redistribution Mechanism

Huajian Li [1], Ming Xu[1]*

[1] *School of Materials Science and Engineering, Huazhong University of Science and Technology, Wuhan, China…*

Achieving high sensitivity across a wide pressure range remains a fundamental challenge in pressure sensing due to the inherent trade-off between sensitivity and structural stability. Conventional sensors, including piezoresistive and capacitive types, often suffer from nonlinear responses, mechanical fatigue, or limited adaptability. Here, we introduce a novel sensing principle that leverages electric double-layer (EDL) charge redistribution, where pressure-induced variations in interfacial geometry dynamically modulate local charge density and electric potential, ensuring highly stable and tunable signal output (Figure 1) [1-3]. To further enhance signal transduction and mechanical adaptability, we integrate a hierarchical interlocking architecture in carbon nanotube (CNT) networks, where macro- and micro-scale groove structures regulate stress distribution and interfacial charge transport. This approach mitigates stress concentration and preserves effective charge storage, achieving an unprecedented detection range spanning six orders of magnitude. Our sensor demonstrates record-breaking sensitivity (2437.1 kPa^{-1}) and weak pressure detection (190 mPa) at 100-meter depths**,** surpassing existing deep-sea sensors and rivaling air-based counterparts. Supported by Poisson's equation modeling, stress distribution simulations, and experimental validation**,** this framework provides a universal strategy for next-generation pressure sensors, with applications spanning underwater exploration, biomedical monitoring, and robotic tactile sensing [4].

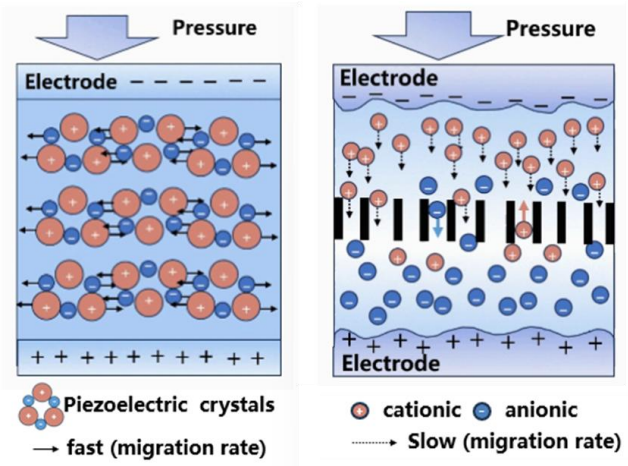

Figure 1: Comparison of Piezoelectric Sensing and Electric Double-Layer Charge Redistribution Sensing Mechanisms

References (if desired)

[1] Zhang M, *et al.*, *Advanced Functional Materials* **30**, 2004564 (2020).
[2] Wu S, *et al.*, *Advanced Materials*, **34**, 2201046 (2022).
[3] Li H, *et al.*, *Device*, **1**, 100223 (2024)
[4] Li H, *et al. submitted* (2025)

Progress in CNT Pellicle Development and Future Prospects

Yosuke. Ono[1]

[1]*Mitsui Chemicals, Inc. (Japan)*

In this presentation, the history of CNT pellicle development, the latest development status, and future challenges will be highlighted.

Pellicles are dust-proof membrane used to protect photomasks for photo lithography from particle and defects in the environment.

Mitsui Chemicals has been commercially producing EUV pellicles since 2021. Currently, silicon-based thin membrane are used for EUV pellicle, but as the EUV scanner light source power increase, higher heat resistance are required for pellicle membrane. Under such situation, CNT pellicles, which have both very high heat resistance and high EUV transmittance, are attracting much interest as the top candidate for next-generation EUV pellicle.

We began basic research on CNT pellicles in 2015, and since 2017, in collaboration with the National Institute of Advanced Industrial Science and Technology (AIST), we have successfully developed full-size CNT membranes with EUV transmission over 96%. Since 2023, MCI signed a strategic partnership agreement with imec and is also promoting the development of pellicles compatible with next-generation exposure machines equipped with high-power EUV light sources. And now, a factory for the mass production of CNT pellicles is being set up and constructed with a target completion date of the end of 2025. In other words, commercialization of CNT pellicles is just around the corner.

CNT pellicles need to satisfy various performance requirements, for example, imaging, lifetime, defects, and mechanical strength properties. Lifetime is a performance of particular interest, and various approaches, including coatings on CNTs, are being investigated to further improve lifetimes. Factors and challenges affecting the life time will be discussed.

Our CNT pellicles also can prevent the penetration of nanoscale particles, and the cleanliness of the photomask can be kept by controlling the cleanliness of the CNT pellicle itself appropriately. In addition, our CNT pellicles are characterized by almost no dust emission or scattering of μm to nm level small fibers even in the event of membrane rupture.

By taking advantage of the unique characteristics of CNTs and their performance as pellicles, CNT pellicles can contribute to improving the performance of future semiconductor chips and further growth of the semiconductor market.

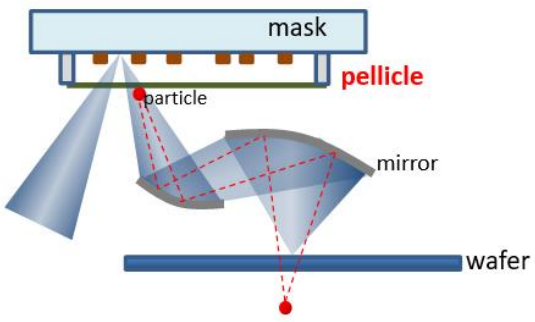

Figure 1: Schematic image of the EUV pellicle in the EUV lithography scanner to prevent defects transfer on the wafer.

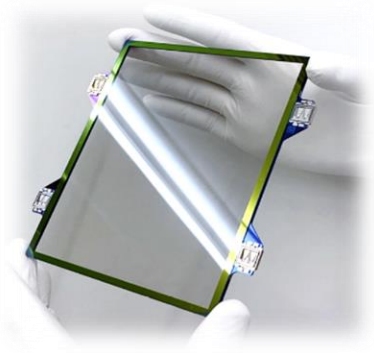

Figure 2: CNT pellicle

Nanofiller effect of single-walled carbon nanotube bundles to elongate and toughen cellulose fibers

K. Kobashi[1], T. Morimoto[1], M. Zhang[1], T. Sugino[1], T. Okazaki[1],
J. Tsujino[2], H. Kajita[2], Y. Isojima[2], Y. Gotoh[3]

[1]*National Institute of Advanced Industrial Science and Technology (Japan),*
[2]*Omikenshi Co., Ltd. (Japan),* [3]*Shinshu University (Japan)*

Regenerated cellulose fibers have been produced from renewable natural resources and widely used, e.g. as a tire cord fabric. However, environmentally burdened chemicals like CS_2 have been required to produce classic cellulose fibers (viscose Rayon) [1]. Thus, we propose an eco-friendly cellulose fiber made by a recyclable ionic liquid, further mechanically toughened by a nanofiller [2]. A synergetic integration of slight amount (0.1 wt%) of single-walled carbon nanotubes (CNT, Zeonano SG101) and cellulose matrix gave the increased (34%) elongation and the retained tensile strength, thus creating the enhanced (39%) toughness (Fig. (a)). Such a filler effect is different from conventional ones generally to decrease the elongation in return for the increased strength. To bring the unique filler effect, control of the bundled CNT particle size was essential. Centrifugal sedimentation was suitable for analyzing the CNT particle sizes in the viscous dispersions of ionic liquid. The elongation and toughness of fibers enhanced in the scope of 400 to 800 nm in CNT particle size (Stokes diameter) (Fig. (b)). To directly visualize the structure of bundled CNT particles in the fibers, both of transverse and longitudinal cross-sections were elaborately made by ion milling. The SEM images displayed the bundled CNT particles possessing ca. 100 nm in width and several micrometers in length, intriguingly resembling a size of cellulose microfibril (Fig. (c, d)). These results demonstrate a smooth transfer of bundled CNT particles from ionic liquid dispersions to cellulose fibers, leading to the nanofiller effect of CNTs. Our findings can give an insight into nanofiller science and expand an environmentally benign use of cellulose.

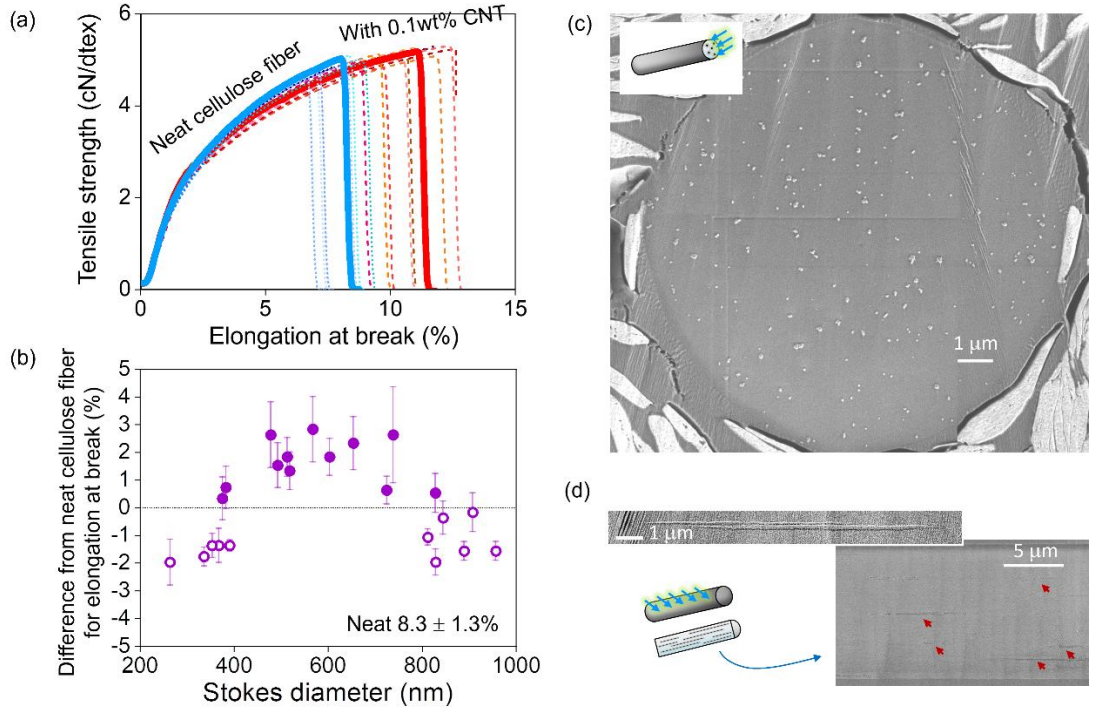

Figure: (a) Stress-strain curves for tensile test of neat cellulose (thin dotted) and CNT/cellulose fibers (thin dashed) with each of the most average ones shown as thick curves, (b) gains and losses in the elongation of the CNT/cellulose fibers plotted versus a CNT particle size in dispersion of ionic liquid (Stokes diameter), and SEM images of (c) transverse, (d) longitudinal cross-sections made by ion milling. These fibers were made by dry-jet wet spinning.

References

[1] H. Shen *et al.* Macromol. Mater. Eng., **308**, 2300089 (2023).
[2] K. Kobashi *et al*. Compos. B Eng., **283**, 111643 (2024).

A New Conductive Network in Concrete: Interfacial Nanoengineering by Graphene

Jing. Zhong

School of Civil Engineering, Harbin Institute of Technology, Harbin, China

The page is limited to one page.Traditionally, conductive fillers are mixed directly with cement matrix before binding with aggregates to develop piezoresistive cement-based sensors. This results in the most vulnerable region, interfacial transition zone (ITZ), from which microcracks are initiated, merely located at the periphery of the conductive network and thus limits the sensitivity of the smart sensor. Recently, we propose a strategy to construct a three-dimensional (3D) conductive network in the mortar with ITZ directly embedded in it, thus greatly increasing both the conductivity and piezoresistivity without significantly sacrificing mechanical property. Highly conductive graphene-coated fine aggregates (termed conductive G@FAg particles) are prepared by adsorption of graphene oxide (GO) onto the fine aggregates (FAg) surface, followed by simple annealing and microwave treatment. The combined usage of conductive G@FAg particles and results in an outstanding electrical conductivity and an excellent fractional change in resistivity under cyclic compressive loading, with a negligible compressive strength loss. The much-improved conductivity and FCR value with such a low weight percentage of conductive carbon materials are attributed to the unique 3D network of conductive channels. Such general strategy of nano-interface engineering with graphene derivatives can also be readily extended to the promotion of other physical properties (strength, EMI, damping, mass transportation, et al), thus opens a new window to optimize properties of cementitious materials.

Session
NT 25（The 25th International Conference on the Science and Applications of Nanotubes and Low-

| Parallel Symposia：17th Symposium on Computational Challenges in Nanotubes, 2D Materials, and Their Macroscopic Assemblies

Tue. Jun 17, 2025 2:00 PM - 5:20 PM JST | Tue. Jun 17, 2025 5:00 AM - 8:20 AM UTC Conference Room IV(Clock Tower Centennial Hall, 2F)

[17ct] Computation and Theory

Chair:Vassili Perebeinos, Mikito Koshino

2:00 PM - 2:40 PM JST | 5:00 AM - 5:40 AM UTC

[17ct-01]

Many-body interactions in optical properties of low-dimensional materials

*Vasili Perebeinos[1] (1. University at Buffalo (United States of America))

2:40 PM - 3:00 PM JST | 5:40 AM - 6:00 AM UTC

[17ct-02]

Contacts to Low-Dimensional Semiconductors: Physics-Based Analytical Model

*Jimmy Qin[1], H. S. Philip Wong[1] (1. Stanford University (United States of America))

3:00 PM - 3:20 PM JST | 6:00 AM - 6:20 AM UTC

[17ct-03]

ELECTRONIC STRUCTURES OF THIN FILMS OF ATOMIC LAYER MATERIALS

*Mina Maruyama[1] (1. University of Tsukuba (Japan))

4:00 PM - 4:20 PM JST | 7:00 AM - 7:20 AM UTC

[17ct-04]

Simulating CVD Carbon Nanotube Growth on Alloy Nanoparticles

*Alister J Page[1] (1. University of Newcastle (Australia))

4:20 PM - 4:40 PM JST | 7:20 AM - 7:40 AM UTC

[17ct-05]

Transient C-O single bond by femtosecond laser on graphene oxide studied by the time-dependent density functional theory

*Yoshiyuki Miyamoto[1], Tokutaro Komatsu[2] (1. National Institute of Advanced Industrial Science and Technology (Japan), 2. School of Medicine, Nihon University (Japan))

4:40 PM - 5:00 PM JST | 7:40 AM - 8:00 AM UTC

[17ct-06]

Topological Design of Low-Dimensional Carbon Materials for Novel Spintronics - Carbon Nanotubes in the Natural Helical Crystal Lattice Scheme

*Elise Yu-Tzu Li[1] (1. National Taiwan Normal University (Taiwan))

5:00 PM - 5:20 PM JST | 8:00 AM - 8:20 AM UTC

[17ct-07]

Exascale transport simulations for the understanding of the switching mechanism in atomically thin memristors

*Liangbo Liang[1], Wenchang Lu[2], Jameela Fatheema[3], Emil Briggs[2], Deji Akinwande[3], Jerzy Bernholc[2], Panchapakesan Ganesh[1] (1. Oak Ridge National Lab (United States of America), 2. North Carolina State University (United States of America), 3. The University of Texas at Austin (United States of America))

Many-body interactions in optical properties of low-dimensional materials

V. Perebeinos
Electrical Engineering Department, University at Buffalo, USA

Atomically thin two-dimensional materials are direct bandgap semiconductors with a rich interplay of the valley and spin degrees of freedom, which offer the potential for electronics and optoelectronics. A strong Coulomb interaction leads to tightly bound electron-hole pairs or excitons and two-electron one-hole quasiparticles or trions. We solve the two-particle and three-particle problems for the wavefunctions for excitons and trions in the basis set of the model- Hamiltonian for single particles. The calculated linear and nonlinear absorptions, photoluminescence spectra, and polariton spectra as a function of doping and temperature explain the experimental data in 2D monolayers and predict novel spectroscopic features due to the many-body Coulomb interactions [1-5]. Exciton lifetime plays a crucial role in optoelectronic applications. I will also discuss the phonon-assisted Auger non-radiative decay mechanism of excitons in doped 2D materials [6]. Finally, I will discuss the role of many-body interactions on second harmonic generation in carbon nanotubes [7].

References

[1] Y.V. Zhumagulov, A. Vagov, N.Y. Senkevich, D.R. Gulevich, V. Perebeinos, “Three-particle states and brightening of intervalley excitons in a doped MoS2 monolayer”, *Phys. Rev. B* **101**, 245433 (2020)

[2] Y.V. Zhumagulov, A. Vagov, P.F. Junior, D.R. Gulevich, V. Perebeinos, “Trion induced photoluminescence of a doped MoS2 monolayer”, *J. Phys. Chem.* **153**, 044132 (2020)

[3] Y. V. Zhumagulov, S. Chiavazzo, D. R. Gulevich, V. Perebeinos, I. A. Shelykh, O. Kyriienko, “Microscopic theory of exciton and trion polaritons in doped monolayers of transition metal dichalcogenides”, *npj Comput. Mater.* **8**, 92 (2022)

[4] Y. V. Zhumagulov, A. Vagov, D. R. Gulevich, V. Perebeinos, “Electrostatic and Environmental Control of the Trion Fine Structure in Transition Metal Dichalcogenide Monolayers”, *Nanomaterials* **12**, 3728 (2022)

[5] V. D. Neverov, A. E. Lukyanov, Y. V. Zhumagulov, D. R. Gulevich, A. V. Krasavin, A. Vagov, V. Perebeinos, “Non-linear spectroscopy of excitonic states in transition metal dichalcogenides”, *Phys. Rev. B* **105**, 239902 (2022)

[6] B. Scharf, V. Perebeinos, “Phonon-Assisted Auger Decay of Excitons in Doped Transition Metal Dichalcogenide Monolayers”, *J. Chem. Phys.* **161**, 134709 (2024)

[7] R. Xu, J. Doumani, V. Labuntsov, N. Hong, A.C. Samaha, W. Tu, F. Tay, E. Blackert, J. Luo, M. El Tahchi, W. Gao, J. Lou, Y. Yomogida, K. Yanagi, R. Saito, V. Perebeinos, A. Baydin, J. Kono, H. Zhu, “Giant Second Harmonic Generation from Wafer-Scale Aligned Chiral Carbon Nanotubes”, arXiv:2407.04514

Contacts to Low-Dimensional Semiconductors: Physics-Based Analytical Model

Jimmy Qin[1], H.-S. Philip Wong[1]
[1] *Department of Electrical Engineering, Stanford University, Stanford, CA 94305, USA*

Understanding the physics of metal contacts to low-dimensional semiconductors, such as transition-metal dichalcogenides (TMD) and carbon nanotubes (CNT), is critical for developing low-resistance contacts required for advanced nanoelectronics. However, it is not well understood how metal-induced gap states (MIGS) and Fermi-level pinning in these contacts depend on the semiconductor, metal, and their interaction. We propose that, in the absence of defects, the MIGS are simply tail states of the semiconductor generated by the metal-semiconductor interaction. We show that Γ(E), the imaginary part of the carrier self-energy, is the key to understanding the physics of MIGS, Fermi-level pinning, Schottky barrier, and contact transfer length. In the limit of small Γ(E), we derive analytical formulas for the MIGS density, charge neutrality level (CNL), Schottky barrier height, transfer length, and overall contact resistance. We show that these simple expressions yield transparent interpretations of recent contact experiments, such as metal-on-CNT [1, 2] and semimetal-on-TMD [3, 4]. The results give new technological insights into contact engineering techniques, such as semimetal-on-semiconductor contacts and doping, and clarify what requirements these techniques must satisfy to yield scalable and low-resistance contacts.

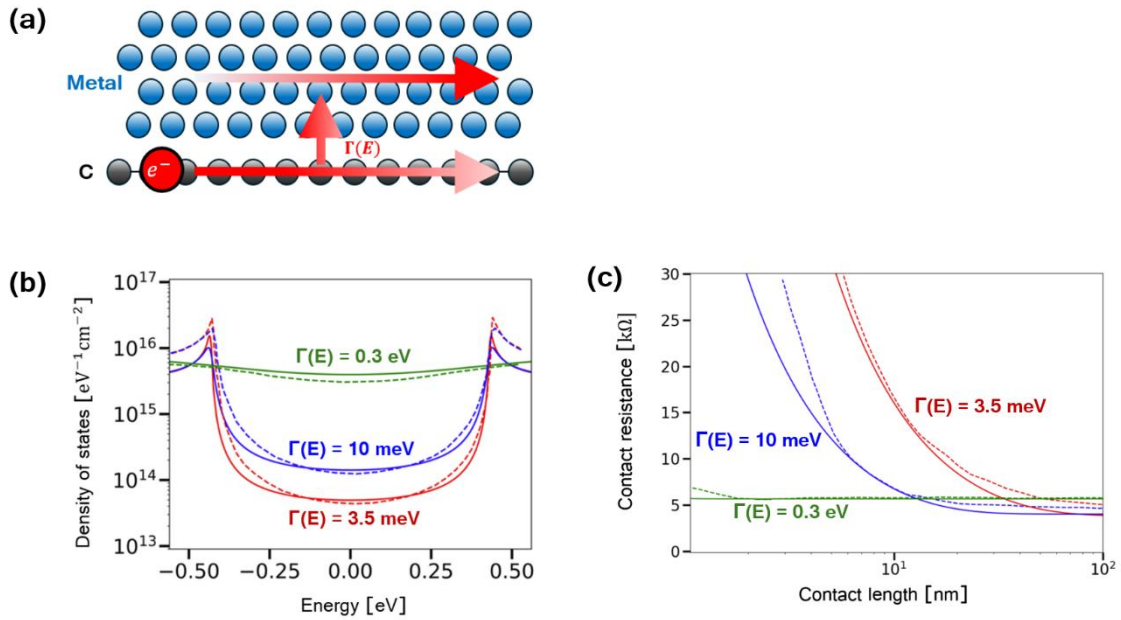

Fig 1. Contact physics in a metal-on-CNT contact. (a) Illustration of electron transport under the contact with nonzero metal-semiconductor interaction Γ(E). The metal is assumed to wrap around the CNT, so only a single layer of carbon atoms in contact with the metal is shown. (b) Comparison of metal-induced gap states (MIGS) density obtained from analytics (solid lines; this work) and from NEGF simulation (dashed lines; ref. [2]). (c) Comparison of contact resistance to a (13,0) single-walled nanotube obtained from analytics (solid lines; this work) and from NEGF simulation (dashed lines; ref [2]).

References

[1] G. Pitner *et al.*, *Nano Letters* **19** (2), 1083-1089 (2019).
[2] S. Su *et al.*, *IEEE Elec. Dev. Lett.*, **43** (8), 1367-1370 (2022).
[3] P. Shen *et al.*, *Nature* **593**, 211–217 (2021).
[4] L. Hoang, *et al.* arXiv:2409.18926 (2024).

ELECTRONIC STRUCTURES OF THIN FILMS OF ATOMIC LAYER MATERIALS

M. Maruyama[1]

[1]*University of Tsukuba (Japan)*

Atomic layer materials can form layered or thin film structures with various interlayer stacking arrangement owing to their chemically inert flat surfaces. The physical properties of these layered materials exceed the simple superposition of those of each layer. For instance, first-principles calculation based on the density functional theory predicted that graphene thin films with the rhombohedral stacking arrangement show surface localized state that causes the spin polarization on the outermost layers [1]. Twisted bilayer graphene with a particular twist angle exhibits superconductivity due to the flat dispersion band at the Fermi level [2]. Bilayer hexagonal boron nitride shows ferroelectricity normal to the layers because of symmetry breaking [3]. Therefore, these facts imply that the stacking arrangement is a new degree of freedom to control the physical properties of such layered materials. In this paper, we reported our recent theoretical calculations on layered structures comprising atomic layer materials, using the density functional theory combined with the effective screening medium method. Our calculations demonstrated that stacking arrangements induce unusual electronic and electrostatic properties on layered structure of atomic layer materials.

References

[1] M. Otani *et al.*, *Phys. Rev. B* **81**, 161403(R) (2010).
[2] Y. Cao *et al.*, *Nature* **556**, 43–50 (2018).
[3] K. Yasuda *et al.*, *Science* **372**, 1458–1462 (2021).

Simulating CVD Carbon Nanotube Growth on Alloy Nanoparticles

A. J. Page,[1] B. McLean[2]

[1]*University of Newcastle, Australia,* [2]*RMIT University, Melbourne, Australia*

For decades, alloy catalyst composition has been employed as a design parameter for improving and controlling chemical vapour deposition carbon nanotube growth. A historical impediment to our mechanistic understanding of CNT growth on alloy nanoparticles, however, has been the lack of computational methods with sufficient accuracy and efficiency to simulate CVD over relevant time scales.

Here, we study the elementary stages of methane chemical vapour deposition on CoRu alloy nanoparticles to gain insights into CNT nucleation and growth. We employ the GFN1-xTB method [1], a tight-binding method that incorporates key quantum chemical phenomena, including polarisation and dispersion, based on one-centred electronic parameters. This provides a key benefit over other tight-binding methods and empirical/machine learning force fields, viz. that two-centre parameters (overlap and Hamiltonian matrix elements etc.) or empirical bond and angle force field parameters do not need to be explicitly parameterised. GFN1-xTB affords a level of accuracy that is qualitatively consistent with full PBE for the systems studied in this work.

We consider Ru loadings between 0 and 30%, relevant to recent experiments [2]. Our simulations (Figure 1) show that, at temperatures relevant to CVD growth of CNTs, the 55-atom CoRu nanoparticles present in our simulation almost immediately phase-separate into a morphology reminiscent of a core-shell structure; Ru is almost entirely located within the nanoparticle core, while Co is located at the nanoparticle surface. Similar phase separation phenomena has been observed experimentally for CoW alloys [3]. The effect of this segregation does not significantly impact the physical state of the nanoparticle (i.e. solid/liquid). However, precursor decomposition and CNT nucleation is driven exclusively by Co in these CoRu alloys. Interestingly, the Ru content in the nanoparticle still has a dramatic, yet indirect, impact on the catalytic efficiency of the nanoparticle overall, as well as the morphology of the nucleating sp^2 carbon network that nucleates prior to CNT growth. We show ultimately these effects derive from Ru's influence on the nanoparticle Fermi level, and therefore catalytic efficiency, which can be understood in terms of established ideas in heterogeneous catalysis, such as d-band theory [4].

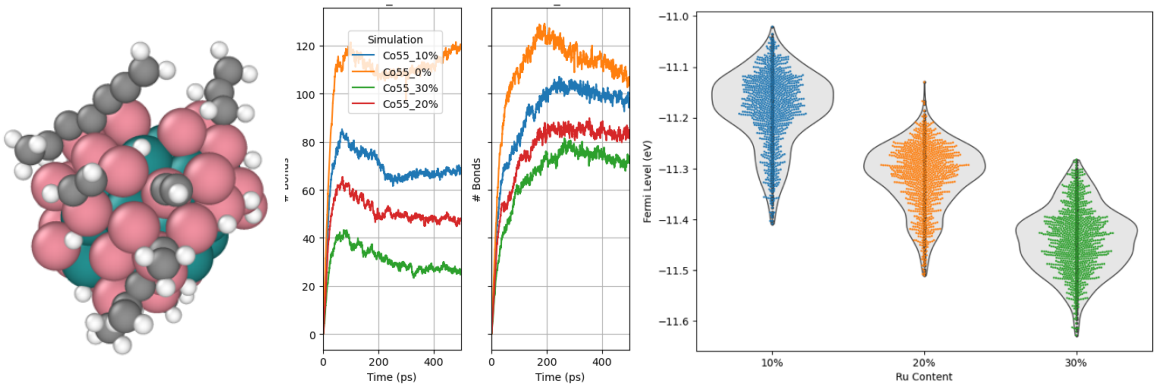

Figure 1. GFN1-xTB/MD simulations of methane CVD on CoRu alloy nanoparticles (left) as a function of Ru loading (0-30%) show that Ru content influences overall catalytic efficiency and CNT nucleation (centre) indirectly via modulation of the nanoparticle Fermi level (right).

References

[1] Grimme et al., *J Chem Theor Comp* **13** 1989-2009 (2017)
[2] Everhart et al., *Chem Mater* **34**, 4548-4559 (2022)
[3] Cui et al., *Nanoscale* **3** 1608-1617 (2016)
[4] Hammer, Nørskov, *Nature* **376** 2238-2240 (1995)

Transient C-O single bond by femtosecond laser on graphene oxide studied by the time-dependent density functional theory

Yoshiyuki Miyamoto[1], and Tokutaro Komatsu[2]

[1]National Institute of Advanced Industrial Science and Technology (Japan), [2]School of Medicine, Nihon University (Japan)

In this presentation we will demonstrate that chemically unstable shape of adsorbate on graphene can appear by shining femtosecond laser with adjusted intensity[1]. Transient formation of C-O single bonds on epoxide of graphene oxide was monitored by performing the *ab-initio* molecular dynamics (MD) by laser irradiation within the scheme of the time-dependent density functional theory (TDDFT)[2]. We have used numerical scheme for solving the time-dependent Kohn-Sham equation with use of the plane-waves[3] and the open-source code FPSEID21[4]. We assumed laser conditions (wavelength and pulse duration) as same as used in experiment for reducing the graphene oxide[5] and found C-O-single bond formation with laser intensity just below the threshold of the reduction. The nature of the single bond was confirmed by analyzing valence wavefunctions of the C-O bond obtained by the constraint DFT and by the complete active space self-consistent (CASSCF) calculations.

The formed C-O bonds were found to be inert by performing further TDDFT-MD simulation with the same laser condition but with presence of water molecules nearby the epoxide. The inert nature of C-O single bond sounds strange, but indeed this is the case only under the electronic excited state. We will discuss how to monitor this transient structure and potential applications.

The figure shows snapshots of the TDDFT-MD simulation with wavelength 266 nm, pulse duration time, 100 fs, and fluence of 0.8 J/cm^2.

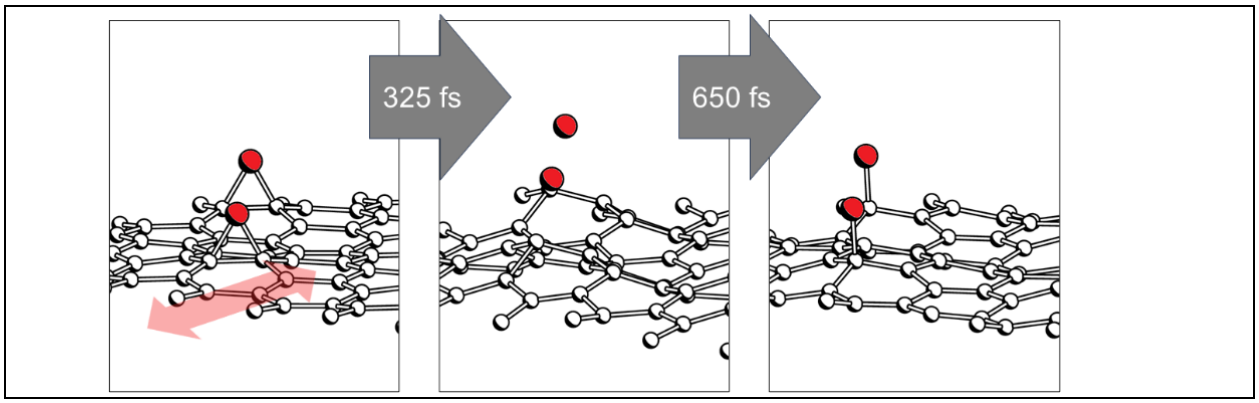

Figure caption: Snapshots of TDDFT-MD simulation with laser conditions mentioned in the main text. The hatched balls denote oxygen atoms while the open ball denote carbon atoms. Red arrow in the left panel shows polarization direction of the laser field.

References (if desired)

[1] Y. Miyamoto and T. Komatsu, *CARBON.* **233**, 119847 (2025).
[2] E. Runge and E. K. U. Gross, *Phys. Rev. Lett.*, **52**, 997-1000 (1984).
[3] O. Sugino and Y. Miyamoto, *Phys. Rev. B* **59**, 2579–2586 (1999).
[4] https://staff.aist.go.jp/yoshi-miyamoto/
[5] M. Hada, *et al.*, *ACS Nano* **13**, 10103–10112 (2019)

Topological Design of Low-Dimensional Carbon Materials for Novel Spintronics - Carbon Nanotubes in the Natural Helical Crystal Lattice Scheme

Elise Y. Li

Department of Chemistry, National Taiwan Normal University (Taiwan)

Low-dimensional carbon allotropes (0D to 2D) exhibit intriguing geometry-dependent electronic and magnetic properties, making them promising candidates for spintronic applications. In this talk, we present our theoretical investigations on all-carbon materials, focusing on their spin separation, combination mechanisms, and band structure modulations. We explore the chemical tuning of spin states through rational molecular design, beginning with zero-dimensional triangulene fragments and their spin combination rules under various connectivity schemes and size amplifications. Extending these concepts, we investigate how superatomic assemblies can form one- and two-dimensional periodic structures, such as magnetic covalent organic frameworks, and analyze their impact on spin-polarized band structures. Furthermore, we introduce our theoretical framework on topological effects in one-dimensional nanoribbons and chiral carbon nanotubes, revealing new possibilities for spin control. Through these studies, we establish design principles for carbon-based spin interactions and assess their potential for next-generation spintronic materials.

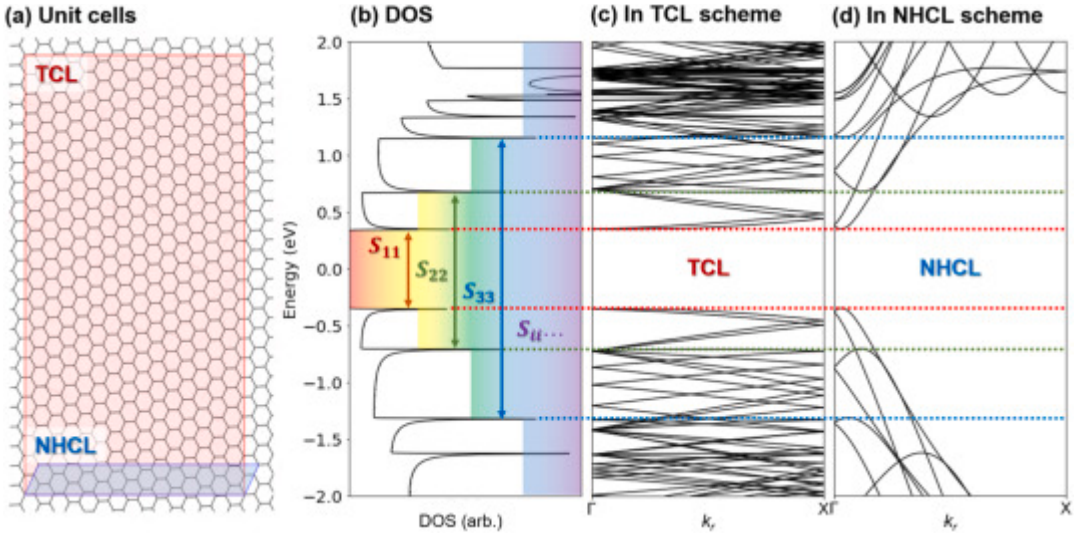

Figure caption: An (8, 7)-CNT in the TCL (red rectangle) and the NHCL (blue parallelogram) schemes.

References

[1] C.-H. Lu and **E. Y. Li***, "A New Graph Theory to Unravel the Bulk-Boundary Correspondence of Graphene Nanoribbons", *Carbon,* **2024**, 230, 119624

[2] J.-Y. Hsiao†, C.-Y. Liu†, and **E. Y. Li***, "Spintronic Interactions Between Topological Edge States in Chiral Carbon Nanotubes: A Natural Helical Symmetry Approach", *J. Mater. Chem. C,* **2023**, 11, 15001-15007

[3] D.-R. Wu, P. Yeh, Y.-T. Chen, C.-H. Lu, J.-Y. Hsiao, and **E. Y. Li***, "Engineering Triangulene Building Blocks with Tunable Magnetic Exchange Coupling for All-Carbon-Based Molecular Spintronics", *J. Phys. Chem. C*, **2023**, 127, 13249-13255

[4] C.-Y. Liu†, J.-J. Hsiao†, and **E. Y. Li***, "A global prediction of the Kataura plot for chiral carbon nanotubes: Topological family effect revealed in the natural helical crystal lattice scheme", *Carbon*, **2023**, 208, 72-81

Exascale transport simulations for the understanding of the switching mechanism in atomically thin memristors

Liangbo Liang[1], Wenchang Lu[2], Jameela Fatheema[3], Emil Briggs[2], Deji Akinwande[3], Jerzy Bernholc[2], Panchapakesan Ganesh[1]

[1]*Center for Nanophase Materials Sciences, Oak Ridge National Laboratory, Oak Ridge, Tennessee 37831, USA*

[2]*Department of Physics, North Carolina State University, Raleigh, NC 27695, USA*

[3]*Microelectronics Research Center, The University of Texas at Austin, Texas 78758, USA*

Non-volatile resistive switching (NVRS) has emerged as an important concept in the development of high-density information storage and computing. The recent discovery of NVRS in two-dimensional (2D) monolayer structures, such as MoS_2 and hexagonal boron nitride (hBN), open a new avenue for memory/computing devices at the ultrathin scale. The fundamental switching mechanism in 2D monolayers, however, is not yet fully understood. It is hypothesized that vacancies in 2D monolayers mediate formation of conducting filamentary channels leading to a high- to low resistance state. However, questions remain as to why the current on/off ratio and switching voltage are both strongly device-dependent and vary significantly among different experimental works. To address these questions, it is highly desirable to simulate the electronic transport in a realistic device geometry using *ab initio* approaches for comparison with experimental data. This is rather challenging as quantum transport simulations are computationally demanding. Here, for the first time, we report results from simulations of electronic transport of ~1000 atom systems consisting of a hBN monolayer sandwiched by top and bottom gold electrodes and compute *I-V* curves. These large quantum transport simulations are made possible by implementing the non-equilibrium Green's function (NEGF) method in a highly scalable first-principles DFT code: the Real-space MultiGrid (RMG) that runs efficiently in the first exascale supercomputer, Frontier, at Oak Ridge National Laboratory. Systematic calculations reveal that experimental devices exhibit a wide range of on/off ratios due to variations in interface distances between the electrode and h-BN that significantly modulates the gold/h-BN wavefunction overlap. In addition, DFT calculations demonstrate that the energy barrier of a gold atom to dissociate from the electrode and bind with h-BN increases dramatically with the interface distance, thereby explaining the strong dependence of the switching voltage on distance. Our work provides a deeper understanding of the resistive switching mechanism in atomically thin memristors and demonstrates the significance of interface distance in governing the current on/off ratio and switching voltage.

Session
NT 25（The 25th International Conference on the Science and Applications of Nanotubes and Low-

| Parallel Symposia：6th Symposium on Synthesis, Purification, Functionalization, and Manufacturing of Carbon Nanotubes and Low-Dimensional Materials

Tue. Jun 17, 2025 2:00 PM - 5:20 PM JST | Tue. Jun 17, 2025 5:00 AM - 8:20 AM UTC HORIBA Symposium Hall (INNOVATION BLDG., 5F)

[17sy] Synthesis

Chair:Don N Futaba, Guohai Chen

2:00 PM - 2:20 PM JST | 5:00 AM - 5:20 AM UTC

[17sy-01]

Salt-Assisted Growth of Transition Metal Dichalcogenide Nanotubes: Mechanisms from Molecular Dynamics

*Alister J Page[1], Daniel S Vadseth[1], Shigeo Maruyama[2] (1. University of Newcastle (Australia), 2. Tokyo University (Japan))

2:20 PM - 2:40 PM JST | 5:20 AM - 5:40 AM UTC

[17sy-02]

Transforming the Synthesis of Carbon Nanotubes with Machine Learning Models and Automation

*Yue Yuri Li[1], Liu Qian[1], Jin Zhang[1] (1. Peking University (China))

2:40 PM - 3:00 PM JST | 5:40 AM - 6:00 AM UTC

[17sy-03]

An Autonomous, Closed Loop Experimentation system for Floating Catalyst Carbon Nanotube Synthesis

*Arthur William Newton Sloan[1,2], Morgen Smith[1,3,4], Robert Waelder[1,4], John Bulmer[1,2], Rahul Rao[1], Benji Maruyama[1] (1. Air Force Research Laboratory (United States of America), 2. National Research Council (United States of America), 3. Kansas State University (United States of America), 4. BlueHalo LLC (United States of America))

3:00 PM - 3:20 PM JST | 6:00 AM - 6:20 AM UTC

[17sy-04]

Carbon Nanotube Synthesis Mechanism for Deep-Injection Floating Catalyst Chemical Vapor Deposition

Raj Kumar[1,2], Ji Hong Park[1], Seung-Yeol Jeon[1,2], Young Shik Cho[1], *Seung Min Kim[1,2] (1. Korea Institute of Science and Technology (Korea), 2. Jeonbuk National Univ. (Korea))

4:00 PM - 4:20 PM JST | 7:00 AM - 7:20 AM UTC

[17sy-05]

High-speed screening of growth conditions for carbon nanotube thin films using an aerosol jet printing system

*Keigo Otsuka[1], Ryuji Fujiwara[1], Shigeo Maruyama[1] (1. The University of Tokyo (Japan))

4:20 PM - 4:40 PM JST | 7:20 AM - 7:40 AM UTC

[17sy-06]

Synthesis of boron nitride nanotubes and applications into electrochemical catalysis

*Myung Jong Kim[1] (1. Gachon University (Korea))

4:40 PM - 5:00 PM JST | 7:40 AM - 8:00 AM UTC

[17sy-07]

Session

NT 25（The 25th International Conference on the Science and Applications of Nanotubes and Low-

Controlled Synthesis of Single-Walled Carbon Nanotubes: Microplasma-Assisted Multi-Step Reactor and Catalyst Precursor Effects

*Guohai Chen[1], Takashi Tsuji[1], Jinping He[1], Maho Yamada[1], Yoshiki Shimizu[1], Hajime Sakakita[1], Kenji Hata[1], Don N. Futaba[1], Shunsuke Sakurai[1] (1. AIST (Japan))

5:00 PM - 5:20 PM JST | 8:00 AM - 8:20 AM UTC

[17sy-08]

Aerosol CVD Carbon Nanotube Thin Films: From Synthesis to Advanced Applications

*Ilya V. Novikov[1], Dmitry V. Krasnikov[2], Albert G. Nasibulin[2], Il Jeon[1] (1. Sungkyunkwan University (Korea), 2. Skolkovo Institute of Science and Technology (Russia))

Salt-Assisted Growth of Transition Metal Dichalcogenide Nanotubes: Mechanisms from Molecular Dynamics

Daniel S. Vadseth[1], Shigeo Maruyama,[2] Alister. J. Page[1],
[1.] *School of Environmental and Life Sciences, University of Newcastle, Newcastle, Australia*
[2.] *Department of Mechanical Engineering, School of Engineering, The University of Tokyo, Tokyo, 113-8656, Japan*

The use of inorganic salts to increase the yield and quality of 2D transition metal dichalcogenide (TMD) monolayers during CVD has become well established in recent years [1-2]. While 2D van der Waals (vdW) heterostructures have been extensively studied since the late 2000's, their 1D counterpart, the 1D nanotube vdW heterostructure, was first reported in 2020 [3]. Salt assisted growth has become a strategy for synthesising 1D heterostructures as well, highlighting the importance of a better understanding of these salts in the synthesis of TMD nanomaterials. Proposed mechanisms for this type of salt assisted growth feature lower melting temperature salts (compared to for example MoO_3/WO_3) such as Na_2WO_4 and $NaMoO_3$, which provide a steady flux of TMD metal to the substrate, thereby increasing yield and quality [2,4]. Similarly, Na_2MoO_4 has been proposed to form a eutectic with the chalcogen, before monolayer TMDs are precipitated [3]. The formation of transition metal oxychlorides as intermediates that more readily reduces has also been investigated as an explanation of these effects [4]. However, the precise atomistic mechanism by which the salt acts to make these improvements remains unclear.

Here we present quantum chemical molecular dynamics (MD) simulations using the GFN1-xTB [5] method to explore the role of NaCl in the formation of MoS_2. MoO_3, S_2 and varying amounts of NaCl were modelled in the gas phase to better understand the intermediates that form and the individual role of Na and Cl on the formation of these intermediates. We show that adding NaCl doubles the rate of oxidation/reduction of Mo and O, with gas-phase Na^+ cations being the main facilitator of this change. Our results show new insights highlighting the role of Na, which has so-far been neglected in attempting to understand salt assisted growth, as a key reduction agent and catalyst driving bond rearrangement between Mo, O and S.

References (if desired)

[1] S. Li, et al., *Applied Materials Today*, 2015, **1**, 1.
[2] S. Li, et al., *Chem. Mater.*, 2021, **33**, 18.
[3] R. Xiang, et al., *Science*, 2020, **367**, 6477.
[4] J. Lei, et al., *J. American Chem. Soc.*, 2022, **144**, 16.
[5] S. Grimme, et al., *Journal of Chemical Theory and Computation*, 2017, **13**, 5

Transforming the Synthesis of Carbon Nanotubes with Machine Learning Models and Automation

Yue Li[1], Liu Qian[1*], Jin Zhang[1*]

[1]*Peking University (China)*

Carbon-based nanomaterials (CBNs) are showing significant potential in various fields, such as electronics, energy, and mechanics. However, their practical applications face synthesis challenges stemming from complexities in structural control, large-area uniformity, and consistency, unaddressed by current research methodologies. Here we introduce Carbon Copilot (CARCO), an artificial intelligence (AI)-driven platform that integrates transformer-based language models for carbon materials, robotic chemical vapor deposition (CVD), and data-driven machine learning models, driving a paradigm shift in CBNs research. Employing CARCO, we discovered a novel Titanium-Platinum bimetallic catalyst for high-density horizontally aligned carbon nanotube (HACNT) array synthesis, outperforming traditional iron-based catalysts. Furthermore, leveraging millions of virtual experiments, we achieved an unprecedented 56.25% precision in synthesizing predetermined densities of HACNT arrays. All were accomplished within just 43 days. This work not only advances the field of CBNs but also exemplifies the integration of AI with human expertise to overcome the limitations of traditional experimental approaches, marking a paradigm shift in nanomaterials research and paving the way for broader applications.

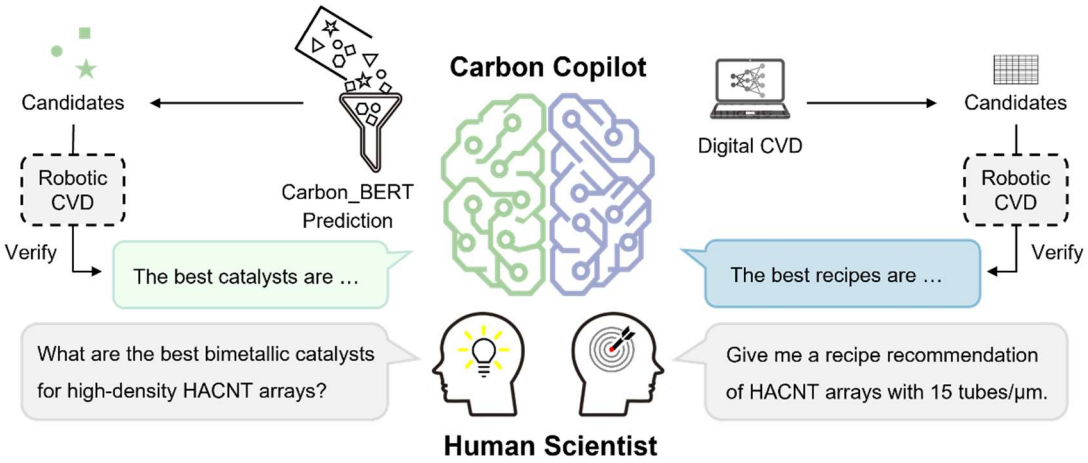

Figure caption: Interactive workflows with CARCO. Two workflows, catalyst prediction (left side) and controlled-density growth (right side), demonstrating CARCO's capabilities in innovation and precision manufacturing within CBNs synthesis research.

References

[1] Yue Li *et al.*, *Matter.* **8**, 101913 (2025).

An Autonomous, Closed Loop Experimentation system for Floating Catalyst Carbon Nanotube Synthesis

A. W. N. Sloan[1,2], M. Smith[1,3,4], R. Waelder[1,4], J. Bulmer[1,2], R. Rao[1], and B. Maruyama[1]

[1]*Air Force Research Laboratory (USA),* [2]*National Research Council (USA),* [3]*Kansas State University (USA),* [4]*BlueHalo LLC (USA)*

Autonomous experimentation systems are an increasingly prevalent tool in the field of materials science to accelerate discovery and development of new materials, with demonstrated utility across diverse research problems. These systems combine three key capabilities: robotic execution of experiments, integrated analysis techniques, and the use of artificial intelligence (AI) and machine learning (ML) to plan subsequent experiments based on the collected data. By iterating through this experiment-analyze-plan cycle, autonomous research systems can achieve research goals an order of magnitude more efficiently than traditional design of experiment (DOE) techniques, reducing the number of experiments, experimental materials, and human researcher time required.[1]

We have previously demonstrated the value of our autonomous research system (ARES) approach for studying the substrate growth of CNTs in a cold-wall chemical vapor deposition (CVD) reactor using laser heating.[2-4] These results have provided key insights into factors affecting the growth rate of CNTs; however, a gulf remains between these results and the scalable synthesis of high quality single-walled CNTs. To address this shortcoming, we demonstrate the operation of a new ARES systems based on the floating catalyst chemical vapor deposition (FCCVD) process for CNT synthesis. FCCVD is a substrateless process that can be operated continuously and is thus a promising route for scaling the production of high-quality single or few-walled CNTs to commercially viable levels.[5,6]

In this work, we present the floating catalyst ARES (FC-ARES). The FC-ARES, shown schematically in Figure 1, consists of a benchtop FCCVD reactor with computer control of reactor temperature and the flow rates of up to three gas phase and four liquid phase feedstock species through our open-source ARES OS™ software. CNT samples are collected on a reel-to-reel tape at the reactor outlet and advanced through one or more analysis stations to collect metrics such as the presence and distribution of CNT radial breathing modes or the yield of the experiment.[7,8] We present initial results comparing ML planned autonomous operation to traditional DOE approaches. Additionally, we build upon our previous work in the in cold-wall CVD reactor ARES and examine our ability to transfer knowledge between reactor systems.[4]

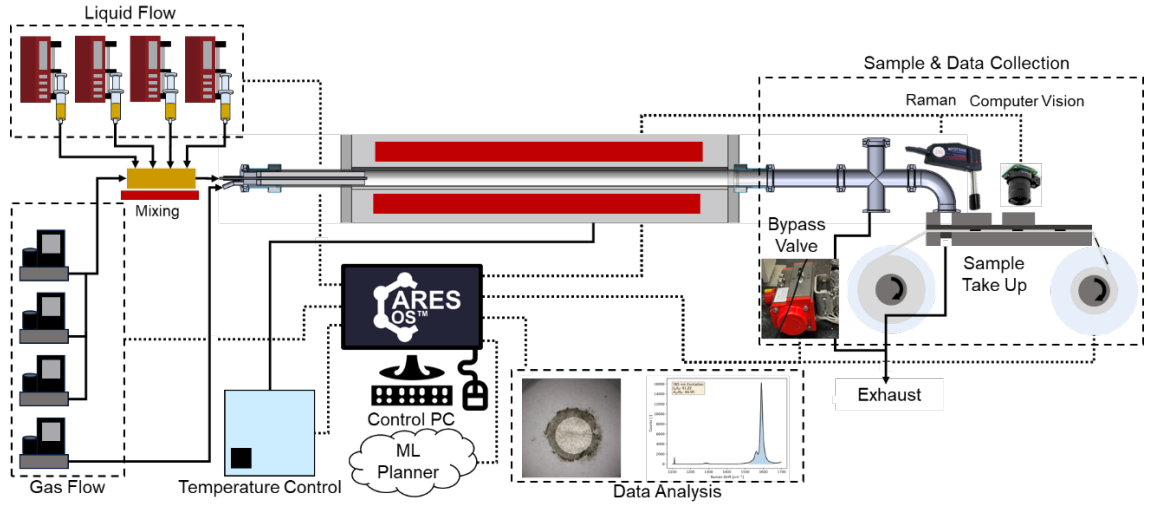

Figure 1: Schematic representation of the FC-ARES reactor developed for this work.

References

[1] Stach, E. et al. *Matter* **4**, 2702–2726 (2021).
[2] Nikolaev, P. et al. *npj Comput Mater* **2**, 16031 (2016).
[3] Rao, R. et al. *npj Comput Mater* **7**, 157 (2021).
[4] Waelder, R. et al. *Carbon* **228**, 19356 (In Review)
[5] Weller, L. et al. *Carbon* **146,** 789–812 (2019).
[6] Glerum, M. & Boies, A. *Advances in Chemical Engineering* **61**, 133-192 (2023)
[7] Rao, R., and Maruyama, B. *U.S. Patent No. 10,994,990*. (2021).
[8] Bulmer, J. et al. *Carbon* **201**, 719–733 (2023).

Carbon Nanotube Synthesis Mechanism for Deep-Injection Floating Catalyst Chemical Vapor Deposition

Raj Kumar[1,2], Ji Hong Park[1], Seung-Yeol Jeon[1,2], Young Shik Cho[1], Seung Min Kim[1,2]

[1]Korea Institute of Science and Technology (Republic of Korea), [2]Jeonbuk National University (Republic of Korea)

In this presentation, a new synthesis mechanism of carbon nanotubes (CNTs) by a deep-injection floating catalyst chemical vapor deposition (DI-FCCVD) will be dealt with [1]. In 2021, our group developed DI-FCCVD method by which CNTs with high crystallinity (I_G/I_D ~60) and high aspect ratio (>17,000) were successfully synthesized at a relatively high production rate (~ 6 mg/min) [2]. The critical factor of DI-FCCVD is to deliver the reactants rapidly into a hot reaction zone through a thin injection tube. Another interesting point is that a larger amount of Ar is used with H_2 as a carrier gas. Here, we investigated the roles of a heavier inert gas, such as Ar, in simultaneously improving the crystallinity and productivity of CNTs or CNTFs. Heavier inert gases have lower thermal conductivities than lighter inert gases. Hence the addition of heavier inert gases in H_2 ambient leads to the formation of a larger space at an exit of the injection tube with a lower temperature gradient to the synthesis temperature. This larger space allows carbon and catalyst precursors to decompose and prevents decomposed catalyst particles from agglomerating into too large catalyst particles, resulting in the significantly enhanced synthesis of CNTs.

References

[1] R. Kumar *et al.*, *Carbon.* 234, 119929 (2025).
[2] S. Lee *et al.*, *Carbon.* **173**, 901–909 (2021).

High-speed screening of growth conditions for carbon nanotube thin films using an aerosol jet printing system

K. Otsuka, R. Fujiwara, S. Maruyama

The University of Tokyo (Japan)

Unique properties of semiconducting carbon nanotubes (s-CNTs), such as low dimensionality and optical/electrical/thermal properties, offer opportunities in various device applications [1]. Requirements for their quantity and quality are usually in a trade-off relationship, and the requirement level highly depends on the application. To optimize the growth condition of CNTs, it is essential to understand growth mechanisms and explore the huge space of synthesis parameters. Although in-depth mechanistic studies and autonomous research approaches have been reported [2,3], additional constraints imposed by such specific experimental designs often limit the growth yield and the parameter space that can be tuned. In this study, we developed an aerosol jet printing method for CNTs grown *via* conventional floating catalyst chemical vapor deposition to realize high-throughput screening of various synthesis parameters, which will readily provide application-oriented CNT films once growth conditions are optimized.

Ethanol containing ferrocene was filled into a syringe and supplied [4] at a tunable rate along with various carrier gases. We collected CNTs floating in gas on glass filter paper using a homemade aerosol jet printer (Fig. 1a). A nozzle and the filter paper mounted on a vacuum chuck were moved by a three-axis stage to deposit CNT films in a 1-mm-diameter area, whereas dry-transferable films were deposited when collected on membrane filters (Fig. 1b). For example, we deposited CNTs on the paper grown under 61 conditions within 2 hours by automatically scanning the nozzle synchronized with parameter modulations. Figure 1c shows the representative Raman spectra of CNTs grown with elevated CO_2 concentration while fixing the other parameters, showing a nontrivial diameter shift upon the CO_2 supply, including the narrowed diameter distribution (Fig. 1d). We found even more complex trends when considering the multiple parameters (Fig. 1e), which underline the importance of comprehensively exploring a vast parameter space for CNT growth using our nanotube printer.

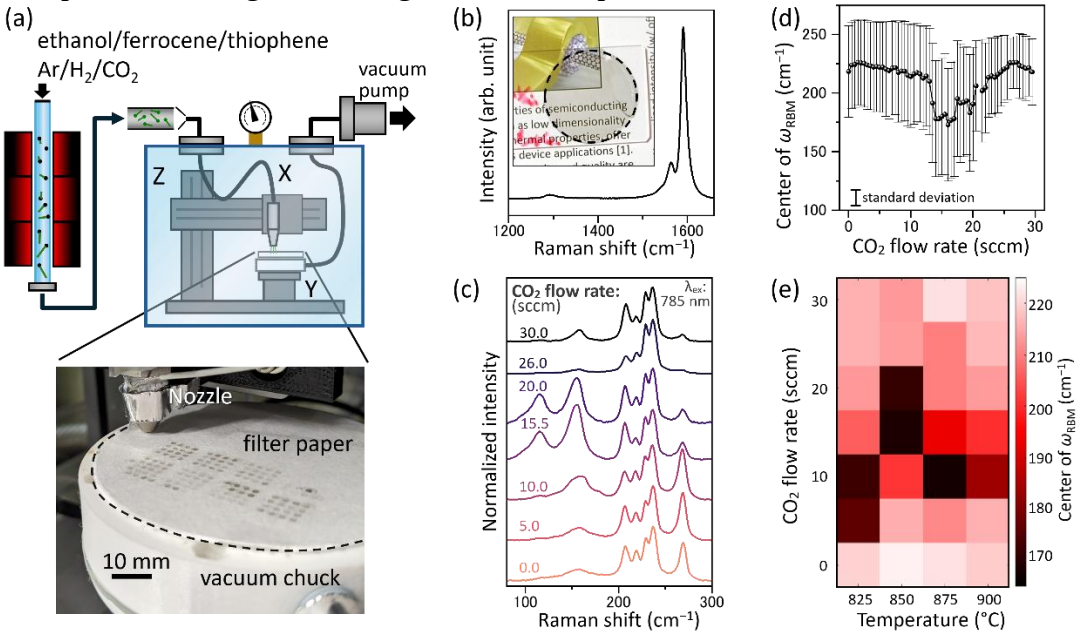

Figure 1: (a) Schematic and photograph of the nanotube printing system. (b) Raman spectrum of a dry-transferable CNT film. Inset: Photograph of the 25-mm diameter CNT film on a glass side. (c,d) Normalized Raman spectra (c) and weighted center of radial breathing mode ω_{RBM} (d) of CNT films grown with elevated CO_2 flow rates. (e) Heat map of ω_{RBM} as a function of reactor temperature and CO_2 flow rate.

References

[1] D.-M. Tang *et al.*, *Nat. Rev. Electr. Eng.* **1**, 149 (2024).
[2] P. Nikolaev *et al.*, *npj Comput. Mater.* **2**, 16031 (2016).
[3] K. Otsuka *et al.*, *ACS Nano* **16**, 5627 (2022).
[4] E.-X. Ding *et al.*, *Nanoscale* **9**, 17601 (2017).

Synthesis of boron nitride nanotubes and applications into electrochemical catalysis

Myung Jong Kim[1*]

[1]*Gachon University, Department of Chemistry, 1342 Seongnam-daero, Sujeong-gu, Seongnam-si, Gyeonggi-do 13120, Republic of Korea.*

**myungjongkim@gachon.ac.kr*

Boron nitride nanotubes (BNNTs) are structural analogues of carbon nanotubes, where alternating boron and nitrogen atoms replace carbon atoms in a hexagonal lattice structure. This elemental change results in a number of potential advantages over carbon nanotubes. These includes a uniform band gap (~ 5 eV) that is insensitive to either diameter or chirality, electrical insulation, thermal conduction, radiation shielding, piezoelectricity and oxidation resistance up to 900 °C. These properties make BNNTs attractive for nanoscale applications. However, facile methods for large scale synthesis of BNNTs remains as a challenge. In this presentation, we will mainly discuss about synthesis methods including laser ablation [1], high temperature plasma [2], and CVD [3] for high crystalline BNNTs, and the applications into electrochemical catalysis will be briefly discussed [4].

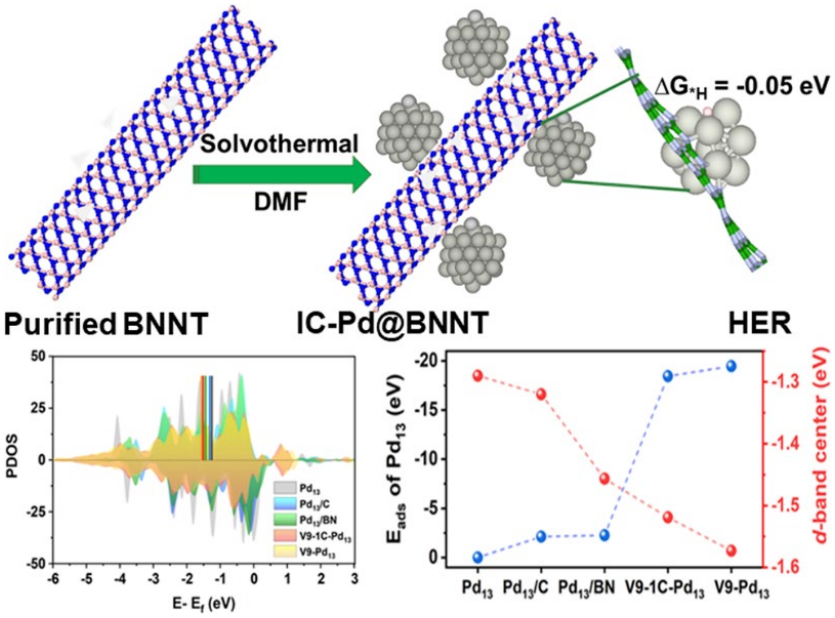

Figure. HER characteristics of BNNT-Pd hybrid catalysts.

References

[1] M. J. Kim *et al.*, Nano Convergence, **9**, 20 (2022)
[2] M. J. Kim *et al.*, ACS Omega, **8**, 21514 (2023)
[3] M. J. Kim *et al.*, Submitted
[4] M. J. Kim *et al.*, *Applied Catalysis B: Environment and Energy*, **345**, 123609 (2024)

Controlled Synthesis of Single-Walled Carbon Nanotubes: Microplasma-Assisted Multi-Step Reactor and Catalyst Precursor Effects

Guohai Chen[1], Takashi Tsuji[1], Jinping He[1], Maho Yamada[1], Yoshiki Shimizu[2,3], Hajime Sakakita[4], Kenji Hata[1], Don N. Futaba[1], Shunsuke Sakurai[1]

[1]*Nano Carbon Device Research Center, National Institute of Advanced Industrial Science and Technology (AIST), Tsukuba, Ibaraki 305-8565, Japan*

[2]*Nanomaterials Research Institute, AIST, Tsukuba, Ibaraki 305-8565, Japan*

[3]*AIST-UTokyo Advanced Operando-Measurement Technology Open Innovation Laboratory (OPERANDO-OIL), AIST, Kashiwa, Chiba 227-8589, Japan*

[4]*Innovative Plasma Processing Group, Research Institute for Advanced Electronics and Photonics, AIST, Tsukuba, Ibaraki 305-8568, Japan*

Achieving precise control over nanoparticle (NP) formation and single-walled carbon nanotube (SWCNT) synthesis is essential for optimizing nanomaterial properties and productivity, leveraging their exceptional characteristics [1-4]. However, achieving precise control over NP growth and uniformity remains a challenge, directly impacting CNT quality and yield. To address this, we present a multi-step chemical vapor synthesis (CVS) reactor that enables independent control of NP nucleation and SWCNT growth [5]. The reactor—centered on an atmospheric, continuous-flow microplasma—incorporates abrupt interaction steps to precisely regulate the start and stop of NP aggregation, ensuring well-defined growth conditions even at high NP densities. By applying this framework to gas-phase SWCNT synthesis, we demonstrate that the precise initiation and termination of catalyst NP nucleation can be controlled using the microplasma reactor (start) and a carbon reactant gas (stop) to suppress further aggregation and promote SWCNT growth. As a result, we achieved the production of highly crystalline SWCNTs [5-6].

Furthermore, we used this framework to systematically investigate the impact of catalyst precursor ligands—ferrocene ($Fe(C_5H_5)_2$) and iron pentacarbonyl ($Fe(CO)_5$)—on NP growth kinetics and CNT quality [7]. Our results reveal that $Fe(CO)_5$ produces smaller, more uniform NPs compared to $Fe(C_5H_5)_2$, leading to higher-purity CNTs with improved yield, despite similarities in CNT structural properties such as diameter, chirality, and crystallinity [5-7]. This result demonstrates that the catalyst precursor ligands in significantly influence NP growth rates and sizes, directly impacting CNT quality, highlighting their crucial role in CNT synthesis.

Our work demonstrates the feasibility of precise structural control of nanomaterials using a multi-step CVS reactor by finely regulating aggregation time in high-density particle flow. When applied to CNT synthesis, our results provide deeper insights into the role of catalyst precursor ligands in NP formation and CNT synthesis, offering pathways for optimizing CNT synthesis.

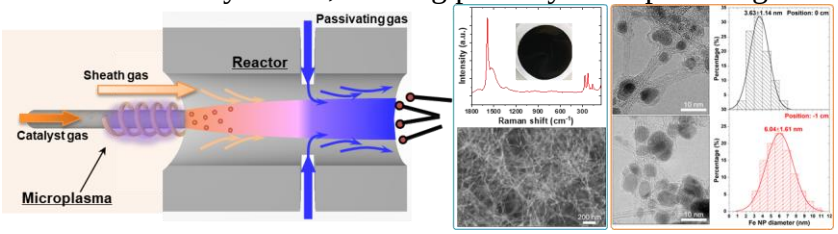

Figure caption: Microplasma-assisted multi-step CVS reactor for synthesizing highly crystalline SWCNTs and controlling NP formation.

Acknowledgements

G.H. Chen acknowledges support from JSPS KAKENHI Grant Number JP23K04552.

References

[1] G. H. Chen, *et al.*, *ACS Nano* **7**, 10218-10224 (2013).
[2] D.-M. Tang, *et al.*, G. H. Chen, *et al.*, *Science* **374**, 1616-1620 (2021).
[3] G. H. Chen, et al., *Nanomaterials* **14**, 1688 (2024).
[4] G. H. Chen, et al., *J. Mat. Sci. Technol.* **In Press** (2025).
[5] G. H. Chen *et al.*, *Chem. Eng. J.* **444**, 136634 (2022).
[6] T. Tsuji†, G. H. Chen†, *et al.*, *Nanomaterials* **11**, 3461 (2021).
[7] T. Tsuji†, G. H. Chen† *et al.*, *Mater. Today Chem*. **44**, 102576 (2025).

Aerosol CVD Carbon Nanotube Thin Films: From Synthesis to Advanced Applications

Ilya V. Novikov[1], Dmitry V. Krasnikov[2], Albert G. Nasibulin[2], Il Jeon[1]

[1] *Sungkyunkwan University (SKKU) (Republic of Korea),* [2] *Skolkovo Institute of Science and Technology (Russia)*

Carbon nanotubes (CNTs) produced by the floating catalyst chemical vapor deposition (FCCVD) method are among the most promising nanomaterials today, attracting interest from both academic and industrial sectors since FCCVD enables continuous and scalable synthesis of CNTs with exceptional properties due to their binder-free and low-defect structure [1]. Among the methodological FCCVD variations, aerosol CVD is distinguished by its operation with a low catalyst concentration resulting in the production of thin films comprising macroscale networks of individual nanotubes and their small bundles, which can be fabricated in both on-substrate and free-standing forms (**Figure 1**) and exhibit superior performance and practical applicability [2].

This presentation will elucidate the complex interrelations between aerosol CVD reactor synthesis conditions and the resulting properties of CNT films by providing a guide map that connects all the phases from the reactor engineering to the applications: reactor → catalyst → nanotube → film → device (**Figure 1**). Thus, it will review the latest progress in the chemical engineering of aerosol CVD reactors followed by the impact of synthesis process design on the mechanism of the nanotube growth in the flow reactor and, as a result, on the properties of the synthesized nanotubes. In particular, characterization methodologies specific to aerosol-CVD-synthesized CNTs will be covered. Then, the correlations between CNT structural parameters (length, diameter, defectiveness, etc.) and resulting film properties (conductivity, optical and mechanical characteristics, mechanical and chemical sensing, etc.) will be briefly discussed to establish a comprehensive framework for optimizing CNT thin film synthesis. Finally, the influence of CNT properties on applications in diverse domains, from energy devices to optoelectronics will be evaluated. The review will conclude with a comparison of the aerosol CVD with other production methods for CNT thin film, addressing current challenges and prospects in this field, including mass production and overcoming the yield/performance trade-off, and exploring new promising directions, such as multilevel engineering and rational design of CNT films to expand their advanced applications.

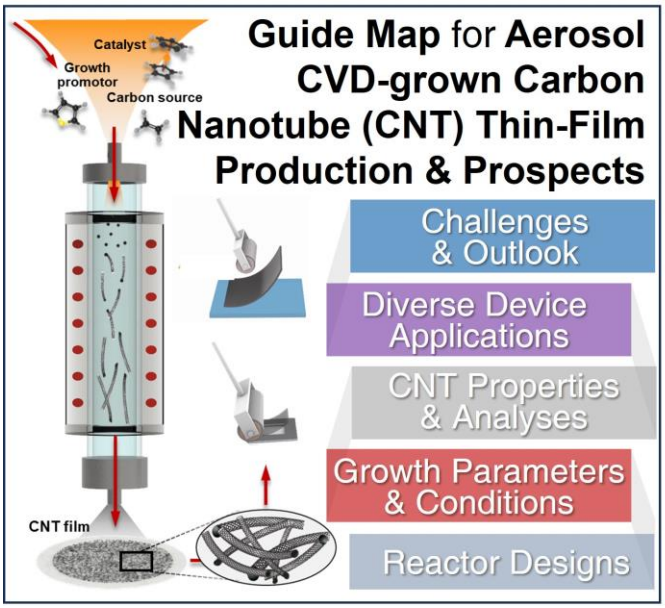

Figure 1: Representation of the aerosol CVD reactor and the guide map**.**

References:

[1] P.X. Hou *et al.*, *Adv. Func. Mat.* **32**, 2108541 (2022).
[2] I.V. Novikov *et al.*, *Adv. Mat.* 2413777 (2025).

Session
NT 25（The 25th International Conference on the Science and Applications of Nanotubes and Low-

| Parallel Symposia：Symposium on Fundamental, Structural and Optical Properties of 1D and 2D Materials and their Heterostructures

Tue. Jun 17, 2025 2:00 PM - 5:20 PM JST | Tue. Jun 17, 2025 5:00 AM - 8:20 AM UTC International Exchange Hall III (Clock Tower Centennial Hall, 2F)

[17fn] Fundamental Properties

Chair:Yasumitsu Miyata, Antoine RESERBAT-PLANTEY

2:00 PM - 2:40 PM JST | 5:00 AM - 5:40 AM UTC

[17fn-01]

TEM-EELS of low-D materials combining high energy and momentum resolution

*Thomas Pichler[1] (1. University of Vienna (Austria))

2:40 PM - 3:00 PM JST | 5:40 AM - 6:00 AM UTC

[17fn-02]

Energy transfer in mixed-dimension heterostructures based on super-radiant Dyes@BNNT and 2D semiconductors

*Juliette Le Balle[1,2], Jean-Baptiste Marceau[2], Frédéric Fossard[1], Gaëlle Recher [2], Annick Loiseau [1], Etienne Gaufrès[2] (1. Université Paris-Saclay, ONERA, CNRS, Laboratoire d'étude des microstructures (LEM), 92322 Châtillon, France. (France), 2. Laboratoire Photonique Numérique et Nanosciences, CNRS-Institut d'Optique - Université de Bordeaux, 33400 Talence, France. (France))

3:00 PM - 3:20 PM JST | 6:00 AM - 6:20 AM UTC

[17fn-03]

Creation and Control of Quantum Light Emitters in 2D Flatland

*Han Htoon[1] (1. Los Alamos National Laboratory (United States of America))

4:00 PM - 4:20 PM JST | 7:00 AM - 7:20 AM UTC

[17fn-04]

Anharmonicity and confinement effects in Carbyne-like Materials

*Sebastian Heeg[1] (1. Humboldt-Universität zu Berlin (Germany))

4:20 PM - 4:40 PM JST | 7:20 AM - 7:40 AM UTC

[17fn-05]

Unraveling the Origin of B-Type Photoluminescence Blinking at 2D/3D Heterojunction Interface

*Tao Zhou[1], Dongyang Wan[1], Junpeng lu[1], Zhenhua Ni[1] (1. Southeast University (China))

4:40 PM - 5:00 PM JST | 7:40 AM - 8:00 AM UTC

[17fn-06]

Strain and defects engineering in transition metal dichalcogenide nanostructures

*Yasumitsu Miyata[1] (1. Tokyo Metropolitan University (Japan))

5:00 PM - 5:20 PM JST | 8:00 AM - 8:20 AM UTC

[17fn-07]

Moiré Superlattice in Twisted Transition Metal Dichalcogenide Trilayers

*Hao Ou[1], Kota Tanaka[2], Koshi Oi[2], Jiang Pu[1], Taishi Takenobu[2] (1. Institute of Science Tokyo (Japan), 2. Nagoya Univ. (Japan))

TEM-EELS of low-D materials combining high energy and momentum resolution

T. Pichler

[1] *University of Vienna, Faculty of Physics, Botzmanngasse 5, 1090 Vienna (Austria)*

A major mission of condensed-matter physics is to understand material properties via the knowledge of the energy vs. momentum (q) dispersion and lifetime of fundamental excitations. Recent developments of EELS in TEM with a combined high energy & q-resolution is a perfect tool to determine them. This opens the so-far unexplored possibility to investigate dispersion and lifetime of phonons, plasmons & excitons in nanomaterials including molecules, 1D & 2D materials and heterostructures with few nm of lateral resolution on samples as thin as an atomic monolayer. In this presentation I give an overview on our recent progress in analysing fundamental excitations such as phonons, excitons, and plasmons in 2D materials such as graphene, h-BN and transition metal dichalcegonides (TMDC), and graphite intercalation compounds (GIC) using EELS with complementary high energy and momentum resolution in comparison to previous results. I will show how we can understand the full phonon dispersion of an apolar material like graphene [1] and use the ultrahigh momentum resolution to make the link to surface phonon polaritons close to the optical limits in h-BN. For graphene we also show new results on the plasmon dispersion including the gap opening close to the optical limit unravelling the Dirac cone in the excitation spectrum [2] concomitant to the direct observation of a vanishing EELS cross section approaching the optical limit [3]. For monolayer TMDC using ultra high q resolution we determined the exciton dispersion and deciphered the intense postgap absorptions and disentangling plasmon from excitons from their different momentum dependence [4-6]. For GIC we analyse how few layer stage I GIC single crystals and its slow evolution with time can be explained by high resolution EELS [7].

We thank the MORE-TEM consortium for support and the EU for funding from the European Research Council (ERC) under the European Union's Horizon 2020 research and innovation program grant agreements No 951215 (MORE-TEM).

References

[1] R. Senga, K. Suenaga, P. Barone, S. Morishita, F. Mauri, T. Pichler, *Nature* **573** (2019) 247
[2] A. Guandalini, R. Senga, Y.C. Lin, K. Suenaga, A. Ferretti, D. Varsano, A. Recchia, P. Barone, F. Mauri, T. Pichler, C. Kramberger, *Nanoletters* **23**, 11835 (2023)
[3] A. Guandalini, R. Senga, Y.C. Lin, K. Suenaga, P. Barone, F. Mauri, T. Pichler, C. Kramberger, Phys. Rev. B 111, L041401 (2025).
[4] J. Hong, R. Senga, T. Pichler, K. Suenaga, *Phys. Rev. Lett.* **124** (2020) 087401.
[5] J. Hong, M. Koshino, R. Senga, T. Pichler, H. Xu, K. Suenaga, *ACSNano* **15** (2021) 7783.
[6] J. Hong, M.K. Svendsen, M. Koshino, T. Pichler, H. Xu, K. Suenaga, K.S Thygesen, *ACSNano* **16**, (2022) 12328.
[7] R. Senga et al., in preparation.

Energy transfer in mixed-dimension heterostructures based on super-radiant Dyes@BNNT and 2D semiconductors

J. Le Balle[1,2] , J-B. Marceau[2], F. Fossard[1], G. Recher[2], A. Loiseau[1] and E. Gaufrès[2]

[1]*Université Paris-Saclay, ONERA, CNRS, Laboratoire d'étude des microstructures (LEM), 92322 Châtillon, France.*

[2]*Laboratoire Photonique Numérique et Nanosciences, CNRS-Institut d'Optique – Université de Bordeaux, 33400 Talence, France.*

Since the discovery of graphene, the assembling of 2D semiconductors in van der Waals (VdW) heterostructures results in the emergence of fascinating properties[1] with potential applications in photonics and optoelectronics. However, the presence of intrinsic structural defects and inhomogeneities, associated to indirect band gaps in their bulk form, leads to non-radiative process and low fluorescence quantum yields. In contrast, 0D materials such as luminescent organic molecules can act as quasi pure quantum emitters with strong light/matter interaction. However, these molecules are fragile and difficult to arrange and position at the nanoscale.

In this presentation we show that boron nitride nanotubes (BNNTs) can be used as a template for integrating a 1D chain of luminescent molecules[2-5] onto 2D semiconductors in the van der Waals regime. Different heterostructures are fabricated by either modifying the nature of the 2D material (MoS_2, WSe_2 and WS_2), their thickness or the nature and spacing of the encapsulated molecules. We present the methods for fabricating mixed-dimension heterostructures and fingerprints of optical interactions between molecules inside the BNNTs as well as between molecules and the 2D semiconductors in heterostructures, using polarized and time-resolved fluorescence imaging and spectroscopy.

References

[1] Novoselov, K. S., Mishchenko, A., Carvalho, A. & Castro Neto, A. H. 2D materials and van der Waals heterostructures. *Science* **353**, aac9439 (2016). A. K. Geim, *Science* **324**, 1530–1534 (2009).

[2] Gaufrès, E. *et al.* Giant Raman scattering from J-aggregated dyes inside carbon nanotubes for multispectral imaging. *Nature Photon* **8**, 72–78 (2014).

[3] Allard, C. *et al.* Confinement of Dyes inside Boron Nitride Nanotubes: Photostable and Shifted Fluorescence down to the Near Infrared. *Adv. Mater.* **32**, 2001429 (2020).

[4] Badon, A., J.-B. Marceau et al. Fluorescence anisotropy using highly polarized emitting dyes confined inside BNNTs. Mater. Horiz. 10, 983–992 (2023).

[5] J-B. Marceau, J. Le Balle et al, Shaping and Spacing Dye J-aggregates by Activated Molecular Diffusion in BNNTs (2024) arXiv:2402.17537

Creation and Control of Quantum Light Emitters in 2D Flatland

Han Htoon
Center for Integrated Nanotechnologies, Los Alamos National Laboratory.

In this talk, I will highlight our recent efforts on the development of new class of 2D material-based quantum light emitters and exploit of proximity interactions in realization of chiral quantum light emitters. 2D-Quantum emitters have generated a lot of excitement for their potential in quantum information technologies. Most of the QE realized to date operate at wavelengths shorter than 1 micron. Here I will present three new 2D quantum emitters capable of wavelength tunable single photon emission across 1000-1600 nm NIR spectral range and operation at liquid nitrogen temperatures. The QEs were realize via strain engineering of $MoTe_2$,[1] WSe_2/MoS_2,[2] and $InSe_2$[3] 2D materials. Next, I will show that circularly polarized single photon emission can be achieved without the application of a high external magnetic field, injection of spin-polarized carriers and coupling to complex chiral metamaterial structures. Our experiment shows that QE created at the same location as the magnetic defect in 2D correlated antiferromagnet, $NiPS_3$, can borrow magnetic properties of the magnetic defect through proximity induced exchange interaction and emit circularly polarized single photons.[4]

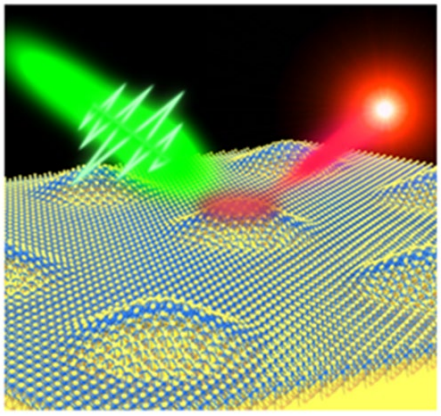

Fig. 1. Strain engineering of 2D TMD layer via use of nanopillar array leads to formation of quantum light emitters

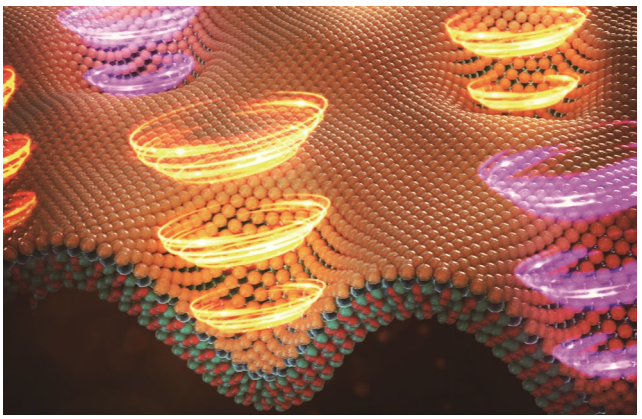

Fig. 2. Chiral quantum light emitters are created by nano indentations of $WSe_2/NiPS_3$, TMD/2D antiferromagnetic heterostructure .

References:

1. Zhao, H., Pettes, M. T., Zheng, Y. & Htoon, H. Site-controlled telecom-wavelength single-photon emitters in atomically-thin MoTe2. *Nature Communications* **12**, 1-7 (2021).
2. Zhao, H. *et al.* Manipulating Interlayer Excitons for Near-Infrared Quantum Light Generation. *Nano Letters* **23**, 11006-11012 (2023).
3. Zhao, H. *et al.* Telecom-wavelength Single-photon Emitters in Multi-layer InSe. Submitted to ACS Nano. (2024)
4. Li, X. et al. Proximity-induced chiral quantum light generation in strain-engineered WSe2/NiPS3 heterostructures. *Nature Materials* **22**, 1311-1316 (2023).

Anharmonicity and confinement effects in Carbyne-like Materials

S. Heeg[1]

[1]*Humbolt-Universität zu Berlin (Germany)*

Carbyne, an infinite linear chain of carbon atoms, is the truly 1D allotrope of carbon that has remained elusive to date. While carbyne-like materials like long linear carbon chains encapsulated in carbon nanotubes or short carbon atomic wires are available for study, the transition between the two systems and common properties that can be linked to carbyne are poorly understand. In this talk, I will present our Raman spectroscopy study of the C-mode of individual confined carbyne chains up to the third overtone. We find a strong vibrational anharmonicity that increases with decreasing C-mode frequency. Upon comparison to carbon atomic wires, we find that this relation between vibrational anharmonicity and C-mode frequency is universal to carbyne-like materials [1]. Finally, I will show that the collective LO-phonon mode of carbon atomic wires confined inside carbon nanotube approaches the frequency of confined carbyne's C-mode, suggesting that convergence to length-independent properties of long linear carbon chain inside carbon nanotubes occurs at shorter chain lengths than previously thought [2].

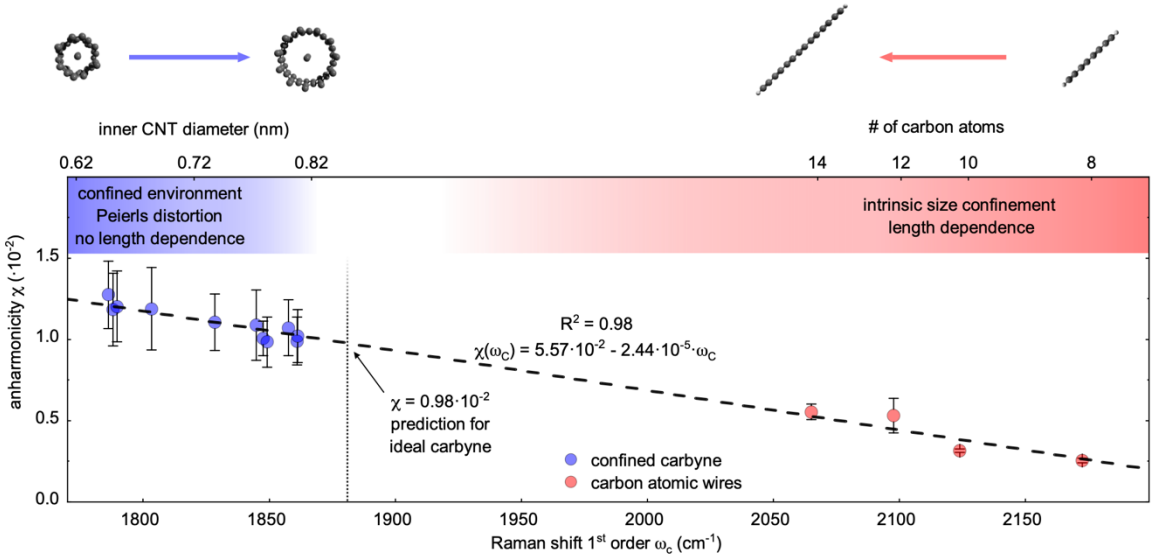

Universal Vibrational Anharmonicity in Carbyne-like Materials: Anharmonicity χ as a linear function of the first-order BLA oscillation Raman mode frequency ω_C for confined carbyne (C mode, blue dots) and carbon atomic wires (ECC mode, red dots). χ is calculated from Vibrational Perturbation Theory 2 (VPT2). The linear correlation (dashed black line) between χ and the Raman mode frequency is given in the figure. The values of the inner nanotube diameter, which parametrizes the C mode/BLA of confined carbyne chains, are calculated from Eq. 1 in Ref. [3] The correlation between the chain lengths of carbon atomic wires and the ECC mode/BLA is described in Ref. [4]. Figure adapted from Ref. [1]

References

[1] J.A.M. Lechner *et al.*, *in print in Nature Communications* (2025).
[2] P. Marabotti, *in preparation* (2025).
[3] S. Heeg *et al., Nano Letters* **18,** 5426 – 5431 (2018).
[4] P. Marabotti *et al.*, *Carbon* **216**, 118503 (2024).

Unraveling the Origin of B-Type Photoluminescence Blinking at 2D/3D Heterojunction Interface

Tao Zhou[1], Dongyang Wan[1], Junpeng Lu[1], Zhenhua Ni[1]

[1]*Southeast University (China)*

Fluorescence blinking is a random perturbation phenomenon, which commonly occurs across zero-dimensional quantum dots, one-dimensional nanowires.[1–4] Fundamental researches on blinking dynamics have revealed its critical role in manipulating radiative recombination processes and optimizing emitter performance.[1,5] While extensive mechanistic frameworks exist for zero-dimensional systems, the origins of blinking in two-dimensional materials remain barely explored. Here, we identify a distinctive B-type blinking at the WS_2/Si heterointerface through statistics of fluorescence lifetime-intensity distribution. Temperature dependent photoluminescence and transient absorption spectroscopies demonstrate its genesis from the competition between A exciton and localized exciton. Moreover, Förster resonance energy transfer dominates exciton density at the 2D/3D interface, preventing saturation of localized states and promoting the competition. This discovery not only expends blinking mechanism in two dimensional systems but also provides design principles for suppressing optical instability in 2D-based quantum light sources.

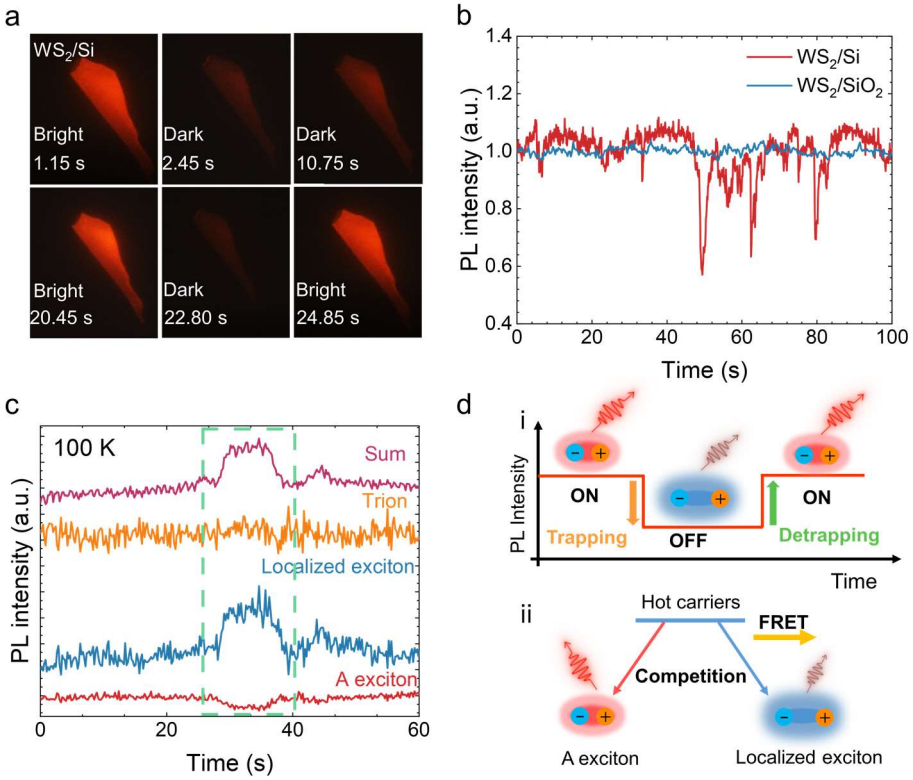

Figure caption: a, Snapshots from a video recorded by fluorescence microscope, with a series of timestamps of the typical bright and dark PL status of the WS_2/Si heterojunction. **b**, Photoluminescence(PL) intensity trace of WS_2/Si (red) and WS_2/SiO_2 (blue) with a time resolution of 100 ms. **c,** PL intensity trace of total PL intensity (sum), A exciton, trion and localized exciton as a function of time at 100 K. The dashed green box indicates one typical blinking process. **d,** The upper panel (**i**) shows PL intensity changes. The bright ON state is governed by A exciton radiative recombination. When photo generated carriers are trapped by localized states, nonradiative recombination occurs, leading to the OFF state. Detrapping process restores the ON state. The lower panel (**ii**) illustrates the competition between A exciton and localized exciton recombination channels.

References

[1] Galland, C. et al. Nature **479**, 203–207 (2011).
[2] Xu, W. et al. Nature **541**, 62–67 (2017).
[3] Luo, X. et al. Adv. Funct. Mater. **34**, 2312335 (2024).
[4] Godiksen, R. H. et al. Nano Lett. **20**, 4829–4836 (2020).
[5] Javaux, C. et al. Nat. Nanotechnol. **8**, 206–212 (2013).

Strain and defects engineering in transition metal dichalcogenide nanostructures

Y. Miyata

Department of Physics, Tokyo Metropolitan University, Hachioji, 192-0397 (JAPAN)

Transition metal dichalcogenides (TMDs) serve as attractive building blocks for a wide variety of nanostructures due to their atomically-thin forms and exceptional physical properties. Some examples of these nanostructures include moiré superlattices and tubular structures, where their properties can be modulated by quantum confinement and symmetry reduction. However, to fully harness their potential, it is essential to develop advanced methods for producing high-quality, defect-controlled samples. In this presentation, we report our recent progress in strain and defect engineering aimed at the controlled fabrication of nanostructures with enhanced quality.

First, we demonstrate the rolling-up of both monolayer and multilayer TMDs into scrolls spanning a wide range of diameters [1,2]. This process is driven by the built-in strain in Janus MoSSe (or WSSe), which promotes the spontaneous formation of tubular structures (Fig.1a). Next, we present our work on transfer-free fabrication of moiré superlattices. By applying a plasma-assisted substitution process, bilayer $MoSe_2$ was converted into Janus MoSSe/$MoSe_2$ heterobilayers that display moiré patterns arising from a slight lattice mismatch (Fig.1b) [3]. Moreover, we investigated TMDs grown directly on atomically-flat hBN substrates, demonstrating that strain suppression is critical for achieving uniform moiré superlattices. Similar strain suppression also plays a key role in enhancing the device performance of tunnel field-effect transistors based on in-plane heterostructures [4,5]. Finally, we discuss our efforts to characterize and control point defects to minimize unintentional impurities in CVD-grown TMDs, paving the way for improved material performance in future device applications.

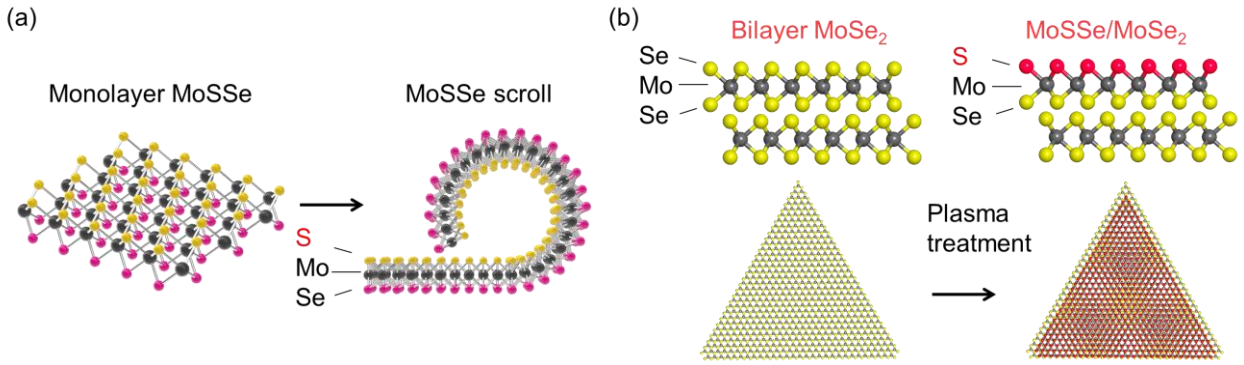

Figure 1: Schematics of (a) the planar and scroll structures of monolayer MoSSe and (b) bilayer $MoSe_2$ and MoSSe/$MoSe_2$ heterobilayers.

References

[1] M. Kaneda et al., ACS Nano 18 (2024) 2772.
[2] M. Kaneda et al., in preparation.
[3] W. Zhang et al., Small Structures 5 (2024) 2300514.
[4] H. Ogura, et al., ACS Nano 17 (2023) 6545.
[5] S. Toida et al., Appl. Phys. Lett. 124 (2024) 263101.

Moiré Superlattice in Twisted Transition Metal Dichalcogenide Trilayers

H. Ou[1], K. Tanaka[2], K. Oi[2], J. Pu[1], T. Takenobu[2]

[1] *Institute of Science Tokyo (Japan),* [2] *Nagoya University (Japan)*

Moiré superlattice forms when vertically stacking van der Waals materials. The study of moiré superlattice unveils many exotic low-dimensional phenomena, including strongly correlated electron behavior, unconventional superconductivity, and topological transport. The material system has manifested itself as a highly tunable platform for exploring new physics. When stacking two monolayer transition metal dichalcogenides (TMDCs), which lacks inversion symmetry center, the obtained moiré superlattice exhibits a two-dimensional array with alternatively polarized domains. Such a stacking-induced polarization opens a new gate for investigating the interfacial ferroelectricity/antiferroelectricity of the superlattice, and inspires the fabrication of next-generation non-volatile memory devices [1]. Currently, most related studies focus on the moiré superlattice of twisted bilayer TMDCs, revealing a triangular lattice with polarized domain array (Fig. a; top). On the other hand, twisted multi-layer TMDCs could possibly exhibit moiré superlattice with more sophisticated domain structure (Fig. a; bottom), which probably leads to more exotic physical phenomena, such as multiple polarization states, robust electronic correlation, *et al*. thus deserving in-depth investigation.

Here, we present the fabrication and observation of moiré superlattices in twisted trilayer WSe_2. We controlled the twisted angle between adjacent layers during fabrication, to tune the moiré superlattice period and relaxation. To observe the resulting superlattices, we employed the piezoresponse force microscope (PFM) to directly resolve the polarized domain structure [2]. The observed moiré superlattice (trilayer superlattice) is shown to be the composition of the superlattices from two pairs of adjacent monolayers (bilayer superlattices). We present trilayer superlattices under two conditions: 1) one bilayer superlattice has a much longer period than the other, and 2) two bilayer superlattices have similar periods. For the first case (Fig. b), the trilayer superlattice shows a generally triangular structure with AA domains within AB/BA domains, due to the combination of relaxed and unrelaxed bilayer superlattices. For the second case (Fig. c), we found that the AA domains form an approximately hexagonal lattice. This is the result of multiscale lattice relaxation, in which relaxation occurs in both atomic scale and moiré scale, when the two bilayer superlattices have similar periods [3]. We analyzed the formation of the two types of trilayer superlattices and their domain structures. Our results reveal the huge potential of twisted multi-layer TMDCs as functional ferroelectric device applications based on van der Waals materials.

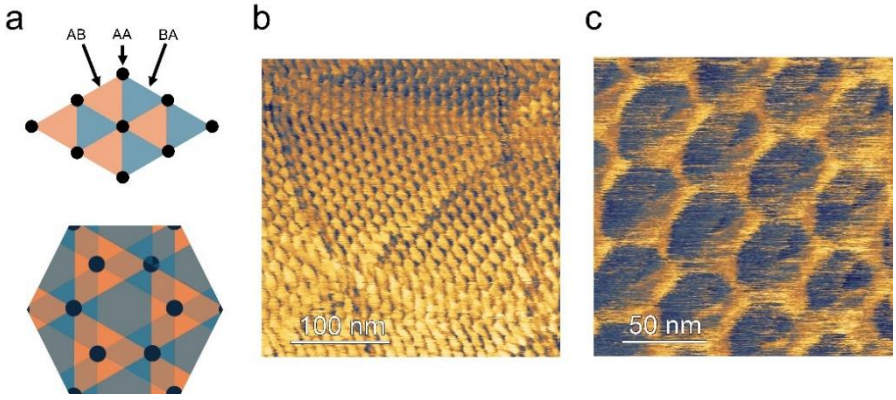

Figure: a. (Top) moiré superlattice in twisted bilayer TMDC. (Bottom) one possible moiré superlattice in twisted trilayer TMDC. (b, c) PFM phase images of trilayer moiré superlattice when the two bilayer superlattices have diverse periods (b) and similar periods (c).

References

[1] X, Wang *et al.*, *Nat. Nanotechnol.* **17**, 367–371 (2022).
[2] H. Ou *et al.*, *Small*, 2407316 (2025), in press.
[3] N. Nakatsuji *et al.*, *Phys. Rev. X*, **13**, 041007, 2023.

Session
NT 25（The 25th International Conference on the Science and Applications of Nanotubes and Low-

| Main conference：Main conference

Tue. Jun 17, 2025 6:00 PM - 8:00 PM JST | Tue. Jun 17, 2025 9:00 AM - 11:00 AM UTC Poster 1(International Exchange Hall III, Clock Tower Centennial Hall, 2F)

[17psa] Poster 1

[17psa-01]

Hybrid silicon all-optical switching devices integrated with 2D material

*Daiki Yamashita[1,2], Nan Fang[1], Shun Fujii[1,3], Yuichiro K Kato[1] (1. RIKEN (Japan), 2. AIST (Japan), 3. Keio Univ. (Japan))

[17psa-02]

Optical resolution of single-walled carbon nanotubes through wrapping with chiral metal coordination polymers followed by interlocking with metal-tethered tetragonal nanobrackets

Sicong Dai[1], Guoqin Cheng[1], Takuya Hayashi[2], Xinyi Fu[1], *Naoki Komatsu[1] (1. Graduate School of Human and Environmental Studies, Kyoto University (Japan), 2. Carbon Science Division, Research Institute for Supra Materials, Shinshu University (Japan))

[17psa-03]

Perpendicular electronic transport in twisted 3D graphite and twisted 3D superconductors

*Tenta Tani[1], Takuto Kawakami[1], Mikito Koshino[1] (1. Osaka Univ. (Japan))

[17psa-04]

Correlation between Flow-induced Electricity Generation on Graphene and Flow Dynamics

*Takeru Okada[1], Mitsuhiro Honda[2], Masaki Tanemura[2], Ichiro Yamashita[3], Atsuki Komiya[4] (1. Graduate School of Engineering, Tohoku University (Japan), 2. Naogya Institute of Technology (Japan), 3. Osaka University (Japan), 4. Institute of Fluid Science, Tohoku University (Japan))

[17psa-05]

Surface-Dependent Graphene Growth Kinetics on Cu Foil in Low-Pressure Chemical Vapor Deposition

*Jiyun Kim[1], Ji-Yong Park[1] (1. Ajou Univ. (Korea))

[17psa-06]

Automated evaluation and counting of nanofibers in SEM micrographs

*Torben Peters[1], John Schumann[1], Asmus Meyer-Plath[1] (1. Federal Institute for Occupational Safety and Health (Germany))

[17psa-07]

Suspended SWCNT arrays by transfer with sublimable materials

*Yuuki Kanai[1], Kaito Sakakibara[1], Riku Fujiwara[1], Ryotaro Kaneda[1], Waka Miyata[1], Keigo Otsuka[1], Shigeo Maruyama[1], Chiashi Shohei[1] (1. The University of Tokyo (Japan))

[17psa-08]

Hydrogenolysis of Graphene Oxide

*Moe Kitamura[1], Akiho Horibe[1], Koji Nakabayashi[2], Toshihira Irisawa[3], Yoshiyuki Nonoguchi[1] (1. Kyoto Institute of Technology (Japan), 2. Kyushu University (Japan), 3. Gifu University (Japan))

[17psa-09]

Chemical Vapor Deposition of Large Area Single-Walled Carbon Nanotubes Films Using Ethanol as the Carbon Precursor

*Afzal Khan[1], Abid .[1], Lingfeng Wang[1], Yongjia Zheng[1], Nduwarugira Bill Herve[1], Salman Ullah[1], Hafiz Bilal Naveed[1], Rong Xiang[1] (1. Zhejiang University (China))

[17psa-10]

Viral detection platform: portable graphene-derived biosensor

*Ana Champi[1] (1. Federal University of ABC (Brazil))

[17psa-11]

Optimizing CVD Growth of Monolayer MoS 2 through Relative Configurations of Substrate and Gas flows

*hoyeon Jung[1], jiyong Park[1] (1. Ajou University (Korea))

[17psa-12]

Energetics and electronic property of Janus WSSe nanoscroll

*Yanlin Gao[1], Susumu Okada[1] (1. University of Tsukuba (Japan))

[17psa-13]

Electrical and thermal transport properties of individual carbon nanotubes by in situ TEM

*Daiming Tang[1,2], Hai-Bo Zhao[3,4], Ovidiu Cretu[1], Chang Liu[3,4] (1. National Institute for Materials Science (NIMS) (Japan), 2. Faculty of Pure and Applied Sciences, University of Tsukuba (Japan), 3. Institute of Metal Research (IMR), Chinese Academy of Sciences (CAS) (China), 4. School of Materials Science and Engineering, University of Science and Technology of China (China))

[17psa-14]

Investigation and Mitigation of the Electron-Hole Conduction Asymmetry in Graphene Field-Effect Transistors

*MINSANG KIM[1], Ji-Yong Park[1] (1. AJOU UNIV. (Korea))

[17psa-15]

Signle-step SH group termination of epitaxial graphene and graphene oxide

*Yuya Miyake[1], Jun Ishii[1], Taisei Suzuoka[1], Yoshiaki Matsuo[2], Kazuyuki Takai[1] (1. Hosei Univ. (Japan), 2. Univ. of Hyogo (Japan))

[17psa-16]

Aggregation effect on exciton binding energies of single-chirality single-walled carbon nanotubes

*Zhirui Liu[1], Taishi Nishihara[1], Vasili Perebeinos[2], Yuhei Miyauchi[1] (1. Institute of Advanced Energy, Kyoto University (Japan), 2. Department of Electrical Engineering and Center for Advanced Semiconductor Technologies, University at Buffalo (United States of America))

[17psa-17]

Solvent acoustic coupling governs non-covalent bonding at the interface of ultra-long carbon nanotubes

*Yuxuan Tian[1] (1. Beijing Key Laboratory of Green Chemical Reaction Engineering and Technology, Department of Chemical Engineering, Tsinghua University, Beijing 100084, China. (China))

[17psa-18]

Fabrication of Near-Infrared Perfect Absorber Using Chirality-Sorted Carbon Nanotubes

*Mioko Kawakami[1], Sota Takasu[1], Taishi Nishihara[1], Yuhei Miyauchi[1] (1. Kyoto University (Japan))

[17psa-19]

One-pot Electrochemical Exfoliation/Functionalization of graphite for N-Functionalized Graphene

Yuta Konno[1], Sota Ishizu[1], Ryo Watanabe[1], *Haruya Okimoto[1] (1. Yamagata University (Japan))

[17psa-20]

Self-winding ultra-long carbon nanotube rings and their potential functional applications

*Sibo Chen[1], Fei Wei[1] (1. Tsinghua University (China))

[17psa-21]

A High-Performance High-Temperature Accelerometer Based on the Improved Graphene Aerogel

*Yanchun Wang[1], Zibo Wang[1], Weiya Zhou[1] (1. Institute of Physics, Chinese Academy of Sciences (China))

[17psa-22]

Early-Stage Au Deposition Morphology on Graphene and Its Effect on Graphene Field Effect Transistors

*SungYeon Kim[1], Ji-Yong Park[1] (1. Ajou university (Korea))

[17psa-23]

A statistical assessment of the semiconducting proportion in single-wall carbon nanotubes based on electrostatic force microscopy

Yuki Kuwahara[1], Indra M Khoris[1], Fahmida Nasrin[1], *Ryota Yuge[2,1], Takeshi Saito[1] (1. AIST (Japan), 2. NEC (Japan))

[17psa-24]

Diameter Dependence of Phase Transition and Phases Coexistence of Water Confined Inside Carbon Nanotubes

*Wenjie Liu[1], Ikuma Kohata[1], Yuki Maekawa[2], Takihiro Yamamoto[2], Yoshikazu Homma[2], Shohei Chiashi[1] (1. The University of Tokyo (Japan), 2. Tokyo University of Science (Japan))

[17psa-25]

Carbon Nanotube-based Spectrally Selective Solar Absorber: Design and Fabrication

*Hengkai Wu[1], Taishi Nishihara[1], Takeshi Tanaka[2], Hiromichi Kataura[2], Yuhei Miyauchi[1] (1. Kyoto University (Japan), 2. National Institute of Advanced Industrial Science and Technology (AIST) (Japan))

[17psa-26]

Achieving High Thermal Conductivity with Lower Filler Loading: Direct CNT Growth on AlN in Silicone Rubber Composites

*Naoyuki Matsumoto[1], Don N. Futaba[1], Takeo Yamada[1], Ken Kokubo[1] (1. National Institute of Advanced Industrial Science and Technology (AIST) (Japan))

[17psa-27]

Oxidation Mechanism on Single-Walled Carbon Nanotubes Analyzed by Photo-Induced Force Microscopy

*Kaori Fujii[1], Kazufumi Kobashi[1], Yasuhiko Fujita[1], Takahiro Morimoto[1], Hideaki Nakajima[1], Toshiya Okazaki[1] (1. Advanced industrial science and technology (Japan))

[17psa-28]

Large-scale separation of micrometer-long single-chirality single-wall carbon nanotubes in aqueous surfactant systems

*Zimeng An[1], Sayuki Oka[1], Kazuki Nagashima[1], Yohei Yomogida[1] (1. Hokkaido University (Japan))

[17psa-29]

Automatic Transfer of Carbon Nanotubes: from Growth to Device Performance

*Luca Ornago[1], Frederik H. van Veen[2,3], Jorien van der Meulen[4,1], Seoho Jung[1], Natanael Lanz[1], Andre Butzerin[1], Marko Nikolic[1], Mikael L. Perrin[2,3], Maria El Abbassi[1] (1. Chiral Nano AG (Switzerland), 2. Empa (Switzerland), 3. ETH Zürich (Switzerland), 4. TU Delft (Netherlands))

[17psa-30]

Ultraclean carbon nanotube transistors via robotic assembly

*Seoho Jung[1], Frederik van Veen[2,3], Jorien van der Meulen[1,4], Luca Ornago[1], Marko Nikolic[1], Andre Butzerin[1], Natanael Lanz[1], Mickael Perrin[2,3], Maria El Abbassi[1] (1. Chiral Nano AG (Switzerland), 2. Empa (Switzerland), 3. ETH Zurich (Switzerland), 4. Delft Univ. of Technology (Netherlands))

[17psa-31]

NIR photoluminescence of single-wall carbon nanotubes by the biochemical reaction of luciferin/luciferase

*Takeshi Tanaka[1], Mahoko Higuchi[1], Mayumi Tsuzuki[1], Atsunori Hiratsuka[1], Hiromichi Kataura[1] (1. Nanomaterials Research Institute, National Institute of Advanced Industrial Science and Technology (AIST) (Japan))

[17psa-32]

Reconfigurable physical unclonable functions from carbon nanotube transistors for secure vehicle communications

*Yang Liu[1], Jingfang Pei[1], Yingyi Wen[1], Lekai Song[1], Songwei Liu[1], Pengyu Liu[1], Teng Ma[2], Guohua Hu[1] (1. the Chinese University of Hong Kong (Hong Kong), 2. the Hong Kong Polytechnic University (Hong Kong))

[17psa-33]

MXene Quantum Dots/ Metal Organic Framework Hybrid for Photocatalytic Applications

*MUHAMMAD ANNAS SYHUKRI BIN MOHD ARIFFIN[1], ANIR SYAHMI BIN SHARBIRIN[1], AFRIZAL LATHIFUL FADLI[1], JEONGYONG KIM[1] (1. SUNGKYUNKWAN UNIVERSITY (Korea))

[17psa-34]

Theoretical study on photo thermoacoustic phenomena in carbon nanotubes based on Tyndall model

*Akari Sudo[1], Takahiro Yamamoto[1] (1. Tokyo University of Science (Japan))

[17psa-35]

Semiconducting Transport Characteristics and Performance of Large-Bundle SWCNT FETs

*Md Abu Taher Khan[1], Nan Wei[2], Esko I. Kauppinen[1] (1. Aalto University (Finland), 2. Peking University (China))

[17psa-36]

Armchair-Oriented Synthesis of Tin Disulfide Nanotubes (SnS_2 NT)

*Abid .[1], Yongjia Zheng[1], Luneng Zhao[2], Ju Huang[3,4], Yuta Sato[5], Qingyun Lin[6], Zheng Han[7], Chunxia .[1], Tianyu Wang[1], Kazu Suenaga[10], Yige Zheng[1], Hang Wang[1], Salman Ullah[1], Mohd Taazeem Ansari[8], Feng Ding[9], Afzal Khan[1], Wenbin Li[3,4], Junfeng Gao[2], Shigeo Maruyama[11], Rong Xiang[1] (1. State Key Laboratory of Fluid Power and Mechatronic Systems, Zhejiang Provincial Key Laboratory for Atomic-level Manufacturing, School of Mechanical Engineering, Zhejiang University (China), 2. Key Laboratory of Material Modification by Laser, Ion and

Session
NT 25（The 25th International Conference on the Science and Applications of Nanotubes and Low-Electron Beams (Dalian University of Technology), Ministry of Education, Dalian, 116024, China (China), 3. Key Laboratory of 3D Micro/Nano Fabrication and Characterization of Zhejiang Province, School of Engineering, Westlake University, 310030, Hangzhou, China (China), 4. Institute of Advanced Technology, Westlake Institute for Advanced Study, 310024, Hangzhou, China (China), 5. Nanomaterials Research Institute, National Institute of Advanced Industrial Science and Technology (AIST), Tsukuba 305-8565, Japan (Japan), 6. Center of Electron Microscopy, State Key Laboratory of Silicon and Advanced Semiconductor Materials, School of Material Science and Engineering, Zhejiang University, Hangzhou 310027, China (China), 7. College of Chemistry and Molecular Engineering, Peking University, Beijing 100871, P. R. China (China), 8. Department of Applied Sciences & Humanities, Faculty of Engineering & Technology, Jamia Millia Islamia, New Delhi, India (India), 9. Institute of Technology for Carbon Neutrality, Shenzhen Institute of Advanced Technology, Chinese Academy of Sciences, Shenzhen, China (China), 10. The Institute of Scientific and Industrial Research, Osaka University, 8-1 Mihogaoka, Ibaraki, Osaka, Japan (Japan), 11. Department of Mechanical Engineering, The University of Tokyo, Tokyo 113-8656, Japan (Japan))

[17psa-37]

Overcoming Van der Waals Bundling: Molecular Wedges Enable Sonication-Free Dispersion of Single-Walled Carbon Nanotubes

*Seungyeop Lee Lee[1], Ziyi Wang[1], Ebenezer Afriyie[1], Jiajun Wang[2], Ayman Alibrahim[1], Anand Jagota[2], YuHuang Wang[1] (1. University of Maryland, College Park (United States of America), 2. Lehigh University (United States of America))

[17psa-38]

Hydrogen storage by carbon nanohorns enhanced by dispersion with metallic nanoparticles

*Noriaki Sano[1] (1. Kyoto Univerisity (Japan))

[17psa-39]

Synthesis of H_2-rich syngas and CNTs from CH_4/CO_2 using Ni-Mo_2C/MgO catalyst: Impact of biogas impurities and catalyst regeneration

*Supanida Saconsint[1], Noriaki Sano[1], Sakhon Ratchahat[2] (1. Kyoto Univerisity (Japan), 2. Mahidol University (Thailand))

[17psa-40]

Geometric structure and electronic properties of bilayer graphene with a Moire superlattice by interlayer asymmetric tensile strain

Mina Maruyama[1], Nadia Sultana[1], Yanlin Gao[1], *Susumu Okada[1] (1. UNiversity of Tsukuba (Japan))

[17psa-41]

Structural and Electrical Properties of 3D CNT Networks in CNT-Oxide Ceramic Composites

*Akinobu Shibuya[1,2], Tomo Tanaka[1,2], Noriyuki Tonouchi[1,2], Toshie Miyamoto[1,2], Ryota Yuge[1,2] (1. NEC Corporation (Japan), 2. National Institute of Advanced Industrial Science and Technology (Japan))

[17psa-42]

Composite of Carbon Nanotubes and Activated Carbon as Air Electrode in Zn-air Battery

*Munsuree Kalong[1], Noriaki Sano[1], Tetsuo Suzuki[1] (1. Kyoto Univerisity (Japan))

[17psa-43]

Quantitative insights into the correlation between sp^3 defects and functional groups in oxidized single-walled carbon nanotubes

*Hideaki Nakajima[1], Kazufumi Kobashi[1], Ying Zhou[1], Minfang Zhang[1], Toshiya Okazaki[1] (1. National Institute of Advanced Industrial Science and Technology (Japan))

[17psa-44]

Preferential growth of (7,5) SWCNTs by enhanced direct-injection pyrolytic synthesis method

Yuki Kuwahara[1], Yuta Nishiwaki[2], Kei Takano[2], *Takeshi Hashimoto[2], Ryota Yuge[1,3], Takeshi Saito[1] (1. AIST (Japan), 2. Meijo Nano Carbon Co. Ltd. (Japan), 3. NEC (Japan))

[17psa-45]

Vacuum electronics of carbon nanotubes and its applications in aerospace

*Peng Liu[1], Lian Liu[1], Kaili Jiang[1], Shoushan Fan[1] (1. Tsinghua University (China))

[17psa-46]

Machine learning force field driven exploration of 992 binary alloy metal clusters for carbon nanotube growth

*Daniel Hedman[1], Daisuke Asa[2], Ryo Yoshikawa[2], Ikuma Kohata[2], Kaoru Hisama[3], Christophe Bichara[4], Keigo Otsuka[2], Shigeo Maruyama[2] (1. Center for Multidimensional Carbon Materials (CMCM), Institute for Basic Science (IBS) (Korea), 2. Department of Mechanical Engineering, The University of Tokyo (Japan), 3. Center for Research Initiative for Supra-Materials, Shinshu University (Japan), 4. Aix-Marseille Univ, CNRS, CINaM (France))

[17psa-47]

Impact of Twisted angle on Thermal Transport Property of Graphene/h-BN Moiré Superlattice

*SHINICHIRO MOURI[1], Yusuke Kodama[1], Abdul Kuddus[2] (1. Graduate of School of Science and Engineering (Japan), 2. R-GIRO, Ritsumeikan University (Japan))

[17psa-48]

Structure and Fabrication Process Optimization of Microbolometer Array using Semi-conducting Single-walled Carbon Nanotube Networks

*Tomo Tanaka[1,2], Masahiko Sano[1], Masataka Noguchi[1,2], Megumi Kanaori[2], Toshie Miyamoto[1,2], Ryota Yuge[1,2] (1. NEC Corporation (Japan), 2. AIST (Japan))

[17psa-49]

Gate Voltage Dependence of Low-Frequency Noise in Carbon Nanotube Networks

*Noriyuki Tonouchi[1,2], Norika Fukuda[2], Tomo Tanaka[1,2], Ryota Yuge[1,2] (1. NEC (Japan), 2. AIST (Japan))

[17psa-50]

Terahertz wave detection using P/N carbon nanotube fiber at room temperature

*Koki Shiba[1], Shigeki Saito[1], Satoshi Kusaba[1,2], Ryo Tamaki[2], Shizuka Tsuduki[3], Tsukasa Matsuura[3], Jun Takeda[2], Ikufumi Katayama[2], Kazuhiro Yanagi[1] (1. Tokyo Metroplitan Univ. (Japan), 2. Yokohama National Univ. (Japan), 3. TOKAI RIKA Co., LTD. (Japan))

[17psa-51]

Growth of Isolated Carbon Nanotubes Wrapped by Homogeneous Amorphous Carbon

Zeyu Liu[1], Xinrui Zhang[1], Yanzhao Liu[1], Zilong Qiu[1], Jian Sheng[1], Zeyao Zhang[1], *Yan Li[1] (1. Peking University (China))

[17psa-52]

DIRECT GRAPHENE GROWTH BETWEEN ELECTRODES BY JOULE HEATING

*Koki Nakane[1], Agus Subagyo[1], Kazuhisa Sueoka[1] (1. Graduate School of Information Science and Technology, Hokkaido University (Japan))

Hybrid silicon all-optical switching devices integrated with 2D material

Daiki Yamashita[1,2], Nan Fang[3], Shun Fujii[1,4] and Yuichiro K. Kato[1,3]

[1]*Quantum Optoelectronics Research Team, RIKEN Center for Advanced Photonics, Saitama 351-0198, Japan*
[2]*Platform Photonics Research Center, National Institute of Advanced Industrial Science and Technology (AIST), Ibaraki 305-8568, Japan*
[3]*Nanoscale Quantum Photonics Laboratory, RIKEN Cluster for Pioneering Research, Saitama 351-0198, Japan*
[4]*Department of Physics, Faculty of Science and Technology, Keio University, Kanagawa 223-8522, Japan*

Silicon photonics has garnered attention as a platform for photonic integrated circuits (PICs), which monolithically integrate electronic and photonic devices in the same chip. On-chip all-optical switching is an essential component for the PICs. Fast and energy-efficient all-optical switches based on microcavities have been demonstrated, and currently, the performance is limited by the substrate material which is silicon. Here we propose and demonstrate hybrid all-optical switching devices that combine silicon nanocavities and two-dimensional (2D) semiconductors [1]. By exploiting the refractive index modulation caused by photo-induced carriers in the 2D material instead of the silicon substrate, we offer a new pathway for overcoming the switching performance limitation imposed by the substrate material. Photonic crystal nanobeam cavities capable of efficient interaction with 2D materials are fabricated, and molybdenum ditelluride ($MoTe_2$), a 2D material with rapid carrier recombination, is transferred onto the cavities. The $MoTe_2$ flake is excited by an optical pump pulse to shift the resonant wavelength of the cavity for switching operation. We have successfully achieved all-optical switching operations on the time scale of tens of picoseconds while requiring a low switching energy of a few hundred femtojoules.

This work is supported in part by JSPS (KAKENHI JP22K14624, JP22K14625, JP20H02558, JP23H00262), and MEXT (ARIM JP-MXP1223UT1141). N.F. is supported by RIKEN Special Postdoctoral Researcher Program. The FDTD calculations are performed using the HOKUSAI BigWaterfall supercomputer at RIKEN. We acknowledge the Advanced Manufacturing Support Team at RIKEN for technical assistance.

References

[1] D. Yamashita, N. Fang, S. Fujii, Y. K. Kato, Hybrid silicon all-optical switching devices integrated with 2D material, *Adv. Opt. Mater.* 13, 2402531 (2024).

Optical resolution of single-walled carbon nanotubes through wrapping with chiral metal coordination polymers followed by interlocking with metal-tethered tetragonal nanobrackets

Guoqing Cheng[1], Sicong Dai[1], Takuya Hayashi[2], Xinyi Fu[1], Naoki Komatsu[1]

[1] Graduate School of Human and Environmental Studies, Kyoto University (Japan), [2] Carbon Science Division, Research Institute for Supra Materials, Shinshu University (Japan)

Since the optically active carbon nanotubes (CNTs) were first separated in 2007 [1], many CNTs have been optically resolved mostly by use of chiral surfactants [2], (bio)polymers [3] and host molecules [4]. In this work, simple metal salts consisting of chiral ligands and metal ions successfully discriminate the handedness or helicity of single-walled carbon nanotubes (SWNTs). Actually, optically active SWNTs were separated with sequential addition of copper (*R*)- or (*S*)-mandelate ((*R*)- or (*S*)-Cu**L**$_2$, respectively) and dipyrrin nanobracket (**NB**). After removal of the metal salt and **NB**, a pair of dispersions gave symmetrical CD spectra, indicating that the small chiral molecules or mandelates discriminate the handedness of SWNTs. The following two steps are conceivable in this optical resolution; 1) the helicity of SWNTs was discriminated through selective wrapping with chiral coordination polymers formed by (*R*)- and (*S*)-Cu**L**$_2$, and 2) the SWNTs wrapped with the coordination polymers were selectively dispersed through interlocking by dipyrrin **NB** copper complexes. The experimental results are supported by the theoretical calculations; van der Waals interaction of (*R*)-Cu**L**$_2$ with (*P*)-(6,5)-SWNTs is stronger than that with (*M*)-(6,5)-SWNTs.

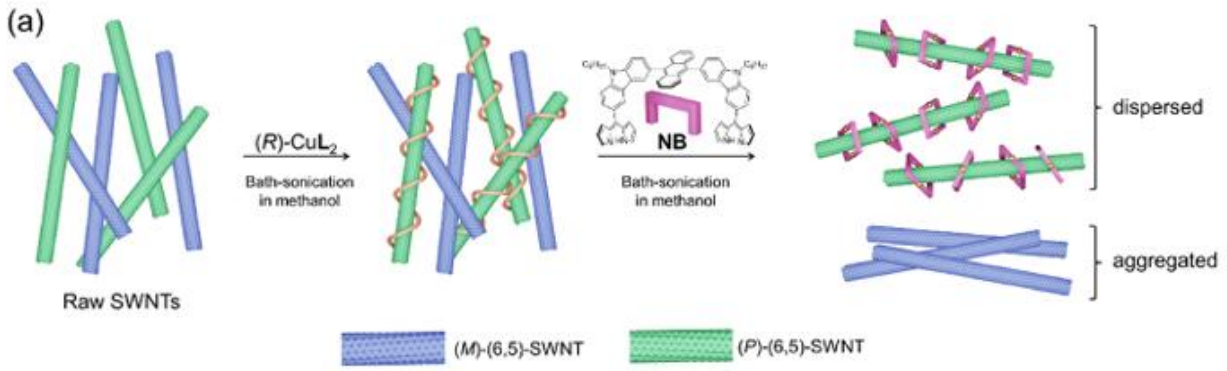

Figure 1: Procedure of SWNT separation with (*R*)-Cu**L**$_2$ and nanobracket (**NB**)

References

[1] X. Peng, N. Komatsu, et al., *Nat. Nanotechnol*. **2007**, 2, 361; X. Peng, N. Komatsu, et al., *J. Am. Chem. Soc*., **2007,** 129, 15947; F. Wang, N. Komatsu, et al., *J. Am. Chem. Soc*., **2010**, 132, 10876.
[2] Lin P, Cong Y, et al., *ACS Appl. Mater*, **2015**, 7, 6724.
[3] Akazaki K, Toshimitsu F, Ozawa H, et al., *J. Am. Chem. Soc*. **2012**, 134, 12700.
[4] G. Liu, N. Komatsu, et al., *J. Am. Chem. Soc*. **2013**, 135, 4805; G. Liu, N. Komatsu, et al., *J. Mater. Chem. A*, **2014**, 2, 19067; G. Liu, Y. Miyake, N. Komatsu, *Org. Chem. Front*, **2017**, 4, 911.

Perpendicular electronic transport in twisted 3D graphite and twisted 3D superconductors

Tenta Tani, Takuto Kawakami, Mikito Koshino

Department of Physics, Osaka University (Japan)

We theoretically study a perpendicular electronic transport in twisted three-dimensional (3D) systems using the effective continuum model and recursive Green's function method [1].

Recently, twisted two-dimensional (2D) systems, where a pair of 2D materials are stacked with a twist, have attracted significant attentions. Our research question is what are the properties of a twisted 3D system, which is a pair of 3D materials stacked with a twist?

Here we study how the perpendicular electronic transport depends on the twist angle in twisted 3D systems. The perpendicular electric conduction in twisted systems was probed in a recent experiment [2] while the transmission across the twisted interface has not been well examined theoretically. In this study, we develop a formulation for the electronic transport in the twisted 3D system, which is a pair of 3D materials stacked with a twist angle, by using the effective continuum model and recursive Green's function method.

We apply the method to twisted graphite (rotationally-stacked graphite pieces), which is one of the simplest twisted 3D systems.

In the twisted graphite, we found that the perpendicular conductivity depends on the twist angle non-monotonously, and it cannot be explained by a simple picture based on the Fermi-surface overlap. We reveal that the anomalous twist-angle dependence is due to the Fano resonance by an interface-localized state, which is a remnant of the flat state of magic-angle twisted bilayer graphene. The existence of the interface-localized state is confirmed by calculating the local density of states using the recursive Green's function method. In addition, we will report the extension of our formulation to 3D superconductors, and the Josephson current calculated by our method.

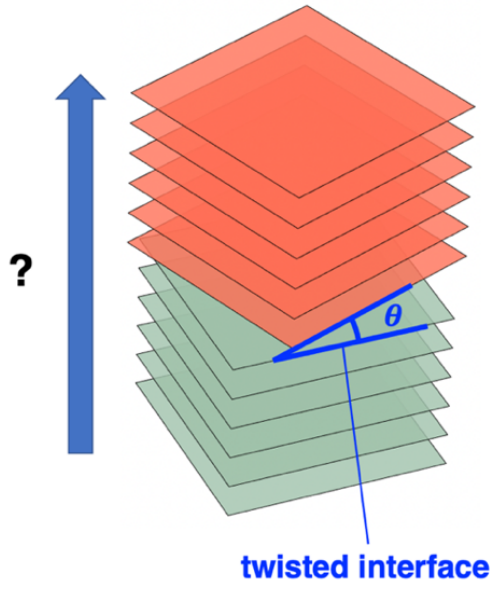

Figure 1: The schematic figure of twisted 3D system.

References

[1] T. Tani, T. Kawakami, M. Koshino, Phys. Rev. B **108**, 165422 (2023).

[2] A. Inbar *et al.*, Nature **614**, 682 (2023).

Correlation between Flow-induced Electricity Generation on Graphene and Flow Dynamics

T. Okada[1], M. Honda[2], M. Tanemura[2], I. Yamashita[3], and A. Komiya[4]

[1]*Department of Electronic Engineering, Tohoku University (Japan),* [2]*Naogya Institute of Technology (Japan),*

[3]*Osaka University (Japan),* [4]*Institute of Fluid Science, Tohoku University (Japan)*

The transfer of liquid media over or through nanocarbons has shown potential for various applications, which have been extensively explored due to the development of techniques that leverage the nearly ideal nanocarbon surfaces. Over the past decade, experimental achievements in interfacial electricity generation by flowing liquids over nanocarbons have been reported by several groups. Recently, theories have been proposed for graphene in a liquid medium that involve the interaction between the charge fluctuations of the liquid's molecules, called as hydrons, and the electronic excitations in graphene. This "quantum friction" mechanism has the potential to control nanofluid behavior and could have significant impact across various fields. The mechanism is based on the condition that the flow near the interface (graphene) is not considered. However, some experimental results do not satisfy the condition, hence the mechanism is still debatable issue, especially in terms of flow conditions. In this study, we investigated the correlation between the electricity of graphene and the flow conditions of liquid water through both experiments and numerical calculations.

We used micro-fluidic chips that consist of PDMS fluidic channel, graphene/glass substrate, electrical connections, and water supply ports. The generated voltage was measured in several points in the flow channel along flow direction by applying water flow over graphene.

The voltage generation responds water-flow and is repeatable and reproducible as shown in Fig. 1. In addition, the position along flow direction in the channel greatly affects magnitude of the generated voltage, indicating that flow conditions corelates the voltage generation. Since flow conditions in the channel are complex, we investigated the effects of flow conditions using numerical simulation. As a result, near the inlet, the irregular flow is observed as asymmetric flow speed profiles. These profiles gradually change to symmetric shapes as the flow develops in the middle region of the channel, indicating that a feature of laminar flow in the channels. The profiles observed in the middle region of the channel indicate that the flow condition not only becomes laminar but also fully developed in this region. Figure 2 shows the plot of the experimentally obtained Electromotive Force (EMF, E) versus the flow transition ratio estimated by numerical calculation. As the figure indicates, the EMF is low at the inlet region, then increases as flow develops towards the middle region. As flow develops further to nearly laminar, the EMF drops significantly and is approximately zero. This observed relationship suggests that the middle region is suitable for generating the EMF due to the flow transition. The magnitude and gradient of the flow velocity change are correlated with the generated EMF. Considering the length of graphene, the transition ratio also exists on graphene, indicating that moderate transition of flow conditions plays a role in the electrical conduction of graphene[1]. Thus, our results indicate that the spatial transition region from irregular to laminar flow plays a crucial role in electricity generation.

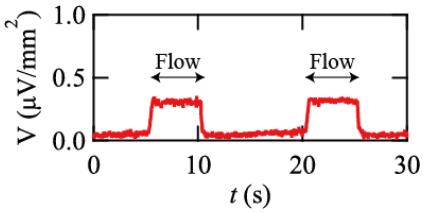

Figure 1: The generated voltage from graphene by flowing water.

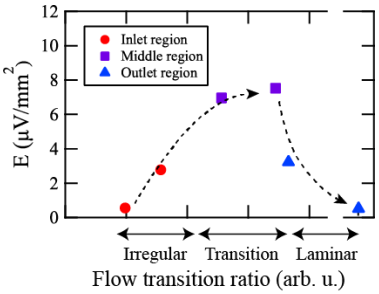

Figure 2: Correlation between the generated Electromotive Force and flow transition ratio obtained by numerical calculation.

References

[1] H. Takeda, N. Iwamoto, M. Honda, M. Tanemura, I. Yamashita, A. Komiya, and T. Okada, *Appl. Phys. Lett.* **125**, 184101 (2024).

Surface-Dependent Graphene Growth Kinetics on Cu Foil in Low-Pressure Chemical Vapor Deposition

Jiyun Kim[1], Ji-Yong Park[*]

[1] *Department of Physics and Energy Systems Research, Ajou University, Suwon 16499, Korea*

In this study, we investigate and compare graphene growth characteristics on the top and bottom surfaces of Cu foil using low-pressure chemical vapor deposition (LPCVD). When the Cu foil is loaded, it conforms to the curvature of the quartz tube in the LPCVD setup, resulting in the top and bottom surfaces of Cu foil encountering different gas environments in terms of gas flow rate and residence time during the LPCVD growth process. Consequently, graphene grown on the top surface achieves full monolayer coverage in as fast as 1 minute, approximately 10 times faster than on the bottom surface. The top surface, being more directly exposed to the gas flow, facilitates rapid monolayer formation. However, prolonged growth times exceeding 5 minutes also lead to the secondary nucleation for multilayer growth. Conversely, graphene grown on the bottom surface proceeds at a slower rate, involving the expansion of graphene islands to gradually form a monolayer. We systematically investigated these growth characteristics and differences using optical and electron microscopy, Raman spectroscopy, and atomic force microscopy. Additionally, we also investigated the device characteristics of field effect transistors based on graphene grown on both surfaces.

Automated evaluation and counting of nanofibers in SEM micrographs

T. Peters[1], J. Schumann[1], A. Meyer-Plath[1]

[1]*Federal Institute for Occupational Safety and Health (Germany)*

Determination of size and diameter distributions of fibers in electron microscope images is a central requirement both of fibre synthesis quality control and of workplace exposure measurements. As visual morphological evaluation is a tedious and time-consuming task, we have developed an automated fiber characterization, classification and counting method. It employs a convolutional neural network of U-Net-like architecture that recognizes fiber-occupied image pixels and returns fibre image areas as masks. These masks are then subjected to classic image processing algorithms that trace and morphologically analyze contained fibers. The U-Net was trained on a large data set of more than 20 gigapixels of manually annotated high-resolution SEM micrographs. A comparative analysis, conducted to assess the reliability of our method, reveals a great level of agreement between the automated results generated by our method and those obtained manually by human experts.

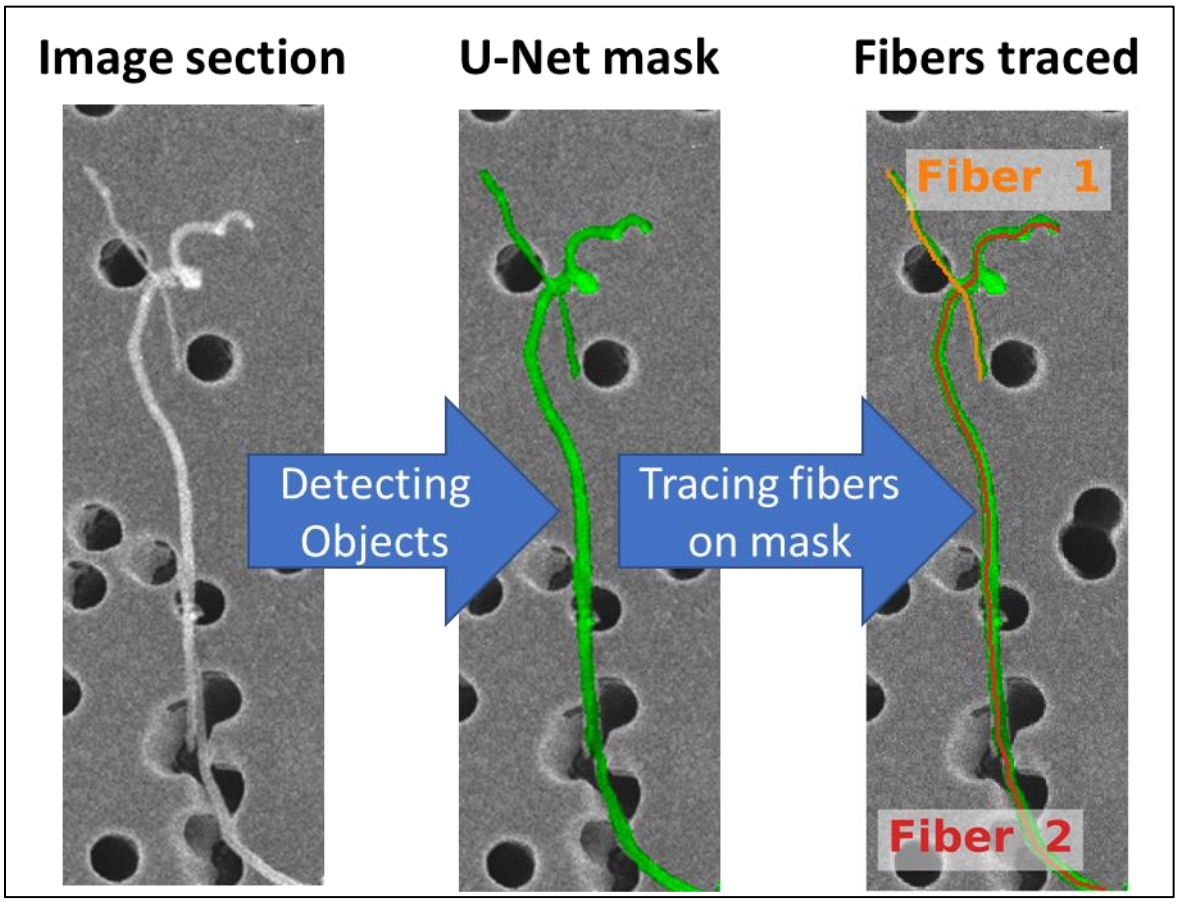

Figure: Our method applied to a section of a SEM micrograph.

Suspended SWCNT arrays by transfer with sublimable materials

Yuuki Kanai[1], Kaito Sakakibara[1], Riku Fujiwara[1], Ryotaro Kaneda[1], Waka Miyata[1], Keigo Otsuka[1], Shigeo Maruyama[1], Chiashi Shohei[1]

[1]*Department of Mechanical Engineering, The University of Tokyo, Tokyo 113-8656, Japan*

The suspended structure of single-walled carbon nanotubes (SWCNTs) eliminates the influence of the substrate, suitable for device applications and spectroscopy analysis. Cyclododecane (CDD), which is sublimable at room temperature, is expected to be a transfer agent that is less likely to leave impurities and thus less likely to affect SWCNTs. In this study, we have successfully fabricated suspended structures of horizontally aligned SWCNT (HA-SWCNT) arrays by transferring them onto a slit keeping parallel using CDD as a transfer agent and evaluated.

To synthesize HA-SWCNTs, R-cut quartz substrates were used and iron catalysts were deposited on them. Then HA-SWCNTs were grown by an alcohol CVD method at 800°C. CDD/HA-SWCNT/quartz substrate structure was fabricated by spin-coating a hexane solution of CDD onto the synthesized HA-SWCNTs and recrystallizing the CDD on a hot plate. The substrate was then immersed in potassium hydroxide solution and ammonia [2] solution at room temperature. The quartz substrate was etched by potassium hydroxide solution and the recrystallized CDD/HA-SWCNT film was exfoliated by ammonia solution. The peeled film floating on the liquid surface was scooped up with a SiO_2/Si slit substrate, and the CDD was sublimated at room temperature to form a suspended SWCNT structure on the slit. Samples were analyzed by scanning electron microscopy (SEM) and optical spectroscopy.

Figure 1 shows SEM images of the fabricated suspended SWCNT array structure. The density of SWCNTs on substrate is 0.83 μm^{-1} and those suspend is 0.73 μm^{-1}. So, approximately 88% of transferred SWCNTs on slit are suspended. Figure 2 shows the results of Raman scattering spectroscopy of the suspended SWCNTs and the SWCNTs on the substrate excited by 532 nm. The G-band intensity of the suspended SWCNTs was 5 times larger than that on the substrate when comparing the G-band intensity 1592 cm^{-1}. This indicates that the decrease in optical intensity of SWCNTs due to contact with the substrate is avoided in the suspended area. Figure 3 shows the mapping of SWCNT's G-band around suspended area. Not only on substrate but also on slit, suspended SWCNT' G-band can be seen.

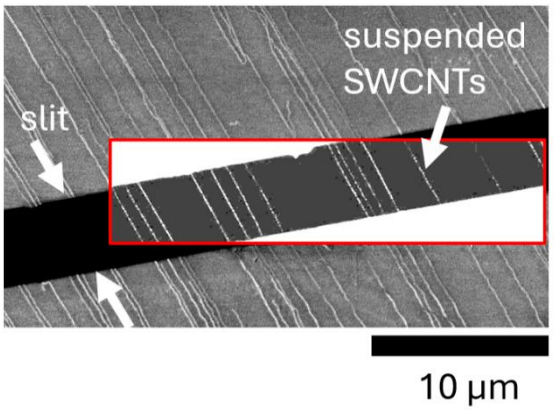

Fig. 1 SEM image of suspended SWCNTs on SiO_2/Si slit substrate.

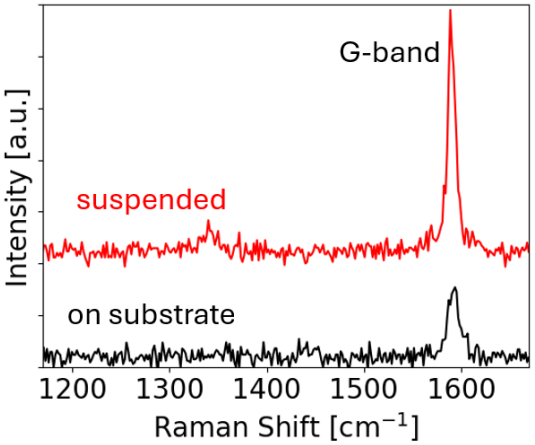

Fig. 2 Raman scattering spectra from suspended SWCNT and SWCNT on SiO_2/Si substrate. The excitation wavelength was 532 nm.

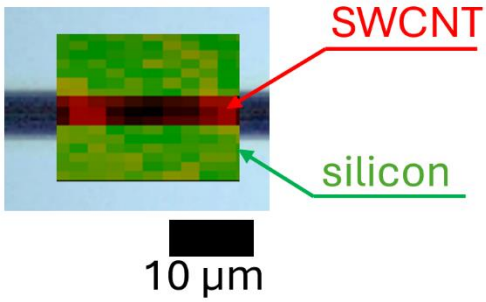

Fig. 3 Raman mapping image. Red indicate G-band of SWCNT and green indicate Si substrate.

References

[1] Kim, M. J. et al., *Appl. Phys. Lett.*, **123** (2023) 211602.

[2] X. Zheng et al. , NT'24 conference (2024) 300.

Hydrogenolysis of Graphene Oxide

○Moe Kitamura[1], Akiho Horibe[1], Koji Nakabayashi[2], Toshihira Irisawa[3], Yoshiyuki Nonoguchi[1]

[1]Faculty of Materials Science& Engineering, Kyoto Institute of Technology, Kyoto 606-8585, Japan, [2]Institute for Materials Chemistry and Engineering, Kyushu University, 819-0395, Fukuoka, Japan, [3]Gu Composite Center, Institute for Advanced Study, Gifu University, Gifu 501-1193, Japan

Currently, the development of recycling technologies for carbon materials is underway to prevent the depletion of fossil resources. Carbon materials, carbon fiber and graphite, are persistent due to their polycyclic aromatics with layered structure, and due to their remarkable stability, and then, their recycling still remains difficult. It is therefore important to establish advanced decomposition technology for carbon materials. Herein we use hydrogenolysis in hydrogenated solvents (i.e. 1,2,3,4-tetrahydronaphthalene (tetralin)), known as “direct coal liquefaction” for the production of petroleum alternatives.1 We examined the decomposition of carbon materials by a combination of chemical oxidation and hydrogenolysis. Graphene oxide (GO) with controlled oxidation degree was added to tetralin and autoclaved at 400℃ for 1 hour using a high temperature and high pressure reactor. Waxy solids were extracted from the autoclaved solution by vacuum distillation and dissolved in toluene and tetrahydrofuran (THF). The precipitates were further subject to Soxhlet extraction using THF, and toluene.

After autoclaving, the tetralin solution changed from colorless to yellow. In addition, the mass of GO decreased after autoclaving while the distillation of reaction solutions yielded wax like solids at the yields ranging from 10 to 15% (Table.1). Absorption and photoluminescence spectra showed distinct shoulders in the range from 300 nm to 400 nm for the toluene soluble portion, and with GO oxidation degree increased, the absorption and photoluminescence peaks were more isolated. These results suggest that the obtained solid contains polycyclic aromatics. Dynamic light scattering (DLS) showed that most of the toluene soluble portions were distributed in the range from 1 to 2 nm. This result suggests that the direct coal liquefaction has advanced degradation of GO to small molecules. NMR showed CH3 and CH2 of aliphatic, and aromatic peaks. The integral ratio showed more aliphatic peaks compared to aromatic peaks, suggesting that aliphatic peaks were the main components of the degradant2. FTIR also revealed that the obtained solids were composed mainly of alkanes with a small portion of aromatic species. In the presentation, we will report on the oxidation degree dependence on hydrogenolysis.

Table 1. Yields of various samples

GO Oxidation degree	Supply (mg)	Filtrate (mg)	Distilled & extracted in THF (mg)	Distilled & extracted in PhMe (mg)	Soxhlet extracted in THF (mg)	Soxhlet extracted in PhMe (mg)
20%	50.25	37.29	0.22	1.24	2.65	0.98
30%	49.96	32.93	2.43	0.87	1.14	1.37
40%	49.5	29.13	4.01	1.42	1.78	0.53
50%	50.35	23.94	0.44	2.88	1.38	1.99

References
[1] R. Malhotra, D. F. McMillen, Energy Fuels, 4, 184-193 (1990)
[2] Organic Spectra Analysis (in Japanese), Shokabo (2021)

Chemical Vapor Deposition of Large Area Single-Walled Carbon Nanotubes Films Using Ethanol as the Carbon Precursor

Afzal Khan[1], Abid[1], Lingfeng Wang [1], Yongjia Zheng[1], Nduwarugira Bill Herve[1], Salman Ullah[1], Hafiz Bilal Naveed[1], Rong Xiang[1*]

[1]*State Key Laboratory of Fluid Power and Mechatronic Systems, Zhejiang Provincial Key Laboratory for Atomic-level Manufacturing, School of Mechanical Engineering, Zhejiang University, Hangzhou-310058 (China)*

Abstract: Transparent conductive electrodes have influenced modern technologies as they represent an integral component of various optoelectronic devices. At present, indium tin oxide (ITO) is the most commonly used transparent conductive material. However, its brittle nature and the limited resource of indium pose many challenges for ITO applications, especially in flexible electronics. Therefore, alternative transparent conductive material such as single-walled carbon nanotubes (SWCNTs) as transparent conductive films (TCFs) show great potential owing to their outstanding mechanical, electrical, and optical properties coupled with excellent flexibility and environmental stability [1-3]. Herein, we report the synthesis of SWCNTs films using the floating-catalyst chemical vapor deposition (FCCVD) technique. A vertical wall quartz tube reactor is used coupled with the custom-built outlets to deposit large area SWCNTs films on A4 size filter papers. The ferrocene is used as a catalyst precursor, ethanol as a carbon precursor, and thiophene as a growth promoter. The ferrocene and thiophene are dissolved in ethanol, followed by injection with a syringe pump at an optimized rate. The injected solution is introduced into the growth reactor along with the mixed gas flow of hydrogen (H_2) and Argon (Ar) in a fixed ratio at a set growth temperature. The aerosol-grown SWCNTs travelled to the outlet of the reactor and deposited as a film on A4 size filter papers at room temperature. Raman analysis confirmed the high-quality growth of SWCNTs, and the film's thickness, density, and transparency are tuned by varying the deposition time. Since ethanol is environment and user friendly, it is a better choice to be used as the carbon precursor for producing high-quality and large-area SWCNTs films. Moreover, such large-area SWCNTs films could easily be press-transferred to any substrates like glass, silicon, paper, plastic, polymers, and metals. Hence, it will enable us to fabricate a variety of large-area devices such as flexible sensors and optoelectronic devices, including photodetectors and solar cells, transparent conducting electrodes, etc.

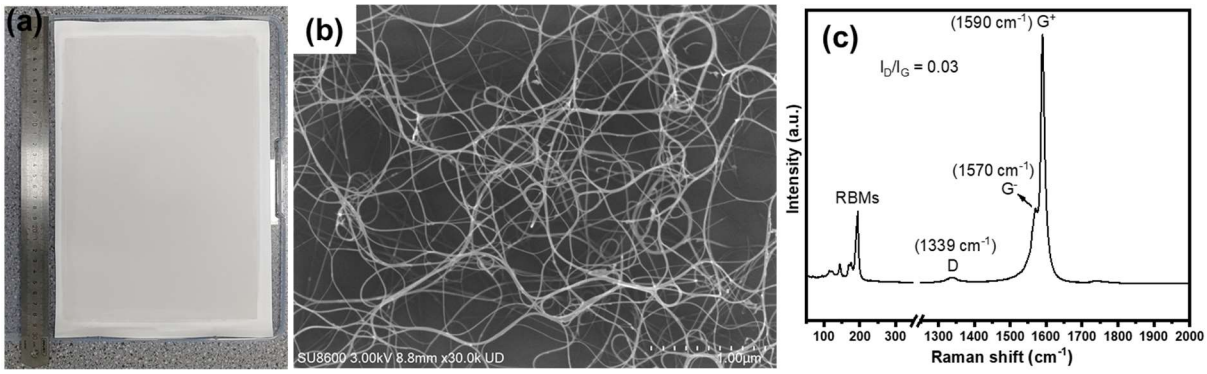

Figure-1: (a) A large-area SWCNTs film deposited on A4 size filter paper using floating catalyst CVD method (b) corresponding SEM image, and (c) Raman spectrum showing clean and high-quality SWCNTs, respectively.

References

[1] Q. Zhang *et al.*, *Adv. Mater.* **32**, 2004277 (2020).
[2] D. A. Ilatovskii *et al.*, *Adv.Sci.* **9**, 2201673 (2022).
[3] P. Liu *et al.*, *ACS Nano,* **18 (29)**, 18900-18909 (2024)

Viral detection platform: portable graphene-derived biosensor

A. Champi
Laboratory of New Carbon Materials: Graphene
Center of Natural and Human Sciences, Federal University of ABC,
Santo André, SP 09210-580, Brazil

Graphene and its derivatives has shown an easy functionalization with biological molecules such as DNA, enzymes, antibodies, RNA, c-DNA, viruses and bacteria among other biological systems generating a wide range of applications in order to develop new disease biosensing devices due to the low cost and speed to obtain results compared to conventional techniques. In this study we report on a novel platform electrochemical portable biosensor for viruses' detection and quantification based on reduced oxide graphene films. The working electrode was built following the synthesis of lysozyme-reduced graphene oxide (rGO) films proposed by Graphene oxide is synthesized using modified Hummer's method and chemically reduced using hydrazine and lysozyme. Thin-films were produced by dip-coating deposition using rGO solution onto a gold substrate pre-treated with cysteine. We report the successful application for RNA virus detection using cDNA functionalization on the working electrode surface and quantification of RNA concentration with a linearly dependency of chronoamperometric current. Also, it shows selectivity against an RNA different from the one used for electrode functionalization. The novel biosensor was applicated for RABV and Sars Cov-2 in-situ detection in nasopharyngeal swab samples of bat and humans showing a difference in response of positive samples from negative samples. A portable detector was performed using nasopharyngeal swab samples and clustered in three groups according to electrochemical response using PBS solution and surface characterization after PBS response. Several groups of graphene derivatives biosensors were due to characterization and surface analysis. This new biosensor proved to be an innovative electrochemical method for in-situ virus diagnosis including machine learning to improve efficiency.

References:

[1] Champi Ana et. al., Biosensors & Bioelectronics, 232, 115291, 2023.

[2] Champi Ana et. al. Microchemical Journal, 205, 111074, 2024.

Optimizing CVD Growth of Monolayer MoS_2 through Relative Configurations of Substrate and Gas flows

Ho-yeon Jung*, Ji-Yong Park*

* Department of Physica and Department of Energy Systems Resaerch, Ajou University, Suwon 16499, Republic of Korea

Monolayer molybdenum disulfide (MoS_2), a representative two-dimensional (2D) semiconductor with a direct bandgap of ~1.8 eV, is a highly promising material for electronic applications. The strong quantum confinement effects in MoS_2 enable MoS_2 field-effect transistors (FETs) to achieve exceptional room-temperature operation characteristics, such as on/off ratios exceeding 10^8.[1] These remarkable properties have garnered extensive research to synthesize high-quality monolayer MoS_2. Chemical vapor deposition (CVD) using perylene-3,4,9,10-tetracarboxylic acid tetrapotassium salt (PTAS) as a seeding promoter has been shown to produce large-area monolayer MoS_2 with superior optical quality and enhanced electrical mobility compared to other promoters.[2]

In this study, we optimized the CVD process by vertically aligning the growth substrate with the carrier gas (Ar) flow, contrasting with the conventional horizontal arrangement above the MoO_3 source. This vertical configuration significantly improves nucleation uniformity, resulting in more consistent growth. Our CVD approach allows for precise control over key growth parameters, such as growth time, temperature, gas flow rate, and the distance between the growth substrate and the Mo source. We systematically investigated the morphological and electrical properties of MoS_2 flakes synthesized under varying CVD conditions.

References

[1] Radisavljevic, Branimir, and Andras Kis. "Mobility engineering and a metal–insulator transition in monolayer MoS2. " *Nature materials* 12.9 (2013): 815-820.

[2] Yang, Peng, et al. "Influence of seeding promoters on the properties of CVD grown monolayer molybdenum disulfide." Nano Research 12 (2019): 823-827.

Energetics and electronic property of Janus WSSe nanoscroll

Y. Gao and S. Okada

University of Tsukuba (Japan)

Janus transition metal dichalcogenides (JTMD) exhibit structural asymmetry due to their unique in-plane heterostructures, where different chalcogen layers sandwich the transition metal layer. This structural asymmetry causes the dipole moment across its layer, leading to unique geometric structure and electronic properties. For instance, Janus WSSe tends to favor a curved structure as its ground state [1]. Additionally, van der Walls interaction between JTMD layers stabilized its bilayer structure [2]. Recently, JTMDs have been reported to be able to form scrolled structures [3]. These scrolled structures include curvature and interlayer interaction, which are expected to modulate the stability and electronic structure of JTMD. To explore this, we studied the energetics and electronic structures of Janus WSSe nanoscroll in terms of their innermost radii and the number of shells using the density functional theory. Here, Janus WSSe nanoscrolls was constructed by rolling up a WSSe nanoribbon with W-terminated zigzag edges and a width of 3.3 nm containing 100 W lines. we considered WSSe nanoscroll with innermost radii r_i of 1.3, 1.6, 2.0, 2.5, 3.2 and 4.4 nm [Fig.1(a)].

Our calculations revealed that WSSe nanoscrolls are more stable than the corresponding WSSe nanoribbon, because the van der Walls interaction between adjacent shells and the strain relaxation by the scrolling cooperatively stabilize their structures. The most stable nanoscroll considered in this work has an innermost radius of 2.5 nm [Fig.1(b)]. The electronic structure of WSSe nanoscrolls depends on both their scroll conformation and the atomic position along the scroll. WSSe nanoscrolls are semiconductors exhibiting a band bending along the scroll, where the band edges of W on the inner shell are shallower than those on the outer shell. This band bending results in a type II band edge alignment between the inner and outer shells, where the length of p-n interfaces depends on the length of shell connecting the inner and outer shells [Fig.1(c)]. This band bending is ascribed to the radial dipole moment induced by curvature and asymmetric chalcogen arrangement across the shell.

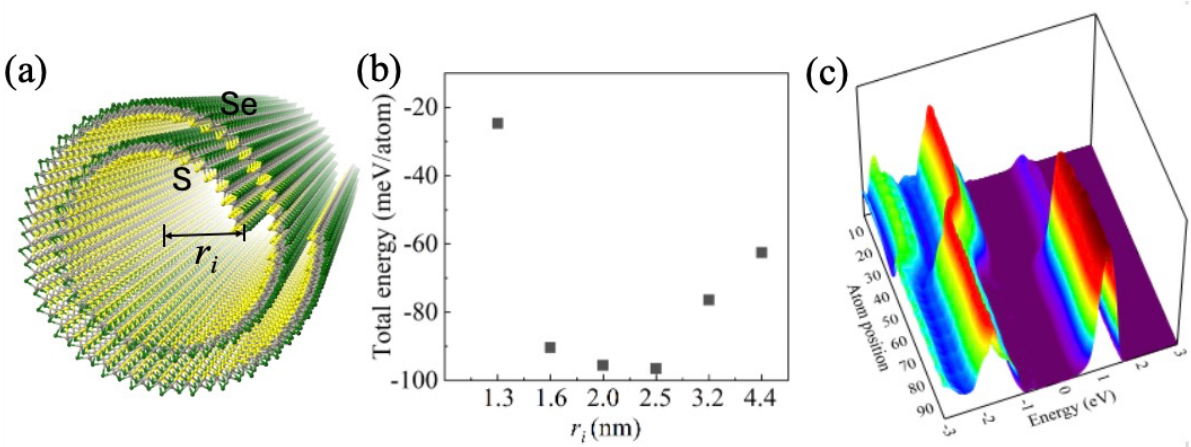

Figure 1: (a) The optimized WSSe nanoscroll with r_i=1.6 nm. (b) Total energy of Janus WSSe nanoscrolls relative to the corresponding isolated flat WSSe nanoribbon. (c) Projected density of states of W atoms along the shell from the inner most to outermost scroll with r_i=1.6 nm.

References

[1] Y. Gao and S. Okada, *Phys. Rev. B* **110**, 035414 (2024).
[2] Y. Gao and S. Okada, *Appl. Phys. Express* **16**, 075004 (2023).
[3] M. Kaneda *et al*. *ACS Nano* **18**, 2772 (2024).

Electrical and thermal transport properties of individual carbon nanotubes by in situ TEM

Daiming Tang[1,2], Hai-Bo Zhao[3,4], Ovidiu Cretu[1], Chang Liu[3,4]

[1]*National Institute for Materials Science (NIMS), Tsukuba 305-0044, Japan*

[2]*Faculty of Pure and Applied Sciences, University of Tsukuba, Tsukuba 305-8573, Japan*

[3]*Institute of Metal Research (IMR), Chinese Academy of Sciences (CAS), Shenyang 110016, China*

[4]*School of Materials Science and Engineering, University of Science and Technology of China, Hefei 230026, China*

Single-wall carbon nanotubes (SWCNTs) have a one-dimensional helical tubular molecular structure made up of hexagonally bonded sp2 carbon atoms. Conceptually, a SWCNT could be formed by rolling up a graphene sheet along a so-called chiral vector. The chirality of a SWCNT uniquely determines its atomic geometry and electronic structure, i.e. metallic or semiconducting. Semiconducting SWCNTs have been considered as ideal candidate for channel materials of energy-efficient nanotransistors.

There are two challenges to apply SWCNTs for energy-efficient transistors. One is to control the chirality of individual SWCNTs [1], the other is to dissipate heat efficiently. We developed an in situ transmission electron microscopy (TEM) probing method to monitor the chirality transition and transport properties of individual SWCNTs. Controlled metal-to-semiconductor transition was realized to create nanotube transistors with a semiconducting nanotube channel bonded between metallic nanotube source and drain.[2] In addition, we developed in situ STEM-EELS and plasmon spectroscopy method to map the temperature distribution of Joule heated individual carbon nanotubes.[3-4] Diffusive transport was observed for microscale MWCNTs, while a transition to ballistic transport was revealed for SWCNTs with length shorter than 100 nm. Finally, an outlook of the ultimate SWCNT electronics enabled by chirality engineering will be presented.[5]

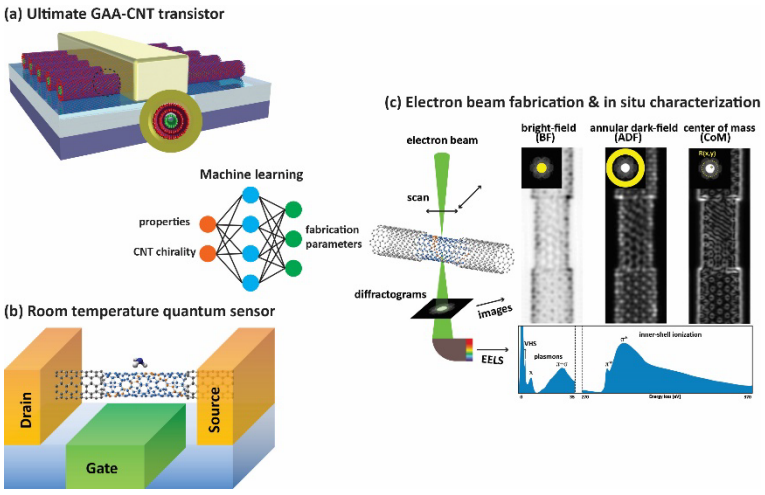

Figure 1 in situ TEM for fabricating, characterizing and measuring individual CNT electronic devices.

References

[1] Snowdon et al., ACS Appl. Nano Mater, 8, 944-951 (2025).
[2] Tang, et al., Science, 374, 1616-1620, (2021).
[3] Cretu, et al., Carbon, 201, 1025-1029, (2023).
[4] Zhao et al., J Mater Sci Technol 221, 46-53 (2025).
[5] Tang, et al., Nat. Rev. Electr. Eng., 1, 149-162, (2024).

Acknowledgments JSPS Kakenhi (JP20K05281, JP25820336, JP23H01796), JST-FOREST (JPMJFR223T), ARIM (JPMXP1223NM5306).

Investigation and Mitigation of the Electron-Hole Conduction Asymmetry in Graphene Field-Effect Transistors

Min-sang Kim[1], Ji-Yong Park[*]
[1]*Department of Physics and Department of Energy Systems Research, Ajou University, Suwon 16499 KOREA*

Due to its excellent electrical properties, such as high mobility and large saturation current, graphene has been actively explored for electronic applications. As a basic building block for such applications, graphene field effect transistor (GFET) has been the focus of many research efforts. In GFETs, asymmetric transfer characteristics are often observed, where the field effect mobility of holes is usually larger than that of electrons.[1] This asymmetry is usually attributed to the metal-induced doping of graphene at the contacts.

In this study, we investigated the electron-hole conduction asymmetry in GFETs with Au contacts. We found that this asymmetry arises from p-type doping of graphene under the Au contacts, leading to different kinds of junctions when the graphene channel is field-doped using a back gate. However, the doping is not directly induced by Au metal, but rather by photoresist residues remaining on the graphene under contacts during the fabrication process.[2] By removing the photoresist residue with oxygen plasma, the electron-hole asymmetry can be significantly reduced.

References
[1] Frank schwierz, Nature Nanotechnol. 5, 487–496 (2010)
[2] Eduardo Nery Duarte de Araujo et al**.,** Beilstein J. Nanotechnol. 10, 349–355. (2019)

Single-step SH group termination of epitaxial graphene and graphene oxide

Y. Miyake[1], J. Ishii[1], T. Suzuoka[2], Y. Matsuo[3], K. Takai[1,2]

[1]Department of Chemical Science and Technology, Hosei University (Japan), [2] Graduate School of Science and Technology, Hosei University (Japan), [3]Department of Applied Chemistry, University of Hyogo (Japan)

SH group termination of graphene is a promising strategy for forming covalent bonds to metal surface and organic molecules [1]. Due to the chemical stability of graphene, graphene oxide (GO) has been studied in covalent chemistry utilizing rich oxygen-containing functional groups (OFGs) as reactive sites. However, little is known about the dependence of thiol functionalization efficiency on the structure and electronic state of GO. In addition, reported SH termination proceeds two steps: the addition of thioester and followed by hydrolysis in a strong base [1].

In this work, we report single-step SH group termination of GO powder and wafer forms of epitaxial graphene (**EG**) using 1,4-benzenedithiol (BDT) as a straight rigid linker. To elucidate the GO structure dependence, different types of GO prepared from natural graphite powder (**Gr**) by the reported method developed by Hummers, Brodie, and Bhagavathsingh [2], labeled as **HGO**, **BGO**, and **BhGO** as starting materials for SH termination by BDT. **HGO-BDT**, **BGO-BDT**, **BhGO-BDT**, and **Gr-BDT** were obtained by reacting the corresponding GO in BDT solution deprotonated by Et_3N in *N*,*N*-dimethylformamide (DMF) at room temperature for a day and following washing by DMF and ethanol based on the reported procedure for cysteine amine [3]. Gas phase thiol functionalization of **EG** grown on 4H-SiC wafer at 2050 ºC under Ar and its oxide (**EGO**) prepared by plasma treatment for different duration (t = 1, 5 and 10 s) under oxygen flow (0.5 Pa and 1.0 sccm) was also investigated by adsorbing sublimated BDT, nebulizing Et_3N in DMF and washing by DMF and EtOH (**EG-BDT**, **EGO*t*s-BDT**, and **EGO1s-0.2Pa-BDT**).

The XPS spectra shown in Fig. 1 (a, b) indicate successful BDT functionalization for powder and wafer forms of graphene and GO. **BhGO-BDT**, **Gr-BDT**, **EG-BDT**, and **EGO-BDT** showed clear peaks with spin-orbit splitting around 164 eV in the S_{2p} region, assigned as single C-SR or C-SH state or their anion. **HGO-BDT** and **BGO-BDT** showed increments of the ratio of oxidized sulfur species to carbon (SO_x / C) at 167 eV by 0.32×10^{-2} and 0.13×10^{-2} respectively, decreasing SH termination efficiency. These GO showed little π-π* plasmon peaks in C1s spectra due to electron-deficient nature, in contrast to **BhGO-BDT**, **Gr-BDT**, **EG-BDT**, and **EGO-BDT** showing clear π–π* plasmon loss (6.6×10^{-2}, 8.5×10^{-2}, 14×10^{-2}, $12 \sim 6.4 \times 10^{-2}$) with high conductivity. The reaction efficiency showed a logarithmic correlation to oxygen abundance ($R^2 = 0.96$) only for such conductive species except for **HGO** and **BGO** as seen in Fig. 1 (c), different from the reaction on **HGO** by aliphatic thiol in the literature [1, 3]. From this tendency, it was revealed that not only the O / C ratio but also the electronic state was a crucial factor for efficient SH termination by BDT, relating to the low stability of sulfide in electron-deficient or defective GO.

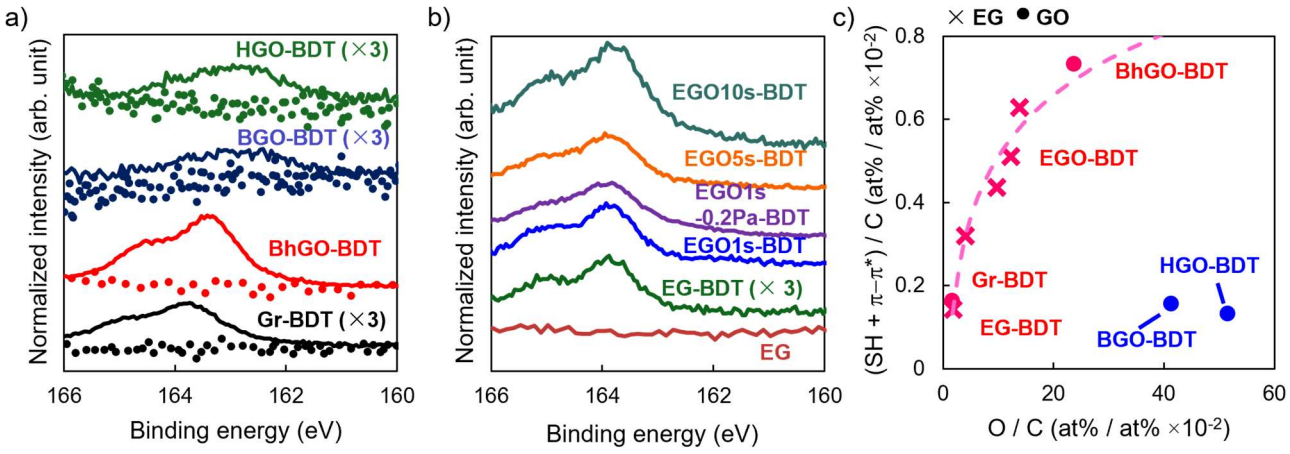

Fig. 1. S2p spectra of XPS (a, b); a) Before (dotted line) and after (solid line) SH termination for powder forms of different type of GO. b) S2p spectra of wafer forms of EG and EG-BDT for different O / C ratio. c) Correlation between oxygen abundance and the total concentration of C-SH state and π–π* plasmon loss in S2p spectra.

References [1] Thomas, H. R. *et al. Angew. Chem. Int. Ed Engl.**53***, 7613 (2014).
[2] Matsuo, Y. *et al. ChemSusChem* **16**, e202201127 (2023).
[3] Piñeiro-García, A. *et al. FlatChem* **26**, 100230 (2021).

Aggregation effect on exciton binding energies of single-chirality single-walled carbon nanotubes

Z. Liu[1], T. Nishihara[1], V. Perebeinos[2], Y. Miyauchi[1]

[1] *Institute of Advanced Energy, Kyoto University (Japan),* [2] *Department of Electrical Engineering and Center for Advanced Semiconductor Technologies, University at Buffalo (United States)*

Single-walled carbon nanotubes (SWCNTs) have attracted lots of attentions because of their intrinsic sharp optical resonances arising from the highly stable quasi one-dimensional (1D) excitons [1,2,3]. In isolated SWCNTs, the excitons possess a high binding energy of 0.3–0.5 eV due to weak Coulomb screening characteristic of 1D systems, leading to their high thermal stability even at 2,000 K [4]. Moreover, recent developments of the chirality separation techniques have enabled fabrication of single-chirality SWCNT membranes as novel opto-functional materials that allows one to take advantage of the excellent exciton feature of SWCNTs at a macroscopic scale [5]. Exciton binding energy, as a fundamental parameter of excitons, is expected to vary depending on the dielectric environment of SWCNTs [3,6]. Therefore, the exciton binding energies in bundled SWCNTs in the aggregation is expected to be considerably different from that in isolated ones, and the extent to which the exciton binding energy is preserved in aggregation is particularly critical for excitonic applications of SWCNTs. However, how the exciton binding energy is affected by aggregation of the SWCNTs with the identical chirality have remained to be clarified.

Here, we study the aggregation effect of single-chirality (6,5) SWCNTs on exciton binding energies using two-photon photoluminescence excitation spectroscopy. (6,5) SWCNT dispersion in toluene was prepared from CoMoCAT SWCNTs using PFO-BPy as a dispersing agent, followed by the membrane fabrication via vacuum filtration [7]. The residual dispersant was reduced as far as possible by applying redispersion and rapid annealing and cooling procedures [8]. We measured the one-photon absorption and two-photon excitation spectra of the dispersion and the membrane. The change in the energy difference of the one-photon and the two-photon absorption peaks reflects variations in the energy levels of exciton Rydberg series of 1u and 2g states due to differences of the dielectric environments [1,2]. From the comparison of the experimental results with calculated two-photon absorption spectra using various effective dielectric constants [3], we found that the exciton binding energy in the membrane decreased for about 20% than that in the isolated condition in the dispersion, down to ~0.25 eV. This value is about 0.1 eV smaller than that of isolated SWCNTs, but indicates that the excitons in the aggregated SWCNTs are still thermally stable even at very high temperatures.

References

[1] F. Wang, G. Dukovic, L. E. Brus, T. F. Heinz, *Science* **308**, 838–841 (2005).
[2] J. Maultzsch *et al*., *Phys. Rev. B* **72**, 241402 (2005).
[3] V. Perebeinos, J. Tersoff, P. Avouris, *Phys. Rev. Lett*. **92**, 257402 (2004).
[4] T. Nishihara, A. Takakura, Y. Miyauchi, K. Itami, *Nature Commun.* **9**, 3144 (2018).
[5] T. Nishihara, A. Takakura, M. Shimasaki, K. Matsuda, T. Tanaka, H. Kataura, Y. Miyauchi, *Nanophotonics* **11**, 1011–1020 (2022).
[6] Y. Miyauchi *et al.*, *Chem. Phys. Lett.* **442**, 394–399 (2007).
[7] T. Nishihara, Z. Liu, Y. Miyauchi, *J. Heat Transfer Soc. Jpn.* **62**, 36–42 (2023).
[8] J. Yao *et al*., *Carbon* **184**, 764–771 (2021).

Solvent acoustic coupling governs non-covalent bonding at the interface of ultra-long carbon nanotubes

A. Yuxuan Tian[1], B. Hongjie Yue[1], C. Chenxi Zhang[1], D. Xiao Chen[1], E. Fei Wei[1,*]

[1] *Beijing Key Laboratory of Green Chemical Reaction Engineering and Technology, Department of Chemical Engineering, Tsinghua University (China).*

Abstract text: The spatial arrangement of ultra-long carbon nanotubes is severely limited by their mechanical strength, among which regulating the interaction between tubes is a key factor. We have designed a method to regulate the interface structure of ultra-long carbon nanotubes by coupling solvent dispersion and acoustic vibration, achieving the regulation of the interaction between ultra-long carbon nanotubes. The reconfiguration of non-covalent bonds at the interface between small molecule solvents and ultra-long carbon nanotubes effectively reduces the interaction strength between carbon nanotubes. Through acoustic vibration, the mass transfer efficiency of solvent molecules at the interface is further improved, effectively enhancing the uniformity of the distribution of non-covalent bonds at the interface of ultra-long carbon nanotubes, thereby improving interface stability and facilitating the spatial arrangement control of ultra-long carbon nanotubes. This study analyzed the synergistic regulation mechanism of solvent dispersion and acoustic vibration on the number and distribution of non-covalent bonds at the interface, providing an important theoretical basis for the array control technology of ultra-long carbon nanotube bundles and promoting a new breakthrough in the mechanical strength of ultra-long carbon nanotubes.

Keywords: Ultra-long carbon nanotubes, Interface structure, Non-covalent interaction, Tube bundle array, Mechanical property.

References (if desired)

[1] Y. X. Bai *et al.*, *Science* **369**, 1104–1106 (2020).
[2] V. A. Davis *et al.*, *Nature Nanotechnology* **4**, 830–834 (2009).
[3] Y. F. Guo *et al.*, *Nature Nanotechnology* 17, 278–284 (2022).
[4] X. S. Zhang *et al.*, *Science* **384**, 1318–1323 (2024).

Fabrication of Near-Infrared Perfect Absorber Using Chirality-Sorted Carbon Nanotubes

M. Kawakami, S. Takasu, T. Nishihara, Y. Miyauchi

Kyoto University (Japan)

Enhancing absorptance of a thin film in a specific wavelength band in the near-infrared region is crucial for various optical devices such as optical sensors, detectors, and thermal emitters. Therefore, near-infrared perfect absorbers which can perfectly absorb the incident light at the operating wavelength have attracted much attention. Previous studies focused on designs incorporating microstructures such as photonic crystals and meta-surfaces. On the other hand, in the far-infrared region, it is known that perfect absorption can be achieved with a simple layered structure known as Salisbury screen [1], which consists only of a thin absorbing layer, a lossless dielectric layer, and a metal reflecting layer. In this structure, perfect absorption is achieved by interference-based antireflection and strong absorption by the thin absorbing layer. In principle, this strategy is also applicable to the near infrared region. However, an absorption coefficient α satisfying $\alpha \gtrsim 10/\lambda$, where λ is wavelength, is required for the thin absorbing layer, and the limitation of absorption coefficient of conventional materials (Fig. 1a) has prevented the realization of near-infrared perfect absorbers based on the similar strategy as in the far-infrared region.

In contrast to conventional semiconductors, low-dimensional materials such as transition metal dichalcogenides and carbon nanotubes exhibit strong absorption in the visible to near-infrared region originating from excitonic resonance. Particularly, an assembled thin film of single-chirality single-walled carbon nanotubes (SWCNTs) was recently reported to have a strong absorption in the near-infrared region (Fig. 1a) [2]. Here, we propose an all-dielectric near-infrared perfect absorber with a Salisbury screen-inspired structure. We designed the perfect absorber utilizing SWCNT thin films not only as the absorbing layer, but also as a lossy mirror that reflects light for the destructive interference and simultaneously absorbs residual transmitted light, at the S_{11} exciton resonance (Fig. 1b). Calculations using the optical transfer method revealed that nearly perfect absorption can be achieved only with the four-layer structure composed of (7,5) SWCNT thin films and lossless dielectric materials (Fig. 1c). This is impossible with a single-layer SWCNT film of the same total thickness whose absorptance is limited to ~0.5 due to the strong reflection at the excitonic resonance. The absorber proposed in this study is composed of simple layers of dielectric thin films. Therefore, it is scalable, heat-resistant, and thus suitable for devices operating at high temperatures such as wavelength-selective emitters. The design, fabrication methods, and experimental results will be discussed in detail.

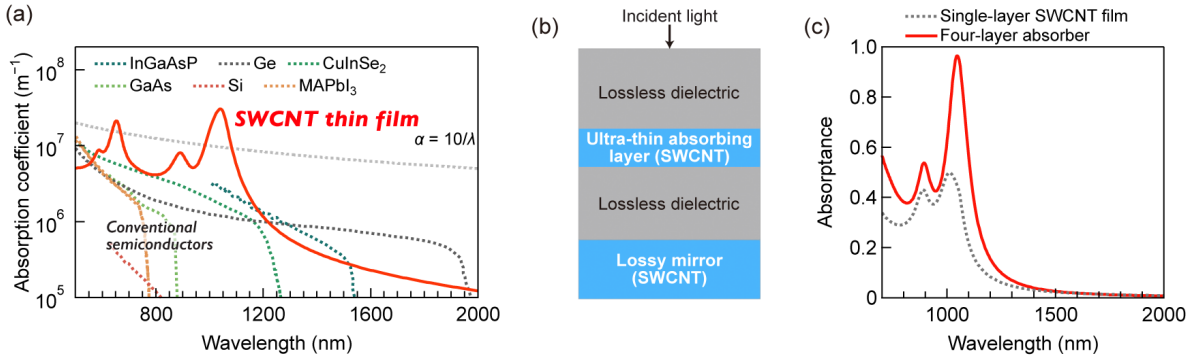

Figure 1: (a) The absorption coefficients of conventional semiconductors and single-chirality single-walled carbon nanotube (SWCNT) thin film. (b) Schematic of the four-layer SWCNT-based absorber. (c) Calculated absorptance of single-layer SWCNT thin film and the four-layer absorber. The total thickness of the SWCNT films is consistent (70 nm).

References

[1] R. L. Fante *et al*. *IEEE Trans. Antennas. Propag.*, **36**, 1443–1454 (1988).

[2] T. Nishihara *et al*. *Nanophotonics*, **11**, 1011–1020 (2022).

One-pot Electrochemical Exfoliation/Functionalization of graphite for N-Functionalized Graphene

Konno Yuta, Sota Ishizu, Ryo Watanabe and ○Haruya Okimoto

Department of Polymeric and Organic Materials Engineering, Yamagata University, Yamagata 992-8510, Japan

Functionalized Graphene such as N-doped graphene and metal functionalized graphene is expected to be used as a sensor and a catalyst for fuel cells. The nitrogen and oxygen content in this graphene significantly affects its functionality. Ideally, a high nitrogen content with minimal unwanted oxidation is desirable. For example, the N/C ratio of N-Gr prepared from GO ranges from 0.1 to 0.8. However, since this reaction goes through the Hummers method (O/C ratio of 0.34), the oxygen content is high. Additionally, a reduction process is necessary to decrease the oxidation level. In this study, we report a one-pot electrochemical exfoliation and modification method that enables exfoliation and modification under milder conditions to produced N-functionalized graphene, metal/N-functionalized graphene. This method involves applying a positive potential to graphite in an amine/electrolyte aqueous solution, allowing simultaneous electrochemical exfoliation and amine modification. With this approach, oxidation can be suppressed while maintaining the same modification levels (N/C ratio: 0.1, O/C ratio: 0.20). On the other hand, conventional electrochemical reactions require fixing graphite to an electrode, making it difficult to exfoliate and modify a large amount of powdered graphite particles. To address this, we applied bipolar electrochemistry, a non-contact electrochemical reaction using an external electric field, and successfully developed a non-contact exfoliation and modification method. This approach increased the modification level up to an N/C ratio of 0.52. When we examined the ORR potential of the obtained nitrogen-doped graphene, we found that it exhibited higher catalytic activity than typical electrochemically exfoliated graphene. Furthermore, we also report an electrochemical exfoliation and modification method for metal/nitrogen-doped graphene by combining metal particle deposition with electrochemical exfoliation.

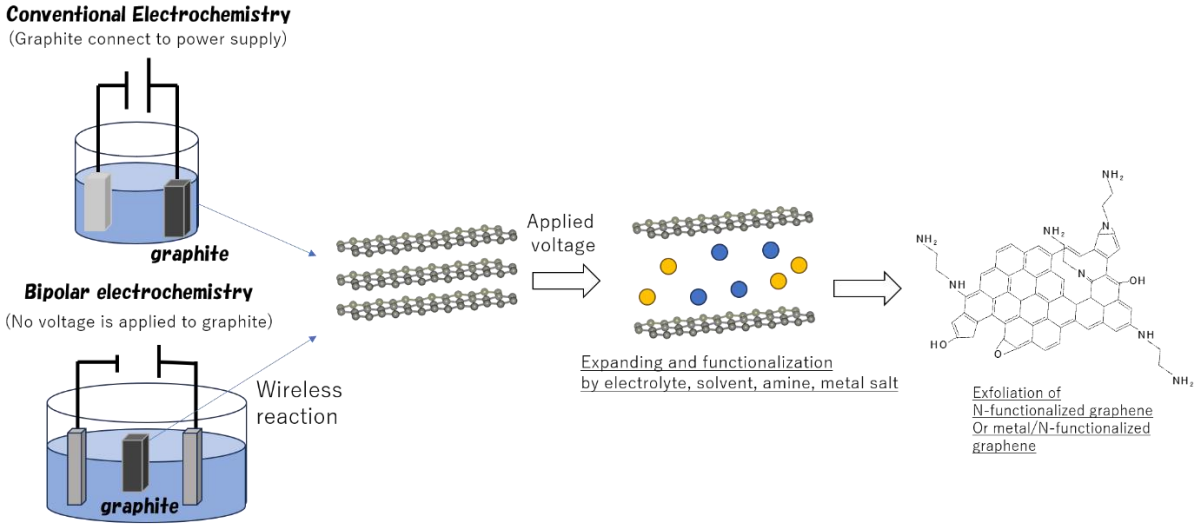

Figure. Schematic illustration of exfoliation/functionalization using conventional electrochemistry and bipolar electrochemistry

Self-winding ultra-long carbon nanotube rings and their potential functional applications

Sibo Chen[1], Fei Wei[1]
[1]*Tsinghua University (China)*

Abstract: Ultra-long carbon nanotubes (ULCNTs) have excellent mechanical and electrical properties and typical optical research value. The various assembly forms of ULCNTs, such as ULCNTs bundle fibers, films, arrays, etc., make them have great applications in the fields of ultra-strong materials and electronic/optical devices. However, self-assembly at the microscopic level is a challenge to control the preparation of hierarchical structures of ULCNTs, but it implies more interesting microscopic topology. Here, we demonstrate that ULCNTs with a floating growth mechanism exist in a toroidal hierarchical self-assembly form. Centimeter-scale ULCNTs can form perfect rings with many turns of winding in the micron-scale. We observed these ULCNTs rings using advanced optical microscopy and dark-field microscopy, and confirmed their structural perfection and optical enhancement by Raman and Rayleigh spectra. Most of them are perfectly semiconducting ULCNTs. Meanwhile, Raman demonstrated that ULCNTs rings have the same RBM peaks as the source and tail ends, indicating their possible chirality consistency. FIB reveals the stacking patterns and types of ULCNTs in the rings, especially the more rigid multi-walled carbon nanotube (MWCNT) can also be assembled into a ring structure. SEM shows that there are many kink structures in the rings, which make the ULCNTs rings like Mobius band. The formation of kink may be due to the gas flow or the inherent chiral correlation. At the same time, due to the unique circular winding structure of ULCNTs, we can use them to construct novel semiconductor electrical devices or micro electromagnetic coil element. It is worth emphasizing that this involves deep thinking about the effect of electron tunneling between tubes. The study of its growth mechanism will also help to understand the interphase interaction between substrate and fluid during the growth of ULCNTs. In conclusion, self-winding ULCNTs rings will be a unique self-assembly form that can help us understand the growth mechanism and structural basis of ULCNTs, and have the potential to develop novel functional applications.

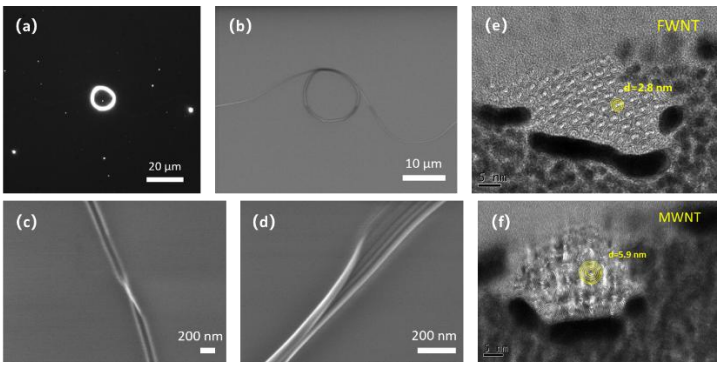

Figure caption: (a) ULCNTs ring image in the dark-field microscopy; (b) SEM image of ULCNTs ring; (c-d) Kink structures in the ULCNTs rings; (e-f) FIB-TEM image of ULCNTs rings.

A High-Performance High-Temperature Accelerometer Based on the Improved Graphene Aerogel

Yanchun Wang, Zibo Wang, Weiya Zhou

Institute of Physics, Chinese Academy of Sciences, Beijing 100190, China

Vibration sensors play a crucial role in detecting fluctuating acceleration, velocity, and other vibration signals across various fields, including aerospace, automobiles, industrial machinery, consumer electronics, transportation, power generation, and infrastructure. As the aerospace industry continues to advance, there is an increasing demand for sensors capable of operating under extreme conditions [1].

Among these sensors, high-temperature accelerometers are particularly vital for ensuring the normal operation of equipment in aerospace applications, such as monitoring and identifying abnormal vibrations in aircraft engines. However, current high-temperature accelerometers face significant limitations when operating continuously above 973 K, primarily due to phase transitions in piezoelectric crystals, mechanical failure, and current leakage in piezoresistive/capacitive materials. It is a great challenge to develop a new type of vibration sensor to meet the crucial demands at high temperature.

In this study, we report a novel high-temperature accelerometer working with a contact resistance mechanism. This device is based on an improved graphene aerogel (GA) synthesized through a modulated treatment process. The resulting accelerometer can stably operate at 1073 K in continuous mode and intermittently at 1273 K. The developed sensor is lightweight (sensitive element <5 mg) and has high sensitivity (an order of magnitude higher than MEMS accelerometers) and wide frequency response range (up to 5 kHz at 1073 K) with marked stability, repeatability and low nonlinearity error (<1%). These outstanding properties are attributed to the excellent mechanical performance of the improved GA in the temperature range of 299–1073 K [2]. The accelerometer could be a promising candidate for high-temperature vibration sensing in space stations, planetary rovers and others.

References

[1] Z. Wang *et al*., *Nano Res.* **16**, 11342-11349 (2023).
[2] Z. Wang *et al*., *ACS Appl. Mater. Interfaces* **15**, 19337-19348 (2023).

Early-Stage Au Deposition Morphology on Graphene and Its Effect on Graphene Field Effect Transistors

Sungyeon Kim[1], Ji-Yong Park*

[1]*Department of Physics and Department of Energy Systems Research, Ajou University, Suwon 16499 KOREA*

Graphene has garnered significant interest in nanoelectronics due to its exceptional electrical and mechanical properties. As metal junctions are inherent in graphene-based devices, understanding the initial deposition morphology of metals is crucial for optimizing their integration into high-performance graphene electronic devices.

In this study, we systematically investigated the early-stage deposition characteristics of Au on graphene via electron beam evaporation under controlled conditions. By varying deposition times, we analyzed the initial nucleation and growth mechanisms of Au nanostructures using scanning electron microscopy (SEM) and atomic force microscopy (AFM), revealing distinct growth patterns. Furthermore, we explored the influence of Au nanoparticle deposition on the electrical properties of graphene field-effect transistors (FETs). This demonstrates how Au nanoparticle deposition on the graphene channel affects charge carrier doping, mobility, and electric field enhancement. Additionally, we utilize Raman spectroscopy, including surface-enhanced Raman scattering (SERS), to elucidate the electronic structure modifications induced by Au deposition, providing insights into the relationship between Au morphology and graphene's electronic properties.

A statistical assessment of the semiconducting proportion in single-wall carbon nanotubes based on electrostatic force microscopy

Yuki Kuwahara[1], Indra M. Khoris[1], Fahmida Nasrin[1], Ryota Yuge [1,2], Takeshi Saito[1]

[1]National Institute of Advanced Industrial Science and Technology (Japan), [2]NEC Corporation (Japan)

Single-wall carbon nanotubes (SWCNTs) possess interesting characteristics predicted from their ideal one-dimensional electronic system [1], in addition to their flexibility and chemical stability. Because SWCNTs prepared by general productions are a mixture of metallic (m-) and semiconducting (s-) types, the performance of devices that utilize their semiconducting property is supposed to be significantly affected by the s-type proportion [2]. Therefore, a quantitative and accurate method for assessing the s-type proportion is of great importance.

In this presentation, we report the statistical assessment of SWCNTs to determine the s-type proportion with emphasis on the precise quantification purpose based on their atomic and electrostatic force microscopies (AFM/EFM) images shown in Fig. 1 that can distinguish the types [3]. Our analysis of 1826 as-grown SWCNTs (total tube length ~ 4.92×10^5 nm) in AFM/EFM images based on the tube length showed that the s-type proportion in the as-grown SWCNTs was 67.3 %. On the other hand, that of s-type enriched SWCNTs separated from the same as-grown ones was 98.6 %.

In addition, we carried out the random sampling of 100 SWCNTs from 619 as-grown SWCNTs measured in one AFM/EFM image-set with 1000 iterations. The iteration result showed the s-type proportion around 68% with the mean of standard errors 8.6%, that supports the pretty good certainty even in the analysis using a limited number of SWCNTs.

This work was supported by Innovative Science and Technology Initiative for Security Grant No. JPJ004596, ATLA, Japan.

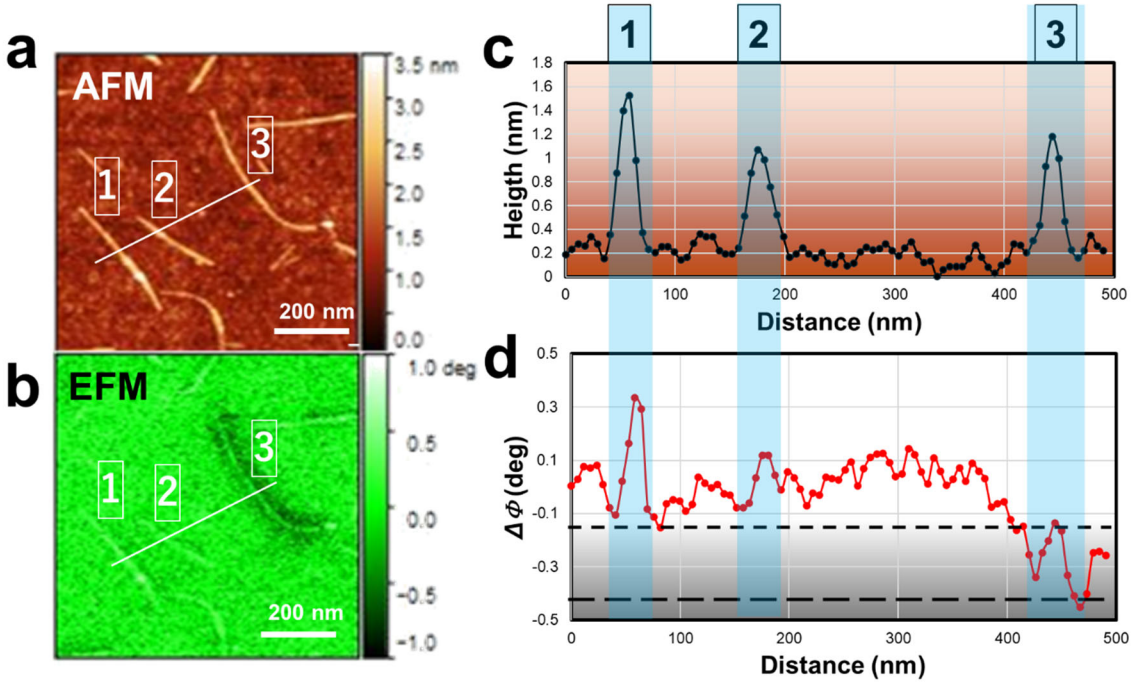

Figure 1. A typical AFM/EFM image-set; (a) topographic and (b) EFM images, and the cross-section profiles of height (c) and EFM signal (d) along the line across SWCNTs shown in (a) and (b).

References

[1] R. Saito *et al.*, Physical Properties of Carbon Nanotubes, (Imperial College Press, 1998), ISBN 1-86094-093-5.
[2] K. Ihara *et al.*, J. Phys. Chem. C, **115** (2011) 22827
[3] I. M. Khoris Y. Kuwahara *et al.*, Carbon, **229** (2024) 119540.

Diameter Dependence of Phase Transition and Coexistence of Water Confined Inside Carbon Nanotubes

Wenjie Liu[1], Ikuma Kohata[1], Yuki Maekawa[2], Takahiro Yamamoto[2],
Yoshikazu Homma[2], Shohei Chiashi[1]

[1] *Department of Mechanical Engineering, The University of Tokyo, Tokyo 113-8656, Japan*

[2] *Department of Physics, Tokyo University of Science, Shinjuku, Tokyo 162-8601, Japan*

liuwenjie@photon.t.u-tokyo.ac.jp

Low-dimensional confinement can significantly alter the thermodynamic and dynamic properties of substances, giving rise to novel phase behaviors such as highly shifted transition temperatures [1], solid-liquid critical behaviors [2], and even phase oscillations [3]. In this study, we performed classical MD simulations to investigate the phase behavior of water confined within open-ended carbon nanotubes (D = 0.95–1.25 nm, $L \approx$ 20 nm), which were placed at the center of simulation boxes filled with fully equilibrated water vapor (P = 1 kPa). We systematically examined the observed phase behaviors across different water potentials and water-carbon Lenard-Jones interactions to ensure neutrality in potential and parameterisation effects.

Structural (Fig. 1a, parameter definition is in Fig. 1e) and dynamical (Fig. 1b) analyses confirm the presence of liquid species and multiple phase coexistence states with fluctuating phase ratios (Fig. 1a) and temperature-dependent domain sizes and lifetimes. The melting temperature exhibits non-monotonic dependence on nanotube diameter, consistent with previous studies [1,4]. Notably, the temperature ranges for phase coexistence also show considerable diameter dependence: they broaden near the local minimum of the phase transition temperature, where two different ice nanotube phases are similarly stable and coexist, likely due to the complexity of the free energy landscape, while narrowing sharply for D > 1.2 nm or D < 1.0 nm, ruling out finite-size effects as the sole origin of rounded phase transitions.

Further analysis of confined liquid states reveals broad, bimodal distributions in both rotational dynamics and local structure (Fig. 1d, e), with a strong statistical correlation between the two. This suggests the presence of continuous phase transitions or the coexistence of two distinct liquid species: one well-structured and dynamically slow, and the other less structured and dynamically fast.

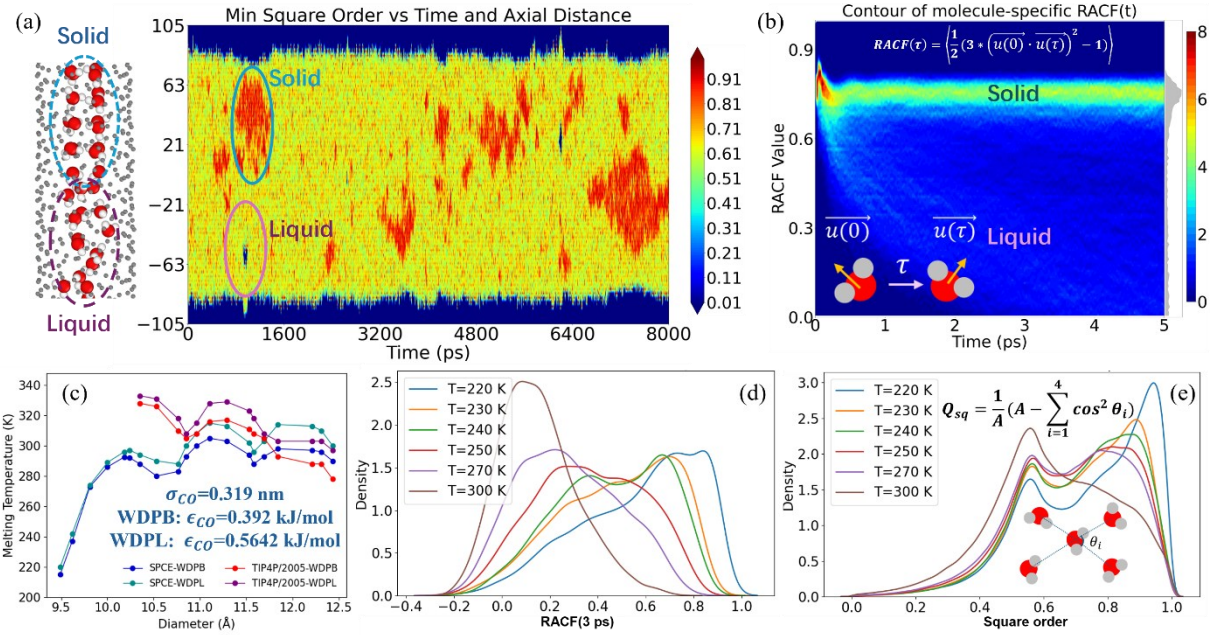

Fig. 1: (a, b) Phase coexistence illustrated by (a) structural; (b) molecule-specific dynamics analysis; (c) temperature dependence of CNTs' diameter; (d, e) bimodal distribution of (d) dynamics, (e) local structure.

References

[1] Agrawal, K., *et al.*, *Nat. Nanotech.* **12**, 267–273 (2017).
[2] Mochizuki, K., *et al.*, *Proc. Natl. Acad. Sci. U.S.A.* **112(27)**, 8221-8226 (2015).
[3] Kastelowitz, N., *et al.*, *ACS Nano* **12(8)**, 8234-8239 (2018).
[4] Chiashi, S., *et al.*, *ACS Nano* **13(2)**, 1177-1182 (2019).

Carbon Nanotube-based Spectrally Selective Solar Absorber: Design and Fabrication

Hengkai Wu[1], Taishi Nishihara[1], Takeshi Tanaka[2], Hiromichi Kataura[2], Yuhei Miyauchi[1*]

[1]Institute of Advanced Energy, Kyoto University (Japan), [2]Nanomaterials Research Institute, AIST (Japan)

Solar-thermal energy harvesting plays a significant role in meeting the growing heat demand of human society in a sustainable approach. Spectral selective solar absorbers (SSAs), which can suppress thermal radiation loss while maintaining maximized sunlight absorption, are critical for achieving high operation temperature and high conversion efficiency without the reliance on the expensive, land-occupying optical concentrators. An ideal SSA requires broadband high absorption across the sunlight region (mainly 300–2500 nm), minimal absorption in the mid-infrared region (and hence minimal emission according to Kirchhoff's law), and an appropriately located cutoff wavelength in near-infrared where the transition of absorption feature occurs rapidly. The absorber-reflector bilayer is the simplest structure to achieve such selective absorption, where the absorber should be highly absorptive in the UV-visible region and transparent in the infrared region (semiconductors, transition-metal compounds, etc.), and the reflector should be highly reflective in the infrared region (aluminum, silver, gold, etc.) [1]. However, the performance of such SSA is constrained by the limited intrinsic properties of the naturally existing absorber materials. Therefore, complicated structures and additional mechanisms such as thin film interference, optical cavity, photonic crystal, and textured surface are usually required to further enhance solar absorption and suppress thermal radiation [2, 3].

Single-walled carbon nanotubes (CNTs) are promising materials with strong light-matter interactions originating from their quasi-1D excitons, which are stable even at extremely high temperatures [4,5]. They exhibit sharp absorption cutoff in the near-infrared regions depending on their chirality [6,7] and weak absorption in the mid-infrared region, indicating their huge potential for SSA applications. In our previous research, we reported the complex refractive index spectrum of single-chirality CNT assemblies, enabling the optical design of CNT-based devices [8,9].

In this work, we theoretically design and experimentally fabricate SSA that can achieve high sunlight absorptance ($\alpha = 0.84$) and low infrared emissivity ($\varepsilon_{300^\circ\mathrm{C}} = 0.03$) spontaneously with the simple CNT-metal bilayer structure. Furthermore, both simulations and measurements indicate that these properties are maintained at incident angles up to 60º, which is also important for SSAs. Under unconcentrated sunlight, the CNT-SSA reaches 188 ºC, which is much higher than the 100 ºC of a pseudo-blackbody absorber ($\alpha/\varepsilon_{300^\circ\mathrm{C}} = 1.0/0.94$) under the same conditions. The details of the design concept and sample demonstration will be discussed.

References

[1] A. Donnadieu and B. O. Seraphin, *J. Opt. Soc. Am.* **68**, 292 (1978).
[2] M. Bello and S. Shanmugan, *J. Alloys Compd.* **839**, 155510 (2020).
[3] L. Feng *et al., Adv. Mater.* **32**, 1903787 (2020)
[4] H. Kataura *et al., Synth. Met.* **103**, 2555 (1999).
[5] K. Liu *et al., Nat. Nanotechnol.* **7**, 325 (2012).
[6] T. Nishihara *et al.*, *Nat. Commun.* **9**, 3144 (2018).
[7] S. Konabe *et al.*, *Opt. Lett*. **46**, 3021 (2021).
[8] T. Nishihara *et al*., *Nanophotonics* **11**, 1011 (2022).
[9] H. Wu *et al.*, *Carbon* **218**, 118720 (2024).

Achieving High Thermal Conductivity with Lower Filler Loading: Direct CNT Growth on AlN in Silicone Rubber Composites

N. Matsumoto[1], Don N. Futaba[1], T. Yamada[1], K. Kokubo[1]

[1] *Nano Carbon Device Research Center, National Institute of Advanced Industrial Science and Technology (AIST) (Japan)*

Research and development of composite materials using carbon nanotubes (CNTs) as fillers can be broadly divided into two main directions. The first is to exploit the high electrical and thermal conductivity of CNTs to significantly improve electrical and thermal properties. For example, the incorporation of CNTs as conductive pathways can reduce electrical resistance and improve the operating efficiency of devices, while the establishment of heat-conducting channels can greatly improve heat dissipation. The second direction focuses on exploiting the high strength, high aspect ratio, and low weight of CNTs to increase Young's modulus and mechanical strength, and to achieve material benefits such as weight reduction and lower thermal expansion coefficients. In recent years, this area of research has moved from basic laboratory studies to demonstration phases, with an increasing emphasis on simultaneously optimizing mechanical properties and functionality, rather than targeting just one property.

Despite these developments, CNTs remain expensive, and no “killer application” justifying their cost has yet been identified. Consequently, there is a need to move beyond simply “adding” CNTs as a reinforcing or conductive component. A deeper understanding of the intrinsic properties of CNTs and the technical challenges they pose is crucial. In addition, a comprehensive integration of “materials design,” “process design,” and “evaluation technology” is required to fully unlock the potential of CNTs and create high-value-added composite materials.

Meanwhile, the demand for thermal interface materials (TIMs) with superior heat dissipation capabilities has surged in step with the dramatic rise in the information processing power of servers and power devices. Typically, adequate thermal conductivity is achieved by loading base materials such as rubber or resin with more than 60 vol% of highly thermally conductive ceramic fillers. However, such high filler loading significantly impairs the base material’s intrinsic flexibility, mechanical strength, and sealing properties.

In this study, our research has developed a composite filler by directly growing CNTs on the surface of aluminum nitride (AlN) particles—well-known for their excellent thermal conductivity—using a high-efficiency CNT synthesis technique (Super-growth method [1]). Specifically, after optimizing the coating conditions for the Fe catalyst and the synthesis parameters, we mixed the resulting CNT/AlN composite filler with silicone rubber to produce a composite material. Evaluation results suggest that this approach can retain a level of thermal conductivity comparable to using conventional AlN fillers alone while mitigating the deterioration of the base material’s mechanical properties [2].

Our findings offer a promising strategy for simultaneously enhancing the performance of TIMs and preserving the intrinsic properties of base materials, thus providing a vital technological pathway for further miniaturization and performance advances in electronic and power devices. Through advanced materials design and process engineering that fully exploit the unique characteristics of CNTs, future composite materials may demonstrate practical value on par with, or even surpassing, the current costs associated with CNTs—garnering increasing attention in the field.

References

[1] K. Hata *et al.*, *Science* **306**, 1362-1365 (2004).
[2] N. Matsumoto *et al.*, *Nanomaterials* **14**, 528 (2024).

Oxidation Mechanism on Single-Walled Carbon Nanotubes Analyzed by Photo-Induced Force Microscopy

Kaori Fujii[1], Kazufumi Kobashi[1], Yasuhiko Fujita[2], Takahiro Morimoto[1], Hideaki Nakajima[1], Toshiya Okazaki[1]

1 Nano carbon device research center, AIST, Ibaraki, 305-8565, Japan

2 Research Institute for Sustainable Chemistry, AIST, Hiroshima 739-0046, Japan

The oxidation process of carbon nanotubes (CNTs) is a critical step in their industrial applications. Understanding the distribution of functional groups on CNTs will accelerate reproducible and precise development of CNT-based materials [1]. In this study, photo-induced force microscopy (PiFM, see Figure 1), which combines infrared spectroscopy and atomic force microscopy (AFM), was utilized to visualize the functional groups on oxidized single-walled CNT bundles.

We selected two types of commercially available CNTs synthesized by eDIPS and water assisted super-growth (SG) method. They were treated in HNO_3 aqueous solution or a mixed aqueous solution of H_2SO_4/$KMnO_4$ to introduce oxygen-containing functional groups [2]. PiFM images of as-grown and oxidized CNTs drop-casted on Si substrate were acquired at various wavenumbers corresponding to resonant frequencies of functional groups.

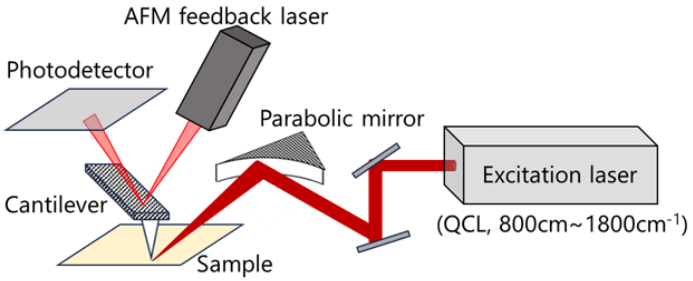

Figure 1 Schematic illustration of the photo-indued force microscopy.

For oxidized eDIPS-CNTs, several oxygen-functional groups, including epoxides, alcohols, ketone, and carboxylic acids were observed on the surface of CNT bundles. Moreover, PiFM signal contrast of epoxides and other groups (alcohols, ketones and carboxylic acids) showed distinct differences, as shown in Fig. 2. These differences suggests that a sequential chemical reaction involving epoxide cleavage and oxidation of alcohols. Notably, PiFM signal contrast within bundles were heterogeneous, and differences in the distribution were observed for several functional groups. This indicates that functionalization progresses simultaneously with debundling of CNTs.

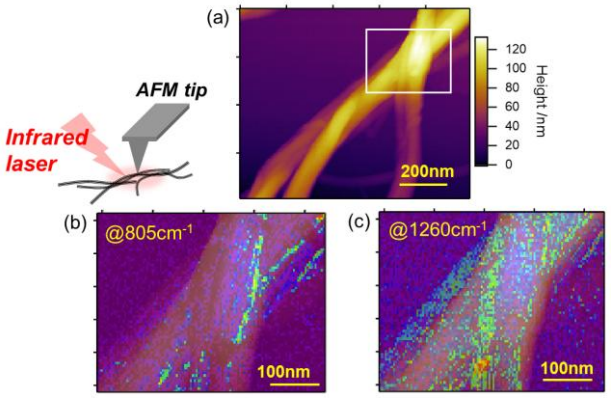

Figure 2 (a) Topographic and PiFM images of oxidized eDIPS-CNT at (b) 805 cm^{-1} and (c) 1260 cm^{-1}.

In contrast, PiFM images of as-grown SG-CNTs showed increased signal count especially for epoxides and alcohols. They are introduced during the CNT growth and will be converted to carbonyl groups through subsequent oxidation treatment.

We will present the PiFM mapping images of oxidized SG-CNT bundles and discuss changes in the functional group distribution with respect to the oxidation treatment time.

References

[1] L. Qian *et al*., *J. Am. Chem. Soc*. **143**, 18805 (2021)

[2] H. Nakajima *et al*., Carbon, **216**, 118495 (2024)

Large-scale separation of micrometer-long single-chirality single-wall carbon nanotubes in aqueous surfactant systems

An Zimeng[1], Sayuki Oka[1,2], Kazuki Nagashima[1,2], Yohei Yomogida[1,2]

[1]*Department of Chemistry, Hokkaido University（Japan）*

[2]*Research Institute for Electronic Science, Hokkaido University（Japan）*

Large-scale separation of single-chirality single-wall carbon nanotubes (SWCNTs) is crucial to utilize their intrinsic performance for applications [1]. Among these, separation methods employing aqueous surfactant systems have advantages for separation of various (n,m) species and enantiomers of SWCNTs [2]. However, in most cases, the separated SWCNTs are shortened by ultrasonic dispersion process before separation, leading to degraded performance in applications. Thus, separation of long single-chirality SWCNTs has been desired. Recently, a method has been developed to extract long single-chirality SWCNTs with polymers in organic solvent systems using a mild dispersion technique called shear force mixing (SFM) [3]. In this study, we applied this technique to the aqueous surfactant systems, which have advantages for separation, and tried separation of long, single-chirality SWCNTs.

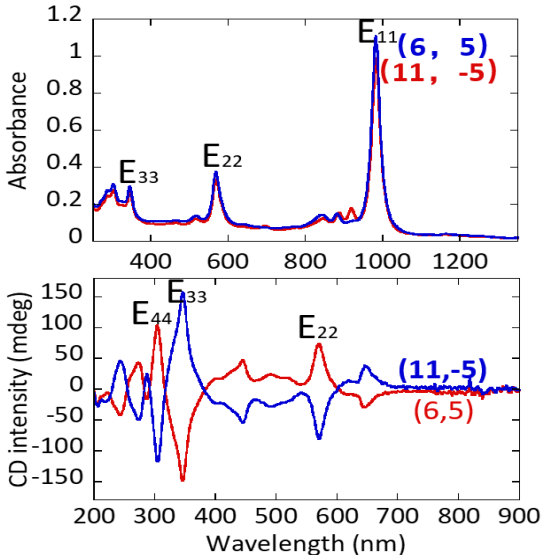

Fig. 1 Absorption and CD spectra of SWCNTs.

SWCNTs were dispersed by SFM using sodium cholate or deoxycholate surfactant and subsequently separated by gel chromatography. By properly selecting the surfactant, we efficiently dispersed SWCNTs in aqueous surfactant systems and successfully separated various (n,m) species and enantiomers in large quantities. Figure 1 shows absorption and CD spectra. Clear peaks indicate the separated SWCNTs are high-purity single-chirality enantiomers. Average lengths of the chirality-sorted SWCNTs were found to be greater than 1 micrometer (1.0 ± 0.5 μm) and could be further enhanced in length (1.8 ± 0.9 μm) by size exclusion chromatography.

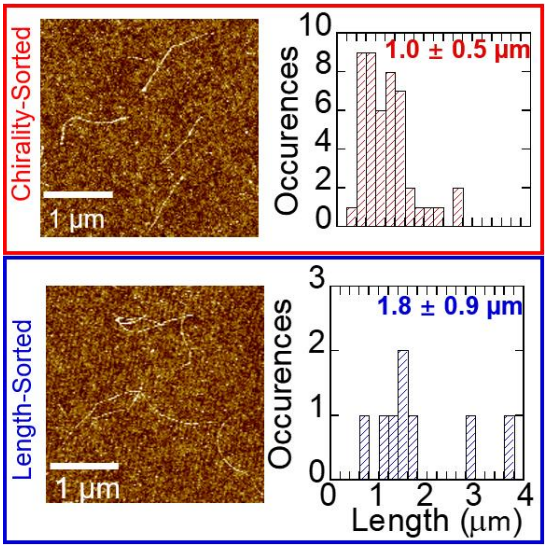

Fig. 2 AFM images and length distributions of SWCNTs, chirality-sorted (red) and length-sorted (blue).

[1] Y. Yomogida et al, *Nat. Commun.* (2016).

[2] Y. Yomogida et al, *ACS Appl. Nano Mater.* (2020).

[3] A. Graf et al, *Carbon* 105 (2016) 593.

Automatic Transfer of Carbon Nanotubes: from Growth to Device Performance

L. Ornago[1], F.H. van Veen[2,3], J. van der Meulen[1,4], S. Jung[1], N. Lanz[1], A. Butzerin[1], M. Nikolić[1], M.L. Perrin[2,3], M. El Abbassi[1]

[1]Chiral Nano AG (Switzerland), [2]Empa (Switzerland), [3]ETH Zürich (Switzerland), [4]TU Delft (The Netherlands)

The integration of Carbon Nanotubes (CNTs) on large-scale and high-volume has been the focus of applied research for years, following the promise of unparalleled performances of CNT based devices for applications spanning from semiconductors to quantum devices. Researchers developed several strategies to grow, select and deposit CNTs on the desired devices, such as direct Chemical Vapor Deposition (CVD) growth, Floating Catalyst CVD, and self-assembly methods [1-4].

This poster will present the approach that Chiral Nano, a Swiss-made spinoff of ETHZ and Empa, is taking on facing such challenges. The core of our technology consists of an automated robotic machine to mechanically transfer CNTs from a growth substrate to a target device wafer. In this way, high-quality nanotubes can be synthesized ex-situ by CVD [5] and transferred with no contamination or degradation of the final devices [6].

Furthermore, Chiral Nano strongly leverages on post-growth Raman characterization to select which CNTs are most suitable for the application [7,8]. For this, we leverage extensive characterization of the electronic properties of the final devices. Here we will present our latest progress and results on suspended carbon nanotube devices with different channel lengths at room temperature, as well as ultra-high-quality quantum devices at cryogenic temperatures.

References (if desired)

[1] F. Yang et al., *Chem. Rev.*, **120**,5, 2693-2758, (2020).
[2] Y. Lin et al., *Nat. Electon.*, **6**, 7,506-515, (2023).
[3] S. Rathinavel et al., *Mater. Sci. Eng. B*, **268**, 115095, (2021).
[4] K. de Almeida Barcelos et al., *J Drug Deliv Sci Technol*, **87**, 104834, (2023).
[5] L. Durrer et al., *Nanotec*, **20**, 35, 355601, (2009).
[6] S. Jung et al., *Sens Actuators B Chem*, **331**,129406, (2021).
[7] M.S. Dresselhaus et al, *Phys. Rep.*, **409**, 2, 47-99, (2005).
[8] J. Zhang et al., *Microsyst. Nanoeng.*, **8**,1, 19, (2022).

Ultraclean carbon nanotube transistors via robotic assembly

S. Jung[1], F. van Veen[2,3], J. van der Meulen[1,4], L. Ornago[1], M. Nikolic[1], A. Butzerin[1], N. Lanz[1], M. Perrin[2,3], M. El Abbassi[1]

[1]Chiral Nano AG (Switzerland), [2]Transport at Nanoscale Interfaces Laboratory, Empa (Switzerland), [3]Department of Information Technology and Electrical Engineering, ETH Zurich (Switzerland), [4]Delft University of Technology (The Netherlands)

Ultraclean carbon nanotube field-effect transistors (CNTFETs) have demonstrated exceptional potential for low-power electronics, quantum applications, and others [1], yet controlled and scalable fabrication remains a bottleneck for commercialization. Previously reported carbon nanotube integration methods do not allow thorough nanotube selection and controlled placement, leading to device variability. Chiral Nano AG is a nanotechnology startup company producing electronic devices with ultraclean nanomaterials with its unique fabrication workflow addressing these issues. Our process begins with the catalytic CVD growth of >10,000 individual CNTs suspended between cantilevers, followed by fully automated Raman spectroscopy and machine-learning-based selection of nanotubes with desired properties. A robotic nanoassembly system then transfers the selected CNTs onto device substrates in a contamination-free, deterministic manner [2]. This approach enables wafer-scale fabrication of ultraclean CNTFETs with unprecedented reproducibility. This work presents the performance of such carbon nanotube transistors, with its statistics gathered from thousands of devices characterized at room temperature and from a subset of devices measured at low temperature. Device quality—as demonstrated by unprecedented low contact resistance [3], systematic observation of 4-fold degeneracy at low temperatures, etc—and reproducibility will be discussed in detail.

References

[1] A. Franklin, Nat. Electron. 7 (2024) 1068-1069.
[2] A. Butzerin et al., Precis. Eng. 89 (2024) 328-337.
[3] S. Jung et al., Sens. Actuators B Chem. 331 (2021) 129406.

NIR photoluminescence of single-wall carbon nanotubes by the biochemical reaction of luciferin/luciferase

Takeshi Tanaka, Mahoko Higuchi, Mayumi Tsuzuki, Atsunori Hiratsuka, Hiromichi Kataura

Nanomaterials Research Institute, National Institute of Advanced Industrial Science and Technology (AIST), Tsukuba 305-8565 (Japan)

We present the near-infrared (NIR) photoluminescence of single-wall carbon nanotubes (SWCNTs) generated through chemical energy derived from enzymatic reactions. NIR photoluminescence from SWCNTs has garnered significant attention for medical applications, such as bioimaging and biosensors, due to its high transparency and low scattering in biological tissues. However, visible excitation light cannot penetrate deep tissue regions. In this study, we developed a novel method where the NIR photoluminescence of SWCNTs is driven by the biochemical reaction of luciferin/luciferase from fireflies, eliminating the need for external excitation light. The photoluminescence was detected using a highly sensitive IR camera system, and optimal conditions for photoluminescence were investigated. Spectroscopic analysis of the NIR photoluminescence using chirality-sorted SWCNTs [1] confirmed that the photoluminescence originated from SWCNTs. This is the first report of achieving NIR photoluminescence of SWCNTs using chemical energy, which does not require external energy sources such as excitation light or electronic power, and holds potential for biological imaging and sensing applications [2]. This work was supported by JSPS KAKENHI Grants 19H02539, 20H05668, and 24K01282 and by the Suzuken Memorial Foundation.

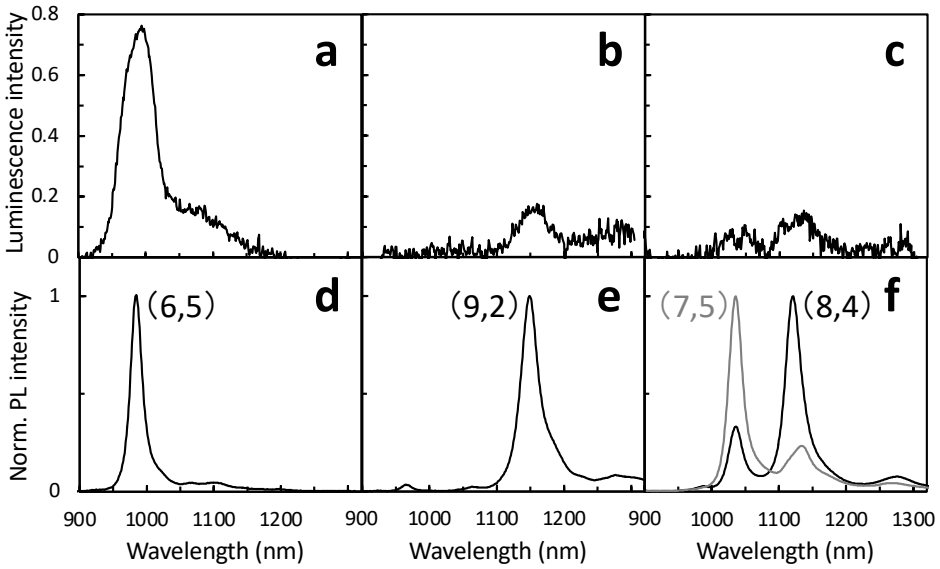

Fig. 1 (a−c) Luminescence spectra by SWCNTs and luciferase reaction and (d−f) photoluminescence (PL) spectra of the corresponding SWCNTs: (a, d) (6,5) SWCNTs, (b, e) (9,2) SWCNTs, and (c, f) mixture of (7,5) and (8,4) SWCNTs. (d−f) The excitation wavelengths for the PL measurements were set to S_{22} of the respective SWCNTs as follows: 570 nm for (6,5) (d), 555 nm for (9,2) (e), 650 nm for (7,5) (f, gray line), and 595 nm for (8,4) (f, black line).

References

[1] Y. Yomogida *et al.* Nat. Commun. **7**, 12056 (2016).
[2] T. Tanaka *et al*. J. Phys. Chem. Lett., **14**, 5955 (2023).

Reconfigurable physical unclonable functions from carbon nanotube transistors for secure vehicle communications

LIU Yang[1,2] , PEI Jingfang[1] , SONG lekai[1] , LIU Songwei[1] , LIU Pengyu[1] , WEN Yingyi[1,3] , MA Teng[3] , HU Guohua[1]

[1]Department of Electronic Engineering, CUHK, HKSAR, China, [2]The Shun Hing Institute of Advanced Engineering, HKSAR, China, 3Department of Applied Physics, PolyU, HKSAR, China.

Hardware security is critical in the era of information and IoT, as the hardware is now transmitting and processing exponential amounts of data. Physical unclonable functions (PUF) are an emerging technology to secure hardware communications. Here we report scalable PUF design and implementation using wafer-scale carbon nanotube charge-trapping transistors. Arising from the unique electronic properties of carbon nanotubes and the intrinsic dynamics of charge trapping, the transistors exhibit trivial yet robust transferring dynamics in their non-volatile memory states, thereby enabling reconfigurable PUFs. Notably, a PUF consisting of 9 transistor arrays allows secure and stable 32^9 mathematically and physically unclonable primitives. Our analyses prove an excellent resilience of the PUFs against attacks. For example, a 108-bit PUF may take up to 10^{16} years to attack in brute force method. Given this unclonable capability, as well as the scalability, the PUFs hold great potential in enabling hardware security in, for instance, vehicle communications. As an example, we demonstrate secure key exchange in autonomous vehicle communications on OMNET++ using the PUFs.

MXene Quantum Dots/ Metal Organic Framework Hybrids for Photocatalytic Applications

Annas S. Ariffin[1], Anir S. Sharbirin[1], Afrizal L. Fadli[1], Jeongyong Kim[1]

[1]*Department of Energy Science, Sungkyunkwan University, Suwon 16417 (Rep. of Korea),*

Fragmentation of two-dimensional (2D) MXene allows the broadening of bandgap of MXene, thus allowing the metallic 2D MXene to possess semiconductor-like properties [1]. These MXene quantum dots (MQDs) have gained much interest and are being studied in various applications like sensors, photovoltaics and optoelectronic devices. Same as its precursor MXene, MQDs also possess excellent conductivity and electrochemical stability [2]. Also, owing to its superior conductivity and adequate active sites, MQDs show great potential in photocatalytic field. In this work, we incorporate titanium nitride (Ti_2N) MQDs into MIL-125-NH_2, a type of titanium-based metal organic framework (MOF) known for efficient charge separation, abundance of active sites and modifiable pores and framework, and study the photocatalytic activities of the hybrid [3]. By introducing Ti_2N MQDs as co-catalyst, the interfacial contact and charge extraction can increase, hence enhancing the photocatalytic activities [4]. Through the embedding of MQDs in MOF strategy, it will further increase the internal contact and building the heterostructure, which are favorable for charge separation and built of heterojunctions [5]. We evaluate the catalytic performance of the hybrid by observing the photodegradation performance of rhodamine 6G by the MQDs/MOF hybrid. This work aimed at exploring the workability of Ti_2N) MQDs as photocatalyst and understanding the dynamic of charge transfer in Ti_2N MQDs/ MOF hybrid.

References

[1] Sharbirin, A.S., et al., *Adv, Optical Material.* **13**(4), 2402379 (2024).
[2] Deng, H., et al. *Chinese Chemical Letters*. **35**(6), 109078 (2024).
[3] Zhu, C., et al, *Chemical Engineering Journal*. **497**, 154689 (2024).
[4] Nie, J., et al, *Separation and Purification Technology.* **354**, 128961 (2025).
[5] Xu, Q., et al, *Journal of Materials Chemistry A.* **11**(10), 5309-5319 (2023).

Theoretical study on photo thermoacoustic phenomena in carbon nanotubes based on Tyndall model

Akari Sudo[1] and Takahiro Yamamoto[1,2]

[1] *Department of Physics, Tokyo University of Science, Tokyo 162-8601, Japan*

[2] *RIST, Tokyo University of Science, Tokyo 162-8601, Japan*

Recently, Iijima discovered a novel photo thermoacoustic (PTA) phenomenon in which sound is generated by irradiating carbon nanotubes (CNTs), such as vertically aligned CNTs (VA-CNTs) and eDIPS-CNTs, with pulse light (white LED light) [1]. Interestingly, the frequency response of the sound emitted by CNTs contains more harmonic components than fundamental. In the case of VA-CNTs, the sound volume differs depending on the length of the CNTs.

In this study, we have carried out simulations to investigate how the heating of the air and the pressure waves generated vary with the shape of the incident pulsed light, the pulse interval and the pulse width. We adopt Tyndall's model to understand the PTA phenomena in CNTs and assumed that the heat generated in the CNT diffuses radially. The temperatures of the CNT and the air are expressed by the following equations:

$$\frac{dT_{\mathrm{CNT}}(t)}{dt} = \frac{P_{\mathrm{in}}(t)}{mc} - \frac{\alpha}{mc}\left(T_{\mathrm{CNT}} - T_{\mathrm{air}}(0,t)\right), \qquad \frac{\partial T_{\mathrm{air}}(r,t)}{\partial t} = \kappa_{\mathrm{air}}\left(\frac{1}{r}\frac{\partial}{\partial r}\left(r\frac{\partial T_{\mathrm{air}}(r,t)}{\partial r}\right)\right),$$

where T_{CNT} is the temperature of CNT, $P_{\mathrm{in}}(t)$ the power of pulse light, α the resistance between CNTs and air, $T_{\mathrm{air}}(0,t)$ the temperature at the interface between air and the CNT, T_{air} the temperature of air, and κ_{air} the thermal diffusivity. $T_{\mathrm{air}}(\infty,t) = T_0$ $(= 300\mathrm{K})$ and $T_{\mathrm{CNT}}(0) = T_{\mathrm{air}}(r,0) = T_0$ are imposed as the boundary and initial conditions, respectively. In addition, the presser wave is calculated using the following equation:

$$\left(\nabla^2 - \frac{1}{v_s^2}\frac{\partial^2}{\partial t^2}\right)p(\vec{r},t) = -\frac{\beta}{\kappa v_s^2}\frac{\partial^2 T(\vec{r},t)}{\partial t^2},$$

where $p(\vec{r},t)$ is sound pressure at position and time, $T(\vec{r},t)$ is air temperature rise at position and time, v_s is speed of sound, κ is isothermal compression ratio, and β is volumetric expansion coefficient.

We performed a Fourier analysis of the calculated pressure waves and compared the data with the experimental data reported by Iijima [1]. We also studied how the CNT length depends on the amplitude of sound from VA-CNTs. To do this, we extended the above equation to solve for finite length CNTs. As a result, we found that the sound amplitude is determined by the temperature distribution in the CNT, which depends on the CNT length and the contact thermal resistance between the CNTs and the substrate.

In the presentation, we will show the details of the calculation results and how they compare to the experiment.

References

[1] S. Iijima (For example, The 68th Fullerenes-Nanotubes-Graphene General Symposium, Meijo University, Nagoya).

Semiconducting Transport Characteristics and Performance of Large-Bundle SWCNT FETs

Abu Taher Khan[1], Nan Wei [2], Esko I. Kauppinen [1]

[1]Aalto University (Finland), [2]Peking University (China)

When carbon nanotubes grow in a floating catalyst CVD (FCCVD) reactor, they agglomerate due to Brownian diffusion [1] and form bundles as predicted by simple aerosol models [2]. Generally, as one third of as-synthesized SWCNTs are metallic, bundles, too, consist of a mixture of metallic and semiconducting tubes. While significant research efforts have been devoted to exploring the electrical performance of field-effect transistors (FETs) based on individual SWNTs, less attention has been given to investigating the electrical performance of bundles and the underlying transport properties of these bundles [3,4].

In this study, we investigated the transport behavior of SWCNT bundles with a mean bundle diameter of 7.1 nm, formed from tubes with a mean diameter of 1.9 nm. As-grown SWCNT bundles were composed of 53.7% semiconducting and 46.3% metallic nanotubes as determined by electron diffraction. Ideally, the transistor is expected to lose its gate modulation efficiency due to the presence of a metallic tube in the bundle. Thus, one would expect that all SWCNT bundles that contain metallic tubes, exhibit poor switching characteristics. Surprisingly, however, our data implies the opposite, and in fact, we observe a higher fraction of semiconducting FETs than the fraction of as-grown semiconducting SWCNTs. A total of ~2000 transistors were studied. Of these, 62% exhibit semiconducting characteristics. In this study, we examine the transport characteristics and charge transport mechanisms of large-bundle SWCNT FETs as a function of bias voltage. Our results reveal that the metallic tubes in the bundle have less influence on the transport characteristics, while the surface conductive tubes determine whether the transistor is metallic or semiconducting. However, the charge carrier mobility is a key performance metric and ohmic contact single bundle SWCNT FETs exhibited a mean mobility of 5378 $cm^2V^{-1}S^{-1}$, among the highest reported. Furthermore, the FETs exhibited a high on-off ratio up to 10^8 making them ideal for high-speed digital electronics.

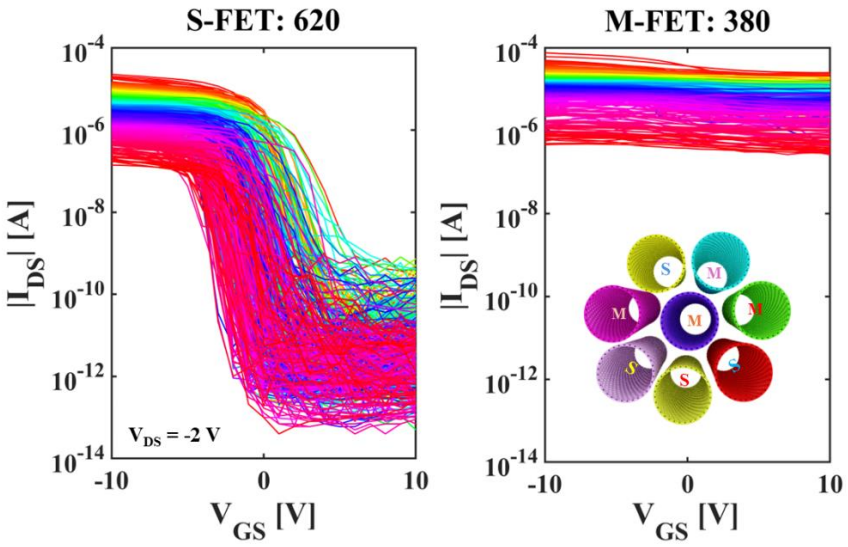

Figure : The figure presents the transfer curves of SWCNT bundle FETs, highlighting both semiconducting and metallic properties. The inset in the right panel shows a large bundle composed of both metallic and semiconducting nanotubes.

References:
[1] A. Moisala *et al. Chem. Eng. Sci.* **61(13)**, 4393–4402 (2006).
[2] K. Mustonen *et al. Apple. Phys. Lett.* **107**, 013106 (2015).
[3] A. Kaskela *et al. Appl. Mater. Inter.* **7**, 28134-28141 (2015).
[4] P. Laiho *et al. Appl. Mater. Inter.* **9**, 20738-20747 (2017).

Armchair-Oriented Synthesis of Tin Disulfide Nanotubes (SnS_2 NT)

Abid[1], Yongjia Zheng[1], Luneng Zhao[2], Ju Huang[3,4], Yuta Sato[5], Qingyun Lin[6], Zheng Han[7], Chunxia[1], Tianyu Wang[1], Bill Herve Nduwarugira[1], Yige Zheng[1], Hang Wang[1], Salman Ullah[1], Mohd Taazeem Ansari[8], Hafiz Bilal Naveed[1], Afzal Khan[1], Wenbin Li[3,4], Junfeng Gao[2], Bingfeng Ju[1], Feng Ding[9], Yan Li[7], Kazu Suenaga[10], Shigeo Maruyama[11], Huayong Yang[1], Rong Xiang*[1]

[1]*State Key Laboratory of Fluid Power and Mechatronic Systems, Zhejiang Provincial Key Laboratory for Atomic-level Manufacturing, School of Mechanical Engineering, Zhejiang University, Hangzhou 310027, China*
[2]*Key Laboratory of Material Modification by Laser, Ion and Electron Beams (Dalian University of Technology), Ministry of Education, Dalian, 116024, China*
[3]*Key Laboratory of 3D Micro/Nano Fabrication and Characterization of Zhejiang Province, School of Engineering, Westlake University, 310030, Hangzhou, China*
[4]*Institute of Advanced Technology, Westlake Institute for Advanced Study, 310024, Hangzhou, China*
[5]*Nanomaterials Research Institute, National Institute of Advanced Industrial Science and Technology (AIST), Tsukuba 305-8565, Japan*
[6]*Center of Electron Microscopy, State Key Laboratory of Silicon and Advanced Semiconductor Materials, School of Material Science and Engineering, Zhejiang University, Hangzhou 310027, China*
[7]*College of Chemistry and Molecular Engineering, Peking University, Beijing 100871, P. R. China*
[8]*Department of Applied Sciences & Humanities, Faculty of Engineering & Technology, Jamia Millia Islamia, New Delhi, India*
[9]*Institute of Technology for Carbon Neutrality, Shenzhen Institute of Advanced Technology, Chinese Academy of Sciences, Shenzhen, China*
[10]*The Institute of Scientific and Industrial Research, Osaka University, 8-1 Mihogaoka, Ibaraki, Osaka, Japan*
[11]*Department of Mechanical Engineering, The University of Tokyo, Tokyo 113-8656, Japan*

Abstract: In this work, we present the chiral angle preferred synthesis and detailed characterization of tin disulfide nanotubes (SnS_2 NTs) encapsulated within boron nitride nanotubes (BNNTs) using a tailored chemical vapor deposition (CVD) technique. Chirality control of the NTs at the atomic level precisely controls their electronic, optical, and quantum properties [1]. However, synthesizing chirality-preferred TMD NTs remains a formidable challenge, as traditional approaches, such as CVD, often produce mixtures of zigzag (ZZ) and armchair (AC) configurations due to stochastic growth dynamics [1]. To address this, we proposed a four-step synthesis approach using BNNT as a template to grow SnS_2 NTs inside [2]. High-resolution electron microscopy and spectroscopy reveal these heterostructures' structural complexity and high compositional purity. The chirality of individual SnS_2 nanoribbon (NR) and nanotube (NT) is determined using nano-area electron diffraction (NAED). Statistical evaluations show that the 85% AC configuration dominates NT chirality distributions, but ZZ or near ZZ stands out as the primary configuration for NRs. Our theoretical (DFT and MD) calculations agreed well with the experimental results that AC SnS_2 NT growth is most favorable, enabling systematic chirality modulation during nanoribbons (NRs) transformation into nanotubes (NTs) inside the BNNT. By advancing chirality-resolved synthesis and 1D heterostructure engineering, this work bridges a critical gap in nanomaterials innovation, offering a scalable pathway toward tailored quantum materials for optoelectronic, catalytic, and quantum applications.

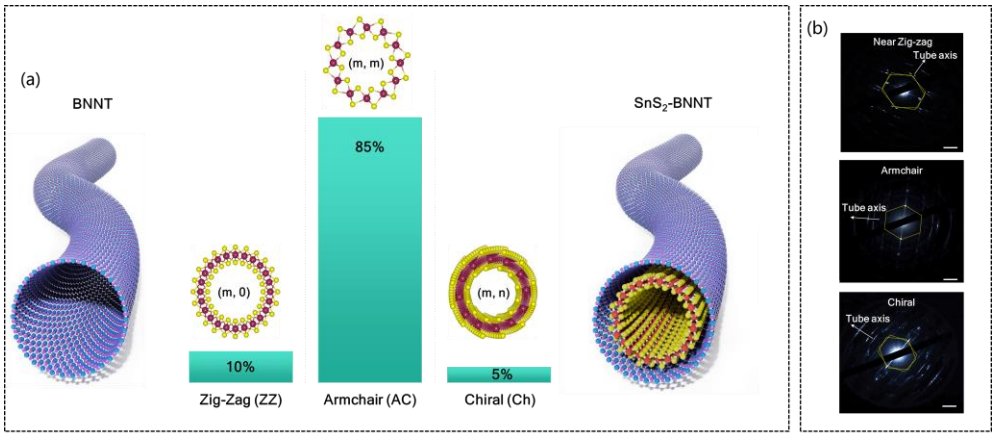

Figure 1: (a) Schematic representation of SnS_2 NT encapsulation inside the BNNT along with the chiral angle preference statistics and (b) NAED illustrating the different chirality configuration.

References

[1] Liu, B., et al. ACS Nano vol. 11 31–53 (2017).
[2] Abid et al.., *Nature Materials* (communicated).

Overcoming Van der Waals Bundling: Molecular Wedges Enable Sonication-Free Dispersion of Single-Walled Carbon Nanotubes

Seungyeop Lee[1], Ziyi Wang[1], Ebenezer Afriyie[1], Jiajun Wang[2], Ayman Alibrahim[1], Anand Jagota[2,3], YuHuang Wang[1,4,5*]

[1]Department of Chemistry and Biochemistry, University of Maryland, College Park, Maryland, United States

[2]Department of Bioengineering, Lehigh University, Bethlehem, PA, 18015, United States

[3]Department of Chemical and Biomolecular Engineering, Lehigh University, Bethlehem, PA, 18015, United States

[4]Chemical Physics Program, University of Maryland, College Park, Maryland, United States

[5]Maryland NanoCenter, University of Maryland, College Park, Maryland, United States

*Correspondence should be addressed to Y.H.W. at yhw@umd.edu

Single-walled carbon nanotubes (SWCNTs) strongly bundle due to van der Waals interactions, posing a significant challenge to their individualization and wide-ranging applications. Current dispersion strategies rely on extended shear force mixing or ultrasonication, which are energy-intensive and can damage nanotubes. Here, we present a sonication-free strategy that uses small "molecular wedges" to intercalate between nanotubes and overcome these bundling forces. By combining minimal amounts of superacids (e.g., chlorosulfonic acid) with wedge precursors (e.g., 1-octanol or ammonia), we chemically drive wedge molecules into the nanotube bundles, markedly reducing van der Waals interactions. Classical mechanics modeling reveals that even a small wedge (e.g., 0.8 nm in diameter) can effectively split nanotube aggregates. The resulting "wedged" SWCNTs show a 40-fold increase in dispersion efficiency with sodium deoxycholate and a two-fold improvement with single-stranded DNA, all while preserving nanotube length. Furthermore, we demonstrate a one-pot synthesis that introduces sp^3 quantum defects into these SWCNTs with improved uniformity. This molecular wedge approach thus addresses key challenges in SWCNT dispersion and should be broadly adaptable to other van der Waals materials.

HYDROGEN STORAGE BY CARBON NANOHORNS ENHANCED BY DISPERSION WITH METALLIC NANOPARTICLES

N. Sano

Department of Chemical Engineering, Kyoto University, Kyoto 615-8510, Japan

It is known that carbon nanomaterials dispersed with metallic nanoparticles can store hydrogen by softly-dissociative adsorption of hydrogen, and their hydrogen storage capacity is higher than pure carbon materials. This enhancement is reported to be contributed by so-called hydrogen spillover. The present study reports that carbon nanohorns synthesized by arc discharge in water with gas-injection can be dispersed with various metallic nanoparticles when the electrode in the arc discharge system contains carbon and metallic species. Also, it reports that the metal-dispersed carbon nanohorns can exhibit significantly higher hydrogen storing capacity than ordinal carbon nanohorns and the metal species and its amount dispersed in carbon nanohorns essentially affects the hydrogen storage capacity. It is observed that titanium is the appropriate metallic species and there is an optimized amount of it in carbon nanohorns. In addition, chemical modification on metal-dispersed carbon nanohorns can exhibit high hydrogen storage capacity. Theoretically, the metal dispersion on carbon nanohorns can reduce activation energy to dissociate hydrogen molecule in hydrogen spillover scheme, and the present study elucidate this mechanism by a modeled molecular-orbital calculations.

Synthesis of H_2-rich syngas and CNTs from CH_4/CO_2 using Ni-Mo_2C/MgO catalyst: Impact of biogas impurities and catalyst regeneration

S. Saconsint[1], N. Sano[1], S. Ratchahat[2]

[1]Kyoto University (Japan), [2]Mahidol University (Thailand)

Biogas dry reforming presents a promising approach for utilizing renewable resources while reducing greenhouse gas emissions. However, impurities such as H_2S, NH_3, and moisture (H_2O) present challenges by poisoning nonprecious metal catalysts like Ni, leading to activity loss and increased maintenance costs [1]. Transition metal carbides (TMCs), particularly Ni-Mo_2C, have shown potential as cost-effective alternatives to noble metals due to their resistance to sulfur, nitrogen, and oxygen compounds [2-4]. Despite this, the impact of poisoned gases on Ni-Mo_2C for simultaneous syngas and carbon nanotube (CNT) production remains insufficiently understood. In this study, the performance of Ni-Mo_2C/MgO catalyst was evaluated under biogas conditions containing varying concentrations of CH_4, CO_2, H_2O, including NH_3, and trace amounts of H_2S at 800°C and atmospheric pressure over a 3-hour reaction period. The results demonstrate a noticeable reduction in CH_4 and CO_2 conversion rates at the onset of sulfur poisoning, followed by a stabilization phase where CH_4 conversion maintained at 46% and CO_2 conversion reached up to 80%, indicating partial sulfur tolerance of the catalyst. With the introduction of water vapor into the sulfur-induced system, the gas conversion rates significantly improved, suggesting that water mitigates sulfur's deactivating effects by facilitating sulfur species oxidation and enabling partial catalyst regeneration. Additionally, the investigation into varying impurity concentrations provided deeper insights into the poisoning mechanisms and catalyst behavior, supported by advanced characterization techniques.

References

[1] M. A. Osachoque *et al., Mater. Chem. Phys*. **69**, 76 (2016).
[2] J. G. Chen, *Chem. Rev*. **1477**, 1498 (1996).
[3] J. S. Lee *et al., J. Catal*. **126**, 136 (1991).
[4] P. Da Costa, C. Potvin, J. M. Manoli, M. Breeysse, and G. Djega-Mariadassou, *Catal. Lett*. **133**, 138 (2003).

Geometric structure and electronic properties of bilayer graphene with a Moire superlattice by interlayer asymmetric tensile strain

Mina Maruyama, Nadia Sultana, Yanlin Gao, and Susumu Okada

University of Tsukuba (Japan)

An external electric field or excess carrier affects the geometric and electronic structures of graphene and its thin films [1]. The lattice parameter of graphene increases with the increase of the hole concentration, while that remains approximately constant against the electron doping. Furthermore, the injected hole in bilayer graphene and graphene thin films is primarily distributed in the outermost layer below the electrode. These facts imply that graphene thin films can form a Moire superlattice, of which periodicity is continuously tunable by controlling the hole concentration and the external electric field. Therefore, in this work, we aim to investigate the geometric and electronic structures of bilayer graphene, one of which layers has tensile strain ranging from 5 to 7.6%, using the density functional theory combined with an effective screening medium method.

We consider bilayer graphene consisting of $(n-1) \times (n-1)$ supercell with tensile strain and $n \times n$supercell with the equilibrium lattice constant (n=13~20). The asymmetry in the atomic density between the layers induces the internal electric field across the layers. This asymmetry also causes upward and downward shifts of the Dirac cone of $(n-1) \times (n-1)$ and $n \times n$ supercells, respectively, leading to the charge redistribution between the layers. The charge redistribution strongly depends on the interlayer atomic arrangement where the accumulated carrier is absent at the AA stacking region. The potential difference between layers shows the family pattern with the triple periodicity of n [2].

References

[1] N. Sultana, M. Maruyama, Y. Gao, and S. Okada, *Appl. Phys. Express* **17**, 035001 (2024).
[2] M. Maruyama, N. Sultana, Y. Gao, and S. Okada, Jpn. J. Appl. *Phys.* **63**, 115003 (2024).

Structural and Electrical Properties of 3D CNT Networks in CNT-Oxide Ceramic Composites

A. Shibuya[1,2], T. Tanaka[1,2], N. Tonouchi[1,2], T. Miyamoto[1,2], and R. Yuge[1,2]

[1] NEC Corporation (Japan), [2] National Institute of Advanced Industrial Science and Technology (Japan)

Our research group is engaged in the research and development of infrared image sensors using semiconducting carbon nanotubes (CNTs) as bolometer materials [1-2]. By using semiconducting single-walled CNTs separated by the electric-field-induced layer formation (ELF) method [3] and controlling the manufacturing condition of the CNT network, we have reported a temperature coefficient of resistance (TCR) of -6%/K, which is three times larger than that of the conventional bolometer material, VOx [4].

In this study, we developed composite materials of semiconducting CNTs and oxide ceramics with the aim of forming a three-dimensional (3D) CNT network and evaluating its properties. The manufacturing method of the composite is as follows: a suspension of ceramic particles with an average grain size of approximately 1 μm was prepared and drop-casted onto a substrate, dried, and solidified to form an oxide porous film. Subsequently, a silane coupling self-assembled monolayer was formed on the surface of the oxide ceramic particles in the porous film, a CNT dispersion liquid was dropped and infiltrated into the porous film, attempting to form a CNT network on the surface of the oxide particles and the substrate. P-type Si substrate with a thermally oxidized film was used, and electrodes forming a back-gate field-effect transistor (FET) structure were pre-formed on the substrate, then the CNT-oxide ceramics composites were formed using the above manufacturing method. Then a polymethyl methacrylate (PMMA) solution was dropped on the channel portion and solidified to fix the composite, after which the oxide particles and CNTs in the areas not supplied with PMMA were removed to produce an FET device for characteristic evaluation.

From microstructural observations using scanning electron microscopy (SEM) and transmission electron microscopy (TEM), it was confirmed that the developed composite materials form 3D networks of CNTs based on oxide ceramic particle films with thickness of 2-3 μm. By evaluating the transport characteristics of FETs using composite with $Zn_{1-x}Mg_xP_2O_7$ as oxide particles, we found the potential to achieve both low resistance and TCR <-10%/K.

Acknowledgments: The study was partly supported by Innovative Science and Technology Initiative for Security Grant No. JPJ004596, ATLA, Japan.

References

[1] T. Tanaka. et. al., 2022 MRS Fall Meeting, NM02.09.08 (2022).
[2] T. Tanaka. et. al., 2023 MRS Fall Meeting, EL07.06.10 (2023).
[3] K. Ihara, et. al., J. Phys. Chem. C, **115**, 22827-22832 (2011).
[4] C. Chen, et. al., Sen. Act. A. Phys. **90**, 212-214 (2001).

Composite of Carbon nanotubes and Activated carbon as air electrode in Zn-air battery

M. Kalong[1], N. Sano[1], T. Suzuki[1]

[1]*Kyoto University (Japan)*

Zn-air batteries (ZABs) have recently gained attention due to their potential advantages, including low cost, high theoretical energy density, safety, and environmental-friendliness. However, the development of efficient air electrodes remains essential for further progress in ZABs technology. From a sustainable perspective, it is important that the air electrodes are efficient, low cost, and composed of abundant resources instead of metals. Due to their excellent conductivity, low cost, and strong durability, carbon-based materials are promising types of electrocatalyst in ZABs. In this study, composite electrodes consisting of carbon nanotube (CNTs) and activated carbon (AC) at varying AC to CNTs ratios were prepared and employed as air cathodes in two-electrode Zn-air battery cells containing an 8 M KOH aqueous electrolyte. The morphology of these composite electrodes observed via scanning electron microscopy (SEM) revealed superior contact between activated carbon particles and carbon nanotubes, and the bundle formation of carbon nanotubes on activated carbon particles also appeared in composite electrode. The power generation in the battery cell increased proportionally with the increase in the amount of AC in composite electrode AC-CNT electrode. The power density reached the maximum, approximately 6.7 mW cm^{-2}, at 50:50 weight ratio of AC to CNTs. CNTs effectively functioned as structural binders to stabilize the electrode structure, while AC provided a high surface area crucial for electrochemical reactions. The synergistic effects of combining CNTs and AC, including their transportation properties within the composite electrodes, are also discussed.

Quantitative insights into the correlation between sp^3 defects and functional groups in oxidized single-walled carbon nanotubes

○Hideaki Nakajima, Kazufumi Kobashi, Ying Zhou, Minfang Zhang, Toshiya Okazaki

National Institute of Advanced Industrial Science and Technology (AIST), Tsukuba 305-8565, Japan

Carbon nanotube (CNT) surface functionalization has been increasingly advanced and diversified in recent years, with the vigorous development of appropriate control techniques for versatile applications. However, the formation of critical defects such as sidewall cleavage has become an increasingly important concern, as it severely degrades the performance of CNTs. Here, we demonstrate a framework for quantitatively evaluating the correlation between sp^3 defects and functional groups on single-walled CNT surfaces by combining recently developed energy dispersive X-ray spectroscopy in scanning electron microscope (SEM-EDS) [1-3] and μ-Raman spectroscopy techniques (Fig. 1a).

Two types of single-walled CNTs (super growth denoted as CNT1 and enhanced direct injection pyrolytic synthesis denoted as CNT2) were oxidized by $KMnO_4/H_2SO_4$ treatment. The D/G ratio and oxygen concentration on the same bundle structure were measured at multiple locations using μ-Raman and SEM-EDS. It allowed a comparative analysis of the trends in sp^3 defects and functional groups between the two types of CNTs.

Figure 1(b) indicates the obtained D/G ratio and oxygen concentration as the average distance of defects (L_D) and the number of carbon atoms of CNTs for every functional group (η), respectively. η decreases with increasing the sp^3 density by oxidation for both types of CNTs. However, the slopes differ between them. To clarify the difference, the variable θ defined as the ratio of the degree of functionalization/defect density is introduced. θ=1 corresponds to the ideal state where one functional group is anchored for each sp^3 site. The measured results are appropriately explained by θ values of 0.01-0.02 for CNT1 and 0.001-0.001 for CNT2. It implies the different trends between the two types of CNTs regarding forming structural disruptions during the oxidation reaction. Since this consideration precisely aligns with the transmission electron microscope (TEM) observation, our analytical model is capable of quantitatively evaluating nm-sized sidewall cleavage [2]. Details of the analysis and TEM observation will be discussed at the conference.

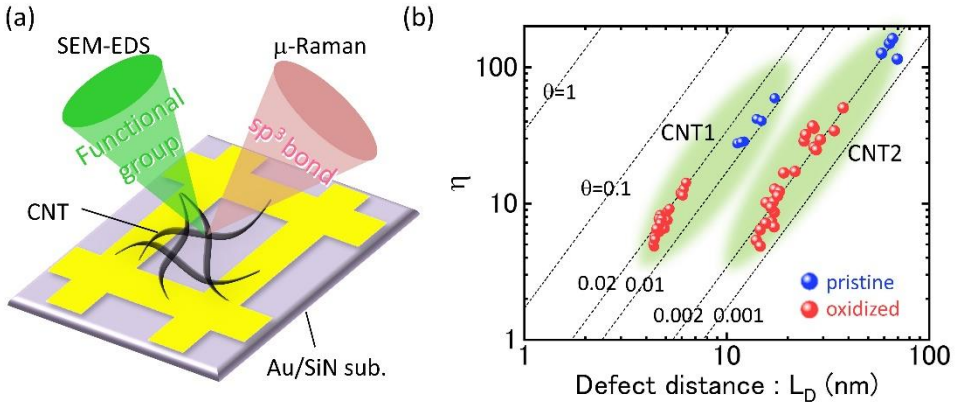

Fig. 1 (a) Conceptual illustration of this study. (b) Correlation between sp^3 defect distance (L_D) and the number of carbon atoms for every functional group (η).

References

[1] H. Nakajima *et al.*, *Nanoscale* **11**, 21487-21492 (2019).
[2] H. Nakajima *et al.*, *J. Phys. Chem. C* **124**, 25142-25147 (2020).
[3] H. Nakajima et al., *Appl. Surf. Sci.* **624**, 157077 (2023).
[4] H. Nakajima *et al.*, *Carbon* **216**, 118495 (2024).

Preferential growth of (7,5) SWCNTs by enhanced direct-injection pyrolytic synthesis method

Yuki Kuwahara[1], Yuta Nishiwaki[2], Kei Takano[2], Takeshi Hashimoto[2], Ryota Yuge [1,3], Takeshi Saito[1]

[1]*National Institute of Advanced Industrial Science and Technology (Japan),* [2]*Meijo Nano Carbon Co. Ltd. (Japan),* [3]*NEC Corporation (Japan)*

Synthesis of single-wall carbon nanotubes (SWCNTs) with the control of their structural characteristics is an enabling step for their many potential applications and fundamental studies. Hitherto we had been developing the continuous growth system for SWCNT production with the controllability of tube diameter, “enhanced direct-injection pyrolytic synthesis (eDIPS) CVD” [1], that is one of the technologies adopted to produce commercially available SWCNTs [2]. Because the tube diameter is closely correlated with chirality, diameter controllability would be a key to achieving chirality-selectivity in SWCNT growth.

In this presentation, we report a preferential growth of (7,5) SWCNTs by eDIPS method. The optimization of reaction conditions such as reaction temperature, carbon source gas and its flow rate were carried out to control the growth. Semiconducting chiralities of the as-grown SWCNTs were characterized by using the photoluminescence-excitation (PLE) mapping. The result of the typical sample is shown in Fig. 1 with chirality assignments. As shown in Fig. 1, predominant peaks of (7,5) and (8,4) SWCNTs were observed with several weak peaks of (6,5), (8,3), (7,6) and (9,2). In particular, the intensity of (7,5) was ca. two times larger than that of (8,4) that suggests the preferential growth of (7,5) in the present reaction condition. We will also discuss about the detailed analysis of chiralities including the metallic one by using optical absorption spectroscopy.

This work was supported by Innovative Science and Technology Initiative for Security Grant No. JPJ004596, ATLA, Japan.

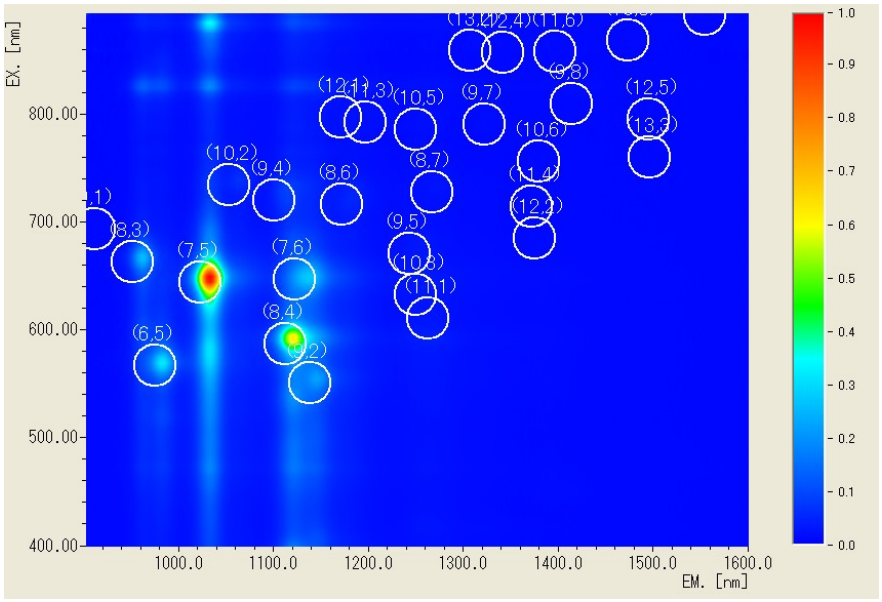

Figure 1. PLE mapping of a typical SWCNT sample produced by eDIPS-CVD.

References

[1] T. Saito, S. Ohshima, T. Okazaki, S. Ohmori, M. Yumura, *et al*., Selective Diameter Control of Single-Walled Carbon Nanotubes in the Gas-Phase Synthesis, J. Nanosci. Nanotechnol., **8** (2008) 6153–6157.

[2] https://www.meijo-nano.com/en/home

Vacuum electronics of carbon nanotube and its applications in aerospace

Peng Liu[1], Liang Liu[1], Kaili Jiang[1], Shoushan Fan[1]

[1] *Tsinghua University (China)*

For their excellent physical and chemical properties such as high mechanical strength, high melting point, extreme aspect ratio, carbon nanotubes show outstanding performance in vacuum electronics. We will report our researches about the elementary properties of carbon nanotube vacuum electronics such as work function measurement, electron emission and transport mechanism at high temperature, influence of adsorption[1, 2]. Furthermore, the related applications of carbon nanotube in other vacuum electronic parts such as gate and anode will also be reported[3]. It was found that the carbon nanotube gate can realize the high electric field uniformity and high electron transparency simultaneously[4]. The carbon nanotube anode shows as electron absorption coefficient above 90% and can be viewed as electron blackbody. The carbon nanotube lights can used as NDIR source to monitoring the greenhouse gases[5]. The carbon nanotube neutralizer has worked in the Taiji-1 satellite[6]. We will also report our researches about the crystalline characterization of large area 2-D materials with a low energy transmitted electron diffraction and imaging technology[7, 8]. Due the high aspect ratio of carbon nanotube, an electrostatic catalysis method can be used to control the synthesis of high purity semiconducting carbon nanotubes by combining the their unique DOS state[9, 10].

References (if desired)

[1]. Yang, X.H., et al., Phys Status Solidi A, 2020. **217**(15). 2000069.
[2]. Yang, X.H., et al., Phys Status Solidi B, 2020. **257**(9). 2000103.
[3]. Liu, P., et al., Nano Lett, 2018. **18**(8). 4691-4696.
[4]. Zhang, K., et al., P Natl Acad Sci USA, 2023. **120**(6). e2209670120.
[5]. Lai, L.W., et al., Adv Funct Mater, 2022. **33**. 2208891.
[6]. Liu, P., Nature Reviews Electrical Engineering, 2024. **1**(2). 73-74.
[7]. Zhao, W., et al., Sci Adv, 2017. **3**(9). e1603231.
[8]. Zhao, W., P. Liu, and K.L. Jiang, J Phys D Appl Phys, 2020. **53**(40). 403001.
[9]. Liu, Z.B., et al., J Am Chem Soc, 2021. **143**(42). 17607-17614.
[10]. Wang, J.T., et al., Nat Catal, 2018. **1**(5). 326-331.

Machine learning force field driven exploration of 992 binary alloy metal clusters for carbon nanotube growth

Daniel Hedman[1], Daisuke Asa[2], Ryo Yoshikawa[2], Ikuma Kohata[2], Kaoru Hisama[3], Christophe Bichara[4], Keigo Otsuka[2] and Shigeo Maruyama[2]

[1]*Center for Multidimensional Carbon Materials (CMCM), Institute for Basic Science (IBS), Ulsan 44919 (Korea),*
[2]*Department of Mechanical Engineering, The University of Tokyo, Tokyo 113-8656 (Japan),*
[3]*Center for Research Initiative for Supra-Materials, Shinshu University, Nagano 380-8553 (Japan),*
[4]*Aix-Marseille Univ, CNRS, CINaM, Marseille 13288 (France)*

Single-walled carbon nanotubes (SWCNTs) are cylindrical nanostructures with remarkable electronic properties that vary with their atomic arrangement (chirality), making them promising candidates for next-generation integrated circuits. The selective synthesis of SWCNTs with specific chirality remains challenging, as traditional catalysts typically produce broad chirality distributions. High-melting-point solid metal nanoparticles could be promising catalysts for selective growth, as their well-defined crystalline structure may promote specific nanotube chiralities.

The central challenge addressed in this study is identifying binary metal alloy combinations that form stable, high-melting-point nanoparticles suitable for chirality-selective SWCNT growth. Here we trained a neuroevolution potential (NEP) on data from on-the-fly machine learning force field accelerated ab initio molecular dynamics and used it to perform long-timescale cooling and melting simulations of 992 binary clusters formed from combinations of 32 different metals. Our results show that only 9 out of the 992 binary alloy clusters formed vertex-Mackay (v-Mackay) icosahedral structures, see Figure 1, during cooling, with the rest forming core-shell, segregated or random alloy clusters. We found that the major factors determining binary alloy cluster structure are the differences in surface energy and atomic size of the constituent elements, see Figure 1. Through slow melting simulations, we identified exceptional thermodynamic stability in specific core-shell compositions including $Cu_{42}Fe_{13}$, $Pt_{42}Fe_{13}$, $Ni_{42}Fe_{13}$ and $Pt_{42}Cu_{13}$, which could enable precise control over SWCNT chirality during synthesis.

This comprehensive exploration of binary alloy clusters establishes a foundation for rational design of catalyst nanoparticles with high melting point for controlled SWCNT growth. We anticipate these results will accelerate progress toward chirality-selective synthesis of SWCNTs by guiding experimental efforts toward the most promising binary catalyst systems.

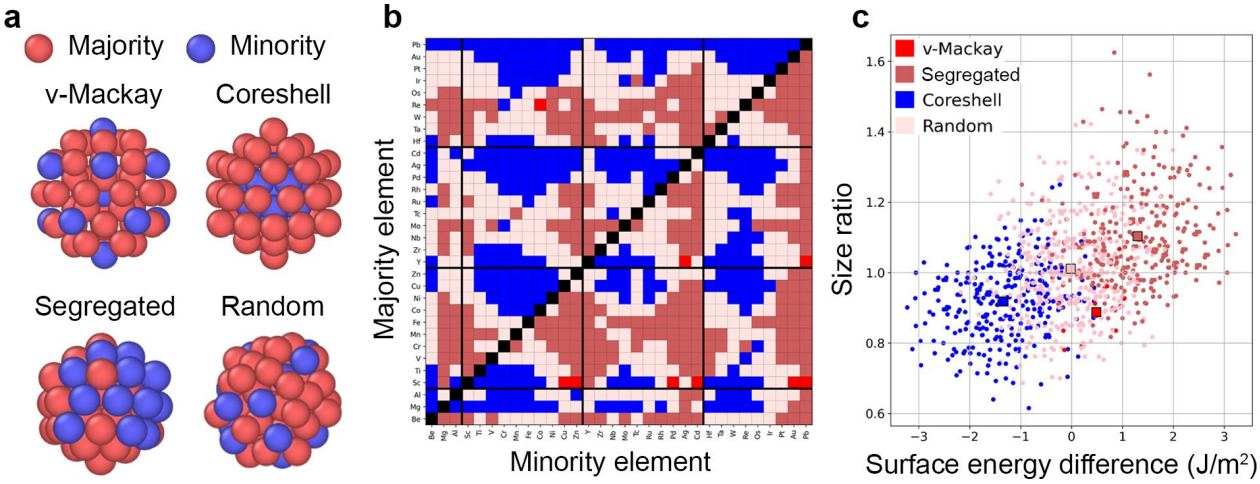

Figure 1. a schematic representation of four distinct structures of binary alloy metal clusters. **b** heatmap depicting the structure for each of the 992 binary alloy metal clusters obtained from cooling simulations. **c** clustering of different structural types as a function of size ratio and surface energy differences between the majority and minority elements.

Impact of Twisted angle on Thermal Transport Property of Graphene/h-BN Moiré Superlattice

S. Mouri[1], Y. Kodama[1], A. Kuddus[2]
Graduate of School of Science and Engineering, Ritsumeikan University, Shiga 525-8577, Japan
[2] *R-GIRO, Ritsumeikan University, Shiga 525-8577, Japan*

Graphene (Gr) and related two-dimensional (2D) layered materials exhibit distinct electronic characteristics, including exceptionally high electron mobility [1] and high thermal conductivity [2], with a band structure that depends on the number of layers. Stacking Gr with insulating h-BN is a promising approach for achieving high-mobility electronic devices. While several studies have investigated the thermal transport properties of stacked structures [3][4], the twist-angle-dependent thermal conductivity of Gr/h-BN stacks and its implications for thermal management in electronic devices remain largely unexplored.

In this study, we investigate the thermal properties of twisted Gr/h-BN and Gr/Gr moiré superlattices depending on their twisted angles using laser heating while monitoring Raman shift. We prepared suspended Gr/h-BN heterostructures on a Si_3N_4 grid with 5.0 μm diameter holes using a wet transfer process with PMMA. The twist angles were determined through selected area electron diffraction pattern measured by TEM setup.

We conducted Raman spectroscopy while varying the excitation laser power, estimating the temperature increase (ΔT) from the redshift of the spectral peak. The thermal conductivity was calculated using a 2D heat equation analysis [5]. Figure 1(a) presents the thermal conductivity of Gr/h-BN with a twist angle of 14°, plotted as a function of temperature. The thermal conductivity tends to decrease with increasing temperature, with an average value of approximately 330 W/mK in the range of 350°C to 450°C. Figure 1(b) compares the average thermal conductivity for Gr/h-BN and Gr/Gr as a function of the twist angle. In general, the thermal conductivity of twisted samples tends to decrease with increasing twist angle. This is likely due to enhanced phonon scattering caused by the increased overlap between optical and acoustic phonon branches in twisted structures. On the other hand, in Gr/h-BN, an increasing trend in thermal conductivity is observed around 20°. According to MD simulations, the interlayer distance is expected to decrease near 20° due to stacking [6], which may contribute to the observed increase in thermal conductivity.

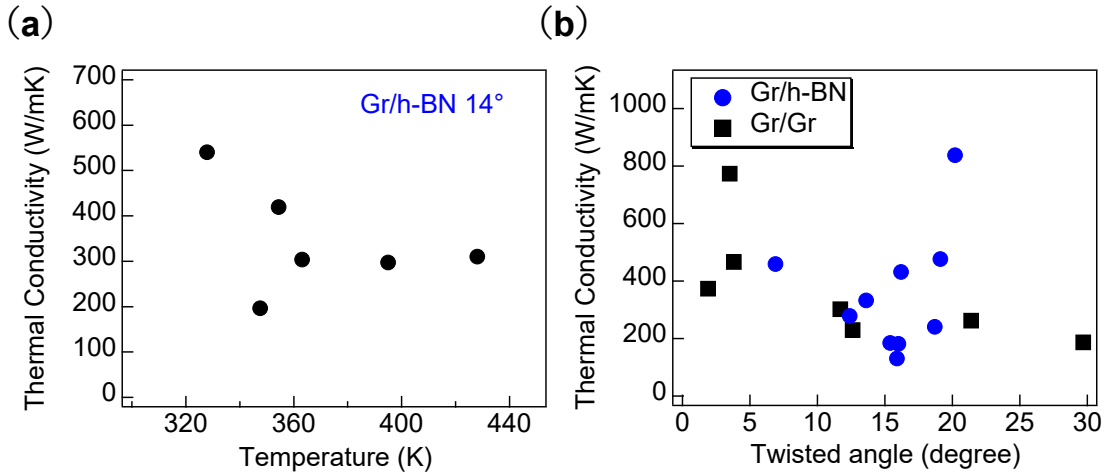

Figure1 (a) The thermal conductivity of Gr/h-BN is presented as a function of temperature. The sample's twisted angle is measured at 14°. (b) Thermal conductivity as a function of the twist angle for Gr/h-BN (Blue circles) and Gr/Gr (Black squares), with the average value calculated between 350°C and 450°C.

References (if desired)
[1] K. I. Bolotin et al., Sol. Stat. Commun. **146**, 351 (2008).
[2] A. A. Balandin et.al., Nano Lett **8**, 902 (2008).
[3] C. C.Chen et.al.,n Appl. Phys. Lett. **104**, 081908 (2014).
[4] A. J. Pak and G. S. Hwang., Phys. Rev. Applied **6**, 034015 (2016).
[5] W. W. Cai et al., Nano Lett. **10**, 1645 (2010).
[6] Z. Zhang et al., Nanotechnology **28**, 225704 (2017).

This work was supported by JSPS KAKENHI grant number 22H05471、21H01017、21K18913.

Structure and Fabrication Process Optimization of Microbolometer Array using Semi-conducting Single-walled Carbon Nanotube Networks

T. Tanaka[1,2], M. Sano[1], M. Noguchi[1,2], M. Kanaori[2], T. Miyamoto[1,2], R. Yuge[1,2]

[1]NEC Corporation (Japan), [2]National Institute of Advanced Industrial Science and Technology (Japan)

Uncooled infrared sensors of the bolometer type have a wide range of applications such as security, food inspection, health care and automotive night vision systems. The bolometer is a long-wave infrared (LWIR) detector of radiant heat using an infrared absorber with a temperature-sensitive electrical resistive material. Infrared radiation strikes the absorber material, heating it and thus changing the electrical resistance of the resistive material. Therefore, the performance of the bolometer is severely limited by the temperature coefficient of resistance (TCR) of the resistor. NEC has developed microbolometer array by Micro Electro Mechanical System fabrication process with vanadium oxide (VO_X) for high TCR electrical resistance. The conventional electrical resistors for microbolometers are generally based on VO_X or amorphous silicon with TCR of about -2%/K[1], and an excellent electrical resistor is essential to achieve highly sensitive infrared detectors.

Recently, semi-conducting single-walled carbon nanotubes (SWCNTs) are expected to be promising materials with high TCR. We have reported that semi-conducting SWCNT networks extracted by the "Electric-field inducing Layer Formation (ELF)" method[3] and formed on Si wafer by dip coat process shows high TCR, which is close to -6%/K[3]. The ELF method is the remarkable promising technique to obtain high-purity semi-conducting SWCNTs, which show stable device performance and excellent electrical transport property. In a previous study, it was demonstrated that the TCR of a semi-conducting SWCNT network was responsible for the increased sensitivity of the microbolometer. We have established a fabrication process for Video Graphics Array (VGA) format microbolometer focal plane allays (FPAs) with semi-conducting SWCNTs on the 6-inch read out integrated circuit wafer for VO_X microbolometer[4]. To evaluate the detectivity of the bolometer pixel, responsivity and noise characteristics of a test element group installed in the liquid nitrogen cryostat ware measured. The responsivity was estimated to be over 10^5 V/W at 0.2 V bias voltage. At frequencies up to 200 Hz, the noise power density exhibited an inverse proportionality to frequency. This shows that the noise is predominantly characterized by 1/f noise at the operating frequency of a standard microbolometer camera. The black body detectivity, D* calculated from the responsivity and the noise was equal to or better than microbolometer using VO_X fabricated by a similar fabricating process. In this study, we report on recent efforts to improve the uniformity of characteristics and detectivity of microbolometer pixels on 6-inch wafers. Details will be reported on the day.

Acknowledgments: The study was partly supported by Innovative Science and Technology Initiative for Security Grant No. JPJ004596, ATLA, Japan.

Reference

[1] C. Chen, et. al., *Sen. Act. A. Phys.* **90**, 2001, 212.
[2] Y. Tanaka, et. al., *Proc. SPIE* **5074**, Infrared Technology and Applications XXIX, (10 October 2003).
[3] K. Ihara, et. al., *J. Phys. Chem. C*, **115**, 2011, 22827.
[4] T. Tanaka. et. al., 2022 MRS Fall Meeting, NM02.09.08.
[5] T. Tanaka. et. al., *Proc. SPIE* **13046**, Infrared Technology and Applications L, 130460X (7 June 2024).

Gate Voltage Dependence of Low-Frequency Noise in Carbon Nanotube Networks

N. Tonouchi[1, 2], N. Fukuda[2], T. Tanaka[1, 2], and R. Yuge[1, 2]

[1]NEC Corporation (Japan), [2]National Institute of Advanced Industrial Science and Technology (Japan)

Our group is engaged in the research and development of uncooled bolometers using carbon nanotubes, which are reported to have high temperature coefficients of resistance (TCRs) [1]. The performance of uncooled bolometers depends on the TCR and the noise of the resistor. It is therefore essential to increase the TCR and reduce the noise in order to improve the detection capability.

We have previously demonstrated that the TCR can be controlled by applying gate voltages using a thin film transistor structure [2]. In this study, we investigated the gate voltage dependence of TCR and noise to determine the optimal gate voltage for maximizing detection performance. Figure 1 shows the measured transport characteristics and calculated TCRs at a drain voltage of -0.2 V. The transport characteristics showed a normally on characteristic, where the device is in the off state when a positive gate voltage is applied. We confirmed that the TCR is maximized in the off-state at around 8V (Figure 1). Figure 2 shows the gate voltage dependence of the normalized noise power density. We found that the normalized noise power density exhibits 1/f noise behavior at low frequencies and increases as the off-state is approached. We will report the detailed experimental and analytical results, as well as guidelines for maximizing detection performance.

Acknowledgments: The study was partly supported by Innovative Science and Technology Initiative for Security Grant No. JPJ004596, ATLA, Japan.

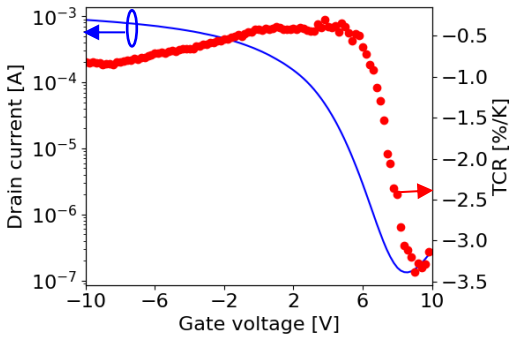

Figure 1. I_d-V_g curve and estimated TCR

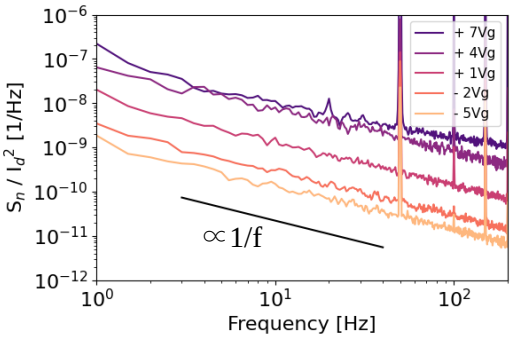

Figure 2. Gate voltage dependence of low frequency noise

References

[1] T. Tanaka et al. *Proc. SPIE* **12534**, 125341U (2023)

[2] N. Tonouchi et al. *70rd Annual Meeting of the Japan Society of Applied Physics*, 15p-A205-11 (2023).

Terahertz wave detection using P/N carbon nanotube fibers at room temperature

○K. Shiba[1], S. Saito[1], S. Kusaba[1,2], R. Tamaki[2], S. Tsuzuki[3], T. Matsuura[3], J. Takeda[2], I. Katayama[2], and K. Yanagi[1]

[1] *Department of Physics, Tokyo Metropolitan University, Tokyo 192-0397, Japan*
[2] *Department of Physics, Graduate School of Engineering Science, Yokohama National University, Yokohama 240-8501, Japan*
[3]*Production Engineering Development Division, TOKAI RIKA Co., LTD. Aichi 480-0195, Japan*

Terahertz (THz) optoelectronic technology is expected to be applied in various fields, such as communication, medicine, security, and astronomy [1]. The development of efficient THz detection devices plays a key role for the application of THz in various fields, however, it has not yet been found for devices such as compact, high-performance, and robust [2]. Carbon nanotubes (CNTs) are promising candidates for the material of THz detection devices because they absorb electromagnetic waves over a wide frequency range and exhibit excellent thermoelectric properties, and THz detections using CNTs have been demonstrated [3, 4]. Recently, we succeeded to produce P-type and N-type CNT fibers with high electricity (> 10^6 S/m) and relatively large Seebeck coefficient (~ 40 μVK^{-1}). In this study, we fabricated PN junctions using the P-type and N-type fibers, and evaluated the THz detection characteristics. Figure 1(a) and (b) show the setups of devices made from 1-pair and 2-pairs CNT fiber PN junctions, and the THz response characteristics (1.7 mW, ~1 THz). As shown in Fig. 1(c), clear THz responses are observed. Additionally, the device made from 2-pairs CNT fibers exhibits stronger signal intensity and faster response time compared to the 1-pair device, as shown in the graph, which would be due to the larger junction area and cross section area contribute more efficient THz absorption and enhancement of thermal conductance. The results suggest further optimization of texture will improve the responses.

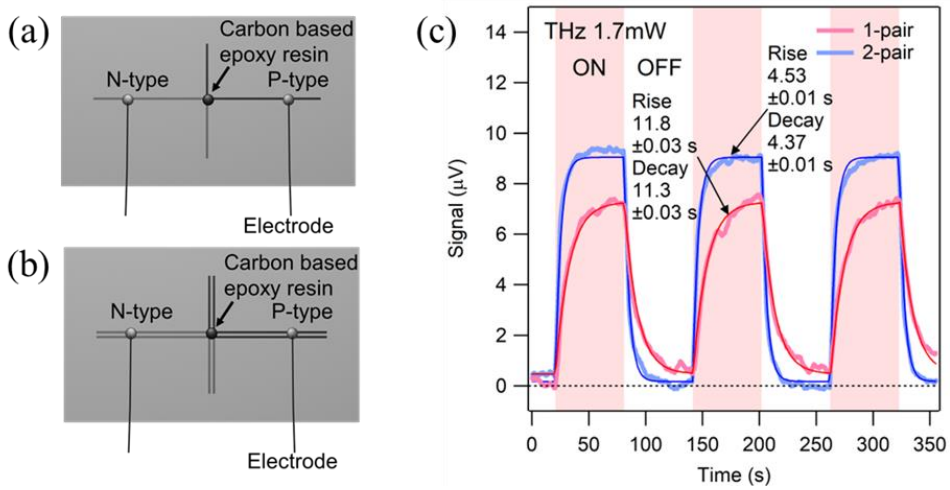

Fig. 1: (a), (b): Device setups for 1-pair and 2-pairs CNT PN junctions. (c): Voltage responses under THz ON/OFF radiation for every 50 seconds.

[1] A. Leitenstorfer *et al.*, *J. Phys. D* **56**, 223001 (2023). [2] R. A. Lewis, *J. Phys. D* **52**, 433001 (2019). [3] X. He *et al.*, *Nano Lett.* **14**, 3953–3958 (2014). [4] K. Li *et al.*, *Nat. Commun.* **12**, 3009 (2021).

Corresponding Author: K. Yanagi, E-mail: yanagi-kazuhiro@tmu.ac.jp

Growth of Isolated Carbon Nanotubes Wrapped by Homogeneous Amorphous Carbon

Zeyu Liu[1], Xinrui Zhang[1], Yanzhao Liu[1], Zilong Qiu[1], Jian Sheng[1], Zeyao Zhang[1,*], Yan Li[1,*]

[1]*College of Chemistry and Molecular Engineering, Peking University, Beijing 100871, China*

Abstract: It is challenging to grow isolated carbon nanotubes (CNTs) directly through floating catalyst chemical vapor deposition (FCCVD) method. Here, we synthesize isolated CNTs coated with long-range homogeneous amorphous carbon through FCCVD method using toluene and methane as carbon sources. With a rapid pyrolysis process of toluene, the cracked carbon atoms can feed the catalyst particles whenever they emerge as relatively small sizes and immediately activate the growth of CNTs. Spontaneously, large amount of pyrolyzed carbon species deposit onto the outer wall of each CNT into amorphous carbon layers along the growth of nanotube to avoid the formation of bundles. This unique structure will open new application potentials for nanocarbon materials.

Keywords: floating catalyst chemical vapor deposition, isolated carbon nanotube, amorphous carbon, toluene

DIRECT GRAPHENE GROWTH BETWEEN ELECTRODES BY JOULE HEATING

K. Nakane[1], A. Subagyo[1], K. Sueoka[1]
[1] *Graduate School of Information Science and Technology, Hokkaido University, Sapporo, Japan*

Graphene-based electronic device performances are highly dependent on the junction properties between graphene and metal electrodes, and low contact resistance is essential for high-performance graphene devices [1,2]. Compared to conventional graphene devices with side contact structures, graphene devices with edge (or end) contact structures exhibit low contact resistance [3,4]. Graphene devices with edge-contact structures were first realized by encapsulating graphene with hBN, a two-dimensional material, and forming electrodes at the cut edges [5]. This method was widely applied to devices with edge-contact structures of two-dimensional and one-dimensional materials [6-9]. In general, resist residues and contamination during the transfer of graphene to device substrates and device fabrication processes have a significant impact on graphene device fabrication. Graphene can be grown directly on the device substrate by heating Ni/C bilayers in a vacuum or a hydrogen atmosphere, allowing the fabrication of graphene devices without the need for graphene transfer [10-12]. However, in many cases, electrode formation takes place after graphene growth, so contamination of graphene by resist and other contaminants is inevitable. Focusing on device fabrication using a resist-free process, this study investigated a method for simultaneous graphene growth and electrode junctions by Joule heating during electromigration of pre-patterned bilayer films made of nickel and carbon.

The devices were first patterned on SiO_2/Si substrates using electron beam lithography, followed by carbon and nickel deposition. The thickness of nickel films was 26nm, while carbon thickness ranged from 1.5nm to 2.5 nm. Then 30nm of nickel and 40nm of Au were deposited as electrodes for electrical connection. Electromigration was performed in a vacuum to simultaneously form electrode gaps and directly grow graphene on the gaps. The thin section of the bilayer films ranged from 300-1000nm. Electromigration breaks the bilayer films caused by the increase of the Joule heating when voltage is gradually increased. Simultaneously, graphene grows between the bilayer gaps, similar to the graphene growth mechanism by rapid heating effect[12]. The size and shape of the gaps depend on the increasing time of the applied voltage. Interestingly, we found that the graphene properties depend on the structure of the bilayer films, i.e., better graphene can be obtained when using bilayer films with carbon layers on the top.

References (if desired)

[1] K. S. Novoselov *et al.*, *Science* **306**, 666 (2004).
[2] G. Fiori *et al*., *Nature Nanotechnology* **9**, 768 (2014).
[3] Y. Matsuda, *et al.*, *J. P. C. C* **114,** 17845 (2010).
[4] H. Liu, H. Kind and T. Ohno, *Phys. Rev. B* **86**, 155434 (2012).
[5] L. Wang *et al.*, *Science* **342**, 614(2013).
[6] S. Das *et al*., *Nano Lett.* **13**, 100 (2012).
[7] Y. Du *et al.*, *IEEE Electron Dev. Lett.* **35**, 599 (2014).
[8] S. McDonnell *et al.*, *ACS Nano* **8**, 2880 (2014).
[9] Y. Cao *et al.*, *Nature* **556**, 43 (2018).
[10] S. Kim *et al*., *Appl. Phys. Lett.* **94**, 062107–1 (2009).
[11] T. Chu and Z. Chen, *ACS Nano* **8**, 3584 (2014).
[12] Rodriguez-Manzo *et.al.*, *ACS Nano* **5**, 1529 (2011).

Session
NT 25（The 25th International Conference on the Science and Applications of Nanotubes and Low-

| Main conference：Main conference

Tue. Jun 17, 2025 6:00 PM - 8:00 PM JST | Tue. Jun 17, 2025 9:00 AM - 11:00 AM UTC Poster 2(International Exchange Hall I&II, Clock Tower Centennial Hall, 2F)

[17psb] Poster 2

[17psb-01]

Fabrication of High-Density Arrays of Single-Chirality and Enantiomer-Pure Single-Walled Carbon Nanotubes

*Yanzhao Liu[1], Zilong Qiu[1], Yiran Ma[1], Min Lyu[1], Zeyao Zhang[1,2], Yan Li[1,2] (1. Peking University (China), 2. Institute of Carbon-Based Thin Film Electronics, Peking University, Shanxi (China))

[17psb-02]

Photovoltaic devices with wide operating temperature ranges based on large-area, freestanding, transparent and conductive G-SWCNT films

*Weiya Zhou[1,2], Ying Yue[1,2], Mingming Li[1,2] (1. Beijing National Laboratory for Condensed Matter Physics and Institute of Physics, Chinese Academy of Sciences (China), 2. University of Chinese Academy of Sciences (China))

[17psb-03]

Multi-level organization of carbon nanotubes for advanced THz optics

*Dmitry V. Krasnikov[1], Nikita I. Raginov[1], Arina V. Radivon[2], Alexey S. Ezersky[3], Gleb M. Katyba[4,5], Sergey A. Kuznetsov[6], Maria G. Burdanova[2], Albert G. Nasibulin[1] (1. Skolkovo Institute of Science and Technology (Russia), 2. Moscow Institute of Physics and Technology (Russia), 3. ITMO University (Russia), 4. Prokhorov Institute of General Physics of the Russian Academy of Sciences (Russia), 5. Institute of Solid State Physics of the Russian Academy of Sciences (Russia), 6. Novosibirsk State University (Russia))

[17psb-04]

Coupling TiO_2 with Low-Dimensional Materials for Efficient Photocatalytic Oxidation of NOx

Morgen L Smith[1], Brian M Everhart[1], Ahmed Al Mayyahi[1], *Placidus B Amama[1] (1. Kansas State University (United States of America))

[17psb-05]

Continuous Synthesis and Fiber Spinning of Nitrogen-Doped SWCNTs

*Zhikai Li[1], Toshihiko Fujimori[1,2], Samuel Jeong[1], Jun-ichi Fujita[1] (1. University of Tsukuba (Japan), 2. Sumitomo Electric Industries, Ltd (Japan))

[17psb-06]

Dielectric-assisted transfer using single-crystal antimony oxide for two-dimensional material devices

*Junhao Liao[1] (1. Peking University (China))

[17psb-07]

Graphene Tamed Supercooling in Plastic Crystals

*Xinyu Zhang[1], Yuanlong Shao[1,2], Jin Zhang[1,2] (1. Peking University (China), 2. Beijing Graphene Institute (China))

[17psb-08]

Nano-seeding method for preparing arrays of horizontally aligned carbon nanotube wafers

*Ying Xie[1], Yue Li[1], Zhisheng Peng[1], Liu Qian[1], Ziqiang Zhao[1], Jin Zhang[1] (1. Peking University (China))

[17psb-09]

Direct Crystallization of one-dimensional Van der Waals Semiconductor WTe_2 Nanowires via Chemical Vapor Transport

*Hang Wang[1], Tianyu Wang[1], Yongjia Zheng[1], Shanhe Xue[2], Abid .[1], Yige Zheng[1], Qingyun Lin[1], Afzal Khan[1], Qi Zhang[2], Rong Xiang[1] (1. Zhejiang Univ (China), 2. Hangzhou Dianzi Univ (China))

[17psb-10]

Janus MoSSe nanotubes on one-dimensional SWCNT-BNNT van der Waals heterostructures

*Chunxia Yang[1,2], Qingyun Lin[2], Yuta Sato[3], Yanlin Gao[4], Yongjia Zheng[2], Tianyu Wang[2], Yicheng Ma[2], Wanyu Dai[1], Wenbin Li[5], Mina Maruyama[4], Susumu Okada[4], Kazu Suenaga[6], Shigeo Maruyama[1,2], Rong Xiang[2] (1. The University of Tokyo (Japan), 2. Zhejiang University (China), 3. National Institute of Advanced Industrial Science and Technology (AIST) (Japan), 4. University of Tsukuba (Japan), 5. Westlake University (China), 6. Osaka University (Japan))

[17psb-11]

A Simple Equipment-Free Method for Length Sorting of Carbon Nanotubes

*Xiaojun Wei[1,2], Shuang Ling[1,3], Xin Luo[1], Xiao Li[1,2], Feibing Xiong[3], Weiya Zhou[1,2], Sishen Xie[1,2], Huaping Liu[1,2] (1. Institute of Physics, Chinese Academy of Sciences (China), 2. University of Chinese Academy of Sciences (China), 3. Xiamen University of Technology (China))

[17psb-12]

In-Situ Observation of Vapor-Liquid-Solid Growth of WS_2 in a Substrate-Stacked Microreactor for Mechanistic Investigation

*Hiroo Suzuki[1], Yutaro Senda[1], Yuta Takahashi[2], Shun Fujii[2], Yasuhiko Hayashi[1] (1. Okayama Univ. (Japan), 2. Keio Univ. (Japan))

[17psb-13]

Tailoring Oxidation States for Selective CVD Growth of Boron Nitride Nanotubes on Supported Catalysts

*Chunghun Kim[1], Myung Jong Kim[1] (1. Gachon university (Korea))

[17psb-14]

Interlocking of SWNTs with Metal-Tethered Tetragonal Nanobrackets to Enrich a Few Hundredths of Nanometer Range in Their Diameters

*Guoqing Cheng[1], Takuya Hayashi[2], Hiroshi Tabata[3], Mitsuhiro Katayama[3], Naoki Komatsu[4] (1. SINANO, CAS (China), 2. Shinshu Univ. (Japan), 3. Osaka Univ. (Japan), 4. Kyoto Univ. (Japan))

[17psb-15]

Novel BNNT-Tungsten Oxide Hybrid Structures for Enhanced Energy Storage Applications

*Honggu Kim[1], Chandan Kumar Maity[1], Myung Jong Kim[1] (1. Gachon University (Korea))

[17psb-16]

Reductive functionalization and purification of single-walled carbon nanotubes for controlling near-infrared photoluminescence properties

*Yutaka Maeda[1], Kentaro Kawada[1], Atsushi Suwa[1], Yui Iguchi[1], Yasuhiro Suzuki[1], Yui Konno[1], Michio Yamada[1], Pei Zhao[2], Masahiro Ehara[2] (1. Tokyo Gakugei University (Japan), 2. Institute for Molecular Science (Japan))

[17psb-17]

Divide and Functionalize: Sorting and Brightening of Single-Walled Carbon Nanotubes

Dominik Just[1], Patrycja Taborowska[1], Andrzej Dzienia[1], *Dawid Janas[1] (1. Silesian University of Technology (Poland))

[17psb-18]

Ultra clean (6,5) SWCNT film with perfect vdW spacing and its 1D heterostructures

*Lingfeng Wang[1], Yicheng Ma[1], Zhirui Liu[2], Yongjia Zheng[1], Tianyu Wang[1], Yuhei Miyauchi[2], Rong Xiang[1] (1. Zhejiang University (China), 2. Kyoto University (Japan))

[17psb-19]

Metal chloride-intercalated pnictogens. Unexplored field full of possibilities

*Cristina Madrona[1], Gonzalo Abellán[1] (1. ICMol - Universidad de Valencia (Spain))

[17psb-20]

TERPYRIDINE-FUNCTIONALIZED SINGLE-WALLED CARBON NANOTUBES AS SELECTIVE ELECTROCATALYST

*Ioanna Sideri[1], Nikos Tagmatarchis[1] (1. National Hellenic Research Foundation, Theoretical and Physical Chemistry Institute (Greece))

[17psb-21]

FUNCTIONALIZED MoS_2 ELECTROSTATICALLY ASSOCIATED WITH PHOTOACTIVE CHROMOPHORES

*Eleni Nikoli[1], Marina Tsigkou[1], Ioanna Sideri[1], Michalis Kardaras[1], Hiram Joazet Ojeda Galvan[2], Mildred Quintana[2], Nikos Tagmatarchis[1] (1. National Hellenic Research Foundation, Theoretical and Physical Chemistry Institute (Greece), 2. Universidad Autonóma de San Luis Potosi, High Resolution Microscopy-CICSaB and Faculty of Science (Mexico))

[17psb-22]

Transition Metal Dichalcogenide Nanotubes with Diameters Below 3 nm

*Runze Lai[1], Zhen Han[1], Xinrui Zhang[1], Yan Li[1] (1. College of Chemistry and Molecular Engineering, Peking University (China))

[17psb-23]

Large-scale complementary carbon nanotube integrated circuits for harsh radiation environments

Ke Zhang[1], *Daming Zhou[1], Ningfei Gao[2,3], Zhongzhen Tong[1], Xiaoyang Lin[1], Haitao Xu[2,3,4], Lianmao Peng[2], Weisheng Zhao[1] (1. School of Integrated Circuit Science and Engineering, Beihang University (China), 2. Key Laboratory for the Physics and Chemistry of Nanodevices, Center for Carbon-based Electronics, School of Electronics, Peking University (China), 3. Beijing Institute of Carbon-based Integrated Circuits (China), 4. Institute of Carbon-based Thin Film Electronics, Peking University (China))

[17psb-24]

Architecting Host−Guest Synergistic Solid-State Electrolytes Enables Unobstructed Li-Ion Interphase Migration for Lithium Metal Batteries

*lixiang li[1] (1. University of Science & Technology Liaoning (China))

[17psb-25]

Optimizing Metal Contacts for Low Contact Resistance in Graphene Field Effect Transistors

*Duc Chung Nguyen[1], Yi Yong Park[1] (1. Ajou University (Korea))

[17psb-26]

Diameter Adjustment of Single-Walled Carbon Nanotubes by Ni-Based Bimetallic Catalysts in Laser Ablation

Shaochuang Chen[1], *Zeyao Zhang[1,2], Yan Li[1,2] (1. Peking University (China), 2. Institute of Carbon-Based Thin Film Electronics, Peking University, Shanxi (China))

[17psb-27]

Marangoni-Flow-Induced Self-Assembly of Single Walled Carbon Nanotubes into High Density Arrays

Zilong Qiu[1], Yuguang Chen[1], *Yanzhao Liu[1], Zeyao Zhang[1,2], Yan Li[1,2] (1. Peking University (China), 2. Institute of Carbon-Based Thin Film Electronics, Peking University, Shanxi (China))

[17psb-28]

Intrinsic High-Semiconducting-Purity Carbon Nanotube Array Films for High-Performance Electronics

*Lan Bai[1,2] (1. Peking University (China), 2. Shanxi Institute of Carbon-Based Thin Film Electronics, Peking University (China))

[17psb-29]

h-BN/Graphene Heterostructure-Decorated Copper Current Collector for Long-Cycle Anode-Free Lithium Metal Batteries

*Lingchen Kong[1], Chaofan Zhou[1], Xuanguang Ren[1], Li Lin[1,2], Xin Gao[1,2] (1. Peking University (China), 2. Beijing Graphene Institute (China))

[17psb-30]

Research on Semiconducting SWCNTs with clean surfaces in Dispersions and Thin-Films

*Song Qiu[1] (1. Suzhou Institute of Nano-Tech and Nano-Bionics, Chinese Academy of Sciences (China))

[17psb-31]

Gas Phase Chemistry of Salt Assisted MoS_2 Growth

*Daniel Stormer Vadseth[1], Shigeo Maruyama[2], Alister Page[1] (1. University of Newcastle (UoN) (Australia), 2. University of Tokyo (UTokyo) (Japan))

[17psb-32]

On the use of seeding for chirality-controlled growth of carbon nanotubes

*Kim-Jonas Mikael Ylivainio[1], Daniel Hedman[2], Andreas Larsson[1] (1. Luleå university of technology (Sweden), 2. Institute for basic science (Korea))

[17psb-33]

Super graphene-skinned material: From epitaxial growth to property calculations

*Sun Xiu cai[1], Liu Zhong fan[2,1] (1. Beijing Graphene Institute (BGI) (China), 2. Peking University (China))

[17psb-34]

Graphene Layers Folded Many Times

*Kazuyuki Uchida[1] (1. Kyoto Sangyo University (Japan))

[17psb-35]

Anomalous Electrostatic Properties of Double-walled BN Nanotubes

*Nadia Sultana[1], Yanlin Gao[1], Mina Maruyama[1], Susumu Okada[1] (1. University of Tsukuba (Japan))

[17psb-36]

Machine Learning-Assisted Computational Exploration of the Electronic Structures of MoS_2 Nanotubes

*Wenbin Li[1], Ju Huang[1] (1. Westlake University (China))

[17psb-37]

Observation of Topological Nodal-Ring Phonons in Monolayer Hexagonal Boron Nitride

*Zhiyu Tao[1] (1. Institute of Physics, Chinese Academy of Sciences (China))

[17psb-38]

On-Chip Metasurface-Mediated $MoTe_2$ Photodetector with Electrically Tunable Polarization-Sensitivity

*Ruizhi Li[1], Xinlei Zhang[1], Fan Zhong[1], Zhenhua Ni[1] (1. Southeast University (China))

[17psb-39]

Synthesis of Rhenium Doped WS_2 Nanotubes and their electrical properties

*Abdul Ahad[1,2], M. A. Afzal[1], R. Higashinaka[1], M. Kikuchi[1], S. Saito[1], S. Kusaba[1], Z. Liu[4], Y. Miyata[1], Y. Hirose[3], K. Yanagi[1] (1. Department of Physics, Tokyo Metropolitan University (Japan), 2. Department of Physics, Comilla University (Bangladesh), 3. Department of Chemistry, Tokyo Metropolitan University (Japan), 4. National Institute of Advanced Industrial Science and Technology (AIST) (Japan))

[17psb-40]

Interband Scattering via Effective-Diameter Modulation in Single-Wall Carbon Nanotubes

*Nikita Gavrilov[1], Eden Levi[1], Alon Strugatsky[1], Michael Shlafman[1], Kenji Watanabe[2], Takashi Taniguchi[2], Yuval E. Yaish[1] (1. Technion - Israel Institute of Technology (Israel), 2. National Institute for Materials Science (Japan))

[17psb-41]

Thermal characterization of highly thermally conductive SWCNT films employing two-laser Raman thermometry

*Timm Swoboda[1], Martin Magg[2], Cristian Borja Peña[3], Pu Tan[1], Jiaqi Yang[1], Daniel Capolat Palomar[1], Wim Wenseleers[4], Sofie Cambré[3], Benjamin Flavel[2], Javier Rodriguez-Viejo[1,5], Marianna Sledzinska[1] (1. Catalan Institute of Nanoscience and Nanotechnology (ICN2), 08193, Barcelona, Spain (Spain), 2. Institute of Nanotechnology, Karlsruhe Institute of Technology, 76344, Eggenstein-Leopoldshafen, Germany (Germany), 3. Theory and Spectroscopy of Molecules and Materials, Department of Physics, University of Antwerp, 2610. Antwerp, Belgium (Belgium), 4. Nanostructured and Organic Optical and Electronic Materials, Department of Physics, University of Antwerp, 2610, Antwerp, Belgium (Belgium), 5. Physics department, Autonomous University of Barcelona (UAB) Campus UAB, Bellaterra, 08193, Barcelona, Spain (Spain))

[17psb-42]

ANISOTROPIC OPTICAL PROPERTIES OF MONOLAYER ALIGNED SINGLE-WALLED CARBON NANOTUBES

G A Ermolayev[1], M G Burdanova[2], Y Xie[3], L Qian[3], M Tatmyshevskiy[2], A Slavich[2], A Arsenin[1], V Volkov[1], J Zhang[3], *Alexander Chernov[2,4] (1. Emerging Technologies Research Center XPANCEO Emmay Tower (United Arab Emirates), 2. Moscow Institute of Physics and Technology (Russia), 3. Peking University (China), 4. Russian Quantum Center (Russia))

[17psb-43]

Fluctuations, dynamics and structure of the crystal edge of growing carbon nanotubes

Session

NT 25（The 25th International Conference on the Science and Applications of Nanotubes and Low-

Daniel Hedman[1], *Christophe Bichara[2] (1. CNRS and Aix-Marseille Univ. (Korea), 2. Institute for Basic Science (France))

Fabrication of High-Density Arrays of Single-Chirality and Enantiomer-Pure Single-Walled Carbon Nanotubes

Yanzhao Liu[1], Zilong Qiu[1], Yiran Ma[1], Min Lyu[1], Zeyao Zhang[1,2], Yan Li[1,2]*

[1]*College of Chemistry and Molecular Engineering, Peking University, Beijing, China*

[2]*Institute of Carbon-Based Thin Film Electronics, Peking University, Shanxi, Taiyuan 030012, China*

Corresponding author: yanli@pku.edu.cn

Single-walled carbon nanotubes (SWCNTs) possess one-dimensional hollow structures and diverse carbon atom configurations, endowing them with strong anisotropy and chirality-dependent optical and electronic characteristics. When assembled into macroscale arrays with uniform chirality, these single-chirality arrays not only preserve the intrinsic anisotropic nature of individual nanotubes but also demonstrate enhanced signal responses. In this work, we have prepared (9,8), (7,5) and (6,5)-enriched single-chirality SWCNT arrays from organic dispersions, along with (-)(6,5) and (+)(6,5) enantiomeric SWCNT arrays from aqueous dispersions. Systematic characterization through polarized spectroscopic measurements and microscopic imaging has confirmed both the high degree of alignment and high packing density of the arrays. The ability to obtain single chirality and enantiomeric SWCNT arrays allows us to further explore their special optical and electronic properties in the future.

Photovoltaic devices with wide operating temperature ranges based on large-area, freestanding, transparent and conductive G-SWCNT films

W.Y. Zhou[1,2], Y. Yue[1,2], M.M. Li[1,2]

[1]Beijing National Laboratory for Condensed Matter Physics and Institute of Physics, Chinese Academy of Sciences (China), [2]University of Chinese Academy of Sciences (China)

Transparent conductive film (TCF) is an important part of a lot of advanced equipment such as electronic, photoelectric and energy devices in modern technology and has received widespread research. Among the emerging transparent conductive materials, carbon nanofilms (graphene, carbon nanotubes, hybrid films) are considered to be the most potential alternatives for traditional ITO due to their excellent electrical, optical, mechanical, flexible and stable properties [1]. However, at the present stage, developing high-quality carbon nanofilms that can be scaled up in large-area and at large-scale remains a formidable challenge. For this purpose, we have proposed a faceted driven carbon nanotube network reorganization (FD-CNNR) strategy to produce large area, freestanding, flexible, transparent and conductive reorganized carbon nanofilms with A3 size or even up to meter-length [2]. The key properties of as-prepared G-SWCNT TCFs, such as transparent conductivity and mechanical strength, have been improved synergistically, enabling it to achieve sheet resistance as low as 69 Ω/sq at 86% transmittance, and the Young's modulus of ~45 MPa, which can meet the demand for flexible TCFs in industry to a certain extent.

In the application field of TCFs, with the development of emerging electronic devices, optoelectronic devices have attracted increasing attention. In the face of the lack of photovoltaic devices at low temperatures, we have investigated heterojunction solar cells (HSCs) and transparent photovoltaic devices (TPVDs) based on the large area and freestanding G-SWCNT TCF prepared by FD-CNNR technique.

(1) Design and fabrication of a TPVD as a photodetector, realizing the development of TPVDs with long time air stability and wide operating temperature range [3], fills the research gap in this area. The as-obtained TPVD has high performance not only, but also excellent environmental stability and service stability which will be attributed to the G-RSWNT TCF with air stability and molecular blocking effect, with no degradation of its main performance parameters after being placed in the air for 3 months and undergoing 20000 photo-switching cycles. Particularly, it manifests stable performance and remarkable serviceability over a wide temperature range from low to high temperatures (-180°C~300°C). As a demonstration, self-powered solar-blind UV optical communication is performed using as-obtained TPVD under -180°C~300°C. The research provides important scientific reference for promoting the process of practical application of TPVDs.

(2) Design and preparation of a G-SWCNT/Si HSC, which can operate at room temperature, low temperature and wide temperature (-269°C ~ room temperature). On the basis of the HSC with stable and high photoelectric conversion efficiency (PCE) of up to 12.5% at room temperature prepared by pure G-SWCNT TCF, combined with surface passivation, doping improvement and interface optimization, a novel HSC is designed and achieves significantly improved PCE to 17.8%, 28.5% and 26.3% at room temperature, liquid nitrogen temperature and liquid helium temperature, respectively. The reasons for its modified performance are also discussed. This result breaks through the application bottleneck of traditional silicon-based HSCs in extremely cold conditions and demonstrates the research and development value of our HSCs in some important fields and the potential of practical applications at low or even extremely low temperatures.

References

[1] Q. Zhang *et al.*, *Adv. Mater.* **32**, 2004277 (2020).
[2] Y. Yue *et al.*, *Adv. Mater.* **36**, 2313971 (2024).
[3] Y. Yue *et al., Nano Res.* **17**, 6582−6593 (2024).

MULTI-LEVEL ORGANIZATION OF CARBON NANOTUBES FOR ADVANCED THZ OPTICS

Raginov N.I.[1], Radivon A.V.[2], Ezersky A.S.[3], Chernykh A.V.[3], Terentyev A.V.[2], Zhivetyev K.V.[2], Rakov I.I.[1], Katyba G.M.[4,5], Novikov I.V.[1], Tsiplakova E.G.[3], Paukov M.I.[2], Starchenko V.V.[2], Arsenin A.V.[2], Spector I.E.[4], Kuznetsov S.A.[6], Zaitsev K.I.[4], Petrov N.V.[3], Burdanova M.G.[2,4], Kopylova D.S.[1], Gorshunov B.P.[2], Volkov V.[2], Nasibulin A.G.[1], **Krasnikov D.V.[1]**

[1] Skolkovo Institute of Science and Technology (Russia), [2] Moscow Institute of Physics and Technology (Russia),

[3] ITMO Universit (Russia) [4] Prokhorov Institute of General Physics of the Russian Academy of Science (Russia)

[5] Institute of Solid State Physics of the Russian Academy of Science (Russia) [6] Novosibirsk State University, (Russia)

The unique set of mechanical, electrical, and optical features of carbon nanotubes has inspired scientists and engineers for several decades to create new materials and devices in various fields of our civilization: from medicine to aerospace, from telecommunications to construction technologies. Significant progress in the field of functional materials ensures the gradual introduction of nanotubes into such scientific and technological products as antistatic coatings, lithium-ion batteries and polymer composites; nevertheless, the development of carbon nanotube-based devices in optoelectronics and biomedicine lacks in performance. This is mostly related to insufficient control on nanotube properties. Here we report our recent advances on tuning carbon nanotubes to create an element base in the THz range. By identifying five levels (Figure 1) of nanotube organization [1] ("individual nanotubes" [2, 3], "nanotube agglomerates" [4], "network of agglomerates" [5], "structured assembly" [6, 7], "system of assemblies" [8]), we transform the polyphony of properties of carbon nanotubes to THz create modulators, sensors *etc*.

.

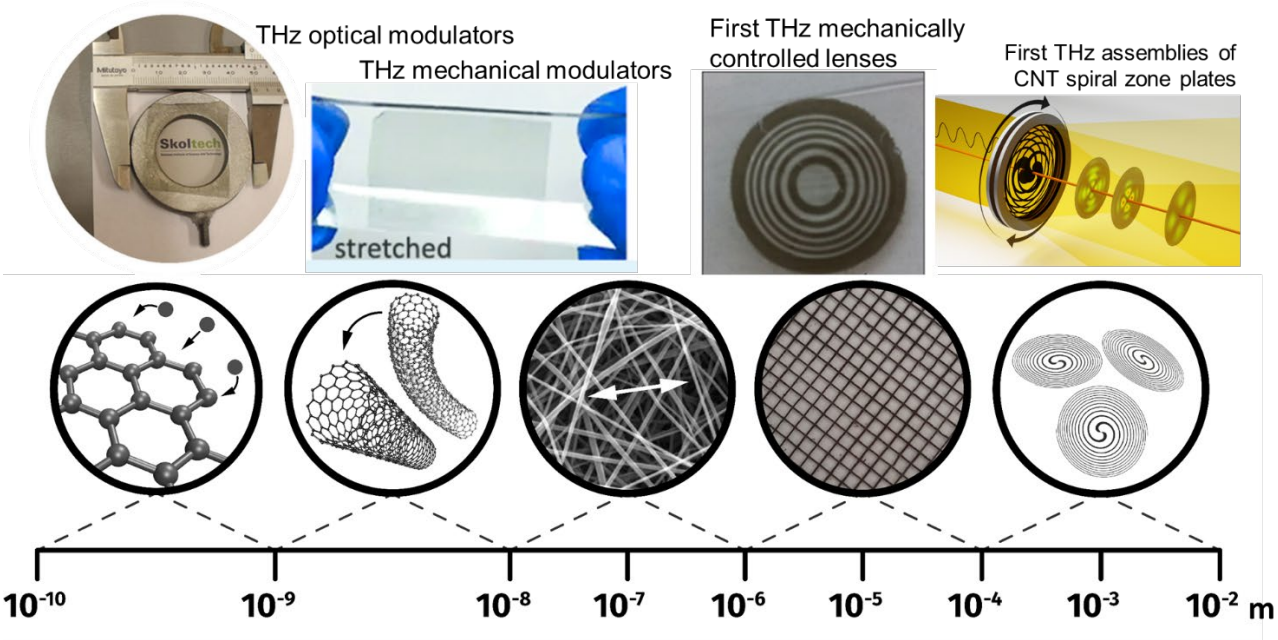

Figure1: Multi-level organization of carbon nanotube films and corresponding THz devices.

References

[1] I.V. Novikov, *et al. Adv. Mat. 2413777, (2025)*
[2] Maria G. Burdanova, *et al.*, *Carbon* **173**, 245-252 (2021).
[3] Daria S. Kopylova *et al.*, *Carbon* **167**, 244-248 (2020).
[4] Novikov I.V., *et al.* (2022). *ACS applied materials and interfaces* 14, 18866–18876
[5] Maksim I. Paukov, *et al. Ultrafast Science* **3**, 1-9 (2023).
[6] G. M. Katyba, *et al. Optica* **10**, 53-61 (2023).
[7] I. V. Novikov, *et al. Chemical Engineering Journal* **485** 149733-149732(2024).
[8] A.V. Radivon, *et al. Advanced Optical Materials*, **12,** 2303282 (2024).

Coupling TiO_2 with Low-Dimensional Materials for Efficient Photocatalytic Oxidation of NOx

Morgen L. Smith, Brian M. Everhart, Ahmed Al Mayyahi, Placidus B. Amama

[1]*Tim Taylor Department of Chemical Engineering, Kansas State University, United States*

To address the limitations of TiO_2 in photocatalysis, we have investigated the modification of TiO_2 using carbon nanotubes (CNTs) and MXene (Ti_3C_2) to form TiO_2-CNT and TiO_2-Ti_3C_2 hybrid photocatalysts. The resulting hybrid photocatalyst films (TiO_2-CNT and TiO_2-Ti_3C_2) were systematically investigated in NOx oxidation under relevant conditions that will enable their implementation as part of a flue gas treatment system, downstream of selective catalytic reduction (SCR) and prior to emission to the atmosphere. Utilizing the De-NOx index, an objective figure of merit for photocatalytic NOx abatement, in tandem with relative NOx oxidation, has provided a deeper understanding of the performance of the novel hybrid photocatalysts. Our results show substantial photocatalytic enhancement of TiO_2 and improved conversion of NO_x to benign products (nitrates) by coupling with CNTs or MXenes. We have investigated the effects of initial concentration, humidity, and reactor headspace on De-NOx for commercial TiO_2 (P25) and TiO_2-based hybrids under practical conditions. Additionally, we have examined, for the first time, the primary mechanism of the oxidation reaction on each hybrid photocatalyst by creating scenarios that hindered different mechanisms. Our results reveal the complex interplay between nanomaterial properties in the hybrid, humidity, and primary mechanistic pathways. This study shows that the NOx degradation mechanism is far more nuanced than assumed for most works and is heavily dependent on the hybrid properties.

References

[1] A. Al Mayyahi et al. *J. Photochem. Photobiol. A: Chem*. **444**, 114965 (2023).
[2] B.M. Everhart et al. *Chem. Eng. J*. **446**, 136984 (2022).
[3] A. Al Mayyahi et al. *J. Phys. Chem. Solids* **170**, 110875 (2022).
[4] A. Al Mayyahi et al. *Mater. Today Comm.* **32**, 103835 (2022).
[5] A. Al Mayyahi et al. *RSC Adv.* **11**, 11702 (2021).
[6] J.O. Ighalo et al. *2D Mater.* **12**, 022001 (2025).
[7] J.O. Ighalo et al. *Appl. Catal. B: Environ. Energy* **358**, 124352 (2024).
[8] D. Austin et al. Adv. Func. Mater. 2310469 (2023).

Continuous Synthesis and Fiber Spinning of Nitrogen-Doped SWCNTs

Zhikai Li[1], Toshihiko Fujimori[1,2], Samuel Jeong[1], Jun-ichi Fujita[1]

[1] Institute of Applied Physics, Graduate School of Pure and Applied Sciences, University of Tsukuba, Tsukuba 305-8573 (Japan), [2] Sumitomo Electric Industries, Ltd, 1-1-3 Shimaya, Konohana-ku, Osaka 554-0024, (Japan).

Nitrogen-doped single-walled carbon nanotubes (N-SWCNTs) enable bandgap modification of semiconducting SWCNTs through the regulation of Fermi level [1]. Specifically, the graphitic nitrogen configuration provides a potential to induce n-type doping in SWCNTs. In addition, the N-doped sites could modify electron transport behavior between intra-fiber nanotube bundles. In our previous work, we reported that N-SWCNTs can be highly dispersed in chlorosulfonic acid (CSA) at concentrations higher than 8 wt%, resulting in the continuous spinning of N-SWCNTs fibers with enhanced electric conductivity. The high dispersibility of N-SWCNTs in CSA originates from the nitrogen substituted sites which facilitate additional protonation centers during dispersion. To address scalability challenges in the production of N-SWCNTs fibers, this study combines controlled N-SWCNTs synthesis via floating-catalyst chemical vapor deposition (FC-CVD) with CSA-based wet-spinning technology. We systematically investigated large-scale synthesis parameters using acetonitrile and pyridine as the nitrogen precursors with methane and ethylene as the carbon sources. In this presentation, we demonstrate that our optimized conditions yield N-SWCNTs (average diameter: 2.4 nm) with 0.75 at% graphitic nitrogen content at production rates exceeding 3.5 mg/min. Continuous fibers spun from 8 wt% N-SWCNTs solution in CSA exhibit the electric conductivity of 3.5 MS/m and tensile strength of 1.4 GPa after the post-annealing process to remove remaining acids. This work establishes a foundation for the scalable production of high-performance N-SWCNTs fibers.

References

[1] Z. K. Li *et al.*, *Applied Physics Express*. **16**, 095001(2023).

Dielectric-assisted transfer using single-crystal antimony oxide for two-dimensional material devices

Junhao Liao[1,3], Yanfeng Zhang[1,2,3*], Li Lin[1,2,3*], Zhongfan Liu[1,3*]

[1]Academy for Advanced Interdisciplinary Studies, Peking University (China), [2]School of Materials Science and Engineering, Peking University (China), [3]Beijing Graphene Institute (China).

By confining the electrons in the two-dimensional (2D) channel, 2D materials have become promising for next-generation electronics. Despite recent breakthroughs in synthesizing single-crystal 2D channel material wafers, critical challenges still exist in the preparation of single-crystal dielectric wafers and reliable methods to integrate dielectric on 2D semiconductors with ultraclean interfaces, sufficiently large gate capacitance, and low leakage current. Here we achieved the epitaxial growth of transferable, ultrathin, single-crystal Sb_2O_3 dielectric wafers on graphene-covered Cu(111) surface, which exhibited a fine gate controllability with equivalent oxide thickness (EOT) of 0.60 nm. The conformal growth of Sb_2O_3 enabled the crack and wrinkle-free transfer of graphene onto application-specific substrates and highly improved graphene device performance across 4-inch wafers with a maximum carrier mobility of 29,000 $cm^2\ V^{-1}\ s^{-1}$ and long-term stability. By minimizing the interfacial traps and defects, the clean interface and single-crystal nature of Sb_2O_3 allow for an on/off ratio of 10^8 and minimum subthreshold swing (SS) of 64 mV dec^{-1} in MoS_2 devices. This study offers a reliable method for growing single-crystal dielectric wafers with outstanding gate capacitance and fabricating wafer-scale 2D material devices with fine device yield and satisfactory performance, which would propel advancements in electronic applications of 2D materials.

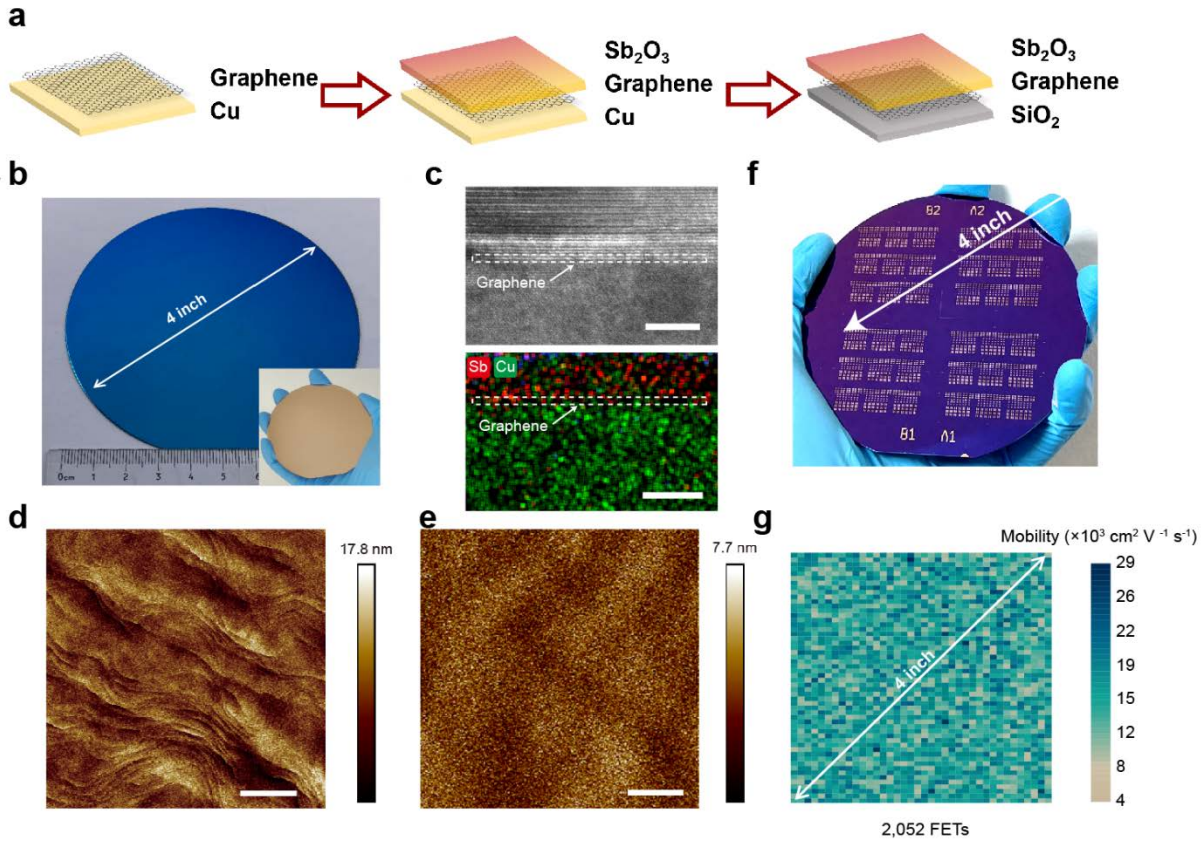

Figure caption: a, Schematic of the graphene transfer process using Sb_2O_3. **b,** Photograph of 4-inch sized graphene wafer transferred onto the SiO_2/Si substrate assisted by Sb_2O_3 films. Inset: Photograph of graphene wafer. **c,** HAADF-STEM cross-section image (top) and related X-ray (EDX) spectroscopy mapping of Sb and Cu elements (bottom) of the as-deposited Sb_2O_3 on graphene covered Cu(111). **d,** AFM image of graphene on Cu(111) after the deposition of Sb_2O_3 films with a thickness of 10 nm. Scale bar, 10 μm. **e,** AFM image of the transferred graphene on SiO_2/Si substrate, after being laminated onto the SiO_2/Si substrates. Scale bar, 10 μm. **f,** Photograph of the graphene FET arrays over an entire 4-inch wafer. **g,** Mapping of the extracted carrier mobilities across the entire wafer.

Graphene Tamed Supercooling in Plastic Crystals

Xinyu Zhang[1,2], Yuanlong Shao[1,3], Jin Zhang[1,3*]

[1]School of Materials Science and Engineering, Peking University, Beijing 100871, China, [2]Academy for Advanced Interdisciplinary Studies, Peking University, Beijing, 100871, China, [3]Beijing Graphene Institute (BGI), Beijing 100095, China

Email: jinzhang@pku.edu.cn

Plastic crystals are characterized by reversible phase transitions between low temperature ordered and high temperature disorder states driven by the rotatable molecule orientational dynamics, which the substantial phase transition energy barriers involved in phase transition result in pronounced supercooling[1,2]. To address this issue, graphene was introduced as a template to promote nucleation by forming a nanoscale ordered layer on its surface. It is demonstrated that a small amount of graphene can significantly reduce supercooling. Tris(hydroxymethyl)-aminomethane to form a transient state comprising a thin ordered layer adhering to the graphene surface. These confined Tris molecules mimic the low-temperature ordered rhombohedral phase, which effectively reduces the rotational freedom and facilitates the ordered molecular layer formation. The graphene additive acts as a heterogeneous nucleation site and structure ordering template to promote nucleation and inhibit supercooling. These findings suggest an efficient strategy that inhibits the phase transition hysteresis in plastic crystals and pave the way to future solid-state thermal regulation technologies

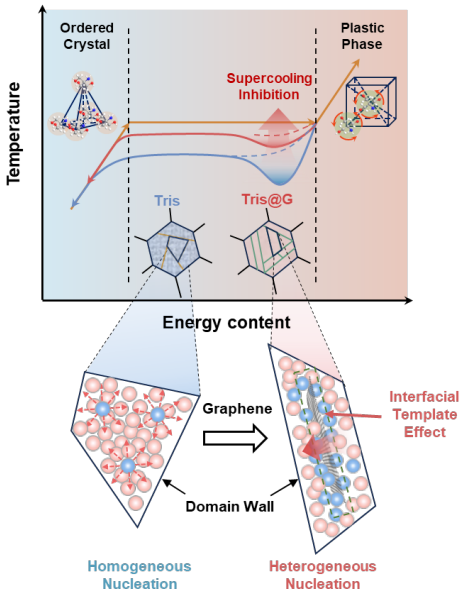

Schematic diagram of the supercooling properties of Tris, Tris@G and graphene-induced changes in the crystal domain structure and nucleation mechanism.

Reference

[1] Matuszek, K., Kar, M., Pringle, J. M. & MacFarlane, D. R. Phase Change Materials for Renewable Energy Storage at Intermediate Temperatures. *Chem. Rev.* **123**, 491-514 (2023).

[2] Das, S., Mondal, A. & Reddy, C. M. Harnessing molecular rotations in plastic crystals: a holistic view for crystal engineering of adaptive soft materials. *Chem. Soc. Rev.* **49**, 8878-8896 (2020).

Nano-seeding method for preparing arrays of horizontally aligned carbon nanotube wafers

Y. Xie,[1 §] Y. Li,[1 §] Z.S. Peng,[1 §] L. Qian,[1 *] Z.Q. Zhao,[1 *] J. Zhang[1 *]

[1] *Peking University, Beijing, 100871, China.*

[§]*These authors contributed equally to this work: Ying Xie, Yue Li and Zhisheng Peng.*
[*]*E-mail: jinzhang@pku.edu.cn; zqzhao@pku.edu.cn; qianliu-cnc@pku.edu.cn*

In the realm of modern materials science, horizontally aligned carbon nanotube arrays (HACNT arrays) stand as promising materials for the development of next-generation integrated circuits. However, their large-scale integration has been impeded by the constraints of current fabrication techniques, which struggle to achieve the necessary uniformity, density, semiconducting purity and size control of HACNT arrays. Overcoming this challenge necessitates a significant shift in fabrication approaches. Herein, we present a nano-seeding method that not only revolutionized the preparation of catalyst nanoparticles for growing high-density HACNT arrays, but also functionalized the substrate for regulating semiconducting purity of HACNT arrays. By implantation of metal ions, uniform catalyst nanoparticles were formed in situ, and catalyzed the growth of one-inch HACNT-array wafers with the highest density of 140 tubes μm^{-1}. The high density and uniformity of the as-prepared HACNT-array wafers are validated through an advanced high-throughput characterization technique. By further combined implantation with oxygen ions, etchants were released synergistically with catalyst nanoparticles, and enriched the growth of semiconducting HACNT arrays effectively. The electrical properties of high on-state current, high on/off ratio and low subthreshold swing are demonstrated in field-effect transistors based on the arrays. This study shows the potential in customized synthesis of HACNT arrays, and propels the scalability of carbon-nanotube-array fabrication for future carbon-based electronics.

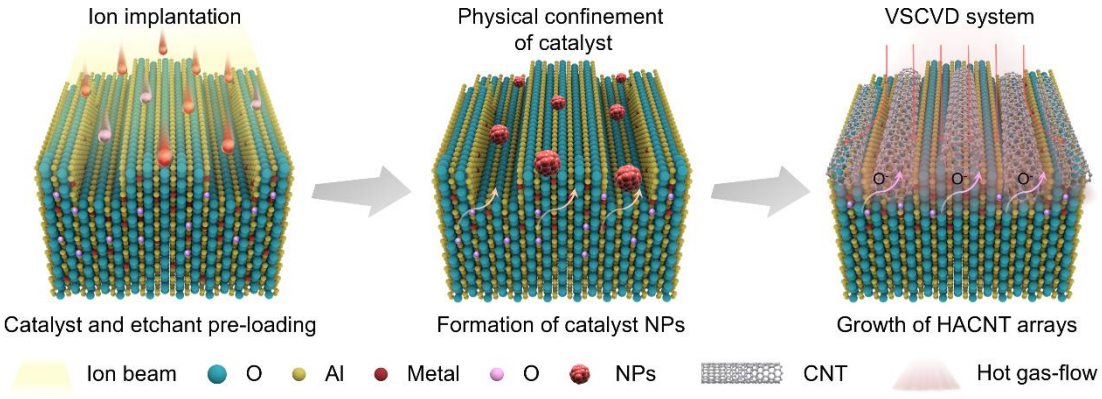

Growth of HACNT arrays through the nano-seeding method: Schematic of the nano-seeding method: the precise loading of catalyst and etchant precursors by ion implantation, the physical confining of catalyst nanoparticles by substrate processing and the controlled growth of HACNT arrays by VSCVD system.

Direct Crystallization of one-dimensional Van der Waals Semiconductor WTe_2 Nanowires via Chemical Vapor Transport

Hang Wang[1], Tianyu Wang[1], Yongjia Zheng[1], Shanhe Xue[3], Abid[1], Yige Zheng[1], Qingyun Lin[2], Afzal Khan[1], Qi Zhang[3] and Rong Xiang[1*]*

[1]*Affiliated Institution1State Key Laboratory of Fluid Power and Mechatronic System, School of Mechanical Engineering, Zhejiang University, Hangzhou 310027, (China)*

[2]*Center for Advanced Optoelectronic Materials, College of Materials and Environmental Engineering, Hangzhou Dianzi University (HDU), Hangzhou 310018, (China)*

[3]*Center of Electron Microscopy, State Key Laboratory of Silicon and Advanced Semiconductor Materials, School of Materials Science and Engineering, Zhejiang University, Hangzhou, 310027, (China)*

Abstract

The rediscovery of one-dimensional (1D) and quasi-1D (q-1D) van der Waals (vdW) crystals ushered the realization of nascent physical properties in 1D that are suitable for applications in photonics, electronics, and sensing.[1-3] However, despite renewed interest in the creation and understanding of the physical properties of 1D and q-1D vdW crystals, the lack of accessible synthetic pathways for growing well-defined nanostructures that accurately controlled number of layers.[4-5] Using the highly anisotropic 1D vdW WTe_2 crystal as a model phase, we present a catalyst-free and bottom-up synthetic approach to access different diameter WTe_2 nanowires, with uniform thicknesses ranging from 2 to 20 nm between individual nanowires. Control over the synthetic parameters enabled the modulation of controlled WTe_2 nanowires. These nanowires exhibit an anisotropic 1D optical response and SHG properties. Additionally, through a specially designed oxide heterostructure the fi ndings not only shed light on the suppression of photoexcitation conductivity but also provide a platform for the study on physics and device applications of nanowire-based 2D and 3D crystals.

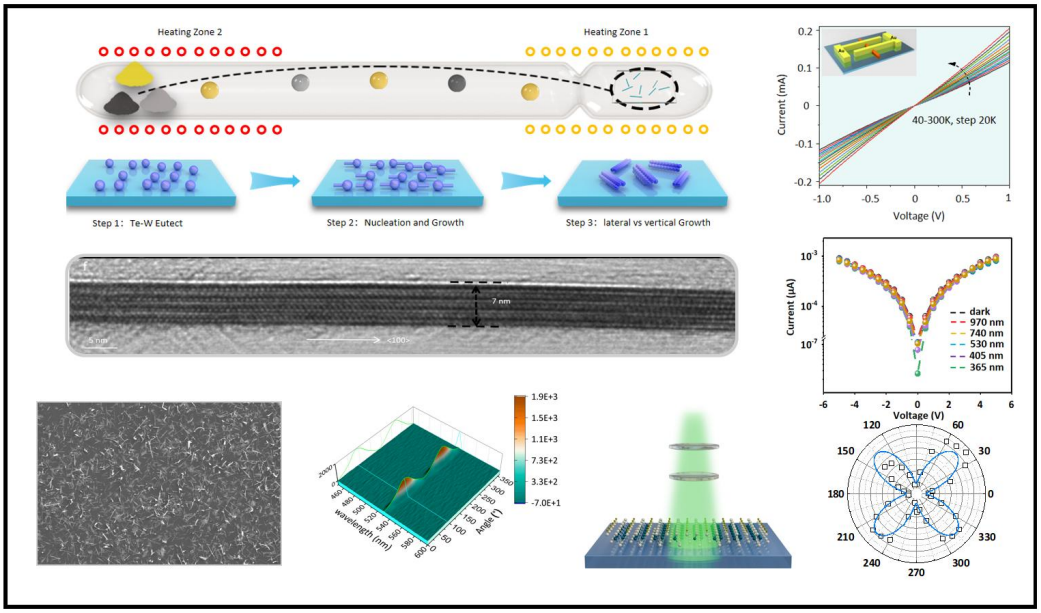

Figure caption: We propose a chemical vapor transport (CVT) synthesis route to produce 1D WTe_2 vdW crystals with diameters ranging from 2 to 20 nm, exhibiting an anisotropic 1D optical response. We also give rise to a negative photoconductive effect, resulting in two different transport properties in the temperature range of 40-300K.

References

[1] Q. Zhang et al., *ACS Nano*. **12 (3),** 2634-2642 (2018).
[2] S. Meyer et al., *Physical Review B*. **100,** 041403 (2019).
[3] M. Nagata et al., Nano Letters. **19,** 4845-4851 (2019).
[4] T. Pham rt al., Science. **361,** 262-264(2018).
[5] Z. Liu et al., The Journal of Physical Chemistry C. **125,** 12730-12737 (2021).

Janus MoSSe nanotubes on one-dimensional SWCNT-BNNT van der Waals heterostructures

Chunxia Yang[1,2], Qingyun Lin[2], Yuta Sato[3], Yanlin Gao[4], Yongjia Zheng[2], Tianyu Wang[2], Yicheng Ma[2], Wanyu Dai[1], Wenbin Li[5], Mina Maruyama[4], Susumu Okada[4], Kazu Suenaga[6], Shigeo Maruyama[1,2*], Rong Xiang[2*]

[1] The University of Tokyo, (Japan), [2] Zhejiang University, (China), [3] National Institute of Advanced Industrial Science and Technology (AIST), (Japan),[4] University of Tsukuba, (Japan), [5] Westlake University, (China), [6] Osaka University, (Japan)

Two-dimensional (2D) Janus TMDC layers with broken mirror symmetry exhibit giant Rashba splitting and unique excitonic behavior. For their one-dimensional (1D) counterparts, the Janus nanotubes possess curvature, which introduce an additional degree of freedom to break the structural symmetry. This could potentially enhance these effects or even give rise to novel properties [1-3]. Moreover, Janus MSSe nanotubes (M=W, Mo), with diameters surpassing 40 Å and Se positioned externally consistently demonstrate lower energy states compared to their Janus monolayer counterparts [4]. However, there have been limited studies on the preparation of Janus nanotubes, due to the synthesis challenge and limited sample quality. In this study, we first synthesize MoS_2 nanotubes based on single-walled carbon nanotubes and boron nitride nanotube (SWCNT-BNNT) heterostructure and then explore the growth of Janus MoSSe nanotubes from MoS_2 nanotubes at room temperature with the assistance of H_2 plasma. The successful formation of the Janus structure is confirmed by Raman spectroscopy, and microscopic morphology and elemental distribution of the grown samples were further characterized [5]. The synthesis of Janus MoSSe nanotubes based on SWCNT-BNNT heterostructure paves the way for further exploration of novel properties in Janus TMDC nanotubes.

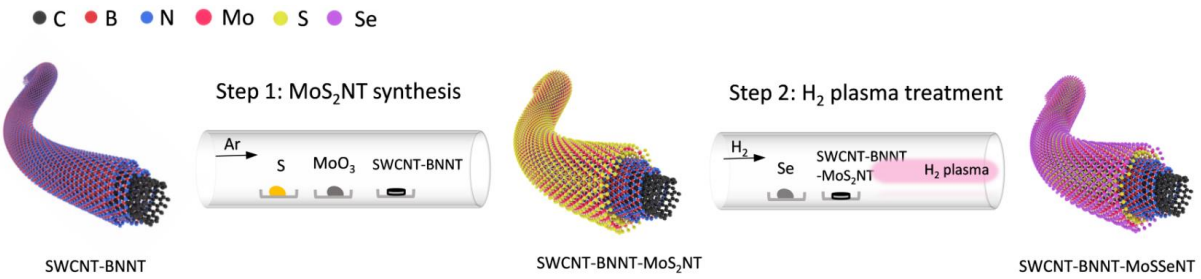

Figure 1: Schematic illustration of the fabrication process of Janus MoSSe nanotubes based on 1D SWCNT-BNNT heterostructures.

References

[1] R. Xiang *et al.*, *Natl Sci Open*, **1**, 20220016 (2022).
[2] N. T. Hung *et al.*, *ACS Nano*, **17** 19877 (2023).
[3] B. Cai *et al.*, *Phys. Rev. B*, **108** 045416 (2023).
[4] R. A. Evarestov *et al.*, *Physica E*, **115** 113681 (2020).
[5] C. Yang *et al.*, *Small*, in press.

A Simple Equipment-Free Method for Length Sorting of Carbon Nanotubes

Xiaojun Wei[1,2,*], Shuang Ling[1,3], Xin Luo[1], Xiao Li[1,2], Feibing Xiong[3], Weiya Zhou[1,2], Sishen Xie[1,2], and Huaping Liu[1,2,*]

[1] *Beijing National Laboratory for Condensed Matter Physics, Institute of Physics, Chinese Academy of Sciences, Beijing 100190, China*

[2] *Department of Physics and Center of Materials Science and Optoelectronics Engineering, University of Chinese Academy of Sciences, Beijing 100049, China*

[3] *Department of Optoelectronic, Xiamen University of Technology, Xiamen, Fujian 361024, China*

Corresponding authors: weixiaojun@iphy.ac.cn; liuhuaping@iphy.ac.cn

As-grown single-wall carbon nanotubes (SWCNTs) usually exist in the form of bundles due to strong van der Waals interactions. Therefore, an additional sonication treatment is widely used to prepare efficiently dispersed SWCNT dispersion for their further purification and application. Unfortunately, the vigorous external force generated by sonication inevitably introduces defects on the surface of SWCNTs and then results nanotube length shortening, degrading their inherent properties. How to extract the long SWCNTs with excellent optoelectronic properties from SWCNT dispersion is critical for enabling their application in high-performance optoelectronic devices [1].

In this work, we show a simple, high-efficiency, and equipment-free method for length separation of SWCNTs. Only by modulating the concentrations of binary surfactants in SWCNT solution, the long SWCNTs can spontaneously precipitate [2]. This effect is attributed to the formation of compound micelles by binary surfactants that squeeze the free space of long SWCNTs due to their large excluded volumes. Interestingly, the precipitated SWCNTs are redispersible upon shaking vessels by hand without additional sonication treatment. With this technique, it can readily separate near-pure long (⩾500 nm in length, 99% in content) and short (⩽500 nm in length, 98% in content) SWCNTs with separation efficiencies of 26% and 64%, respectively, exhibiting markedly greater length resolution and separation efficiency than those of previously reported methods (including size exclusion chromatography [3]). Thin-film transistors fabricated from extracted semiconducting SWCNTs with lengths >500 nm exhibit significantly improved electrical properties, including a 10.5-fold on-state current and 14.7-fold mobility, compared with those with lengths <500 nm. The present length separation technique is perfectly compatible with various surfactant-based methods for structure separations of SWCNTs and is significant for fabrication of high-performance electronic and optoelectronic devices.

References

[1] X. Wei *et al.*, *Adv. Sci.* **9**, 2200054 (2022).

[2] S. Ling, X. Wei *et al*., *Small* **20**, 2400303 (2024). (Front Cover)

[3] X. Wei *et al.*, *ACS Nano* **17**, 8393-8402 (2023).

In-Situ Observation of Vapor-Liquid-Solid Growth of WS_2 in a Substrate-Stacked Microreactor for Mechanistic Investigation

Hiroo Suzuki[1], Yutaro Senda[1], Yuta Takahashi[2], Shun Fujii[2], Yasuhiko Hayashi[1]

[1]*Life, Natural Science and Technology, Institute of Academic and Research, Okayama University (Japan),*

[2]*Department of Physics, Faculty of Science and Technology, Keio University (Japan)*

Transition metal dichalcogenides (TMDCs), a class of two-dimensional semiconducting materials, have attracted attention for optoelectronic device applications due to their high flexibility, strong light absorption, and high emission coefficient with a direct bandgap. The growth of high-quality TMDC crystals is crucial for realizing their various applications. We have previously reported the chemical vapor deposition (CVD) growth of monolayer WS_2 based on the vapor-liquid-solid (VLS) method using metal salts in a microreactor constructed with two stacked growth substrates [1]. Using this method, we have successfully grown extremely large WS_2 crystals, up to ~1100 μm in size. The growth mechanism of monolayer WS_2 has been investigated based on the energetic estimation of the rate-limiting step. We found that the growth mechanism is governed by a surface diffusion-limited process of sulfur atoms in the confined space. However, the detailed mechanism of the VLS growth process in the microreactor remains unclear.

In-situ observation of crystal growth is a powerful technique for investigating growth mechanisms. In this study, we constructed a CVD system equipped with an *in-situ* optical observation setup using a microscope. A substrate-stacked microreactor was configured using a bottom SiO_2/Si substrate and a top transparent sapphire substrate, allowing direct observation of the microreactor's interior. Using this system, we successfully achieved direct observation of the VLS growth of monolayer WS_2 in the substrate-stacked microreactor. We observed a liquid-state molten intermediate at the edge of epitaxially growing WS_2. Furthermore, we identified an abnormal growth behavior—ribbon-shaped growth—under sulfur-rich conditions. Under alkali metal oxide-rich conditions, both particle-driven ribbon-shaped growth and continuous film growth were observed. To gain deeper insights into the crystal growth regimes, we investigated the influence of molten liquid dynamics by combining the *in-situ* observation with elemental and thermal analysis. We analyzed the crystal properties using optical measurements such as photoluminescence and second-harmonic generation, which provide insights into crystallinity and crystal orientation. Furthermore, we examined the influence of WS_2 crystallinity, grown under various conditions, on these optical properties.

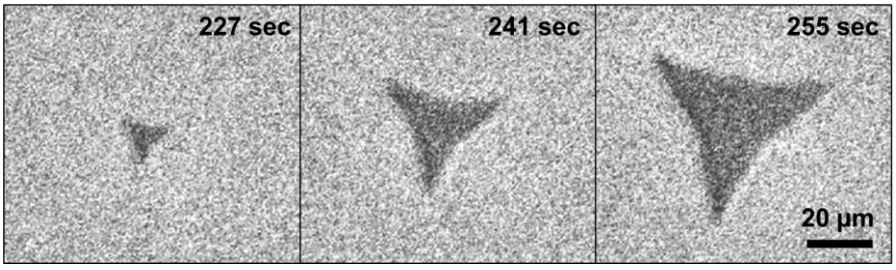

Figure 1: Time-series micrographs of monolayer WS_2 captured during *in-situ* observation.

Reference

[1] H. Suzuki *et al*., *ACS Nano* **16**, 11360 (2022).

Tailoring Oxidation States for Selective CVD Growth of Boron Nitride Nanotubes on Supported Catalysts

Chunghun Kim[1], Myung Jong Kim[1*]

[1]*Gachon University,1342 Seongnam-daero, Sujeong-gu, Seongnam-si, Gyeonggi-do 13120, Republic of Korea.*

**myungjongkim@gachon.ac.kr*

Carbon nanotubes have been commercialized via chemical vapor deposition using supported catalysts for large-scale production, yet supported catalyst-based synthesis of boron nitride nanotubes remains largely unexplored. Here, a Ni-Pd alloy supported on magnesium oxide enabled selective growth of highly crystalline BNNTs and MgO-BN core/shell nanowires at 1100°C. The MgO-BN nanowires, exceeding 50 micrometers in length, can be converted into BNNTs via simple acid treatment and annealing or directly utilized due to their enhanced oxidation resistance. Transmission electron microscopy and density functional theory analyses revealed a tip-growth mechanism driven by a reduced eutectic point, quasi-liquid catalyst deformation, and strong interactions with boron nitride. This tailored catalyst design provides a viable route for the low-temperature mass production of BNNTs, expanding their potential applications in high-temperature environments and advanced composites [1].

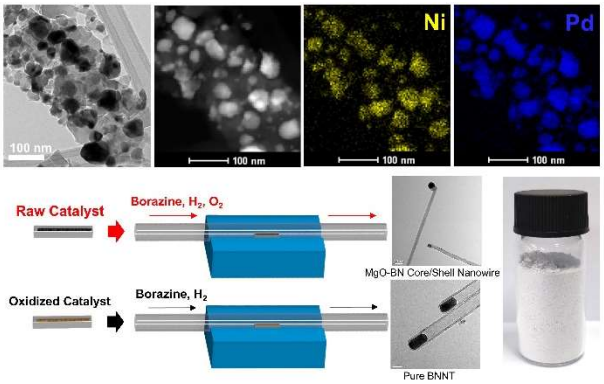

Figure: Structural and compositional analysis of Ni-Pd (MgO) catalysts and their oxidation state-controlled selective CVD synthesis of BNNTs and MgO-BN core/shell nanowires.

References

[1] C. Kim *et al. Selective CVD Growth of Boron Nitride Nanotubes via Oxidation Control of Supported Catalysts.* submitted.

Interlocking of SWNTs with Metal-Tethered Tetragonal Nanobrackets to Enrich a Few Hundredths of Nanometer Range in Their Diameters

G. Cheng[1], T. Hayashi[2], H. Tabata[3], M. Katayama[3], N. Komatsu[4]

[1]Suzhou Institute of Nano-Tech and Nano-Bionics, Chinese Academy of Sciences (China), [2]Shinshu University (Japan), [3]Osaka University (Japan), [4]Kyoto University (Japan)

We have separated CNTs through host-guest complexation using host molecules named “nanotweezers” and “nanocalipers” [1]. In this work, a new host molecule named tetragonal “M-nanobrackets”, consisting of a pair of dipyrrin nanocalipers corresponding to two square brackets “[” and “]” tethered by two metals (M), is designed, synthesized and employed for separating SWNTs (Figure 1a) [2]. Three-step facile process, including one-pot Suzuki coupling, from a carbazole derivatives gave M-nanobrackets in 37% total yield (M = Cu). Upon extraction of SWNTs in the presence of the square nanobracket and Cu(II), *in situ* formed tetragonal M-nanobrackets is found to interlock SWNTs to disperse in 2-propanol. After concentrating the extract, the residual extracted SWNTs was washed several times with dichloromethane to remove the host molecules weakly bound to the SWNT surface. The resulting interlocked SWNTs (i-SWNTs) were demetallized with dithiothreitol in dichloromethane, giving pristine SWNTs (p-SWNTs) as solid and the square nanobracket in the washings (Figure 1a). The interlocking is confirmed mainly by TEM observation (Figure 1b) and Raman spectra (Figure 1c). While Cu-nanobrackets are found to show inherent resonance Raman signals (green trace in Figure 1c), similar signals remain in i-SWNTs (blue trace) and disappear in p-SWNTs (red trace), supporting the interlocking structure. The facile unlocking enables precise evaluation of the diameter selectivity to SWNTs by Raman, photoluminescence and absorption spectroscopies, revealing the diameter enrichment of only three kinds of SWNTs, (7,6), (9,4) and (8,5), in the 0.02 nm diameter range from 0.90 nm to 0.92 nm among ~20 kinds of SWNTs from 0.76 nm to 1.17 nm in their diameter range.

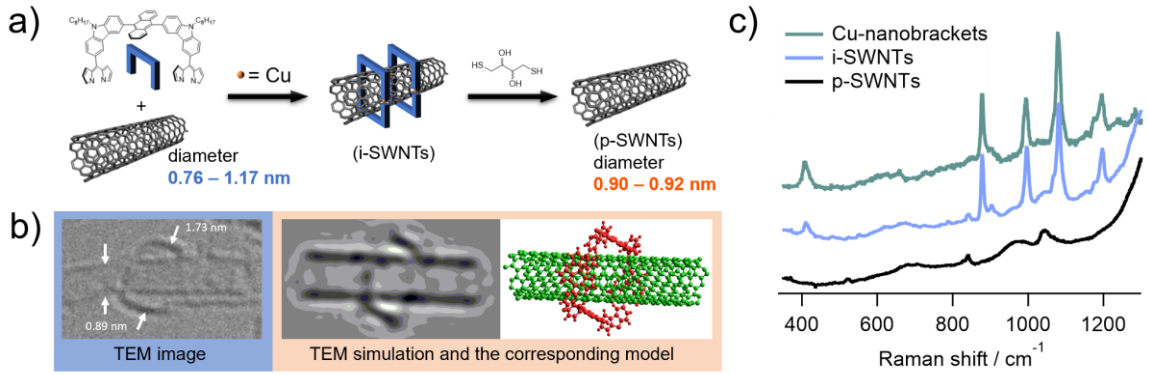

Figure 1: a) Extraction of SWNTs with Cu-nanobrackets and their removal with dithiothreitol; b) TEM image of the mechanically interlocked SWNT, TEM simulation and computer generated model; c) Raman spectra of Cu-nanobrackets, i-SWNTs and p-SWNTs (λ_{ex} = 488 nm). Raman intensities of all SWNTs are normalized at the G-band.

References

[1] G. Liu, N. Komatsu, *et al. J. Am. Chem. Soc.*, **135**, 4805 (2013); *J. Mater. Chem. A*, **2**, 19067 (2014); *Org. Chem. Front.*, **4**, 911 (2017).

[2] G. Cheng, T. Hayashi, Y. Miyake, T. Sato, H. Tabata, M. Katayama, N. Komatsu *ACS Nano*, **16**, 12500 (2022).

Novel BNNT-Tungsten Oxide Hybrid Structures for Enhanced Energy Storage Applications

Honggu Kim[1], Chandan Kumar Maity[1], Myung Jong Kim[1] *

Department of Chemistry, Gachon University Global Campus (South Korea)

**myungjongkim@gachon.ac.kr*

This research introduces a breakthrough approach for energy storage materials by demonstrating precise selective attachment of tungsten oxide both inside and on the surface of boron nitride nanotubes (BNNT). Our innovative synthesis methodology represents a significant advancement, enabling unprecedented control over the placement of functional materials—either as internal filling or external coating—creating customized hybrid nanoarchitectures with location-specific properties. This selective attachment capability proves critical, as our comprehensive characterization reveals distinct performance advantages from each configuration: interior tungsten oxide filling dramatically enhances long-term stability, while exterior tungsten oxide coating maximizes capacitive performance. The BNNT framework serves dual roles as both an electrolyte transport channel and tungsten oxide stabilizer, with the spatial relationship between components directly influencing electrochemical behavior. The tungsten oxide-coated BNNT configuration offers impressive specific capacitance along with improved energy density, while the tungsten oxide-filled BNNTs exhibit superior cycling durability compared to surface-coated BNNTs. These findings highlight how precise control over material placement within and upon BNNT structures enables tailored performance characteristics, offering a versatile platform for next-generation energy storage system development with customizable property profiles.

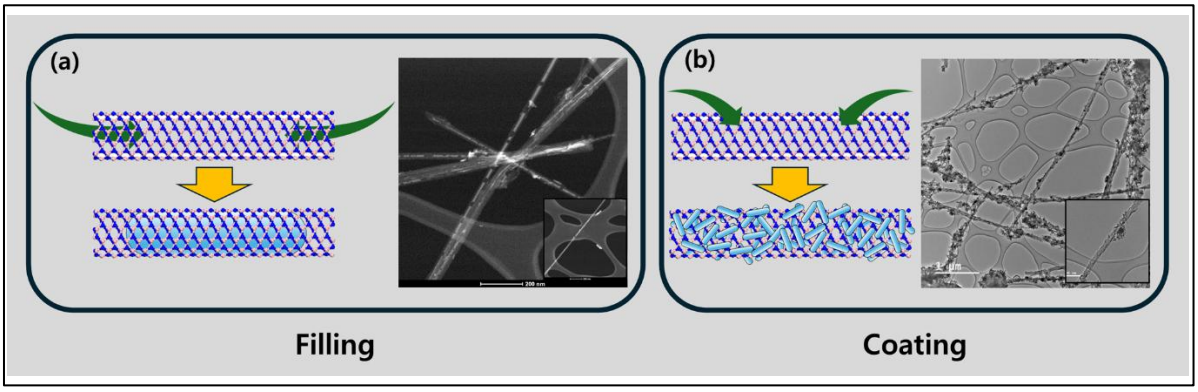

Figure. 1 (a) Schematic diagram of the BNNT filling process and TEM image of a sample in which BNNTs were filled with tungsten oxide. (b) Schematic diagram of the coating process and TEM image of a sample in which BNNTs were coated with tungsten oxide.

References

[1] Kim, Honggu, et al. "Alternative inner filling and outer surface coating of BNNT by Tungsten (VI) oxide for supercapacitor electrode." Composites Part B: Engineering 279 (2024): 111436.

Reductive functionalization and purification of single-walled carbon nanotubes for controlling near-infrared photoluminescence properties

Y. Maeda[1], K. Kawada,[1] A. Suwa,[1] Y. Iguchi[1], Y. Suzuki,[1] Y. Konno[1], M. Yamada[1], P. Zhao, M. Ehara

[1]*Department of Chemistry, Tokyo Gakugei University (Japan)*

[2]*Research Center for Computational Science, Institute for Molecular Science (Japan)*

The functionalization of single-walled carbon nanotubes (SWCNTs) has received considerable attention in the last decade since high-efficiency near-infrared photoluminescence (PL) has been observed red-shifted compared with the intrinsic PL peak of pristine SWCNTs. The PL wavelength has been manipulated using arylation reactions with aryldiazonium salts and aryl halides.[1] Additionally, oxidation and alkylation reactions are also effective in adjusting the PL wavelength extensively, with the resulting PL efficiency varying based on the chosen reaction techniques and molecular structures.[2] In this presentation will discuss the relationship between the reaction reagents and PL wavelength emerged by the reductive functionalization.[3-7]

The functionalized SWCNT was synthesized using sodium naphthalenide and bromoalkane, dibromoalkane, or iodobenzene in tetrahydrofuran. The reaction mixture was washed by filtration and dispersed in 1 wt% sodium cholate solution of D_2O for optical characterization. Two new PL paeks were observed from (6,5) SWCNT upon functionalization with bromoalkane or iodobenzene. As a control experiment, the optical properties of the product obtained by the two-step reaction using butyllithium were also evaluated. On the other hand, single PL peak around 1230 nm emerged from (6,5) SWCNT by functionalization with dibromoalkanes depending on the alkyl chain length. The PL wavelengths were significantly shifted to the longer wavelength region by replacing the hydrogen atoms on the alkyl chain to fluorine atoms. These adducts were separated by gel chromatography depending on their chiral index, and the PL properties of SWCNTs with different chiral indices were evaluated. The relationship between PL characteristics and structure of SWCNT adducts was considered through theoretical calculations using model compounds.

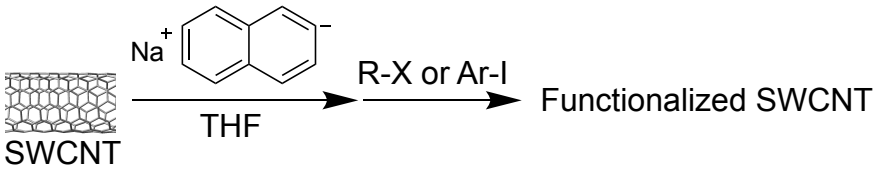

References

[1] A. H. Brozena *et al.*, *Nat. Rev. Chem.*, **3**, 375-392 (2019).
[2] Y. Maeda *et al.*, *Chem. Commun.* **59**, 14497-14508 (2023).
[3] Y. Maeda *et al.*, *Commun. Chem.* **6**, 159 (2023).
[4] Y. Maeda *et al.*, *J. Phys. Chem. C* **127**, 2360-2370 (2023).
[5] Y. Maeda *et al.*, *Chem. Commun.* **59**, 11648-11651 (2023).
[6] Konno, Y *et al.*, *Chem. Eur. J.* **29**, e202301766 (2023).
[7] Konno, Y *et al.*, *Chem. Eur. J.* **29**, e202300766 (2023).
[8] Y. Maeda *et al.*, *Chem. Eur. J.* **31**, e202401111 (2025).

Divide and Functionalize: Sorting and Brightening of Single-Walled Carbon Nanotubes

D. Just[1], P. Taborowska[1], A. Dzienia[1], D. Janas[1]

[1]*Silesian University of Technology (Poland)*

There is a pressing need to develop methods for producing pure SWCNTs in high concentrations with notably improved PLQYs to facilitate their broad application in real-world scenarios. Exciton engineering via mild covalent functionalization of SWCNTs currently stands out as the most promising approach for enhancing their optical properties [1-3]. However, diazonium chemistry, a commonly utilized method for chemically modifying SWCNTs, has several limitations, including unstable reactants and extensive processing times without external stimulation. Furthermore, this grafting technique is essentially limited to aqueous environments unless the solubility of diazonium salts is improved with certain chemical agents [4]. Other modification strategies also exhibit considerable restrictions.

This study illustrates how we can overcome these constraints, achieving both long-desired objectives previously outlined. By incorporating PFO-BPy as a self-synthesized selective extractor for SWCNTs and utilizing dual-function additives in a liquid medium, we significantly enhanced the sorting capacity of SWCNTs, resulting in highly concentrated and well-modified monochiral SWCNTs. The innovative functionalization platform enabled quick attachment of various functional groups to the SWCNTs, thus precisely tuning their emission properties. Notably, the approach discussed proved to be versatile, allowing for the rapid production of chemically modified pure SWCNTs, whether in aqueous or organic environments. The new protocol's simplicity and efficiency make it highly beneficial for optimizing the luminescence of SWCNTs for various applications [5].

Interestingly, this contribution reveals the previously unrecognized role of solvents and dispersants (used for SWCNT solubilization) in the process of generation of luminescent defects on the surface of SWCNTs [6,7].

The authors would like to acknowledge the support of the National Science Centre, Poland (under the OPUS and SONATA programs, Grant agreements UMO-2019/33/B/ST5/00631 and UMO-2020/39/D/ST5/00285)

References

[1] D. Janas, *Mater. Horiz.* **2020**, 7, 2860-2881.
[2] J. Zaumseil, *Adv. Optical Mater.* **2022**, 10, 2101576.
[3] T. Shiraki et al., *Acc. Chem. Res.* **2020**, 53, 1846-1859.
[4] F. Berger et al., *ACS Nano* **2019**, 13, 9259-9269.
[5] D. Just et al., *Adv. Optical. Mater.*, in revision.
[6] P. Taborowska et al., *Chem. Sci.* **2025**, 16, 1374-1389.
[7] D. Just et al., in preparation.

Ultra clean (6,5) SWCNT film with perfect vdW spacing and its 1D heterostructures

Lingfeng Wang[1], Yicheng Ma[1], Zhirui Liu[2], Yongjia Zheng[1], Tianyu Wang[1],
Yuhei Miyauchi[2], Rong Xiang[1]

[1] *School of Mechanical Engineering, Zhejiang University, Hangzhou 310003, China*

[2]*Institute of Advanced Energy, Kyoto University, Uji, Kyoto 611-0011, Japan*

Semiconducting (s-) SWCNTs play a critical role in next-generation electronic devices. In particular, application of high-purity s-SWCNTs in thin-film transistors (TFTs) has attracted widespread interest which motivated a number of sorting techniques. Among various sorting techniques, conjugated polymer wrapping is regarded as one of the most effective ways for isolating pure semiconducting SWCNTs. However, the residual polymer, whether wrapping around the s-SWCNTs or remaining in the solution, can significantly affect the properties of the s-SWCNTs and ultimately degrade the performance of the s-SWCNTs devices [1-3].

In this work, we optimize the process of the s-SWCNTs film cleaning and obtain a high- quality s-SWCNTs film with ultra clean individual s-SWCNT. We use PFO-BPy combined with tip-sonication to sort high-purity (6,5) SWCNTs. Rather than moving impurities in solution, we transfer the film to the substrate firstly to avoid aggregation of clean s-SWCNTs. $Re(CO)_5Cl$ is utilized as a removal agent for PFO-BPy, where selective chelation with the BPy unit in the copolymer results in the unwrapping of PFO-BPy. By subsequent annealing and polar solution cleaning treatment, the quality of the film has been substantially improved. TEM images directly demonstrate the quality of both individual SWCNT and the entire film. The perfect van der Waals spacing observed in ultra-clean SWCNTs further substantiates their cleanliness. Additionally, we use the obtained film to grow SWCNT@BN heterostructure. Clean film template can also enable the growth of high quality one-dimensional (1D) van der Waals (vdW) heterostructures[4]. Furthermore, we fabricate thin film transistors respectively, using pre-cleaning, post-cleaning and post-BN growth film. These films exhibit markedly different electrical properties, highlighting the need for improved s-SWCNTs film quality to meet the requirements of next-generation thin-film transistors applications.

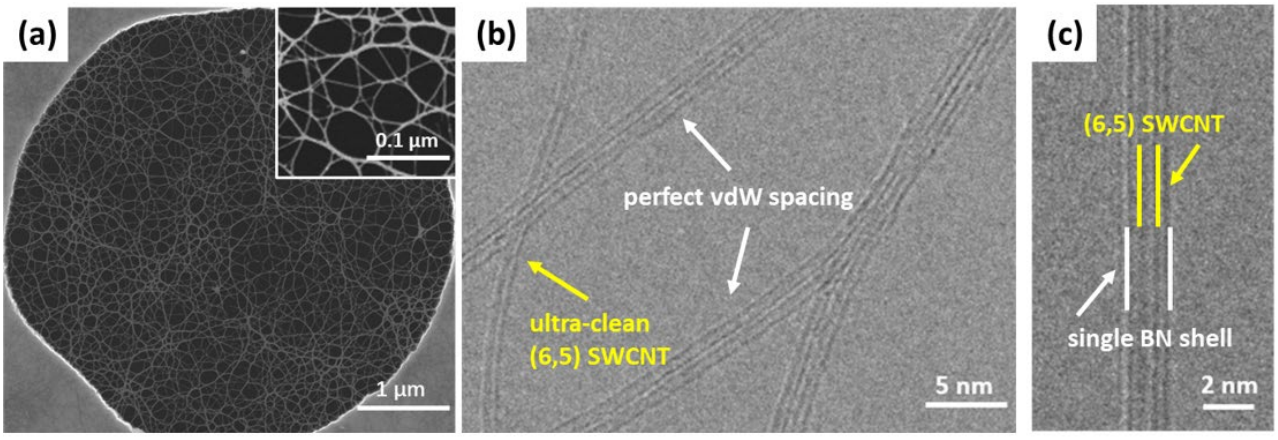

Figure.1 (a) SEM image of clean (6,5) SWNCT thin film. (b)TEM image shows ultra clean individual (6,5) SWCNT and (6,5) SWCNT with perfect vdW spacing. (c)TEM image of high quality SWCNT@BN 1D vdW heterostructure.

References

[1] A. Nish et al., Nat. Nanotechnol. 2, 640 (2007).
[2] Y. Joo et al., ACS Nano 9, 10203 (2015).
[3] S. Qiu et al., Adv. Mater. 31, 1800750 (2019).
[4] R. Xiang et al., Science 367, 537 (2020).

Metal chloride-intercalated pnictogens. Unexplored field full of possibilities

C. Madrona[1], G. Abellán[1]

[1]*ICMol – Universidad de Valencia (Spain)*

In this work, we present the intercalation of the antimony layered pnictogen (group XV) with a metal chloride (MC) for the very first time. In the formed intercalation compound (IC), the intercalate is distributed across the entire material, as demonstrated by XRD through the disappearance of the interlayer (003) Sb peak, and the asymmetric shape of the in-plane ones.

When compared to their graphite analogues, this also layered MC-Sb IC is far more stable in terms of intercalate retention due to the formation of Lewis acid-base adducts between the empty p orbital of the MC Lewis acid and the lone pair of electrons present at the pnictogens. The importance of the acidic strength of the MC with respect to bonding and diffusion of intercalate will be discussed.

The appearance of a new peak at 529 eV in X-ray photoelectron spectrum (XPS) of the Sb 3d orbital proves the bonding between Sb and MC (see figure below). Furthermore, and to our surprise, this MC removes most of the surface oxide layer present in the as-received Sb powder (important for applications such as battery anodes, due to the inactivity of the oxide) and decreases the oxidation rate of the otherwise highly reactive antimony.

Our results provide a glimpse into the very first steps of a new family of intercalation compounds, with a distinct behavior as compared to its graphite analogues. Whether the large MCs can somehow ‘isolate’ the Sb layers (as in GICs) [1] so that they behave as functionalized 2D structures remains unexplored.

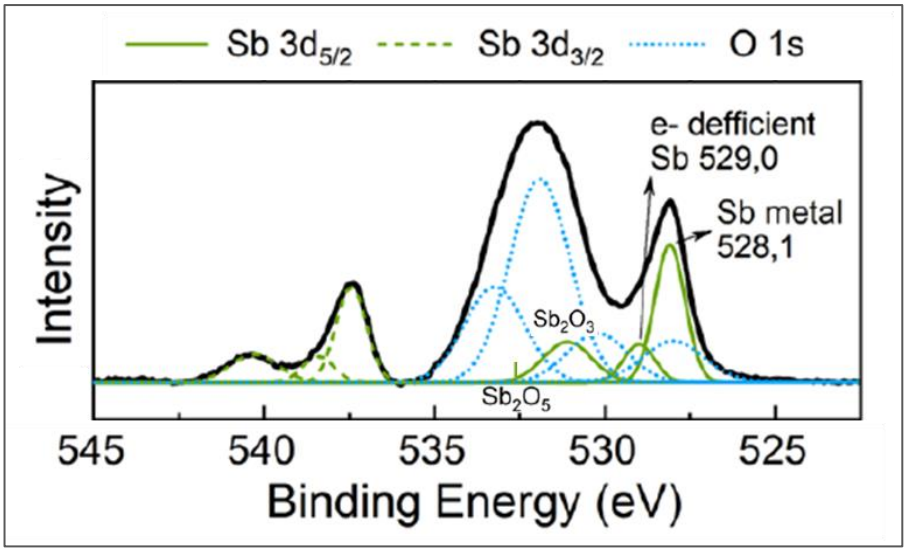

Figure caption: XPS of the MC-Sb IC showing the appearance of a new peak at the Sb 3d orbital. Its occurrence at larger binding energy respect to pure Sb metal is in accordance with the pulling of valence electrons by the MC acceptor.

References

[1] Dresselhaus, M. S. (1987). Intercalation in layered materials. *MRS Bulletin*, *12*, 24-28.

TERPYRIDINE-FUNCTIONALIZED SINGLE-WALLED CARBON NANOTUBES AS SELECTIVE ELECTROCATALYST

Ioanna K. Sideri,[1] and Nikos Tagmatarchis[1]

[1]*National Hellenic Research Foundation, Theoretical and Physical Chemistry Institute (Greece)*

Single-walled carbon nanotubes (SWCNTs) have been extensively utilized as electrocatalysts due to their mechanical strength and electronic properties, despite lacking inherent catalytic centers.[1] The current scientific focus aims in enhancing their catalytic activity through their modification with organometallic chelate complexes, particularly terpyridine ligands, for controlled molecular-level structuring and improved performance in Proton Exchange Membrane Fuel Cells (PEMFCs) applications.[2] The in-depth mechanistic study of the electrocatalytic reactions involved in PEMFCs in terms of molecular structure, is still in a premature stage, although highly enlightening towards the design of efficient electrocatalysts. Herein, the stepwise chemical modification of SWCNTs with terpyridines in the absence of metal, as well as in the presence of Ru in two different oxidative states, is investigated.[3] The SWCNTs-based prepared nanomaterials were characterized by IR, Raman and UV-Vis spectroscopy, while the degree of functionalization was determined by thermogravimetric analysis (TGA). Extensive electrocatalytic study revealed the impact of covalent modification on the lattice of SWCNTs with terpyridine complexes of Ru^{2+} and Ru^{3+} on the mechanistic pathway of oxygen reduction reaction (ORR). This comparative study highlights the importance of the first sphere of substituents of precious metals on both the thermodynamics and kinetics of ORR when anchored on the lattice of carbon nanomaterials, therefore provides valuable insights towards the nanostructure design of carbon-based effective electrocatalysts.

This project is funded by the European Union under the Grant Agreement 101084131. Views and opinions expressed are however those of the author(s) only and do not necessarily reflect those of the European Union or CINEA. Neither the European Union nor CINEA can be held responsible for them.

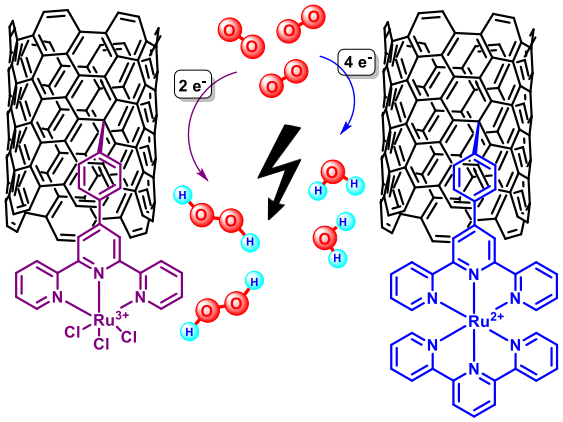

Figure 1: The effect of different oxidation states of ruthenium-metalated terpyridine-functionalized SWCNTs on the ORR activity.

References

[1] J. Sheng *et al.*, *ACS Appl. Mater. Interfaces* **14**, 20455-20462 (2022).
[2] S. Li *et al.*, *Chem. Sci.* 15, 11188 (2024).
[3] I. K. Sideri *et al.*, Submitted (2025).

FUNCTIONALIZED MoS_2 ELECTROSTATICALLY ASSOCIATED WITH PHOTOACTIVE CHROMOPHORES

E. Nikoli[1], M. Tsigkou[1], I. K. Sideri[1], Michalis Kardaras[1], Hiram Joazet Ojeda Galvan[2], Mildred Quintana[2], and Nikos Tagmatarchis*[1]

[1]Theoretical and Physical Chemistry Institute National Hellenic Research Foundation, 48 Vassileos Constantinou Avenue, 11635 Athens (Greece), [2]High Resolution Microscopy-CICSaB and Faculty of Science, Universidad Autonóma de San Luis Potosi, Av. Sierra Leona 550, Lomas de San Luis Potosi, 78210 SLP (Mexico)

The functionalization of transition metal dichalcogenides (TMDs), particularly MoS_2, with photoactive molecules has expanded their potential for optoelectronic and energy-related applications. While covalent functionalization has been extensively studied, electrostatic interactions remain comparatively underexplored, despite their ability to spatially accommodate chromophores in ways that influence electronic communication. In this work, we investigate the photophysical characteristics of three distinct nanoensembles, where MoS_2 electrostatically hosts Zn-phthalocyanine (ZnPc), Zn-porphyrin (ZnP), and boron-dipyrromethene (BODIPY), covering a broad range of visible light absorption. UV-Vis and photoluminescence spectroscopy reveal strong excited-state interactions across all chromophores, while ground-state interactions vary significantly. Notably, ZnPc and BODIPY exhibit opposite absorption shifts—bathochromic for ZnPc and hypsochromic for BODIPY—indicating distinct electronic interactions, while ZnP remains largely unaffected in the ground state. Emission studies confirm significant quenching across all nanoensembles, suggesting charge or energy transfer mechanisms. The observed tunability of optical properties based on chromophore selection highlights the potential of these systems for light-harvesting applications. Furthermore, the electrostatic functionalization strategy ensures both strong and potentially reversible interactions, offering a versatile approach to modulating TMD-based hybrid materials. [1]

The research project was supported by the Hellenic Foundation for Research and Innovation (H.F.R.I.) under the “2nd Call for H.F.R.I. Research Projects to support Faculty Members & Researchers” (Project Number 2482).

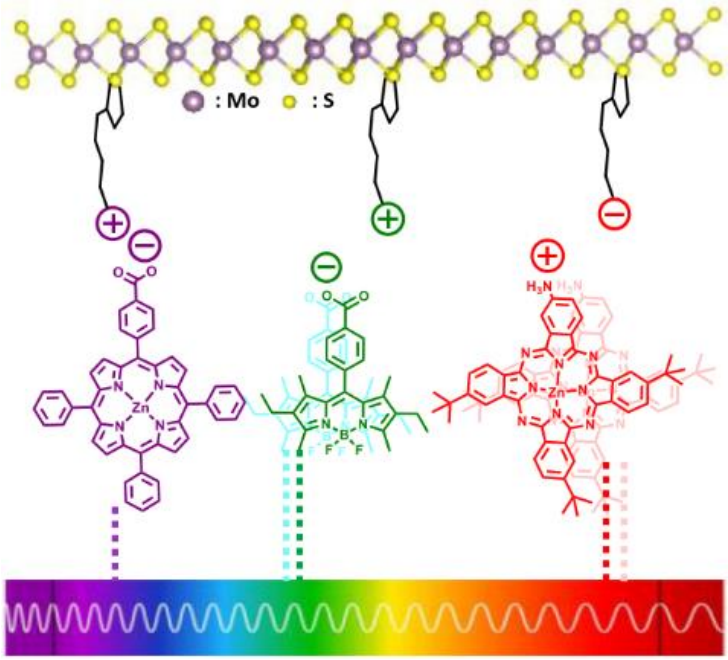

References

[1] M.Tsigkou *et al, Chem. Eur. J.*, e202404746 (2025).

Transition Metal Dichalcogenide Nanotubes with Diameters Below 3 nm

Runze Lai[1], Zhen Han[1], Xinrui Zhang[1], Yan Li[1*]

[1]*College of Chemistry and Molecular Engineering, Peking University, Beijing, (China)*

One-dimensional transition metal dichalcogenide nanotubes (TMDNTs) with additional degrees of freedom in both diameter and chirality exhibit unique physical and chemical properties.[1,2] However, synthesizing TMDNTs with diameters below 3 nm remains a significant challenge due to the high strain energy involved.[3] In this work, we employed multi-walled carbon nanotubes (MWCNTs) as templates to synthesize single-walled TMDNTs with diameters below 3 nm through a filling-conversion method. Transmission electron microscopy (TEM) characterization revealed that TMDNTs exhibit high crystallinity, with diameters as small as ~1 nm. By varying the precursor materials, we successfully synthesized several kinds of monometallic dichalcogenide nanotubes, such as ReS_2, WS_2, and $MoSe_2$, as well as alloyed metal dichalcogenide nanotubes. The crystallinity of the template and the reaction kinetics played crucial roles in the formation of TMDNTs. The inner cavity of MWCNTs endowed the possibility for TMDNTs to overcome ultra-high strain energy at extremely small diameters. The TMDNTs with diameters below 3 nm provided an ideal platform for investigation into their electronic and phonon modulation under high curvature.

References

[1] J. Guo, R. Xiang, T. Cheng *et al*., *ACS Nanosci. Au*, **2**, 3–11 (2022).
[2] R. Xiang, S. Maruyama, Y. Li, *Natl. Sci. Open*, **1**, 20220016 (2022).
[3] R. Xiang, T. Inoue, Y. Zheng, *et al*. *Science* **367**, 537–542 (2020).

Large-scale complementary carbon nanotube integrated circuits for harsh radiation environments

Ke Zhang[1,#], Daming Zhou[1,#], Ningfei Gao[2,3,#], Zhongzhen Tong[1], Xiaoyang Lin[1,*], Haitao Xu[2,3,4,*], Lianmao Peng[2], Weisheng Zhao[1,*]

[1]School of Integrated Circuit Science and Engineering, Beihang University (Beijing, China), [2]Key Laboratory for the Physics and Chemistry of Nanodevices, Center for Carbon-based Electronics, School of Electronics, Peking University (Beijing, China), [3]Beijing Institute of Carbon-based Integrated Circuits (Beijing, China), [4]Institute of Carbon-based Thin Film Electronics, Peking University (Taiyuan, China).

Advanced silicon-based integrated circuits (ICs) are facing significant risks in radiation-heavy environments [1], such as deep-space exploration, nuclear power facilities, and radiation-based medical treatments. High-energy photons and ions can penetrate shielding layers, causing damage to channel materials and even triggering reactions within packaging materials, which exacerbating the impact of irradiation. Irradiation-induced malfunctions or permanent damage to transistors significantly reduce the performance and reliability of these circuits, posing potential risks to critical equipment. Carbon nanotubes (CNTs), known for their ultra-strong chemical bonds and nanoscale dimensions, have been identified as ideal materials for achieving high radiation performance [2]. However, existing radiation-tolerant carbon nanotube field-effect transistors (CNTFETs) face several challenges, including the degradation of electrical performance due to trapped charges in the substrate, the lack of uniformly high-quality N-type devices, and have not yet been implemented in the large-scale level [3-5]. In this work, we employed an electrostatic doping strategy to fabricate local bottom-gate (LBG) complementary CNTFETs. By leveraging these high-yield, high-uniformity, and high-symmetry CMOS building blocks, we successfully demonstrated various logic gates, including inverters, NAND, and XOR gates, all of which exhibited correct rail-to-rail Boolean functionalities even after the irradiation dose of 6 Mrad(Si). Furthermore, ultra-low stage delay (~10 ns) can still be maintained for a 501-stage ring oscillator comprised of 1,004 transistors during the irradiation exposure. These results demonstrate the potential of complementary CNTFETs for practical, radiation-tolerant electronic systems and suggest a promising pathway for the development of reliable ICs in extreme environments.

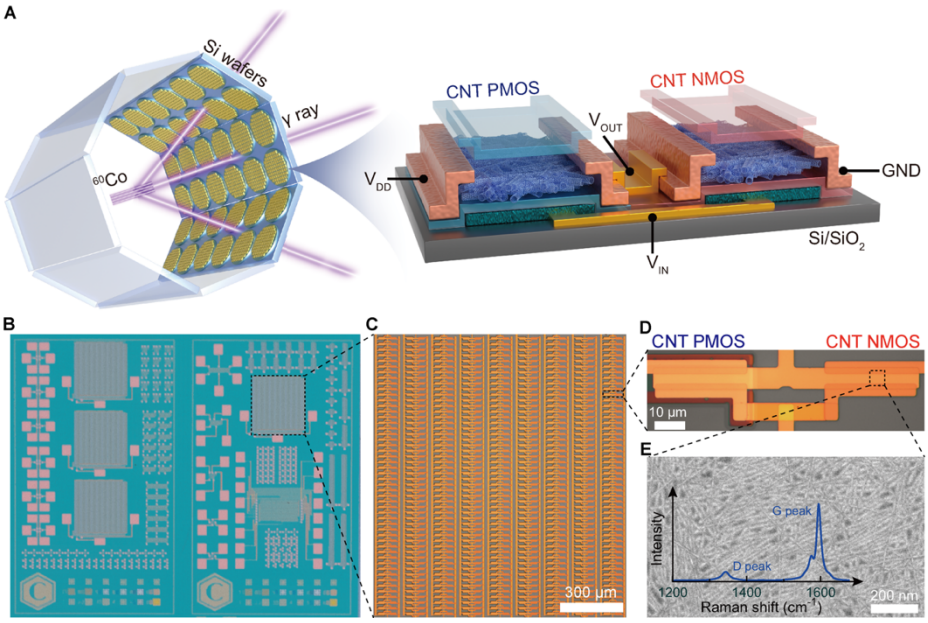

Figure 1: Large-scale radiation-tolerant complementary carbon nanotube (CNT) integrated circuits**.**

References

[1] J. Prinzie, et al., *Nat Electron,* **4**, 243-253 (2021).
[2] M. Zhu, et al., *Nat Electron,* **3**, 622-629 (2020).
[3] L. Liu, et al., *Science*, **368**, 850-856 (2020).
[4] Q. Cao, *et al.*, *Nature,* **454**, 495-500 (2008).
[5] B. Chen, *et al.*, *Nano Letter,* **16**, 5120-5128 (2016).

Architecting Host−Guest Synergistic Solid-State Electrolytes Enables Unobstructed Li-Ion Interphase Migration for Lithium Metal Batteries

L. Li[1], J.G. Zheng[1], H.X. Zhou[1], H. Huang[1]…, C.G. Sun[1,2] , B.G. An[1]

[1] *School of Chemical Engineering, University of Science and Technology Liaoning, Anshan, Liaoning 114051(People's Republic of China),*
[2] *School of Chemical Engineering, Nanjing University of Science and Technology, Nanjing, Jiangsu 210094 (People's Republic of China)*

Abstract text. Composite solid-state electrolytes inherit the intrinsic merits of each polymer and the inorganic solid-state electrolyte. However, their combined products are still unsatisfactory due to the unmatched Li-ion transport properties and the absence of structural integrity. Herein, an architectural inorganic−organic solid-state electrolyte (AIOSE) was constructed with highly coordinated Li-ion transport mode, where the primary Li6.4La3Zr1.4Ta0.6O12 particles were reconstructed as a continuous fast Li-ion transport skeleton, and the assisted organic components, including poly(ethylene glycol) diacrylate, ethylene carbonate, dimethyl carbonate, and lithium difluoro(oxalato) borate, were *in situ* polymerized into an elastic fast ion filler. The principles of "host−guest synergistic regulating Li-ion transport" and "Li-ion conductivity matched in order of magnitude" can provide continuous two-phase Li-ion transfer channels, achieving a high Li-ion conductivity of 0.58 mS cm−1 and Li-ion transference number of 0.66 at 25 °C. The Li||AIOSE||Li symmetric cells can be cycled for 1200 h at 0.35 mA cm−2 without an internal short circuit and hysteresis potential rise. The Li||AIOSE||LiNi0.8Co0.1Mn0.1O2 solid-state batteries can operate properly at −20 °C with 91.6% capacity retention and maintain 1000 cycles at 20 and 60 °C with 73% capacity retention. Our fabricated strategy validates the effectiveness of the design and showcases enormous potential in solid-state lithium batteries.

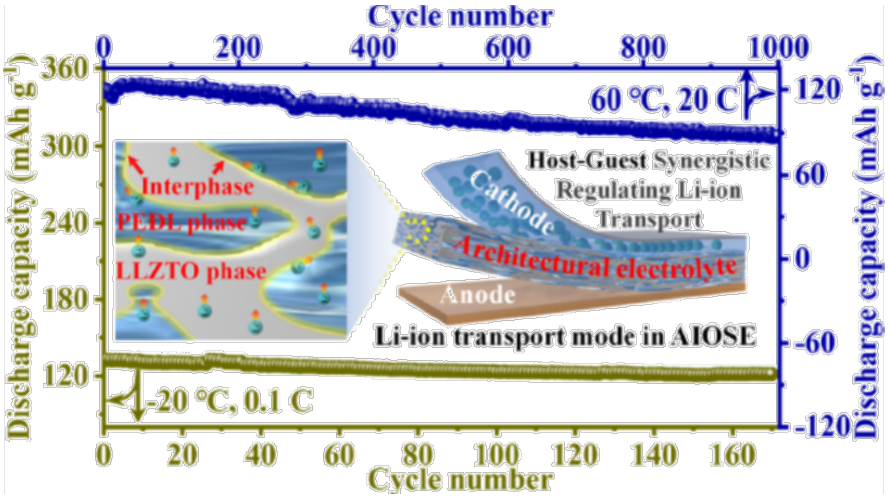

Figure 1. Schematic illustration and Charge and discharge curves of NCM811||AIOSE||Li cells in the range from −20 to 60 °C.

Optimizing Metal Contacts for Low Contact Resistance in Graphene Field Effect Transistors

Duc Chung Nguyen[1], Ji-Yong Park[1]

[1] *Department of Physics and Department of Energy Systems Research, Ajou University, Suwon, 16499, Korea*

Abstract

For the past two decades, graphene has been widely recognized for its unique electrical properties, including high charge carrier mobility, zero band gap, and high carrier saturation velocity, making it an ideal material for high-frequency electronic devices. However, the performance of graphene field effect transistors (GFETs) is significantly limited by high contact resistance, which reduces transconductance, gain, and increases power dissipation. Therefore, minimizing contact resistance is crucial for enhancing the performance of graphene-based electronic devices and realizing their full potential in various applications.

In this study, we investigated the impact of various metals on contact resistance in GFETs using the transfer length method (TLM). Through judicious selection of metals, we could achieve an average contact resistance (R_c) of ~90 Ω·μm, with a minimum value of ~50 Ω·μm at a hole carrier density of ~4.0×10^{12} cm^{-2}. This represents a reduction of more than half compared to the average contact resistance obtained with commonly employed Pd metal contacts (R_c ~180 Ω·μm) at a similar hole carrier density. Simultaneously, we could determine the intrinsic electrical properties of graphene, which exhibited a minimum sheet resistance (R_{sheet}) of ~40 Ω/sq with a high hole mobility (μ_p) of ~42,000 $cm^2V^{-1}s^{-1}$ at room temperature and a carrier density of ~4.0×10^{12} cm^{-2}, indicating the high quality of the graphene used in our devices.

Diameter Adjustment of Single-Walled Carbon Nanotubes by Ni-Based Bimetallic Catalysts in Laser Ablation

Shaochuang Chen[1], Zeyao Zhang[1,2,*], Yan Li[1,2,*]

[1]*College of Chemistry and Molecular Engineering, Peking University, Beijing 100871, China*

[2]*Institute of Carbon-Based Thin Film Electronics, Peking University, Shanxi, Taiyuan, 030012, China*

Structure-control in laser ablation (LA) synthesis of single-walled carbon nanotubes (SWCNTs) is challenging. Here, we use bimetallic catalysts based on Ni to regulate the diameter of SWCNTs. By the addition of Ti, SWCNTs with a higher yield and smaller diameters were derived. The Ni/Ti ratio, temperature and atmosphere were the key factors. The additions of Zr, Hf, Cr, Mo and W were also useful to adjust the diameters of SWCNTs. We proposed a possible mechanism about the diameter adjustment based on the melting point of catalysts. When using coal as carbon source, diameters were also adjusted by Ni-Ti catalyst.

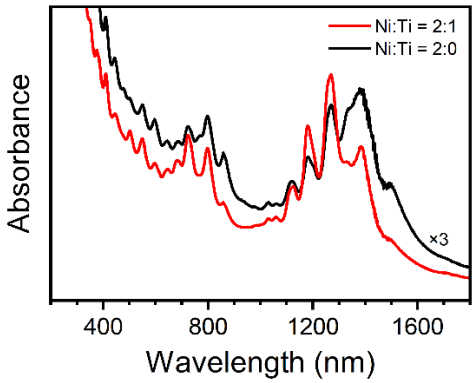

Figure. Absorption spectra of SWCNTs synthesized by Ni-Ti or Ni. Dispersed by 2% DOC.

Marangoni-Flow-Induced Self-Assembly of Single Walled Carbon Nanotubes into High Density Arrays

Zilong Qiu[1], Yuguang Chen[1], Yanzhao Liu[1], Zeyao Zhang[1,2], Yan Li[1,2]

[1]*College of Chemistry and Molecular Engineering, Peking University, Beijing 100871 (China)*

[2]*Institute of Carbon-Based Thin Film Electronics, Peking University, Shanxi, Taiyuan 030012 (China)*

The preparation of high-density semiconducting single-walled carbon nanotube (SWCNT) arrays is a key factor for the fabrication of SWCNT field-effect transistors (FETs) with performance exceeding that of conventional silicon complementary metal oxide semiconductor FETs. It is important to assemble SWCNTs dispersed in solution with different solvents and dispersants into arrays on substrates. Here we demonstrate a general strategy for utilizing Marangoni flow to assemble SWCNTs into high-density arrays. The Marangoni flow is regulated by the surface tension gradient and it might take effect in the assembly process by making SWCNTs concentrate at the meniscus, form nematic ordering, and deposit on lifting substrates as high-density arrays. This strategy is suitable for preparation of wafer scale SWCNT arrays. It can be applied from either aqueous or organic SWCNT dispersions. The densities of arrays assembled from organic and aqueous dispersions are ≥ 128 /μm and ≥ 216 /μm, respectively, and the two-dimensional order parameters are 0.96 and 0.91, respectively.

Intrinsic High-Semiconducting-Purity Carbon Nanotube Array Films for High-Performance Electronics

Lan Bai[1,2]

[1]*Peking University, Beijing (China),* [2] *Shanxi Institute of Carbon-Based Thin Film Electronics, Peking University (SICTFE-PKU), Taiyuan (China)*

Semiconducting carbon nanotubes (S-CNTs) are promising channel materials for field-effect transistors (FETs) due to their unique one-dimension structure and excellent electronic and thermal properties. High-density and high-semiconducting-purity aligned carbon nanotubes (A-CNTs) are required for high performance electronics. Wafer-scale aligned CNTs (A-CNTs) are usually self-assembled based on high-semiconducting-purity CNT solutions prepared by conjugated polymer wrapping. In this work, the chiral selectivity and separation performance of PFO-BPy and PCz for carbon nanotubes with different diameters were systematically studied. While the above two polymer wrappers are difficult to completely removed from the A-CNTs, the intrinsic electronic performance of s-CNTs was degraded. Then degradable conjugated polymer PFO-N-PFO was designed and synthesized, which had similar selectivity and dispersion to PCz, but with better selectivity for small diameter Hipco CNTs. A process for batch preparation of CNT solutions with high semiconductor purity was develop based on PFO-N-PFO, which is also available with a wafer-scale self-assembly technique to prepare high-density (A-CNTs). Due to the presence of C=N bonds in backbone, the polymer wrapped on the CNT film is removed by trifluoroacetic acid (TFA), solvent cleaning and annealing to obtain ultra-clean intrinsic A-CNTs, which is characterized by X-ray photoelectron spectroscopy (XPS) N1s peaks and SEM. Top-gated FETs based on the A-CNTs with a 45 nm channel length exhibit an on-state current (I_{on}) of 2.2 mA/μm, a peak transconductance (g_m) of 1.1 mS/μm, low contact resistance (R_c) of 191 Ω•μm and negligible hysteresis. The results show that intrinsic A-CNT films, which was obtained by polymer structure design, high-semiconducting-purity CNT solution preparation, A-CNT films process, and polymer wrapper removal by post-processing process, showing great potential for high-performance electronics.

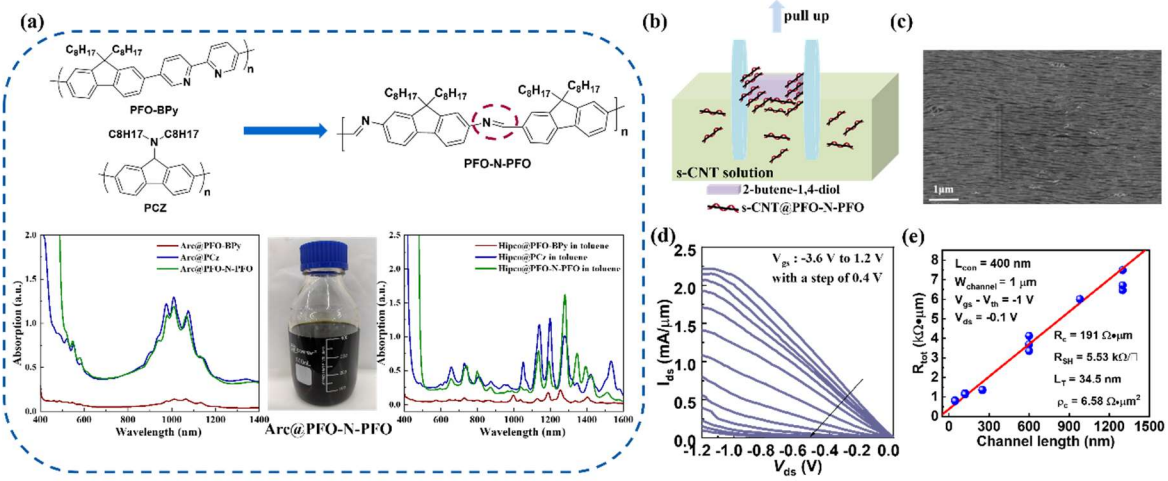

Figure caption: (a) Absorption spectra of Arc and Hicpo CNT solutions prepared in batches using PCz, PFO and degradable PFO-N-PFO; (b) Schematic showing the process of assembling A-CNTs; (c) SEM image of ultra-clean and high-semiconducting-purity A-CNTs; (e) Output transconductance characteristics of top-gated FETs with channel length of 45 nm; (f) Contact resistance extraction for A-CNT FETs with L_{con} of 400nm.

h-BN/Graphene Heterostructure-Decorated Copper Current Collector for Long-Cycle Anode-Free Lithium Metal Batteries

Lingchen Kong[1], Chaofan Zhou[1], Xuanguang Ren[1], Li Lin[1, 2,*], Xin Gao[1, 2,*]

[1]*School of Materials Science and Engineering, Peking University, Beijing 100871, China*

[2]*Beijing Graphene Institute (BGI), Beijing 100095, China*

Abstract: Anode-less lithium metal batteries (ALLMBs) offer exceptional energy density and cost-efficiency, making them prime candidates for next-generation energy storage [1-2]. However, the natural oxide layer on commercial copper current collectors (CuCCs) significantly hampers lithium-ion mobility, causing uneven deposition, solid electrolyte interphase (SEI) structure instability, and capacity decay—a critical issue that has been overlooked [3-4]. Based on this, we designed an anode-free copper current collector modified with an atomic-scale BNG heterostructure (BNG@Cu), where the BNG architecture consists of a hybridized boron nitride (BN) and graphene (Gr) framework deposited on copper foil via atomic layer deposition (ALD). The insulating BN component effectively suppresses continuous parasitic reactions by blocking direct contact between Li and the electrolyte, while simultaneously buffering volume fluctuations during cycling. In contrast, the conductive Gr domains act as lightweight mechanical pivots, enhancing the mechanical toughness of the SEI and improving the lithiophilicity of the hybrid structure through electron delocalization effects. Electrochemical tests of ALLMBs fabricated with BNG@Cu demonstrate an average Coulombic efficiency of 98.9% and superior capacity retention of 70% for 60 cycles. This is a 1.4-fold increase in cycle life compared with conventional CuCCs. This study highlights the critical role of ALD in surface and interface modification, establishing it as a transformative and scalable technique for engineering CuCCs in advanced battery systems.

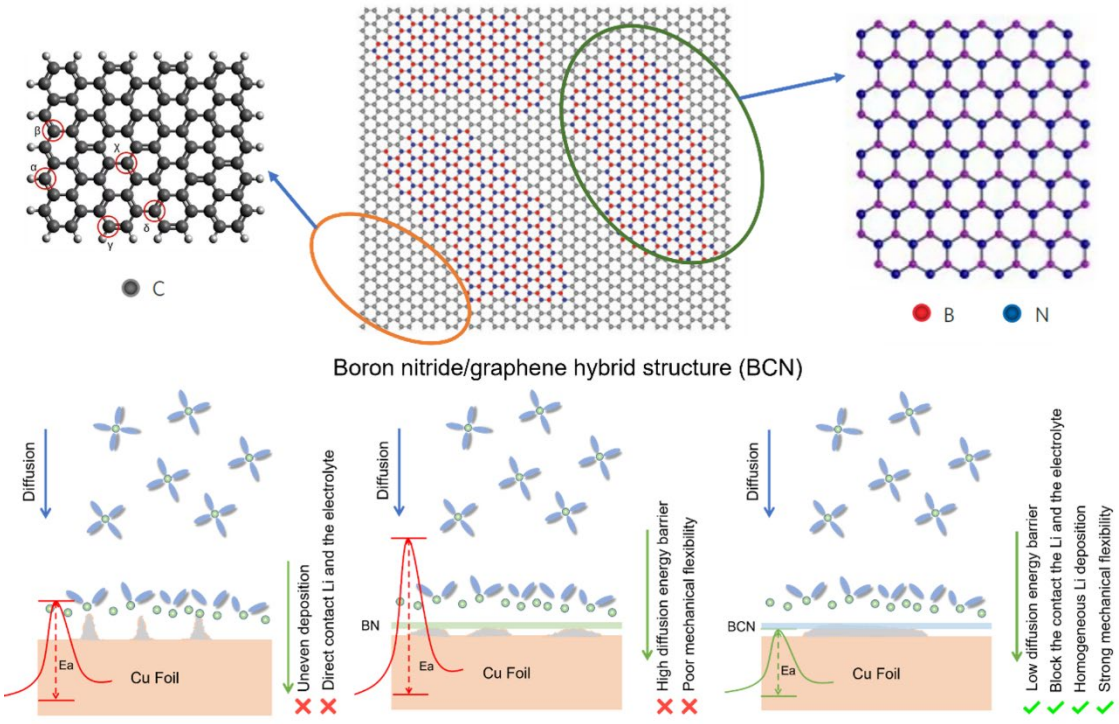

Figure caption: Schematic diagram of BNG and the Li+ transfer and deposition process

References

[1] P. Albertus *et al.*, *Nat. Energy* **3**, 16–21 (2017).
[2] J. Liu *et al.*, *Adv. Energy Mater.* **11**, 2000804 (2021).
[3] R. Weber *et al., Nat. Energy* **4**, 683–689 (2019).
[4] C. Heubner *et al., Adv. Funct. Materials* **31**, 2106608 (2021).

Research on Semiconducting SWCNTs with clean surfaces in Dispersions and Thin-Films

Song Qiu[1]

[1]*Suzhou Institute of Nano-Tech and Nano-Bionics (SINANO), Chinese Academy of Sciences*

This study investigates surface purification strategies for semiconducting single-walled carbon nanotube (s-SWCNT) dispersions and thin films to mitigate performance degradation caused by residual contaminants. A multi-step purification protocol was systematically examined. This work establishes a scalable surface purification framework critical for advancing carbon nanotube-based nanoelectronics and optoelectronic devices.

Gas Phase Chemistry of Salt Assisted MoS_2 Growth

Daniel S. Vadseth[1], *Shigeo Maruyama*[2], *Alister Page*[1]

1. School of Environmental and Life Sciences, University of Newcastle, Newcastle, Australia

2. Department of Mechanical Engineering, School of Engineering, The University of Tokyo, Tokyo, 113-8656, Japan

DSV: daniel.vadseth@uon.edu.au, AP: alister.page@newcastle.edu.au

Salts, especially alkali metal halides like NaCl, have been used during CVD synthesized to increase the yield and quality of 2D transition metal dichalcogenide (TMD) monolayer materials[1]. The proposed mechanism for this type of salt-assisted growth is that the salt forms intermediates with the metal oxide precursor, e.g. Na_2WO_4 and $NaMoO_3$, have a lower melting point compared to the transition metal oxide, thus increasing the vapor pressure and providing a steady flux of metal to the substrate increasing yield and quality[2,3]. Another method of salt-assisted growth of 2D TMD materials involves using a vapor-liquid-solid (VLS) mechanism where the transition metal + alkali metal salt, e.g. Na_2MoO_4, is put directly on the substrate, melted into droplets which absorb the chalcogen and precipitate out monolayer TMDs[3]. Sodium has also been investigated for its catalytic properties, accelerating the chemistry of making TMD nanomaterials from the metal oxide precursor[4]. While the effects of salt on the precursors and at the substrate have been investigated, the gas phase chemistry of salt assisted growth has not been investigated in the literature to the best of our knowledge.

While 2D van der Waals (vdW) heterostructures have been extensively studied since the late 2000's, their 1D counterpart, the 1D nanotube vdW heterostructure, was first reported in 2020[5]. Salt-assisted growth has proven to be an important part of the synthesis of 2D TMD materials but has not yet been properly investigated as a way of increasing yield and quality of 1D TMD nanotubes and heterostructures.

To address this knowledge gap, molecular dynamics (MD) using GFN1-xTB[6] is used to explore the role of NaCl in the formation of MoS_2 nanomaterials, as well as investigating the possibility of salt-assisted growth of MoS_2 nanotubes. MoO_3, S_2 and LiCl, NaCl, KCl were modelled in various gas phase chemical environments to better understand the intermediates that form and how affects the chemistry.

References

[1] S. Li, et al., *Applied Materials Today*, 2015, **1**, 1.

[2] S. Li, et al., *Chem. Mater.*, 2021, **33**, 18.

[3] J. Lei, et al., *J. of American Chem. Soc.*, 2022, **144**, 16.

[4] P. Yang, et al., *Nature Communications*, 2018, **9**, 1.

[5] R. Xiang, et al., *Science*, 2020, **367**, 6477.

[6] S. Grimme, et al., *Journal of Chemical Theory and Computation*, 2017, **13**, 5

On the use of seeding for chirality-controlled growth of carbon nanotubes

Kim-Jonas Ylivaino[1], Daniel Hedman[2], Andreas Larsson[1]

[1]*Applied Physics, Division of Materials Science, Department of Engineering Sciences and Mathematics, Luleå, University of Technology, Luleå, SE-97187 (Sweden),*
[2]*Center for Multidimensional Carbon Materials (CMCM), Institute for Basic Science, (IBS), Ulsan 44919 (Korea)*

Single-walled carbon nanotubes (SWCNTs) exhibit exceptional electronic properties that are highly sensitive to their chirality, making them promising candidates for next-generation electronics. However, achieving chirality-specific synthesis remains difficult. One potential strategy to address this is to seed SWCNT growth using preformed caps or short SWCNT segments (seeds) with the desired chirality [1, 2].

A major challenge here is to ensure that these seeds remain stable long enough for additional carbon atoms to be added to the seed-catalyst interface, thereby elongating the seed into a tube. This requires careful optimization of the catalyst and growth conditions. In this work, we employed the second generation of the DeepCNT-22 machine learning force field previously used to simulate defect-free SWCNT growth [3]. We performed 100 ns molecular dynamics (MD) simulations to determine the catalyst carbon concentration required to prevent seed dissolution. Subsequently, we simulated seeds with chiralities (5,5), (6,4), (7,3), (8,1), and (9,0) on Fe_{50}, as well as seeds with chiralities (7,7), (8,6), (10,4), (12,0), and (12,1) on Fe_{113}. For both nanoparticle sizes, the simulations were conducted at carbon concentrations of 34% and 40%. See Figure 1a for examples of the simulation setups. The carbon concentrations were selected based on the equilibrium between the tube and nanoparticle that prevents dissolution, see Figure 1b.

Stability of the seeds was evaluated by measuring their structural evolution during the MD simulation by calculating a similarity kernel from local descriptors using the Smooth Overlap of Atomic Positions (SOAP). Additionally, we tracked the number of carbon atoms in the nanoparticle and the change in the edge structure of the seed over time. Our results indicate that the (9,0) SWCNT seed is particularly stable up to 1200 K, suggesting its suitability as an optimal seed for chirality-controlled growth, see Figure 1c.

By exploring the stability of nanotube seeds with various chiralities, our study advances the understanding of catalyzing chirality-specific SWCNT growth, a critical step toward overcoming current synthesis challenges.

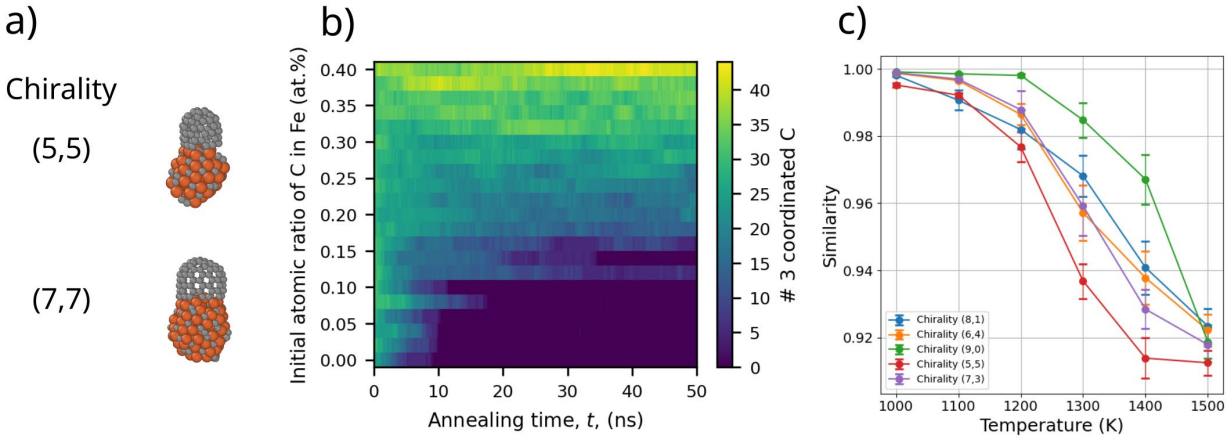

Figure 1. a) Example of seeds attached to saturated nanoparticles used for molecular dynamics simulations. b) Heatmap illustrating the evolution over time of the seed size, measured as the number of three-coordinated carbon atoms, when attached to Fe_{50} nanoparticles with varying initial carbon concentrations. c) Similarity index versus temperature at the final timestep, averaged over 20 MD simulations. Here seeds are placed on a Fe_{50} catalyst with a carbon concentration of 40%.

References

[1] H. Wang *et al*., *Nano Lett.* **5**, 301 (2005).
[2] J. R. Sanchez-Valencia *et al., Nature* **515**, 61 (2014).
[3] D. Hedman *et al., Nat. Commun.* **15**, 4076 (2024).

Super graphene-skinned material: From epitaxial growth to property calculations

Xiucai Sun[1], Zhongfan Liu[1,2]

[1] *Beijing Graphene Institute (BGI), Beijing 100095, China*

[2]*Center for Nanochemistry, Beijing Science and Engineering Center for Nanocarbons, Beijing National Laboratory for Molecular Science, College of Chemistry and Molecular Engineering, Peking University, Beijing 100871, China*

As a new member of graphene materials family, super graphene-skinned material is a type of graphene composite materials made by directly depositing continuous graphene layers on traditional materials *via* chemical vapor deposition (CVD) process. By growing high-performance graphene "skin", the traditional materials are given new functionalities. The atomically thin graphene hitches a ride on the traditional material carriers to market. The experimental progress has been driven by theoretical insights. Using methods such as first-principles calculations, molecular dynamics, and high-throughput machine learning, we have conducted in-depth research on the key issues of graphene-skinned materials, from growth to applications. Based on the gas-phase and surface reaction mechanisms in CVD graphene growth, we have established a theoretical framework for the growth of graphene on both metallic and non-metallic materials. By investigating the oxidation resistance, water and oxygen barrier properties, and thermal conductivity of graphene, we have opened new avenues for the practical application of continuous graphene films, providing fresh momentum for the accelerated industrialization of graphene materials.

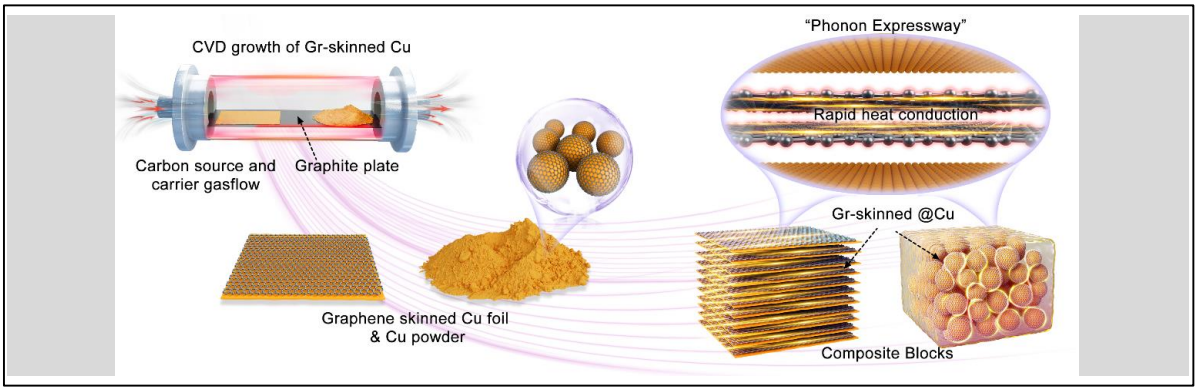

Figure caption: Design and preparation process of high thermal conductivity graphene-skinned Cu materials**.**

References (if desired)

[1] Qi Y, Sun L, Liu Z. Super graphene-skinned materials: an innovative strategy toward graphene applications. *ACS Nano* **18**, 4617 (2024).

[2] Qi Y.; Sun L.; Liu Z. Super Graphene-Skinned Material: A New Member of Graphene Materials Family. *Acta Phys. Chim. Sin.* **39**, 2307028 (2023).

[3] Sun, X.; Lou, S.; Wang, W.; Liu, X.; Sun, X.; Song, Y.; Yang, W.; Liu, Z. Kinetics of Hydrogen Constrained Graphene Growth on Cu Substrate. *Nano Res.* **17**, 9284-9292 (2025).

[4] Lou S.; Ma X.; Wang Z.; Wang W.; Song L.; Sun X.; Ding Y.; Yin W.; Yang W.; Tan J.; Sun, X.; Liu Z. Interfacial coupling induced discrete orientation of epitaxial graphene on high-index Cu substrates. *Adv. Funct. Mater.* **35**, 2415972 (2025).

[5] Sun, X.; Lou, S.; Wang, W.; Liu, X.; Sun, X.; Song, Y.; Yang, W.; Liu, Z. Kinetics of Hydrogen Constrained Graphene Growth on Cu Substrate. *Nano Res.* **17**, 9284-9292 (2024).

[6] Sun, X.; Liu, X.; Sun, Z.; Zhang, X.; Wu, Y.; Zhu, Y.; Song, Y.; Jia, K.; Zhang, J.; Sun, L.; Yin, W.-J.; Liu, Z. Invisible Vapor Catalysis in Graphene Growth by Chemical Vapor Deposition. *Nano Res.* **17**, 4259-4269 (2024).

Graphene Layers Folded Many Times

Kazuyuki Uchida

Department of Physics, Kyoto Sangyo University (Japan)

Experimental techniques for folding graphene at the desired position and into the desired direction have been reported [1]. An interesting research question is to understand what kind of nanoscale structures and electronic properties can be obtained by folding graphene in such ways. In this work, we present the results of our computer simulations of the atomic structure of graphene folded multiple times on a flat substrate. We use the Tersoff potential to describe the covalent bonds within a graphene layer and the Lennard-Jones potential to describe the van der Waals interactions between layers.

Our calculations show that, in multi-folded graphene, the interactions between the folds form a characteristic atomic structure that is not seen in single-folded ones [2]. Furthermore, the atomic structure was found to change qualitatively with the size of the folds. We show that void structures of various shapes and sizes appear in the gaps between the folds, and we discuss that various floating electron states [3] may arise reflecting these void structures. We also show that moiré patterns appear depending on the bend angle, exploring unique electronic properties [4] that reflect this moiré.

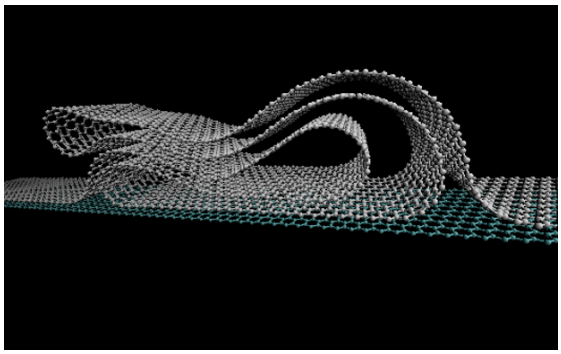

Fig.1: Atomic structure of a single graphene layer folded four times on a flat substrate.

References

[1] K. Kim et al., Phys. Rev. B **83**, 245433 (2011).
[2] T. Shimizu, D. Kamihara, and K. Uchida, J. Phys. Soc. Jpn. **92**, 074602 (2023).
[3] Th. Fauster et al., Phys. Rev. Lett. **51**, 430 (1983). M. Posternak et al., Phys. Rev. Lett. **52**, 863 (1984). A. F. Hebard et al., Nature **350**, 600 (1991). Y. Miyamoto et al., Phys. Rev. Lett. **74**, 2993 (1995). S. Okada et al., Phys. Rev. B **62**, 7634 (2000). M. S. Dresselhaus et al., Advances in Physics, **51**, 1 (2002). Y.-I. Matsushita et al., Phys. Rev. Lett. **108**, 246404 (2012).
[4] Z. Ni et al., Phys. Rev. B **77**, 235403 (2008). G. Trambly de Laissardie`re et al., Nano Letters **10**, 804 (2010). K. Uchida et al., Phys. Rev. B **90**, 155451 (2014). O. Arroyo-Gascon et al., Nano Lett. **20**, 7588 (2020). Y. Cao et al., Nature **556**, 43 (2018).

Anomalous Electrostatic Properties of Double-walled BN Nanotubes

°N. Sultana, Y. Gao, M. Maruyama, S. Okada

Department of Physics, University of Tsukuba, Tsukuba 305-8571, Japan

Hexagonal boron nitride (hBN) is a key supporting substrate for atomic layer materials to investigate their physical properties precisely. Like a carbon nanotube from a graphene sheet, hBN also forms a tubular structure with insulating electronic properties and remarkable stability [1]. Thus, BN nanotubes (BNNTs) can be a template for synthesizing other tubular forms of atomic layer materials [2]. BNNTs have a multi-walled structure for these template applications where the inter-wall atomic arrangement is expected to play a decisive role because of the inter-wall polarity as is the bilayer hBN [3]. The electronic properties of double-walled BNNTs (DW-BNNTs) are unclear yet, although the physical properties of their single-walled form are well established. Thus, in this work, we investigate the electronic properties of DWBNNT in terms of mutual inter-wall arrangement, using the density functional theory (DFT).

Fig. 1 shows contour plots of the electrostatic potential of DW-BNNTs comprising (5,5) and (10,10) BNNTs with various inter-wall arrangements. The electrostatic potential outside the outer nanotube is sensitive to the mutual orientation of the inner nanotube, although the orientation of the outer nanotube is fixed during the calculation. Moreover, we found that potential between the walls also strongly depends on the inter-wall atomic arrangements. In contrast, the electronic structure near the band edges is insensitive to the mutual orientation of walls.

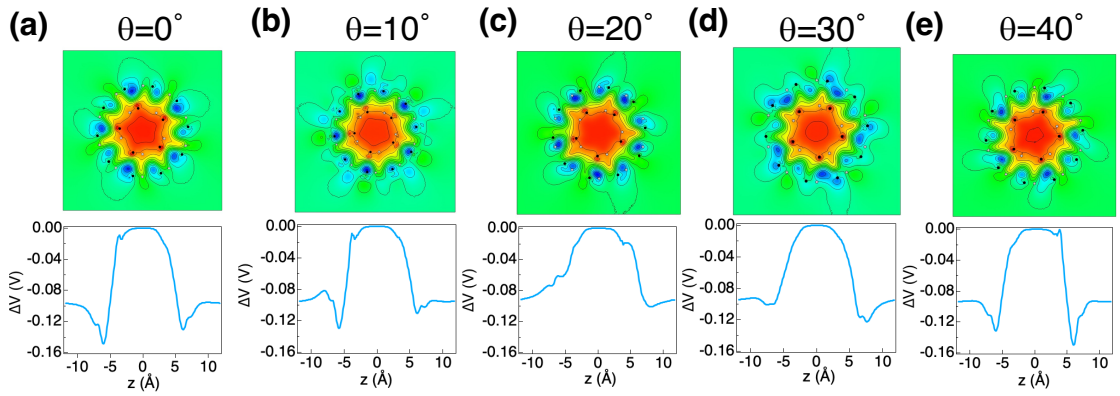

Figure 1: Contour plots of electrostatic potential of (5,5) @ (10,10) BNNT with the mutual stacking angles of (a) 0, (b) 10, (c) 20, (d) 30, and (e) 40 deg. The bottom of each panel indicates the electrostatic potential as a function of z axis. Red and blue in the plots correspond to the higher and lower potentials, respectively. Black and gray circles indicate N and B atoms, respectively.

References

[1] D. Golberg et al. Adv. Mater. **19**, 2413−2432 (2007).
[2] R. Xiang et al. Science **367**, 537-542 (2020).
[3] M. Maruyama and S. Okada FlatChem **372**, 1458-1462 (2021).

Machine Learning-Assisted Computational Exploration of the Electronic Structures of MoS_2 Nanotubes

Ju Huang[1], Wenbin Li[1]

[1] *School of Engineering, Westlake University, 310030, Hangzhou, China*

Transition-metal dichalcogenide (TMDC) nanotubes (NTs) exhibit exceptional physical and chemical properties, making them promising candidates for future electronic and optoelectronic devices. The electronic properties of these one-dimensional structures are tunable through their structural chirality, diameter, and elemental composition, highlighting the importance of understanding chiral-dependent properties for performance optimization. However, the high computational cost associated with first-principles calculations of tubular systems limits the exploration of their structure-property space. While previous studies focused on the electronic properties of non-chiral (zigzag and armchair) NTs with a small number of atoms in a unit cell, high-resolution transmission electron microscopy has revealed a broad distribution of chirality in various single-wall TMDC NTs.

Here, we employ a combined machine learning (ML) and density functional theory (DFT) approach to investigate the relationship between electronic properties and crystal structures of molybdenum disulfide (MoS_2) NTs with various chirality and diameters. By training state-of-the-art ML universal potentials and ML DFT Hamiltonians, we efficiently compute the electronic band structures of optimized MoS_2 NTs with significantly reduced computational demands. Our study reveals that while the band gaps of the NTs are independent of the chiral angles, the effective masses of the electrons and holes depend on both the chiral angles and the diameters of the NTs. When the diameters of the NTs exceed 60 Å, the effective masses converge to those of the MoS_2 monolayer and remain consistent regardless of chiral angles and sizes.

Our findings provide valuable insights into the electronic properties of MoS_2 NTs with diverse chirality and diameters, serving as a reference for their application in electronic devices. Furthermore, our high-accuracy ML models for structural optimization and electronic structure calculations demonstrate the efficiency of ML-assisted approaches in materials physics research.

Observation of Topological Nodal-Ring Phonons in Monolayer Hexagonal Boron Nitride

Zhiyu Tao[1], Jiandong Guo[1], Xuetao Zhu[1]

[1]*Institute of Physics, Chinese Academy of Sciences (China)*

Topological physics has evolved from its initial focus on Fermionic systems to uncover fascinating phenomena in Bosonic systems, particularly in phonons within crystalline materials. Notably, topological phonons in two-dimensional insulating materials hold significant promise for future technological applications. In this work, we expand a new dimension to this field by investigating topological phonons in monolayer hexagonal boron nitride (MhBN) using advanced high-resolution electron energy loss spectroscopy with two-dimensional energy-momentum mapping. Our high-resolution experimental data explicitly demonstrate two topological nodal rings in monolayer hexagonal boron nitride, protected by mirror symmetry, thus expanding the understanding of 2D topological phonons beyond graphene. This research not only deepens fundamental knowledge of 2D topological phonons but also paves the way for innovative phononic devices utilizing a wide-bandgap insulating material, crucial for advancements in electronics and photonics.

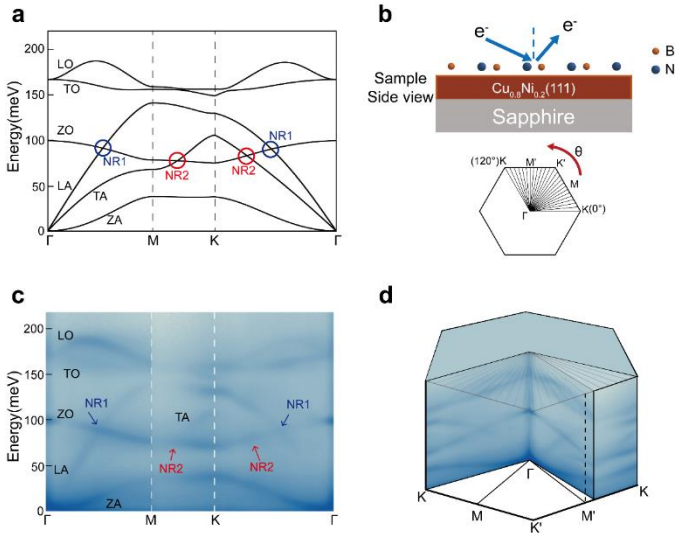

Fig. 1 | Sample structure and phonon spectra of MhBN. a, Calculated MhBN phonon spectra along the high-symmetry paths. **b**, MhBN sample structure and Brillouin zone of MhBN, with black radial lines indicating the scattering angles measured in the HREELS experiment. **c**, Experimental MhBN phonon spectra corresponding to a. **d**, 3D HREELS mapping of the MhBN phonon spectra.

References

[1] Xu, Y. *et al.* Catalog of topological phonon materials. *Science* **384**, eadf8458 (2024).
[2] Li, J.D. *et al*. Direct observation of topological phonons in graphene. *Phy.Rev. Lett.*, **131**, 116602 (2023).
[3] Tao, Z.Y. *et al.* Observation of topological nodal-ring phonons in monolayer hexagonal boron nitride. *Chin. Phys. Lett.* **42**,027405 (2025).

On-Chip Metasurface-Mediated $MoTe_2$ Photodetector with Electrically Tunable Polarization-Sensitivity

Ruizhi Li[1, #], Xinlei Zhang[1,#], Fan Zhong[1,#,*], Zhenhua Ni[1,2,*]

[1] *School of Physics, Key Laboratory of Quantum Materials and Devices of Ministry of Education, Southeast University, Nanjing 211189, China*

[2] *Purple Mountain Laboratories, Nanjing 211111, China*

Abstract text: Photodetectors with tunable polarization sensitivity play a significant role in decoding signals in optical communications, extracting polarization-encrypted information, and the environmental monitoring of polarization variations. Metasurfaces are widely used in polarized photodetectors, while the responses for different polarization incidences follow a determinable and consistent correspondence. In this paper, an electrically tunable polarization photodetector composed of $MoTe_2$ and gold metasurface is proposed for on-chip polarization-sensitive near-infrared (900–1200 nm) detection. Through contact engineering and electro-tuning, highly-tunable Schottky barriers are achieved. This enables the modulation of photoelectric conversion via the excitation of surface plasmon polaritons, which in turn allows for continuous adjustment on the degree of linear polarization of a settled metasurface ranging from 0.2 to an ultimate value of 1.0. The results outline a paradigm to achieve a polarization-dependent electrically tunable response, which is promising for on-chip information processing in integrated optics.

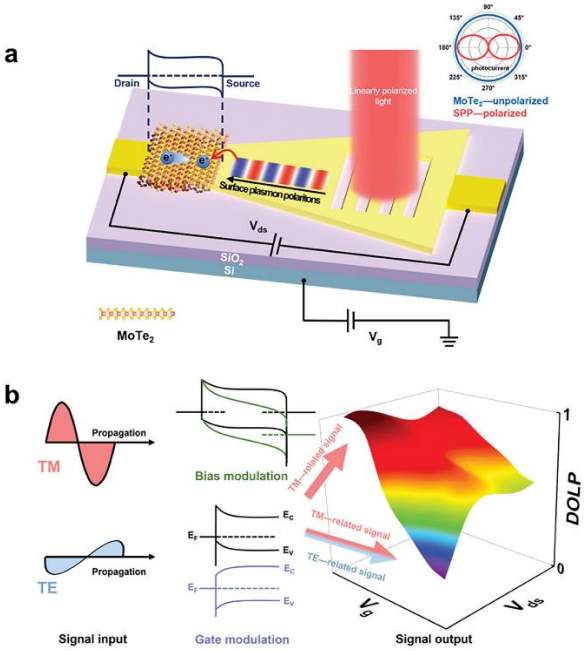

Figure caption: Schematic diagram of our system. a) Highly efficient polarization detection with the on-chip SPP-mediated isotropic $MoTe_2$-based photodetector. The incidence illuminating the polarization-sensitive grating is transferred into the SPPs and detected by the $MoTe_2$-based photodetector, and the SPPs induce the electron-hole pairs separated by applying a bias voltage. The bottom p-doped silicon serves as the back gate to set gate the voltage. Through the polarization-sensitive structure, the isotropic $MoTe_2$-based photodetector has an anisotropic photoresponse for different linear polarizations, as shown by the red curve comparison with the blue curve in the inset. b) By varying the bias and the gate voltage, the input polarization mixed signals are transferred into output photocurrents with tunable polarization-dependence, which provides a large range of tunability in the DOLP.

Synthesis of Rhenium Doped WS_2 Nanotubes and their electrical properties

A. Ahad[1,2], M. A. Afzal[1], R. Higashinaka[1], M. Kikuchi[1], S. Saito[1], S. Kusaba[1], Z. Liu[4], Y. Miyata[1], Y. Hirose[3], and K. Yanagi[1]

[1]*Department of Physics, Tokyo Metropolitan University, Hachioji, Tokyo 192-0397, Japan*
[2]*Department of Physics, Comilla University, Cumilla-3506, Bangladesh*
[3]*Department of Chemistry, Tokyo Metropolitan University, Hachioji, Tokyo 192-0397, Japan*
[4]*National Institute of Advanced Industrial Science and Technology (AIST), Tsukuba 305-8565, Japan*

Tungsten disulfide nanotubes (WS_2-NTs) exhibit semiconducting properties irrespective of their chiralities. The advancement of synthesis techniques to control their structure and functionalize their properties is of great importance for their application in electronic and optoelectronic devices. One of the approaches to tune the electronic structure of WS_2-NTs is hetero-atom doping, such as rhenium (Re) and niobium (Nb) [1-2]. It is reported that Re-doped WS_2-NTs have shown a transition from the stable semiconducting 2H phase to the metallic 1T phase [3]. However, the doping level reported in the literature is extremely low (<0.1 at.%), and the synthesis processes remain highly complex and challenging for the scale-up.

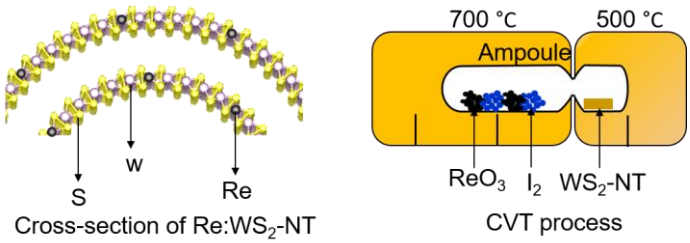

Fig. 1 Schematic illustration for synthesizing Re:WS_2-NT.

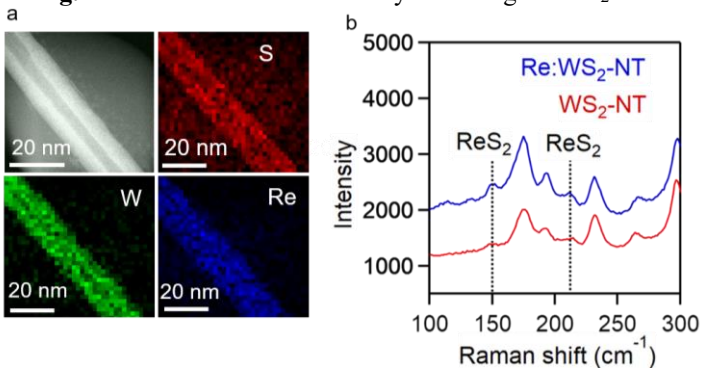

Fig. 2 (a) EELS mapping, (b) Raman shift of Re:WS_2-NTs.

In this study, we employed a chemical vapor transport (CVT) method and successfully synthesized Re-doped WS_2-NTs with higher doping levels (Figure 1). First, we prepared WS_2-NTs with a diameter of 15-20 nm through our reported CVD method. Then, we employed the CVT process to dope the Re into the WS_2-NTs using rhenium oxide. In the CVT, synthesis parameters, such as temperature gradient, reaction time, and the amount of reagent, were optimized to achieve uniform doping. Figure 2 (a) shows the EELS mapping of STEM, confirming the substitutions of Re atoms in the NTs' layer with doping levels up to 1.5 at.% and figure 2 (b) depicts the Raman shift of the pristine and Re-doped WS_2-NTs. We fabricated two terminal electrodes on a single rope of the NTs to evaluate electrical properties and observed the enhancement of current density in the doped sample compared to pristine WS_2-NTs.

References: [1] Yadgarov, *et al.*, Angew. Chem. Int. Ed. 2012, 51, p.1148-1151. [2] Yadgarov, *et al.*, 2013.Wear, 297, p.1103-1110. [3] Enyashin, *et al.*, J. Phys. Chem. C,115, p.24586-24591. **Corresponding Authors K. Yanagi, E-mail**: yanagi-kazuhiro@tmu.ac.jp.

Interband Scattering via Effective-Diameter Modulation in Single-Wall Carbon Nanotubes

Nikita Gavrilov[1], Eden Levi[1], Alon Strugatsky[1], Michael Shlafman[1], Kenji Watanabe[2], Takashi Taniguchi[2], and Yuval E. Yaish[1]

[1]*Andrew and Erna Viterbi Faculty of Electrical and Computer Engineering, Technion, Haifa 32000, Israel*

[2]*National Institute for Materials Science, 1-1 Namiki, Tsukuba 305-0044, Japan*

Usually, electrical transport through small-diameter single-wall carbon nanotube (SWCNT) is dominated by its lowest subband, and participation of higher subbands in transport is either negligible or hard to observe. However, by modifying the shape and electrostatic environment of a carbon nanotube (CNT) transistor one can alter the appearance of the next Van-Hove singularity and increase the rate for interband scattering. We fabricate CNT field effect transistors (CNTFETs) with different environments for different segments of the same CNT. In those segments encapsulated by hexagonal boron nitride (hBN), we observe a reduction of interface scattering, allowing the observation of a clear current step near room temperature. Using the Landauer formalism, we develop a model for transport in CNTFETs that considers interband scattering [1]. The model suggests that the encapsulation increases the effective diameter of the encapsulated CNT, thus decreasing the gaps between consequent bands and allowing the observation of higher bands at lower gate values. This observation alludes to the importance of taking the electrical and mechanical influence of the CNT's environment on its electrical performance.

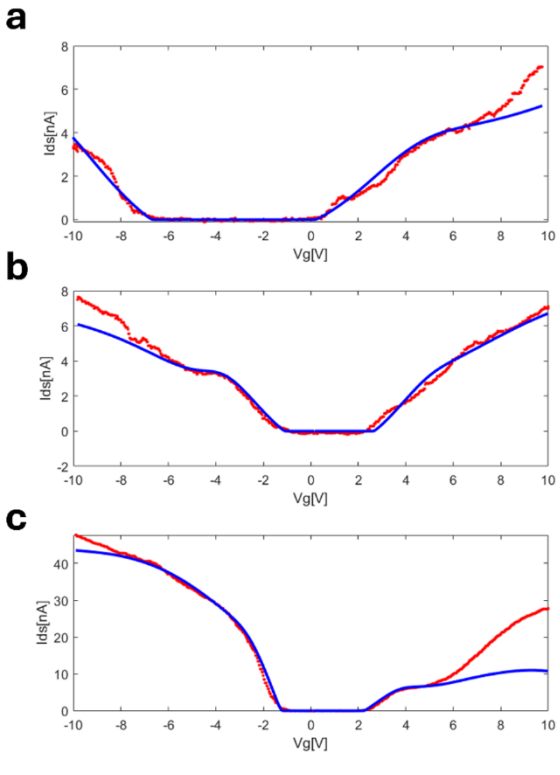

Figure: Transfer characteristics (red) and the model's fitting (blue) to three different sections of the same CNT. A good fit is obtained up to the second band

References

[1] Zhou, Xinjian, et al. *Physical Review Letters* **95**.14 (2005).

Thermal characterization of highly thermally conductive SWCNT films employing two-laser Raman thermometry

T. Swoboda[1], M. Magg[2], C. Borja Peña[3], P. Tan[1], J. Yang[1], D. Capolat Palomar[1], W. Wenseleers[4], S. Cambré[3], B. Flavel[2], J. Rodriguez-Viejo[1,5], M. Sledzinska[1]

[1]*Catalan Institute of Nanoscience and Nanotechnology (ICN2), 08193, Barcelona, Spain*

[2]*Institute of Nanotechnology, Karlsruhe Institute of Technology, 76344, Eggenstein-Leopoldshafen, Germany*

[3]*Theory and Spectroscopy of Molecules and Materials, Department of Physics, University of Antwerp, 2610. Antwerp, Belgium*

[4]*Nanostructured and Organic Optical and Electronic Materials, Department of Physics, University of Antwerp, 2610, Antwerp, Belgium*

[5]*Physics department, Autonomous University of Barcelona (UAB) Campus UAB, Bellaterra, 08193, Barcelona, Spain*

Carbon nanotubes (CNT) display significant potential for future electronic devices.[1] Beyond their excellent electronic properties, such as their high carrier mobility, CNT are gaining interest due to their heat spreading capabilities.[2] Despite this potential, experimental studies on the thermal properties of CNT films remain scarce. In 2023, Mehew *et.al.* investigated the thermal conductivity in various CNT structures based on the temperature decay of heated films using a two-laser Raman thermometry (2LRT) approach.[2] This opens the field for further studies on material modification, such as the alignment or the functionalization of the films, which are essential for the optimization of their heat spreading characteristics.

In this study, we measure the thermal conductivity in free standing single walled CNT (SWCNT) films by employing 2LRT. Randomly oriented endohedral doped SWCNT films were transferred onto a substrate with various openings, resulting in suspended areas of the film. This allows us to heat the films from below with a static laser, while a second laser from above probed the resulting temperature profile of the heated area, as illustrated in Figure 1 **a**. Figure 1 **b** displays a 2D temperature map of the heated films and Figure 1 **c** presents the corresponding 1D temperature profile. From these images we extract the temperature decay away from the hot spot, allowing us to calculate the thermal conductivity of the films. Other relevant sample characteristics are measured with SEM and AFM. For the investigated CNT films, we observed a relatively high thermal conductivity of 28.5 ± 1.4 W/(m·K). Based on these results, we fitted the measured temperature profile with finite element method (FEM) simulations.

These findings provide insights into the potential impact of doping on the heat spreading characteristics of CNT films and pave the way for a deeper understanding of the functionalization in these films. Future studies on the doping and the CNT characteristics will further contribute to the exploration of the thermal properties in CNT films.

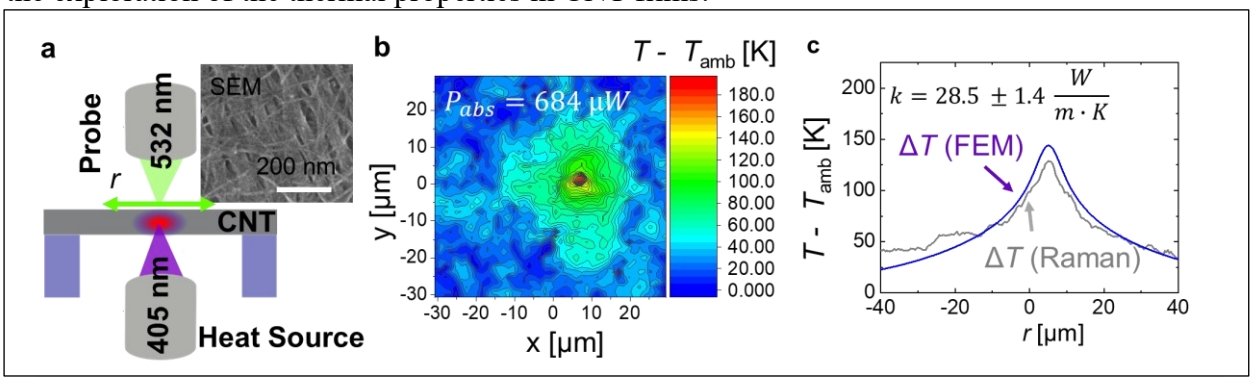

Figure 1: a Schematic drawing of the two laser Raman (2LRT) setup, the green arrow is illustrating the scan line direction with the coordinate *r* of the probe laser, the inset figure shows a SEM image of the sample surface, **b** 2D temperature map obtained in the suspended area of the film with an absorbed power of P_{abs} = 684 µW, **c** Temperature profile of the measurements and FEM simulation across the hot spot as a function of *r*.

References

[1] L. Peng *et al.*, *Nature Electronics*, **2**, 499-505 (2019).
[2] J. D. Mehew *et al., ACS Appl. Mater. Interfaces,* **15**, 51876−51884 (2023).

ANISOTROPIC OPTICAL PROPERTIES OF MONOLAYER ALIGNED SINGLE-WALLED CARBON NANOTUBES AND 2D MATERIALS

G.A. Ermolaev[1], M.G. Burdanova[2], Y. Xie[3], L. Qian[3], M.K. Tatmyshevskiy[2], A.S. Slavich[2], A.V. Arsenin[1], V.S. Volkov[1], J. Zhang[3], A.I. Chernov[2,4]

[1]Emerging Technologies Research Center XPANCEO Emmay Tower Dubai (United Arab Emirates), [2]Center for Photonics and 2D Materials Moscow Institute of Physics and Technology Dolgoprudny (Russia), [3]Beijing National Laboratory for Molecular Sciences College of Chemistry and Molecular Engineering Peking University Beijing, (P. R. China), [4]Russian Quantum Center Skolkovo Innovation City (Russia)

The 2D materials are the fundamental building blocks for modern optoelectronics and photonics. Optically anisotropic monolayers give even more flexibility in device design and performance. However, the random orientation of optical axes in the large-scale samples prevents anisotropic monolayers from widespread use. The alternative structure is a monolayer of aligned single-walled carbon nanotubes (SWCNTs) with an anisotropic dielectric tensor. Herein, aligned SWCNTs monolayer anisotropic optical constants in a broad spectral range (250–1700 nm) are measured for the first time. It is discovered that it has a large birefringence of $\Delta n = 0.2$ and a high dichroism of $\Delta k = 0.4$. Moreover, it is demonstrated that aligned SWCNTs monolayer optical response can be described by an effective medium approximation using the graphene dielectric function. In addition, it gives a universal approach for a determination of carbon concentration in nanotubes structures. It also applies for other types of carbon nanotubes, such as multi-walled and randomly oriented carbon nanotubes arrays. As the result, aligned SWCNTs monolayer optical constants are added to the optical anisotropy database, which facilitates the longstanding challenge of using 1D structures in two dimensions, and a rapid characterization method for carbon nanotubes is provided [1].

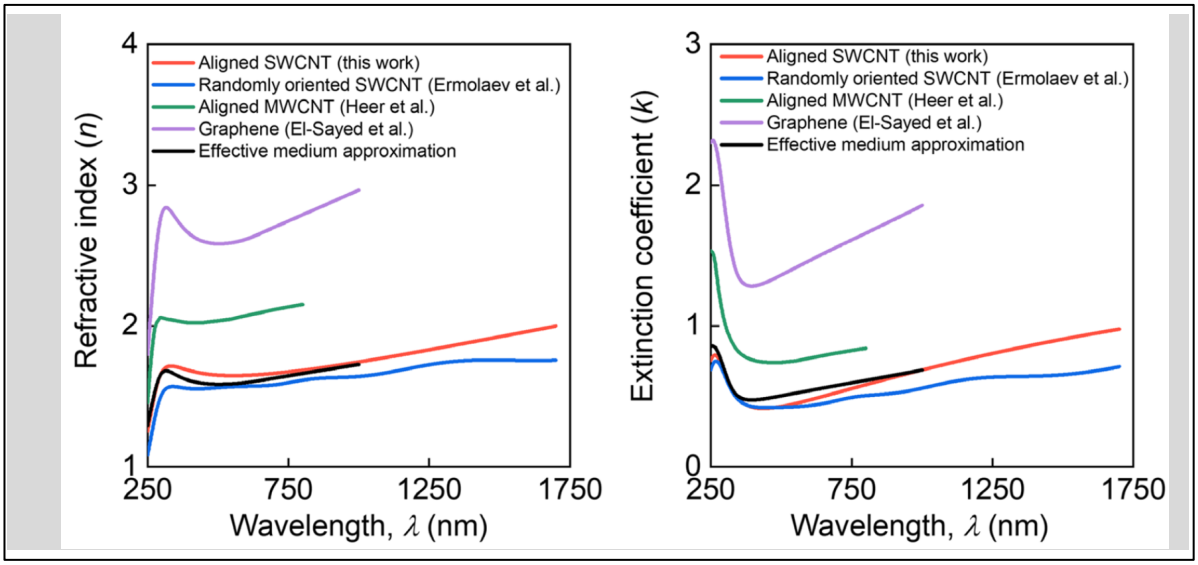

Figure caption: Refractive index and extinction coefficient of carbon-based materials

Moreover, carbon nanotube networks serve as an example of a system with controllable orientation achieving on-demand optical properties. Such a network allows programming their optical response depending on the orientation of the constituent carbon nanotubes and leads to the switching of its dielectric tensor from isotropic to anisotropic [2]. Furthermore, it also allows for the achievement of wavelength-dispersion for their principal optical axes. The results originate from two unique carbon nanotubes features: uniaxial anisotropy from the well-defined cylindrical geometry and the intersection interaction among individual carbon nanotubes.

The work was supported by by the MESR, Agr. 075-15-2024-680.

References

[1] G. A. Ermolayev *et al.*, *Phys. Stat. Sol. RRL 2300199 (2023).*
[2] K. V. Voronin *et al.*, *Adv. Sci.* 2404694 (2024).

Fluctuations, dynamics and structure of the crystal edge of growing carbon nanotubes

Daniel Hedman[1] and Christophe Bichara[2]

[1] *CMCM, IBS, Ulsan, 44919,(Republic of Korea),* [2]*CINaM, Aix-Marseille Univ and CNRS, Marseille (France).*

Three decades of unrelenting research have suggested that understanding the interactions between the few dozens of carbon atoms forming the tube's open edge and the metal catalyst in contact with them is essential for the effective control carbon nanotube growth (1). Recent experiments showing that the observed growth is more complex (2-4) than previously thought raised new questions and required to significantly improve the accuracy and capabilities of our computer simulations tools.

In this poster we improve the Machine Learning based Interatomic Potentials (MLIP) used previously (5, 6) to study how the large fluctuations due to the high synthesis temperature and small size of the tube edge influences the mechanisms leading to a net elongation or receding of the tube. Microsecond scale Molecular Dynamics (MD) and Grand Canonical Monte Carlo simulations coupled with MD (GCMC/MD) are used to simulate the catalytic growth or etching that are driven by the carbon chemical potential fixed by the synthesis conditions.

The close agreement between the activation energies for SWNT growth measured experimentally by Pimonov et al. (3) and obtained by Molecular Dynamics demonstrates the quality of our MLIP. We then show that the partial rates of carbon attachment/detachment and rings closure/opening events at the edge, measured by either MD or GCMC/MD, depend linearly on the chiral angle of the SWNT. This implies that the overall rate, the sum of these two contributions, is also linear. Large error bars are observed, which can be explained by the fact that this overall rate is the difference between partial quantities that are up to 20 times larger, themselves affected by error bars.

Our most striking result is that when considering chemical potentials symmetrical with respect to the equilibrium potential, the chiral angle dependences of the measured growth and etching rates are not symmetrical. This difference may suggest ways of kinetically influencing the chiral distribution by alternating growth and etching sequences.

References

1) Magnin Y., *et al.* Entropy-driven stability of chiral single-walled carbon nanotubes. *Science*, *362*(6411), 212–215 (2018).
2) Koyano, B *et al.*, Regrowth and catalytic etching of individual single-walled carbon nanotubes studied by isotope labeling and growth interruption. *Carbon*, *155*, 635–642 (2019).
3) Pimonov V. *et al*. Dynamic Instability of Individual Carbon Nanotube Growth Revealed by In Situ Homodyne Polarization Microscopy. *Nano Letters*, *21*(19), 8495–8502 (2021).
4) Förster G. D., *et al.* Swinging Crystal Edge of Growing Carbon Nanotubes. *ACS Nano*, *17*(8), 7135–7144 (2023).
5) Hedman D. *et al.* Dynamics of growing carbon nanotube interfaces probed by machine learning-enabled molecular simulations, *Nature Comms*, 15(1), 4076 (2024).
6) Sun S. *et al.* Chirality-Dependent Kinetics of Single-Walled Carbon Nanotubes from Machine-Learning Force Fields, *JACS* 147, 8, 7103–7112 (2025).

Session
NT 25（The 25th International Conference on the Science and Applications of Nanotubes and Low-

| Main conference：Main conference

Wed. Jun 18, 2025 9:30 AM - 10:40 AM JST | Wed. Jun 18, 2025 12:30 AM - 1:40 AM UTC Centennial Hall (Clock Tower Centennial Hall)

[18ma] Main Conference

Chair: Toshiaki Kato

9:30 AM - 10:10 AM JST | 12:30 AM - 1:10 AM UTC

[18ma-01]

Ultra-clean interfaces in atomically thin materials for electronics

*Manish Chhowalla[1] (1. University of Cambridge (UK))

10:10 AM - 10:40 AM JST | 1:10 AM - 1:40 AM UTC

[18ma-02]

Flexoelectricity in Self-Assembled Graphene Nanowrinkles

Sathvik Ajay Iyengar[2,3], James G McHugh[3], Jonathan P Salvage[4], Alan Dalton[5], Manoj Tripathi[5], P M Ajayan[2], *Vincent Meunier[1] (1. The Pennsylvania State University (United States of America), 2. Rice University (United States of America), 3. University of Manchester (UK), 4. University of Brighton (UK), 5. University of Sussex (UK))

Ultra-clean interfaces in atomically thin materials for electronics

Manish Chhowalla

University of Cambridge, UK

In this presentation I will summarise our work on ultra-clean van der Waals (vdW) contacts on atomically thin semiconductors. We have demonstrates that vdW contacts on two dimensional transition metal dichalcogenides (2D TMDs) enables the realisation of field effect transistors with low contact resistance and high mobility. We have also adopted the strategy of vdW contacts for efficient spin injection and collection. We show that the vdW gap between magnetic metal electrodes and graphene is an efficient tunnel barrier for spin injection. Very recently, we have demonstrated high efficiency WSe_2 solar cells with vdW contacts. Specifically, we can achieve near ideal diodes with vdW contacts with high on/off ratio and an ideality factor of 1.1. These diodes results in solar cells with very high current density and open circuit voltage resulting in efficiency values of > 10%. My presentation will summarise methods for achieving vdW contacts and their fundamental properties that enable the high performance devices described above.

Flexoelectricity in Self-Assembled Graphene Nanowrinkles

Sathvik Ajay Iyengar[1], James G. McHugh[2], Jonathan P. Salvage[3], Robert Vajtai[1], Alan Dalton[4], Manoj Tripathi[4], P.M. Ajayan[1], Vincent Meunier[5]

[1]Department of Materials Science and NanoEngineering, Rice University (USA); [2]National Graphene Institute, University of Manchester, (UK);[3]School of Pharmacy and Biomolecular Science, University of Brighton (UK); [4] Department of Physics and Astronomy, University of Sussex (UK); [5] Department of Engineering Science and Mechanics, Pennsylvania State University (USA)

Flexoelectricity—the polarization induced by strain gradients—manifests with remarkable intensity in two-dimensional materials due to their extraordinary mechanical flexibility and structural sensitivity. This phenomenon reaches peak expression in highly curved nanostructures, where extreme charge redistribution creates measurable electrostatic effects.

Our presentation will begin with an introduction to flexoelectricity's fundamental principles in 2D materials. [1] We will then explore its microscopic origins in graphene nanowrinkles (NW) through density functional theory (DFT), demonstrating how intense curvature at top of the NWs generates significant local Gaussian curvature values, producing observable macroscopic effects.

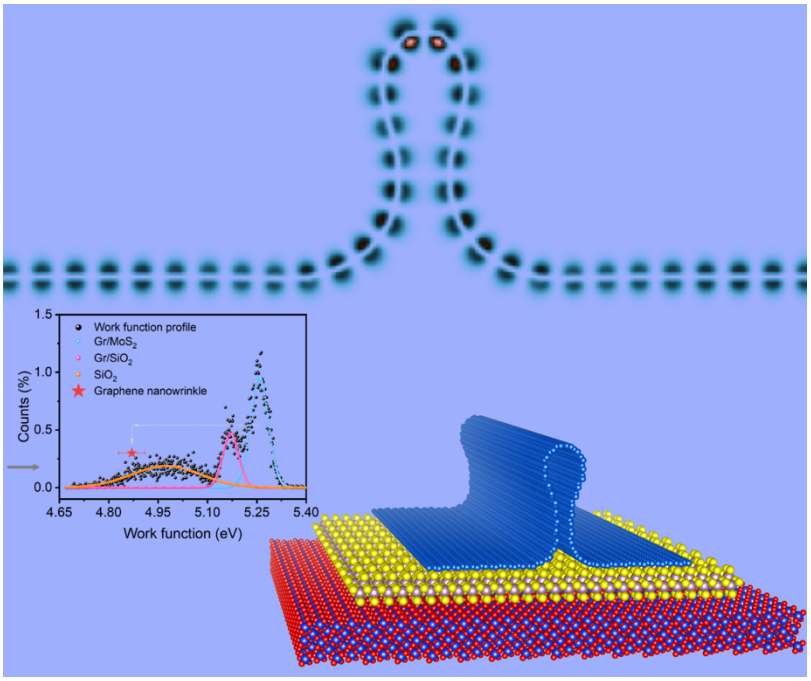

Figure: (Top) Low-energy charge distribution in a section of NW, as calculated by DFT. (Bottom Right) The experimental setup consists of a self-assembled NW on top of an MoS_2 slab deposited on a silica substrate. (Bottom Left: measurement of work function.

Our experimental observations focus on self-assembled graphene NWs formed on flat MoS_2 substrates. The mismatch in elastic properties between these materials creates strain gradients, which we mapped using sub-micro Raman spectroscopy. Conductive atomic force microscopy (c-AFM) measurements revealed consistent, reproducible flexoelectric currents under appropriate bias potential across extensive networks of dense NWs.

Our research establishes graphene NWs as an ideal system for investigating strong flexoelectric effects. The findings highlight significant potential applications in strain-engineered nanoscale electronic and electromechanical devices, opening new avenues for harnessing this phenomenon in future technologies. This work bridges theoretical predictions with experimental validation, advancing our understanding of how nanoscale structural deformations in 2D materials can be leveraged for novel electronic properties and functionalities. [2]

References

[1] S. Kalinin and V. Meunier, Phys. Rev. B, 77(3), 033403 (2008)
[2] Sathvik Ajay Iyengar et al, manuscript in preparation (2025)

Session
NT 25（The 25th International Conference on the Science and Applications of Nanotubes and Low-

| Main conference：Main conference

Wed. Jun 18, 2025 11:00 AM - 12:10 PM JST | Wed. Jun 18, 2025 2:00 AM - 3:10 AM UTC Centennial Hall (Clock Tower Centennial Hall)

[18ss] Special panel session of 35 Years of Carbon Nanotubes –Past, current and future applications in industry—

Kenji Hata (AIST)
Shigeo Maruyama (Zhejiang University, The University of Tokyo, Nagoya University)

Round 1: (15 min. presentation)
Kohei Arakawa (Zeon Corporation)
Morinobu Endo (Shinshu University)
Sumio Iijima (Meijo University)

Round 2: (5 min. presentation)
Fei Wei (Tsinghua University)
James Elliot (University of Oxford)
Esko Kauppinen (Aalto University)
Michael Arnold (University of Wisconsin-Madison)

Round 3: Panel discussion

This special session is Sponsored by NEC, UNI ROOT, and Zeon.

Session
NT 25（The 25th International Conference on the Science and Applications of Nanotubes and Low-

| Main conference：Main conference

Thu. Jun 19, 2025 9:30 AM - 12:10 PM JST | Thu. Jun 19, 2025 12:30 AM - 3:10 AM UTC Centennial Hall (Clock Tower Centennial Hall)

[19ma] Main Conference

Chair: Ryo Kitaura, Susumu Okada

9:30 AM - 10:10 AM JST | 12:30 AM - 1:10 AM UTC

[19ma-01]

Luminescent Defects in Single-Wall Carbon Nanotubes: Chemistry & Applications

*Jana Zaumseil[1] (1. Heidelberg University (Germany))

10:10 AM - 10:40 AM JST | 1:10 AM - 1:40 AM UTC

[19ma-02]

Electroluminescence From Monochiral Carbon Nanotubes With Quantum Defects

*Ralph Krupke[1] (1. Institute of Nanotechnology, Karlsruhe Institute of Technology (Germany))

11:00 AM - 11:30 AM JST | 2:00 AM - 2:30 AM UTC

[19ma-03]

Infrared Image Sensor using Carbon Nanotubes

*Ryota Yuge[1,2], Tomo Tanaka[1,2], Masahiko Sano[1], Noriyuki Tonouchi[1,2], Akinobu Shibuya[1,2], Taizo Shibuya[1,2], Masataka Noguchi[1,2], Toshie Miyamoto[1,2], Naoki Oda[1] (1. NEC Corporation (Japan), 2. National Institute of Advanced Industrial Science and Technology (Japan))

11:30 AM - 11:50 AM JST | 2:30 AM - 2:50 AM UTC

[19ma-04]

Nanofluidic transport in narrow single-wall carbon nanotube pores

*Aleksandr Noy[1] (1. Lawrence Livermore National Laboratory (United States of America))

11:50 AM - 12:10 PM JST | 2:50 AM - 3:10 AM UTC

[19ma-05]

Thermal rectification using Tesla valve structure in graphite microribbon

*Masahiro Nomura[1,3], Roman Anufriev[2,3], Laurent Jalabert[3], Kenji Watanabe[4], Takashi Taniguchi[4], Sebastian Volz[3] (1. The University of Tokyo (Japan), 2. Universite de Lyon (France), 3. LIMMS, CNRS-IIS UTokyo (Japan), 4. NIMS (Japan))

LUMINESCENT DEFECTS IN SINGLE-WALL CARBON NANOTUBES: CHEMISTRY & APPLICATIONS

J. Zaumseil

Institute for Physical Chemistry, Heidelberg University (Germany)

The functionalization of semiconducting single-wall carbon nanotubes (SWCNTs) with luminescent oxygen or sp^3 defects leads to exciton trap-states with new red-shifted emission features in the near-infrared (see **Figure 1**) and enhanced overall photoluminescence (PL) quantum yields. Over the past decade they have become a highly promising material platform for next-generation in-vivo imaging, metabolite sensing, and single-photon emission. The growing interest in the application of SWCNTs with luminescent defects drives the development of more efficient and selective functionalization methods where the choice of reactants and reaction parameters enables precise control of the type of defect and thus emission wavelengths and PL quantum yields.

Here, I will give an overview of the different methods that were developed to introduce luminescent defects into SWCNTs and the current understanding of their electronic and optical properties. I will then focus on analytical methods to precisely quantify the number of introduced defects [1,2] and our recent efforts to tune the chemistry of luminescent defects for single-photon emission [3], optical sensing of biomolecules [4] and enhanced PL quantum yields of ultrashort nanotubes as near-infrared emitters for bioimaging [5]. I will further highlight the role of optimized and scalable functionalization procedures to observe and investigate the circular dichroism of luminescent quantum defects in enantiomer-sorted SWCNT dispersions.

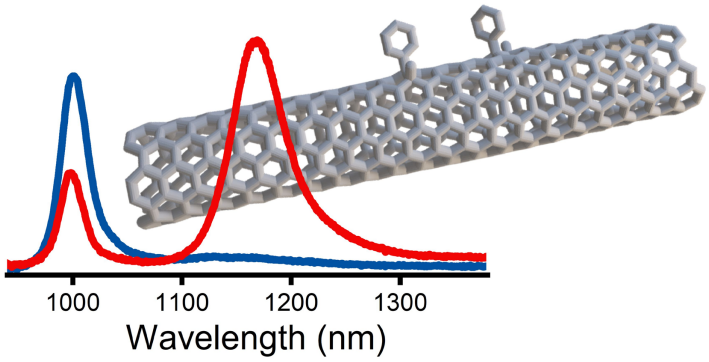

Figure 1: Near-infrared PL spectra of pristine (blue) and functionalized (6,5) SWCNTs (red) in dispersion.

References

[1] F.L. Sebastian *et al., ACS Nano* **17**, 21771-21781 (2023).
[2] F.L. Sebastian *et al., Nanoscale Horizons* ***9****, 2286-2294 (2024).*
[3] S. Settele *et al., Nature Communications* **12**, 2119 (2021).
[4] S. Settele *et al., Nature Communications* **15**, 706 (2024).
[5] S. Settele *et al., ACS Nano* **18**, 20667-20678 (2024).

Electroluminescence From Monochiral Carbon Nanotubes With Quantum Defects

R. Krupke[1]

[1]*Institute of Nanotechnology and Institute of Quantum Materials and Technologies, Karlsruhe Institute of Technology, Germany*

We present electroluminescence spectroscopy data from single-tube devices based on (7,5) carbon nanotubes functionalized with dichlorobenzene molecules and connected to graphene electrodes. We observe electrically generated, defect-induced emissions that are controllable by electrostatic gating and are strongly red-shifted compared to emissions from pristine nanotubes. These defect-induced emissions are attributed to excitonic and trionic recombination processes, as determined by correlating electroluminescence excitation maps with electrical transport and photoluminescence data. Under cryogenic conditions, additional gate-dependent emission lines are identified as phonon-assisted hot-exciton electroluminescence from quasi-levels. Furthermore, we report single-photon defect-state emission observed via second-order correlation function measurements in a Hanbury Brown and Twiss experiment. Additionally, we demonstrate the integration of electroluminescent semiconducting carbon nanotubes into hybrid 2D-3D photonic circuits and outline our initial steps towards picosecond pulsed excitation.

References

[1] Min-Ken Li et al., ACS Nano 2022
[2] Min-Ken Li et al., ACS Nano 2024
[3] A. Ovvyan et al., Nat Commun 2023

Infrared Image Sensor using Carbon Nanotubes

Ryota Yuge[1, 2], Tomo Tanaka[1, 2], Masahiko Sano[1], Noriyuki Tonouchi[1, 2], Akinobu Shibuya[1, 2], Taizo Shibuya[1, 2], Masataka Noguchi[1, 2], Toshie Miyamoto[1, 2], Naoki Oda[1]

[1]NEC Corporation (Japan), [2]National Institute of Advanced Industrial Science and Technology (Japan)

A bolometer-type infrared image sensor is a technology that converts infrared radiation into electrical signals to obtain temperature information and can detect thermal images radiated from people and objects. Recently, the utilization in industrial fields has been activated, including thermography, inspection equipment for structures and foodstuffs, night vision to support nighttime automobile driving, and security cameras. One of the current challenges is to increase sensitivity. The effective means is to improve the resistance temperature coefficient (TCR) or lower the resistance of the bolometer material.

Single-walled carbon nanotubes (CNTs) exhibit semiconducting and metallic properties depending on the arrangement of carbon hexagons. We have succeeded in developing an original technology to separate semiconducting components from single-walled CNTs with high purity by the electric field-induced layer formation method [1-2]. Using this technology and the printing fabrication technique we have developed in our CNT flexible thin-film transistor research [3], we fabricated a bolometer film with controlled orientation of semiconducting CNTs and achieved a TCR of -6%/K, which is three times higher than that of VO_x, a conventional material [4]. In this study, we realized a new device structure by integrating CNT printing and fabrication technologies and our original MEMS (Micro Electro Mechanical Systems) device fabrication technology [5], and succeeded in fabricating a high-resolution infrared image sensor with 640 × 480 pixels by arraying these devices [6]. The thermal separation structure was realized by making a void between the infrared absorbing layer and the substrate, and connecting the infrared absorbing layer and the contact electrode only with beam wiring. Basic characterization of the fabricated sensor single element showed that a responsivity (R_v) of 10^5 V/W or higher was obtained at a bias voltage of 0.2 V. In the noise measurements, the 1/f characteristic was mainly observed, indicating that 1/f noise is dominant at the assumed sensor operating speed. The specific detectivity D* calculated from the responsivity and noise was higher than that of the VO_x element used for comparison. Details will be reported on the day.

Acknowledgments: The study was partly supported by Innovative Science and Technology Initiative for Security Grant No. JPJ004596, ATLA, Japan.

References

[1] K. Ihara et al., *J. Phys. Chem. C*, **115**, 22827-22832 (2011).
[2] K. Ihara et al., *ACS Appl. Nano Mater*. **2**, 4286−4292 (2019).
[3] H. Numata et al., *Proc. 16th. Inter. Cof. IEEE-NANO*, 849-852 (2016).
[4] T. Tanaka et al., *Proc. SPIE*, **12534**, 125341U (2023).
[5] S. Tohyama, et al., *Opt. Eng*. **45**, 014001 (2006).
[6] T. Tanaka et al., *Proc. of SPIE*, **13046** 130460X (2024).

Nanofluidic transport in narrow single-wall carbon nanotube pores

A. Noy[1,2]

Lawrence Livermore National Laboratory (USA), University of California Merced (USA).

Spatial confinement is important for many transport phenomena ranging from industrial membrane separations to biological transport, where confinement effects help to achieve exquisite selectivity and high transport efficiency. Carbon nanotube pores have well-defined dimensions and a smooth chemically-inert surface that make them an idea channel structure for studying effects of strong spatial confinement on transport of water and ions. I will show that carbon nanotube porins—pore channels formed by ultra-short carbon nanotubes assembled in a lipid membrane matrix—can exploit spatial confinement to transport water, protons, and ions with high efficiency. In particular, I will focus on the unusual mechanism of ion transport in these pores, as well as on the electronic properties of the channel walls on the transport efficiency [1,2]. Overall, nanotube porins represent simple, precise, and versatile model membrane pores that could be ideal for exploring the physical principles for next generation of separation technologies.

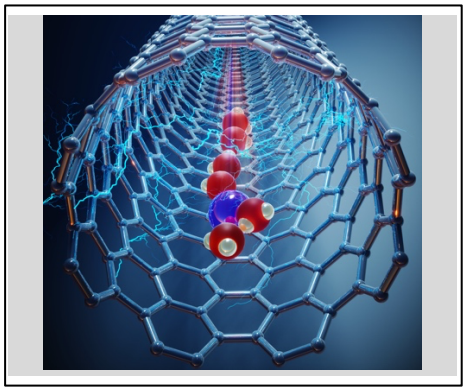

Illustration showing ion-water cluster inside a carbon nanotube channel.

References

[1] Z. Li *et al.*, *Nature Nanotechnol.* **18**, 177-183 (2023).

[2] Y. Li *et al.*, *Nature Mater.* **23**, 1123-1130 (2024).

Thermal rectification using Tesla valve structure in graphite microribbon

X. Huang[1], R. Anufriev[1,2], L. Jalabert[1,3], K. Watanabe[4], T. Taniguchi[5], S. Volz[1,3] and M. Nomura[1,3]

[1]Institute of Industrial Science, The University of Tokyo (Japan), [2]Universite de Lyon, INSA Lyon, CNRS, CETHIL, UMR5008, Villeurbanne (France), [3]LIMMS, CNRS-IIS IRL 2820, The University of Tokyo (Japan), [4]Research Center for Electronic and Optical Materials, National Institute for Materials Science (Japan), [5]Research Center for Materials Nanoarchitectonics, NIMS (Japan)

Phonon hydrodynamics is a macroscopic quantum thermal phenomenon from the collective behavior of quantized vibrational excitations (phonons) in solids, similar to fluid dynamics. As a long-standing topic that has been revisited recently, phonon hydrodynamics motivates theoreticians and experimentalists to explore it at micro-and nanoscale and at elevated temperatures. Graphitic materials, with their intensive normal process in nature, are currently considered as perfect hosts to establish the hydrodynamic flow. We investigated phonon Poiseuille flow in graphite samples with both natural (98.9% ^{12}C, 1.1% ^{13}C) and purified (99.98% ^{12}C, 0.02% ^{13}C) carbon isotope concentrations and demonstrated hydrodynamic heat transfer in graphite microribbon in the temperature range of 40 to 90 K [1].

We further consider its potential applications in thermal management. Inspired by the Tesla valve, which benefits the rectification of fluid flow in microfluidic systems (Fig. 1a), we design and fabricate the Tesla valve structure in graphite for modern solid-state thermal rectifiers, as shown in Fig. 1(b). In the forward direction (top), hydrodynamic phonons predominantly travel from the heat source to the sink via the main channel. Conversely, in the backward case (bottom), two distinct hydrodynamic phonon flows diverge from the heat source. The convergence of these two flows leads to a loss of phonon momentum and introduces resistance to thermal transport. In Fig. 1(c), we define the diodicity of the heat flow as the ratio of κ_f to κ_r. This phenomenon results in a pronounced diode effect in the hydrodynamic temperature range of 20-65 K, wherein κ_f surpasses κ_r by 15.4% at 45 K. This demonstration extends the concept of Tesla valve from fluid to heat transfer after 100 years of the invention in 1920 by Nicola Tesla [2].

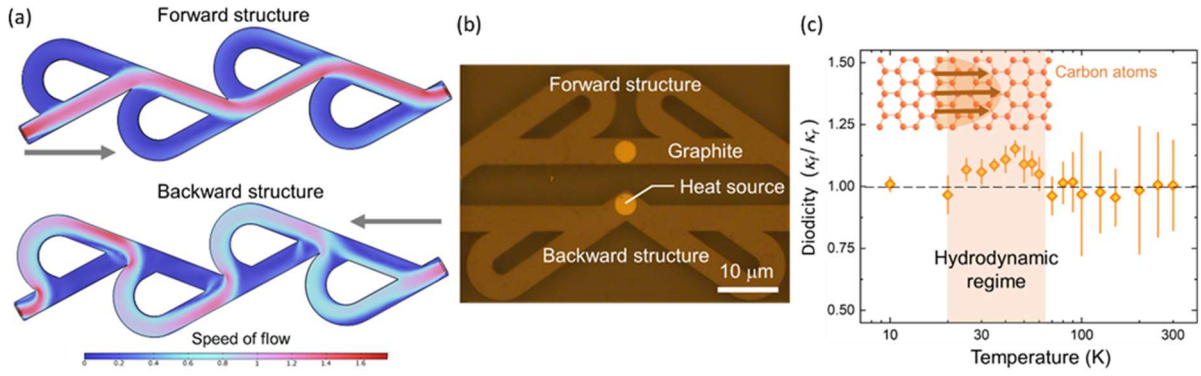

Fig. 1. (a) Illustration of the liquid flow in a Tesla valve structure. (b) Optical microscope image of the fabricated graphite Tesla valve structures. (c) Observed thermal rectification in the hydrodynamic regime.

References

[1] X. Huang, …, and M. Nomura, *Nat. Commun*. **14**, 2044 (2023).
[2] X. Huang, …, and M. Nomura, *Nature* **634**, 1086 (2024).

Session
NT 25（The 25th International Conference on the Science and Applications of Nanotubes and Low-

| Parallel Symposia：Symposium on Nanomaterials for Energy and Electronics

Thu. Jun 19, 2025 2:00 PM - 5:20 PM JST | Thu. Jun 19, 2025 5:00 AM - 8:20 AM UTC Conference room 5a/5b(INNOVATION BLDG., 5F)

[19en] Energy & Electronics

Chair:Yutaka Matsuo, Yutaka Takaguchi

2:00 PM - 2:40 PM JST | 5:00 AM - 5:40 AM UTC

[19en-01]

MIXED-DIMENSIONAL HETEROSTRUCTURES FOR ELECTRONIC AND ENERGY TECHNOLOGIES

*Mark Hersam[1] (1. Northwestern University (United States of America))

2:40 PM - 3:00 PM JST | 5:40 AM - 6:00 AM UTC

[19en-02]

Automated processing and transfer of two-dimensional materials with robotics

*Yixuan Zhao[1] (1. Peking university (China))

3:00 PM - 3:20 PM JST | 6:00 AM - 6:20 AM UTC

[19en-03]

Single-Walled Carbon Nanotubes in Artificial Photosynthesis

*Yutaka Takaguchi[1], Linh Thi Pham[1], Kazushi Mukai[1], Kazutaka Gomado[1] (1. University of Toyama (Japan))

4:00 PM - 4:20 PM JST | 7:00 AM - 7:20 AM UTC

[19en-04]

Semiconducting Carbon Nanotube-Polythiophene Composites Showing Large Thermoelectric Power Factors

*Yoshiyuki Nonoguchi[1] (1. Kyoto Inst. Tech. (Japan))

4:20 PM - 4:40 PM JST | 7:20 AM - 7:40 AM UTC

[19en-05]

Suspended carbon nanotube quantum dot heat engines

*Frederik van Veen[1,2], Jordi Picó Cortés[3], Seoho Jung[4], Bhaskar Ghawri[1], Natanael Lanz[4], Marko Nikolic[4], Andre Butzerin[4], Luca Ornago[4], Michel Calame[1,6], Andrea Donarini[3], Milena Grifoni[3], Herre van der Zant[5], Maria El Abbassi[4], Mickael Perrin[1,2] (1. Transport at Nanoscale Interfaces Laboratory, Empa (Switzerland), 2. Department of Information Technology and Electrical Engineering, ETH Zurich (Switzerland), 3. Institute for Theoretical Physics, University of Regensburg (Germany), 4. Chiral Nano AG (Switzerland), 5. Delft University of Technology (Netherlands), 6. Department of Physics, University of Basel, (Switzerland))

4:40 PM - 5:00 PM JST | 7:40 AM - 8:00 AM UTC

[19en-06]

STRUCTURE-DEFINED THERMOELECTRIC PERFORMANCE OF THIN SINGLE-WALLED CARBON NANOTUBE FILMS

*Dmitry V. Krasnikov[1], Jiraphat Khongthong[1], Nikita I. Raginov[1], Anastasia E. Goldt[1], Vladislav A. Kondrashov[1], Albert G. Nasibulin[1] (1. Skolkovo Institute of Science and Technology (Russia))

5:00 PM - 5:20 PM JST | 8:00 AM - 8:20 AM UTC

[19en-07]

SiO-$LiNi_{0.8}Co_{0.1}Mn_{0.1}O_2$ Full Cell Realized by Three-Dimensional Current Collectors of Carbon Nanotubes

Session
NT 25（The 25th International Conference on the Science and Applications of Nanotubes and Low-
*Tomotaro Mae[1], Suguru Noda[1] (1. Waseda University (Japan))

MIXED-DIMENSIONAL HETEROSTRUCTURES FOR ELECTRONIC AND ENERGY TECHNOLOGIES

Mark C. Hersam[1]

[1]*Department of Materials Science and Engineering, Northwestern University, Evanston, IL 60208, USA*

Layered two-dimensional (2D) materials interact primarily via van der Waals bonding, which has created opportunities for heterostructures that are not constrained by epitaxial lattice matching requirements [1]. However, since any passivated, dangling bond-free surface interacts with another via non-covalent forces, van der Waals heterostructures are not limited to 2D materials alone. In particular, 2D materials can be integrated with a diverse range of other materials, including those of different dimensionality, to form mixed-dimensional van der Waals heterostructures. Furthermore, chemical functionalization provides additional opportunities for tailoring the properties of 2D materials and the degree of coupling across heterointerfaces. In this manner, a variety of optoelectronic and energy applications can be enhanced including photodetectors, optical emitters, supercapacitors, and batteries [2-4]. Furthermore, mixed-dimensional heterostructures enable unprecedented electronic device function to be realized that exploit neuromorphic, opto-spintronic, and quantum phenomena [5-8]. In addition to technological implications for electronic and energy technologies, this talk will explore several fundamental issues including band alignment, doping, trap states, and charge/energy transfer across mixed-dimensional heterointerfaces.

References

[1] S. Hadke, *et al.*, *Chemical Reviews*, **125**, 835 (2025).
[2] M. I. B. Utama, *et al.*, *Nature Communications*, **14**, 2193 (2023).
[3] S. V. Rangnekar, *et al.*, *ACS Nano*, **17**, 17516 (2023).
[4] L. E. Chaney, *et al.*, *Advanced Materials*, **37**, 2305161 (2024).
[5] X. Yan, *et al.*, *Nature Electronics*, **6**, 862 (2023).
[6] H. Liu, *et al.*, *Nature Electronics*, **7**, 876 (2024).
[7] J. T. Gish, *et al.*, *Nature Electronics*, **7**, 336 (2024).
[8] X. Yan, *et al.*, *Nature*, **624**, 551 (2023).

Automated processing and transfer of two-dimensional materials with robotics

Yixuan Zhao[1,3], Li Lin[2,3]*, Zhongfan Liu[1,3]*

[1]College of Chemistry and Molecular Engineering, Peking University, Beijing 100871, P. R. China, [2]School of Materials Science and Engineering, Peking University, Beijing 100871, P. R. China, [3]Beijing Graphene Institute, Beijing 100095, P. R. China.

The mature and well-developed chemical vapor deposition (CVD) growth technologies have enabled two-dimensional (2D) materials and their heterostructures to take the centre stage in developing material platforms for next-generation electronics and advanced photonic devices for the semiconductor industry, quantum technologies, etc. However, the gap between 2D material production and end-user applications is the lack of a scalable technique to transfer the high-quality CVD-grown materials from their growth substrates to target substrates.

Herein, by engineering the interfacial adhesion and strain, we have achieved an automatic processing and the transfer of 2D materials with robotics. The deep insights into common challenges in delamination and lamination processes of 2D materials were discussed and addressed by introducing an ultrathin layer of Al coating and an Al oxidation step, which facilitate the fine tuning and precise control of interfacial adhesion and strain. The developed transfer technique and automated system are industrially compatible for batch production, which are demonstrated by the enhanced production capability, highly reliable transfer quality, and high uniformity and repeatability of the transferred 2D materials.

Demonstrated by life-cycle assessment (LCA), the automated robotic system delivers a green and sustainable transfer route with advantages in all environmental impact categories This automatic processing technique bridges the gap between 2D material production industry and the industry of advanced electronics and photonics, and has the potential to be extended to other material and nanotechnology system, thus, could boost the rapid development of the whole industry of 2D material manufacture and application industries.

Single-Walled Carbon Nanotubes in Artificial Photosynthesis

Y. Takaguchi[1], L. T. Pham[1], K. Mukai[1], K. Gomado[1]

[1]*Department of Materials Design and Engineering, University of Toyama (Japan)*

Photocatalytic water splitting ($2H_2O \rightarrow 2H_2 + O_2$), an endergonic reaction ($\Delta G = 237$ kJ/mol), is a key process in artificial photosynthesis for converting solar energy into chemical energy. Single-walled carbon nanotubes (SWCNTs) possess excellent light-harvesting properties,[1] making them promising candidates for a photosensitizer in artificial photosynthesis. However, examples of SWCNTs employed as solar-light absorbers in photocatalytic water splitting are limited. We have discovered that physical modification of SWCNTs by an amphiphilic C_{60}-dendron leads to a formation of a nano-hybrid with a SWCNT/C_{60} heterojunction that acts as an efficient photocatalyst for hydrogen evolution from water.[2,3] The external quantum yield (EQY) of SWCNT-photocatalyst having (8,3)tube as the core reached 13% upon illumination of 1000-nm-light, although conventional photocatalysts are inactive upon such near-IR illumination.[4] Furthermore, we have achieved overall water splitting using a Z-scheme photocatalytic system incorporating $BiVO_4$ as an oxygen evolution photocatalyst (OEP).

In this context, we will highlight several of our recent advances in SWCNT photocatalysts.[5-7] For example, we succeeded overall water splitting using commercially availableWO_3 as an OEP and iodide ions (I^-) as a redox mediator. Upon photoexcitation of the SWCNT, electron extraction from the exciton in SWCNTs to C_{60} take place to form charge separated state ($SWCNT^{+\bullet}/C_{60}^{-\bullet}$), subsequently the electron in C_{60} migrate to co-catalyst ($RuCl_3$) to generate H_2 via two-electron reduction of H+. The holes in the CNT photocatalyst are consumed by I^- ions to form I_3^-. The I_3^- ions subsequently receive electrons from WO_3, regenerating I^-. Consequently, we observed efficient H_2 evolution (2.2 μmol/h) and O_2 evolution (1.2 μmol/h) with the stoichiometric ratio 2 : 1 (H_2 : O_2) after 4 hours of visible light irradiation ($\lambda > 422$ nm). This result underscores the potential of cost-effective, SWCNT-photocatalyst systems for overall water splitting. Moreover, this approach can also be extended to water splitting reactions using TMDs as photosensitizers [8].

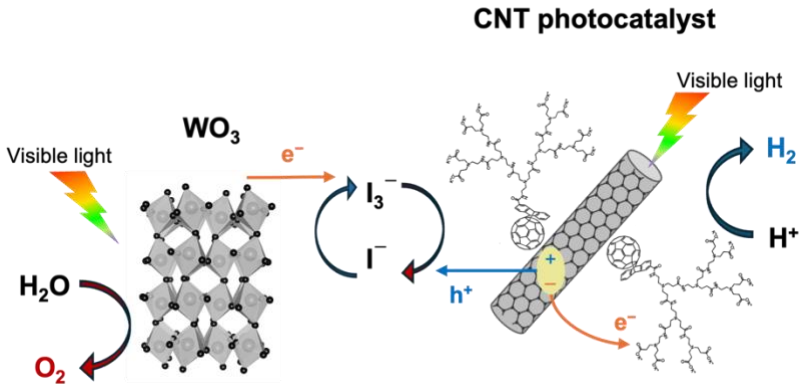

Figure 1. Overall water splitting using SWCNT/C_{60}-dendron nanohybrid (CNT-photocatalyst) and WO_3.

References

[1] J. L. Blackburn, *ACS Energy Lett.* **2017**, 2, 1598−1613.
[2] T. Tajima, W. Sakata, Y. Takaguchi *et al.*, *Adv. Mater.* **2011**, 23, 5750–5754.
[3] N. Murakami, Y. Takaguchi *et al.*, *Sci. Rep.* **2017**, 7, 43445.
[4] T. Izawa, Y. Takaguchi *et al.*, *Chem. Lett.* **2019**, 48, 410–413.
[5] M. Yamagami, T. Tajima, Y. Takaguchi *et al.*, *Nanomaterials* **2022**, 12, 3826.
[6] H. Watanabe, Y. Takaguchi, A. Orita *et al.*, *Bull. Chem. Soc. Jpn.* **2023**, 96, 57–64.
[7] T. Tajima, K. Yano, K. Mukai, Y. Takaguchi, *Catalysts* **2024**, 14, 715.
[8] T. Tajima, T. Matsuura, A. Efendi, M. Yukimoto, Y. Takaguchi, *Chem. Eur. J.* **2024**, e202402690.

Semiconducting Carbon Nanotube-Polythiophene Composites Showing Large Thermoelectric Power Factors

Yoshiyuki NOnoguchi[1]

[1]*Kyoto Institute of Technology (Japan)*

The thermoelectric properties of semiconducting carbon nanotubes (SWCNTs) have attracted attention due to recent developments in purification, doping technology, and transport theory. Although the relationship between primary structure and thermoelectric properties has been reported, the impact of their morphology on the transport is rarely demonstrated. Herein we show that a composite of purified semiconducting SWCNTs and polythiophene exhibits a large thermoelectric power factor (PF).

A trade-off relationship was observed between conductivity and Seebeck coefficient for both SWCNT/ethyl cellulose (EC) and SWCNT/poly(3-dodecylthiophene) (P3DDT) films; the SWCNT/P3DDT film exhibited more than 2-fold higher conductivity compared to SWCNT/EC,[1] where the maximum PF reached 309 μW/mK^2 for SWCNT/EC films and 1024 μW/mK^2 for SWCNT/P3DDT films (Fig. 1 (a)). The former is comparable to the previously reported arc-SWCNT film, and the latter is the highest level ever achieved for the similar material (Fig. 1 (b)). Since there is no significant difference in the primary structures of SWCNTs used in the two films, we are currently investigating the morphology effects, such as contact points between SWCNTs, on PF modulation. In the presentation, we will compare the results with various conducting polymer-supported films, and discuss the relationship between the observed structure and carrier transport.

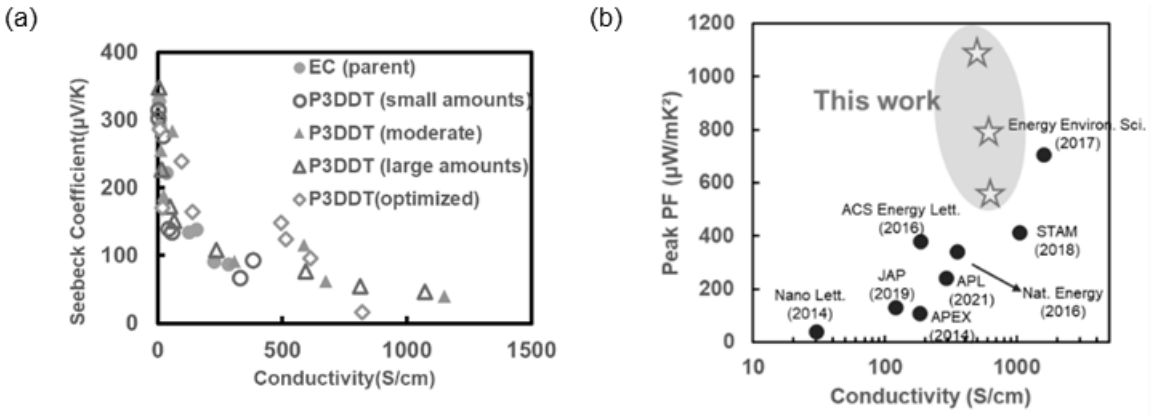

Figure 1: (a) Thermoelectric properties of CNT/EC and CNT/P3DDT films. (b) This work's peak PF compared to previous research for conductivity.

References

[1] T. Yagi, K. Yoshida, S. Sakurai, T. Kawai, Y. Nonoguchi, *J. Am. Chem. Soc.* **146**, 20913–20918 (2024).

Suspended carbon nanotube quantum dot heat engines

F. van Veen[1,2], J. Picó Cortés[3], S. Jung[4], B Ghawri[1], N. Lanz[4], M. Nikolic[4], A. Butzerin[4], L. Ornago[4,] M. Calame[1,6], A. Donarini[3], M. Grifoni[3], H.S.J. van der Zant[5], M. El Abbassi[4], M.L. Perrin[1,2],

[1]Transport at Nanoscale Interfaces Laboratory, Empa (Switzerland), [2] Department of Information Technology and Electrical Engineering, ETH Zurich (Switzerland), [3] Institute for Theoretical Physics, University of Regensburg (Germany),[4] Chiral Nano AG (Switzerland), [5] Delft University of Technology (The Netherlands), [6] Department of Physics, University of Basel,(Switzerland)

Low-dimensional nanoscale materials have long been proposed as ideal thermoelectric building blocks[1]. Recent studies have demonstrated excellent thermoelectric performance and high conversion efficiencies using quantum dots in particle-exchange heat engines[2].

In this work, we demonstrate the operation of a particle-exchange quantum dot heat engine based on ultra-clean, suspended carbon nanotubes (CNTs). Using Raman spectroscopy, we select pristine, individual CNTs and mechanically transfer them onto thermoelectric devices equipped with embedded heater lines and four-point resistance thermometers. Cryogenic transport measurements over a wide electrostatic gate range confirm the exceptional cleanliness of our devices and the high quality of the CNTs, as evidenced by clear observations of four-fold symmetry and distinct electronic coupling regimes (Coulomb blockade, Kondo, and Fabry-Perot).

We measure the steady-state power output of the CNT heat engine through external load resistors across a broad range of energy levels. This allows us to experimentally determine the optimal electronic coupling conditions necessary for maximising quantum dot heat engine performance. Furthermore, we observe a significant enhancement in thermoelectric power output due to the four-fold degeneracy of CNTs, far surpassing values reported in previous studies[2]. Our findings underline the critical role of entropy in enhancing thermoelectric engine efficiency.

Finally, we systematically explore heat engine performance across an extensive temperature range and investigate how vibrational excited states influence thermoelectric transport.

References

1. Hicks, L. D. & Dresselhaus, M. S. *Phys. Rev. B* **47**, 12727–12731 (1993)
2. M. Josefsson et al., Nature Nanotechnology 12, 920-924 (2018)

STRUCTURE-DEFINED THERMOELECTRIC PERFORMANCE OF THIN SINGLE-WALLED CARBON NANOTUBE FILMS

J. Khongthong[1], N. I. Raginov[1], A.E. Goldt[1], V.A. Kondrashov[1], A.G. Nasibulin[1], **D. V. Krasnikov[1]**

[1] *Skolkovo Institute of Science and Technology (Russia)*

Outstanding properties of single-walled carbon nanotubes (SWCNTs), such as excellent mechanical stability, high electrical conductivity, and high Seebeck coefficient, make this material promising for flexible thermoelectric generators (TEGs) – principal components for self-powered, wearable, and stretchable devices. However, a restricted understanding of the relationship between SWCNT properties and thermoelectric characteristics significantly limits their thermoelectric applications. Here, for the first time, we highlight the key role of bundle size and defectiveness in single-walled carbon nanotubes for thermoelectric applications Moreover, we employ the aerosol (floating catalyst) chemical vapor deposition (CVD) to achieve the state-of-the-art power factor (Figure 1a) of 534 μW/mK^2 – the highest registered for pristine SWCNT films. Furthermore, to highlight the potential of SWCNT films with smaller bundles, we developed an aerosol method for p-type and n-type doping [1] of the films consisting of the individual high-quality SWCNTs. This allowed us to achieve superior power factor values (Figure 1b) as high as 729 and 926 μW/mK^2, respectively [2].

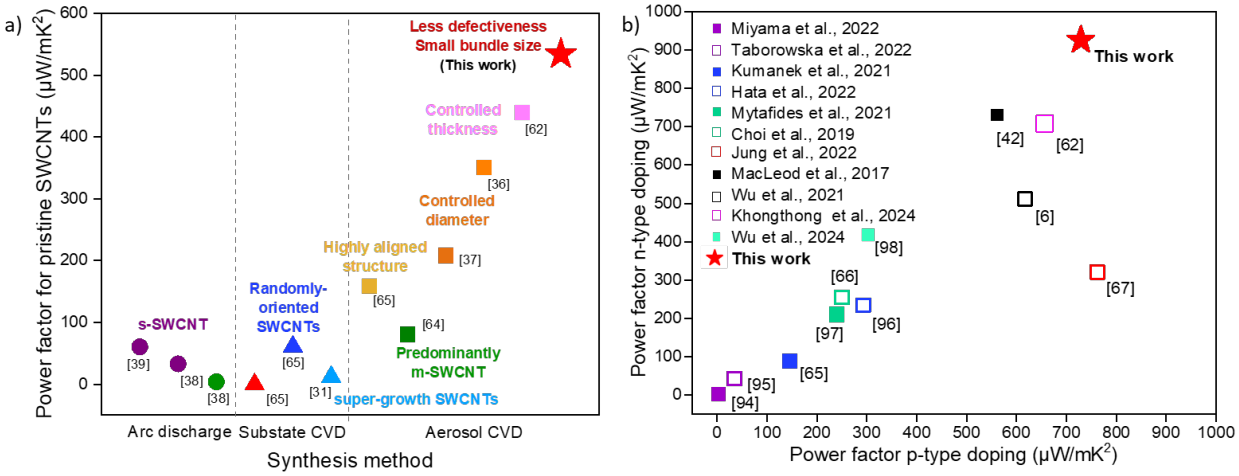

Figure1: Performance plots for pristine (a) and p- and n- doped SWCNT thin films (b).

This work was supported by Russian Science Foundation grant No. 20-73-10256. The authors thank Dr. Eldar M. Khabushev for the invaluable contribution.

References

[1] J. Khongthong, *et al. Carbon* ***218*** 118670 *(2024)*
[2] J. Khongthong, *et al. Carbon* ***in press***

SiO-$LiNi_{0.8}Co_{0.1}Mn_{0.1}O_2$ Full Cell Realized by Three-Dimensional Current Collectors of Carbon Nanotubes

T. Mae[1], S. Noda[1,2*]

[1] *Department of Applied Chemistry, Waseda University, 3-4-1 Okubo, Shinjuku-ku, Tokyo, 169-8555, (Japan),*

[2] *Waseda Research Institute for Science and Engineering, Waseda University, 3-4-1 Okubo, Shinjuku-ku, Tokyo, 169-8555, (Japan).*

The development of high-energy-density Li-ion batteries (LIBs) is actively progressing. In this study, we focused on a carbon-coated SiO (SiO/C) anode, which exhibits high capacity and excellent cycle stability. However, in academic research, conventional electrodes are typically prepared by coating a small amount of active material onto heavy current collectors of metal, limiting the capacity based on electrode mass. To address this issue, we applied a light-weight three-dimensional current collector of carbon nanotubes (CNTs), developed SiO||NCM ($LiNi_{0.8}Mn_{0.1}Co_{0.1}O_2$) full cell, and achieved high-energy density based on the total electrode mass through a partial prelithiation of the SiO/C-CNT anode [1,2]. However, the prelithiation process posed challenges such as a long processing time (24 h) and increased electrode thickness due to a high electrolyte to SiO mass ratio (E/SiO ratio, 20 $\mu L/mg_{SiO}$) [1]. In this study, we optimized the E/SiO ratio and the prelithiation time using half-cells to address these issues. The electrodes achieved small/large capacities (~0/>1600 mA h/g_{SiO}) for initial lithiation/delithiation with E/SiO >6.9 $\mu L/mg_{SiO}$, indicating sufficient prelithiation in 24 h (Fig. 1a). At a fixed E/SiO ratio of 6.7–6.9 $\mu L/mg_{SiO}$, the initial lithiation capacity decreased with prelithiation time and reached 93.3–138 mA h/g_{SiO} at 4 h with large initial delithiation capacities of 1660–1669 mA h/g_{SiO} (Fig. 1b). Therefore, the optimal prelithiation condition was determined to be an E/SiO ratio of 6.9 $\mu L/mg_{SiO}$ with a prelithiation time of 4 h. This optimized condition was applied in making the CNT-based SiO||NCM full cell that achieved a high-energy density based on the total electrode mass of 346–377 W $h/kg_{electrode}$ after 300 cycles, surpassing the conventional LIB value (346 W $h/kg_{electrode}$, calculated by [3]) (Fig. 1c). Although the SiO/C-CNT electrode increased its thickness from 41 to 83 µm upon prelithiation (Fig. 1d,e), the thickness was 26% smaller than the electrode prelithiated under the previous condition (Fig. 1f). This was possibly due to suppression of excessive solid electrolyte interphase (SEI) formation between the electrolyte and CNTs.

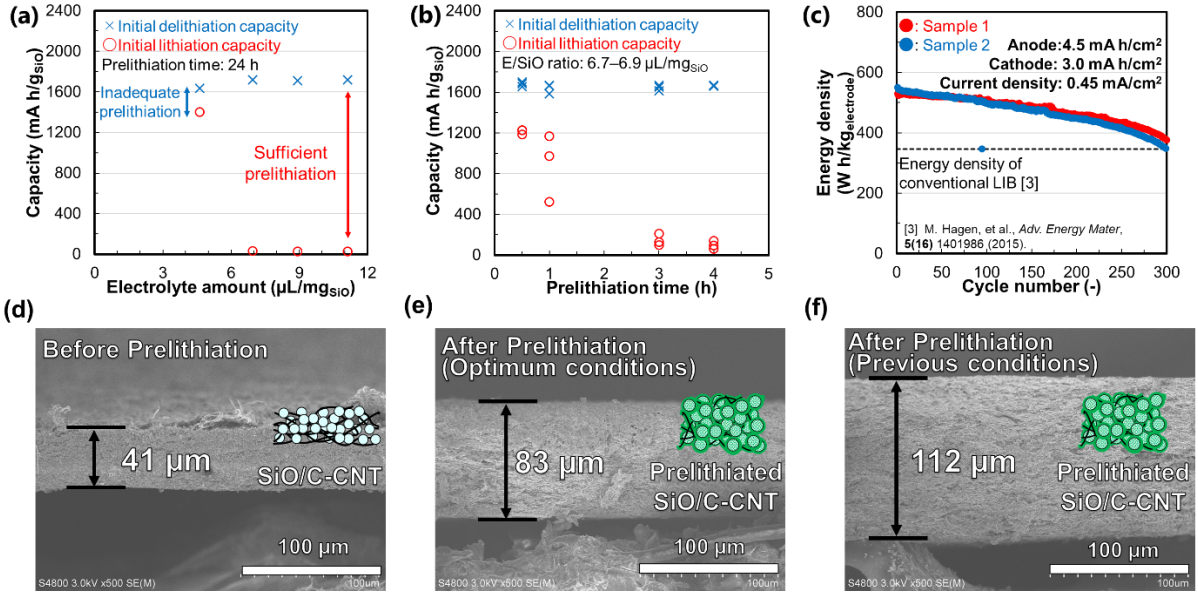

Fig. 1. (a,b) Initial lithiation and delithiation capacity for (a) the E/SiO ratio and (b) the prelithiation time. (c) Cycle performance of CNT-based SiO||NCM full cells. (d-f) Cross-sectional scanning electron microscope images of the SiO/C-CNT electrodes before the prelithiation (d), and after the prelithiation under (e) optimal conditions (6.9 $\mu L/mg_{SiO}$, 4 h) and (f) previous conditions (20 $\mu L/mg_{SiO}$, 24 h).

Acknowledgements
This research was supported by Grant-in-Aid for Scientific Research (A) (JP21H04633), JST Spring (JPMJSP2128), JST ASPIRE (JPMJAP2312), and Zeon Corporation.

References
[1] T. Mae et al., *Carbon* **218**, 118663 (2024). [2] T. Mae et al., *Carbon* **209**, 118014 (2023).

Session
NT 25（The 25th International Conference on the Science and Applications of Nanotubes and Low-

| Parallel Symposia：Symposium on Thin Films, Fibers, 3-D Materials and their Properties

Thu. Jun 19, 2025 2:00 PM - 5:00 PM JST | Thu. Jun 19, 2025 5:00 AM - 8:00 AM UTC Conference Room III(Clock Tower Centennial Hall, 2F)

[19mm] Macromaterials

Chair:Yoshiyuki Nonoguchi, Suguru Noda

2:00 PM - 2:40 PM JST | 5:00 AM - 5:40 AM UTC

[19mm-01]

Multifunctional Carbon Nanotube Films for Advanced Protective Applications

*Qingwen Li[1] (1. Suzhou Institute of Nano-Tech and Nano-Bionics, Chinese Academy of Sciences (China))

2:40 PM - 3:00 PM JST | 5:40 AM - 6:00 AM UTC

[19mm-02]

Large-area and long-length single-wall carbon nanotube transparent conductive film strengthened by carbon welding

*Peng-Xiang Hou[1], Yi-Ming Zhao[1], Chang Liu[1], Hui-Ming Cheng[2] (1. Shenyang National Laboratory for Materials Science, Institute of Metal Research, Chinese Academy of Sciences (China), 2. Shenzhen Key Laboratory of Energy Materials for Carbon Neutrality, Shenzhen Institute of Advanced Technology, Chinese Academy of Sciences (China))

3:00 PM - 3:20 PM JST | 6:00 AM - 6:20 AM UTC

[19mm-03]

Aerosol-synthesized Surfactant-free Single-walled Carbon Nanotube-based chemical sensors: Unprecedentedly High Sensitivity, Fast Recovery, and In-fluid (transformer oil) Applicability

*IL JEON[1] (1. Sungkyunkwan University (SKKU) (Korea))

4:00 PM - 4:20 PM JST | 7:00 AM - 7:20 AM UTC

[19mm-04]

Unlocking the Full Potential of Carbon Nanotubes: A Trans-Scale Approach from Nanoscale to Macroscale

*Yasuhiko Hayashi[1], Hiroo Suzuki[1] (1. Okayama University (Japan))

4:20 PM - 4:40 PM JST | 7:20 AM - 7:40 AM UTC

[19mm-05]

Electrical and Thermal Properties of Aligned CNT Materials at Extreme Temperatures

*Kadyn Tackett[1], Brice Hall[1], Jake Blue[1], Sabrina Eddy[1], Timothy Haugan[1], John Bulmer[1,2] (1. Air Force Research Laboratory (United States of America), 2. National Research Council (United States of America))

4:40 PM - 5:00 PM JST | 7:40 AM - 8:00 AM UTC

[19mm-06]

High-performance carbon nanotube fiber actuators driven by electrochemical intercalation

*Jiangtao Di[1] (1. Suzhou Institute of Nano-Tech and Nano-Bionics, Chinese Academy of Sciences (China))

Multifunctional Carbon Nanotube Films for Advanced Protective Applications

Qingwen Li[a,*]

[a] *Suzhou Institute of Nano-Tech and Nano-Bionics, Chinese Academy of Sciences, 398 Ruoshui Road, Suzhou, 215123*

*Corresponding author(s): qwli2007@sinano.ac.cn

The demand for lightweight, robust and multifunctional protective materials is growing rapidly due to the fast development of various high-power electronic equipment for communication, transportation and wearable health monitoring etc., as well as more outdoor activities for extreme-environmental sports etc.. Carbon nanotube films synthesized from floating CVD methods, have demonstrated tunable aggressive structures and superior physicochemical properties covering chemical stability, mechanical, electronic, thermal, magnetic and intrinsic anti-flaming characteristics etc., which enable them as promising lightweight and multifunctional candidates in many advanced protection applications. In my talk, I will report our recent progress in the following aspects:1) Scalable and low-cost CVD synthesis of CNT films; 2) Tailoring CNT network structures for high-energy absorption and impact protection; 3)Structural modification of CNT films for excellent EMI shielding performance; 4) Fabrication of CNT based electrothermal devices for smart and extreme-environmental thermal management. Finally, I will summarize the advantages and disadvantages of CNT films for advance protections compared to traditional materials, and its future developments in intelligent protection systems combing self-sensing, adaptive or interactive capability will be prospected as well.

Large-area and long-length single-wall carbon nanotube transparent conductive film strengthened by carbon welding

P.X. Hou[1*], Y. Meng[1], C. Liu[1], H.M. Cheng[2]

[1] Shenyang National Laboratory for Materials Science, Institute of Metal Research, Chinese Academy of Sciences, Shenyang 110016, China, [2] Shenzhen Key Laboratory of Energy Materials for Carbon Neutrality, Shenzhen Institute of Advanced Technology, Chinese Academy of Sciences, Shenzhen, 518055, P.R.China.

Single-wall carbon nanotubes (SWCNTs) are ideal for fabricating transparent conductive films because of their small diameter, good optical and electrical properties, and excellent flexibility. We have prepared ultrahigh-performance transparent conductive films of carbon-welded isolated SWCNT films[1] and successfully used them in solar cells as transparent electrodes[2-3]. However, it is difficult to obtain large-area freestanding SWCNT film, which limit their applications. In this work, we breakthrough this limitation and synthesized large-area suspended SWCNT film (Figure 1a) by prolonging the catalyst lifetime. The atomic force microscopy (AFM) image (Figure 1b) of the as-prepared SWCNT film shows a random SWCNT network consisting of straight and long SWCNTs. Both AFM image and transmission electron microscopy (TEM) image show carbon-welded junction structure. The Raman spectrum shows a very high G band and an almost invisible D band with a I_G/I_D value of 180 for a 633-nm laser, indicative of a well-crystallized sp^2 C-C structure, which are further confirmed by 532- and 785-nm laser Raman spectra with high I_G/I_D. This unique structure endows SWCNT film with high strength, which can support an overweight object.

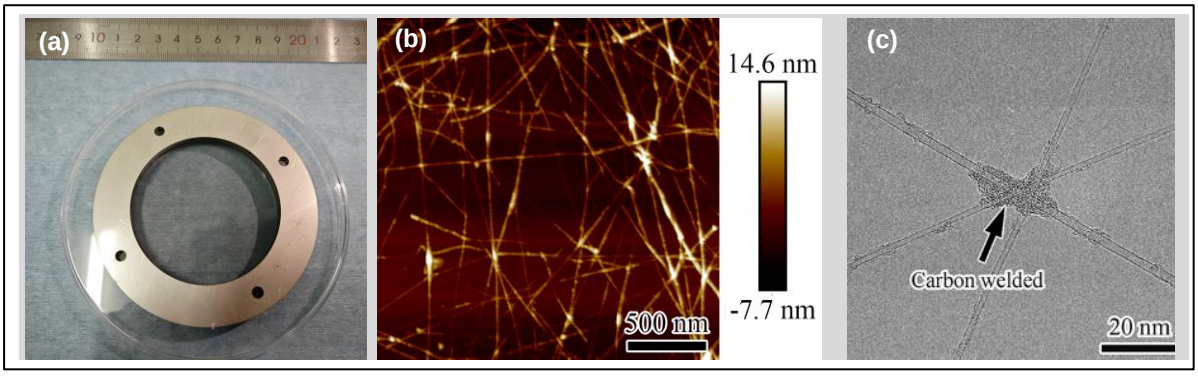

Figure 1. (a) A photo of suspended SWCNT film on Cu frame. Typical (b) AFM and (TEM) image of SWCNT film.

References (if desired)
[1] P. X. Hou *et al.*, *Sci. Adv*. **4**, eaap9264 (2018).
[2] P. X. Hou *et al.*, *Adv. Funct. Mater.* **31**, 2104396 (2021).
[3] P. X. Hou *et al.*, *Nat. Commun.* **15**, 2245 (2024).

Aerosol-synthesized Surfactant-free Single-walled Carbon Nanotube-based chemical sensors: Unprecedentedly High Sensitivity, Fast Recovery, and In-fluid (transformer oil) Applicability

S. Kim[1], Esko I. Kauppinen[2], Keekeun Lee,[3] I. Jeon[1,4,5]

[1]SKKU Advanced Institute of Nano Technology (SAINT) (Republic of Korea), [2]Aalto University (Finland), [3]Ajou University, (Republica of Korea), [4]SKKU Global Research Center (SGRC) (Republic of Korea), [5]Tohoku University (Japan)

This study presents an acetylene gas sensor capable of in situ monitoring transformer oils. This sensor utilizes carbon nanotubes (CNTs) embedded in polyimide (PI) synthesized by floating catalyst chemical vapor deposition. Unlike conventional sensors that target hydrocarbon gases dissolved in oil and measure the gas extracted from the oil, the proposed CNT-PI sensor detects gas within the oil in real time. The PI embedding technique effectively anchors and shields the CNT network against fluidic damage, ensuring stable sensing performance over 6 months, even under friction stress caused by oil convection. Decorating CNTs with gold nanoparticles further enhances the sensitivity and response of the sensor. The sensor achieves a high response (10.5% at 30 ppm) and fast response/recovery times (28 s/77 s), Furthermore, the sensor demonstrates good response (10.4% at 30 ppm) and moderate response/recovery times (444 s/670 s) in an oil medium, which qualifies for industrial applications. Additionally, a CNT-PI-based heater is integrated into the sensor as a multilayer component, maintaining an optimal operating temperature of 90 °C. The CNT-PI sensor demonstrates consistent gas-sensing performance even after 10,000 bending cycles and exhibits superior characteristics, indicating its compatibility with various forms of transformers.

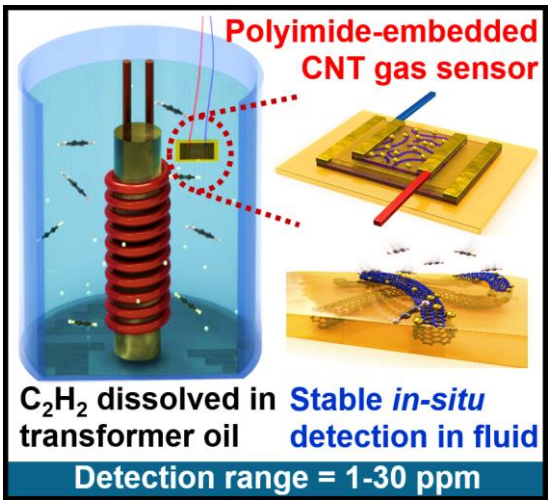

References
[1] I. Jeon *et al.*, *Adv. Mater*. 2313830 (2024).
[2] I. Jeon *et al.*, *Adv. Mater*. 2410179 (2024).

Unlocking the Full Potential of Carbon Nanotubes: A Trans-Scale Approach from Nanoscale to Macroscale

Y. Hayashi[1], H. Suzuki [1]

[1] *Life, Natural Science and Technology, Institute of Academic and Research, Okayama University, Japan*

We are exploring ways to effectively transfer the exceptional properties of carbon nanotubes (CNTs) from the nanoscale to the macroscale, facilitating the development of CNT dry-spun yarns and CNT sheets for practical applications. In this presentation, I will discuss our research on high-strength, few-walled CNT (FWCNT) dry-spun yarn as a promising alternative to high-strength carbon fiber [1,2].

We have identified the critical CNT height, density, and quantity necessary for the highly reproducible and continuous production of CNT dry-spun yarn through direct pulling and twisting from a CNT forest. High drawability was observed only when the CNT number density was below 15,000 per μm². During dry spinning, the average diameter of CNT bundles extracted from the CNT forest remained constant, regardless of drawability. This result indicates that the CNT number density is proportional to the bundle number density, and the spacing between CNT bundles, as determined by the number density, influences the drawability of the CNT forest. Furthermore, we clarified that even if the overall bulk density of the forest does not meet the necessary conditions for enhanced drawability, drawability can still be improved if the CNT number density per mm² satisfies the required criteria.

The untreated CNT dry-spun yarn exhibits a tensile strength of approximately 1.5 GPa with Young's modulus of ~100 GPa. A key challenge is to surpass the tensile strength of high-performance aerospace-grade carbon fibers, such as Toray's T1100G (7 GPa tensile strength, 320 GPa Young's modulus) [3]. To address this, we developed a high-speed Joule annealing (JA) treatment, applying an electric current to CNT dry-spun yarn at a rate of 1 cm/s. Above 3000 K, the principal Raman intensity ratio G at 1350 cm^{-1} and D at 1590 cm^{-1} increases significantly, enhancing strength. During Joule annealing above 3000 K, residual amorphous carbon, which did not contribute to CNT synthesis, at the boundary between the CNTs underwent graphitization or sublimation based on analysis of Raman 2D band (approximately 2650 - 2680 cm^{-1}) originates from the double-resonance processes in graphene and CNTs [2].

To further enhance strength, it is crucial to minimize slippage between CNTs and CNT bundles. To achieve this, we developed a technique that introduces fine graphene oxide or graphene flakes into the nanoscale voids within CNT dry-spun yarn using a solution immersion method. By combining this approach with Joule annealing (JA) treatment, we achieved a tensile strength of 6.4 GPa and a Young's modulus of 320 GPa, approaching the performance of T1100G. Molecular dynamics simulations were conducted to analyze the insertion of graphene (derived from amorphous carbon) between CNTs, followed by heating. At 3000 K, the edges of the graphene flakes between CNTs were found to chemically bond with the CNTs. This result suggests that cross-linking through graphene flakes suppresses CNT slippage during tensile testing, leading to high-strength CNT dry-spun yarn.

This research demonstrates that fine graphene and graphene oxide can be incorporated into CNT dry-spun yarn through an immersion process, followed by Joule annealing at temperatures of 3000 K or higher. This treatment enhances the strength of the CNT dry-spun yarn, bringing it closer to serving as a high-strength carbon fiber substitute.

References

[1] H. Inoue *et al*., *Carbon* **158**, 662-671 (2020).
[2] R. Shikata *et al*., *Nanotechnol*. paper235707 (2022).
[3] https://www.toraycma.com/products/carbon-fiber/

Electrical and Thermal Properties of Aligned CNT Materials at Extreme Temperatures

K. Tackett, B. Hall, J. Blue, S. Eddy, T. Haugan, J. Bulmer

Air Force Research Laboratory (USA)

Aligned carbon nanotube (CNT) materials are an emerging strategic resource, offering copper-like conductivity on a weight basis and carbon-fiber-level strength. The high-temperature regime (>1700 °C) is particularly exciting, with recent studies highlighting partial molecular coalescence[1] and circularly polarized IR radiation[2]. Here, we examine the electrical, thermal, and emissivity responses of aligned CNTs (up to 2100 °C) using a custom-built Joule graphitization platform. This setup rapidly heats CNT ribbons via direct current injection, while contactless pyrometers and thermal cameras monitor temperatures in real time under vacuum or ultra-purified argon. Computer models then convert the measured temperature gradients and partitioned resistances into temperature-dependent material properties. As a result, the platform can thermally treat conductive carbon materials within seconds—versus hours in conventional furnaces above 1500 °C—and measure their thermal and four-wire electrical conductivities in subsequent temperature sweeps.

Using this platform, we heat-treated solution-spun CNT ribbons (provided by Dexmat and the CarbonHub) from 1500 to 2100 °C with DC currents up to 15 A (≈17 kA cm^{-2}). Continuous operation at 1500 °C was routine, and 2100 °C was sustained for over five minutes. Raman spectroscopy showed no structural modifications or added defects. However, the likelihood of failure increased with both dwell time and temperatures above 1700 °C. We hypothesize that the onset of structural changes triggers hotspot formation, thermal runaway, and eventual breakage. Such break events often produced a stable low-voltage plasma (~7 cm long, <50 V, 1 atm), likely due to the sooty argon atmosphere and the low work function of CNTs. Similar low-voltage, ambient-pressure plasmas have recently been demonstrated with carbon fiber and are relevant for high-temperature materials processing[3].

After reaching a maximum temperature, subsequent ramps stayed below 1500 °C to prevent further modifications to the carbon conductor. Because the temperature profile varied for each current setting, we could not simply assign a single resistance value to a single temperature. Instead, we derived temperature-dependent specific conductivity by combining four-wire resistance measurements with spatial temperature profiles at multiple DC current settings, then solved the resulting system of equations. We observed metallic-like conduction up to 2100 °C, with specific conductivity comparable to graphite, tungsten, and molybdenum. By measuring emissivity carefully and accounting for radiation and convection in our in-house solver (validated by Ansys Multiphysics simulations) we extracted temperature-dependent thermal conductivity. Finally, we discuss hybrid CNT ribbons infused with beneficial constituents for enhanced performance.

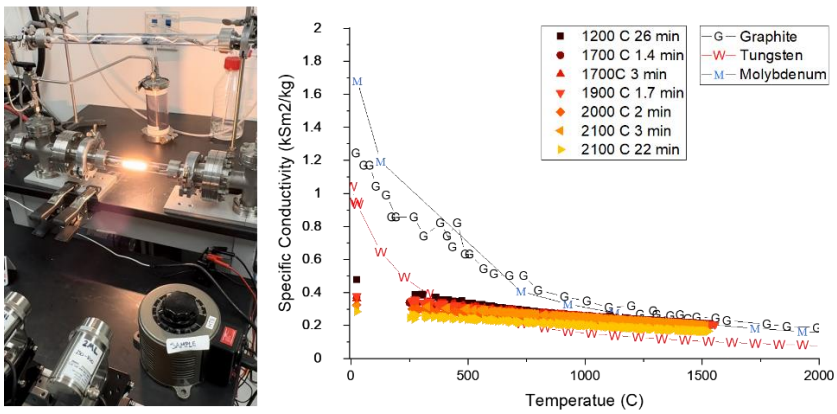

Left, the Joule Graphitization Platform and, right, Specific Conductivity versus Temperature of various CNT materials compared to benchmarks.

[1] D. Lee *et al.*, *Sci. Adv. 2022, 8 (16), 1–9.*
[2] J. Lu *et al.*, *Science, 2024, **386**, 1400-1404.*
[3] H. Xie *et al.*, Nature 2023, 623 (7989), 964–971.

High-performance carbon nanotube fiber actuators driven by electrochemical intercalation

Jiangtao Di[1]

[1] *Suzhou Institute of Nano-Tech and Nano-Bionics, Chinese Academy of Sciences*

Fiber-type actuators, also known as artificial muscle yarns, have recently emerged as a new type of intelligent material and attracted considerable attention. This talk focuses on addressing the challenges of actuation precision control and actuation feedback of fiber-type actuators. We utilized the faradaic intercalation and extraction to drive a carbon nanotube (CNT) fiber. Two types of selected ions of ctetrachloroaluminate ($AlCl_4^-$) and hexafluorophosphate (PF_6^-) can act as strong but dynamic "lockers" when they electrochemically intercalated into the CNT fiber. This allowed the CNT fiber to have the important features of an energy-free high-tension catch state and programmable stepwise actuation. When powered off, the CNT fiber nearly 100% maintained any achieved strokes under loads of 96,000 times the muscle weight. This mechanism allowed the programmable control of stroke steps down to 1%. By wrapping a CNT fiber core in sequence with an elastomer layer, a nanofiber network, and an MXene/CNT thin sheath, we prepared an artificial neuromuscular fiber that achieves an ingenious sense-judge-act intelligent system in an elastic fiber. This would provide a promising solution for closed-loop control for future intelligent soft robots.

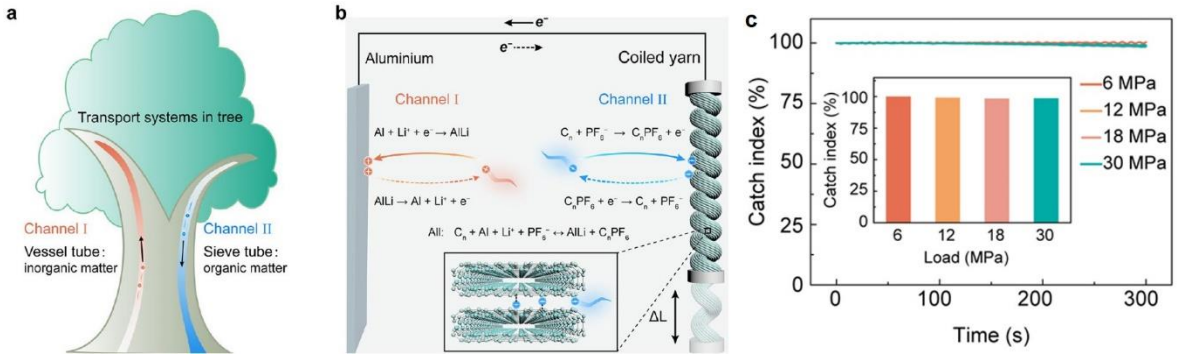

Figure caption: (a-b) The actuation mechanism of the carbon nanotube fiber actuator by electrochemical intercalation using PF_6^-. (c) The catch state of the fiber actuator that holds different loads when the input electricity power is turned off.

References (if desired)

[1] J. Di *et al.*, *Nano-Micro Letters* **15,** 162 (2023).
[2] J. Di *et al.*, *ACS Nano* **17**, 12809–12819 (2023).
[3] J. Di *et al.*, *Science Advances* **8**, eabq7703 (2022).
[4] J. Di *et al.*, *ACS Nano* **16**, 15850–15861 (2022).
[5] J. Di *et al.*, *Nano Energy* **102**, 107609 (2022).

Session
NT 25（The 25th International Conference on the Science and Applications of Nanotubes and Low-

| Parallel Symposia：6th Symposium on Synthesis, Purification, Functionalization, and Manufacturing of Carbon Nanotubes and Low-Dimensional Materials

Thu. Jun 19, 2025 2:00 PM - 5:20 PM JST | Thu. Jun 19, 2025 5:00 AM - 8:20 AM UTC HORIBA Symposium Hall (INNOVATION BLDG., 5F)

[19sy] Synthesis

Chair:Minfang Zhang, Shigeo Maruyama

2:00 PM - 2:20 PM JST | 5:00 AM - 5:20 AM UTC

[19sy-01]

Ultra-Pure Synthesis of (6,5) Carbon Nanotubes with Multiphase Catalysts

*Toshiaki Kato[1] (1. Tohoku Univ. (Japan))

2:20 PM - 2:40 PM JST | 5:20 AM - 5:40 AM UTC

[19sy-02]

Catalytic rapid Joule heating synthesis of carbon nanotubes in seconds

*Jian Sheng[1], Yifan Xu[1], Yan Li[1] (1. Peking University (China))

2:40 PM - 3:00 PM JST | 5:40 AM - 6:00 AM UTC

[19sy-03]

Synthesis and Characterization of One-Dimensional van der Waals Heterostructures with Radial, Axial and Alloy Configurations

*Yongjia Zheng[1], Wanyu Dai[2], Akihito Kumamoto[3], Yuta Sato[4], Keigo Otsuka[2], Qiang Zhang[5], Esko I. Kauppinen[5], Yuichi Ikuhara[3], Kazu Suenaga[6], Shigeo Maruyama[2], Rong Xiang[1] (1. State Key Laboratory of Fluid Power and Mechatronic Systems, School of Mechanical Engineering, Zhejiang University (China), 2. Department of Mechanical Engineering, The University of Tokyo (Japan), 3. Institute of Engineering Innovation, The University of Tokyo (Japan), 4. Nanomaterials Research Institute, AIST (Japan), 5. Department of Applied Physics, Aalto University School of Science (Finland), 6. The Institute of Scientific and Industrial Research (ISIR), Osaka University (Japan))

3:00 PM - 3:20 PM JST | 6:00 AM - 6:20 AM UTC

[19sy-04]

Preparation of Highly Ordered CNT Fiber and Its Application on Nanofiltration

*Xiao Zhang[1], Weiya Zhou[1], Huaping Liu[1], Michael De Volder[2], Adam Boies[2] (1. Institute of Physics, Chinese Academy of Sciences (China), 2. Department of Engineering, University of Cambridge (UK))

4:00 PM - 4:20 PM JST | 7:00 AM - 7:20 AM UTC

[19sy-05]

Oxidation Saturation in Carbon Nanotubes: General Understanding of Functionalization Methods

*Minfang Zhang[1], Mei Yang[1], Makoto Yaguchi[1], Hirokuni Jintoku[1], Shunsuke Sakurai[1], Don Futaba[1] (1. National Institute of Advanced Industrial Science and Technology (AIST) (Japan))

4:20 PM - 4:40 PM JST | 7:20 AM - 7:40 AM UTC

[19sy-06]

Confined Assembling Chemistry within Single-Walled Carbon Nanotubes

*Feng Yang[1] (1. Southern University of Science and Technology (China))

4:40 PM - 5:00 PM JST | 7:40 AM - 8:00 AM UTC

Session

NT 25（The 25th International Conference on the Science and Applications of Nanotubes and Low-

[19sy-07]

Precise Partitioning of Single-Wall Carbon Nanotubes and Enantiomers Through Aqueous Two-Phase Extraction

*Han Li[1], Ming Zheng[2], Jeffrey Fagan[2] (1. University of Turku (Finland), 2. National Institute of Standards and Technology (United States of America))

5:00 PM - 5:20 PM JST | 8:00 AM - 8:20 AM UTC

[19sy-08]

Quantifying Enantiomeric Purity Of Sorted Single-Walled Carbon Nanotubes Using Combined Chiroptical Spectroscopy And Hyperspectral Fluorescence Microscopy

Miguel Ángel López Carrillo[1], Filip Desmet[1], Maksiem Erkens[2], Jeffrey A. Fagan[3], Ming Zheng[3], Han Li[4,5], Benjamin S. Flavel[4], Wim Wenseleers[2], Wouter Herrebout[1], Sofie Cambré[1], *Dmitry Levshov[1] (1. Theory and Spectroscopy of Molecules and Materials, Department of Chemistry and Department of Physics, University of Antwerp, Antwerp (Belgium), 2. Nanostructured and Organic Optical and Electronic Materials, Department of Physics, University of Antwerp, Antwerp (Belgium), 3. Materials Science and Engineering Division, National Institute of Standards and Technology, 20899 Gaithersburg, Maryland (United States of America), 4. Institute of Nanotechnology, Karlsruhe Institute of Technology, 76344 Eggenstein-Leopoldshafen (Germany), 5. Department of Mechanical and Materials Engineering, University of Turku, FI-20014 Turku (Finland))

Ultra-Pure Synthesis of (6,5) Carbon Nanotubes with Multiphase Catalysts

T. Kato[1, 2]

[1]*Grad. School of Engineering, Tohoku Univ. (Japan),* [2]*WPI-AIMR, Tohoku Univ. (Japan)*

The controlled synthesis of carbon nanotubes (CNTs) with specific chirality represents a significant challenge in the field. In this study, we investigated complex multiphase catalysts consisting of three or more components, which remain largely unexplored in CNT synthesis, with the goal of elucidating their correlation with chirality selection. Utilizing nickel (Ni) as the base catalyst and incorporating over 40 different second elements, we performed chemical vapor deposition (CVD) synthesis and assessed chirality distribution. Our results indicate that pure Ni yields a (6,5) CNT purity of 34%, whereas the addition of tin (Sn) in the Ni catalyst enhances this purity to 84%. Furthermore, by introducing a new third component into the NiSn catalyst for ternary catalyst exploration, we discovered that the NiSnFe catalyst, containing iron (Fe), increases the synthesis quantity of (6,5) CNTs by approximately sixfold. Through the optimization of synthesis conditions with this newly developed NiSnFe ternary catalyst, we achieved an ultra-high purity of 95% for (6,5) CNTs [1]. Comprehensive structural analyses conducted via scanning transmission electron microscopy (STEM) and X-ray diffraction (XRD), along with first-principles calculations, demonstrated that the Ni_3Sn structure formed within the NiSnFe catalyst plays a critical role in achieving the ultra-high purity synthesis of (6,5) CNTs. This innovative multiphase catalyst for CVD synthesis is anticipated to pave the way for the selective synthesis of other chiralities in the future.

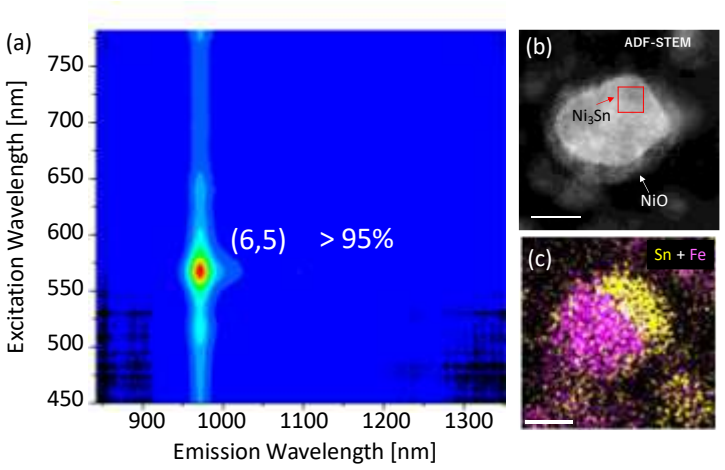

Fig. : (a) Photoluminescence-excitation mapping of ultra-high purity (6,5) CNTs grown from NiSnFe catalysts. (b) STEM and (c) element mapping images of NiSnFe catalysts.

References

[1] S. Shiina, *et al.*, *ACS Nano* **18,** 23979–23990 (2024).

Catalytic rapid Joule heating synthesis of carbon nanotubes in seconds

Jian Sheng[1†], Yifan Xu[1†], Yan Li[1]

[1]*Beijing National Laboratory for Molecular Sciences, Key Laboratory for the Physics and Chemistry of Nanodevices, College of Chemistry and Molecular Engineering, Peking University, Beijing 100871, China*

Corresponding author: shengjian@pku.edu.cn; yanli@pku.edu.cn

The efficient and controllable synthesis of high-quality carbon nanotubes (CNTs) remains a critical challenge for their practical applications. Herein, we demonstrate a Joule heating strategy for the rapid synthesis of carbon nanotubes (CNTs) from solid carbon sources (e.g., polyethylene). The extreme heating rates (>10^3 °C/s) inherent to Joule heating selectively facilitates the generation of small carbon species (C_1–C_3) while suppressing the formation of long-chain carbon species during polyethylene pyrolysis, thereby enhancing the accessibility of carbon sources on catalyst surfaces. Concurrently, rapid heating process stabilizes CoMo nano-catalysts by inhibiting thermal sintering, enabling uniform growth of multi-walled CNTs (Diameter: 8.8 ± 2.1 nm; 5.3 ± 1.2 nm) and single-walled CNTs (Diameter: 1.8 ± 0.3 nm). Transient high temperature promotes the catalytic conversion of the polyethylene to CNTs while kinetically limiting amorphous carbon formation through rapid quenching of side reactions. Moreover, this method markedly enhances production efficiency by achieving a rapid yield of 0.6 g of multi-walled CNTs within seconds. This represents a significant advancement compared to conventional furnace-based methods. The unique thermal conditions of Joule heating simultaneously activate the catalysts and optimize the distribution of carbon species, resolving the conflicts between catalyst stability and growth efficiency. This work establishes a new paradigm for time- and energy-efficient synthesis of CNTs.

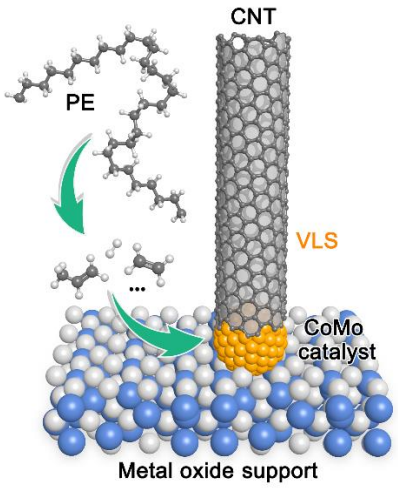

Figure 1: Schematic illustration of the rapid conversion process from polyethylene to CNTs.

Synthesis and Characterization of One-Dimensional van der Waals Heterostructures with Radial, Axial and Alloy Configurations

Yongjia Zheng[1], Wanyu Dai[2], Akihito Kumamoto[3], Yuta Sato[4], Keigo Otsuka[2], Qiang Zhang[5], Esko I. Kauppinen[5], Yuichi Ikuhara[3], Kazu Suenaga[6], Shigeo Maruyama[2], Rong Xiang[1]

[1]State Key Laboratory of Fluid Power and Mechatronic Systems, School of Mechanical Engineering, Zhejiang University (China), [2]Department of Mechanical Engineering, The University of Tokyo (Japan), [3]Institute of Engineering Innovation, The University of Tokyo (Japan), [4]Nanomaterials Research Institute, AIST (Japan), [5]Department of Applied Physics, Aalto University School of Science (Finland), [6]The Institute of Scientific and Industrial Research (ISIR), Osaka University (Japan)

Abstract: The achievement of synthesizing high-quality one-dimensional van der Waals (1D vdW) heterostructures through chemical vapor deposition in 2020, exemplified by the radial junction configuration of single-walled carbon nanotubes (SWCNTs) wrapped with boron nitride nanotubes (BNNTs) and molybdenum disulfide (MoS_2), has revealed new possibilities for transforming conventional 2D vdW architectures into their tubular counterparts [1-3]. While substantial research efforts have since focused on 1D vdW systems, current progress remains constrained by limited structural diversity in existing heterostructure designs.

This study breaks new ground by developing three distinct categories of heteronanotubes: (1) Single-element modified systems (MoS_2-WS_2 and MoS_2-$MoSe_2$), (2) Dual-element substituted structures ($MoSe_2$-WS_2), and (3) Compositionally mixed MoS_2-WS_2 alloy nanotubes. The first category demonstrates precise elemental substitution at fixed chalcogen positions, while the second achieves simultaneous transition metal and chalcogen replacement. Additionally, the third category show a platform for continuous elemental modulation along the nanotube. These advances not only expand the material genome of 1D vdW heterostructures but also provide fundamental insights for engineering next-generation electronic and optoelectronic devices with tailored quantum confinement effects and bandgap engineering capabilities.

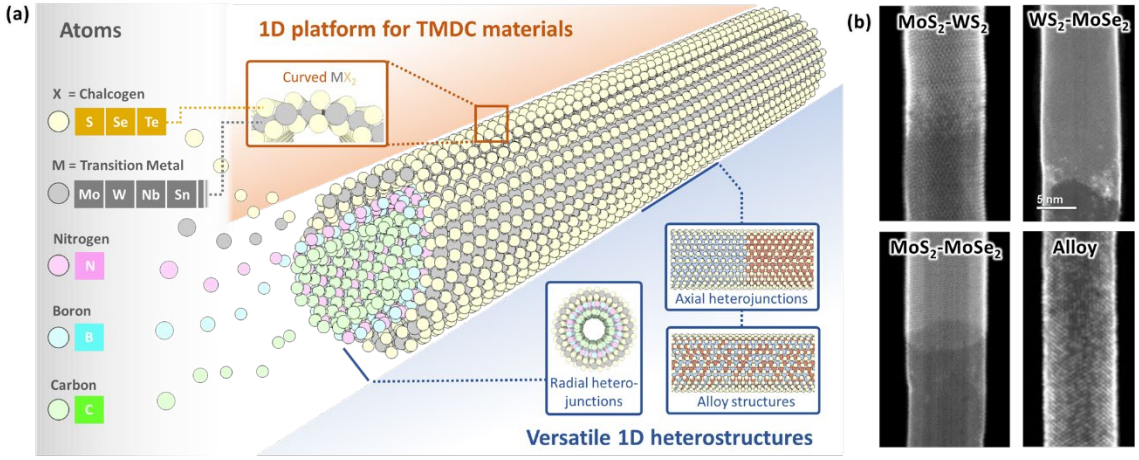

Figure 1. (a) Overview of three categories of heteronanotubes, and (b) High-angle annular dark-field scanning transmission electron microscopy (HAADF-STEM) images of MoS_2-WS_2, WS_2-$MoSe_2$, MoS_2-$MoSe_2$ and alloy structures.

References

[1] R. Xiang *et al., Science,* **367**(6477), 537 (2020).
[2] Y. Zheng, *et al., PNAS*, **118**(37), e2107295118 (2021).
[3] R. Xiang, et al., *National Science Open* **1**(3), 20220016 (2022).

X. Zhang[1]*, W.Y. Zhou[1], H.P. Liu[1], M. De Volder[2], Adam Boies[2]

[1]*Beijing National Laboratory for Condensed Matter Physics, Institute of Physics, Chinese Academy of Sciences, Beijing 100190 (China)*

[2]*Department of Engineering, University of Cambridge, Cambridge CB2 1PZ (UK)*

Individual carbon nanotube (CNT) is superior to the polymer chain on the mechanical and thermal properties; Its atomic smooth inner wall and well defined 0.8-3 nm diameter channel also owe it to ultrahigh penetrations of solvents and sub-nm selectivity for nanofiltration.

However, the macroscopic CNT fibers (CNTF) remain inferior to many advanced synthetic fibers. There is still significant room for further performance improvement, up to the excellent performance of individual CNT. The degradation on CNTFs is believed to originate from the failure of embedding CNTs effectively in superstructures, that is, the alignment or compaction. In this talk, a double-drawing technique we developed will be discussed, which rearrange the constituent CNTs and enhance the interfacial interaction. Consequently, with the newly developed techniques, the mechanical and thermal properties of the resulting CNTFs can simultaneously reach their highest performances with specific strength ~3.30 N tex^{-1}, work of rupture ~70 J g^{-1}, and thermal conductivity ~354 W m^{-1} K^{-1} despite starting from low-crystallinity (I_G:I_D ~ 5) and thick raw materials. The processed CNTFs are more versatile than comparable carbon fiber, Zylon and Dyneema. In the end, with all the experimental evidence, we find that, despite of the known dependence of fiber properties on CNT alignment and stacking, new evidence of the load transfer efficiency on individual CNTs measured with in situ stretching Raman highlights the importance of (i) straightening of CNT bundles, which increases the proportion of effective bundles jointly sharing the load, and (ii) the higher barrier of slippage activation within bundles, which originates from the effective tube length increase within effective bundles.

In recent years, based on the above highly ordered CNTFs, we realized the batch production of nanofiltration membranes. Leveraging the dense stacking of CNTs, the low tortuosity, and the extended length endowed by the FCCVD method in the CNTFs, we have achieved a high water permeability coefficient and excellent selectivity by regulating the diameter of CNTs in the CNTFs.

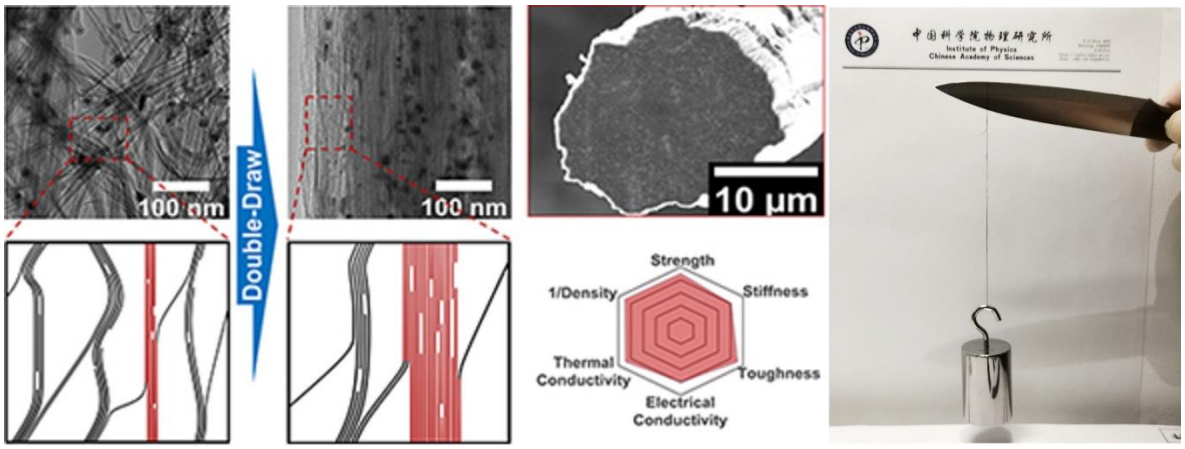

References

[1] X. Zhang *et al.*, *Science Adv.* **8**, eabq3515 (2022).
[2] J. L. Sun *et al.*, *Nano Res.* **17**, 7522-7532 (2024).
[3] X. Zhang *et al.*, *Nano Res.* **16**, 12821-12829 (2023).
[4] X. Zhang *et al.*, *Science Adv.* **6**, eabb6010 (2020).

Oxidation Saturation in Carbon Nanotubes: General Understanding of Functionalization Methods

Minfang Zhang[1], Mei Yang[1], Makoto Yaguchi[1], Hirokuni Jintoku[1], Shunsuke Sakurai[1], Don Futaba[1]

[1]*National Institute of Advanced Industrial Science and Technology (AIST), Tsukuba, Japan*

In carbon nanotube (CNT) processing, surface chemical modification is crucial for imparting desired functionalities to the typically inert graphitic surface [1]. This modification can strengthen CNT fibers by enhancing bonding, increase electrical conductivity through doping, or improve chemical affinity with host materials. Oxidation is a fundamental technique for purifying and modifying CNTs, introducing functional groups that improve dispersibility, reactivity, and expand their potential applications, but it involves breaking the graphitic surface and creating defects to which ligands can attach. Although harsher conditions—such as stronger acids, longer treatment durations, and higher temperatures—can improve functionalization efficiency, they also risk causing significant damage to the CNT structure. Balancing optimal functionalization with minimal structural damage remains a key challenge.

In this presentation, I will discuss our work to explore the limitations of oxidation in carbon nanotube (CNT) functionalization, highlighting a method-specific saturation point beyond which further treatment leads to the decomposition of functional groups and structural degradation [2]. We compare three common oxidation methods—hydrogen peroxide (H_2O_2), nitric acid (HNO_3), and a sulfuric/nitric acid mixture (H_2SO_4/HNO_3)—reveals distinct functionalization behaviors. The reaction rates and saturation points vary across methods, with the mixed acid treatment achieving the highest degree of functionalization while minimizing structural damage. In contrast, HNO_3 and H_2O_2 result in significant degradation at their respective saturation points. By identifying these saturation limits, this study provides insights into optimizing CNT functionalization for maximum performance with minimal structural compromise. A generalized oxidation model is introduced, offering guidance for advancing applications in nanotechnology, composites, and electronics.

References

[1] A. Hirsch, O. Vostrowsky, *Top Curr Chem.* **245,** 193–237 (2005).
[2] M. Zhang, M. Yang, M. Yaguchi, H. Jintoku, S. Sakurai, D. Futaba, *Carbon* **237**, 120132 (2025).

Confined Assembling Chemistry within Single-Walled Carbon Nanotubes

Feng Yang

Department of Chemistry, Southern University of Science and Technology, Shenzhen, 518055, China

Studying the molecular assembly behavior in confined spaces is of great significance for understanding mass transfer in microenvironments, chemical reactions, exploring novel metastable structures, and investigating material properties. Single-walled carbon nanotubes (SWCNTs) and clusters with well-defined structures provide ideal models for visualizing atomic-scale confined chemistry. The nearly transparent, single-layer curled sp^2 carbon atom layer also enables the transmission of properties of substances encapsulated within the carbon nanotubes.

We proposed a solution-phase host-guest confinement assembly strategy for SWCNTs [1,2], selecting clusters with electron-donating/accepting capabilities as guests. Through size confinement effects and electrostatic interactions, these clusters were driven to form ordered assemblies within the SWCNT cavities. This nanoconfined assembly approach opens new avenues for precisely constructing one-dimensional atomic crystals with ultimate unit-cell dimensions and metastable structures [3-5]. We developed a two-solvent-phase SWCNT-extraction method, achieving the confined growth of one-dimensional single-unit-cell-chain halide perovskites [6]. Atomic-resolution electron microscopy and spectroscopy revealed the unconventional structure of these single-unit-cell chain crystals and uncovered the strong "π-cation" interaction between the chain and the SWCNT. These single-unit-cell-chain perovskites, protected by a single conductive graphene-like layer, exhibit unique electronic structures and stable crystal configurations. The constructed X-ray detectors demonstrate outstanding and long-term stable performance.

References

[1] X. Yang, F. Yang, et al, J. Am. Chem. Soc. **143**, 10120 (2021).
[2] X. Zhao, F. Yang, et al, J. Am. Chem. Soc. **145**, 25242 (2023).
[3] K. Wang, F. Yang, et al, J. Am. Chem. Soc. **145**, 12760 (2023).
[4] H.-J. Liu, F. Yang, et al, J. Am. Chem. Soc. **146**, 20193 (2024).
[5] X. Zhao, F. Yang. et al, J. Am. Chem. Soc. **147**, 7028 (2025).
[6] M. Song, F. Yang. et al, Nat. Synth. 10.1038/s44160-025-00785-9 (2025).

Precise Partitioning of Single-Wall Carbon Nanotubes and Enantiomers Through Aqueous Two-Phase Extraction

H. Li[1,2], M. Zheng[3], J.A. Fagan[3]

[1]Department of Mechanical and Materials Engineering, University of Turku (Finland), [2]Turku Collegium for Science, Medicine and Technology, University of Turku (Finland), [3]Materials Science and Engineering Division, National Institute of Standards and Technology (USA)

Separation of single-chirality single-wall carbon nanotubes (SWCNTs) and their enantiomers holds significant promise for materials science and a range of applications, yet both scalability and precision remain challenging. In this work, we present a systematic strategy to define the separation conditions for various SWCNT types via aqueous two-phase extraction (ATPE). By introducing the concept of a partition coefficient change condition (PCCC), which can be extended beyond the photoluminescence-based measurements typical of semiconducting tubes, we make these separation parameters applicable to non-emissive metallic SWCNTs, enabled through presorted fractions and real ATPE procedures.

Through fine-tuning of binary and ternary surfactant mixtures, we demonstrate effective isolation of high-purity armchair nanotubes, such as (6,6), (7,7), (8,8), and (9,9), as well as more elusive non-armchair metallic species (9,3), (8,5), (7,4), (10,4), and (10,7) and some of their enantiomers. Our results reveal atypical partition behaviors, particularly among “outlier” tubes like (6,6) and (8,8), which highlight the crucial role of surfactant–nanotube interactions in defining solvation energies. Moreover, sharp transition profiles with high Hill coefficients underscore the importance of cooperative surfactant adsorption for achieving higher resolution and reproducibility in sorting.

These findings expand our fundamental understanding of co-surfactant-driven ATPE and set the stage for designing surfactant-specific protocols to separate SWCNTs more systematically. Ultimately, producing well-defined, high-purity nanotube ensembles will enable deeper investigations of their properties and broaden their deployment in fields including nanophotonics, optoelectronics, and biomedicine.

Quantifying Enantiomeric Purity Of Sorted Single-Walled Carbon Nanotubes Using Combined Chiroptical Spectroscopy And Hyperspectral Fluorescence Microscopy

Miguel Ángel López Carrillo[1], Filip Desmet[1], Maksiem Erkens[2], Jeffrey A. Fagan[3], Ming Zheng[3], Han Li[4,5], Benjamin S. Flavel[4], Wim Wenseleers[2], Wouter Herrebout[1], Sofie Cambré[1], Dmitry I. Levshov[1]

[1]Theory and Spectroscopy of Molecules and Materials, Department of Chemistry and Department of Physics, University of Antwerp, 2020 Antwerp (Belgium), [2]Nanostructured and Organic Optical and Electronic Materials, Department of Physics, University of Antwerp, 2610 Antwerp (Belgium), [3]Materials Science and Engineering Division, National Institute of Standards and Technology, 20899 Gaithersburg, Maryland (United States), [4]Institute of Nanotechnology, Karlsruhe Institute of Technology, 76344 Eggenstein-Leopoldshafen (Germany), [5]Department of Mechanical and Materials Engineering, University of Turku, FI-20014 Turku (Finland)

Recent advancements in sorting techniques have enabled the ultimate separation of as-synthesized single-walled carbon nanotube (SWCNT) samples into their two distinct mirror-image structures, known as enantiomers [1]. These SWCNT enantiomers hold great potential for a wide range of cutting-edge applications [2], including the detection and separation of chiral molecules in biology and chemistry, as well as circularly polarized light detection and emission — key functionalities for quantum computing, spintronics, and optoelectronics.

For many of these applications, maintaining precise control over the enantiomeric purity or enantiomeric excess (*ee*) of SWCNTs is crucial. In chemistry, chiroptical spectroscopy — particularly electronic circular dichroism (ECD) and Raman optical activity (ROA) — is the most effective method for such characterization. However, while these techniques are widely used in the SWCNT field, their full potential for characterization remains largely underexplored.

In this study, we combine ECD and ROA with hyperspectral fluorescence microscopy, UV-Vis-NIR absorption, and fluorescence excitation spectroscopy to analyze enantiomer-sorted (6,5) SWCNTs from different synthesis sources (HiPCO or CoMoCAT) with varying enantiomeric purities (Figure 1). By leveraging fluorescence shifts in hyperspectral data [3], we quantify the *ee* of (6,5) SWCNTs and calibrate ECD and ROA intensities. Our findings reveal that the synthesis source significantly influences the optical properties of SWCNTs, particularly in differentiating between (+)- and (−)-(6,5) enantiomers in hyperspectral fluorescence images. Additionally, we identify the critical role of SWCNT concentration in accurately estimating *ee* through chiroptical spectroscopy, addressing challenges such as photon reabsorption and the ECD-Raman effect [4]. Our results provide a reliable approach for quantifying the *ee* of SWCNTs using chiroptical spectroscopy, paving the way for improved characterization and more efficient enantiomeric sorting techniques.

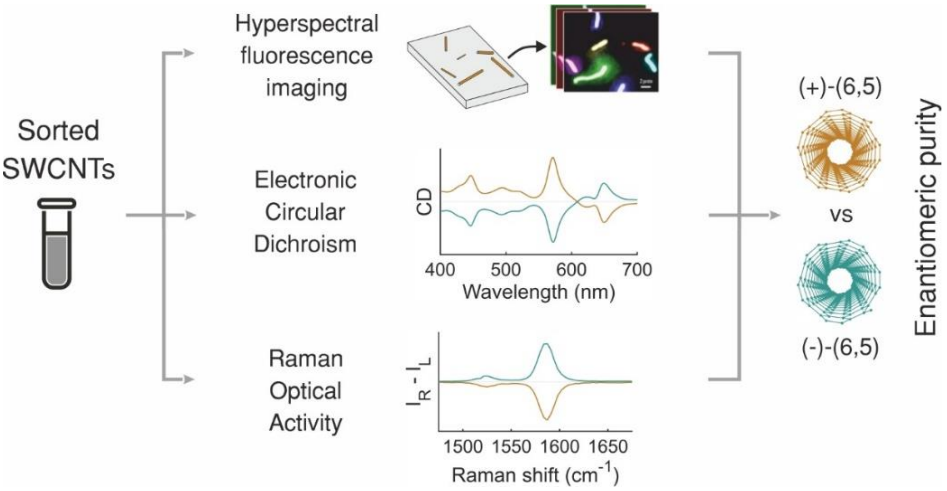

Figure 1: Characterization of enantiomer-sorted SWCNT samples by combining hyperspectral data, ECD and ROA.

References: Yang *et al.*, Chem Rev 2020, 120 (5), 2693–2758 ; [2] Wei *et al.*, Advanced Science 2022, 9 (14), 1–42; [3] Erkens *et al.*, ACS Nano 2024, 18 (22), 14532–14545 ; [4] Machalska *et al.*, Angew. Chemie 2021, 133 (39), 21375–21380.

Session
NT 25（The 25th International Conference on the Science and Applications of Nanotubes and Low-

| Parallel Symposia：Symposium on Fundamental, Structural and Optical Properties of 1D and 2D Materials and their Heterostructures

Thu. Jun 19, 2025 2:00 PM - 5:00 PM JST | Thu. Jun 19, 2025 5:00 AM - 8:00 AM UTC International Exchange Hall III (Clock Tower Centennial Hall, 2F)

[19fn] Fundamental Properties

Chair:Sebastian Heeg, Shohei Chiashi

2:00 PM - 2:20 PM JST | 5:00 AM - 5:20 AM UTC

[19fn-01]

Optical Absorption in Layered Semiconductor to Semimetal Platinum Diselenide

*Marin Tharrault[1], Sabrine Ayari[1,2], Mehdi Arfaoui[3], Eva Desgué[4], Romaric Le Goff[1], Sihem Jaziri[3,5], Bernard Plaçais[1], Pierre Legagneux[4], Francesca Carosella[1], Christophe Voisin[1], Robson Ferreira[1], Emmanuel Baudin[1] (1. Laboratoire de Physique de l'Ecole normale supérieure, ENS, Université PSL, CNRS, Sorbonne Université, Université Paris Cité (France), 2. De Vinci Higher Education, Research Center (France), 3. Laboratoire de Physique de la Matière Condensée, Faculté des Sciences de Tunis, Université Tunis El Manar (Tunisia), 4. Thales Research & Technology (France), 5. Laboratoire de Physique des Matériaux : Structure et Propriétés, Faculté des Sciences de Bizerte, Université de Carthage (Tunisia))

2:20 PM - 2:40 PM JST | 5:20 AM - 5:40 AM UTC

[19fn-02]

THERMAL TRANSPORT ACROSS TWISTED BI-LAYERS OF 2D TRANSITION METAL DICHALCOGENIDES

*Marianna Sledzinska[1], Jiaqi Yang[1,2], Daniel Capolat Palomar[1], Onurcan Kaya[1], Aron W Cummings[1], Aitor Lopeandia[1,2], Javier Rodríguez Viejo[1,2], Stephan Roche[1,3] (1. Catalan Institute of Nanoscience and Nanotechnology (ICN2) (Spain), 2. UAB (Spain), 3. ICREA (Spain))

2:40 PM - 3:00 PM JST | 5:40 AM - 6:00 AM UTC

[19fn-03]

Chiral Stacking Identification of Two-Dimensional Triclinic Crystals Enabled by Machine Learning

*He Hao[1], Kangshu Li[1], Xujing Ji[1], Xiaoxu Zhao[1], Lianming Tong[1], Jin Zhang[1] (1. Peking University (China))

3:00 PM - 3:20 PM JST | 6:00 AM - 6:20 AM UTC

[19fn-04]

Probing strong electron-phonon coupling in graphene by resonance Raman spectroscopy with infrared excitation energy

*Simone Sotgiu[1,2], Tommaso Venanzi[2], Lorenzo Graziotto[2], Francesco Macheda[3], Taoufiq Ouaj[1], Elena Stellino[2], Guglielmo Marchese[2], Claudia Fasolato[4], Paolo Postorino[2], Vaidotas Mišeikis[3], Marvin Metzelaars[1], Paul Kögerler[1], Bernd Beschoten[1], Camilla Coletti[3], Stefano Roddaro[5], Matteo Calandra[6], Michele Ortolani[2], Christoph Stampfer[1], Francesco Mauri[2], Leonetta Baldassarre[2] (1. RWTH Aachen Univ. (Germany), 2. Sapienza Univ. (Italy), 3. IIT (Italy), 4. CNR (Italy), 5. Pisa Univ. (Italy), 6. Trento Univ. (Italy))

4:00 PM - 4:20 PM JST | 7:00 AM - 7:20 AM UTC

[19fn-05]

Intrinsic process for upconversion photoluminescence via *K*-momentum phonon coupling in carbon nanotubes

Session
NT 25（The 25th International Conference on the Science and Applications of Nanotubes and Low-
*Daichi Kozawa[1,2], Shun Fujii[1,3], Yuichiro K. Kato[1] (1. RIKEN (Japan), 2. NIMS (Japan), 3. Keio University (Japan))

4:20 PM - 4:40 PM JST | 7:20 AM - 7:40 AM UTC

[19fn-06]

EXPERIMENTAL DETERMINATION OF PHASE TRANSITIONS OF WATER MOLECULES ENCAPSULATED INSIDE THIN SWCNTs

*Aina Fitó-Parera[1], Miles Martinati[1,2], Wim Wenseleers[2], Sofie Cambré[1] (1. TSM2, University of Antwerp (Belgium), 2. NANOrOPT, University of Antwerp (Belgium))

4:40 PM - 5:00 PM JST | 7:40 AM - 8:00 AM UTC

[19fn-07]

Multi-modal carbon nanotube characterization for nano-confined thermodynamics

*Matthias Kuehne[1] (1. Brown University (United States of America))

OPTICAL ABSORPTION IN LAYERED SEMICONDUCTOR TO SEMIMETAL PLATINUM DISELENIDE

M. Tharrault[1], S. Ayari[1,2], M. Arfaoui[3], E. Desgué[4], R. Le Goff[1], S. Jaziri[3,5], B. Plaçais[1], P. Legagneux[4], F. Carosella[1], C. Voisin[1], R. Ferreira[1], and E. Baudin[1]

[1]Laboratoire de Physique de l'Ecole normale supérieure, ENS, Université PSL, CNRS, Sorbonne Université, Université Paris Cité (France), [2]De Vinci Higher Education, Research Center (France), [3]Laboratoire de Physique de la Matière Condensée, Faculté des Sciences de Tunis, Université Tunis El Manar (Tunisia), [4]Thales Research & Technology (France), [5]Laboratoire de Physique des Matériaux : Structure et Propriétés, Faculté des Sciences de Bizerte, Université de Carthage (Tunisia)

The transition metal dichalcogenide $PtSe_2$ exhibits the surprising property of transitioning from a semimetal to a semiconductor as it is thinned down to a few monolayers [1]. This strongly thickness-dependent 2D material hence allows the tuning of its electronic properties to address specific applications—such as near-infrared photodetection for fiber optics telecommunications. Yet, the light absorption mechanism in such materials is still not well understood.

In this talk, I will rely on broadband optical absorption spectroscopy (0.8–3.0 eV) of high-quality $PtSe_2$ few-layer crystals obtained by the Au exfoliation technique [2]. While previous studies conjectured that their absorption threshold originates from interband indirect transitions, we will rule out such a mechanism by studying the dependence of optical absorption on temperature and material quality. The quantitative comparison with *ab initio* density functional theory (DFT) simulations will allow us to conclude that the optical absorption arises solely from direct transitions, and to identify the transitions at play [3]. Based on this understanding, I will revisit the $PtSe_2$ semiconductor-to-semimetal transition with respect to the number of layers.

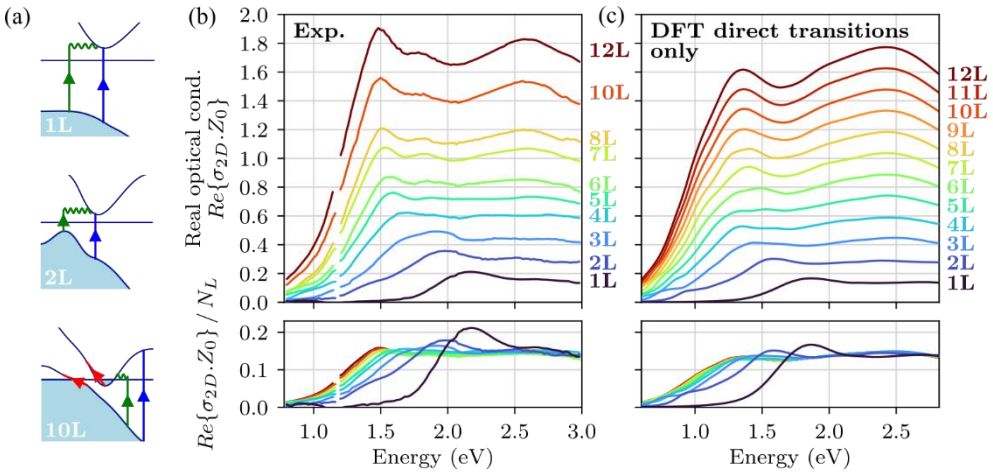

Figure caption: (a) Schematic of photon absorption mechanisms considered—depicting intraband (red), indirect interband (green), and direct interband (blue) transitions. (b) Experimental and (c) theoretical real 2D optical conductivities $Re\{\sigma_{2D}.Z_0\}$ (top plots), and their values normalized by the layer count N_L (bottom plots). $Z_0 = 377\Omega$ is the impedance of free space. Adapted from [3].

References

[1] Y. Zhao, J. Qiao, Z. Yu *et al.*, *Adv. Mater.* **29**, 1604230 (2017).
[2] M. Tharrault, E. Desgué, D. Carisetti *et al.*, *2D Mater.* **11,** 025011 (2024).
[3] M. Tharrault, S. Ayari, M. Arfaoui *et al.*, *Phys. Rev. Lett.* **134**, 066901 (2025).

THERMAL TRANSPORT ACROSS TWISTED BI-LAYERS OF 2D TRANSITION METAL DICHALCOGENIDES

J. Yang[1,2], T. Swoboda[1], D. Capolat Palomar[1], O. Kaya[1], A.W. Cummings[1], A. Lopeandia[1,2], J. Rodríguez Viejo[1,2], S. Roche[1,3], M. Sledzinska[1].

[1] *Catalan Institute of Nanoscience and Nanotechnology (ICN2), CSIC and BIST, Campus UAB, Bellaterra, 08193 Barcelona, Spain*

[2]*Autonomous University of Barcelona (UAB,) Campus UAB, Bellaterra, 08193 Barcelona Spain.*

[3]*ICREA - Institució Catalana de Recerca i Estudis Avançats, 08010 Barcelona, Spain*

marianna.sledzinska@icn2.cat

Two-dimensional transition metal dichalcogenides (TMDs) are promising for next-generation thermal management applications due to their atomically layered structures, which introduce rotational degrees of freedom. Theoretical studies suggest that both cross-plane and in-plane thermal transport in stacked 2D materials are highly dependent on twist angle, as it modulates interlayer phonon coupling, thereby affecting phonon transmission and scattering. These effects are particularly pronounced at small twist angles (0–5°). However, precise fabrication of high-quality, twisted bilayers with small angles remains challenging, and experimental validation of theoretical predictions is still limited [1,2].

Here, we discuss synthesis strategies for high-quality, large-area monolayers of TMDs, such as MoS_2 and WS_2, via capping-assisted CVD growth and fabrication techniques for obtaining clean, twisted bilayers. Thermal transport across the mono and bi-layers was studied using frequency-domain thermoreflectance, together with molecular dynamics simulations. Our findings provide insights into how interlayer coupling influences phonon transport in twisted bilayers of homo- and hetero-stacking, particularly in the small-angle regime. These results are crucial for phonon engineering strategies in 2D materials and the design of tunable thermal management systems for nanoscale devices.

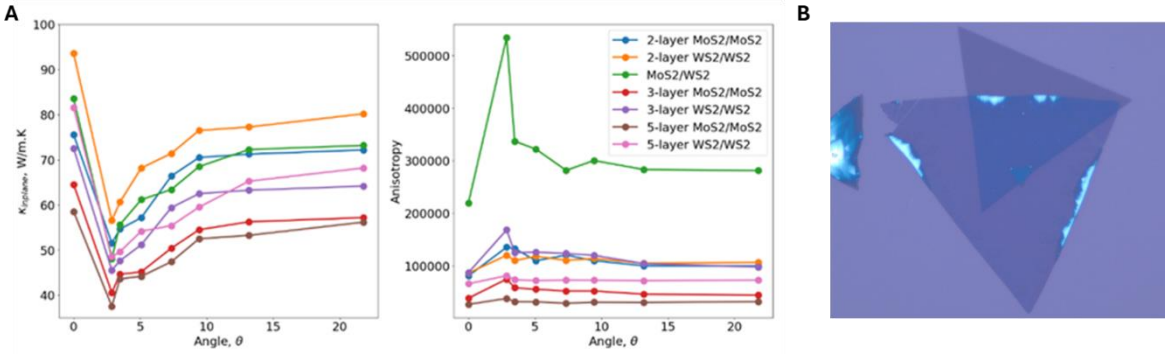

Figure 1: (A) In-plane thermal conductivity and thermal anisotropy of twisted multilayers with respect to the applied twist angles, from molecular dynamics simulations of the in-plane and cross-plane thermal conductivity of both homo- and heterogeneous stacks of TMDCs. (B) Twisted WS_2 with an angle of 15° fabricated in this study.

References

[1] L, Zhang et. al. Nano Lett. 2023, 23, 17, 7790–7796.
[2] L, Xiong et. al. ACS Appl. Nano Mater. 2023, 6, 17, 15685–15696.

Acknowledgements This work was supported by EIC-Japan project PETITE (PCI2023-143399).

Chiral Stacking Identification of Two-Dimensional Triclinic Crystals Enabled by Machine Learning

He Hao[1], Kangshu Li[2], Xujing Ji[2], Xiaoxu Zhao[2], Lianming Tong[1], and Jin Zhang[1]

[1]*Center for Nanochemistry, Beijing Science and Engineering Center for Nanocarbons, Beijing National Laboratory for Molecular Sciences, College of Chemistry and Molecular Engineering, Peking University, 100871 Beijing (China),*
[2]*School of Materials Science and Engineering, Peking University, 100871 Beijing (China)*

Chiral materials possess broken inversion and mirror symmetry and show great potential in the application of next-generation optic, electronic, and spintronic devices. Two dimensional (2D) chiral crystals have planar chirality, which is nonsuperimposable on their 2D enantiomers by any rotation about the axis perpendicular to the substrate [1, 2]. The degree of freedom to construct vertical stacking of 2D monolayer enantiomers offers the possibility of chiral manipulation for designed properties by creating multilayers with either a racemic or enantiomerically pure stacking order. However, the rapid recognition of the relative proportion of two enantiomers becomes demanding due to the complexity of stacking orders of 2D chiral crystals. Here, we report the unambiguous identification of racemic and enantiomerically pure stackings for layered $ReSe_2$ and ReS_2 using circular polarized Raman spectroscopy [3]. The chiral Raman response is successfully manipulated by the enantiomer proportion, and the stacking orders of multilayer $ReSe_2$ and ReS_2 can be completely clarified with the help of second harmonic generation and scanning transmission electron microscopy measurements. Finally, we trained an artificial intelligent Spectra Classification Assistant to predict the chirality and the complete crystallographic structures of multilayer $ReSe_2$ from a single circular polarized Raman spectrum with the accuracy reaching 0.9417±0.0059.

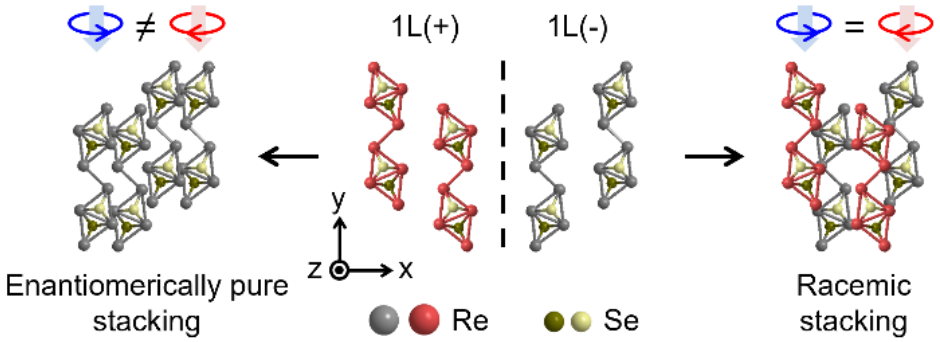

Figure caption: Enantiomerically pure and racemic stacking of bilayer $ReSe_2$ and their chiral Raman response under excitation of left-handed (blue arrows pointing anticlockwise) and right-handed (red arrows pointing clockwise) circularly polarized light.

References

[1] S. Zhang *et al.*, *Nat. Commun.* **13**, 1254 (2022).
[2] Y. Zhao *et al.*, *Nat. Commun.* **14**, 2223 (2023).
[3] H. Hao *et al.*, *ACS Nano* **18**, 13858−13865 (2024).

Probing strong electron-phonon coupling in graphene by resonance Raman spectroscopy with infrared excitation energy

S. Sotgiu[1,2], T. Venanzi[2], L. Graziotto[2], F. Macheda[3], T. Ouaj[1], E. Stellino[2], G. Marchese[2], C. Fasolato[4], P. Postorino[2], V. Mišeikis[3,5], M. Metzelaars[6], P. Kögerler[6], B. Beschoten[1], C. Coletti[3,5], S. Roddaro[7], M. Calandra[8], M. Ortolani[2], C. Stampfer[1], F. Mauri[2] and L. Baldassarre[2]

[1] *JARA-FIT and 2nd Institute of Physics, RWTH Aachen University (Germany),*

[2] *Department of Physics, Sapienza University of Rome (Italy)*

[3] *Istituto Italiano di Tecnologia, Graphene Labs (Italy)*

[4] *Institute for Complex System, National Research Council (Italy)*

[5] *Istituto Italiano di Tecnologia, Center for Nanotechnology Innovation @NEST (Italy)*

[6] *Institute of Inorganic Chemistry, RWTH Aachen University, (Germany)*

[7] *Department of Physics, University of Pisa (Italy)*

[8] *Department of Physics, University of Trento (Italy)*

Resonance Raman spectroscopy has been a key asset to study the interplay between electronic and vibrational properties of graphene and other two-dimensional materials [1].

Here, we report on resonance Raman spectroscopy measurements with an excitation photon energy down to 1.16 eV on mono and bilayer graphene, to study how low-energy carriers interact with lattice vibrations. Thanks to the excitation energy close to the Dirac point, we unveil in the monolayer a giant increase of the intensity ratio between the double-resonant 2D and 2D' Raman peaks with respect to that measured in graphite (Fig.1a) [2].

In bilayer graphene, the low excitation energy hampers some of the resonant Raman processes giving rise to the 2D Raman peak. Consequently, the sub-features composing the 2D mode are spectrally more separated with respect to visible excitations (Fig.1b and c). We follow the excitation-energy dependence of the intensity of each sub-structure and, comparing experimental measurements on bilayer graphene with ab initio theoretical calculations, we trace back such modifications on the joint effects of probing the electronic dispersion close to the band splitting and enhancement of electron-phonon matrix elements [3].

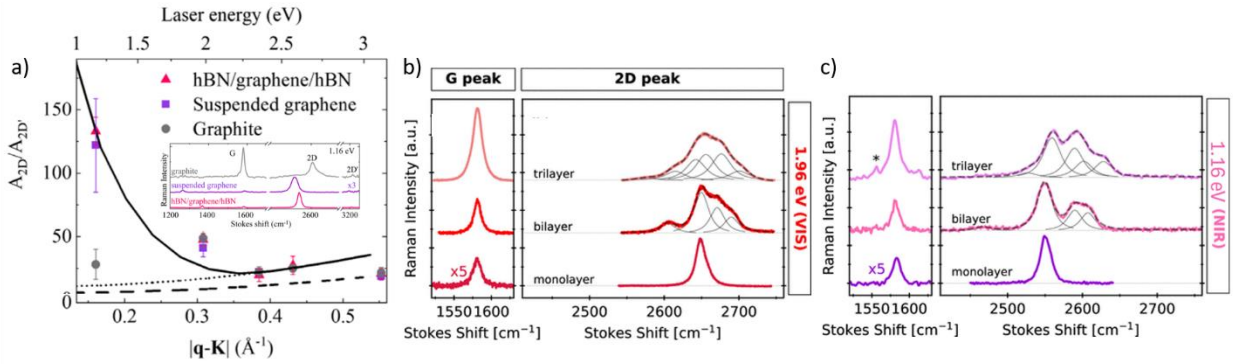

Figure 1: a) Intensity ratio of the resonant peaks 2D and 2D' at several laser excitation energies. In the inset the spectra obtained at 1.16 eV for graphite and graphene samples are reported. b) 2D peaks for mono, bi and trilayer graphene measured for red and c) infrared laser excitation energies.

References

[1] D. Graf *et al. Nano Lett.* **238**-242 (2007)
[2] T. Venanzi *et al., Phys. Rev. Lett.* **130**, 256901 (2023)
[3] L. Graziotto *et al., Nano Lett.* **24**-1867 (2024)

Intrinsic process for upconversion photoluminescence via *K*-momentum phonon coupling in carbon nanotubes

Daichi Kozawa[1,2,3], Shun Fujii[1,4], Yuichiro K. Kato[1,2]

[1] *Quantum Optoelectronics Research Team, RIKEN Center for Advanced Photonics, Wako, Saitama, Japan*

[2] *Nanoscale Quantum Photonics Laboratory, RIKEN Cluster for Pioneering Research, Wako, Saitama, Japan*

[3] *Research Center for Materials Nanoarchitectonics, National Institute for Materials Science, Tsukuba, Ibaraki, Japan*

[4] *Department of Physics, Keio University, Yokohama, Kanagawa, Japan*

We investigate the intrinsic microscopic mechanism of photon upconversion in air-suspended single-walled carbon nanotubes through photoluminescence and upconversion photoluminescence spectroscopy (Fig. 1) [1]. Nearly linear excitation power dependence of upconversion photoluminescence intensity is observed, indicating a one-photon process as the underlying mechanism. In addition, we find a strongly anisotropic response to the excitation polarization which reflects the intrinsic nature of the upconversion process. In upconversion photoluminescence excitation spectra, three peaks are observed which are similar to photoluminescence sidebands of the *K*-momentum dark singlet exciton. The features in the upconversion photoluminescence excitation spectra are well reproduced by our second-order exciton-phonon interaction model, enabling the determination of phonon energies and relative amplitudes. The analysis reveals that the upconversion photoluminescence can be described as a reverse process of the sideband emission linked to the *K*-momentum phonon modes. The validity of our model is further reinforced by temperature-dependent upconversion photoluminescence excitation measurements reflecting variations in the phonon population. Our findings underscore the pivotal role of the resonant exciton-phonon coupling in pristine carbon nanotubes and presents potential for advanced optothermal technologies by engineering the excitation pathways.

This work is supported in part by JSPS (KAKENHI 23K23161, JP22K14625, JP23H00262, JP20H02558), JST (ASPIRE JPMJAP2310), the Precise Measurement Technology Promotion Foundation (PMTP-F), and MEXT (ARIM JPMXP1222UT1136). We thank the Advanced Manufacturing Support Team at RIKEN for technical assistance.

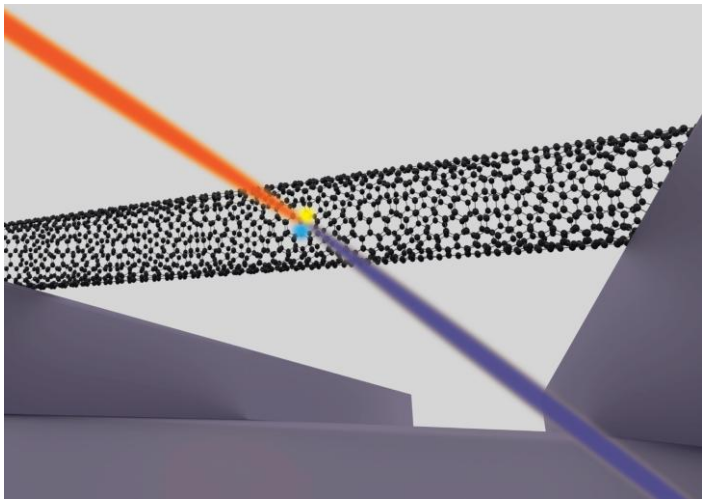

Figure 1: A carbon nanotube suspended across a Si trench. The red ray is the excitation laser and the blue ray is the upconversion photoluminescence.

References

[1] D. Kozawa, S. Fujii, Y. K. Kato Intrinsic process for upconversion photoluminescence via K-momentum-phonon coupling in carbon nanotubes Phys. Rev. B 110, 155418 (2024).

EXPERIMENTAL DETERMINATION OF PHASE TRANSITIONS OF WATER MOLECULES ENCAPSULATED INSIDE THIN SWCNTs

Aina Fitó-Parera[1], Miles Martinati[1, 2], Wim Wenseleers[2], Sofie Cambré[1]
[1]*Theory and Spectroscopy of Molecules and Materials (TSM²), Department of Physics, University of Antwerp (Belgium)*

[2]*Nanostructured and Organic Optical and Electronic Materials (NANOrOPT), Department of Physics, University of Antwerp (Belgium)*

The experimental determination of the behaviour of water under one-dimensional confinement has been a topic of interest in recent years [1]–[5]. While molecular dynamics simulations have predicted the solid-liquid phase transition of water to occur at different temperatures depending on the SWCNT diameter [1-2], experimental results have only been achieved for a few discrete chiral structures with diameters above 1.0178 nm [3,5], and one demonstration for water encapsulated inside the (6,5) chirality [4], Previous studies detected the phase transitions through a change in vibrational or optical properties of the SWCNTs, but relied on measuring single- or few-tube samples, making a full diameter-dependent analysis unfeasible. Ensemble measurements on mixed-chirality SWCNTs could provide a solution for this, however, were for a long time hindered by the difficulty of finding the correct experimental conditions, where the influence of the surrounding environment can be completely uncoupled from the quasi-phase transitions occurring in the internal core of the SWCNT.

In this work, I describe temperature-dependent photoluminescence-excitation (PLE) measurements performed directly in mixed-chirality, yet empty/water-filled sorted, ensemble samples combined with detailed fitting of these PLE maps, able to disentangle external and internal environmental changes of the optical transitions as a function of temperature. To achieve this, the measurements were performed by immobilizing the SWCNTs in a PVA matrix that prevented unnecessary quenching of the PL to maintain a sufficiently high signal-to-noise ratio, allowing for accurate extraction of peak positions and line widths of both the first and second optical transitions of a number of SWCNTs as a function of temperature. These PLE measurements revealed the phase transition of 6 chiralities within a diameter range between 0.77 and 0.95 nm, exactly in a range where experimental observations were still lacking (see **Figure 1** for an example of the (8,3) chirality). These new experimental results confirm previous theoretical calculations and reveal the highly complex behaviour of water molecules at the nanoscale.

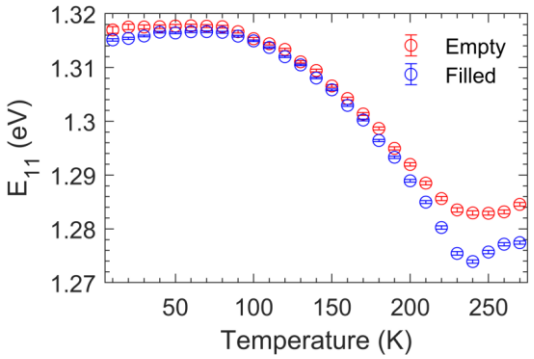

Figure 1: E_{11} (8,3) peak positions of empty (red) and water-filled (blue) SWCNTs for a range of 10 to 270 K.

References

[1] D. Takaiwa *et al.*, *PNAS.* **105**, 39–43 (2008).
[2] H. Kyakuno *et al.*, *J. Chem. Phys.* **134**, 244501 (2011).
[3] K. V. Agrawal *et al.*, *Nat. Nanotechnol.* **12**, 267-273 (2017).
[4] X. Ma *et al.*, *Phys. Rev. Lett.* **118**, 027402 (2017).
[5] S. Chiashi *et al.*, *ACS Nano* **12**, 267-273 (2019).

Multi-modal carbon nanotube characterization for nano-confined thermodynamics

M. Kuehne[1]

[1]*Brown University, Providence, RI (United States)*

Recent pioneering work has leveraged optical spectroscopy to investigate fluids under extreme nanoscale confinement in carbon nanotubes (CNTs) [1,2]. These studies have revealed breakthroughs including the observation of discontinuous trends in phase transition temperatures in the single-digit nanopore regime. However, quantitative disagreements among different experimental techniques and platforms, as well as among molecular dynamics simulations [3,4], highlight the need for more comprehensive investigation approaches. I will discuss progress in developing an integrated multi-modal characterization platform that extends beyond the capabilities of conventional optical spectroscopy approaches.

Our work centers on the implementation and integration of complementary measurement techniques for individual carbon nanotubes. Specifically, we combine optical spectroscopy with electromechanical measurements and electrothermal methods. I will detail our progress in establishing these techniques, addressing the significant instrumentation challenges involved, and demonstrating initial validation experiments. Key advancements include integration of electromechanical measurements with individual ultralong carbon nanotubes, and the development of a modified electrothermal method—initially qualified on micrometer-diameter nanofibers—that may enable thermal characterization of nanotubes with relevant diameters on the nanometer scale.

While future applications of this platform will include detailed investigations of molecular phase transitions, our current focus is on establishing the measurement infrastructure itself. This foundational work represents an important advance in nanofluidics instrumentation, with potential implications for fields including materials science, chemical separations, and energy applications where molecular behavior under extreme confinement plays a critical role.

References

[1] K. V. Agrawal *et al.*, *Nat. Nanotechnol.* **12**, 267–273 (2017).
[2] S. Chiashi *et al.*, *ACS Nano* **13**, 1177–1182 (2019).
[3] D. Takaiwa *et al.*, *Proc. Natl. Acad. Sci. U.S.A.* **105**, 39-43 (2008).
[4] M. Raju et al., *Sci. Rep.* **8**, 3851 (2018).

Session
NT 25（The 25th International Conference on the Science and Applications of Nanotubes and Low-

| Parallel Symposia：15th Symposium on Carbon Nanomaterials, Biology, Medicine and Toxicology

Thu. Jun 19, 2025 2:00 PM - 5:00 PM JST | Thu. Jun 19, 2025 5:00 AM - 8:00 AM UTC Meeting Room E/F(INNOVATION BLDG., 5F)

[19nb] NanoBio

Chair:Tomohiro Shiraki, Anton Naumov, Mijin Kim

2:00 PM - 2:40 PM JST | 5:00 AM - 5:40 AM UTC

[19nb-01]

Functionally Programmed Medical Nanodevices for Cancer

*Naoki Komatsu[1] (1. Kyoto University (Japan))

2:40 PM - 3:00 PM JST | 5:40 AM - 6:00 AM UTC

[19nb-02]

Engineered Muti-Walled Carbon Nanotubes for tumor microenvironment modulation and melanoma metastasis suppression

*LORENA GARCÍA HEVIA[1], Rym Soltani[2], Jesús González[3], Olivier Chaloin[2], Cecilia Ménard-Moyon[2], Alberto Bianco[2], Mónica L. Fanarraga[3] (1. CINBIO, UNIVERSITY OF VIGO, IISGS (Spain), 2. University of Strasbourg (France), 3. Universidad de Cantabria-IDIVAL (Spain))

3:00 PM - 3:20 PM JST | 6:00 AM - 6:20 AM UTC

[19nb-03]

Evidence-based, systematic design of machine perception nanosensors for disease detection

*Mijin Kim[1] (1. Georgia Institute of Technology (United States of America))

4:00 PM - 4:20 PM JST | 7:00 AM - 7:20 AM UTC

[19nb-04]

Wrapping Polymer-dependent Microenvironment Responses of Near-infrared Photoluminescence from Color Centers in Single-walled Carbon Nanotubes

*Tomohiro Shiraki[1,2], Yoshiaki Niidome[1], Ryo Hamano[1], Hiromu Matsumoto[1], Koichiro Kato[1,3], Tsuyohiko Fujigaya[1,2,3] (1. Dept. of Applied Chem., Kyushu Univ. (Japan), 2. WPI-I2CNER, Kyushu Univ. (Japan), 3. CMS, Kyushu Univ. (Japan))

4:20 PM - 4:40 PM JST | 7:20 AM - 7:40 AM UTC

[19nb-05]

Toward Non-Invasive Real-Time Detection of Neurotransmitters and Hormones Using Near-Infrared Fluorescent Graphene Quantum Dots

*Anton Naumov[1], Floyd Wormley[1], Alina Valimukhametova[1], Natalia Castro Lopez[1], Alyssa Dickens[1], Pramita Sharma[1] (1. Texas Christian University (United States of America))

4:40 PM - 5:00 PM JST | 7:40 AM - 8:00 AM UTC

[19nb-06]

The Design and Application of Carbon Dots-Based Prodrug Conjugates

*Jia-Yaw Chang[1] (1. National Taiwan University of Science and Technology (Taiwan))

Functionally Programmed Medical Nanodevices for Cancer

Naoki Komatsu

Graduate School of Human and Environmental Studies, Kyoto University, Sakyo-ku, Kyoto 606-8501 (Japan)

Nanomedicine is promising to improve conventional cancer medicine by making diagnosis and/or therapy more precise and more efficient in a more personalized manner. A key for cancer nanomedicine is construction of medical nanodevices by programming most of the following functions to nanomaterials; A) high dispersibility in a physiological environment, B) high stealth efficiency to slip through the trap by mononuclear phagocyte system (MPS) in liver and spleen, C) high targeting efficiency to tumor tissue and/or cells, D) clear visualization of tumor for diagnosis, and E) high antitumor activity for therapy (Figure 1) [1].

In my talk, I will present rational design and facile construction of medical nanodevices for cancer, based on organic chemistry and nanoscience, especially novel "RadioNano" sensitizers in boron neutron capture therapy (BNCT) for cancer [2-8].

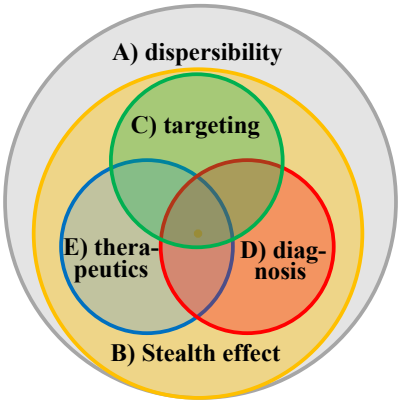

Figure 1. Requisite functions in medical nanodevices for cancer [1].

References

[1] N. Komatsu* *Acc. Chem. Res.*, **56**, 106 (2023).
[2] L. Zhao, T. Takimoto, M. Ito, N. Kitagawa, T. Kimura, N. Komatsu,* *Angew. Chem. Int. Ed.*, **50**, 1388 (2011) [highlighted at the back cover].
[3] Y. Zou, S. Ito, F. Yoshino, Y. Suzuki, L. Zhao, N. Komatsu,* *ACS Nano*, 1**4**, 7216 (2020).
[4] F. Yoshino, T. Amano, Y. Zou, J. Xu, F. Kimura, Y. Furusho, T. Chano, T. Murakami, L. Zhao,* N. Komatsu,* *Small*, **15**, 1901930 (2019) [highlighted at the back cover].
[5] L. Zhao, Y.-H. Xu, H. Qin, S. Abe, T. Akasaka, T. Chano, F. Watari, T. Kimura, N. Komatsu,* X. Chen* *Adv. Funct. Mater.*, **24**, 5348 (2014) [highlighted at the inside front cover].
[6] Y. Wang, G. Reina, H. G. Kang, X. Chen, Y. Zou, Y. Ishikawa, M. Suzuki, N. Komatsu* *Small*, **18**, 2204044 (2022).
[7] Y. Zhang, H. G. Kang, H. Xu, H. Luo, M. Suzuki, Q. Lan,* X. Chen,* N. Komatsu,* L. Zhao* *Adv. Mater.*, **35**, 2301479 (2023).
[8] Y. Zou, S. Ito, M. Fujiwara, N. Komatsu,* *Adv. Funct. Mater.*, **32**, 2111077 (2022) [highlighted at the inside front cover].

Engineered Muti-Walled Carbon Nanotubes for tumor microenvironment modulation and melanoma metastasis suppression

L. García-Hevia[1], R. Soltani[2], J. González[3], O. Chaloin[2], C. Ménard-Moyon[2], A. Bianco[2] and M. L. Fanarraga[3]

[1]*The Hybrid Nanomaterials Group, CINBIO, University of Vigo, IIS Galicia Sur, Estrada de Marcosende, 36310 Vigo, Pontevedra, (Spain)*

[2]*CNRS, Immunology, Immunopathology and Therapeutic Chemistry, UPR 3572, University of Strasbourg, ISIS, 67000 Strasbourg, (France)*

[3]*The Nanomedicine Group, Universidad de Cantabria-IDIVAL, University of Cantabria, Avda Herrera Oria s/n, 39011, Santander, (Spain)*

Metastasis, the complex biological process through which cancer cells spread from their original site to establish secondary tumors in distant organs, remains a major obstacle in cancer treatment, significantly increasing disease severity and mortality rates.

Multi-walled carbon nanotubes (MWCNTs) have demonstrated a unique ability to interact with cytoskeletal nanofilaments upon cellular and tissue penetration, exerting intrinsic antitumor effects comparable to microtubule-targeting chemotherapies such as Taxol® [1-5].

This study explores the potential of oxidized MWCNTs as selective inhibitors of vascular endothelial growth factor receptors (VEGFR), assessing their capacity to suppress metastatic progression by inducing anti-proliferative, anti-migratory, and cytotoxic effects on both tumor cells and their surrounding microenvironment. Our results reveal a striking reduction of over 80% in melanoma lung metastases following intravenous administration of biodegradable, targeted MWCNTs. Additionally, combining these nanomaterials with the standard chemotherapeutic agent Taxol® amplified the antimetastatic efficacy by an impressive 90% [6]. This combinatorial therapeutic strategy holds significant promise in combating metastatic cancer, as demonstrated by these compelling findings. Given that metastasis accounts for nearly 60,000 deaths annually, these results highlight a potential breakthrough in metastatic disease treatment, paving the way for novel nanotechnology-based interventions.

References

[1] L. Rodríguez-Fernández, et al. ACS Nano. 6 (2012) 6614–6625.
[2] L. García-Hevia, et al. Nanomedicine. 9 (2014) 1581–1588.
[3] L. Garcia-Hevia, et al. Curr Pharm Des. 21 (2015) 1920–1929.
[4] L. García-Hevia, R. et al. Curr Pharm Des. 21 (2015).
[5] L. García-Hevia, M.L. Fanarraga, J Nanobiotechnology. 18 (2020) 1–11.
[6] L. García-Hevia, et al. Bioactive Materials 34 (2024) 237-247.

Evidence-based, systematic design of machine perception nanosensors for disease detection

Mijin Kim[1]

[1]*Georgia Institute of Technology (USA)*

A *machine perception liquid biopsy (MPLB)* approach can detect and identify disease states from blood rapidly, inexpensively, and without prior knowledge of biomarkers, and the method enables the discovery of biomarkers responsible for the detection. MPLB synergizes optical nanosensors with artificial intelligence capabilities. Sensor arrays, comprised of *quantum defect-modified carbon nanotubes (QTs),* transduce subtle differences in the physicochemical properties of molecules in biofluids, such as serum and plasma. The diverse responses of the QT array, processed by machine learning, collectively produce a disease-specific “spectral fingerprint.” While variations in functional defect type, density, and excipients would modulate diverse physicochemical interactions between biomolecules and nanoparticles, the design principle of the QT arrays to improve chemical diversity and molecular interactions remains underexplored. In this talk, I will discuss how chemical modification of nanoparticles impacts biomolecular corona composition and facilitates the development and optimization of an evidence-based, systematic design of MPLB for disease detection.

Wrapping Polymer-dependent Microenvironment Responses of Near-infrared Photoluminescence from Color Centers in Single-walled Carbon Nanotubes

T. Shiraki[1,2], Y. Niidome[1], R. Hamano[1], H. Matsumoto[1], K. Kato[1,3], T. Fujigaya[1,2.3]

[1]Department of Applied Chemistry, Kyushu University (Japan); [2] WPI-I2CNER, Kyushu University (Japan); [3] CMS, Kyushu University (Japan)

Polymer wrapping techniques of single-walled carbon nanotubes (SWCNTs) are used for not only their solubilization in solvents but also near-infrared (NIR) biosensor fabrication including corona phase molecular recognition−based nanosensors [1]. Luminescent color centers (CCs) formed in SWCNTs by local chemical functionalization (The resultant SWCNTs are named as locally functionalized SWCNTs: lf-SWCNT) show bright and red-shifted NIR photoluminescence (PL) (E_{11}* PL) compared to the original PL (E_{11} PL) of pristine SWCNTs [2-5]. The E_{11}* PL shows sensitive and remarkable PL energy shifts in response to changes in their surrounding dielectric environments [6]. Based on the unique E_{11}* PL microenvironment responses, the polymer-wrapped lf-SWCNTs with CCs have been used to develop various biosensors, which allow to differentiate protein structure differences [7] and to detect a bioactive protein [8] and a proinflammatory biomarker through a ligand-induced protein folding phenomenon [9]. Accordingly, further understanding of local environments formed around CCs in the polymer-wrapped lf-SWCNTs would contribute to enhance the sensor performance and develop other types of biosensors.

In this study, we systematically analyzed the emission property changes of E_{11}* PL from CCs of lf-SWCNTs when vinyl polymers with four different side chains were used for the wrapping. The observed E_{11}* PL energy shifts clarify the unique microenvironment formation at the CCs based on the polymer wrapping fashion differences: Namely, the side chains of the used polymers modulate the polymer wrapping tightness that changes the amounts of D_2O molecules accessing to the nanotube surfaces for local polarity variation near the CCs, which induces the polymer-dependent PL shifts. Moreover, the substituents of the modified aryl groups on the CCs of lf-SWCNTs contribute to the polarity and hydrophobicity of the CCs, by which a clear correlation between the substituent structures and the induced PL shifts is found. Therefore, the CCs of lf-SWCNTs can produce unique molecular interaction fields showing E_{11}* PL shift responses. This finding would contribute to further development of advanced biosensors using CCs of lf-SWCNTs.

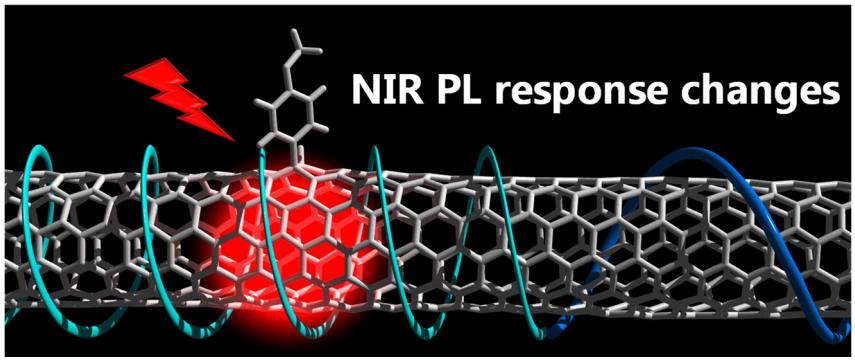

Figure 1: Polymer wrapping structures change at the CCs in lf-SWCNTs, by which NIR PL responses to dielectric microenvironments are sensitively modulated depending on the chemical structures of the wrapping polymers**.**

References

[1] J. Zhang *et al.*, *Nat. Nanotechnol.* **8**, 959–968 (2013).
[2] A. H. Brozena *et al., Nat. Rev. Chem.* **3**, 375–392 (2019)
[3] T. Shiraki *et al.*, *Acc. Chem. Res.* **53**, 1846–1859 (2020).
[4] B. J. Gifford *et al.*, *Acc. Chem. Res.* **53**, 1791-1801 (2020).
[5] J. Zaumseil, *Adv. Opt. Mater.* **10**, 2101576 (2022).
[6] Y. Niidome *et al.*, *Chem. Commun.* **55**, 3662-3665 (2019).
[7] Y. Niidome *et al.*, *Nanoscale* **14**, 13090–13097 (2022).
[8] Y. Niidome *et al.*, *Carbon* **216**, 118533 (2024).
[9] M. Kim *et al.*, *J. Am. Chem. Soc.* **146**, 12454–12462 (2024).
[10] Y. Niidome *et al.*, *J. Phys. Chem. C* **128**, 5146–5155 (2024).

Toward Non-Invasive, Real-Time Detection of Neurotransmitters and Hormones Using Near-Infrared Fluorescent Graphene Quantum Dots

A. Naumov[1], F. Wormley[1], A. Valimukhametova[1], N. Castro Lopez[1] A. Dickens[1], P. Sharma[1]

[1]*Texas Christian University (USA)*

Accurate detection of neurotransmitters and hormones such as dopamine, serotonin, oxytocin, and cortisol is essential for understanding their roles in physiological and psychological processes. Dysregulation of these biomarkers is associated with neurological disorders, including Parkinson's disease, schizophrenia, depression, and anxiety. Conventional diagnostic methods such as high-performance liquid chromatography (HPLC) and mass spectrometry (MS) are highly sensitive but invasive, expensive, and impractical for continuous monitoring. In the recent work we aim to develop a novel non-invasive sensor system utilizing near-infrared (NIR) fluorescent graphene quantum dots (GQDs) for real-time detection of these critical biomarkers. GQDs synthesized via a top-down approach exhibit high for nanocarbons (up to 8%) quantum yield near-infrared (NIR) fluorescence, *in vitro* biocompatibility at over 1 mg/mL, and substantial water solubility, making them suitable for *in vivo* applications. They successfully perform NIR *in vivo* imaging with 808 nm laser excitation when injected intravenously into Balb/C mice, while showing no behavioral or histological signs of toxicity for 21 days at concentrations order of magnitude above the imaging doses. Post injection, GQDs experience efficient clearance primarily through renal and reticuloendothelial pathways. When subject to the analytes GQDs show progressive quenching response sensitive to blood-relevant hormone/neurotransmitter concentration. Analyte specificity is realized here not through the sensor design, but rather via the Artificial Intelligence-based signal recognition algorithms. This simplifies sensor development and expands detection capabilities allowing for the detection of multiple analyte species with the same sensor construct. When imbedded into biocompatible hydrogels, GQDs still experience concentration-dependent NIR fluorescence quenching upon the introduction of the analyte, indicating their capacity for use in the implantable hydrogel-based NIR sensors. Considering the high animal tissue penetration depth of their NIR fluorescence shown in this work, GQDs can become prospective candidates for non-invasive multi-analyte detection *in vivo*.

The Design and Application of Carbon Dots-Based Prodrug Conjugates

Jia-Yaw Chang

Department of Chemical Engineering, National Taiwan University of Science and Technology, Taipei, 10607, Taiwan, Republic of China

This study presents an innovative therapeutic platform that utilizes carbon dots (CDs) for image-guided photodynamic therapy (PDT) and chemotherapy involving camptothecin (CPT) [1]. The authors synthesized heteroatom-doped CDs through a rapid microwave heating method. These CDs produce reactive oxygen species (ROS) upon exposure to laser light, making them highly effective for PDT. A significant highlight of the research is the creation of the CD-CPT nanoplatforms, which successfully link CPT via a thioketal, enabling controlled drug release triggered by ROS in acidic environments similar to those found in tumors. In vitro tests on HeLa and 4T1 cancer cells showed low cytotoxicity for CD-CPT prior to laser exposure, but a marked increase in cancer cell death occurred following laser treatment. Additionally, the heteroatom-doped CDs were biofunctionalized with glucose oxidase (GOx) and camptothecin (CPT) to construct multifunctional nanoplatforms [2]. Under acidic conditions, the release of Cu^{2+} and S^{2-} ions from this nanoplatform encourages the generation of hydroxyl (•OH) radicals and hydrogen sulfide (H_2S) gas, enhancing chemodynamic therapy (CDT) and gas therapy (GT) for cancer treatment. Importantly, this nanoplatform exhibits ROS-responsive release of CPT when activated by hydrogen peroxide and glucose, achieving approximately 66% drug release in this study. Overall, the development of a multifunctional nanoplatform that integrates ROS generators with stimuli-responsive drugs shows promising potential for clinical applications.

References

[1] G. Getachew *et al.*, *J. Colloid Interf. Sci.*, **623**, 396–410 (2023)
[2] A. Wibrianto e*t al.*, *Carbon* **208**, 191-207 (2023)

Session
NT 25（The 25th International Conference on the Science and Applications of Nanotubes and Low-

| Main conference：Main conference

Thu. Jun 19, 2025 6:00 PM - 8:00 PM JST | Thu. Jun 19, 2025 9:00 AM - 11:00 AM UTC Poster 1(International Exchange Hall III, Clock Tower Centennial Hall, 2F)

[19psa] Poster 1

[19psa-01]

Laser fabrication of hBN single photon emitters on silicon nitride waveguides

*Daiki Yamashita[1], Masaki Yumoto[1], Aiko Narazaki[1], Makoto Okano[1] (1. AIST (Japan))

[19psa-02]

Sorting of Single-Walled Carbon Nanotubes in the Tri-Surfactant System Using Aqueous Two-Phase Extraction

Cheng Li[1], Min Lyu[1], *Yan Li[1,2] (1. Peking Univ. (China), 2. Institute of Carbon-Based Thin Film Electronics, Peking University, Shanxi (China))

[19psa-03]

Evaluation of cross-plane Seebeck coefficient of single-walled carbon nanotube thin films using AC heating

*Shigeki Saito[1], Yoshihiko Kaneko[1], Shojiro Asatori[1], Satoshi Kusaba[1], Kan Ueji[1,2], Takashi Yagi[2], Kazuhiro Yanagi[1] (1. Tokyo Metropolitan University (Japan), 2. National Institute of Advanced Industrial Science and Technology (Japan))

[19psa-04]

The origin of the negative linear temperature dependence of resistance in nano-carbon materials

*Takahiro Morimoto[1], Takumi Inaba[1], Satoshi Yamazaki[2], Kazufumi Kobashi[1], Toshiya Okazaki[1] (1. AIST (Japan), 2. ADMAT (Japan))

[19psa-05]

Visualization of exciton modulation in monolayer WSe2 under dynamic strain

*Yuta Takahashi[1], Takumi Yamamoto[1], Kazuki Maezawa[1], Hajime Kumazaki[1], Shinichi Watanabe[1], Shun Fujii[1] (1. Keio University (Japan))

[19psa-06]

Non-catalytic direct synthesis of graphene and h-BN on sapphire substrates

*Waka Miyata[1], Hodaka Nishimura[1], Keigo Otsuka[1], Shigeo Maruyama[1], Shohei Chiashi[1] (1. Department of Mechanical Engineering, the University of Tokyo (Japan))

[19psa-07]

Development of In-Situ Electrical Observation System for Janus TMDs

*Dingkun Bi[1,2], Tianyishan Sun[1,2], Weizi Lu[1,2], Hiroto Ogura[1,2], Toshiaki Kato[1,2] (1. Grad. School of Engineering, Tohoku Univ. (Japan), 2. WPI-AIMR, Tohoku Univ. (Japan))

[19psa-08]

Formation of hBN-Encapsulated Janus TMDs without Air Exposure

*Tianyishan Sun[1,2], Dingkun Bi[1,2], Hiroto Ogura[1,2], Weizi Lu[1,2], Toshiaki Kato[1,2] (1. Grad. School of Engineering, Tohoku Univversity (Japan), 2. WPI-AIMR, Tohoku University (Japan))

[19psa-09]

Direct Fabrication of Graphene-Bridged Superconductor Junctions

*Zhuoqun Li[1,2], Yuto Tsukidate[1,2], Hiroto Ogura[1,2], Toshiaki Kato[1,2] (1. Grad. School of Engineering, Tohoku Univ. (Japan), 2. WPI-AIMR, Tohoku Univ. (Japan))

[19psa-10]

Boundary-Directed Epitaxy of Block Copolymers Guided by Graphene Nanoribbon Templates via Boundary-Directed Epitaxy

*Michael S. Arnold[1] (1. University of Wisconsin-Madison (United States of America))

[19psa-11]

Electrical contact formation of CNT@BNNT heteronanotubes with metal electrodes through heat treatment

*Atsutaka Watanabe[1], Makoto Shimizu[1], Yoshinori Murase[1], Taiki Inoue[1], Yoshihiro Kobayashi[1] (1. Osaka University (Japan))

[19psa-12]

Synthesis and Evaluation of High-Quality BNNT Growth on SWCNTs

*Xiyang Qiu[1], Shuhui Wang[1], Dmitry I Levshov[2], Ming Liu[1], Waka Miyata[1], Bowen Zhang[1], Yongjia Zheng[1,3], Esko I Kauppinen[4], Keigo Otsuka[1], Vasili Perebeinos[5], Shohei Chiashi[1], Rong Xiang[1,3], Shigeo Maruyama[1,3,6] (1. The University of Tokyo (Japan), 2. University of Antwerp (Belgium), 3. Zhejiang University (China), 4. Aalto University (Finland), 5. University at Buffalo (United States of America), 6. Nagoya University (Japan))

[19psa-13]

Weighing Transport of CNT Conductors in Extreme Environments

*John Bulmer[1,7], Chris Kovacs[1,8], Thomas Bullard[1,5], Charlie Ebbing[1,6], Kadyn Tackett[1], Sabrina Eddy[1], Michael Susner[1], Ganesh Pokharel[2,4], Stephen Wilson[2], Fedor Balakirev[3], Oscar Valenzuela[3], Timothy Haugan[1] (1. Air Force Research Laboratory (United States of America), 2. University of California, Santa Barbara (United States of America), 3. National High Magnetic Field Laboratory, Los Alamos (United States of America), 4. University of West Georgia (United States of America), 5. Blue Halo (United States of America), 6. University of Dayton Research Institute (United States of America), 7. National Research Council (United States of America), 8. Scintillating Solutions LLC (United States of America))

[19psa-14]

SAW-guided Reconfigurable Memristor using 2D MoS_2

*Sihyeok Kim[1], Jang Woo Lee[1], Hyeonseung Ryu[2], Taehoon Kim[1], Il Hyun Lee[1], Soo Ho Choi[1], Hyunho Lee[2], Yeong Hwan Ahn[2], Keekeun Lee[2], Il Jeon[1] (1. Sungkunkwan university (Korea), 2. Ajou university (Korea))

[19psa-15]

CNT-PP composite spacers for Reverse Osmosis Technology: A promising strategy to reduce positive organic fouling

*Armando David Martinez Iniesta[1], Kenji Takeuchi[1], Juan Fajardo-Diaz[1], Hiroki Kitano[3], Takahiro Kawakatsu[4], Syogo Tejima[5], Rodolfo Cruz-Silva[1,6], Morinobu Endo[1,2] (1. Institute for Aqua Regeneration, Shinshu University (Japan), 2. Global Aqua Innovation Center, Shinshu University (Japan), 3. Kitagawa Industries Co. (Japan), 4. Kurita Water Industries Ltd (Japan), 5. Research Organization for Information Science & Technology. (Japan), 6. Center for Applied Research in Chemistry, Plastic Transformation department (Mexico))

[19psa-16]

Efficient thermal defect healing of single-walled carbon nanotubes using a multiple-cycle approach

*Man Shen[1], Taiki Inoue[1], Yoshihiro Kobayashi[1] (1. Osaka Univ. (Japan))

[19psa-17]

Photo-induced thermal effects on the bandgap of monolayer WSe_2 integrated with ultrahigh-Q optical microcavities

*Hidetoshi Kanzawa[1], Ryo Sugano[1], Hajime Kumazaki[1], Shun Fujii[1] (1. Keio University (Japan))

[19psa-18]

Magnetic bulk photovoltaic effect in $MoS_2/CrPS_4$ artificial heterostructure device.

*Shuichi Asada[1], Keisuke Shinokita[1], Kazunari Matsuda[1] (1. Kyoto University Institute of Energy Science (Japan))

[19psa-19]

Magnetic brightening of defect-localized single-photon emission in monolayer WSe_2

*Yubei Xiang[1], Keisuke Shinokita[1], Kenji Watanabe[2], Takashi Taniguchi[3], Kazunari Matsuda[1] (1. Institute of Advanced Energy, Kyoto University (Japan), 2. Research Center for Electronic and Optical Materials, NIMS (Japan), 3. Research Center for Materials Nanoarchitectonics, NIMS (Japan))

[19psa-20]

Study on Alignment Control Method of Carbon Nanotube Network Films and Their Electrical Properties

*Norika Fukuda[1], Noriyuki Tonouchi[1,2], Tomo Tanaka[1,2], Toshie Miyamoto[1,2], Megumi Kanaori[1], Ryota Yuge[1,2] (1. National Institute of Advanced Industrial Science and Technology (Japan), 2. NEC Corporation (Japan))

[19psa-21]

Catalytic rapid Joule heating synthesis of one-dimensional nanomaterials in seconds

*Jian Sheng[1], Yifan Xu[1], Zhen Han[1], Xinrui Zhang[1], Chi Xu[1], Hai-Gang Lu[2], Si-Dian Li[2], Yan Li[1] (1. Peking University (China), 2. Shanxi University (China))

[19psa-22]

Stacking structure of epitaxial growth graphene on reduced graphene oxide

*Satoshi Kanda[1], Shunji Kurosu[2], Fumitaka Sakamoto[2], Tatsuro Hanajiri[1,2], Yuta Nishina[3], Ryota Negishi[1,2] (1. Graduate School of Toyo Univ. (Japan), 2. BNC (Japan), 3. Okayama univ. (Japan))

[19psa-23]

Circular dichroism of Trion in enantiopure carbon nanotubes

*Hiroyuki Fujinami[1], Koki Shiba[1], Yuya Hosokawa, Yohei Yomogida[2], Kazuhiro Yanagi[1] (1. Department of Physics, Tokyo Metropolitan University (Japan), 2. Department of Chemical Sciences and Engineering, Hokkaido University (Japan))

[19psa-24]

Direct Growth of Graphene on Hexagonal Boron Nitride under a Catalyst-Free Condition

*Yunosuke Miyashita[1], Hayato Watanabe[2], Yusei Terada[2], Aoi Sasanuma[2], Ryosuke Takatsuka[1], Keiichi Yanagisawa[3], Tomofumi Ukai[3], Shunji Kurosu[3], Kenji Watanabe[4], Takashi Taniguchi[4], Tatsuro Hanajiri[1,2,3], Toru Maekawa[1,2,3], Ryota Negishi[1,2,3] (1. Graduate School of Toyo Univ. (Japan), 2. Toyo Univ. (Japan), 3. BNC (Japan), 4. NIMS (Japan))

[19psa-25]

Doping-dependent valley polarization induced by Mott transition in WSe_2/WS_2 moiré superlattice

Session
NT 25 (The 25th International Conference on the Science and Applications of Nanotubes and Low-

*Zhiwei Li[1], Kenji Watanabe[2], Takashi Taniguchi[3], Kazunari Matsuda[1] (1. Institute of Advanced Energy, Kyoto University, Uji, Kyoto (Japan), 2. Research Center for Electronic and Optical Materials, NIMS (Japan), 3. Research Center for Materials Nanoarchitectonics, NIMS (Japan))

[19psa-26]

Development of a Dual-Functional Device for Rapid Detection of NO_2 Gas and Long-Term Cumulative Exposure Memory using Optimized Single-Walled Carbon Nanotubes

*Sihyeok Kim[1], Ilya V. Novikov[1], Peng Liu[2], Jang Woo Lee[1], Il Hyun Lee[1], Artem Dudorov[3], Dmitry V. Krasnikov[3], Esko I. Kauppinen[2], Albert G. Nasibulin[3], Keekeun Lee[4], Il Jeon[1] (1. Sungkunkwan university (Korea), 2. Aalto university (Finland), 3. Skolkovo Institute of Science and Technology (Russia), 4. Ajou university (Korea))

[19psa-27]

Bending Effect on Thermoelectric performance of carbon nanotubes

*Akari Yoshida[1], Takahiro Yamamoto[1,2] (1. Tokyo University of Science, Department of Physics (Japan), 2. RIST, Tokyo University of Science (Japan))

[19psa-28]

POROUS SILICON-BASED NANOCOMPOSITES FOR EFFICIENT ELECTROCHEMICAL SENSORS

*Abdullah Saeed Jalalah[1], Fahad Hussain Albaqami[1] (1. Institute of Microelectronics and Semiconductor Technologies, King Abdulaziz City for Science and Technology, Saudi Arabia (Saudi Arabia))

[19psa-29]

Optical Absorption of Fermi Level-Cotrolled Multilayer Graphene:Effects of Stacking Structure and Spacer Insertion

*Shinnosuke Yoshida[1], Takuo Mizuno[1], Taiki Inoue[1], Yuta Nishina[2], Yoshihiro Kobayashi[1] (1. Osaka Univ. (Japan), 2. Okayama Univ. (Japan))

[19psa-30]

EVALUATION OF MOLYBDENUM DISULFIDE PREPARED BY HEATING SULFUR-CAPPED MOLYBDENUM THIN FILMS

Kazushi Inoue[1], Yuto Kimura[1], Koki Nakane[1], *Agus Subagyo[1], Kazuhisa Sueoka[1] (1. Graduate School of Information Science and Technology, Hokkaido University (Japan))

[19psa-31]

Detection of process-induced contaminants on carbon nanotubes using Raman spectroscopy

*Haruki Uchiyama[1], Yudai Yoshikawa[1], Hiromichi Kataura[2], Yutaka Ohno[1,3] (1. Nagoya Univ. (Japan), 2. AIST (Japan), 3. IMaSS, Nagoya Univ. (Japan))

[19psa-32]

Peptide-modified Carbon Nanotube Biosensor

*Asahi Nagamine[1], Haruki Uchiyama[1], Hiromichi Kataura[2], Chishu Homma[3], Yuhei Hayamizu[3], Yutaka Ohno[1,4] (1. Department of Electronics, Nagoya Univ. (Japan), 2. Nanomaterials Research Institute, National Institute of Advanced Industrial Science and Technology (Japan), 3. Tokyo Institute of Technology (Japan), 4. Institute of Material and Systems for Sustainability, Nagoya Univ. (Japan))

[19psa-33]

METAL OXIDE/METAL SELENIDE NANOSTRUCTURE ELECTRODE FOR SOLID-STATE SYMMETRIC SUPERCAPACITOR WITH EXCELLENT CAPACITANCE RETENTION

*Mohammed Jalalah[1], Arpan Nayak[2] (1. Promising Centre for Sensors and Electronic Devices (PCSED), Najran University, P.O. Box: 1988, Najran 11001, Saudi Arabia (Saudi Arabia), 2. Department of Energy Engineering, Konkuk University, 120 Neungdong-ro, Seoul-05029, Republic of Korea (Korea))

[19psa-34]

Electronic transport in CNT thin films and PBTTT films:Crossover between weak and strong localization

*Yuki Hiyama[1], Hiroki Kaya[1], Manaho Matsubara[1], Hidetoshi Fukuyama[2], Takahiro Yamamoto[1] (1. Department of Physics, Tokyo University of Science (Japan), 2. RIST, Tokyo Univerity of Science (Japan))

[19psa-35]

Characterization of carbon nanotube thin-film transistors with inorganic polymer insulator

*Eito Kuromiya[1], Haruki Uchiyama[1], Masahiro Matsunaga[2], Shunto Arai[3], Hiromichi Kataura[4], Yutaka Ohno[1,2] (1. Department of Electronics, Nagoya University (Japan), 2. Institute of Material and Systems for Sustainability, Nagoya University (Japan), 3. National Institute for Materials Science (Japan), 4. National Institute of Advanced Industrial Science and Technology (Jersey))

[19psa-36]

Floating Catalyst Chemical Vapour Deposition (FCCVD)-Based CNT Electrodes for Metal Halide Perovskite Memristors in Neuromorphic Synaptic Applications

*Jang Woo Lee[1], Yasir Shafi Mir[1], Taehoon Kim[1], Sihyeok Kim[1], Ilya Novikov[1], Sungjoo Lee[1], Il Jeon[1] (1. SKKU Advanced Institute of Nano-Tech. (Korea))

[19psa-37]

Durable Organic and Perovskite Solar Cells Using Single-walled Carbon Nanotubes Transparent Thin-film Electrodes

*Yutaka Matsuo[1] (1. Nagoya University (Japan))

[19psa-38]

Structural changes in semiconducting CNT networks by coating conditions

*Toshie Miyamoto[1,2], Tomo Tanaka[1,2], Megumi Kanaori[2], Norika Fukuda[2], Shunta Doi[1], Noriyuki Tonouchi[1,2], Ryota Yuge[1,2] (1. NEC Corporation (Japan), 2. National Institute of Advanced Industrial Science and Technology (Japan))

[19psa-39]

Bayesian optimization for the synthesis of small-diameter single-walled carbon nanotubes using the eDIPS method

*Taizo Shibuya[1,2], Noriyuki Tonouchi[1,2], Yuta Nishiwaki[3], Satoru Hashimoto[3], Takeshi Hashimoto[3], Takeshi Saito[2], Ryota Yuge[1,2] (1. NEC Corporation (Japan), 2. AIST (Japan), 3. Meijo Nano Carbon Co., Ltd (Japan))

[19psa-40]

POROUS SILICON-BASED NANOCOMPOSITES FOR EFFICIENT ELECTROCHEMICAL SENSORS

*Fahad Hussain Albaqami[1], Abdullah Saeed Jalalah[1] (1. Institute of Microelectronics and Semiconductor Technologies, King Abdulaziz City for Science and Technology, Riyadh, Saudi Arabia (Saudi Arabia))

[19psa-41]

Optical Properties of Interlayer Excitons in TMD-based vdw Stacks

Session
NT 25 (The 25th International Conference on the Science and Applications of Nanotubes and Low-

*Sudhanshu Kumar Nayak[1,2], Hiroo Suzuki[3], Daichi Kozawa[2], Sai Santosh Kumar Raavi[1], Ryo Kitaura[2] (1. Ultrafast Photophysics and Photonics Laboratory, Department of Physics, Indian Institute of Technology Hyderabad, Kandi, Telangana, India (India), 2. Research Center for Materials Nanoarchitectonics (MANA)National Institute for Materials Science (NIMS)Tsukuba 305-0044, Japan (Japan), 3. Life, Natural Science and Technology, Institute of Academic and Research, Okayama University (Japan) (Japan))

[19psa-42]

Carbon Nanotube Electrode-Based Reconfigurable Metal Halide Perovskite Memristors for Reservoir Computing Applications

*Jang Woo Lee[1], Taehoon Kim[1], Naoumi Hasumi[2], Ryosuke Nakajima[2], Sihyeok Kim[1], Sungjoo Lee[1], Suguru Noda[2], Il Jeon[1] (1. SKKU Advanced Institute of Nano-Tech. (Korea), 2. Waseda University (Japan))

[19psa-43]

Collapsed carbon nanotubes: Raman signal and flattening control

*Emmanuel Picheau[1], Daiming Tang[1] (1. NIMS (Japan))

[19psa-44]

Exploration for the Optimized Double-Layer Catalyst Support Structure for the Synthesis of Vertically Aligned Carbon Nanotube Arrays

*Shunsuke Sakurai[1], Takashi Tsuji[1], Don N Futaba[1] (1. National Institute of Advanced Industrial Science and Technology (Japan))

[19psa-46]

Activated Diffusion of 1D J-Aggregates in Boron Nitride Nanotubes by Curvature Patterning

Jean-Baptiste Marceau[1], Juliette Le Balle[1,4], Duc-Minh Ta[2], Alberto Aguilar[2], Annick Loiseau[4], Richard Martel[5], Pierre Bon[2], Raphael Voituriez[3], Gaelle Recher[1], *Etienne Gaufrès[1] (1. CNRS-University of Bordeaux (France), 2. CNRS-University of Limoges (France), 3. CNRS-University of Sorbonne (France), 4. CNRS-Onera (France), 5. University of Montreal (Canada))

[19psa-47]

Flexible electronics based on conjugated polymers, oxides, and carbon nanostructures

*Lucimara Stolz Roman[1] (1. Universidade Federal do Paraná (Brazil))

[19psa-48]

Graphene nano-electromechanical mass sensor with high resolution at room temperature

*SangWook Lee[1], Dong-Hoon Shin[2,3], Sunghyun Kim[1], Peter Steeneken[3], Chirlmin Joo[3] (1. Ewha Womans University (Korea), 2. Korea University (Korea), 3. Delft University of Techology (Netherlands))

[19psa-49]

Carbon Nanotube Schottky Diode-Based Millimeter-Wave Frontends: Enabling Silicon-Compatible Flexible RF Systems from 10 GHz to W-Band

*Defu Wang[1] (1. Peking University (China))

[19psa-50]

Upcycling Waste Plastics into Carbon Nanotube Wirings and Synaptic Devices for Physical Reservoir Computing

*Takashi Ikuno[1], Kotaro Takanashi[1] (1. Tokyo University of Science (Japan))

[19psa-51]

CNTFET-Metal Contact Investigations via Voltage Controlled Material Deposition

*Martin Hartmann[1,2], Martin Ernst[1,2], Simon Böttger[1,2], Sascha Hermann[1,2] (1. Center for Microtechnologies, Chemnitz University of Technology (Germany), 2. Center for Materials Architecture and Integration of Nanomembranes, Chemnitz University of Technology (Germany))

[19psa-52]

AM I TOO FAT? CNT ASKED. DIFFERENCES IN MORPHOLOGY OF CARBON NANOTUBES FOR TRIBOLOGICAL APPLICATION

*Szymon Tomasz Ruczka[1,2,3], Adam Marek[1,4], Artur Terzyk[5], Magdalena Skrzypek[6], Łukasz Wojciechowski[6], Sławomir Boncel[1,2,3] (1. NanoCarbon Group; Department of Organic Chemistry, Bioorganic Chemistry and Biotechnology, Silesian University of Technology, Bolesława Krzywoustego 4, 44-100 Gliwice, Poland (Poland), 2. Centre for Organic and Nanohybrid Electronics (CONE), Silesian University of Technology, Stanisława Konarskiego 22B, 44-100 Gliwice, Poland (Poland), 3. NanoCarbonGroup.com Ltd., Ks. Marcina Strzody 7, 44-100 Gliwice, Poland (Poland), 4. Department of Chemical Organic Technology and Petrochemistry, Silesian University of Technology, Bolesława Krzywoustego 4, 44-100 Gliwice, Poland (Poland), 5. Department of Materials Chemistry, Adsorption and Catalysis, Nicolaus Copernicus University in Toruń, Gagarina 7, 87-100 Toruń, Poland (Poland), 6. Institute of Construction Machines and Automotive Vehicles, Poznań University of Technology, Piotrowo 3, 60-959 Poznań (Poland))

[19psa-53]

FROM DOTS TO TUBES – THE *REVERSE* SCENARIO
OF BOTTOM-UP CATALYST-FREE SYNTHESIS OF *N*-DOPED CNTs

*Slawomir Boncel[1], Anna Kolanowska[1,2] (1. Silesian University of Technology (Poland), 2. University of Silesia (Poland))

Laser fabrication of hBN single photon emitters on silicon nitride waveguides

Daiki Yamashita[1], Masaki Yumoto[2], Aiko Narazaki[2] and Makoto Okano[1]

[1]*Hybrid Photonics Research Team, Platform Photonics Research Center, National Institute of Advanced Industrial Science and Technology (AIST), Ibaraki 305-8568, Japan*
[2]*Innovative Laser Processing Group, Research Institute for Advanced Electronics and Photonics, National Institute of Advanced Industrial Science and Technology (AIST), Ibaraki 305-8568, Japan*

Single-photon emitters (SPEs) are fundamental components in the field of quantum photonics. Among various photon-emitting materials, hexagonal boron nitride (hBN) has recently emerged as a promising SPE host. hBN is a two-dimensional wide-bandgap semiconductor with optically active defects capable of emitting stable single photons at room temperature. These defects can be conveniently introduced through chemical reactions, electron beam irradiation, ion implantation, or laser writing [1]. Moreover, hBN flakes can be dry-transferred onto arbitrary substrates, expanding their compatibility with existing photonic platforms and broadening their potential applications.

Here we demonstrate a deterministic post-fabrication method for integrating hBN SPEs with a silicon nitride (SiN) photonic platform. Exfoliated hBN flakes are transferred onto SiN waveguides with grating couplers at their ends. Defects in the hBN are created using laser processing [2], which allows precise control of the defect positions on the waveguides. The optical properties of the fabricated defects are characterized, and single-photon emission is confirmed. Next, we demonstrate the on-chip excitation of the SPE via the waveguide. The excitation laser is coupled into the waveguide through the grating coupler and excites the defect in the hBN flake. The defect exhibits single-photon emission when excited through the waveguide. This successful waveguide-mediated excitation highlights the potential for integrating such emitters into photonic circuits.

This work is supported in part by JSPS (KAKENHI JP22K14624, JP24K08296), MEXT (ARIM JPMXP1224AT0098, JPMXP1224UT1040), and Amada Foundation (AF-2024235-C2, AF-2023209-B2).

References

[1] C. Su, E. Janzen, M. He, C. Li, A. Zettl, J. D. Caldwell, J. H. Edgar, and I. Aharonovich, "Fundamentals and emerging optical applications of hexagonal boron nitride: a tutorial," Adv. Opt. Photonics 16, 229 (2024).
[2] L. Gan, D. Zhang, R. Zhang, Q. Zhang, H. Sun, Y. Li, and C.-Z. Ning, "Large-Scale, High-Yield Laser Fabrication of Bright and Pure Single-Photon Emitters at Room Temperature in Hexagonal Boron Nitride," ACS Nano 16, 14254 (2022).

Sorting of Single-Walled Carbon Nanotubes in the Tri-Surfactant System Using Aqueous Two-Phase Extraction

Cheng Li[1], Min Lyu[1], Yan Li[1,2]

[1]*Beijing National Laboratory for Molecular Science, Key Laboratory for the Physics and Chemistry of Nanodevices, College of Chemistry and Molecular Engineering, Peking University, Beijing, China*
[2]*Institute of Carbon-Based Thin Film Electronics, Peking University, Shanxi, Taiyuan, China*

Abstract: The structure of single-walled carbon nanotubes (SWCNTs) determines all of its intrinsic properties. Structurally uniform or single-chirality SWCNTs have demonstrated promising applications in electronics, defect-induced luminescence, sensing, and imaging [1]. However, commercially available SWCNT samples are typically a mixture of various structural species. Therefore, the preparation ((i.e., synthesis or separation) of SWCNTs with consistent structure is of great significance. Recently, aqueous two-phase (ATP) extraction has been found to be applicable for the sorting of SWCNTs, with the separation based on the differential partition of complexes formed by dispersants and SWCNTs of different chiralities in the top and bottom phases with minimal hydrophobicity/hydrophilicity differences. The sorting of SWCNTs by aqueous two-phase extraction has become an important research direction due to its convenient and efficient characteristics. We realized the bandgap-based separation in SDS (sodium dodecyl sulfate)-SC (sodium cholate)-DOC (sodium deoxycholate) tri-surfactant system using ATP extraction. Under oxidative conditions, we achieved efficient and stable bandgap-based separation of two different SWCNT samples with different diameter distributions: CoMoCAT-SG65i and HiPco in PEG/DX ATP system. This separation method showed higher resolution than traditional metallic/semiconducting separation. For HiPco SWCNTs, semiconducting SWCNTs with small-bandgap first partitioned into top phase, followed by large-bandgap semiconducting SWCNTs, and finally metallic SWCNTs were distributed into top phase. For CoMoCAT-SG65i SWCNTs, we achieved high-purity separation of (8,4), (9,2) and (8,3) species. The separation was realized by combined effects of SC, SDS, and the oxidant NaClO, especially the introduction of SC, which has a higher affinity for large chiral-angle SWCNTs [2], leaving SWCNTs with small chiral angles such as (8,4), (9,2) and (8,3) in top phases. After a further second-stage separation, each species was isolated.

References

[1] Yang. F *et al*., *Chem. Rev.* **120**, 2693–2758 (2020).
[2] Kawai. M *et al*., *J. Am. Chem. Soc.* **134**, 9545–9548 (2012).

Evaluation of cross-plane Seebeck coefficient of single-walled carbon nanotube thin films using AC heating

○Shigeki Saito[1], Yoshihiko Kaneko[1], Shojiro Asatori[1], Satoshi Kusaba[1], Kan Ueji[1,2], Takashi Yagi[2], Kazuhiro Yanagi[1*]

[1]*Department of Physics, Tokyo Metropolitan University, Tokyo 192-0397, Japan*

[2]*National Institute of Advanced Industrial Science and Technology, Ibaraki 305-8560, Japan*

Flexible thermoelectric materials have attracted considerable attention for efficient energy harvesting from the environment and batteries of flexible devices. Single-walled carbon nanotubes (SWCNTs) are well known for their high thermoelectric performance. The internal structure of SWCNT thin films can be modified by controlling their alignment and chirality, enabling significant changes in their physical properties. For example, adjusting the stacking angle of aligned SWCNT thin films has the potential to enhance energy filtering and phonon transport suppression [1]. Therefore, understanding the correlation between the internal structure of SWCNT films and thermoelectric performance is important. For this purpose, the development of techniques to evaluate the cross-plane thermoelectric properties of thin films is crucial. However, compared to electrical and thermal conductivity [2], there were few studies on the evaluation of the Seebeck coefficient in cross-plane direction. In this study, we have developed a technique to evaluate the Seebeck coefficient in cross-plane direction using AC heating and then tried to determine the figure of merit of the thin film in cross-plane direction. The samples used in this study were highly aligned semiconducting SWCNT thin films (diameter of 1.4 nm, ~100 nm thickness). As shown in Figure 1(a) and 1(b), this film was placed between the top and bottom gold electrodes for evaluation of temperature and thermoelectric voltage. To measure the Seebeck coefficient in cross-plane direction, we employed 2ω method. The temperature difference was induced by an AC current with a modulation frequency of ω on the back side of the substrate, and then the temperature gradient was measured using the temperature dependence of the gold resistance with the frequency of 2ω. We were able to measure <30 mK temperature differences and the Seebeck coefficient of this film was 113.1±8.7 μV/K (Figure 2), consistent with values reported in previous research [3]. We will also discuss the effects of electrical doping using ionic liquids for controlling chemical potential, as well as the results of similar measurements conducted on (6,5) chirality-enriched CNTs thin films.

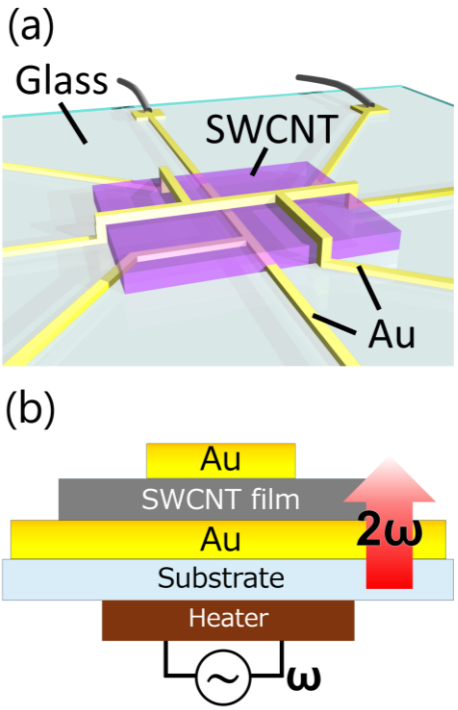

Figure 1(a), (b): schematic images of Seebeck measurement in cross-plane direction.

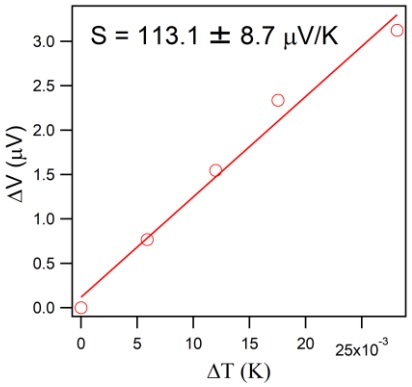

Figure 2: The result of relationship between voltage and temperature differences in cross-plane direction.

References

[1] W. Yu, *et al., Materials Today Physics,* **20**, 100447 (2021)

[2] K. Ueji, *et al., ACS Applied Nano Materials,* **5**, 5, 6100-6105 (2022)

[3] K. Yanagi, *et al.*, *Nano Letter*, **14**, 11, 6437-6442 (2014)

E-mail: saitou-shigeki@ed.tmu.ac.jp

The origin of the negative linear temperature dependence of resistance in nano-carbon materials

T. Morimoto[1], T. Inaba[1], S. Yamazaki[2], K. Kobashi[1] and Toshiya Okazaki[1]

[1]AIST (Japan), [2]ADMAT (Japan)

Understanding electronic and electric behaviors is important for the application of nano-carbon materials. For the last few decades, many research efforts have concentrated on revealing the fundamental behavior of nano-carbon materials, including carbon nanotubes, graphene, and these derivatives. Temperature dependence is of great importance for gaining insights into electronic conduction and the impacts of material/electrode interface on electronic transport. The positive linear temperature dependence of resistance is well understood as scattering between transport electron and phonon. Meanwhile, some nano-carbon materials exhibited a unique temperature dependence of resistance, characterized by a negative linear relationship between resistance and temperature [1], and its' details are unclear. The negative linear temperature dependence of resistance (NLTR) is attractive for applications that establish stable and wide-range temperature sensors, such as thermistors [2]. Such devices can pave the way for applying nano-carbon materials in broad research and industrial fields, including quantum technology.

Recently, we suggested that the NLTR is originated from the scattering and interfering phenomena around the defects embedded in the flattened graphitic structures in nano-carbon materials [3,4]. The NLTR behavior was only observed in MWCNTs with the flattened region in their cross-section structures. Moreover, we investigated the effects of high-temperature annealing on this phenomenon by observing structural changes in nano-carbon materials. The figure shows the typical behavior of SWCNTs under different annealing conditions. The temperature dependence of resistance of the pristine sample shows the general behavior of the hopping conduction and phonon scattering. In the case of higher-temperature annealed samples, the NLTR was clearly observed in a wide range of temperatures from a few K to room temperature. This behavior correlates well with the theoretical expression by the scattering and interference via the Fridel oscillation at the defect in flattened graphitic structures [5]. In this presentation, we will present the details of the mechanism and the various dependencies of this phenomenon. Moreover, we will discuss the importance of NLTR for applying stable and wide temperature range thermistors.

This work is based on results obtained from a project (No. JPNP16010) commissioned by the New Energy and Industrial Technology Development Organization (NEDO).

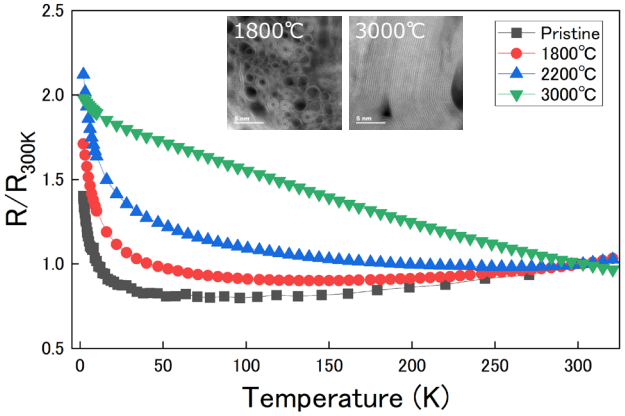

Figure: The temperature dependence of resistance at different annealing samples of CNT films is compared. The NRL dependence gradually smears the typical hopping and phonon scattering behavior. Inset: The cross-section TEM images in 1800 and 3000 degrees Celsius.

References

[1] C. Yan, J. Wang and P. S. Lee, *ACS Nano*, **9**, 2130–2137 (2015).
[2] D. Yang, *et al., Adv. Funct. Mater.*, **2024,** 2411257 (2024).
[3] T. Inaba, T. Morimoto, S. Yamazaki and T. Okazaki, *Nano Res.* **15,** 889-897 (2022).
[4] T. Morimoto, Takumi Inaba, Satoshi Yamazaki, Kazufumi Kobashi and Toshiya Okazaki, Submitted.
[5] V. V. Cheianov and V. I. Fal 'ko, *Phys. Rev. Lett.,* **97**, 226801 (2006).

Visualization of exciton modulation in monolayer WSe_2 under dynamic strain

Y. Takahashi[1], T. Yamamoto[1], K. Maezawa[1], H. Kumazaki[1], S. Watanabe[1] and S. Fujii[1]

[1] *Department of Physics, Faculty of Science and Technology, Keio University (Japan)*

Transition metal dichalcogenides (TMDCs) are at the forefront of atomically-thin semiconducting materials and exhibit unique physical phenomena that are not observed in their bulk counterparts. These materials exhibit the indirect-to-direct band gap transition when exfoliated to a monolayer, and excitons can exist even at room temperature due to their strong binding energy and the reduced screening of Coulomb interactions [1,2]. In recent years, manipulation of excitons in TMDCs via surface acoustic waves (SAWs) is attracting great attention [3-5]. SAWs are acoustic waves which propagate on the surface of an elastic material, and thus the strain and piezoelectric fields induced by SAWs dynamically modulate the bandgap of TMDCs and their emission properties. Although exciton transport under traveling SAWs [3] and exciton dissociation due to piezoelectric field-induced modulation [4,5] have been reported, the relationship between band edge modulation and local dynamic strain remains incompletely understood.

Here we visualize the exciton modulation in monolayer tungsten diselenide (WSe_2) under dynamic strain induced by SAWs. By combining microscopic photoluminescence (PL) measurements with Michelson optical interferometry, we demonstrate sinusoidally modulated excitonic luminescence in synchronization with SAW propagation. To resolve the spatial-temporal exciton modulation, we employ a femtosecond pulse laser, with a repetition rate synchronized to an integer multiple of the frequency of electrically driven SAWs as an excitation source. This synchronization technique enables stroboscopic PL measurements, where the pulsed laser optically excites the WSe_2 at the same phase of the SAW in each cycle. A lock-in measurement with a Michelson optical interferometer [6] allows us to simultaneously measure the amplitude of the SAW. Additionally, we investigate the transient dynamics of exciton lifetimes under dynamic strain using time-correlated single-photon counting (TCSPC) measurements. Our results indicate that the traveling SAW spatially modulates the emission energy, linewidth, and intensity within the exciton lifetimes. These findings open new avenues for manipulating excitons in TMDCs using acoustic waves.

Part of this work was supported by JSPS KAKENHI (JP24H01202), the Precise Measurement Technology Promotion Foundation (PMTP-F), Iketani Science and Technology Foundation, and The Hattori Hokokai Foundation. We thank Dr. Y. K. Kato for valuable discussions.

References

[1] K. F. Mak, C. Lee, J. Hone, J. Shan, and T. F. Heinz, Atomically thin MoS_2 : a new direct-gap semiconductor, Phys. Rev. Lett. **105**, 136805 (2010).

[2] A. Splendiani, L. Sun, Y. Zhang, T. Li, J. Kim, C. Y. Chim, G. Galli, and F. Wang, Emerging photoluminescence in monolayer MoS_2, Nano Lett. **10**, 1271–1275 (2010).

[3] K. Datta, Z. Lyu, Z. Li, T. Taniguchi, K. Watanabe and P. B. Deotare, Spatiotemporally controlled room-temperature exciton transport under dynamic strain, Nat. Photon. **16**, 242–247 (2022).

[4] K. Datta, Z. Li, Z. Lyu, and P. B. Deotare, Piezoelectric modulation of excitonic properties in monolayer WSe_2 under strong dielectric screening, ACS Nano **15**, 12334–12341 (2021).

[5] A. R. Rezk, B. Carey, A. F. Chrimes, Desmond W. M. Lau, Brant C. Gibson, Changxi Zheng, Michael S. Fuhrer, Leslie Y. Yeo, and Kourosh Kalantar-zadeh, Acoustically-driven trion and exciton modulation in piezo electric two-dimensional MoS_2. Nano Lett. **16**, 849 (2016).

[6] L. Shao, V. J. Gokhale, B. Peng, P. Song, J. Cheng, J. Kuo, A. Lal, W. M. Zhang and J. J. Gorman, Femtometer-amplitude imaging of coherent super high frequency vibrations in micromechanical resonators. Nat Commun **13**, 694 (2022).

Non-catalytic direct synthesis of graphene and h-BN on sapphire substrates

Waka Miyata[1], Hodaka Nishimura[1], Keigo Otsuka[1], Shigeo Maruyama[1], Shohei Chiashi[1]

[1]*Department of Mechanical Engineering, the University of Tokyo (Japan)*

Two-dimensional graphene has excellent electrical properties, such as high mobility. The graphene/h-BN stacked heterostructure is obtained by synthesizing h-BN and graphene in this order on a substrate, but this process cannot use metal catalysts. Therefore, a CVD synthesis technique for graphene and h-BN without metal catalysts is essential to directly synthesize this heterostructure by CVD.

In the experiment, R-, M-, C- and A-plane sapphire were used as substrates. Acetylene gas and pyrolysis gas (130 °C) of ammonia borane were used as precursors for graphene and h-BN synthesis, respectively. The effects of sapphire surface orientation, substrate annealing conditions, and CVD conditions on the synthesis were investigated. The synthesized graphene and h-BN were characterized by SEM, AFM, Raman and UV-Vis-NIR spectroscopic analysis.

High quality graphene was synthesized on H_2-annealed M-plane sapphire. The Raman spectra showed that I_G/I_D was 12.7 and I_{2D}/I_G was 1.5, indicating that the synthesized graphene was of high quality and monolayer. Figure 1 shows the correlation between ω_G and ω_{2D} of the graphene. The peak position data show that the strain and the carrier density of the graphene were -0.170 % and 4.45×10^{12} cm^{-2}, respectively [1]. The sheet resistance of the synthesized monolayer graphene was 1173 Ω/sq. Hall measurement showed that the carrier mobility was 1075 $cm^2/(V\ s)$ and the carrier density was 5.19×10^{12} cm^{-2} at room temperature.

h-BN was synthesized on sapphire. In the Raman spectra shown in Figure 2(a), h-BN synthesized on M-plane sapphire exhibited a narrow E_{2g} peak at 1371 cm^{-1}. The FWHM of the E_{2g} peak was 16 cm^{-1}. It was narrower than that of h-BN synthesized directly on sapphire in previous studies [2] and was as narrow as that of h-BN grown on copper surface and transferred to a silicon substrate [3]. The narrow E_{2g} peak indicates that the synthesized h-BN was of high quality and highly crystalline. Figure 2(b) shows the AFM image of h-BN synthesized on M-plane sapphire. The wrinkles in h-BN indicate that h-BN was synthesized on the whole surface, as the wrinkles were caused by the difference in thermal expansion coefficient of h-BN and sapphire. Since the E_{2g} peak of the heat-treated h-BN monolayer is 1372 cm^{-1}[4], the synthesized h-BN was high quality monolayer.

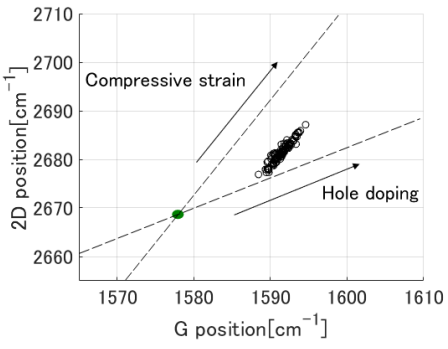

Fig. 1 Correlation between the frequencies of the G and 2D Raman modes of graphene on M-plane sapphire. The green dot shows the data of strain-free and charge-neutral graphene [1].

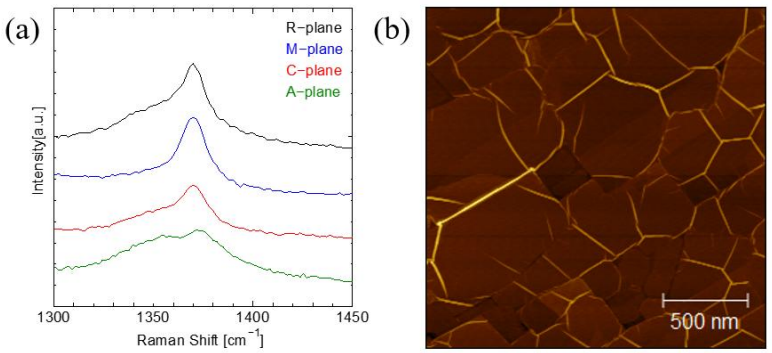

Fig. 2 (a)Raman spectra of h-BN on R-, M-, C- and A-plane sapphire. (b)AFM image of M-plane sapphire.

References

[1] J. E. Lee, *et al.*, *Nat. Commun.*, **3**, 1024 (2012).
[2] K. Ahmed, *et al.*, *Mater. Res. Express* **4**, 015007 (2017).
[3] R. Chang, *et al.*, *Chem. Mater.* **29**, 6562 (2017).
[4] Q. Cai, *et al.*, *Nanoscale*, **9**, 3059 (2017).

Development of In-Situ Electrical Observation System for Janus TMDs

D. Bi[1, 2], T. Sun[1, 2], W. Lu[1, 2], H. Ogura[1, 2] and T. Kato[1, 2]

[1]*Grad. School of Engineering, Tohoku Univ. (Japan),* [2]*WPI-AIMR, Tohoku Univ. (Japan)*

Janus transition metal dichalcogenides (TMDs), which consist of different chalcogen atoms on the upper and lower surfaces, have garnered significant attention due to their theoretically predicted novel properties, such as spontaneous polarization in the out-of-plane direction, which are not found in conventional TMDs. Synthesizing Janus TMDs requires atomic-level substitution reaction techniques, and thus far, experimental research has made little progress globally. We have developed an “In-situ plasma-assisted Janusization equipment” that allows direct observation of the photoluminescence (PL) spectrum of TMDs during the Janusization process, and successfully acquired the time evolution of the PL spectrum. Using this high-precision Janusization technology, we have reported the creation of Janus TMD nanotubes [1], Janus TMD nanoscrolls [2], and heterobilayer moiré superlattices in Janus TMDs and conventional TMDs [3]. These new Janus TMD materials are expected to be applied to various optoelectronic devices through spatial patterning. While significant progress has been made in the study of optical properties of Janus TMDs, there have been very few experimental reports regarding their electrical transport properties. This lack of data is primarily due to the fact that, during device fabrication after Janus formation, effects such as intrinsic strain can cause the crystals to either scroll or fragment. In this study, we conducted Janus treatment on pre-fabricated TMD devices structured as field-effect transistors (FETs) and developed a system to monitor the changes in their electrical transport properties in real-time. This approach is expected to yield insights into the previously unexplored detailed electrical transport characteristics of Janus TMDs as well as the mechanisms underlying the Janus formation reaction.

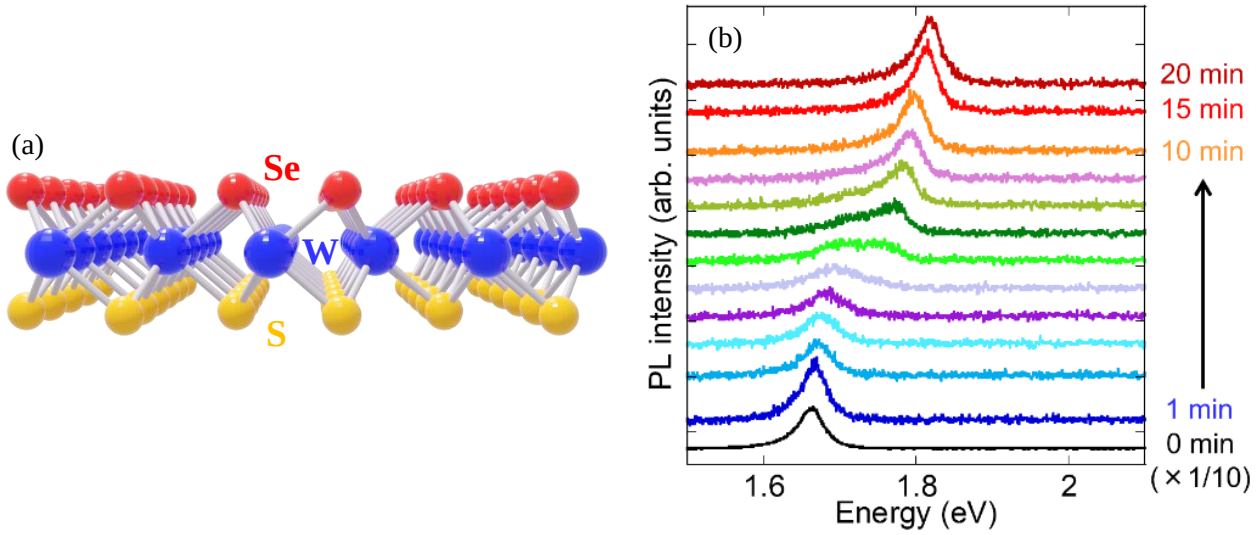

Fig.: (a) Schematic of WSSe, a typical Janus TMDs. (b) Typical time-evolution PL spectra obtained by our in-situ Janusization process.

References

[1] Y. Nakanishi, *et al.*, Adv. Mater. **35**, 2306631-1-11 (2023).

[2] M. Kaneda, *et al.*, ACS Nano **18**, 2772−2781 (2024).

[3] W. Zhang, *et al.*, Small Structures **5**, 2300514-1-8 (2024).

Formation of hBN-Encapsulated Janus TMDs without Air Exposure

T. Sun[1,2], D. Bi[1,2], H. Ogura[1,2], W. Lu[1,2], T. Kato[1,2]

[1]*Grad. School of Engineering, Tohoku Univ. (Japan),* [2]*WPI-AIMR, Tohoku Univ. (Japan)*

As one of the newly synthesized materials, two-dimensional (2D) Janus transition metal dichalcogenides (TMDs) have attracted attention in recent years Fig. (a) [1-3]. Unlike normal TMDs, the different atomic species on the upper and lower facets induce an intrinsic dipole moment in Janus TMDs, indicating much more unique physical properties. Due to the dipole moment, Janus TMDs are expected to absorb impurities, such as oxygen and water molecules, which tend to change their optical and electrical characteristics.

To investigate the original properties of Janus TMDs, a novel method to form hBN-encapsulated Janus TMDs without air exposure has been developed. In this new method, the WSeS/hBN stack was covered with hBN without air exposure to avoid oxygen adsorption. Because of the weak bonding between the upper replaced chalcogen atoms and metal atoms, Janus TMDs themselves cannot withstand high temperatures. However, with the protection of top hBN layers, thermal annealing can be carried out to improve the contact between hBN and Janus TMDs as well as enhance the excitonic properties of Janus TMDs. In this study, the optical properties of hBN-encapsulated WSeS without air exposure were explored, as shown in Fig. (b). It is noteworthy that the photoluminescence (PL) peak intensity is enhanced two times after vacuum thermal annealing, which is not observed for air-exposed Janus TMDs. Based on the corresponding PL mapping of the peak at 1.82 eV, the relatively good uniformity of WSeS can be obtained by this method. Moreover, the peak energy also shows a slight downshift (~ 10 meV), thanks to the introduced strain during the annealing process. This novel method for the formation of hBN-encapsulated Janus TMDs without air exposure makes it possible to investigate the original properties of Janus TMDs monolayers as well as their superlattices.

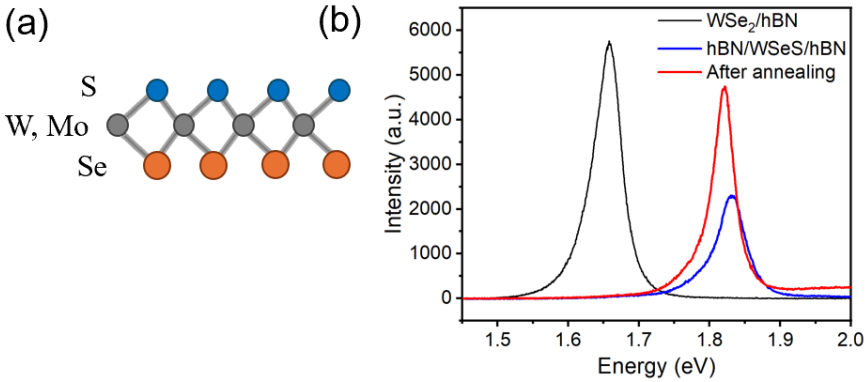

Fig.: (a) Schematic of Janus TMDs. (b) PL spectra of WSe_2/hBN, hBN/WSeS/hBN, and hBN/WSeS/hBN after vacuum thermal annealing, respectively.

References

[1] Y. Nakanishi, et al., Adv. Mater. **35**, 2306631-1-11 (2023).

[2] M. Kaneda, et al., ACS Nano **18**, 2772−2781 (2024).

[3] W. Zhang, et al., Small Structures **5**, 2300514-1-8 (2024).

Direct Fabrication of Graphene-Bridged Superconductor Junctions

Z. Li[1, 2], Y. Tsukidate[1, 2], H. Ogura[1, 2], and T. Kato[1, 2]
[1]*Grad. School of Engineering, Tohoku Univ. (Japan),* [2]*WPI-AIMR, Tohoku Univ. (Japan)*

Josephson junction (JJ) consisting of superconductor electrodes and various channel materials represents a promising structure for advanced electronic applications. Previous studies have demonstrated that graphene is a feasible candidate for ballistic JJs that offer advantages in minimizing thermal noise in superconducting quantum devices such as Josephson parametric amplifiers [1]. Although JJs based on exfoliated graphene crystals have been demonstrated, bottom-up synthesis and high-density integration of graphene JJs have not been achieved. On the other hand, our lab-built plasma-enhanced chemical vapor deposition (PECVD) system can realize position-selective and wafer-scale growth of graphene and graphene nanoribbons [2-6]. In this study, to realize direct synthesis of graphene JJs, we performed position-selective growth of graphene between superconducting MoRe electrodes by the PECVD system.

We synthesized the graphene from Ni or Cu nanobars between superconducting MoRe electrodes (Fig.). The Ni or Cu nanobars and MoRe electrodes were prepared by conventional electron-beam lithography process. The position-selective growth of graphene can be realized because graphene is grown from only Ni or Cu nanobars. By optimizing the synthesis conditions and conducting systematic experiments, it was found that, in devices synthesized without any post-processing such as electrode fabrication or nanobar etching, the current flowing between the superconducting electrodes MoRe can be clearly modulated by the gate voltage. This indicates that graphene has been directly synthesized between the superconducting MoRe electrodes. These results are important steps for future applications of graphene-superconductor JJs.

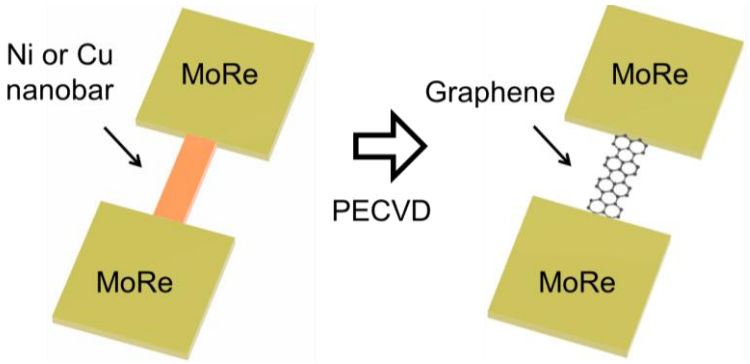

Fig.： Schematic illustration of position-selective growth of graphene between superconducting MoRe electrodes.

References

[1] J. Sarkar *et al.*, *Nat. Nanotechnol.* **17**, 1147–1152 (2022).
[2] T. Kato and R. Hatakeyama, *Nat. Nanotechnol.* **7**, 651–656 (2012).
[3] H. Suzuki *et al.*, *Nat. Commun.* **7**, 11797 (2016).
[4] H. Suzuki *et al.*, *Sci. Rep.* **8**, 11819-1-9 (2018).
[5] Q.-Y. Li *et al.*, *ACS Nano* **13**, 9182-9189 (2019).
[6] T. Kato *et al.*, *Commun. Mater.* **3**, 103-1-7 (2022).

Boundary-Directed Epitaxy of Block Copolymers Guided by Graphene Nanoribbon Templates via Boundary-Directed Epitaxy

M. S. Arnold

[1]*University of Wisconsin-Madison (USA)*

The directed self-assembly (DSA) of block copolymers (BCPs) can be used to produce nanometer-scale patterns without the cost and process complexity of state-of-the-art EUV nanolithography. Thus, DSA is of potential use in a wide variety of semiconductor technologies, such as finFETs and biosensors. Here, we show how lithographically patterned and atomically thin monolayers of graphene can be leveraged to control the position and orientation of BCP domains to create technologically useful BCP patterns. The BCP domains are organized via "boundary-directed epitaxy" – which utilizes the chemical contrast at the boundaries between a substrate and relatively wide chemical stripe (in this case a monolayer of graphene) to induce ordering.[1-2] Aligned and high density-multiplied BCP nanopatterns with half-pitch of 6.4 nm have been created using graphene stripes as wide as 100 nm.

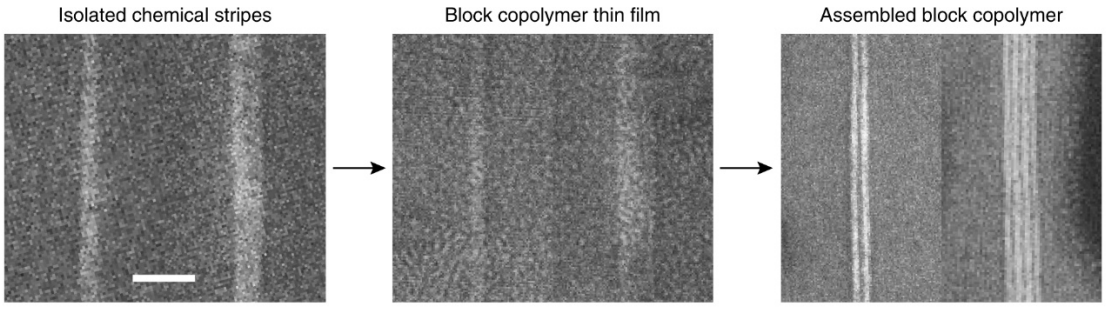

Fig. 1: (Left) Isolated graphene nanoribbons grown on Ge(001). (Middle) BCP thin film after spin-coating on the template. (Right) BCP assembly into sub-10 nm domains via boundary-directed epitaxy. Scalebar = 100 nm.

References

[1] Boundary-directed epitaxy of block copolymers. R.M. Jacobberger, V. Thapar, G.-P. Wu, T.-H. Chang, V. Saraswat, A.J. Way, K.R. Jinkins, Z. Ma, P.F. Nealey, S.-M. Hur, S. Xiong, M.S. Arnold, *Nature Communications* 11, 4151 (2020), 10.1038/s41467-020-17938-3.

[2] K.A. Su, M.S. Arnold, et al. *In Preparation* (2025).

Electrical contact formation of CNT@BNNT heteronanotubes with metal electrodes through heat treatment

A. Watanabe[1], M. Shimizu[1], Y. Murase[1], T. Inoue[1], Y. Kobayashi[1]

[1]*Osaka University (Japan)*

E-mail: a.watanabe@ap.eng.osaka-u.ac.jp

A heteronanotube structure in which a carbon nanotube (CNT) is wrapped by a boron nitride nanotube (BNNT) [1], termed CNT@BNNT, is expected to exhibit superior transport properties. However, for device applications of CNT@BNNTs, a key challenge is establishing electrical contact between the CNT and a metal electrode, which is hindered by the insulating BNNT. A previous study of CNT@BNNT has demonstrated that selective removal of BNNTs using XeF_2 gas enables direct contact between CNT sidewalls and electrodes [2]. In conventional CNT devices, an end-bonded contact (EBC), where covalent bonds are formed between CNT edges and metal via heat-induced dissolution of CNTs beneath the metal, has been established as an effective approach for reducing contact resistance in miniaturized electrodes [3]. In this study, we investigated electrical contact formation in CNT@BNNT heteronanotubes through heat-induced dissolution into metal electrodes (Fig. 1(a)). Back-gate field-effect transistors (FETs) of CNT@BNNTs were fabricated on SiO_2/Si substrates using a sequential growth and transfer process [4], followed by metal electrode deposition (Fig. 1(b)). The source-drain current (I_{DS}) was measured before and after heating at 600–700 °C in an Ar/H_2 atmosphere. Figure 1(c) shows the changes in maximum I_{DS} of devices with Al/Ni bimetallic electrodes after heating at different temperatures. Before heating, the current was ~10^{-11} A, indicating insulation caused by the BNNT. After heating at 660 °C, the current increased to ~10^{-7} A, confirming the electrical contact formation. The results can be explained by two possible mechanisms: (i) dissolution of only the BNNT, enabling CNT sidewall–electrode contact (Fig. 1(a) left), or (ii) dissolution of both the BNNT and CNT, leading to EBC formation (Fig. 1(a) right). Further investigations are required to distinguish them. Nevertheless, these results demonstrate that heat-induced dissolution into metal is promising for forming electrical contacts in CNT@BNNT heteronanotubes.

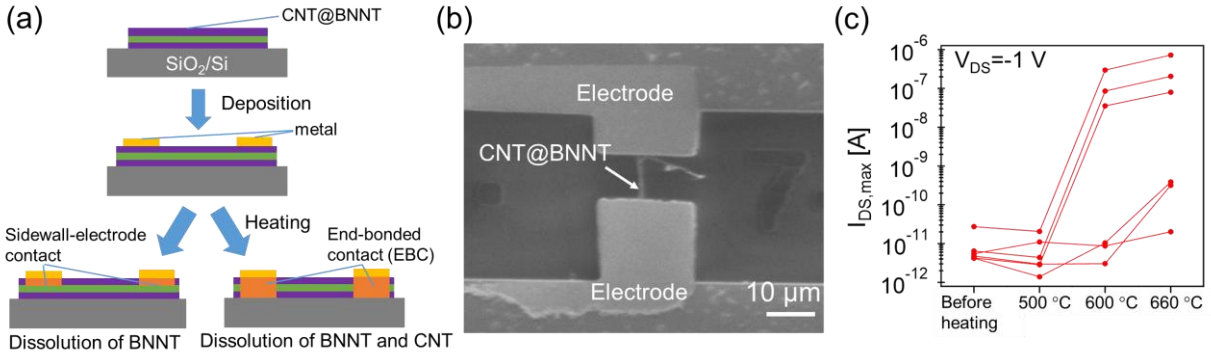

Fig. 1 (a) Schematic images of electrical contact formation by dissolution of CNT@BNNTs. (b) SEM image of a CNT@BNNT-FET. (c) Changes in maximum drain currents of CNT@BNNT-FETs after heat treatment.

References

[1] R. Xiang et al., *Science* **367**, 537 (2020).
[2] K. Otsuka et al., *Nano Res*. **16**, 12840 (2023).
[3] Q. Cao et al., *Science* **350**, 68 (2015).
[4] T. Inoue et al., manuscript in preparation.

Synthesis and Evaluation of High-Quality BNNT Growth on SWCNTs

X. Qiu[1], S. Wang[1], D. Levshov[2], M. Liu[1], W. Miyata[1], B. Zhang[1], Y. Zheng[1,3], E. Kauppinen[4], K. Otsuka[1], V. Perebeinos[5], S. Chiashi[1], R. Xiang[1,3], S. Maruyama[1,3,6]

[1] The University of Tokyo (Japan), [2] University of Antwerp (Belgium),[3] Zhejiang University (China), [4] Aalto University (Finland), [5] University at Buffalo (USA),[6] Nagoya University (Japan)

Single-walled carbon nanotube (SWCNT) films exhibit exceptional optical and electrical properties. In addition, the experimental realization of one-dimensional van der Waals (1D vdW) heterostructures based on SWCNTs further extends their potential for diverse applications [1,2]. In particular, SWCNTs encapsulated in Boron Nitride Nanotubes (SWCNT@BNNTs) have been proposed for a range of advanced applications: back-gate field-effect transistors [1], the smallest coaxial cables [3], low-power nanodevices [4]. In this work, we investigated a range of synthesis conditions and analyzed the resulting growth using multiple optical characterization methods [5].

First, floating-catalyst-dry-deposited SWCNTs [6] with diameters of approximately 2 nm were used for BN synthesis under various conditions. The results showed that higher growth temperatures generally improved BNNT quality, as evidenced by FT-IR measurements. Next, switching the BN source from ammonia borane powder to borazine gas enabled more precise control over the gas flow rate, leading to further enhancements in BNNT quality [7]. Finally, HiPCO SWCNTs [8] and arc-discharged SWCNTs with smaller tube diameters were also employed for BNNT growth. Stronger interactions between the inner and outer layers in these small-diameter SWCNTs significantly influenced the optical measurement results.

In summary, we investigated various BNNT growth conditions and systematically analyzed the resulting structures and properties. Further optimization of synthesis parameters may enable additional improvements in BNNT quality. Additionally, using density functional theory (DFT) we explore how growth-induced defects in BNNTs influence optical properties of SWCNTs wrapped by BNNTs, such as photoluminescence (PL) measurements [9].

References

[1] R. Xiang *et al.*, *Science* **367**(6477), 537−542 (2020).
[2] R. Xiang *et al.*, *National Science Open* **1** (3), 20220016 (2022).
[3] K. E. Walker *et al.*, *SmallMethods* **1** (9), 1700184 (2017).
[4] C. Hu *et al.*, *Nano Lett.* **19** (6), 4146−4150 (2019).
[5] S. Wang *et al.*, *ACS Nano* **18** (14), 9917-9928 (2024).
[6] A. Kaskela *et al.*, *Nano Letters* **10** (11), 4349-4355 (2010).
[7] Waka Miyata, Graduation Thesis, The University of Tokyo (2024).
[8] J. Cui *et al.*, *ACS Appl. Nano Mater* **2** (1)**,** 343-350 (2019).
[9] D. Gulo *et al.*, *J. Phys. Chem. Lett.* **16** (7)**,** 1711–1719 (2025).

Weighing Transport of CNT Conductors in Extreme Environments

John Bulmer[1], Chris Kovacs[1], Thomas Bullard[1], Charlie Ebbing[1], Kadyn Tackett[1], Sabrina Eddy[1], Michael A. Susner[1], Ganesh Pokharel[2], Stephen D. Wilson[2], Fedor F. Balakirev[3], Oscar A. Valenzuela[3], Timothy Haugan[1]

[1]*Air Force Research Laboratory (USA),* [2]*University of California, Santa Barbara (USA),* [3]*National High Magnetic Field Laboratory, Los Alamos (USA)*

Cables made from carbon nanotubes (CNTs) with aligned microstructures are an emerging strategic material that are currently more conductive by weight than copper and can be as strong as carbon fiber, with further improvements anticipated through increased aspect ratio and the incorporation of ordered dopants. It is possible that CNT conductors will become a bendable, mechanically resilient analog of a graphitic intercalation compound (GIC)—the brittle form of bulk graphite with ordered doping that can exceed copper's conductivity by up to 50%. Notably, both GICs and their host graphites exhibit a completely metallic-like resistivity that decreases with temperature down to liquid helium levels, whereas CNT conductors show a well-known U-shaped resistance–temperature response that behaves metallic-like at high temperature, but becomes semi-conducting-like at lower temperatures. The origin of this semi-conducting-like upturn in CNT resistivity is an underappreciated controversy: many transport physicists invoke homogeneous models (e.g., variable-range hopping and weak localization), while polymer physicists rely on heterogeneous transport models such as fluctuation-induced tunneling. A deeper understanding of this upturn will enable the development of CNT wires with a fully metallic-like temperature response, allowing them to better compete with GICs.

Here, we explore the electrical transport of CNT conductors whose doping degree and molecular aspect ratio are systematically controlled, with electrical measurements carried out down to 65 mK and in magnetic fields up to 60 T. We find that, in doped CNT conductors, resistance plateaus as the temperature approaches absolute zero, demonstrating for the first time that heterogeneous fluctuation-induced tunneling explains much of the semi-conducting-like upturn. Low-field magnetic measurements show that homogeneous weak localization provides a smaller contribution, but accounts for the low-field negative magnetoresistance. Completely de-doped CNT conductors, by contrast, exhibit variable-range hopping, starkly differing from pure graphite. Hall measurements reveal holes as the dominant carriers in acid-doped samples and nearly compensated conduction for de-doped samples, with an abrupt crossing of the charge neutrality point near room temperature. While quantitative mobility could not be directly extracted from Hall data, it was determined from the quadratic response of high-field magnetoresistance. Magnetic-field orientation studies uncovered 2-fold and 4-fold symmetries, including large magnetoresistance (+22% longitudinal MR at 270 K) when the field aligns with the CNT axis.

These results are notable because: (1) they confirm that heterogeneous fluctuation-induced tunneling must be invoked to explain the majority of the room-temperature resistance, (2) they establish a much-needed methodology for mobility characterization, and (3) they enable estimates of CNT cables' ultimate conductivity. We conclude by highlighting our group's recent work on converting these CNT cables into superconductors.

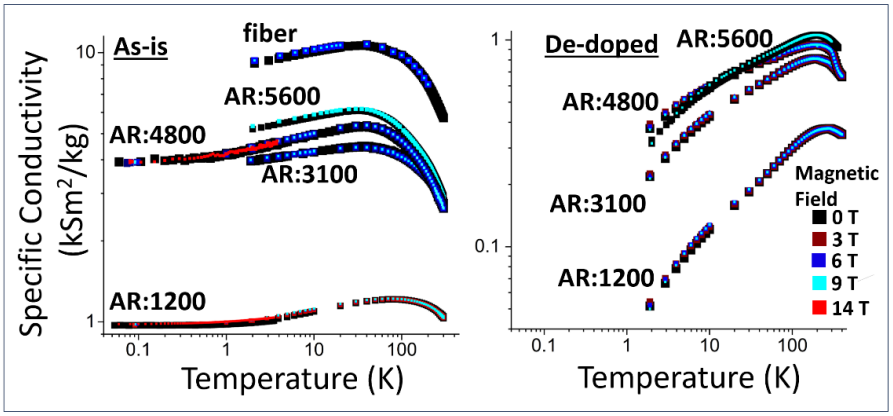

Specific conductivity of CNT fibers and ribbons in the as-is/ doped (left) or de-doped (right) state. AR specifies the aspect ratio and color indicates the magnetic field.

SAW-guided Reconfigurable Memristor using 2D MoS_2

Sihyeok Kim[1], Jang Woo Lee[1], Hyeonseung Ryu[2], Taehoon Kim[1], Il Hyun Lee[1], Soo Ho Choi[1], Hyunho Lee[3], Yeong Hwan Ahn[2], Keekeun Lee[3], Il Jeon[1,*]

[1] *Department of Nano Engineering, Department of Nano Science and Technology, SKKU Advanced Institute of Nanotechnology (SAINT), Sungkyunkwan University (SKKU), Suwon 16419, Republic of Korea,*

[2]*Department of Physics and Department of Energy Systems Research, Ajou University, Suwon 16499, Republic of Korea*

[3]*Department of Electrical and Computer Engineering, Ajou University, Suwon, Gyeonggi-do, 16499, Republic of Korea*

Memristors based on two-dimensional (2D) semiconductor materials are emerging as promising candidates for next-generation memory devices, thanks to their remarkable electrical characteristics, such as ultrafast switching speeds, high on/off-current ratio (I_{on}/I_{off}), and excellent mechanical flexibility, along with superior scalability [1-2]. Owing to the unique and exceptional properties of 2D materials, memristors utilizing materials such as WS_2, MoS_2, and graphene have been extensively explored. However, most of these devices focus on either volatile or non-volatile characteristics, with limited studies addressing integrated reconfigurable properties. Furthermore, 2D materials can suffer from reliability issues when exposed to electrical signals for extended periods, particularly under high-voltage stress or frequent switching, which could hinder their long-term reliability in memory device applications. Additionally, repeated short-term electrical stimuli can lead to the degradation of the device, causing unwanted changes into long-term memory.

To address these issues, a new 2D MoS_2-based reconfigurable memristor driven by surface acoustic waves (SAW) has been demonstrated for the first time. SAW induces mechanical strain on the MoS_2 flake, which generates an acoustoelectric current. Unlike traditional electrical stimuli, the inherent non-destructive nature of the SAW signal preserves the intrinsic properties of the device, ensuring sustained operational reliability over 10,000 seconds of SAW stimulation without any degradation. Additionally, it was demonstrated that the device returns to its initial state without any changes even after repeated application of numerous SAW pulses. To maximize the strain effect of SAW on MoS_2, an ultrathin monoflake with a thickness of approximately 0.3 nm, formed by chemical vapor deposition (CVD), was applied as the memristive material, allowing for significant deformation even with small mechanical energy. Additionally, a SAW device with an optimized design centered at 221 MHz was employed to minimize the insertion loss of the acoustic wave. Vacuum annealing was used to create sulfur (S)-vacancies, which maximized the hysteresis window of the memristor. The proposed reconfigurable memristor demonstrated an endurance of over 10^3 cycles and a retention time exceeding 10^3 seconds, with an I_{on}/I_{off} ratio greater than 10^3. Additionally, by leveraging the volatile memory characteristics through SAW, 4-bit based reservoir computing was performed, exhibiting an accuracy of over 95%. The non-destructive SAW-assisted neuronic control technology proposed in this study is expected to be widely applied in future reconfigurable memristor applications.

References

[1] M. Wang, S. Cai, C. Pan *et al.*, *Nat. Elec.*, **1**, 130–136 (2018).
[2] S. S. Teja Nibhanupudi *et al.*, *Nat. Comm.*, **15**, 2334, 1-6 (2024).

CNT-PP composite spacers for Reverse Osmosis Technology: A promising strategy to reduce positive organic fouling

Armando D. Martinez-Iniesta[1], Kenji Takeuchi[1], Juan L. Fajardo-Diaz[1], Hiroki Kitano[3], Takahiro Kawakatsu[4], Syogo Tejima[5], Rodolfo Cruz-Silva[1,6], Morinobu Endo[1,2]

[1] Institute for Aqua Regeneration, Shinshu University (Nagano, Japan), [2]Global Aqua Innovation Center, Shinshu University (Nagano, Japan), [3]Kitagawa Industries Co. (Aichi, Japan), [4]Kurita Water Industries Ltd. (Tokyo, Japan), [5]Research Organization for Information Science & Technology. (Tokyo, Japan), [6]Center for Applied Research in Chemistry, Plastic Transformation department. (Coahuila, Mexico),

Reverse Osmosis (RO) technology is one of the most used methods for water purification at industrial scale [1]. However, performance like ion rejection and water permeation, is strongly affected by Fouling. In those systems used to purify water at very low pressure (< 1 MPa), organic fouling has a significative impact which is mostly promoted by proteins that are deposited or absorbed on the membrane surface[2]. This fouling layer negatively impacts the performance of RO modules and reduces their operational lifetime. To prevent and mitigate this problem, a variety of strategies have been proposed in the literature, including the modification of the feed spacers by the incorporation of carbon nanomaterials to improve antifouling behavior and improve mass transfer [3].

In this work, we evaluated the antifouling performance of a multi-walled carbon nanotube-polypropylene (CNT-PP) composite spacer in a RO system against a positively charged Lysozyme (LYS) protein. Our findings demonstrate that the CNT-PP spacer improved antifouling behaviour compared with a plain-PP spacer. By fluorescence microscopy, we have monitored the interaction between protein and spacer, finding that the PP spacer has a stronger interaction with the LYS compared with the low adhesion behavior of the protein with the CNT-PP spacer. AFM and contact angle measurements reveal a higher roughness on the CNT-PP spacer and a decrease in the hydrophobic properties compared with the commercial PP spacer. These surface changes provide a larger surface area for water molecules, allowing the formation of an interfacial water layer that prevents the LYS adsorption over the CNT-PP spacer. By molecular dynamics simulation, we demonstrate a stronger binding affinity between the protein and the PP structure than the CNT-PP model, as well as the formation of an interfacial water layer on the CNT-PP surface.

Finally, we evaluate the permeation performance of the CNT-PP spacer on a full-scale reverse osmosis module. Our findings revealed a 2 times higher mass transfer coefficient for the CNT-PP composite against the plain PP spacer. This demonstrates the enhancement characteristics of this new technology which is a promising strategy to reduce fouling caused by LYS protein in water treatment, particularly for industrial wastewater recycling.

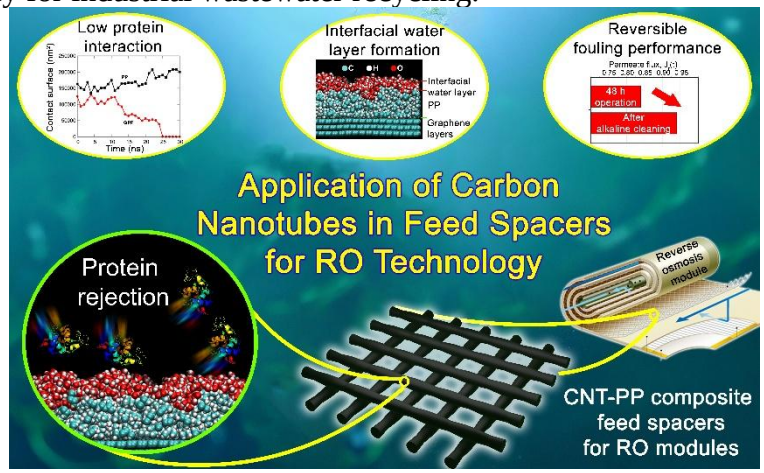

Graphical abstract: Carbon nanotubes applied into feed-spacer for reverse osmosis technology. Enhanced protein rejection, reduced protein-CNT-PP molecular interaction, and high antifouling performance**.**

References

[1] A. Bodalo-Santoyo et al., *Desalination.* **160,** 151-158, (2004).
[2] A. Martin et al., *Sci. Total Environ* **765**, 142721, (2021).
[3] H. Kitano et al., *ACS Omega* ***4***, 15496-15503, 2019.

Efficient thermal defect healing of single-walled carbon nanotubes using a multiple-cycle approach

Man Shen, Taiki Inoue, and Yoshihiro Kobayashi

Department of Applied Physics, Osaka University (Japan)

Single-walled carbon nanotubes (SWCNTs) are renowned for their exceptional mechanical, electrical, and thermal properties. However, these excellent properties can be significantly degraded by defects. Effective defect healing is crucial for unlocking the full potential of SWCNTs. In this study, we developed a C_2H_2-assisted multiple-cycle process combined with air exposure [1] or CO_2 treatment, achieving highly efficient defect healing. SWCNTs were synthesized using nanodiamond as the seed material for growth. [1,2] As shown in Figure 1(a) and (b), during the multiple-cycle defect-healing process, the SWCNTs were heated in a CVD furnace under an C_2H_2, or CO_2 flow for several cycles. Raman spectroscopy (λ_{ex} = 633 nm) was used to characterize the defect density of the grown SWCNTs by analyzing the G-band to D-band intensity ratio (I_G/I_D). Figure 1(c) and (d) shows the Raman spectra before and after each cycle of defect healing with air exposure and normalized I_G/I_D based on the pristine I_G/I_D after different defect healing. Air exposure significantly influences multiple-cycle defect healing. Without air exposure, the ratio increases after the first and second cycles but decreases after the third cycle. With air exposure, the ratio increases through the first three cycles before decreasing, indicating its positive effect on defect healing. Additionally, introducing CO_2, effectively replaces air exposure and shortens the healing time from three cycles to two cycles. This suggests that the beneficial effect of air exposure may result from the etching action of gas molecules. Besides, we successfully healed commercially available bulk-scale SWCNTs (super-growth SWCNTs) with the assistance of C_2H_2. Overall, our study demonstrates that a multiple-cycle defect-healing approach with air exposure or with the assistance of CO_2 is an effective strategy for enhancing the quality of SWCNTs.

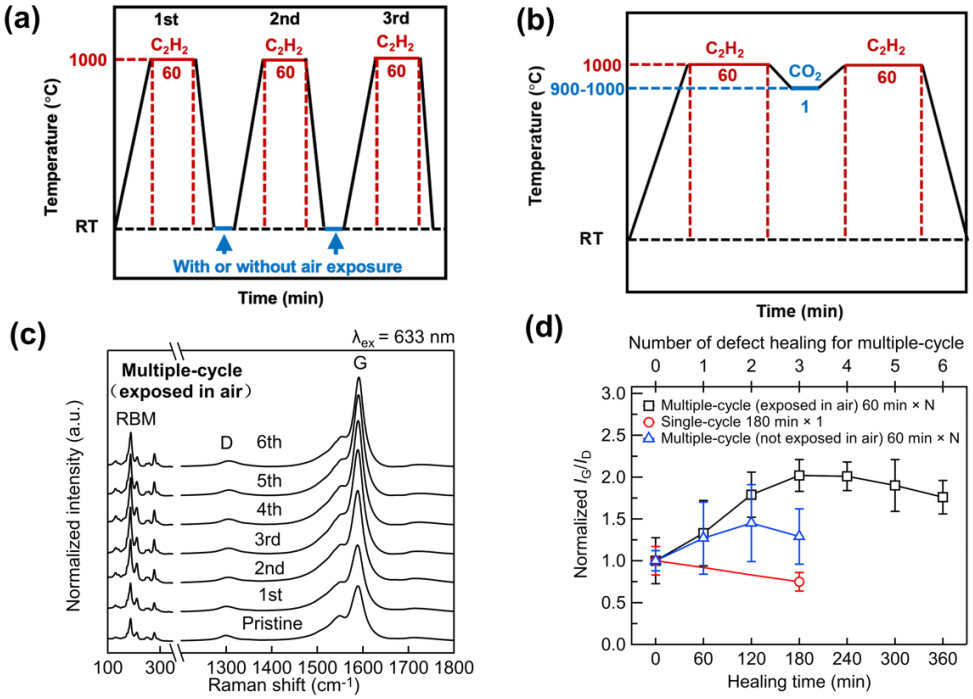

Figure 1: (a, b) Temperature-time schematic diagram of multiple-cycle defect healing (a) with or without air exposure; (b) with the assistance of CO_2; (c) Raman spectra of SWCNTs before and after each cycle of multiple-cycle defect healing with air exposure; (d) Changes in normalized I_G/I_D with increasing healing time during multiple-cycle defect healing.

References

[1] M. Shen *et al.*, under revision.
[2] M. Wang, M. Shen et *al.*, *Appl. Phys. Express* **16**, 015002 (2023).

Photo-induced thermal effects on the bandgap of monolayer WSe_2 integrated with ultrahigh-Q optical microcavities

H. Kanzawa[1], R. Sugano[2], H. Kumazaki[1,2], and S. Fujii[1]

[1] *Department of Physics, Faculty of Science and Technology, Keio University (Japan), 2 Department of Electronics and Electrical Engineering, Faculty of Science and Technology, Keio University (Japan),*

High-quality-factor (Q) optical microcavities have garnered significant interest across diverse research fields, including nonlinear optics [1], optomechanics [2], and quantum optics [3]. In recent years, there has been increasing attention on leveraging optical microcavities to bring out unique optical properties of atomically-thin two-dimensional materials. The ability of microcavities to confine light for a long period in a small mode volume significantly enhances light-matter interactions with graphene and transition metal dichalcogenides (TMDs). This enhancement holds promise for the development of practical optoelectronic devices, such as photodetectors [4], lasers [5], and single-photon sources [6]. Monolayer TMDs are known to exhibit direct bandgap photoluminescence due to their large exciton binding energy, which reaches several hundred meV at room temperature [7,8]. As a result, hybrid platforms integrating TMDs with optical microcavities enable cavity-enhanced photoluminescence (PL) emission and lasing behaviors. Recently, cavity-enhanced second-harmonic generation has also been observed in high-Q silica microcavities decorated with monolayer tungsten diselenide (WSe_2) [9] thanks to the large second-order nonlinearity. In such devices, thermal effects play a vital role in optical properties of TMDs because thermal radiation from excited optical modes cannot be negligible.

In this study, we investigate photo-induced thermal effects on the PL properties of monolayer WSe_2 integrated with ultrahigh-Q silica microcavities. We observe a distinct redshift in the PL emission wavelength, which is proportional to the increase in intracavity power. To analyze this phenomenon, we develop a theoretical model that accounts for the dynamic thermal behavior of a cavity resonant mode.

We employ a WSe_2-integrated silica microsphere cavity with a diameter of approximately 70 μm. The hybrid cavity is fabricated by transferring mechanically exfoliated monolayer WSe_2 using the dry-transfer technique. High-Q factors in the range of 10^6–10^7 are maintained even after surface decoration. In the experiment, optically excited PL emission of monolayer WSe_2 is monitored while a continuous-wave (CW) laser with a wavelength of ~1550 nm is coupled to a cavity mode via an optical tapered fiber. As the laser wavelength is scanned towards the resonant wavelength, leading to an increase in intracavity power, the central wavelength of the PL spectrum exhibits a linear redshift of up to a few meV. By estimating the temperature increase due to photoinduced heat generation using the developed theoretical model, we found that the observed PL redshift is consistent with the estimated bandgap change induced by heat dissipation from the optical cavity modes. Our findings offer valuable insights for the design and optimization of 2D-material-integrated nanophotonic devices.

Part of this work was supported by KAKENHI (JP24H01202), Inamori Foundation, and Nippon Sheet Glass Foundation for Materials Science and Engineering. We thank Dr. Y. K. Kato for valuable discussions.

References

[1] G. Lin, A. Coillet, & Y. K. Chembo, *Adv. Opt. Photonics* **9**, 828 (2017).
[2] M. Aspelmeyer, T.J. Kippenberg, & F. Marquardt, *Rev. Mod. Phys.* **86**, 1391 (2014).
[3] I. Shomroni, *et al.*, *Science* **345**, 903 (2014).
[4] M. Furchi, *et al.*, *Nano Lett.* **12**, 2773 (2012).
[5] S. Wu, *et al.*, *Nature* **520**, 69 (2015).
[6] K. Parto, *et al.*, *Nano Lett.* **22**, 9748 (2022).
[7] K.F. Mak, *et al.*, *Phys. Rev. Lett.* **105**, 136805 (2010).
[8] A. Splendiani, *et al.*, *Nano Lett.* **10**, 1271 (2010).
[9] S. Fujii *et al.*, *Nano Lett.* **24**, 4209 (2024).

Magnetic bulk photovoltaic effect in $MoS_2/CrPS_4$ artificial heterostructure device.

S. Asada[1], K. Shinokita[1], K. Matsuda[1]

[1]*Institute of Advanced Energy, Kyoto Univ. (Japan)*

Recently, artificial van der Waals heterostructures with different two-dimensional materials have attracted attention, due to the combination of various materials and the emergence of new physical properties not seen in individual materials, they are very promising research subjects for optical and electrical device applications. It has been reported that when two-dimensional layered materials with different rotational symmetries are stacked at a specific angle, at the interface of such an artificial heterostructure, the spatial symmetry at the heterostructure interface is degenerated to only one mirror symmetry, and the *P*-symmetry is broken, resulting in in-plane polarization and the generation of spontaneous photocurrent without p-n junction or bias voltage [1]. However, there are still many unknowns about the shift current that is thought to be the cause of the photovoltaic effect, especially the correlation with magnetism and the effect of the breaking of *T*-symmetry on the shift current.

In this study, we fabricated $MoS_2/CrPS_4$ heterostructures that are expected to exhibit spontaneous photovoltaic properties, and investigated their device characteristics. $CrPS_4$ is layered semiconductor known for its high air stability [2], and has 2-fold symmetry and 1-axis mirror symmetry. Therefore, by stacking $CrPS_4$ at an appropriate angle with MoS_2, which has 3-fold symmetry and 3-axis mirror symmetry, the *P*-symmetry is broken at the interface, and shift current is predicted to occur. When a laser was irradiated onto the $MoS_2/CrPS_4$ heterostructure device and its *I*-*V* characteristics were measured, the finite photocurrent was confirmed at a bias voltage of 0 V, as shown in Fig. 1. $CrPS_4$ has also attracted attention for its magnetic properties, and in the bulk state used in this study, it exhibits anti-ferromagnetism with a magnetic phase transition temperature of approximately 40 K [3]. In this study, we measured the photovoltaic properties in the range of 10 K – 300 K, which includes the magnetic phase transition temperature of $CrPS_4$, and conducted research with the aim of clarifying the correlation between the shift current and magnetism (Fig. 1). It is known that the shift current is not temperature dependent because it is not affected by the carrier mobility, and only the open circuit voltage changes with the change in resistivity [4]. However, as shown in Fig. 1, a sudden change in the spontaneous photocurrent was observed in the low temperature region below the magnetic phase transition temperature. In this poster, we will discuss the cause of this change in the spontaneous current.

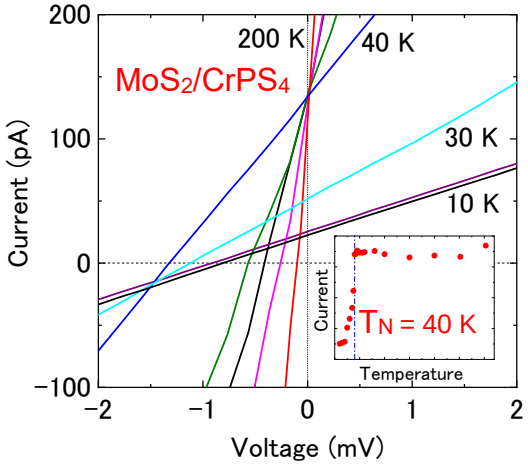

Fig.1: Temperature dependence of *I*-*V* properties of $MoS_2/CrPS_4$ heterostructure device (Inset: Temperature dependence of spontaneous photocurrent, T_N = magnetic transition temperature of $CrPS_4$)

References

[1] T. Akamatsu *et al.*, *Science*, **372**, 68 (2021)
[2] J. Son *et al.*, *ACS Nano*, **15**, 16904 (2021)
[3] J. Lee *et al.*, *ACS Nano*, **11**, 10935 (2017)
[4] M. Nakamura *et al.*, *Appl. Phys. Lett.*, **113**, 232901 (2018)

Magnetic brightening of defect-localized single-photon emission in monolayer WSe_2

Yubei Xiang[1], Keisuke Shinokita[1],
Kenji Watanabe[2], Takashi Taniguchi[3] and Kazunari Matsuda[1]

[1] *Institute of Advanced Energy, Kyoto University,* [2] *Research Center for Electronic and Optical Materials, NIMS,* [3] *Research Center for Materials Nanoarchitectonics, NIMS*

Quantum light sources, in particular solid-state single-photon emitters, have garnered considerable attention due to their crucial essential role in quantum information technologies. Recently, defects in two-dimensional monolayer transition metal dichalcogenides, such as tungsten diselenide (WSe_2), have been demonstrated to be promising candidates for stable and bright quantum light sources. [1,2] However, the external controllability of single-photon emission remains not fully understood.

In this study, we investigated the nature and dynamics of defect-localized exciton emission in monolayer WSe_2 under magnetic fields for novel single-photon emitters with external tunability. Figure 1(a) shows the typical photoluminescence (PL) spectra of monolayer WSe_2 at low temperature, revealing strong and sharp PL peaks attributed to defect-localized exciton emissions. Figure 1(b) presents the polarization-resolved PL spectra under an in-plane magnetic field, where each PL spectrum is normalized by the peak intensity of the higher energy states for each magnetic field. Notably, the PL intensity of the lower energy states increases significantly with increasing magnetic field within a small range below 1 T.

Moreover, Figure 1(c) shows the photon correlation measurements under a magnetic field, performed using defect-localized exciton emission in monolayer WSe_2 with the Hanbury-Brown and Twiss experimental setup. This result confirms the preserved antibunching characteristic, indicating that the single-photon purity is maintained under the magnetic field. In addition, the decrease near zero delay time occurs more rapidly under the magnetic field of 1 T, and the characteristic dip at zero delay time becomes sharper in contrast to the case without the magnetic field, reflecting a reduction in the effective lifetime of the defect-localized single-photon emission under the magnetic field.

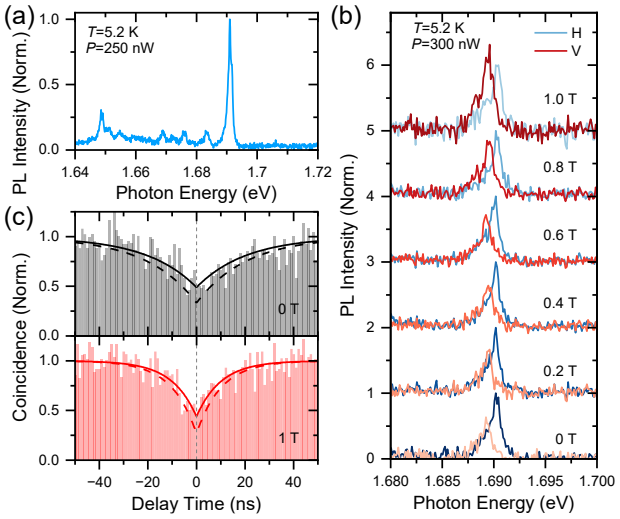

Figure 1 (a) Typical low temperature PL spectra of monolayer WSe_2. (b) Polarization-resolve PL spectra with the increasing in-plane magnetic fields. (c) Second-order correlation measurement of the localized exciton emission under the magnetic field of 0 and 1 T.

We discuss the dynamics of the magnetic brightening of defect-localized exciton emission in monolayer WSe_2. Our findings on the physical nature of defect-localized exciton states in monolayer WSe_2 and the dynamics of magnetic brightening provide a novel approach for controlling single-photon emitters using an external magnetic field in the field of quantum optics applications.

References

[1] Linhart, L. et al. *Phys. Rev. Lett.*, **123**, 146401 (2019).
[2] Jadczak, J. et al. *ACS Nano*., **15**, 19165–19174 (2021).

Study on Alignment Control Method of Carbon Nanotube Network Films and Their Electrical Properties

Norika Fukuda[1], Noriyuki Tonouchi[1, 2], Tomo Tanaka[1, 2], Toshie Miyamoto[1, 2], Megumi Kanaori[1] and Ryota Yuge[1, 2]

[1]National Institute of Advanced Industrial Science and Technology (Japan), [2]NEC Corporation (Japan)

Single-walled carbon nanotubes (CNTs) are cylindrical carbon allotropes with a diameter of about 1 nm consisting of a sheet made of six-membered carbon rings. We are developing an uncooled infrared microbolometer using CNT network films, which is expected to be applied to security surveillance cameras, human body thermography, and cameras for mobile objects. Recently, we reported that high-purity semiconducting CNT network films isolated by the electric field-induced layer formation (ELF) method have a high temperature coefficient of resistance (TCR) [1]. The detectivity of uncooled infrared microbolometers depends linearly on the TCR of the resistive element. To suppress noise, the resistance of the resistor element must be reduced. To improve these characteristics, the CNT network structure should be optimized to have a larger TCR and smaller resistance. In this study, we developed a deposition process to control the CNT network films and a new method to evaluate the network structure, and measured the electrical properties of the resulting CNT network structure.

CNT orientation was quantified by an orientation angle evaluation algorithm using a Gabor filter [2]. As a result, we found that the domain size of the local orientation changes depending on the formation conditions. The evaluation of these resistances indicted that the CNT network films with a moderately ordered structure had the lowest resistance (Fig. 1). The TCR was also found to be independent of the degree of orientation. The details of this process and the mechanism of the difference in orientation and electrical properties will be discussed in the day's session.

This work was partially supported by the ATLA Innovative Security Technology Research Grant JPJ004596.

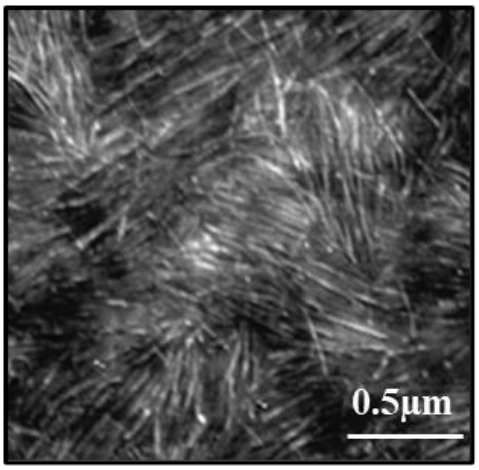

Fig. 1 AFM images of CNT networks (moderately ordered structure).

References

[1] T. Tanaka et al., *Proc. SPIE*, **12534**, 125341U (2023).
[2] N. Fukuda et al. *71st Annual Meeting of the Japan Society of Applied Physics*, 22p-P07-13 (2024).

Catalytic rapid Joule heating synthesis of one-dimensional nanomaterials in seconds

Jian Sheng[1†], Yifan Xu[1†], Zhen Han[1], Xinrui Zhang[1], Chi Xu[1], Hai-Gang Lu[2], Si-Dian Li[2], Yan Li[1]*

[1]*Beijing National Laboratory for Molecular Sciences, Key Laboratory for the Physics and Chemistry of Nanodevices, College of Chemistry and Molecular Engineering, Peking University, Beijing 100871, China*

[2]*Institute of Molecular Science, Shanxi University, Taiyuan 030006, China*

Corresponding author: yanli@pku.edu.cn

Rapid Joule heating (RJH) has shown its great power and rapid development in materials synthesis, attributing to its simple procedure, extremely fast reaction speed, and high energy efficiency. To improve the controllability and versatility of RJH, we introduce nano-catalysts and develop a catalytic RJH route for the synthesis of nanomaterials. In the RJH growth of one-dimensional (1D) nanomaterials, we verify the validity of vapor-liquid-solid (VLS) mechanism at temperatures beyond 2500 °C. Nanowires of refractory carbides, high entropy carbides, II-VI and III-V group semiconductors are synthesized in seconds, showing the great feasibility of catalytic RJH strategy. The ultrahigh heating rate of RJH (>10^3 °C/s) breaks the equilibrium limitations, inhibits catalyst agglomeration, and enhances the supersaturation of the precursor, thereby yielding uniform 1D morphologies. With a general applicability to various material types, a short synthesis time, a low energy consumption of kilojoules per gram of nanomaterials, and more importantly a potential in morphology and structure control endowed by the nano-catalysts, this catalytic RJH strategy presents great perspectives in material synthesis and production.

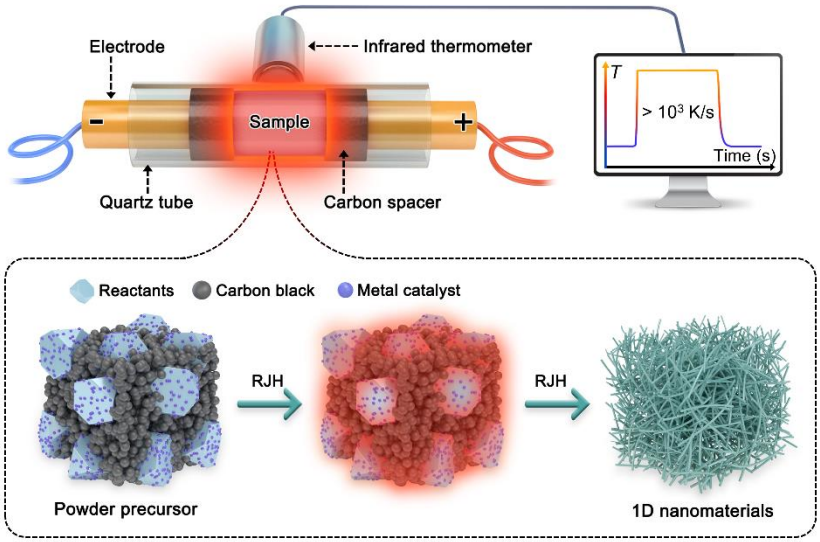

Figure 1: Schematic of the RJH reactor and synthesis process of 1D nanomaterials.

References

[1] J. Sheng *et al.*, ChemRxiv: 10.26434/chemrxiv-2024-5pp4t.

Stacking structure of epitaxial growth graphene on reduced graphene oxide

°S. Kanda[1], S. Kurosu[2], F. Sakamoto[2], T. Hanajiri[1,2], Y. Nishina[3], R. Negishi[1,2]

[1]*Graduate School of Science and Engineering, Toyo Univ., Kawagoe 350-8585, Japan*

[2]*Bio-nanoelectronics Research Centre, Kawagoe 350-8585, Japan* [3]*Okayama Univ., Okayama 700-8530, Japan*

s36C02400048@toyo.jp

Multilayer graphene with weak interlayer coupling is a promising candidate for channel materials in high-performance electron devices. This structure provides both high conductivity and high carrier mobility due to its shielding effect [1] and the linear dispersion of the electronic band structure [2]. Graphene oxide (GO) can be synthesized at low cost and in high yield [3]. Due to its high scalability, which facilitates the feasible fabrication of large-area multilayer graphene thin films, it has been actively studied for applications in electron devices [4]. It was reported that high-temperature reduction in an ethanol atmosphere leads to the formation of multilayer reduced graphene oxide (rGO) thin films [5]. However, the specific reduction mechanism remains unclear, posing a critical challenge in the application of GO to turbostratic multilayer graphene. In this study, we investigated the stacking structure of rGO thin films prepared by high temperature annealing in an ethanol vapor as a carbon source for the restoration of graphitic structure in GO.

Fig. 1 shows the Raman spectra of rGO films prepared at various thermal annealing temperatures. The results indicate that the crystallinity of the rGO films exhibits a marked improvement at annealing temperatures above 1300°C. As shown in Fig. 2, deconvoluting the peaks in the 2D band of rGO prepared at 1400°C into three components [6] enables the estimation of the turbostratic ratio R' [7] at 64.3%, indicating a high-yield formation of turbostratic stacking. Fig. 3 shows atomic force microscopy (AFM) images of rGO surfaces annealed at (a) 1200°C and (b) 1400°C. At 1400°C, multilayer graphene islands with monolayer step heights are observed. At higher temperatures, ethanol undergoes pyrolysis, generating carbon radicals. The aggregation of these carbon radicals on the rGO surface is believed to initiate gas-solid phase epitaxial growth. The analysis of the orientation angles of individual islands in Fig. 4 indicates that a distribution of orientation angles exists. This variation is considered to induce turbostratic stacking at the interface between the rGO and the islands. This result provides a foundation for elucidating the formation mechanism of turbostratic stacking structures associated with the high crystallization of rGO. Additionally, it suggests the potential for the application of turbostratic multilayer graphene derived from rGO to electron devices.

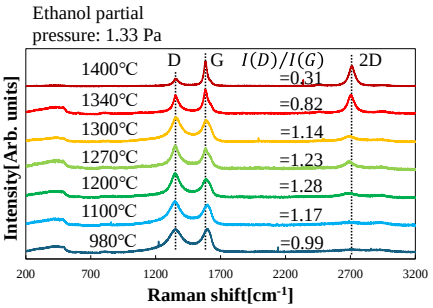

Fig. 1 Raman spectra of rGO prepared at various thermal annealing temperatures.

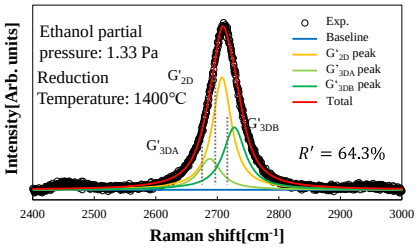

Fig. 2 Peak deconvolution of the 2D band obtained from the rGO prepared by thermal annealing at 1400°C.

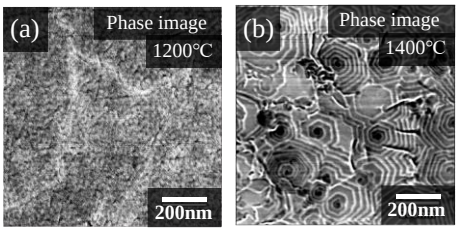

Fig. 3 AFM phase images of the rGO surfaces prepared by thermal annealing at (a) 1200°C and (b) 1400°C.

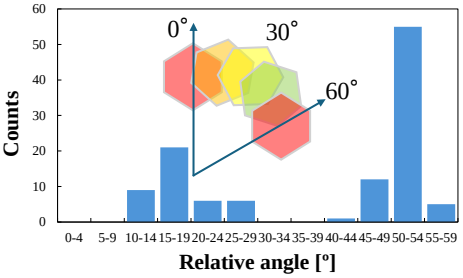

Fig. 4 Orientation angle distribution of the island in Fig. 3(b).

Acknowledgments

We gratefully thank Dr. J. Xu for experimental supports in XRD measurements. This research was supported by Grants-in-Aid for Scientific Research (C) (No. 22K04865) from the Japan Society for the Promotion of Science (JSPS). This work was partly supported by the Inoue Enryo Memorial Grant, Toyo University.

References

[1] K. Uemura, *et al.*, *Jpn. J. Appl. Phys.* **57**, 030311 (2018).
[2] J. A. Garlow, *et al.*, *Sci. Rep.* **6**, 19804 (2016).
[3] N. Morimoto, *et al.*, *Chem. Mater.* **29**, 2150-2156 (2017).
[4] R. Chen, *et al.*, *Carbon* **187**, 35-46 (2022).
[5] T. Ishida, *et al.*, *Appl. Phys. Express* **9**, 025103 (2016).
[6] L. G. Cançado *et al.*, *Carbon* **46**, 272-275 (2008).
[7] C. Wei, *et al.*, *Jpn. J. Appl. Phys.* **58**, SIIB04 (2019).

Circular dichroism of Trion in enantiopure carbon nanotubes

Hiroyuki Fujinami[1], Shiba Koki[1], Yuya Hosokawa, Yohei Yomogida[2], Kazuhiro Yanagi[1*]

[1]*Department of Physics, Tokyo Metropolitan University, Hachioji, Tokyo, Japan*

[2]*Department of Chemical Sciences and Engineering, Hokkaido University, Hokkaido 060-0808, Japan*

Chirality has been an intensive research subject since a large number of objects in nature exhibit chirality, such as amino acids, proteins, sea shells, and so on. The chiral structure has demonstrated various non-trivial physical phenomena such as no-reciprocal transport, photo-galvanic effect, chirality-induced spin selectivity. In the field of carbon nanotubes, handedness is also important. Recently, various purification methods made it possible to prepare enantiopure carbon nanotubes, and the enantiopure carbon nanotubes are expected to exhibit unique properties. Chiral structure has different responses to right-handed and left-handed circularly polarized light. Circular dichroism (CD) is a powerful tool for studying the chiral state of materials and also in the carbon nanotubes, which exhibit clear CD spectra reflecting their handedness. Here we discuss the CD of trions in enantiopure carbon nanotubes. Because of the strong binding energy reflecting the one-dimensionality of carbon nanotubes, the trion state is uniquely formed at room temperature in carbon nanotubes at a controlled doping level, and we investigated whether the trion state can also exhibit the handedness of carbon nanotubes.

We prepared randomly oriented (6, 5) and (11, -5) SWCNT films, set up an electrolyte gating device on the films during CD measurements, and clarified the CD spectra as a function of gate voltage. We identified the presence of optical absorption due to CD of tirons and found the formation of CD peak in the trion. The sign of CD peak of the trion is the same as that of CD of E11 exciton state and is opposite between the trions of (6, 5) and (11, -5) SWCNTs. In the poster, the details are discussed.

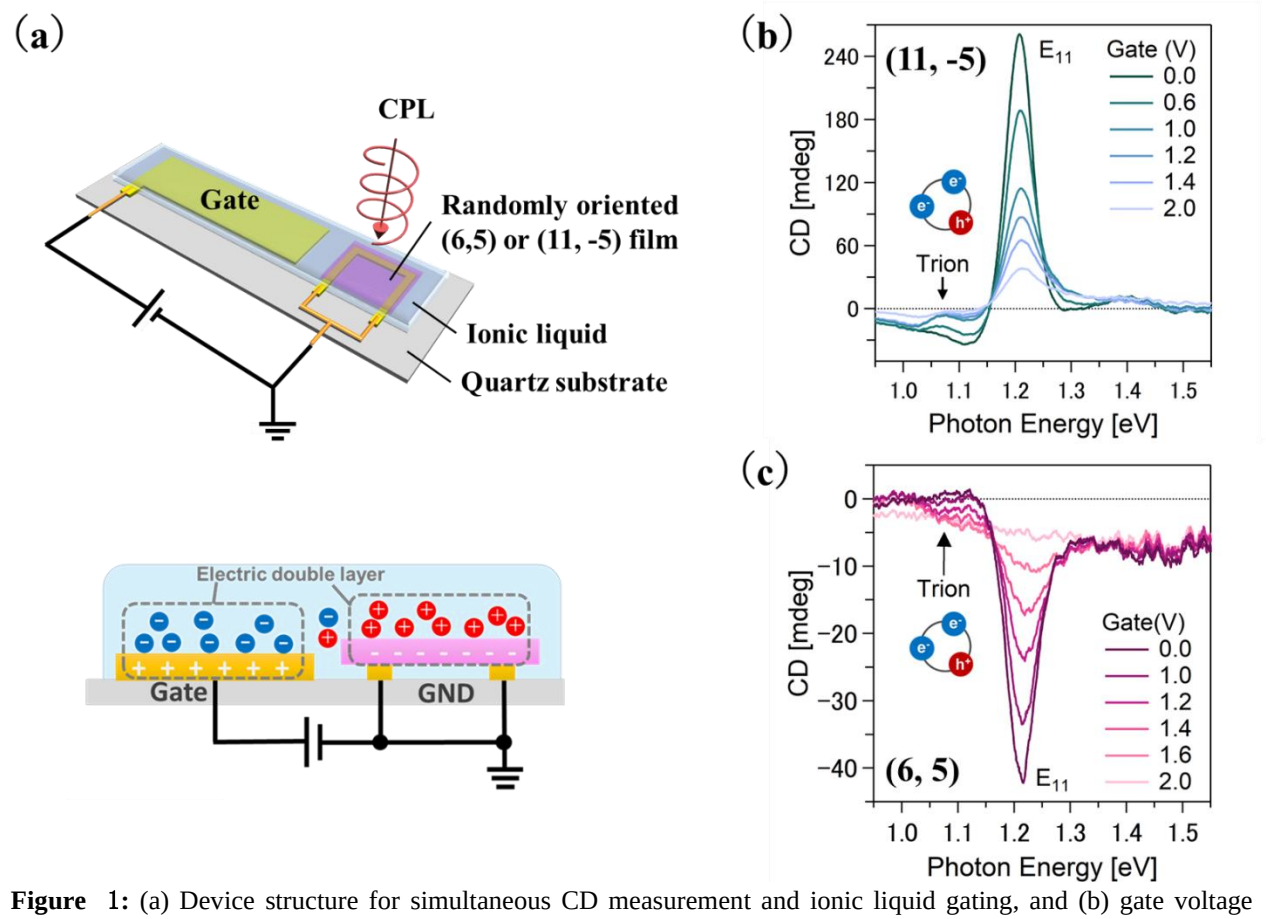

Figure 1: (a) Device structure for simultaneous CD measurement and ionic liquid gating, and (b) gate voltage dependence of near-infrared CD spectra of (11, -5) SWCNT, and (c) gate voltage dependence of near-infrared CD spectra of (6, 5) SWCNT.

Direct Growth of Graphene on Hexagonal Boron Nitride under a Catalyst-Free Condition

Y. Miyashita[1], H. Watanabe[2], Y. Terada[2], A. Sasanuma[2], R. Takatsuka[1], K. Yanagisawa[3], T. Ukai[3], S. Kurosu[3], K. Watanabe[4], T. Taniguchi[4], T. Hanajiri[1,2,3], T. Maekawa[1,2,3], R. Negishi[1,2,3]

[1]*Graduate School of Science and Engineering, Toyo University, 2100 Kujirai, Kawagoe-city, Saitama 350-8585, Japan*

[2]*Department of Electrical, Faculty of Science and Engineering, Toyo University, 2100 Kujirai, Kawagoe-city, Saitama 350-8585, Japan*

[3]*Bio-nanoelectronics research center, 2100 Kujirai, Kawagoe-city, Saitama 350-8585, Japan*

[4]*National Instirute for Material Science, 1-2-1 Sengenm Tsukuba, 305-0047, Japan*

Graphene is a two-dimensional (2D) material composed of carbon atoms bonded via sp^2 hybridization, forming a hexagonal crystal structure[1]. Currently, the chemical vapor deposition method using copper foil (Cu-CVD) is widely used for the large-area synthesis of highly crystalline graphene. However, when graphene is applied to devices, a challenge arises due to the damage caused during the transfer of graphene grown on copper foil onto an insulating device substrate[2].

In this study, we report the establishment of a catalyst-free and transfer-free graphene synthesis method via a direct growth approach using insulating hexagonal boron nitride (h-BN) flakes as a solid template, and we also investigate its formation mechanism in detail.

Figures 1(a) and 1(b) show the atomic force microscopic (AFM) images of graphene grown at 1280℃ and 1400℃, respectively. At the lower growth temperatures, a three-dimensional (3D) graphene islands are formed, whereas at the higher growth temperatures, 2D islands with a monolayer step height are formed, of which the diameters reach the microscale. Figure 2 shows the temperature dependence of the grown island size under the conditions of constant growth time and constant amount of carbon supply. The average diameter of the grown graphene islands increases dramatically with increasing growth temperature, which means that the different mechanisms of graphene island formation work in the temperature ranges of 1220–1280℃ and 1300–1450℃.

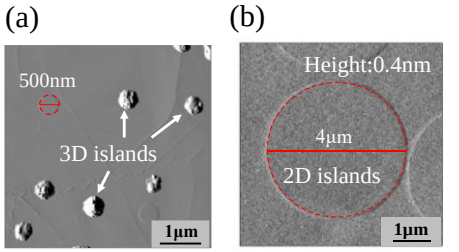

Figure 1: AFM images of graphene islands grown on h-BN flake at (a) 1280°C and (b) 1400°C.

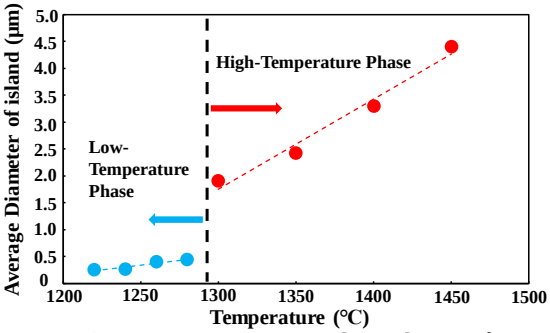

Figure 2: Temperature dependence of graphene island size.

Figures 3(a) and 3(b) show the schematic diagrams of growth mechanism at lower or higher temperatures. At lower temperatures, the re-evaporation of carbon atoms on the h-BN substrate is suppressed, which allows many surface-diffused carbon atoms and molecules to aggregate, and predominantly contributes to the formation of amorphous 3D islands.

In contrast to this, at higher growth temperatures, the re-evaporation of carbon atoms is activated and the diffusion length increases, which results in a higher probability of carbon incorporation at the edges and thus promoting a layer-by-layer growth mode. Actually, the Raman spectra obtained from graphene islands grown at high temperatures exhibits a low I_D/I_G ratio and a high I_{2D}/I_G ratio, indicating high crystallinity. From these results, we conclude that the formation of highly crystalline, monolayer graphene islands on the h-BN flake as a solid-template is dominant under high-temperature growth conditions.

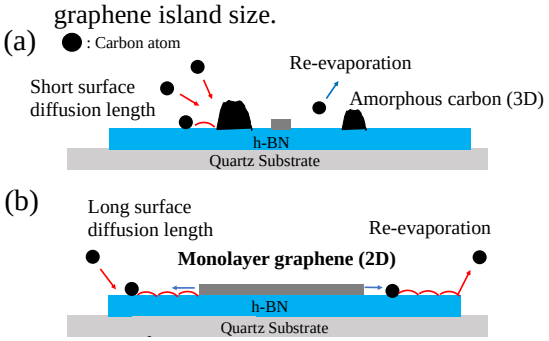

Figure 3: Schematic drawings of the growth mechanism at (a) lower and (b) higher temperatures.

Acknowledgments

This research was supported by Grants-in-Aid for Scientific Research (C) (No. 22K04865) from the Japan Society for the Promotion of Science (JSPS). This work was partly supported by the Inoue Enryo Memorial Grant, Toyo University.

References

[1] K.S. Novoselov, et al., Science **306**, 666 (2004). [2] M. Nakatani et al., Nature Electronics **7**, 119 (2024).

Doping-dependent valley polarization induced by Mott transition in WSe_2/WS_2 moiré superlattice

Zhiwei Li[1], Kenji Watanabe[2], Takashi Taniguchi[3] and Kazunari Matsuda[1]

[1]*Institute of Advanced Energy, Kyoto University, Uji, Kyoto 611-0011 (Japan),* [2]*Research Center for Electronic and Optical Materials, NIMS,* [3]*Research Center for Materials Nanoarchitectonics, NIMS.*

The stacking of monolayer metal dichalcogenides (MX_2: M=Mo, W, X=S, Se) with slight lattice mismatch, creates a periodic moiré potential array capable of confining electron-hole pairs (excitons) between the layers in the heterostructures. Among these heterostructures, the material combination of WSe_2/WS_2 system exhibits the intriguing electronic properties arising from strong electron-electron interaction by the presence of moiré flat minibands, effectively described by the Hubbard model [1]. These distinctive properties facilitate the exploration and realization of intriguing many-body phenomena, including Mott transitions [2], light-induced ferromagnetism [3] and generalized Wigner crystal [4]. Such rich physics highlights the potential application of WSe_2/WS_2 system as a novel platform for tunable electronic and optical devices. The valley polarization of interlayer excitons has drawn significant attention due to its controllability through external electric- and magnetic-fields. The previous study has reported drastic changes in valley polarization in WSe_2/WS_2 heterostructure during the electron/hole doping conditions [5]. Nevertheless, the underlying mechanisms governing valley polarization during the Mott transition and generalized Wigner crystal formation remain elusive. The understanding of these physical mechanisms is essential for controlling of novel excitonic many-body states, further enriching the functionalities of moiré-based quantum systems.

Here, we investigate the change of valley polarization in WSe_2/WS_2 system associated with the Mott transition via electron/hole doping conditions. **Figure 1a** shows the two-dimensional photoluminescence (PL) of moiré exciton peak in WSe_2/WS_2 heterostructure with R-type stack. The significant blueshift of 10 meV at electron-doped region (filling factor n, n=1) was observed (**Fig. 1(a)**), which is well consistent with the previous report [5]. The polarization- and time-resolved PL spectroscopy were carried out for investigation. We found significant enhancement in the degree of circular polarization (DOCP), which reached up from 15% at n=0 to 50% at n=1, in **Fig. 1(b)**. The enhanced valley polarization indicates the strong exciton correlation at the electron-doping condition, which could be ascribed to the suppression of valley scattering with the formation of Wigner crystal. Moreover, the unusual peak splitting behavior observed at n>1, depicted in **Fig. 1(c)**. After the formation of Wigner crystal at n=1, newly doped electrons would occupy the Γ valley instead of the -K valley and contribute to the broken symmetry and valley splitting.

Our work establishes WSe_2/WS_2 moiré heterostructure as a tunable testbed for controlling the valley polarization through the Mott transitions and the formation of Wigner crystal by doping process. Moreover, the valley splitting without the external magnetic field is also observed in the heterostructure system, which could contribute to the direct implications for designing the new generation quantum devices.

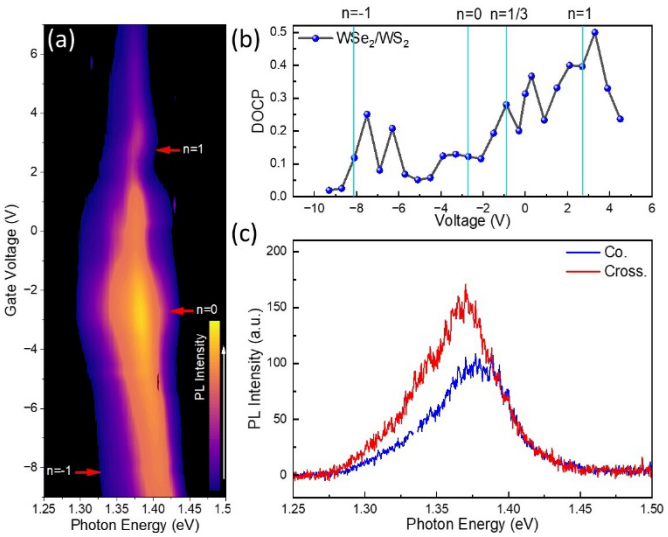

Figure 1. (a) Voltage-dependent PL spectra for R-stacked WSe_2/WS_2 device, (b) Voltage-dependent CP of WSe_2/WS_2 device, (c) Valley splitting at n>1.

References

[1] B. Gao et al., Nat. Commun. 15, 2305 (2024).
[2] Y. Shimazaki et al., Nature 580, 472–477 (2020).
[3] X. Wang et al., Nature 604, 468–473 (2022).
[4] E. C. Regan et al., Nature 579, 359–363 (2020).
[5] Z. Lian et al., Nat. Phys. 20, 34–39 (2024).

Development of a Dual-Functional Device for Rapid Detection of NO_2 Gas and Long-Term Cumulative Exposure Memory using Optimized Single-Walled Carbon Nanotubes

Sihyeok Kim[1], Ilya V. Novikov[1], Peng Liu[2], Jang Woo Lee[1], Il Hyun Lee[1], Artem Dudorov[3], Dmitry V. Krasnikov[3], Esko I. Kauppinen[2], Albert G. Nasibulin[3], Keekeun Lee[4], Il Jeon[1],*

[1] *Department of Nano Engineering, Department of Nano Science and Technology, SKKU Advanced Institute of Nanotechnology (SAINT), Sungkyunkwan University (SKKU), Suwon 16419, Republic of Korea*

[2] *Department of Applied Physics, School of Science Aalto University, Aalto 15100, Finland*

[3] *Skolkovo Institute of Science and Technology (Russia)*

[4]*Department of Electrical and Computer Engineering, Ajou University, Suwon, Gyeonggi-do, 16499, Republic of Korea*

Nitrogen dioxide (NO_2) gas is emitted from a variety of industrial sources and vehicle exhausts, and sustained exposure to elevated concentrations of NO_2 poses significant health risks, including respiratory and dermatological conditions [1]. Consequently, the development of highly sensitive and rapid sensors capable of detecting NO_2 gas is of paramount importance. In addition to exposure to high concentrations of NO_2 gas, chronic and repeated exposure to even low levels of NO_2 may contribute to the onset of debilitating and life-threatening diseases, such as Parkinson's disease, emphasizing the urgent need for advanced systems that can monitor and retain a record of cumulative exposure and its associated damage. However, existing studies have focused primarily on the rapid detection of toxic gases, with limited research on detecting the cumulative effects of repeated exposure.

This study presents a dual-functional device that integrates an ideal sensor for quick and precise real-time detection of NO_2 gas, along with a memory-based component capable of tracking long-term or repeated exposure to low concentrations. To implement these functions, single-walled carbon nanotube (SWCNT) films were synthesized by the CO-based (Boudouard reaction aerosol CVD, a particular case of floating catalyst CVD (FCCVD) method. Thickness of CNT films, proportional to its absorbance was simply tuned by the collection time. Diameter of nanotubes was adjusted by controlling the concentration of CO_2 added as a growth promoter, whereas enrichment by semiconducting SWCNTs (s-SWCNTs) was performed by N_2O-etching in the tandem reactor design. Properties of SWCNT films were studied by UV-vis-NIR optical absorbance and Raman spectroscopies.

A CNT layer composed of 98% low transmittance, relatively low s-SWCNTs)was used as the sensing layer, where rapid gas response and recovery are crucial. A microheater was integrated into this layer. The low CNT density maximized the surface-to-volume ratio, contributing to faster gas response, while the microheater elevated the surface temperature to facilitate gas adsorption and desorption. In contrast, for the persistent memory device, samples with 94% high s-SWCNT content and 60% low transmittance CNTs were used to minimize gas desorption. The thick CNTs reduced the surface area, which slowed the desorption process. The high proportion of s-SWCNTs further delayed gas desorption due to the strong binding energy with NO_2 molecules, enhancing long-term memory retention. These results suggest that by adjusting the composition and density of s-SWCNTs, it is possible to develop devices that not only enable rapid detection of harmful gases but also incorporate memory functions to record cumulative exposure to these gases.

[1] S. Kim, *et al*., Adv. Mater., (2024) 2313830.

Bending Effect on Thermoelectric performance of carbon nanotubes

A. Yoshida[1] and T. Yamamoto[1,2]

[1] *Department of Physics, Tokyo University of Science, Shinjuku, Tokyo 162-8601 (Japan),*

[2] *RIST, Tokyo University of Science, Shinjuku Tokyo 162-8601 (Japan)*

Recently, carbon nanotubes (CNTs) with high thermoelectric performance [1] have been successfully synthesized in large quantities using the super growth (SG) method, attracting significant interest for their applications in thermoelectric devices. However, the inherently high thermoelectric power factor (PF) of SG-CNTs is not fully realized due to structural disorder introduced during synthesis or device fabrication. In particular, the impact of CNT bending during thinning on thermoelectric performance remains unclear. A previous study [2] demonstrated that the resistance and Seebeck coefficient of CNTs vary with changes in curvature through repeated bending and stretching experiments. However, the physical mechanism underlying this phenomenon remains poorly understood, necessitating theoretical investigation. This study aims to analyze the effect of CNT bending on thermoelectric properties using simulations and to elucidate the fundamental physical mechanisms governing this behavior.

In this study, we bend semiconductor and Metal CNT by giving a Tersoff potential based on molecular statics and calculate the thermoelectric responses of the systems using first-principles calculations based on the π-orbital tight-binding model combined with the nonequilibrium Green's function method. The results show that semiconductor and metal CNT have different conductivity behaviors near the band edge. Furthermore, the PF of semiconductor one increases with bending depending on the value of the chemical potential. These causes are discussed in the presentation. Thus, it is clear that the thermoelectric performance of CNTs can be controlled by bending them.

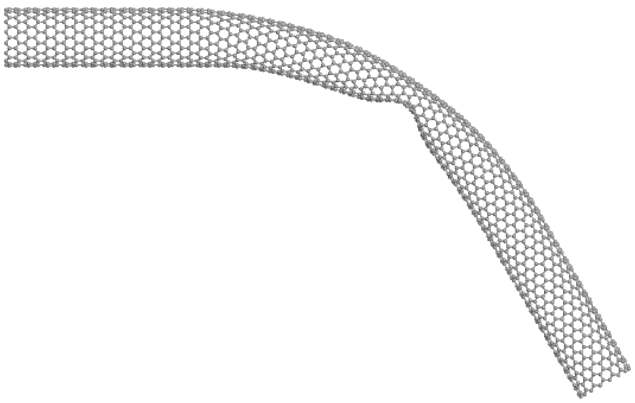

Schematic of bent (14,0) CNT.

References

[1] Y. Nakai, *et al*., Phys. Express **7**, 025103 (2014).
[2] C. W. Chang, *et al.*, Phys. Rev. Lett. **99**, (2007).

POROUS SILICON-BASED NANOCOMPOSITES FOR EFFICIENT ELECTROCHEMICAL SENSORS

A. Jalalah[1], F.H. Albaqami[1]

[1]*Institute of Microelectronics and Semiconductor Technologies, King Abdulaziz City for Science and Technology (Saudi Arabia)*

Sensors are extensively employed in a wide range of applications including environmental monitoring and food industry, safety-related issues, diagnostic and drug discovery, etc. Great efforts have been made to develop a wide range of sensing materials for the detection of chemical analytes either in vapor or liquid phases. Particularly, there is increased interest in using nano-structured porous silicon (n-PSi) arrays in sensing based-devices. The rationale for using n-PSi in sensor applications is the ease of fabrication, large specific surface area and controllable surface modification and reactivity. The sensing principle is based mainly on the changes in optical or electrical characteristics of n-PSi upon adsorption of target chemical analytes. This presentation describes a simple chemical etching approach to fabricate n-PSi nanopowder as a sensing material to detect and quantify various biomolecules by the electrochemical technique. An overview of our recent research being done in the area of silicon nanotechnology, with an emphasis on sensing systems that harness the n-PSi-based electrochemical sensors will be provided. The presentation will discuss some of the practical issues and challenges with the fabrication of nanocomposites-based PSi, with an example of coupling n-PSi with a conducting polymer and precious metallic nanoparticles. Modification of Glassy Carbon Electrode (GCE), as a working electrode, with the active n-PSi nanocomposites will be described. Furthermore, results of electrochemical detection of biomolecules using cyclic voltammetry (CV), Amperometry (i-t curves) and Electrochemical Impedance Spectroscopy (EIS) will be demonstrated. In addition, the sensor parameters including sensor sensitivity, linear dynamic range and limit of detection will be evaluated. Finally, the sensing mechanism, storage and long-term stability as well as sensor durability and reproducibility will be presented and thoroughly discussed.

Optical Absorption of Fermi Level-Cotrolled Multilayer Graphene: Effects of Stacking Structure and Spacer Insertion

○S. Yoshida[1], T. Mizuno[1], T. Inoue[1], Y. Nishina[2], Y. Kobayashi[1]

[1] *Osaka Univ. (Japan),* [2] *Okayama Univ. (Japan)*
E-mail: s.yoshida@ap.eng.osaka-u.ac.jp

Single-layer graphene (SLG) exhibits a linear dispersion electronic state, which leads to broadband and uniform optical absorption, making it a promising candidate for optoelectronic applications [1]. However, for practical device applications, low absorption and the loss of uniform absorption due to doping from the substrate and charge impurities remain significant challenges. To address these issues, Fermi level control of random stacking graphene (RSG) [2], which maintains a linear dispersion and exhibits high absorption, is considered effective. However, it has been reported that Fermi level control through the application of gate voltage from the surface is ineffective due to the strong interlayer screening effect, resulting in non-uniform Fermi level modulation across the layers. In this study, we examined the effect of the short screening length of RSG on the optical absorption spectrum. Furthermore, as a novel method to uniformly control the Fermi level across multilayer films, we investigated the effect of expanding the interlayer distance with spacers and introducing ionic liquids into the multilayer film (Fig. (a)). Thin and thick RSG was fabricated by transferring CVD graphene and thermally treating graphene oxide, respectively. Spacer-inserted bilayer graphene was fabricated by transferring SLG and coating nanodiamond (ND) as a spacer. The screening effect was analyzed by fitting of infrared absorption spectra. Fig. (b) shows the dependence of the screening length of RSG on the random stacking ratio. The screening length decreases with increasing random stacking ratio, indicating that RSG exhibits a stronger screening effect than AB-stacked graphene. Moreover, the screening length of RSG with a high random-stacking ratio was found to be as short as 0.19 nm, suggesting that the effect of Fermi level control through gate voltage application from the surface is limited to a few layers. Fig. (c) shows the gate voltage dependence of optical absorption. The modulation of absorption by gate voltage increased with spacer insertion. This is attributed to the fact that the ionic liquid was introduced between the expanded layers, which allowed the gate voltage to be applied to each layer uniformly. These results are expected to contribute to the realization of broadband and uniform optical absorption in multilayer graphene.

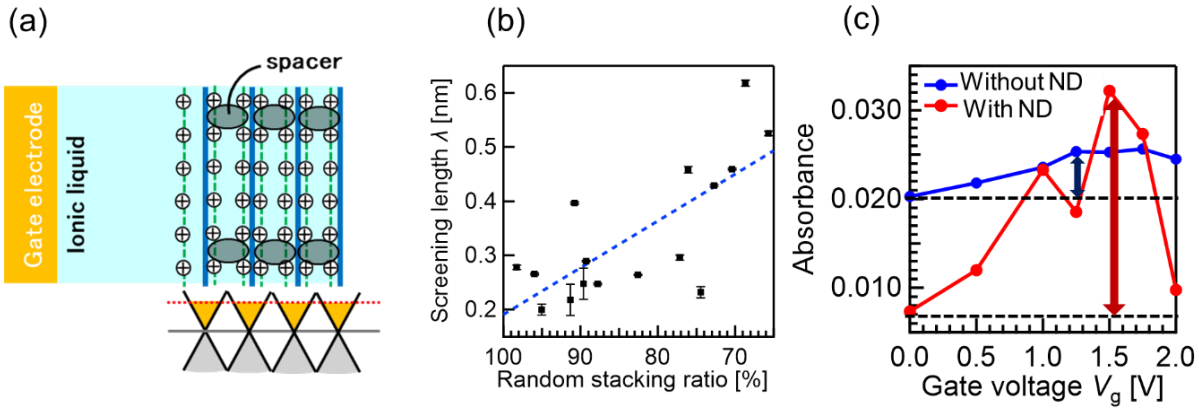

Fig. (a) Schematic illustration of Fermi level control in spacer-inserted graphene. (b) Dependence of screening length on the random stacking ratio. (c) Gate voltage dependence of the absorbance of two-layer graphene at a photon energy of 0.62 eV.

References

[1] K. F. Mak et al., Phys. Rev. Lett. **101** (2008) 196405.
[2] S. Latil et al., Phys. Rev. B **76** (2007) 201402.

EVALUATION OF MOLYBDENUM DISULFIDE PREPARED BY HEATING SULFUR-CAPPED MOLYBDENUM THIN FILMS

K. Inoue[1], Y. Kimura[1], K. Nakane[1], A. Subagyo[1], K. Sueoka[1]
[1] *Graduate School of Information Science and Technology, Hokkaido University, Sapporo, Japan*

In the next-generation electronic devices, new materials are required to replace or complement silicon, with the 2D materials graphene and transition metal dichalcogenides (TMDCs) in particular attracting attention [1-3]. Due to its high carrier mobility, thinness, and high transparency, graphene is expected to find a variety of applications, including flexible devices, transparent electrodes and integrated circuits [4,5]. However, the gapless band structure of graphene at the Fermi energy makes it unsuitable for applications such as transistors [6]. On the other hand, TMDCs such as molybdenum disulfide (MoS_2) have been shown to have an indirect energy gap of 1.2 eV in the bulk and a direct energy gap of 1.8 eV in the monolayer MoS_2, and are expected to be used in transistors with high on/off ratios, optoelectronics and energy harvesting [7-9]. For device applications, it is essential to produce MoS_2 of sufficient size and high quality and various fabrication methods have been proposed. The most common method to produce high-quality MoS_2 is thin-film fabrication by exfoliation of bulk crystals, but only small crystals can be obtained and the thickness and position are difficult to control [10]. The widely used thermal CVD growth method can produce single or bilayer high-quality MoS_2 by selecting the growth substrate and other factors [11]. However, because transfer to the device substrate is usually required, degradation of MoS_2 due to transfer has been observed, therefore, direct growth on device substrates, which does not require transfer, is required. The preparation of MoS_2 by direct sulfurization of Mo thin films is one such method, but it requires improvement due to its small grain size and non-uniform shape [12]. In this study, the sulfurization of Mo thin films was carried out by vacuum heating the Mo thin film sample with preformed sulfur films on the Mo thin film surface by immersing the Mo thin film in a sulfur solution.

Mo was deposited on SiO_2/Si and c-Al_2O_3 substrates with thicknesses ranging from 0.5 nm to 3 nm by EB evaporation. The Mo thin films were then immersed in a sulfur solution heated at 175°C for 30 seconds and immediately dried with a nitrogen blow. Heating was carried out in a vacuum of about $1x10^{-3}$ Pa with temperatures ranging from 500°C to 700°C in 10 min. Raman spectra showed that 2-3 layers of MoS_2 can be fabricated at 500°C on both substrates [13]. There was little dependence on the Mo film thickness, which suggests that a non-sulfurized Mo remains beneath the MoS_2 film. For Mo thin films thicker than 1 nm, the number of layers increased as the temperature increased to 600 °C and 700 °C, indicating that Mo was increasingly sulfurized. To assess the electrical properties, electrode arrays were formed on the MoS_2 film; the MoS_2 film was found to be continuously formed between electrode gaps up to 200 μm. Transistor characteristics were also investigated using the silicon substrate as a gate. For comparison, direct sulfurization of Mo thin films by CVD with heated sulfur as a precursor was also carried out.

References

[1] P.A Packan, *Science* **285**, 2079–2081 (1999)
[2] Q. H. Wang *et al., Nat. Nanotech*. **7**, 699-712 (2012).
[3] G. Fiori *et al., Nat. Nanotech*. **9**, 768 (2014).
[4] K. S. Novoselov *et al., Science* **306**, 666 (2004).
[5] D. Akinwande *et al., Nat. Commun*. **5**, 5678 (2014).
[6] T. G. Pedersen, *et al. Phys. Rev. B* **98**, 195416 (2018)
[7] A. Splendiani *et al., Nano Lett.* **10**, 1271-1275 (2010).
[8] K. F. Mak *et al., Phys. Rev. Lett*. **105**, 136805 (2010).
[9] B. Radisavljevic *et al., Nat. Nanotech*. **6**, 147-150 (2011).
[10] M. G. Stanford, P. D. Rack, D. Jariwala, *NPJ 2D Mater. Appl.* **2**, 20 (2018).
[11] A. Yan *et al. Nano Lett*. **15**, 6324–6331 (2015).
[12] M. H. Heyne *et al., J. Mater. Chem. C.* **4**, 1295–1304 (2016).
[13] C. Lee *et al*., *ACS Nano*, **4**, 2695 (2010)

Detection of process-induced contaminants on carbon nanotubes using Raman spectroscopy

○Haruki Uchiyama[1], Yudai Yoshikawa[1], Hiromichi Kataura[2] and Yutaka Ohno[1,3]

[1]*Department of Electronics, Nagoya University, Nagoya 464-8603, Japan*
[2]*National Institute of Advanced Industrial Science and Technology, Ibaraki 305-8565, Japan*
[3]*Inst. of Material and Systems for Sustainability, Nagoya University, Nagoya 464-8601, Japan*

The critical issue in controlling property of carbon nanotube (CNT) thin-film transistors (TFTs) is the formation of clean interfaces between the CNTs and the contact metal and gate oxide. [1] Recently, the yttrium oxide coating and decoating (YOCD) method has been reported to be effective in removing polymers from polymer-wrapped CNTs. [2] In this study, we applied the YOCD method to remove surfactants and photoresist residues from the CNT thin film of transistors. Additionally, we investigated a possibility to detect the contaminants with Raman scattering spectroscopy.

Semiconducting CNTs dispersed in water with sodium cholate (SC) was deposited on a Si substrate by the immersion deposition method. The double-layered photoresists of a lift-off resist (Kayaku, LOR) and positive photoresist (MICROPOSIT, S1813G) were spin-coated on the CNT film and then removed by immersing in the remover (MICROPOSIT, Remover 1165). For YOCD process, yttrium (3 nm) was deposited by electron-beam evaporation, thermally oxidized at 250°C in air, and removed by immersing in hydrochloric acid. Atomic force microscopy (AFM) images confirmed the effective removal of photoresist residues after the YOCD process. Raman spectroscopy revealed small peaks in as-deposited CNTs and additional peaks after lithography, which disappeared following YOCD process. These results indicate that YOCD effectively removes SC and photoresist residues from CNT TFTs.

References

[1] Z. Zhang *et. al.*, *ACS Appl. Nano Mater.* **6**, 3293 (2023).

[2] Z. Ma *et. al.*, *ACS Appl. Mater. Interfaces* **11**, 11736 (2019).

Peptide-modified Carbon Nanotube Biosensor

A. Nagamine[1], H. Uchiyama[1], H. Kataura[2], C. Homma[3], Y. Hayamizu[3], Y. Ohno[1,4]

[1]Department of Electronics, Nagoya University (Japan), [2]Nanomaterials Research Institute, National Institute of Advanced Industrial Science and Technology (Japan), [3]Tokyo Institute of Technology (Japan), [4]Institute of Material and Systems for Sustainability, Nagoya University (Japan)

Semiconducting carbon nanotube (CNT) thin films have high mobility and a one-dimensional structure, making them promising materials for the realization of highly sensitive biosensors. Surface modification of CNTs is essential for the selective detection of specific biomolecules. Peptides, which are molecules composed of amino acid chains, can be designed to obtain high selectivity in the detection of biomolecules. [1] In this study, we report the fabrication of a peptide-modified carbon nanotube biosensor and the demonstration of its ability to detect streptavidin (SA) with the aim of achieving a highly sensitive and selective biosensor.

As a biosensor platform, we fabricated a semiconductor CNT thin-film field-effect transistor on a Si/SiO_2 substrate using a conventional photolithography-based microfabrication process. The semiconducting CNTs were extracted using gel chromatography technology. The substrate was immersed in a dispersion of semiconducting CNTs to form a CNT thin film. [2] In the device manufacturing process, the CNT surface was protected with an Al_2O_3/PMMA layer to prevent contamination from photoresist and other materials. [3]

To modify the CNT surface with peptides, an aqueous peptide solution (500 nM) was dropped onto the device and left for one hour. In this study, two types of peptides were used: Bio-SSS-Y3Y and Y3Y, respectively. [4] Bio-SSS-Y3Y contains biotin, which strongly interacts with SA. In the case of CNTs modified with Bio-SSS-Y3Y, the threshold voltage in the transfer characteristics shifted in the negative direction with the SA concentration. This result is consistent with the existence of positive charge of SA.

References

[1] T. Wasilewski *et al.*, *CSCEE* **5**, 100197 (2022).
[2] W. Su *et al.*, *Carbon* **163**, 370 (2020).
[3] N. X. Viet *et al.*, *ACS Appl. Mater. Interfaces* **11**, 6389 (2019).
[4] H. Noguchi *et al.*, *ACS Appl. Mater. Interfaces* **15**, 14058 (2023)

METAL OXIDE/METAL SELENIDE NANOSTRUCTURE ELECTRODE FOR SOLID-STATE SYMMETRIC SUPERCAPACITOR WITH EXCELLENT CAPACITANCE RETENTION

A. Author1[1], A.Nayak[2]

[1]*Department of Electrical Engineering, College of Engineering, Najran University (Saudi Arabia),*

[2]*2Department of Energy Engineering, Konkuk University (Republic of Korea)*

Metal oxide/selenide nanostructures have emerged as promising electrode materials for symmetric supercapacitors due to their unique structural, electrical, and electrochemical properties. In this study, a facile two-step process was applied to synthesize cobalt oxide/cobalt selenide nanostructure arrays on titanium sheet via a wet anion-exchange resin approach. The morphology and structure of the prepared electrodes were investigated using XRD, Raman, SEM, HR-TEM, SAED, EDX, and XPS techniques. The electrochemical CV, GCD, and EIS three-electrode measurements were carried out on the prepared electrodes. The optimized electrodes were then used to fabricate the solid-state symmetric supercapacitor devices (SSSD) via assembling two identical electrodes with PVA-based gel polymer electrolytes. Finally, the electrochemical two-electrode measurements were performed on the fabricated SSSD devices at room temperature. The energy density of the built SSSD device achieves more than 20 Wh/kg at a power density of half kW/kg. In addition, the capacitance retention of the built SSSD device achieves outstanding capacitance retention of about 97% over five thousand of charge-discharge cycles, revealing the excellent stability of the prepared electrode. This work highlights the potential of metal oxide/selenide nanostructures as advanced electrode materials for durable SSSD devices, which might pave the way for next-generation energy storage systems.

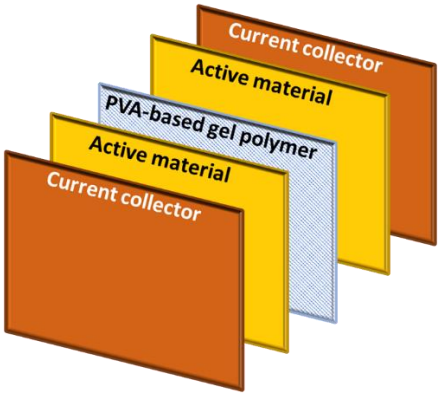

Figure: Schematic illustration of the fabricated solid-state symmetric supercapacitor devices (SSSD) device**.**

Electronic transport in CNT thin films and PBTTT films: Crossover between weak and strong localization

Y. Hiyama[1], H. Kaya[1], M. Matsubara[1], H. Fukuyama[2], and T. Yamamoto[1]

[1] *Department of Physics, Tokyo University of Science, Tokyo 162-8601, Japan*

[2] *RIST, Tokyo University of Science, Tokyo 162-8601, Japan*

Recently, two-dimensional (2D) nanomaterial semiconductors - such as carbon nanotubes (CNT) thin films and poly[2,5-bis(3-alkylthiophen-2-yl)thineo(3,2-b)thiophene] (PBTTT) thin films – have attracted attention for organic semiconductors because of mechanical flexibility and electrical properties [1-3]. However, their structural disorder makes it hard to fully understand their charge transport properties in these materials at low temperature (T). First, by using electric double-layer transistors, the T dependence of their bipolar electrical conductivity (σ) was measured [1]. These experiments have showed some interesting and unexpected features. Specifically, there is a smooth crossover from week localization (WL) to strong localization (SL), where T dependences of σ follows respectively a logarithmic and exponential function. This is a characteristic feature of charge transport in two-dimensional (2D) systems. The original scaling theory of Abrahams *et al.* [4] revealed that in 2D, all electronic states become localized, and smooth crossover from WL to SL can happen as the system size L increases. However, to compare with experiments, this theory needs to be extended to systems with finite T and macroscopic system (*i.e.,* infinite-L systems). This was proposed by Anderson *et al* [5] immediately after the publication of Ref. [4]. Although, this finite-T scaling theory addressed only the WL regime ,where σ follows a ln$T$ dependence, and it does not describe the crossover from WL to SL as T decreases.

In this study, we develop a theory to describe the crossover WL and SL for the first time by extending the present scaling theory [6]. We introduce a continuous and monotonic scaling function with respect to the electrical conductance, which smoothly connects the WL limit and SL limit when T=0. As an extension of the finite-T framework proposed by Anderson *et al* [3], we assumed that the diffusion phenomenon in WL regime remains valid even in SL regime, and introduced a dephasing length that changes continuously with T. Applying our framework to CNT thin films and PBTTT thin films, we successfully reproduced the experimental T dependence of σ at various carrier densities. This was done by using three independent parameters: the carrier density, the dephasing length and the scaling parameter. Interestingly, the scaling parameter changes gradually from 1/3 to 1/2 with decreasing the carrier density, which means the electron-electron interaction becomes essential for low carrier density transport in the thin films.

References

[1] K. Yanagi, 2023 Spring Meeting of the Japan Society of Applied Physics (JSAP), 18a-D511-7, (2023).
[2] S. Watanabe, et al., Phys. Rev. B 100, 241201(R) (2019).
[3] H. Ito, et al., Commun. Phys. 4, Article number: 8 (2021).
[4] E. Abrahams *et al*., Phys. Rev. Lett., **42**, 673 (1979).
[5] P.W. Anderson, *et al*., Phys. Rev. Lett., **43**, 718 (1979).
[6] T. Yamamoto, *et al*., arXIv:2411.01127.

Characterization of carbon nanotube thin-film transistors with inorganic polymer insulator

○Eito Kuromiya[1], Haruki Uchiyama[1], Masahiro Matsunaga[2], Shunto Arai[3], Hiromichi Kataura[4], Yutaka Ohno[1,2]

[1]*Department of Electronics, Nagoya University, Nagoya 464-8603, Japan*
[2]*Institute of Material and Systems for Sustainability, Nagoya University, Nagoya 464-8601, Japan*
[3]*National Institute for Materials Science, Ibaraki 305-0044, Japan*
[4]*National Institute of Advanced Industrial Science and Technology, Ibaraki 305-8565, Japan*

Carbon nanotube (CNT) thin-film transistors (TFTs) are promising for applications in flexible electronics due to high mobility and mechanical flexibility. While analog front-end circuits using CNT TFTs for sensing devices have been demonstrated [1], it is needed to reduce low-frequency noise for more accurate physiological signal measurements such as ECG and EEG. In this study, we report the flexible CNT TFTs with an inorganic polymer insulator, which are expected as a gate insulator material with low trap density.

Bottom-gate CNT TFTs were fabricated on a polyethylene naphthalate (PEN) substrate by a self-align process. The gate insulator of polymeric SiO_2 was formed by spin-coating perhydropolysilazane as a precursor. [2] The thickness of the polymeric SiO_2 layer was 400 nm. A semiconductor CNT film was formed by the immersion deposition method, achieving uniform device characteristics. [3] The channel length (L_{Ch}) and channel width (W_{Ch}) are both 100 μm.

The CNT TFT with the polymeric SiO_2 exhibited the high on-current as 0.2 mA/mm at V_{DS} = –2 V and steep subthreshold swing as 130 mV/dec, while one with an Al_2O_3 gate insulator exhibited 0.05 mA/mm and 870 mV/dec. The device also exhibited 1/f noise with the noise power density reduced compared to one with an Al_2O_3 gate insulator.

[1] T. Kashima et al., Research Square (2020) DOI:10.21203/rs.3.rs-68702/v1.

[2] Y. H. Kang et al., ACS Appl. Mater. Interfaces 12, 15396 (2020).

[3] W. Su et al., Carbon 163, 370 (2020).

Floating Catalyst Chemical Vapour Deposition (FCCVD)-Based CNT Electrodes for Metal Halide Perovskite Memristors in Neuromorphic Synaptic Applications

Jang Woo Lee[1], Yasir Shafi Mir[1], Taehoon Kim[1], Sihyeok Kim[1], Ilya Novikov, Sungjoo Lee[1] and Il Jeon[1†]

[1] *Department of Nano Engineering and Department of Nano Science and Technology, SKKU Advanced Institute of Nanotechnology (SAINT), Sungkyunkwan University (SKKU), Suwon 16419, Republic of Korea*

[2] *Department of Applied Chemistry and Waseda Research Institute for Science and Engineering, Waseda University, 3-4-1 Okubo, Shinjuku-ku, Tokyo 169-8555, Japan*

Metal halide perovskite (MHP)-based memristors are emerging candidates for next-generation neuromorphic synaptic devices due to their high on-/off-current ratio (I_{on}/I_{off}), low operating voltage, tunable bandgap properties, high mechanical flexibility, and solution processability [1-3]. Recently, low-energy-consuming (~10 fJ/synaptic operation) neuromorphic synaptic devices have garnered significant attention, highlighting a key advantage of MHP-based memristors. However, there have been few reports on MHP-based memristors for enhancing the linearity and symmetricity [4]. To achieve both high linearity and symmetricity, increasing the work function of the electrodes, which controls the Schottky energy barrier height (E_{SB}) between the metal and MHP, is crucial. Typically, the electrodes for MHPs are limited to indium tin oxide (ITO), fluorine-doped tin oxide (FTO), Au, Ag, and Cu. This limitation is due to the intrinsic instability of MHPs to oxidation, ion migration, and humidity, as well as the material cost.

Carbon nanotubes (CNTs) have gained attention as alternative electrodes due to their advantages of no metal-ion migration, mechanical flexibility, natural abundance, and, most importantly, adjustable work function through facile chemical doping [5]. There are two mainstream types of CNT electrodes: solution-type enhanced direct injection pyrolytic synthesis (e-DIPS) and dry-type floating catalyst chemical vapour deposition (FCCVD). Although e-DIPS CNTs are suitable for low-cost and large-scale mass production, FCCVD CNTs possess an incomparably low defect density and, unlike solution-type CNTs, do not require a separate dispersion process, thereby eliminating the need for surfactants.

In this work, we employed FCCVD CNT electrodes for MHP-based memristors and achieved high linearity by fine-tuning the work function of CNTs using nitric acid vapour doping. For synaptic memristor applications, FCCVD CNT electrodes were a better choice over e-DIPS CNTs owing to the surfactant-free characteristic. The optimized devices exhibited low synaptic current of ~10^{-7} μA, while maintaining $I_{on}I_{off}$ >10^3, which is suitable for the low-energy synaptic devices. Moreover, low variation effect was confirmed for our the MHP-based memristors by the statistical analysis.

[1] R. A. John *et al*. Nature Communications, **13**, 2074 (2022)
[2] Y. Fang *et al*. ACS Applied Materials & Interfaces, **13** (2021)
[3] Y. Park *et al*. Journal of Physical Chemistry Letters, **13** (2022)
[4] S. -U. Lee *et al*. ACS Nano Letters, **24** (2024)
[5] J. W. Lee *et al*. ACS Nano Letters, **19** (2019)

Durable Organic and Perovskite Solar Cells Using Single-walled Carbon Nanotubes Transparent Thin-film Electrodes

Yutaka Matsuo[1,2]

[1]1 Department of Chemical Systems Engineering, Nagoya University (Japan),
[2] Institute of Materials Innovation, Institutes of Innovation for Future Society, Nagoya University (Japan)

e-mail: matsuo.yutaka.h7@f.mail.nagoya-u.ac.jp

In recent years, research on solar power generation technology has progressed to achieve carbon neutrality. Organic thin-film solar cells (OPVs) and perovskite solar cells (PSCs) have been attracting attention as lightweight and flexible next-generation solar cells. While OPVs and PSCs have unique characteristics not found in conventional inorganic solar cells, they face challenges in terms of durability and cost due to the use of metal and metal oxide electrodes. To address these issues, our research group has reported the fabrication of OPVs (CNT-OPVs) and PSCs (CNT-PSCs) using single-walled carbon nanotubes (CNT) electrodes instead of metal or metal oxide electrodes.

CNT-OPVs have not yet progressed beyond laboratory-scale sizes. Therefore, we attempted to scale up from conventional cell sizes to semi-modules (Figure 1) in order to move towards the practical application of CNT-OPVs. In this paper, we discuss the results and the prospects of CNT-OPVs.

PSCs have particular issues with durability. It has been shown that using CNT electrodes for the top electrode significantly improves the durability of PSCs. Thus, CNT electrodes offer a feasible alternative to the unstable and brittle metal electrodes (Au, Ag, and Cu) in traditional perovskite solar cells (PSCs). CNT electrodes serve as excellent hole transporting electrodes due to their p-type semiconducting properties when exposed to air and oxygen. To change its transport characteristic, this study implements a facile n-type molecular doping approach to increase the electron conductivity of CNTs, enabling their use as electron-transporting electrodes in PSCs.

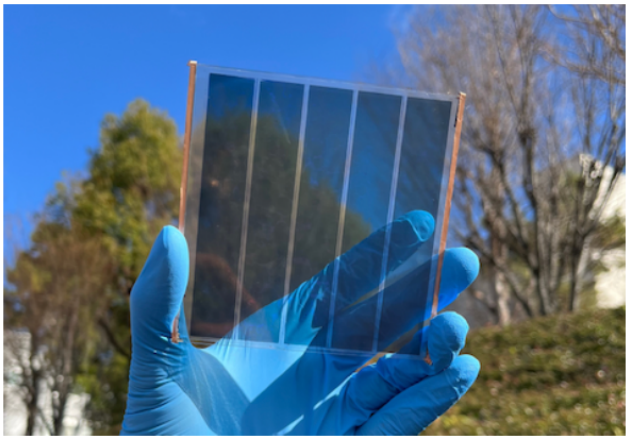

Figure 1. 10 cm square, double-sided light-receiving, translucent CNT-OPV semi-module

References

[1] Q.-J. Shui, S. Shan, Y.-C. Zhai, S. Aoyagi, S. Izawa, M. Huda, C.-Y. Yu, L. Zuo, H. Chen, H.-S. Lin, Y. Matsuo, J. Am. Chem. Soc., 145, 27307 (2023).
[2] H.-S. Lin, R. Hatomoto, D. Miyata, M. Huda, I. Jeon, S. Hashimoto, T. Hashimoto, Y. Matsuo, Appl. Phys. Express, 15, 046505 (2022).
[3] Y. Matsuo, Bull. Chem. Soc. Jpn., 94, 1080 (2021).
[4] I. Jeon, A. Shawky, H.-S. Lin, S. Seo, H. Okada, J.-W. Lee, A. Pal, S. Tan, A. Anisimov, E. I. Kauppinen, Y. Yang, S. Manzhos, S. Maruyama, Y. Matsuo, J. Am. Chem. Soc., 141, 16553 (2019).
[5] I. Jeon, K. Cui, T. Chiba, A. Anisimov, A. Nasibulin, E. Kauppinen, S. Maruyama, Y. Matsuo, J. Am. Chem. Soc., 137, 7982 (2015).

Structural changes in semiconducting CNT networks by coating conditions

Toshie Miyamoto[1, 2], Tomo Tanaka[1,2], Megumi Kanaori[2], Norika Fukuda[2],
Shunta Doi[1], Noriyuki Tonouchi[1, 2], Ryota Yuge[1, 2]

[1]NEC Corporation (Japan), [2]National Institute of Advanced Industrial Science and Technology (Japan)

The industrial use of bolometer-type infrared image sensors has been revitalized with various applications such as security surveillance, thermography of the human body, and automatic driving. We have conducted research and development of uncooled infrared image sensors with semiconducting single-walled carbon nanotubes (SWCNTs) using our original extracting method, the ELF method[1]. Our semiconducting SWCNT networks show a high resistance temperature coefficient, and strongly contributes to improving the responsivity of bolometer-type detectors[2]. To improve imaging sensor performance, the electrical resistance of each pixel must be highly uniform. With the conventional dip-coating method, it is difficult to control the SWCNT network morphology and uniformity for large scale. In this study, we investigated how to control the morphology and uniformity of SWCNT networks by process conditions.
The high-purity semiconducting SWCNTs were extracted from commercial SWCNT (Meijo Nano Carbon Co., Ltd.: EC1.5) by the ELF method[3] and formed SWCNT networks on Si substrates under different conditions. The morphology of the SWCNT networks was observed by SEM and AFM, and the electrical properties were measured by semiconducting parameter analyzer. It was found that the morphology of the CNT network, such as local orientation and domain size, can be controlled by the coating conditions. It was also found that the uniformity of large-area substrates changes by changing the coating conditions. Details will be reported on the day.

Acknowledgments: The study was partly supported by Innovative Science and Technology Initiative for Security Grant No. JPJ004596, ATLA, Japan.

References

[1] T. Tanaka et al. *Proc. SPIE* **12534**, 125341U (2023).
[2] T. Tanaka. et. al., *Proc. SPIE* **13046**, 130460X (2024).
[3] K. Ihara et al, *J. Phys. Chem. C*, **115**, 22827 (2011).

Bayesian optimization for the synthesis of small-diameter single-walled carbon nanotubes using the eDIPS method

T. Shibuya[1, 2], N. Tonouchi[1, 2], Y. Nishiwaki[3], S. Hashimoto[3], T. Hashimoto[3], T. Saito[2], R. Yuge[1,2]

[1]NEC Corporation (Japan), [2]National Institute of Advanced Industrial Science and Technology (Japan)

[3]Meijo Nano Carbon Co. Ltd. (Japan)

Uncooled bolometers have various applications including security, military, food inspection, health care, and automotive cameras. The bolometer detects temperature changes in the infrared receiving area as changes in the electrical resistance of a resistor. For a high-performance bolometer, a high temperature coefficient of resistance (TCR) is required. With a focus on the high TCR of semiconducting single-walled carbon nanotube network[1-2], we are developing bolometers using it as a resistor. Our previous research has shown that the TCR of SWCNT networks increases as the band gap of the SWCNT increases. It is known that the smaller the diameter of the SWCNT, the larger the band gap. Therefore, to further improve the performance of the bolometer, we are aiming at fabricating small-diameter SWCNTs. In particular, we are focusing on the eDIPS method[3], which is excellent for continuous production, and are searching for conditions that will allow us to selectively synthesize SWCNTs with a diameter smaller than existing products such as EC 1.0 (1.0 nm in diameter) with a high yield. The eDIPS method is a type of chemical vapor deposition that uses two kinds of carbon sources with different decomposition temperatures, thereby improving the controllability of the diameter.

In this study, decalin and ethylene were used as carbon sources, and ferrocene and thiophene were used as catalysts. More than 250 samples were synthesized using the flow rate of the carrier gas, the flow rate of ethylene, the mixing ratio of the liquid raw materials, and the temperature of the furnace as the variable parameters. The samples were characterized mainly using Raman spectroscopy with excitation wavelengths of 532 and 633 nm. The quantities that correlate with diameter selectivity and SWCNT yield were extracted from the Raman spectra, and the conditions for a single diameter of 0.9 nm or less and high yield were searched for using Bayesian optimization. In the presentation, we also discuss clustering of Raman spectra and combinations of synthesis conditions that well explain the features of Raman spectra.

Acknowledgments: The study was partly supported by Innovative Science and Technology Initiative for Security Grant No. JPJ004596, ATLA, Japan.

References

[1] T. Tanaka *et al. The MRS FALL MEETING* 2022, NM02.09.08.
[2] T. Miyamoto *et al. The 63th FNTG general symposium*, 2022, 3P-8.
[3] T. Saito *et al., J. Nanosci. Nanotechnol.* **8**, 6153 (2008).

POROUS SILICON-BASED NANOCOMPOSITES FOR EFFICIENT ELECTROCHEMICAL SENSORS

A. Jalalah[1], F.H. Albaqami[1]

[1]*Institute of Microelectronics and Semiconductor Technologies, King Abdulaziz City for Science and Technology (Saudi Arabia)*

Sensors are extensively employed in a wide range of applications including environmental monitoring and food industry, safety-related issues, diagnostic and drug discovery, etc. Great efforts have been made to develop a wide range of sensing materials for the detection of chemical analytes either in vapor or liquid phases. Particularly, there is increased interest in using nano-structured porous silicon (n-PSi) arrays in sensing based-devices. The rationale for using n-PSi in sensor applications is the ease of fabrication, large specific surface area and controllable surface modification and reactivity. The sensing principle is based mainly on the changes in optical or electrical characteristics of n-PSi upon adsorption of target chemical analytes. This presentation describes a simple chemical etching approach to fabricate n-PSi nanopowder as a sensing material to detect and quantify various biomolecules by the electrochemical technique. An overview of our recent research being done in the area of silicon nanotechnology, with an emphasis on sensing systems that harness the n-PSi-based electrochemical sensors will be provided. The presentation will discuss some of the practical issues and challenges with the fabrication of nanocomposites-based PSi, with an example of coupling n-PSi with a conducting polymer and precious metallic nanoparticles. Modification of Glassy Carbon Electrode (GCE), as a working electrode, with the active n-PSi nanocomposites will be described. Furthermore, results of electrochemical detection of biomolecules using cyclic voltammetry (CV), Amperometry (i-t curves) and Electrochemical Impedance Spectroscopy (EIS) will be demonstrated. In addition, the sensor parameters including sensor sensitivity, linear dynamic range and limit of detection will be evaluated. Finally, the sensing mechanism, storage and long-term stability as well as sensor durability and reproducibility will be presented and thoroughly discussed.

Optical Properties of Interlayer Excitons in TMD-based vdw Stacks

Sudhanshu Kumar Nayak[a,b], Hiroo Suzuki[c], Daichi Kozawa[b], Sai Santosh Kumar Raavi[a,*], and Ryo Kitaura[b,*]

[a]*Ultrafast Photophysics and Photonics Laboratory, Department of Physics, Indian Institute of Technology Hyderabad, Kandi, Telangana, India*
[b]*Research Center for Materials Nanoarchitectonics (MANA)National Institute for Materials Science (NIMS)Tsukuba 305-0044, Japan*
[c] *Life, Natural Science and Technology, Institute of Academic and Research, Okayama University (Japan)*

Two-dimensional (2D) semiconductors, such as transition metal dichalcogenides (TMDs) and halide perovskites, provide a fascinating platform for investigating exciton physics in two-dimensional systems, where strong Coulomb interaction leads to significant excitonic effects in optical transitions.[1, 2] 2D semiconductors also offer opportunities to explore interlayer excitons by optically exciting van der Waals stacks of 2D structures, resulting in various emerging interlayer excitonic states (Fig. 1). In this work, we have focused on investigating excitonic responses from several 2D stacked systems, such as TMD/halide-perovskite, TMD/TMD, etc. using cryogenic microspectroscopy technique. TMDs host 2D mobile excitons whereas halide perovskites can have localized excitons, called self-trapped excitons.[3, 4] Interlayer excitons formed between systems with different nature probably cause unique excitonic states in TMD/halide-perovskite systems. In our study, we selected $Cs_2AgBiBr_6$ as a halide perovskite and WS_2 as 2D TMD. $Cs_2AgBiBr_6$ and WS_2 were synthesized using the space-confinement method[5] and the chemical vapor deposition (CVD) method, respectively. $WS_2/Cs_2AgBiBr_6$ heterostructures were prepared using the PDMS-assisted wet transfer method. Temperature dependence in Photoluminescence (PL) intensity measured with 488 nm excitation indicates larger activation energy in the heterostructure compared to its pristine perovskite material counterpart. Additionally, we measured PL of the heterostructure using a 590 nm laser for excitation. At 50 K, we detected a broad peak alongside the WS_2 PL peak, which is absent in both pristine materials. This broad peak may result from interlayer coupling between the two materials, leading to the formation of interlayer excitons. In the presentation, in addition to the origin of the broad peak in WS_2/perovskite, we will also discuss results about TMD/TMD in details.

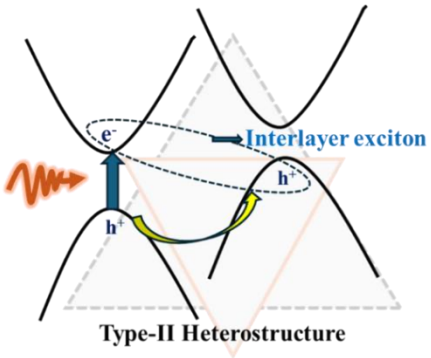

Fig. 1: Schematic representation of interlayer exciton formation in a type-II van der Waals heterostack.

References

1. K. Xiao, T. Yan, C. Xiao, F.-R. Fan, R. Duan, Z. Liu, K. Watanabe, T. Taniguchi, S. S. Parkin and W. Yao, ACS nano **18** (46), 31869-31876 (2024).
2. D. Van Tuan, M. Yang and H. Dery, Physical Review B **98** (12), 125308 (2018).
3. M. S. Ahmed, L. Sireesha, S. K. Nayak, R. Bakthavatsalam, D. Banerjee, V. R. Soma, J. Kundu and S. S. K. Raavi, Nanoscale **15** (21), 9372-9389 (2023).
4. C. Chakraborty, L. Qiu, K. Konthasinghe, A. Mukherjee, S. Dhara and N. Vamivakas, Nano Letters **18** (5), 2859-2863 (2018).
5. F. Fang, H. Li, S. Fang, B. Zhou, F. Huang, C. Ma, Y. Wan, S. Jiang, Y. Wang and B. Tian, Advanced Optical Materials **9** (9), 2001930 (2021).

Carbon Nanotube Electrode-Based Reconfigurable Metal Halide Perovskite Memristors for Reservoir Computing Applications

Jang Woo Lee[1], Tae Hoon Kim[1], Naoumi Hasumi[2], Ryosuke Nakajima[2], Sihyeok Kim[1], Sungjoo Lee[1], Suguru Noda[2†], and Il Jeon[1†]

[1] *Department of Nano Engineering and Department of Nano Science and Technology, SKKU Advanced Institute of Nanotechnology (SAINT), Sungkyunkwan University (SKKU), Suwon 16419, Republic of Korea*

[2] *Department of Applied Chemistry and Waseda Research Institute for Science and Engineering, Waseda University, 3-4-1 Okubo, Shinjuku-ku, Tokyo 169-8555, Japan*

Recently, reconfigurable neuromorphic devices, particularly memristors capable of operating in both non-volatile and volatile memory modes, have garnered significant attention [1]. Since these memory characteristics are determined by the thickness of the conductive filament (CF), precise modulation of the operating current or voltage is essential for achieving reconfigurable memristors. However, implementing volatile memory that mimics the spontaneous rupture of CF remains challenging. Previous studies have explored multilayer structures combining materials specialized for each memory type [2] or integrating Ag nanowire bundles with non-volatile memory [3], but these methods face challenges in interfacial optimization and device integration. Meanwhile, recent studies have reported that the electric-field crowding effect can effectively induce volatile memory behavior [4], yet no research has applied this effect directly to electrode design. Therefore, developing electrode materials that incorporate both a random network structure and the electric-field crowding effect is essential, though research in this area remains unexplored.

Metal halide perovskite (MHP)-based memristors have recently gained attention as promising candidates for next-generation neuromorphic synaptic devices due to their high on/off current ratio (I_{on}/I_{off}), low operating voltage, mechanical flexibility, and solution processability [1]. Furthermore, the low ion migration energy of MHP makes it particularly suitable for volatile memory applications. However, despite these advantages, research on MHP-based memristors for volatile memory remains extremely limited, with only one study reported to date [1].

In this work, we employed solution-processable e-DIPS CNT electrodes for MHP-based memristors and successfully achieved reconfigurable operation exhibiting both volatile and non-volatile characteristics. The wavy surface of the CNTs facilitates the formation of thin CFs, thereby enhancing volatile memory implementation. Additionally, to maximize the reconfigurable characteristics, we applied HNO_3 doping and compared our devices with conventional indium tin oxide (ITO)-based memristors. Proposed devices highlight the potential of these devices for neuron-synapse co-integrated low-power reconfigurable synaptic applications.

[1] R. A. John *et al*. Nature Communications, **13**, 2074 (2022)
[2] S. -U. Lee *et al*. ACS Nano Letters, **24** (2024)
[3] G. Milano *et al.* Nature Materials, **21** (2022)
[4] D. Ju *et al*. The Journal of Chemical Physics, **161** (2024)

Collapsed carbon nanotubes: Raman signal and flattening control

E. Picheau[1], D. Tang[1]

[1] *Research Center for Materials Nanoarchitectonics (MANA), National Institute for Materials Science (NIMS) (Japan)*

Carbon nanotubes (CNTs) are generally considered cylindrical objects. However, under certain circumstances a flattened geometry is more stable than the cylindrical counterpart. It is for instance possible to collapse a cylindrical CNT into its flattened shape by applying pressure, or to obtain spontaneously flattened CNT if its diameter is large enough (~ 5 nm for a single wall CNT[1]). Being identical to bilayer graphene nanoribbons but closed on their edges by atomically smooth cavities, flattened carbon nanotubes possess interesting properties of great potential.[2]

After a brief review of the last 25 years of literature about flattened CNTs, the presentation will report the obtaining of spontaneously flattened CNTs from multi-walled samples and remind their Raman signal.[3] Our recent attempts to flatten medium-range diameter CNTs by applying external stimuli and using “Through Silicon Via” devices will be also reported, as well as the devices fabrication process allowing advanced in-situ TEM experiments of CNT.

References

[1] He, M. et al. ACS Nano 8, 9657–9663 (2014).
[2] He, M. et al. Small 15, 1804473 (2019).
[3] Picheau, E. et al. ACS Nano 15, 596–603 (2021).

Exploration for the Optimized Double-Layer Catalyst Support Structure for the Synthesis of Vertically Aligned Carbon Nanotube Arrays

S. Sakurai[1], T. Tsuji[1], D. N. Futaba[1]

[1]*Nano Carbon Device Research Center, National Institute of Advanced Industrial Science and Technology (AIST), Tsukuba, Ibaraki 305-8565, Japan*

Metal nanoparticle catalysts are widely used in chemical reactions due to their high surface area and unique reactivity, but they suffer from structural degradation, especially at high temperatures. Key deactivation mechanisms include Ostwald ripening and subsurface diffusion, which reduce catalyst lifetime. A critical application requiring stable catalysts is the synthesis of single-walled carbon nanotube (SWNT) forests, where catalysts must endure extreme conditions. Despite research efforts, no single support material effectively prevents both surface and subsurface diffusion. In SWNT synthesis, aluminum oxide (Al_2O_3) [1,2] and magnesium oxide (MgO) [3] are commonly used, with studies highlighting the impact of support properties on catalyst stability.

Recently, we proposed a strategy to mitigate this limitation by maintaining structural stability and thus chemical reactivity using a double-layer (DL) support architecture [4]. The DL support is composed of a top “anchor layer” to impede surface diffusion, and a high crystallinity “sealing layer” to inhibit subsurface diffusion. We demonstrated the growth of millimeter-tall single-walled carbon nanotube (SWNT) forests from MgO/Al_2O_3 DL support layer, and also centimeter-tall CNT forest from Al_2O_3/SiO_2 DL support. We also explored the fabrication process parameters of the double-layer (DL) catalyst support and investigated the key factors contributing to CNT growth efficiency. Analysis using a machine learning model revealed that the thickness of the MgO layer has a significant impact on SWNT forest synthesis efficiency.

References

[1] K. Hata, D. N. Futaba, K. Mizuno, T. Namai, M. Yumura, S. Iijima, *Science* **306**, 1362 (2004).
[2] S. Sakurai et al., *J. Am. Chem. Soc.* **134**, 2148, (2012).
[3] T. Tsuji, K. Hata, D. N. Futaba, S. Sakurai, *J. Am. Chem. Soc.* **138**, 16608, (2016).
[4] S. Sakurai, T. Tsuji, J. He, M. Yamada, D. N. Futaba, *ACS Appl. Nano Mater.* **7**, 12745 (2024).

Activated Diffusion of 1D J-Aggregates in Boron Nitride Nanotubes by Curvature Patterning

J.-B. Marceau[1], J. Le Balle[1,2], D.-M. Ta[3], A. Aguilar[3], A. Loiseau[2], R. Martel[4], P. Bon[3], R. Voituriez[5], G. Recher[1], and E. Gaufrès[1*]

[1] Laboratoire Photonique Numérique et Nanosciences, Institut d'Optique, CNRS, Université de Bordeaux, France, [2] Laboratoire d'Étude des Microstructures, ONERA-CNRS, Université Paris-Saclay, France, [3] XLIM, CNRS, Limoges, France, [4] Département de chimie et Institut Courtois, Université de Montréal, Canada, [5] Lab. de Physique Théorique de la Matière Condensée CNRS Sorbonne Université, Paris, France

Single walled carbon nanotubes (SWCNTs) have been used as a 1D template for assembling various organic and inorganic compounds thanks to their hollow, crystalline and cylindrical architectures. In the context of fluorescent molecules assembly, it was unfortunately demonstrated that the overlap of the emission bands of the adsorbed dyes with the absorption bands of semiconducting nanotubes in the visible range (2-3 eV) leads to effective energy transfers that both readily quench the dyes fluorescence and sensitize the nanotube host. As an alternative, boron nitride nanotubes (BNNTs) have been identified as a promising dielectric host template for fluorescent molecules because of their wide-gap semiconductors of ~5.5 eV, opening the way for the design of fluorescent nano-hybrids. [1,2]

In this presentation, we will first present an activated and guided diffusion mechanism of luminescent dyes molecules initially confined inside boron nitride nanotubes.4,5 This mechanism leads to the formation of periodic luminescent chains of aligned molecules with chain lengths ranging from 500 nm to 2 microns [3]. Correlative measurements between BNNT bending and the position of molecules along the BNNT axis reveal an efficient and long-range migration of molecules from the curved to the straight parts of a BNNT. We combined a phenomenological model of the molecular transport in 1D with the description of the bending properties of BNNTs to decipher this mechanism and to predict the position and morphologies of a cluster as a function BNNT length. This mechanism leads to the formation of bright J-aggregates with periodic spacing and defined lengths.

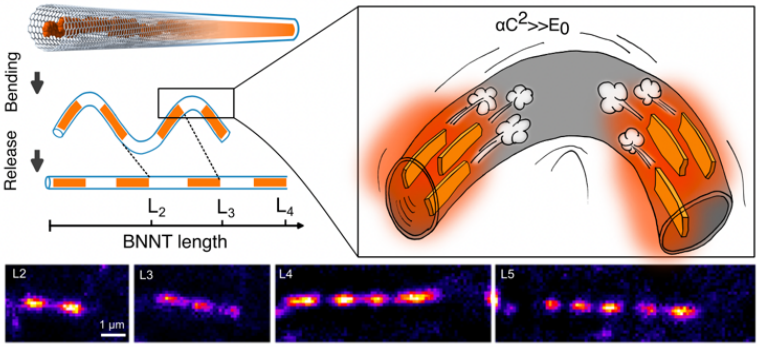

Figure caption: Curvature in 1D activates the diffusion of dye J-aggregates in Boron Nitride Nanotubes to form deterministic fluorescent patterns.

References (if desired)

[1] C. Allard et al, Advanced Materials, 32,29 (2020)
[2] A. Badon & J.-B Marceau et al, Materials Horizons 10, 983-992 (2023)
[3] J-B Marceau et al, ACS Nano, just accepted (2025)

FLEXIBLE ELECTRONICS BASED ON CONJUGATED POLYMERS, OXIDES AND CARBON NANOSTRUCTURES

Lucimara Stolz Roman

Physics department - Universidade Federal do Paraná (UFPR) (Brazil)

The combination of conjugated polymers, oxides and carbon nanostructures can be an interesting way of organizing the nanostruture of thin films and develop new optoelectrical properties. The development of electronic devices based on thin films as electrodes or active layers offers some processing advantages and new possibilities in the manufacture of these devices, such as flexibility and large areas. The interest in this research area has grown significantly, presenting many innovations, whether in the synthesis of new materials, in the understanding of optoelectronic properties or in new device geometries allowing the increase of their efficiencies. The solution processed devices can take advantage of nanostructured inks to allow their fabrication using spin coating or slot die coating in flexible substrates. In this work, some examples of the combination of these materials in thin films, the optoelectrical properties and morphology will be discussed. Additionally, examples of these films used in the fabrication of electronic devices, such as gas sensors, electrodes, and active layers of solar cells, will be presented. The active thin films can be obtained by simple mixture in a common solvent; generated by interfacial synthesis; slot-die printing (see Figure below) and by miniemulsion technique.

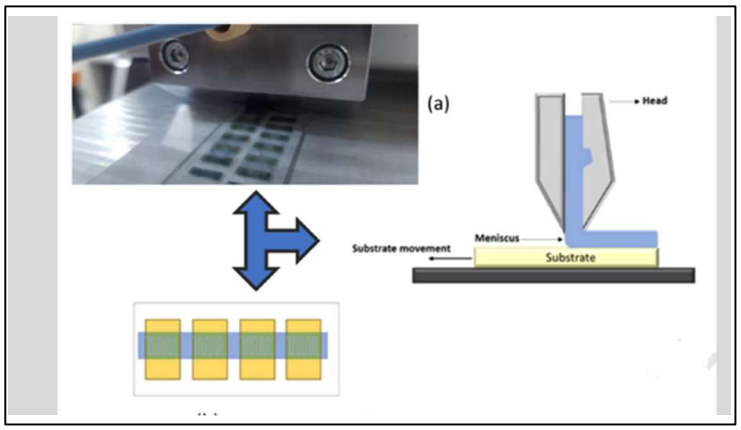

Figure caption: (a) Photo of the slot-die printing the devices and the schematic diagram of the functioning of the printer on interdigitated electrodes on glass or PET substrates.

Graphene nano-electromechanical mass sensor with high resolution at room temperature

Dong-Hoon Shin[1,3], Sung Hyun Kim[2], Peter G Steeneken[3], Chirlmin Joo[3], SangWook Lee[2]

[1]*Department of Electronics and Information Engineering, Korea University, Sejong (Korea),*

[2]*Department of Physics, Ewha Womans University, Seoul (Korea),*

[3]*Department BioNanoSci, Delft Univ Tech, Delft, (Netherlands)*

The inherent properties of 2D materials—light mass, high out-of-plane flexibility, and large surface area—promise great potential for precise and accurate nanomechanical mass sensing, but their application is often hampered by surface contamination. Here we demonstrate a tri-layer graphene nanomechanical resonant mass sensor with sub-attogram resolution at room temperature, fabricated by a bottom-up process. We found that Joule-heating is effective in cleaning the graphene membrane surface, which results in a large improvement in the stability of the resonance frequency. We characterized the sensor by depositing Cr metal using a stencil mask and found a mass-resolution that is sufficient to weigh very small particles, like large proteins and protein complexes, with potential applications in the fields of nanobiology and medicine.

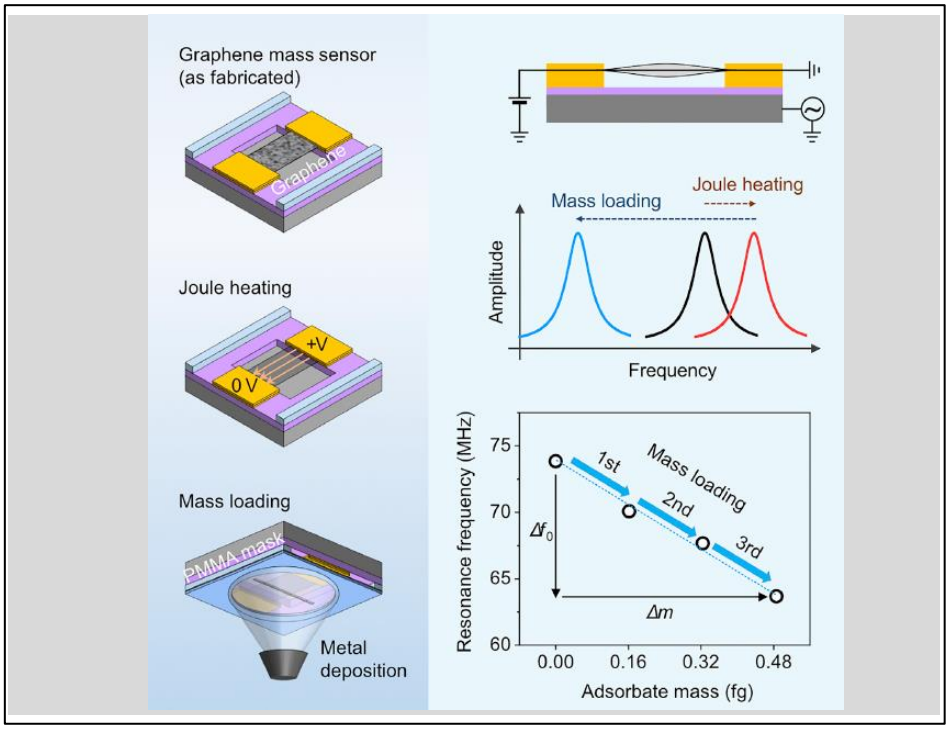

Figure 1: Schematics of experimental process of suspended graphene based mass change detection (left) and results on each process (right)

References

[1] Dong Hoon Shin, Hakseong Kim, Sung Hyun Kim, Hyeonsik Cheong, Peter G. Steeneken, Chirlmin Joo, and Sang Wook Lee "Graphene Nano-Electromechanical Mass Sensor with High Resolution at Room Temperature" iScience 26, 105958 February 17 (2023)

Carbon Nanotube Schottky Diode-Based Millimeter-Wave Frontends: Enabling Silicon-Compatible Flexible RF Systems from 10 GHz to W-Band

Defu Wang[1], Hongrong Qiu[2], Murong Zhuo[3], Zhiyong Zhang[1], Lian-Mao Peng[1]
[1]*Peking University (China),* [2]*Xiangtan University (China),* [3]*Beijing University of Posts and Telecommunications (China)*

This report presents high-performance millimeter-wave front-end technology based on carbon nanotube (CNT) Schottky diodes. By leveraging interface engineering, ultrafast switching response and ultra-high cutoff frequency are achieved, leading to the groundbreaking development of a multi-platform-compatible RF system. Frequency multipliers on silicon, quartz, and flexible substrates cover the 30–60 GHz, 45–90 GHz, and 10–20 GHz bands, respectively. The W-band phase shifter (including a W-band reflective 30° continuous phase shift and a 40 GHz T-type phase shifter) demonstrates high phase accuracy and low insertion loss. Additionally, CNT-based RF devices enable the realization of differential negative impedance amplifiers (with gain in the Ka-band) and reconfigurable notch filters with innovative architectures. These advancements surpass traditional semiconductor solutions in terms of conversion loss, low power consumption, and mechanical flexibility, providing highly integrated solutions for flexible IoT (harmonic tags), millimeter-wave communications (6G/W-band), and intelligent phased array systems.

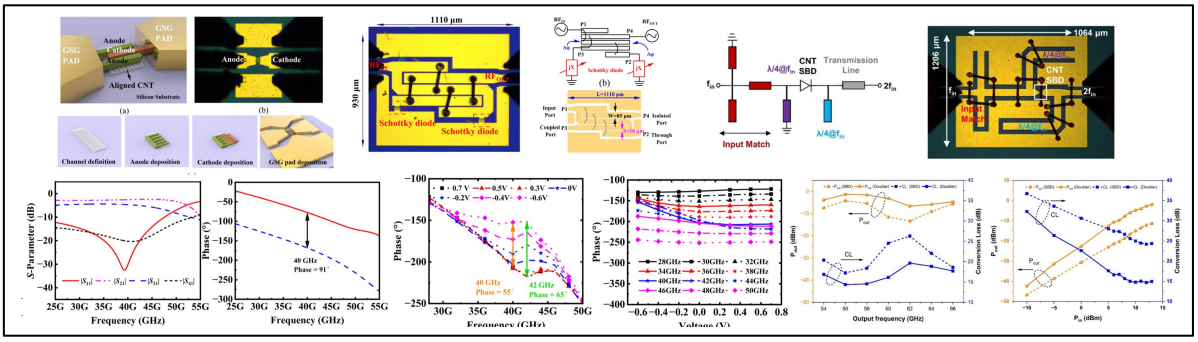

Upcycling Waste Plastics into Carbon Nanotube Wirings and Synaptic Devices for Physical Reservoir Computing

T. Ikuno[1] and K. Takanashi[1]

[1]*Tokyo University of Science (Japan)*

In recent years, marine pollution has become increasingly severe, with approximately eight million tons of plastic waste entering the ocean annually. It is projected that by 2050, the mass of plastics in the ocean will exceed that of fish. From an upcycling perspective, we aim to convert waste plastics into high-value carbon nanotubes (CNTs). Although previous studies have reported the conversion of virgin plastics into multi-walled CNTs (MWNTs) via chemical vapor deposition (CVD), the conversion efficiency (η) was low (a maximum of 4%), and only a limited range of plastic types could be used. Furthermore, the correlation between plastic types and MWNT properties has not been well understood.

In this study, we developed a novel CVD system capable of efficiently converting various types of plastic waste into MWNTs. Our method consists of three distinct regions: a plastic pyrolysis region, a metal-organic catalyst sublimation region, and an MWNT growth region. This approach offers two key advantages: a significantly higher conversion efficiency ($\eta > 50\%$) compared to previous reports and compatibility with a wider range of plastic feedstocks. Additionally, we successfully fabricated patterned CNT wirings on plastic films using upcycled MWNTs via a laser-induced transfer method [1]. Furthermore, we applied the upcycled MWNTs as synaptic devices in the physical reservoir layer for physical reservoir computing (PRC). Moreover, we demonstrated the feasibility of further upcycling plastic films with CNT wirings back into MWNTs.

In this presentation, I will introduce the details of our conversion method. Specifically, I will discuss the relationship between pyrolysis gas species—analyzed via infrared and mass spectroscopy—and the properties of the resulting MWNTs. Furthermore, I will present demonstrations of MWNT synthesis from "real" marine debris, such as fishing nets collected from beaches and inland areas, achieving a conversion efficiency of over 30%.

Reference

[1] H. Komatsu, T. Ikuno *et al. Sci. Rep*. **13** (2023) 2254.

CNTFET-Metal Contact Investigations via Voltage Controlled Material Deposition

M. Hartmann, M. Ernst, S. Böttger, S. Hermann

Center for Microtechnologies, Chemnitz University of Technology, Chemnitz, Germany

Center for Materials Architecture and Integration of Nanomembranes, Chemnitz University of Technology, Chemnitz, Germany

martin.hartmann@zfm.tu-chemnitz.de

Carbon nanotube-based (CNT) field effect transistors (FETs) with high frequency capabilities present a highly promising solution for advancing future communication electronics, due to their exceptional charge carrier mobility and low intrinsic capacitance. In 2019, it was firstly demonstrated that this technology outperforms comparable silicon-based radio frequency FETs, particularly in terms of extrinsic current gain cut-off frequencies and maximum oscillation frequencies [1]. Furthermore, in recent years, their performance has continued to improve, nearing the THz range [2,3].

However, this technology is still in its early stages, and advancements in the CNT-to-metal contacts, the device geometry, CNT alignment and density, CNT quality, as well as CNT encapsulation and doping, will further improve the high-frequency performance of CNTFETs.

In this study, we investigate the impact of various metal deposition processes on the properties of CNT layers and the performance of CNTFETs fabricated from them. While existing literature often discusses the influence of different metals on CNTFET properties [4], we have found that the deposition process itself plays a significant role as well. Specifically, we examine the effects of deposition methods, such as sputtering and electron beam deposition, along with key process parameters like the acceleration energy of metal clusters onto the CNTs. These factors are analyzed in relation to defect formation on the CNT sides and their impact on the CNTFET performance. Interestingly, the highest on-currents are not achieved with the least defective CNTs.

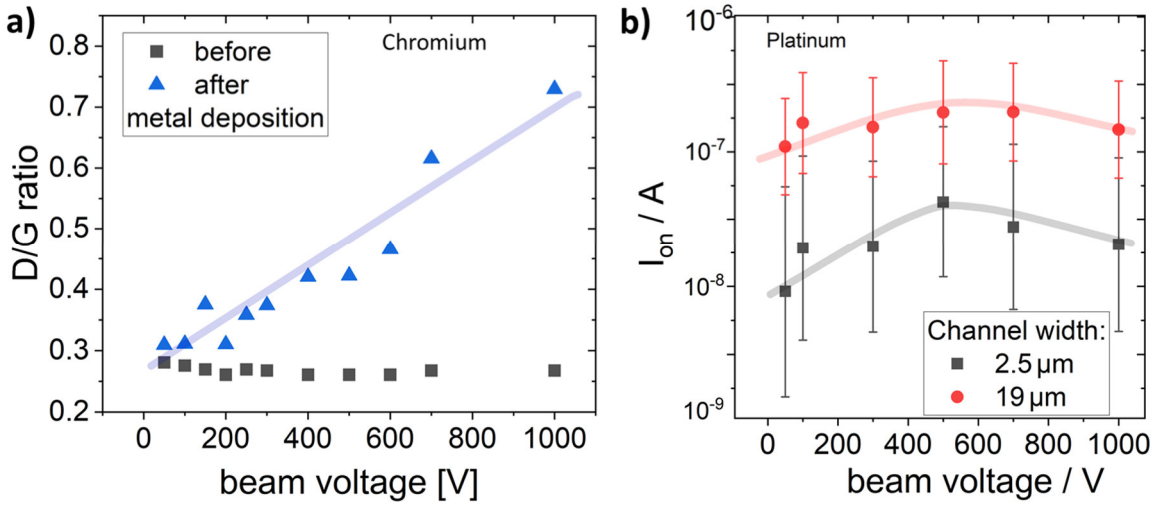

Overview of the impact of different Chromium deposition voltages on the D/G ratio extracted from Raman spectroscopy measurements of CNT layers in a) and the impact of various Platinum deposition voltages onto the on-current of CNTFETs.

References

[1] C. Rutherglen *et al.*, *Nature Electronics* **2**, 530–539 (2019).
[2] J. Zhou *et al.*, *IEEE Electron Device Letters* **44** (2), 329–332 (2023).
[3] X. Cheng. *et al.*, *Science Advances* **10** (12), 1-9 (2024).
[4] A. Fediai *et al.*, *Nanoscale*, **8**, 10240-10251 (2016).

AM I TOO FAT? CNT ASKED. DIFFERENCES IN MORPHOLOGY OF CARBON NANOTUBES FOR TRIBOLOGICAL APPLICATION

Sz. Ruczka[1,2,3], A. Marek[1,4], A. Terzyk[5], M. Skrzypek[6], Ł. Wojciechowski[6], S. Boncel[1,2,3]

1 NanoCarbon Group, Department of Organic Chemistry, Bioorganic Chemistry and Biotechnology, Silesian University of Technology, Bolesława Krzywoustego 4, 44-100 Gliwice, Poland

2 Centre for Organic and Nanohybrid Electronics (CONE), Silesian University of Technology, Stanisława Konarskiego 22B, 44-100 Gliwice, Poland

3 NanoCarbonGroup.com Ltd., Ks. Marcina Strzody 7, 44-100 Gliwice, Poland

4 Department of Chemical Organic Technology and Petrochemistry, Silesian University of Technology, Bolesława Krzywoustego 4, 44-100 Gliwice, Poland

5 Department of Materials Chemistry, Adsorption and Catalysis, Nicolaus Copernicus University in Toruń, Gagarina 7, 87-100 Toruń, Poland

6 Institute of Construction Machines and Automotive Vehicles, Poznań University of Technology, Piotrowo 3, 60-959 Poznań

Carbon nanotubes (CNTs) are studied as additives to various lubricants such as polyalphaolefins or ionic liquids. The introduction of CNTs can improve their properties such as reduction in wear and friction thus improving rheological properties [1]. Therefore, their efficiency depends on the morphology of their structure such as aspect ratio, metallic residue, no. of walls, and overall carbon purity. Within those parameters, one can tailor CNTs for targeted applications. The existing literature shows significant differences between CNTs in the case of tribological properties [2]. In this work, we focus on describing the morphology influence of CNTs on their impact on the tribological and rheological properties of IoNanoFluids (INFs). Analysis of rheological and tribological parameters of in-house synthesized high-purity MWCNTs can lead to a more reliable description of such systems. As was proven in the latest work, even a small addition of CNTs can lead to drastic changes in the rheological parameters of INFs [3]. To parametrize CNTs, we apply thermogravimetric analysis (TGA), scanning and transmission electron microscopy with energy-dispersive X-ray spectroscopy (TEM, SEM/EDX), Raman spectroscopy, and X-ray photoelectron spectroscopy (XPS). At the same time, to quantify functional characteristics IoNanoFluids we implement rheological (viscosity, shear rate and shear stress) and tribological measurements on polymer-steel (UHMWPE/steel AISI 4130) tribo-pairs, including coefficient of friction (COF).

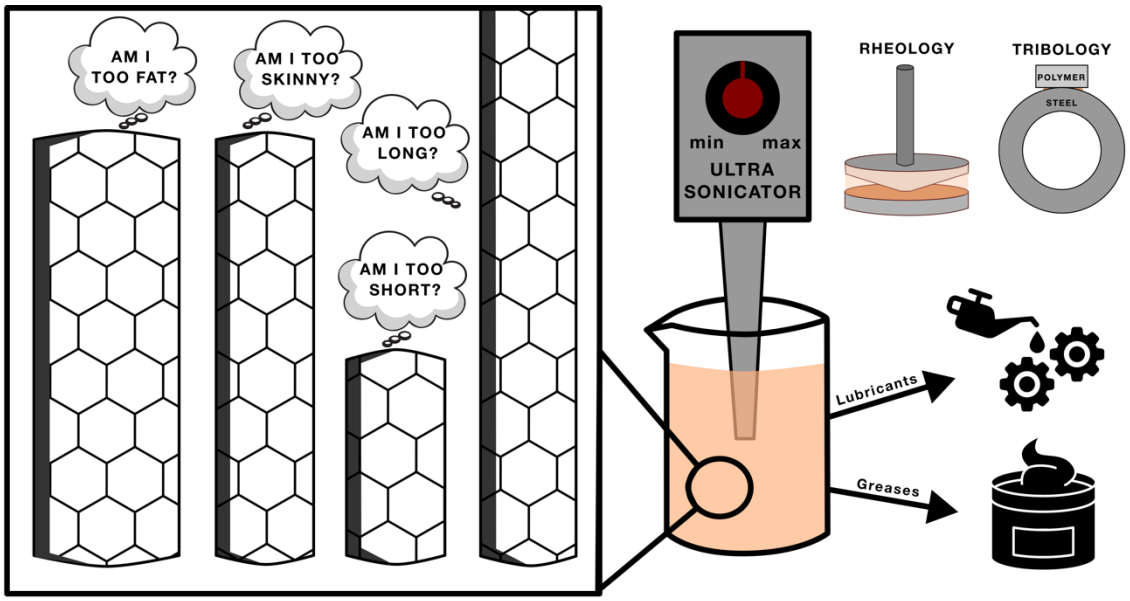

Figure 1: Various morphology of carbon nanotubes in tribological application

References

[1] N. Nyholm, N. Espallargas, *Carbon,* **201**, 1200-1228, (2023)
[2] Ł. Wojciechowski *et al.*, *Tribol. Int* **191**, 109203 (2024).
[3] S. Boncel, *J. Mol. Liq.* **391**, 1-10 (2023).

FROM DOTS TO TUBES – THE *REVERSE* SCENARIO OF BOTTOM-UP CATALYST-FREE SYNTHESIS OF *N*-DOPED CNTs

S. Boncel[1], A. Kolanowska[1,2]

[1]*Silesian University of Technology, CONE, NanoCarbon Group (Poland),* [2]*University of Silesia*

In 2004, the family of carbon nanoallotropes, with the reborn in 1991 1D carbon nanotubes (CNTs), grew to include 0D carbon quantum dots (CQDs) [1]. While intrinsically fluorescent CQDs vary in their chemical nanoarchitecture, one of their most important representatives is nanoparticles with a nanocarbon core and polar, shell O/N functionalities. In general, CQDs, as carbon nanomaterials unique *per se*, might serve as fluorescent probes, drug delivery systems, sensors, light emitters, and photocatalysts [2], but they are generally not considered as versatile substrates in the synthesis. At the same time, nitrogen-doped CNTs (*N*-CNTs), including n-doped, i.e., electron-enriched single-walled CNT semiconductors, can be applied as supercapacitors, electrodes, active 1D fillers of reinforced, thermo- and electroconductive composites, separation membranes, superhydrophobic surfaces, and sensors [3].

The synthetic interrelationships between CQDs and CNTs have been represented so far only by a top-down strategy based on progressive, oxidation-driven degradation of CNTs toward CQDs [4]. Indeed, there are no reports on the synthesis of *N*-CNTs from CQDs: only the *reverse* scenario was realized. And although the synthesis of CNTs and *N*-CNTs has been studied for more than three decades, the catalyst-free methods were elaborated almost exclusively for CNTs.

Here, we report a novel, sustainable method for the synthesis of *N*-CNTs from amino-acid-derived CQDs in the absence of an external catalyst [5]. *Yucca*-like *N*-CNTs, containing from 4 to 26 at.% of N, were comprehensively analyzed using complementary methods, such as SEM, EDX, TEM, XPS, Raman spectroscopy, and ICP-AES. The elaborated strategy enables protocols for the synthesis of novel materials applicable as, for instance, from-transparent-to-translucent electrodes, multifunctional coatings/self-standing films of enhanced electroconductivity [6], and needle-like drug delivery systems, while the above list has rather only a tentative character.

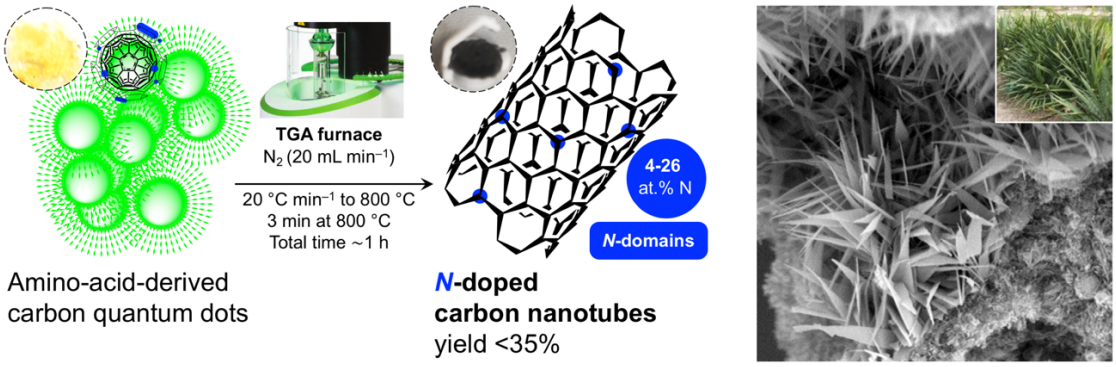

Figure: Synthesis of N-CNTs from amino-acid-derived CQDs (*left*); SEM image of *Yucca*-like N-CNTs (*right*)

Acknowledgements

The authors are very grateful for the financial support from the National Science Centre (Poland) Grant No. 2021/43/B/ST5/00421 in the framework of the OPUS-22 program.

References

[1] S. Y. Lim *et al.*, *Chem. Soc. Rev.* **44**, 362–381 (2015).
[2] A. Kolanowska *et al.*, *ACS Omega* **7**, 41165–41176 (2022).
[3] S. Boncel *et al.*, *Beilstein J. Nanotechnol.* **5**, 219–233 (2014).
[4] A. Kolanowska *et al.*, *RSC Adv.* **9**, 37608–37613 (2019).
[5] A. Kolanowska *et al.*, *Chem. Commun.* **59**, 7659–7662 (2023).
[6] S. Boncel *et al.*, *ACS Appl. Nano Mater.* **5**, 15762–15774 (2022).

Session
NT 25（The 25th International Conference on the Science and Applications of Nanotubes and Low-

| Main conference：Main conference

Thu. Jun 19, 2025 6:00 PM - 8:00 PM JST | Thu. Jun 19, 2025 9:00 AM - 11:00 AM UTC Poster 2(International Exchange Hall I&II, Clock Tower Centennial Hall, 2F)

[19psb] Poster 2

[19psb-01]

Investigation of Co Nanoparticle Formation Mechanisms on MgO and Al_2O_3 supports for Carbon Nanotube Synthesis

*Jiwoo Kim[1], Jaegeun Lee[1,2] (1. School of Chemical Engineering, Pusan National University (Korea), 2. Department of Organic Material Science and Engineering, Pusan National University (Korea))

[19psb-02]

Hybrid bismuthene hexagons by molecular interface engineering

*Gonzalo Abellán[1] (1. University of Valencia (Spain))

[19psb-03]

Carbon nano-onions: Potassium intercalation and reductive covalent functionalization

María Eugenia Pérez-Ojeda[1], Matteo Andrea Lucherelli[2], *Gonzalo Abellán[2] (1. FAU Erlangen-Nürnberg (Germany), 2. University of Valencia (Spain))

[19psb-04]

Orientation of MoS_2 Flakes Grown on Twisted Bilayer Graphene

*SHINICHIRO MOURI[1], Shun Tonegawa[1], Abdul Kuddus[2] (1. Graduate of School of Science and Engineering, Ritsumeikan University (Japan), 2. R-GIRO, Ritsumeikan University (Japan))

[19psb-05]

Growth of MoS_2 on $Al_{(1-x)}Ti_xO_y$ by Chemical Vapor Deposition

*Koshiro Kawakami[1], Syunsuke Yamamura[1], Abdul Kuddus[1], Shinichiro Mouri[1] (1. Ritsumeikan Univ. (Japan))

[19psb-06]

In situ XAFS measurements on the formation process of single-walled carbon nanotubes from Fe catalyst

*Jumpei Horiuchi[1], Shinya Mizuno[1], Takahiro Saida[1], Shigeya Naritsuka[1], Takahiro Maruyama[1] (1. Meijo Univ. (Japan))

[19psb-07]

Chirality Selective Growth of Bulk Single-walled Carbon NanotubesUsing Cobalt-sulfur Catalyst

Zihan Xu[1], *Zeyao Zhang[1,2], Yan Li[1,2] (1. Peking University (China), 2. Institute of Carbon-Based Thin Film Electronics, Peking University, Shanxi (China))

[19psb-08]

Understanding the role of molybdenum in carbon nanotube growth using layered double hydroxides

*Yeon Su Shin[1], Yoon Seo Kim[2], Seungho Cho[2,3], Jaegeun Lee[1,4] (1. School of Chemical Engineering, Pusan National University, Busan 46241 (Korea), 2. Department of Materials Science and Engineering, Ulsan National Institute of Science and Technology (UNIST), Ulsan 44919 (Korea), 3. Graduate School of Semiconductor Materials and Devices Engineering, Center

for Future Semiconductor Technology (FUST), Ulsan National Institute of Science and Technology (UNIST), Ulsan 44919 (Korea), 4. Department of Organic Material Science and Engineering, Pusan National University, Busan 46241 (Korea))

[19psb-09]

Harnessing Metal-Support Interaction in Catalytic Synthesis of Carbon Nanotubes

Chi Xu[1], *Sida Sun[1], Zeyao Zhang[1], Yan Li[1] (1. Peking University (China))

[19psb-10]

Chirality and Enantiomer Based Sorting of Single-Walled Carbon Nanotubes by PEG/Salt Aqueous Two-Phase Systems

Min Lyu[1], Cheng Li[1], *Yanzhao Liu[1], Yan Li[1,2] (1. Peking University (China), 2. Institute of Carbon-Based Thin Film Electronics, Peking University, Shanxi (China))

[19psb-11]

General Synthesis Strategy of Alloy Transition Metal Dichalcogenide Nanotubes

*Runze Lai[1], Zhen Han[1], Xinrui Zhang[1], Yan Li[1] (1. College of Chemistry and Molecular Engineering, Peking University (China))

[19psb-12]

Remote salt enabling metallic NbS_2 one-dimensional van der Waals heterostructures

*Wanyu Dai[1], Yongjia Zheng[1,2], Akihito Kumamoto[3], Yanlin Gao[4], Sijie Fu[5], Sihan Zhao[5], Ryo Kitaura[6], Esko I Kauppinen[8], Keigo Otsuka[1], Slava V Rotkin[7], Yuichi Ikuhara[3], Mina Maruyama[4], Susumu Okada[4], Rong Xiang[1,2], Shigeo Maruyama[1,2] (1. Department of Mechanical Engineering, The University of Tokyo (Japan), 2. State Key Laboratory of Fluid Power and Mechatronic System, School of Mechanical Engineering, Zhejiang University (China), 3. Institute of Engineering Innovation, The University of Tokyo (Japan), 4. Department of Physics, Graduate School of Pure and Applied Sciences, University of Tsukuba (Japan), 5. School of Physics, Zhejiang University (China), 6. Research Center for Materials Nano architectonics (MANA), National Institute for Materials Science (NIMS) (Japan), 7. Materials Research Institute and Department of Engineering Science & Mechanics The Pennsylvania State University (United States of America), 8. Department of Applied Physics, Aalto University School of Science (Finland))

[19psb-14]

Fundamental investigation of monolayer graphene modification by low-pressure Argon Plasma

*Pierre Vinchon[1], Lucas Spiske[1], Nicolas Mauchamp[1], Yoshiyuki Miyamoto[2], Satoshi Hamaguchi[1] (1. Osaka University (Japan), 2. National Institute of Advanced Industrial Science and Technology (Japan))

[19psb-15]

Development of an autonomous 2D semiconductors production system driven by Bayesian optimization

*Wataru Idehara[1], Fan Yang[1], Keisuke Shinokita[1], Kazunari Matsuda[1] (1. Institute of Advanced Energy Science, Kyoto University (Japan))

[19psb-16]

Analysis roles of Fe and Co binary catalysts in chemical vapor deposition growth of single-walled carbon nanotubes

*Qingmei Hu[1], Ya Feng[2,1], Wanyu Dai[1], Daisuke Asa[1], Daniel Hedman[3], Aina Fitó Parera[4], Yixi Yao[5], Yongjia Zheng[6,1], Kaoru Hisama[7], Christophe Bichara[8], Shohei Chiashi[1], Yan Li[5], Wim Wenseleers[4], Dmitry Levshov[4], Sofie Cambré[4], Keigo Otsuka[1], Rong Xiang[1,6], Shigeo

Maruyama[1,6] (1. The University of Tokyo (Japan), 2. Dalian University of Technology (China), 3. IBS-CMCM (Korea), 4. University of Antwerp (Belgium), 5. Peking University (China), 6. Zhejiang University (China), 7. Shinshu University (Japan), 8. Aix-Marseille University and CNRS (France))

[19psb-17]

Single-crystal Graphene Wafers: Controlled Synthesis and Mass Production

*Kaicheng Jia[1] (1. Beijing Graphene Institute (China))

[19psb-18]

HIGH-TEMPERATURE ADSORPTION OF NITROGEN DIOXIDE FOR STABLE, EFFICIENT, AND SCALABLE DOPING OF CARBON NANOTUBES

*Dmitry V. Krasnikov[1], Nikita I. Raginov[1], Anastasia E. Goldt[1], Stanislav S. Fedotov[1], Albert G. Nasibulin[1] (1. Skolkovo Institute of Science and Technology (Russia))

[19psb-19]

Synthesis of Tunable Fluorescent Carbon Dots from Dairy Whey for Advanced Cancer Nanomedicine: Bioimaging and Theranostic Applications

*Mónica L Fanarraga[1], Rafael Valiente[1], Jesús González[1], Marina Candela[1], Lorena García-Hevia[1] (1. Grupo de Nanomedicina, Universidad de Cantabria-IDIVAL (Spain))

[19psb-22]

Robust carbon nanotube composite coatings for perfect absorption in harshenvironmental applications

*Yuanhao Jin[1] (1. Tsinghua University (China))

[19psb-23]

Synthesis of Single-Walled Carbon Nanotubes/Graphene Nanoflakes Hybrid Nanostructures Utilizing Fe-Re Bimetallic Catalysts by Floating Catalyst Chemical Vapor Deposition

*Anastasios Karakasidis[1], Hirotaka Inoue[1,2], Ghulam Yasin[1], Hua Jiang[1], Esko I. Kauppinen[1] (1. Aalto University (Finland), 2. Sumitomo Electric Industries (Japan))

[19psb-24]

Magnetically Aligned All-Solid-State Ionic-Liquid Crystal Elastomer based Electrochemical Artificial Muscles

*Guang Yang[1,2] (1. University of Science and Technology of China (China), 2. Suzhou Institute of Nano-Tech and Nano-Bionics, Chinese Academy of Sciences (China))

[19psb-25]

Sequential Assembly of Low-Dimensional Materials on Arbitrary Fiber Substrates for Electromagnetic Interference Shielding

*Jiayi Liu[1,2], Quanfen Guo[1,2], Huahui Tian[2], He Hao[3], Xin Gao[1], Jin Zhang[3] (1. School of Materials Science and Engineering, Peking Univ. (China), 2. Beijing Graphene Institute (China), 3. Beijing Science and Engineering Center for Nanocarbons, Beijing National Laboratory for Molecular Sciences, College of Chemistry and Molecular Engineering, Peking Univ. (China))

[19psb-26]

Facile and scalable concentration method for surfactant-assisted carbon nanotube dispersion

*Jaegyun Im[1], Jaegeun Lee[1,2] (1. School of Chemical Engineering, Pusan National University (Korea), 2. Department of Organic Material Science and Engineering, Pusan National University (Korea))

[19psb-27]

Wet-spinning of high strength and high thermal conductivity carbon nanotube fibers

*Yuanlong Shao[1], Jin Zhang[1] (1. Peking University (China))

[19psb-28]
Exploring the Role of Sulfur Promoter from Carbon Disulfide in Carbon Nanotubes Synthesis
*Ghulam Yasin[1], Otto Salmela[1], Hirotaka Inoue[1,2], Anastasios Karakassides[1], Hua Jiang[1], Esko I. Kauppinen[1] (1. Aalto University (Finland), 2. Sumitomo Electric Industries (Japan))

[19psb-29]
Selective Semiconducting Carbon Nanotube Extraction with Cellulose Acetate
*Kazuhiro Yoshida[1], Yoshiyuki Nonoguchi[1] (1. Kyoto Institute of Technology (Japan))

[19psb-30]
Estimating key factors for self-organized, aligned CNT film formation by machine learning
*Miki Ikeda[1], Tomoyuki Miyao[2], Yoshiyuki Nonoguchi[1] (1. Kyoto Institute of Technology (Japan), 2. Nara Institute of Science and Technology (Japan))

[19psb-32]
Preparation, properties and applications of carbon nanomaterial flexible transparent conducting films
*Hong-Zhang Geng[1] (1. Tiangong University (China))

[19psb-33]
Beyond d-spacing: The critical role of defects in graphene oxide membranes
*Nima Zakeri[1], Kirill Levin[1], Marta Cerruti[1] (1. McGill University (Canada))

[19psb-34]
Structure Dependence of CNT Forests on the Lateral Memristive Resistance
*Hiroshi Furuta[1,2], Yuki Sato[1], Ryuichi Shinsei[1] (1. School of Systems Engineering, Kochi Univ. Technol. (Japan), 2. Research Inst., Kochi Univ. Technol. (Japan))

[19psb-35]
Direct identification and manipulation of valley coherence in monolayer semiconductor WSe_2
*Haonan Wang[1], Kenji Watanabe[2], Takashi Taniguchi[2], Satoru Konabe[3], Kazunari Matsuda[1] (1. Kyoto University (Japan), 2. NIMS (Japan), 3. Hosei University (Japan))

[19psb-36]
High-Density Polarization Dots in Short-Period Moiré Superlattices Enabled by Flexoelectric Effects
*Kota Tanaka[1], Hao Ou[2], Taishi Takenobu[1] (1. Nagoya University (Japan), 2. Institute of Science Tokyo (Japan))

[19psb-37]
High current density in electric double layer light-emitting devices of WSe_2 monolayers
*Koshi Oi[1], Taiga Aridome[1], Hao Ou[2], Jiang Pu[2], Takahiko Endo[3], Yasumitsu Miyata[3], Taishi Takenobu[1] (1. Department of Applied Physics, Nagoya University (Japan), 2. Department of Physics, Institute of Science Tokyo (Japan), 3. Department of Physics, Tokyo Metropolitan University (Japan))

[19psb-38]
Novel Interface Effects in Fe2O3@CNT
AAkanksha Kapoor[1], Avirup Dey[1], Sunil Nair[1], *Ashna Bajpai[1] (1. Indian Institute of science education and Research (India))

Session
NT 25（The 25th International Conference on the Science and Applications of Nanotubes and Low-

[19psb-39]

Reconfigurable nonlinear losses of nanomaterial covered waveguides

*Ayvaz Davletkhanov[1,2], Daniil Ilatovskii[3], Aram Mkrtchyan[4], Alexey Bunkov[4], Dmitry Krasnikov[4], Albert Nasibulin[4], Yuriy Gladush[4], Ralph Krupke[1,2,5] (1. Institute of Quantum Materials and Technologies, Karlsruhe Institute of Technology, 76131 Karlsruhe (Germany), 2. Institute of Materials Science, Technische Universität Darmstadt, 64827 Darmstadt (Germany), 3. Okinawa Institute of Science and Technology, 1919-1 Tancha, Onna-son, Kunigami-gun Okinawa (Japan), 4. Skolkovo Institute of Science and Technology, Moscow 121205 (Russia), 5. Institute of Nanotechnology, Karlsruhe Institute of Technology, 76131 Karlsruhe (Germany))

Investigation of Co Nanoparticle Formation Mechanisms on MgO and Al_2O_3 supports for Carbon Nanotube Synthesis

Jiwoo Kim[1], Jaegeun Lee[1,2*]

[1]*School of Chemical Engineering, Pusan National University, Busandaehak-ro 63beon-gil, Geumjeoung-gu, Busan, Republic of Korea, 46241*

[2]*Department of Organic Material Science and Engineering, Pusan National University, Busandaehak-ro 63beon-gil, Geumjeoung-gu, Busan, Republic of Korea, 46241*

As the demand for precisely tailored carbon nanotube (CNT) properties increases, the role of catalyst design becomes more critical. This study examines how support materials influence the formation of metal nanoparticles and catalytic performance in CNT synthesis. Cobalt-based catalysts supported on MgO and Al_2O_3 were prepared using the wet impregnation method. Their catalytic activity was evaluated based on CNT synthesis and crystallinity analysis using Raman spectroscopy, while X-ray diffraction (XRD), X-ray photoelectron spectroscopy (XPS), transmission electron microscopy (TEM), and temperature-programmed reduction (TPR) were utilized for catalyst characterization. As a result, the state of metal particles varied depending on the type of support due to the influence of the metal-support interaction, and solid solution played a key role in achieving a small and uniform metal distribution. Furthermore, we proposed metal particle formation mechanisms for each support and successfully synthesized SWCNTs at 750°C through MSI regulation. These findings highlight the pivotal role of support materials in CNT synthesis and offer valuable insights for optimizing catalyst design to achieve precise control over CNT production.

Acknowledgement

This work was supported by the development project for high-performance carbon nanotube composite fiber manufacturing technology (RS-2023-00258521) Ministry of Trade, Industry & Energy (MOTIE) of Republic of Korea.

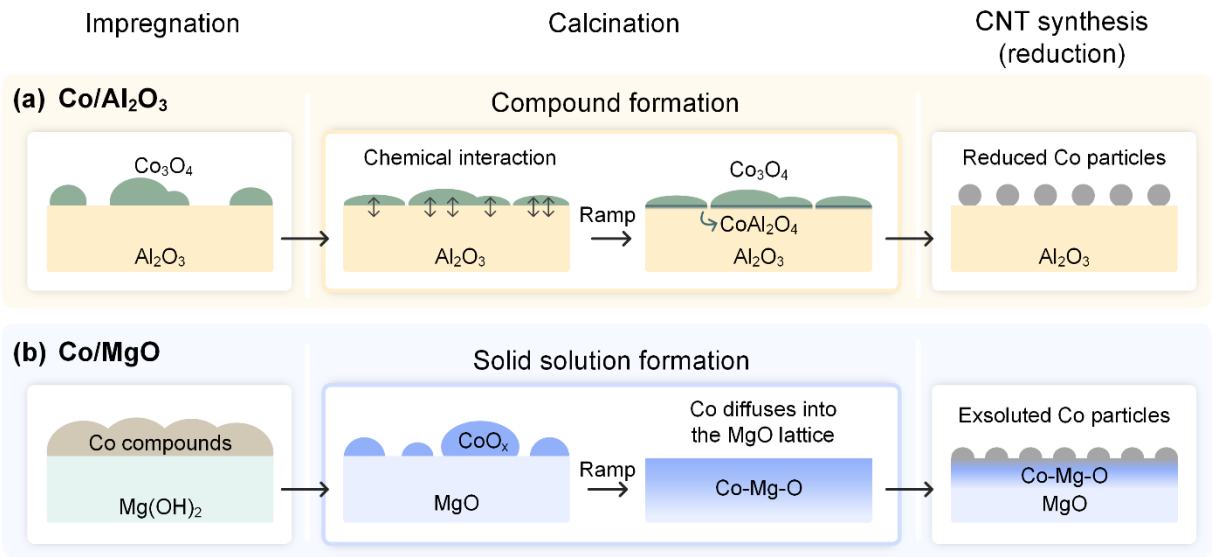

Figure caption: Fig. 1 Schematic of Co/Al_2O_3 and Co/MgO catalyst evolution for CNT growth. (a) In Co/Al_2O_3, Co forms $CoAl_2O_4$ compound during calcination and reduces to Co nanoparticles. (b) In Co/MgO, Co dissolves into MgO, forming a Co-Mg-O solid solution, with Co nanoparticles exsolving upon reduction.

Hybrid bismuthene hexagons by molecular interface engineering

G. Abellán[1]

[1]*ICMol – University of Valencia*

High-quality devices based on layered heterostructures typically require materials obtained through complex solid-state physical approaches or laborious mechanical exfoliation and transfer. Despite the ability to obtain large lateral sizes, wet-chemically synthesized 2D materials are not commonly used due to their surface residuals and intrinsic defects. Here, we introduce a new 2D member to the pnictogen family (group 15 of the Periodic Table), synthetized by a colloidal approach [1,2], that consists of a coherent sandwich of beta-bismuth, encapsulated by sulfur-alkyl-functionalized flat bismuthene interfaces [3,4]. While an unprecedented degree of structural quality is demonstrated, an altered atomic arrangement of the outermost, functionalized bismuthene layers leads to a drastic change in the chemical reactivity and band structure. Beyond electronics, this 2D hybrid material may be of interest in organic catalysis [5], biomedicine, or energy storage and conversion [2].

Our findings indicate how surface reconstructions in 2D systems can promote unexpected properties that can pave the way to new functionalities. Moreover, this scalable synthetic process opens new avenues for applications in plasmonics or electronic (and spintronic) device fabrication. In this regard, our large-scale production strategy will be introduced [6].

References

[1] Carrasco, J. A., *et al*. Chemical Society Reviews, **52**, 1288-1330 (2023).
[2] Lucherelli, M. A., *et al*. Chemical Communications, **59**, 6453-6474 (2023).
[3] Dolle, C., *et al*. Journal of the American Chemical Society, **145**, 12487-12498 (2023).
[4] Patent: WO 2023/007051
[5] Lloret, V., et al. Nature communications, **10**, 509 (2019).
[6] Torres. I., *et al*. Advanced Functional Materials, **31**, 2101616 (2021).

Carbon nano-onions: Potassium intercalation and reductive covalent functionalization

M. E. Pérez-Ojeda[1], M. A. Lucherelli[2], G. Abellán[2]

[1]FAU Erlangen-Nürnberg (Germany), [2]ICMol – University of Valencia (Spain)

Functionalization of carbon nanomaterials is a promising approach to controllably engineer the band gap structure, create novel architectures, and manipulate the interfacial characteristics of graphene and carbon nanotubes, increasing their processability [1,2].

Herein we report the synthesis of covalently functionalized carbon nano-onions (CNOs) via a reductive approach using unprecedented alkali-metal CNO intercalation compounds. For the first time, an in-situ Raman study of the controlled intercalation process with potassium has been carried out revealing a Fano resonance in highly doped CNOs. The intercalation was further confirmed by electron energy loss spectroscopy and X-ray diffraction. Moreover, the experimental results have been rationalized with DFT calculations. Covalently functionalized CNO derivatives were synthesized by using phenyl iodide and n-hexyl iodide as electrophiles in model nucleophilic substitution reactions. The functionalized CNOs were exhaustively characterized by statistical Raman spectroscopy, thermogravimetric analysis coupled with gas chromatography and mass spectrometry, dynamic light scattering, UV–vis, and ATR-FTIR spectroscopies. This work provides important insights into the understanding of the basic principles of reductive CNOs functionalization and will pave the way for the use of CNOs in a wide range of potential applications, such as energy storage, photovoltaics, or molecular electronics [3].

References

[1] Abellán, G., *et al*. Am. Chem. Soc. **139**, 5175 (2017).
[2] Schirowski, M., *et al*. J. Am. Chem. Soc. **140**, 3352 (2018).
[3] Pérez-Ojeda, M.E., *et al*. J. Am. Chem. Soc. 143, 18997 (2021).

Orientation of MoS_2 Grown on Twisted Bilayer Graphene

S. Mouri[1], S.Tonegawa[1], A. Kuddus[2]

[1] *Graduate of School of Science and Engineering, Ritsumeikan University, Shiga 525-8577, Japan*

[2] *R-GIRO, Ritsumeikan University, Shiga 525-8577, Japan*

Van der Waals epitaxy is a key technology for the integration of 2D materials, but achieving uniform orientation in large area samples remains challenging. In graphene, small potential variations in the number of layers and the underlying substrate significantly affect the crystal growth on it [1,2]. Following this analogy, the stacking angle of bilayer graphene could introduce subtle potential variations that significantly affect crystal growth. In this study, we prepared twisted bilayer graphene (tBGr) with different stacking angles on the Si_3N_4 TEM grid (EM Japan Co.) and grew MoS_2 flakes on them by CVD to investigate how the number of layers or the angle difference affects the growth. It has been reported that MoS_2 grows aligned with the orientation of the monolayer graphene [3]. This system provides a suitable experimental setup to investigate the effects of layer number and stacking angle.

The growth was carried out in a three-zone tubular furnace, using sulfur and MoO_3 as precursors along with argon gas, and the growth was carried out for 20 min at a growth temperature of 750 °C. The small triangular flakes of MoS_2 with a scale of 100 nm were grown on tBGr under this condition, as shown in the TEM image of Fig. 1(a). Figure 1(b) shows the corresponding selected area electron diffraction (SAED) pattern of the grown MoS_2 flakes. Hexagonal symmetry of the diffraction pattern was observed. The intensity of the graphene and MoS_2 spots was plotted along the circumference from the center of the hexagonal pattern as shown in Fig.1(c). The MoS_2 peaks are observed at positions corresponding to the sixfold symmetric pattern rotated by 14° in graphene, but one peak appears stronger while the other is weaker.These results indicate that MoS_2, although in small amounts, grows not only aligned with the upper graphene layer but also with the lower layer. A magnified view is shown in Fig. 1(d). The MoS_2 spots appear wider than those of graphene, reflecting the smaller flake size and strain effects. Although there is a slight misalignment of about 1-3°, the two peaks correspond well. This trend has been observed in different samples with different stacking angles, suggesting that it is a universal phenomenon. Given the experimental conditions, intercalation and backside growth are unlikely to occur. Therefore, remote epitaxy mediated by the lower graphene layer is the most plausible mechanism. In this talk we will discuss the validity of this mechanism together with a detailed analysis of the stacking angle dependence.

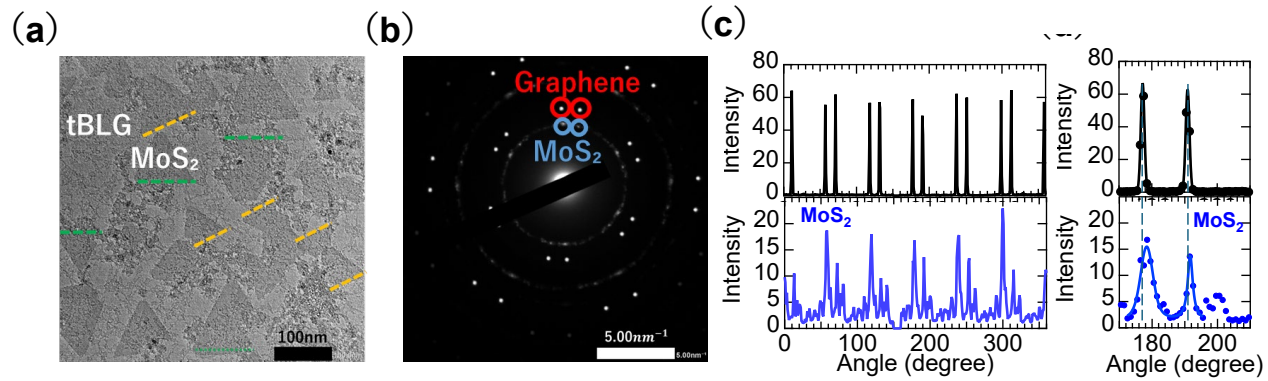

Figure1 (a) TEM image of MoS_2 flakes grown on tBLGr. (b) SAED pattern of MoS_2 flakes grown on tBLGr with a twist angle of 14°. (c) Diffraction spot intensity of graphene and MoS_2 flakes as a function of the oriented angle. (d) Magnified view of Fig. 1(c), highlighting a specific region.

References (if desired)

[1] Y. Kim, Y., Cruz, S., Lee, K. *et al., Nature* **544**, 340–343 (2017).
[2] W. Kong, H. Li, K. Qiao, *et al. Nature Mater* **17**, 999 (2018).
[3] Y. Shi *et al.*, *Nano Lett.* **12**, 2784 (2012).

This research was conducted with the support of KAKENHI (#22H05471, #21H01017, #21K18913) and the Kyoto Prefectural Technology Center for Small and Medium Enterprises.

Growth of MoS_2 on $Al_{(1-x)}Ti_xO_y$ by Chemical Vapor Deposition

◦Koshiro Kawakami[1], Syunsuke Yamamura[1], Abdul Kuddus[2], Shinichiro Mouri[1]

1 Graduate School of Science and Engineerring, Ritsumeikan University, Shiga 525-8577, Japan

2 Ritsumeikan Global Innovation Research Organization, Ritsumeikan University, Shiga 525-8577, Japan

Monolayer MoS_2 possesses outstanding properties, including high mobility, a large on-off current ratio, and a high absorption coefficient, making it a promising material for various electronic and photonic applications such as transistors, light-emitting diodes, and solar cells. In a high-κ dielectric environment, the screening of Coulomb scattering is known to enhance its mobility considerably at room temperature.[1] However, identifying a suitable high-κ dielectric material free of minor metals remains a major challenge for industrial applications. $Al_{(1-x)}Ti_xO_y$ is considered a potential candidate for use as a high-κ gate material in transition metal dichalcogenide-based devices.[2]

Therefore, in this work, we investigated the growth of MoS_2 on $Al_{(1-x)}Ti_xO_y$ using chemical vapor deposition (CVD). $Al_{(1-x)}Ti_xO_y$ was prepared on the P^+-Si substrate by mist CVD method. The Al/Ti ratio in the precursor solution for mist CVD was set to 7:3. MoS_2 was then grown on $Al_{(1-x)}Ti_xO_y$ /P^+-Si substrate using CVD method. 600mg of S powder and 35mg of MoO_3 powder were used as precursors, and Ar gas was used as carrier gas. The growth time and temperature were 30 min and 750°C, respectively.

Fig1.a shows an optical microscope image of MoS_2 growth on high-k $Al_{(1-x)}Ti_xO_y$ substrate. Fig1.b shows the Raman spectrum of it before and after growth. The characteristics out-of plane A_{1g} peak at 406 cm^{-1} and the in-plane E^1_{2g} peak at 385 cm^{-1} indicate the successful growth of MoS_2. Fig. 1c depicts the peak interval between the E^1_{2g} and A_{1g} modes against location on the surface measured at equal intervals from the top to the bottom of the substrate marked with an X in Fig. 1a. The peaks spacing is around 21 cm^{-1} at the most locations, indicating that a nearly uniform bilayer MoS_2 have grown over a scale of several millimeters in most locations, with single layer in edge regions. In the presentation, we will also discuss the PL properties and FET performance using this direct growth ultrathin MoS_2 films.

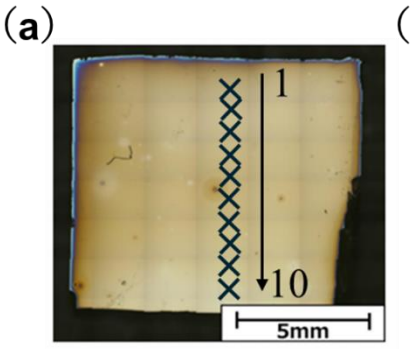

Fig1.(a): Optical microscope image of MoS_2 film grown on high-k substrate $Al_{(1-x)}Ti_xO_y$

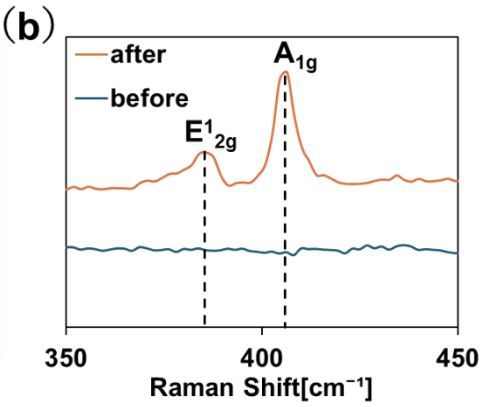

Fig1.(b): Raman spectra before and after MoS_2 growth on a high-k substrate $Al_{(1-x)}Ti_xO_y$

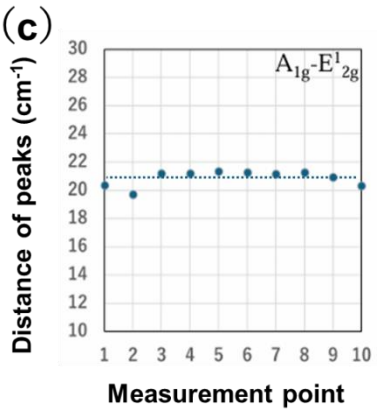

Fig1.(c): Plots of the peak distance between the A_{1g} and E^1_{2g} modes in the Raman signal at different positions of the grown MoS_2 film

References

[1] P. Xia et al., Sci. Rep.**7**,40669(2017).

[2] K. Yokoyama et al., ACS Appl. Electron. Mater. **4**, 2516–2524 (2022).

Corresponding Author: Koshiro Kawakami E-mail: re0152sr@ed.ritsumei.ac.jp

This work was supported by JSPS KAKENHI grant number 22H05471, 21H01017, 21K18913.

In situ XAFS measurements on the formation process of single-walled carbon nanotubes from Fe catalyst

J. Horiuchi[1], S. Mizuno[1], T. Saida[1,2], S. Naritsuka[3], T. Maruyama[1,2]

[1]*Department of Applied Chemistry, Meijo University (Nagoya, Japan)*

[2] *Nanomaterial Research Center, Meijo University (Nagoya, Japan)*

[3]*Department of Materials Science and Engineering, Meijo University (Nagoya, Japan)*

Single-walled carbon nanotubes (SWCNTs) are nanomaterials that are expected for applications in the electronics field. However, the formation mechanism of SWCNTs has not been clarified sufficiently, which hinders the practical use. To clarify it, in situ analysis during SWCNT growth is essential. In this study, we focused on X-ray absorption fine structure (XAFS) measurements, which enable analysis of the neighboring elements around the target one even under high pressure and high temperature [1-3]. We aimed to clarify the SWCNT growth process by analyzing the chemical state of the Fe catalyst during SWCNT growth using in situ XAFS measurements.

Iron nitrate nonahydrate, alumina slurry, and purified water were mixed and sintered to obtain powders where Fe nanoparticles were deposited on Al_2O_3 micropowders. Then, they were molded into a pellet to use as a sample for XAFS measurements. After the sample was placed in a CVD reactor, carrier gas (Ar/H_2) was introduced and the temperature was raised to 800 °C. Then, the supply of Ar/H_2 was stopped, and N_2/C_2H_2 (1000 sccm) was supplied to grow SWCNTs for 10 min. Fe K edge XAFS spectra were taken every minute during the temperature rise and SWCNT growth. The XAFS measurements were performed at beamline BL11S2 of Aichi SR. After in situ XAFS analysis, the samples were characterized using Raman, SEM, TEM and XRD.

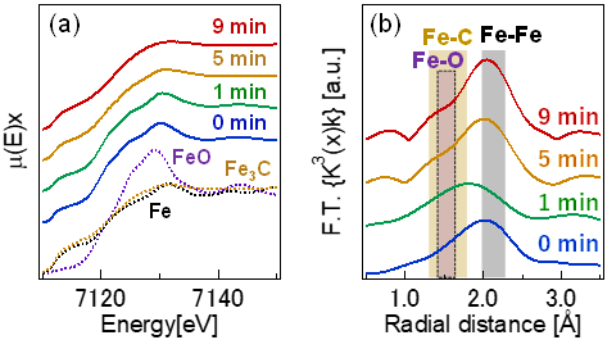

Fig.1 (a) XANES and (b) RSF during CNT growth using Ar/H_2.

Raman spectroscopy, SEM, and TEM observations showed that SWCNTs were grown during in situ XAFS measurements. Figure 1(a) and (b) shows XANES spectra and RSFs during SWCNT growth. Upon heating under Ar/H_2 supply, a mixture of FeO and metallic Fe was formed just before the start of SWCNT growth (0 min). After C_2H_2 supply, Fe catalysts were partially carbonized, but the composition of Fe-Fe bonds increased as the growth proceeded. XRD results showed formation of Fe_3C during SWCNT growth, suggesting that SWCNTs were grown from Fe_3C particles. We will also discuss the effect of carrier gases containing O_2 on SWCNT growth.

This work was partially supported by KAKENHI (B) 19H02563 and Meijo University Nanomaterial Research Center. TEM analysis was conducted in Institute for Molecular Science (IMS), supported by ARIM of the MEXT.

References (if desired)

[1] S. Karasawa *et al.*, *Chem. Phys. Lett.* **804**, 139889 (2022).
[2] S. Karasawa *et al.*, *Chem. Phys. Lett.* **808**, 140135 (2022).
[3] S. Karasawa *et al.*, *Jpn. J. Appl. Phys.* **62**, SG1036 (2023).

Chirality Selective Growth of Bulk Single-walled Carbon Nanotubes Using Cobalt-sulfur Catalyst

Zihan Xu[1], Zeyao Zhang[1, 2, *], Yan Li[1, 2, *]

[1]*College of Chemistry and Molecular Engineering, Peking University (China),*

[2]*Institute of Carbon-Based Thin Film Electronics, Peking University (China)*

High-performance carbon-based electronics require single-walled carbon nanotubes (SWCNTs) with extremely high semiconducting purity and similar band gaps. The combination of chirality-controlled growth of bulk SWCNTs and selective extraction by conjugated polymer is currently the most promising way to prepare materials that meet these requirements.

Yuan Chen et al reported a method for selective growth of (9,8)-enriched SWCNTs using $CoSO_4$ as the catalyst precursor and SiO_2 as the catalyst support.[1] Here, Co precursor together with sulfate additive were loaded on MgO by co-precipitation combining impregnation. (6,5) and (9,8)-enriched SWCNTs were grown using such catalyst, where (6,5) and (9,8) accounted for 28% and 30%, respectively, by absorption spectrum. The diameter distribution corresponding to TEM images was consistent with the chirality distribution obtained from absorption spectrum. Due to the significant difference in diameter, (6,5) and (9,8) could be easily separated. Therefore, our SWCNTs are promising for the preparation of high-purity (9,8) dispersions, whose diameter (1.17 nm) meets the requirement for high-performance electronic devices.

We studied the effect of several factors on the chirality distribution, including the growth temperature, the reduction temperature, the carbon source, and the catalyst support. When using CO as the carbon source, increasing the growth temperature from 740 °C to 860 °C or increasing the reduction temperature from 540 °C to 820 °C both led to a shift in the chirality distribution toward SWCNTs of smaller diameters. At higher temperatures, more subsurface cobalt species may be reduced by CO or H_2 to form smaller cobalt nanoparticles, thereby catalyzing the growth of SWCNTs with smaller diameters. It is noteworthy that under higher reduction temperatures, sulfur loss in the form of H_2S may increase, so that fewer Co nanoparticles with relatively large diameters were formed through Co_9S_8 intermediates, which may cause the chirality distribution to further move toward SWCNTs with smaller diameters.

Compared with CO, when using CH_4 as the carbon source, the chirality distribution became much wider. When SiO_2 was used as the catalyst support instead of MgO, the enriched chirality was only (9,8). The difference in chirality distribution is likely to be caused by different alkalinity of MgO versus SiO_2.

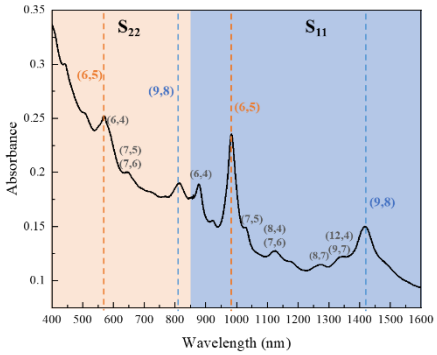

Figure 1: UV-vis absorption spectroscopy of dispersion of SWCNTs grew under optimized condition with Co-S precursor system loaded on MgO**.**

References

[1] H. Wang *et al*., ACS Nano **7(1)**, 614–626 (2013).

Understanding the role of molybdenum in carbon nanotube growth using layered double hydroxides

Yeon Su Shin[1,‡], Yoon Seo Kim[2,‡], Seungho Cho[2,3,*], and Jaegeun Lee[1,4,*]

[1] *School of Chemical Engineering, Pusan National University, Busan 46241 (Republic of Korea),*
[2] *Department of Materials Science and Engineering, Ulsan National Institute of Science and Technology (UNIST), Ulsan 44919 (Republic of Korea),*
[3] *Graduate School of Semiconductor Materials and Devices Engineering, Center for Future Semiconductor Technology (FUST), Ulsan National Institute of Science and Technology (UNIST), Ulsan 44919, (Republic of Korea),*
[4] *Department of Organic Material Science and Engineering, Pusan National University, Busan 46241, (Republic of Korea),*

‡ *These authors equally contributed to the work.*
* *Corresponding authors: scho@unist.ac.kr (Seungho Cho), jglee@pusan.ac.kr (Jaegeun Lee)*

The role of molybdenum (Mo) in carbon nanotube (CNT) synthesis catalysts has been widely reported [1-3] . However, conventional catalyst preparation methods often result in non-uniform metal ion distribution, making it challenging to determine Mo's intrinsic role. To accurately elucidate Mo's function, a catalytic system with uniformly dispersed components is essential. Layered double hydroxides (LDHs), a type of clay with tunable metal compositions and homogeneously distributed metal ions at the atomic scale, offer a promising alternative for controlled catalyst design [4,5]. In this study, CoMgAl LDHs with varying Mo content were synthesized to investigate Mo's role in CNT growth. X-ray diffraction (XRD) and X-ray photoelectron spectroscopy (XPS) analyses revealed that Mo_2C forms beyond a specific Mo threshold, significantly enhancing CNT yield. Mo_2C acts as a carbon reservoir, stabilizing Co particles and preventing deactivation. Our findings demonstrate that Mo_2C formation is essential for optimizing CNT growth, providing a deeper mechanistic understanding of Mo's catalytic function. Further studies using Fe and Fe-Co LDH systems confirmed that Mo's role can be extended to complex and diverse multimetallic catalyst systems. This study highlights the advantages of Mo-LDH catalysts for achieving high-yield CNT synthesis and offers valuable insights into multimetallic catalyst design.

Acknowledgement

This work was supported by the development project for high-performance carbon nanotube composite fiber manufacturing technology (RS-2023-00258521) Ministry of Trade, Industry & Energy (MOTIE) of Republic of Korea.

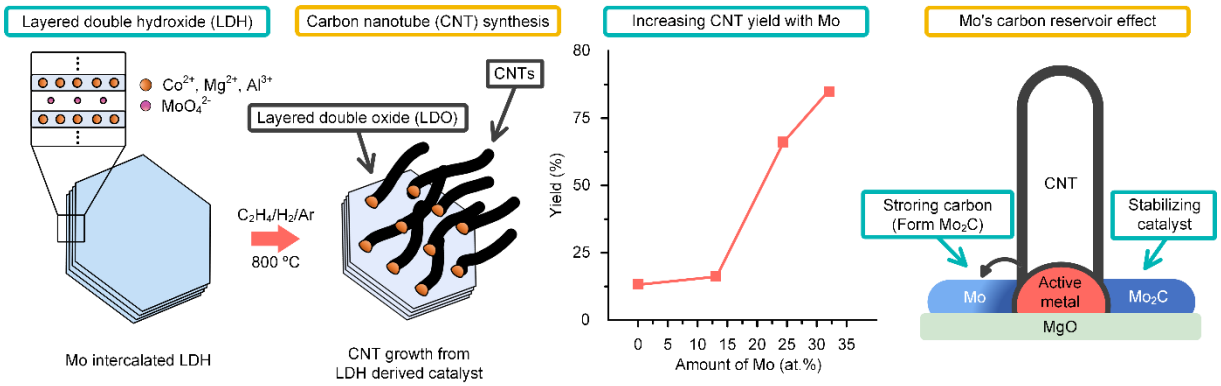

Figure 1: Research flow of finding Mo's intrinsic role via LDH as catalyst precursor.

References (if desired)

[1] W.E. Alvarez *et al*, Carbon 39.4 (2001): 547-558.
[2] X. Xu *et al*, Mater Chem Phys 127 (2011) 379–384.
[3] P. Dubey *et al*, Carbon Letters 13 (2012) 99–108.
[4] J.H. Lee *et al*, Nano Lett 24 (2024) 9322–9330.
[5] K.Y. Kim *et al*, ACS Catalysis 14 (2024) 7020–7031.

Harnessing Metal-Support Interaction in Catalytic Synthesis of Carbon Nanotubes

Chi Xu, Sida Sun, Zeyao Zhang*, Yan Li*

College of Chemistry and Molecular Engineering, Peking University (China),

Abstract

Carbon nanotubes (CNTs) possess unique properties, depending on their wall numbers and diameters. Catalysts play important roles in CNT synthesis. Previous studies have shown that by manipulating the composition and size of catalysts and reaction condition, multi-/few-/single-walled CNTs (MWCNTs/FWCNTs/SWCNTs) can be facilely synthesized by chemical vapor deposition. However, there are few reports about the effect of catalyst supports on CNT growth. Herein, we found that the addition of Al into MgO supports resulted in the decrease in the wall numbers and diameters of grown CNTs. It was observed that the Al species are well dispersed in the MgO matrix and the crystallinity of MgO is deceased. XPS and H_2-TPR characterization indicate that Al can enhance the metal-support interaction, thus generating smaller metal nanoparticles after reduction and preventing their aggregation during the high temperature process, and eventually resulting in the formation of SWCNTs and FWCNTs. Our results show the important influence of metal-catalyst support on the catalytic growth of CNTs.

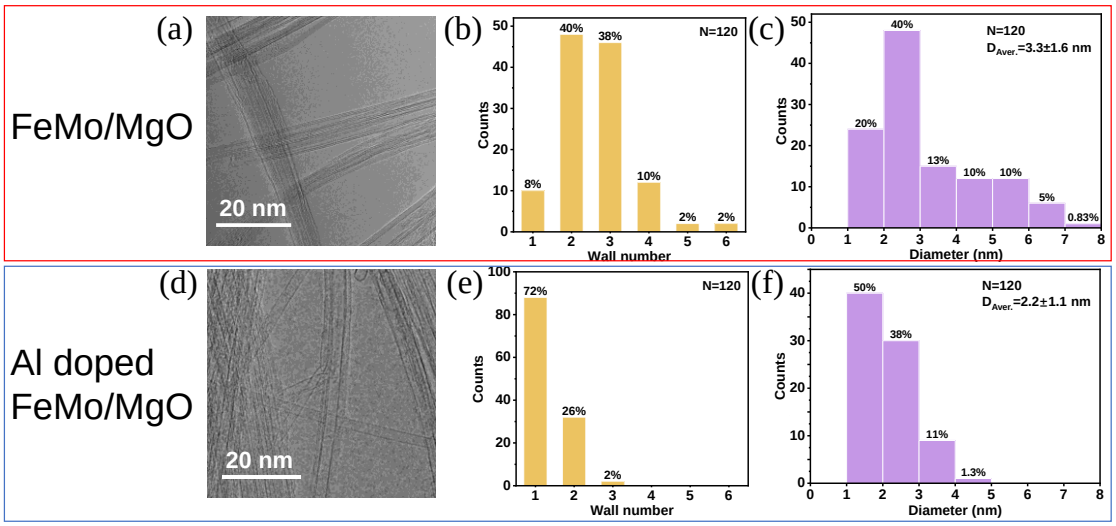

(a, d) HRTEM images, distribution of (b, e) wall numbers and (c, f) diameters of CNTs grown on (a-c) $Fe_{0.4}Mo_{0.1}/Mg_{30}O$ and (d-f) $Fe_{0.4}Mo_{0.1}/Mg_{25}Al_5O$, respectively.

Chirality and Enantiomer Based Sorting of Single-Walled Carbon Nanotubes by PEG/Salt Aqueous Two-Phase Systems

Min Lyu[1], Cheng Li[1], Yanzhao Liu[1], Yan Li[1,2]

[1]*Beijing National Laboratory for Molecular Science, Key Laboratory for the Physics and Chemistry of Nanodevices, College of Chemistry and Molecular Engineering, Peking University, Beijing, China*
[2]*Institute of Carbon-Based Thin Film Electronics, Peking University, Shanxi, Taiyuan, China*

Abstract: Aqueous two-phase extraction (ATPE) is very effective for the sorting of single-walled carbon nanotubes (SWCNTs).[1] DNA has been proven to wrap and disperse SWCNTs in a stable and efficient manner and specific DNA sequences are able to recognize SWCNTs of certain chirality.[2] Here we report that the PEG/salt ATP systems could be used to realize chirality and enantiomer sorting of SWCNTs. The partition of DNA-SWCNTs was significantly affected by the type of phase-forming salt, especially the cation of the salt. The order of cations from largest to smallest trend for DNA-SWCNT distributed in the top phase is: NH_4^+ > K^+ > Li^+ > Na^+. By controlling the cation composition in the system, we were able to obtain single-chirality (6,5) and (8,3) SWCNTs from the top phase in a single step. By multistage extraction or changing the salt composition of the system, another (6,5) enantiomer can also be purified from the bottom phase without using extra modulating agent.

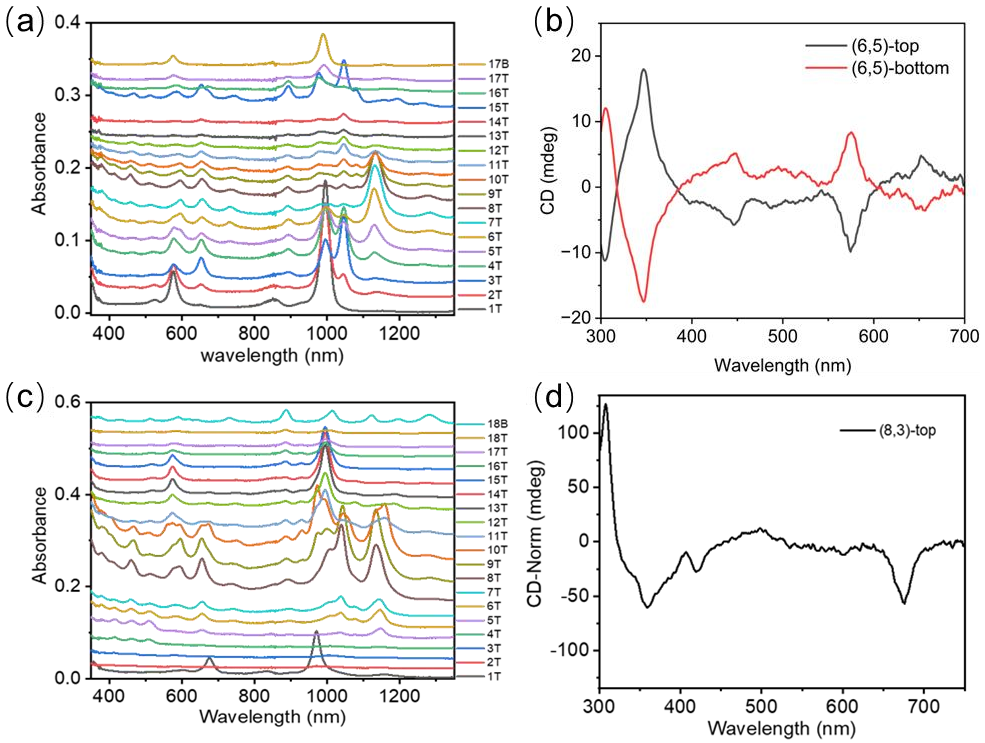

Figure caption: (a) Absorbance spectra of each fraction obtained during the sorting of TTA TAT TAT ATT-SG65i (65ss-SG65i) in PEG6k/salt ATP system. (b) Circular dichroism spectra of (6,5) species. (c) Absorbance spectra of each fraction obtained during the sorting of TTT CCC TTT CCC CCC-SG65i (83ss-SG65i) in PEG6k/salt ATP system. (d) Circular dichroism spectra of (8,3) species.

References

[1] Khripin. C. Y, Fagan. J. A, Zheng. M, *J. Am. Chem. Soc*. **135**, 6822–6825 (2013).
[2] Zheng. M *et al*, *Nature Mater* **2**, 338–342 (2003).

General Synthesis Strategy of Alloy Transition Metal Dichalcogenide Nanotubes

Runze Lai[1], Zhen Han[1], Xinrui Zhang[1], Yan Li[1*]

[1]*College of Chemistry and Molecular Engineering, Peking University, Beijing, (China)*

One-dimensional transition metal dichalcogenide nanotubes (TMDNTs) with structural and chemical diversity offer an exceptional platform for investigating electronic and optical properties. [1,2] Despite the successful synthesis of various TMDNTs, [3,4] this class of materials continues to present abundant opportunities for exploring novel chemical compositions and topological structures. In this study, we introduce a general synthesis strategy for TMDNTs using multi-walled carbon nanotube (MWCNT) templates. By selecting appropriate precursors, we successfully synthesized monometallic dichalcogenide nanotubes such as MoS_2NT, WS_2NT, and $ReSe_2$NT, as well as alloyed metal dichalcogenide nanotubes, including (MoW)S_2NT, （MoWRe)S_2NT, and (MoWRe)Se_2NT. Transmission electron microscopy (TEM) characterization revealed the high crystallinity of the TMDNTs. Energy dispersive spectrometer (EDS) mapping confirmed the uniform distribution of metal elements within the nanotubes, thereby verifying their alloy characteristics. This study enriches the compositional diversity of TMDNTs and provides a material foundation for exploring the relationship between chemical composition and material properties.

References

[1] J. Guo, R. Xiang, T. Cheng *et al*., *ACS Nanosci. Au*, **2**, 3–11 (2022).
[2] R. Xiang, S. Maruyama, Y. Li, *Natl. Sci. Open*, **1**, 20220016 (2022).
[3] R. Xiang, T. Inoue, Y. Zheng, *et al*., *Science* **367**, 537–542 (2020).
[4] Y. Nakanishi, S. Furusawa, Y. Sato, *et al*., *Adv. Mater.*, **23**, 2306631 (2023)

Remote salt enabling metallic NbS_2 one-dimensional van der Waals heterostructures

Wanyu Dai[1], Yongjia Zheng[2], Akihito Kumamoto[3], Yanlin Gao[4], Sijie Fu[5], Sihan Zhao[5], Ryo Kitaura[6], Esko I. Kauppinen[8], Keigo Otsuka[1], Slava V. Rotkin[7], Yuichi Ikuhara[3], Mina Maruyama[4], Susumu Okada[4], Rong Xiang[2*], Shigeo Maruyama[1,2*]

[1]Department of Mechanical Engineering, The University of Tokyo (Japan), [2]State Key Laboratory of Fluid Power and Mechatronic System, School of Mechanical Engineering, Zhejiang University (China), [3]Institute of Engineering Innovation, The University of Tokyo(Japan), [4]Department of Physics, Graduate School of Pure and Applied Sciences, University of Tsukuba (Japan), [5]School of Physics, Zhejiang University (China), [6]Research Center for Materials Nano architectonics (MANA), National Institute for Materials Science (NIMS) (Japan), [7]Materials Research Institute and Department of Engineering Science & Mechanics The Pennsylvania State University (The United States), [8]Department of Applied Physics, Aalto University School of Science (Finland)

The first experimental realization of one-dimensional (1D) van der Waals (vdW) heterostructures which include single-walled carbon nanotubes (SWCNTs), boron nitride nanotubes (BNNTs), and molybdenum disulfide nanotubes (MoS_2NTs) was demonstrated in 2020, indicating the great potential of acquiring 1D forms of candidate materials from 2D vdW heterostructures [1-3]. As MoS_2/WS_2 nanotubes behaved as semiconducting, BNNT being insulating, introducing metallic materials into the 1D vdW heterostructures would be of great research interest for potential device applications of 1D vdW heterostructures.

In this work, by employing a "remote salt" strategy, precise control over NaCl supply was achieved, enabling the growth of high-quality coaxial NbS_2 nanotubes on SWCNT-BNNT templates. Structural characterization via high-resolution transmission electron microscopy (HRTEM) and scanning transmission electron microscopy (STEM) confirms the formation of crystalline NbS_2 nanotubes, revealing a distinct bi-layer preference compared to monolayer-dominated semiconducting TMDCs analogs. With Raman analysis, oxidation studies demonstrate relative higher degradation rate of 1D NbS_2 under ambient conditions. Density functional theory (DFT) calculations with a mechanical stability model further elucidate the stabilization mechanism of bi-layer NbS_2 nanotubes, emphasizing interlayer charge transfer and Coulomb interactions. This work establishes a robust framework for synthesizing metallic 1D vdW heterostructures, advancing their potential applications in optoelectronics and nanodevices.

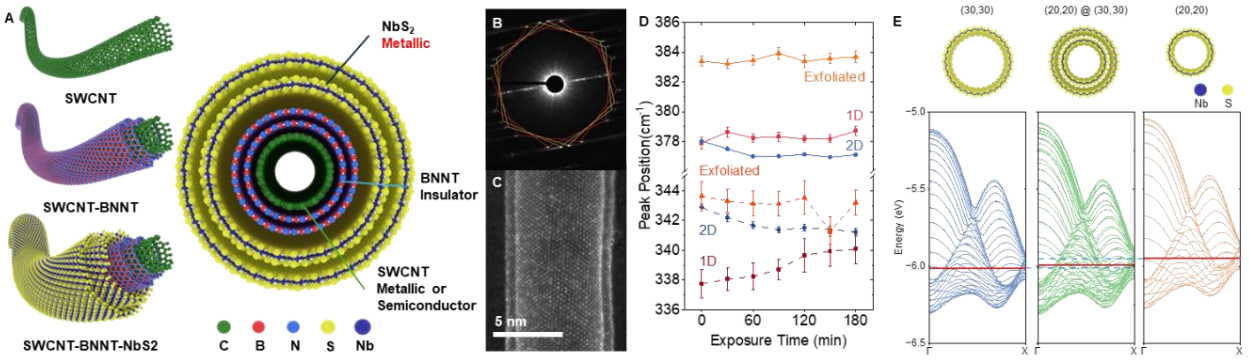

Figure 1(A) Scheme of SWCNT-BNNT-NbS_2NT. (B) Electron diffraction pattern of bilayer NbS_2 nanotubes @ SWCNT-BNNT, (C) STEM image of bilayer NbS_2 nanotubes @ SWCNT-BNNT, (D) Raman peak shift of NbS_2 when exposed in the atmosphere. (E) The electronic energy bands near the Fermi level of (30,30), (20,20) @ (30,30), and (20,20) nanotubes. The energies are measured from the vacuum level. The red horizontal line in each panel indicates the Fermi level energy.

References

[1] R. Xiang, *et al.*, Science, **367**, 537 (2020).
[2] Y. Zheng, *et al.*, PNAS, **118**, e2107295118 (2021).
[3] S. Cambre, *et al.*, Small, **17**, 2102585 (2021)

Fundamental investigation of monolayer graphene modification by low-pressure Argon Plasma

P. Vinchon[1], L. Spiske[1], N. Mauchamp[1],Y. Miyamoto[2], S. Hamaguchi[1]

[1]*Division of Materials and Manufacturing Science, Graduate School of Engineering, Osaka University, 2-1 Yamadaoka, Suita, Osaka 565-0871, Japan,*
[2]*National Institute of Advanced Industrial Science and Technology (AIST) 1-1-1 Umezono, Tsukuba, Ibaraki 305-8560 Japan*
vinchon@ppl.eng.osaka-u.ac.jp

Low-pressure plasma plays a central role in the ever-decrease in semiconductor device dimensions as they allow material etching and deposition at the nanometer scale. As 2D materials are considered for semiconductor devices, the precise understanding of plasma-surface interactions becomes crucial. Upon contact with the sample, plasma excited species generate out-of-equilibrium phenomena on surfaces, of which influences are difficult to quantify. This leads to defect generation which can strongly affect the final devices' performance and lifetime.

In monolayer graphene, a strict energy threshold at 18-22 eV has been established for defect generation both experimentally and theoretically [1]. However, it has been shown that low-pressure Ar plasma with low-energy ions (<15 eV) can generate defects in graphene [2]. Ion neutralization on the surface is expected to happen at a similar timescale as ion impact, providing a significant amount of potential energy to the surface that might contribute to defect generation. Even though classical Molecular Dynamics (MD) simulation is limited to the observation of neutral atoms, it can provide significant insight into defect generation dynamics. However, to properly study the real-time dynamics of ion neutralization, it is necessary to look at electron dynamics coupled to the MD simulation. First-principal calculations such as Time-Dependent Density Functional Theory (TD-DFT) allow us to look at the fundamental mechanisms at play.

When defects are generated by sub-threshold ions impact, the released carbon adatoms remain on the surface. Their diffusion on the surface provokes significant defect healing at room temperature. [3,4]. Furthermore, plasma generates a large amount of Argon Metastable (Ar*) which influences 2D material is scarcely understood. Experiments show that defective graphene exposure to Ar* leads to a significant decrease in defect concentration. From those results, Ar* may provide a new way to tune defect density in monolayer graphene. More generally, a precise understanding of plasma-surface interactions would enable the use of plasma-excited species for 2D materials modification or synthesis.

References

[1] F. Banhart, J. Kotakoski, A.V. Krasheninnikov, Structural Defects in Graphene, ACS Nano 5 (2011) 26–41..
[2] P. Vinchon, X. Glad, G. Robert-Bigras, R. Martel, A. Sarkissian, L. Stafford, A combination of plasma diagnostics and Raman spectroscopy to examine plasma-graphene interactions in low-pressure argon radiofrequency plasmas, Journal of Applied Physics 126 (2019) 233302.
[3] P. Vinchon, X. Glad, G. Robert Bigras, R. Martel, L. Stafford, Preferential self-healing at grain boundaries in plasma-treated graphene, Nat. Mater. 20 (2021) 49–54.
[4] P. Vinchon, S. Hamaguchi, S. Roorda, F. Schiettekatte, L. Stafford, Self-healing kinetics in monolayer graphene following very low energy ion irradiation, Carbon 233 (2025) 119852.

Development of an autonomous 2D semiconductors production system driven by Bayesian optimization

W. Idehara, F. Yang, K. Shinokita, K. Matsuda

Institute of Advanced Energy, Kyoto University, Uji 611-0011 (Japan)

In recent years, the rapid advancement of artificial intelligence (AI) technologies, including machine learning, has brought a new paradigm to fundamental physics research. In particular, researchers utilizing AI technologies such as deep learning and large language models have achieved innovative results in the field of two-dimensional semiconductor materials and their artificial van der Waals (vdW) heterostructures [1]. In the fabrication of artificial vdW heterostructures, the efficient production of high-quality 2D semiconductor monolayers with areas exceeding 100 μm² using mechanical exfoliation methods with bulk single crystals and exfoliation tape is one of the key technical challenges in this research field. However, the mechanical exfoliation method remains a complex process involving numerous microscopic parameters and strongly depends on researchers' experience. In particular, establishing reproducibility and optimal experimental conditions for large-area monolayer production is widely recognized as a fundamental challenge [2].

In this study, we developed an autonomous robotic system that systematically performs all processes from the production to detection of two-dimensional semiconductor monolayers [3]. Furthermore, by implementing a Bayesian optimization algorithm in this system to sequentially update experimental parameters, we identified optimal experimental parameters for high-quality and large-area monolayer WSe_2 with only 2.5% of the total experimental conditions. Figure 1(a) shows a histogram of the number and area of produced WSe_2 monolayers, and Figure 1(b) shows how the maximization index (LEAP) in the Bayesian optimization algorithm is updated with each experiment. LEAP is an indicator of how efficiently large-area monolayers exceeding 100 μm² are produced. Under optimized conditions, we achieved a 40% probability for producing large-area monolayer WSe_2 exceeding 100 μm² for monolayers larger than 10 μm². Furthermore, systematic analysis of experimental data revealed the dominant parameters in the production of large-area monolayer WSe_2. This approach not only advances the reproducible production of 2D semiconductor materials but also demonstrates the potential of AI-driven experimental optimization in materials science.

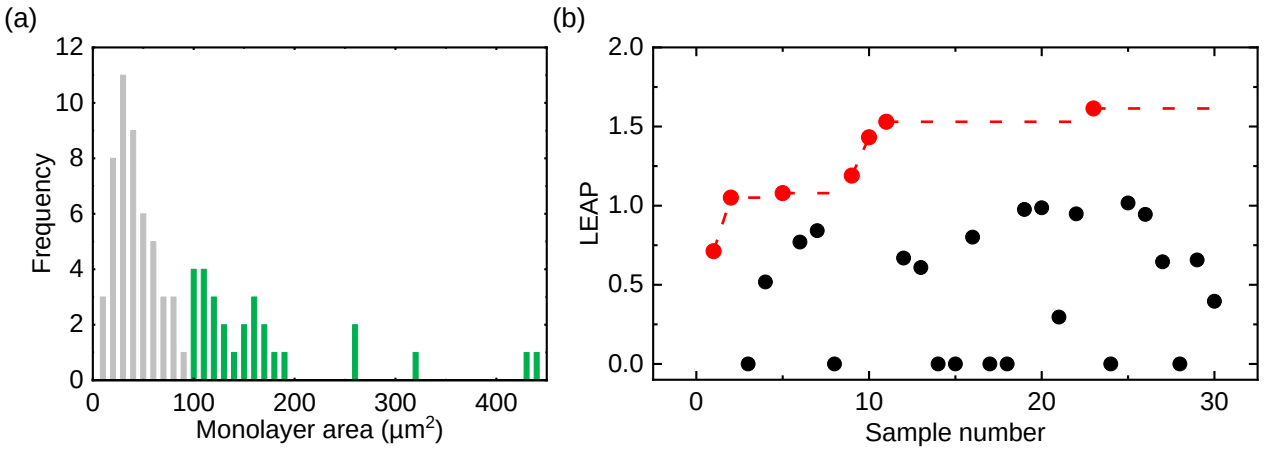

Figure. 1 (a) Histogram showing the number and area of monolayers. The histogram represents monolayers produced under optimized conditions. (b) Update of the maximization index (LEAP) with each experiment (red dotted line).

References (if desired)

[1] R. Rampi *et al.*, *npj Comput. Mater.* **3**, 54 (2017)
[2] E. Gao *et al.*, *J. Mech. Phys. Solids.* **115**, 248 (2018)
[3] F. Yang, W. Idehara, *et al.*, arXiv. *2411.06891* (2024)

Analysis roles of Fe and Co binary catalysts in chemical vapor deposition growth of single-walled carbon nanotubes

Qingmei Hu[1], Ya Feng[1,2*], Wanyu Dai[1], Daisuke Asa[1], Daniel Hedman[3], Aina Fitó Parera[4], Yixi Yao[5], Yongjia Zheng[1,6], Kaoru Hisama[7], Christophe Bichara[8], Shohei Chiashi[1], Yan Li[5], Wim Wenseleers[4], Dmitry Levshov[4], Sofie Cambré[4], Keigo Otsuka[1], Rong Xiang[1,6], Shigeo Maruyama[1,6*]

[1] *Department of Mechanical Engineering, The University of Tokyo, Tokyo, 113-8656, Japan*
[2] *Key Laboratory of Ocean Energy Utilization and Energy Conservation of Ministry of Education, School of Energy and Power Engineering, Dalian University of Technology, Dalian, Liaoning 116024, China*
[3] *Center for Multidimensional Carbon Materials (CMCM), Institute for Basic Science (IBS) (Republic of Korea), Ulsan, 44919, Republic of Korea*
[4] *Department of Physics, University of Antwerp, Antwerp 2610, Belgium*
[5] *Center Beijing National Laboratory for Molecular Science, Key Laboratory for the Physics and Chemistry of Nanodevices, State Key Laboratory of Rare Earth Materials Chemistry and Applications, College of Chemistry and Molecular Engineering, Peking University, Beijing, 100871, China*
[6] *School of Mechanical Engineering, Zhejiang University, Hangzhou, 310058, China*
[7] *Interdisciplinary Cluster for Cutting Edge Research, Research Initiative for Supra-Materials, Shinshu University, Japan*
[8] *The Interdisciplinary Nanoscience Centre of Marseille (CINaM), Aix-Marseille University and CNRS, Marseille, France*

Investigating the structure and role of metal catalysts is crucial for the controlled synthesis of single-walled carbon nanotubes (SWCNTs) via chemical vapor deposition. Iron (Fe) and cobalt (Co), as well-known transition metals, are widely employed in SWCNT growth. However, most studies use Fe-Co binary catalysts with a fixed 1:1 atomic ratio, leaving the influence of varying Fe-Co ratios largely unexplored. This study investigates the effect of different Fe-Co ratios on SWCNT growth. We found that a monometallic Co catalyst at 600 °C 50Pa (The partial pressure of ethanol gas in the ethanol-argon mixed gas) (Fig. (a-b)) and a binary catalyst with 25% Co at 850 °C and 50Pa (Fig. (c-d)) exhibited exceptional growth efficiency compared to other ratios. Transmission electron microscopy confirms those composition (pure Co at 600 °, and 25% Co at 850 °C) also has the smallest catalyst diameter. We speculate that this size reduction contributes to their superior growth performance (Fig. (f)). Energy-dispersive X-ray spectroscopy (EDS) mapping showed uniform Fe-Co mixing, with Co atoms preferentially occupying surface sites, while the catalyst core formed a Fe-Co alloy—consistent with our simulations (Fig. (e)). Molecular dynamics simulations showed that catalyst clusters with identical sizes, but different Fe-Co ratios exhibited variations in melting point, directly affecting their stability. The 297-atom cluster has the highest melting point around 75% Fe and 25% Co. These findings align well with our experimental results

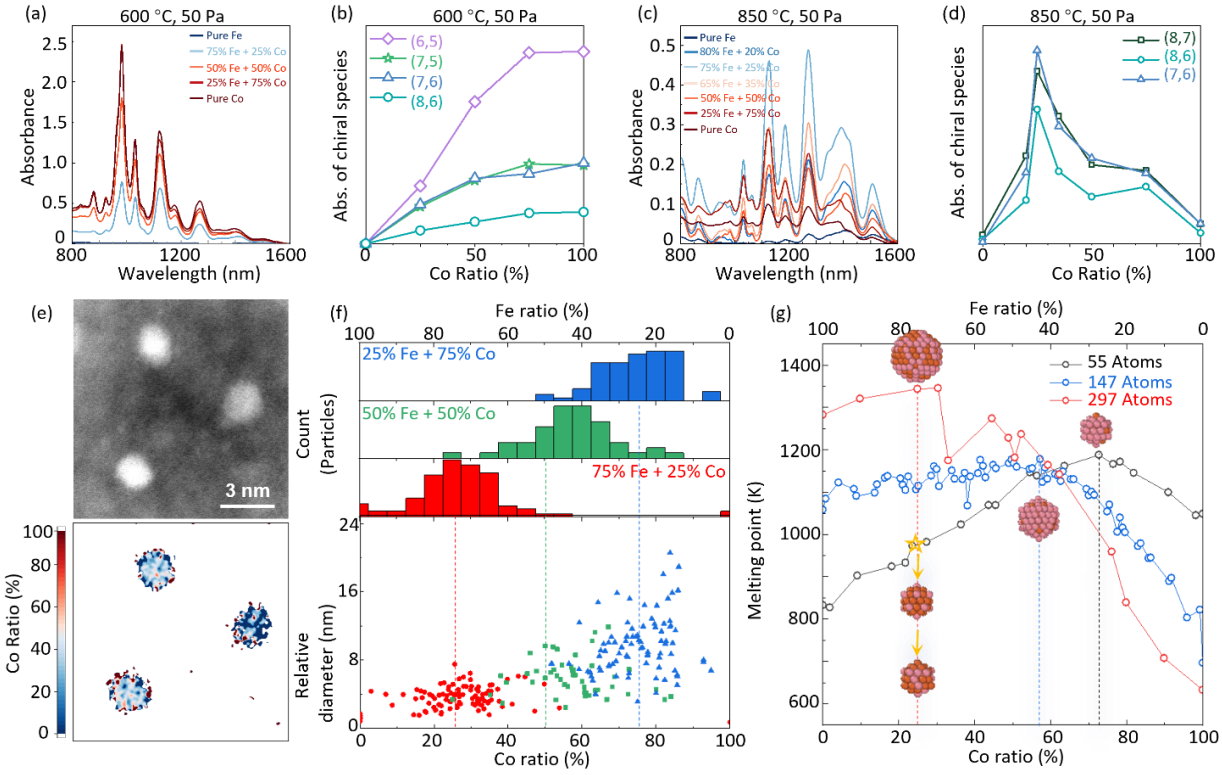

Figure: The absorbance spectrum of catalyst with different Fe-Co ratio grown at (a) 600 °C and (c) 850 °C; The dependence of quantity of each chiral species on Co atomic percentage for catalyst grown at (b) 600 °C and (d) 850 °C; (e) EDS mapping and calculated Fe-Co ratio mapping of catalyst with 75% Fe and 25% Co grown at 850 °C; (f) The statistics and analysis of real Co ratio of sample grown at 850 °C; (g) Melting point of Mackay clusters with different total atoms at varied Fe-Co ratio obtained from molecular dynamics simulations .

Single-crystal Graphene Wafers: Controlled Synthesis and Mass Production

Kaicheng Jia[1]

[1]*Beijing Graphene Institute (BGI), Beijing 100095 (P.R.China)*

Single-crystal graphene wafers have been proven to be compelling candidates for post-silicon semiconductor technology, owing to the excellent carrier mobility, wafer-scale performance uniformity, and fine compatibility with silicon-based integration. Controlled synthesis of high-quality and single-crystal graphene wafers has been regarded as the key guarantee to bridge graphene materials close to high-performance electronic and optoelectronic devices. However, current graphene wafers grown by chemical vapor deposition approach still suffer from the presence of twin boundaries on Cu substrates, which would highly degrade the aligned epitaxial growth of graphene domains. Herein, we demonstrated efficient methods to fabricate 4 to 8-inch Cu(111) single crystals without the existence of in-plane twin boundaries. Graphene wafers grown on as-obtained Cu(111) substrates exhibit improved crystallinity, which contributes an enhancement in the electrical properties such as carrier mobility and sheet resistance. Based on the above research, we have built two pilot-scale lines for the scalable production of 4 to 8-inch single-crystal graphene wafers. And the capacity of our designed equipment is about 20,000 pieces per year. Our work provides a new insight into the fabrication of single-crystal Cu(111) wafers without lattice defect, and exciting opportunities for the utilization of single-crystal graphene wafers for advanced applications..

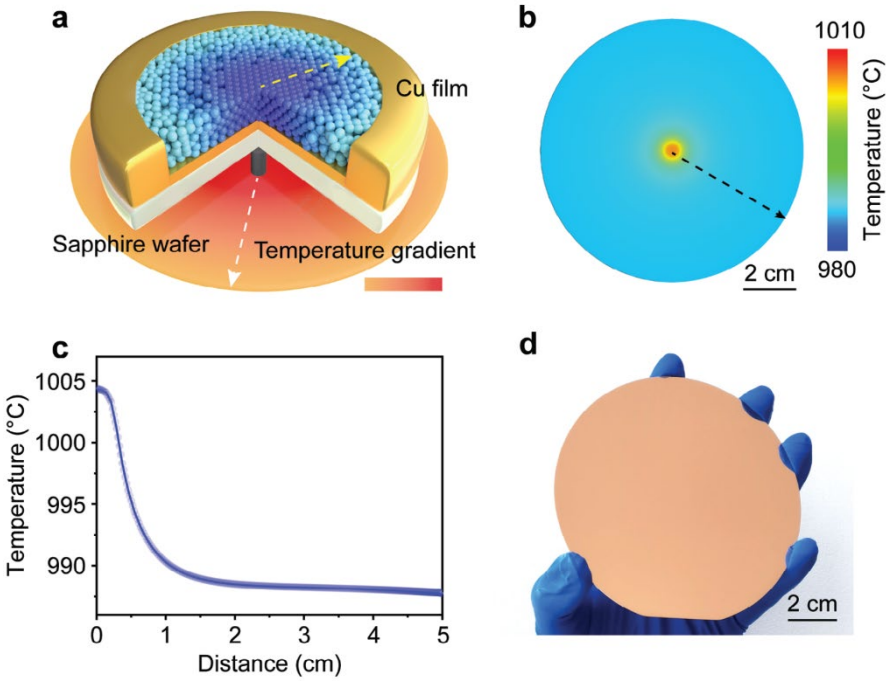

Figure caption: Schematic illustration for the fabrication of 4-inch single-crystal Cu(111) wafer**.**

References

[1] Y. Zhu *et al.*, *Adv. Mater.* **36**, 2308802 (2024).

HIGH-TEMPERATURE ADSORPTION OF NITROGEN DIOXIDE FOR STABLE, EFFICIENT, AND SCALABLE DOPING OF CARBON NANOTUBES

D. V. Krasnikov[1], I.V. Novikov[1], A.E. Goldt[1], S.S. Fedotov[1], A.G. Nasibulin[1],

[1] *Skolkovo Institute of Science and Technology (Russia)*

This work is devoted to a novel efficient strategy for single-walled carbon nanotube doping based on heat treatment with nitrogen dioxide [1]. Unlike numerous reports of powerful but unstable NO_2 doping at room temperature, the proposed method combines high efficiency and stability, enabled by a phenomenon of a temperature-dependent adsorption of nitrogen dioxide on the nanotube surface. We reveal that doping stability increases with the treatment temperature reaching maxima at 300°C without any detrimental effect on nanotube structure and optical transmittance. As a result, we demonstrate doped carbon nanotube transparent conductive films exhibiting competitive performance (to films treated with other dopants) with a less than 50% drop in conductive characteristics for over a year (Figure 1). Thermo-programmed desorption analysis confirms the preferential formation of long-living adsorbed nitrogen species, such as NO_3-groups, after high-temperature treatment of the samples. We believe the current work provides a basis for the robust and technologically efficient doping of single-walled carbon nanotubes and related structures at industrial scales, as the developed method could be easily coupled with a floating-catalyst synthesis reactor (or any other continuous technology) in a tandem manner.

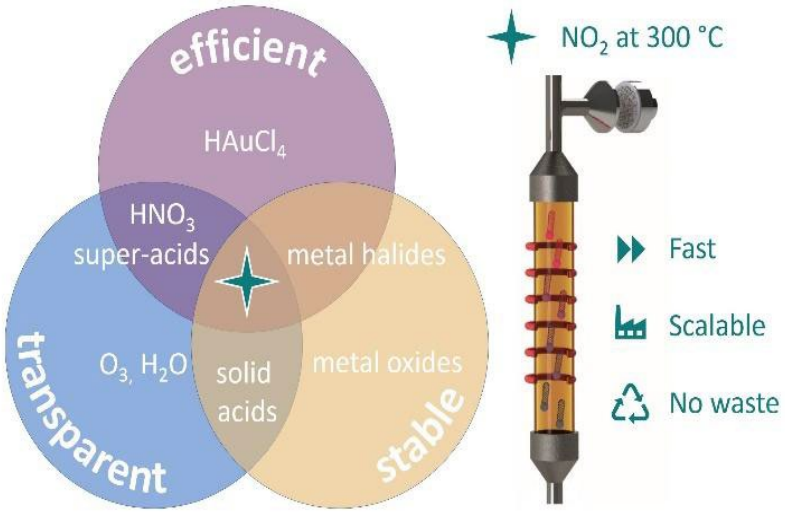

Figure1: Comparison of the developed technology with other SWCNT doping methods in terms of key performance indicators of the doping procedure.

D.V.K. and A.G.N. acknowledge Russian Science Foundation grant No. 22-13-00436. The authors thank Dr. Eldar M. Khabushev for the invaluable contribution.

References

[1] E. M. Khabushev, *et al. Carbon* ***224*** 119082 *(2024)*

Synthesis of Tunable Fluorescent Carbon Dots from Dairy Whey for Advanced Cancer Nanomedicine: Bioimaging and Theranostic Applications

M.L. Fanarraga, R. Valiente, J. González, M.T. Candela, L. García-Hevia.

The Nanomedicine Group, IDIVAL- Universidad de Cantabria (Spain)

Carbon nanomaterials have emerged as pivotal tools in cancer nanomedicine, with carbon dots (CDots) standing out as a secure, biocompatible, and versatile option for a wide range of biomedical applications. These applications include drug and gene delivery, toxin absorption, nanosensors, and hyperthermia. CDots are semiconductor nanoparticles, typically 2 to 10 nm in diameter, renowned for their exceptional biocompatibility, optical absorption, chemical stability, low toxicity, and radiation resistance. These properties make them particularly promising for cancer treatment and diagnostics.

This study focuses on the synthesis of CDots with tunable fluorescence emission, leveraging a green chemistry approach to transform dairy whey, a by-product of the dairy industry, into high-quality CDots. Whey, with its uniform composition of approximately 63-75% lactose (a disaccharide of glucose and galactose) and 11-15% globular proteins rich in sulfur-containing amino acids such as cysteine and methionine, serves as an ideal precursor. These components play a crucial role in enhancing the quantum yield, surface functionalization, and catalytic properties of CDots during a one-step synthesis process.

The project specifically aims to harness the potential of CDots for bioimaging in the diagnosis of brain cancer and as theranostic agents for cancer treatment through photo-hyperthermia in preclinical models. By exploring the conversion of dairy whey into CDots, this research offers a sustainable and environmentally friendly synthesis route and a versatile solution for advancing safer and more effective biomedical interventions in cancer nanomedicine.

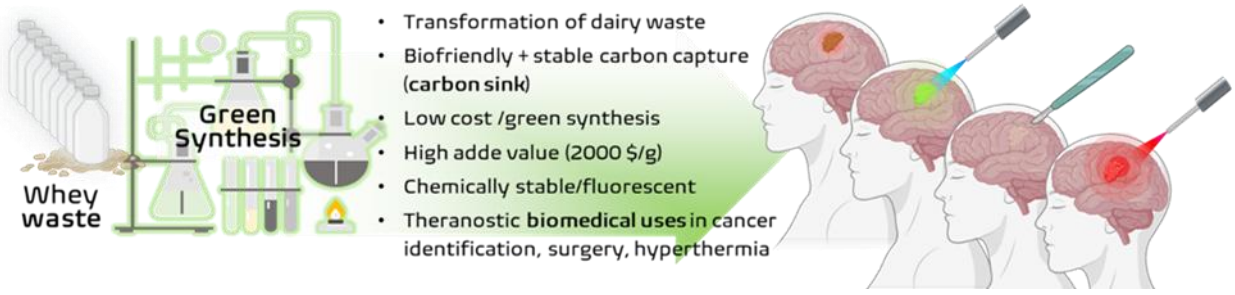

Figure: Vision of the study**.**

Robust carbon nanotube composite coatings for perfect absorption in harsh environmental applications

Yuanhao Jin, Qunqing Li, Shoushan Fan

Department of Physics, Tsinghua-Foxconn Nanotechnology Research Center, Tsinghua University, 100084, Beijing, China

We have successfully developed a nearly perfect absorber coating designed for extreme environmental conditions, utilizing a spray coating process that facilitates easy, cost-effective and large-scale production. The coating is formulated with carbon nanomaterials, enhanced by the incorporation of epoxy resin-coated carbon nanotubes that serve as a binding agent within the carbon black particle matrix. This strategic integration effectively 'freezes' the micro- and nanostructures of the surface, thereby substantially improving the coating's durability and stability. The coating delivers omnidirectional high absorption efficiency, exceeding 99.9 % across a broad wavelength range from 400 nm to 20 μm. It exhibits excellent adhesion and abrasion resistance, ensuring the maintenance of its absorptive performance under extreme conditions such as high and low temperatures, UV radiation, water impact and prolonged outdoor exposure. Carbon nanotubes have demonstrated their effectiveness as ideal connecting materials for perfect absorber coatings and their application has paved the way for new opportunities in the development of smart coatings. This robust and stable perfect absorber coating addresses the theoretical mechanical limitations inherent in conventional perfect absorber, significantly expanding their potential applications.

References (if desired)

[1] Jin, Y.; Li, M.; Yang, H.; Zhang, L.; Liu, C.; Song, J.; Hao, X.; Wang, J.; Fan, S.; Li, Q. Robust carbon nanotube composite coatings for perfect absorption in harsh environmental applications. *Carbon* **2025**, *233*, 119900.

Synthesis of Single-Walled Carbon Nanotubes/Graphene Nanoflakes Hybrid Nanostructures Utilizing Fe-Re Bimetallic Catalysts by Floating Catalyst Chemical Vapor Deposition

Anastasios Karakassides[1], Hirotaka Inoue[1,2], Ghulam Yasin[1], Hua Jiang[1], Esko I. Kauppinen[1]

[1]Aalto University (Finland), [2]Sumitomo Electric Industries (Japan)

The catalyst plays a fundamental role in carbon nanotubes (CNTs) synthesis and has been extensively studied. In particular, multi-metallic catalysts-comprising two or more metal species that form alloys—have demonstrated significant influence over the controlled synthesis of CNTs. These catalysts impact key factors such as CNT growth rate [1], catalyst lifetime [2], chirality distribution [3], and diameter distribution [4]. Understanding the interplay between metal composition, alloying behavior, and CNT growth mechanisms is essential for optimizing CNT synthesis. While previous studies have explored bimetallic catalysts in substrate-supported chemical vapor deposition (CVD), their implementation in floating catalyst CVD (FC-CVD) remains largely unexplored. In this study, we investigate the use of an iron-rhenium (FeRe) bimetallic catalyst for single-walled CNTs (SWCNTs) synthesis in FC-CVD, systematically tuning the Fe/Re ratio to optimize growth conditions. Under specific Fe/Re ratios, we report the high-yield synthesis of novel hybrid SWCNT/graphene nanoflake (GNFs) structures. Comprehensive characterization using high-resolution transmission electron microscopy (HRTEM), Raman spectroscopy, and UV–Vis–NIR absorption spectroscopy confirms the structure, morphology, and electronic properties of the synthesized materials. This work demonstrates the potential of Fe-Re catalysts in FC-CVD for scalable, controlled synthesis of SWCNT-based hybrid nanomaterials, advancing their applicability in energy storage and environmental remediation applications and beyond.

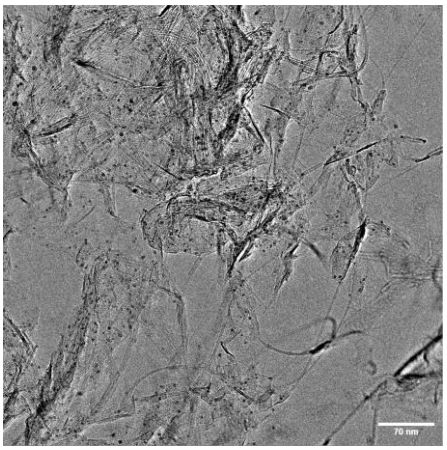

Figure 1. TEM micrograph of the SWCNTs/GNFs hybrid nanostructures.

References

[1] N.G. Shang *et al.*, *Nanotechnology* **21**, 505604 (2010).
[2] M. He *et al.*, *Carbon* **52**, 590-594 (2013).
[3] F. Yang *et al.*, *Nature* **510**, 522-524 (2014).
[4] F. Yang *et al.*, *Sci. Adv.* **8**, eabq0794 (2022).

Magnetically Aligned All-Solid-State Ionic-Liquid Crystal Elastomer based Electrochemical Artificial Muscles

Guang Yang[1, 2], Jiangtao Di[1, 2]

[1] *University of Science and Technology of China (China),* [2] *Suzhou Institute of Nano-Tech and Nano-Bionics, Chinese Academy of Sciences (China)*

Oriented liquid crystal elastomers (LCE), which possess the entropic elasticity and reversible actuation, have received immense attention as artificial muscle fibers in soft robotics. However, actuation and sensing in nature are carried out through ionic conduction between nerves and muscles. Currently, most of the studies on LCE artificial muscle fibers are based on thermotropic and photoisomerization actuation mechanisms. Herein, we improve the affinity of LCE with ionic liquids by introducing the imidazole cations as chain extender into the soft segment of LCE. In addition, magnetic fields are employed to align ionicLCE, and oriented molecular networks provide the rapid ion transport pathways. Parallel aligned CNT fibers were composited with ionicLCE, and all-solid-state electrochemically actuated LCE-based artificial muscle fibers were developed. The CNT/oriented ionicLCE artificial muscle fibers output favorable actuation performance (15% maximum contraction and 1 Hz maximum actuation frequency). Furthermore, the artificial muscle fibers maintain favorable actuation properties in vacuum due to the low saturation vapor pressure of the ionic liquid. The deployment of solar panels in the vacuum was demonstrated to show the potential application of the all-solid-state electrochemical artificial muscle fibers in space deformation structures.

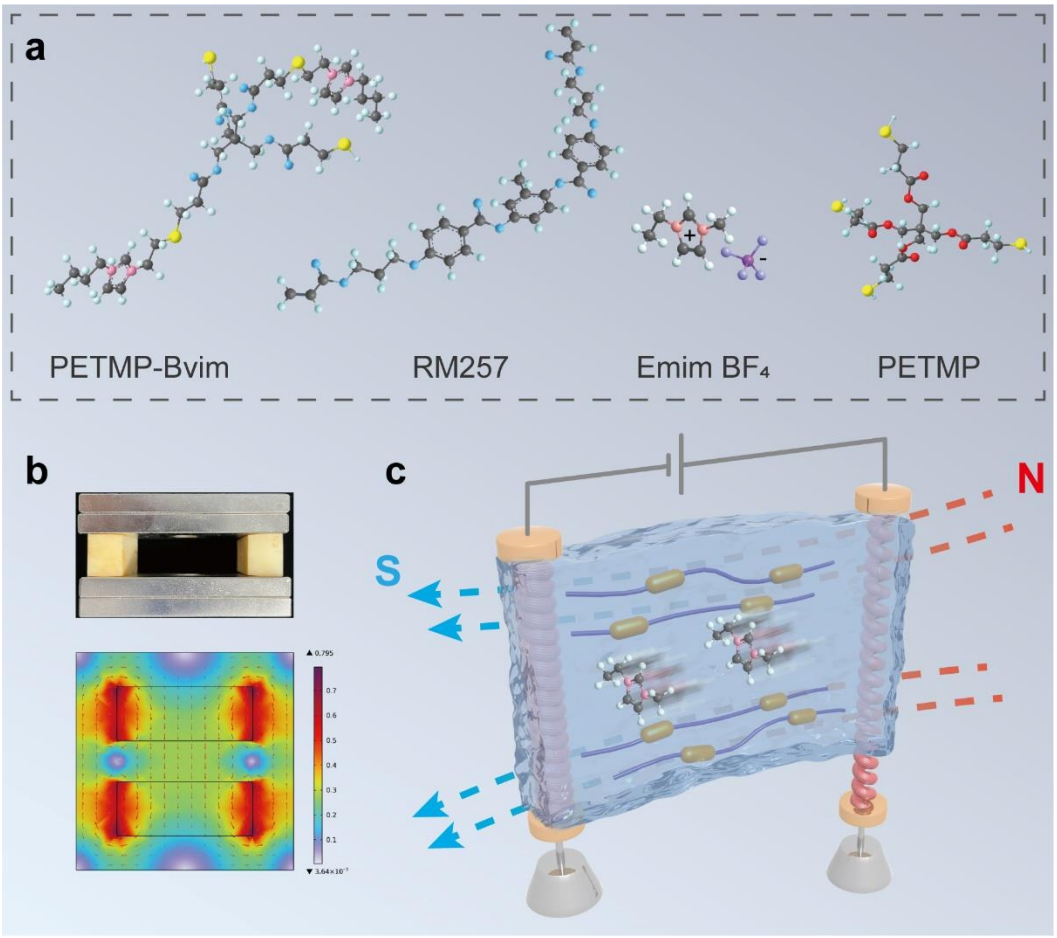

Figure caption: (a) The molecular composition of ionic liquid crystal elastomers. (b) Photographs and simulation studies of magnetic field induced LCE orientation. (c) All-solid-state electrochemical actuation of CNT/ionicLCE artificial muscle fibers by rapid transport imidazole cations.

Sequential Assembly of Low-dimensional Materials on Arbitrary Fiber Substrates for Electromagnetic Interference Shielding

Jiayi Liu[1,2], Quanfen Guo[1,2], Huahui Tian[1,2], He Hao[3], Xin Gao[1,2*], Jin Zhang[1,2,3*]

[1] *School of Materials Science and Engineering, Peking University (China),* [2] *Beijing Graphene Institute (China),*

[3] *Beijing Science and Engineering Center for Nanocarbons, Beijing National Laboratory for Molecular Sciences, College of Chemistry and Molecular Engineering, Peking University (China).*

Electromagnetic shielding fabrics are ideal functional materials to address electromagnetic interference (EMI) while offering multifunctional properties, but suffer from a range of challenges in their fabrication steps [1, 2]. Graphene and carbon nanotubes (CNTs), collectively referred to as carbonene materials, are advanced branches of low-dimensional nanomaterials. They possess exceptional electrical and mechanical properties, making them highly promising as coating layers for EMI shielding in fibers or fabrics [3,4]. However, assembling hydrophobic and chemically inert carbonene from dispersions onto hydrophilic or inert fiber surfaces often requires surface treatments or chemical modifications [5]. In this work, we propose a dimension-engineering strategy to fabricate universal carbonene coatings with superior mechanical stability and tunable conductivity on diverse fiber substrates. The approach employed a wet-chemistry assembly process to deposit two-dimensional graphene sheets as a base layer, followed by the integration of one-dimensional CNTs. This sequential assembly effectively flattens the wrinkles of graphene, increasing the sp^2-carbon coverage area and synergistically enhancing conductivity. This is the first demonstration highlighted the critical role of dimensional effects in the liquid-phase assembly of nanomaterials. A 400 nm-thick carbonene coating significantly boosted the conductivity of aramid fibers from 0 to 641 S/cm while maintaining a high tensile strength of 5.92 GPa. Fabrics woven from graphene/CNT-coated aramid fibers (GCAFs) showed an average EMI shielding effectiveness (SE) of 85 dB in the X-band. Moreover, the GCAF fabrics exhibited robust EMI shielding performance under extreme conditions. This novel strategy of dimension-engineered wet-chemistry assembly represents a promising direction for developing universal carbonene coatings with high stability, conductivity, and multifunctionality, and paves the way for the development of low-dimensional nanomaterials in more fields.

References (if desired)

[1] Li W, *et al., Science* **385**, 62–68 (2024).
[2] Yang Y, *et al., Nature* **576**, 248-252 (2019).
[3] Wen Y, *et al., Nano Letters* **22**, 6035-6047 (2022).
[4] H. Kashani, *et al., Matter* **1**, 1077-1087 (2019).
[5] Zhao L, *et al., Nature Communications* **15**, 10027 (2024).

Facile and scalable concentration method for surfactant-assisted carbon nanotube dispersion

Jaegyun Im[1], and Jaegeun Lee[1,2]

[1] *School of Chemical Engineering, Pusan National University, Busan, Republic of Korea, 46241 (Republic of Korea),*
[2] *Department of Organic Material Science and Engineering, Pusan National University, Busan, Republic of Korea, 46241 (Republic of Korea)*

In solution processing of carbon nanotubes (CNTs), achieving homogeneous and high-concentration CNT dispersions is necessary. Although high-crystalline single-walled CNTs can be well dispersed using superacids, commercial grade low-crystalline multi-walled CNTs still have difficulty in achieving high-concentration and uniform dispersion. Herein, we present a facile osmotic dialysis-induced concentration method for surfactant-assisted CNT dispersions. Focusing on the colloidal characteristics of surfactant-assisted CNT dispersion, we successfully demonstrated the selective absorption of dispersed components in CNT dispersions maintaining the stable dispersion state, resulting in an entropy-driven phase transition from isotropic to nematic phase. This facile, fast, and scalable osmotic dialysis-induced concentration method enabled us to process various macroscopic CNT assemblies. Our surfactant-system-specialized engineering paves the way for a new chapter in the solution processing of surfactant-assisted CNT dispersions.

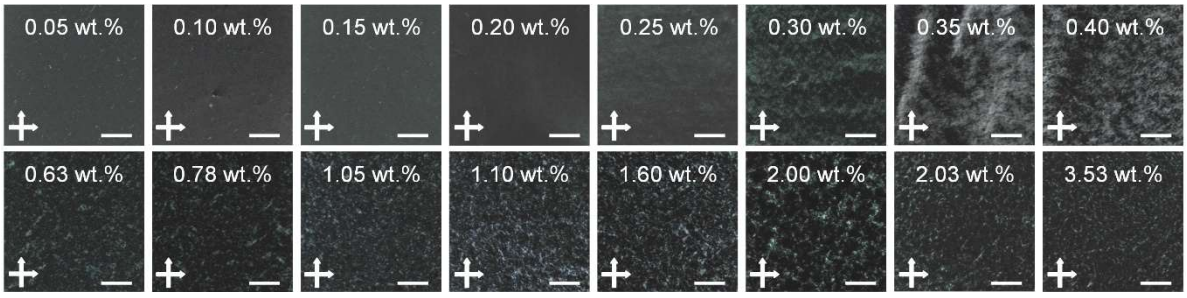

Figure: Polarized optical microscopic images of concentrated CNT dispersions. Scale bar: 250 μm.

Wet-spinning of high strength and high thermal conductivity carbon nanotube fibers

Yuanlong Shao[1,3], Jin Zhang[1,3]

[1]School of Materials Science and Engineering, Peking University, Beijing 100871, China, [2]Academy for Advanced Interdisciplinary Studies, Peking University, Beijing, 100871, China, [3]Beijing Graphene Institute (BGI), Beijing 100095, China

The development of carbon nanotube (CNT) fibers integrating high mechanical strength and exceptional thermal conductivity is critical for advanced applications in aerospace, electronics, and wearable technologies.[1-3] Traditional fabrication methods often struggle to simultaneously optimize these properties due to challenges in CNT alignment, interfacial interactions, and defect minimization.[4,5] Here, we present a polyimide assisted wet-spinning approach employing optimized processing parameters, including a precisely formulated coagulation bath and post-densification treatments, to fabricate CNT fibers. By utilizing a chlorosulfonic acid-based spinning dope and controlled coagulation conditions, we achieve highly aligned CNT bundles, reducing voids and enhancing inter-tube stress transfer. Subsequent mechanical stretching and solvent-assisted densification further improve packing density and phonon transport efficiency. The resulting fibers exhibit a tensile strength exceeding 3.0 GPa and a thermal conductivity of up to about 600 W/mK. In addition, we also build a continuous wet-spinning line with the capability to fabricate thousand meter-length multifilament fibers with consistent performance, suitable for weaving into textiles or integration into composites. Structural and thermal analyses confirm that the reduced inter-filament voids and improved phonon pathways in the multifilament architecture enable efficient stress distribution and heat dissipation. These findings demonstrate the efficacy of wet-spinning in producing multifunctional CNT fibers, offering promising potential for next-generation thermal management systems and high-strength composites.

References:

[1] Yang, Z. *et al.*, *Natl. Sci. Rev.* **11**, nwae203 (2024).
[2] Huang, J. *et al.*, *ACS Nano* **18**, 14377-14387 (2024).
[3] Zhang, X. *et al.*, *Science* **384**, 1318-1323 (2024).
[4] Behabtu, N. *et al.*, *Science* **339**, 182-186 (2013).
[5] Behabtu, N., Green, M. J. & Pasquali, M., *Nano Today* **3**, 24-34 (2008).

Exploring the Role of Sulfur Promoter from Carbon Disulfide in Carbon Nanotubes Synthesis

Ghulam Yasin[1], Otto Salmela[1], Hirotaka Inoue[1,2], Anastasios Karakassides[1], Hua Jiang[1], Esko I. Kauppinen[1]

[1] *Aalto University (Finland),* [2] *Sumitomo Electric Industries (Japan)*

Carbon nanotubes (CNTs) possess a family of promising structural properties, enabling multifunctional applications in various fields, and have been shown promises currently in commercial uses [1]. Despite decades of rigorous research since their discovery in 1991, many challenges remain today in synthesizing CNTs particularly selective growth, quality, and scalability of CNTs. Floating catalyst chemical vapor deposition (FC-CVD) offers a promising synthesis method that tackles multiple challenges through, for instance, high quality and the continuous production of CNTs [2]. To advance the scalability and selective growth strategy, it is vital to probe the mechanism of CNT growth and how the various synthesis conditions and parameters affect the overall production process [3,4].

Therefore, the addition of sulfur and/or sulfur-containing compounds is an important strategy to tune the growth and characteristics of CNTs, because sulfur-containing compounds can promote the growth of CNTs and thereby influence their structure and various properties, such as yield, length, diameter, and sheet resistance of the CNTs. We explore particularly the effect of carbon disulfide (CS_2) as a sulfur source in the synthesis and characteristics of transparent conducting films (TCFs) of CNTs. CS_2, with its high volatility and simple molecular structure, facilitates efficient dissociation into reactive sulfur species, enhancing its interaction to catalyst particles and homogenous sulfur incorporation with less redundant byproducts. In contrast, thiophene's aromatic stability leads to complex decomposition pathways that could limit sulfur availability and cause unwanted carbonaceous byproducts, hindering the controlled growth of CNT [5]. In this work, the CNTs were found to minimize in diameter to about 1.3 nm and a higher yield of 3.19 cm^2/L with an optimum content of sulfur promoter (Fig. 1). Additionally, the lowest sheet resistance of 77 Ω/sq. at 90 % transmittance was attained for the TCFs doped with $AuCl_3$. We investigate the effect of sulfur content and other synthesis parameters on the growth and corresponding characteristics of CNTs, typically in the FC-CVD method. The diameter decrease could be due to the collision restriction of catalyst particles with early availability of sulfur from CS_2, unscrewing the carbon capping to cylindrical growth with smaller particles, and eventually yielding smaller CNTs and vice versa is observed with insufficient content of promoter for diameter and yield. Similarly, the higher yield at an optimum sulfur content of 0.9 (Fig. 1b) reveals the maximum contribution of the promoter in CNTs nucleation and further increasing the sulfur content causes a decline in yield owing to the rapid deactivation of catalyst particles. We believe that these findings will open a new avenue in the optimization and scalable synthesis of high-quality CNTs for impending functional applications and next-generation technologies.

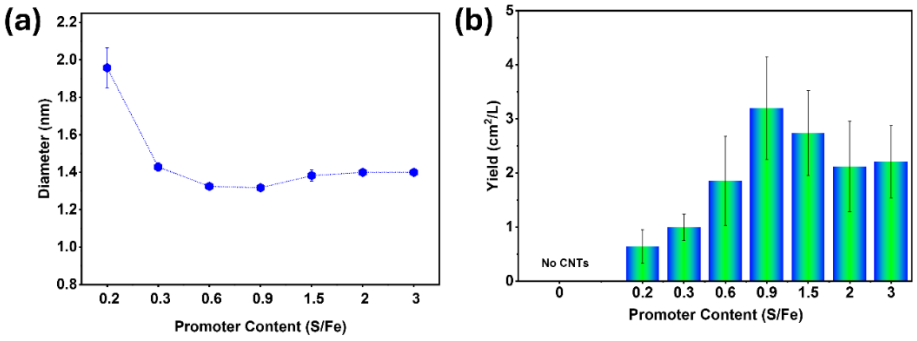

Figure 1. The relationship between promoter content and (a) diameter, (b) synthesis yield of CNTs.

References

[1] A. Cao *et al.*, *ACS Nano* **15**, 7946–7974 (2021).
[2] E. I. Kauppinen *et al.*, *Chem. Eng. J.* **378**, 122010 (2019).
[3] A. G. Nasibulin *et al.*, *Carbon* **210**, 118051 (2023).
[4] E. I. Kauppinen *et al.*, *J. Am. Chem. Soc.* **133**, 1224–1227 (2011).
[5] Z. L. Wang *et al.*, *J. Phys. Chem. C* **39**, 14293–14298 (2007).

Selective Semiconducting Carbon Nanotube Extraction with Cellulose Acetate

K. Yoshida[1], Y. Nonoguchi[1]

[1] *Faculty of Materials Science and Engineering, Kyoto Institute of Technology, (Japan)*

The post-synthetic extraction of semiconducting carbon nanotubes (CNTs) using hydrophobic polymers is in principle advantageous for achieving high purity, crystallinity, and yields over other purification methods. However, the use of highly dry hydrophobic solvents is required in this process, making it difficult to develop practical processes such as scaleup and continuous flow associated with acceptable reproducibility. Herein we propose the purification of semiconducting CNTs using cellulose acetate (CA) as a surfactant in polar organic solvents, which tolerates environmental impurities such as water.

UV-Vis-NIR absorption spectroscopy revealed that CA-assisted ethyl lactate dispersion shows a trace amount of absorption derived from metallic CNTs (arc discharge), in contrast to non-selective, aqueous Pluronic F127 dispersion (Fig. 1(a)). Resonant Raman spectroscopy also supported the decreased amount of metallic CNTs in CA-supported CNT films. These results strongly indicate that semiconducting CNTs are selectively extracted in CA-containing ethyl lactate solution. To take advantage of the present selective extraction, we examined thermoelectric properties of extracted CNTs, that exhibited 9 times larger thermoelectric power factors for appropriate doping conditions than those of unsorted CNTs.

It should be noted that conventional methods involving conducting polymers require the use of dehydrated solvents to achieve selective extraction.[1] Contrastingly, the CA-assisted extraction demonstrated here worked well in the presence of water without significant loss of semiconducting CNTs' purity (Fig. 1(b)). Higher concentrations of CA in the extract increased the yield of semiconducting CNTs without compromising their purity (Fig. 1(c)). This result is in contrast to the ethyl cellulose dispersion reported recently.[2] The addition of THF, a poor solvent for CA-assisted dispersion, reduced the contents of metallic CNTs without significantly decreasing the yields of semiconducting CNTs. As such, CA-assisted dispersion is recognized as a robust and efficient way for selectively extracting semiconducting CNTs in organic solvents.

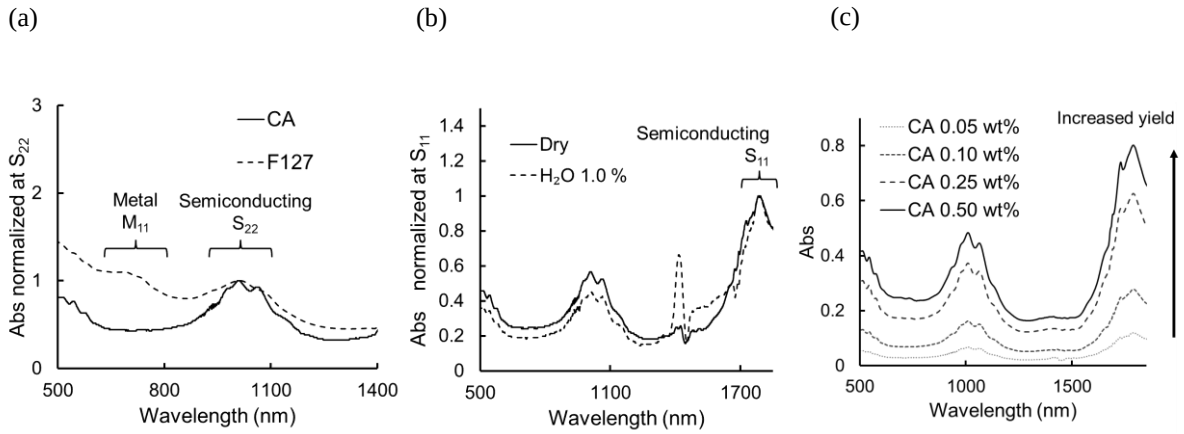

Figure 1. Absorption spectra of (a) F127- and CA-assisted SWNT dispersion, (b) CA-assisted SWNT dispersion in the presence of water, and (c) at various CA concentrations.

References

[1] A. Nish, J. Y. Hwang, J. Doig, R. J. Nicholas, *Nat. Nanotechnol.*, **2**, 640–646 (2007).

[2] T. Yagi, K. Yoshida, S. Sakurai, T. Kawai, Y. Nonoguchi, *J. Am. Chem. Soc*., **146**, 20913–20918 (2024).

Corresponding Author: Yoshiyuki Nonoguchi

Tel: +81-75-724-7515

E-mail: nonoguchi@kit.ac.jp

Estimating key factors for self-organized, aligned CNT film formation by machine learning

Miki Ikeda[1], Tomoyuki Miyao[2], Yoshiyuki Nonoguchi[1]

[1] Kyoto Institute of Technology (Japan), [2] Nara Institute of Science and Technology (Japan)

Carbon nanotubes (CNTs) are known for their exceptional mechanical, thermal, and electrical properties, and controlling their orientation is important for maximizing the use of these properties on a macroscopic scale. In the past, large-area orientation methods for CNTs self-assembly have been reported, using droplet capillary effect,[1] or liquid crystalline dispersant.[2] These methods are thought to make use of the gregarious and cohesive of CNTs and dispersants. We recently discovered that CNT-butyral resin composites form liquid crystal-like long-period structures through evaporation self-assembly from colloidal CNTs dispersions using non-liquid crystalline butyral resin as a dispersant.[3] We have found that CNTs are dispersed independently in the resin and that the elongation in the orientation direction of CNT-resin composite films are improved, but the examination of the preparation conditions has relied on exhaustive search. In this study, we used machine learning to extract solvent parameters related to CNT self-assembly. By feeding solvent predictions back into the experiment, we discovered many new combinations of dispersants and solvents that enable the CNT self-assembly.

The orientation degree of CNT drop-cast films was estimated using the literature method based on scanning electron microscopy images.[4] The orientation degree is the orientation ratio obtained by Fourier transform of the image, and is defined as a value greater than 1, where the values above 1.2 indicate significant anisotropy. Four machine learning models were introduced to predict the orientation degree: Partial Least Squares (PLS), Support Vector Machine, Random Forest, and XGBoost. Using these models, we learned and predicted the orientation degree of CNTs in various solvents obtained from our recent study,[3] and finally, we adopted the Random Forest as the prediction model because it showed the highest validity in all indicators of R^2, RMSE, and MAE (Table 1). Feature importance analyses using the Random Forest estimated that, among the descriptors based on molecular structure information, the three descriptors PEOE_VSA7, BCUT2D_CHGLO, and FpDensityMorgan3 contribute significantly to the alignment. These descriptors suggest that the local charge and electronegativity of the solvent molecules and the asymmetry of the molecules contribute to the self-assembly of CNTs. Furthermore, using this model, we further predicted new solvents that would give a high degree (> 1.2) of CNT orientation, with a probability of 50%. This suggests that it is possible to control this orientation phenomenon by using solvent parameters.

Table. 1 Comparison of the prediction performance of four machine learning models.

Model	Training Metrics			Test Metrics		
	R^2	RMSE	MAE	R^2	RMSE	MAE
Partial Least Squares	0.547	0.109	0.083	0.269	0.137	0.116
Support-Vector Machine	0.631	0.098	0.052	0.383	0.126	0.067
Random Forest	0.703	0.088	0.054	0.510	0.112	0.075
XGBoost	0.698	0.089	0.057	0.507	0.113	0.073

References

[1] Y. Joo et al. *Langmuir* **30**, 3460–3466 (2014).
[2] MD. Lynch et al. *Nano Lett.* **2**, 1197–1201 (2002).
[3] Y. Tsuchie, Y. Nonoguchi et al., in preparation (2025)
[4] T. Enomae, Y.-H. Han, A. Isogai, *Nord. Pulp Pap. Res. J.* **21**, 253-259 (2006)

Preparation, properties and applications of carbon nanomaterial flexible transparent conducting films

Hong-Zhang Geng[1,2]

[1]*School of Material Science and Engineering, Tiangong University (China)*

[2]*Tianji Zhencai Technology (Hebei) Co., Ltd. (China)*

In recent years, flexible optoelectronic devices have attracted extensive attention. Indium tin oxide (ITO) film electrode is used as the conductive film of traditional optoelectronic devices. ITO film has high production cost, high resistance, poor transparency and poor flexibility on the flexible substrate, and it is easy to crack when bending, resulting in device failure. Carbon nanotubes and graphene have many excellent and unique optical, electrical, and mechanical properties. A small amount of carbon nanotubes can form a transparent conductive film with high light transmittance and low surface resistance and a random network structure[1]. Due to its good characteristics in conductivity, light transmittance, strength and flexibility, It can replace the traditional conductive material ITO and be used in transparent flexible heaters[2] and flexible organic light-emitting devices[3]. It has a broad application prospect in flexible display, touch screen and other aspects, and its research interest has been growing. This report summarizes the author's research achievements in the transparent conductive films of carbon nanomaterials in recent years, and discusses the methods to improve the conductivity of the films from the types, purification, dispersion, film preparation, and post-treatment of carbon nanotubes[4], as well as the application in organic light-emitting devices, flexible heating films, and high-performance EMI shielding[5]. For wide application, industrial mass production method of films will be introduced. It is expected to provide reference for the research, promotion and application of carbon nanomaterial thin films.

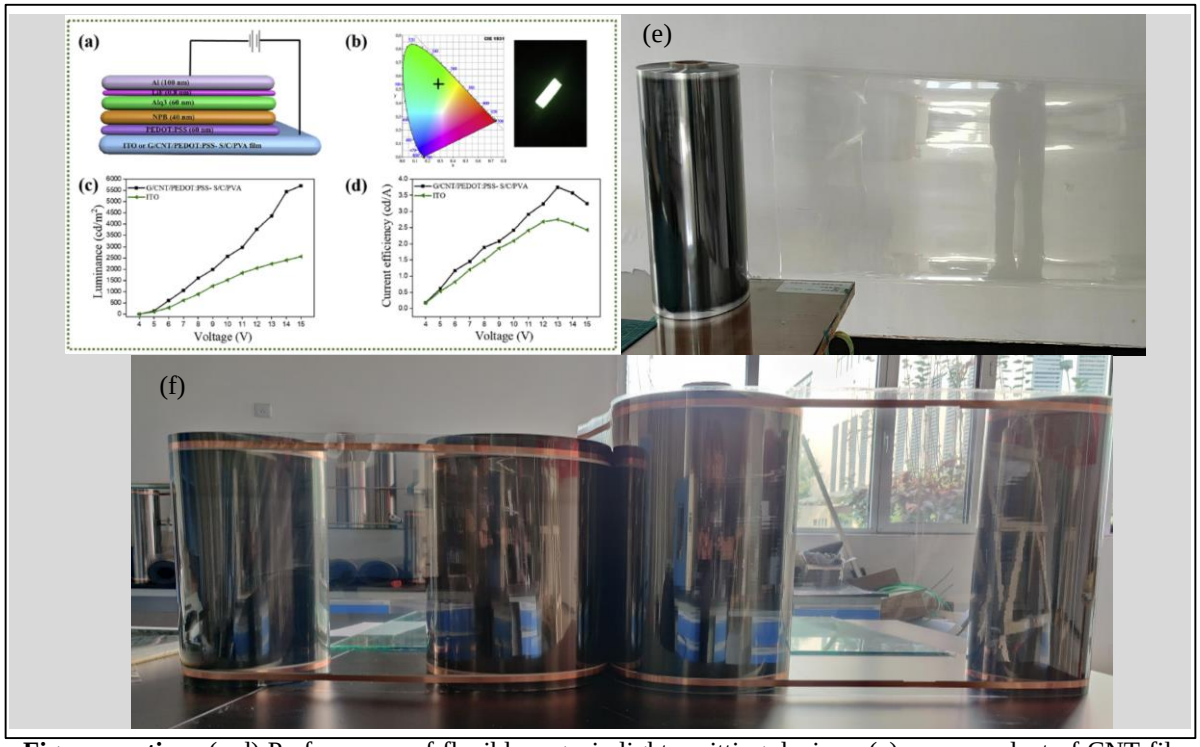

Figure caption: (a-d) Performance of flexible organic light-emitting devices, (e) mass product of CNT film, (f) flexible transparent heating film.

References

[1] H.-Z. Geng *et al.*, *J. Am. Chem. Soc.* **129**, 7758-7759 (2007).
[2] H.-Z. Geng *et al.*, *J.Coll. Interf. Sci*. **577**, 300–310 (2020).
[3] H.-Z. Geng *et al.*, *Carbon* **172**, 379-389 (2021).
[4] H.-Z. Geng *et al.*, *Carbon* **207**, 210-229 (2023).
[5] H.-Z. Geng *et al.*, *J.Coll. Interf. Sci*. **665**, 376–388 (2024).

BEYOND D-SPACING: THE CRITICAL ROLE OF DEFECTS IN GRAPHENE OXIDE MEMBRANES

Nima Zakeri[1], Kirill Levin[2], Marta Cerruti[1]
[1]*Biointerface Lab, Department of Mining and Materials Engineering, McGill University (Canada)*
[2]*Magnetic Resonance Facility, Department of Chemistry, McGill University (Canada)*

Graphene oxide membranes (GOMs) are recognized for their efficient molecular and ionic sieving with ultrafast water transport. They consist of highly ordered nanochannels arranged in crystalline domains separated by defective regions. The size distribution of nanochannels is widely assumed as the main factor determining the selective permeability of the membranes. The reported nanochannel sizes (d-spacing) for pristine GOMs range from 7.4 to 11.5Å[1]. This wide range is concerning as the membrane selectivity is affected by minute changes (~angstrom) in d-spacing.

Variations in d-spacing stem from both intrinsic differences in GO flake properties and differences in fabrication parameters. While some of these effects have been studied, others (e.g. the impact of membrane size) are still completely unexplored. Additionally, current studies largely focus on the d-spacing and overlook the effect of defects in explaining the filtration behavior.

This study explores how fabrication methods (vacuum filtration, VF; air drying, AD), membrane size (0.0314–12.56 cm²), and thickness (500 nm–7.6 µm) influence crystalline domains, defect structures, and filtration efficiency. Crystallite domains were characterized using XRD, Raman spectroscopy, and TGA, while structural defects were analyzed using SAXS and NMR relaxometry. Ethanol vapor permeation tests were also used to assess membrane performance.

Contrary to common beliefs [1], our results revealed that AD does not lead to higher d-spacing, as we found similar d-spacings between VF membranes (VF-GOMs) and AD membranes (AD-GOMs). Despite the similar d-spacings between VF-GOMs and AD-GOMs, diffusion tests showed higher ethanol permeation rates for AD-GOMs. To evaluate if this result could be explained by differences in microstructural defects, we employed both SAXS and NMR relaxometry.

SAXS results showed that AD-GOMs have a higher defect density than VF-GOMs, and defects in AD-GOMs have a more irregular interface with the crystalline domains compared to VF-GOMs. NMR relaxometry enabled assessing the distribution of crystalline domains and defects by studying water mobility, since water mobility is lower in the nanochannels than in the defects due to higher molecular confinement[2]. AD-GOMs showed larger defects compared to VF-GOMs. Also, more water was found in the defect sites than in the nanochannels of VF-GOMs, while a similar amount of water was found in nanochannels and defects in AD-GOMS. This suggests that in VF-GOMs, it is harder for water to infiltrate the nanochannels, where water tends to remain in the defects instead.

To explain these results, we hypothesize that in AD, uneven drying causes the water residues remain within the structure; this may induce local stresses on the GO sheets, curving them to maximize the number of hydrophilic interactions with the water residues. This would explain the presence of larger defects with irregular interfaces in the AD-GOMs; also, upon complete water evaporation at the end of drying, the resulting defects would have a high density of oxygen-rich domains on their interface. The presence of these oxygenated groups may make it easier for water to infiltrate the nanochannels in AD-GOMs compared to VF-GOMs. These observations could also explain the higher ethanol permeation rates in AD-GOMs, as the defects facilitate molecular transport between nanochannels. Overall, our study highlights the critical role of defects in transport in GOMs, advocating for a broader perspective that goes beyond nanochannel size per se.

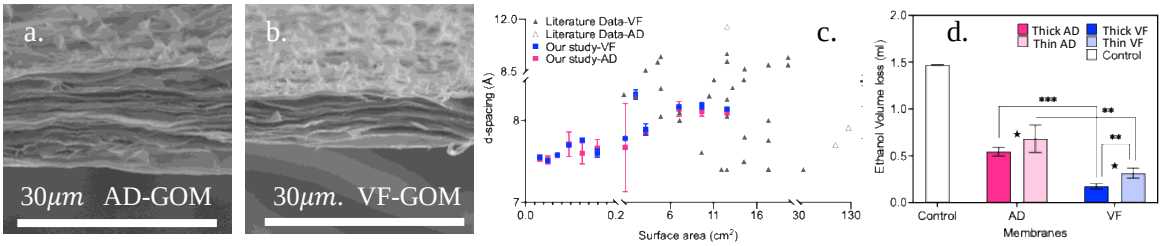

SEM images of GOM cross-section (a,b), d-spacing vs. surface area of membranes (c), ethanol permeation test (d)

References

[1] Tsou, Chi-Hui, et al. *Journal of Membrane Science*, (2015).
[2] Zhang, W.-H., et al., Carbon, (2021).

Structure Dependence of CNT Forests on the Lateral Memristive Resistance

H. Furuta[1, 2], Y. Sato[1], R. Shinsei[1]

[1]*School of Systems Engineering, Kochi Univ. Technol. (Japan),* [2]*Research Inst., Kochi Univ. Technol. (Japan)*

The high-surface-are CNT films are expected to serve as electrodes in reservoir computing devices for neuromorphic applications [1]. The mechanism of conductance in arrays of CNT forests remains an open question, particularly regarding electron transport, contact resistance, and the influence of structural variations. This study examines the impact of CNT forest morphology on lateral electrical resistance and memristive properties. CNT forests were synthesized at 730°C using C_2H_2 gas source with different Fe catalyst annealing times, leading to variations in CNT alignment and growth height. Figure 1 shows memristive R-V characteristics of CNT forest films with different structural properties [2]. The results show that structural differences significantly affect hysteresis behavior and memory effects, with vertically oriented CNTs exhibiting pronounced memristive characteristics. A strong correlation was observed between CNT growth conditions—specifically, catalyst annealing time, and CNT growth height—and electrical response, highlighting the importance of controlled structural engineering for optimizing CNT-based memristors. These findings provide valuable insights for advancing CNT-based neuromorphic device technologies.

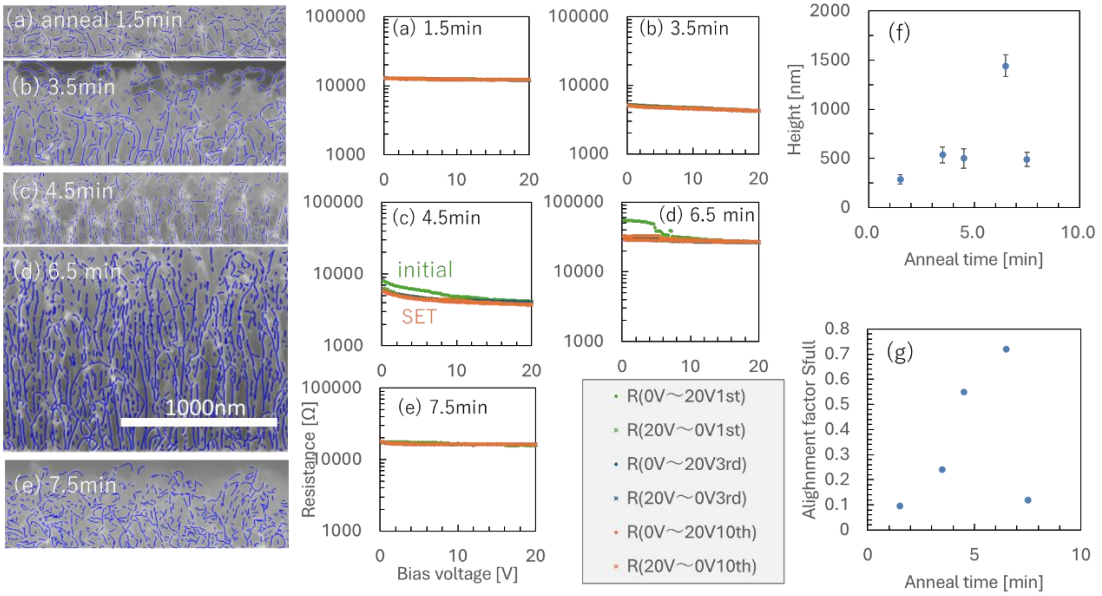

Figure 1: Memristive R-V characteristics of CNT forest films with different structural properties [2]. Cross-sectional SEM images for alignment analysis and R-V characteristics with various annealing time of Fe catalysts for (a) 1.5 min, (b) 3.5 min, (c) 4.5 min, (d) 6.5 min, and (e) 7.5 min. (f) Growth height and (g) alignment factor of CNT forests with various catalyst annealing time.

Acknowledgements: This work was supported by Grant-in-aid for Scientific Research (KAKENHI) 23K04383 (PI: Hiroshi Furuta)

References

[1] T. Shingu, H. Uchiyama, T. Watanabe, Y. Ohno, Carbon **214**, (2023).
[2] Y. Sato, H. Furuta, FNTG68, (Meijo Univ. Nagoya, 2025.03.01-03).

Direct identification and manipulation of valley coherence in monolayer semiconductor WSe_2

Haonan Wang[1], Kenji Watanabe[2], Takashi Taniguchi[2], Satoru Konabe[3] and Kazunari Matsuda[1]

[1]Institute of Advanced Energy, Kyoto University (Japan), [2]NIMS (Japan),
[3]Department of Chemical Science and Technology, Hosei University (Japan).

Monolayer transition metal dichalcogenides (TMDs) are granted with valley degree of freedom due to broken inversion symmetry, and strong spin-orbit coupling. The degenerated states at band-edges of K(K') valley possess information of valley pseudospin, which experiences intervalley decoherence process during emission [1]. With valley decoherence not coupling to any radiative dipole, direct probing or manipulation of valley coherence in the time domain has remain a challenge. Here we propose a method of optically exploring the valley coherence time in the time-domain measurement.

In this study, we have developed a method of direct measuring valley coherence time of the free exciton in monolayer WSe_2. By adopting photon-correlation Fourier spectroscopy, the decoherence process between K and K' valley excitons under various temperature and excitation power are directly measured with polarized interferometry. **Figure 1(a)** shows the typical interferogram arising from valley coherence under 4 K and 7 μW. The exacted valley coherence times from the interferogram are plotted in **Figure 1(b)**. It can be seen that the values of valley coherence time remain stable under temperature from 4 to 30 K, which is consistent with the previous result [2]. Moreover, the valley coherence time gradually decreases due to increased exciton-exciton collision with increasing excitation power condition [3]. We also explored the valley coherence of monolayer (1L) WSe_2 device with changing carrier density in the spectral and time domain. A wide tuning range of degree of linear polarization (DOLP) as well as valley coherence time are observed. Theoretical studies based on the Maialle-Silva-Sham (MSS) approach are conducted for elucidating the decoherence dynamics of valley pseudospin under various doping, which will be further discussed in detail.

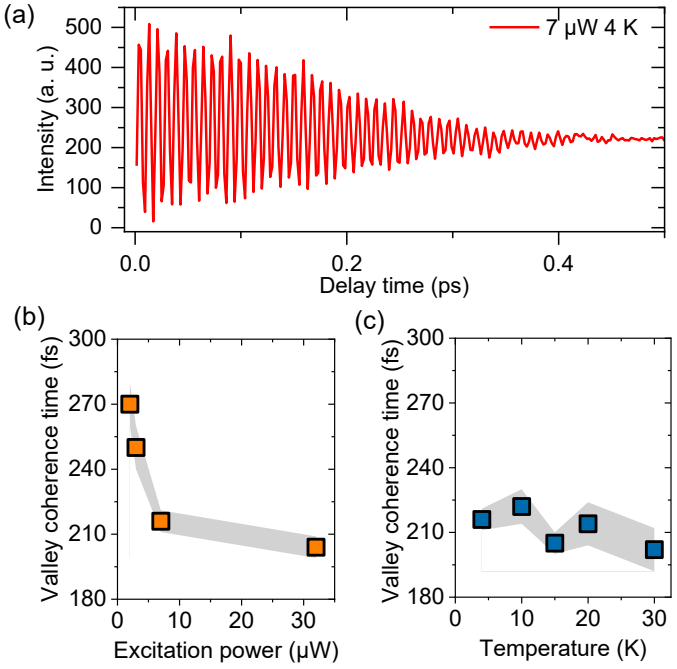

Figure 1 (a) Interferogram of intervalley decoherence process of free exciton in 1L-WSe_2 under 7 μW and 4 K. **(b)** Extracted valley coherence time of free exciton in 1L-WSe_2 under various temperature and excitation power

In conclusion, a new direct method for identification of exciton valley coherence has been applied to 1L-WSe_2 in the time-domain. The detail of intervalley decoherence process is explored under various temperature, excitation power and carrier doping condition, which will facilitate further understanding of valleytronics in 1L-TMDs.

References
[1] A. Jones, *et al. Nat. Nanotech.* **8**, 634–638 (2013).
[2] K. Hao, *et al. Nat. Phys.* **12**, 677–682 (2016).
[3] H. Wang, *et al. Nat. Commun.* **15**, 4905 (2024).

High-Density Polarization Dots in Short-Period Moiré Superlattices Enabled by Flexoelectric Effects

K. Tanaka[1], H. Ou[2], T. Takenobu[1]

[1]*Nagoya University (Japan),* [2]*Institute of Science Tokyo (Japan)*

Moiré superlattices emerge in two-dimensional (2D) materials when a small twist angle or slight lattice mismatch is introduced, resulting in periodic modulations that have attracted significant attention for phenomena such as superconductivity [1] and moiré ferroelectricity [2]. In transition metal dichalcogenides (TMDs), “long-period” moiré patterns (ranging from tens to hundreds of nanometers) have been extensively studied in the context of ferroelectric domains. However, research on “short-period” moiré patterns (~10 nm) remains scarce, and their properties are largely unexplored.

In this work, we investigated both long-period (Fig. 1) and short-period (Fig. 2(a)) moiré superlattices in twisted bilayer WSe_2 using piezoresponse force microscopy (PFM) [3] combined with atomic force microscopy (AFM). In particular, for short-period moiré superlattices, as shown in Fig. 2(b), we identified AA-stacked regions based on a slight increase in surface height observed via AFM. In these regions, as shown in Fig. 2(a), we detected strong PFM signals. Since these signals coincide with the AFM-identified AA regions, we conclude that strong PFM signals originate from AA-stacked domains. Furthermore, the clear correlation between local topographical bumps and signals suggests that flexoelectric effects arising from strain gradients play a dominant role in these short-period structures.

The strong PFM signals attributed to flexoelectric effects contrast with the relatively weak out-of-plane polarization typically expected from MX and XM stacking, which has been actively studied in recent years. Notably, the dense arrays of polarization dots observed in Fig. 2(a) at the nanometer scale hold promise for next-generation memory devices. In this presentation, we will also discuss the details of the observed flexoelectric effects and potential methods for controlling polarization in the future.

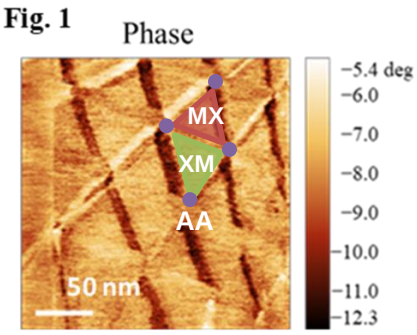

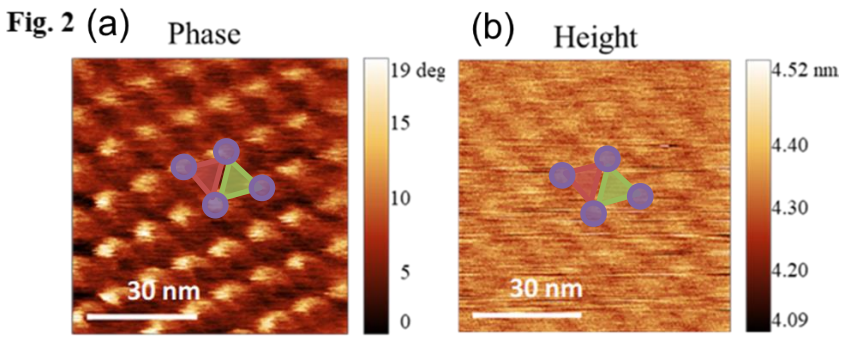

Figure 1: PFM image of long-period moiré superlattice.
Figure 2: (a) PFM image and (b) AFM (Height) image of short-period moiré superlattice.

References

[1] Y. Cao, et al., *Nature* **556,** 43-50 (2018)
[2] K. Yasuda, et al., *Science* **372,** 1458-1462, (2021)
[3] L. J. McGilly, et al., *Nat. Nanotechnol.* **15**, 580-584, (2020)

High current density in electric double layer light-emitting devices of WSe_2 monolayers

K. Oi[1], T. Aridome[1], H. Ou[2], J. Pu[2], T. Endo[3], Y. Miyata[3], T. Takenobu[1]

[1]Nagoya University (Japan), [2]Institute of Science Tokyo (Japan), [3]Tokyo Metropolitan University (Japan)

Group-VIB transition-metal dichalcogenides (TMDCs; MX_2, M = Mo or W, X = S or Se) are promising candidates for next-generation light-emitting materials due to their direct band gap, atomically thin structure, and excellent exciton stability at room temperature. Leveraging these properties, we have developed novel light-emitting devices (LEDs), including electric double-layer LEDs (EDLEDs), and demonstrated various electroluminescence (EL) devices, such as chiral and color-tunable light sources [1-5].

Although EDLEDs enable high-density carrier doping (~10^{14} /cm²) and low electrical resistance, the applicable voltage and current density are severely constrained by the redox potential of the electrolyte. Currently, the highest current density among monolayer TMDC LEDs is 517 kA/cm², achieved using an EDLED [2]. To surpass this record, increasing the applicable voltage is essential.

In this work, we explored multiple strategies to achieve the highest possible current density. First, EDLEDs were cooled to their glass transition temperature to suppress redox reactions, enabling the application of voltages significantly exceeding the redox potential. Additionally, pulsed voltages were utilized to circumvent redox reactions while still allowing for high-voltage application. Furthermore, optimizing the electrolyte composition enabled pulsed voltage application near room temperature while maintaining the system below the glass transition. By combining these approaches, we successfully achieved a current density exceeding MA/cm². In this presentation, we will detail our strategies and further discuss luminescence characteristics at high current densities.

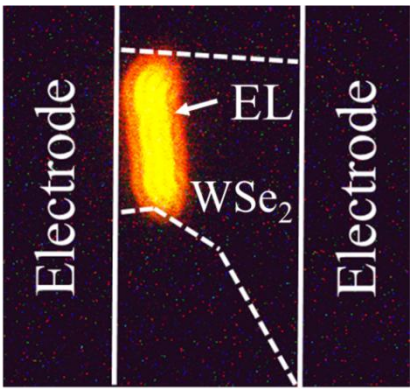

Fig1: Photo of WSe_2 EL

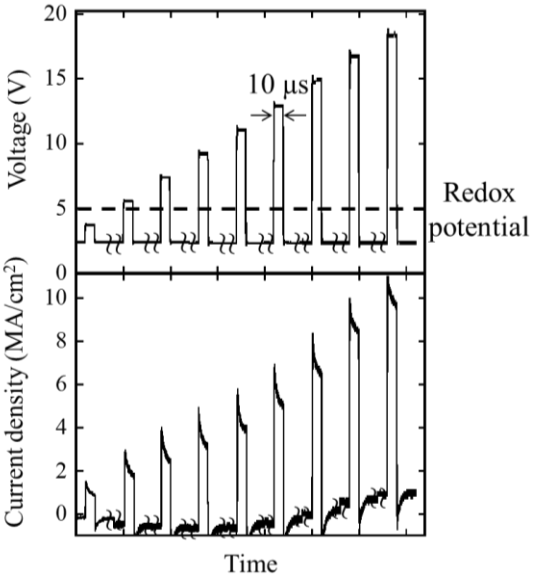

Fig2: Current density response to pulse voltage application of WSe_2 EL devices

References

[1] J. Pu, T. Takenobu *et al.*, *Adv. Mater.* **29**, 1606918 (2017).
[2] J. Pu, T. Takenobu *et al.*, *Adv. Mater.* **33**, 2100601 (2021).
[3] H. Ou, K. Oi, Y. Miyata, T. Takenobu *et al.*, *ACS Nano* **15**, 12911 (2021).
[4] J. Pu, Y. Miyata, T. Takenobu *et al.*, *Adv. Mater.* **34**, 2203250 (2022).
[5] N. Wada, T. Takenobu, Y. Miyata *et al.*, *Adv. Funct. Mater.* **32**, 2203602 (2022).

Novel Interface effects in Fe_2O_3@CNT

Aakanksha Kapoor[1], Avirup. Dey[1], Sunil Nair [1] and Ashna Bajpai[1]

[1]*Indian Institute of Science education and Research(IISER) Pune, Dr. Homi Bhabha Road, Pashan, Pune, India. 411 008 India*

Interface between two dissimilar materials is known for surprises in condensed matter system. We have been investigating hybrids of carbon nanotube (CNT) and functional magnetic oxides, in an attempt to uncover new functionalities that arise at the interface of the graphitic shells of multiwall CNT and functional magnetic oxides [1-4].The magnetic oxide which is encapsulated inside the core cavity of CNT is α-Fe_2O_3 or hematite. Here hematite is a well know Dyaloshinskii Moriya Interaction (DMI) driven canted antiferromagnet (AFM) and also a symmetry allowed piezomagnet/5/. While the Neel temperature (T_N) for hematite is ~950 K, there is another magnetic transition, known as the Morin transition (T_M ~260K). Hematite turns to a routine AFM from canted –AFM below the Morin Transition. Though hematite is a room temperature spin-canted AFM, the spin-canting angle is small due to very high T_N. We find that the manifestations of spin –canting effect & piezomagnetism are significantly enhanced, once it is encapsulated inside CNT/2,3/. The sample is in the form of long carpets of aligned CNT filled with α-Fe_2O_3 in the form of nano-wires inside the core cavity of the CNT (Fig1). Measurements have also been done in samples with entangled geometry. We would present experimental results on magnetization, remanent magnetization & Anomalous Nernst Effect (ANE) on α-Fe_2O_3@CNT along with reference data on bare α-Fe_2O_3. Significant enhancement in magnetization and remanent magnetization is observed due to strain at the interface in α-Fe_2O_3@CNT. This is corroborated through temperature variation of synchrotron XRD /3/ and Raman in the vicinity of T_M. ANE is the emergence of a transverse electric field in a magnetic material perpendicular to both the applied temperature gradient and the sample magnetization. It is to be noted that ANE is not expected to be significant in routine AFM as the effect is proportional to magnetization. However, α-Fe_2O_3@CNT shows significantly enhanced ANE[6]. Overall, encapsulation of hematite inside CNT leads to novel interface effects that can be important from both fundamental and application point of view.

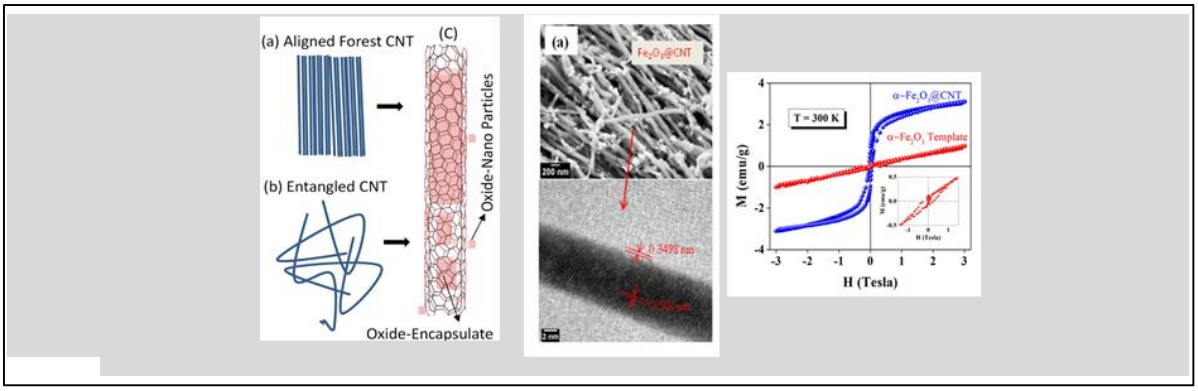

Figure 1:(a) & (b) in left figure *display schematic for oxide@CNT in "aligned forest" and "entangled" morphology* ***(c)*** *schematic for oxide emasculate inside CNT in the form of long and short nano-wires.* ***Middle Figure****:* SEM and TEM images of ***α***-Fe_2O_3@CNT formed in aligned forest geometry. **Right figure** is M vs H measured on ***α***-Fe_2O_3@CNT (blue dots) and corresponding template (bare ***α***-Fe_2O_3 nano-particles) formed in the same morphology (red dots)

References

[1] A.Bajpai et.al, A carbon-nanotube based nano-furnace for in-situ restructuring of a magnetoelectric oxide, 114, 291 (2017).
[2] A. Kapoor et,al, 3d transition metals and oxides within carbon nanotubes by co-pyrolysis of metallocene & camphor: High filling efficiency and self-organized structures, Carbon,733, (2018).
[3] A. Kapoor et.al, Enhanced magnetism and time-stable remanence at the interface of hematite and carbon nanotubes, Nanotechnology, 30, 385706, (2019).
[4] A. Kapoor et.al, Synthetically encapsulated & self-organized transition metal oxide nano-structures inside carbon nanotubes as robust: Li-ion battery anode materials, J. Phys. D: applied physics, 58,425504, (2023)
[5] I. E. Dzyaloshinskii, JETP 32, 1259 (1957).
[6] A.De, A. Kapoor, S. Nair and A.Bajpai (manuscript under preparation)

RECONFIGURABLE NONLINEAR LOSSES OF NANOMATERIAL COVERED WAVEGUIDES

Ayvaz Davletkhanov [1,2], Daniil Ilatovskii[3], Aram Mkrtchyan[4], Alexey Bunkov[4], Dmitry Krasnikov[4], Albert Nasibulin[4], Yuriy Gladush[4], Ralph Krupke[1,2,5]

[1]Institute of Quantum Materials and Technologies, Karlsruhe Institute of Technology (Germany), [2]Institute of Materials Science, Technische Universität Darmstadt (Germany), [3]Okinawa Institute of Science and Technology (Japan), [4]Skolkovo Institute of Science and Technology (Russia) ,[5] Institute of Nanotechnology, Karlsruhe Institute of Technology (Germany),

Devices for controlling propagating light are a necessity in all optical systems, spanning from optical communications to all-optical computing systems. In systems where light travels in waveguides, one effective method for light control involves covering the waveguide with nanomaterial. The idea of nanomaterial covered waveguides has already led to many practical demonstrations from saturable absorbers and modulators to optical sensors [1, 2]. Further development of this approach implies the creation of reconfigurable devices granting more freedom for light manipulation. In the present study, we show that the nonlinear response of the nanomaterial covered waveguide, exemplified by the case of a polished optical fiber covered with single-walled carbon nanotube film, can be reversed to act as an optical limiter, which means increased losses at higher intensities [2]. This behavior is rather unexpected and uncommon, as the carbon nanotube film is well-known as a saturable absorber material, implying reduced losses at higher intensities. Moreover, the device can exhibit non-monotonic relationships between losses and intensity, and these characteristics can be adjusted by varying the thickness of the nanotube film. By utilizing electrochemical gating of the nanotube film, we demonstrate the applicability of the observed effect by fabricating the device whose nonlinear optical response can be controllably switched between saturable absorbing and optical limiting. The findings are supported by an analytical approach extending the phenomenon to planar waveguides and revealing the conditions for its observation. It should be emphasized that the effect under consideration is a general phenomenon that can be observed in various waveguide types and covering materials, once the requirements on material thickness and refractive index are met. These introduce possibilities for engineering the complex nonmonotonic nonlinear optical response of nanomaterial covered waveguides, which could be implemented in all-optical computing and neuromorphic integrated photonic systems. In addition, our study highlights the importance of optimization of the parameters of saturable absorbers on a waveguide and presents a theoretical framework for it.

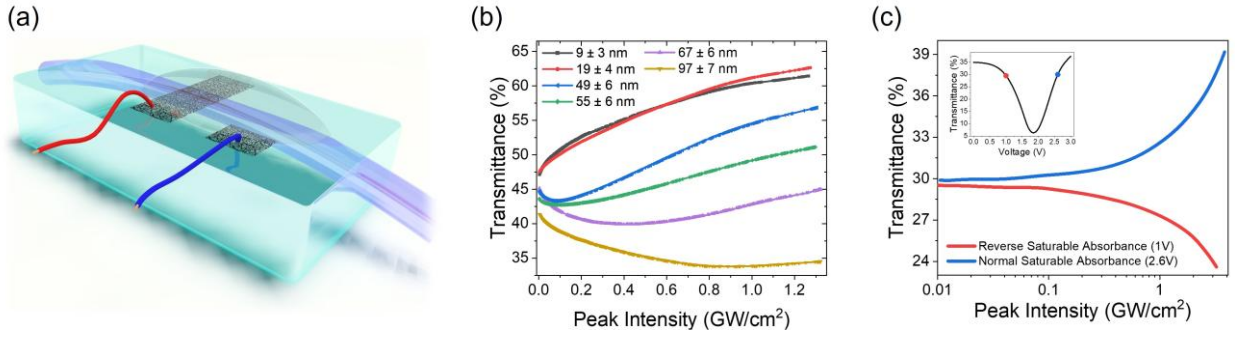

Figure caption: (a) Graphical illustrations of the polished fiber with carbon nanotube film gated with ionic liquid, (b) nonlinear transmittance curves for different film thicknesses and (c) gate voltage.

References

[1] Zhipei Sun *et al.*, *Nat. Photonics* **10**, *227–238 (2016)*.
[2] Yong-Won Song, *Opt. Lett.* **32**, 148–150 (2007).
[3] Ayvaz Davletkhanov *et al.*, *Nanophotonics* **12**, *4229–4238 (2023)*.

Session
NT 25（The 25th International Conference on the Science and Applications of Nanotubes and Low-

| Main conference：Main conference

Fri. Jun 20, 2025 9:30 AM - 12:10 PM JST | Fri. Jun 20, 2025 12:30 AM - 3:10 AM UTC Centennial Hall (Clock Tower Centennial Hall)

[20ma] Main Conference

Chair: Taishi Takenobu, Suguru Noda

9:30 AM - 10:10 AM JST | 12:30 AM - 1:10 AM UTC

[20ma-01]

Synthesis and Characterization of Janus Transition Metal Dichalcogenide Materials

*Jing Kong[1] (1. MIT (United States of America))

10:10 AM - 10:40 AM JST | 1:10 AM - 1:40 AM UTC

[20ma-02]

Synthesis and scalable transfer of research-grade CVD graphene

*James Hone[1] (1. Columbia University (United States of America))

11:00 AM - 11:30 AM JST | 2:00 AM - 2:30 AM UTC

[20ma-03]

CARBON-BASED MULTI-VIEW TERAHERTZ AND INFRARED IMAGERS

*Yukio Kawano[1,2,3], Kou Li[1] (1. Chuo University (Japan), 2. National Institute of Informatics (Japan), 3. Kanagawa Institute of Industrial Science and Technology (Japan))

11:30 AM - 11:50 AM JST | 2:30 AM - 2:50 AM UTC

[20ma-04]

Stepwise Engineering of van der Waals Heterostructures for High Current Density in Light Emitting Devices

Rei Usami[1], Koshi Oi[1], Keisuke Yamada[1], Jiang Pu[2], Hao Ou[2], Takahiko Endo[3], Yasumitsu Miyata[3], *Taishi Takenobu[1] (1. Nagoya University (Japan), 2. Institute of Science Tokyo (Japan), 3. Tokyo Metropolitan University (Japan))

11:50 AM - 12:10 PM JST | 2:50 AM - 3:10 AM UTC

[20ma-05]

CARBON AND BORON NITRIDE MATERIALS: BASIC SCIENCE AND BROADER IMPACT

*Rodney Ruoff[1,2] (1. IBS CMCM (Korea), 2. UNIST (Korea))

Synthesis and Characterization of Janus Transition Metal Dichalcogenide Materials

Jing Kong

Department of Electrical Engineering and Computer Science, MIT

In recent years, 2D Janus transition metal dichalcogenide (TMD) materials have attracted a lot of attention due to their unique structures, remarkable properties, and potential applications. It is a type of 2D material that cannot be obtained by exfoliation from its bulk counterparts but has to be obtained chemically from its parent TMD monolayer. Compared with the original TMD monolayer, structurally it adds an additional dipole moment and a broken mirror symmetry in the out of plane direction. This enables a variety of unprecedented properties, such as large Rashba spin splitting and enhanced piezoelectric and nonlinear optical response and induced built in electric field, etc. In this talk I will present our research efforts in synthesizing Janus TMD monolayers, characterizing their properties and exploring their potential applications.

Synthesis and scalable transfer of research-grade CVD graphene

James Hone

Columbia University, USA

This talk will review our recent achievements in synthesis and transfer of CVD-grown graphene. We have recently demonstrated that controlling trace oxygen at the parts-per-million level is the key to achieving highly repeatable graphene CVD synthesis. [1] Oxygen-free CVD (OF-CVD) synthesis displays straightforward kinetics that can be understood within a simple model that predicts growth rate over a wide range of conditions. OF-CVD graphene is defect-free and free of surface contamination, with high electronic quality. In more recent work, we have demonstrated a facile method for transfer of OF-CVD graphene that yields arrays of arbitrary shapes with identical crystal orientation. When incorporated into heterostructures, the transferred OF-CVD graphene yields devices with performance indistinguishable from exfoliated graphene, including fully developed integer quantum Hall states at B=10 mT, and highly detailed fractional quantum Hall spectrum at high fields. This work points the way to going 'beyond scotch tape' for even the most demanding of applications.

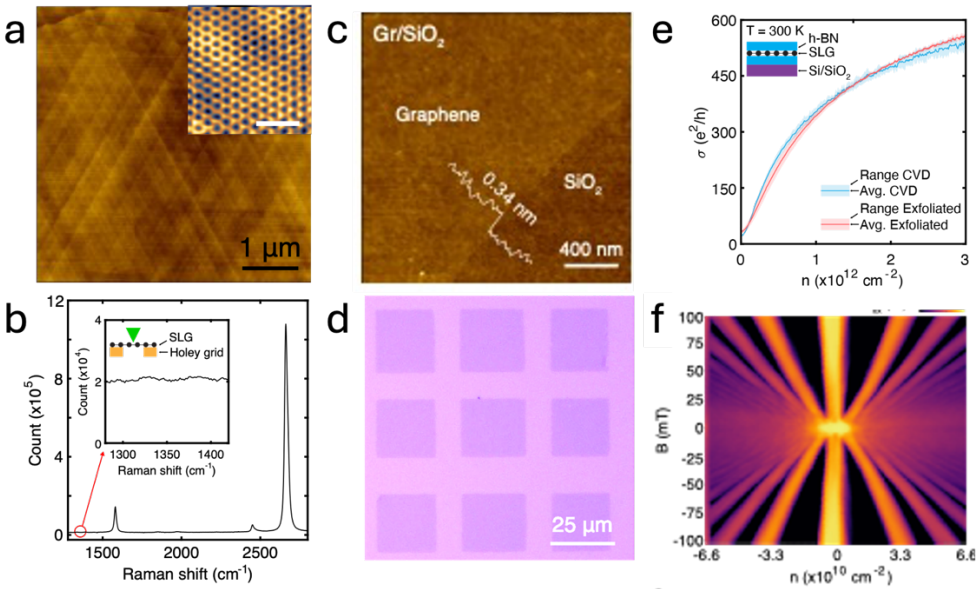

Research-quality OF-CVD graphene: (a) AFM image of graphene grown on Cu(111) film. Inset shows STM image of graphene lattice. (b) Raman spectrum of OF-CVD graphene. Inset shows magnified view in the vicinity of the D peak. (c) AFM image of graphene after transfer to Si/SiO_2 substrate. Profile shows step height at edge. (d) Optical image of array of identical graphene squares after transfer. (e) Measured room-temperature conductivity of OF-CVD graphene compared to exfoliated. (f) Low-temperature Landau fan showing emergence of fully developed quantum Hall states in the mT range.

References

[1] Amontree, J., et al. *Nature* **630**, 636-642, (2024).

CARBON-BASED MULTI-VIEW TERAHERTZ AND INFRARED IMAGERS

Y. Kawano[1-3] and K. Li[1]

[1]Chuo University (Japan), [2]National Institute of Informatics (Japan), [3]Kanagawa Institute of Industrial Science and Technology (Japan)

We present flexible terahertz (THz) and infrared (IR) imaging sheets based on carbon nanotube (CNT) films with broadband optical absorption properties [1-10]. We demonstrated multi-view THz and IR visualization (Figs. 1 a-c), which enabled omni-directional analysis for various forms of objects. As industrial applications of the imagers, we showed nondestructive detection of impurities concealed inside coating [4] and non-sampling and label-free chemical monitoring [5]. In order to improve the detection sensitivity, the use of plasmon-based technologies is promising because of their plasmon-mediated ability to strongly confine an electromagnetic wave [11]. We previously reported on a continuously frequency-tunable plasmonic structure in THz region and its application to non-invasive inspections [12]. By developing a non-circular shaped structure with a subwavelength aperture surrounded by continuously varied, concentric plasmonic grooves (Figs. 2 a,b), we demonstrated that the resonant frequency of the plasmon-mediated THz concentration becomes freely tunable (Fig. 2 c), which would largely enhance its usefulness for the CNT sensor.

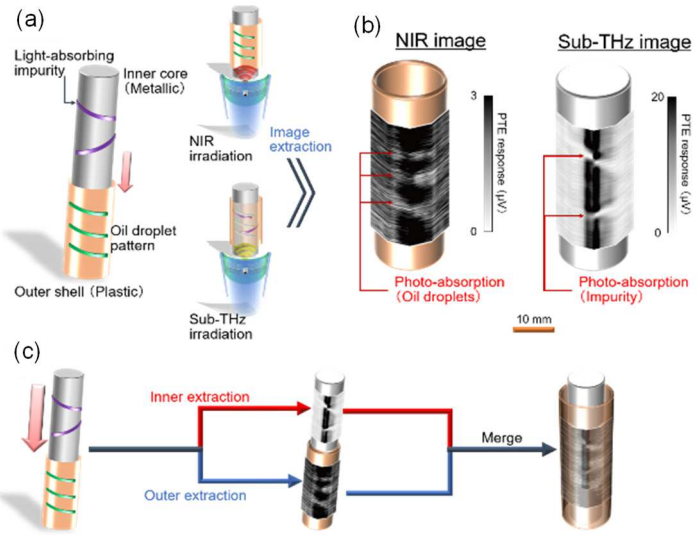

Figure 1: (a) Hierarchical image extraction of a multi-layered columnar object with the reflective multi-view multi-frequency band imaging in sub-THz (λ = 1.15 mm) and NIR (λ = 870 nm) regions. (b) Image extractions of the outer shell (NIR) and the inner core (sub-THz). (c) Image restoration of the multi-layered columnar object by covering the inner hierarchical image with the outer hierarchical one. Reprinted with permission from [4]. Copyright 2021, Springer Nature.

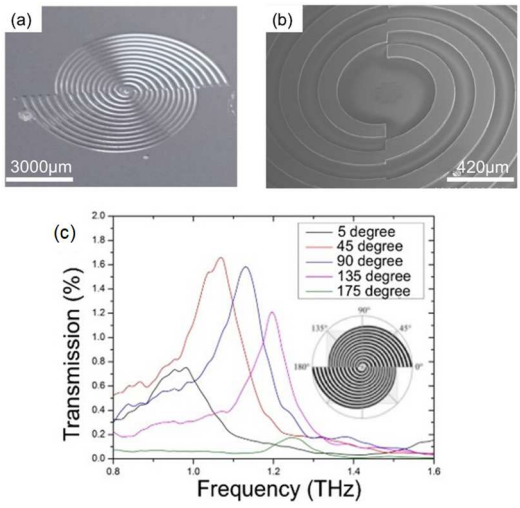

Figure 2: (a) Photograph of the frequency-tunable non-circular plasmonic structure. (b) Magnified image of (a). (c) Transmission spectra for (a) with different polarization direction of the incident THz wave. Reprinted with permission from [12]. Copyright 2019, Springer Nature.

References

[1] D. Suzuki, S. Oda, and Y. Kawano, *Nature Photonics* **10**, 809–813 (2016).
[2] D. Suzuki and Y. Kawano, *Carbon* **162**, 13–24 (2020).
[3] D. Suzuki *et al.*, *Advanced Functional Materials* **31**, 2008931 (2021).
[4] K. Li *et al.*, *Nature Communications* **12**, 3009 (2021).
[5] K. Li *et al.*, *Science Advances* **8**, eabm4349 (2022).
[6] K. Li *et al.*, *Advanced Materials Interfaces* **10**, 2300528 (2023).
[7] T. Araki *et al.*, *Advanced Materials* **36**, 2304048 (2024).
[8] R. Kawabata *et al.*, *Advanced Materials* **36**, 2309864 (2024).
[9] K. Li *et al.*, *Advanced Optical Materials* **12**, 2302847 (2024).
[10] Y. Matsuzaki *et al.*, *Small Science*, early view, 2400448 (2025).
[11] T. Iguchi, T. Sugaya, and Y. Kawano, *Appl. Phys. Lett.* **110**, 151105 (2017).
[12] X. Deng, L. Li, M. Enomoto, and Y. Kawano, *Scientific Reports* **9**, 3498 (2019).

Stepwise Engineering of van der Waals Heterostructures for High Current Density in Light Emitting Devices

R. Usami[1], K. Oi[1], K. Yamada[1], J. Pu[2], H. Ou[2], T. Endo[3], Y. Miyata[3], T. Takenobu[1]

[1]Nagoya University (Japan), [2]Institute of Science Tokyo (Japan), [3]Tokyo Metropolitan University (Japan)

Van der Waals (vdW) heterostructures of transition metal dichalcogenides (TMDs) have attracted significant attention in optoelectronic applications, including light-emitting devices (LEDs) and lasers [1]. However, realizing high current density in PN-junction-based vdW LEDs has been hindered by the challenges associated with efficient doping techniques, leading to limited carrier injection and high device resistance [2]. In this study, we present a novel approach that leverages stepwise engineering of vdW heterostructures combined with electric double-layer (EDL) doping to achieve enhanced carrier injection and reduced resistance.

We fabricated a WS_2/WSe_2 heterostructure LED where both P-type and N-type materials are in direct contact with an electrolyte, allowing for efficient high-density carrier doping via the EDL effect. This unique stepwise-engineered structure facilitates improved charge transport by ensuring direct electrolyte access to both materials, forming a well-defined PN junction with stable electroluminescence (EL) emission. Importantly, our approach addresses a key limitation of conventional electrolyte-based LEDs, where the EL emission position often shifts with applied bias [2-4]. Our design ensures fixed-position EL at the heterostructure interface (see figure), a crucial advantage for future integration with optical resonators and laser applications.

Electrical and optical characterizations revealed non-linear current-voltage characteristics with clear rectification behavior, confirming PN junction formation at the WSe_2/WS_2 interface. The EL spectrum predominantly corresponds to the direct bandgap transition of WS_2, suggesting efficient hole injection from WSe_2 into WS_2. Notably, our device achieved a peak current density of 8.4×10^4 A/cm², significantly exceeding previously reported values for vdW heterostructure LEDs and approaching the requirements for laser operation. This improvement is attributed to the stepwise-stacked structure, which minimizes series resistance while enhancing charge accumulation at the junction.

Our findings demonstrate the potential of vdW heterostructures for high-performance light-emitting applications, providing a viable pathway toward current-driven lasing in two-dimensional materials. The combination of stepwise engineering and electrolyte gating represents a promising strategy for overcoming doping challenges in vdW semiconductors, paving the way for advanced nano-optoelectronic devices.

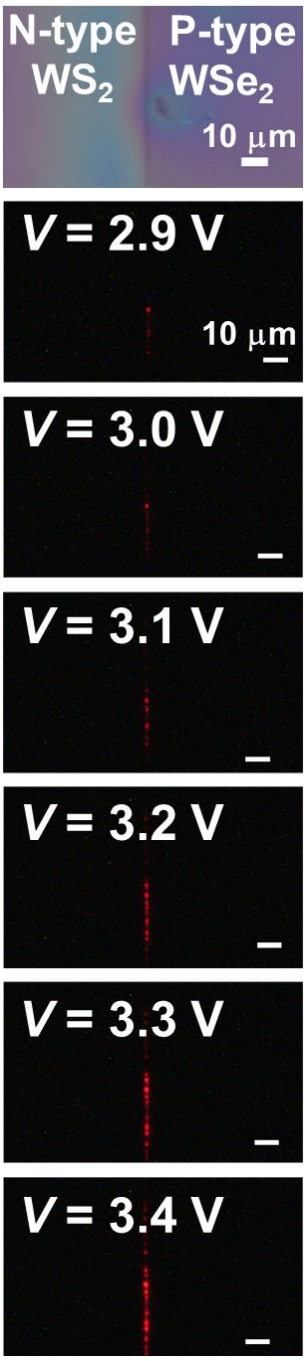

Figure Fixed-position EL at the heterostructure interface

References

[1] Y. Liu *et al.*, *Nat. Rev. Mater.* **1**, 16042 (2016).
[2] J. Pu, T. Takenobu, *Adv. Mater.* **30**, 1707627 (2018).
[3] J. Pu *et al.*, *Adv. Mater.* **29**, 1606918 (2017).
[4] H. Henck *et al.*, *Nat. Commun.* **13**, 3917 (2022).

CARBON AND BORON NITRIDE MATERIALS: BASIC SCIENCE AND BROADER IMPACT

Rodney S. Ruoff[1,2]

[1]*Center for Multidimensional Carbon Materials (CMCM), Institute for Basic Science (IBS) (Republic of Korea),*
[2]*Department of Chemistry, Ulsan National Institute of Science and Technology (UNIST) (Republic of Korea)*

We have discovered some quite interest things about the macroscale strength of single crystal graphene. Many materials exhibit very high strength including ideal strength values, at microscale. We have CVD-grown single crystal and large area graphene (SCG) on Cu(111) and Ni(111) substrates. The centimeter-length scale tensile strength, strain-at-failure, and toughness modulus, are quite literally "out of this world" with strength values 5x to 6x that of the highest strength macroscale material commercially available (Toray ultra-strength carbon fibers (TORAYCA™ T1200 that Toray states has tensile strength of 8.0 GPa, Young's modulus 317 GPa; https://www.toraycma.com/toray-develops-torayca-t1200-the-ultra-high-strength-carbon-fiber/), and see [1]. Both the basic science and practical applications of macroscale SCG tensile mechanics are extremely intriguing (such as potentially enabling a 100,000 km tether for the space elevator, it's use in solar sails, and many earth-based uses for astonishingly high specific strength materials). In addition to discussing this in detail I will also outline the macroscale strength possibilities for single crystal hBN.

Diamond & graphite are essentially isoenergetic at STP (298K, 1 atm) as are hexagonal-boron nitride (hBN) & cubic boron nitride (cBN), and the same is true at higher temperatures. For a sample containing only graphite and diamond that is at chemical equilibrium the mass percentage of each is about 50 wt% diamond and about 50 wt% graphite. And yet there is a perception that it 'must be' more difficult to form diamond, and also cubic boron nitride, than graphite and hBN, respectively. Why? Because to date, this has been true. Also, on Earth there seems to be much more natural graphite than natural diamond, and there is (now) much more synthetic graphite annually produced than synthetic diamond. But must this always be so, going forward? I describe how one might synthesize diamond and cBN in new ways, and see [2]. *Supported by the Institute for Basic Science (IBS-R019D1).*

References

[1] Anirban Kundu , Seyed Kamal Jalali, Minhyeok Kim , Meihui Wang, Da Luo, Sun Hwa Lee, Nicola M.Pugno, Won Kyung Seong, Rodney S. Ruoff. The Mechanical Behaviour of Macroscale Single-Crystal Graphene. https://arxiv.org/abs/2411.01440v111.01440v1

[2] Yan Gong, Da Luo, Myeonggi Choe, Won Kyung Seong, Pavel Bakharev, Meihui Wang, Seulyi Lee, Tae Joo Shin Zonghoon Lee, Rodney Ruoff. Growth of diamond in liquid metal at 1 atmosphere pressure. *Nature*. 2023, 629, 348-354.